

ZOOLOGICAL SCIENCE

An International Journal

VOLUME 7
1990

published by

The Zoological Society of Japan



CONTENTS OF VOLUME 7

NUMBER 1, FEBRUARY 1990

REVIEWS

- Gotoh, T. and T. Suzuki: Molecular assembly and evolution of multi-subunit extracellular annelid hemoglobins 1
- Lawrence, J. M.: The effect of stress and disturbance on echinoderms 17

ORIGINAL PAPERS

Cell Biology and Morphology

- Low, W. P., Y. K. Ip and D. J. W. Lane: A comparative study of the gill morphology in the mudskippers - *Periophthalmus chrysophilus*, *Boleophthalmus boddarti* and *Periophthalmodon schlosseri* 29
- Kondo, H., Y. Yonezawa and T. A. Nomaguchi: Difference in migratory ability between human lung and skin fibroblasts 39

Immunology

- Kono, H., A. Mizoguchi, H. Nagasawa, H. Ishizaki, H. Fugo and A. Suzuki: A monoclonal antibody against a synthetic carboxyl-terminal fragment of the eclosion hormone of the silkworm, *Bombyx mori*: characterization and application to immunohistochemistry and affinity chromatography 47

Biochemistry

- Michibata, H., T. Uyama and J. Hirata: Vanadium-containing blood cells (vanadocytes) show no fluorescence due to the tunichrome in the ascidian, *Ascidia sydneiensis samea* 55

Developmental Biology

- Ma, Y. K. and S. B. Ramaswamy: Histochemistry of yolk formation in the ovaries of the tarnished plant bug, *Lygus lineolaris* (Palisot de Beauvois) (Hemiptera: Miridae) (COMMUNICATION) 147
- Kamishima, Y.: Organization and development of reflecting platelets in iridophores of

- the giant clam, *Tridacna crocea* Lamarck 63
- Ishikawa, T.: Effects of puromycin and α -amanitin on the activity of alkaline phosphatase in early preimplantation mouse embryos (COMMUNICATION) 153
- Uchiyama, M., T. Murakami and H. Yoshizawa: Notes on the development of the crab-eating frog, *Rana cancrivora* 73

Reproductive Biology

- Asada, N. and T. Fukumitsu: Reaction mass formation in *Drosophila*, with notes on a phenoloxidase activation 79
- Jarosz, S. J. and W. R. Dukelow: Embryo transfer and pregnancy rate in the golden hamster (*Mesocricetus auratus*) 85

Endocrinology

- Tagawa, M., S. Miwa, Y. Inui, E. G. de Jesus and T. Hirano: Changes in thyroid hormone concentrations during early development and metamorphosis of the flounder, *Paralichthys olivaceus* 93
- Tasaki, Y. and S. Ishii: Effects of thyroidectomy, hypophysectomy, temperature and humidity on the occurrence of nocturnal locomotor activity in the toad, *Bufo japonicus*, during the breeding season 97
- Uchiyama, M. and T. Murakami: Effects of hypophysectomy and replacement therapy with several hormones on plasma sodium concentrations in bullfrog tadpoles 105

Taxonomy and Systematics

- Abé, H.: Two species of the genus *Actacarus* (Acari, Halacaridae) from Japan 111
- Yunxia, T. and Y. Shaoyi: Comparative study on LDH isozymes in different subfamily of teleost fish - grass carp (*Ctenophryngodon idellus*) and blunt snout-bream (*Megalobrama amblycephala*) 127

Watabe, H., X. C. Liang and W. X. Zhang: The <i>Drosophila robusta</i> species-group (Dip- tera: Drosophilidae) from Yunnan Pro- vince, southern China, with the revision of its geographic distribution.....	133
Ando, A., S. Shiraishi and T. A. Uchida: Reexamination on the taxonomic position of two intraspecific taxa in Japanese <i>Eothe- nomys</i> : evidence from crossbreeding experi- ments (Mammalia: Rodentia)	141
Instructions to authors	159

NUMBER 2, APRIL 1990

REVIEWS

Yasugi, S. and T. Mizuno: Mesenchymal- epithelial interactions in the organogenesis of digestive tract	159
Tiedemann, H.: Cellular and molecular aspects of embryonic induction.....	171

ORIGINAL PAPERS

Physiology

Ip, Y. K., S. F. Chew and R. W. L. Lim: Ammoniogenesis in the mudskipper, <i>Periophthalmus chrysospilos</i>	187
Niida, A. and T. Ohono: Tectal visual affer- ents from fish dorsolateral tegmental cells (COMMUNICATION)	327
Mizutani, A. and Y. Toh: Morphological and physiological characterization of the para-ocellar nerve of the cockroach, <i>Peri- planeta americana</i> (COMMUNICATION)	331

Cell Biology

Fu, Y., K. Sato, K. Hosokawa and K. Shioka- wa: Expression of circular plasmids which contain bacterial chloramphenicol acetyl- transferase gene connected to the promoter of polypeptide IX gene of human adenovirus type 12 in oocytes, eggs and embryos of <i>Xenopus laevis</i>	195
Kusakabe, T.: Ultrastructural studies of the carotid labyrinth in the newt, <i>Cynops pyr- rhogaster</i>	201

Genetics

Niwa, M. and N. Wakasugi: Abnormal development of preimplantation embryos derived from intersubspecific hybrids be-	
---	--

tween <i>Mus musculus molossinus</i> and <i>M. m. domesticus</i>	209
--	-----

Immunology

Saad, A. H. and E. Cooper: Evidence for a Thy-1-like molecule expressed on earth- worm leucocytes	217
---	-----

Developmental Biology

Sivasubramanian, P. and D. R. Nässel: Neu- ral control of flight muscle differentiation in the fly, <i>Sarcophaga bullata</i>	223
Tonegawa, Y., E. Hojiro and K. Takahashi: Effect of pH on the participation of calcium ion in the cell aggregation of sea urchin embryos.....	229

Reproductive Biology

Tachi, C. and S. Tachi: Mechanisms under- lying regulation of local immune responses in the uterus during early gestation of eutherian mammals. III. Possible functional dif- ferentiation of macrophages cultured together with blastocyst <i>in vitro</i> , with special reference to the cellular shape and produc- tion of leukotriene C ₄	235
--	-----

Endocrinology

Tasaki, Y. and S. Ishii: Effects of thyroxine on locomotor activity and carbon dioxide release in the toad, <i>Bufo japonicus</i>	249
Yamada, C., S. Noji, S. Shioda, Y. Nakai and H. Kobayashi: Intragranular colocalization of arginine vasopressin- and angiotensin II- like immunoreactivity in the hypothalamo- neurohypophysial system of the goldfish, <i>Carassius auratus</i>	257

- Polzonetti-Magni, A. M., R. Curini, O. Carnevali, C. Novara, M. Zerani and A. Gobetti: Ovarian development and sex steroid hormones during the reproductive cycle of *Rana esculenta* complex 265
- Mugiya, Y.: Long-term effects of hypophysectomy on the growth and calcification of otoliths and scales in the goldfish, *Carassius auratus* 273
- Kobayashi, Y. and M. Okada: Urea stimulation of pituitary pars intermedia cells of suckling mice under copious drinking 281

Morphology

- Itow, T., T. Masuda and K. Sekiguchi: Formation of ganglions and stomodaeum in normal and separate embryos of horseshoe crab,

- Tachypleus tridentatus* 287

Taxonomy

- Wynn, S., M. J. Toda and T. X. Peng: The genus *Phorticella* Duda (Diptera: Drosophilidae) from Burma and southern China 297
- Fukuda, Y.: Early larval and postlarval morphology of the soldier crab, *Mictyris brev-dactylus* Stimpson (Crustacea: Brachyura: Mictyridae) 303
- Okajima, S.: Some *Nesothrips* (Insecta, Thysanoptera, Phlaeothripidae) from east Asia 311
- Miura, T. and L. Laubier: Nautiliniellid polychaetes collected from the Hatsushima cold-seep site in Sagami Bay, with descriptions of new genera and species 319

NUMBER 3, JUNE 1990

REVIEWS

- Plisetskaya, E. M.: Recent studies of fish pancreatic hormones: Selected topics 335
- Suzuki, N.: Structure and function of sea urchin egg jelly molecules 355

ORIGINAL PAPERS

Physiology

- Nakashima, H. and Y. Kamishima: Regulation of water permeability of the skin of the treefrog, *Hyla arborea japonica* 371
- Hori, K., Y. Furukawa and M. Kobayashi: Regulatory actions of 5-hydroxytryptamine and some neuropeptides on the heart of the African giant snail, *Achatina fulica* Férussac 377
- Kanui, T. I., K. Hole and J. O. Miaron: Nociception in crocodiles: Capsaicin instillation, formalin and hot plate tests (COMMUNICATION) 537

Cell Biology and Morphology

- Tamamaki, N.: Evidence for the phagocytotic removal of photoreceptive membrane by pigment cells in the eye of the planarian, *Dugesia japonica* 385

- Sato, M., H. Mitani and A. Shima: Eurythermic growth and synthesis of heat shock proteins of primary cultured goldfish cells 395
- Iga, T., J. Kinutani and N. Maeno: Motility of cultured iridophores from the freshwater goby, *Odontobutis obscura* 401

Biochemistry

- Ryuzaki, M. and M. Oonuki: Changes in lipid composition in the tail of *Rana catesbeiana* larvae during metamorphosis 409

Genetics

- Phang, V. P. E., A. A. Fernando and E. W. K. Chia: Inheritance of the color patterns of the blue snakeskin and red snakeskin varieties of the guppy, *Poecilia reticulata* 419

Developmental Biology

- Irisawa, S., T. Iguchi and N. Takasugi: Critical period of induction by tamoxifen of genital organ abnormalities in male mice (COMMUNICATION) 541

Reproductive Biology

- Pandey, S. C. and S. D. Pandey: Photo-periodic influences on pheromonal delay of puberty in young female wild mice (COMMUNICATION).....547

Endocrinology

- Oota, Y.: Immunocytochemical and ultra-structural characterization of the cells in the pars tuberalis of the turtle, *Geoclemys reevesii* (COMMUNICATION)551
- Taniguchi, Y., S. Tanaka and K. Kurosumi: Distribution of immunoreactive thyrotropin-releasing hormone in the brain and hypophysis of larval bullfrogs with special reference to nerve fibers in the pars distalis427
- Takei, Y. and T. X. Watanabe: Vasodepressor effect of atrial natriuretic peptides in the quail, *Coturnix coturnix japonica*.....435

Taxonomy and Systematics

- Tanabe, T.: A new milliped of the genus *Riukiaria* from Is. Yaku-shima, Japan (Diplopoda; Polydesmida; Xystodesmidae)443
- Ito, A. and S. Imai: Ciliate Protozoa in the

- rumen of Holstein-Friesian cattle (*Bos taurus taurus*) in Hokkaido, Japan, with the description of two new species449
- Watabe, H., X. C. Liang and W. X. Zhang: The *Drosophila polychaeta* and the *D. quadri-setata* species-groups (Diptera: Drosophilidae) from Yunnan Province, southern China459
- Sawada, I. and M. Harada: Cestodes of field micromammals (Insectivora) from central Honshu, Japan.....469
- Takeda, M. and N. Shikatani: Crabs of the genus *Calappa* from the Ryukyu Islands, with description of a new species.....477
- Ito, T. and M. J. Grygier: Description and complete larval development of a new species of *Baccalaureus* (Crustacea: Ascothoracida) parasitic in a zoanthid from Tanabe Bay, Honshu, Japan.....485
- Abé, H.: Three new species of the genus *Rhombognathus* (Acari, Halacaridae) from Japan517
- Inger, R. F. and R. J. Wassersug: A centrolenid-like anuran larva from southeast Asia (COMMUNICATION).....557

NUMBER 4, AUGUST 1990

REVIEWS

- Koolman, J.: Ecdysteroids563
- Yoshizaki, N.: Functions and properties of animal lectins581

ORIGINAL PAPERS

Physiology

- Lin, J. T., Toh, Y., Mizutani, M. and H. Tateda: Putative neurotransmitter in the ocellar neuropil of American cockroaches593
- Okamoto, K. and T. Tagawa: Aminergic, cholinergic and peptidergic innervation of hepatic portal vein in the anuran amphibians605

Cell Biology

- Waku, Y., Koike, M. and N. Yoshida: Cell

- culture of the antennal imaginal disc of the silkworm, *Bombyx mori* L. and differentiation of neurons from the culture613
- Uchiyama, M., Yoshizawa, H., Wakasugi, C. and C. Oguro: Structure of the internal gills in tadpoles of the crab-eating frogs, *Rana cancrivora*.....623

Biochemistry

- Tamanai, I., Fujii, N., Muraoka, S., Harada, K., Joshima, H. and T. Ishihara: The induction of D-aspartic acid in mouse lens protein by continuous gamma-irradiation (COMMUNICATION)763

Immunology

- Saad, A. H.: Estradiol-induced lymphopenia in the lizard, *Chalcides ocellatus*

-631
 Nunomura, W., Watanabe, H. K. and H. Hirai: Interaction of C-Reactive protein with macrophages in rat (COMMUNICATION)767

Developmental Biology

- Yang C.-H. and R. Yanagimachi: Changes in the rigidity of the hamster egg during meiotic maturation and after fertilization ..639
 Kanayama, M. and Y. Kamishima: Role of symbiotic algae in hatching of gemmules of the freshwater sponge, *Radiospongilla cerebellata*.....649
 Tacke, L. and H. Grunz: Effect of cytochalasin B, nocodazol and procaine on binding and fate of concanavalin A in competent ectoderm of *Xenopus laevis*657
 Tanaka, A. and M. H. Ross: Instability of the number of segments of unoperated and regenerated maxillary palpi in the maxillary-palp-elongate (*mpe*) German cockroach mutant671

Reproductive Biology

- Ueda, J., Hirano, T. and S. Fujimoto: Changes in protein secretory patterns during the development of the rat epididymis681
 Ueda, H., Fukui, Y., Araki, H. and S. Fujimoto: Protein secretory patterns during the development of the rat ovary.....691

Endocrinology

- Endo, K., Fujimoto, Y., Masaki, T. and K. Kumagai: Stage-dependent changes in the activity of the prothoracicotropic hormone (PTTH) in the brain of the Asian comma butterfly, *Polygonia c-aureum* L.697
 Yamanouchi, H. and S. Ishii: Effects of gonadotropin-specific antibodies on the interaction

- of follicle-stimulating hormone and luteinizing hormone with testicular receptors in the bullfrog, *Rana catesbeiana*705
 Kobayashi, M. and N. E. Stacey: Effect of ovariectomy and steroid hormone implantation on serum gonadotropin levels in female goldfish715
 Holmes, W. N., Cronshaw, J. and J. L. Redondo: Stress-induced adrenal steroidogenesis in neonate mallard ducklings and domestic chickens723
 Tomooka, Y., Edery, M., Mills, K. T., Bern, H. A. and J. A. McLachlan: Effects of androgen on mouse seminal vesicle epithelial cells in serum-free culture.....731
 Koshimizu, I. and Y. Oota: A scanning electron microscopic study of the blood vascular architecture of the snake hypophysis (COMMUNICATION).....771

Morphology

- Ohtsuki, H.: Inner structures of the cerebral vesicle in the ascidian larva, *Styela plicata*: an SEM study.....739
 Atoji, Y., Takayanagi, K., Suzuki, Y. and M. Sugimura: Immunohistochemical demonstration of S-100 protein in the chick non-nervous tissue747
 Atoji, Y., Takada, Y., Suzuki, Y. and M. Sugimura: Immunocytochemical identification of four cell types in the pancreatic islets of the Japanese serow, *Capricornis crispus* (COMMUNICATION)779

Taxonomy

- Yoshimura, K.: Two new species of the genus *Monhystrium* Cobb, 1920 (Monhysteridae: Nematoda) from terrestrial crabs of subfamily Sesarminae (Brachyura) in Japan755

NUMBER 5, OCTOBER 1990

REVIEWS

- Omura, Y., K. Horst-W., M. Oguri and A. Oksche: Properties of the blood-brain and blood-cerebrospinal fluid (CSF) barrier in

- the circumventricular organs of the diencephalic roof of teleosts.....783
 Kobayashi, M. and Y. Muneoka: Structure and action of molluscan neuropeptides.....801

ORIGINAL PAPERS

Physiology

- Burton, D. and B. A. Everard: *In vitro* characteristics of K^+ and Na^+ induced melanophore responses in a cold ocean teleost, *Pseudopleuronectes americanus*.....815
- Toh, Y.: Diurnal structural changes in rhabdomeric microvilli of the compound eye in the blue crab, *Callinectes sapidus* (COMMUNICATION).....961
- Uchiyama, M., T. Ogasawara, T. Hirano, S. Kikuyama, Y. Sasayama and C. Oguro: Serum and urine osmolyte concentrations during acclimation to various dilutions of seawater in the crab-eating frog, *Rana canticivora* (COMMUNICATION).....967

Cell Biology

- Devi, S. A., S. Kan and S. Kawashima: Effect of culture age on lipofuscin accumulation and creatine phosphokinase activity in spontaneously beating rat heart cells, and its modifications by tocopherol821

Biochemistry

- Suyemitsu, T., Y. Tonegawa and K. Ishihara: Similarities between the primary structures of exogastrula-inducing peptides and peptide B purified from embryos of the sea urchin, *Anthocidaris crassispina*831

Developmental Biology

- Kurabuchi, S. and Y. Kishida: Comparative study of the influence of head and tail grafts on axial polarity in regeneration of the freshwater planarian841
- Fujishima, M., K. Nagahara and Y. Kojima: Changes in morphology buoyant density and protein composition in differentiation from the reproductive short form to the infectious long form of *Holospora obtusa*, a macro-nucleus-specific symbiont of the ciliate *Paramecium caudatum*849
- Aoki, K., M. Nakamura, H. Namiki, S. Okinaga and K. Arai: The effect of glucose and phosphate on mouse two-cell embryos to develop *in vitro* (COMMUNICATION)973

Reproductive Biology

- Takahashi, N., N. Sato, N. Ohtomo, A. Kondo, M. Takahashi and K. Kikuchi: Analysis of the contraction-inducing factor for gonadal smooth muscle contraction in sea urchin861
- Dukelow, W. R., C. S. T. Pow, J. H. Kennedy and L. Martin: Stress effects on late pregnancy in the flying-fox, *Pteropus scapulatus*871

Endocrinology

- Kato, Y., T. Ezashi, T. Hirai and T. Kato: Strain difference in nucleotide sequences of rat glycoprotein hormone subunit cDNAs and gene fragment879

Behavior Biology

- Hayashi, S.: Social condition influences sexual attractiveness of dominant male mice889
- Chiba, Y., Y. Yamamoto, C. Shimizu, M. Zaitu, M. Uki, M. Yoshii and K. Tomioka: Insemination-dependent modification of circadian activity of the mosquito, *Culex pipiens pallens*895
- Yamanouchi, K.: Role of the medullary raphe nucleus in regulating sexual behaviors in female rats907

Morphology

- Atoji, Y. and Y. Suzuki: Apocrine gland of the infraorbital gland of the Japanese serow, *Capricornis crispus*913
- Meyer, W. and A. Tsukise: Structural and carbohydrate histochemical aspects of the snout skin of the opossum, *Didelphis virginiana* Kerr923

Taxonomy

- Shimazu, T.: Trematodes of the genus *Orientocreadium* (Digenea: Orientocreadiidae) from freshwater fishes of Japan933
- Higgins, R. P. and Y. Shirayama: Dracoderidae, a new family of the cyclorhagid Kinorhyncha from the Inland Sea of Japan939
- Mukai, H.: Systematic position of *Stephanella*

- hina* (Bryozoa: Phylactolaemata), with special reference to the budding site and the attachment of sessoblasts.....947
- Hirayama, A.: A new species of the genus *Paramoera* (Crustacea: Amphipoda) from the intertidal zone of Hokkaido, northern Japan955
- Ohkubo, N.: A new species of *Ramusella* (Acari: Oribatei) from Japan.....979
- Sakagami, S. F. and M. Munakata: *Lasioglossum blackstoni* sp. nov., the northernmost representative of the palaeotropical subgenus *Ctenonomia* (Insecta, Hymenoptera, Halictidae)985

NUMBER 6, DECEMBER 1990

REVIEWS

- Fukumoto, M.: Morphological aspects of ascidian fertilization.....989
- Hill, R. B. and K. Kuwasawa: Neuromuscular transmission in molluscan hearts.....999
- Proceedings of the 61st Annual Meeting of the Zoological Society of Japan 1103
- Announcements 1186
- Acknowledgments..... 1186, 1206
- Author Index..... 1187
- Erratum..... 1209
- Contents of Zoological Science, Vol. 7, Nos. 1-6 i

Vol. 7 No. 1

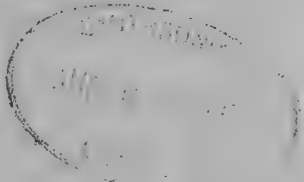
February 1990

864
H

ZOOLOGICAL SCIENCE

An International Journal

PHYSIOLOGY
CELL and MOLECULAR BIOLOGY
GENETICS
IMMUNOLOGY
BIOCHEMISTRY
DEVELOPMENTAL BIOLOGY
REPRODUCTIVE BIOLOGY
ENDOCRINOLOGY
BEHAVIOR BIOLOGY
ENVIRONMENTAL BIOLOGY
ECOLOGY and TAXONOMY



published by Zoological Society of Japan

distributed by Business Center for Academic Societies Japan
VSP, Zeist, The Netherlands

ISSN 0289-0003

ZOOLOGICAL SCIENCE

The Official Journal of the Zoological Society of Japan

Editors-in-Chief:

Seiichiro Kawashima (Tokyo)

Hideshi Kobayashi (Tokyo)

Managing Editor:

Chitaru Oguro (Toyama)

Assistant Editors:

Yuichi Sasayama (Toyama)

Hitoshi Michibata (Toyama)

Miéko Komatsu (Toyama)

The Zoological Society of Japan:

Toshin-building, Hongo 2-27-2, Bunkyo-ku,
Tokyo 113, Japan. Tel. (03) 814-5675

Officers:

President: Hiromichi Morita (Fukuoka)

Secretary: Hideo Namiki (Tokyo)

Treasurer: Tadakazu Ohoka (Tokyo)

Librarian: Masatsune Takeda (Tokyo)

Editorial Board:

Howard A. Bern (Berkeley)

Horst Grunz (Essen)

Susumu Ishii (Tokyo)

Koscak Maruyama (Chiba)

Tokindo S. Okada (Okazaki)

Hiroshi Watanabe (Tokyo)

Walter Bock (New York)

Robert B. Hill (Kingston)

Yukiaki Kuroda (Mishima)

Roger Milkman (Okazaki)

Andreas Oksche (Giessen)

Mayumi Yamada (Sapporo)

Aubrey Gorbman (Seattle)

Yukio Hiramoto (Chiba)

John M. Lawrence (Tampa)

Kazuo Moriwaki (Mishima)

Hidemi Sato (Nagoya)

Ryuzo Yanagimachi (Honolulu)

ZOOLOGICAL SCIENCE is devoted to publication of original articles, reviews and communications in the broad field of Zoology. The journal was founded in 1984 as a result of unification of Zoological Magazine (1888-1983) and *Annotationes Zoologicae Japonenses* (1897-1983), the former official journals of the Zoological Society of Japan. ZOOLOGICAL SCIENCE appears bimonthly. An annual volume consists of six numbers of more than 1200 pages including an issue containing abstracts of papers presented at the annual meeting of the Zoological Society of Japan.

MANUSCRIPTS OFFERED FOR CONSIDERATION AND CORRESPONDENCE CONCERNING EDITORIAL MATTERS should be sent to:

Dr. Chitaru Oguro, Managing Editor, Zoological Science, Department of Biology, Faculty of Science, Toyama University, Toyama 930, Japan, in accordance with the instructions to authors which appear in the first issue of each volume. Copies of instructions to authors will be sent upon request.

SUBSCRIPTIONS. ZOOLOGICAL SCIENCE is distributed free of charge to the members, both domestic and foreign, of the Zoological Society of Japan. To non-member subscribers within Japan, it is distributed by Business Center for Academic Societies Japan, 6-16-3 Hongo, Bunkyo-ku, Tokyo 113. Subscriptions outside Japan should be ordered from the sole agent, VSP, Utrechtseweg 62, 3704 HE Zeist (postal address: P. O. Box 346, 3700 AH Zeist), The Netherlands. Subscription rates will be provided on request to these agents. New subscriptions and renewals begin with the first issue of the current volume.

All rights reserved. No part of this publication may be reproduced or stored in a retrieval system in any form or by any means, without permission in writing from the copyright holder.

© Copyright 1990, The Zoological Society of Japan

[Publication of Zoological Science has been supported in part by a Grant-in-Aid for
Publication of Scientific Research Results from the Ministry of Education, Science
and Culture, Japan.]

REVIEW

**Molecular Assembly and Evolution of Multi-Subunit
Extracellular Annelid Hemoglobins**TOSHIO GOTOH and TOMOHIKO SUZUKI¹

Department of Biology, College of General Education, University of Tokushima,
Tokushima 770 and ¹Department of Biology, Faculty of Science,
Kochi University, Kochi 780, Japan

ABSTRACT—An extracellular annelid hemoglobin is a multi-subunit protein with a molecular weight of $3\text{--}4 \times 10^6$ and exhibits a hexagonal bilayer of twelve submultiples. Recent advances in studies on the molecular evolution and assembly of the huge annelid hemoglobins are summarized. Sequence determinations of the eight polypeptide chains of the multi-subunit hemoglobins of the polychaete *Tylorrhynchus heterochaetus* and the oligochaete *Lumbricus terrestris* have provided fundamental information on the common molecular architecture and the phylogeny of these huge dioxygen-carrying proteins. In addition, morphological studies using scanning transmission electron microscopy and conventional transmission electron microscopy with image analysis have revealed the tetrahedral structure of the submultiple. A new nomenclature 'a', 'A', 'b', and 'B', is proposed for the four basic constituent chains common to oligochaete and polychaete hemoglobins based on their homology. Phylogenetically, these heme-containing chains can be separated into two strains 'A', and 'B'. According to the symmetrical '192-chain' model, the multi-subunit hemoglobins might be represented as '(aAbB)₄₈'. The minimum entity 'aAbB' that consists of a monomeric chain 'a' and a disulfide-bonded trimer 'AbB' may correspond to one unit in the tetrahedral of the submultiple in electron microscopic appearance. On the basis of recent information, earlier models are evaluated as well as the 'bracelet' model, in which the minor subunits D1 and D2 without heme have a key role in linking the complexes of subunit a and subunit AbB together.

INTRODUCTION

Ever since Svedberg [1–3] found that an extracellular annelid hemoglobin is a huge protein and consists of either about 144 or 192 polypeptide chains, an outstanding problem has been to construct a common model for the molecular architecture of annelid hemoglobins.

Ten years ago, we decided to determine the molecular weight of each constituent chain of hemoglobin of the polychaete *Tylorrhynchus heterochaetus* by analyzing its amino acid sequence [4, 5]. Our results have provided much information on the molecular architecture and the evolution of giant annelid hemoglobins [6–11]. Similar studies on hemoglobin of the oligochaete *Lumbri-*

cus terrestris have progressed concurrently in other laboratories [12–14]. Four major species of constituent chains with heme have been isolated from each of these polychaete and oligochaete hemoglobins and have been sequenced. Moreover, Vinogradov and his colleagues recently reported that non-heme chains with molecular masses of 31–37 kDa act as a scaffold for the complexes of two types of heme-containing subunits 'monomers' and disulfide-bonded 'trimers' [15–17]. Morphological studies by scanning transmission electron microscopy (¹STEM) [18–20] and conventional transmission electron microscopy (CTEM) with image

¹ Abbreviations used: STEM, scanning transmission electron microscopy; CTEM, conventional transmission electron microscopy; SDS-PAGE, sodium dodecyl sulfate-polyacrylamide gel electrophoresis; SAXS, small-angle X-ray scattering.

analysis technique [21, 22] have also provided information for constructing of a common model of giant hemoglobins.

These recent findings are all consistent with a common model for the molecular architecture of multi-subunit annelid hemoglobins consisting of about 200 polypeptides including four species of 192 heme-containing chains and some non-heme chains, although the detailed subunit assembly is still controversial. In particular, it is still uncertain whether annelid hemoglobins contain common non-heme chains with molecular masses of about double those of heme-containing chains. The 288 disulfide bonds present in the heme-containing chains of a molecule must be important for interlocking the whole complex [11, 14] and perhaps the non-heme chains may link the complexes of heme-containing subunits together [16, 23]. With regard to molecular phylogeny, two globin strains have been found in both polychaete and oligochaete hemoglobins [9, 23, 24]. In this article we introduce a new nomenclature for the four main heme-containing chains common to oligochaete and polychaete hemoglobins so that future 'monomeric' and 'trimeric' globin chains can be readily compared. Although non-heme chains are expected to be 'linkers' that consist of two domains of globin and conserve the drastic evolutionary history of the hemoglobins, these chains must be examined further, especially in terms of amino acid or DNA sequences, to be identified as real components. Since the major constituent chains with heme have all been found to be homologous with a vertebrate myoglobin, the old name for giant annelid hemoglobins, 'erythrocrutorin', is no longer appropriate.

HISTORICAL BACKGROUND

Sixty years ago, Svedberg [1] developed a method for determining the molecular weight of a protein by centrifugation, and using this method he found a variety of globins ranging in molecular weight from 17,000 for myoglobin to about 3 million for annelid extracellular hemoglobins. As the annelid extracellular hemoglobin is a huge protein, Svedberg and Eriksson [2] thought that its protein portion have completely different chemical

properties from those of vertebrate hemoglobins, and they revived the name "erythrocrutorin", originally used for the red blood pigment of the invertebrates by Ray Lankester in 1868 [25]. No satisfactory explanation of the evolutionary relationships between different sizes and forms of globins was proposed for many years. But in 1960, in X-ray diffraction studies Perutz [26] observed similarity in the three dimensional structures of vertebrate myoglobin and hemoglobin. Now, more than 250 globin chains have been sequenced [27] and a phylogenetic tree for their molecular evolution has been constructed [28]. Thus the homologies of diverse hemoglobins have been established and these molecules have been shown to be members of the globin family.

Kimura [29] proposed the neutral theory for molecular evolution based largely on the primary structures of vertebrate globin chains. Recently, however, attention has been directed into the structural diversity of invertebrate hemoglobins, with the expectation of finding some drastic mutations besides the point mutations that have already been analyzed in vertebrate globin chains. Based on the quarternary structures, Vinogradov [30] has classified hemoglobins into four types: (a) Single-domain, single-subunit molecules consisting of a single polypeptide chain of about 16 kDa containing one heme group; (b) two domain, multi-subunit hemoglobins, ranging in size from 250 to 800 kDa and consisting of 30–40 kDa chains, each containing two heme-binding domains; (c) multi-domain, multi-subunit hemoglobins, consisting of two or more long polypeptide chains each containing 8–20 heme-binding domains connected lineally; (d) Single-domain, multi-subunit hemoglobins, consisting of aggregates of several small subunits, some of which are disulfide-bonded and not all of which contain heme. The giant extracellular annelid hemoglobins are of type *d*. Oligochaetes have only this type of hemoglobin. On the other hand, polychaetes have various types of pigments such as monomeric and polymeric intracellular hemoglobins, monomeric extracellular hemoglobins, and multi-subunit extracellular hemoglobins and chlorocruorins. In some cases, two types of hemoglobins are present in a single species [31–33]. Chlorocruorins are green, but they are considered to be

homologous with multi-subunit hemoglobins because of their similarities to the latter in size and shape [3, 34]. Annelid multi-subunit hemoglobins and chlorocruorins can also be characterized by the appearance of a double-layered hexagonal array of twelve submultiples [34–36]. These hemoproteins appear to consist of ‘monomers’, ‘dimers’, disulfide-bonded ‘trimers’ and disulfide-bonded ‘tetramers’ in various proportions and combinations depending upon the species [30]. The molecular masses of unit chains in all these forms except ‘dimers’ are comparable to those of vertebrate myoglobins [4, 12, 30]. Most preparations of these hemoglobins and chlorocruorins exhibit the presence of some ‘dimer’ components with molecular masses of 31–37 kDa, but they have not yet been well characterized. The relationships between the oxygen-dissociation curve and the structure of the annelid hemoglobins has been studied extensively [37–46]. The present review is, however, limited mainly to recent progress in studies on the molecular evolution and assembly of the multi-subunit extracellular annelid hemoglobins.

Many workers have studied different hemoglobins and have proposed models for their molecular assembly based on their results obtained by various methods [for earlier reviews, see Refs. 47–52]. For analysis of the whole molecule, precise measurements of basic parameters, such as the molecular weight of the whole molecule and the constituent chains, and the iron or heme content are necessary. The values reported for the molecular masses of whole molecules vary from about 3,000 kDa to 4,000 kDa [3, 40, 53]. The molecular masses of major constituent chains estimated by sodium dodecyl sulfate-polyacrylamide gel electrophoresis (SDS-PAGE) range from 11 kDa to 19 kDa [54–56], whereas the molecular masses of the constituent chains estimated by centrifugation are 22–23 kDa [57, 58]. The minimum molecular mass per heme observed also ranges from 17 kDa to 28 kDa [54, 59–61]. Thus, even very recently it was difficult to justify the reported values of these parameters and to assign the heme group to the disulfide-bonded ‘trimer’ [15]. As pointed out by many workers [62], it is also difficult to determine the exact number of chains per whole molecule,

because in estimating the molecular weight of the whole molecule any error in the minimum molecular weight is multiplied by about ‘144’ or ‘192’.

MOLECULAR SHAPE

Figure 1 shows typical STEM images of polychaete and oligochaete hemoglobins, which consist of double layered hexagonal submultiples [11]. In the central cavity of the molecule, there are faint indications of protein masses that appear to be anchored to the surface of all 12 submultiples. In the view of *Tylorrhynchus* hemoglobin from the top (Fig. 1A), each submultiple appears to be composed of three globular units with a tiny hole at the center. The side view of a submultiple (Fig. 1B) also shows three identical units. From these findings the simplest steric model of a submultiple is a tetrahedral structure, the fourth unit being masked by the others both in the top and side views. The size of *Tylorrhynchus* hemoglobin is 28.4 nm in vertex-to-vertex diameter and 18.2 nm in height, as listed in Table 1 with the values for *Lumbricus* hemoglobin for comparison [19]. The high resolution STEM method was developed by Crewe of Chicago University [63] and first used to examine *Lumbricus* hemoglobin by Kapp and Crewe in the collaboration with Vinogradov of Wayne State University [18]. Recently, Vinogradov and his collaborators [15–17, 20] suggested a role of the filament structure in the central cavity of the hemoglobin molecule as a scaffolding or linker for the submultiples. By two dimensional image analysis and reconstruction by optical and computed methods of electron micrographs, Ghiretti Magaldi and her colleagues [21, 22, 64] demonstrated the tetrahedral structure of the each submultiple of an extracellular hemoglobin and a chlorocruorin as shown in Figure 2. These electron microscopic studies indicated the existence of 48 tetrahedral units in the whole molecule. However, the materials found by STEM in the central cavity could not be observed by CTEM with image analysis [22].

Several multi-subunit annelid hemoglobins have been examined by small-angle X-ray scattering (SAXS) [65–70], which is a useful method for obtaining information on the quaternary structure

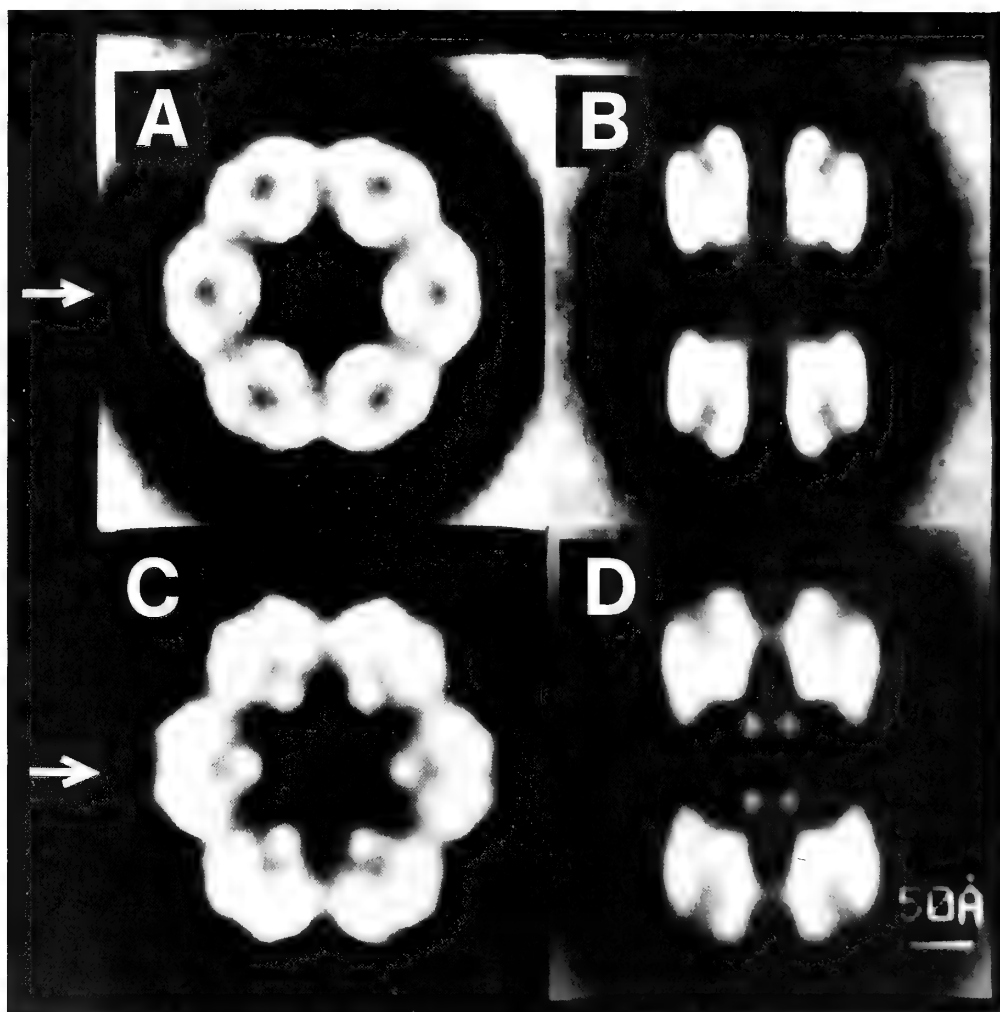


FIG. 1. STEM images of *Tylorrhynchus* (A and B) and *Lumbricus* (C and D) hemoglobins. A and C, and B and D are top and side views, respectively. Note the faint protein mass in the central cavity. (from Suzuki, T., Kapp, O. H. and Gotoh, T. [11]. Reprinted with permission from the American Society for Biochemistry & Molecular Biology.)

TABLE 1. Molecular dimensions of *Tylorrhynchus* and *Lumbricus* hemoglobins determined by STEM

Hemoglobin	Vertex-to-vertex diameter (nm)	Height (nm)	Central hole (nm)	Ref.
<i>Tylorrhynchus</i>	28.4	18.2	8.8	[11]
<i>Lumbricus</i>	30.7	20.1	8.8	[19]

(from Suzuki, T., Kapp, O. H. and Gotoh, T. [11]. Reprinted with permission from the American Society for Biochemistry and Molecular Biology.)

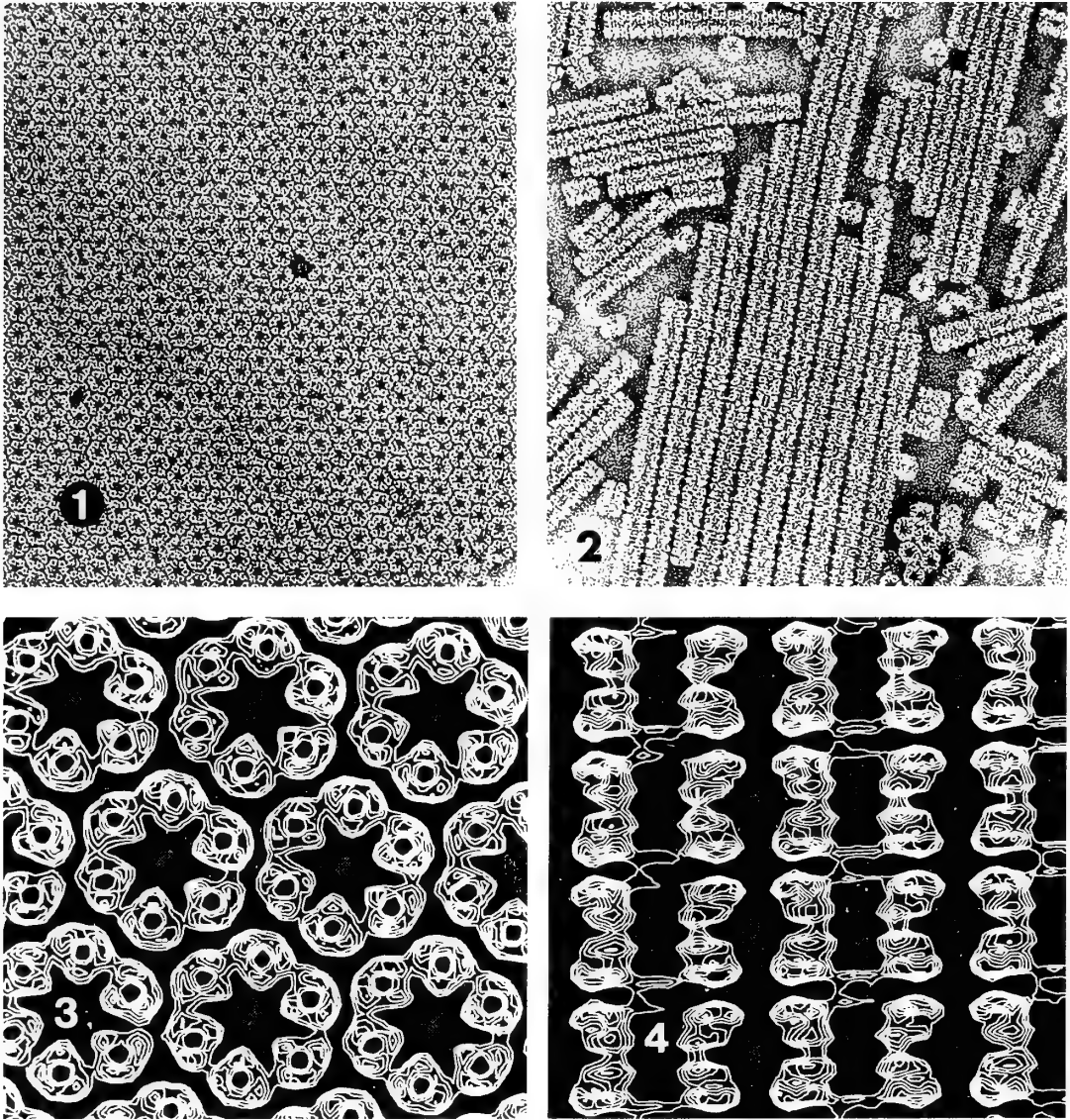


FIG. 2. Electron microscopic images of *Spinographis chlorocruorin*. 1 and 2 are bidimensional crystals in the axial and lateral projections, respectively. 3 and 4 are the relative computed reconstructions for the axial and lateral projections, respectively. Magnification electron micrographs $90,000\times$. Note the tetrahedral structure of each submultiple. (By courtesy of Dr. Ghiretti Magaldi, A. [22]. Reprinted with permission from Springer Verlag.)

of biological macromolecules in solution. For instance, the radius of gyration and maximum dimension of *Tylorrhynchus* hemoglobin have been determined to be 10.8 ± 0.2 nm and 29.6 ± 0.5 nm, respectively, as listed in Table 2 in comparison with values for *Lumbricus* hemoglobin [70]. These molecular parameters are in good agreement with

the values obtained from the STEM images. A model that fits the X-ray scattering curve of *Tylorrhynchus* hemoglobin is shown in Figure 3 [70]. This model indicates some protein masses in the center of the molecule as well as between submultiples consistent with STEM images. However, it should be noted that in this model the small

TABLE 2. Radii of gyration and maximum dimensions of *Tylorrhynchus* and *Lumbricus* hemoglobins determined by small-angle X-ray scattering

Hemoglobin	Radius of gyration (nm)	Maximum dimension (nm)	Ref.
<i>Tylorrhynchus</i>	10.8 ± 0.2	29.5 ± 0.5	[70]
<i>Lumbricus</i>	11.2 ± 0.2	29.0 ± 1.0	[67]

(from Pilz, I., Schwarz, E., Suzuki, T. and Gotoh, T. [70]. Reprinted with permission of the publishers, Butterworth & Co. Ltd. ©.)

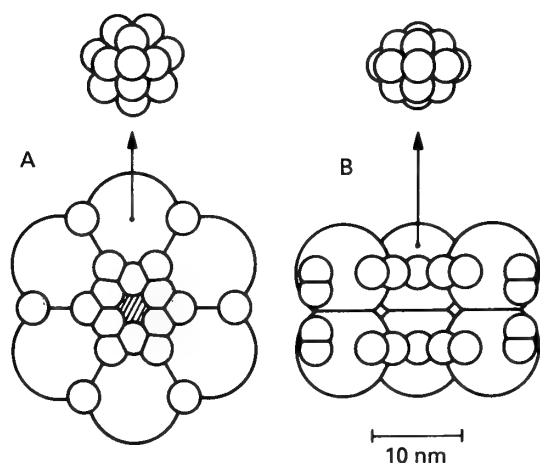


FIG. 3. A model of *Tylorrhynchus* hemoglobin based on the X-ray scattering curve. A and B are top and side views, respectively. Each submultiple indicated by a large sphere is composed of 17 small spheres arranged in five tiers containing one, four, seven, four and one spheres, respectively. There are also four small spheres per submultiple located between the large spheres. Thus the whole model contains $12 \times 21 = 252$ small spheres. (from Pilz, I., Schwarz, E., Suzuki, T. and Gotoh, T. [70]. Reprinted with permission of the publishers, Butterworth & Co. Ltd. ©.)

spheres used to simulate the quaternary structure have no relation to the real number and size of the subunits or polypeptide chains forming the molecule. Furthermore, the model in which each submultiple consists of four tetramers of ellipsoids in a tetrahedral arrangement also fits all the SAXS data fairly well [70]. According to the SAXS analysis, the protein mass in the central hole of *Tylorrhynchus* hemoglobin is less than that *Lumbricus* hemoglobin [70]. In sharp contrast, measurement of the pixel intensity of STEM images indicates more protein mass in the central

hole of *Tylorrhynchus* hemoglobin than in that of *Lumbricus* hemoglobin [11]. Thus, the technical limitations of STEM, CTEM and SAXS must be taken into account in considering the filamentous structure in the central cavity.

MOLECULAR PHYLOGENY

The hemoglobin of the polychaete *Tylorrhynchus* was the first multi-subunit extracellular hemoglobin to be sequenced completely [9]. Soon afterwards, the corresponding chains of the oligochaete *Lumbricus* hemoglobin were sequenced [13, 14]. These sequencings provided much information on the phylogeny of giant annelid hemoglobins. Two chains from other multi-subunit oligochaete hemoglobins have subsequently been sequenced [71, 72]. Figure 4 shows the amino acid sequences of the four chains of *Tylorrhynchus* hemoglobin [5–7, 9]. Nine of the 25 invariant residues are also conserved in the human β chain. In vertebrate hemoglobins [73, 74], all these residues except Val (A8) and Trp (A12) belong to the central exonic regions, which are known to be the minimal functional entity for O_2 binding [75]. It is noteworthy that the invariants of *Tylorrhynchus* hemoglobin involve the residues corresponding to the distal (E7) His, distal (E11) Val, and proximal (F8) His of vertebrate hemoglobins, which are the most important residues for maintaining the functional properties. The fifth coordination position of the iron atom in the heme is known to be histidine F8 (the proximal His); O_2 is bound at the sixth coordination position. In sperm whale myoglobin, the distal (E7) His is known to be the only residue capable of interacting directly with bound dioxygen and stabilizing it [76]. All eight chains of *Tylorrhynchus* and *Lum-*

bricus hemoglobins are clearly homologous with those of vertebrate hemoglobins [9, 13, 14]. In fact, each of the isolated chains shows a typical absorption spectrum of a globin chain [46, 77, 62]. Jhiang *et al.* [78] found that the gene of a heme-containing chain of *Lumbricus* hemoglobin has a two intron-three exon structure like those of vertebrate globin chains [73]. Therefore, there is no reason to maintain the old name 'erythrocrucorin' for invertebrate hemoglobins except familiarity with this name, as pointed out by Garlick and Riggs [12]. The heme moiety of 'erythrocrucorin' is the same as that of a vertebrate hemoglobin [79].

As the giant annelid hemoglobins differ from other hemoglobins in possessing disulfide-bonded 'trimers' or 'tetramers', the sites of half-cystine residues in *Tylorrhynchus* and *Lumbricus* hemoglobins are noted to be all located in the side exonic regions [8, 9, 11, 14, 78], as shown in Figure 4.

These residues all participate in forming either intra- or inter-chain disulfide bridges [11, 14], as shown in Figure 5. There is one intra-chain disulfide bridge in each chain of *Lumbricus* and *Tylorrhynchus* hemoglobins including the monomers [11, 14]. As the multi-subunit annelid hemoglobins dissociate completely into separate chains in the presence of a reducing agent without any other protein-denaturant [21, 81, 82], the disulfide bonds appear to have a key role in the *in vivo* assembly of the giant molecule [11]. Namely, point mutations at the positions now having Cys residues must have been a major factor in bringing about formation of these huge proteins. The side exons can also be considered to have evolved with a special role of stabilizing the molecular assembly.

High homologies are seen between *Tylorrhynchus* chains *b* and *B* (74 identical residues, 50% homology), and *Tylorrhynchus* chains *a* and *A* (57

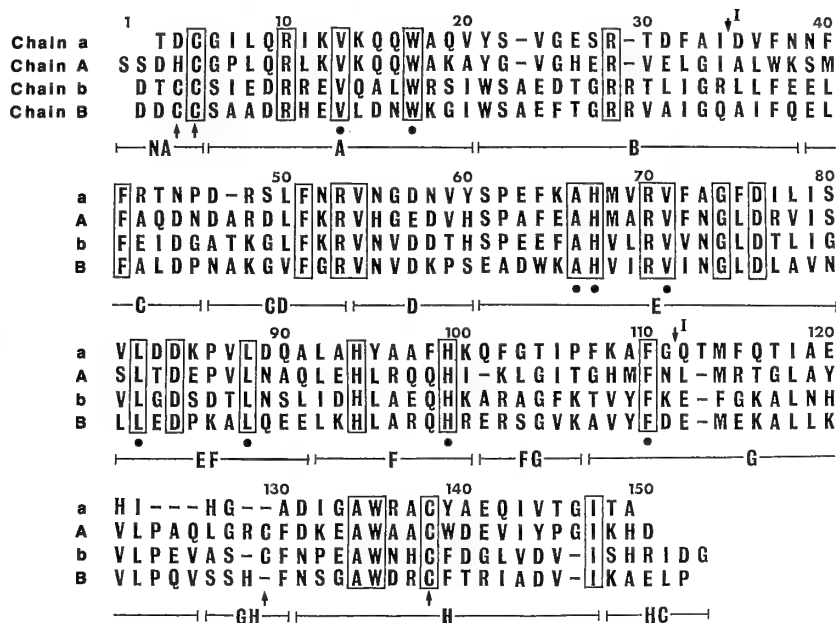


FIG. 4. Amino acid sequences of the constituent chains of *Tylorrhynchus* hemoglobin. The alignment is based on the assumption that the helical segments present in most other globins are also present in the constituent chains of the multi-subunit annelid hemoglobin. The boxed residues indicate the 25 invariable residues in four globin chains. The residues indicated by a dot are homologous with those of the human β chain. Arrows without a suffix indicate the positions of half-cystine residues. Arrows with the suffix 'I' indicate intronic positions assuming that the intronic positions in *Tylorrhynchus* hemoglobin are the same as those in vertebrate globins [73] and *Lumbricus* hemoglobin [78]. (from Suzuki, T. and Gotoh, T. [9]. Reprinted with permission from the American Society for Biochemistry and Molecular Biology.)

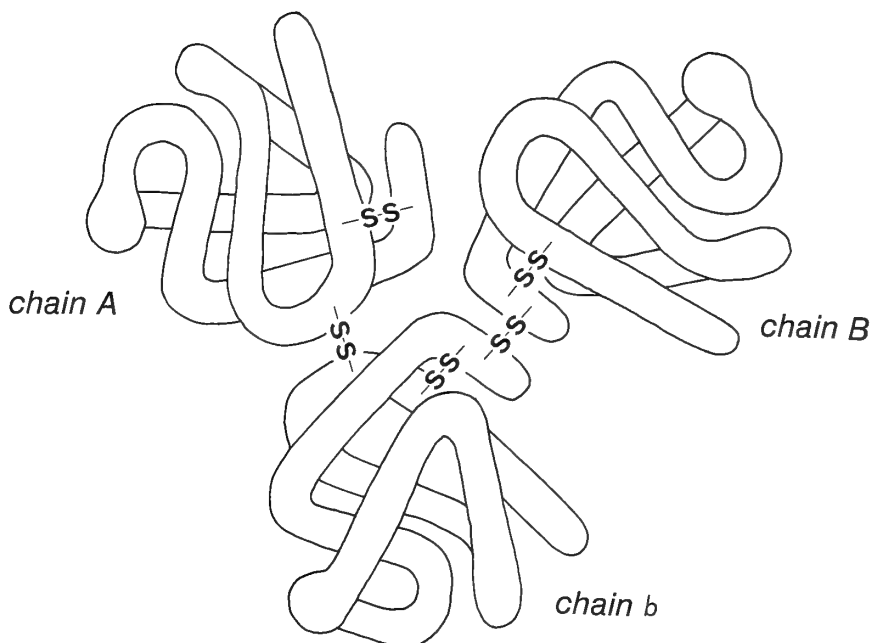


FIG. 5. A model for the steric assembly of the disulfide-bonded 'trimer' of chains A, b and B in *Tylorrhynchus* hemoglobin. 'Globin folding' was cited from that of the human β chain [80]. (from Suzuki, T., Kapp, O. H. and Gotoh, T. [11]. Reprinted with permission from the American Society for Biochemistry and Molecular Biology.)

	1	2	3	4	5	6	7	8	9	10	11	12	13	14	15	16	17	18	19	20	21	22
Lum. a						Glu	CYS	Leu	Val	Thr	Glu	Gly	Leu	Lys	VAL	Lys	Leu	Gln	TRP	Ala	Ser	Ala
Lum. A				Lys	Lys	Gln	CYS	Gly	Val	Leu	Glu	Gly	Leu	Lys	VAL	Lys	Ser	Glu	TRP	Gly	Arg	Ala
Tyl. a				Thr	Asp	CYS	Gly	Ile	Leu	Gln	Arg	Ile	Lys	VAL	Lys	Gln	Gln	TRP	Ala	Gln	Val	
Tyl. A			Ser	Ser	Asp	His	CYS	Gly	Pro	Leu	Gln	Arg	Leu	Lys	VAL	Lys	Gln	Gln	TRP	Ala	Lys	Ala
Lum. b	Asp	Glu	His	Glu	His	Cys	CYS	Ser	Glu	Glu	Asp	His	Tyr	Ile	VAL	Gln	Lys	Gln	TRP	Asp	Ile	Leu
Lum. B	Ala	Asp	Glu	Glu	Ser	Cys	CYS	Ser	Tyr	Glu	Asp	Arg	Arg	Glu	VAL	Arg	His	Ile	TRP	Asp	Asp	Val
Tyl. b			Asp	Thr	Cys	CYS	Ser	Ile	Glu	Asp	Arg	Arg	Glu	VAL	Gln	Ala	Leu	TRP	Arg	Ser	Ile	
Tyl. B			Asp	Asp	Cys	CYS	Ser	Ala	Ala	Asp	Arg	His	Glu	VAL	Leu	Asp	Asn	TRP	Lys	Gly	Ile	

← NA → ← A →

FIG. 6. Alignment of NH_2 -terminal sequences of *Tylorrhynchus* and *Lumbricus* chains. The boxed residues indicate invariant residues in the eight chains and either the upper strain (strain A) or the lower strain (strain B). The residues indicated by a dot are homologous with those of the human β chain. Others are as for in Fig. 4. (from Gotoh, T., Shishikura, F., Snow, J. W., Ereifej, K. I., Vinogradov, S. N. and Walz, D. A. [24]. Reprinted with permission from the Biochemical Society and Portland Scientific Press.)

identical residues, 40% homology). Therefore, phylogenetically, the 'trimeric' chain A is more closely related to the 'monomeric' chain a than to either of the other 'trimeric' chain, b and B [9]. This finding has been extended to the idea that there are in general two distinct groups, strain A

and B, of chains in multi-subunit annelid hemoglobins, as clearly seen in Figure 6 [24]. The separation of these strains must have been derived from the gene duplication [24]. In fact, using the unweighted pair-group clustering method [83], Fushitani *et al.* [14] clearly demonstrated two

TABLE 3. Proposed common nomenclature for the chains of multi-subunit annelid hemoglobins, and the corresponding names for *Tylorrhynchus* and *Lumbricus* hemoglobins used hitherto

Hemoglobin	Chain		name		Ref.
<i>Tylorrhynchus</i>	I	IIA	IIC	IIB	[6]
<i>Lumbricus</i>	I	II	III	IV	[55]
<i>Lumbricus</i>	<i>d</i>	<i>b</i>	<i>c</i>	<i>a</i>	[77]
Common name	<i>a</i>	<i>A</i>	<i>b</i>	<i>B</i>	This paper
No. of Cys	2	3	4	3	[9, 14]

The arbitrary names were given according to either the order of mobility on SDS-PAGE [6, 55] or the elution order on column chromatography [6, 77]. The proposed nomenclature is based on the homology between different hemoglobins.

subfamilies in the phylogenetic tree for *Lumbricus* and *Tylorrhynchus* hemoglobins. Furthermore, they used the type of inter-chain disulfide bonding and the number of half-cystine residues to distinguish two types of chains in the same strain [14]. Thus the correspondence of the four constituent chains in these two hemoglobins has been established.

Here, we would like to propose a new nomenclature for common names of the sequenced chains to facilitate comparison of the 'monomeric' and 'trimeric' globin chains of different species. We have used the new nomenclature without definition in Figures 4, 5 and 6. The smaller and 'monomeric' chain in strain *A* is named chain '*a*', and the other one in strain *A* is named chain '*A*'. Chain *a* (139 residues) of *Tylorrhynchus* hemoglobin is smaller than all the other constituent chains: chain *A*, 146 residues; *b*, 149 residues; *B* 148 residues. *Lumbricus* chain *a* is also the smallest constituent and exists as a 'monomer' [13, 14, 55]. Chains *a* and *A* can also be distinguished by the number of half-cystine residues [9, 14]: they have 2 and 3 half-cystine residues, respectively, as seen in Figure 4. Similarly, chains '*b*' and '*B*' in strain *B* can be defined as those having 4 and 3 half-cystine residues, respectively. Chains *b* was shown experimentally to be situated in the center of the trimer '*AbB*', as shown in Figure 5 [11, 14]. Employing the myoglobin-fold for each chain in the steric model of disulfide-bonded 'trimer', five disulfide bridges can easily be located without any bending or stretching [11]. Chain *a* exists as a 'monomer' because it has only two half-cystine

residues and forms one intra-chain disulfide bond [9, 11, 14]. The distributions of half-cystine residues in *Lumbricus* and *Tylorrhynchus* hemoglobins are the same [9, 14]. The relationships between the new names and the arbitrary ones used previously for the *Tylorrhynchus* and *Lumbricus* chains are summarized in Table 3. As the polychaete *Tylorrhynchus heterochaetus* and the oligochaete *Lumbricus terrestris* are very different species each other in the phylum Annelida, the proposed nomenclature can be extended to many other annelid hemoglobins. A slight modification of the proposed nomenclature will, however, be necessary in the future because some annelid hemoglobins and chlororuorins contain disulfide-bonded 'tetramers' [30].

Figure 7 shows the phylogenetic tree of the nine globin chains of the multi-subunit annelid hemoglobins from the polychaete *Tylorrhynchus* and the oligochaete *Lumbricus* and *Pheretima sieboldi* according to the unweighted pair-group clustering method. Strains *A* and *B* are clearly separated. According to the unweighted pair-group clustering method [83], the amino acid substitution rate for the 'functionally essential' central exonic region is about 1.5 times slower than that for the 'structurally essential' side exonic regions [71]. The observed identities of the nine chains of *Tylorrhynchus*, *Lumbricus* and *Pheretima* hemoglobins range from 32 to 51%, as shown in Figure 7. Some of these identities are comparable to that (44%) between the α and β chains of human hemoglobin, which were separated by gene duplication about 450 million years ago in the Ordovician period [84].

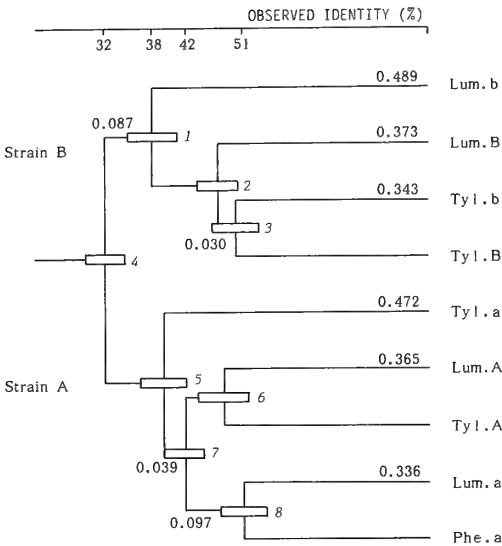


FIG. 7. Phylogenetic tree of the nine heme-containing chains from multi-subunit annelid hemoglobins. The tree was constructed from a homology matrix by comparison of 137 amino acid residues common to all chains [71], by an unweighted pair-group clustering method [83]. The standard errors at the branching points 1–8 are 0.045, 0.038, 0.042, 0.035, 0.041, 0.044, 0.036 and 0.042, respectively.

Assuming comparable evolutionary rates for extracellular and vertebrate hemoglobins, Fushitani *et al.* [14] suggested that the divergence of the Oligochaeta and Polychaeta occurred around the time of the gene duplication that led to the α and β gene families in vertebrates. On the other hand, from the maximum parsimony tree, Goodman *et al.* [28] calculated the times when the annelid globin chains were separated more exactly. For instance, they reported that the *Tylorrhynchus* chain *b* and *B* were separated about 140 million years ago in the Cretaceous period, the *Tylorrhynchus* chain *a* and other *Tylorrhynchus* chain were separated about 380 million years ago in the Devonian period, and the *Glycera* intracellular monomeric chain and extracellular globin chains were separated about 575 million years ago in the Cambrian period. Although it is of great biological interest to know the time when the Polychaeta and Oligochaeta were separated, fossil records of annelids, and particularly of oligochaetes are very incomplete [85].

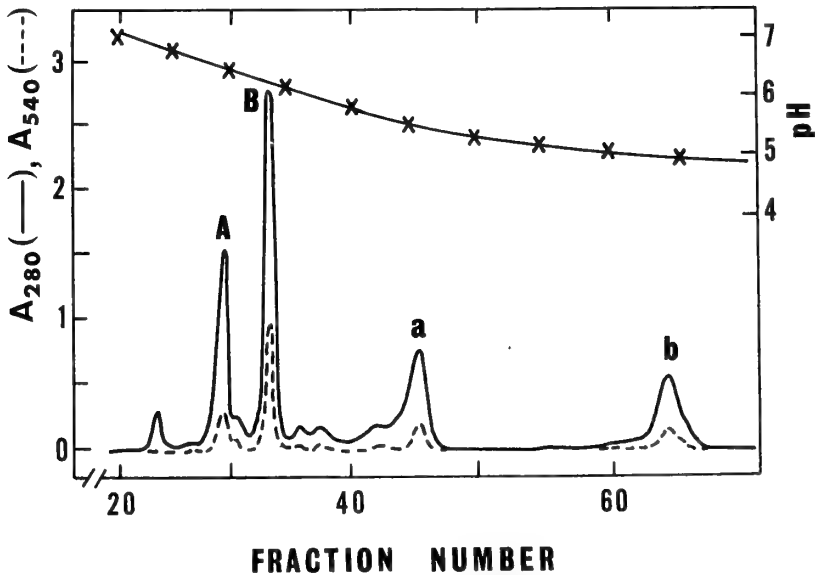
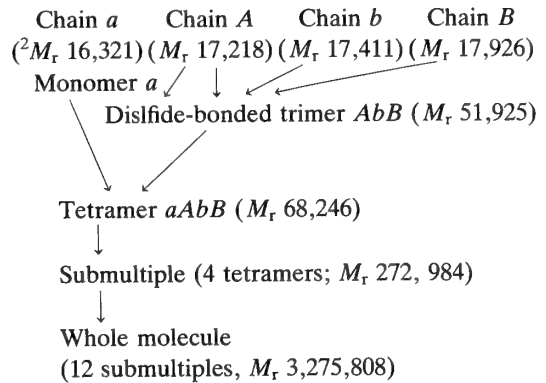


FIG. 8. Elution profile on chromatofocussing of *Tylorrhynchus* cyanomethemoglobin. Hemoglobin solution was reduced with dithiothreitol and applied to a PBE94 column equilibrated with a imidazole buffer (pH 7.4). Material was eluted with Polybuffer 74 (pH 5). Peaks A, B, a and b are those of chains A, B, a and b, respectively. Note that all four chains isolated carry a heme. (from Suzuki, T., and Gotoh, T. [6]. Reprinted with permission from the American Society for Biochemistry and Molecular Biology.)

'192-CHAIN' MODEL OF THE SUBUNIT ASSEMBLY

Sequence analyses of the multi-subunit annelid extracellular hemoglobins have indicated the precise molecular weight of protein moiety in each constituent chain, which is essential for construction of a model of the molecular architecture. The heme content of each chain has been clarified directly by column chromatographic isolation procedures [6, 24, 77, 86]. Figure 8 shows the elution profile of each constituent chain of *Tylorrhynchus* hemoglobin on chromatofocussing [6]. The isolated chains exhibit the typical absorption spectrum of a vertebrate myoglobin. Therefore, it is concluded that all four chains, *a*, *A*, *b* and *B*, contain one heme group per chain. In fact, these four chains have a histidine residue, which corresponds to the proximal one (F8) of vertebrate hemoglobins [26], as shown in Figure 4.

The molar ratio of the four *Tylorrhynchus* chains *a*:*A*:*b*:*B* was determined to be nearly 1:1:1:1 by statistical comparison of the exact amino acid compositions calculated from the sequence of each chain and the observed composition measured by amino acid analysis of the whole molecule [10]. Considering the apparent molecular masses of the whole molecule (3, 370 kDa), submultiple (250 kDa), unstable tetramer (72 kDa) and disulfide-bonded trimer (50 kDa) [9, 87, 88], we proposed that the formation of *Tylorrhynchus* hemoglobin may be as follows [10].



Therefore, our model proposed for *Tylorrhynchus* hemoglobin consists of 192 polypeptide chains containing heme. According to the new nomenclature proposed above, *Tylorrhynchus* hemoglobin can be represented as '(aAbB)₄₈'. aAbB is the minimum structural entity, which may correspond to one unit in the tetrahedral structure of the submultiple observed in the STEM image (Fig. 1). This giant protein consists of 27,936 amino acid residues and 192 heme groups, and is linked by 288 disulfide bridges, 192 intra- and 96 inter-chain disulfide bonds. These are the contents of our symmetrical '192-chain' model. The salient point of this model is that the subunit assembly is based on the exact molecular weight and strict molar ratio of each constituent polypeptide chain. The '192-chain' model is in good agreement with electron microscopic observations for the tetrahedral structure of a submultiple [21, 22, 61, 64, 89].

TABLE 4. Earlier models of annelid multi-subunit hemoglobins

Hemoglobin	Minimum M_r per heme	No. of units	M_r of whole molecule ($\times 10^{-6}$)	Ref.
<i>Lumbricus</i>	17,250	144	2.48	[1]
<i>Lumbricus</i>	17,600	192	3.38	[3]
<i>Arenicola</i>	27,000	192	2.59	[54]
<i>Octolasion</i>	23,000	144	3.30	[57]
<i>Lumbricus</i>	17,000	192	3.26	[90]
earthworm	22,000	192	3.84	[58]
<i>Tylorrhynchus</i>	17,062	192	3.275808	[10]

All models except those reported in refs. [10] and [54] consist of a single species of unit protein containing a heme moiety.

² The M_r of each constituent chain of *Tylorrhynchus* hemoglobin including a heme group was recalculated.

However, this model does not explain the filamentous structure in the central hole of the molecule, shown in Figure 1. Two further other problems about the '192-chain' model are that the measured value of the minimum molecular mass per heme is much higher than the value calculated from the model, and that the SDS-PAGE pattern often shows one or two extra minor components with molecular masses of about double those of the chains containing heme [88].

Table 4 shows some earlier models of annelid hemoglobins compared with our '192-chain' model. Chiancone *et al.* [57] and David and Daniel [58] reported higher values for the minimum molecular weight. These values might be reasonable for the minimum molecular weight per heme, but not for the molecular weight of a minimum unit, because sequence analyses of *Tylorrhynchus* [9] and *Lumbricus* hemoglobins [14] revealed that the size of each chain containing heme is comparable with that of myoglobin. Chiancone *et al.* considered the '144-chain' model based on the relationships of the molecular weights of the minimum unit and whole molecule. On the other hand, David and Daniel proposed a '192-chain' model by which the calculated molecular weight of the whole molecule reached the measured value of 3.84×10^6 , in contrast to the others clustered in the first half of 3 million. Anyway, it is now obvious that these models overestimated the molecular weight of a minimum unit. On the other hand, in most cases, the molecular mass of a constituent chain was underestimated by SDS-PAGE. Waxman [54] examined *Arenicola cristata* hemoglobin by SDS-PAGE and he found two major components with molecular masses of 13 kDa and 14 kDa. As the minimum molecular mass per heme was estimated to be 27 kDa, he proposed a '192-chain' model for *Arenicola* hemoglobin with a relatively lower molecular mass of 2,590 kDa, which consists of

two species of constituent chains, half of which do not contain a heme group. Vinogradov and his colleagues have maintained the idea that not all chains contain a heme group [16, 55, 91].

'BRACELET' MODEL OF THE SUBUNIT ASSEMBLY

Shlom and Vinogradov [55] noted fifth and sixth components of multi-subunit hemoglobins that can always be observed as faint bands V and VI on SDS-PAGE of a preparation of *Lumbricus* hemoglobin. As these components are about twice the size of the major components, chains *a*, *A*, *b* and *B*, they are designated as 'D1' ($M_r = 31,000$) and 'D2' ($M_r = 37,000$) and called "dimers" arbitrarily (15). Recently, Vinogradov's group [15-17] proposed a 'bracelet' model for the subunit assembly of a giant annelid hemoglobin in which D1 and D2 have the remarkable role of linking 12 submultiples. In the novel 'bracelet' model, subunits D1 and D2 are assumed to form a closed circular collar or bracelet decorated with 12 complexes of several 'monomers' *a* and 'trimers' *AbB*, providing the electron microscopic appearance of a symmetrical hexagonal bilayer. There is no inter-chain disulfide bridge between 'dimers' D1 and D2, and these and heme-binding subunits *a* and *AbB* [55]. The 'bracelet' model was deduced from extensive studies on the dissociation and reassociation of *Lumbricus* hemoglobin either at an extreme of pH [17, 19] or in the presence of a dissociating agent at neutral pH [16]. The existence of subunits D1 and D2 appeared to be essential for complete reassociation of the molecule of *Lumbricus* hemoglobin from the dissociated products under physiological conditions. Although the experimental results did not provide direct proof of the existence of a bracelet structure, the filamentous structure in the central hole of the giant hemoglobin may corres-

TABLE 5. Models of annelid hemoglobins with none-heme chains

Hemoglobin	No. of chain	No. of heme	$M_r (\times 10^{-6})$	Ref.
<i>Arenicola</i>	192	96	2.59	[54]
<i>Lumbricus</i>	204	144	3.77	[91]
<i>Lumbricus</i>	ca. 200	156	3.8	[16, 20]
<i>Lumbricus</i>	204	192	3.77	[23]

pond to the bracelet [20]. An alternative explanation is that subunits D1 and D2 do not form a continuous bracelet structure but may act as linkers between submultiples [16].

Table 5 summarizes the models of multi-subunit annelid hemoglobins that include non-heme chains. These models depend greatly upon the estimated value for the heme content, which varied significantly in different laboratories. Vinogradov *et al.* [15, 91] assumed that one chain of the 'trimer' of *Lumbricus* hemoglobin did not contain heme. However, this idea was disproved by the finding that all chains isolated by chromatography under mild conditions contained a heme group [24, 77]. Recently, Fushitani *et al.* [23] determined the heme content of *Lumbricus* hemoglobin to be one mole per 19,000 g of protein. Their model consists of 48 'aAbB' and 12 chains of D1 and D2, as shown in Table 5. This model appears to be the most consistent with all data so far obtained on *Lumbricus* hemoglobin. Fushitani and Riggs [23] assumed that D1 and D2 contain no heme, and reported that the amounts of D1 and D2 constitute 11.2% of the total. On the other hand, Mainwaring *et al.* [17] reported that D2 exhibits a reduced capacity to bind heme. The relative proportions of D1 and D2 in *Lumbricus* hemoglobin are reported to be 25 and 10%, respectively [17, 55]. D1 was separated into two fractions [92]. There are no homologies in the reported NH₂-terminal sequences of D2 and two D1 chains or between these and those of other globins [23, 92]. If D1 and D2 have evolved as heterogeneous components with the same function of linking the complexes of subunits *a* and *AbB* together, they should exhibit high homology in terms of amino acid sequences. The natures of chains D1 and D2 are still unclear. Comparative studies revealed diversity in the appearance of D1 and D2 components [30]. In *Nephtys incisa* hemoglobin, no dimer component can be seen in the absence of a reducing agent, but two dimers are seen on SDS-PAGE in the presence of a reducing agent [93]. On the other hand, in the case of *Potamia leptochaeta* chlorocruorin, one band of dimer is seen in the absence of a reducing agent, but no dimer is seen in reduced conditions [94]. Waxman [54, 61] suggested that the faint bands of

D1 and D2 might be those of partially reduced dimers derived from disulfide-bonded 'tetramers'. Pionetti and Pouyet [95] thought that the two bands with molecular masses of about 30 kDa must be due to contaminants with some non-heme chains. At present, it can not be concluded that D1 and D2 are common to all multi-subunit annelid hemoglobins, although several lines of evidence support the 'bracelet' model.

According to the '192-chain' model and the 'bracelet' model, the values for the calculated molecular weight of *Lumbricus* hemoglobin are 3,343,872 and 3,770,000, respectively [23]. Ghirelli Magaldi *et al.* [21] stated, "we have absolutely no reason to believe that these M_r values are underestimated by even 25%". They determined the relative molecular weights of *Ophelia bicornis* hemoglobin and *Spirographis sparanzani* chlorocruorin to be about 3×10^6 . In contrast, Vinogradov and Kolodziej [53] stressed that the recent values reported for the molecular weight of *Lumbricus* hemoglobin are clustered at about 3.8×10^6 . Furthermore, Vinogradov *et al.* [16] stated in the 'bracelet' model, "it is postulated that the stoichiometries of some of the subunits need not be constant". Due to the symmetrical appearance of 12 submultiples, however, we believe that there are at least 6 or 12 units for each constituent in the whole molecule. From an X-ray crystallographic study, Royer and Hendrickson [96] reported that self-rotation function calculations of *Lumbricus* hemoglobin reveal D₆ symmetry to a resolution of at least 6 Å.

PERSPECTIVE

Which is correct, the '192-chain' model or the 'bracelet' model? At present neither can be disregarded. The discrepancy between these models will be explained in part by the results of sequencing the D1 and D2 chains from at least two species of hemoglobins. Immuno-electron microscopy might be a suitable method to determine the loci of D1 and D2 in the molecule, if it is possible to distinguish D1 and D2 from the other chains *a*, *A*, *b* and *B* immunologically [97]. The fine three-dimensional structure of the multi-subunit hemoglobin can of course be determined by X-ray

crystallography, which is currently in progress using crystals of *Lumbricus* hemoglobin [96, 98]. Comparative study will also be of great importance in considering D1 and D2. In fact, it is noteworthy that the deep-sea tube worm *Lamellibrachia* sp. contains two kinds of hemoglobins with molecular masses of 440 kDa and 3,000 kDa, the latter having the characteristic quarternary structure of multi-subunit annelid hemoglobins [99, 100]. Suzuki *et al.* [101] found that the larger one contains components corresponding in molecular size to 'linkers' D1 and D2, whereas the smaller one does not contain 'linker' proteins. Although the tube worm has been assigned to the phylum Vestimentifera [102], the NH₂-terminal amino acid sequences of its four chains containing heme exhibit high homology with those of polychaete and oligochaete chains *a*, *A*, *b* and *B* [101, 103]. Even more important, the 'linker' chain D1 of the tube worm hemoglobin shows slight, but significant homology with at least one of the four heme-binding chains sequenced completely [103, 104]. The alignment of the D1 chain with the heme-binding chain suggests that the linker resulted from gene duplication and exon shuffling of a globin chain with a three exon-two intron structure. The D1 chain consists of two domains and the first exon of domain 1 and the last exon of domain 2 are deleted. Therefore, there is a high possibility that in *Lumbricus* hemoglobin either D1 and D2 is also a real member of the molecule. Anyway, to find a rare protein, it is essential to scrutinize any possible candidates thoroughly. Conversely, when morphologists agree with the idea of biochemists that tube worms belong to the phylum Annelida, the sequences of the D1 chain of *Lamellibrachia* hemoglobin [104] will be recognized as the first 'dimer' chain of annelid hemoglobins sequenced.

In order to understand much clearly about the evolution of multi-subunit annelid hemoglobins, it is necessary to investigate the locus of each gene of the constituent chains in the DNA molecules (S). There are many challenging problems on invertebrate hemoglobin molecules to be solved in terms of DNA sequences. In the near future, the drastic mutations occurred in soluble proteins during the course of evolution can be explained in large parts by the knowledge of invertebrate hemoglobins

because they contain treasures of diversity not only in the primary and quarternary structures [30, 32, 105–107] but also in the biosyntheses including the regulation [108, 109]. On the other hand, it will also be of great interest to design disulfide-bonded trimers and tetramers such as ' $\alpha\beta\alpha$ ', ' $\beta\alpha\beta$ ', and ' $\alpha_2\beta_2$ ' of vertebrate hemoglobins, which might be synthesized with the technique of DNA recombinant [110] by inserting half-cystine residues at sites corresponding to those of Cys-4, 5, 129 and 148 in multi-subunit annelid hemoglobins.

ACKNOWLEDGMENTS

This paper is dedicated to Professor Kazuhiko Konishi of the Department of Biology, Faculty of Science, Tohoku University on the occasion of his retirement. He has encouraged us throughout this work.

REFERENCES

- 1 Svedberg, T. (1933) *J. Biol. Chem.*, **103**: 311–325.
- 2 Svedberg, T. and Eriksson, I. -B. (1933) *J. Am. Chem. Soc.*, **55**: 2834–2841.
- 3 Svedberg, T. (1937) *Nature*, **139**: 1051–1062.
- 4 Suzuki, T., Takagi, T., Shikama, K. and Gotoh, T. (1981) *Zool. Mag. (Tokyo)*, **90**: 549. (Abstr.)
- 5 Suzuki, T., Takagi, T. and Gotoh, T. (1982) *Biochim. Biophys. Acta*, **708**: 253–258.
- 6 Suzuki, T., Furukohri, T. and Gotoh, T. (1985) *J. Biol. Chem.*, **260**: 3145–3154.
- 7 Suzuki, T., Yasunaga, H., Furukohri, T., Nakamura, K. and Gotoh, T. (1985) *J. Biol. Chem.*, **260**: 11481–11487.
- 8 Suzuki, T. and Gotoh, T. (1986) In "Invertebrate Oxygen Carriers". Ed. by B. Linzen, Springer Verlag, Berlin/Heidelberg, pp. 69–72.
- 9 Suzuki, T. and Gotoh, T. (1986) *J. Biol. Chem.*, **261**: 9257–9267.
- 10 Suzuki, T. and Gotoh, T. (1986) *J. Mol. Biol.*, **190**: 119–123.
- 11 Suzuki, T., Kapp, O. H. and Gotoh, T. (1988) *J. Biol. Chem.*, **263**: 18524–18529.
- 12 Garlick, R. L. and Riggs, A. F. (1982) *J. Biol. Chem.*, **257**: 9005–9015.
- 13 Shishikura, F., Snow, J. W., Gotoh, T. Vinogradov, S. N. and Walz, D. A. (1987) *J. Biol. Chem.*, **262**: 3123–3131.
- 14 Fushitani, K., Matsuura, M. S. A. and Riggs, A. F. (1988) *J. Biol. Chem.*, **263**: 6502–6517.
- 15 Vinogradov, S. N. (1986) In "Invertebrate Oxygen Carriers". Ed. by B. Linzen, Springer Verlag, Berlin/Heidelberg, pp. 25–36.

- 16 Vinogradov, S. N., Lugo, S. D., Mainwaring, M. G., Kapp, O. H. and Crewe, A. V. (1986) *Proc. Natl. Acad. Sci. U.S.A.*, **83**: 8034–8038.
- 17 Mainwaring, M. G., Lugo, S. D., Fingal, R. A., Kapp, O. H. and Vinogradov, S. N. (1986) *J. Biol. Chem.*, **261**: 10899–10908.
- 18 Kapp, O. H., Vinogradov, S. N., Ohtsuki, M. and Crewe, A. V. (1982) *Biochim. Biophys. Acta*, **704**: 546–548.
- 19 Kapp, O. H., Polidori, G., Mainwaring, M. G., Crewe, A. V. and Vinogradov, S. N. (1984) *J. Biol. Chem.*, **259**: 628–639.
- 20 Kapp, O. H., Mainwaring, M. G., Vinogradov, S. N. and Crewe, A. V. (1987) *Proc. Natl. Acad. Sci. U. S. A.*, **84**: 7532–7536.
- 21 Ghiretti Magaldi, A., Zanotti, G., Tognon, G. and Mezzasalma, V. (1985) *Biochim. Biophys. Acta*, **829**: 144–149.
- 22 Ghiretti Magaldi, A., Ghiretti, F., Tognon, G. and Zanotti, G. (1986) In "Invertebrate Oxygen Carriers". Ed. by B. Linzen, Springer Verlag, Berlin/Heidelberg, pp. 45–55.
- 23 Fushitani, K. and Riggs, A. F. (1988) *Proc. Natl. Acad. Sci. U.S.A.*, **85**: 9461–9463.
- 24 Gotoh, T., Shishikura, F., Snow, J. W., Ereifej, K. I., Vinogradov, S. N. and Walz, D. A. (1987) *Biochem. J.*, **241**: 441–445.
- 25 Ray Lankester, E. (1868) *J. Anat. Physiol.*, **2**: 114–116.
- 26 Perutz, M. F., Rossmann, M. G., Cullis, A. F., Muirhead, H., Will, G. and North, A. T. C. (1960) *Nature*, **185**: 422–427.
- 27 Kleinschmidt, T. and Sgouros, J. G. (1987) *Biol. Chem. Hoppe Seyler*, **367**: 223–228.
- 28 Goodman, M., Pedwaydon, J., Czelusniak, J., Suzuki, T., Gotoh, T., Moens, L., Shishikura, F., Walz, D. A. and Vinogradov, S. N. (1988) *J. Mol. Evol.*, **27**: 236–249.
- 29 Kimura, M. (1983) *The Neutral Theory of Molecular Evolution*. Cambridge Univ. Press, Cambridge.
- 30 Vinogradov, S. N. (1985) *Comp. Biochem. Biophys.*, **82B**, 1–15.
- 31 Ochi, O. (1969) *Mem. Ehime Univ. Sci. B.*, **6**: 23–91.
- 32 Terwilliger, R. (1980) *Am. Zool.*, **20**: 53–67.
- 33 Fushitani, K., Ochi, O. and Morimoto, H. (1982) *Comp. Biochem. Physiol.*, **72B**: 267–273.
- 34 Roche, J. (1965) In "Studies in Comparative Biochemistry". Ed. by K. D. Munday, Pergamon Press, Oxford, pp. 62–80.
- 35 Roche, J., Bessis, M. and Thiéry, J. P. (1960) *Biochim. Biophys. Acta*, **41**: 182–184.
- 36 Levin, O. (1963) *J. Mol. Biol.*, **6**: 95–101.
- 37 Haughton, T. M., Kerkut, G. A. and Munday, K. A. (1958) *J. Exp. Biol.*, **35**: 360–368.
- 38 Mangum, C. P., Lykkeboe, G. and Johansen, K. (1975) *Comp. Biochem. Physiol.*, **52A**: 477–482.
- 39 Giardinia, B., Chiancone, E. and Antonini, E. (1975) *J. Mol. Biol.*, **93**: 1–10.
- 40 Wood, E. J., Mosby, L. J. and Robinson, M. S. (1976) *Biochem. J.*, **153**: 589–596.
- 41 Ochiai, T. (1984) *Arch. Biochem. Biophys.*, **231**: 136–143.
- 42 Igarashi, Y., Kimura, K. and Kajita, A. (1985) *Biochem. Int.*, **10**: 611–618.
- 43 Imai, K. and Yoshikawa, S. (1985) *Eur. J. Biochem.*, **147**: 453–463.
- 44 Fushitani, K., Imai, K. and Riggs, A. F. (1986) *J. Biol. Chem.*, **261**: 8414–8423.
- 45 Bunn, H. F. and Forget, B. G. (1986) *Hemoglobin: Molecular, Genetic and Clinical Aspects*. pp. 126–167. W. B. Saunders Co., Philadelphia.
- 46 Tsuneshige, A., Imai, K., Hori, H., Tyuma, I. and Gotoh, T. (1989) *J. Biochem. (Tokyo)*, **106**: 406–417.
- 47 Mungum, C. (1976) In "Adaptation to Environment: Physiology of Marine Animals". Ed. by P. C. Newell, Butterworth's London, pp. 191–278.
- 48 Antonini, E., and Chiancone, E. (1977) *Annu. Rev. Biophys. Bioeng.*, **6**: 239–271.
- 49 Chung, M. C. M. and Ellerton, H. D. (1979) *Prog. Biophys. Mol. Biol.*, **35**: 53–102.
- 50 Weber, R. E. (1978) In "Physiology of Annelids". Ed. by P. J. Mill, Academic Press, New York, pp. 393–478.
- 51 Weber, R. E. (1980) *Am. Zool.*, **20**: 79–101.
- 52 Vinogradov, S. N., Shlom, J. M., Kapp, O. H. and Frossard, P. (1980) *Comp. Biochem. Physiol.*, **67B**: 1–16.
- 53 Vinogradov, S. N. and Kolodziej, P. (1988) *Comp. Biochem. Physiol.*, **91B**: 577–579.
- 54 Waxman, L. (1971) *J. Biol. Chem.*, **246**: 7318–7327.
- 55 Shlom, J. M. and Vinogradov, S. N. (1973) *J. Biol. Chem.*, **248**: 7904–7912.
- 56 Ochiai, T. and Enoki, Y. (1981) *Comp. Biochem. Physiol.*, **68B**: 275–279.
- 57 Chiancone, E., Vecchini, P., Rossi-Fanelli, M. R. and Antonini, E. (1972) *J. Mol. Biol.*, **70**: 73–84.
- 58 David, M. M. and Daniel, E. (1974) *J. Mol. Biol.*, **87**: 89–101.
- 59 Partel, S. and Spencer, C. P. (1963) *Comp. Biochem. Physiol.*, **8**: 65–82.
- 60 Yamagishi, M., Kajita, A., Shukuya, R. and Kajiro, K. (1966) *J. Mol. Biol.*, **21**: 467–472.
- 61 Waxman, L. (1975) *J. Biol. Chem.*, **250**: 3790–3795.
- 62 Terwilliger, R. C., Terwilliger, N. B. and Roxby, R. (1975) *Comp. Biochem. Physiol.*, **50B**: 225–232.

- 63 Crewe, A. V. (1983) *Science*, **221**: 325–330.
- 64 Mezzasalma, V., Di Stefano, L., Piazzese, S., Zagra, M., Salvato, B., Tognon, G. and Ghirelli Magaldi, A. (1985) *Biochim. Biophys. Acta*, **829**: 135–143.
- 65 Stockel, P., Mayer, A. and Keller, R. (1973) *Eur. J. Biochem.*, **37**: 193–200.
- 66 Pilz, I., Schwarz, E. and Vinogradov, S. N. (1980) *Int. J. Biol. Macromol.*, **2**: 279–283.
- 67 Wilhelm, P., Pilz, I. and Vinogradov, S. N. (1980) *Int. J. Biol. Macromol.*, **2**: 383–384.
- 68 Messerschmidt, U., Wilhelm, P., Pilz, I., Kapp, O. H. and Vinogradov, S. N. (1983) *Biochim. Biophys. Acta*, **742**: 366–373.
- 69 Theuer, M., Pilz, I., Schwarz, E., Wilhelm, P., Mainwaring, G. M. and Vinogradov, S. N. (1985) *Int. Biol. Macromol.*, **7**: 25–29.
- 70 Pilz, I., Schwarz, E., Suzuki, T. and Gotoh, T. (1988) *Int. J. Biol. Macromol.*, **10**: 356–360.
- 71 Suzuki, T. (1989) *Eur. J. Biochem.*, **185**: 127–134.
- 72 Stern, M., Snow, J. W., Ereifej, K., Mainwaring, M. G., Vinogradov, S. N. and Walz, D. A. (1987) *Fed. Proc. Fed. Am. Soc. Exp. Biol.*, **46**: 2266. (Abstr.)
- 73 Nishioka, Y., and Leder, A. (1879) *Cell*, **18**: 875–882.
- 74 Gö, M. (1981) *Nature*, **291**: 90–92.
- 75 Craik, C. S., Buchman, S. R. and Beychok, S. (1980) *Proc. Natl. Acad. Sci. U.S.A.*, **77**: 1384–1388.
- 76 Phillips, S. E. V. and Schoenborn, B. P. (1981) *Nature*, **292**: 81–82.
- 77 Fushitani, K., Imai, K. and Riggs, A. F. (1986) In "Invertebrate Oxygen Carriers". Ed. by B. Linzen, Springer Verlag, Berlin/Heidelberg, pp. 77–79.
- 78 Jhiang, S. M., Garey, J. R., and Riggs, A. F. (1988) *Science*, **240**: 334–336.
- 79 Keilin, D. and Hartree, E. F. (1951) *Nature*, **168**: 266–269.
- 80 Dickerson, R. E. and Geis, I. (1983) *Hemoglobin*. The Benjamin/Cumming Publishing Co., Menlo Park, CA.
- 81 Fushitani, K., Morimoto, H. and Ochi, O. (1982) *Arch. Biochem. Biophys.*, **218**: 540–547.
- 82 Suzuki, T., Takagi, T., Furukohri, T. and Gotoh, T. (1983) *Comp. Biochem. Physiol.*, **75B**: 567–570.
- 83 Nei, M., Stephens, J. C. and Saitou, N. (1985) *Mol. Biol. Evol.*, **2**: 66–85.
- 84 Goodman, M., Weiss, M. L. and Czelusniak, J. (1982) *Syst. Zool.*, **31**: 375–399.
- 85 Tasch, P. (1980) *Paleobiology of the Invertebrates*. pp. 441–470. Wiley, New York.
- 86 Fushitani, K., Bonaventura, J. and Bonaventura, C. (1986) *Comp. Biochem. Physiol.*, **84B**: 137–141.
- 87 Gotoh, T. and Okada, K. (1975) *J. Sci. Univ. Tokushima*, **13**: 1–7.
- 88 Gotoh, T. and Kamada, S. (1980) *J. Biochem. (Tokyo)*, **87**: 557–562.
- 89 Gueritore, D., Bonaci, M. L., Brunori, M., Antonini, E., Wyman, J. and Rossi-Fanelli, A. (1965) *J. Mol. Biol.*, **13**: 234–237.
- 90 Wiechelman, K. J. and Parkhurst, L. J. (1972) *Biochemistry*, **11**: 4515–4520.
- 91 Vinogradov S. N., Shlom, J. M., Hall, B. C., Kapp, O. H. and Mizukami, H. (1977) *Biochim. Biophys. Acta*, **492**: 136–155.
- 92 Walz, D. A., Snow, J., Mainwaring, M. G. and Vinogradov, S. N. (1987) *Fed. Proc. Fed. Am. Soc. Exp. Biol.*, **46**: 2266. (Abstr.)
- 93 Vinogradov S. N., Van Gelderen, J., Polidori, G. and Kapp, O. H. (1983) *Comp. Biochem. Physiol.*, **76B**: 207–214.
- 94 Vinogradov, S. N. and Orii, Y. (1980) *Comp. Biochem. Physiol.*, **67B**: 183–185.
- 95 Pionetti, J.-M. and Pouyet, J. (1980) *Eur. J. Biochem.*, **105**: 131–138.
- 96 Royer, W. E., Jr., Hendrickson, W. A. (1988) *J. Biol. Chem.*, **263**: 13762–13765.
- 97 Lightbody, J. J., Ziaja, E. L., Lugo, S. D., Mainwaring, M. G., Vinogradov, S. N., Shishikura, F., Walz, D. A., Suzuki, T. and Gotoh, T. (1986) *Biochim. Biophys. Acta*, **873**: 340–349.
- 98 Royer, W. E., Jr., Hendrickson, W. A. and Love, W. E. (1987) *J. Mol. Biol.*, **197**: 149–153.
- 99 Terwilliger, R. C., Terwilliger, N. B. and Schab-tach, E. (1980) *Comp. Biochem. Physiol.*, **65B**: 531–535.
- 100 Arp, A. J., Childress, J. J. and Vetter, R. D. (1987) *J. Exp. Biol.*, **128**: 139–158.
- 101 Suzuki, T., Takagi, T. and Ohta, S. (1988) *Biochem. J.*, **255**: 541–545.
- 102 Jones, M. L., (1985) *Biol. Soc. Wash. Bull.*, **6**: 117–158.
- 103 Suzuki, T., Takagi, T. and Ohta, S. (1990) *Biochem. J.*, **266**: 221–225.
- 104 Suzuki, T., Takagi, T. and Ohta, S. (1990) *J. Biol. Chem.*, **265**: 1551–1555.
- 105 Iwaasa, H., Takagi, T. and Shikama, K. (1989) *J. Mol. Biol.*, **208**: 355–358.
- 106 Usuki, I., Hino, A. and Ochiai, T. (1989) *Comp. Biochem. Physiol.*, **93B**: 555–559.
- 107 Ochiai, T., Enoki, Y. and Usuki, I. (1989) *Comp. Biochem. Physiol.*, **93B**: 935–940.
- 108 Antonie, M. and Niessing, J. (1984) *Nature*, **310**: 795–797.
- 109 Kobayashi, M. and Hoshi, T. (1984) *Zool. Sci.*, **1**: 523–532.
- 110 Nagai, K., Perutz, M. F. and Poyart, C. (1985) *Proc. Natl. Acad. Sci. U. S. A.*, **82**: 7252–7255.

REVIEW

The Effect of Stress and Disturbance on Echinoderms

JOHN M. LAWRENCE

Department of Biology, University of South Florida, Tampa,
Florida 33620, U. S. A.

1. INTRODUCTION

Grime [1, 2] proposed that two types of external factors limit biomass. One, *stress*, was defined as any factor that limited production; the second, *disturbance*, as any factor that partially or totally caused destruction of biomass. Habitat productivity and habitat duration, and growth rate and mortality (parameters of fitness) have been used in a similar manner [3, 4]. Stress and disturbance can be either biotic or abiotic. Grime's definition of stress is consistent with Levitt's [5] analogy of biological to physical stress: a stress produces a strain. In biological systems, the strain would be a decrease in production [6]. Levitt [5] pointed out that stresses in biological systems differ from physical ones in that the stress must be measured not in units of force, but in units of energy. Similarly, since production is best expressed in units of energy [7, 8], biological stress would result in a decrease in deposition of energy in the organism (a decrease in production). It is in this context that low levels of resources, including food for animals, may be stresses as they limit production.

Grime [1, 2] identified three primary strategies in plants, corresponding to three of the four possible permutations of high and low stress and disturbance (Figs. 1, 2). Distinct types of life-history strategies would be associated with these three strategies. *Competitive plants* (C-strategy) are adapted to low stress and low disturbance in habitats of high productivity and long duration; *stress-tolerant plants* (S-strategy), to high stress and

low disturbance in habitats of low productivity and long duration; *ruderal plants* (R-strategy, from Latin meaning "rubble" and thus, growing in a disturbed habitat), to low stress and high disturbance in habitats of high productivity and short duration. High stress would prevent recovery in highly disturbed habitats, and this strategy would not be possible.

The three primary strategies are the results of extreme levels of stress and disturbance, and Grime proposed that intermediate conditions would result in secondary strategies. *Competitive ruderals* (CR strategy) are adapted to low stress, with competition being restricted by moderate disturbance; *stress-tolerant ruderals* (SR strategy), to lightly disturbed, unproductive habitats; *stress-tolerant competitors* (CS strategy), to relatively undisturbed conditions and moderate intensities of stress; and *CSR species*, to habitats with moderate intensities of both stress and disturbance that restrict competition, or which have temporal or spatial variation in intensities of competition, stress, and disturbance.

A suite of characteristics would be associated with each strategy (Table 1). According to Grime [2, 3, 9-11], these characteristics involve the way in which energy and matter are allocated for somatic and gonadal production, maintenance, and protection from disturbance.

Competitors have access to large amounts of resources over considerable periods of time, and a high potential for resource capture. In terrestrial animals, competitors are active foragers over large areas. In aquatic animals, competitors may also be less active foragers or even stationary if productiv-

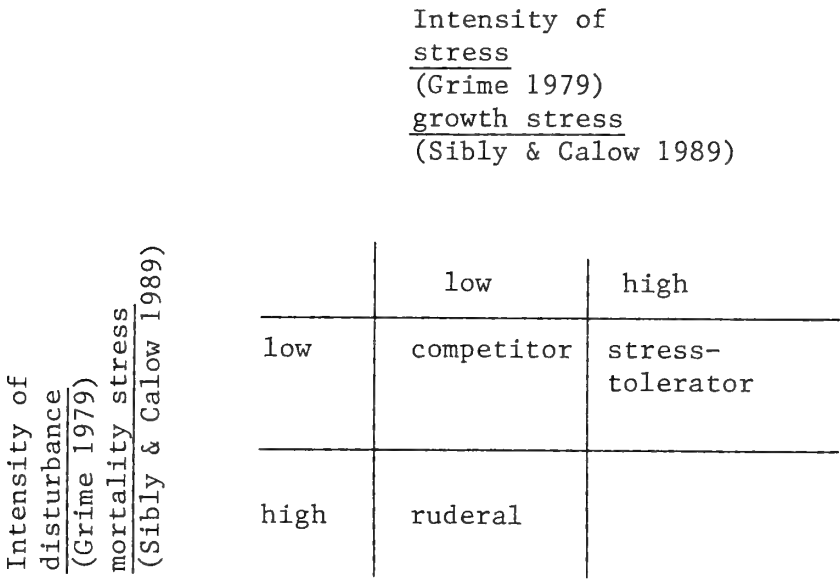


FIG. 1. Strategies resulting from combinations of different levels of stress and disturbance.

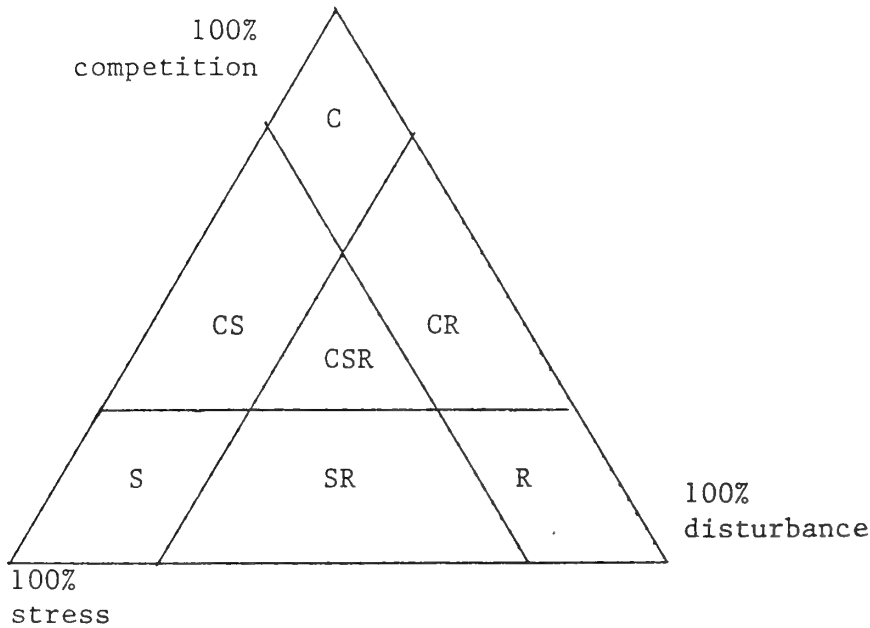


FIG. 2. Triangular model indicating the strategies resulting from combinations of different levels of stress and disturbance. C: competitor, S: stress-tolerator, R: ruderal, CS: stress-tolerant competitor, CR: ruderal competitor, SR: stress-tolerant ruderal, CRS: CRS strategist. (modified from Grime 1977)

ity is high and food is brought to them by currents. Competitors are fast growing, long-lived, and iteroparous. They reinvest captured resources in continued somatic production and activity. Be-

cause of these characteristics, Grime [3] also referred to this as a “capitalistic” strategy. *Stress-tolerators* have access to small amounts of resources (either because of the small amounts

TABLE 1. Characteristics of competitive, stress-tolerant, and ruderal echinoderms

	Competitive	Stree-tolerant	Ruderal
<i>Characteristic</i>			
<i>Habitat</i>			
Potential productivity	high	low	high
Duration	long	long	short
Stability	high	high	low
Disturbance	low	low	high
<i>Life history</i>			
Longevity	long or relatively short	long or very long	short, or very short
Phenology of reproduction	annual, pronounced cycle	many types, may be intermittent, continuous, or asexual	early in life, annual
Reproductive effort	low	low	high
Reproductive output	high	low	low or high, depending on body size
Developmental type*	2.1 (2.2?)	1, 2	1,2
<i>Physiology</i>			
Maximal relative potential for resource capture	high	low	high
Maximal relative potential growth rate	rapid	slow	rapid
<i>Miscellaneous</i>			
Defense against predation (structural, chemical, bchavioral)	relatively specialized, often ineffective	if present, constitutive	relatively specialized, often ineffective
Palatability	high	if predation occurs, low	high

* Developmental types [107]: 1, Direct; 2, Indirect; 2.1, planktotrophic and pelagic; 2.2; lecithotrophic and pelagic, 2.3, lecithotrophic and benthic; 2.4, lecithotrophic and brooded; 2.5, lecithotrophic and viviparous.

available or of their mode of resource capture). In animals, stress-tolerators are passive in feeding or have limited active foraging over limited areas. Resources are captured at a low rate over a long period or time, or in brief, infrequent, unpredictable pulses. They are slow growing, and long or very long-lived. Although iteroparous, their reproduction may be irregular in time and nature; it may be suspended with chronic, severe stress.

Ruderals have access to large amounts of resources but their longevity is limited by disturbance (food exhaustion, predation, abiotic factors). They have rapid growth and early reproduction at an early age. As they are short lived, they are

semelparous or have limited iteroparity. They tend to sustain reproduction even when under stress.

Grime [2, 9] suggested that heterotrophic organisms also have the three primary strategies attributed to autotrophic plants. He placed primary significance on the response of the organism to stress, and asserted that evolutionary responses to stress fall into basic types that correspond to widely-recurrent ecological strategies that would allow all organisms, regardless of taxonomic or trophic group, to be placed in a common framework of basic functional types. His proposal has not been systematically evaluated for any

major group of heterotrophs. This review applies the triangular model to the Echinodermata, a major animal phylum of great importance in the ocean world.

2. PRIMARY STRATEGIES

2.1 *Competitive echinoderms*

The only echinoderms that clearly fit the criterion of being active foragers are some asteroids. *Acanthaster planci* of the Indo-Pacific coral reefs may be an example. It is found in a region of high resource availability and long duration, has a high potential for resource acquisition, is long lived, iteroparous with a high fecundity, and has relatively ineffective protection against disturbance [12, 13]. *Pycnopodia helianthoides* and *Meyenaster gelatinosus* are probably other examples [14, 15]. These are very active species found on the highly productive west coasts of North and South America respectively where abundant prey are available.

Among the regular echinoids, the diadematids have the highest capacity for active foraging but are not always found in habitats of high production and low disturbance. The other regular echinoids are less active. Although many are found in areas of high productivity, the temporal and spatial variation in intensities of competition, stress, and disturbance suggests that they are not competitors as a primary strategy.

Whether particulate-feeding echinoderms have the potential for a sufficiently high rate of food capture to be a competitor as a primary strategy is debatable. Dense, persistent shallow-water epifaunal ophiuroid beds are found in various parts of the world ocean [16]. These occur where flow and levels of suspended organic matter are high and the incidence of predation is low and sublethal. The dendrochirotid holothuroid *Aslia lefevrei* forms dense aggregates off the west coast of Europe where moderately strong water-flow supplies seston continuously [17, 18]. It can have a longevity of ca. 10 years or more. As a result of their susceptibility to predation, few crinoids are found in shallow-water habitats of high productivity and low disturbance. *Antedon rosaceus* may be

an exception.

It is unlikely that deposit-feeding echinoderms (spatangoids, and aspidochirotid and molpadid holothuroids) are competitors. The ingestion of inorganic sediment should reduce their potential for a high rate of resource capture.

2.2 *Stress-tolerating echinoderms*

Although their feeding mode may limit the potential for resource capture in many echinoderms, those with stress-tolerance as a primary strategy are found where food availability is very low. This occurs in the deep sea which receives only 1 to 3% of the surface primary productivity [19]. Many echinoderm species occur in the deep sea, and no class is always dominant [20]. All should be stress-tolerant strategists as a result of the low availability of food. This is correlated with their passive or low level of activity in feeding.

Perhaps the best known representatives are the stalked crinoids, now restricted to deeper waters [21]. Crinoids are passive, rheophilic suspension-feeders restricted to low-energy water habitats [22] and have little potential for capturing even the limited resources in the deep sea. Meyer and Macurda [23] suggested that the appearance of predatory teleosts led to the restriction of stalked crinoids to the deep sea. It would seem that the combination of high stress (low capacity for production) and disturbance (predation), Grime's fourth non-permissible permutation, would be responsible. Nothing is known of their life histories, but one would predict that they would be slow-growing and long-lived.

Growth of deep-sea holothuroids, echinoids and ophiuroids is slow and the echinoids there are long lived [24–32] as expected. *Echinus affinis* are thought to live up to ca. 28 years. Several holothuroid, ophiuroid, and asteroid species have low fecundity [30, 33–36], but not necessarily less than that characteristic for their taxon, size, and reproductive mode. The deep-sea pelagic holothuroid *Scotoanassa* has occurrence patterns that have been interpreted to result from reproductive responses to short-term environmental changes (probably in food availability) [37].

The tropical shallow-water asteroids are microphagous. They may be stressed by the low levels of

resources available. Blake [38] concluded that the primarily tropical valvatids and echiniasterids have extensive development of structural protection that is related to the high predation pressure in the region, and suggested that the microphagous mode of feeding was the consequence of this. To the contrary, the protection against predation may be the consequence of the stress of the low rate of resource capture and the advantage of allocating resources to increase longevity.

The echinoids *Colobocentrotus atratus* and *Heterocentrotus mammillatus* (Echinometridae) are found in extremely high-energy water in the tropics and have a low detrital food supply that constitutes an additional stress to that of physical exposure. These species have an extremely heavy test and spines that constitute a greater proportion of the body weight [39] and energy [40] than in most regular echinoids. They also have a long life-span [39, 41]. Ebert [39] noted that the survivorship of regular echinoids increases with an increase in the relative size of the body wall. He related this to the degree of exposure to high-energy habitats. The long life-span was associated with a slow rate of growth. Ebert suggested that these observations supported the hypothesis that survival is related to allocation of resources to maintenance. Rather than attributing the long life-span and slow growth to the rigors of the physical environment, one might attribute them to low resource availability or acquisition.

The suspension-feeding ophiuroid *Amphiura filiformis* would seem best classified as a stress-tolerant species based on estimated life-spans of 20 to 25 years [42, 43]. Yet a number of reports indicates life spans of only ca. 5 years [see 43]. Indeed, Buchanan [44] concluded that the species was fast growing and short-lived, dying soon after reproduction. He contrasted it to *Amphiura chiajei*, which he found to be slow growing and long-lived. This difference in characteristics reported for *A. filiformis* has been attributed to underrepresentation of juveniles in sampling [42]. It would seem that the maximal longevity found best indicates the strategy for the species. The high incidence of sublethal predation of *A. filiformis* in Galway Bay that should require a major allocation of resources [45] is not that expected to be associ-

ated with such a long-lived species. In this regard, it may be that the other suspension-feeding ophiuroids that form dense, persistent beds but suffer little predation [16, 46, 47] are also stress-tolerators. They would be comparable to the stalked crinoids that apparently cannot exist in shallow-water because of predation [23] as it combines high stress and disturbance.

Deposit-feeding echinoids (Atelostomacea and Gnathostomacea), ophiuroids (Ophiocomidae, Amphiuridae, Ophiactida, Ophiothrichidae), holothuroids (Aspidochirotida, Elaspodida, Apodida, Molpadida), and asteroids (some Paxillosida) ingest sediment that should reduce nutrient levels and should be stress-tolerators. The ophiuroid *Amphiura chiajei* shows no evidence of lethal predation, has a slow rate of growth, and is long-lived and iteroparous [43]. The spatangoid *Echinocardium cordatum* has a relatively long life-span estimated to be ca. 15 years [48]. As it lives in deep burrows [49], it should be relatively free from predation, but mortality in shallow waters as a result of storms occurs [50].

It is possible that the Antarctic echinoderms are stress-tolerant strategists. Pearse *et al.* [51] characterized the Antarctic shallow-water environment as being extremely oligotrophic most of the year, with the shallow benthos being seasonally very productive and unstable and the deeper benthos being very stable. They characterized the benthic invertebrates as having very slow gonadal development and somatic growth, and attributed this to lack of adaptation to the low temperatures. These characteristics may instead be responses to low food availability or quality. Either would result in a decrease in productivity.

Stressed echinoderms may have unusual reproductive characteristics such as little seasonality (asynchrony within and/or among individuals), intermittent reproduction, asexual reproduction, and direct development over a long life-span. The asteroid *Asterina miniata*, which feeds most commonly on detrital plant material that may limit its production [52], seems to have no predators [53] and has asynchronous reproduction [54]. The asteroid *Ctenodiscus crispatus*, which feeds non-selectively on deposits, shows asynchronous gametogenesis and aseasonal, continuous reproduction

[55]. Shick *et al.* [55] noted that the reproductive pattern in the eurybathic *C. crispatus* is similar to that of deep-sea echinoderms and suggested that it may be related to the constancy of the population's detrital food source. Similarly, Tyler [19, 29] and Tyler *et al.* [56] suggested that the high frequency of reproductive asynchrony in deep-sea ophiuroids and asteroids results from the constant level of food that provides no seasonal cues for reproduction. To the contrary, the low level of food, and not its constancy, may be responsible.

Asexual reproduction by fission occurs in a few species of asteroids, ophiuroids, and holothuroids [57]. Asexual reproduction in these species seems to be associated with low availability of food [57, 58] and thus would be a stress response.

2.3 Ruderal echinoderms

Several shallow-water, tropical regular echinoids of the family Toxopneustidae (*Lytechinus*, *Tripleneustes*) seem to be ruderals. They are found in habitats of high primary production, have a rapid growth rate, high reproductive output and fecundity, and short life-spans that are associated with both biotic and abiotic disturbance [59–62].

Among the ophiuroids, several species along the French coast of the English Channel have life spans of ca. 5 years or less [63–66]. These species are found in current-washed habitats, and abiotic disturbance could be the cause of the short longevity in this productive area. The longevity of *Ophiura texturata* is less in the Mediterranean Sea than in the North Sea [66] which may result from a difference in predation levels.

Some ophiuroids have longevities of only slightly more than 1 year. *Ophiothrix fragilis* lives ca. 15 months [64]. *Amphipholis squamata* has a longevity of ca. 1 to 2.5 years [see 47]. The shorter longevities reported for this species were in tide-pool populations and were thought to result from higher stress. The simultaneous hermaphroditism and brooding habit of this species may be related to the small size of individuals and rigors of the habitat. Somatic and gonadal growth occur simultaneously in *A. squamata*, which is not a characteristic one would predict for a ruderal species as most resources should be put into reproduction, but whether the reproductive effort is actually

small is not known.

Amphipholis squamata is found in habitats with high production [67]. High production would not be associated with rubble habitats. Hendler and Littman [68] noted that the rarity of small ophiuroids in rubble remained to be explained. The rubble habitat is probably the non-permissible fourth permutation of Grime: high stress (low food availability) and high disturbance.

If the potential for high resource capture is a requisite for the ruderal strategy, it seems contradictory to conclude that some ophiuroids could be assigned to this primary strategy and not to the competitive one which also requires that potential. Differences in sizes or mode of feeding may be the explanation.

Several species of asteroids have characteristics of ruderals. *Asterina phylactica* is a small, simultaneous hermaphrodite that lives in moderate to strong currents along the coasts of the British Isles [69]. It first reproduces at 2 years, produces 1 to 3 broods, and has a longevity of up to 4 years [70]. In contrast, the closely related *Asterina gibbosa* is larger, a protandric hermaphrodite that lives in more sheltered habitats although it overlaps with *A. phylactica*. It first reproduces at 4 years, produces 4 to 7 broods, and has a longevity of 7 or more years. *A. phylactica* has a greater reproductive effort than *A. gibbosa*, a characteristic of a ruderal species. Emson and Crump [69, 70] related the life-history characteristics of *A. phylactica* to a more stressful habitat than that of *A. gibbosa* but they may be more related to a disturbed habitat.

3. SECONDARY STRATEGIES

3.1 Competitive ruderal echinoderms

Echinoderms with this strategy would have a high potential to obtain food but would be subject to moderate disturbance. This restricts the possibilities to asteroids and regular echinoids. Suspension-feeding ophiuroids and holothuroids in highly productive habitats may also have this strategy.

Leptasterias hexactis coexists with *Pisaster ochraceus* on the west coast of North America. Whereas *P. ochraceus* has characteristics of a CS

strategy, *L. hexactis* has characteristics of a CR strategy. It matures at a smaller size at ca 2 years of age and has a moderate, but shorter longevity [71, 74]. Menge [72] calculated that the energetic reproductive output of *P. ochraceus* was less than that of *L. hexactis*, but this is not indicative of the reproductive effort. He suggested that the small size and brooding habit of *L. hexactis* made it more susceptible to disturbance than *P. ochraceus* in the high water-energy intertidal habitat. As *L. hexactis* is found in a productive region and grows larger in the absence of *P. ochraceus*, it may be classified as having a CR strategy.

Another forcipulatid that seems to experience high disturbance is *Asterias*. *Asterias amurensis* has a longevity of only ca. 3 years [75], and actually becomes reproductively mature in less than 1 year under favorable conditions [76]. *Asterias vulgaris* and *Asterias forbesi* also mature at a small size in less than 1 year [77–79]. Menge suggested that massive mortality of these species results from disease and storms, and that their density consequently is less than the carrying capacity of their habitat. As with other echinoderms, growth is greatly affected by the availability of food. One population of *Asterias rubens* off the coast of Brittany grows slowly to a small size and has a longevity of more than 5 years while another grows rapidly to a large size and has a longevity of 3 years [80]. Thus *Asterias* seems to be another asteroid with a CR strategy.

3.2. Stress-tolerating ruderal echinoderms

Abiotic stress such as sublethal but non-optimal levels of temperature, salinity, exposure to air and wave-energy can affect intertidal and shallow-water echinoderms. Much stress, however, may be due to low levels of resources, either in their availability and/or in the ability of the organism to obtain it rapidly. The latter case can occur in those taxa that feed passively or have a low level of activity, and also in those whose potential for feeding is restricted by the potential for predation.

The reproductive characteristics of two species of Caribbean ophiuroids differ according to their level of exposure to abiotic disturbance and possibly to stress [81]. *Ophiocomella ophiactoides* in protected areas reproduce asexually except in a

few large individuals. Those in exposed areas have a high rate of asexual reproduction at all sizes. *Ophiatis savignyi* found in sponges reproduce asexually except for the few large individuals. Epiphytic ones are all asexual. Both of these species are small. The early reproduction at such a small size could be related to the high level of disturbance. The asexual reproduction could be an adaptation to a high level of stress (either low levels of food, the rigors of a shallow-water tropical habitat, or from the small body-size itself that limits resource capture). However, many echinoderms of similar size reproduce sexually.

Shallow-water tropical crinoids also seem to be SR-strategists. Crinoids in the tropical shallow-waters not only are stressed by the low level of resource availability and their passive mode of acquiring the resource, but suffer disturbance from predation as well. Although these crinoids have some behavioral, structural, and chemical deterrents to predation, they are not effective [82]. Predation on the crinoids is usually sublethal and the lost parts are regenerated.

Suspension-feeding ophiuroids have a similar situation of stress from low resource availability or acquisition and of disturbance from predation. Species found on coral-reef flats, Caribbean lagoons, and subtidal rocky reefs off the English coast are cryptic and show high incidences of sublethal predation [16, 46].

Representatives of several orders of echinoids are stress-tolerating ruderals. In the clypeasteroids *Mellita* and *Dendraster* the rate of feeding and growth, longevity, and relative gonadal-somatic production [83–87] are suggestive of stress-tolerant ruderals. The regular echinoid *Echinometra* is found in tropical intertidal and very shallow-water habitats, and experiences the stress of exposure and low food availability [88, 89] along with predation [61, 90, 91].

Intertidal dendrochirotid holothuroids in areas of low production can have SR characteristics. *Cucumaria curata* has delayed sexual maturity (at 3 years), moderate longevity ca. 5 years and low fecundity [92].

3.3. Stress-tolerating competitive echinoderms

These echinoderms would be subject to low

resource availability but have an active mode of resource capture. Several asteroids seem to fit this category. *Pisaster ochraceus* is mobile, if not highly active. It has delayed onset of reproduction, high fecundity, a potential high rate of growth, and a long life-span [73, 93], but is usually food limited [93, 94]. A related species *Pisaster giganteus* allocates energy to the pyloric caeca and to maintenance when stress is increased by low food availability [95].

3.4. CSR echinoderms

These echinoderms should be found where resources are relatively abundant and have an active mode of feeding, but also experience disturbance. As the potential for feeding is restricted by the presence of predators, the availability of the resources may be more apparent than real.

The asteroid *Luidia clathrata* is an active predator [96] that is subject to arm loss that affects its reproductive capacity [97]. It has a nocturnal feeding cycle, presumably predator-induced, that results in its being resource limited in the field [96, 98]. With limited food, it allocates resources to nutrient storage and reproduction rather than to arm regeneration [99]. With abundant food, it allocates resources to both arm regeneration and growth of the internal organs [100]. With limited food, not only is development of the gonads reduced, but also the capacity for egg fertilization and development [101].

The regular echinoids associated with lush algal florae of temperate waters are CSR strategists. They show temporal and spatial variation in intensities of competition, stress, and disturbance. *Strongylocentrotus* species have been studied most [see 53, 102–105]. These species have delayed onset of reproduction followed by annual reproduction for a number of years, a low gonadal: somatic production but a high potential maximal rate of feeding and production. Their protection against predation is not highly effective and their life-history characteristics are greatly affected by the level of predation. Predation by fish and sea otters on *Strongylocentrotus* species can be great on the west coast of North America. In this situation, they have low stress and low or moderate disturbance. Without this predation, stress

may become extreme as the strongylocentrotids eliminate their food resource by overgrazing. In this situation, they have high stress and low disturbance, and adopt the foraging strategy of “mobile-active search” rather than the “sit-and-wait” one used when food is abundant. An increase in the relative size of the Aristotle’s lantern in *Strongylocentrotus purpuratus* in such situations is thought to be an adaptive phenotypic response [106]. Strongylocentrotids survive low food availability with no or minimal somatic and gonadal production. Other Echinidae (*Echinus*, *Loxechinus*, *Paracentrotus*, *Parechinus*, *Psammechinus*, *Sterechinus*), and some Echinometridae (*Heliocidaris*, *Evechinus*) also seem to be CSR-strategists.

4. DISCUSSION

Grime’s model predicts that species adapted to different types of habitats will have different suites of characters. These characters sort into primary and secondary strategies involving differences in life history and physiology (Table 1). Life history characters involve reproduction and mortality. Physiological characters involve feeding, growth, and maintenance activities. Competitive and ruderal species are similar physiologically in the high potential for resource capture and growth rates, but differ in life histories as competitive species have greater longevity, a smaller reproductive effort, and a higher fecundity. Competitive and stress-tolerant species overlap in longevity (although the latter may be very long-lived) and are similar in their small reproductive effort, but stress-tolerant species have a lower potential for resource capture and growth rate, and a lower fecundity.

The criterion of longevity can be used to separate ruderal echinoderms from the competitive and stress-tolerant echinoderms. Ruderal, CR, and SR echinoderms seem to have life-spans of up to 5 years; competitive, CR, and CS echinoderms, from 5 to 15 years; and stress-tolerant and CS echinoderms, of many more years. The overlapping of longevity of the echinoderms in the different groups except for the extremes makes use of longevity as a criterion difficult.

Basic criteria separating the groups should in-

volve size at first reproduction, reproductive effort, reproductive output, and fecundity. It is important to recognize that reproductive effort is the proportion of the energy acquired by an organism that is allocated to reproduction. This is different from the reproductive output, which is simply the amount of energy allocated to reproduction, even if expressed in terms of body weight. Competitive echinoderms have a high reproductive output and fecundity. Ruderal echinoderms may have these characteristics also, but only in those that attain a large size. CS, and CR echinoderms similarly vary in their reproductive output and fecundity with individual size. Those few values for CS and CR echinoids suggest that reproductive effort is low. They continue to grow asymptotically. Fecundity is the result of both egg size and number, and is high in these groups. In contrast, fecundity is low in SR echinoderms, often involving the production of fewer, larger eggs and culminating, in those groups where the potential exists, in a few fissiparous species that produce a single new individual with asexual reproduction. The body form and location of the gonads may limit fecundity in crinoids and ophiuroids and affect their potential for the competitive or ruderal strategies.

The potential to acquire resources is the result of the quantity or quality of food and/or the ability to acquire it. The latter can result from the level of activity and/or effectiveness of the feeding mechanism. A basic criterion that immediately separates echinoderms is whether they are active or passive or relatively inactive feeders. Active feeders, defined as those that actively forage over large areas, are found only in Asteroidea and regular Echinoidea. Only they have the functional morphology that enables this behavior. The other groups range from the completely passive (suspension-feeding stalked Crinoidea and functionally pelmatozoan Dendrochirotida and Ophiuroidea) to the minimally vagile (suspension-feeding Comatulida, and some Ophiuroidea, Dendrochirotida, and deposit-feeding Atelostomacea, Gnathostomacea, Aspidochirotida, Molpadida, and Ophiuroidea). This low level of activity correlated with microphagous feeding limits the potential for resource acquisition and often involves ingestion

of low quality food.

Although this major division can be made on a broad scale, individual species within any taxon with characteristic size, functional morphology, or trophic type, will differ in their ability to acquire food. Thus, species in groups that are passive or relatively inactive in feeding can increase their feeding ability and/or be found in habitats of high production that increase their capacity to acquire resources. This is the probable basis for the appearance of some suspension- or deposit-feeding echinoderms as competitors or ruderals. For animals in general, it is necessary to take into account the particular characteristics of feeding behavior and predation in relation to production [107].

The maximal potential relative growth rate is another criterion that separates the competitive and ruderal strategies from the stress tolerant strategy. As echinoderms do not always recruit to habitats in which a maximal growth rate results, a wide range of growth rates for several species has been reported. One generally concludes that the fastest rate is the maximal potential rate. Although growth rates are usually based on linear dimensions or weights, comparisons of groups that differ in body forms, structures, and composition are difficult. If production is the criterion, growth should be measured in energy units. In no other way can the growth rate of a holothuroid be compared to that of an asteroid, or a regular echinoid to a spatangoid. Competitive, CS, CR, and ruderal echinoderms within taxa do have more rapid growth rates.

A basic characteristic of echinoderms important to understanding their strategies is their overall susceptibility to predation. Fish and crustaceans are the primary predators of echinoderms although some gastropods are also. Defense against predation can be structural, chemical, or behavioral. Structural and chemical defense uses energy that is not available for growth in size or for reproduction. Behavioral defense invariably reduces feeding and consequently production. As great longevity is important to the strategy, the presence of an effective defensive system against predation is found in stress-tolerant echinoderms. Less effective systems are found CS, CR, and ruderal echinoderms. Those stress-tolerant echinoderms

found in habitats that have less predation, such as the deep-sea, seem to lack structural defenses and should lack chemical ones as well. Similarly, those spatangoids burrowing at a depth sufficient to avoid predation do not have deterrent spines.

5. CONCLUSION

Studies on echinoderms have not considered the life-history and physiological characteristics in terms of the relative levels of stress and disturbance that echinoderms experience. Grime's model provides a context that can be used to interpret these characteristics. Most of the data available for echinoderms involve life-history characteristics such as longevity and reproductive output. Fecundity has not been documented for many species. An important characteristic that has not been studied for many species is reproductive effort. Most studies of the pertinent physiological characteristics involve the rate of growth, but even these are primarily for regular echinoids and asteroids and almost invariably are not in energetic units. Few studies except for regular echinoids and asteroids report the potential for resource capture and the quantify the availability of food. Data on both the life-history and physiological characteristics of a species are necessary before a complete understanding of their way of life is possible.

REFERENCES

- Grime, J. P. (1974) *Nature*, **250**: 26–31.
- Grime, J. P. (1977) *Am. Nat.*, **111**: 1169–1194.
- Grime, J. P. (1989) *Biol. J. Linn. Soc.*, **37**: 3–17.
- Sibley, R. M. and Calow, P. (1989) *Biol. J. Linn. Soc.*, **37**: 101–116.
- Levitt, J. (1972) *Responses of Plants to Environmental Stress*, Academic Press, New York.
- Fry, F. E., (1947) *Publ. Ontario Fish. Res. Lab.*, **68**: 1–62.
- Brody, S. (1945) *Bioenergetics and Growth*. Hafner, New York.
- Winberg, G. G. (1956) *Fish. Res. Bd. Can. Trans. Ser. No. 194*.
- Grime, J. P. (1979) *Plant Strategies and Vegetation*, John Wiley & Sons, Chichester.
- Grime, J. P., Cuick, J. C. and Rincon, R. E. (1986) In "Plasticity in Plants". Ed. by D. H. Jennings and A. J. Trewaras, *Soc. Exp. Biol.*, Cambridge, pp. 7–29.
- Grime, J. P., Hodgson, J. G. and Hunt, R. (1988) *Comparative Plant Ecology*. Unwin Hyman, London.
- Birkeland, C. (1989) *Echinoderm Studies*, **3**: 1–79.
- Moran, P. J. (1986) *Oceanogr. Mar. Biol. Ann. Rev.*, **24**: 379–480.
- Dayton, P. K. (1975) *Ecol. Monogr.*, **45**: 137–159.
- Dayton, P. K., Rosenthal, R. J., Mahen, L. C., and Antezana, T. (1977) *Mar. Biol.*, **39**: 361–370.
- Aronson, R. B. (1989) *Ecology*, **70**: 856–865.
- Costelloe, J. (1988) *Mar. Biol.* **99**: 535–545.
- Costelloe, J. and Keegan, B. F. (1984) *Mar. Biol.* **84**: 135–142.
- Tyler, P. A. (1988) *Oceanogr. Mar. Biol. Ann. Rev.*, **26**: 227–258.
- Sibuet, M. (1987) *Structure des Peuplements Benthiques en Relation avec les Conditions Trophiques en Milieu Abyssal sans l'Océan Atlantique*, Thesis, Univ. de Paris VI.
- Roux, M. (1987) *Echinoderm Studies*, **2**: 1–53.
- Meyer, D. L. (1982) In "Echinoderm Nutrition". Ed. by M. Jangoux and J. M. Lawrence, Balkema, Rotterdam, pp. 25–42.
- Meyer, D. L. and Macurda, D. B., Jr. (1977) *Paleobiology*, **3**: 74–82.
- Gage, J. D. (1984) *J. Mar. Biol. Ass. U. K.*, **64**: 157–170.
- Gage, J. D. (1987) *Mar. Biol.*, **96**: 19–30.
- Gage, J. D. and Tyler, P. A. (1981) *Mar. Biol.*, **64**: 163–172.
- Gage, J. D. and Tyler, P. A. (1982) *Oceanol. Acta*, **5**: 73–83.
- Gage, J. D. and Tyler, P. A. (1985) *Mar. Biol.*, **90**: 41–53.
- Tyler, P. A., (1980) *Oceanogr. Mar. Biol. Ann. Rev.*, **18**: 125–153.
- Tyler, P. A. and Gage, J. D. (1979) In "Cyclic Phenomena in Marine Plants and Animals". Ed. by E. Naylor and R. G. Hartnoll, Pergamon, Oxford, pp. 215–222.
- Tyler, P. A. and Gage, J. D. (1980) *Oceanol. Acta*, **3**: 177–185.
- Tyler, P. A. Muirhead, A., Billett, D. S. M., and Gage, J. D. (1985) *Mar. Ecol. Prog. Ser.*, **23**: 269–277.
- Tyler, P. A. and J. D. Gage (1982) *J. Mar. Biol. Ass. U. K.*, **62**: 45–55.
- Tyler, P. A. and J. D. Gage (1983) *J. Mar. Biol. Ass. U. K.*, **63**: 609–616.
- Tyler, P. A., Billett, D. S. M. and Gage, J. D. (1987) *J. Mar. Biol. Ass. U. K.*, **67**: 385–397.
- Tyler, P. A. and Pain, S. L. (1982) *J. Mar. Biol. Ass. U. K.*, **62**: 869–887.
- Childress, J. J., Gluck, D. L., Carney, R. S. and

- Gowing, M. M. (1989) *Limnol. Oceanogr.*, **34**: 913-930.
- 38 Blake, D. B. (1983) *Bull. Mar. Sci.*, **33**: 703-712.
- 39 Ebert, T. A. (1982) *Ecol. Monogr.*, **52**: 353-384.
- 40 Lawrence, J. M. (1985) In "Echinoderms". Ed. by B. F. Keegan and B. D. S. O'Connor, Balkema, Rotterdam, pp. 47-67.
- 41 Ebert, T. A. (1975) *Am. Zool.*, **15**: 755-775.
- 42 Muus, K. (1981) *Ophelia*, **20**: 153-168.
- 43 O'Connor, B., Bowmer, T. and Grehan, A. (1983) *Mar. Biol.*, **75**: 279-286.
- 44 Buchanan, J. (1964) *J. Mar. Biol. Ass. U. K.*, **44**: 565-576.
- 45 Bowmer, T. and Keegan, B. F. (1983) *Mar. Biol.*, **74**: 65-71.
- 46 Aronson, R. B. (1987) *Paleobiology*, **13**: 187-192.
- 47 Aronson, R. B. (1988) *Bull. Mar. Sci.*, **43**: 93-97.
- 48 Buchanan, J. (1966) *J. Mar. Biol. Ass. U. K.*, **46**: 97-114.
- 49 Nichols, D. (1959) *Pubs. System. Ass. Lond.*, **3**: 61-80.
- 50 Beukema, J. J. (1985) *Neth. J. Sea Res.*, **19**: 129-134.
- 51 Pearse, J. S., J. B. McClintock and I. Bosch. (1990) *Amer. Zool.* (In press)
- 52 Gerard, V. A. (1976) Some Aspects of Material Dynamics and Energy Flow in a Kelp Forest in Monterey Bay, California, Thesis, Univ. of California, Santa Cruz.
- 53 Harrold, C., and Pearse, J. S. (1987) *Echinoderm Studies*, **2**: 137-233.
- 54 Farmanfarmanian, A., Giese, A. C., Boolootian, R. A. and Bennett, J. (1958) *J. Exp. Zool.*, **138**: 355-367.
- 55 Shick, J. M., Taylor, W. F. and Lamb, A. N. (1981) *Mar. Biol.*, **63**: 51-66.
- 56 Tyler, P. A., Pain, S. L. and Gage, J. D. (1982) *J. Mar. Biol. Ass. U. K.*, **62**: 57-69.
- 57 Emson, R. H. and Wilkie, I. E. (1980) *Oceanogr. Mar. Biol. Ann. Rev.*, **18**: 155-250.
- 58 Lawrence, J. M. (1987) *A Functional Biology of Echinoderms*, Croom and Helm, London.
- 59 Bacolod, P. T. and Dy, D. T. (1986) *Philipp. Sci.*, **23**: 1-14.
- 60 Dafni, J. and Tobol, R. (1986/87) *Isr. J. Zool.*, **34**: 191-204.
- 61 Hendler, G. (1977) *Proc., Third Internat. Coral Reef Symp.*, Univ. of Miami, pp. 217-223.
- 62 Scheibling, R. E. and Mladenov, P. V. (1988) *Mar. Fish. Rev.*, **49**: 62-69.
- 63 Bourgoïn, A. (1987) *Ecologic et Demographie d'Acronida branchiata* (Montague) (Echinodermata: Ophiuroidea) en Baie de Douarnenez (Bretagne), Thesis, Univ. de Bretagne Occidentale.
- 64 Davoult, D. (1989) *Vie Mar., Hors serie no. 10*: 116-127.
- 65 Gentil, F. and Zakardjian, B. (1989) *Vie Mar., Hors serie no. 10*: 148.
- 66 Guillou, J. and Robert, R. (1979) In "Echinoderms: Present and Past". Ed. by M. Janguoux, Balkema, Rotterdam, pp. 171-177.
- 67 Emson, R. H. and Whitfield, P. J. (1989) *J. Mar. Biol. Ass. U. K.*, **69**: 27-41.
- 68 Hendler, G. and Littman, B. S. (1986) *Coral Reefs*, **5**: 31-42.
- 69 Emson, R. H. and Crump, R. G. (1984) *J. Mar. Biol. Ass. U. K.*, **64**: 35-53.
- 70 Emson, R. H. and Crump, R. G. (1979) *J. Mar. Biol. Ass. U. K.*, **59**: 77-94.
- 71 Menge, B. A. (1972) *Ecology*, **53**: 635-644.
- 72 Menge, B. A. (1974) *Ecology*, **55**: 84-93.
- 73 Menge, B. A. (1975) *Mar. Biol.*, **31**: 87-100.
- 74 Menge, J. L. and Menge, B. A. (1974) *Ecology*, **44**: 189-209.
- 75 Hatanaka, M. and Kosaka, M. (1958) *Tohoku J. Agric. Res.*, **9**: 159-178.
- 76 Nojima, S., Soliman, F. El-S., Kondo, Y., Kuwana, Y., Nasu, K. and Kitajima, C. (1986) *Pub. Amakusa Mar. Biol. Lab.*, **8**: 90-112.
- 77 Galtsoff, P. S. and Loosanoff, V. L. (1939) *Bull. Bur. Fish. U. S.*, **49**: 75-132.
- 78 Menge, B. A. (1979) *Oecologia*, **41**: 245-272.
- 79 Menge, B. A. (1986) *Bull. Mar. Sci.*, **39**: 467-476.
- 80 Guillou, M. and Guillaumin, A. (1985) In "Echinodermata". Ed. by B. F. Keegan and B. D. S. O'Connor, Balkema, Rotterdam, pp. 513-521.
- 81 Mladenov, P. V. and Emson, R. H. (1988) *Mar. Erol. Prog. Ser.*, **42**: 181-194.
- 82 Meyer, D. L. (1985) *Paleobiology*, **11**: 154-164.
- 83 Birkeland, C. and Chia, F. -S. (1971) *J. Exp. Mar. Biol. Ecol.*, **6**: 265-278.
- 84 Ebert, T. A. and Dexter, D. M. (195) *Mar. Biol.*, **32**: 397-407.
- 85 Lane, J. M. (1977) *Bioenergetics of the Sand Dollar, Mellita quinquesperforata*, Theses, Univ. of South Florida, Tampa.
- 86 Morin, J. G., Kastendiek, J. E., Harrington, A. and Davis, N. (1985) *Mar. Ecol. Prog. Ser.*, **27**: 163-185.
- 87 Timko, P. L. (1976) *Biol. Bull.*, **151**: 247-259.
- 88 Lawrence, J. M. and Kafri, J. (1979) *Mar. Biol.*, **52**: 87-91.
- 89 Russo, A. R. (1977) *Aust. J. Mar. Freshwater Res.*, **28**: 693-702.
- 90 McClanahan, T. R. and Muthiga, N. A. (1989) *J. Exp. Mar. Biol. Ecol.*, **126**: 77-94.
- 91 Menge, B. A. and Lubchenko, J. (1981) *Ecol. Monogr.*, **51**: 429-450.
- 92 Rutherford, J. C. (1973) *Mar. Biol.*, **22**: 167-176.
- 93 Feder, H. (1970) *Ophelia*, **8**: 161-185.

- 94 Castilla, J. C. and Paine, R. T. (1987) Rev. Chilena Hist. Nat., **60**: 131–151.
- 95 Harrold, C. and J. S. Pearse (1980) J. Exp. Mar. Biol. Ecol., **48**: 169–183.
- 96 McClintock, J. B. (1984) An Optimization Study on Feeding Behavior of *Luidia clathrata* (Say) (Echinodermata: Asteroidea), Univ. of South Florida, Tampa.
- 97 Lawrence, J. M. and Dehn, P. F. (1979) Fla. Sci., **42**: 9–12.
- 98 Lawrence, J. M., Klinger, T. S., McClintock, J. B., Watts, S. A., Chen, C. -P., Marsh, A. and Smith, L. (1986) J. Exp. Mar. Biol. Ecol., **102**: 47–53.
- 99 Lawrence, J. M., and Ellwood, A. (unpubl.)
- 100 George, S., Lawrence, J. M. and Fenaux, L. (unpubl.)
- 101 Lawrence, J. M. (1975) Oceanogr. Mar. Biol. Ann. Rev., **13**: 213–286.
- 102 Lawrence, J. M. and Sammarco, P. W. (1982) In "Echinoderm Nutrition". Ed. by M. Jangoux and J. M. Lawrence, Balkema, Rotterdam, pp. 331–371.
- 103 Estes, J. A. and Harrold, C. (1988) In "The Community Ecology of Sea Otters". Springer-Verlag, Berlin, pp. 116–150.
- 104 Ebeling, A. W. and Laur, D. R. (1988) In "The Community Ecology of Sea Otters". Springer-Verlag, Berlin, pp. 169–191.
- 105 Ebert, T. A. (1980) Bull. Mar. Sci., **30**: 467–474.
- 106 Dickie, L. M., Kerr, S. R., Boudreau, P. R., (1987) Ecol. Monogr., **57**: 233–250.
- 107 Chia, F. S. (1974) Thal. Jugoslav., **10**: 121–130.

A Comparative Study of the Gill Morphometry in the Mudskippers-*Periophthalmus chrysospilos*, *Boleophthalmus boddaerti* and *Periophthalmodon schlosseri*

WAI P. LOW, YUEN K. IP AND DAVID J. W. LANE

Department of Zoology, National University of Zoology, Kent Ridge,
Singapore 0511, Republic of Singapore

ABSTRACT—The gill and skin morphometries of three mudskippers-*Periophthalmus chrysospilos*, *Boleophthalmus boddaerti* and *Periophthalmodon schlosseri* were studied and compared. Correlations were made between the morphometric parameters of these respiratory surfaces and the different terrestrial and aquatic affinities of the mudskippers with special reference to their capabilities to respire terrestrially.

The natural preference of *B. boddaerti* for an aquatic environment can be explained by their having the longest and greatest number of gill filaments amongst the three mudskippers studied. It also has the largest gill area and gill area: skin area ratio, indicating a greater role of its gills than its skin in respiration.

Both *P. chrysospilos* and *P. schlosseri* have relatively lesser affinity to water as their gills are not well adapted for aquatic respiration. *P. chrysospilos* has the smallest total number of filaments and shortest total filament length. It also has smaller gill area: skin ratio than *B. boddaerti*, and exhibits the most rapid increase in skin area with respect to body weight. Thus, its skin appears to have a greater role in gaseous exchange than its gills. In *P. schlosseri*, the gill area: skin area ratio increases as the fish grows, suggesting that small fish depends more on its skin for gaseous exchange whilst branchial respiration is more important in bigger individuals.

INTRODUCTION

Much of the information available on air-breathing fish generally deals with their diverse respiratory adaptations to their mode of life. Accessory breathing organs of air-breathing fish eg. *Channa*, *Saccobranchus*, *Clarias*, *Anabas* [1] and *Heteropneustes fossilis* [2] have been examined and described. The various respiratory areas of air-breathing fish have also been measured [1, 3]. In general, the gill area in air-breathing fish is smaller than non air-breathing aquatic fish. Even air-breathing fish which never leave water have relatively small gill area [4, 5].

Much interest has also been centered on amphibious fishes, mainly the mudskippers. Mudskippers are unique in being some of the most terrestrial fishes [6]. Hence, most of the information

collected on mudskippers had placed major emphasis on their physiological [7–10] and biochemical [11–15] adaptations to terrestrial exposure.

The three major genera of mudskippers in Singapore are *Periophthalmus chrysospilos*, *Boleophthalmus boddaerti* and *Periophthalmodon schlosseri*. They live in the same vicinity at Pasir Ris estuary, off the east coast of Singapore, but differ markedly in behavior and microhabitat. *B. boddaerti* and *P. schlosseri* are found on the intertidal zone of the mudflats whereas *P. chrysospilos* inhabits the littoral zone of the seashore nearby. Of the three mudskippers, *B. boddaerti* has the greatest affinity for water. At low tide, it is found on the mudflats and it periodically enters the water. But, as the tide rises, it retreats into its burrows which are on the lower region of the mudflats and remains submerged until the tide ebbs. *P. schlosseri* and *P. chrysospilos* have less affinity for water compared to *B. boddaerti*. At low tide, *P. schlosseri* comes onto the mudflats; at

high tide, they are usually found swimming along the water's edge with their snout above water. *P. chrysopilos* is almost invariably found on land next to water at both high and low tides. When agitated, *B. boddaerti* dives and remains submerged for some time whereas *P. schlosseri* and *P. chrysopilos* skim away at the water surface through several bounces. Low *et al.* [16] studied the gill morphologies of these three genera of mudskippers in Singapore by scanning electron microscopy and reported their structural adaptations to be very different.

One of the problems mudskippers face upon terrestrial exposure is that their gills may collapse and their secondary lamellae tend to coalesce, resulting in a major reduction in functional respiratory area available for gaseous and ionic exchange. The gill morphometry of the mudskippers *B. boddaerti* [17, 18], *B. chinensis* and *P. cantonensis* [19] have been studied. Although the gill morphometry of *B. boddaerti* from the Arabian Gulf has been studied by Hughes and Al-Kadhomy [18], the behavior reported in their investigation was very different from that observed in our local species. In contrast to the local *B. boddaerti*, the specimens studied by Hughes and Al-Kadhomy [18] were found at the water's edge during high tide. Moreover, the local mudskipper is herbivorous [20] whereas the Arabian Gulf *B. boddaerti* is reported to be omnivorous. Since no detailed information on the gills of *P. schlosseri* is available and the most recent report on those of *P. chrysopilos* concerned more about the gill morphology than morphometry [16], the presence of the three local mudskippers in Pasir Ris therefore presented the authors with a unique opportunity to compare their gill morphometries and skin areas in relation to body sizes and their variable capabilities to respire terrestrially. It is hoped that this study can explain the very different behavioral strategies of these mudskippers in their natural habitats.

MATERIALS AND METHODS

Mudskippers ranging from young to fully grown adults, (2 to 13 g for *P. chrysopilos*, 2 to 35 g for *B. boddaerti* and 3 to 111 g for *P. schlosseri*) were captured from August to September in 1986, at

Pasir Ris, Singapore. These mudskippers were identified according to Khoo [20]. Normal breeding period of the mudskippers in Singapore was observed to be between May and July. No measurement was made on gravid specimens and no attempt was made to separate the sexes. They were maintained in the laboratory in 50% seawater (18‰ salinity). Fish were killed by pithing, lightly blotted dry and their weights recorded by a Shimadzu Libror EB 280M electronic animal balance to the nearest milligram.

Skin morphometry

The skin area was obtained by rolling one side of the mudskipper flat onto a piece of paper and tracing its outline. This outline was retraced onto a piece of paper of even thickness, cut out, and its area determined. This value was doubled to obtain the bilateral skin area of the specimen.

Gill morphometry

Dissected gills were rinsed with 0.85% NaCl solution and immersed in 5% formalin made with 50% sea water. Measurements were made on all four right gill arches. Exposure of the gills to formalin for various periods of time might cause artificial changes to some of the morphometric parameters measured, especially the secondary lamellar area. Therefore, attempt was made to standardise the period of exposure of all the gill samples to formalin before measurement of a specific gill parameter was made. Such procedure ensured that comparison of the specific gill parameters between specimens was valid. The total number of filaments were counted after preservation for one day. On the second day, the total filament length was measured, whilst the number of secondary lamellae/mm and lamellar area were obtained on the third and fourth day respectively.

The method of filament sampling was according to Hughes [21]. The gill parameters were obtained from measurements of every fifth filament in *P. chrysopilos* and *B. boddaerti*. In *P. schlosseri*, however, a substantial number of branched filaments occurred at the centre of the arch [16]. If measurements of the filament length were made on every fifth filament, some of them being branched and others not, it would give rise to a considerable

amount of error. Therefore, measurements of filament length were made on every filament on all four right arches in this mudskipper. To measure the number of secondary lamellae/mm, two counts were made near the base and tip of the unbranched or branched filaments. This was performed on every other filament on all four arches. These values were averaged and doubled as there were secondary lamellae on both sides of the filament. They were next multiplied by the total filament length of that gill arch to obtain the number of secondary lamellae.

To determine the secondary lamellar area, the arches of all three species were stained with methylene blue. Four lamellae were excised from the base, four from the tip and four from the middle of the filaments. These were mounted on glass slides. Their outlines were traced by a WILD camera lucida onto even thickness paper which was cut, and the average bilateral areas calculated. This was performed on every fifth filament of *P. chrysopilos* and *B. boddaerti* from which the filament length was obtained. For *P. schlosseri*, three filaments were chosen for this determination—one from the centre (usually branched), and two from the mid-point between the centre and the dorsal and ventral aspects of the arch. The averaged bilateral lamellar area was then multiplied by the number of secondary lamellae to give the gill area of that particular arch. This value was next doubled to account for the left arch as well. The total gill area was obtained by summing the gill area of all the gill arches.

RESULTS

The results of the skin and gill parameters fit the logarithmic equation:

$$\text{Log } Y = \log a + b \log W$$

or

$$Y = aW^b$$

where Y is the parameter measured; W=weight of the fish; a=intercept on the Y axis giving the parameter for a 1 g fish; b=regression coefficient (slope), with correlation coefficients (r) greater than 0.95 for most of the parameters measured (Table 1). The standard deviations of the Y intercept (S_a) and the slope (S_b), are also given in the

same table. Unlike most gill morphometric studies, various dimensions for 1, 10 and 100 g fish and 95% confidence limits are not given as these values can be calculated from the equations in Table 1. Bilogarithmic plots of the skin and various gill parameters against body weight are presented in Figures 1, 2, 3 and 4.

The total filament number and total filament length decrease in the order *B. boddaerti* > *P. schlosseri* > *P. chrysopilos* (Fig. 1, Table 1). From the bilogarithmic plots of secondary lamellae/mm against body weight, it can be seen that the decrease in this parameter is slight in *P. schlosseri* and *B. boddaerti* but marked in *P. chrysopilos* (Fig. 2, Table 1). Although the total number of secondary lamellae (N) decrease in the order *B. boddaerti* > *P. schlosseri* > *P. chrysopilos* (Fig. 2), the slope of increase in this gill parameter with body size is the greatest in *P. schlosseri* (Table 1). The regression coefficient in enlargement of bilateral secondary lamellar area (bl) with body

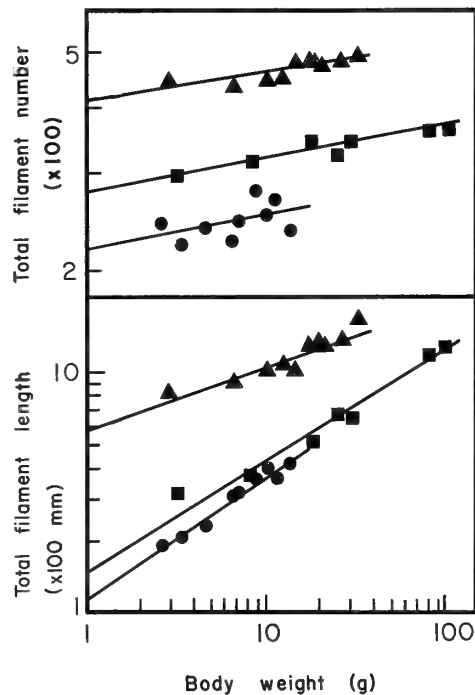


Fig. 1. Bilogarithmic plot of total filament number and total filament length of *P. chrysopilos* (●), *B. boddaerti* (▲) and *P. schlosseri* (■) against body weight.

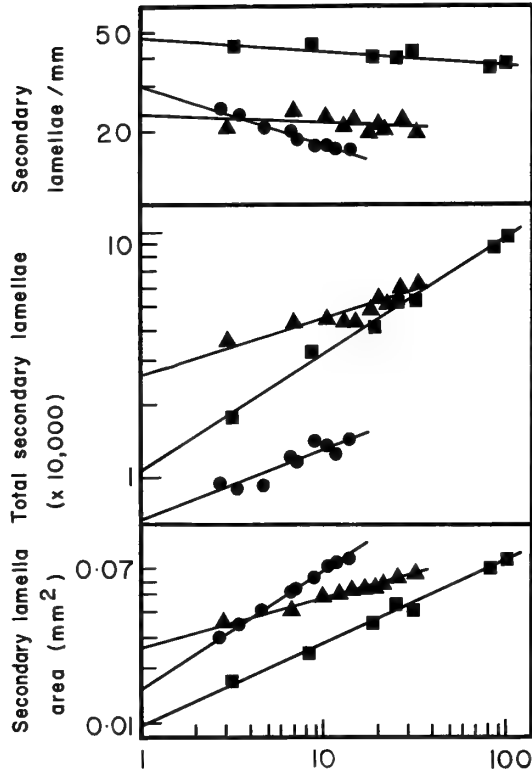


FIG. 2. Bilogarithmic plot of number of secondary lamellae/mm on one side of the filament, total secondary lamellae and average secondary lamella area of *P. chrysopilos* (●), *B. boddaerti* (▲) and *P. schlosseri* (■) against body weight.

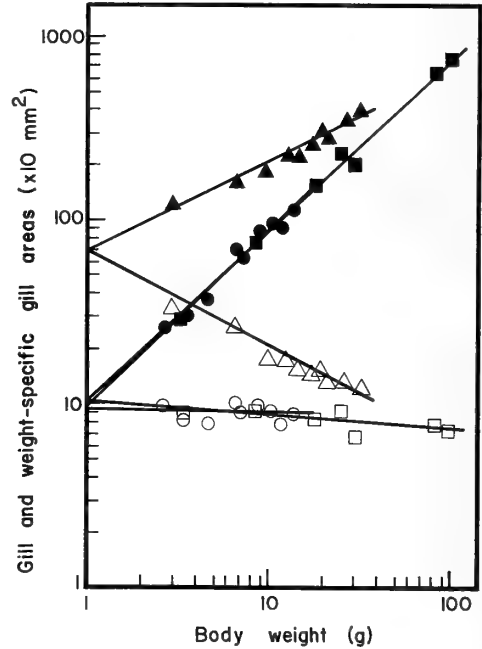
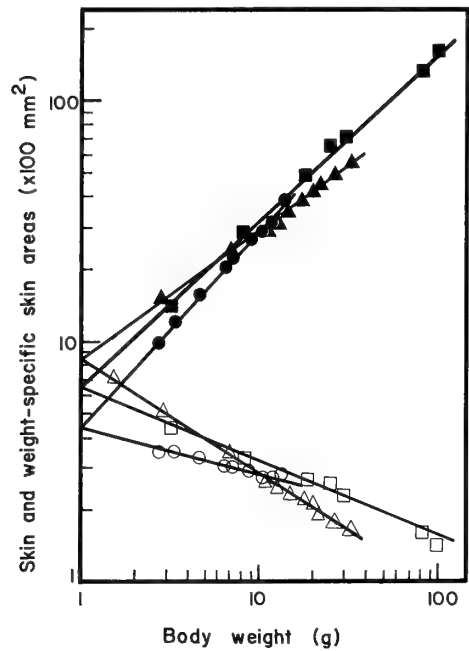


FIG. 3. Bilogarithmic plot of gill area *P. chrysopilos* (●), *B. boddaerti* (▲) and *P. schlosseri* (■) against body weight. Open symbols represent the corresponding weight-specific gill areas of the mudskippers.

TABLE 1. Summary of equations obtained from regression analysis of the *P. schlosseri*

Parameter	<i>P. chrysopilos</i>	<i>S_a</i>	<i>S_b</i>	<i>r</i>
Skin area (mm ²)	Log SA=2.6423+0.8077 log W SA=439 W ^{0.8077}	1.0319	0.01582	0.9985
Weight-specific skin area (mm ² /g)	Log S=2.6206-0.1696 log W S=417 W ^{-0.1696}	1.0345	0.01712	0.9659
Total number of filaments	Log F=2.3376+0.0629 log W F=218 W ^{0.0629}	1.0975	0.04689	0.4517
Total filament length (mm)	Log L=2.0568+0.5033 log W L=114 W ^{0.5033}	1.0819	0.03968	0.9788
Number of secondary lamellae/mm (one side)	Log n=1.4802-0.2367 Log W n=30.2 W ^{-0.2367}	1.0322	0.01599	0.9844
Total number of secondary lamellae	Log N=3.8209+0.2933 log W N=6620 W ^{0.2933}	1.1171	0.05584	0.8933
Average bilateral secondary lamella area (mm ²)	Log bl=-1.8275+0.6456 log W bl=0.01488 W ^{0.6456}	1.0211	0.01051	0.9990
Gill area (mm ²)	Log GA=1.9895+0.9577 log W GA=97.6 W ^{0.9577}	1.1518	0.07126	0.9813
Weight-specific gill area (mm ² /g)	Log G=1.9679-0.0198 log W G=92.9 W ^{-0.0198}	1.1436	0.06765	0.1095



weight is smallest in *B. boddaerti* and greatest in *P. chrysospilos* (Fig. 2, Table 1).

B. boddaerti has larger gill area than *P. schlosseri* and *P. chrysospilos* (Fig. 3), but smaller slopes of increase in *N* and *bl* with respect to weight. These result in its smallest slope of increase in gill area, and hence its largest slope of decrease in weight-specific gill area with body size among the three mudskippers (Fig. 3, Table 1). In contrast, *P. chrysospilos* and *P. schlosseri* have regression coefficients of increase in gill area with body weight approaching 1, indicating only slight change in weight-specific gill area as the fish grows larger (Fig. 3, Table 1).

The slopes of increase in skin area with body weight increase in the order *B. boddaerti* > *P. schlosseri* > *P. chrysospilos* (Fig. 4, Table 1). Calculated gill area: skin area ratios are plotted against body weight in Figure 5. The ratios for *P. chrysospilos*, which range from 0.27 to 0.36, are smaller than those for *B. boddaerti* (0.67 to 0.77). *P. schlosseri* is unusual in having ratios that increase from 0.22 in small specimens to 0.50 in larger ones (Fig. 5).

A comparison has been made between some gill parameters of the mudskippers with those of various fish species (Table 2) and mudskippers (Table 3) reported elsewhere.

FIG. 4. Bilogarithmic plot of skin area of *P. chrysospilos* (●), *B. boddaerti* (▲) and *P. schlosseri* (■) against body weight. Open symbols represent the corresponding weight-specific skin area of the mudskippers.

skin areas and the various gill parameters with body weight of *P. chrysospilos*, *B. boddaerti* and

<i>B. boddaerti</i>	<i>S_a</i>	<i>S_b</i>	<i>r</i>	<i>P. schlosseri</i>	<i>S_a</i>	<i>S_b</i>	<i>r</i>
Log SA=2.9250+0.5299 log W SA=841 W ^{0.5299}	1.0197	0.00753	0.9990	Log SA=2.8015+0.6889 log W SA=633 W ^{0.6889}	1.0559	0.01627	0.9985
Log S=2.9252-0.4701 log W S=842 W ^{-0.4701}	1.0197	0.00754	0.9990	Log S=2.8015-0.3112 log W S=633 W ^{-0.3112}	1.0559	0.01626	0.9920
Log F=2.6109+0.0521 log W F=408 W ^{0.0521}	1.0221	0.00843	0.9000	Log F=2.4423+0.0615 log W F=277 W ^{0.0615}	1.0347	0.01021	0.9247
Log L=2.7553+0.2567 log W L=569 W ^{0.2567}	1.0614	0.02301	0.9659	Log L=2.1629+0.4600 log W L=146 W ^{0.4600}	1.0898	0.02570	0.9910
Log n=1.3636-0.0307 log W n=23.1 W ^{-0.0307}	1.0620	0.02323	0.4025	Log n=1.6803-0.0518 log W n=47.9 W ^{-0.0518}	1.0506	0.01475	0.8432
Log N=4.4162+0.2290 log W N=26074 W ^{0.2290}	1.0685	0.02557	0.9482	Log N=4.0289+0.4759 log W N=10687 W ^{0.4759}	1.0723	0.02088	0.9950
Log bl=-1.6002+0.2650 log W bl=0.02511 W ^{0.2650}	1.0197	0.00718	0.9970	Log bl=-2.0262+0.4491 log W bl=0.00942 W ^{0.4491}	1.0646	0.01870	0.9955
Log GA=2.8319+0.4812 log W GA=679 W ^{0.4812}	1.1032	0.03618	0.9783	Log GA=2.0012+0.9312 log W GA=100 W ^{0.9312}	1.1257	0.03539	0.9965
Log G=2.8325-0.5194 log W G=680 W ^{-0.5194}	1.1029	0.03607	0.9798	Log G=2.0012-0.0688 log W G=100 W ^{-0.0688}	1.1257	0.03540	0.6557

TABLE 2. Comparison of the computed values of total filament number (F), total filament length (L) and gill area (GA) obtained in the present studies for 10 g mudskippers and various species of fish of equivalent weight reported elsewhere

Fish species at 10 g	F	L ($\times 100$ mm)	GA ($\times 1000$ mm ²)	Reference
Aquatic fishes				
<i>Cyprinus carpio</i>	1110	23.2	5.17	25
<i>Katsuwonus pelamis</i>	—	137	262	26
<i>Thunnus</i> sp.	—	135	200	26
Air-breathing fishes				
<i>Anabas testudineus</i>	1049	11.2	2.29	1
<i>Channa punctuata</i>	1111	14.9	1.84	3
Mudskippers				
<i>P. chrysopilos</i>	251	3.63	0.89	Present study
<i>B. boddaerti</i>	460	10.28	2.06	Present study
<i>P. schlosseri</i>	547	4.21	0.86	Present study

— value is not available as regression analyses were not performed on this gill parameter

TABLE 3. Comparison of gill measurements of the local mudskippers *P. chrysopilos* (*P. chry.*), *B. boddaerti* (*B. b.*) and *P. schlosseri* (*P. s.*) with the *B. boddaerti* studied by Niva *et al.* (17) and Hughes and Al-Kadhomiy (18). The measurements of 8.8 g *Periophthalmus cantonensis* (*P. can.*) and 53 g *Boleophthalmus chinensis* (*B. c.*) by Tamura and Moriyama (19) are also given

Gill measurement	Tamura & Moriyama			Present study			Niva <i>et al.</i>	Hughes & Al-Kadhomiy
	8.8 g <i>P. can.</i>	53 g <i>B. c.</i>	8.8 g <i>P. chry.</i>	8.8 g <i>P. s.</i>	53 g <i>B. b.</i>	53 g <i>P. s.</i>	53 g <i>B. b.</i>	53 g <i>B. b.</i>
Total filament number	306	486	249	317	502	354	630	—
Total filament length (mm)	495–510	2500–2969	340	396	1577	904	2179	3678
Number of secondary lamellae/mm (one side)	21–26	12–16	18.1	42.8	11.8	39.0	17.7	10.7
Average bilateral secondary lamella area (mm ²)	0.040	0.080	0.061	0.025	0.072	0.056	0.061	0.076
Total secondary lamellae	23617	77532	12529	30085	64723	70706	77975	78870
Gill area (mm ²)	1050–1150	5020–5551	783.5	759.8	4587	4044	4695	5979

DISCUSSION

The amphibious nature of all three genera of mudskippers is undisputable. However, their relative success in terrestrial adaptation and their strategies for terrestrial respiration may be very different. *B. boddaerti* enters and submerges itself in water frequently whereas *P. chrysopilos* and *P. schlosseri* stay on land most of the time. Thus, the mudskippers have marked differences in their dependence on an aquatic environment. Tamura and Moriyama [19] pointed out that a small gill area

necessarily leads to a smaller role of branchial respiration. Hence, the relationship between the skin and gill area may explain the behavioral differences in these mudskippers.

P. chrysopilos has a smaller gill area than *B. boddaerti* (Fig. 3) and the fewest and shortest filaments of the three mudskippers (Fig. 1). As its filaments are bent and twisted [16], not all of its secondary lamellae will be oriented parallel to the respiratory water current, making the counter-current distribution mechanism for oxygen absorption inefficient. Therefore, oxygen uptake in this

mudskipper has to be supplemented by other surfaces such as the skin, be it in water or on land. In general, the respiratory medium-blood distance of skin is much thicker than that of gill epithelia. Nevertheless, cutaneous respiration in *P. chrysopilos* could be more efficient in air where the medium is less dense and the diffusion rate of oxygen would be higher as relatively more oxygen is available ($200 \mu\text{l}$ oxygen/ml air compared to $5 \mu\text{l}$ oxygen/ml water). The importance of cutaneous respiration in *P. chrysopilos* is further reflected in its small gill: skin area ratio (Fig. 5) as compared to *B. boddaerti*. Since cutaneous respiration is important for this mudskipper, it exhibits the greatest slope of increase in skin area and the smallest slope of decrease in weight-specific skin area with respect to weight (Fig. 4, Table 1). The results of Tamura *et al.* (22) are in support of our hypothesis of the importance of cutaneous respiration in this genera of mudskipper. Their studies showed that *P. cantonensis* relies on its skin for 76% and its gills for 27% of its oxygen uptake on land. When confined to water, the oxygen uptake by the skin and gills were about equal (48% and 52% respectively). Thus, for respiratory reasons, *P. chrysopilos* may remain on land most of the time. Furthermore, the gills of *P. chrysopilos*

have adaptive features to withstand aerial exposure. Graham [23] suggested that greater spacing between secondary lamellae reduces collapse of the respiratory surfaces in air. Secondary lamellar frequency in *P. chrysopilos* is indeed lower and decreases markedly body weight as compared to the other two mudskippers (Fig. 2, Table 1).

In contrast, *B. boddaerti* has the longest and greatest number of filaments (Fig. 1) of the three mudskippers. Long filaments are more likely to collapse when removed from water. Although *B. boddaerti* of body weights greater than 4 g have smaller secondary lamellar area than *P. chrysopilos* of similar weight (Fig. 2), the former have comparatively greater number of lamellae/mm (Fig. 2). Thus, the secondary lamellae may tend to coalesce upon removal from water. All these factors lead to the reduced preference of *B. boddaerti* for land compared to the other two mudskippers. However, its filaments are more aligned [16], hence, most of the secondary lamellae may be in the optimal position to fully utilise the counter-current mechanism for aquatic gaseous exchange. Also, since it has the largest gill area (Fig. 3), weight-specific gill area (Fig. 3) and gill area: skin area ratio of the three mudskippers (Fig. 5), its greater affinity for water can be easily appreciated. The results of the present studies are in agreement with those reported by Tamura and Moriyama [19] for *B. chinensis*. Since the gills of *B. boddaerti* are playing a greater role in respiration, therefore measurements reveal that the slope of increase in skin area with respect to weight in this fish is the smallest of the three mudskippers (Table 1, Fig. 4).

The bilogarithmic plots of gill area and weight-specific gill area of *B. boddaerti* against body weight are notably different from those of *P. chrysopilos* and *P. schlosseri*. The gill area of a fish is determined by its total number of secondary lamellae and average secondary lamellar area. As the regression coefficients of the increase in these two gill parameters with body weight in *B. boddaerti* is the smallest of the three mudskippers (Table 1, Fig. 2), it thus results in its smallest slope of increase in total gill area with body weight (Fig. 3, Table 1). A consequence of its small slope of increase in gill area is the rapid reduction in its

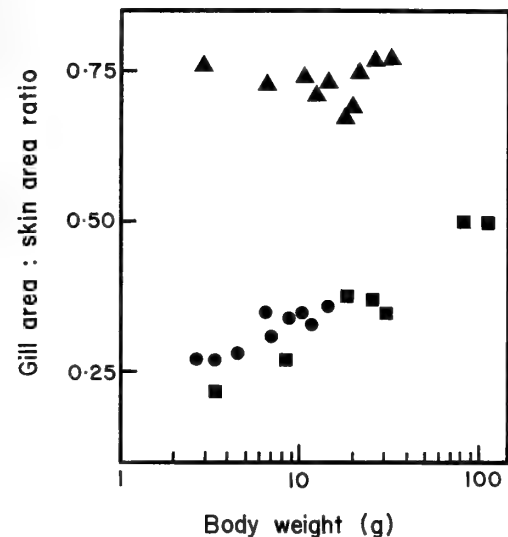


FIG. 5. Plot of gill area: skin area ratio of *P. chrysopilos* (●), *B. boddaerti* (▲) and *P. schlosseri* (■) against logarithmic body weight.

weight-specific gill area as the fish grows larger (Fig. 3, Table 1). A greater slope of increase in gill area may restrict the terrestrial capability of *B. boddaerti*, for it necessarily result from a greater increase in either total number of secondary lamellae, or average bilateral lamellar area, or both of these gill parameters with body weight. If its regression coefficient of increase in secondary lamellar area with body weight is similar to that of *P. chrysopilos*, its secondary lamellae will be so large that they may fold over removed from water and thus reduce the respiratory area. An increase in the total number of secondary lamellae without a concomitant increase in filament length would lead to a high lamellar frequency. A high lamellar frequency implies closely spaced secondary lamellae which will tend to coalesce upon aerial exposure. If the filament length were to increase to accommodate these secondary lamellae, these longer filaments will have a greater tendency than shorter ones to collapse when the fish emerges from water.

The gills of *P. schlosseri* are not well adapted for aquatic respiration. Low *et al.* [16] reported the presence of intrafilamentary secondary lamellar fusions in the gills of *P. schlosseri*. This may prevent water from flowing between the lamellae and impede oxygen uptake by the counter-current mechanism of the gills. Its total filament length (Fig. 1) and gill area (Fig. 3) are similar to those of *P. chrysopilos*. *P. schlosseri* is also frequently found out of water in its natural habitat. In addition, the gills of *P. schlosseri* can withstand desiccation as the fenestrae formed by the tissue fusions between secondary lamellae may trap water, reducing the risk of gill dehydration upon terrestrial exposure [16].

Small *P. schlosseri* have smaller gill area: skin area ratio (Fig. 5) as compared to bigger ones. This suggests that small *P. schlosseri*, like *P. chrysopilos*, may have greater dependence on cutaneous than branchial respiration. *P. schlosseri*, on the other hand, can attain a size of greater than 100 g. At 100 g, presumably its skin would be much thicker than those of the other two mudskippers at their respective maximum sizes. Furthermore, the surface area: volume ratio would be smaller in a large fish compared to a small one.

Cutaneous respiration in bigger *P. schlosseri* may thus be relatively inefficient. However, it has branched filaments (16) which naturally have more filament tips than unbranched ones. As secondary lamellae are added towards the tip of gill filament, more tips would therefore increase the potential of generating a greater total number of secondary lamellae and, hence, gill area as the fish grows. This potential is clearly shown in its large slopes of increase in total secondary lamellae and gill area with weight (Figs. 2, 3, and Table 1). The gill area: skin area ratio of *P. schlosseri* increases with size from 0.22 until it reaches 0.50 in larger specimens (Fig. 5). This indicates that its gills play a bigger role than its skin in respiration as this mudskipper grows.

Comparison with aquatic fishes, air-breathing fishes and other mudskippers

Schottle [24] and Graham [23] found that air-breathing and amphibious fishes have reduced and length of filaments as well as gill area relative to aquatic fishes. Indeed, these parameters in the mudskippers are smaller than both aquatic and air-breathing fishes (Table 2). The exception is *B. boddaerti*, which has slightly longer filament length and greater gill area than *Channa punctata* (Table 2). These air-breathing fishes spend most of their time in water and occasionally surface to breathe whereas mudskippers come on land often. Thus, the fewer and shorter filaments of mudskippers may be correlated to their greater terrestrial capabilities [23].

When similar weight *Periophthalmus* (8.8 g) were compared, it is notable that *P. chrysopilos* has many smaller gill parameters than *P. cantonensis* [19], resulting in a smaller gill area (Table 3). It is possible that the *B. boddaerti* studied by Niva *et al.* [17] and Hughes and Al-Kadhomy [18] are of a dissimilar species from the local counterpart as they have different observed swimming and feeding behaviors. Most of the gill parameters of the local species are considerably divergent from those of *B. boddaerti* in previous studies (Table 3), pointing also towards this possibility. No detailed data has been collected on the gill morphometry of *Periophthalmodon*.

P. schlosseri at 8.8 g have comparable total

filament length and gill area to *P. chrysospilos* whilst its total filament number approximates that of *P. cantonensis* of similar weight (Table 3). However, *P. schlosseri* has fewer and shorter filaments, and smaller gill area than a similar sized *Boleophthalmus* (Table 3). In addition to its unique gill morphology of branched filaments and intrafilamentary secondary lamellar fusions, *P. schlosseri* has smaller lamellae but higher lamellar frequency than *Periophthalmus* and *Boleophthalmus*.

ACKNOWLEDGMENTS

This study was supported by grants RP 70/85 and RP 860337 from the National University of Singapore.

REFERENCES

- 1 Hughes, G. M., Dube, S. C. and Munshi, J. S. D. (1973) Surface area of the respiratory organs of the climbing perch, *Anabas testudineus* (Pisces: Anabantidae). *J. Zool.*, **170**: 227–243.
- 2 Munshi, J. S. D. (1962) On the accessory respiratory organs of *Heteropneustes fossilis* (Bloch). *Proc. R. Soc. Edinb. (B)*, **68**: 128–146.
- 3 Hakin, A., Munshi, J. S. D. and Hughes, G. M. (1978) Morphometrics of the respiratory organs of the Indian green snake-headed fish, *Channa punctata*. *J. Exp. Zool.*, **184**: 519–543.
- 4 Carter, G. S. (1957) Air-breathing. In "The Physiology of Fishes", Vol. 1. Ed. by Brown, M. E., Academic Press, New York/London, pp. 65–79.
- 5 Hughes, G. M. and Morgan, M. (1973) The structure of fish gills in relation to their respiratory function. *Biol. Rev.*, **48**: 419–475.
- 6 Gordon, M. S., Gabaldon, D. J. and Yip, A. Y. W. (1985) Exploratory observations on microhabitat selection within the intertidal zone by the Chinese mudskipper *Periophthalmus cantonensis*. *Mar. Biol.*, **85**: 209–215.
- 7 Gordon, M. S., Boetius, J., Evans, D. H., McCarthy, R. and Oglesby, L. C. (1969) Aspects of physiology of the terrestrial life in the amphibious fishes. I. The mudskipper *Periophthalmus sobrinus*. *J. Exp. Biol.*, **50**: 141–149.
- 8 Gordon, M. S., Ng, W. W. S. and Yip, A. Y. W. (1978) Aspects of the physiology of terrestrial life in amphibious fishes. III. The Chinese mudskipper *Periophthalmus cantonensis*. *J. Exp. Biol.*, **72**: 57–75.
- 9 Lee, C. G. L., Low, W. P., and Ip, Y. K. (1987) Na^+ , K^+ and volume regulation in the mudskipper, *Periophthalmus chrysospilos*. *Comp. Biochem. Physiol.*, **87A**: 439–448.
- 10 Lee, C. G. L. and Ip, Y. K. (1987) Environmental effect on plasma thyroxine (T_4), 3, 5, 3'-triiodo-L-thyronine (T_3), prolactin and cyclic adenosine 3', 5',-monophosphate (cAMP) content in the mudskippers *Periophthalmus chrysospilos* and *Boleophthalmus boddarti*. *Comp. Biochem. Physiol.*, **87A**: 1009–1014.
- 11 Gregory, R. B. (1977) Synthesis and total excretion of waste nitrogen by fish of the *Periophthalmus* (mudskipper) and *Scartelaos* Families. *Comp. Biochem. Physiol.*, **57A**: 33–36.
- 12 Morii, H., Nishikata, K. and Tamura, O. (1978). Nitrogen excretion of mudskipper fish *Periophthalmus cantonensis* and *Boleophthalmus pectinirostris* in water and on land. *Comp. Biochem. Physiol.*, **60A**: 189–193.
- 13 Morii, H. (1979) Changes with time of ammonia and urea concentrations in the blood and tissue of mudskipper fish, *Periophthalmus cantonensis* and *Boleophthalmus pectinirostris* transferred from land to water. *Comp. Biochem. Physiol.*, **63A**: 23–28.
- 14 Chew, S. F. and Ip, Y. K. (1987) Ammoniogenesis in mudskippers *Boleophthalmus boddarti* and *Periophthalmodon schlosseri*. *Comp. Biochem. Physiol.*, **87B**: 941–948.
- 15 Siau, H. and Ip, Y. K. (1987) Activities of enzymes associated with phosphoenolpyruvate metabolism in the mudskippers, *Boleophthalmus boddarti* and *Periophthalmodon schlosseri*. *Comp. Biochem. Physiol.*, **88B**: 119–125.
- 16 Low, W. P., Lane, D. J. W. and Ip, K. Y. (1988) A comparative study of terrestrial adaptations of the gills in three mudskippers-*Periophthalmus chrysospilos*, *Boleophthalmus boddarti* and *Periophthalmodon schlosseri*. *Biol. Bull. (In press)*.
- 17 Niva, B., Ojha, J. and Munshi, J. S. D. (1981) Morphometrics of the respiratory organs of an estuarine goby, *Boleophthalmus boddarti*. *Jpn. J. Ichthyol.*, **27**: 316–326.
- 18 Hughes, G. M. and Al-Kadhomiy, N. K. (1986) Gill morphometry of mudskipper *Boleophthalmus boddarti*. *J. Mar. Biol. Ass. U. K.*, **66**: 671–682.
- 19 Tamura, O. and Moriyama, T. (1976) On the morphological feature of the gill of amphibious and air-breathing fishes. *Bull. Fac. Fish. Nagasaki Univ.*, **41**: 1–8.
- 20 Khoo, K. G. (1966) Studies on the biology of Periophthalmidae fishes in Singapore. Honours thesis. National University of Singapore. Singapore.
- 21 Hughes, G. M. (1984) Measurement of gill area in fishes: Practices and problems. *J. Mar. Biol. Ass. U. K.*, **64**: 637–655.
- 22 Tamura, S. O., Morii, H. and Yuzuriha, M. (1976) Respiration of the amphibious fishes *Periophthal-*

- mus cantonensis* and *Boleophthalmus chinensis* in water and on land. J. Exp. Biol., **65**: 97–107.
- 23 Graham, J. B. (1976) Respiratory adaptations of marine air-breathing fishes. In "Respiration of Amphibious Vertebrates" Ed. by Hughes, G. M., Academic Press, New York, pp. 165–187.
- 24 Schottle, E. (1932) Morphologie und Physiologie der Atmung bei wassers-, schlamm- und landlebenden Gobiiformes. Z. Wiss. Zool., **140**: 1–114.
- 25 Oikawa, S., and Itazawa, Y. (1985) Gill and body surface areas in the carp in relation to body mass, with special reference to the metabolism-size relationship. J. Exp. Biol., **117**: 1–14.
- 26 Muir, B. S., and Hughes, G. M. (1969) Gill dimensions for three species of tunny. J. Exp. Biol., **51**: 271–285.

Difference in Migratory Ability between Human Lung and Skin Fibroblasts

HIROSHI KONDO, YUMIKO YONEZAWA and TAKASHI A. NOMAGUCHI

*Department of Biology, Tokyo Metropolitan Institute
of Gerontology, Tokyo 173, Japan*

ABSTRACT—TIG-3 human lung fibroblasts were found to differ in their migratory ability from TIG-3S human skin fibroblasts derived from the same fetus: (1) TIG-3 cells migrated in medium supplemented with 10% fetal bovine serum (FBS) more slowly than TIG-3S cells. (2) TIG-3 cells migrated in serum-free medium as effectively as in medium supplemented with 10% FBS, whereas TIG-3S cells migrated in serum-free medium much more slowly than in medium supplemented with 10% FBS. (3) The migration of TIG-3S cells was changed more markedly by the pH of the culture medium than that of TIG-3 cells. The second was the most striking difference in migratory ability between the TIG-3 and TIG-3S cells, and was also the case when several human fetal lung fibroblasts (TIG-1, TIG-7, WI-38, IMR-90, MRC-5), and skin fibroblasts from adult and elderly donors were tested. The monovalent ionophore, monensin, inhibited the migration of TIG-3 and TIG-3S cells in our experimental system according to monensin concentration, and immunofluorescence staining for fibronectin demonstrated that monensin inhibited the secretion of fibronectin. This implies that secreted substances including fibronectin regulate cell migration. However, the migration of TIG-3S cells was not decreased to the same degree as that of TIG-3 cells after monensin treatment. The role of the extracellular matrix in this difference of migratory ability between human lung and skin fibroblasts is discussed.

INTRODUCTION

Since human fibroblasts have an intrinsic limit of cell division potential, they are often used as a model system of cellular aging *in vitro* [1, 2]. Human fibroblasts derived from different tissues seem to possess similar features. However, it has been reported that human fibroblasts show heterogeneity and tissue differences [3–8]. Our previous study on the effects of serum from human subjects of various ages on cell migration demonstrated a difference in migratory ability between human fetal lung fibroblasts (TIG-1) and skin fibroblasts from adult donors: Adult donor skin fibroblasts migrated in serum-free medium much more slowly than in medium supplemented with 10% FBS, whereas TIG-1 cells migrated in serum-free medium as effectively as in medium supplemented with 10% FBS [9]. There has been no previous report of any tissue difference in the

migratory ability of human fibroblasts. The present study was therefore carried out to confirm and generalize the differences in migratory ability between human lung and skin fibroblasts.

MATERIALS AND METHODS

Cells

Several human fetal lung fibroblast lines (TIG-1, TIG-3, TIG-7, WI-38, IMR-90, MRC-5) were used. TIG-1, TIG-3 and TIG-7 cells were established at a project team of the Tokyo Metropolitan Institute of Gerontology [10, 11]. WI-38 and IMR-90 cells were obtained from the Institute for Medical Research (Camden, USA), and MRC-5 cells were obtained from the American Type Culture Collection (Rockville, USA). Several human skin fibroblast lines (TIG-3S, ASF-4, ASF-5, ASF-3, ASF-2) were also used. Human fetal skin fibroblasts (TIG-3S) were established at a project team of the Tokyo Metropolitan Institute of Gerontology, and skin fibroblasts from adult (ASF-

4, ASF-5) and elderly (ASF-2, ASF-3) donors were kindly supplied by Drs. K. Kaji and M. Matsuo [12]. The cells were cultured in Eagle's basal medium (BME) (GIBCO) supplemented with 10% FBS and antibiotics, as described in a previous paper [13].

Mycoplasma contamination in these cell cultures was measured by the method of Kihara *et al.* [14], but none was detected.

Serum

One lot of FBS (Hyclone, #100394) was used throughout all experiments.

Measurement of cell migration

Cell migration was measured by a slight modification of the method of Stenn [15]. Before cell preparation, cover glasses (22×22 mm, No. 1, Matsunami Glass Ind., Ltd, Japan) were cleaned, and coated by dipping them in 1,2-dichloroethane (Dojindo Lab., Japan) solution containing 1% Formvar powder (Polyvinyl Formal, Oken Shoji Co., Japan) and 0.2% Scarlet red (Sudan IV, Chroma-Gesellschaft Schmid GMBH & Co., DDR). The coated cover glasses were placed in 35-mm plastic Petri dishes (Falcon, 3001) and secured to the bottom of the dishes with sterile silicone. Confluent cells, obtained 1 week after subcultivation with a split ratio of 1:4, were harvested from 60-mm plastic culture dishes (Falcon, 3002) by treatment with 0.25% trypsin (Difco, 1:250) in Mg^{2+} -, Ca^{2+} - free phosphate-buffered saline (PBS), pH 7.4. Confluent cells (split ratio 1:1) or 1×10^6 cells per dish were poured into the 35-mm plastic culture dishes containing the previously prepared cover glasses. The cells covered the bottom of the dish as a monolayer. The cell numbers were determined with a Coulter counter (Coulter Electronics, Hialeah, FL). After culture for 1 day at 37°C in a 5% CO₂ incubator, the cultures were washed once with BME. Each cover glass was placed on a sterile glass slide and the cell sheet on the cover glass was marked by cutting off the cell-Formvar coat along the midline of the cover glass with a sterile stainless steel blade (Disposable Dermatome, Feather Ind., Ltd., Japan). Then, the cell-coated cover glass was secured to the bottom of a new 35-mm culture dish containing culture medium with or without 10%

FBS. On the second day after re-culture, the outgrowths were stained by removing the culture medium and flooding the cover glass for 2 min with a staining solution composed of 0.73% toluidine blue and 0.27% basic fuchsin in 30% ethanol. Outgrowths were quantified using a calibrated ocular micrometer by measuring the maximal linear distance of cell movement from the cut edge.

Immunofluorescence staining of fibronectin

In order to detect extracellular fibronectin, immunofluorescence staining of human fibroblasts was performed by the method described previously [16]. Cell sheets on Formvar-coated cover glasses were washed three times with PBS, pH 7.2, and incubated with rabbit antibody to human fibronectin (E-Y Laboratories, Inc., USA) at 1:20 dilution without fixation or drying. Control cultures were incubated with nonimmune rabbit serum or PBS. After incubation for 30 min at room temperature, the cell sheets were washed three times with PBS, and then fluorescein isothiocyanate (FITC)-conjugated goat anti-rabbit IgG (E-Y Laboratories, Inc., USA) as a second antibody at 1:20 dilution was poured over the cell sheets and incubated at room temperature for 30 min. The cell sheets on Formvar-coated cover glasses were washed three times with PBS and then embedded with glycerol solution (glycerol/PBS:9/1).

RESULTS

Migratory ability of human fetal lung and skin fibroblasts derived from the same fetus

The previous study showed that human fetal lung fibroblasts (TIG-1) migrated linearly during 3 days of incubation [9]. Figure 1 also demonstrates that human lung (TIG-3) and skin (TIG-3S) fibroblasts derived from the same fetus migrated linearly for 3 days in culture medium supplemented with 10% FBS. TIG-3 cells migrated in serum-free medium as effectively as in medium supplemented with 10% FBS (Fig. 1A), although the number of migrating cells seemed to be much larger in serum-supplemented medium than in

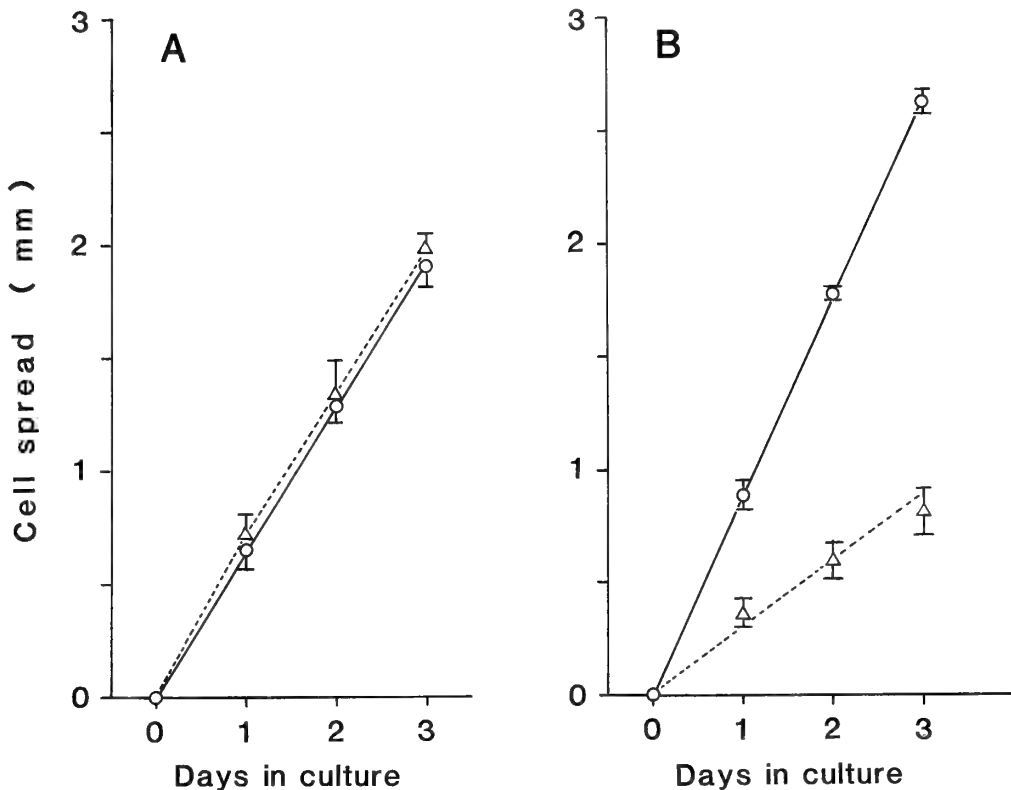


FIG. 1. Time course of migration of human lung (TIG-3) and skin (TIG-3S) fibroblasts derived from the same fetus. TIG-3 (A) and TIG-3S (B) cells were cultured in BME supplemented with 10% FBS in a humidified CO₂ incubator (5% CO₂) at 37°C and cell migration experiments were carried out as described in Materials & Methods. TIG-3 cells at PD29 and TIG-3S cells at PD25 were treated with 0.25% trypsin and suspended in culture medium. Two ml (1×10^6 cells) of each cell suspension was inoculated into a 35-mm plastic culture dish containing a Formvar-coated cover glass. After culture for 1 day, each culture was washed once with BME. The cell sheets on cover glasses were cut off, and the cell-coated cover glasses were re-cultured in BME with or without 10% FBS and stained at regular time intervals. Values represent the means of at least triplicate determinations. Vertical bars show standard deviations of means. ○—○, medium supplemented with 10% FBS; △-----△, serum-free medium.

serum-free medium (Fig. 2). On the other hand, the migration rate of TIG-3S cells decreased remarkably when serum was removed from the culture medium (Figs. 1B, 2). TIG-3 cells migrated more rapidly than TIG-3S cells.

A study was carried out to determine whether the difference in the migratory ability between TIG-3 and TIG-3S cells was observed in culture media containing various concentrations of FBS (Fig. 3). TIG-3S cells migrated in media containing 2.5–50% FBS much more rapidly than TIG-3 cells, although the opposite result was obtained in serum-free medium. The migratory ability of

TIG-3 and TIG-3S cells gradually decreased according to increased serum concentration, and the slope of the decline in migration rate was more rapid for TIG-3S cells than for TIG-3 cells. Next, the effects of culture medium pH on the migration of TIG-3 and TIG-3S cells were measured (Fig. 4). When culture medium containing 10% FBS was used, the migration rate of TIG-3 and TIG-3S cells was lower at pH 6.8 than at pH 7.4–8.2. The migration rates of TIG-3 cells were the same within a pH range of 6.8–8.2, even when serum was removed from the culture medium. On the other hand, the migration rate of TIG-3S cells at

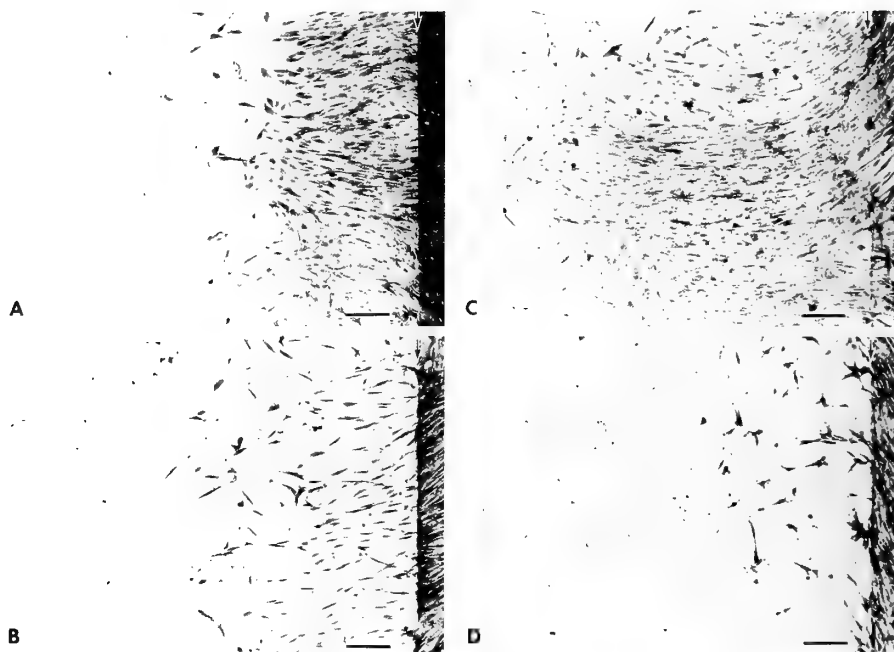


FIG. 2. Photomicrographs of migrating TIG-3 (A, B) and TIG-3S (C, D) cells.

Cell migration experiments were carried out using TIG-3 cells at PD29 and TIG-3S cells at PD25, as described for Fig. 1. Cells were stained after 2 days of re-culture and photographs of the cells were taken. Arrow designates cut edge from which cells began to migrate. Bar shows 200 μ m. A, C: medium supplemented with 10% FBS; B, D: serum-free medium.

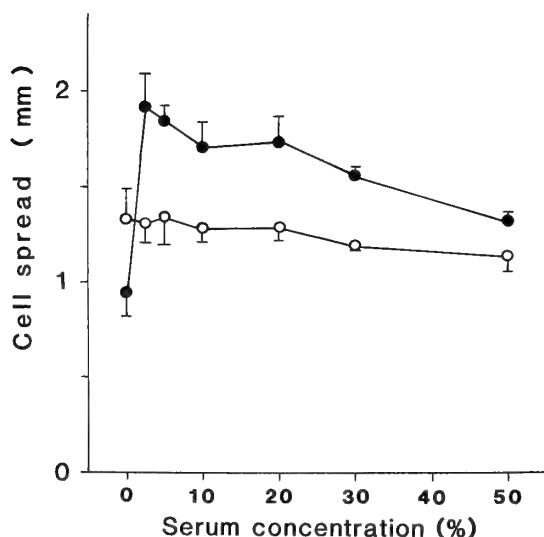


FIG. 3. Effects of serum concentration on migration of human lung (TIG-3) and skin (TIG-3S) fibroblasts derived from the same fetus.

The migration of TIG-3 cells at PD29 and TIG-3S cells at PD25 was determined as described for Fig. 1. Two ml of each cell suspension (1×10^6 cells) was inoculated. After 1 day of culture, the cell sheets on cover glasses were washed with BME and cut off, and cell-coated cover glasses were re-cultured in BME containing various concentrations of FBS and stained on the second day. Values represent the means of at least triplicate determinations. Vertical bars show standard deviations of means. \circ — \circ , TIG-3 cells; \bullet — \bullet , TIG-3S cells.

pH 6.8 was much lower in serum-free medium than in medium supplemented with 10% FBS. However, TIG-3S cells migrated rapidly at pH 7.8 and 8.2, although the migration of TIG-3S cells was lower in serum-free medium than in medium

supplemented with 10% FBS.

Comparison of migratory ability of several fibroblast cell lines cultured from lung and skin

When FBS was removed from the culture

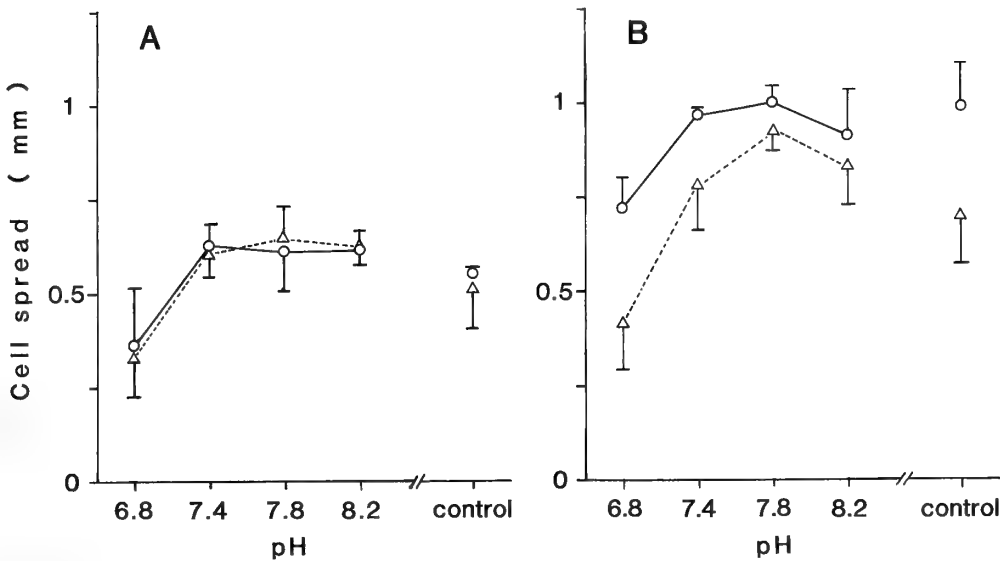


FIG. 4. Effects of pH of culture medium on migration of human lung (TIG-3) and skin (TIG-3S) fibroblasts derived from the same fetus.

The migration of TIG-3 cells (A) at PD29 and TIG-3S cells (B) at PD25 was determined as described for Fig. 3. Two ml of each cell suspension (1×10^6 cells) was incubated in a 5% CO_2 atmosphere. After 1 day of culture, the cell sheets on cover glasses were washed and cut off, and cell-coated cover glasses were re-cultured in medium containing 30 mM Hepes buffer adjusted to each pH (6.8, 7.4, 7.8 and 8.2) in a CO_2 incubator (0% CO_2), and stained on the first day. For the control experiment, cell sheets on cover glasses were washed and cut off, and cell-coated cover glasses were re-cultured in medium without Hepes buffer in a CO_2 incubator (5% CO_2). Values represent the means of at least triplicate determinations. Vertical bars show standard deviations of means. \circ — \circ , medium supplemented with 10% FBS; \triangle — \triangle , serum-free medium.

TABLE 1.. Migration of human lung and skin fibroblast lines in media with or without FBS

Cells (Donor age, Sex)	PD used/ Total PD	(No.)	Cell spread (μm)		10% FBS/ No serum
			No serum	10% FBS	
Lung					
TIG-1 (Fetus, F)	(26/67)	(7)	1126 \pm 99	1223 \pm 84	(+ 9%)
TIG-3 (Fetus, M)	(25/75)	(1)	1026 \pm 198	1212 \pm 84	(+ 18%)
TIG-7 (Fetus, M)	(23/63)	(1)	912 \pm 90	939 \pm 85	(+ 3%)
WI-38 (Fetus, F)	(39–41/52)	(2)	902 \pm 7	1159 \pm 1	(+ 28%)
IMR-90(Fetus, F)	(24/62)	(1)	758 \pm 85	1052 \pm 81	(+ 39%)
MRC-5(Fetus, M)	(42–44/55)	(2)	928 \pm 53	1047 \pm 61	(+ 13%)
Skin					
TIG-3S(Fetus, M)	(25–29/69)	(2)	677 \pm 162	1723 \pm 60	(+155%)
ASF-5 (21Y, M)	(26/66)	(1)	519 \pm 11	1420 \pm 64	(+174%)
ASF-4 (36Y, M)	(32–34/74)	(2)	450 \pm 7	1330 \pm 33	(+196%)
ASF-2 (65Y, F)	(25/56)	(1)	587 \pm 74	1642 \pm 140	(+180%)
ASF-3 (77Y, M)	(24–26/43)	(2)	407 \pm 37	1050 \pm 75	(+158%)

Migration experiments were carried out as described for Fig. 1. The numbers of cells inoculated onto each 35-mm culture dish were 1×10^6 cells for TIG-1 cells and confluent cells (split ratio 1 : 1) for other cell lines. After 1 day of culture, the cell sheets on cover glasses were washed and cut off. The cell-coated cover glasses were re-cultured in BME with or without 10% FBS, and stained on the second day. Values represent the means (\pm S.D.) of at least triplicate determinations.

medium, the migration rate of TIG-3S cells decreased whereas that of TIG-3 cells did not change (Figs. 1, 2). A study was carried out to clarify whether the same result was obtained when many other fibroblast lines derived from lung and skin were tested. Table 1 shows that the migratory abilities of five human fetal lung fibroblast lines were the same as that of TIG-3 cells, whereas the migratory abilities of four human skin fibroblast lines derived from adult and elderly donors were the same as that of TIG-3S cells. These results imply that human lung fibroblasts differ from human skin fibroblasts in migratory ability.

Effects of monensin on migration of human fetal lung and skin fibroblasts

In order to clarify whether substances in the extracellular matrix contribute to the difference in migratory ability between human lung and skin fibroblasts, the effects of monensin on cell migration were measured (Fig. 5). Migration of both

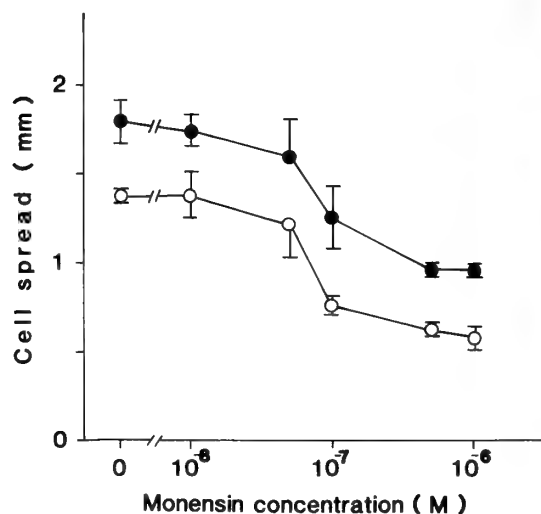


FIG. 5. Effects of monensin on migration of human fetal lung (TIG-3) and skin (TIG-3S) fibroblasts.

The migration of TIG-3 cells (A) at PD35 and TIG-3S cells (B) at PD25 was determined as described for Fig. 3. Two ml of cell suspension (1×10^6 cells) was inoculated. After 1 day of culture, the cell sheets on cover glasses were washed and cut off, and cell-coated cover glasses were re-cultured in BME containing 10% FBS and various concentrations of monensin, and stained on the second day. Values represent the means of duplicate determinations. Vertical bars show standard deviations of means. ○—○, TIG-3 cells; ●—●, TIG-3S cells.

cell types was inhibited according to increased monensin concentration (5×10^{-8} – 1×10^{-6} M). However, the migration rate of TIG-3S cells did not become the same as that of TIG-3 cells even when monensin at 1×10^{-6} M was used. Since it has been reported that monensin inhibits the secretion of substances constituting the extracellular matrix, such as procollagen and fibronectin [17, 18], an attempt was made to detect the secretion of fibronectin after monensin treatment, using im-

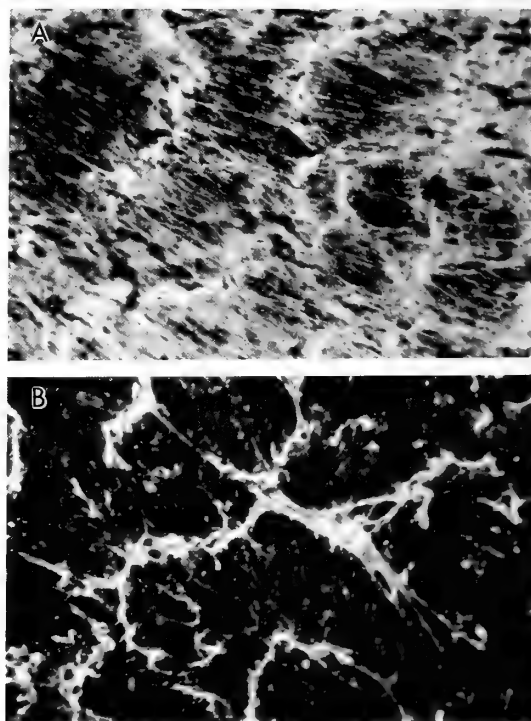


FIG. 6. Immunofluorescence staining of the monolayers of TIG-3 human fetal lung fibroblasts with antibodies to human fibronectin.

Cell migration experiments were carried out using TIG-3 cells at PD37, as described for Fig. 5. Two ml of cell suspension (1×10^6 cells) was inoculated. After 1 day of culture, the cell sheets on cover glasses were washed and cut off, and the cell-coated cover glasses were re-cultured in culture medium with (B) or without (A) 5×10^{-7} M monensin. On the second day, the cell sheets on cover glasses were incubated with antibodies to human fibronectin, and extracellular fibronectin was stained, as described in Materials and Methods. Monolayer cells were microscopically photographed. Control cultures which were incubated with nonimmune rabbit serum or PBS were not stained (data not shown). $\times 50$.

munofluorescence staining of fibronectin. The result showed that monensin strongly inhibited the secretion of fibronectin from TIG-3 cells (Fig. 6). The same result was also obtained when TIG-3S cells were tested (data not shown).

DISCUSSION

When measuring the migration of human lung and skin fibroblasts, we observed a difference in migratory ability between the two fibroblast lines employed (Table 1). It has been reported that human lung fibroblasts differ from human skin fibroblasts in cell morphology, growth rate and cell density at confluence [6], the capacity to change cortisone into hydrocortisone [7], and the K_d value for the binding reaction of dexamethasone to cells [8]. However, a difference in migratory ability between these two fibroblast lines has not been reported. Therefore the findings of our present study seem to be the first evidence of a tissue difference in the migration of human fibroblasts.

The migration rate of human skin fibroblasts (TIG-3S) changed greatly upon removal of FBS from the culture medium, range of pH of serum-free medium and change in the serum concentration of culture medium, unlike the case of human lung fibroblasts (TIG-3) derived from the same fetus (Figs. 1, 3, 4). This result was also obtained when skin fibroblasts from adult and elderly donors were used. This implies that human skin fibroblasts seem to be sensitive to stimuli or environmental change. For skin fibroblasts to perform their role in wound healing, a high sensitivity to many forms of stimulus may be an essential feature. However, the mechanism by which human skin fibroblasts migrate more rapidly than human lung fibroblasts is unclear.

Using relatively early passaged cells, we demonstrated that human lung fibroblasts (TIG-3) differ from human skin fibroblasts (TIG-3S) with regard to migration rate and pH and serum dependency. A study was therefore carried out to clarify whether this phenomenon changed during the *in vitro* aging of human fibroblasts. The same result was obtained, although the migratory ability of cells decreased with successive passages (unpublished data). These results show that TIG-3 cells

differ from TIG-3S cells in migratory rate at all stages of passage in addition to showing serum dependency (and perhaps pH dependency).

The number of migrating TIG-3 cells seemed to be much greater in serum-supplemented medium than serum-free medium (Fig. 2A, B). This may have been due partly to cell proliferation because dividing cells were often observed in serum-supplemented medium. However, the migration rate of TIG-3 cells did not change when serum was removed from the culture medium (Fig. 1). These results are consistent with our previous study, i.e., a loss of cell division potential, which was induced by exposure to ⁶⁰Co-γ-rays, did not change the migration rate of TIG-1 cells [9].

It has been reported that monensin inhibits the secretion of procollagen and fibronectin from cultured human fibroblasts but does not inhibit protein synthesis [17, 18]. Also, since monensin inhibits the spreading of human fibroblasts [19–21], we determined the effects of monensin on cell migration using our present experimental system. Monensin inhibited the migration of TIG-3 and TIG-3S cells according to its concentration (Fig. 5). Immunofluorescence staining for extracellular fibronectin revealed that monensin strongly inhibited the secretion of fibronectin from TIG-3 (Fig. 6) and TIG-3S cells (data not shown). This implies that monensin inhibits the secretion of secretory proteins including fibronectin. The finding that a relatively low concentration of monensin produced an effect is compatible with the action of monensin on cell attachment and spreading [17, 18]. The monensin concentration effective for inhibition of cell migration was the same in both TIG-3 and TIG-3S cells. However, the migration of TIG-3S did not decrease to the same extent as that of TIG-3 cells even when 1×10^{-6} M monensin was used. In other words, the difference in migratory ability between TIG-3 and TIG-3S cells could not be explained by the quantitative and qualitative differences in extracellular matrix secreted from the two cell types. Rather, it may reflect differences in the cell-specific events necessary for cell migration.

ACKNOWLEDGMENTS

We wish to thank Dr. M. Osanai for helpful discussion during the course of this work. We also thank Drs. H. Okumura and K. Kihara, National Institute of Health, Tokyo, for the mycoplasma testing of cultures.

REFERENCES

- 1 Hayflick, L. and Moorhead, P. S. (1961) The serial cultivation of human diploid cell strains. *Exp. Cell Res.*, **25**: 585-621.
- 2 Hayflick, L. (1965) The limited *in vitro* lifetime of human diploid cell strains. *Exp. Cell Res.*, **37**: 614-636.
- 3 Pinsky, L., Finkelberg, R., Straisfeld, C., Zilahi, B., Kaufman, M. and Hall, G. (1972) Testosterone metabolism by serially subcultured fibroblasts from genital and nongenital skin of individual human donors. *Biochem. Biophys. Res. Commun.*, **46**: 364-369.
- 4 Griffin, J. E., Punyashtiti, K. and Wilson, J. D. (1976) Dihydrotestosterone binding by cultured human fibroblasts. *J. Clin. Invest.*, **57**: 1342-1351.
- 5 Kaufman, M., Pinsky, L., Straisfeld, C., Shanfield, B. and Zilahi, B. (1975) Qualitative differences in testosterone metabolism as an indication of cellular heterogeneity in fibroblast monolayers derived from human preputial skin. *Exp. Cell Res.*, **96**: 31-36.
- 6 Schneider, E. L., Mitsui, Y., Au, K. S. and Shorr, S. S. (1977) Tissue specific differences in cultured human diploid fibroblasts. *Exp. Cell Res.*, **108**: 1-6.
- 7 Aronson, J. F., McClaskey, J. W. and Cristofalo, V. J. (1983) Human fetal lung fibroblasts: Observation on origin and stability in culture. *Mech. Ageing Dev.*, **21**: 229-244.
- 8 Kondo, H., Kasuga, H. and Noumura, T. (1985) The heterogeneity of human fibroblasts as determined from the effects of hydrocortisone on cell growth and specific dexamethasone binding. *Exp. Cell Res.*, **158**: 342-348.
- 9 Kondo, H., Nomaguchi, T. A. and Yonezawa, Y. (1989) Effects of serum from human subjects of different ages on migration *in vitro* of human fibroblasts. *Mech. Ageing Dev.*, **47**: 25-37.
- 10 Ohashi, M., Aizawa, S., Ooka, H., Ohsawa, T., Kaji, K., Kondo, H., Kobayashi, T., Noumura, T., Matsuo, M., Mitsui, Y., Murota, S., Yamamoto, K., Ito, H., Shimada, H. and Utakoji, T. (1980) A new human diploid cell strain, TIG-1, for the research on cellular aging. *Exp. Gerontol.*, **15**: 539-549.
- 11 Matsuo, M., Kaji, K., Utakoji, T. and Hosoda, K. (1982) Ploidy of human embryonic fibroblasts during *in vitro* aging. *J. Gerontol.*, **37**: 33-37.
- 12 Kondo, H., Nomaguchi, T. A., Sakurai, Y., Yonezawa, Y., Kaji, K., Matsuo, M. and Okabe, H. (1988) Effects of serum from human subjects of various ages on proliferation of human lung and skin fibroblasts. *Exp. Cell Res.*, **178**: 287-295.
- 13 Kondo, H., Kasuga, H. and Noumura, T. (1983) Effects of various steroids on *in vitro* lifespan and cell growth of human fetal lung fibroblasts (WI-38). *Mech. Ageing Dev.*, **21**: 335-344.
- 14 Kihara, K., Ishida, S. and Okumura, H. (1981) Detection of mycoplasmal contaminants in sera. *J. Biol. Stand.*, **9**: 243-251.
- 15 Stenn, K. S. (1980) Quantitative assay of dissociated tissue cell motility *in vitro*. *In Vitro*, **16**: 357-360.
- 16 Kuhl, U., Timpl, R. and von der Mark, K. (1982) Synthesis of type IV collagen and fibronectin from cultured human fibroblasts. *Dev. Biol.*, **93**: 344-354.
- 17 Uchida, N., Smilowitz, H. and Tanzer, M. L. (1979) Monovalent ionophores inhibit secretion of procollagen from cultured human fibroblasts. *Proc. Natl. Acad. Sci. USA*, **76**: 1868-1872.
- 18 Uchida, N., Smilowitz, H., Ledger, P. W. and Tanzer, M. L. (1980) Kinetic studies of the intracellular transport of procollagen and fibronectin in human fibroblasts. *J. Biol. Chem.*, **255**: 8638-8644.
- 19 Virtanen, I., Vartio, T., Badley, R. A. and Lehto, V.-P. (1982) Fibronectin in adhesion, spreading and cytoskeletal organization of cultured fibroblasts. *Nature*, **298**: 660-663.
- 20 Pizzey, J. A., Bennet, F. A. and Jones, G. E. (1983) Monensin inhibits initial spreading of cultured human fibroblasts. *Nature*, **305**: 315-317.
- 21 Pizzey, J., Witkowski, J. and Jones, G. (1984) Monensin-induced inhibition of cell spreading in normal and dystrophic human fibroblasts. *Proc. Natl. Acad. Sci., USA*, **81**: 4960-4964.

A Monoclonal Antibody against a Synthetic Carboxyl-Terminal Fragment of the Eclosion Hormone of the Silkworm, *Bombyx mori*: Characterization and Application to Immunohistochemistry and Affinity Chromatography

TAKAHARU KONO, AKIRA MIZOGUCHI¹, Hiromichi Nagasawa, Hironori Ishizaki¹, HAJIME FUGO² and Akinori Suzuki

Department of Agricultural Chemistry, Faculty of Agriculture, The University of Tokyo, Tokyo 113, ¹Biological Institute, Faculty of Science, Nagoya University, Nagoya 464, ²Faculty of Agriculture, Tokyo University of Agriculture and Technology, Tokyo 183, Japan

ABSTRACT—Monoclonal antibodies were produced using as antigen a synthetic fragment corresponding to the C-terminal portion of the eclosion hormone (EH) of the silkworm, *Bombyx mori*. The characterization of these antibodies using ELISA revealed that one of them recognized specifically both the synthetic fragment and native eclosion hormone. Immunohistochemistry using this antibody indicated that EH was produced in two pairs of median neurosecretory cells of the brain. Affinity chromatography of a partially purified EH using a column on which this antibody had been immobilized showed that EH activity was completely adsorbed to this column and eluted with the synthetic fragment with about 60% recovery.

INTRODUCTION

The adult eclosion in the silkworm, *Bombyx mori*, occurs during a specific period of the day [1] as in other lepidopteran insects. The timing of pupal-adult eclosion is controlled by the neurosecretory hormone designated eclosion hormone (EH) [2] which triggers a series of eclosion behaviors. EH acts not only at the adult ecdysis but also at the larval and pupal ecdyses [3]. In *B. mori*, EH might also be involved in the egg hatching behavior [4]. Recently, using the tobacco hornworm, *Manduca sexta*, Copenhaver and Truman have succeeded in identifying a cluster of ipsilaterally projecting cells (group Ia) that contain EH by a sensitive behavioral bioassay and, more specifically, five cells in this group in each brain hemisphere by immunological techniques using an anti-EH antiserum [5].

We have recently determined the amino acid sequence (61 residues) of the *Bombyx* EH [6]. At almost the same time, Marti *et al.* [7] and Kataoka *et al.* [8] determined the whole amino acid sequence (62 residues) of the *Manduca* EH independently, showing 80% sequence homology with the *Bombyx* EH.

The clarification of the amino acid sequence permitted us to attempt to make monoclonal antibodies against a synthetic peptide fragment. In this paper we describe the characterization of a highly specific monoclonal antibody raised against a synthetic peptide corresponding to the C-terminal portion of EH and its application to immunohistochemical study and affinity chromatography.

MATERIALS AND METHODS

Peptide synthesis

A C-terminal synthetic peptide corresponding to

EH (49-61), H-Cys-Glu-Ser-Phe-Ala-Ser-Ile-Ser-Pro-Phe-Leu-Asn-Lys-OH, was synthesized as follows. The protecting groups for the functional side chains of the amino acids were cyclohexyl ester for glutamic acid, benzyl ether for serine, and 2-chlorobenzoyloxycarbonyl (2ClZ) for lysine. Starting with Boc-Lys(2ClZ)-OCH₂-Pam resin, the stepwise solid-phase synthesis was performed on an Applied Biosystems model 430 A peptide synthesizer using dicyclohexyl carbodiimide/1-hydroxybenzotriazole as a coupling reagent. After removal of the protecting groups and resin in HF, the residue was washed several times with diethylether and chloroform by turns. Then the deblocked peptides were extracted with 2 M acetic acid, lyophilized, and finally purified by preparative reverse phase HPLC. Amino acid sequence of the synthetic peptide was checked by an Applied Biosystems model 470 A protein sequencer.

Preparation of antigen

Four mg (0.06 μ mol) of bovine serum albumin (BSA) was mixed with 0.3 mg (1 μ mol) of N-hydroxysuccinimidyl 3-(2-pyridyldithio) propionate (SPDP, Pharmacia Fine Chemicals) in 0.1 M phosphate-buffered saline (pH 7.5) at 23°C for 30 min, allowing the amino groups of BSA to react with N-hydroxysuccinimide ester moiety of SPDP. After removal of reagents by gel filtration on Sephadex G-25, synthetic EH (49-61) (1.3 mg, 1 μ mol) was added to the resulting BSA-SPDP conjugate fraction at 25°C for 20 min. The free sulfhydryl group of cysteine of the synthetic peptide was treated with the 2-pyridyldisulfide moiety of SPDP [9]. After removal of the reagents with Sephadex G-25, about 5.3 mg of EH(49-61)-BSA conjugate were obtained. N-Terminal sequence analysis after purification by HPLC indicated that more than 5 mol of EH(49-61) were coupled with 1 mol of BSA.

Production of monoclonal antibodies

Three female BALB/c mice were immunized four times at a 2-week interval by the intraperitoneal injection of EH(49-61)-BSA (20 μ g/mouse) in Freund's complete adjuvant. Three days after each injection, the mice were bled from the tail vein and the blood was centrifuged to remove

cells. The antibody detection in each mouse serum was carried out by the dot-immunobinding assay, essentially according to Hawkes *et al.* [10]. After four times of antigen injection, the antibody activity of one mouse detected by the dot immunobinding assay using the synthetic EH(49-61) fragment was positive at 5,000 fold dilution of the antiserum, and this mouse was used to produce monoclonal antibodies.

The splenocytes collected (8×10^7 cells) were fused with mouse myeloma NS-1 cells using polyethyleneglycol. Hybridoma cells obtained were seeded into 96-well microplates (Falcon, 3072) and cultured in the presence of 1×10^4 peritoneal macrophages per well as a feeder layer. The supernatant of each well was primarily screened by dot-immunobinding assay using EH(49-61)-BSA conjugate or EH(49-61) fragment as an antigen. Positive colonies on this assay were again cultured in 24-well plates, and further screened in the same manner, and positive hybridomas were cloned by limit dilution.

The cloned hybridomas secreting anti-EH(49-61) antibody were intraperitoneally injected into a mouse previously injected with 0.5 ml of pristane, and after two weeks, about 5 ml of an ascites fluid was collected. The monoclonal antibody was partially purified from this ascites by ammonium sulfate precipitation at 20-33% saturation, Sephadex G-25 gel filtration, and DEAE-Sephadex CL-6B ion exchange chromatography.

Competitive enzyme-linked immunosorbent assay (competitive ELISA)

Wells of a 96-well ELISA plate (Sumitomo bakelite, MS-3596F) were coated with 50 μ l of 5×10^{-10} M EH(49-61)-BSA conjugate in 0.1 M sodium carbonate buffer (pH 9.6) for 2 hr at 25°C. After washing with 50 mM Tris-buffered saline (pH 7.4) (TBS) and blocking with 3% gelatin (Bio Rad), 50 μ l of the monoclonal antibody solution corresponding to 1:200,000 dilution of the ascites and 50 μ l of serially diluted test materials were added into each well, and the plate was incubated overnight at 4°C.

The plate was washed with TBS containing 0.05% Tween-20 (TTBS), and reincubated with 50 μ l of 1:1,000 diluted horseradish peroxidase

(HRP)-linked anti-mouse immunoglobulin goat serum (AMS, Kirkegaard & Perry Laboratories Inc.) at 25°C for 2 hr. Wells were developed with *o*-phenylenediamine as a substrate for HRP. The enzyme reaction was stopped by addition of 50 μ l of 2 M H₂SO₄, and the absorbance at 492 nm was measured.

Affinity chromatography

Partially purified monoclonal antibody obtained from ascites was linked to CNBr-activated Sepharose 4B (Pharmacia Fine Chemicals) by the standard method. About 5 mg of the partially purified antibody was immobilized to the gel (1 g dry weight) and 3.5 ml of affinity gel was obtained. EH was partially purified from 80,000 heads of *B. mori* through the 11 step purification procedure according to the methods as described previously [11]. This partially purified EH in 100 ml of 0.1 M ammonium acetate (pH 8.5) was applied to the affinity column. The column was sufficiently washed with 0.2 M ammonium acetate (pH 8.5) until the absorbance at 280 nm became below 0.005. Adsorbed materials were eluted successively with 0.2 M ammonium acetate containing 100 μ M of S-carboxamidomethyl EH(49-61) fragment, 0.25 M sodium carbonate containing 0.5 M NaCl (pH 8.5), and 0.2 M Gly-HCl (pH 2.5).

The active fraction after the affinity chromatography was acidified to pH 2, and directly subjected to a reverse phase HPLC using VP-318 (Senshu Kagaku). Chromatography was performed by applying a linear gradient of acetonitrile (0.5%/min) in the presence of 0.1% trifluoroacetic acid.

Immunohistochemistry

The *Bombyx* brains from freshly ecdysed pupae, 3-, 5-, and 7-day developing adults were dissected out and fixed in Bouin's solution for 4 hr. The specimens were dehydrated with graded ethanol and embedded in paraffin. Serial sections (7 μ m thick) were cut on a rotary microtome and affixed on slide glasses. The sections were deparaffinized by xylene, washed with absolute ethanol, soaked in methanol containing 0.03% H₂O₂ for 30 min to inhibit the endogenous peroxidase activity in the tissue, and washed with TBS. The anti-EH(49-61)

IgG of 1:500 diluted solution was applied to the rehydrated tissue section after blocking with 3% gelatin, and incubated overnight at 4°C. Subsequently, the extra antibody solution was removed by washing with TTBS. The tissue sections were incubated with the 500-fold diluted solution of HRP-linked AMS for 2 hr, and rinsed again with 50 mM Tris-buffered saline (pH 7.4) (TBS). Then the sections were mounted with 2.2 mM of 4-chloro-1-naphthol in TBS containing 0.03% H₂O₂.

Whole mount staining was performed using *Bombyx* pharate adult brains. The procedure followed essentially the protocol of Bollenbacher *et al.* (personal communication). The brain was fixed with Bouin's solution for 4 hr. After washing with TTBS, the fixed brain was desheathed and exposed to the 500-fold diluted antibody solution containing 2% Triton X-100 overnight at 4°C. After washing with TTBS, the tissue was incubated with 500-fold diluted solution of HRP-linked AMS for 2 hr at room temperature. The tissue was washed with TBS, and incubated with 1.3 mM of diaminobenzidine in TBS containing 0.02% H₂O₂ for 10 min. Then the reaction was terminated by removing the enzyme substrate solution and washed successively with TBS, water, 70% ethanol, 95% ethanol, and 100% ethanol. Finally, the tissue was cleared by methylsalicylate overnight and mounted on a slide.

RESULTS

Generation of the monoclonal antibody recognizing EH

During the first screening of the hybridoma colonies using EH(49-61)-BSA conjugate as an antigen, 10 colonies gave positive immunoreaction. On the second screening using EH(49-61) synthetic fragment, however, only one hybridoma colony among them appeared to produce antibody that recognized this fragment. This hybridoma was cloned and the antibody was produced by the intraperitoneal injection of the hybridoma cells into a mouse. The monoclonal antibody obtained from the ascites fluid was purified partially and characterized.

The class of the immunoglobulin produced by

this clone was identified as IgG by its reactivity to the class-specific goat anti-mouse immunoglobulin sera. The characterization of the immunobinding specificity of this antibody was further accomplished by the competitive ELISA using BSA-EH(49-61) conjugate as a coated antigen on a

solid phase. The binding of the antibody to the solid phase was inhibited in a dose-dependent manner when BSA-EH(49-61), EH(49-61) fragment, and "highly purified EH" [11] were used as a competitive antigen added to the liquid phase (Fig. 1), but this antibody did not recognize BSA.

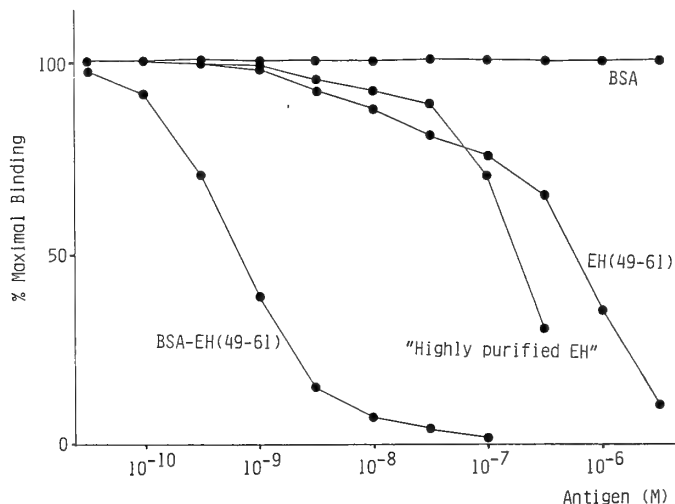


FIG. 1. Binding activity of an EH(49-61) monoclonal antibody as assessed by competitive ELISA to EH(49-61)-BSA. ELISA plate was precoated with $50 \mu\text{l}$ of 5×10^{-10} M of EH(49-61)-BSA as a competitive antigen and competitive ELISA was performed on this plate with the presence of the monoclonal antibody corresponding to 1 : 200,000 dilution of ascites in liquid phase.

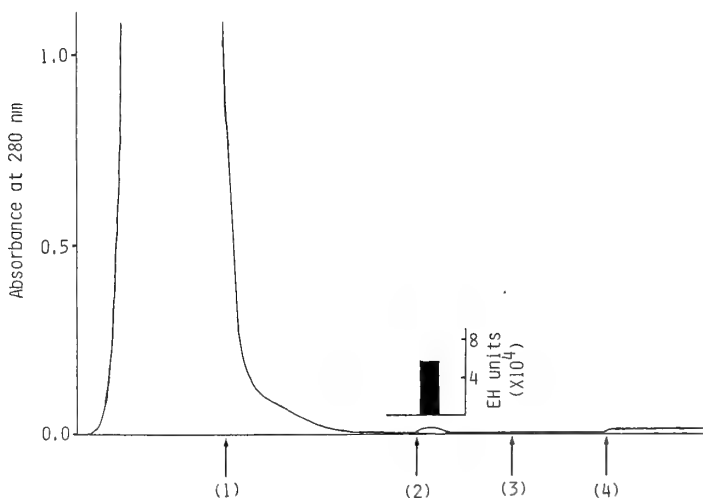


FIG. 2. Affinity chromatography using an EH(49-61) monoclonal antibody-Sepharose 4B column. As a sample solution, 80,000 head equivalents of the partially purified EH preparation was used. After application of the sample, the column was washed with (1) 0.2 M $\text{CH}_3\text{COONH}_4$ (pH 8.5), (2) 100 μM S-carboxamidomethyl EH(49-61)/0.2 M $\text{CH}_3\text{COONH}_4$ (pH 8.5), (3) 0.5 M $\text{NaCl}/0.25$ M Na_2CO_3 (pH 8.5) and (4) 0.2 M Gly-HCl (pH 2.5) in order. Flow rate was 3 ml/hr and EH activity detected is shown as a solid bar.

Therefore, this antibody not only bound to EH(49–61) portion at a concentration of 10^{-7} M, but also cross-reacted with partially purified native EH. The content of EH in this “highly purified EH” sample was estimated to be about 0.1%.

Affinity chromatography

Partially purified EH was obtained by the usual 11-step purification procedure [11], and this material was applied to the affinity column. Biological activity was completely adsorbed to this column and eluted with 100 μ M of synthetic S-carboxamidomethyl EH(49–61) fragment in 0.2 M ammonium acetate buffer (pH 8.5) with about 60% recovery. The column was eluted successively with 0.5 M NaCl containing 0.25 M Na_2CO_3 (pH 8.5) and 0.2 M Gly-HCl (pH 2.5), but EH activity was not detected in either of these two fractions (Fig. 2).

The active fraction was acidified and directly subjected to reverse phase HPLC. Activity was detected in a single peak with a shoulder shown in the painted peak in Figure 3, and Table 1 shows the summary of the purification efficiency. Sequence analysis of the peptide in the main part of the peak for N-terminal portion (up to the 5th residue) assessed the substance in this fraction to be EH.

Immunohistochemical localization of EH in the *Bombyx* brain

Immunohistochemical staining was performed on various stages of *Bombyx* pupal brains. In the usual immunohistochemical procedures using serial sections with 7 μ m thick, two pairs of median neurosecretory cells were found to be im-

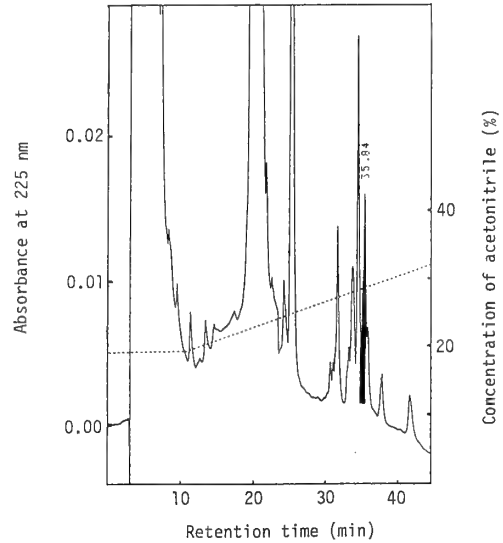


FIG. 3. Reverse phase HPLC of the affinity-purified EH. The result from 10,000 head equivalents of active fraction is shown. The dotted line shows the concentration of acetonitrile in 0.1% trifluoroacetic acid. The shaded peak at 35.84 min indicate fraction containing EH activity and the peak at 22 min is S-carboxamidomethyl EH(49–61).

munoreactive to the antibody in all stages (Fig. 4A). These cells were about 10 μ m in diameter, and their cytoplasm was densely filled with immunoreactive material.

To assess the topographical distribution of these cells further, whole mount staining was carried out on the brains from the pharate adult 2 days before ecdysis. As shown in Figure 4B, two pairs of median neurosecretory cells were stained, and some immunoreactive nerve fibers were derived from these cells. From various angles of observa-

TABLE 1. Summary of the purification of EH from 80,000 head equivalents of EH sample

Purification step	Weight (μ g)	Total activity (EH units)	Specific activity (ng/EH unit)
8th Ppt. with 80% acetone ("Crude EH")	4,400,000	110,000	40,000
9th Sephadex G-50 (fine)	1,960,000	100,000	19,600
11th SP-Sephadex C-25	332,000	90,000	3,700
12th EH(49–61) antibody-Sepharose 4B*	460	55,000	8.4
13th VP-318 (TFA)	4	20,000	0.2

* Activity was eluted with 100 μ M S-carboxamidomethyl EH(49–61) synthetic fragment/0.2 M $\text{CH}_3\text{COONH}_4$ (pH 8.5).

tion, these four cells were supposed to localize in the anterior portion of the brain as illustrated in Figure 4C and 4D.

DISCUSSION

In our previous study to isolate EH, we obtained

only about 30 μg of EH from the extract of 770,000 *Bombyx* pharate adult heads. Because of the limited availability of pure EH, it seemed to be quite difficult to use natural EH for raising anti-EH antibody. Therefore, we took the strategy to make a fragment peptide of EH and to immunize mice with this synthetic peptide after conjugation with BSA. EH has six cysteine residues and these residues were supposed to make three intramolecular disulfide bonds in the molecule to form a globular tertiary structure. Therefore, we decided to make synthetic fragments corresponding to the N-terminal 14 residues and the C-terminal 13 residues, respectively, because these parts would be localized at the surface of the molecule and, therefore, have a rather flexible structure. The study to make monoclonal antibodies against the N-terminal fragment is now in progress.

The attempt to raise the monoclonal antibody against the C-terminal synthetic fragment succeeded in getting one hybridoma clone which secreted an antibody capable of recognizing the native EH as well as EH(49-61) fragment. According to the results from the competitive ELISA, the antibody recognized a partially purified native EH designated "highly purified EH" in a dose-dependent manner. The results showed that our antibody detected the EH molecule in "highly purified EH" at concentrations higher than 10^{-8} M. This assay needs only 50 μl of the sample solution, and so, the amount of EH in 10^{-8} M of the sample solution is about 3 ng. That is to say, this assay system can detect a several hundred femto mole level of EH molecule considering the molecular weight of EH to be about 7,000. This sensitivity is quite satisfactory for immunolo-

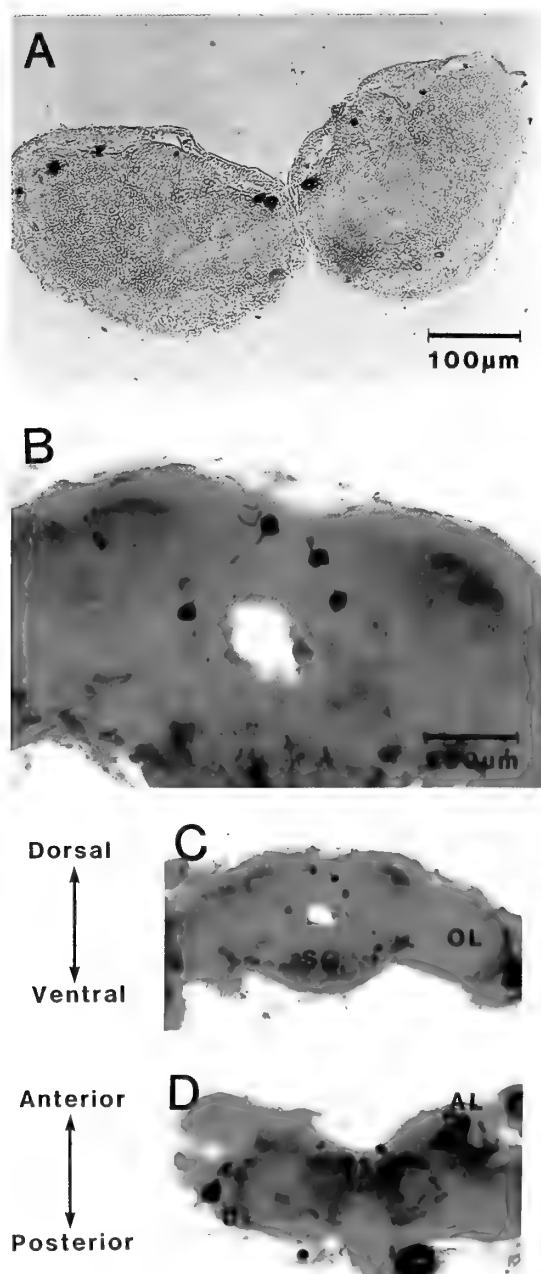


FIG. 4. Immunohistochemical localization of EH in *Bombyx* brain. (A) Transverse section of day-0 pupal brain. In the median part, two pairs of immunoreactive cells are seen. (B, C, D) Whole mount staining of pharate adult brain. (B) Two pairs of neurosecretory cells are stained, and immunoreactive nerve fibers are seen to start from these cells. Anterior view (C) and dorsal view (D) of the pharate adult brain-suboesophageal ganglion complex show that the immunoreactive four cells are supposed to localize in the anterior portion of the brain. AL: antennal lobe. OL: optic lobe. SG: suboesophageal ganglion.

gical assay, but is still less sensitive than biological assay using *Bombyx* pharate pupa, which can detect 0.1 ng of EH.

In our previous study, 18 steps of purification procedure were necessary to isolate EH from the extract of *Bombyx* heads. However, by the use of immunoaffinity chromatography with this antibody, the purification procedure could be simplified considerably by omitting several steps of open column chromatographies and HPLCs.

The EH activity was adsorbed to the affinity column completely. Elution of the active material with the eluant of pH 2.5 did not give a good yield, and the solution containing the synthetic EH(49–61) fragment was concluded to be the best in recovery. Consecutive elution with the solutions of 0.5 M NaCl or of pH 2.5 did not give any active material, indicating that most of the activity was eluted by substitution with the synthetic fragment. In purification by the affinity chromatography using the sample of 80,000 head equivalents, the recovery estimated from total activity was about 60%, and about 440 fold purification could be attained. The specific activity after this affinity chromatography was about 8.4 ng/unit. Considering that specific activity of pure EH is 0.1–0.2 ng/unit, an about 80-fold purification was necessary to isolate EH after this step. By the use of an ODS column, EH was separated from a large amount of S-carboxamidomethyl EH(49–61) and the activity was detected in a single peak. Because the specific activity of this peak was estimated to be 0.2 ng/EH unit and, in addition, the amino acid sequence analysis showed that a peptide in this peak coincided with EH at least for the N-terminal portion, we think EH was isolated by this HPLC step. This immunoaffinity chromatography followed by one-step reverse phase HPLC can considerably simplify the isolation procedure for EH.

Immunohistochemistry using the antibody revealed that two pairs of brain median neurosecretory cells had immunoreactive material in the perikarya (Fig. 4A). Therefore, it is highly possible that these four cells produce EH. Whole mount staining showed that the immunoreactive nerve fibers were originated from these cells as shown in Fig. 4B, and these fibers did not seem to cross at the middle part of the brain. Fugo *et al.*

examined the distribution of EH activity in the brain-suboesophageal ganglion (SG) complex of pharate adult *Bombyx* by the surgical cutting into three pieces (median and lateral pieces of brain and SG) and showed that EH activity was highest in the brain median part [12]. Thus, the present immunohistochemical results agree well with this previous report.

Copenhaver *et al.* have already identified EH-producing cells in the moth, *Manduca sexta* [5]. By an immunohistochemical study using an antiserum against *Manduca* EH, they revealed that 5 pairs of group Ia cells that project to ipsilateral corpus cardiacum and corpus allatum contained EH. It is of interest that there is such a great difference in the number of EH producing cells between the two lepidopteran insects, *Bombyx* and *Manduca*.

Recently, Mizoguchi *et al.* [13] reported four pairs of *Bombyx* median neurosecretory cells contained bombyxin, a *Bombyx* neurosecretory peptide that activates the prothoracic glands of the saturniid moth *Samia cynthia ricini*, by immunohistochemistry using a monoclonal antibody against a synthetic fragment of bombyxin. By a whole mount immuno-staining study using the anti-bombyxin antibody, the bombyxin cells were located in the dorsal-posterior position and proven different from the EH immunoreactive cells (photographs not shown).

ACKNOWLEDGMENTS

We are grateful to Drs. M. Nagata and A. Takenaka of The University of Tokyo, for their technical advice in immunohistochemistry, and to Mr. K. Soma and Miss I. Kubo for their technical assistance. This work was partly supported by Grants-in-Aid for Scientific Research (Nos. 61560135, 62560117 and 63430021) from the Ministry of Education, Science and Culture of Japan.

REFERENCES

- 1 Fugo, H. (1982) The eclosion behaviour of the silkworm, *Bombyx mori* and its hormonal control. *J. Seric. Sci. Jpn.*, **51**: 523–527.
- 2 Truman, J. W. (1985) In "Comprehensive Insect Physiology, Biochemistry, and Pharmacology," Vol. 8, Ed. by G. A. Kerkut and L. I. Gilbert, Pergamon Press, Oxford, pp. 413–440.

- 3 Truman, J. W., Taghert, P. H., Copenhaver, P. F., Tublitz, N. J. and Schwartz, L. M. (1981) Eclosion hormone may control all ecdysis in insects. *Nature*, **291**: 70–71.
- 4 Chen, J. H., Fugo, H., Nakajima, M., Nagasawa, H. and Suzuki, A. (1986) The presence of neurohormonal activities in embryos of the silkworm, *Bombyx mori*. *J. Seric. Sci. Jpn.*, **55**: 54–59.
- 5 Copenhaver, P. F. and Truman, J. W. (1986) Identification of the cerebral neurosecretory cells that contain eclosion hormone in the moth *Manduca sexta*. *J. Neurosci.*, **6**: 1738–1747.
- 6 Kono, T., Nagasawa, H., Isogai, A., Fugo, H. and Suzuki, A. (1987) Amino acid sequence of eclosion hormone of the silkworm, *Bombyx mori*. *Agric. Biol. Chem.*, **51**: 2307–2308.
- 7 Marti, T., Takio, K., Walsh, K., Terzi, G. and Truman, J. W. (1987) Microanalysis of the amino acid sequence of the eclosion hormone from the tobacco hornworm *Manduca sexta*. *FEBS Lett.*, **219**: 415–418.
- 8 Kataoka, H., Troetschler, R. G., Kramer, S. J., Cesarin, B. J. and Schooley, D. A. (1987) Isolation and primary structure of the eclosion hormone of the tobacco hornworm, *Manduca sexta*. *Biochem. Biophys. Res. Commun.*, **146**: 746–750.
- 9 Carlsson, J., Drevin, H. and Axen, R. (1978) Protein thiolation and reversible protein-protein conjugation. *Biochem. J.*, **173**: 723–737.
- 10 Hawkes, R., Niday, E. and Gordon, J. (1982) A dot-immunobinding assay for monoclonal and other antibodies. *Anal. Biochem.*, **119**: 142–147.
- 11 Nagasawa, H., Kamito, T., Takahashi, S., Isogai, A., Fugo, H. and Suzuki, A. (1985) Eclosion hormone of the silkworm, *Bombyx mori*: purification and determination of the N-terminal amino acid sequence. *Insect Biochem.*, **15**: 573–578.
- 12 Fugo, H. and Iwata, Y. (1983) Change of eclosion hormone activity in the brain during the pupal-adult development in the silkworm, *Bombyx mori*. *J. Seric. Sci. Jpn.*, **52**: 79–84.
- 13 Mizoguchi, A., Ishizaki, H., Nagasawa, H., Kataoka, H., Isogai, A., Tamura, S., Suzuki, A., Fujino, M. and Kitada, C. (1987) A monoclonal antibody against a synthetic fragment of bombyxin (4K-prothoracicotropic hormone) from the silkworm, *Bombyx mori*: characterization and immunohistochemistry. *Mol. Cell. Endocrinol.*, **51**: 227–235.

Vanadium-Containing Blood Cells (Vanadocytes) Show No Fluorescence Due to the Tunichrome in the Ascidian, *Ascidia sydneiensis samea*

HITOSHI MICHIBATA, TARO UYAMA and JUNKO HIRATA¹

*Biological Institute, Faculty of Science, Toyama University,
Toyama 930, Japan*

ABSTRACT—Ascidians belonging to the family Ascidiidae are known to accumulate vanadium ions from seawater to levels in excess of one million times the level in seawater and to maintain the vanadium ions in a reduced form. A tunichrome which appears to be involved in the accumulation and reduction of vanadium ions produces an autonomous fluorescence upon excitation with blue-violet light. Among six different types of ascidian blood cell, the morula cell, which emits fluorescence brightly, has been thought to be the vanadium-containing blood cell (vanadocyte) and, consequently, it has been suggested that the intensity of fluorescence is indicative of the concentration of vanadium ions in the blood cell.

In the present experiments, after ascidian blood cells were fractionated into the various subpopulations by means of Ficoll density gradient centrifugation, the level of vanadium in each subpopulation was determined to ascertain which type of blood cell is the true vanadocyte in *Ascidia sydneiensis samea*. The autonomous fluorescence from the vanadocyte was also monitored with a fluorescence microscope. Consequently, we found that the subpopulation of morula cells that fluoresced brightly did not contain vanadium, whereas the subpopulation of signet ring cells, which did not emit fluorescence, contained high levels of vanadium.

INTRODUCTION

The ability of ascidians to concentrate vanadium ions, to levels in excess of one million times the level in seawater, is a source of special fascination [1, 2]. A tunichrome, which can be extracted from the blood cells of *Ascidia nigra*, has been proposed to be involved in the accumulation of vanadium ions from seawater [1, 3–5]. This substance has been reported to emit a specific autonomous fluorescence upon excitation with blue-violet light [4, 6]. Among several different types of ascidian blood cell examined, the strongest fluorescence that could be ascribed to the tunichrome was observed in the morula cell. Thus, it was suggested that the intensity of fluorescence is indicative of the concentration of vanadium ions in the cells [4].

However, we have already verified that the morula cell contains no vanadium, whereas the signet ring cell contains a very high level of vanadium ions, in the case of *A. ahodori*. We based our conclusions on the results of cell fractionation techniques, neutron activation analysis and electron spin resonance spectrometry (ESR) [7].

In the present experiments, we examined whether the signet ring cell (vanadocyte), separated by Ficoll density gradient centrifugation, emits an autonomous fluorescence due to the tunichrome, in order to verify any participation by this substance in the accumulation of vanadium ions in ascidian blood cells from seawater.

MATERIALS AND METHODS

Ascidia sydneiensis samea were collected in the bay of Nanao, Ishikawa Prefecture, Japan, and were maintained in an aerated seawater aquarium at 18° C. Blood, drawn by making an incision through the lower part of the tunic and puncturing

Accepted February 20, 1990

Received December 21, 1989

¹ Present address : Faculty of Pharmaceutical Sciences,
University of Tokushima, Tokushima 770.

the mantle, was suspended in artificial seawater (ASW) that contained 460 mM NaCl, 9 mM KCl, 33 mM Na_2SO_4 , 6 mM NaHCO_3 , 1 mM EDTA(ethylenediamine-tetraacetic acid) and 5 mM HEPES (N-2-hydroxyethylpiperazine-N'-2-ethanesulfonic acid) buffer (pH 7.0) to avoid clotting. The suspension was separated into blood cells and plasma by centrifugation at $300\times g$ for 10 min at 10°C . The pellet obtained was resuspended at a concentration of about 10^7 cells/ml in ASW and is referred to as "washed cells". Thereafter, cell fractionation by Ficoll density gradient centrifugation was carried out in a manner similar to that described previously [7]. Ficoll type 400 (Pharmacia Fine Chemicals) was dissolved in ASW to final concentrations of 34.0, 18.0, 14.5 and 4.0% (w/v) and discontinuous gradients were prepared in 10-ml centrifuge tubes. One ml of washed cells was layered onto each gradient and tubes were centrifuged at $300\times g$ for 20 min at 10°C . Layers of cells were gently pipetted from the top of the tubes. Each layer of cells obtained in this way was washed twice with ASW by centrifugation at $350\times g$ for 10 min in order to remove Ficoll 400 and was resuspended in a small amount of ASW. The fractionated populations of cells were subsequently used for determination of levels of vanadium by neutron activation analysis at the Institute for Atomic Energy of Rikkyo University, Yokosuka, Japan [2]. The blood cells which were resuspended in a small amount of ASW were observed with a standard bright field microscope and a fluorescence microscope (Nikon). They were also observed after vital staining with neutral red, Nile blue and Janus green.

RESULTS

Morphology and fluorescence of blood cells

We were able to recognize six different types of cell: the giant cell, signet ring cell, morula cell, compartment cell, pigment cell and hyaline leucocyte. These types of cell were classified mainly according to the criteria of Wright [8] and Rowley [9].

Subpopulations of the blood cells are present at variable proportions in individuals in this species.

The giant cell was the second most abundant cell type accounting for 21 to 30% of the total cells. This cell was very large and spherical or irregularly shaped. It was 40 to $80\ \mu\text{m}$ in diameter and contained a single, very large, fluid-filled vacuole which occupied most of the cell (Fig. 1A). The vacuole was coloured faint red and faint violet after staining with neutral red and Nile blue, respectively. The cell weakly emitted a pale green fluorescence (Fig. 1a). The giant cell is probably analogous to the nephrocyte [8]. It seems however reasonable that the cell should be designated as a giant cell because it is not apparent that the giant cell is involved in excretion.

The morula cell was round to ovoid, 8 to $10\ \mu\text{m}$ in diameter. As shown in Figure 1B, the morula cell in this species exhibited refractive cytoplasm under bright field illumination and a few cells appeared typical berry-like shape, differing from the morula cell in the other species. It was accounted for 6 to 12% of the total population. This cell appeared red, blue-green and green after staining with neutral red, Nile blue and Janus green, respectively, and emitted autonomous fluorescence with a yellow green colour upon excitation with blue-violet light (Fig. 1b).

The signet ring cell, 10 to $12\ \mu\text{m}$ in diameter, which comprised about 32 to 44% of the total population of cells, predominated. This cell was characterized by a single and fluid-filled vacuole which displaced the nucleus and cytoplasm to the periphery of the cell (Fig. 1C). A single, small, refractive vesicle was suspended in the vacuole. Such vacuole was coloured a faint red after staining with neutral red. The small vesicle was dyed a red and green with neutral red and Janus green, respectively. No fluorescence was detected from this cell upon excitation with blue-violet light (Fig. 1c).

The compartment cell, was ovoid, $6\ \mu\text{m}$ in diameter, and accounted for 15 to 21% of the total population of cells (Fig. 1D). This cell was dyed a red with neutral red. The granules in the cytoplasm appeared deep red and green after staining with neutral red and Janus green, respectively. No fluorescence was detected from the compartment cell (Fig. 1d).

Pigment cells (Fig. 1E) were relatively rare. The

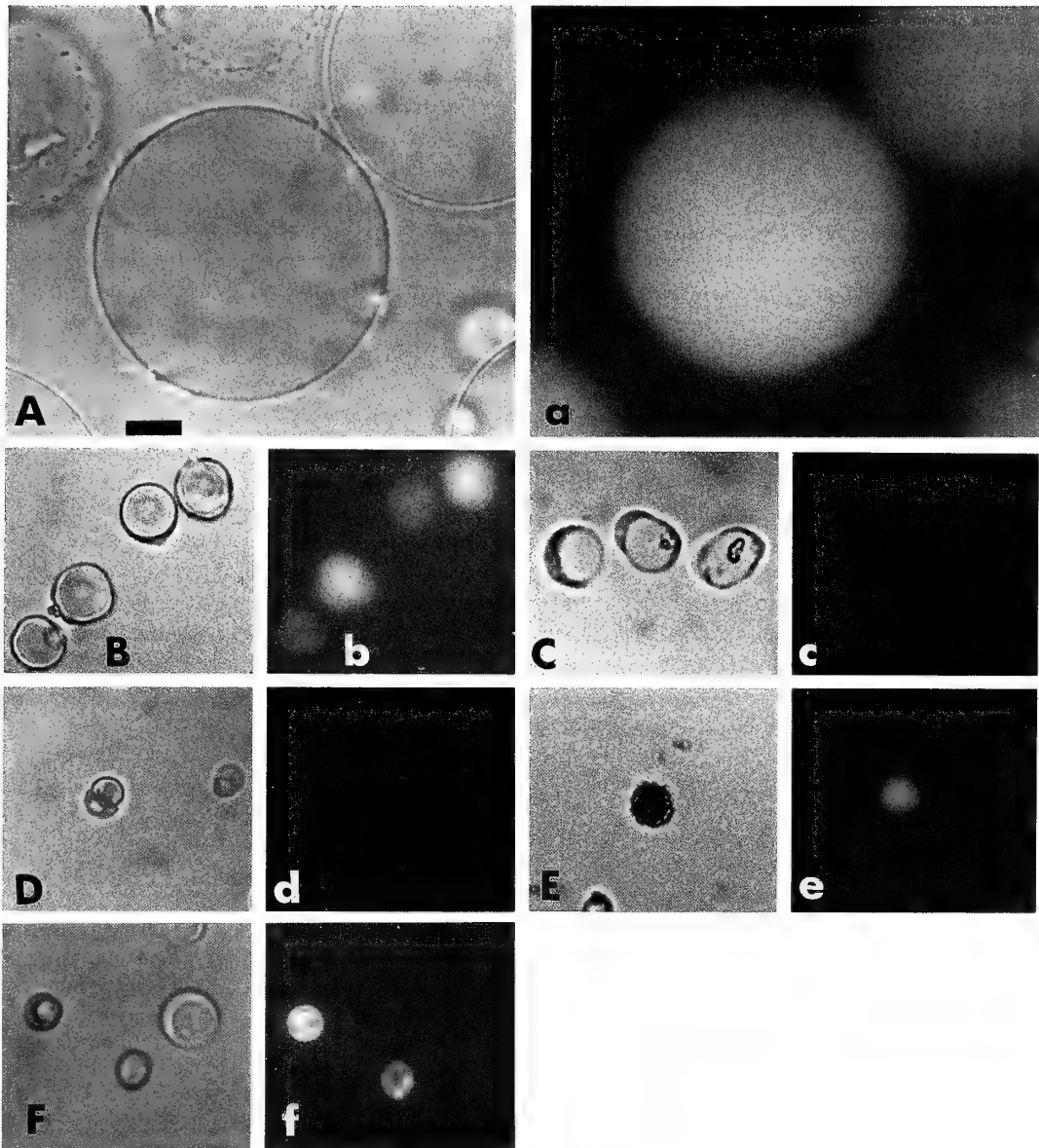


FIG. 1. Blood cells of *Ascidia sydneiensis samea* were observed with a bright field microscope (A-F) and a fluorescence microscope (a-f). The giant cell, the second most abundant cell type, was 40 to 80 μm in diameter and contained a single, very large, fluid-filled vacuole (A). This cell weakly emitted a pale green fluorescence upon excitation with blue-violet light (a). The morula cell had refractive cytoplasm (B) and a few cells appeared typical berry-like shape. This cell emitted autonomous fluorescence with a yellow green colour (b). The signet ring cell, which contained large amounts of vanadium, was characterized by a single and fluid-filled vacuole and refractive vesicle in the vacuole (C). This cell type was predominant in the blood cells. From this cell no fluorescence was detected upon excitation with blue-violet light (c). The compartment cell was small and ovoid, accounting for 15 to 21% of the total population of cells (D). No fluorescence was also detected from this cell (d). The pigment cell shows red, dark orange or brown colour (E) and emitted bright coloured fluorescence (e). The hyaline leucocyte (F) fluoresced most brightly among the blood cells in this species (f). Scale bar indicates 10 μm .

pigment cell emitted bright orange coloured fluorescence (Fig. 1e). The cells shown in Figure 1f seem to be hyaline leucocytes and fluoresced most brightly among the blood cells in this species (Fig. 1f).

Cell flactionation

The blood cells were partitioned into four discrete layers that contained various subpopulations, after Ficoll density gradient centrifugation. Most

TABLE 1. Distribution of each subpopulation of blood cells prior to and following separation by centrifugation on a Ficoll density gradient

	Total cell number	Giant cells	Signet ring cells	Morula cells	Compartment cells
Washed cells	79,422±16,250 (100.0)	20,545±10,789 (63.9)	29,398±7,274 (14.0)	8,344±1,210 (3.2)	13,936±2,370 (8.5)
Layer 1	2,294±808 (100.0)	1,466±555 (63.9)	321±179 (14.0)	73±66 (3.2)	194±59 (8.5)
Layer 2	3,096±1,189 (100.0)	—	2,816±1,119 (91.0)	—	217±70 (7.0)
Layer 3	875±164 (100.0)	—	465±171 (53.1)	—	396±56 (45.3)
Layer 4	517±167 (100.0)	—	—	471±159 (91.1)	—
Total number of cells recovered	6,782	1,466	3,602	544	807

Each number of blood cells is shown in 1,000 cells and as the mean±standard error. Figures in the parenthesis express % of total number of blood cells in the washed cells and each layer.

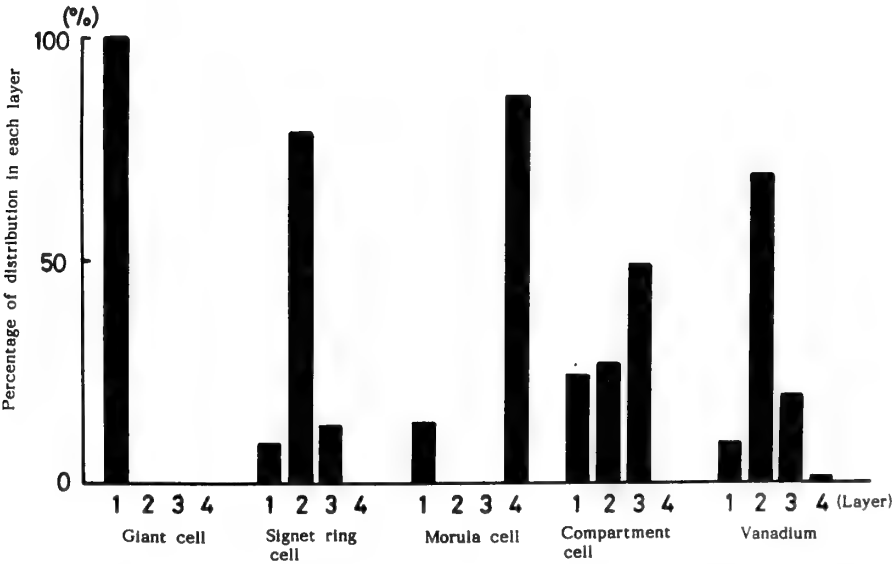


FIG. 2. Comparison of the patterns of distribution of giant cells, signet ring cells, morula cells and compartment cells with that of vanadium ions after density gradient centrifugation of blood cells of *A. sydneyensis samea*. Histograms depict the relative numbers of each type of cell and the amounts of vanadium distributed in the four layers of cells as percentages of the total number of cells and the total amount of vanadium. Each bar represents the average of results of five trials. The pattern of distribution of vanadium is similar to that of the signet ring cells but is different from those of the other cell types.

of the separated blood cells in each layer did not take up eosin Y, indicating that they were still alive. The results obtained represent the average of results of five trials \pm S.E. (standard error) and are shown in Table 1. About 6 to 12% of each subpopulation were recovered from the various layers, which low rates were due to sacrifice the recovery rate to obtain purer subpopulation of blood cells.

The percentages of giant cells, signet ring cells, morula cells and compartment cells distributed among each of four layers, are presented graphically in Figure 2. All of the giant cells were gathered in layer 1, suggesting that they were of low density. About 79% of the signet ring cells were present in layer 2 and the remaining 8% and 13% were found in layer 1 and 3, respectively. Almost all of the morula cells (88%) were present in layer 4, indicating that this cell type has highest density among the blood cells in this species. Half of the subpopulation of the compartment cells was found in layer 3 and the other half was divided between layer 1 and 2.

Vanadium content

Neutron activation analysis revealed that 127.5 μ g of vanadium was contained in the washed blood cells and 14.7 μ g of the metal, which corresponded to about 12% of the initial amount in the washed cells, was recovered from the fractioned blood

cells as shown in Table. 2. The highest percentage of vanadium distributed among four layers was found in layer 2, in which about 70% of the vanadium was present. The remaining 9 and 20% of vanadium were distributed in layer 1 and 3, respectively.

The pattern of distribution of vanadium was compared with those of blood cells in Figure 2. This pattern was very similar to that of the signet ring cells, but was clearly different from that of the morula cells and of the other cell types. Furthermore, the following data strengthen evidence that the signet ring cell is the vanadocyte. As has been pointed out, the proportion of each type of blood cell varied in individuals in this species. Hence, the signet ring cells recovered from layer 2 also varied in number through 1,664,000 to 4,867,000 cells and vanadium content in layer 2 rose and fell in proportion to the cell number. When the vanadium content per 1000 signet ring cells in layer 2 was calculated in each trial, the values were of a very narrow range of 3.04 to 4.11 ng/1000 cells (average value \pm S.E. was 3.71 ± 0.4 ng/1000 cells). Such tight correlation of vanadium content with the cell number could not be found out in the other type of blood cell.

DISCUSSION

The vanadium ion dissolved in seawater is in the +V oxidation state at concentrations of about 35 nM [10, 11]. Some ascidians concentrate these ions 10^6 -fold in their blood cells and store the metal ion in its reduced +III and/or +IV states [7, 12-16]. Macara *et al.* [1] isolated a tunichrome from the ascidian blood cells, which serves as a good agent for forming complexes with vanadium ions and which reduces the metal ion to its reduced form. The tunichrome emits fluorescence when it is excited with blue-violet light and is present with vanadium at approximately equimolar concentrations [1]. The concentration of vanadium has, therefore, been estimated from the intensity of fluorescence of the tunichrome in each type of blood cell. In consequence, concentrations of both vanadium and tunichrome were thought to be in the order, morula cell > compartment cell > signet ring cell [4].

TABLE 2. Vanadium content of layers separated by Ficoll density gradient centrifugation

	Total content (ng)
Washed cells	127,540 \pm 32,240
Layer 1	1,370 \pm 640 (9.3%)
Layer 2	10,220 \pm 3,640 (69.4%)
Layer 3	2,900 \pm 820 (19.7%)
Layer 4	230 \pm 150 (1.6%)
Recovered vanadium after separation	14,720

Each value represents the average of five trials \pm standard error. Figures in the parenthesis express % of recovered vanadium.

Although the morula cell unequivocally emitted fluorescence in this experiment (Fig. 1), the combined results of cell fractionation and neutron activation analysis have revealed that the morula cell does not contain vanadium, while the signet ring cell which does not fluoresce contains large amounts of vanadium (Tables 1 and 2). In fact, the pattern of distribution of vanadium among the fractionated layers corresponded clearly to that of the signet ring cells as shown in Figure 2. Moreover, the vanadium content per 1000 signet ring cells in layer 2 was almost consistent in each trial. Based on these results, it could be concluded that the actual vanadocyte involved in the accumulation of vanadium must be the signet ring cell in *A. sydneiensis samea*.

If the tunichrome is involved in the reduction and accumulation of vanadium ions in the ascidian blood cells, it would be necessary that the tunichrome should be contained in the signet ring cell, which is the vanadocyte. However, no fluorescence due to the tunichrome was detected in this cell (Fig. 1). In a different species of *A. ahodori*, a similar finding that the signet ring cell did not emit fluorescence was obtained from preliminary experiments in which the blood cells were not fractionated [17]. Tunichrome B-1, one of the tunichromes, has been isolated from non-separated blood cells of *A. nigra* and its chemical structure has been determined. It consists of three units of hydroxy-DOPA (3, 4-dehydroxy-phenylalanine) [18], and it must have the ability to reduce an oxide to its reduced state, as shown in the report by Macara *et al.* [1]. There is, however, no evidence that this substance is involved in the reduction and accumulation of vanadium ions in the vanadocytes in ascidian blood.

The fluorescence emitted by ascidian blood cells [1, 3, 4, 6] cannot be attributed solely to the tunichrome. It is well known that there are several kinds of autonomous fluorescent substance, for example, lipids, vitamins and porphyrins, in living cells. Therefore, the finding of fluorescence does not always provide evidence for the presence of a tunichrome.

We have extracted a vanadium-binding substance which we have called vanadobin from the blood cells of *A. sydneiensis samea*. This substance

is colourless and can maintain the vanadium ion in the vanadyl form (VO(IV)), even under aerobic conditions. Moreover, this substance has an affinity for exogenous vanadium ions (V) and contains a reducing sugar [16]. Taking all the above data into account, we suggest that it is not the tunichrome but rather the vanadobin that is the substance involved in the accumulation of vanadium ions from seawater in ascidian blood cells.

ACKNOWLEDGMENTS

We are grateful to Profs. M. Yoneda and N. Satoh of Kyoto University for providing help in the use of fluorescence microscope. This work was supported in part by a grant-in-aid from the Ministry of Education, Science and Culture, Japan (No. 62540540) and was also supported financially by the Japan Securities Scholarship Foundation and the Ito Science Foundation. Neutron activation analysis was carried out under the Cooperative Programs of the Institute for Atomic Energy of Rikkyo University.

REFERENCES

- 1 Macara, I. G., McLeod, G. C. and Kustin, K. (1979) Isolation, properties and structural studies on a compound from tunicate blood cells that may be involved in vanadium accumulation. *Biochemical J.*, **181**: 457-465.
- 2 Michibata, H., Terada, T., Anada, N., Yamakawa, K. and Numakunai, T. (1986) The accumulation and distribution of vanadium, iron, and manganese in some solitary ascidians. *Biol. Bull.*, **171**: 672-681.
- 3 Macara, I. G., McLeod, G. C. and Kustin, K. (1979) Tunichromes and metal ion accumulation in tunicate blood cells. *Comp. Biochem. Physiol.*, **63B**: 299-302.
- 4 Robinson, W. E., Agudelo, M. I. and Kustin, K. (1984) Tunichrome content in the blood cells of the tunicate, *Ascidia callosa* Stimpson, as an indicator of vanadium distribution. *Comp. Biochem. Physiol.*, **78A**: 667-673.
- 5 Oltz, E. M., Bruening, R. C., Smith, M. J., Kustin, K. and Nakanishi, K. (1988) The tunichromes. A class of reducing blood pigments from sea squirts: Isolation, structures, and vanadium chemistry. *J. Am. Chem. Soc.*, **110**: 6162-6172.
- 6 Oltz, E. M. (1987) Biorganic studies of the tunichromes: A class of reducing blood pigments obtained from sea squirts. Thesis of Columbia University.
- 7 Michibata, H., Hirata, J., Uesaka, M., Numakunai, T. and Sakurai, H. (1987) Separation of vanado-

- cytes: Determination and characterization of vanadium ion in the separated blood cells of the ascidian, *Ascidia ahodori*. J. Exp. Zool., **244**: 33-38.
- 8 Wright, K. R. (1981) Urochordates. In "Invertebrate Blood Cells". Ed. by Ratcliffe, N. A. and Rowley, A. F., Academic Press, London, Vol. 2, pp. 565-626.
- 9 Rowley, A. F. (1981) The blood cells of the sea squirt, *Ciona intestinalis*: Morphology, differential counts, and *in vitro* phagocytic activity. J. Invertebr. Pathol., **37**: 91-100.
- 10 Cole, P. C., Eckert, J. M. and Williams, K. L. (1983) The determination of dissolved and particulate vanadium in sea water by X-ray fluorescence spectrometry. Anal. Chim. Acta, **153**: 61-67.
- 11 Collier, R. W. (1984) Particulate and dissolved vanadium in the North Pacific Ocean. Nature, **309**: 441-444.
- 12 Swinehart, J. H., Biggs, W. R., Halko, D. J. and Schroeder, N. C. (1974) The vanadium and selected metal contents of some ascidians. Biol. Bull., **146**: 302-312.
- 13 Dingley, A. L., Kustin, K., Macara, I. G. and McLeod, G. C. (1981) Accumulation of vanadium by tunicate blood cells occurs via specific anion transport system. Biochim. Biophys. Acta, **649**: 493-502.
- 14 Bell, M. V., Pirie, B. J. S., McPhail, D. B., Goodman, B. A., Falk-Petersen, I. -B. and Sargent, J. R. (1982) Contents of vanadium and sulphur in the blood cells of *Ascidia mentula* and *Ascididiella aspersa*. J. Mar. Biol. Ass. U. K., **62**: 709-716.
- 15 Frank, P., Carlson, R. M. K. and Hodgson, K. O. (1986) Vanadyl ion EPR as a non-invasive probe of pH in intact vanadocytes from *Ascidia ceratodes*. Inorg. Chem., **25**: 470-478.
- 16 Michibata, H., Miyamoto, T. and Sakurai, H. (1986) Purification of vanadium binding substance from the blood cells of the tunicate, *Ascidia sydneiensis samea*. Biochem. Biophys. Res. Commun., **141**: 251-257.
- 17 Michibata, H., Hirata, J., Terada, T. and Sakurai, H. (1988) Autonomous fluorescence of ascidian blood cells with special reference to identification of vanadocytes. Experientia, **44**: 906-907.
- 18 Bruening, R. C., Oltz, E. M., Furukawa, J., Nakanishi, K. and Kustin, K. (1985) Isolation and structure of tunicchrome B-1, a reducing blood pigment from the tunicate *Ascidia nigra* L. J. Am. Chem. Soc., **107**: 5298-5300.

Organization and Development of Reflecting Platelets in Iridophores of the Giant Clam, *Tridacna crocea* Lamarck

YOSHIHISA KAMISHIMA

*Department of Biology, Faculty of Science, Okayama University,
Okayama 700, Japan*

ABSTRACT—Giant clams show brilliant coloration on the mantle. The color comes from iridophores which are distributed in the mesenchyme. Each iridophore contains thin reflecting platelets which are aligned uniformly in rows. The platelet is bound with a membrane and has a fine substructure with a 7 nm lattice. A flat cistern intervenes two neighbouring platelets to keep the interspace constant.

In developing iridoblast, the reflecting platelets are formed in a confined area around the nucleus. Various types of vacuoles representing transitional forms from the ER to a mature reflecting platelet are seen in the area. Golgi vesicles are involved in the platelet formation. They are incorporated onto the vacuolar membrane while accumulation of the dense reflecting substance takes place in the vacuolar lumen. The dense substance is condensed in the vacuoles. The vacuoles are then fashioned into thin rectangular platelets and aligned in rows to form an alternating reflecting surface. The intervening cistern is formed from vesicles which fuse with one another to become a flat, thin cistern.

INTRODUCTION

In molluscs, two types of iridophores (iridocytes) have been identified. The first type is the iridophore which contains small granular or vesicular organelles by which the incident light is split and sent backwards to effect the Tyndall phenomenon. This type of iridophore has been observed in the mantle of opisthobranchiate gastropods [1]. The second type is the iridophore which shows a color by reflection and interference through multilayered platelets arranged uniformly in the cytoplasm. Cells of the second type are observed in the skin of cephalopods [2, 3], and in the mantle tissue of some bivalved shells [4, 5]. Because of their poorly arranged platelets, some of these cells display less effective coloration and have been referred to as reflector cells [6].

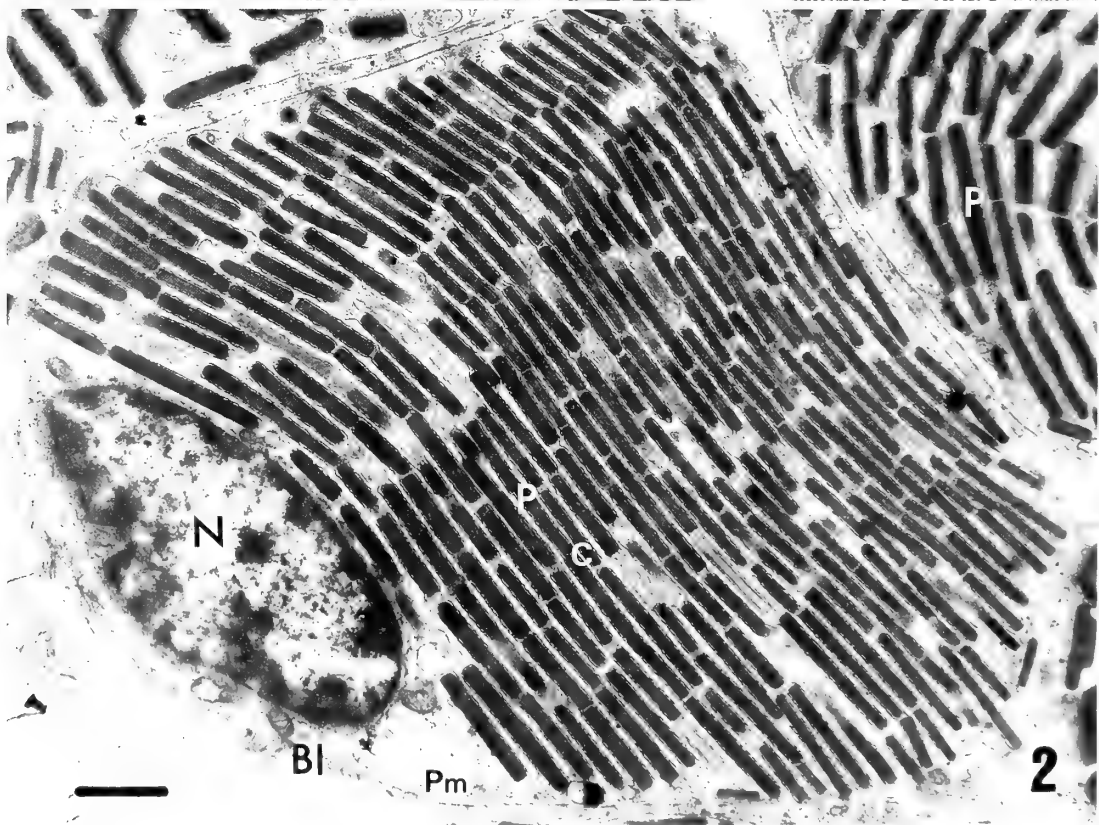
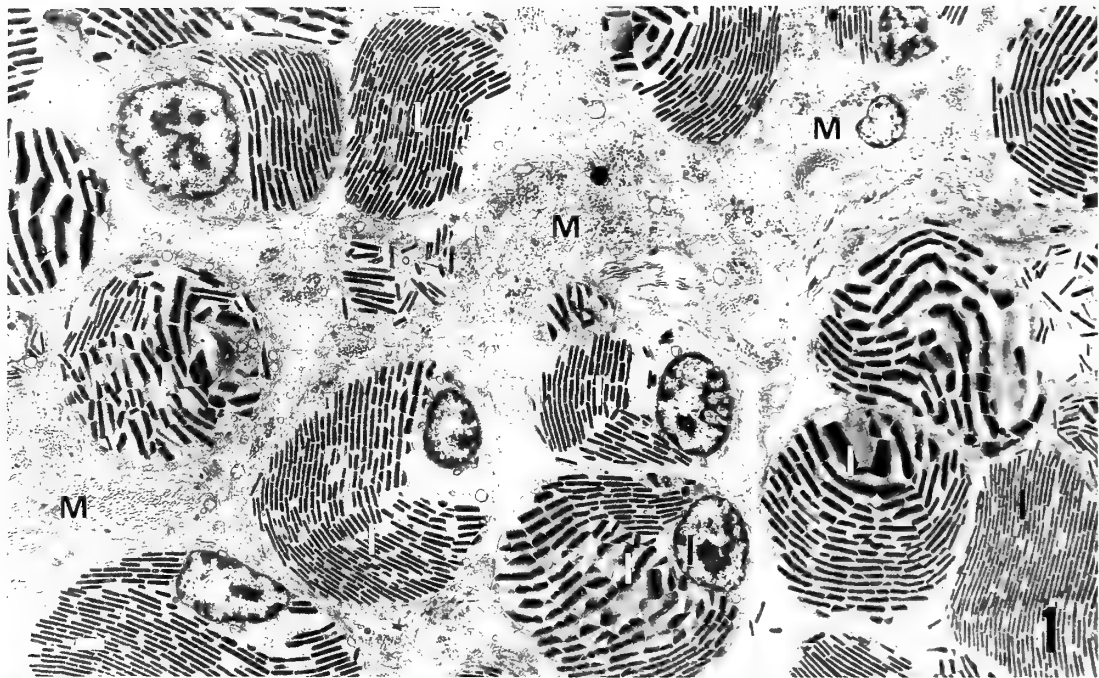
Iridophores of the giant clam show a clear monochromatic coloration in various spectral ranges according to the anatomical location of the cell. These iridophores contain multiple rows of reflecting platelets, each of which is uniform in thickness [4, 7]. The precision with which the

platelets are arranged is reflected in a narrow range of spectrum, which leads to the giant clam producing one of the prominent colorations among molluscs.

In spite of their high efficiency as chromatophores, no detailed studies have so far been reported on the structure and development of the clam iridophores. This study intends to show the ultrastructural organization and the development of reflecting platelets in iridophores of the giant clam.

MATERIALS AND METHODS

Giant clams (*Tridacna crocea*) were collected from the Ryukyu Islands, the south-western archipelago of Japan. The brilliantly colored portion of the mantle tissue was excised and minced into small blocks in 3% glutaraldehyde fixative buffered to pH=7.4 with 0.1 M phosphate solution. Tissue blocks were further fixed in the same solution at room temperature for 2 hr and then transferred into 1% osmium tetroxide solution buffered with 0.1 M phosphate to pH 7.4. After the post osmification for 1.5 hr in the solution at the room temperature, tissue blocks were dehydrated through the ethanol series and embedded in



epoxy resin. Thin sections obtained on the LKB ultramicrotome 4800 A or the Porter-Blum MT-I ultratome mounted with glass knives were examined under the Hitachi Electron Microscope HU-11E.

RESULTS

Morphology of the iridophore

Mantle iridophores of the giant clam were observed in the mesenchyme. They were distributed mostly in clusters among muscle cells and positioned to cover the outer layer of digestive glands in which zooxanthellae, the algal symbionts, were colonized (Fig. 1). The iridophore was spherical or oval in shape. A round nucleus was usually located in the peripheral cytoplasm and the rest of the cell was filled with rows of reflecting platelets (Fig. 2). Mitochondria, vesicles and ribosomes were observed around the nucleus. A small number of vesicles and ribosomes were also found in the interspaces between the platelets.

The reflecting platelets were rectangular in shape (Fig. 5). Thickness of the platelet was uniform within each cell (Fig. 2), although it differed from cell to cell, ranging from 80 nm to 120 nm. The platelet was enveloped with a single limiting membrane, which measured 7 nm in thickness and was slightly thinner than the plasma or ER membrane (Figs. 3 and 4). At the end of the platelet, vesicles and ribosomes were often seen closely associated with the platelet (Figs. 3~6). The reflecting body mass of the platelet was electron dense and had a substructure of fine lattice (Fig. 6). The lattice consisted of an alternate arrangement of dense and light lines (2.0 nm and 5.0 nm in thickness, respectively) at 7.0 nm intervals. There was a narrow marginal space of 3 nm

between the envelope and the inner reflecting body mass (Fig. 6). All platelets in a mature iridophore faced one direction and were aligned in parallel rows with a set interval (Figs. 2~3). In each row, the platelets were arranged end to end, forming a broad reflecting plane (Fig. 5).

Flat and long cisterns lay between the platelet rows. The cistern was tightly secured between two platelets, ensuring a constant interspace (Figs. 2~4). The width of the cistern was uniform within each cell but differed slightly according to the cell. The width ranged from 50 nm to 60 nm in most cases, so that the distance between the dense reflecting masses of the platelets measured from 80 nm to 100 nm. The lumen of the cistern appeared to be empty, although a few granular substances were detected on the internal surface of the cisternal membrane. Cisterns were found only between the platelet rows, so that no cisterns were found along the outer side of the platelets at the extremity of the row (Figs. 3 and 11). Cisterns were often seen fusing with the cell membrane at the marginal end, so that their lumina were directly opened to the extracellular space (Fig. 4). The opening was always covered with the solid basal lamina which did not invaginate concomitantly with the plasma membrane.

Development of the iridoblast

In iridoblasts, especially in those in earlier developmental stages, many endoplasmic reticula and Golgi complexes were seen around the nucleus (Fig. 7). Numerous vacuoles and vesicles of various shapes and sizes were also observed in this area (Figs. 7~13). Developing platelets were observed in the vicinity of this area. The developing platelets were smaller than mature ones and often lacked the associating cisterns along them (Figs. 8, 11 and 12).

FIG. 1. Electron micrograph of the mantle tissue of a giant clam. Iridophores (I) are observed in clusters among muscle cells (M). The iridophore is spherical and has a nucleus in the periphery. Most part of the cytoplasm is occupied with reflecting platelets. Each cell contains 20 to 30 rows of reflecting platelets which are aligned in parallel one another and are arranged around the nucleus. The orientation of the platelets differs in each cell. Bar indicates 1 μ m. $\times 3,500$

FIG. 2. Transverse profile of the platelet in a giant clam iridophore. Each row consists of a series of platelets (P) arranged end to end. Interspace between the platelet rows is kept in uniform distance by an intervening cistern (C). Only few organelles such as mitochondria, small vesicles and ribosomes are seen around the nucleus (N). Thick basal lamina (Bl) is seen outside of the iridophore plasma membrane (Pm). Bar indicates 1 μ m. $\times 12,000$

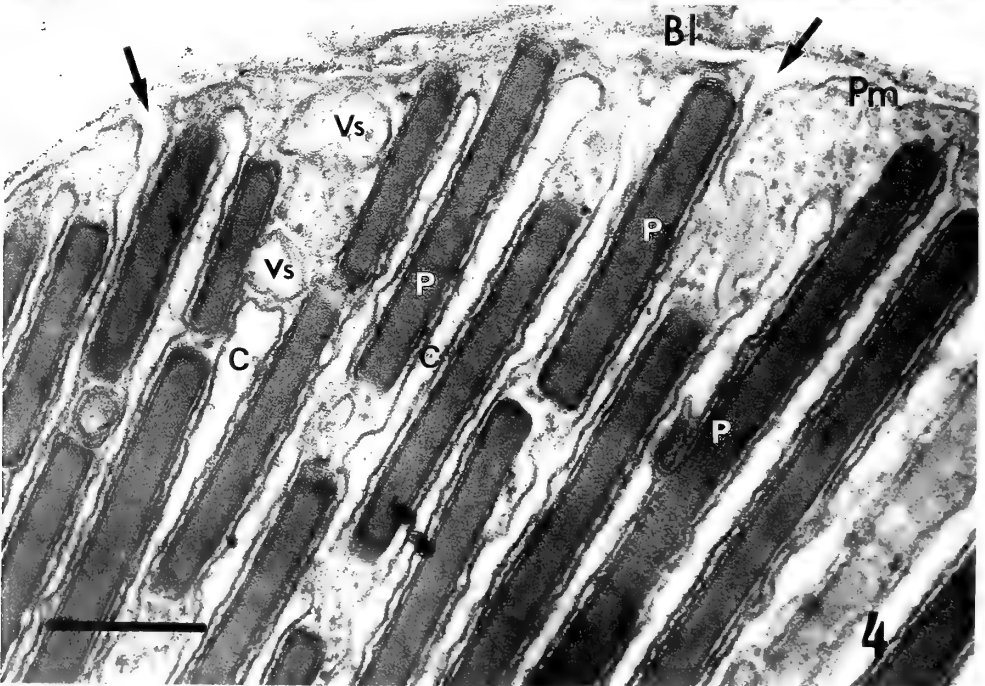
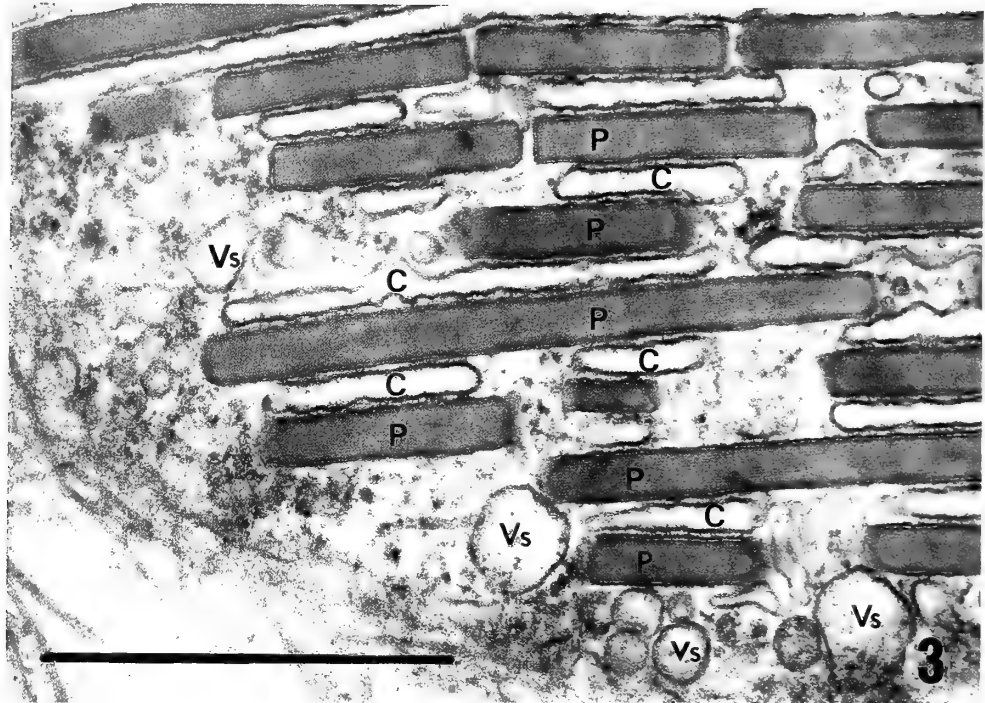


FIG. 3. A portion of platelet forming area near the cell surface showing developing cisterns. A flat cistern (C) with 50 nm to 60 nm width is tightly secured between two platelets (P). No cisterns are seen along the outside of the marginal platelets. Distended vesicles (Vs) are seen along the platelets. Ribosomes are seen among the platelets. Bar indicates 1 μ . $\times 54,000$

FIG. 4. A peripheral portion of an iridophore sectioned transversely to the platelet row. Some of cisterns fuse with the plasma membrane at the periphery, so that the cisternal lumen opens directly to the extracellular space (arrows). Note dilated vesicles (Vs) at the position of the cistern. Thick basal lamina (Bl) is seen outside of the plasm membrane (Pm). Bar indicate 1 μ m. $\times 43,700$.

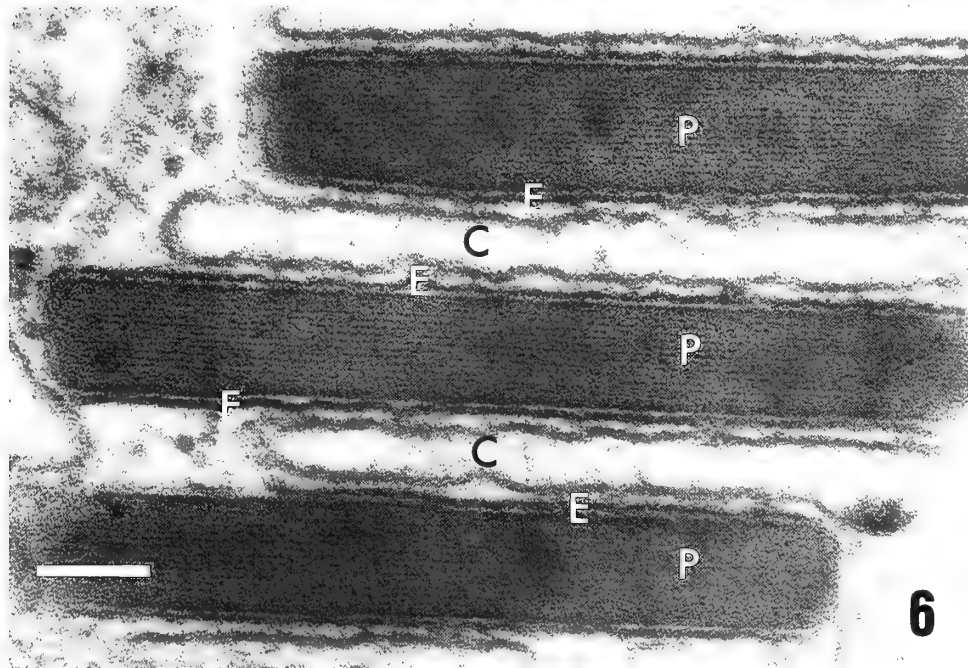
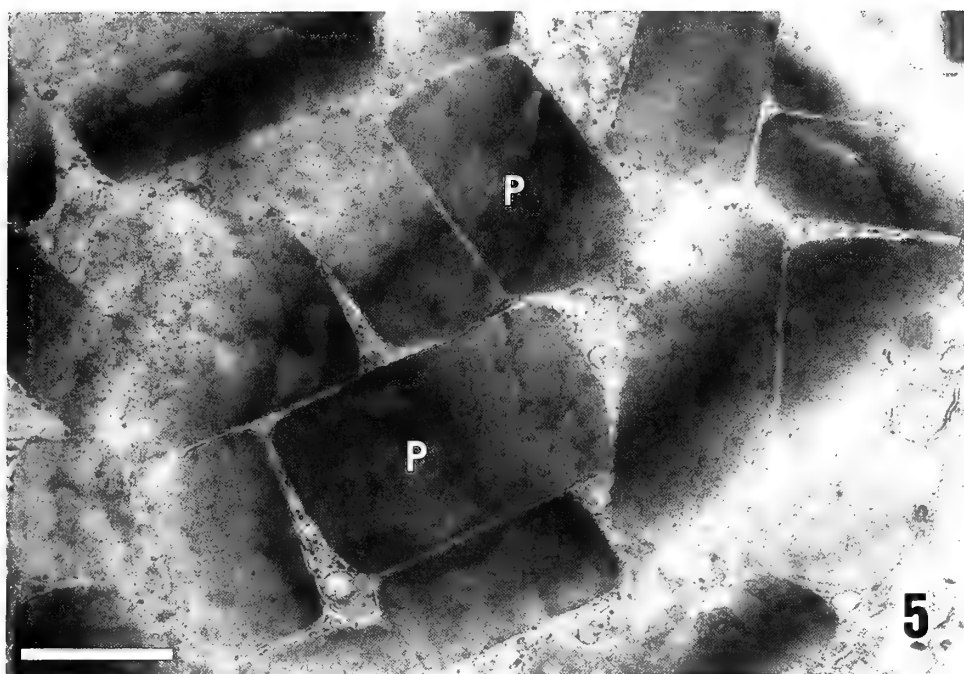
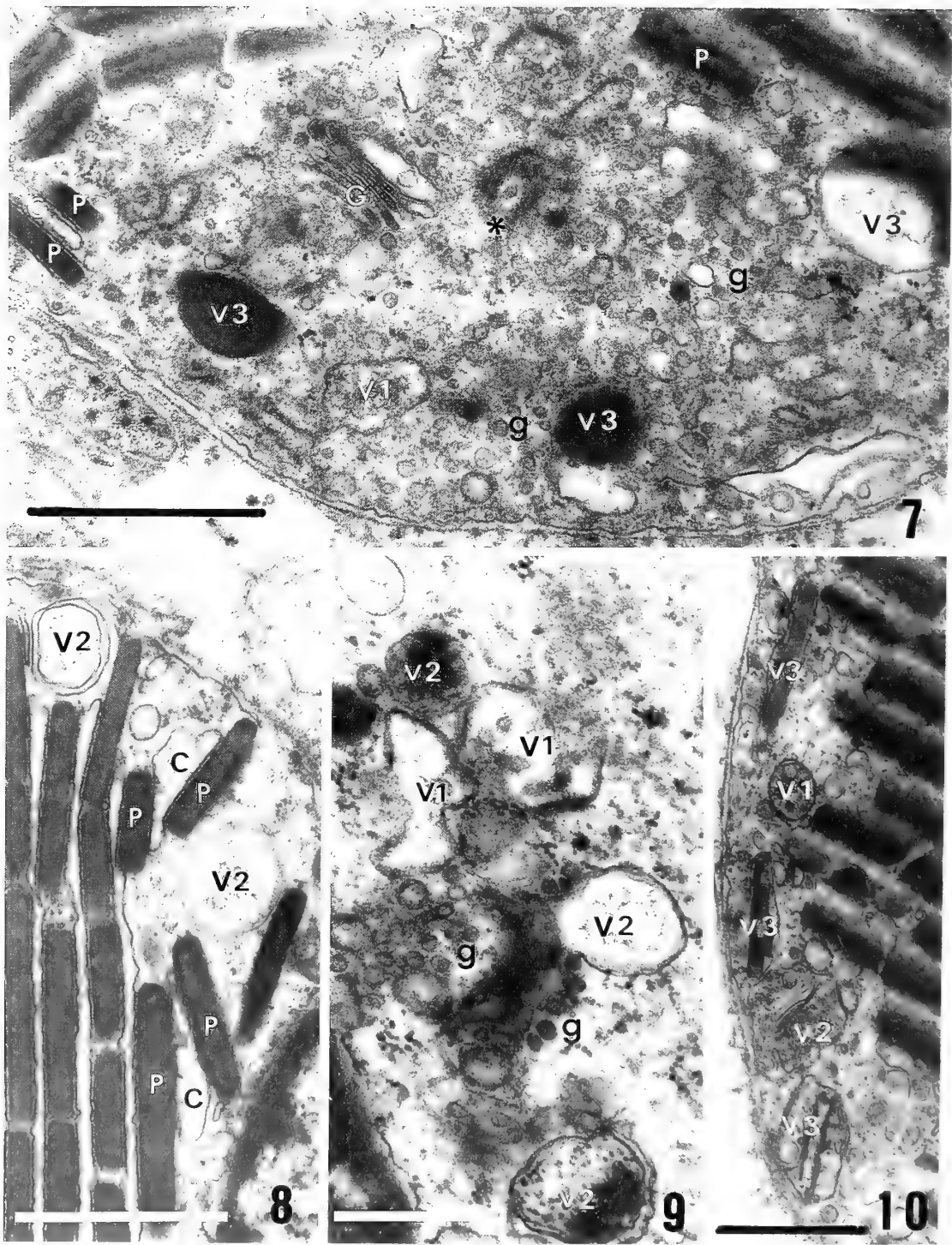


FIG. 5. Para-horizontal section through the platelets (P). Platelets are rectangular in shape and differ in size. They are arranged closely side by side to form a single plane of the reflecting surface. Bar indicates $1\ \mu\text{m}$. $\times 21,000$

FIG. 6. Higher magnification of reflecting platelets in transverse profiles. Each platelet (P) is enveloped with a membrane (E). The envelope is separated from the inner platelet mass by $3\ \text{nm}$. The platelet shows fine substructure of $7\ \text{nm}$ lattice. The cisterns (C) with $60\ \text{nm}$ width are observed between neighbouring platelets. Bar indicates $0.1\ \mu\text{m}$. $\times 150,000$.



In the platelet forming area, three types of vacuoles were observed (Figs. 7–12). The first type of vacuole (marked as V1 in Figs. 7, 9 and 10) was irregular in shape and resembled distended rough surfaced endoplasmic reticulum. Some of these vacuoles contained various cytoplasmic components, such as vesicles and ribosome-like granules. The second type of vacuole (marked as V2 in micrographs) were round in profile and contained fluffy materials in the lumen. The second type of vacuole had a complex internal membrane structure and often appeared as a double walled vacuole (Figs. 8, 10–12). The last type (marked as V3 in micrographs) often had an elipsoidal or even elongated shape and contained a dense amorphous substance which was similar in appearance to the internal mass of the reflecting platelet.

A cluster of vesicles or smaller cisterns (marked as Vs in Figs. 3, 4 and 13) were observed along the developing platelets. These vesicles were aligned in a line at the place of the cistern between neighbouring platelets. Newly formed platelets were often seen in close contact, because of the absence of an intervening cistern (Fig. 12). Golgi bodies were often found in the platelet forming area in iridoblasts (Fig. 7). The outer lamella of the Golgi stack was distended in these cells. Golgi vesicles were also seen associated with the vacuoles or the developing platelets (Figs. 9 and 11). Some of the Golgi vesicles were seen directly fusing with the limiting membrane of the developing platelet (Fig. 11). The lumina of the Golgi lamellae and vesicles were filled with opaque mate-

rial. Centrioles were often detected in close association with the Golgi complex. Microtubules were seen radiating from the centriole.

DISCUSSION

The overall appearance of the clam iridophores resembled those in cephalopods [2] and vertebrates [4, 8, 18]. The cytoplasm of the cell is fully occupied with tightly packed reflecting platelets. Platelets are aligned in rows and form multiple reflecting planes at each interface with the cytoplasm. Each platelet is bound with a membrane: the envelope. The membrane measures 7 nm in thickness and its dimensions are virtually identical to those of the plasma or cisternal membrane. The platelet is rectangular in shape and it has uniform thickness in each cell. The dimension, however, differs from cell to cell, ranging from 80 nm to 120 nm. The reflecting body of the platelet is electron dense and has a fine lattice that resembles the paracrystalline structure of proteins.

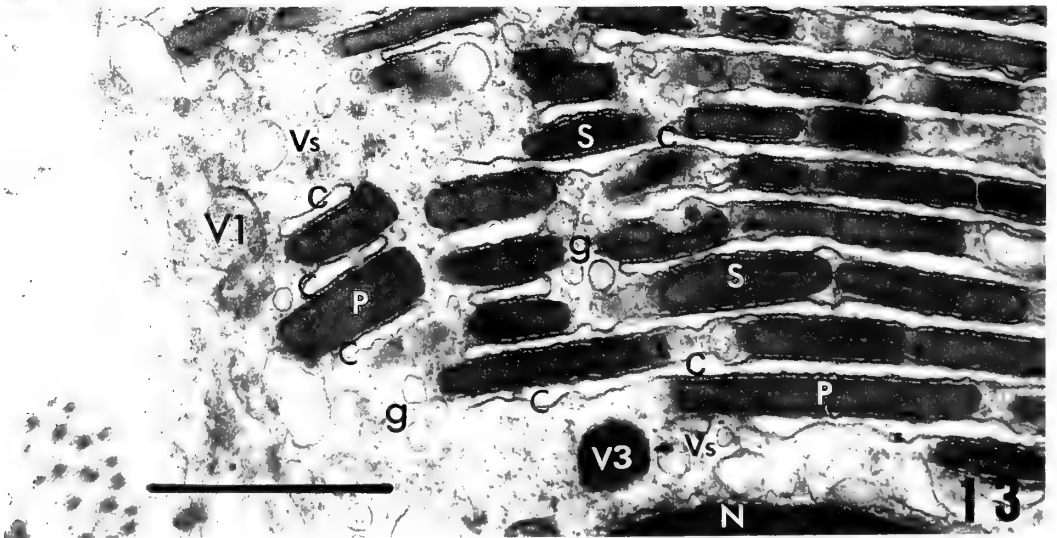
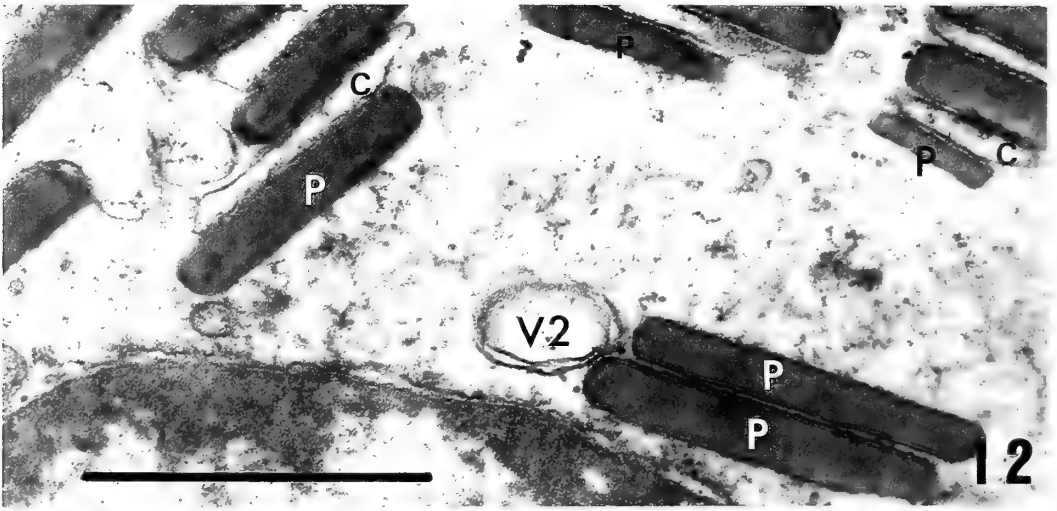
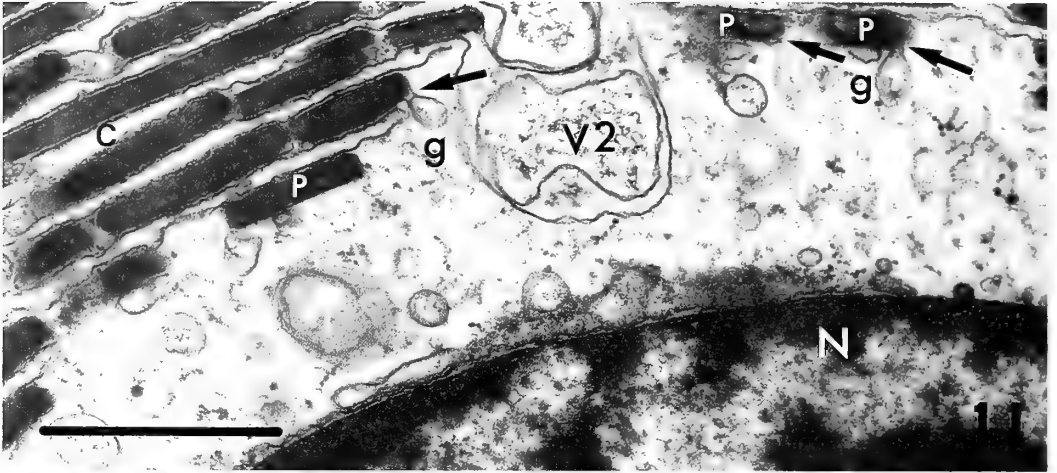
There are long and flat cisterns tightly secured between the rows of membrane bound platelets. Since the cistern is fairly uniform in width measuring 50 nm to 60 nm, the space between platelets is also kept in uniform. The intervening cistern illustrates the mechanism that secures the interplatelet space at a definite distance which is required for the efficient coloration of the iridophores [18]. In this respect, the clam iridophores differ from the cephalopod iridophores, in which the space between the platelets is the

FIG. 7. The platelet forming area near the cell periphery of a developing iridoblast. Diverse forms of vacuoles (V1 and V3) are seen around the Golgi body (G) and the centriole (*). Golgi vesicles (g) are seen associated with vacuoles. Some of vacuoles (V3) show the same internal density with the developing platelets (P). A small cistern (c) is observed between developing platelets on the left of the micrograph. Bar indicates 1 μm . $\times 35,800$.

FIG. 8. Platelet forming area where some of vacuoles are seen double walled (V2). Fluffy material in the vacuoles appears similar to the cytoplasmic matrices. Developing cistern (C) formed by fusion of vesicles are seen between two developing platelets (P). Bar indicates 1 μm . $\times 32,000$

FIG. 9. Another platelet forming area showing condensation of dense material in the vacuole (V1 and V2). Vesicles, ribosome-like granules and fluffy materials are seen in the lumina of the vacuoles. Some vacuoles (V2) are double walled. Golgi vesicles (g) are seen accumulating around the vacuole with dense materials. Bar indicates 0.5 μm . $\times 45,000$

FIG. 10. Vacuoles showing transitional stages of the platelet formation. Condensation process of the dense materials is seen in the developing platelets (marked V1, V2, and V3, which indicate the transitional vacuoles in the numerical order). Vacuole at the final stage (V3) appears almost similar to the platelet, except its loose envelope and less dense internal mass. Cytoplasmic components are seen inside of all vacuoles. Transverse sections through the dense mass of the V3 vacuoles are shown as V3s in Figs. 7 and 13. Bar indicates 1 μm . $\times 23,000$



extracellular, so that the platelet is not bound to membrane and is free in the cytoplasm [3, 9, 6, 10].

As well as the structural organization, the physical or chemical nature of the platelet may influence the coloration of the cell. Clam iridophores are sectioned smoothly on the glass knives, suggesting pliability of the platelet element, while purine (such as guanine) platelets in vertebrate iridophores are brittle, so that well sectioned profiles for electron microscopy are not easily obtainable. Thus, purines do not seem to be the major component of platelets in the clam iridophore. The platelets in cephalopod iridophores are also readily sectioned and appeared similar to those of clam iridophores under the electron microscope [2, 3, 7]. There have been diverse reports on the nature of platelets in cephalopod iridophores, such as guanine [3], purines [7], chitin [11] or protein [6, 9]. The paracrystalline structure with fine lattice observed in this study may indicate that the platelet in clam iridophores is mainly of proteinaceous rather than purine nature, although the latter cannot totally be excluded.

Clam iridophores display various colorations ranging from blue to yellow-green, or sometimes even to red, depending on their distribution. This indicates that the thickness and/or arrangement of reflecting platelets differ according to the cell. As mentioned previously, the thickness differs from cell to cell ranging from 80 nm to 120 nm, although it is fairly uniform within a single cell. Providing that the optical path of the reflecting layer in efficient iridophores equals a quarter wavelength of the reflected spectrum [12, 18], the platelet in clam iridophores which has blue to red interference colors and a thickness ranging from 80 nm to 120 nm seems to have a refractive index (n) of

around 1.5. This is almost the same value as that of chitin [11].

In developing iridoblast, platelets are formed in a confined area around the nucleus. In this platelet forming area various organelles, such as endoplasmic reticula, vesicles and vacuoles are found. The vacuole seems to be derived from the endoplasmic reticulum and finally become a platelet envelope, because various forms that suggest a gradual transition from the distended endoplasmic reticulum (V1) to the envelope (V3) are observed in the area. Vacuoles containing vesicles and ribosome granules (V1) are morphologically similar to the "vesiculo-globular bodies" or the "multivesicular bodies" observed in developing melanoblasts in mouse skin [13] or goldfish fin [14], respectively. These vacuoles seem to be in the earlier stages of the platelet formation in the giant clam iridophores and are considered to be equivalent forms to the primordial vesicle proposed by Bagnara [15, 16] for the common precursor to all pigment organelles in vertebrate chromatophores. Double walled vacuoles are frequently seen in the platelet forming area (V2 in Figs. 9, 11 and 12). The similar structure in vertebrate iridoblasts (double walled saccule) is shown to be formed by an invagination or infolding of a vacuole (7). However, this is not demonstrated in the clam iridoblasts.

The accumulation process of the dense reflecting material is also shown in transitional internal structures of the vacuoles. Since the lumina of the earlier vacuoles are slightly denser than the cytoplasm, the accumulation of the reflecting material in these vacuoles seems to have a low concentration (V1 and V2). In the later stage of the vacuole, dense materials appear at the middle of the vacuole and are gradually condensed into a rec-

FIG. 11. A portion of the platelet forming area. No cistern are observed along the developing platelets (P) at the margin of the row. Golgi vesicles are seen fusing with the limiting membrane of the developing platelets (arrows). Double walled vacuole (V2) with fluffy material in the lumen is seen close to the developing platelets. Bar indicates 1 μ m. $\times 32,500$

FIG. 12. Newly formed platelets (P) which are not yet arranged into a row are seen near the nucleus. These platelets show clear limiting membrane, but have no intervening cistern, so that they are closely contacted each other. Bar indicates 1 μ m. $\times 46,000$

FIG. 13. Platelet forming area where developing platelets (P) dispose at the margin of the platelet row. A series of vesicles (Vs) are seen at the position of the cistern. Newly formed cisterns (c) which still appear as flattened vesicles are positioned both sides of the developing platelets. Developing platelets show transitional forms from spherical one (V3), to spindle (S), or rectangular (P) one. Bar indicates 1 μ m. $\times 32,000$

tagular platelet mass (Fig. 11, V3). When the vacuole in this stage is sectioned through the dense accumulation at the middle, it appears as a dark vacuole (Fig. 7). The incorporation of Golgi vesicles onto the developing platelets is frequently observed (Figs. 7 and 11). The involvement of the Golgi vesicles may indicate the possibility of protein and/or carbohydrate (chitinous) as components of the reflecting platelet in the giant clam.

The intervening cisterns are formed from vesicles (Vs in Figs. 3 and 4). These vesicles are also dilated, but are somewhat smaller than the vacuoles involved in the platelet formation. Dilated vesicles are seen to be depressed between small developing platelets which are not yet assembled in rows (Figs. 8 and 13). These vesicles are opaque in appearance and contain flocculent matters in the lumina. They appear in a line between developing platelets and seem to fuse with each other to form a long and flat cistern (Figs. 3 and 4).

ACKNOWLEDGMENTS

The author is greatly indebted to Professor Siro Kawaguti of Kawasaki Paramedical School for kindly providing the materials, and is also very much grateful for his valuable suggestions during the work.

REFERENCES

- 1 Kawaguti, S. and Kamishima, Y. (1964) Electron microscopic study on the iridophores of opisthobranchiate mollusks. *Biol. J. Okayama Univ.*, **10**: 93–103.
- 2 Kawaguti, S. and Ohgishi, S. (1962) Electron microscopic study on iridophores of a cuttlefish, *Sepia esculenta*. *Biol. J. Okayama Univ.*, **8**: 115–129.
- 3 Arnold, M. (1967) Organellogenesis of the cephalopod iridophore: Cytoembranes in development. *J. Ultrastruct. Res.*, **20**: 410–421.
- 4 Kawaguti, S. (1966) Electron microscopy on the mantle of the giant clam with special references to zooxanthellae and iridophores. *Biol. J. Okayama Univ.*, **12**: 81–92.
- 5 Kawaguti, S. (1968) Electron microscopy on zooxanthella in the mantle and gill of the heart shell. *Biol. J. Okayama Univ.*, **14**: 1–11.
- 6 Brocco, S. L. and Cloney, R. A. (1980) Reflector cells in the skin of *Octopus dofleini*. *Cell Tissue Res.*, **205**: 167–186.
- 7 Kamishima, Y. (1981) Reflecting platelet formation in iridophores. In "Phenotypic Expression in Pigment Cells". Ed. by M. Seiji, Univ. Tokyo Press, Tokyo, pp. 279–284.
- 8 Kawaguti, S. (1965) Electron microscopy on iridophores in the scale of the blue wrasse, *Proc. Japan Acad.*, **41**: 610–613.
- 9 Mirow, S. (1972) Skin color in the squids, *Loligo pealii* and *Loligo opalescens*. II. Iridophores. *Z. Zellforsch.*, **125**: 176–190.
- 10 Cooper, K. M. and Hanlon, R. T. (1986) Correlation of iridescence with changes in iridophore platelet ultrastructure in the squid, *Lolliguncula brevis*. *J. Exp. Biol.*, **121**: 451–455.
- 11 Denton, E. J. and Land, M. F. (1971) Mechanism of reflexion in silvery layers of fish and cephalopod. *Proc. Roy. Soc. Lond.*, **A175**: 43–61.
- 12 Land, M. F. (1966) A multilayer interference reflector in the eye of the scallop, *Pecten maximus*. *J. Exp. Biol.*, **45**: 433–447.
- 13 Takeuchi, T. and Ishiguro, S. and Tamate, H. B. (1981) Gene expression in melanosome formation. In "Phenotypic Expression in Pigment Cells". Ed. by M. Seiji, Univ. Tokyo Press, Tokyo, pp. 139–144.
- 14 Turner, Jr., W. A., Taylor, J. D. and Tchen, T. T. (1975) Melanosome formation in the goldfish: the role of multivesicular bodies. *J. Ultrastruct. Res.*, **51**: 16–31.
- 15 Bagnara, J. T., Turner, W. A., Rothstein, J., Ferris, W. and Taylor, J. D. (1979) Chromatophore organellogenesis. In "Pigment Cell". Ed. by S. N. Klaus, S. Karger, Basel, Vol. 4, pp. 13–27.
- 16 Bagnara, J. T. (1983) Developmental aspects of vertebrate chromatophores. *Amer. Zool.*, **23**: 465–478.
- 17 Kamishima, Y. (1979) Electronmicroscopic study on reflecting platelets in the dorsal iridophores of the sand eel, *Ammodytes personatus* GIRARD. *Proc. Japan Acad.*, **B54**: 634–639.
- 18 Kasukawa, H., Oshima, N. and Fujii, R. (1987) Mechanism of light reflection in blue damselfish motile iridophore. *Zool. Sci.*, **4**: 243–257.

Notes on the Development of the Crab-Eating Frog, *Rana cancrivora*

MINORU UCHIYAMA, TOSHIKI MURAKAMI and HIDEKI YOSHIZAWA¹

Department of Oral Physiology, School of Dentistry at Niigata, The Nippon
Dental University, Niigata 951, and ¹Department of Oral Histology,
Matsumoto Dental College, Shiojiri 399-07, Japan

ABSTRACT—Fertilized eggs were obtained from a pair of crab-eating frogs collected in a mangrove swamp in Thailand at the end of April. The tadpoles grew well when both parents and eggs were maintained in 10% seawater, although eggs from a pair of frogs kept in 50% seawater did not develop in 10% seawater. Clutch size was about 1800. Each egg was 1.2–1.3 mm in diameter. Embryonic development was fairly rapid. Hatching took place 27 hr after fertilization at 24.5–26.0°C. Individual variation in the progress of embryonic and larval development was large. In the most rapidly growing tadpoles, metamorphosis took place 44 days after spawning in 10% seawater. On the other hand, at higher salinities (40–100% seawater) development tended to be delayed and tadpoles remained between stages V and XV (Taylor-Kollros stages) 55 days after fertilization.

INTRODUCTION

The tadpole of the crab-eating frog, *Rana cancrivora*, is the only amphibian larva which lives naturally in brackish water [1, 2]. However, it is not clear what mechanisms make this possible. It is, therefore, important to raise tadpoles of this species in the laboratory as a first step toward elucidating the physiological mechanisms of salt water adaptation. Alcalá [1] described the development of this tadpole raised from eggs collected in the field with two tables and two figures. However, he did not show the correct timetable subsequent to fertilization. Later, Gordon and Tucker [2] reported failure to raise artificially fertilized eggs of this frog in various dilutions of seawater.

In the present study, spawning was induced by injection of pituitary homogenates and development was observed carefully under laboratory conditions. The embryonic stages were judged according to the developmental stages for *R. pipiens* described by Witschi [3] and the subsequent larval stages were those described by Taylor and Kollros [4].

MATERIALS AND METHODS

Adult males and females of the crab-eating frog, *Rana cancrivora*, were captured around prawn culture-ponds (salinity 33‰) located in a mangrove swamp at Ang-Sila near Bangkok, Thailand, in late April 1987. They were shipped by air to the laboratory in Niigata, Japan and maintained in 10–50% seawater (3.5–18‰) at 25.0–26.0°C. Body weight was 20–60 g for both sexes. On June 15 1987, two pairs of the adult frogs kept in 10% seawater were injected with pituitary homogenate (one pituitary gland per frog) of *R. brevipoda porosa* and kept in a plastic tank containing 10% seawater. A pair of frogs was found to be clasping the following day and repeat injections were given to them. At 6 hr after the 2nd injection, spawning took place and the eggs were fertilized simultaneously by the male. The fertilized eggs were maintained in 10% seawater at 24.5–26.0°C. Some of the eggs were kept in small dishes for detailed observations on development. When the embryos reached stage 23, they were divided into small groups (5–20 tadpoles). All observations on developmental stage were made using a binocular dissecting microscope. Tadpoles were anesthetized by means of ice and body length was measured. Pictures were taken through the dissecting

microscope. After the tadpoles had started to swim, they were transferred into tall-skirted dishes kept at 28.0°C. The tadpoles were fed on freshly bioled spinach twice a week, and the water (10% seawater) was changed every day.

Acclimation to various dilutions of seawater

Eggs were transferred into aged tap-water, 10% and 20% seawater. Tadpoles of stages 21-XV were acclimated directly to various dilutions of seawater (tap-water to 100% seawater). Tadpoles of stages 24-XV were also acclimated in steps with 10–20% changes of salinity every 2–7 days.

OBSERVATIONS

Breeding behavior and spawning

As noted above, injection with the pituitary homogenates induced breeding behavior: the clasping is axillary and the male having pigmented vocal sacs pushed rhythmically the female's side and called. This breeding behavior was also observed in mature frogs kept in 50% seawater upon injection of pituitary homogenate and transfer to 10% seawater. Six hr later, eggs were laid. Eggs from parents that had been kept in 10% seawater developed rapidly. On the other hand, eggs from parents that had been kept in 50% seawater did not develop.

Eggs and early developmental stages

Fertilized eggs formed egg masses of 6 to several hundreds of eggs and floated on the surface of the water. Eggs were about 1.2–1.3 mm in diameter and were encapsulated within two transparent layers, the outer layer being very sticky. Clutch size was about 1800. The color of the eggs was brown in the animal hemisphere and yellowish-white in the vegetal one. Embryonic development proceeded fairly rapidly and hatching was

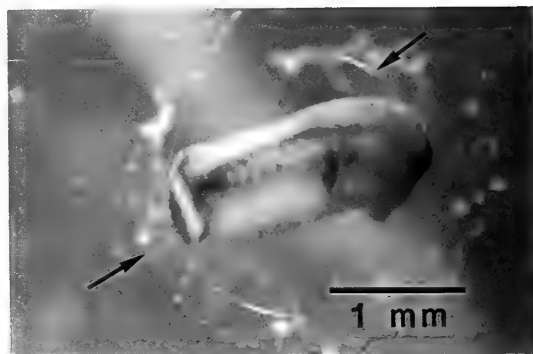


FIG. 1. Stage 20. An embryo moving its tail actively just before hatching. Arrows indicate two layers of the capsule.

observed 27 hr after fertilization. Before hatching, embryos actively moved their tails within the capsule (Fig. 1). After hatching, embryos lay on the bottom of the tank. Thirty hr after fertilization, the external gills were completely developed and the tadpoles swam around. Thereafter, the right external gills began to be covered with the opercular fold, and 96 hr after fertilization both sides of the operculum were completed with a respiratory pore in the left side. The tadpoles at stage 25 were ventro-dorsally compressed. The dorsal and ventral fins were relatively wide. The abdomen was convex and the cloaca opened to the right side. These observations are summarized in Table 1 and Figure 2A-Q.

Larval development (limb bud stage-juvenile)

Fourteen days after fertilization, a pair of hind-limb buds emerged. In tadpoles at stage IV, the tooth row was fully developed with the dental formula, $\frac{1:1+1}{3}$ (Fig. 3).

The tadpoles usually stayed on the bottom of the dish. Before stage I, the skin of the tadpoles was translucent, the color of the back brown, and melanophores were deposited on the dermis of the abdomen. Tadpoles after stage I were yellowish-

FIG. 2. A, Stage I; B, Stage 5; C, Stage 6; D, Stage 7; E, Stage 8; F, Stage 13; G, Stage 14; H, Stage 15; I, Stage 16; J, Stage 18; K, Stage 19; L, Stage 20; M, Stage 21; N, Stage 22; O, Stage 23; P, Stage 24; Q, Stage 25; R, Stage IV; S, Stage XV; T, Stage XX; U, Stage XXII; V, Stage XXIV; W, Stage XXV. Scale bars indicate 1 mm (A-Q), and 1 cm (R-W). Arrow indicates deposit of guanophores on the abdominal skin in tadpole of stage XV.

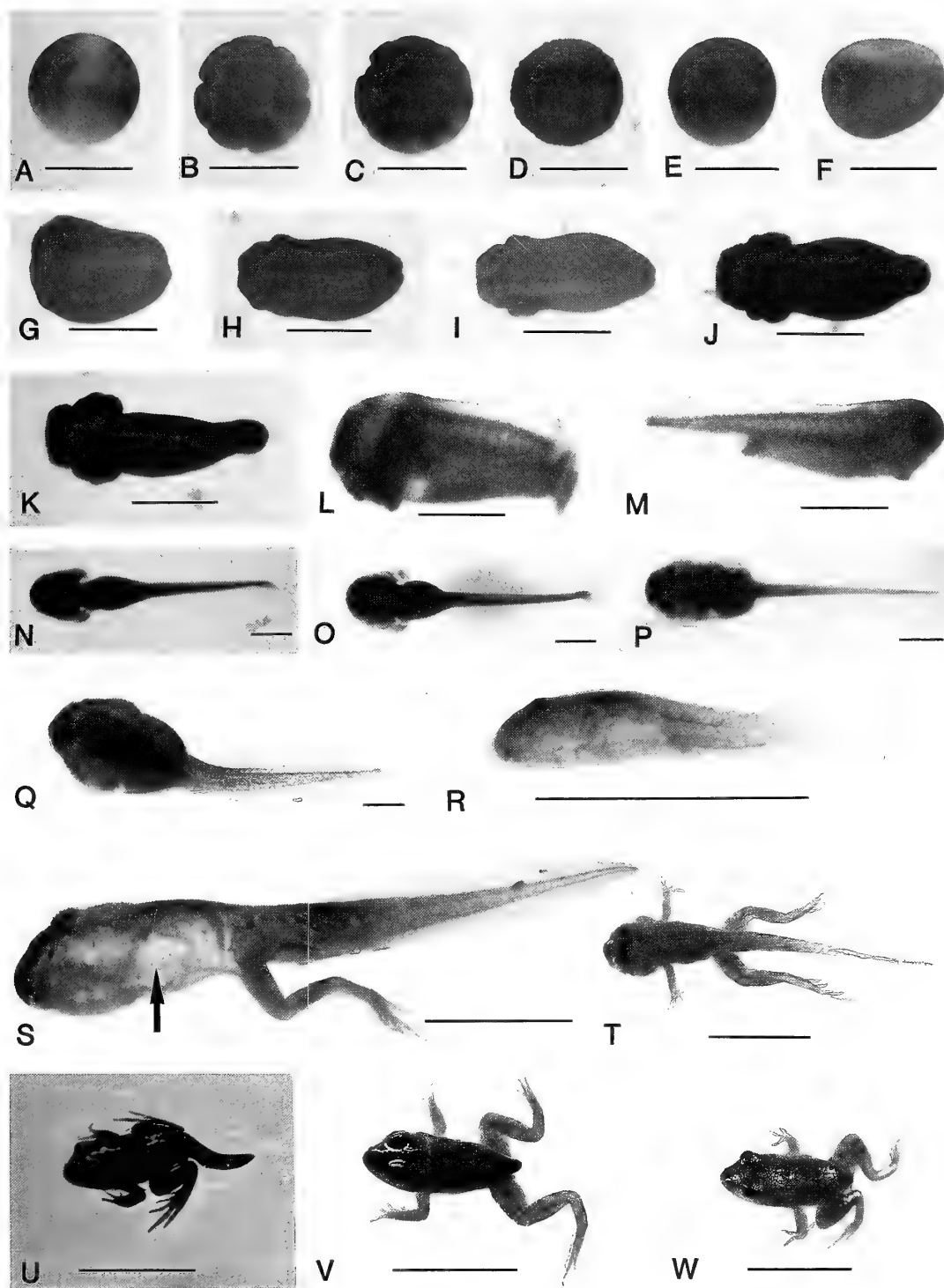


TABLE 1. Early larval development of *Rana cancrivora* in 10% seawater (water temperature 24.5–26°C)

Stage	Time after fertilization (hr:min)	Notes
1	0:05	Egg is encapsulated by two layers. Diameter of egg is 1.2–1.3 mm (Fig. 2A).
4	1:20	Period of cleavage (Fig. 2B-D).
6	3:20	
8	4:30	Blastula stage (Fig. 2E).
11	7:30	Period of gastrulation.
12	8:30	Primitive streak stage.
13	10:30	Embryo elongated. Flattened on dorsal surface of embryo (Fig. 2F).
14	11:30	Blastopore closed (Fig. 2G).
15	12:30	Neural plate stage (Fig. 2H).
16	14:00	Neural tube stage (Fig. 2I).
17	15:30	Tail bud stage. *Total length 1.8 mm.
18	16:30	Tail bud elongated (Fig. 2J). Oral sucker distinct. Total length 1.9 mm.
19	18:00	The 1st and 2nd external gill buds become visible (Fig. 2K). Total length 2.05 mm.
20	25:00	Tail of embryo is curved (Fig. 2L).
21	27:00	Spontaneous hatching (Fig. 2M). Larvae lie on the bottom. Total length 3.4–4.4 mm.
22	30:00	Larvae begin to swim. Body is asymmetrical (Fig. 2N). Total length 4.0–4.2 mm.
23	51:00	Abdomen becomes round (Fig. 2O). Total length 4.0–5.5 mm.
24	62:00	Right external gills are covered by opercular fold. Total length 6.0–6.2 mm.
25	96:00	Left external gills are covered (Fig. 2P, Q). Total length 6.2–6.5 mm.

* Total length is defined as the length from tip of snout to tip of tail.



FIG. 3. Oral part of tadpole at stage X, dental formula being $\frac{1:1+1}{3}$.

gray in color on the back and silver on the abdomen due to guanophore deposition. Development proceeded fairly rapidly. It took 44 days after fertilization to begin metamorphosis in the most rapidly growing tadpole. There were large individual differences in the progress of larval development, but no cannibalism was observed. The froglets at the metamorphic climax (stage XXIII) could not climb the glass wall of the dish. These observations are summarized in Table 2 and Figure 2R-W.

Acclimation to various dilutions of seawater

Fertilized eggs developed well in tap-water, and 10% and 20% seawater. When hatchlings (stage 22) were transferred directly from 10% seawater to

TABLE 2. Larval development of *Rana cancrivora* in 10% seawater (water temperature 28°C)

Stage	Time after fertilization* (days)	Total length** (mm)	Notes
I	15***	6.6–10.0***	Limb buds become visible.
III	33	6.6–12.5	Length of limb bud equal to its diameter.
IV	20	17.0	Horny teeth fully developed (Fig. 2R).
V	24	21.1	Pigmentation evident on abdomen.
VI	27–43	26.0–29.0	Limb buds paddle-shaped.
X	27–52	31.1–32.0	Five toes distinct.
XII	44	28.0	
XIII	50	32.0	
XIV	44	30.0–35.0	Toe pads appear.
XV	30–50	33.0–45.0	Hindlimbs elongate (Fig. 2S).
XVIII	44	37.0–42.0	Cloacal tail-piece disappears.
XIX	39	33.0–40.0	Skin windows become clear.
XX	36		Forelimbs appear (Fig. 2T).
XXI	39		Tail fins absorbed.
XXII	50	26.0–32.0	Tail shorter than hindlimbs (Fig. 2U).
XXIII	42–46	19.0	
XXIV	43	13.0	Stub of tail remains (Fig. 2V).
XXV	44		Metamorphosis accomplished (Fig. 2W).

* Individual variation in the progress of development was large.

** Total length is defined as the length from tip of snout to tip of tail and to vent in tadpole and frog, respectively.

*** Number of animals used for measurements was 1–5.

various dilutions of seawater (tap-water to 100%), they became well acclimated to environments up to 40% seawater. However, tadpoles transferred to 50% seawater or higher concentrations could not acclimated and all died within 8 hr. When environmental salinity was increased stepwise, tadpoles (stages I–XV) were able to adapt to higher salinities (tap-water to 100% seawater). Metamorphosis took place in tadpoles kept in tap-water and 10% seawater. On the other hand, at 55 days after fertilization, tadpoles kept in 40–100% seawater still remained between stages V and XV, without any indication of metamorphosis.

DISCUSSION

This is probably the first report on fertilized eggs of *R. cancrivora* being obtained by artificial induction of spawning and on young frogs being raised in the laboratory. The characteristics, including the size and time of development, of eggs and

tadpoles observed in the present study were fairly consistent with those reported by Alcalá [1]. Therefore, the present observations seem to reflect the normal breeding behavior and development of this species in the field. The developmental process of this species is similar to that of *R. pipiens*, except that development proceeds very rapidly. In the present study, metamorphosis took place in the most rapidly growing tadpoles 44 days after spawning at about 28°C. On the other hand, Taylor and Kollros [4] reported that *R. pipiens* larvae metamorphosed at an age of over 90 days at room temperature (about 20°C).

Gordon and Tucker [2] reported that no development was observed when eggs from frogs kept in 60% seawater were artificially fertilized in 20% seawater. However, the first few cleavages occurred when eggs from adults kept in 20% seawater were artificially fertilized and placed in either fresh water or 20% seawater. They [2] also suggested from their field data that spawning might

occur only during and soon after heavy rains when the salinity of the spawning pools becomes low. In the present study, frogs kept in 50% seawater showed breeding behavior, but eggs were undeveloped even when removed to 10% seawater after fertilization. These results, therefore, suggest that it is necessary for frogs and eggs to be kept in hypoosmotic media in order for them to develop.

In the tolerance experiments, although the tadpoles at developmental stages III-XIX were able to survive well at all salinities from fresh water to full-strength seawater (32‰), eggs and tadpoles before stage 25 could not stay in high salinity [2, 5]. Early development (stages 1-25) proceeded rapidly until 4 days after fertilization, and it then took about 10 days until the appearance of limb buds (stage I). During the period between stage 25 and stage I, the skin grew to be thick. This morphological change may be one of the factors for salt tolerance of tadpoles at these stages. Gordon and Tucker [2] observed that metamorphosis is hindered by salinities higher than 20% seawater, and suggested from the field data that metamorphosis is delayed as long as the pond salinity remains high. The present observations are consistent with their suggestion. Metamorphosis took place in tadpoles kept in tap-water and 10% seawater and development of tadpoles kept in higher salinities (40-100% seawater) was delayed. These results may suggest that a low-salinity environment is necessary for the induction of both metamorphosis and spawning.

According to the previous observations [1, 2] and the present study, it can be speculated that the following may occur in nature. After heavy rain-

fall during the rainy season, spawning occurs and early embryonic development proceeds rapidly in low-salinity and high-temperature water. Then, when the tadpoles acquire salinity tolerance they can survive in higher-salinity water. Thereafter, the development of tadpoles proceeds further and metamorphosis is accomplished when water salinity becomes low after the next heavy rainfall. The rapid advance of development in this species must therefore be favored by an environment where the salinity changes markedly.

ACKNOWLEDGMENTS

This study was supported in part by a Grant-in-Aid for Overseas Scientific Research (No. 62041035) from the Ministry of Education, Science and Culture of Japan. The authors wish to thank Prof. Chitaru Oguro of Toyama University (project leader) for his thoughtful arrangement of the project.

REFERENCES

1. Alcalá, A. C. (1962) Breeding behavior and early development of frogs of Negros, Philippine Islands. *Copeia*, **4**: 679-726.
2. Gordon, M. S. and Tucker, V. A. (1965) Osmotic regulation in the tadpoles of the crab-eating frog (*Rana cancrivora*). *J. Exp. Biol.*, **42**: 437-445.
3. Witschi, E. (1956) Development of Vertebrates. W. B. Saunders Co., Philadelphia, pp. 78-84.
4. Taylor, A. C. and Kollros, J. J. (1946) Stages in the normal development of *Rana pipiens* larvae. *Anat. Rec.*, **94**: 7-23.
5. Uchiyama, M., Murakami, T., Wakasugi, C. and Sudara, S. (1987) Development and salinity tolerance in tadpoles of the crab-eating frog. *Zool. Sci.*, **4**: 1077.

Reaction Mass Formation in *Drosophila*, with Notes on a Phenoloxidase Activation

NOBUHIKO ASADA¹ and TAKASHI FUKUMITSU

Biological Laboratory, Faculty of Science, Okayama University of Science,
Okayama 700, Japan

ABSTRACT—In the supernatant fraction of the adult *Drosophila*, phenoloxidase activity was detected by the use of SDS-PAGE and spectrophotometry. The level of phenoloxidase activity increased within six minutes after the initiation of copulation. The length of time of reaction mass formation corresponded to the increase of phenoloxidase activity after the initiation of copulation in a copulated female. The reaction mass formation in mated female *Drosophila* was, in part, considered to be in relation to phenoloxidase activation after copulation.

Abbreviations

Phenoloxidase: *o*-diphenol: O₂ oxidoreductase, EC 1.10.3.1

SDS-PAGE: Sodium dodecyl sulfate-polyacrylamide gel electrophoresis

p-NPGb: *p*-nitrophenyl-*p*'-guanidinobenzoate

EDTA: Ethylenediaminetetraacetic acid

Dopa: L-3, 4-dihydroxyphenylalanine

Dopa chrome: 2, 3-dioxyindole-5, 6-quinone-2-carboxylic acid

MW: Molecular weight

K: Kilodalton

INTRODUCTION

In *Drosophila*, reaction mass, which is to be found in the female uterus, is formed immediately after copulation associated with the insemination reaction [1–6]. It takes place just after the initiation of copulation, within 10 min, in both intra- and interspecific crosses. Early studies revealed that it played a role that led to preparation of the reproductive tract for oviposition and had a bearing on the problem of speciation process in intraspecific crosses, because reaction mass remained soft and unmelanized then disappeared,

probably by proteolysis, *in vivo* prior to oviposition. On the other hand, in interspecific crosses, reaction mass that remained in the uterus prevented oviposition resulting in a failure of hybrid production. Therefore reaction mass seems to play an important role not only in fecundity, but also as a primitive self-defense response in *Drosophila*. Biochemical studies revealed that reaction mass formation was likely to be a consequence of polymerization and/or conformational change(s) of phenol-containing substance(s) involving the same course of the melanization cascade reaction [6–7]. In this article, the relationship between the reaction mass formation and the key enzyme for melanization, phenoloxidase, is discussed.

MATERIALS AND METHODS

1. Flies

Wild type flies of *Drosophila nasuta* (ADM-1 strain, Andaman, India; MYS-23 strain, Mysore, India; SEZ-2 strain, Seychelles) and *D. pallidifrons* (PNI-74 and PNI-110 strains, Ponape, Caroline Islands) were used in this study. All flies were iso-female strains caught in nature. *D. pallidifrons* has been regarded as an ancestral species and *D. nasuta* has been thought to be a derived species from *D. pallidifrons* [8]. Culture condition and preparation of flies were performed in the same manner as described in Insemination reaction in the *Drosophila nasuta* subgroup [6].

2. Temperature shift

Two experiments were performed. Virgin females and males, four-day-old, were put together in a glass vial (30 mm in diameter, 110

Accepted March 3, 1989

Received August 22, 1989

¹ To whom all correspondence should be addressed.

mm in depth) at 25°C. To observe the copulation, approximately 30 pairs were placed together in the vial. In Experiment-1 (Ex-1), the vials containing the copulating pairs were removed from 25°C and replaced in 2°C within two min after the initiation of copulation. After five hr at 2°C, females were dissected in the *Drosophila* Ringer solution [9] and were examined to determine whether reaction mass was produced in the uterus. In Ex-2, copulating pairs were placed at 2°C in the same manner as Ex-1; then the females were separated to avoid remating, and the culture temperature was raised from 2 to 25°C. After four hr at 25°C, females were dissected and examined. Fifty pairs were run for each experiment.

3. Preparation of samples

A crude extract was prepared to test for the presence of phenoloxidase and to study the kinetics of the activity. Five individuals of four-day-old adult flies were homogenized in the solution containing 50 μ l of a 0.1 M phosphate buffer solution (PBS), pH 6.0, at 0°C. Homogenate was centrifuged at 12,000 round per min (rpm) for five min at 4°C, then supernatant fraction was subjected to SDS-PAGE. To assay the phenoloxidase activity, adult flies were homogenized in the PBS mentioned above adding 25 μ l of a specific serine protease inhibitor, *p*-NPGB dissolved in dimethylformamide and diluted with acetonitrile (final concentration 0.01 M) and 25 μ l of a 10 mM EDTA.

4. SDS-PAGE

The crude extract was dissolved in 50 μ l of a sample buffer solution containing 0.0625 M Tris, 2% SDS, 5% 2-mercaptoethanol, pH 6.0, and a small amount of bromothymol blue. Extracts boiled for two min were also prepared. The samples were separated by 10% SDS-PAGE according to the buffer system of Laemmli [10] for the slab gel (2 mm gel thickness). Electrophoresis was run for about 10 hr at a constant current of 20 mA, 65 V at the initial stage. Phenoloxidase activity was detected by staining with a 0.013 M dopa in a 0.1 M PBS, pH 6.0 used as a substrate buffer solution for several min at 37°C.

5. In vitro melanization and phenoloxidase activity

In vitro melanogenesis of reaction mass was performed. A single reaction mass collected from the uterus of a copulated female was rinsed three times in a PBS, pH 6.8, and then soaked at 25°C in a substrate of 5×10^{-5} M dopa. Melanization of the reaction mass was observed at regular intervals, and the score was expressed in the same manner as Hiruma and Riddiford [11].

Phenoloxidase activity was determined at 2, 5, 10 and 15 min from the beginning of the initiation of copulation. The reason for these specific times being that the average duration of copulation in intraspecific crosses of *D. nasuta* and *D. pallidifrons* and interspecific crosses between *D. pallidifrons* females and *D. nasuta* males was approximately 16, 10 and 12 min, respectively [6]. Phenoloxidase activity was assayed from the supernatant fraction just after adding 1 ml of a PBS and 1 ml of a 30% acetic acid. The color intensity of dopa chrome was measured colorimetrically by a Hitachi Model-101 Spectrophotometer at 475 nm. Two replications were run at each observation time.

RESULTS AND DISCUSSION

Temperature dependency and in vitro melanization of reaction mass

Results of Ex-1 and Ex-2 are summarized in Table 1. In the controled experiment, high frequencies of reaction mass formation was obtained in intraspecific crosses of *D. nasuta* and there were no significant differences in the t-test among the three strains. The frequency being so low, approximately 20.0% in the intraspecific crosses of *D. pallidifrons*, no further analysis was performed.

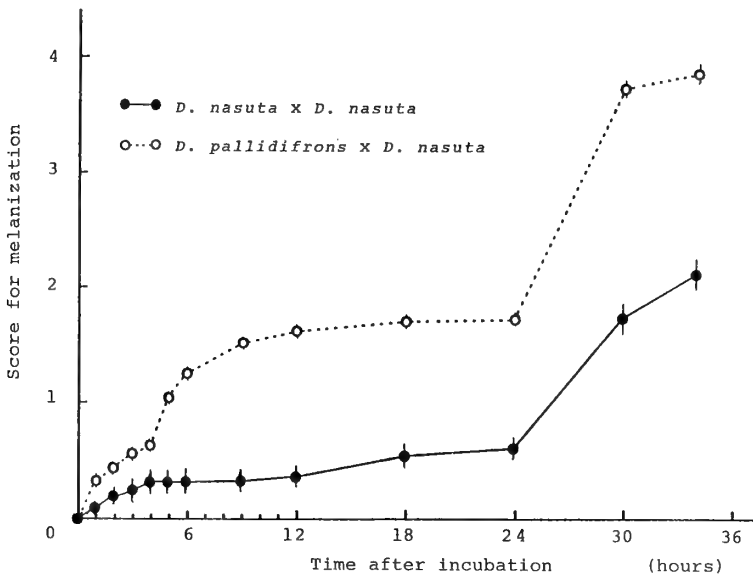
In Ex-1, the difference in the frequency of the reaction mass formation was highly significant in all crosses as compared with the control group. Reduction ranged from 60.0%, ADM-strain, to 33.0%, SEZ-strain, in the intraspecific crosses of *D. nasuta* as compared to the corresponding control figures of 86.0–90.0%. No complete

TABLE 1. Percent of reaction mass formation in temperature shift experiments

Species	Cross type		Number of females	% of formation of reaction mass		
	Female	Male		Control	Ex-1	Ex-2
<i>Drosophila nasuta</i>	ADM-1	ADM-1	50	90.0	36.0	70.0
×	MYS-23	MYS-23	50	90.0	52.0	70.0
<i>D. nasuta</i>	SEZ-2	SEZ-2	50	86.0	58.0	68.0
<i>D. pallidifrons</i>	PNI-74	PNI-74	50	12.0	nd	nd
×	PNI-110	PNI-110	50	20.0	nd	nd
<i>D. pallidifrons</i>	PNI-74	SEZ-2	50	52.0	24.0	46.0
×	PNI-110	SEZ-2	50	94.0	46.0	82.0

* $p < 0.05$, ** $p < 0.01$, *** $p < 0.001$.

ns: not significant, nd: not done.

FIG. 1. Melanization of reaction mass incubated with dopa *in vitro*. Score of melanization is expressed after Hiruma and Riddiford (1984).

inhibition, however, was observed at the low temperature. As shown in Ex-2, recovery of the reaction mass formation observed in all crosses was especially significant in intraspecific crosses of *D. nasuta*, ADM-1 strain, and interspecific crosses between *D. pallidifrons* females, PNI-110 strain,

and *D. nasuta* males, SEZ-2, strain when the copulated females were re-transferred from 2 to 25°C. The frequencies, however, were lower than the control values for all crosses.

In vitro melanogenesis was confirmed after incubation with dopa as shown in Figure 1. Length

of time necessary for melanization was much longer in intraspecific than in interspecific crosses. The larger the score increase, the darker the color of the reaction mass. Length of time of melanization reflects that *in vivo*; the reaction mass is somewhat rigid, then colored dark only in interspecific crosses as shown in the previous study [6]. The present work demonstrates that stimulation by copulation itself of some sexual substances ejaculated by the male play an important role in activation of phenoloxidase *in vivo* as the trigger in a copulated female. Additionally, phenoloxidase plays a key role in the formation of reaction mass. Firstly, because melanization of the reaction mass occurred both *in vivo* [6] and *in vitro* (Fig. 1) especially in interspecific crosses. Secondly, formation of reaction mass was significantly inhibited by a direct injection of phenoloxidase inhibitors, thiourea and sodiumdiethyldithiocarbamate [7].

Detection of phenoloxidase by SDS-PAGE and spectrophotometry

Phenoloxidase activity in the extracts from adult flies were examined by SDS-PAGE. As presented in Figure 2, the arrow indicates active bands for

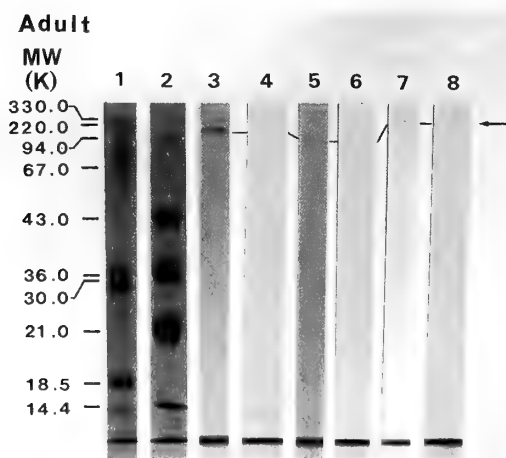


FIG. 2. SDS-polyacrylamide gel electrophoresis of phenoloxidase in adult fly.

Lane-1: marker protein, 2: marker protein, 3: *D. nasuta* (SEZ-2 strain), non-heated, 4: *D. nasuta* (SEZ-2 strain), heated, 5: *D. pallidifrons* (PNI-74 strain), non-heated, 6: *D. pallidifrons* (PNI-74 strain), heated, 7: *D. pallidifrons* (PNI-110 strain), non-heated, 8: *D. pallidifrons* (PNI-110 strain), heated.

phenoloxidase in lanes-3, 5, and 7 appeared within six minutes and then darkened during incubation with dopa at 37°C. Three active bands were distinguishable and molecular weights of each protein were estimated with marker proteins; the major protein was 323,000 daltons, the minor proteins were 339,000, and 302,000 daltons (data not shown). In comparison with active bands in *D. nasuta* and two strains of *D. pallidifrons*, banding patterns were generally similar to one another. No active bands, however, could be detected when the extracts were heated at 100°C as shown in lanes 4, 6, and 8.

Insect phenoloxidase exists as a proenzyme that is processed to become active by protein denaturation and proteases [13]. In *Drosophila*, there are some proenzymes including three A components activated by a natural activator isolated from pupae [14] and one P activating component by 2-propanol [15]. In *D. melanogaster*, three phenoloxidases have been found; one with a monophenoloxidase activity (tyrosinase) and two with dopa oxidase activities [16–17]. The active bands in the gels in this study seems to be dopa oxidase rather than tyrosinase because the extracts obtained from adults were incubated not in tyrosine but in dopa, resulting in the three active bands as given in Figure 2.

Concerning the previous study in *Drosophila*, phenoloxidase activity could be detected in the first-instar-larva, and began to rise, then reached a maximum level at the time of puparium formation. Activity decreased at the stage of pupa, then recovered after eclosion [18–21]. Electropherogram of the present study showed the developmental profile of phenoloxidase activity, that is, the highest activity of phenoloxidase was detected at the late third-instar-larva and not at pupa (data not shown).

Phenoloxidase activity in a supernatant fraction from the whole body of female flies is given in Figure 3. A virgin female was used as the control. The highest level of phenoloxidase activity was presented at five minutes after the initiation of copulation, and no significant differences were observed in all cross types. Then the phenoloxidase activity decreased gradually. The data suggests that the positive correlation between the

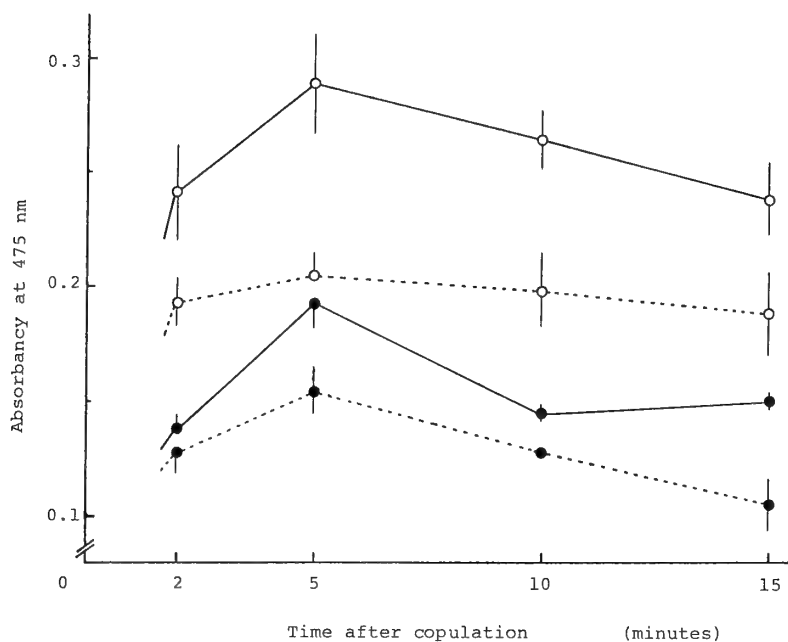


FIG. 3. Phenoloxidase activity in copulated female *in vitro*.

- *D. nasuta* × *D. nasuta*
- *D. nasuta* (♀, control)
- *D. pallidifrons* × *D. nasuta*
- *D. pallidifrons* (♀, control)

formation of reaction mass in the uterus and phenoloxidase activation in the supernatant fraction, and that phenoloxidase seems to make a certain contribution to reaction mass formation. The reaction mass formation was temperature dependent; in other words, the frequency was significantly reduced at a low temperature (2°C), but it recovered when the copulated females were placed again under suitable conditions (Table 1). However, no phenoloxidase activity appeared when the extracts heated at 100°C showed a lack of mass formation. The length of time of phenoloxidase activity was quite similar to that of the reaction mass formation (Fig. 3).

The phenoloxidase system in insects is quite important not only in melanin synthesis and the formation of the cuticle, but also in primitive defense responses in *Drosophila* [7]. In *D. melanogaster*, some mutants which are known to influence melanogenesis, for example, the relationship between *lozenge* (*lz*) and various components of phenoloxidase complex; that is, the A_1 activity is absent in the mutant *lozenge-grossy*

(*lz^g*), the A_2 activity is reduced in *lz* [20] and some electrophoretic variants of phenoloxidase in *lz* mutant have been identified [17]. The phenoloxidase system, however, might be related to reaction mass formation in a manner that may play an important role in preventing gene exchange and interspecific hybridization. Molecular analysis of the phenoloxidase system is needed for further understanding of this system.

ACKNOWLEDGMENTS

The authors wish to express their hearty thanks for invaluable criticism to Prof. Narise, S., Josai University. They also wish to express many thanks for proof reading this manuscript to Dr. Kimble, D. M., Okayama University of Science. This work was partly supported by The National Institute of Genetics, Japan as a cooperative study.

REFERENCES

- 1 Patterson, J. T. (1946) A new type of isolation mechanism in *Drosophila*. Proc. Natl. Acad. Sci. U.S.A., 32: 202-208.

- 2 Patterson, J. T. (1947) The insemination reaction and its bearing on the problem of speciation in the *mulleri* subgroup. Univ. Texas Publ., **4720**: 42–77.
- 3 Wheeler, M. R. (1947) The insemination reaction in the intraspecific matings of *Drosophila*. Univ. Texas Publ., **4720**: 78–115.
- 4 Patterson, J. T. and Stone, W. S. (1952) Evolution in the Genus *Drosophila*, Macmillan, New York.
- 5 Takanashi, E. (1983) Genetic and reproductive differentiation in *Drosophila sulfurigaster*. Jpn. J. Genet., **58**: 463–485.
- 6 Asada, N. and Kitagawa, O. (1988) Insemination reaction in the *Drosophila nasuta* subgroup. Jpn. J. Genet., **63**: 137–148.
- 7 Asada, N. and Kitagawa, O. (1988) Formation and the inhibition of reaction plug in mated *Drosophila*. Study of a primitive defense reaction. Dev. Comp. Immunol., **12**: 521–529.
- 8 Asada, N. and Kitagawa, O. (1982) Reproductive isolating mechanisms in the *D. nasuta* subgroup I. Jpn. J. Genet., **57**: 658–659.
- 9 Ephrussi, B. and Beadle, G. W. (1936) A technique of transplantation for *Drosophila*. Amer. Natl., **70**: 218–225.
- 10 Laemmli, U. K. (1970) Cleavage of structural proteins during the assembly of the head of bacteriophage T4. Nature, **227**: 680–685.
- 11 Hiruma, K. and Riddiford, L. M. (1984) Regulation of melanization of tobacco hornworm larval cuticle *in vitro*. J. Exp. Zool., **230**: 393–403.
- 12 Ashida, M. (1971) Purification and characterization of prephenoloxidase from hemolymph of the silkworm *Bombyx mori*. Arch. Biochem. Biophys., **144**: 749–762.
- 13 Ashida, M. and Dohke, K. (1980) Activation of pro-phenoloxidase by the activating enzyme of the silkworm, *Bombyx mori*. Insect Biochem., **10**: 37–47.
- 14 Mitchell, H. K. and Weber, U. M. (1965) *Drosophila* phenol oxidase. Science, **148**: 964–965.
- 15 Batterham, P. and McKechnie, S. W. (1980) A phenol oxidase polymorphism in *Drosophila melanogaster*. Genetika, **54**: 121–126.
- 16 Rizki, T. M. and Rizki, R. M. (1984) The cellular defense system of *Drosophila melanogaster*. In "Insect Ultrastructure". Ed. by R. C. King, and H. Akai, Plenum Publishing Co., New York, pp. 579–604.
- 17 Rizki, T. M., Rizki, R. M. and Bellotti, R. A. (1985) Genetics of *Drosophila* phenoloxidase. Mol. Gen. Genet., **201**: 7–13.
- 18 Ohnishi, E. (1953) Tyrosinase activity during puparium formation in *Drosophila melanogaster*. Jpn. J. Zool., **11**: 69–74.
- 19 Geiger, H. R. and Mitchell, H. K. (1966) Salivary gland function in phenol oxidase production in *Drosophila melanogaster*. J. Insect Physiol., **12**: 747–754.
- 20 Mitchell, H. K. (1966) Phenol oxidase and *Drosophila* development. J. Insect Physiol., **12**: 755–765.
- 21 Peeples, E., Geisler, A., Whitcraft, C. J. and Oliber, C. P. (1969) Activity of phenol oxidase at the puparium formation stage in development of nineteen *lozenge* mutant of *Drosophila melanogaster*. Biochem. Genet., **3**: 563–569.

Embryo Transfer and Pregnancy Rate in the Golden Hamster (*Mesocricetus auratus*)

S. J. JAROSZ¹ and W. R. DUKELOW²

¹*Akademia Rolnicza im. Eugena Kellqataja, W. Krakowie, Zaklad Hodnell
Zwierzat Futerkowych, Al. Mickiewicza 24/28, 30-059 Krakow,
Poland, and* ²*Endocrine Research Center, Michigan State
University, East Lansing, MI 48824, USA*

ABSTRACT—Two series of experiments were carried out to determine the reason for the low pregnancy rate after embryo transfer in the hamster. Two culture media, TC-199 and TALP plus 20% FCS, were tested for flushing and transfer of embryos. The 4- to 8-cell embryos were recovered from mated females (donors) and transferred to female recipients synchronized by the same hormonal regimen. The pregnancy rate after the use of TC-199 and TALP plus 20% FCS were similar, 36.4% and 39.1% respectively, and compared with control females (80.0%). Only two of eight pregnant females in the TC-199 group and three of nine pregnant females in the TALP group delivered live young. The second series of experiments was carried out on three groups of females. Those in the first group were subjected to embryo transfer (ten, 4- to 8-cell embryos into right uterine horn). Those in the second group were mated and received only medium in the right uterine horn. In the third group, also mated, sham injections were performed in the right uterine horn. All females were autopsied on Day 14 of gestation. The pregnancy rate in females of Groups I, II, and III were 50.0, 59.1, and 60.0% respectively, and the percent of pregnancies with at least one normal developed fetus from the right uterine horn of these three groups were 20.0, 46.2, and 58.3% respectively. In females of Groups II and III, the level of pregnancies in the right uterine horn were 30.8 and 17.7 percentage units less than in the left uterine horn. The number of normally developed fetuses in pregnant females of Group I was 24.4%, similar to that in the first experiment. The numbers of all recovered fetuses and of normally developed fetuses in the right uterine horn of females of Group II were significantly lower (25.8 and 19.5 respectively) than in the left uterine horn (74.2 and 56.6% respectively). A similar tendency was found in females of Group III. Of 174 recovered fetuses from both uteri, 30.5% were from the right uterine horn and 69.5% from the left uterine horn and the levels of normally developed fetuses were 14.9 and 55.2%, respectively.

These results shown that the main reason for a decreased pregnancy rate after embryo transfer in the hamster is due to a trauma of the endometrium of the uterus and medium introduced into uteri, which may induce secretion of prostaglandins.

INTRODUCTION

The technique of embryo transfer has been increasingly used in domestic animals to enhance genetical performance and, improve productivity [1-5]. In humans, this procedure is used in conjunction with *in vitro* fertilization to overcome infertility due to impaired tubal function [6-10]. Embryo transfer has been widely used in laboratory animals for fundamental studies of fertiliza-

tion, blastomere separation, or nuclear transplantation. Primarily these types of experiments have been performed in mice [11-17]. Considerably fewer experiments on embryo transfer have been done in hamsters, a species which seems to be especially suitable for studies on reproduction because of their early maturity, stable cycle length, high prolificacy, and short gestation. Blaha [18] reported that 49.2% of 6- to 8-cell embryos from young hamsters developed to term when transferred into young recipients, but that only 8.3% of the embryos of the same developmental stage developed into fetuses when transferred into old

recipients. Orsini and Psychoyos [19] transferred hamster blastocysts into ovariectomized and progesterone treated females, and found that some of the embryos could develop into live fetuses (7–12 days of gestation). Sato and Yanagimachi [20] transferred 1- to 2-cell embryos into the oviduct or 4- to 8-cell embryos into the uterus (using TC-199 medium) and found that 50 to 100% of the females receiving 4- to 8-cell embryos did become pregnant while none of the females receiving 1- to 2-cell embryos did so. Ridha [21] transferred embryos at different stages of development (1-cell to 8-cell) into the oviduct or uterus of hamsters after induced and natural ovulation and had 53–62% implantation rates in superovulated females. He was not able to produce full term live young. Fan *et al* [22] reported that the culture medium had a strong influence on the success of the embryo transfer. Increased survival rates are obtained in hamster embryo culture with the use of tissue culture medium 199 (TC-199) or Tyrode's solution supplemented with fetal calf serum (FCS) or pregnant hamster serum (PHS). According to Bavister *et al.* [23], the modified Tyrode's solution designated TALP (tyrodes-albumin-lactate-pyruvate) is the most suitable for embryo culture and transfer in hamster.

The objective of the present experiments was to determine whether the type of medium or other factors influence the pregnancy outcome results when 4- to 12-cell embryos are transferred to the hamster uterus.

MATERIALS AND METHODS

Mature golden hamsters (*Mesocricetus auratus*) 8 to 15 weeks old were maintained on a 12 h light: 12 h dark cycle. The estrous of each female was determined according to Orsini [24]. The day of vaginal discharge was designated as Day 1 of the estrus cycle. Hamster females (prospective ovum donors and recipients) were superovulated with an i.p. injection of 30 I.U. of PMSG (Serotropin, Teizo Ltd, Tokyo) on Day 1 of estrus at 0900 h followed by an i.p. injection of 30 I.U. hCG (Sigma Chemical Co., St. Louis, MO) at 1400 h on Day 4 (77 hr after PMS). Females to be used as donors were mated with fertile males and female

recipients with vasectomized males 7–8 hr after the hCG injection. On Day 4 of pregnancy the donor females were killed by cervical dislocation and then the uteri and oviducts were excised from the donors and, during the first series of experiments, were flushed with 0.8 ml of TC-199 or TALP with 20% FCS. Recovered embryos were rinsed once and stored no longer than 35 min at 37°C before transfer to the recipient. FCS was from GIBCO Co., (Grand Island, NY) and TALP was prepared by the method of Bavister *et al.* [23].

Recipient females were anesthetized with 0.12–0.15 ml sodium pentobarbital (60 mg/ml) i.p. and their uteri exposed through a dorsolateral incision. During the first exploratory series of experiments, eight to twenty 4- to 12-cell embryo were drawn into a micropipette with 20 μ l of TC-199 or TALP and injected into the uterine lumen near the utero-tubal junction. Control animals were either a) mated to fertile males, or b) mated and underwent a sham embryo transfer with injection of 20 μ l of medium only. Control animals received the same hormonal regime as the experimental females. All females were allowed to deliver term fetuses, or if no pregnancy was evident by 17 days after mating, the females were killed by cervical dislocation and the uteri were recovered for examination.

During the first series of experiments, it was found that after sham transfer (medium only) into the uterus no pregnancies resulted in the injected horn. Therefore, a second series of experiments were performed on females divided among three groups. The same hormonal regime as described above was used. The right uterine horn of females in Group I (embryo transfer group) received ten 4- to 8-cell embryos in 20 μ l of TALP. In Group II females (medium only transfer group), the right uterine horn received 20 μ l of TALP alone and in Group III females (sham injection group) the right uterine horn received only the tip of micropipette. On Day 14 after hCG and mating, the females were anesthetized, killed by cervical dislocation, and examined for pregnancy. The fetuses were counted and measured for crown-rump (C-R) length, weight, and stage of development.

Student's t-test was used for statistical evaluation.

RESULTS

The results of the first series of experiments demonstrated that the pregnancy rate was 36.4% (8/22) with the use of TC-199 and 39.1% (9/23) with TALP plus 20% FCS. A significantly higher pregnancy rate was found in naturally mated, control females (80.0%, 16/20) which received the same regimen for superovulation ($P < 0.05$). Only two of eight pregnant females with TC-199 and three of nine pregnant females with TALP plus 20% FCS delivered live young. In control females, the delivery rate was 93.8% and was significantly higher than in experimental females ($P < 0.05$). The percent of transferred embryos that developed

to fetuses of the two groups was 54.3 (51/94) and 36.9% (55/149) respectively. The numbers of embryos transferred to each recipient varied from 8 to 20. As mentioned earlier, no implantations occurred in uterine horns of naturally mated females which received an injection of medium alone.

The results of the second series of experiments to determine whether the trauma of transfer had a role in the restriction of pregnancy rate are shown in Tables 1 and 2. Only two of ten pregnant Group I females (20.0%) were pregnant 14 days after embryo transfer. In the females with a medium only transfer (Group II) or a sham injection (Group III) the total pregnancy rate in the right

TABLE 1. Pregnancy rate after embryo transfer, medium only transfer, or sham injection in the right uterine horns of hamsters

Treatment	Females	Embryos in both uterine horns (%)	No. of pregnant females with recovered fetuses on Day 14 of gestation			
			Right uterine horn (treated)		Left uterine horn (untreated)	
			Total (%)	with viable fetuses on Day 14 (%)	Total (%)	With viable fetuses on Day 14 (%)
Group I (embryo transfer)	20 (recipients)	—	10 (50.0)	2/10 (20.0)	0	0
Group II (medium only transfer)	22 (mated)	13 (59.1)	9/13 (69.2)	6/13 (46.2)	13/13 (100.0)	11/13 (84.6)
Group III (sham injection)	20 (mated)	12 (60.0)	10/12 (83.3)	7/12 (58.3)	12/12 (100.0)	10/12 (83.3)

All females were sacrificed on Day 14 of gestation for examination of the fetuses.

TABLE 2. Number of recovered fetuses after embryo transfer, medium only transfer, and sham injection in the right uterine horns of hamsters

Treatment	In both uterine horns	No. of fetuses recovered from females on Day 14			
		In the right uterine horn		In the left uterine horn	
		Total (%)	With viable fetuses	Total (%)	With viable fetuses
Group I (embryo transfer)	44 from 10 pregnant females	44 (100.0)	11 (25.0)	—	—
Group II (medium only transfer)	159 from 13 pregnant females	41 (25.8)*	31 (19.5)*	118 (74.2)	90 (56.6)
Group III (sham injection)	174 from 12 pregnant females	53 (30.5)*	26 (14.9)*	121 (69.5)	96 (55.2)

* Significantly different from control levels ($p < 0.05$).

TABLE 3. Crown-rump length and weights of viable hamster embryos on Day 14 of gestation

Treatment (right uterine horn)	Right uterine horn		Left uterine horn	
	Crown-rump length (mm)	Weight (mg)	Crown-rump length (mm)	Weight (mg)
Group I (embryo transfer)	14.3 ± 2.8 ¹	589 ± 246	—	—
Group II (medium only transfer)	18.1 ± 1.4	816 ± 178	18.6 ± 2.1	679 ± 243
Group III (sham injection)	16.2 ± 1.8	655 ± 198	15.8 ± 2.9	734 ± 177

¹ Values expressed as mean ± (S.D.)

TABLE 4. Ovarian weight and relationship of the number of fetuses to the number of corpora lutea on Day 14 of gestation

Treatment	Ovarian weight (mg)	Right uterine horn (treated) No. of fetuses in relation to no. of corpora lutea		Ovarian weight (mg)	Left uterine horn (control) No. of fetuses in relation to no. of corpora lutea	
		Total (%)	Viable fetuses (%)		Total (%)	Viable fetuses (%)
Group II (medium only transfer)	58.1 ± 0.0	4.8/24.3 (19.4)*	3.8/24.8 (15.5)	62.5 ± 0.0	10.4/28.0 (37.1)	9.6/28.0 (34.3)
Group III (sham injection)	41.3 ± 0.0	4.1/22.0 (18.8)	2.7/22.0 (12.5)	61.5 ± 0.0	11.4/24.0 (47.4)	9.7/24.0 (40.6)

Group I (embryo transfer) not evaluated.

* Significantly different from control levels ($p < 0.05$).

uterine horn in comparison to the left was decreased by 30.8 and 16.8% respectively. The viable pregnancy rate (embryos judged capable of being delivered live two days later) was reduced by 38.4 and 25.0 percentage units in Groups II and III respectively.

Forty-four of the fetuses in 10 pregnant females were identified after embryo-transfer (Group I) but only 25.0% of these were classified as viable (Table 2). This result was similar to that observed in the first series of experiments.

The crown-rump length and weight of normally developed embryos at 14 days of gestation are shown on Table 3. No significant differences were found between groups.

Ovarian weight, the number of corpora lutea, and the relation of the number of fetuses to the number of corpora lutea are shown in Table 4. No statistically significant differences were found between groups for ovarian weight or numbers of corpora lutea as expected. In both Group II and III, the relationship between the number of all fetuses to the number of corpora lutea were, in the

right side, 19.4 and 18.8% respectively and, in the left side, 37.1 and 47.4% respectively, a statistically significant difference reflecting the decreased embryo survival in the treated right side.

DISCUSSION

In the first series of experiments, attention was directed to two culture media, which according to Bavister *et al.* [23] play an important role in the culture of hamster embryos and their successful development after transfer to pseudopregnant females. Work reported by Fan *et al.* [22] has shown that the best results in embryo development were with media TC-199 or Tyrode's solution supplemented with 20–30% of PHS or FCS.

The present results confirm these findings. Pregnancy rates were lower in our experiments than those reported by Blaha [18] who reported 49.2% developed fetuses after transfer of 6- to 8-cell embryos into the uterus, and were also lower than those of Sato and Yanagimachi [20] who reported a 66% pregnancy rate with 48% live fetuses after

transfer of 4- to 8-cell embryos. Ridha [21] reported a 58–59% rate of implantation after unilateral transfer of ten 4- to 8-cell embryos per female. These values are similar to our pregnancy rate (50%) in the second series of experiments, but Ridha was not able to produce live offspring.

Significantly lower pregnancy rates and number of live fetuses were recovered after embryo transfer than in control females. This suggested that factors other than the type of medium, such as trauma to the uterus during the transfer procedure, may play an important role in the restriction of the implantation rate and further development of transferred embryos.

The results of the second series of experiments with sham transfer of medium or the introduction of only the tip of micropipette into the uterine horn show very clearly that these procedures adversely affect the pregnancy rate and the number of implantations.

The pregnancy rates in females with the sham transfer of medium (Group II) and in females with sham micropipette introduction (Group III) are similar- 59.1 and 60.0% respectively (Table 1), but about 20% lower than in control females in the first series of experiments. Comparing the number of pregnancies in the right (treated) horn and the left (untreated) uterine horn to the number of pregnant females, it can be seen that pregnancy rates in term pregnancies with normal and degenerated fetuses as well as those with at least one normal fetus were significantly lower in the treated uterine horn. Significant differences between the treated and untreated uterine horns are seen in the numbers of recovered fetuses on Day 14 of gestation (Table 2). The total number of fetuses (normal and degenerated) in the treated horns were less by about 48 percentage units in females with medium only transfer and by about 39 percentage units in females with sham injection transfer. Similar significant differences were found in the number of normally developed fetuses at Day 14. These results demonstrate that the main factor restricting the implantation and normal development of transferred embryos is trauma of the uterus.

The physiological mechanism of this trauma effect is not known. Pharriss *et al.* [25] noted that

trauma of the endometrium causes release of prostaglandins which, according to Horton *et al.* [26] and Kirton *et al.* [27], stimulate uterine contractility in rabbits and primates, and can induce abortion [28]. Spilman *et al.* [29] studied the effects of two isomers of PGF₂ (19(R)-19(S)-OH) and found that they were considerably less effective than PGF₂ in stimulating motility of the rabbit and monkey reproductive tracts, and that there are different species sensitivities for prostaglandins. Gutknecht *et al.* [30] found that PGF₂ at a dose level of 2 mg/day over any consecutive three-day period from Day 4 after coitus were 100% effective in preventing or terminating pregnancies in the rat. The same author [31], reported that PGF₂ administered subcutaneously at a dose of 0.1 mg/day on Days 5 through 7 post-coitus in the hamster lowered both plasma and ovarian progesterone levels and terminated pregnancy in all animals. He also reported histological evidence of luteal degeneration on Days 6 and 7 post-coitus in treated animals, but that exogenous progesterone maintained pregnancy in PGF₂ treated females. According to Pharriss *et al.* [25] the hamster is the most sensitive species to prostaglandin-induced luteolysis of any examined animals. Thomas *et al.* [32], taking blood and tissue samples from hamsters during estrous cycle and for the first four days of pregnancy, found that maximum steroid and prostaglandin concentrations occurred around ovulation and after that declined to the lowest level on Days 3 and 4 of pregnancy. They reported that a close relationship exists between steroids and prostaglandins. These findings suggest that the trauma which probably releases prostaglandins during embryo transfer, is the main factor decreasing implantation and embryo development.

ACKNOWLEDGMENTS

These studies were supported by REED funds from the state of Michigan and grants from the National Institutes of Health. Appreciation is expressed to Mr. W. E. Roudebush for assistance in the procedures.

REFERENCES

- 1 Williams, T. J., Elsden, R. P. and Seidel, G. E. Jr. (1983) Bisecting bovine embryos: Method applica-

- tions and success rates. Proc. Ann. Conf. on A. I. and Embryo Transfer in Beef Cattle, Denver, Co. pp. 45-51.
- 2 Rorie, R. W., Voelkel, S. A., McFarland, C. W., Southern, L. L. and Godke, R. A. (1984) Another split-embryo transplant in pigs. *Louisiana Agric.*, **28**: 3.
 - 3 Allen, W. R. and Pashen, R. L. (1984) Production of monozygotic (identical) horse twins by embryo micromanipulation. *J. Reprod. Fertil.*, **71**: 607-613.
 - 4 Willadsen, S. M. and Godke, R. A. (1984) A simple procedure for the production of identical sheep twins. *Vet. Rec.*, **114**: 240-243.
 - 5 Tsunoda, Y., Tokunaga, T., Sugie, T. and Katsumata, M. (1985) Production of monozygotic twins following the transfer of bisected embryos in the goats. *Theriogenology*, **24**: 337-342.
 - 6 Mettler, L., Michelman, H. W., Riedel, H. H., Grillo, M., Weisner, D. and Semm, K. (1984) In vitro fertilization and embryo replacement at the Department of Obstetrics and Gynecology, University of Kiel, FRG. *J. In Vitro Fertil. and Embryo Transfer*, **1**: 250-262.
 - 7 Mohr, L. R., Trounson, A. and Freeman, L. (1985) Deep-freezing and transfer of human embryos. *J. In Vitro Fertil. and Embryo Transfer*, **2**: 1-10.
 - 8 Testart, J., Lassalee, B., Belaisch-Allart, J., Hazout, A., Forman, R., Rainbor, J. D. and Frydman, R. (1986) High pregnancy rate after early human embryo freezing. *Fertil. Steril.*, **46**: 268-272.
 - 9 Reinthaler, A., Riss, P., Deutinger, J., Muller-Tyl, E., Fischl, F. and Janish, H. (1986) Factors influencing successful in vitro fertilization and embryo transfer: A matched pair study. *Fertil. Steril.*, **46**: 511-513.
 - 10 Poindexter, A. N., Thomson, D. J., Gibbons, W. E., Findley, W. E., Dodson, M. G. and Young, R. L. (1986) Residual embryos in failed embryo transfer. *Fertil. Steril.*, **46**: 262-267.
 - 11 Tarkowski, A. K. and Wroblewska, J. (1967) Development of blastomeres of mouse eggs isolated at the 4- and 8-cell stage. *J. Embryol. Exp. Morphol.*, **18**: 155-180.
 - 12 Hoppe, P. C. and Illmensee, K. (1977) Microsurgically produced homozygous diploid uniparental mice. *Proc. Natl. Acad. Sci. USA*, **74**: 5657-5661.
 - 13 Illmensee, K. (1982) Experimental genetics of the mammalian embryo. *J. Cellular Physiol. Suppl.*, **2**: 117-129.
 - 14 O'Brien, M. J., Crister, E. S. and First, N. L. (1984) Developmental potential of isolated blastomeres from early murine embryos. *Theriogenology*, **22**: 601-607.
 - 15 Nakagawa, A., Takanashi, Y. and Kanagawa, H. (1985) Studies on developmental potential of bisected mouse embryos in vitro and in vivo. *Jpn. J. Vet. Res.*, **33**: 121-133.
 - 16 Robl, J. M., Gilligan, B., Critser, E. S. and First, N. L. (1986) Nuclear transplantation in mouse embryos: Assessment of recipient cell stage. *Biol. Reprod.*, **34**: 733-739.
 - 17 Papaioannou, V. E. and Ebert, K. M. (1986) Development of fertilized embryos transferred to oviducts of immature mice. *J. Reprod. Fertil.*, **76**: 603-608.
 - 18 Blaha, G. C. (1964) Effect of age of the donor and recipient on the development of transferred hamster ova. *Anat. Rec.*, **150**: 413-416.
 - 19 Orsini, M. W. and Psychoyos, A. (1965) Transplantation of blastocysts transferred into progesterone treated virgin hamsters previously ovariectomized. *J. Reprod. Fertil.*, **10**: 300-301.
 - 20 Sato, A. and Yanagimachi, R. (1972) Transplantation of preimplantation hamster embryos. *J. Reprod. Fertil.*, **30**: 329-332.
 - 21 Ridha, M. T. (1983) Embryo production, freezing and transfer in the golden hamster (*Mesocricetus auratus*). Ph. D. Dissertation. Michigan State University, 95 pp.
 - 22 Fan, B., Ridha, M. T., Demayo, F. J. and Dukelow, W. R. (1986) Culture and transplantation of preimplantation hamster embryos. *J. Agric. Sci., Suppl.*, **2**: 69-77.
 - 23 Bavister, B. D., Leibfried, M. L. and Lieberman, G. (1983) Development of preimplantation embryos of the golden hamster in defined culture medium. *Biol. Reprod.*, **28**: 235-247.
 - 24 Orsini, M. W. (1961) The external vaginal phenomena characterizing the stages of the estrous cycle, pregnancy, pseudopregnancy, lactation, and the anestrus hamster, *Mesocricetus auratus* Waterhouse. *Proc. Animal Care Panel*, **11**: 193-206.
 - 25 Pharriss, B. B., Tillson, S. A. and Erickson, R. R. (1972) Prostaglandins in luteal function. *Recent Progress in Hormone Research*, **28**: 51-80.
 - 26 Horton, E. W., Main, I. H. M. and Thompson, C. J. (1965) Effect of prostaglandins on the oviduct, studied in rabbits and ewes. *J. Physiol.*, **180**: 514-528.
 - 27 Kirton, K. T. and Farbes, A. D. (1972) Activity of 15(S) 15-methyl prostaglandin E₂ and F₂ as stimulants of uterine contractility. *Prostaglandins*, **1**: 319-323.
 - 28 Fuchs, F., Prieto, M. and Marcus, S. (1971) Effect of prostaglandins on uterine activity in pregnant Rhesus monkeys. *Ann. New York Acad. Sci.*, **180**: 531-536.
 - 29 Spilman, C. H., Bergstrom, K. K. and Forbes, A. D. (1977) Effect of 19-hydroxy-prostaglandins on oviductal and uterine motility. *Prostaglandins*, **13**: 795-805.
 - 30 Gutknecht, G. D., Cornette, J. C. and Pharris, B.

- B. (1969) Antifertility properties of prostaglandin F_2 . *Biol. Reprod.*, **1**: 367-371.
- 31 Gutknecht, G. D., Wyngarden, L. J. and Pharris, B. B. (1971) The effect of prostaglandin F_2 on ovarian and plasma progesterone levels in the pregnant hamster. *Proc. Soc. Exp. Biol. Med.*, **136**: 1151-1157.
- 32 Thomas, C. M. G., Bastiaans, L. A. and Rolland, R. (1982) Concentrations of conjugated oestradiol and progesterone in blood plasma and prostaglandins F-2 and E-2 in oviducts of hamsters during oestrous cycle and in early pregnancy. *J. Reprod. Fertil.*, **66**: 469-474.

Changes in Thyroid Hormone Concentrations during Early Development and Metamorphosis of the Flounder, *Paralichthys olivaceus*

MASATOMO TAGAWA, SATOSHI MIWA¹, Yasuo Inui¹,

EVELYN GRACE DE JESUS and TETSUYA HIRANO

Ocean Research Institute, University of Tokyo, Tokyo 164, and

¹Inland Station, National Research Institute of Aquaculture,
Tamaki, Mie 519-04, Japan

ABSTRACT—Changes in the whole body concentrations of thyroid hormones were examined during early development and metamorphosis of the flounder (*Paralichthys olivaceus*). Thyroxine (T4) as well as triiodothyronine (T3) were detected in eggs just after fertilization; concentration of T3 was 6–7 ng/g and that of T4 was about 1 ng/g. Concentration of T3 declined gradually until hatching, decreased sharply from 5 ng/g to 0.5 ng/g within one day after hatching and became non-detectable (below 0.1 ng/g) thereafter. T4 concentration did not show marked changes until 10 days after fertilization. Until the climax of metamorphosis, T3 was undetectable and T4 concentration was less than 1 ng/g. During the climax, T4 concentration increased markedly to 10–15 ng/g, and T3 concentration increased to a detectable level (1–1.5 ng/g). After the completion of metamorphosis, T4 concentration decreased to about a half of the peak level. T3 concentration also decreased slightly. These observations were discussed in relation to the role of T4 and T3 in early development and metamorphosis of the flounder.

INTRODUCTION

Thyroid hormones are known to play an important role in amphibian metamorphosis [1]. Activation of thyroid gland was also observed during metamorphosis in the conger eel [2] and flounder [3], and treatments with thyroid hormones induced metamorphosis in these species [4–6]. Recently, a radioimmunoassay procedure was applied to estimate whole body concentrations of thyroxine (T4) during the metamorphosis of flounder larvae [7, 8], and a significant surge was observed at the climax of metamorphosis. A similar procedure was applied to examine the changes in whole body concentration of triiodothyronine (T3) during early development of chum salmon [9]. Although T3 has been shown to be more effective than T4 in inducing flounder metamorphosis [6], there is no report on the changes in T3 concentrations during the flounder metamorphosis. In this paper, we

report the changes in whole body concentrations of T3 as well as T4 during early development and metamorphosis of the flounder.

MATERIALS AND METHODS

Fertilized eggs of the flounder (*Paralichthys olivaceus*) were obtained from spawning aquarium containing several females and males, and incubated in seawater at 15°C. They hatched 4 days after fertilization. About 600 eggs or larvae were sampled daily until 8 days and on 10th day after fertilization. Larvae were offered rotifers starting from 8 days after fertilization. Another batch of larvae was obtained from a commercial source and reared in a 500 l aquarium. They were fed rotifers and brine shrimp nauplii. Twenty to 40 larvae were sampled at intervals starting from 18 days after hatching until 57 days after hatching. They were stored at –80°C until analyses. Metamorphic stages were identified by the eye migration stage and the length of the 2nd fin ray [7]. Samples of eggs and larvae until 10 days after fertilization

were processed as previously described for the distribution of thyroid hormones in developing chum salmon [9]. The hormone concentrations of metamorphosing larvae were measured from one homogenate made from at least 12 individuals as follows; frozen samples were homogenized in 4 ml of methanol, and the homogenates were divided into halves, one for T4 determination and another for T3 determination, using the half volume of solutions of agents as used in previous studies [9, 10]. The least detectable concentrations of thyroid hormones were 0.1 ng/g for eggs and larvae until 10 days after fertilization and 0.4 ng/g for metamorphosing larvae.

RESULTS

Figure 1 shows the changes in T4 and T3 concentrations until 10 days after fertilization. Both T4 and T3 were detected in eggs just after fertilization; the concentration of T3 was 6.6 ng/g and that

of T4 was 0.8 ng/g. T3 and T4 concentration decreased gradually toward hatching. After hatching, T3 concentration decreased sharply to about 1/10 of the level before hatching within one day, and became non-detectable thereafter. On the other hand, T4 concentration did not show such a marked change at the time of hatching, but a low level less than 1 ng/g was maintained thereafter.

As shown in Figure 2, T4 concentration during the premetamorphosis was less than 1 ng/g, and tended to increase during the prometamorphosis. T3 concentration was still non-detectable (less than 0.4 ng/g) during these periods. During the climax of metamorphosis, when the dorsal fins are being resorbed, T4 concentration increased markedly to 10–15 ng/g. T3 became detectable during the climax, but the level (1–1.5 ng/g) was still lower than the T4 level. During the postclimax of the metamorphosis, T4 concentration decreased to a half of the peak level.

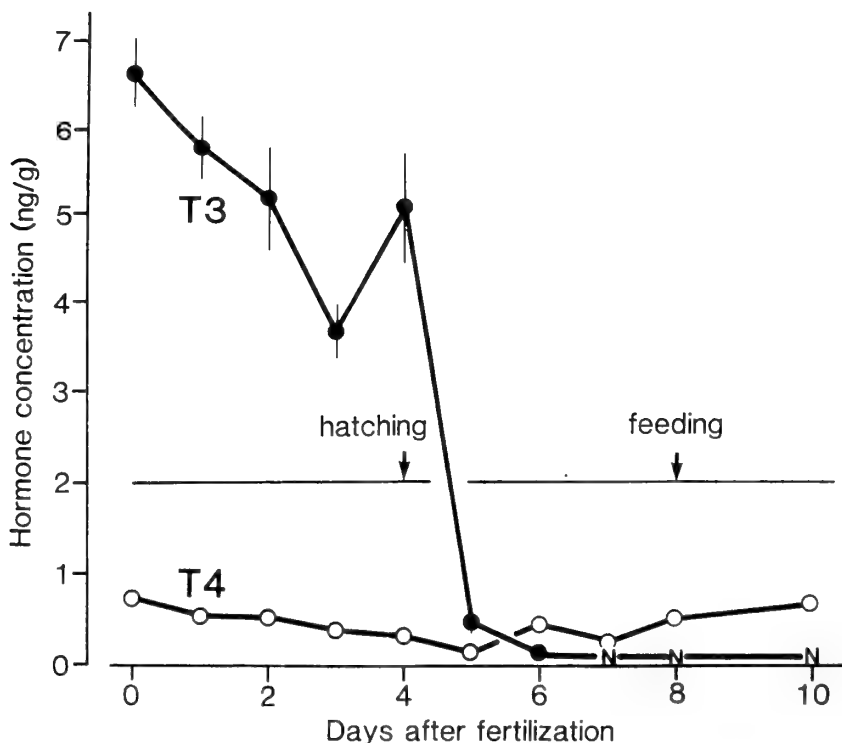


FIG. 1. Changes in T4 and T3 concentrations until 10 days after fertilization in the flounder. Vertical bars represent standard errors of the means of 3 pooled samples. In some cases, the variation was extremely small and within the size of the circle. N: non-detectable (below 0.1 ng/g).

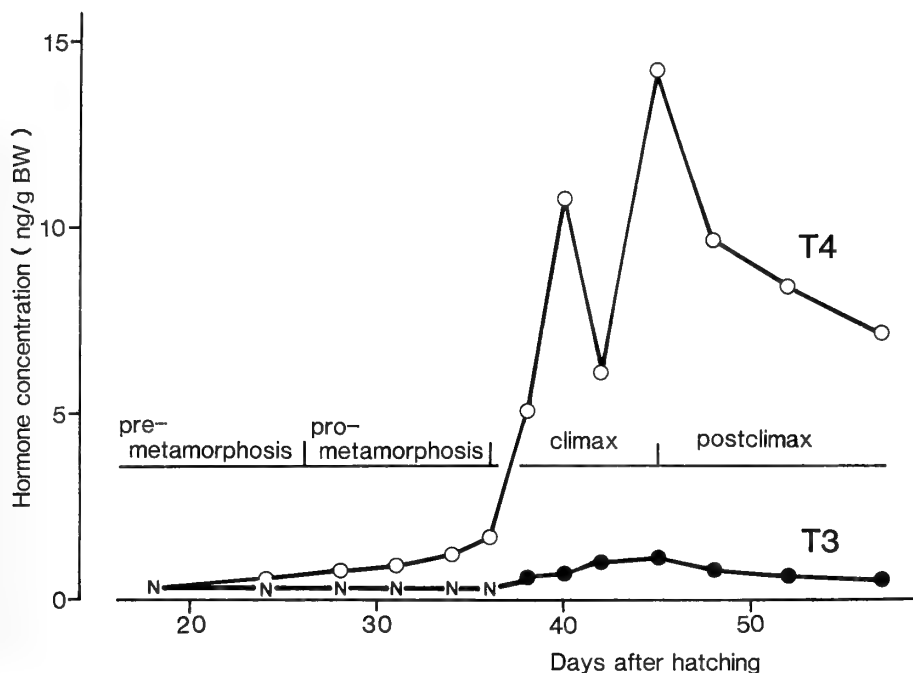


FIG. 2. Changes in T4 and T3 concentrations during metamorphosis of the flounder. Each point represents the average of the duplicate determination of one pooled sample. N: non-detectable (below 0.4 ng/g).

DISCUSSION

Significant quantities of both T4 and T3 have been detected in unfertilized or fertilized eggs of chum salmon (T4; 5–15 ng/g, T3; 4–9 ng/g) [9, 10], coho salmon (T4; 15–30 ng/g, T3; 20 ng/g) [11, 12], chinook salmon (T4; 9 ng/g, T3; 22 ng/g) [12] and striped bass (T4; 4 ng/g, T3; 5 ng/g) [13]. In the flounder eggs, T3 concentration (6.6 ng/g) was higher than T4 (0.8 ng/g) as in chinook salmon [12]. The relative quantities of T4 and T3 in fish eggs may be related to the mechanisms of utilizing thyroid hormones, such as the onset of 5'-deiodinase activity, during early developmental stages.

During the embryonic development of the flounder, whole body concentrations of both T4 and T3 decreased gradually toward hatching. After hatching, however T3 concentration decreased sharply to about 1/10 within 1 day, whereas no marked change was seen in T4 concentration. According to Fukuhara [14], a half of the yolk was resorbed within one day after hatching in the flounder larvae

kept at 14.2°C, and remnant yolk was linearly resorbed to completion in succeeding 3 days. Therefore, the rate of decrease in T3 concentration in the flounder larvae just after hatching seems to be greater than that of the yolk resorption, indicating some selective absorption mechanisms of T3 from the yolk. Selective absorption of thyroid hormones during yolk resorption has also been suggested in salmonid fishes and striped bass [9–13].

Although there is no information on the onset of thyroid hormone receptors during early development of fishes, the higher concentrations of T3 than T4 and the sharp decrease in T3 concentration just after hatching seem to indicate a primary role of T3 in early development of the flounder embryo and larva. According to Eales [15], T3 seems to be the effective thyroid hormone not only in juvenile and adult fishes but also even in early developmental stages.

During the climax of the metamorphosis, T4 concentration increased markedly to 10–15 ng/g, consistent with previous observations [7, 8]. T3

concentration was non-detectable (below 0.4 ng/g) during pre- and prometamorphosis, increased to 1–1.5 ng/g at the climax when T4 surge was observed, and the same level was maintained during postclimax. According to Miwa and Inui [6], T3 was several times more effective than T4 in inducing metamorphosis in the flounder. Therefore, a small increase in T3 concentration might be enough to stimulate the metamorphosis, although it is still possible that T4, but not T3, plays important roles in the flounder metamorphosis. Distribution and development of the thyroid hormone receptors are to be studied in the “metamorphosing” organs or tissues, not only in flounders but also in fishes in general.

ACKNOWLEDGMENTS

This study was supported in part by grants-in-aid from the Ministry of Agriculture, Forestry and Fisheries (BMP-88-II-2-3) to Y. I. and T. H. and also from the Ministry of Education, Science and Culture, Japan (61300014 and 62480022) to T.H.

REFERENCES

- 1 White, B. A. and Nicoll, C. S. (1982) Hormonal control of amphibian metamorphosis. In “Metamorphosis”. Ed. by L. I. Gilbert and E. Frieden, Plenum Press, New York, pp. 363–396.
- 2 Kubota, S. (1961) Studies on the ecology, growth and metamorphosis in conger eel, *Conger myriaster* (Brevoort). J. Fac. Fish. Prefectural Univ. of Mie, **5**: 190–329. (In Japanese)
- 3 Miwa, S. and Inui, Y. (1987) Histological changes in the pituitary-thyroid axis during spontaneous and artificially-induced metamorphosis of larvae of the flounder *Paralichthys olivaceus*. Cell. Tissue Res., **249**: 117–123.
- 4 Kitajima, C., Sato, T. and Kawanishi, M. (1967) On the effect of thyroxine to promote the metamorphosis of a conger eel—preliminary report. Bull. Japan. Soc. Sci. Fish., **33**: 919–922. (In Japanese with English summary)
- 5 Inui, Y. and Miwa, S. (1985) Thyroid hormone induces metamorphosis of flounder larvae. Gen. Comp. Endocrinol., **60**: 450–454.
- 6 Miwa, S. and Inui, Y. (1987) Effects of various doses of thyroxine and triiodothyronine on the metamorphosis of flounder (*Paralichthys olivaceus*). Gen. Comp. Endocrinol., **67**: 356–363.
- 7 Miwa, S., Tagawa, M., Inui, Y. and Hirano, T. (1988) Thyroxine surge in metamorphosing flounder larvae. Gen. Comp. Endocrinol., **70**: 158–163.
- 8 Tanangonan, J. B., Tagawa, M., Tanaka, M. and Hirano, T. (1989) Changes in tissue thyroxine level of metamorphosing Japanese flounder *Paralichthys olivaceus* reared at different temperatures. Nippon Suisan Gakkaishi, **55**: 485–490.
- 9 Tagawa, M. and Hirano, T. (1989) Changes in tissue and blood concentrations of thyroid hormones in developing chum salmon. Gen. Comp. Endocrinol., **76**: 437–443.
- 10 Tagawa, M. and Hirano, T. (1987) Presence of thyroxine in eggs and changes in its content during early development of chum salmon, *Oncorhynchus keta*. Gen. Comp. Endocrinol., **68**: 129–135.
- 11 Kobuke, L., Specker, J. L. and Bern, H. A. (1987) Thyroxine content of eggs and larvae of coho salmon, *Oncorhynchus kisutch*. J. Exp. Zool., **242**: 89–94.
- 12 Greenblatt, M., Brown, C. L., Lee, M., Dauder, S. and Bern, H. A. (1989) Changes in thyroid hormone levels in eggs and larvae and in iodide uptake by eggs of coho and chinook salmon, *Oncorhynchus kisutch* and *O. tshawytscha*. Fish Physiol. Biochem., **6**: 261–278.
- 13 Brown, C. L., Sullivan, C. V., Bern, H. A. and Dickhoff, W. W. (1987) Occurrence of thyroid hormones in early developmental stages of teleost fish. Trans. Am. Fish. Soc. Symp., **2**: 144–150.
- 14 Fukuhara, O. (1986) Morphological and functional development of Japanese flounder in early life stage. Bull. Japan. Soc. Sci. Fish., **52**: 81–91.
- 15 Eales, J. G. (1985) The peripheral metabolism of thyroid hormones and regulation of thyroidal status in poikilotherms. Can. J. Zool., **63**: 1217–1231.

Effects of Thyroidectomy, Hypophysectomy, Temperature and Humidity on the Occurrence of Nocturnal Locomotor Activity in the Toad, *Bufo japonicus*, during the Breeding Season

YOKO TASAKI and SUSUMU ISHII

Department of Biology, School of Education, Waseda University,
Tokyo 169, Japan

ABSTRACT—Toads collected in October 1987 were thyroidectomized or hypophysectomized, and then released into an outdoor pen. Observations were made once a day between 2030 and 2130 hr for 19 days from February 27 to March 16, 1988. Toads found completely exposed above ground at the time of the observation were regarded as active individuals. In males thyroidectomy significantly reduced both the mean number of active individuals each day and the mean number of active days of each individual. Hypophysectomy significantly reduced both of these parameters in males. In females, the effects of the operations were not clear, since the number of active individuals was extremely small in all groups. Significant positive correlations ($r=0.58-0.76$) were observed between the number of active individuals and temperature in both sexes, and between the number of active individuals and the humidity of the air in males. When the temperature and humidity were combined as an independent variable, a highly significant multiple correlation ($r>0.8$) in both sexes was observed. The present results suggest that the pituitary gland plays some role in the migration of the toad toward the pond but thyroid hormone suppresses the migratory activity, and also that the combination of temperature and humidity is the external factor which initiates the migration.

INTRODUCTION

In early spring, adult toads, *Bufo japonicus*, come out of hibernation and begin migration to a particular pond for breeding. This migratory activity occurs only on warm and humid nights and hence, not every day. Temperature and humidity have been proposed as the atmospheric factors which initiate the migration [1, 2]. A possible candidate for the endocrine factor initiating the migration for breeding in amphibians was prolactin, since a number of investigators have shown that prolactin is the water drive factor in newts and salamanders [3–8]. However, one of the present authors and his associates have found that the plasma prolactin level of toads just before or just beginning migration toward a breeding pond was low, and hence, prolactin can not be the migration

inducing factor in the toad [9, 10]. Tasaki *et al.* [11], observing the elevation of plasma thyroxine and triiodothyronine levels during the breeding season in *Bufo japonicus*, suggested the possibility that thyroid hormone is the migration inducing factor in the toad. However, they recently found that thyroxine administration to normal and thyroidectomized male toads suppressed their locomotor activity when measured in a small chamber, and thyroidectomy of male toads increased the activity [12]. These results, though under experimental conditions, suggest that thyroid hormone also can not be the migration inducing factor of the toad.

The purpose of the present study, is to confirm our previous results under conditions which approximate the natural environment, and also to determine the role of the pituitary gland in the migration. The effects of thyroidectomy and hypophysectomy on the occurrence of nocturnal locomotor activity were studied in toads kept in an

outdoor pen during the breeding season.

MATERIALS AND METHODS

Material

Adult male and female toads (*Bufo japonicus*) were used. They were captured in the suburbs of Tokyo in October 1987. The mean body weight was 145.2 g with a standard deviation of 42.0 g.

Operations

After capture, male and female toads were put in separate plastic boxes ($55 \times 40 \times 43 \text{ cm}^3$) with loose fitting tops. Wet pieces of plastic sponge were put in the boxes to maintain humidity. No feeding took place, since toads abstain from food

during the hibernation and breeding periods. Toads were kept in the boxes outdoors for about 2 weeks before the operations. Eight males and eight females were thyroidectomized. Sham-operations were performed on the same number of animals of each sex. Hypophysectomy by the oral approach and corresponding sham-operations were also performed with the same number of male and female toads. MS-222 was used for anesthetization of toads. Each animal was individually marked with a small, numbered plastic sheet which was adhered to its back, and a numbered plastic band which was tied around a forelimb.

Observation of toads

Fourteen to eighteen days after the thyroidectomy and related sham operation or 8 to 11 days

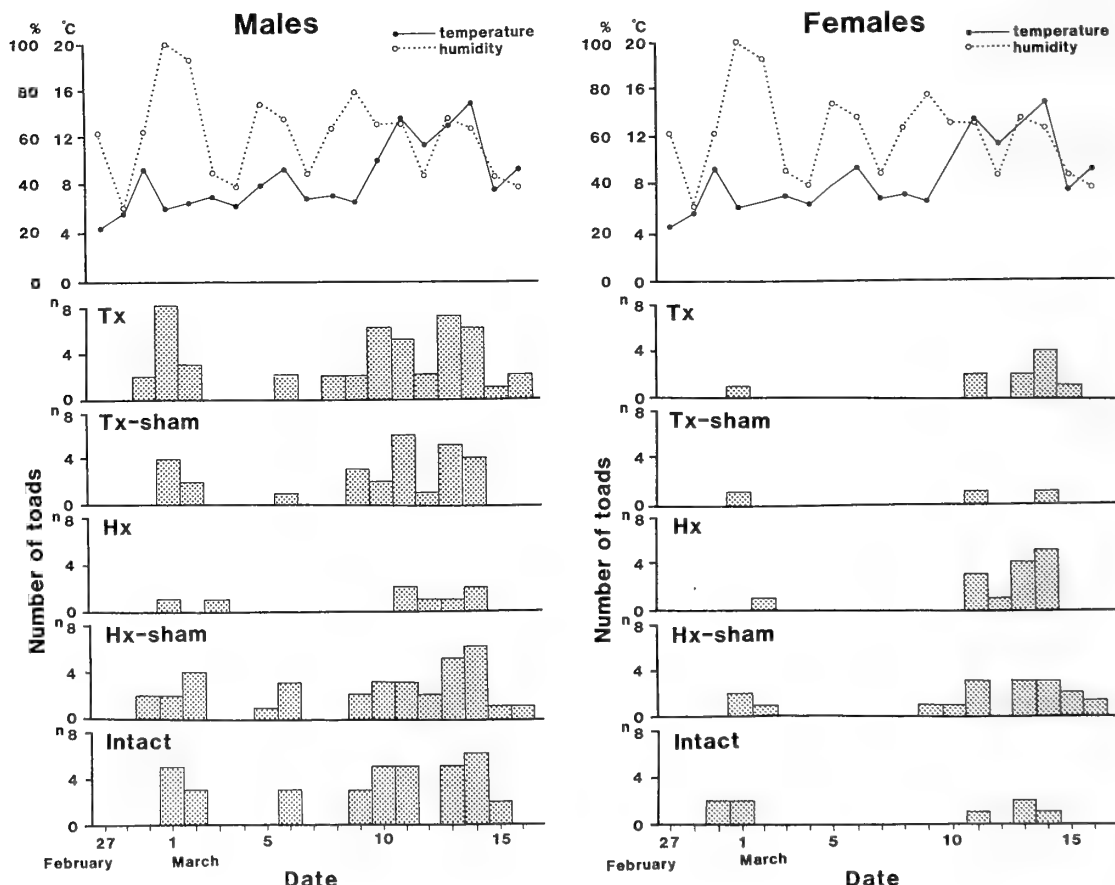


FIG. 1. Atmospheric factors and the number of male (left) and female (right) toads which appeared above ground on each experimental day in each group.

after the hypophysectomy and related sham operation, toads were released into an outdoor pen ($2 \times 26 \text{ m}^2$). As soon as they were released, they buried themselves under the ground. Observations were made in the pen once a day between 2030 and 2130 for 19 days from February 27 to March 16, 1988. When eggs were laid by a female in a pool ($70 \times 42 \times 20 \text{ cm}^3$) in the pen on March 16, observations were terminated. Toads which were found completely exposed above ground were regarded as active individuals, and their identification numbers were recorded. The temperature and relative humidity 10 cm from the ground surface in a corner of the pen were recorded every day at the time of the observation.

Statistical methods

The significant over-all difference in the number of active toads among the groups was determined by Friedman's test. The significant difference in the number of active toads between two groups was determined by the signed-rank test. The randomization test was used to compare the two groups as to the number of days on which toads

showed activity. For these tests, personal computer programs [13] were employed.

RESULTS

Effects of thyroidectomy and hypophysectomy on the occurrence of activity

The daily number of male and female toads of each group which appeared above ground for locomotor activity is shown in Figure 1. The temperature and relative humidity are indicated in the figure. Using the same data, the number of days on which each toad showed activity was calculated, and its distribution is shown in Figure 2.

Males: In males, the locomotor activity was observed relatively frequently, i.e., 15 out of 19 days. However, the number of active toads fluctuated widely over the course of the days and also among the groups (Fig. 1). The over-all difference in the number of active toads each day among the five groups was tested by using Friedman's test. The difference was highly significant ($p < 0.01$).

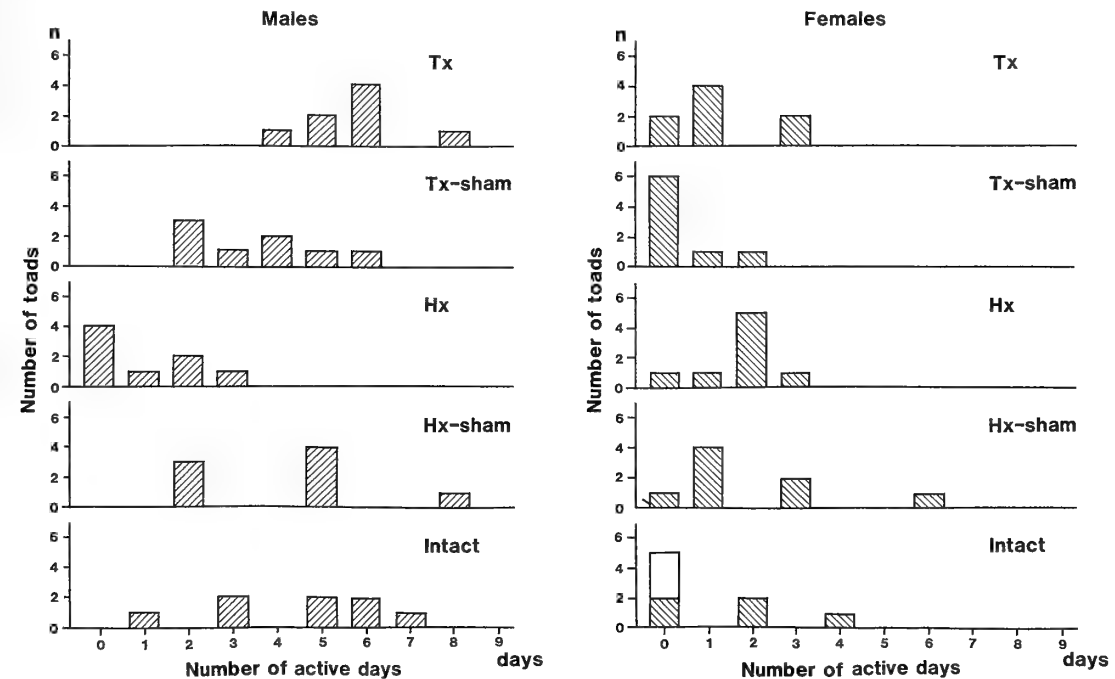


FIG. 2. The distribution of the number of days in which male (left) and female (right) toads showed activity. The open column indicates the number of toads which were not recovered after the observation period.

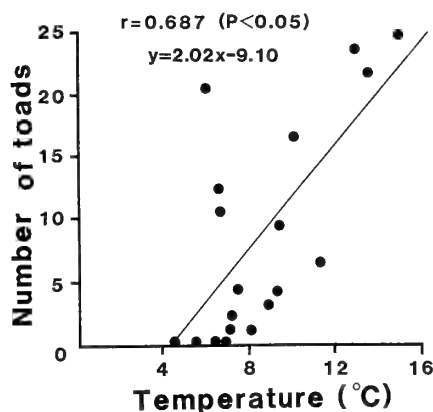
Then, the two-sided signed-rank test was used for paired comparisons between two selected groups. The differences in the number of active males between the thyroidectomized and its sham-operation control groups and also between the hypophysectomized and its sham-operation control groups were highly significant ($p < 0.01$). The differences between each of the sham-operation groups and the intact group were not significant ($p > 0.05$).

The distribution of the number of days on which the toad showed activity is indicated in Figure 2.

The difference in the average number of active days between two groups was tested by the two-sided randomization test. Thyroidectomized males showed activity more frequently than corresponding sham-operation males ($p < 0.008$), but hypophysectomized males showed it less frequently than the corresponding sham-operation males ($p < 0.002$). The frequency did not differ significantly ($p > 0.05$) between each of the sham-operation groups and the intact group.

Females: Compared to males, a fewer number of females showed locomotor activity (cf. Fig. 1).

Males



Females

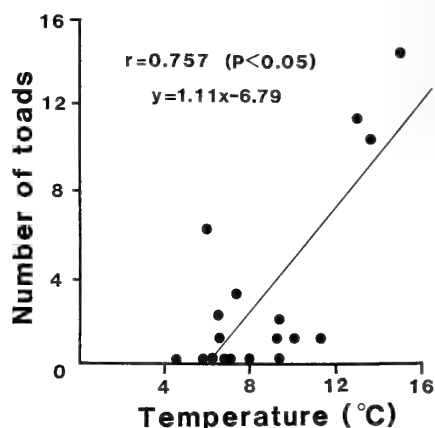
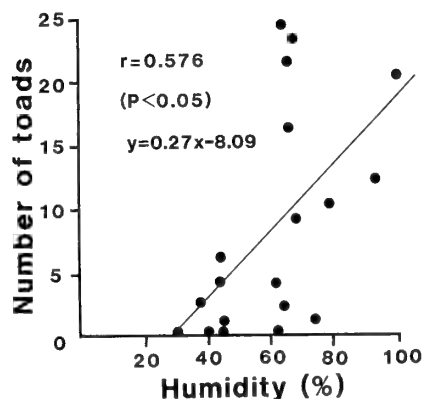


FIG. 3. The single correlation between temperature and the number of active male (left) and female (right) toads. There was a significant ($p < 0.05$) positive correlation in both males and females.

Males



Females

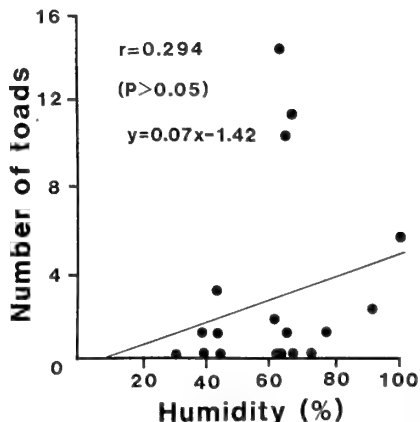


FIG. 4. The single correlation between humidity and the number of active male (left) and female (right) toads. Only in males did the humidity show a significant ($p < 0.05$) positive correlation.

The mean number of active days for females was also less than that for males (cf. Fig. 2). Due to the small number of active individuals, no significant difference was obtained or no statistical test was valid for the comparison of the number of active toads or the number of active days among the

groups.

Correlations between atmospheric parameters and toad activity

The effect of temperature or humidity on the number of active toads was studied by simple

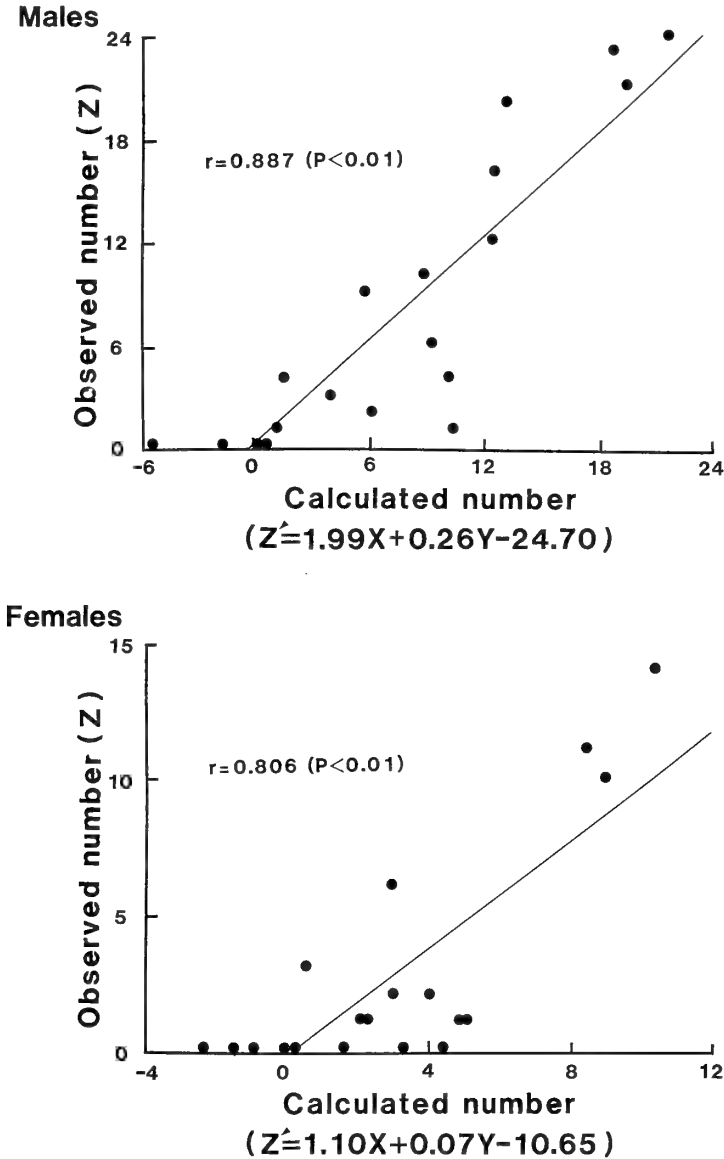


FIG. 5. The multiple correlation among temperature, humidity and the number of active male and female toads. A highly significant multiple correlation was observed between the temperature plus humidity and the number of active toads. On the horizontal axis (Z'), the expected numbers of active toads, which were calculated by using the regression formula with observed temperature (X) and humidity (Y) values, are plotted. On the vertical axis (Z), the observed numbers of active toads are plotted.

correlation analysis. The combined effect of both temperature and humidity was also studied by multiple correlation analysis. Females and males were separately analyzed.

As depicted in Figure 3, temperature showed a significant ($p < 0.05$) positive correlation with the number of active toads in both males and females. Humidity showed a significant positive correlation in males only (Fig. 4). In females, the correlation coefficient was positive, but it was too small to be statistically significant ($p > 0.05$, Fig. 4).

When both temperature and humidity were used as independent variables, a highly significant multiple correlation ($p < 0.01$) with the number of active toads was observed in males as well as in females (Fig. 5).

DISCUSSION

A number of investigations have been published on the role of thyroid hormones in the migration of vertebrates: in fish [14–15], amphibians [5, 7, 16, 17] and birds [18]. Our observations on the annual cycle of plasma thyroxine and triiodothyronine levels in the toad, *Bufo japonicus*, seemed to support the idea that thyroid hormone plays a role in toad migration. On the contrary, we recently observed that the treatment of male *Bufo japonicus* with thyroxine decreased the distance of locomotion of a toad kept in a small experimental chamber [12]. This effect of thyroxine was observed in both normal and thyroidectomized males, and thyroidectomy increased the distance of locomotion. However, we were cautious in concluding that the sedative effect of thyroxine was physiological, since the effect was observed under artificial conditions.

Our former results of the thyroidectomy experiment [12] were confirmed under the quasi-natural conditions in the present study. The thyroidectomy increased both the number of toads which showed activity and the number of days on which the toads showed activity. Accordingly, we conclude that thyroxine decreased both parameters representing the occurrence of locomotor or migratory activity during the breeding season even under the quasi-natural conditions. However, it is not known whether the effect of thyroxine is direct

or indirect. Furthermore, the physiological meaning of this effect is still obscure, although we postulated that it might be related to post-breeding inactiveness [12].

Hypophysectomy clearly suppressed the activity of male toads. This suggests that some hormone(s) of the pituitary gland activates(s) migratory activity in male toads. However, it is difficult to conclude whether this suppressive effect of hypophysectomy is due to the ablation of a specific hormone controlling the migration or the ablation of hormone(s) regulating the general metabolism.

Another problem was the inactiveness of the female toads, which caused difficulty in observing the effect of the operations in females. Only a few females showed activity in the present study as well as in the previous study in the chamber [12]. This may be related to the fact that not all female toads participate in breeding activity every spring [19–21].

It is revealed in the present study that the combination of temperature and humidity is the external factor which initiates locomotor activity in early spring. The high humidity may be advantageous for gas exchange through the skin of the toad and the relatively high temperature, for energy metabolism. A high rate of this external and internal respiration is necessary for muscular activity during the migration of toads in early spring. We can now predict the occurrence of migration in toads from the temperature and humidity by using the regression formula obtained in the present study.

ACKNOWLEDGMENTS

The authors are grateful to Prof. Yasuyuki Oshima for his valuable advice and suggestions. This study was supported by a Grant-in-Aid from the Japanese Ministry of Education, Science and Culture.

REFERENCES

- 1 Hisai, N. and Sugawara, T. (1978) Ecological studies of *Bufo bufo japonicus* Schlegel (V) The relation between appearances and the climatic conditions at breeding season. Miscellaneous Reports of the National Park for Nature Study, **8**: 135–149. (In Japanese)

- 2 Okuno, R. (1985) Studies on the natural history of the Japanese toad, *Bufo japonicus japonicus*. VIII. Climatic factors influencing the breeding activity. Jap. J. Ecol., **35**: 527–535. (In Japanese)
- 3 Reinke, E. E. and Chadwick, C. S. (1940) The origin of the water drive in *Triturus viridescens*. J. Exp. Zool., **83**: 223–233.
- 4 Chadwick, C. S. (1944) Further observations on the water drive in *Triturus viridescens*. J. Exp. Zool., **86**: 175–187.
- 5 Crim, J. W. (1975) Prolactin-induced modification of visual pigments in the eastern red-spotted newt, *Notophthalmus viridescens*. Gen. Comp. Endocrinol., **26**: 233–242.
- 6 Duvall, D. and Norris, D. O. (1977) Prolactin and substrate stimulation of locomotor activity in adult tiger salamanders (*Ambystoma tigrinum*). J. Exp. Zool., **200**: 103–106.
- 7 Duvall, D. and Norris, D. O. (1980) Stimulation of terrestrial-substrate preferences and locomotor activity in newly transformed tiger salamanders (*Ambystoma tigrinum*) by exogenous or endogenous thyroxine. Anim. Behav., **28**: 116–123.
- 8 Moriya, T. (1982) Prolactin induces increase in the specific gravity of salamander, *Hynobius retardatus*, that raises adaptability to water. J. Exp. Zool., **223**: 83–88.
- 9 Yoneyama, H., Ishii, S., Yamamoto, K. and Kikuyama, S. (1984) Plasma prolactin levels of *Bufo japonicus* before, during and after breeding in the pond. Zool. Sci., **1**: 969.
- 10 Ishii, S., Yoneyama, H., Inoue, M., Yamamoto, K. and Kikuyama, S. (1989) Changes in plasma and pituitary levels of prolactin in the toad, *Bufo japonicus*, throughout the year with special reference to the breeding migration. Gen. Comp. Endocrinol., **74**: 365–372.
- 11 Tasaki, Y., Inoue, M. and Ishii, S. (1986) Annual cycle of Plasma thyroid hormone levels in the toad, *Bufo japonicus*. Gen. Comp. Endocrinol., **62**: 404–410.
- 12 Tasaki, Y. and Ishii, S. (1989) Effects of thyroxine on locomotor activity and carbon dioxide release in the toad, *Bufo japonicus*. Zool. Sci. (In press)
- 13 Ishii, S. (1983) "Programs of statistical methods for biologists by N88-BASIC", Baifukan, Tokyo.
- 14 Woodhead, A. D. (1975) Endocrine physiology of fish migration. Oceanogr. Mar. Biol. Annu. Rev., **13**: 287–382.
- 15 Dickhoff, W. W., Folmar, L. C. and Gorbman, A. (1978) Changes in plasma thyroxine during smoltification of coho salmon, *Oncorhynchus kisutch*. Gen. Comp. Endocrinol., **36**: 229–232.
- 16 Grant, W. C., Jr. and Cooper, G. IV (1965) Behavioral and integumentary changes associated with induced metamorphosis in *Diemictylus*. Biol. Bull., **129**: 510–522.
- 17 Dent, J. N. (1985) Hormonal interaction in the regulation of migratory movements in urodele amphibians. In "The Endocrine System and the Environment". Ed. by B. K. Follet, S. Ishii and A. Chandola, Japan Sci. Soc. Press, Tokyo/Springer-Verlag, Berlin, pp. 79–84.
- 18 Berthold, P. (1985) Migration: Control and metabolic physiology. In "Avian Biology", Ed. by D. S. Farner and J. R. King, vol. 5, Academic Press, New York, pp. 77–128.
- 19 Hisai, N. (1981) Ecological studies of *Bufo bufo formosus* Boulenger (VI) Differences of postmetamorphic growth rate and the sexual maturity between sexes in the natural population. Miscellaneous Reports of the National Park for Nature Study, **12**: 103–113. (In Japanese)
- 20 Okuno, R. (1985) Studies on the natural history of the Japanese toad, *Bufo japonicus japonicus*. V. Post-metamorphic survival and longevity. Jap. J. Ecol., **35**: 93–101. (In Japanese)
- 21 Okuno, R. (1986) Studies on the natural history of the Japanese toad, *Bufo japonicus japonicus*. IX. Male behaviors during breeding season. Jap. J. Ecol., **35**: 621–630. (In Japanese)

Effects of Hypophysectomy and Replacement Therapy with Several Hormones on Plasma Sodium Concentrations in Bullfrog Tadpoles

MINORU UCHIYAMA and TOSHIKI MURAKAMI

*Department of Oral Physiology, School of Dentistry at Niigata,
The Nippon Dental University, Niigata 951, Japan*

ABSTRACT—Hypophysectomy significantly decreased plasma sodium concentrations in bullfrog tadpoles kept in low-sodium media (2.5 meq/liter). A study on replacement therapy revealed that administration of tadpole pituitary homogenate corrected this hyponatremia in hypophysectomized tadpoles. These results show that in a low-sodium environment where the tadpoles live in nature, the pituitary gland is important for plasma sodium regulation. AVT and ovine prolactin did not maintain normal plasma sodium levels in hypophysectomized tadpoles, whereas ACTH and corticosteroids (especially cortisol) restrained the sodium decrease. Therefore, in pre-metamorphic tadpoles it seems that the pituitary-adrenal axis plays an important role in plasma sodium regulation.

INTRODUCTION

Among the lower vertebrates, the amphibians, as a group, have been studied extensively with regard to their mechanisms of osmotic and ionic regulation. It is well known that the skin of amphibians can actively take up salt from the surrounding aqueous environment. In these animals, corticosteroids especially aldosterone, and neurohypophysial hormone, arginine vasotocin (AVT), generally show potent natriuretic and osmotic actions [see 1, 2]. It is known that tadpoles also actively transport sodium and chloride ions into their body fluids from a low-concentration external solution [3-6]. The integument of tadpoles, however, has been thought to be inessential for absorption of ions from the environment [7-9]. *In vitro* studies have shown that the main organ for active uptake of ions in tadpoles is not the skin but the gills [4, 10]. On the other hand, in unfed freshwater fish, accumulation of sodium depends almost entirely on the active uptake of sodium across the gill epithelium. It is also known that hypophysectomy results in an increased rate of sodium loss, and that in many

cases, this can be prevented by injection of prolactin [reviewed by 11]. However, injection of ovine prolactin into normal tadpoles acclimated to low aqueous calcium and sodium or high aqueous calcium and sodium does not produce consistent hypernatremia [12], and it has been observed that ovine prolactin does not correct hyponatremia in hypophysectomized tadpoles [13]. In tadpoles, therefore, the role of prolactin in plasma sodium metabolism seems to be minor.

The present study was undertaken to investigate hypernatremic hormone(s) in bullfrog tadpoles, with special reference to the effects of replacement therapy with both pituitary gland and pituitary hormone and corticosteroid on plasma sodium concentration in hypophysectomized tadpoles.

MATERIALS AND METHODS

Tadpoles of the bullfrog, *Rana catesbeiana* Shaw, at T-K stages VI to XIV were obtained from commercial dealers in Niigata [14]. They were kept for at least 1 week in low-calcium and low-sodium water (Ca: 0.85 meq/liter, Na: 2.5 meq/liter) at room temperature and maintained unfed during the experiments. Tadpoles were anesthetized in 0.05% MS 222 (m-aminobenzoic acid ethylester methanesulfonate, Sankyo) prior to

manipulation, hormone injection and blood sampling. The procedures of blood sampling and the method of plasma sodium determination have been described previously [12]. All data are presented as means \pm SE and statistical analysis of differences in means was performed using Student's *t*-test.

Hypophysectomy and autotransplantation or pituitary homogenate injection

Hypophysectomy and autotransplantation or pituitary homogenate injection were done by the methods reported previously [12, 15]. In the autotransplantation experiment, tadpoles were hypophysectomized and then the removed pituitary gland was transplanted under the skin of the head region of the same individual (HYPX+autotransp.). A piece of muscle from each tadpole was transplanted into sham-transplanted tadpoles (HYPX+m. transp.). In the pituitary homogenate injection study, hypophysectomized tadpoles were injected intraperitoneally with a homogenate of tadpole pituitary gland. Each animal received a homogenate of 2 pituitary glands per injection daily for 6 days.

In these experiments, treated tadpoles were maintained in low-sodium water (Na: 2.5 meq/liter) for one more week and then sacrificed for blood sampling.

Hypophysectomy and hormonal treatment

In these experiments, hypophysectomized tad-

poles were divided into several groups and maintained in low-sodium water (Na: 2.5 meq/liter). Then the effects of certain hormones were examined. The following hormones were used: ovine prolactin (NIH-p-S8), aldosterone (Sigma), ACTH (Armour Pharmaceutical Co.), corticosterone (Sigma), cortisol (Merck Sharp & Dohme), and AVT (Sandoz). These hormones were dissolved in 0.6% saline and/or 95% ethanol. Injections (20–25 μ l/animal) were made with a Hamilton microsyringe into the lymph sinus beneath the skin of the back, passing through the tail muscles to prevent leakage. Injections were started one day after the operation. Each group received one of the above-mentioned hormones or the combinations of them daily for 6 days. Two series of experiments were performed.

RESULTS

Hypophysectomy followed by autotransplantation or injection of pituitary homogenates

The results obtained in these experiments are shown in Table 1. It was confirmed that hypophysectomy caused significant hyponatremia, showing that the pituitary gland is important for plasma sodium regulation in bullfrog tadpoles. There was a significant difference between the plasma sodium concentration in the sham operation group and that in the HYPX+muscle transplant group ($P < 0.001$). In the second experiment,

TABLE 1. Effect of hypophysectomy and replacement therapy on plasma sodium in bullfrog tadpoles

Experiment	Treatment	Number	Time after treatment	Na (meq/liter)	Significance compared to: sham operation	Significance compared to: HYPX ^a +m. transp. or saline
1 ^c	sham operation	9	1 week	97.9 \pm 1.4 ^b	—	$P < 0.001$
	HYPX+m. transp.	10	1 week	87.5 \pm 1.3	$P < 0.001$	—
	HYPX+autotransp.	9	1 week	92.2 \pm 2.0	$P < 0.05$	NS
2	sham operation	6	1 week	96.0 \pm 1.0	—	$P < 0.001$
	HYPX+saline	9	1 week	86.8 \pm 1.4	$P < 0.001$	—
	HYPX+pituitary homogenate	12	1 week	93.0 \pm 1.7	NS	$P < 0.05$

^a Abbreviations used: HYPX, hypophysectomy; m. transp., muscle transplantation; saline, saline injection.

^b Values are means \pm SE.

^c Number of experiments conducted: 1, HYPX and autotransplantation; 2, HYPX and injection with pituitary homogenates.

plasma sodium concentration in the sham operation group was significantly higher than that in the HYPX+saline group ($P<0.001$). The plasma sodium concentration in the HYPX+pituitary homogenate group was also significantly higher than that in the HYPX+saline group ($P<0.05$).

Hypophysectomy and hormonal treatment

In the first experiment, the effects of different doses of a hormone or a combination of two hormones were examined on plasma sodium concentration in hypophysectomized tadpoles. Table 2 shows the results obtained from this experiment.

Plasma sodium concentration in the sham operation+saline group was significantly different from those in the HYPX+saline, HYPX+AVT (0.02 ng/g and 0.2 ng/g) and HYPX+ovine prolactin (5 μ g/g) groups ($P<0.05$). Injections of ACTH (50 ng/g), cortisol (0.5 μ g/g, 5 μ g/g), ACTH and ovine prolactin in combination, or aldosterone (50 ng/g) into hypophysectomized tadpoles produced significantly higher plasma sodium concentrations than those in hypophysectomized tadpoles ($P<0.05$), whereas no statistically significant difference was found between the HYPX+saline group and the other experimental groups. In the second experi-

TABLE 2. Effect of hypophysectomy and hormonal replacement therapy on plasma sodium in bullfrog tadpoles

Treatment	Number	Na (meq/liter)	Significance compared to:	
			sham operation +saline	HYPX +saline
sham operation+saline	14	99.9 \pm 1.0 ^a	—	$P<0.05$
HYPX+saline	10	97.0 \pm 0.5	$P<0.05$	—
HYPX+ACTH (50 ng/g)	10	100.4 \pm 0.8	NS	$P<0.01$
HYPX+ACTH (500 ng/g)	10	99.3 \pm 1.1	NS	NS
HYPX+aldosterone (5 ng/g)	8	99.1 \pm 2.1	NS	NS
HYPX+aldosterone (50 ng/g)	12	100.2 \pm 0.9	NS	$P<0.01$
HYPX+corticosterone (0.5 μ g/g)	12	97.5 \pm 0.9	NS	NS
HYPX+corticosterone (5 μ g/g)	10	98.8 \pm 1.2	NS	NS
HYPX+cortisol (0.5 μ g/g)	12	99.8 \pm 1.1	NS	$P<0.05$
HYPX+cortisol (5 μ g/g)	10	100.8 \pm 1.1	NS	$P<0.05$
HYPX+oPRL (5 μ g/g)	9	95.9 \pm 1.4	$P<0.05$	NS
HYPX+oPRL (5 μ g/g)+ACTH (150 ng/g)	12	100.8 \pm 0.9	NS	$P<0.01$
HYPX+AVT (0.02 ng/g)	12	95.7 \pm 1.2	$P<0.05$	NS
HYPX+AVT (0.2 ng/g)	12	96.9 \pm 1.0	$P<0.05$	NS

^a Values are means \pm SE.

TABLE 3. Effect of hypophysectomy and hormonal replacement therapy on plasma sodium in bullfrog tadpoles

Treatment	Number	Na (meq/liter)	Significance compared to:	
			sham operation +saline	HYPX +saline
sham operation+saline	10	98.4 \pm 0.8 ^a	—	$P<0.05$
HYPX+saline	8	91.0 \pm 2.4	$P<0.05$	—
HYPX+ACTH (50 ng/g)	8	96.2 \pm 2.0	NS	NS
HYPX+aldosterone (50 ng/g)	5	94.8 \pm 3.0	NS	NS
HYPX+cortisol (5 μ g/g)	10	100.0 \pm 1.8	NS	$P<0.01$
HYPX+oPRL (5 μ g/g)	8	94.4 \pm 2.8	NS	NS

^a Values are means \pm SE.

ment, ACTH, aldosterone and ovine prolactin failed to maintain normal plasma sodium concentrations. However, cortisol corrected the plasma sodium concentration after hypophysectomy ($P < 0.01$). These results are summarized in Table 3.

DISCUSSION

In bullfrog tadpoles kept in low-sodium water (Na: 2.5 meq/liter), the previous observation that hypophysectomy brought about a significant decrease in plasma sodium concentration was confirmed [12, 13]. In the replacement therapy study, administration of tadpole pituitary homogenate corrected the hyponatremia and pituitary grafts partially prevented this in hypophysectomized tadpoles. These results suggest that the pituitary gland is important for maintaining plasma sodium concentrations in bullfrog tadpoles. The next question to be answered was which pituitary hormones are important for the control of plasma sodium concentration in bullfrog tadpoles.

In the present study, AVT was not able to maintain a normal plasma sodium level after hypophysectomy. Bentley and Greenwald [16] reported that the pituitary gland of the bullfrog tadpole contains only about one-fifth of the neurohypophysial peptides (activity/kg body weight) present in the adult frog. It is also reported that anuran tadpoles exhibit little or no response to AVT, although AVT is an antidiuretic and natriuretic hormone in adult amphibians [8, 16]. Therefore, the present result might be explained by assuming that AVT administration is not sufficient for maintaining a normal plasma sodium level and/or AVT might not be a potent agent for the control of hydromineral balance in young tadpoles. In the present study, prolactin was also unable to restore plasma sodium concentrations in hypophysectomized tadpoles. This result is consistent with the previous report [13]. Brown and Brown [17] suggested that the major role of prolactin in amphibians might be water retention. If this is so in bullfrog tadpoles, it is possible that the increase in plasma sodium concentration caused by prolactin treatment might be masked by hemodilution. On the other hand, Clemons and Nicoll [18] reported that the circulating plasma level and

pituitary content of prolactin were increased significantly during metamorphic climax in bullfrog tadpoles. It was also shown that during the climax stage, prolactin is involved in regulation of the active sodium transport system in the ventral skin of bullfrog tadpoles [19, 20]. The bullfrog tadpoles used in the present study were pre-metamorphic larvae (stages VI-XIV). Therefore, there are two possible explanations for the minimal effect of prolactin on sodium regulation in young tadpoles. One is that prolactin secretion is insufficient in young tadpoles and the other is that the target systems of prolactin sodium transport might be undeveloped. The latter concept is probably true in the case of ACTH (presumably acting through the adrenal gland), since Krug *et al.* [21] showed that a single injection of ACTH failed to elevate the serum level of aldosterone, corticosterone and cortisol in pre-metamorphic larvae (stages X-XIV), whereas the same treatment caused a striking increase in the levels of corticosterone and cortisol in more advanced tadpoles (stages XV-XIX). In the present study, however, it is possible that long-term ACTH treatment might have stimulated the production of corticosteroid in young tadpoles.

It is generally accepted that aldosterone and corticosterone are produced in the interrenal organ, and that corticosteroids, especially aldosterone, are involved in the regulation of electrolytes in adult amphibians. However, little information is available on the influence of corticosteroids on electrolyte regulation in larval anurans. Krug *et al.* [21] reported that serum aldosterone was maintained at fairly low levels in bullfrog tadpoles until a significant increase occurred in the metamorphic climax stage. In the present study, injection of aldosterone was inconsistent in restoring hyponatremia caused by hypophysectomy. Therefore, aldosterone might not be a major sodium-regulating agent in pre-metamorphic bullfrog tadpoles. Krug *et al.* [21] detected very low levels of corticosterone in serum during stages V to X, and then serum corticosterone concentration increased steadily until stage XVII. In the present study, which examined the effects of corticosterone and cortisol in bullfrog tadpoles (stages VII-XII) kept in low-sodium water, the hypernatremic

effect of corticosterone did not exceed that of cortisol at the same dose. It is not yet known whether cortisol is produced in larval amphibians. However, according to Krug *et al.* [21] a cortisol-like substance is present in the serum of young tadpoles (stages V-XXV). In the present study, cortisol was the most potent hypernatremic agent in young tadpoles. In pre-metamorphic bullfrog tadpoles, a cortisol-like substance was detectable [21] and their gills were important site for sodium uptake [4, 10]. Therefore, a cortisol-like substance might be involved in the uptake of sodium by the gills of bullfrog tadpoles. This may also influence the metabolic processes in the body, thus indirectly affecting sodium homeostasis and osmoregulation. In conclusion, it seems that the pituitary-adrenal axis is important for plasma sodium regulation in pre-metamorphic tadpoles.

ACKNOWLEDGMENTS

The authors wish to thank Prof. C. Oguro of Toyama University for his valuable discussions and revision of the manuscript. The authors' thanks are also extended to Prof. P. K. T. Pang, University of Alberta, for his suggestions and encouragement.

REFERENCES

- Bentley, P. J. (1971) The Amphibia. In "Endocrines and Osmoregulation". Ed. by P. J. Bentley, Springer-Verlag, Berlin Heidelberg, New York, pp. 161-192.
- Bentley, P. J. and Baldwin, G. F. (1980) Comparison of trans-cutaneous permeability in skins of larval and adult salamanders (*Ambystoma tigrinum*). *Am. J. Physiol.*, **239**: R505-508.
- Kawada, J., Taylor, R. E. and Barker, S. B. (1968) Measurement of Na-K ATPase in the separated epidermis of *Rana catesbeiana* frogs and tadpoles. *Comp. Biochem. Physiol.*, **30**: 965-975.
- Alvarado, R. H. and Moody, A. (1970) Sodium and chloride transport in tadpoles of the bullfrog *Rana catesbeiana*. *Am. J. Physiol.*, **218**: 1510-1516.
- Casada, J. H. and Nichols, J. R. (1986) Interrelationships among epidermal Na-K ATPase, developmental stage and length of *Rana catesbeiana* tadpoles. *Comp. Biochem. Physiol.*, **3**: 429-433.
- Robinson, D. H. and Mills, J. W. (1987) Ouabain binding in tadpole ventral skin. I. Kinetics and effect on intracellular ions. *Am. J. Physiol.*, **253**: R402-409.
- Taylor, R. E. and Barker, S. B. (1965) Trans-epidermal potential difference: development in anuran larvae. *Science*, **148**: 1612-1613.
- Alvarado, R. H. and Johnson, S. R. (1966) The effects of neurohypophyseal hormones on water and sodium balance in larval and adult bullfrogs (*Rana catesbeiana*). *Comp. Biochem. Physiol.*, **18**: 549-561.
- Cox, T. C. and Alvarado, R. H. (1979) Electrical and transport characteristics of skin of larval *Rana catesbeiana*. *Am. J. Physiol.*, **237**: R74-79.
- Dietz, T. H. and Alvarado, R. H. (1974) Na and Cl transport across gill chamber epithelium of *Rana catesbeiana* tadpoles. *Am. J. Physiol.*, **226**: 764-770.
- Ball, J. N. (1969) Prolactin and osmoregulation in teleost fishes: a review. *Gen. Comp. Endocrinol.*, **Suppl.**, **2**: 10-25.
- Uchiyama, M. and Pang, P. K. T. (1981) Endocrine influence on hypercalcemic regulation in bullfrog tadpoles. *Gen. Comp. Endocrinol.*, **44**: 428-435.
- Sasayama, Y. and Oguro, C. (1982) Effects of hypophysectomy and replacement therapy with pituitary homogenates or ovine prolactin on serum calcium, sodium, and magnesium concentrations in bullfrog tadpoles. *Gen. Comp. Endocrinol.*, **46**: 75-80.
- Taylor, A. C. and Kollros, J. J. (1946) Stages in the normal development of *Rana pipiens* larvae. *Anat. Rec.*, **94**: 7-23.
- Uchiyama, M. and Pang, P. K. T. (1982) Replacement therapy and plasma calcium concentration in hypophysectomized bullfrog tadpoles, *Rana catesbeiana*. *Gen. Comp. Endocrinol.*, **47**: 351-356.
- Bentley, P. J. and Greenwald, L. (1970) Neurohypophyseal function in bullfrog (*Rana catesbeiana*) tadpoles. *Gen. Comp. Endocrinol.*, **14**: 412-415.
- Brown, P. S. and Brown, S. C. (1987) Osmoregulatory actions of prolactin and other adenohypophyseal hormones. In "Vertebrate Endocrinology: Fundamentals and Biomedical Implications, Vol. 2". Ed. by P. K. T. Pang and M. P. Schreibman, Academic Press, San Diego, pp. 45-84.
- Clemons, G. K. and Nicoll, C. S. (1977) Development and preliminary application of a homologous radioimmunoassay for bullfrog prolactin. *Gen. Comp. Endocrinol.*, **32**: 531-535.
- Eddy, L. J. and Allen, R. F. (1979) Prolactin action on short circuit current in the developing tadpole skin: a comparison with ADH. *Gen. Comp. Endocrinol.*, **38**: 360-364.
- Takada, M. (1986) The short-term effect of prolactin on the active Na transport system of the tadpole skin during metamorphosis. *Comp. Biochem. Physiol.*, **85A**: 755-759.
- Krug, E. C., Honn, K. V., Battista, J. and Nicoll, C. S. (1983) Corticosteroids in serum of *Rana catesbeiana* during development and metamorphosis. *Gen. Comp. Endocrinol.*, **52**: 232-241.

Two Species of the Genus *Actacarus* (Acari, Halacaridae) from Japan

HIROSHI ABÉ

*Department of Systematic Zoology, Division of Environmental Structure,
Graduate School of Environmental Science, Hokkaido University,
Sapporo 060, Japan*

ABSTRACT—A new arenicolous halacarid mite, *Actacarus karoensis* sp. nov., is described and another species, *Actacarus illustrans* Newell, 1951, is newly recorded from Japan. *A. karoensis* is easily distinguishable from congeners on the basis of several characters including the shape of the genitoanal plate and length of the ovipositor. As for *A. illustrans*, it was noted that the Japanese specimens differ from the North American specimens in some morphological characters. These differences are regarded here as intraspecific variations.

INTRODUCTION

Taxonomic knowledge of marine halacarid mites in Japan is limited. The first record of the family in Japan was in 1927, when *Halacarus spongiphilus* Kishida, 1927 was described from the abyssal zone in Sagami Bay [1]. An additional species, *Agauopsis okinavensis*, was described by Bartsch [2] from Okinawa, southern Japan. The present paper describes two species of the genus *Actacarus* newly found in Japan.

MATERIALS AND METHODS

Specimens were fixed with modified Imamura's fluid [3], dissected in a drop of pure lactic acid, and mounted in gumchloral medium. Observation was made under a phase-contrast microscope using oil immersion, figures were drawn with the aid of a camera lucida, and measurements were made with an ocular micrometer. Sizes of idiosoma and gnathosoma were measured before dissection, while other parts were measured on dissected specimens.

Terms: The terms for body parts of halacarid mites follow Newell [4–7].

Presentation of numerical data: Metric charac-

ters are always given in micrometers (μm). Meristic characters are sometimes given with ranges. Presentation of leg chaetotaxy and arrangement of subgenital setae follow Newell [7]. In describing positions of certain structures on a plate, the decimal system developed by Newell [6–9] is employed; for example, the statement 'setae at 0.44 on the genitoanal plate' means that the setae are located at a level 0.44 of the interval between the anteromedian point (0.00) and the posteromedian point (1.00) on the plate.

Measured parts (letters in parentheses refer to those given in Fig. 1): **Idiosoma:** Length (a), from the anteriormost margin of the anterior dorsal plate to the terminal end of the anal papilla; width (b), at the level of the lateral coxal margin of leg III. **Plate, genital foramen, and spermatophorotype:** Length (c), from the anterior margin to the posterior margin; width (d), at the widest level. **Gnathosoma:** Length (e), from the posterior margin of the base of the gnathosoma to the anterior tip of the rostrum; width (f), at the widest level of the gnathosoma. **Base of gnathosoma:** Length (g), from the level of the base of the palpal insertions to the posterior margin of the gnathosoma. **Rostrum:** Length (h), from the level of the base of the palpal insertions to the anterior tip of the rostrum; width (i), at the widest level. **Basal cheliceral segment:** Length (j), from the level of the most proximal end of the segment to the level of the tiny

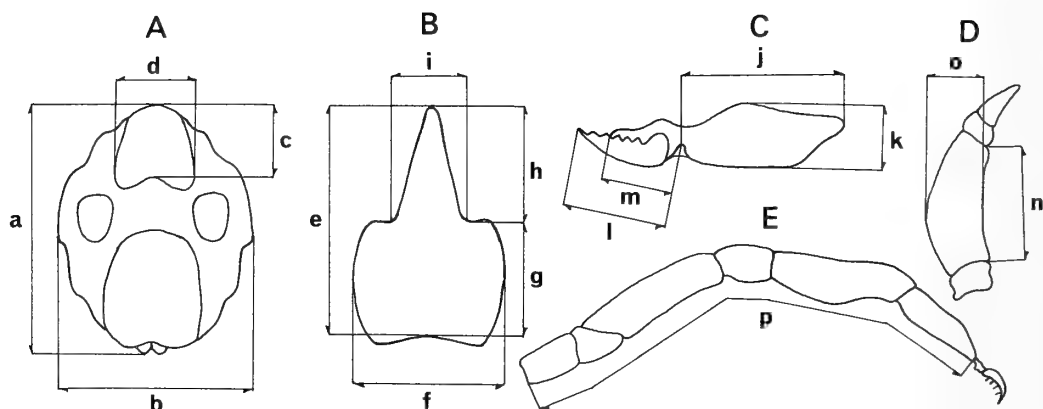


FIG. 1. Diagram of body parts measured. A, idiosoma; B, gnathosoma; C, chelicera; D, palp; E, leg. a-p: Measured parts explained in the text.

ventral gap; height (k), at the highest level. *Movable digit*: Length (l), from the level of the tiny gap to the distal end of the digit. *Fixed digit*: Length (m), from the level of the tiny gap to the distal end of the digit. *Palpal segment*: Length (n), from the proximal end to the distal end along the ventral margin; height (o), at the highest level. *Leg*: Length (p), from the proximal end of the trochanter to the distal end of the tarsal claw fossa along the ventral margin.

Abbreviations: AD, anterodorsal plate; PD, posterodorsal plate; OC, ocular plate; AE, anterior epimeral plate; PE, posterior epimeral plate; GA, genitoanal plate; ds, dorsal setae; aes-i, anterior epimeral setae; aes-ii-lat (-v), lateral (ventral) setae of coxae II; pes-iii-lat (-v), lateral (ventral) setae of coxae III; pes-iv-a (-P), anterior (posterior) setae of coxae IV; P-1 to P-4, first to fourth segment of palp; L/W, the ratio of length to width; Hal-55/etc., specimen codes of the author's personal system. In the present paper the codes are given only to the described specimens.

In addition, the following abbreviations are used in the figure legends: Ds, dorsal view; Vr, ventral view; Lat, lateral view; R, right appendage (or part); L, left appendage (or part).

Family *Halacaridae* Murray, 1987

(Japanese name: Ushiodani-ka)

Subfamily *Actacarinae* Viets, 1939

(Japanese name: Nagisadani-aka, new)

Genus *Actacarus* Schulz, 1937

(Japanese name: Nagisadani-zoku, new)

Actacarus illustrans Newell, 1951

(Japanese name: Kita-nagisadani, new)

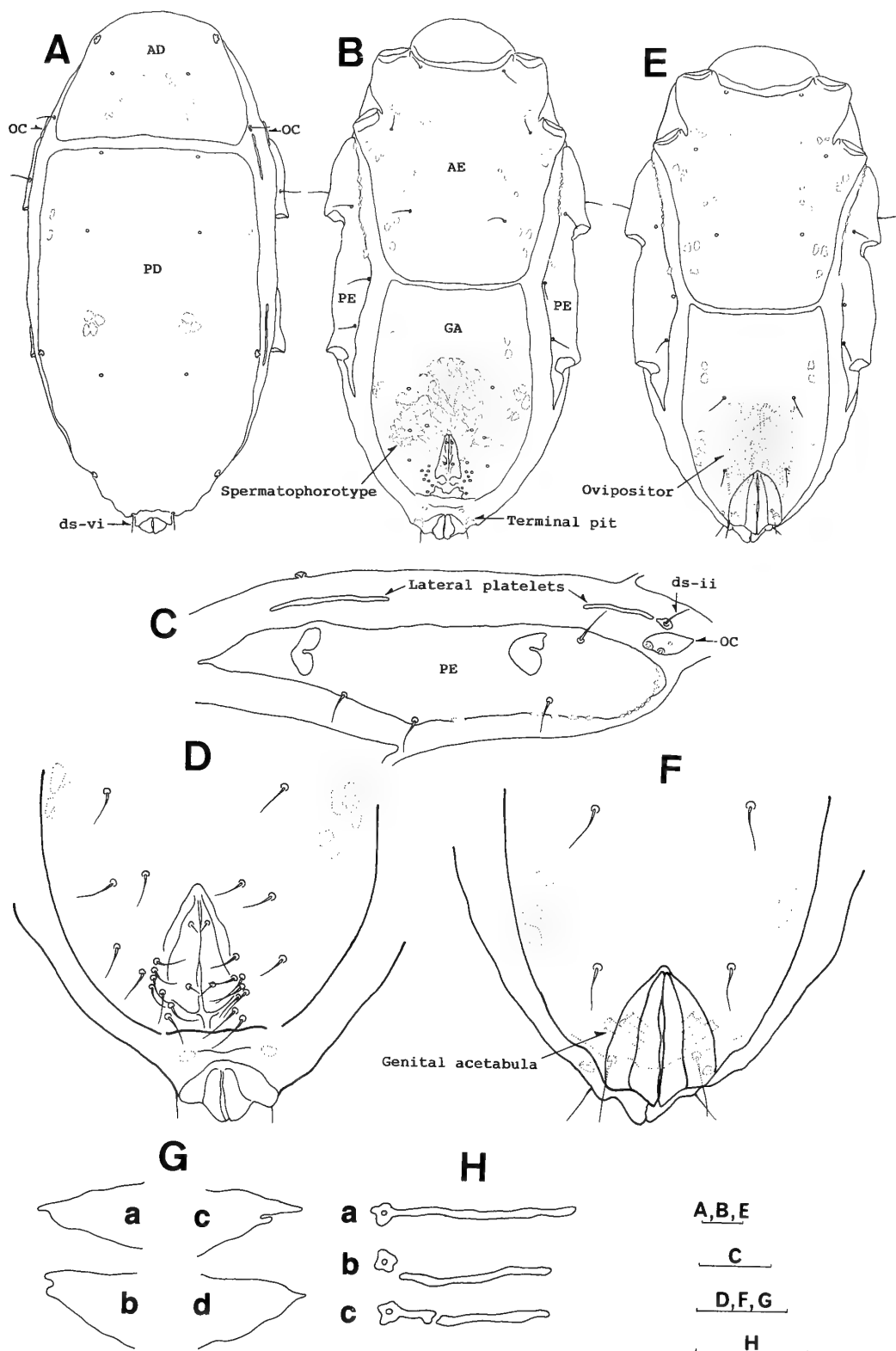
(Figs. 2-6)

Actacarus illustrans Newell, 1951 [4], pp. 33-36, Figs. 126-140. (Holotype: Male, in American Museum of Natural History; type locality, Unalaska Island, Alaska.)

Actacarus illustrans: Krantz, 1976 [10], pp. 255-257, Tab. 5, Figs. 30-32. (Descriptions of immature stages with leg chaetotaxy in adult, record from Oregon.) (nec *A. illustrans* sensu Vorob'yeva and Yaroshenko, 1979 [11].)

Specimens examined. 3 males, 3 females: Intertidal, in coarse sand along shore line at low tide, Uchikabuto, Oshoro Bay (43°12'N, 140°51'E), Hokkaido, Sea of Japan, Japan, 26-VI-1986, H. Abé coll.—1 deutonymph, 1 protonymph, 1 larva:

FIG. 2. *Actacarus illustrans*. Male (Hal-55): A, idiosoma (Ds); B, idiosoma (Vr); C, idiosoma (Lat, R); D, genitoanal region. Female (Hal-1): E, idiosoma (Vr); F, genitoanal region. Males & Females: G, posterior margin of PE (a, b: R; c, d: L); H, anterior lateral platelet (a-c: L). Scale bars=20 μ m.



Intertidal, in coarse sand and gravel along shore line at low tide, Shamodomari, Oshoro Bay, Hokkaido, Sea of Japan, Japan, 19-V-1987, H. Abé coll.—1 male, 1 deutonymph, 2 protonymphs: Intertidal, in coarse sand among boulders along shore line at high tide, Ebisu Rock, Oshoro Bay, Hokkaido, Sea of Japan, Japan, 23-VI-1987, H. Abé coll. The following American specimens were also examined for the purpose of comparison: 1 male, 1 female, 1 deutonymph, 1 protonymph: In coarse sand near bank, mouth of Schooner Creek, Pacific coast of Oregon, U.S.A., 18-VI-1974, G. W. and V. J. Krantz coll.

Description. *Male* (Hal-55): Idiosoma 256 μm long, 128 μm wide, color in life semitransparent with dark brown specks and a longitudinal white dorsal line medially.

Dorsum (Fig. 2A) almost completely covered with two dorsal plates, which are strongly ribbed, uniformly punctate and with small scattered alveoli. AD approximately 1/3 length of PD, L/W 0.66, furnished with a large pore on anterolateral corner on each side, a few minute canaliculi on anterolateral site, and paired weak areolae on surface of posterior half. PD 182 μm long, 114 μm wide, furnished with weak areolae anterolaterally, a cluster of three weak panels medially, and scattered minute canaliculi laterally on each side; two pores near lateral margin. OC (Fig. 2C) 16 μm long, 8 μm wide, lateromarginally placed. Two

lateral platelets (Fig. 2C) lying marginally on each side of idiosoma alongside AD and PD, quite narrow and very weakly sclerotized; the first platelet divided into anterior microplatelet, 3 μm long, 3 μm wide, located dorsally to OC, and posterior microplatelet, 30 μm long, 2 μm wide, extending posteriorly to level about midway between anterior margin of PD and insertion of leg III; the second platelet lying parallel to PD, near insertion of leg IV.

Chaetotaxy of dorsal region: Setae ds-i on AD; ds-ii on anterior microplatelets, seen as if located on membranous cuticle from dorsal view; ds-iii, -iv, -v, -vi (adanal setae) on PD.

Venter (Fig. 2B) covered with four plates which are weakly ornamented in a manner similar to dorsal plates. AE 110 μm long, 106 μm wide, ornamented with tiny triangular epimeral processes, anteriorly with a thin membranous collar, with five sets of lateral and medial subsurface pores of various shapes. PE (Fig. 2C) 136 μm long, 28 μm wide, elongate, marked with some series of marginal subsurface pores ventrally.

Chaetotaxy of epimeral region: Setae aes-i, aes-ii-lat, aes-ii-v on AE; pes-iii-lat, pes-iii-v, pes-iv-a, pes-iv-p each on PE.

Genitoanal region (Fig. 2B, D): GA 180 μm long, 108 μm wide, reaching anteriorly just posterior to level of pes-iv-a, ornamented with two anterolateral subsurface pores and cluster of post-

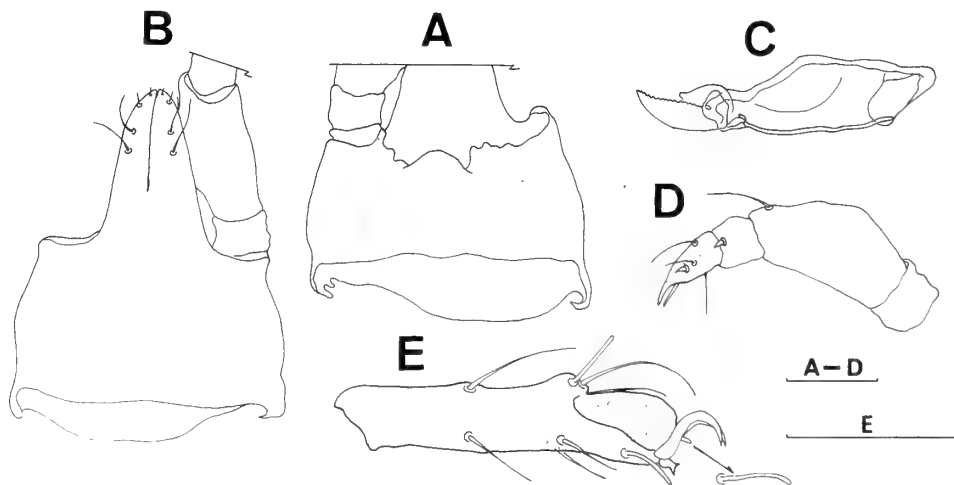


FIG. 3. *Actacarus illustrans*. Male (Hal-55): A, gnathosoma (Ds); B, gnathosoma (Vr); C, chelicera (L); D, palp (R); E, tarsus I (L). Scale bars=20 μm .

erolateral weak panels on each side. Genital foramen about 1/4 length of GA, L/W 1.95, triangular; anterior margin at 0.68 relative to GA length. Anal papilla terminal, well separated from genital foramen. A terminal pit (Fig. 2B) located laterally just adjacent to anal papilla on each side. Spermatophorotype (Fig. 2B) massive, approximately 1/2 length of GA, L/W 1.06.

Chaetotaxy of genitoanal region: One pair of outlying setae at 0.44 on GA; a group of eleven perigenital setae on each lateral side of genital foramen as illustrated in Fig. 2D; two subgenital setae on each genital sclerite, arranged 1-1. No setae on anal papilla.

Gnathosoma (Fig. 3A, B) 70 μm long, 56 μm wide, gnathosomal length/idiosomal length 1.06. Anterior margin of tectum weakly convex. Rostrum 36 μm long, 26 μm wide, furnished with four pairs of delicate rostral setae. Chelicera (Fig. 3C) with basal segment 42 μm long, 16 μm wide, partly punctate, with oblique proximal end. Movable digit approximately 1/2 length of basal segment, slightly inclined dorsally, bearing 16-18 minute denticles along dorsal edge. Fixed digit nearly 1/2 length of movable digit. Palp (Fig. 3D) 61 μm

long, slightly inclined ventrally, with four free segments.

Legs: Length of legs I, II, III, IV=194, 162, 174, 192 μm , respectively. Leg chaetotaxy as follows: Trochanters I-IV, 0-0-1-1; basifemora, 2-2-2-2; telofemora, 2-2-2-2; genua, 5-4-3-3; tibiae, 7-5-5-5. Tarsus I (Fig. 3E) with strongly developed posterior lamella, with three dorsal setae (one at intermediate level on basidorsal limb, others on claw fossa), one solenidion, one famulus, three filiform ventral setae (one intermediately, others distally), and two parambulacral setae (single euphathidai); solenidion fine, setiform, at base of fossary lamella; famulus minute, blade-like in form, with fine canaliculus, lying distally to solenidion; lateral claws small compared with those on other legs, with indistinct combs; median claw bidentate.

Female (Hal-1): Idiosoma 242 μm long, 124 μm wide, resembling male in essential details except for the sculpture of PD and characters of genitoanal region. PD furnished with only one weak panel at about mid-level on each side. **Genitoanal region** (Fig. 2E, F): Genital foramen 32 μm long, 24 μm wide, located terminally and covering anal for-

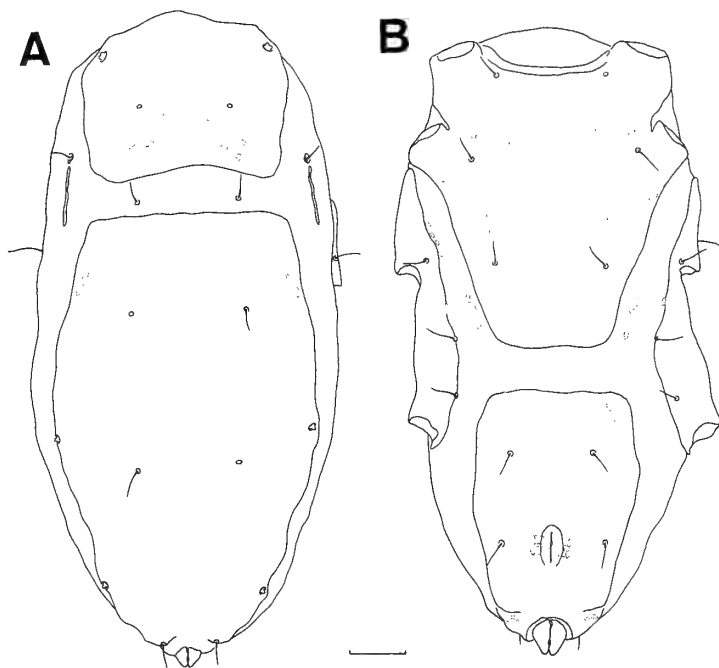


FIG. 4. *Actacarus illustrans*. Deutonymph (Hal-59): A, idiosoma (Ds); B, idiosoma (Vr). Scale bar=20 μm .

men, furnished with three pairs of perigenital setae; the first pair at 0.40, the second at 0.62 (level of anterior margin of genital foramen), and the third at 0.87 (behind genital foramen occupying terminal concavity). Subgenital setae absent. Three pairs of genital acetabula (Fig. 2F) lying inside of genital foramen. Ovipositor (Fig. 2E) short, funnel-like, medially placed.

Immature stages. *Deutonymph* (Hal-59): Idiosoma 228 μm long, 108 μm wide. *Dorsum* (Fig. 4A): AD slightly concave posteriorly. PD extending anteriorly to level about midway between insertions of legs II and III. Setae ds-iii inserted in striated membranous cuticle between AD and PD. *Venter* (Fig. 4B): AE narrowed posteriorly from level of insertion of leg II to level of pes-iv-a. Lateral platelets short and weakly sclerotized. A number of subsurface pores present on membranous cuticle between AE and PE. GA 78 μm long, 60 μm wide, extending anteriorly to level of pes-iv-p, furnished with two pairs of perigenital setae and internal genital acetabula. *Legs*: Basifemur IV has only one seta.

Protonymph (Hal-58): Idiosoma 236 μm long,

108 μm wide. *Dorsum* (Fig. 5A): AD not reaching posteriorly to level of ds-ii. PD extending anteriorly to level of insertion of leg III. *Venter* (Fig. 5B): AE strongly narrowed posteriorly from level of insertion of leg II, with truncated posterior end at level about midway between pes-iii-v and pes-iv-p. Setae pes-iv-a lacking. Several subsurface pores located on membranous cuticle between AE and PE. GA 54 μm long, 46 μm wide, not reaching anteriorly to level of trochanter IV, without setae, bearing one pair of genital acetabula. *Legs*: Basifemur III with only one seta; trochanter IV without setae; femur IV undivided.

Larva (Hal-61): Idiosoma 168 μm long, 92 μm wide. *Dorsum* (Fig. 6A): AD and PD separated from each other by about the same length of AD. Lateral pores on AD and PD relatively large, distinct. Two subsurface pores placed on membranous cuticle dorsoposterior to OC. *Venter* (Fig. 6B): AE lacking aes-ii-lat. PE (Fig. 6C) small, with only one seta ventrally. Two very weakly sclerotized lateral microplatelets lying posterior to each of ds-ii. GA 28 μm long, 32 μm wide, square in outline, lacking both genital setae and genital

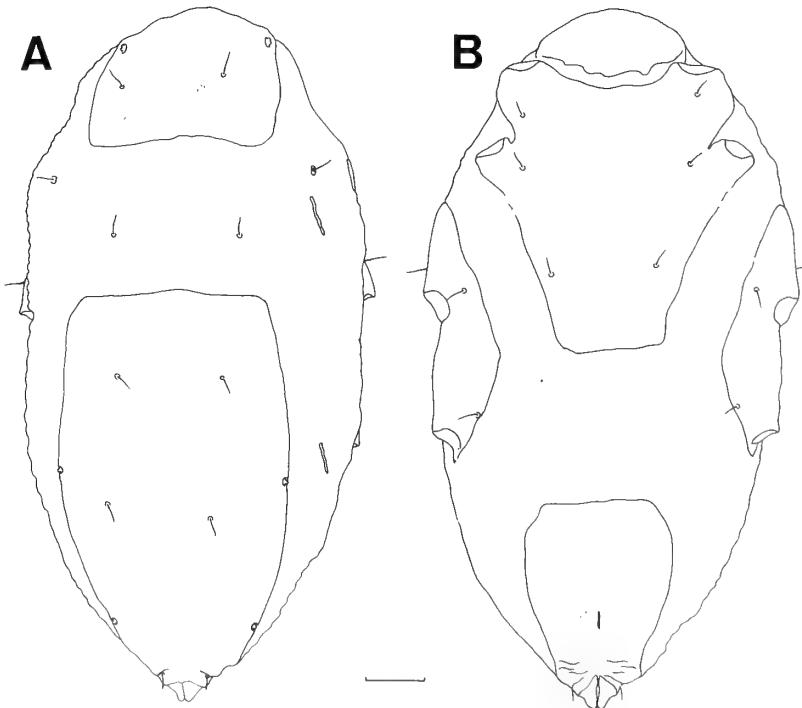


FIG. 5. *Actacarus illustrans*. Protonymph (Hal-58): A, idiosoma (Ds); B, idiosoma (Vr). Scale bar = 20 μm .

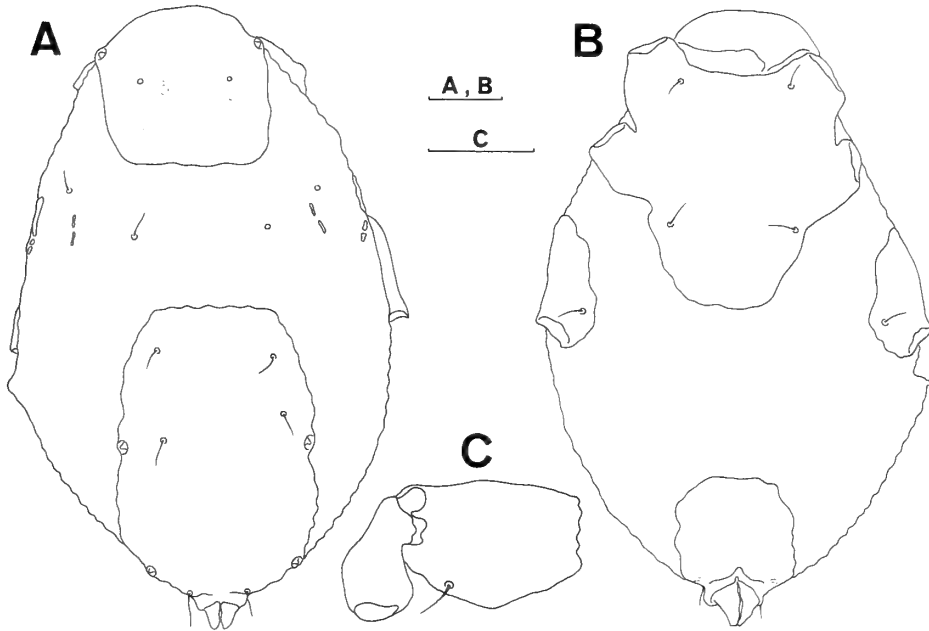


FIG. 6. *Actacarus illustrans*. Larva (Hal-61): A, idiosoma (Ds); B, idiosoma (Vr); C, PE with trochanter of leg III (R). Scale bars=20 μ m.

slit. Legs three pairs; basifemur and telofemur fused. Leg chaetotaxy as follows: Trochanters I-III, 0-0-1; femora, 3-3-3; genua, 4-4-3; tibiae, 5-5-5.

Morphological variation and abnormality: The number of panels comprising a cluster at about mid-level on each side of PD was from two to four in the male, and one to two in the female. The outline of the posterior margin of PE (Fig. 2G; a-d) differed among specimens and even between sides of one specimen. The microplatelets forming the first lateral platelet on each side of the idiosoma usually were separate, but in some cases were fused (Fig. 2H; a-c). Several specimens had three subsurface pores on one side of GA. A few male specimens had only ten perigenital setae on one side of the genital foramen. Basifemur IV had two setae in the described male specimen, but most of the adult specimens examined had only one seta. One deutonymph specimen retained the protonymphal condition in leg segmentation, with leg IV being five-segmented instead of six.

Distribution: Hitherto recorded from the north-eastern Pacific coasts of Alaska and Oregon in U.S.A. This is the first record of *A. illustrans* from

the western part of the northern Pacific.

Actacarus illustrans sensu Vorob'yeva and Yaroshenko [11] from the northwestern part of the Black Sea is identical with *A. bacescui* Konnerth-Ionescu, 1970 (= *A. illustrans* sensu Monniot, 1968 = *A. monniotae* Krantz, 1974) which was originally described from the Black Sea as a subspecies of *A. illustrans* and has been confused with *A. illustrans* Newell, 1951.

Remarks: *Actacarus illustrans* Newell, 1951 was originally described from the intertidal zone at Dutch Harbor, Unalaska Island [4], and its immature stages were described by Krantz [10]. The adult specimens from Hokkaido, northern Japan, accord well with the original description in the following characters: Setae ds-ii on membranous cuticle (on microplatelets forming the first lateral platelets); three pairs of setae on AE; four setae on PE (one dorsally, three ventrally); GA furnished with one pair of outlying setae and eleven perigenital setae in the male; ovipositor funnel-shaped and occupying nearly one third of the distance between each anterior margin of genital foramen and GA.

On the other hand, Japanese adult specimens

deviate from the original description in the following points (corresponding conditions in the original description in parentheses if necessary): (1) Somewhat larger body size: Male 252–260 μm , $n=4$ (240–246 μm , $n=3$); female 242–248 μm , $n=3$ (227–240 μm , $n=3$); (2) idiosoma with weakly sclerotized lateral platelets (no reference to the platelets); (3) anterior margin of tectum weakly convex (bilobed, from illustration); (4) leg chaetotaxy; (5) median claw on tarsus I bidentate (unidentate); (6) tarsus I with ten setae including solenidion and famulus (seven setae; solenidion and famulus lacking); (7) arrangement of perigenital setae in the male: Anterior two pairs of perigenital setae located anteriorly (posteriorly) to level of anterior margin of genital foramen, and one of the remaining nine pairs lying laterally and distant from lateral sides of genital foramen (all nine pairs located in the vicinity of genital foramen); and (8) three pairs of distinct perigenital setae in the female (two pairs).

Of these discrepancies between the specimens under study and the original description, the difference in body size (1) is probably attributable to the individual variation or sampling errors due to the small sample size. Other inconsistencies may reflect the insufficient original description, as shown below: (i) As for the leg chaetotaxy (4), the present material accords well with the description later provided by Krantz [10] on the basis of specimens from Schooner Creek, Oregon; (ii) as regards the anterior margin of the tectum (3) and bidentate median claw on tarsus I (5), the present specimens correspond well with the later description by Krantz [12] based on the *paratype series*; (iii) as for the setae on tarsus I (6) and female perigenital setae (8), Newell [7] later treated these features as found in the Japanese material as the generic characters of the genus *Actacarus*, although he did not specifically emend his original description of these characters in *A. illustrans*; (iv) the lateral platelets of the idiosoma (2) are very slender and lateromarginal in position so that they are not clearly visible in dorsal and ventral views;

these platelets are actually present both in immatures [10] and adults [Abé, the present study] of *A. illustrans* from Schooner Creek. Newell [13] might have overlooked them; (v) the comparison between specimens from Hokkaido and those from Schooner Creek shows the close resemblance in the arrangement of perigenital setae (7) between specimens from these two localities, so that it is probable that Newell [13] figured perigenital setae somewhat insufficiently in his original description.

Krantz [10] described for the first time immature stages of *A. illustrans* on the basis of specimens from Schooner Creek. According to him, deutonymphs have very poorly developed dorsal plates, and this author verified his observation in the deutonymph specimen from Schooner Creek. The Japanese deutonymph specimens have well developed dorsal plates.

Actacarus karoensis sp. nov.

(Japanese name: Karo-nagisadani, new)

(Figs. 7–11)

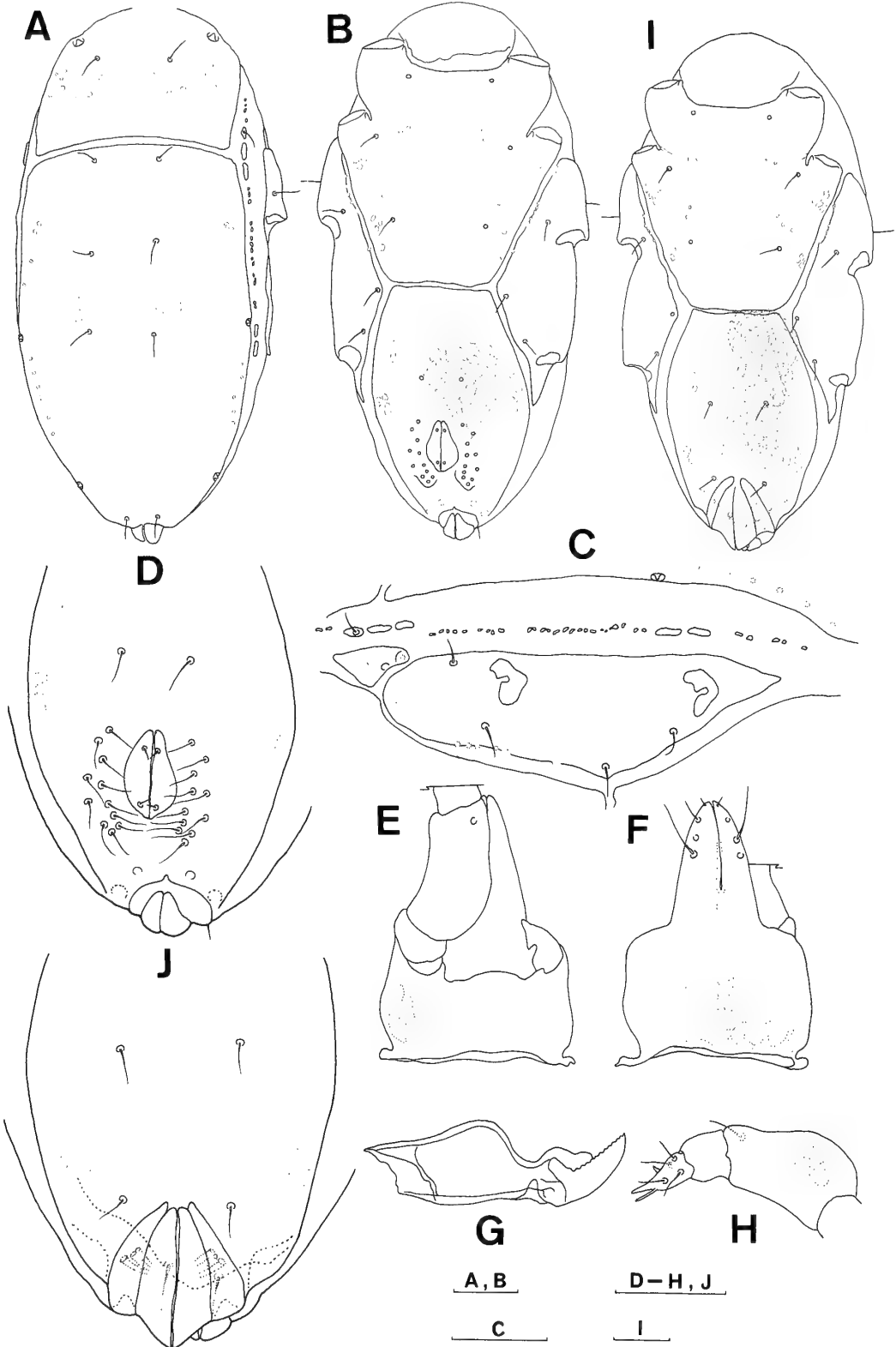
Type series. Holotype: Male, intertidal, in fine sand along shore line, Karo Beach (35°33'N, 134°13'E), Tottori Pref., Sea of Japan, Japan, 6-X-1987, N. Tsurusaki coll. — *Allotype:* Female, data same as the *holotype*. — *Paratypes:* 1 male, 3 protonymphs, 1 larva, data same as the *holotype*; 5 males, 3 females, 1 deutonymph, same locality as the *holotype*, 10-VI-1987, N. Tsurusaki coll.

Type deposition: The type series is deposited in the collections of the National Science Museum, Tokyo, the Zoological Institute, Faculty of Science, Hokkaido University, Sapporo, the National Museum of Natural History, Smithsonian Institution, Washington, DC, U.S.A., and in my private collection.

Description. Male (holotype): Idiosoma small, compact, 174 μm long, 82 μm wide, color semi-transparent after a few weeks preservation in fixative. Color in life unknown.

Dorsum (Fig. 7A) almost completely covered with two dorsal plates which are uniformly punc-

FIG. 7. *Actacarus karoensis* sp. nov. Male (holotype): A, idiosoma (Ds); B, idiosoma (Vr); C, idiosoma (Lat, L); D, genitoanal region; E, gnathosoma (Ds); F, gnathosoma (Vr); G, chelicera (R); H, palp (R). Female (allotype): I, idiosoma (Vr); J, genitoanal region. Scale bars = 20 μm .



tate with fine sparse alveoli. Dorsal setae very fine. AD and PD separated from each other by a narrow strip of finely striated membranous cuticle, opposing portion of AD and PD rectangular. AD approximately 1/3 length of PD, L/W 0.66, moderately convex anteriorly, very slightly concave posteriorly, furnished with a large pore on antero-lateral corner on each side, ornamented with paired weak areolae and a number of laterally scattered minute canaliculi at about mid-level. PD 124 μm long, 76 μm wide, very weakly convex anteriorly, narrow, concave and faintly ribbed posteriorly, ornamented with tiny anterolateral areolae; a pair of weak intermediate panels and a series of lateral minute canaliculi on each side; two pores on each lateral margin; the first pore at 0.50 and the second at 0.88. OC (Fig. 7C) 15 μm long, 8 μm wide, lateromarginally placed, lying at dorsal side of anterior angle of PE, nearly triangular in outline with pointed anterior end, furnished with a small pore medially, a larger pore near posteroventral margin, and an oval apodeme at posterior end. A series of many microplatelets (Fig. 7C) lying marginally on each side of idiosoma alongside AD and PD, of which three anterior and two posterior microplatelets are relatively large and elliptical; anterior three larger microplatelets lying at level between OC and insertion of leg III, all approximately equal in size (4 μm long, 3 μm wide); two larger posterior microplatelets lying at level of insertion of leg IV, each approximately 6 μm long, 3 μm wide.

Chaetotaxy of dorsal region: Setae ds-i on PD at 0.43; ds-ii on the anteriormost larger microplatelets, seen as if placed on membranous cuticle from dorsal view; ds-iii on PD, each separated posteriorly from anterior margin of PD by approximately four alveolar diameters; ds-iv on PD at 0.43; ds-v on PD, at 0.50; ds-vi (adanal setae) on PD, each separated from posterior margin of PD by about five alveolar diameters.

Venter (Fig. 7B) covered with four plates weakly ornamented in a manner similar to dorsal plates. AE 68 μm long, 64 μm wide, subrectangular in outline, reaching posteriorly to level about midway between insertions of legs III and IV, very slightly concave posteriorly, furnished with tiny triangular epimeral processes, with a thin membranous collar

anteriorly, and five sets of lateral and medial subsurface pores of various shapes. PE (Fig. 7C) 82 μm long, 24 μm wide, elongate, tapering posteriorly from 0.57, moderately convex anteriorly, and strongly outcurved ventrally, with bluntly pointing terminal end, marked with a series of marginal subsurface pores ventrally.

Chaetotaxy of epimeral region: Setae aes-i on AE, each separated posteriorly from anterior margin of AE by about six alveolar diameters; aes-ii-lat on AE, posterior and somewhat medial to insertion of leg III; aes-ii-v on AE, at level of insertion of leg III; pes-iii-lat each on PE, on dorsolateral margin of PE at level about midway between anterior margin of PE and insertion of leg III; pes-iii-v each on PE, at level slightly anterior to insertion of leg III, separated from ventral margin of PE by approximately six alveolar diameters; pes-iv-a each on PE, at ventral apex of PE, separated from margin by about three alveolar diameters; aes-iv-p each on PE, at level anterior to insertion of leg IV, separated from ventral margin of PE by about three alveolar diameters.

Genitoanal region (Fig. 7B, D): GA 72 μm long, 54 μm wide, almost truncated anteriorly, extending slightly anterior to level of pes-iv-a, almost touching posterior margin of AE, moderately expanded intermediately and narrowed posteriorly to terminal end; two subsurface pores found anterolaterally and a cluster of lateral weak panels at about mid-level on each side. Genital foramen about 1/4 length of GA, L/W 1.50, pyriform in outline; anterior margin of foramen at 0.60 relative to GA length. Anal papilla terminally placed, well separated from genital foramen. A terminal pit (Fig. 7B) located laterally on each side of anal papilla. Spermatophorotype (Fig. 7B) L/W 1.17, massive, complex in structure, approximately 1/2 length of GA.

Chaetotaxy of genitoanal region: One pair of outlying setae located at 0.42 on GA; a group of eleven perigenital setae on each side of genital foramen as illustrated in Fig. 7D; two subgenital setae on each genital sclerite, arranged 1-1. No setae on anal papilla.

Gnathosoma (Fig. 7E, F): 52 μm long, 36 μm wide, gnathosomal length/idiosomal length 0.30; base of gnathosoma L/W 0.78, slightly expanded

laterally, lacking setae, entirely ornamented with fine punctations, and with a few round panels on dorsolateral and ventroproximal sites. Pharyngeal plate fusiform, with eight visible panels. Anterior margin of tectum weakly convex. Rostrum $24\text{ }\mu\text{m}$ long, $18\text{ }\mu\text{m}$ wide, subtriangular with round tip, just reaching to level of distal end of P-2, bearing four pairs of delicate filiform setae as follows: Protorostral setae minute, near tip; deutorostral setae short, posterior to protorostral setae; tritrostral and basitrostral setae long, approximately four times as long as deutorostral setae, located at 0.14 and 0.21 relative to rostral length, respectively. Rostral sulcus reaching to about $2/3$ level relative to rostral length. Chelicera (Fig. 7G) with

basal segment $30\text{ }\mu\text{m}$ long, $14\text{ }\mu\text{m}$ wide, strongly convex anterodorsally, with oblique proximal end and indistinct ornamentation. Movable digit approximately $2/3$ length of basal cheliceral segment, strongly inclined dorsally, with 16-18 minute denticles along dorsal edge. Fixed digit nearly $1/2$ length of movable digit. Palp (Fig. 7H) $48\text{ }\mu\text{m}$ long, inserted dorsolaterally, slightly inclined ventrally, with four free segments as described below: P-1 short, cylindrical, L/W 1.25; P-2 longest and robust, exceeding combined length of P-3 and P-4, L/W 1.43, slightly expanded dorsoproximally, ornamented with fine faint punctations and a few faint panels, with one distidorsal filiform seta; P-3 about the same length as P-1, L/W 0.75, with one

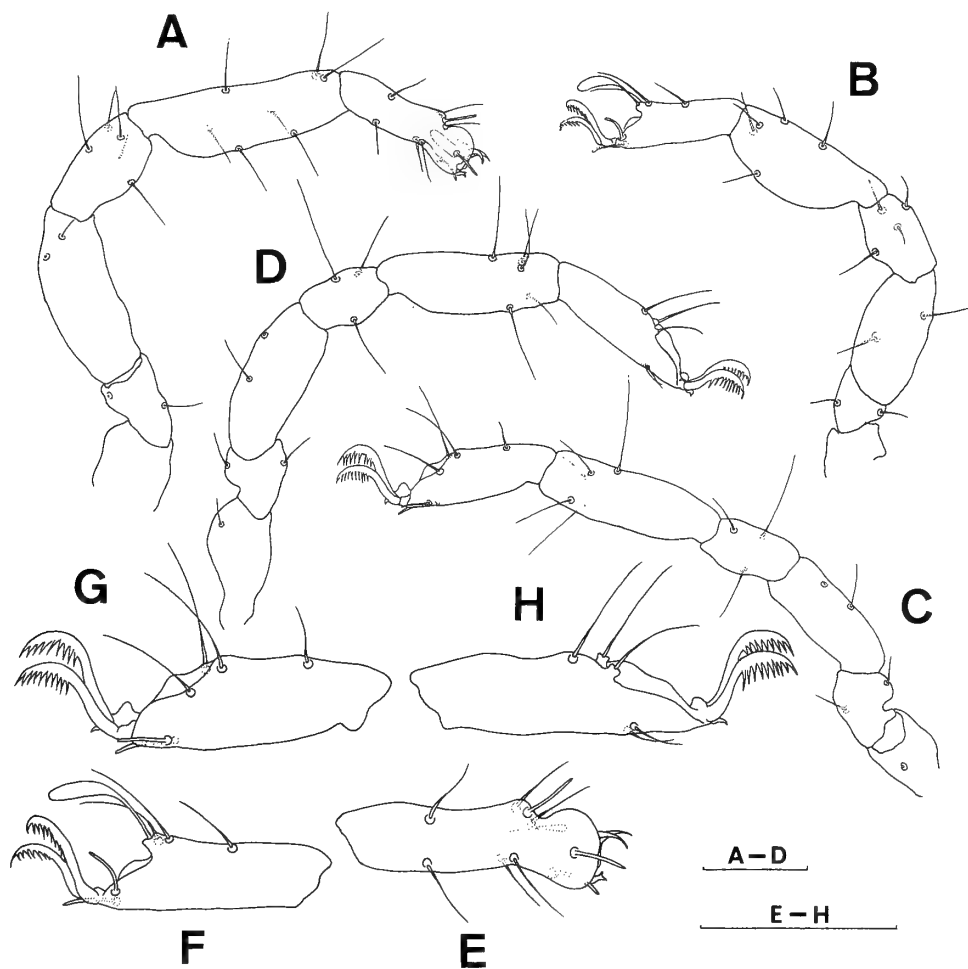


FIG. 8. *Actacarus karoensis* sp. nov. Male (holotype): A, leg I (R); B, leg II (R); C, leg III (L); D, leg IV (L); E, tarsus I (R); F, tarsus II (R); G, tarsus III (L); H, tarsus IV (L). Scale bars = $20\text{ }\mu\text{m}$.

short spiniform seta anterodistally; P-4 conical, slightly curved ventrally, furnished with three slender filiform setae proximally, one slender filiform seta and one short spiniform seta intermediately, and one distal bacilliform seta parallel to terminal blunt spiniform seta.

Legs (Fig. 8A-D): Length of legs I, II, III, IV = 138, 112, 128, 130 μm , respectively, thin, with fine faint punctations on all segments. Each tarsus with claw fossa. Lateral claws with indistinct accessory processes. Median claw of each leg minute, bidentate only in leg I, unidentate in others. Carpite and cavity in claw not clear. Parambulacral setae all single eupathidia.

Leg chaetotaxy as follow: Trochanters I-IV, 0-0-1-1; basifemora, 2-2-2-2; telofemora, 2-2-2-2; genua, 5-4-3-3; tibiae, 7-5-5-5. Tarsus I (Fig. 8E) with strongly developed posterior lamella, with three dorsal setae (one intermediate seta on basidorsal limb, others on claw fossa), one solenidion, one famulus, three filiform ventral setae (one intermediately, others distally), and two parambulacral setae; solenidion fine setiform, at the base of fossary lamella; famulus minute, blade-shaped, with fine canaliculus, lying distally to solenidion; lateral claws small compared with those on other legs, and combs not in visible. Tarsus II (Fig. 8F) with three dorsal setae (one filiform intermediate seta on basidorsal limb, two filiform setae on claw fossa), one distally swollen solenidion at the base of fossary lamella, two parambulacral setae; lateral claws with weakly developed combs. Tarsus III (Fig. 8G) with four dorsal setae (one filiform intermediate seta, one filiform distal seta on basidorsal limb, and two filiform setae on claw fossa), two parambulacral setae; lateral claws with well developed combs. Tarsus IV (Fig. 8H) with three dorsal setae (one filiform distal seta on basidorsal limb, two filiform setae on claw fossa), two parambulacral setae; lateral claws as in tarsus III.

Female (allotype): Idiosoma 190 μm long, 94 μm wide, resembling male in essential details except for the characters of weak panels on PD and genitoanal region. *Dorsum*: PD furnished with only one weak panel near lateral margin on each side.

Genitoanal region (Fig. 7I, J): Genital foramen 26 μm long, 14 μm wide, located terminally and

overlying anal foramen, furnished with three pairs of perigenital setae; the first pair at 0.39, the second at 0.69 (level of anterior margin of foramen), and the third at 0.84 (behind the foramen occupying terminal concavity). Subgenital setae lacking. Genital acetabula (Fig. 7J) internal, three pairs. Ovipositor (Fig. 7I) long, tubular, extending to level near insertion of leg IV, slightly shifted to one side from idiosomal longitudinal median axis, although not reaching to lateral side of idiosoma.

Immature stages: Three immature stages of *A. karoensis* are distinguished. They differ from adults in that 1) plates are less developed and more widely separated from each other by distinctly striated membranous cuticle, 2) smaller lateral microplatelets are almost indistinct, 3) AD and PD more ribbed and furnished with more canaliculi, 4) PD lacks a cluster of weak panels at mid-level on each side, and 5) legs are shorter and more weakly punctate.

Deutonymph (paratype, Hal-63): Idiosoma 180 μm long, 84 μm wide. *Dorsum* (Fig. 9A): Setae ds-iii placed on striated membranous cuticle between AD and PD. PD truncated anteriorly, extending to level of slightly posterior to ds-iii. *Venter* (Fig. 9B): AE strongly narrowed posteriorly from level of insertion of leg II to level of anterior to pes-iv-a. GA 62 μm long, 52 μm wide, reaching anteriorly to level about midway between pes-iv-a and pes-iv-p, furnished with two subsurface pores on each anterolateral corner, bearing two pairs of perigenital setae; the first pair at 0.27; the second at lateral sides of genital field. Primordial genital slit very weakly sclerotized, reaching anteriorly to 0.58 relative to GA length. Subgenital setae lacking. Genital acetabula internal, two pairs. *Legs* (Fig. 9C-F): Basifemur IV with only one seta.

Protonymph (paratype, Hal-90): Idiosoma 160 μm long, 78 μm wide. *Dorsum* (Fig. 10 A): Posterior margin of AD not reaching to mid-level between insertions of legs II and III. Only two lateral microplatelets located dorsoposterior to OC. *Venter* (Fig. 10 B): Posterior margin of AE extending to level about midway between pes-iii-lat and pes-iv-p. Setae pes-iv-a lacking. GA 46 μm long, 34 μm wide, reaching anteriorly to level

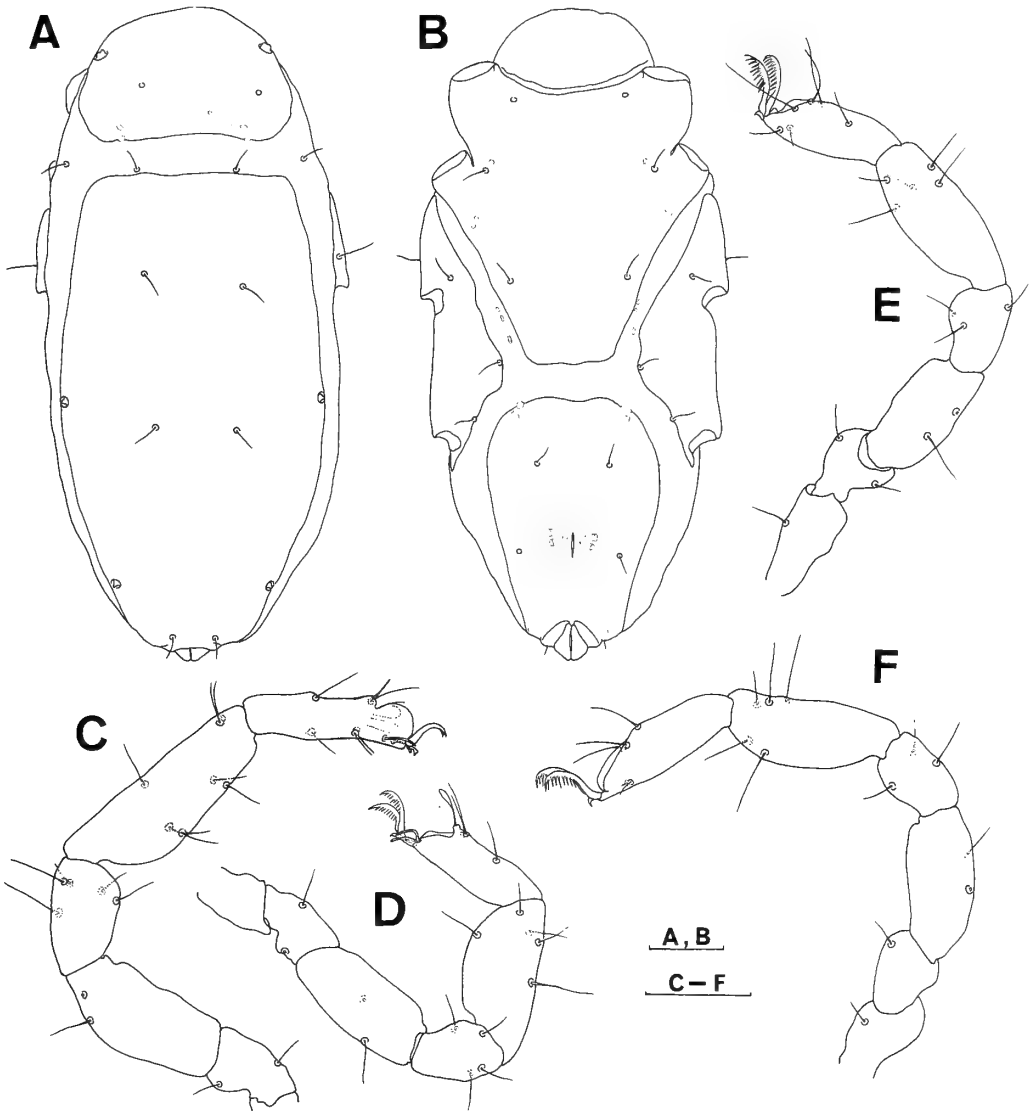


FIG. 9. *Actacarus karoensis* sp. nov. Deutonymph (paratype, Hal-63): A, idiosoma (Ds); B, idiosoma (Vr); C, leg I (R); D, leg II (R); E, leg III (R); F, leg IV (R). Scale bars = 20 μm .

slightly posterior to pes-iv-p, lacking setae, bearing one pair of internal genital acetabula that flank the primordial genital slit. Anterior margin of genital slit at 0.61 relative to GA length. *Legs* (Fig. 10C-F): Basifemur III with only one seta, trochanter IV without setae, femur IV undivided.

Larva (paratype, Hal-93): Idiosoma 140 μm long, 72 μm wide. *Dorsum* (Fig. 11A): AD and PD separated from each other by interval of approximately 2/3 length of PD. Lateral pores on

AD and PD relatively large and distinct. Lateral microplatelets very faint, lying dorsoposteriorly to OC. *Venter* (Fig. 11B): AE lacking aes-ii-lat. PE small, with only one seta and marginal subsurface pores ventrally. Two subsurface pores located on membranous cuticle between AE and PE. GA 22 μm long, 22 μm wide, trapezoidal, weakly protruding anteriorly, lacking both genital setae and genital slit. *Legs* (Fig. 11C-E) three pairs; basifemur and telofemur fused. Leg chaetotaxy as

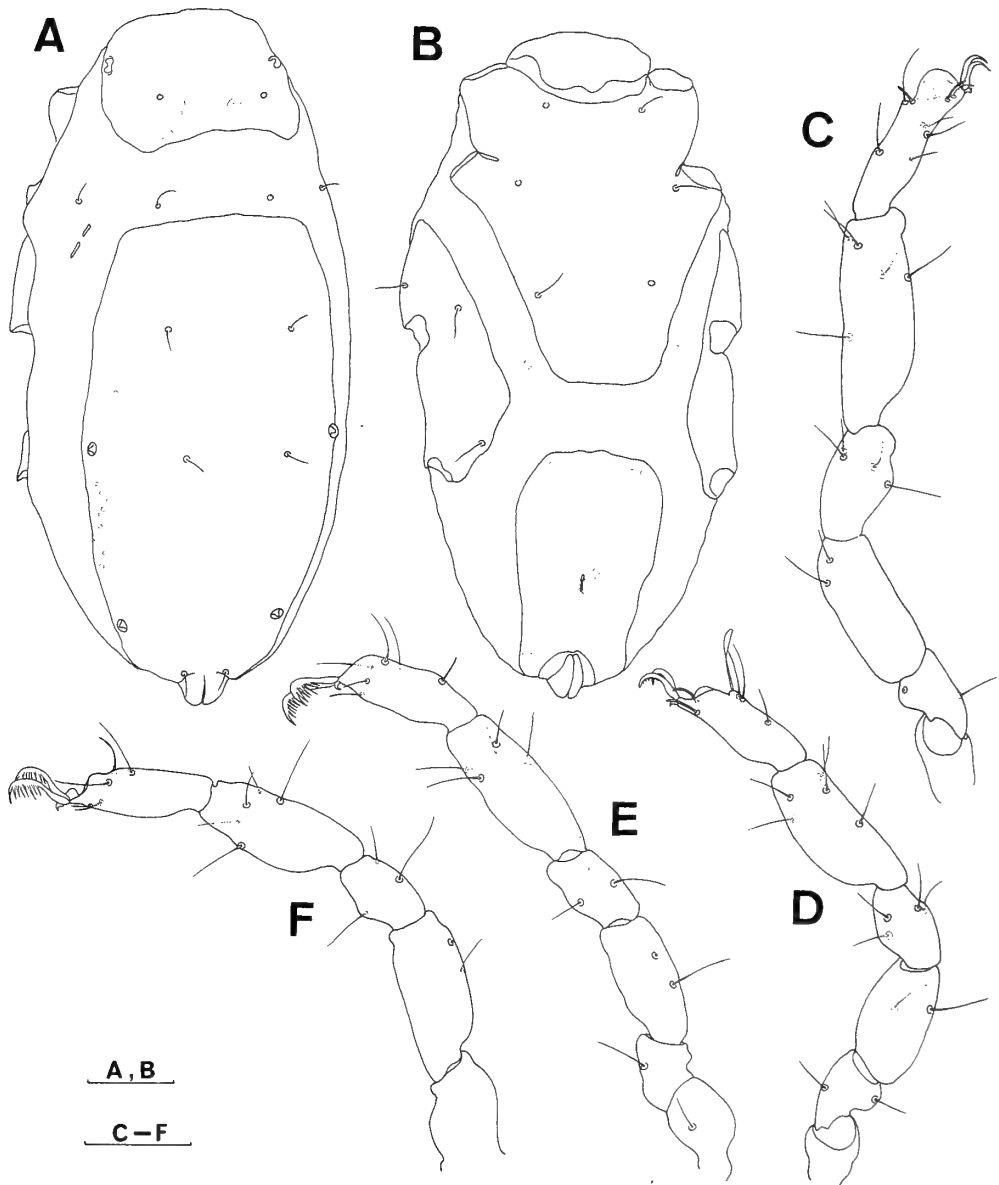


FIG. 10. *Actacarus karoensis* sp. nov. Protonymph (paratype, Hal-90): A, idiosoma (Ds); B, idiosoma (Vr); C, leg I (R); D, leg II (R); E, leg III (R); F, leg IV (R). Scale bars = 20 μ m.

follows: Trochanters I-III, 0-0-1; femora, 3-3-3; genua, 4-4-3; tibiae, 5-5-5.

Morphological variation and abnormality: The number of panels comprising a cluster at the intermediate level on each side of PD was from two to three in the male. The shape and the arrangement of the lateral microplatelets were variable even between sides of one specimen,

although the larger microplatelets were more stable. Two male specimens of the *type series* had only ten perigenital setae on one side of the genital foramen.

Distribution: Tottori Prefecture, Sea of Japan, Japan.

Remarks: *Actacarus karoensis* is distinguished from congeners on the basis of the following

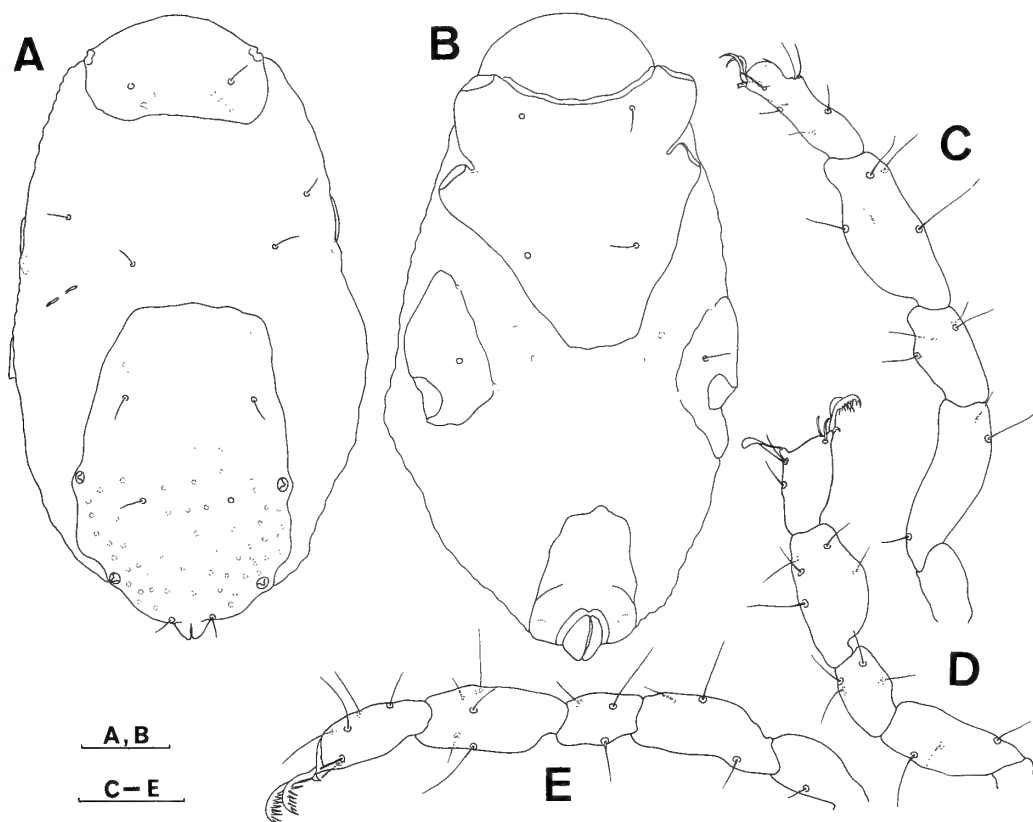


FIG. 11. *Actacarus karoensis* sp. nov. Larva (paratype, Hal-93): A, idiosoma (Ds); B, idiosoma (Vr); C, leg I (L); D, leg II (L); E, leg III (R). Scal bars=20 μ m.

characters: Setae ds-ii on lateral microplatelets; three setae on PE (one dorsally, three ventrally); GA expanded medially, furnished with one pair of outlying setae and eleven pairs of perigenital setae as illustrated in Fig. 7D; anterior margin of tectum very weakly convex; ovipositor extending to level of insertion of leg IV; a series of weakly sclerotized lateral microplatelets laterad from AD and PD on each side of idiosoma.

Morselli and Mari [14] mentioned that *A. clipeolatus* may be distinguished from congeners by the presence of two lateral platelets laterad from AD and PD on each side of the idiosoma. In the present study, however, both the *Actacarus* species examined have the lateral platelets laterad from AD and PD. Therefore, the presence of these platelets cannot be regarded as a critical specific character. It is even possible that the

existence of the lateral platelets or the lateral microplatelets is one of the generic characters of the genus *Actacarus*, and the shape and the size of these platelets might be of specific significance.

The specific epithet is derived from the type locality, "Karo".

ACKNOWLEDGMENTS

The author wishes to express his appreciation to Dr. Haruo Katakura (Hokkaido Univ.) for his valuable advice and revision of the manuscript. Cordial thanks also are due to Professor G. W. Krantz (Oregon State Univ.) for supplying the author with his private collection from Schooner Creek, helpful suggestions on the manuscript, and the correction of English. Dr. Nobuo Tsurusaki (Tottori Univ.) kindly gave the author an opportunity to examine material of value.

REFERENCES

- 1 Kishida, K. (1927) Ushio-dani (*Halacarus spongiophilus* Kishida). In "Nippon Doobutsu Zukan". Hokuryukan, Tokyo, p. 978 (in Japanese).
- 2 Bartsch, I. (1986) Zur gattung *Agauopsis* (Acari, Halacaridae), Beschreibung zweier neuer Arten und Übersicht über Verwandtschaftsgruppen. Zool. Scr., **15**: 165–174.
- 3 Imamura, T. (1965) Hydrachnellae. In "Mites. An Introduction to Classification, Bionomics and Control of Acarina". Ed. by M. Sasa, Univ. of Tokyo Press, Tokyo, pp. 29–30, 34, 216–251 (in Japanese).
- 4 Newell, I. M. (1947) A systematic and ecological study of the Halacaridae of eastern North America. Bull. Bingham Oceanogr. Collect. New Haven, **10**: 1–232.
- 5 Newell, I. M. (1953) The natural classification of the Rhombognathinae (Acari, Halacaridae). Syst. Zool., **2**: 119–135.
- 6 Newell, I. M. (1967) Abyssal Halacaridae (Acari) from the southeast Pacific. Pac. Insects, **9**: 693–708.
- 7 Newell, I. M. (1984) Antarctic Halacaroida. Antarc. Res. Series, **40**: 1–284.
- 8 Newell, I. M. (1957) Studies on the Johnstonianidae (Acari, Parasitengona). Pac. Science, **11**: 396–466.
- 9 Newell, I. M. and Ryckman, R. E. (1966) Species of *Pimeliaphilus* (Acari, Pterygosomidae) attacking insects with particular references to the species parasitizing Triatominae (Hemiptera, Reduviidae). Hilgardia, **37**: 403–436.
- 10 Krantz, G. W. (1976) Arenicolous Halacaridae from the intertidal zone of Schooner Creek, Oregon (Acari: Prostigmata). Acarologia, **18**: 251–258.
- 11 Vorob'yeva, L. V. and Yaroshenko, N. A. (1979) Halacaridae in the north-western Black Sea. Hydrobiol. Jour., **15**: 25–28 (originally in Russian, English translation in 1980).
- 12 Krantz, G. W. (1974) *Actacarus monniotae* n. sp. (= *A. illustrans* sensu Monniot 1968), an arenicolous mite (Acari: Halacaridae) from the Mediterranean region. Vie et Milieu, **24**: 115–118.
- 13 Newell, I. M. (1951) Further studies on Alaskan Halacaridae (Acari). Amer. Mus. Novitates, **1536**: 1–56.
- 14 Morselli, I. and Mari, M. (1986) Researches on the coast of Somalia. The shore and the dune of Sar Uanle. 39. On three interstitial species of Halacaridae (Acari). Italian Jour. Zool., N. S. Suppl., **21**: 137–148.

Comparative Study on LDH Isozymes in Different Subfamily of Teleost Fish - Grass Carp (*Ctenopharyngodon idellus*) and Blunt Snout-Bream (*Megalobrama amblycephala*)

TAO YUNXIA¹ and YAN SHAOYI²

*Institute of Developmental Biology, Academia Sinica,
Beijing, China*

ABSTRACT—Electrophoretic, physico-chemical and immuno-analysis of lactate dehydrogenase isozymes of grass carp (*Ctenopharyngodon idellus*) and blunt snout-bream (*Megalobrama amblycephala*) indicated that although they were rather conservative in evolution, however, some divergences in their gene activities and molecular structures were still remained. So, LDH isozyme can be used as a genetic marker to distinguish these two kinds of fish.

INTRODUCTION

Markert and Faulhaber [1], using starch gel electrophoresis, examined the LDH isozyme patterns in 30 kinds of fish. They found out that the LDH isozymes in fish were more complicated than those in mammals and birds. One to twenty LDH isozymes were found in different fish examined. They were found distributed differently in various tissues in different kinds of fish and were classified into three systems. Among them a major LDH isozyme system was distributed in most tissues corresponding to the A and B gene systems of mammals and birds. Two minor systems were restricted to eye and gonads. Through electrophoresis and immuno analysis, Shaklee *et al.* [2] found that the two minor systems were probably coded by the same gene locus, corresponding to the C gene of mammals and birds. In comparison of the kinetic properties, amino acid content and electrophoretic zymograms of LDH isozymes of Brook trout, lake trout and their hybrid, Splake trout, Wuntch and Goldberg [3] found out that there were some differences of all these properties.

Yan *et al.* [4] reported that the electrophoretic zymograms of LDH isozymes can be used for distinguishing four kinds of subfamily teleost fish in the Family *Cyprininae*. This means that the LDH isozymes not only behave differently in tissue distributions, but also could be performed as a species-specific marker in fish taxonomy.

For accurate comparative study of isozymes in different organisms, purified LDH isozyme fractions must be obtained. In 1967, Okabe *et al.* [5] separated and purified five human LDH isozyme fractions by using the ammonium sulfate fractionation, calcium phosphate gel absorption and DEAE-cellulose separation methods. In 1970, Cuatrecasas [6] using a very simple and rapid method—blue dextran affinity chromatography separated and purified human LDH 1 and LDH 5. Later, Fulton *et al.* [7] using HPLC separated five LDH isozyme fractions in rat. But up to now, the report about the LDH isozymes separation in fish has not been seen.

In this investigation, we have tried to purify LDH isozyme and analyze their divergences in respect to their electrophoretic zymograms, immuno-properties, molecular structures as well as physico-chemical properties in two kinds of fish which belong to a different subfamily—grass carp and blunt snout-bream. Since it has also been known that the LDH 1 is a gene B product and sometimes the divergence of gene B is larger than

Accepted March 20, 1989

Received September 6, 1988

¹ Present address: The Medical College of Pennsylvania, 3300 Henry Ave., Phila., Pa.19129, U.S.A.

² Requests for reprints should be addressed to Yan Shaoyi.

gene A [8], so, the LDH 1 was preferentially to use in this investigation.

MATERIALS AND METHODS

1. Experimental animals: Grass carp (*Ctenopharyngodon idellas*) and blunt snout bream (*Megalobrama amblycephala*) were used for these experiments. Both of them belong to the same family (*Cyprininae*) but to different subfamilies and genera. Grass carp belongs to the Subfamily *Leucinae* and blunt-snout bream belongs to the Subfamily *Abramidae*. They were purchased from Wan Quan Zhuang Fishery Farm, Beijing, and were two years old.

2. Chemicals: Blue dextran and sepharose 4B were purchased from Pharmacia Chemical Co., Sweden; Nitro blue tetrazolium (NBT) and Phenazine methosulfate (PMS) from Buchs Chemical Co., Switzerland; Starch (Lot 387-1) from Cannaught Laboratories Limited Co., Canada; NADH from Boehringer Mannheim Chemical Co., Western Germany; NAD from Yeast Plant of Shanghai, China.

3. Preparation of tissue extracts: Tissues were taken from freshly killed fish, washed with cold 0.75% saline, then homogenized and centrifuged at 15,000 rpm (MSE-18) for 30 min. The supernatants were used for starch electrophoresis.

4. Preparation of blood samples: blood was collected from caudal vein, washed with 0.75% saline containing heparin three times. The red blood cells were hemolysed with 2 ml double distilled water, then centrifuged at 3,000 rpm (k 70, Eastern Germany). The supernatants were used for electrophoresis and affinity chromatography analysis.

5. Electrophoresis and specific stain: Vertical starch gel electrophoresis and LDH isozymes staining were carried out following Xue's improved method [9]. The starch gel electrophoresis was carried out at 4°C for 16 hr. And then the gels were immersed in a specific staining solution at 37°C for 1-2 hr. Every 100 ml staining solution contains 50 mg NAD, 30 mg NBT, 2 mg PMS, 15 ml 0.5 M Tris-HCl buffer, pH 7.2, 10 ml 1 M sodium lactate, and 5 ml 0.1 M NaCl.

6. Purification of LDH: LDH 1-5 and LDH 1

were purified by blue dextran affinity chromatography mainly following Cuatrecasas' method [6] and only the NAD and NADH concentrations of the eluted buffer were changed. The elution buffer for LDH 1-5 was 0.35 mg/ml of NADH, 10 mM of Tris, 0.5 mM of mercaptoethanol, pH 8.6. The elution buffer for LDH 1 was 0.05 mg/ml of NAD, 0.1 mg/ml of lithium lactate, 10 mM of Tris, 0.5 mM mercaptoethanol, pH 8.6.

7. Assay for LDH activity and purity: LDH activity was determined spectrophotometrically by monitoring the formation of NADH at 340 nm in 1 cm quartz cuvettes following the procedure of Holmes *et al.* [10]. LDH purity was determined by enzyme specificity staining with the starch gel, and by measuring the international units (I.U.) per milligram of the extracted LDH. LDH concentration was determined as protein concentration by the method of Lowry *et al.* [11].

8. Amino acid content assay: About 0.5 mg of enzyme were hydrolyzed in 6 N HCl at 110°C for 24 hr. The resultant hydrolysate was washed and evaporated to dryness and then resuspended in 0.2 ml of double distilled water. Amino acid content was determined by HPLC (Waters Company, Model AAA) according to the ion exchange separation method described in Waters Associates Operator's Manual [12].

9. Kinetic parameter determination: The K_m value of LDH 1 was calculated from Lineweaver-Burk plots, with sodium lactate as substrate at pH 8.6 and temperature 25°C. Kinetic of heat activation: The LDH 1 activity was measured at the temperatures ranging from -4°C to 80°C, at pH 8.6. Kinetics of acid and alkali treatment: The LDH 1 activity was measured in the pH range of 6 to 13, at temperature 25°C.

10. Preparation of antibody and investigation on LDH immuno properties: Rabbits were immunized with purified LDH 1-5 isozymes prepared from blunt snout-bream red blood cells following the method of Clausen [13]. A mixture of grass carp and blunt snout-bream LDH 1-5 isozymes and antisera were incubated for 30 min at 30°C prior to starch gel electrophoresis and LDH staining for neutralization or inhibition tests. The immunoprecipitated bands left in the double immuno diffusion agar gels were observed.

RESULTS

LDH isozymes electrophoresis zymograms

The zymograms of LDH isozymes from different tissues of grass carp and blunt snout-bream were displayed by starch gel electrophoresis and they are shown in Figure 1a and 1b. Among them, in the tissues of cardiac muscle, skeletal muscle and eye of both kinds of fish, there existed five LDH isozyme bands, migrating towards the anode, and in liver, there was the C band migrating towards the cathode in both kinds of fish. In kidney tissue there were still five bands in the sample of blunt snout-bream, but seven bands in that of grass carp. The two ‘additional bands’ also migrated towards the anode in between LDH 2 to LDH 3 and LDH 3 to LDH 4.

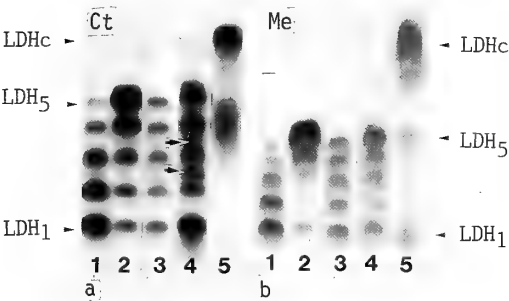


FIG. 1. LDH isozyme zymograms of various tissues of grass carp(Ct) and blunt snout-bream(Me) revealed by starch gel electrophoresis. Ct(a), Me(b). 1. Cardiac muscle, 2. Skeletal muscle, 3. Eye, 4. Kidney, 5. Liver. Arrows show 2 additional bands.

Purification of LDH 1–5 and LDH 1 from blood cells

The optimum concentration of NADH for separating LDH 1–5 was 0.39 mg/ml and the optimum concentration of NAD for separating LDH 1 is 0.05 mg/ml. Figure 2a and 2b shows the purified LDH 1–5 and LDH 1 isozymes of grass carp and blunt snout-bream. The specific activities of these purified LDH isozymes were shown in Table 1 by calculating the international units (I.U.) per milligram for purified LDH protein. The data indicated that all the purified LDH isozymes were over 500 I.U. per milligram.

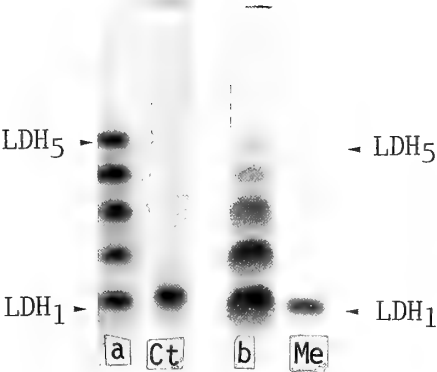


FIG. 2. Purified LDH 1–5 (left) and LDH₁ (right) isozyme zymograms of red blood cell of grass carp(Ct) and blunt snout-bream(Me) revealed by starch gel electrophoresis. Ct(a), Me(b).

TABLE 1. The specific activities of LDH1-5 and LDH1 isozymes extracted and purified from the red blood cells of grass carp (Ct) and blunt snout-bream (Me)

Fish LDH	I.U./mg $\Delta O.D. \ 340 \times 20^*$
	6.2 m
Ct LDH1-5	510
Me LDH1-5	1035
Ct LDH1	515
Me LDH1	1225

* Average value of three times of measurement.

Immuno properties

The antiserum against blunt snout-bream red blood cell LDH 1–5 isozyme were used. After the double diffusion on agar gel with blood sample of grass carp and blunt snout-bream, a complete crossing precipitation line was clearly observed (Fig. 3). When the antisera were mixed with the blood samples of both fish, all the activities of LDH isozymes disappeared. When the antisera were mixed with the extracts from livers and kidneys of the two fish, it was found that the C band remained in both fish, but all the other bands, including two ‘additional bands’ of grass carp disappeared in kidney extracts (Fig. 4a and 4b).

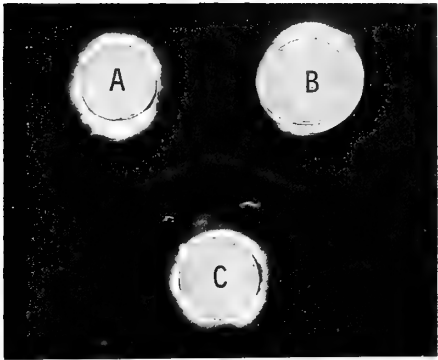


FIG. 3. Double diffusion precipitation lines of the red blood cell LDH 1-5 of Grass carp(A), and Blunt snout-bream(B) against the antiserum of red blood cell LDH 1-5 of Blunt snout-bream(C).

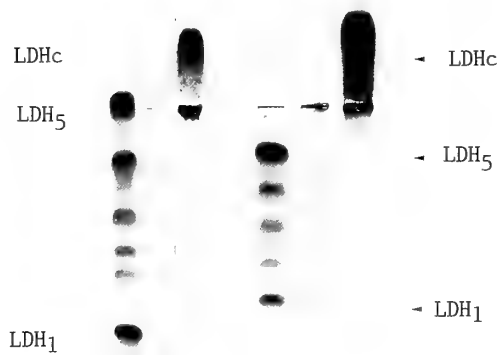


FIG. 4. Starch gel electrophoresis zymograms show, after added the antiserum of blunt snout-bream(Me) blood cell LDH 1-5 to the grass(Cp) and blunt snout-bream(Me) kidney(middle) and liver(right) extracts, the LDHc bands of liver of both fish are still remained, but all the kidney bands disappeared. Both left rows show the Ct and Me kidney LDH 1-5 zymograms without antiserum treatments. A additional bands of Ct kidney LDH isozyme are also showed by arrows.

Physico-chemical properties of LDH 1 isozyme

The starch gel electrophoresis showed that the LDH 1 isozymes of both grass carp and blunt

snout-bream migrated towards the anode but they had different mobility. The LDH 1 isozyme of blunt snout-bream carried more positive charges than the grass carp LDH 1 did. The blue dextran affinity chromatography showed that both of them almost had the same affinity to the blue dextran and could be released from the blue dextran by 0.05 mg/ml of NAD. The optimum pH value, optimum temperature of reaction and denaturing concentration by urea of LDH 1 isozyme are also the same in both fish except their Km values remained different. The Km value of Grass carp LDH 1 is 1.1×10^{-1} and the km value of blunt snout-bream LDH 1 is 5.6×10^{-2} .

The amino acid content of LDH 1 of the two fish are shown in Table 2. It can be seen that some kinds of amino acid content are different in the LDH 1 isozyme of the two fish, i.e. grass carp LDH 1 has more val and blunt snout-bream LDH 1 has more lys and arg.

DISCUSSION

In vertebrates, the LDH isozymes exist as tetrad forms resulting from the random polymerization of different peptides, and having different distribution in different tissues [1]. Obviously, this different distribution is due to the different expression of genes. Comparative studies on fish LDH isozymes in earlier years were carried out mainly by the methods of electrophoresis and they only provided limited evidence for deducing its molecular structure and enzymatic properties. In this paper, some evidences obtained from the kinetic, immuno and amino acid analysis of purified LDH isozymes were observed for indicating the divergences between LDH isozymes of grass carp and blunt snout-bream.

The results of starch gel electrophoretic zymograms indicated that five LDH isozymes existed in most tissues of both grass carp and blunt snout-

TABLE 2. Amino acid contents of red blood cells LDH1 of grass carp (Ct) and blunt snout-bream (Me)

Fish LDH		Amino acid content															
		Asp	Thr	Ser	Glu	Pro	Gly	Ala	Val	Met	Ile	Len	Phe	His	Lys	Arg	Tyr
Ct	LDH 1	116	80	108	132	68	108	144	248	12	28	48	12	40	80	44	0
Me	LDH 1	132	88	124	148	80	124	164	100	12	20	28	8	44	136	92	0

breast, and in liver tissue of both fish, there existed the cathode bands-LDHc. Whitt *et al.* [14] noted that the B gene of LDH isozyme is produced by the duplication of A gene, and the C gene is produced by the duplication of B gene subsequently. Odense *et al.* [15] also found out that, in the evolution of fish, the further LDH gene duplications also existed. For example, in carp, apart from the existence of A, B and C gene loci, there were also B' and C' gene loci. But in grass carp and blunt snout-breast, it seems that a typical major LDH isozyme system encoded by A and B gene loci as well as a minor LDH isozyme system coded by a C gene locus were observed. Carp, grass carp and blunt snout-breast belong to same family, *Cyprininae*. However, as compared with carp, no B' and C' gene duplication could be found in either grass carp or blunt snout-breast. In consideration of the chromosome number differences existing in carp ($2n=100$), grass carp ($2n=48$) and blunt snout-breast ($2n=48$), it could be explained that the less chromosome numbers of grass carp and blunt snout-breast may decrease the possibility of gene duplications on those fish as compared with the carp. However, in the kidney tissue of grass carp, there were seven LDH isozyme bands while in the blunt snout-breast kidney tissue only five LDH isozyme bands were found. Although, at present, it is not clear how the two 'additional bands' of LDH isozyme in grass carp kidney tissue arose, we believe that some minor divergence in the LDH isozymes occurred during the divergent evolution of both fish, even though they have the same chromosome number.

The results obtained from physico-chemical properties analysis of the B gene product—LDH 1 of both fish show that they have almost the same blue dextran affinity, same optimum pH value, same optimum temperature of reaction as well as the same concentration of urea for denaturation except their Km value are different which indicates that an enzymatic property difference exists in the two fish. Table 2 also shows that some amino acid content of LDH 1 have changed in the two fish, i.e. grass carp has more val and blunt snout-breast has more lys and arg. This means that minor molecular structural differences also exist in the LDH isozymes of both fish.

The results of immuno-experiments show that the antiserum against LDH 1–5 isozymes of blunt snout-breast red blood cell not only can precipitate the red blood cell LDH 1–5 isozymes of grass carp and blunt snout-breast but also can neutralize the LDH 1–5 isozyme components of different tissues, for example, the LDH 1–5 isozymes of red blood cell, liver and kidney in both fish even including the two 'additional bands' of grass carp kidney LDH isozyme. However, it can not neutralize the LDH C isozyme either in grass carp or in blunt snout-breast liver tissue. It means that the LDH 1–5 isozymes, the products of A and B gene, in grass carp and blunt snout-breast have a very common immuno property and the cathode band of liver LDH isozyme components in both fish is the product of C gene [14]. It can be also proposed that the two 'additional bands' of grass carp kidney LDH 5 isozyme might be recognized as the sub-bands of its LDH 3 and LDH 4 components, as revealed by electrophoretic zymograms, rather than as the products of other genes, because they can also be neutralized by the antiserum against the purified LDH 1–5 isozyme of blunt snout-breast.

It can be concluded that the LDH isozymes of grass carp and blunt snout-breast have many similarities in general, but some divergences were observed in gene activities, molecular structures as well as some physico-chemical properties according to our above experiments. Therefore, it was confirmed that, as revealed by other authors in fish [3, 4], birds and mammals [1], the LDH isozyme might be used as a genetic marker to distinguish grass carp and blunt snout-breast in addition to their morphological criteria in taxonomy.

ACKNOWLEDGMENTS

The authors wish to thank Professor Huang Gefang of the Institute of Developmental Biology, the Chinese Academy of Sciences, Beijing, China for his reading of this English manuscript. Thanks are also given to Professor Kenjiro Yamagami of the Life Science Institute, Sophia University, Japan and Professor Yoshitaka Nagahama of the National Institute for Basic Biology, Okazaki, Japan for their valuable comments and advices of this manuscript.

The present study was supported by the Important Research Project Grant of the Chinese Academy of

Sciences and the RF 84031 Grant of the Rockefeller Foundation, USA.

REFERENCES

- 1 Markert, C. L. and Faulhaber, I. (1965) Lactate dehydrogenase isozyme patterns of fish. *J. Exp. Zool.*, **159**: 319–322.
- 2 Shaklee, J. B., Kepes, K. L. and Whitt, G. S. (1973) Specialized lactate dehydrogenase isozyme: the molecular and genetic basis for the unique eye and liver LDHs of teleost fishes. *J. Exp. Zool.*, **185**: 217–240.
- 3 Wuntch, T. and Goldberg, E. (1970) A comparative physicochemical characterization of lactated dehydrogenase isozymes in brook trout, lake trout and their hybrid splake trout. *J. Exp. Zool.*, **174**: 233–252.
- 4 Yan, J., Wang G. and Yan, S. (1986) Analysis of starch gel electrophoresis patterns of hemoglobin and red blood cell LDH isozymes of four kinds of fresh water teleost (*Mylopharyngodon piceus*, *Ctenopharyngodon idellus*, *Hypophthalmichthys molitrix*, *Aristichys nobilis*). *Hereditas* (Beijing), **8**: 25–27.
- 5 Okabe, K., Hayakawa, Hamada, M. and Koike, M. (1968) Purification and comparative properties of human lactate dehydrogenase isozymes from uterus, uterine myoma and cervical cancer. *Biochemistry*, **7**: 79–90.
- 6 Cuatrecasas, P. (1970) Protein purification by affinity chromatography. *J. Biol. Chem.*, **245**: 3059–3065.
- 7 Fulton, J. A., Schlabach, T. D., Kerl, J. E., Toren, E. and Clifford, J. (1979) Dual-detector-post-column reactor system for the detection of isozymes separated by high-performance liquid chromatography. II. Evaluation and application to lactate dehydrogenase isozymes. *J. Chromatogr.*, **175**: 283–291.
- 8 Pesce, A., McKay, R. H., Stolzenback, F. R. D. and Kaplan, N. O. (1964) The comparative enzymology of lactate dehydrogenases. I. Properties of the crystalline beef and chicken enzyme. *J. Biol. Chem.*, **239**: 1753–1761.
- 9 Xue, G. (1978) Lactate dehydrogenase isozyme. *Shengwu Kexue Dongtai*, **3**: 10–17.
- 10 Holmes, R. S. and Soopes, R. K. (1974) Immunochemical homologies among vertebrate lactate dehydrogenase isozymes. *Eur. J. Biochem.*, **43**: 167–177.
- 11 Lowry, O. H., Rosebrough, N. J., Farr, A. L. and Randall, R. J. (1951) Protein measurement with the phenol reagent. *J. Biol. Chem.*, **193**: 265–275.
- 12 Amino Acid Analysis System, Operator's Manual. (1983) Waters Associates Publications, Milford, MA, U.S.A. pp. 4–1–4–11.
- 13 Clausen, J. (1981) Immunochemical Techniques for the Identification and Estimation of Macromolecules. Elsevier North-Holl and Biomedical Press, Amsterdam.
- 14 Witt, G. S., Shaklee, J. B. and Markert, C. L. (1975) Evolution of the lactate dehydrogenase isozymes of fishes. *Isozymes*, **4**: 381–400.
- 15 Odense, P. H., Allen, T. M. and Leung, T. C. (1966) Multiple forms of lactate dehydrogenase and aspartate aminotransferase in herring (*Clupea harengus* L.) *Can. J. Biochem.*, **44**: 1319–1326.

The *Drosophila robusta* Species-group (Diptera: Drosophilidae) from Yunnan Province, Southern China, with the Revision of its Geographic Distribution

HIDE-AKI WATABE, XING CHAI LIANG¹ and WEN XIA ZHANG¹

Biological Laboratory, Sapporo College, Hokkaido University of Education,
Sapporo 002, Japan and ¹Kunming Institute of Zoology,
Academia Sinica, Kunming, Yunnan, China

ABSTRACT—Two known and four new species of the *Drosophila robusta* species-group are reported from Yunnan, southern China, and the geographic distribution of the group is revised.

INTRODUCTION

The present paper deals with two known and four new species of the *Drosophila* (*Drosophila*) *robusta* species-group, in Yunnan Province, southern China.

All the holotypes and a part of paratypes are deposited in the Kunming Institute of Zoology, Academia Sinica, Kunming, China, and the remaining paratypes in the Biological Laboratory, Hokkaido University of Education, Sapporo, Japan.

COLLECTION SITES AND METHODS

Dali district covering collection sites of Xiangguan, Dabochin and Butterfly-spring is about 2300 meters above the sea level in northern parts of Yunnan Province, Anning and Kunming in the center of Province, and Simao in subtropical climate. Most of drosophilid flies described here were collected in watersides by using cup-traps baited with fermenting bananas.

D. ROBUSTA SPECIES-GROUP

D. robusta species-group: Sturtevant, 1942, Univ. Texas Publ., 4213: 31.

Diagnosis. Dark brown or black species with 2 pairs of dorsocentrals, body length *ca.* 3.5–4.0 mm (*ca.* 2.5 mm in *D. cheda* Tan *et al.*, 1949). Palpus with several long bristles besides numerous tiny hairs. Acrostichal hairs in 6 regular rows. Preapicals on all three tibiae; apicals on fore and mid tibiae. Wing hyaline, slightly fuscous. Veins dark brown; crossveins clear. R_2+3 straight; R_4+5 and M parallel. C_1 bristles 2, subequal. Cercus fused to pubescent epandrium. Aedeagus curved ventrally. Anterior paramere rudiment or absent, posterior paramere absent.

Drosophila (*Drosophila*) *lacertosa* Okada

Drosophila (*Drosophila*) *lacertosa* Okada, 1956, Syst. Study, 158.

Specimens examined. China: 1 ♂, 1 ♀, Anning, 15. X. 1987, 30 ♂, 28 ♀, Xiangguan, 18. X. 1987, 4 ♂, 8 ♀, Butterfly-spring, 17–18. X. 1987, 1 ♂, Dabochin, 22. IX. 1988, 14 ♂, 18 ♀, Kunming, 16. IX. 1987, 3 ♂, Simao, 4. XI. 1987. Collectors: H. Watabe and X. C. Liang.

Distribution. Japan, Korea, India, Nepal, Burma; China: Taiwan, Guangdong, Yunnan (n. loc.).

Remarks. In Kunming and Dali, *D. lacertosa* has been collected in abundance not only in watersides but also in restaurants and kitchens as a domestic species.

The color patterns of abdominal tergites are

quite variable; yellowish brown with black caudal bands in most specimens [1], but entirely black in Simao specimens.

***Drosophila (Drosophila) neokadai*
Kaneko et Takada**

Drosophila (Drosophila) neokadai Kaneko et Takada 1966, Annot. Zool. Japon., 39:55.

Specimens examined. China: 2♂, Dabochin, 21. IX. 1988; 1♂, 1♀, Xianguan, 22. IX. 1988. Collectors: H. Watabe and X. C. Liang.

Distribution. Japan, China (n. loc.): Yunnan.

Remarks. This species is related to the following new species *D. gani* in the external morphology and in the shape of aedeagus, but distinguishable from the latter by the shapes of surstylus and spermatheca [2].

Drosophila (Drosophila) gani

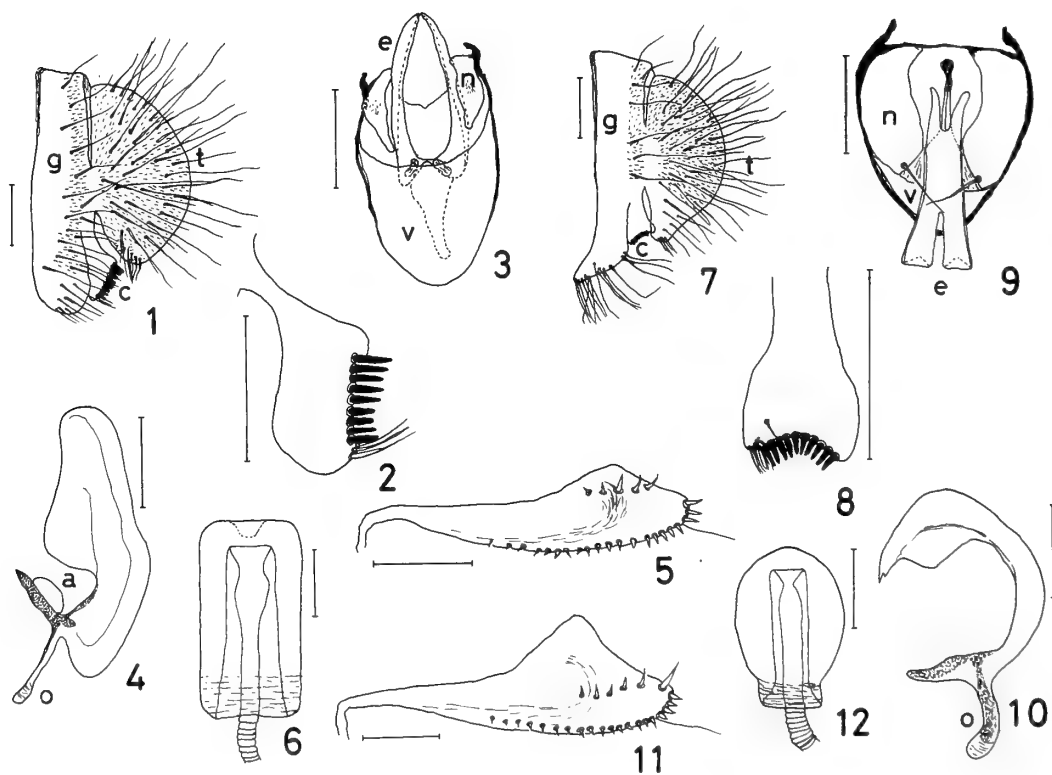
Liang et Zhang, sp. nov.

(Figs. 1–6)

Diagnosis. Body black, largest in this species-group. Arista with ca. 4 upper and ca. 2 lower branches. C index ca. 4.5, C3-fringe ca. 3/4. Epanthrium posteriorly pubescent except lower portion (Fig. 1). Surstylus rectangular, roundish on lower margin (Fig. 2). Spermatheca large, with apical hollow (Fig. 6).

♂, ♀. Body length ca. 4.25 mm (range: 3.7–4.8), thorax length (including scutellum) ca. 1.88 mm (1.8–1.9), wing length ca. 4.40 mm (4.1–4.6).

Head: Eye dark red, with thick piles. Second joint of antenna dark gray, with 2 stout setae; 3rd black, with numerous tiny hairs. Arista with ca. 4 (3–4) upper and ca. 2 lower branches in addition to



FIGS. 1–6. *Drosophila (Drosophila) gani* Liang et Zhang, sp. nov. 1: Periphallallic organs. 2: Surstylus. 3: Phallic organs. 4: Aedeagus (lateral view). 5: Ovipositor. 6: Spermatheca.

FIGS. 7–12. *Drosophila (Drosophila) yunnanensis* Watabe et Liang, sp. nov. 7: Periphallallic organs. 8: Surstylus. 9: Phallic organs. 10: Aedeagus (lateral view). 11: Ovipositor. 12: Spermatheca. Signs: a, anterior paramere; c, surstylus; e, aedeagus; n, novasternum; o, aedeagal apodeme; t, cercus; v, ventral fragma. Scale-line=0.1 mm.

a moderate terminal fork. Frons dark brown, *ca.* 0.50 (0.47–0.53) as broad as head, anteriorly with sparse frontal hairs. Anterior reclinate orbital (Orb 2) *ca.* 0.38 (0.30–0.47) length of posterior reclinate orbital (Orb 1); proclinate orbital (Orb 3) *ca.* 0.56 (0.47–0.67) length of Orb 1. Face reddish brown; carina brown, darker on margin, high, wider below. Clypeus blackish brown. Cheek brown, *ca.* 0.21 (0.17–0.26) as broad as maximum diameter of eye, with *ca.* 3 bristles at lower corner. Second oral (Or 2) *ca.* 0.72 (0.64–0.78) length of vibrissa (Or 1); third oral (Or 3) *ca.* 4/9 length of Or 2. Palpus grayish brown, flattened laterally, with ♂ *ca.* 7 long bristles and ♀ *ca.* 4 bristles.

Thorax: Mesoscutum dark brown, with a longitudinal darker stripe running to scutellum in middle and 1 pair of obscure stripes along notopleural region. Scutellum dark brown; its lateral sides black. Thoracic pleura dark brown. Lower humeral *ca.* 0.83 (0.78–0.91) length of upper one. Length distance of dorsocentrals *ca.* 0.64 (0.60–0.72) cross distance; anterior dorsocentral (DcA) *ca.* 0.71 (0.68–0.73) length of posterior dorsocentral (DcP). Anterior scutellars (SctAs) nearly parallel and posterior scutellars (SctPs) convergent. SctA *ca.* 1.03 (0.98–1.10) length of SctP; distance between SctPs *ca.* 0.50 (0.44–0.53) distance between SctAs. Relative length of anterior/posterior sternopleural (Sterno-index) *ca.* 0.70 (0.53–0.78).

Legs brown; fore femur posteriorly with *ca.* 4 long bristles. Number of small stout bristles on 3rd costa (3Cfr) *ca.* 33 (28–36). Wing indices: C *ca.* 4.47 (3.54–5.21), 4V *ca.* 1.48 (1.43–1.56), 4C *ca.* 0.52 (0.42–0.64), 5x *ca.* 1.07 (0.92–1.17), Ac *ca.* 1.53 (1.17–2.00), C3-fringe *ca.* 0.75 (0.73–0.77). Haltere whitish yellow, basally darker on anterior margin.

Abdomen: Tergites blackish brown, slightly paler in middle of 2nd to 6th tergites. Sternites dark brown; ♂ 5th large, rectangular, with *ca.* 11 long and *ca.* 43 short bristles.

Periphallal organs (Figs. 1 and 2): Epandrium dark brown, paler on lower half, with *ca.* 5 long bristles on upper half and *ca.* 18 bristles on middle to lower half. Surstylus pale brown, with *ca.* 9 primary teeth and *ca.* 3 bristles; basal portion connected to epandrium very narrow. Decaster-

num pale yellow, darker on margin, nearly quadrate. Cercus dark brown, oval, entirely pubescent, with *ca.* 30 long bristles.

Phallic organs (Figs. 3 and 4): Aedeagus orange, bilobed, ventrally curved moderately; apodeme *ca.* 1/4 as long as aedeagus. Anterior paramere pale brown. Novasternum yellowish brown, nearly triangular, with sparse tiny spines in middle of outer surface but without submedian spines.

♀ reproductive organs (Figs. 5 and 6): Lobe of ovipositor brown, with *ca.* 5 light orange discal teeth and *ca.* 21 orange marginal teeth which gradually decrease in size. Spermatheca dark brown, cylindric in lateral view, basally wrinkled; introvert deep; inner duct expanding at 1/4 portion from tip.

Holotype ♂, China: Xianguan, Yunnan Province, 19. IX. 1988. Collector: X. C. Liang.

Paratypes, China: 2 ♂, same data as holotype except 18. X. 1987, 1 ♀, Dabochin, Yunnan Province, 21. IX. 1988. Collector: X. C. Liang.

Distribution. China: Xianguan, Dabochin, Kunming, Yunnan Province, and Meitan, Guichou Province (Prof. Gan, personal. comm.). *Drosophila gani* is the same species as Watabe and Nakata [3] described as *D. sp.* 2, which was collected in Tsugaru district of Honshu Is., northern Japan.

Relationships: This species is related to *D. pullata* Tan *et al.* [4] in the external morphology, but distinguishable from the latter species by the diagnostic characters.

Remarks: This species is dedicated to Prof. Yun Xing Gan (Kunming Institute of Zoology, Academia Sinica), who has introduced the describers (X. C. L., W. X. Z.) into the field of dipteran taxonomy.

Drosophila (Drosophila) yunnanensis

Watabe *et al.* Liang, sp. nov.

(Figs. 7–12)

Diagnosis. Arista with *ca.* 4 upper and *ca.* 2 lower branches. C index *ca.* 4.6, C3-fringe *ca.* 5/9. Tergites with black caudal bands interrupted at middle. Lower margin of epandrium anteriorly convexed, posteriorly rounded (Fig. 7). Aedeagus ventrally curved heavily (Fig. 10). Lobe of ovipo-

sitor broaden caudodorsally (Fig. 11).

♂, ♀. Body color blackish brown. Body length ♂ *ca.* 3.93 mm (3.6–4.2), ♀ *ca.* 4.22 mm (3.3–4.8). Thorax length ♂ *ca.* 1.63 mm (1.5–1.8), ♀ *ca.* 1.78 mm (1.7–1.8). Wing length ♂ *ca.* 3.68 mm (3.4–3.9), ♀ *ca.* 4.22 mm (3.4–4.8).

Head: Eye dark red, with thick piles. Antenna dark brown: 2nd joint with 2–3 stout setae; 3rd with numerous tiny hairs. Arista with *ca.* 4 (4–5) upper and *ca.* 2 lower branches in addition to a terminal fork. Frons blackish brown, ♂ *ca.* 0.47 (0.44–0.51), ♀ *ca.* 0.51 (0.50–0.52) as broad as head, anteriorly with a few frontal hairs. Orb 2 *ca.* 0.36 (0.24–0.53) length of Orb 1; Orb 3 *ca.* 0.69 (0.48–0.84) length of Orb 1. Face reddish brown; carina dark brown, wider below. Cheek light brown, *ca.* 0.18 (0.15–0.22) as broad as maximum diameter of eye. Or 1 long and stout; Or 2 thin, *ca.* 0.58 (0.42–0.75) length of Or 1; Or 3 *ca.* 1/2 length of Or 2. Palpus dark brown, with *ca.* 2–3 long and a few of middle bristles.

Thorax: Mesoscutum dull brown, with 3 longitudinal darker stripes; wide stripe in middle, posteriorly bifurcated, a lateral pair of stripes just outside dorsocentrals, interrupted at transverse suture. Scutellum dark yellow, medially with a broad brown stripe running from mesoscutum. Thoracic pleura dark brown. Humeral plate pale yellow, with 2 humerals; lower one *ca.* 0.71 (0.65–0.87) length of upper one. DcA *ca.* 0.58 (0.51–0.65) length of DcP; length distance of dorsocentrals *ca.* 0.45 (0.41–0.55) cross distance. SptAs nearly parallel; SctPs convergent. SctA *ca.* 0.89 (0.77–0.98) length of SctP; distance between SctPs *ca.* 0.41 (0.36–0.47) distance between SctAs. Sterno-index *ca.* 0.69 (0.47–0.92).

Legs dark brown; fore femur anteriorly with 1 long bristle, posteriorly with *ca.* 4 bristles. Number of 3Cfr *ca.* 20 (16–25). Wing indices: C ♂ *ca.* 4.55 (4.23–4.95), ♀ *ca.* 4.66 (4.36–5.43), 4V ♂ *ca.* 1.59 (1.45–1.79), ♀ *ca.* 1.62 (1.47–1.72), 4C *ca.* 0.57 (0.47–0.63), 5x ♂ *ca.* 1.51 (1.33–1.65), ♀ *ca.* 1.31 (1.14–1.58), Ac ♂ *ca.* 1.63 (1.50–1.78), ♀ *ca.* 1.58 (1.40–1.90), C3-fringe *ca.* 0.57 (0.44–0.65). Haltere yellowish white.

Abdomen: Tergites dark brown, with black caudal bands interrupted at middle; some specimens have entirely black tergites owing to mela-

nization by low temperatures. Sternites brown; ♂ 5th rectangular, posteriorly concaved slightly, with *ca.* 104 bristles; ♀ 6th quadrate, with *ca.* 34 bristles.

Periphallic organs (Figs. 7 and 8): Epandrium posteriorly pubescent except lower half, with *ca.* 7 long bristles on upper half and *ca.* 17 bristles on middle to lower margin. Surstylus distally concaved, with *ca.* 10 apically pointed primary teeth and *ca.* 8 bristles. Decasternum pale yellow, darker on dorsal margin, dorsally rounded and caudally broaden. Cercus pubescent, with *ca.* 40 long bristles; caudoventral corner somewhat pointed, with tuft of several short bristles.

Phallic organs (Figs. 9 and 10): Aedeagus robust, broaden at tip, distally 1/3 bilobed; tip brownish orange, pointed like fook; apodeme *ca.* 2/5 as long as aedeagus. Novasternum broad, with 1 pair of prominent submedian spines on inner margin.

♀ reproductive organs (Figs. 11 and 12): Lobe of ovipositor light orange, apicocaudally broaden, with *ca.* 5 discal teeth and *ca.* 21 marginal teeth; ultimate marginal tooth large, *ca.* 2 times as long as penultimate. Spermatheca dark brown, oval, basally narrowing and wrinkled, with small dark patches on outer surface of capsule, without apical indentation; inner duct narrowed just below tip.

Holotype ♂, China: Dabochin, Yunnan Province, 21. IX. 1988. Collector: X. C. Liang.

Paratypes, China: 5♂, 5♀, same data as holotype.

Distribution. Widely distributed from central to northern parts of Yunnan Province (thus species name).

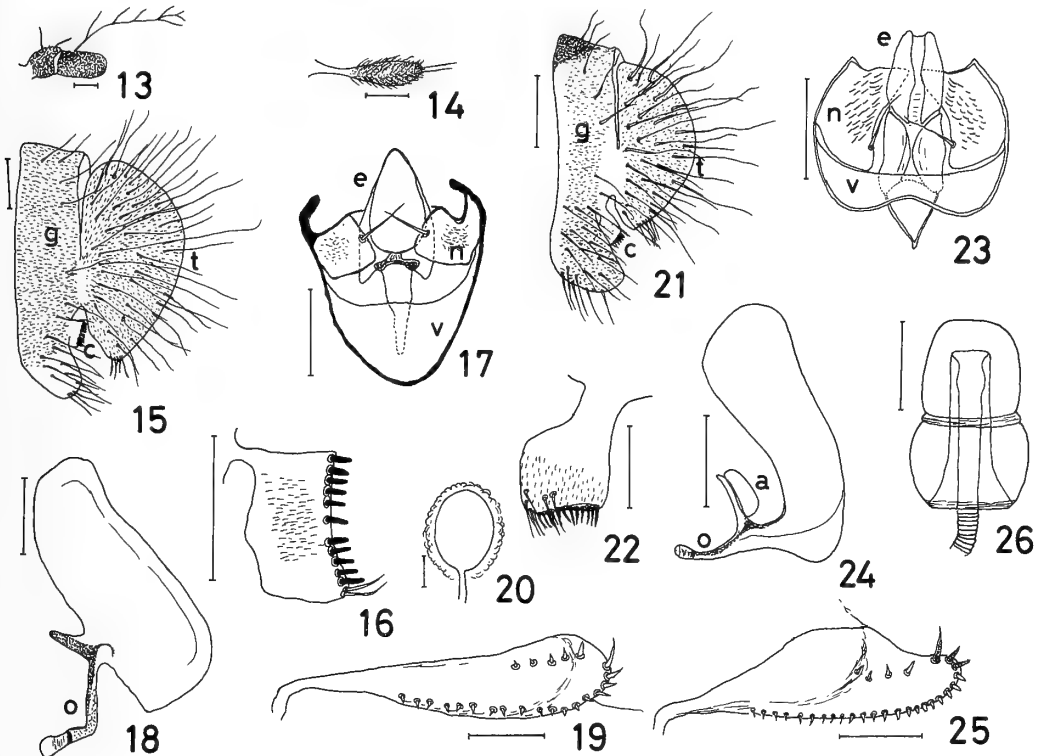
Relationships. *D. yunnanensis* is closely related to *D. lecostosa* in the external appearance, but distinguishable from the latter species by the shapes of aedeagus and spermatheca.

Remarks. In the *robusta* group, novasternum with submedian spines has been found only in *D. lacertosa*, and so *D. yunnanensis* is the second species having such novasternum.

Drosophila (Drosophila) bai

Watabe et Liang, sp. nov.

(Figs. 13–20)



FIGS. 13–20. *Drosophila (Drosophila) bai* Watabe et Liang, sp. nov. 13: Antenna. 14: Palpus. 15: Periphallallic organs. 16: Surstylus. 17: Phallic organs. 18: Aedeagus (lateral view). 19: Ovipositor. 20: Spermatheca. FIGS. 21–26. *Drosophila (Drosophila) medioconstricta*, Watabe, Zhang et Gan, sp. nov. 21: Periphallallic organs. 22: Surstylus. 23: Phallic organs. 24: Aedeagus (lateral view). 25: Ovipositor. 26: Spermatheca. Signs and scales as in Figs. 1–12.

Diagnosis. Arista with *ca.* 4 upper and *ca.* 1 lower branches (Fig. 13). Palpus with 2 long bristles at tip besides numerous tiny hairs (Fig. 14). Or 2 thin, *ca.* 1/3 length of Or 1. C index *ca.* 4.5, C3-fringe *ca.* 4/9. Primary teeth on surstylus sparse, usually separated into two parts (Fig. 15). Aedeagus nearly rectangular (Fig. 18). Lobe of ovipositor slender (Fig. 19); spermatheca less-sclerotized (Fig. 20).

♂, ♀. Body color black. Body length ♂ *ca.* 3.35 mm (3.2–3.6), ♀ *ca.* 3.80 mm (3.4–4.1). Thorax length ♂ *ca.* 1.48 mm (1.4–1.6), ♀ *ca.* 1.61 mm (1.5–1.8). Wing length ♂ *ca.* 3.83 mm (3.8–3.9), ♀ *ca.* 4.25 mm (4.0–4.6).

Head: Eye dark red, with thick piles. Antenna black: 2nd joint with 2 stout setae; 3rd joint with numerous tiny hairs. Arista with *ca.* 4 (3–5) upper and *ca.* 1 (0–2) lower branches in addition to a

small terminal fork. Frons black, *ca.* 0.50 (0.43–0.52) as broad as head, anteriorly with a few frontal hairs. Orb 2 *ca.* 0.34 (0.25–0.41) length of Orb 1; Orb 3 *ca.* 0.68 (0.58–0.91) length of Orb 1. Face brown; carina high, wider below. Cheek dark brown, *ca.* 0.20 (0.13–0.27) as broad as maximum diameter of eye. Or 2 thin, short, *ca.* 0.36 (0.22–0.43) length of Or 1; Or 3 subequal to Or 2. Palpus dark brown, club-shaped.

Thorax: Mesoscutum dark brown, medially with an obscure longitudinal darker stripe; scutellum blackish brown. Thoracic pleura black. Lower humeral *ca.* 0.63 (0.53–0.73) length of upper one. DcA *ca.* 0.67 (0.60–0.73) length of DcP; length distance of dorsocentrals *ca.* 0.46 (0.37–0.53) cross distance. SptAs slightly and SctPs heavily convergent. SctA *ca.* 1.02 (0.93–1.14) length of SctP; distance between SctPs *ca.* 0.40 (0.31–0.45) dis-

tance between SctAs. Sterno-index *ca.* 0.72 (0.54–0.84).

Legs dark brown; fore coxa much darker, anteriorly with *ca.* 2 long bristles. Number of 3Cfr *ca.* 15 (11–20). Wing indices: C ♂ *ca.* 4.51 (4.33–4.63), ♀ *ca.* 4.44 (4.06–4.66), 4V ♂ *ca.* 1.57 (1.48–1.72), ♀ *ca.* 1.53 (1.43–1.66), 4C *ca.* 0.56 (0.51–0.62), 5x ♂ *ca.* 1.30 (1.18–1.44), ♀ *ca.* 1.17 (0.92–1.36), Ac ♂ *ca.* 1.62 (1.55–1.70), ♀ *ca.* 1.75 (1.58–1.80), C3-fringe *ca.* 0.45 (0.40–0.51). Haltere white.

Abdomen: Tergites black, somewhat paler at middle. Sternites brown, paler at middle; ♂ 3rd to 5th large.

Periphallic organs (Figs. 15 and 16): Epandrium black, pubescent except lower margin, caudoventrally convexed, with *ca.* 4 long bristles on upper portion, 1 bristle on middle and *ca.* 13 bristles on lower. Surstylus dark brown, rectangular, medially pubescent on outer surface, with *ca.* 11 primary teeth and *ca.* 2 bristles; basal part connected to epandrium narrow. Decasternum pale brown, darker on margin, medially constricted, ventrally broaden. Cercus black, entirely pubescent, slightly convexed at lower part, with *ca.* 28 long bristles and with several short bristles at caudoventral apex.

Phallic organs (Figs. 17 and 18): Aedeagus yellowish brown, distally bilobed; cross distance *ca.* 3/7 length distance. Novasternum medially pubescent, with submedian spines on inner margin. Ventral fragma blackish brown.

♀ reproductive organs (Figs. 19 and 20): Lobe of ovipositor brown, much darker on ventral margin, with 4–5 discal and *ca.* 18 marginal teeth. Spermatheca small, transparent, without introversion, embedded by adipose tissue.

Holotype ♂, China: Dabochin, Yunnan Province, 19. IX. 1988. Collector: X. C. Liang.

Paratypes, China: 5 ♂, 5 ♀, same data as holotype, except 21. IX. 1988.

Distribution. The distribution of this species has been restricted to Dali (the Autonomous District of Bai Minority, thus species name).

Relationships. *D. bai* is somewhat related to *D. virilis* group species in the external appearance and in having submedian spines, but distinguishable from these species by the diagnostic characters.

Drosophila (Drosophila) medioconstricta

Watabe, Zhang et Gan, sp. nov.

(Figs. 21–26)

Diagnosis. Arista with *ca.* 3 upper and *ca.* 2 lower branches. C index *ca.* 2.82, C3-fringe *ca.* 4/5. Ventral margin of epandrium roundish (Fig. 21). Aedeagus ventrally curved heavily (Fig. 24). Ventral fragma laterally very wide (Fig. 23). Spermatheca gourd-shaped (Fig. 26).

♂, ♀. Body color black. Body length *ca.* 3.57 mm (3.4–3.6), thorax length *ca.* 1.70 mm (1.6–1.8), wing length *ca.* 3.95 mm (3.5–4.2).

Head: Eye dark red, with thick piles. Second joint of antenna black with 2 stout setae; 3rd black, rounded at tip. Arista with *ca.* 3 upper and *ca.* 2 lower branches in addition to a moderate terminal fork. Frons blackish brown, *ca.* 0.51 (0.49–0.52) as broad as head, anteriorly with a few frontal hairs. Orb 2 *ca.* 0.34 (0.24–0.39) length of Orb 1; Orb 3 *ca.* 0.62 (0.58–0.64) length of Orb 1. Face reddish brown; carina high, wider below. Clypeus blackish brown. Cheek brown, *ca.* 0.21 (0.15–0.26) as broad as maximum diameter of eye, with *ca.* 3 bristles at lower corner. Or 2 thin, *ca.* 0.56 (0.45–0.67) length of Or 1; Or 3 *ca.* 1/2 length of Or 2. Palpus dark brown, with ♂ *ca.* 8 long bristles and ♀ *ca.* 4 bristles.

Thorax: Mesoscutum dark brown, medially with a longitudinal darker stripe and laterally 1 pair of obscure broad stripes along notopleurals. Scutellum black, with 1 pair of brown stripes in lateral sides. Thoracic pleura black. Lower humeral *ca.* 0.75 (0.71–0.77) length of upper one. DcA *ca.* 0.67 (0.52–0.73) length of DcP; length distance of dorsocentrals *ca.* 0.49 (0.40–0.62) cross distance. SptA slightly and SctP heavily convergent. SctA *ca.* 0.89 (0.77–1.09) length of SctP; distance between SctPs *ca.* 0.41 (0.40–0.43) distance between SctAs. Sterno-index *ca.* 0.75 (0.55–0.92).

Legs dark brown; fore coxa and femur darker. Number of 3Cfr *ca.* 41 (35–48). Wing indices: C *ca.* 2.82 (2.61–3.20), 4V *ca.* 1.59 (1.55–1.63), 4C *ca.* 0.84 (0.76–0.88), 5x *ca.* 1.23 (1.09–1.40), Ac *ca.* 2.27 (2.08–2.55), C3-fringe *ca.* 0.81 (0.80–0.83). Haltere whitish yellow; basal stalk gray.

Abdomen: Tergites black, medially with small

U-shaped dark yellow area in 2nd to 5th; 1st entirely black. Sternites brown, darker on margin; ♂ 5th nearly rectangular, ♀ 6th quadrate, each with ca. 10–15 long bristles on margin.

Periphallic organs (Figs. 21 and 22): Epandrium dark brown, much darker at antero-dorsal corner, pubescent except anterior margin, with ca. 5 bristles on upper half and ca. 20 bristles on middle to lower half. Surstylus brown, pubescent on distal half of outer surface, with ca. 12 apically pointed primary teeth and ca. 5 bristles at caudoventral corner; basal part connected to epandrium broad, ca. 1/2 maximum width of surstylus. Decasternum pale brown, darker on margin, ladder-shaped. Cercus black, entirely pubescent, with ca. 23 bristles and ca. 9 relatively short bristles on ventral apex.

Phallic organs (Figs. 23 and 24): Aedeagus pale yellow, distally bilobed, ventrally curved strongly, distally swollen in lateral view; apodeme short, ca. 1/4 as long as aedeagus. Anterior paramere pale brown, rectangular in lateral view. Novasternum broad, with small wart-like spines on inner half of surface and with 1 pair of prominent submedian spines on inner margin. Ventral fragma laterally broaden, medially narrowing.

♀ reproductive organs (Figs. 25 and 26): Lobe of ovipositor brown, with ca. 4 light orange discal teeth and ca. 25 orange marginal teeth; ultimate marginal tooth blackish brown, ca. 2.5 times as long as penultimate. Spermatheca constricted at middle (thus, species name), with small dark patches on upper half of outer surface, without apical indentation; introvert ca. 6/7 height of outer capsule; duct distally expanded slightly.

Holotype ♂, China: Dabochin, Yunnan Province, 21. IX. 1988. Collector: X. C. Liang.

Paratypes, China: 3 ♀, same data as holotype.

Distribution. China: Dabochin, Kunming, Yunnan Province.

Relationships. *D. medioconstricta* is related to *D. lacertosa*, *D. yunnanensis* and *D. bai* in having novasternum with submedian spines, but distinguishable from the latter three species by the shapes of aedeagus and ovipositor. Further, this species seems to be related to the *D. melanica* and *D. virilis* species-groups in having a relatively small value of C-index.

Remarks. *D. medioconstricta* inhabits watersides and their surrounding forests.

THE GEOGRAPHIC DISTRIBUTION

The *robusta* species-group is considered to have evolved in the *virilis-repleta* Radiation, and all members have been recorded in temperate to cool regions of Asia and North America: 6 species in Japan, *D. okadai* Takada, *D. neokadai*, *D. moriwakii* Okada et Kurokawa, *D. sordidula* Kikkawa et Peng, *D. pseudosordidula* Kaneko et al. and *D. lacertosa*; 2 species in the mainland of China, *D. cheda* and *D. pullata*; 2 species in North America, *D. colorata* Walker and *D. robusta* Sturtevant. Narayanan [5] examined chromosomes and crossabilities of these American and Japanese members except for *D. okadai* and *D. neokadai*, and proposed an evolutionary phylogeny of the *robusta* group.

From a comparative study of genitalia, however, Beppu [6] has recently transferred *D. moriwakii*

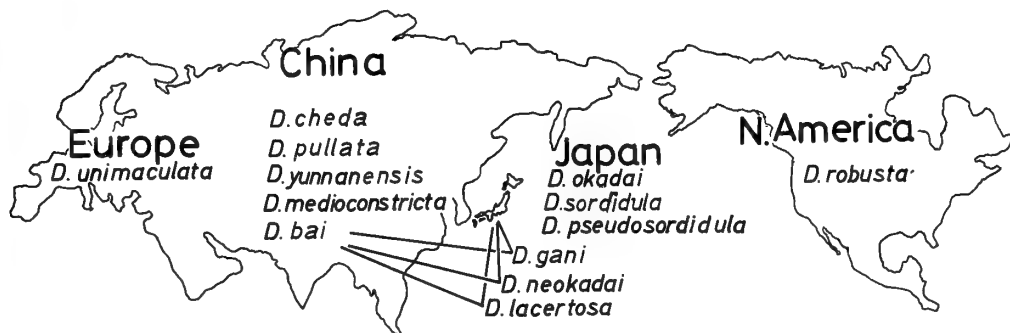


FIG. 27. The geographic distribution of the *Drosophila robusta* species-group.

and *D. colorata* from the *robusta* group to its allied *melanica* species-group, and vice versa *D. unimaculata* Strobl distributed in Europe. The geographic distribution of the *robusta* group is redrawn in Fig. 27, on the basis of recent knowledge including the present new species. The figure shows that China is richest in this fauna and includes three endemic species having submedian spines common to the *melanica* and *virilis* species-groups.

These information indicates that the evolutionary history of the *robusta* group should be reconsidered, and that China is a very important area when considering this.

ACKNOWLEDGMENTS

The authors are grateful to Dr. Masanori J. Toda of Hokkaido University for his advice during this study. This work was supported by a Grant-in-Aid for Overseas Scientific Survey from the Ministry of Education, Science and Culture, Japan (Nos. 62041085, 63043060).

REFERENCES

- 1 Okada, T. (1956) Systematic Study of Drosophilidae and Allied Families of Japan. Gihodo Co. Ltd., Tokyo, pp. 183.
- 2 Kaneko, A. and Takada, H. (1966) *Drosophila* Survey of Hokkaido XXI. Description of a new species, *Drosophila neokadai* sp. nov. (Diptera, Drosophilidae). Annot. Zool. Japon., **39**: 55–59.
- 3 Watabe, H. and Nakata, S. (1989) A comparative study of genitalia in the *Drosophila robusta* and *D. melanica* species-groups (Diptera: Drosophilidae). J. Hokkaido Univ. of Education, Ser. IIB., **40**: 1–18.
- 4 Tan, C. C., Hsu, T. C. and Sheng, T. C. (1949) Known *Drosophila* species in China with descriptions of twelve new species. Univ. Texas Publ., **4920**: 196–206.
- 5 Narayanan, Y. (1973) The phylogenetic relationships of the members of the *Drosophila robusta* group. Genetics, **73**: 319–350.
- 6 Beppu, K. (1988) Systematic positions of three *Drosophila* species (Diptera: Drosophilidae) in the *virilis-repleta* radiation. Proc. Japan. Soc. Syst. Zool., **37**: 55–58.

Reexamination on the Taxonomic Position of Two Intraspecific Taxa in Japanese *Eothenomys*: Evidence from Crossbreeding Experiments (Mammalia: Rodentia)

AKIRO ANDO, SATOSHI SHIRAISHI¹ and TERU AKI UCHIDA

*Zoological Laboratory, Faculty of Agriculture,
Kyushu University 46-06, Fukuoka 812, Japan*

ABSTRACT—As a part of the study in which the taxonomic validity of *E. kageus* is inclusively reexamined, crossbreeding experiments were made between *Eothenomys smithii* with six mammae and *E. kageus* with four mammae, which have been separated by the difference mainly in number of the mammae and in shape of the baculum. Consequently, these two species readily interbred in crosses of both *E. smithii* ♀ × *E. kageus* ♂ and *E. kageus* ♀ × *E. smithii* ♂. F₁ hybrids obtained from the two crosses possessed normal breeding ability. Moreover, F₅ hybrids were produced from the line of the former cross. Some daughters were different from their mothers in number of the mammae, and some litters included both females with four mammae and females with six mammae within a litter. These facts suggest that both species may share an intercommunicating gene pool with each other, and mean that the difference in number of the mammae is an intraspecific variation or a polymorphism. It has been also said that the shape of the bacula is a poor taxonomic character. Therefore, taking the reproductive compatibility between them and the unreliability of the taxonomic characters into account, together with the almost entire identity in their karyotypes previously reported by us, it is concluded that *E. kageus* is synonymous with *E. smithii*.

INTRODUCTION

Taxonomy must be grounded on integrated conclusions which were clarified by investigations from various aspects. Accordingly, when two related forms, which had been separated only by the morphological characters, have given rise to a taxonomic dispute, more extensive studies are desired. In particular, a crossbreeding experiment occupies a great important position in this field and is a useful method of assessing the relationship between such allied forms.

The Smith's red-backed vole with six mammae (*Eothenomys smithii*) and "Kage" red-backed vole with four mammae (*E. kageus*) are said to occur in the western and central parts of Japan, respectively [1]. However, a dispute on the taxonomic position of these two "species" has still remained

unsolved. The dispute began with the separation of *E. kageus* from *E. smithii* by the difference mainly in number of the mammae and in shape of the baculum. Afterwards, many studies have been made on this problem, but restricted to morphological [2-7] and karyological (a conventional staining method) [8, 9] aspects. In this connection, as a part of the broader study in which the taxonomic validity of *E. kageus* is inclusively reexamined, comparisons of the growth and development patterns and the karyotypes (G- and C-band patterns) between *E. smithii* and *E. kageus* revealed that the characteristics of these patterns in *E. kageus* were basically identical with those in *E. smithii* [10, 11]. Then, in order to gain new information on this problem, crossbreeding experiments between them were carried out, although the sample size was small. The aim of the present study is to examine the reproductive compatibility between *E. smithii* and *E. kageus* and the reliability of the number of the mammae as a diagnostic character, and to discuss the taxonomic position of both

Accepted February 20, 1989

Received October 14, 1988

¹ To whom reprint requests should be addressed.

species.

MATERIALS AND METHODS

E. smithii (2 males, 6 females) and *E. kageus* (3 males, 2 females), used as parental generations, were obtained from laboratory colonies which were derived from wild voles live-trapped in Kyushu (Fukuoka Prefecture) and central Honshu (Nagano and Yamanashi Prefectures), respectively. All hybrid generations were originated from four pairs of *E. smithii* ♀ × *E. kageus* ♂ and two pairs of *E. kageus* ♀ × *E. smithii* ♂ (see Table 1).

All animals were housed in stainless steel cages (43×25×23 cm), and given *ad libitum* a commercial diet (NMF or CMF, Oriental Yeast Co., Ltd., Tokyo) and water, and sometimes fresh cabbages. The experimental colonies were maintained at temperatures of 20±1°C on photoperiods of 12 hr light: 12 hr dark. Humidity was not controlled throughout the experimental period. Voles produced litters throughout the year under such rearing conditions. Gravid females were inspected daily for deliveries so that their litters were discovered within 24 hr *post partum*. The day when neonates were found by checking was designated the day of parturition and day 0 of the newborn young. The number of young on the day when they were found was regarded as the litter size. Since the mammae of female young became detectable as about day 7 in both *E. smithii* and *E. kageus* [12, 10], the number of the mammae of female hybrids was determined at this time.

RESULTS

The results of the breeding experiments are given in Table 1. Eleven types of crosses, consisting of eight in the line of *E. smithii* ♀ × *E. kageus* ♂ and three in the line of *E. kageus* ♀ × *E. smithii* ♂, were attempted in this study. Litters were produced from all types of crosses. Mean litter sizes showed 2.5–3.0 in most of the crosses, although the sample size was very small in some cases. The maximum and minimum mean litter sizes were 4.8 and 1.9, respectively.

Regarding the number of the mammae, there were two kinds of crosses; i.e. one was the cross in

which all females of the progeny had six mammae, and the other was the cross in which females of the progeny possessed four or six mammae. Out of the eleven types of crosses, eight types of crosses leading to the former case bore 71 litters *en bloc*, whereas the remaining three types of crosses resulting in the latter case gave birth to 29 litters as a whole. Out of the above 29 litters, five litters contained both females having four mammae and females having six mammae (6 males and 12 females in total; out of 12 females, five had four mammae and six had six mammae, and one was undetermined); the remaining 24 litters involved only females with six mammae. However, no cross existed in which all female hybrids had four mammae. The maximum longevity was 1,354 days in F₁ hybrids between *E. smithii* ♀ and *E. kageus* ♂.

DISCUSSION

1) Reproductive compatibility between *E. smithii* and *E. kageus*.

Isolating mechanisms which are necessary for maintenance of species integrity are classified into two categories, premating and postmating mechanisms; the former category contains seasonal and habitat, ethological and mechanical isolation, while the latter category includes gametic and zygote mortality, hybrid inviability and hybrid sterility [13].

In connection with attempts to obtain interspecific hybrids, crossbreeding (or artificial insemination) experiments between different species have been carried out in some orders of Mammalia, including Rodentia. However, there have been few hybrids with fertility in such cases because of operation of the above postmating mechanisms. As examples of hybrids which die during embryogenesis, the following combinations have been well known: goats (*Capra hircus*) × sheep (*Ovis aries*) [14], ferrets (*Mustela furo*) × minks (*Mustela vison*) [15], rabbits (*Oryctolagus cuniculus*) × hares (*Lepus americanus*) [15] and black rats (*Rattus rattus*) × brown rats (*Rattus norvegicus*) [16,17]. On the other hand, in crosses of horses (*Equus caballus*) × donkeys (*Equus asinus*) [18], horses (*E. caballus*) × zebras (*Equus grevyi*)

TABLE 1. Breeding results

	Types of crosses	No. of pairs	No. of litters	No. of young			Mean litter size	Range	No. of mammae of young
				♂	♀	Ud			
I	<i>E. smithii</i> (♀) × <i>E. kageus</i> (♂)	4	17	27	20	2	2.9	1-5	6
	(<i>smithii</i> × <i>kageus</i>)F ₁ × (<i>smithii</i> × <i>kageus</i>)F ₁	2	16	24	25	4	3.3	1-5	6
	(<i>smithii</i> × <i>kageus</i>)F ₂ × (<i>smithii</i> × <i>kageus</i>)F ₂	5	17	24	19		2.5	2-4	6
	(<i>smithii</i> × <i>kageus</i>)F ₃ × (<i>smithii</i> × <i>kageus</i>)F ₃	3	12	14	15	1	2.5	1-5	4 or 6*
	(<i>smithii</i> × <i>kageus</i>)F ₄ × (<i>smithii</i> × <i>kageus</i>)F ₄	1	2	2	3		2.5	2-3	6
	<i>E. smithii</i> (♀) × (<i>smithii</i> × <i>kageus</i>)F ₁ (♂)	2	7	6	7		1.9	1-3	6
	(<i>smithii</i> × <i>kageus</i>)F ₃ (♀) × (<i>smithii</i> × <i>kageus</i>)F ₂ (♂)	1	1	1	2		3.0	3	4 or 6†
	(<i>smithii</i> × <i>kageus</i>)F ₄ (♀) × (<i>smithii</i> × <i>kageus</i>)F ₃ (♂)	1	2	3	2		2.5	2-3	6
II	<i>E. kageus</i> (♀) × <i>E. smithii</i> (♂)	2	8	13	15	2	3.8	2-6	6
	(<i>kageus</i> × <i>smithii</i>)F ₁ × (<i>kageus</i> × <i>smithii</i>)F ₁	3	16	40	33	3	4.8	3-6	4 or 6‡
	(<i>kageus</i> × <i>smithii</i>)F ₂ × (<i>kageus</i> × <i>smithii</i>)F ₂	1	2	3	3		3.0	3	6

Ud, undetermined.

* Two and eight females have 4 and 6 mammae, respectively, and five have mammae of undetermined number.

† One and the other female have 4 and 6 mammae, respectively.

‡ Four and 23 females have 4 and 6 mammae, respectively, and six have mammae of undetermined number.

[19], Syrian hamsters (*Mesocricetus newtoni*) × golden hamsters (*Mesocricetus auratus*) [20] and Shaw's jirds (*Meriones shawi*) × Libyan jirds (*Meriones libycus*) [21], their hybrids survive to adulthood, but males and/or females are sterile.

As to the present experiments, in crosses of both *E. smithii* ♀ × *E. kageus* ♂ and *E. kageus* ♀ × *E. smithii* ♂, these two species readily interbred. Both sexes of F₁ hybrids obtained from the above two crosses seem to possess, at least under laboratory conditions, normal breeding ability. Further, F₅ hybrids were produced from the line of the former cross. Therefore, these facts demonstrate that almost no barrier caused by postmating isolating mechanisms exists between both species, so far as the crossbreeding experiments are concerned.

In our study mean litter sizes in the crosses were 1.9-4.8, being smaller than the mean litter size (4.5) of *E. smithii* [22], except for the value 4.8. *E. smithii* has wide individual variations in litter size, and the lowest and highest prolificacies were 2.8 and 6.8 young per litter, respectively [22]. Accordingly, when the litter size is discussed, it is necessary to get a larger sample size just in such crossbreeding experiments. Although there is still much to be investigated, very important is the fact

that progeny between *E. smithii* and *E. kageus* were fertile. This fact suggests the probability that both species may share an intercommunicating gene pool with each other, but detailed analyses at the gene level are indispensable with respect to this.

It must be noted that fertility or sterility of hybrids is not the sole criterion of species [13, 23]. For example, coyotes (*Canis latrans*) × dogs (*Canis familiaris*) hybrids are fertile [24]: premating isolating mechanisms seem to play a significant role in such cases [13]. There has been no direct evidence showing the presence or absence of barriers due to premating mechanisms between *E. smithii* and *E. kageus* under natural conditions. However, judging from our success in interbreeding between both species in the laboratory, and from existence of females with four and six mammae under both laboratory and field (as mentioned below) conditions, there is a high possibility that both forms are crossbred under natural conditions.

2) Taxonomic validity of *E. kageus*.

When discussing the taxonomic status of *E. smithii* and *E. kageus*, it is of importance to examine the reliability of the taxonomic characters

(the number of the mammae and the shape of the baculum) which were described by Imaizumi [1].

Imaizumi [1] has stated that the difference in the mammary formula of these two species seems to be fairly important as one of the main diagnostic characters. However, our crossbreeding experiments revealed that some daughters were different from their mothers in number of the mammae, and that some litters included both females with four mammae and females with six ones within a litter. These facts apparently indicate that the number of the mammae is not a constant character at the individual level. Furthermore, in Mt. Yatsugatake (Nagano Pref.), Mt. Kamegamori (Ehime Pref.), Mt. Tsurugi (Tokushima Pref.) and Mt. Hakusan (Ishikawa Pref.), both females with four mammae and females with six mammae are captured at the same locality [3–5, 25]. The difference in number of the mammae has been considered to be individual variation [3, 4]. In this context, it is worthy of note that a pair of voles from Nagano Prefecture (the female with four mammae) produced a litter including a female with four mammae and a female with six mammae in our laboratory [unpublished]; this fact agrees with the results of the above field studies.

In murid mammals, the swamp rat (*Rattus lutreolus*) and the bush rat (*Rattus fuscipes*) inhabiting Australia are known as species in which the numbers of the mammae are different between geographically isolated populations and between subspecies, respectively [26]. In the former species, mainland females have five pairs of teats, while females from Tasmania have only four pairs. *Rattus fuscipes* is divided into four subspecies (*R. f. fuscipes*, *R. f. greyi*, *R. f. assimilis* and *R. f. coracinus*); only *R. f. coracinus* females have four pairs of teats, whereas females of the other three subspecies have five pairs. Thus, the difference in number of the mammae is an intraspecific variation or a polymorphism, being unreliable as a diagnostic character by which *E. kageus* was separated from *E. smithii*. With respect to this problem, Kaneko [7] also has drawn the same conclusion from an investigation on the number of the mammae in pregnant or postpartum wild females.

Regarding the baculum, Imaizumi [1] has mentioned that there are differences in general outline

of the posterior border of its body (semicircular in *E. smithii*, while concave in *E. kageus*) and in shape of the lateral prongs (curved as the letter "c" in *E. smithii*, while double curved as the letter "s" in *E. kageus*). However, Jameson [2] has stated that the difference in the bacula of *E. kageus* and *E. smithii* may be due to individual variation. On the basis of a detailed analysis of the bacula in 71 wild males, Kaneko [7] also has concluded that the above differences in the bacula cannot be employed as a diagnostic character between these two species in question.

Furthermore, the following facts have been reported: in an analysis of the skull, the relative growth coefficient shows no difference among five localities including Kyushu and central Honshu [6]; geographical clines are recognized in the hind foot length, the tail length and the parietal width [4, 6]; the growth and development patterns of both species are basically identical with each other [10]; except for a slight variation in size of the short arm of the Y chromosome, no detectable difference is found in the karyotype (G- and C-band patterns) between both species [11]. All these facts may indirectly adduce negative evidence for the taxonomic validity of *E. kageus*.

From the above consideration, it can be said that *E. kageus* may not be reproductively isolated from *E. smithii*, even under natural condition, and that the taxonomic characters (the number of the mammae and the shape of the bacula) pointed out by Imaizumi [1] are not regarded as diagnostic. Our conclusion reached, therefore, is that *E. kageus* is synonymous with *E. smithii*.

ACKNOWLEDGMENTS

We thank Professor E. W. Jameson, Jr., University of California, for comments on the manuscript.

REFERENCES

- 1 Imaizumi, Y. (1957) Taxonomic studies on the red-backed voles of Japan. Part I. Major divisions of the vole and description of *Eothenomys* with a new species. Bull. Nat. Sci. Mus. (Tokyo), (40): 195–216.
- 2 Jameson, E. W., Jr. (1961) Relationships of the red-backed voles of Japan. Pacific Sci., 15: 594–604.

- 3 Miyao, T., Morozumi, T., Morozumi, M., Hanamura, H., Akahane, H. and Sakai, A. (1964) Small mammals on Mt. Yatsugatake in Honshu. III. Smith's red-backed vole (*Eothenomys smithi*) in the subalpine forest zone on Mt. Yatsugatake. Zool. Mag., **73**: 189–195. (In Japanese with English abstract).
- 4 Miyao, T. (1967) Studies on the geographical variation of the small mammals in Japanese islands. I. Geographical variation of Smith's red-backed vole, *Eothenomys smithi*. (2) Hind-foot length, tail length, number of sacro-caudal vertebrae and breeding activity. J. Growth, **6**: 7–18. (In Japanese with English abstract).
- 5 Tanaka, R. (1971) A research into variation in molar and external features among a population of the Smith's red-backed vole for elucidation of its systematic rank. Jap. J. Zool., **16**: 163–176.
- 6 Aimi, M. (1980) A revised classification of the Japanese red-backed voles. Mem. Fac. Sci. Kyoto Univ., Ser. Biol., **8**: 35–84.
- 7 Kaneko, Y. (1985) Examinations of diagnostic characters (mammary and bacula) between *Eothenomys smithi* and *E. kageus*. J. Mamm. Soc. Japan, **10**: 221–229. (In Japanese with English abstract).
- 8 Tsuchiya, K. (1970) Classification of Japanese cricetid and murid rodents based on their karyotypes (1). Yama to Hakubutsukan (Mountains and Museum), **15**: 2–3. (In Japanese).
- 9 Tsuchiya, K. (1981) On the chromosome variations in Japanese cricetid and murid rodents. Honyurui Kagaku (Mammalian Science), **21**: 51–58. (In Japanese).
- 10 Ando, A. and Shiraishi, S. (1988) Reproduction, growth and development of the so-called "Kage" red-backed vole, *Eothenomys kageus*. Honyurui Kagaku (Mammalian Science), **28**: 13–22. (In Japanese with English abstract).
- 11 Ando, A., Shiraishi, S., Harada, M. and Uchida, T. A. (1988) A karyological study of two intraspecific taxa in Japanese *Eothenomys* (Mammalia: Rodentia). J. Mamm. Soc. Japan, **13**: 93–104.
- 12 Ando, A., Shiraishi, S. and Uchida, T. A. (1987) Growth and development of the Smith's red-backed vole, *Eothenomys smithi*. J. Fac. Agr., Kyushu Univ., **31**: 309–320.
- 13 Mayr, E. (1964) Animal Species and Evolution. Belknap Press of Harvard Univ. Press, Cambridge.
- 14 Alexander, G., Williams, D. and Bailey, L. (1967) Natural immunization in pregnant goats against red blood cells of their sheep×goat hybrid fetuses. Aust. J. Biol. Sci., **20**: 1217–1226.
- 15 Chang, M. C., Pickworth, S. and McGaughey, R. W. (1969) Experimental hybridization and chromosomes of hybrid. In "Comparative Mammalian Cytogenetics". Ed. by K. Benirschke, Springer-Verlag, Berlin, pp. 132–145.
- 16 Hiraiwa, Y. K. and Yoshida, H. (1955) Conception by the cross between *Rattus norvegicus* and *R. rattus*. II. Breeding experiments by the artificial insemination. Sci. Bull. Fac. Agr., Kyushu Univ., **15**: 267–273. (In Japanese with English résumé).
- 17 Yosida, T. H. (1980) Cytogenetics of the Black Rat. University of Tokyo Press, Tokyo.
- 18 Benirschke, K., Brownhill, L. E. and Beath, M. M. (1962) Somatic chromosomes of the horse, the donkey and their hybrids, the mule and the hinny. J. Reprod. Fert., **4**: 319–326.
- 19 King, J. M., Short, R. V., Mutton, D. E. and Hamerton, J. L. (1966) The reproductive physiology of male zebra-horse and zebra-donkey hybrids. In "Comparative Biology of Reproduction in Mammals". Ed. by I. W. Rowlands, Academic Press, New York, pp. 511–527.
- 20 Raicu, P. and Bratosin, S. (1968) Interspecific reciprocal hybrids between *Mesocricetus auratus* and *M. newtoni*. Genet. Res., **11**: 113–114.
- 21 Lay, D. M. and Nadler, C. F. (1969) Hybridization in the rodent genus *Meriones*: I. Breeding and cytological analyses of *Meriones shawi* (♀)×*Meriones libycus* (♂) hybrids. Cytogenetics, **8**: 35–50.
- 22 Ando, A., Shiraishi, S. and Uchida, T. A. (1988) Reproduction in a laboratory colony of the Smith's red-backed vole, *Eothenomys smithi*. J. Mamm. Soc. Japan, **13**: 11–20.
- 23 Futuyama, D. J. (1986) Evolutionary Biology. Sinauer Associate, Inc. Publishers, Sunderland.
- 24 Mengel, R. M. (1971) A study of dog-coyote hybrids and implications concerning hybridization in *Canis*. J. Mamm., **52**: 316–336.
- 25 Shida, T. (1983) Notes on the small mammal fauna in the northern slope of Mt. Hakusan. Annu. Rep. Hakusan Nat. Conserv. Cent., (9): 57–65. (In Japanese with English summary).
- 26 Watts, C. H. S. and Aslin, H. J. (1981) The Rodents of Australia. Angus & Robertson Publishers, London.

[COMMUNICATION]

Histochemistry of Yolk Formation in the Ovaries of the Tarnished Plant Bug, *Lygus lineolaris* (Palisot de Beauvois) (Hemiptera: Miridae)

W. K. MA¹ and S. B. RAMASWAMY

Department of Entomology, Drawer EM, Mississippi State University,
Mississippi State, MS 39762, USA

ABSTRACT—The ovaries of *Lygus lineolaris* were studied using histochemical techniques. Three types of yolk bodies, YB I, YB II and YB III, are recognizable in vitellogenic oocytes. YB I granules were determined to be lipid by Sudan black B staining and YB II and YB III were protein/carbohydrate complexes based on bromophenol blue and periodic acid-Schiff staining. During early vitellogenesis, YB I and YB II are predominant, while in mature oocytes, YB I and YB III predominate suggesting that YB II may be a precursor for YB III. The germarium remains unchanged histochemically throughout the gonotrophic cycle.

INTRODUCTION

Insect eggs contain a large amount of yolk which is incorporated during vitellogenesis. In most insects, yolk consists mainly of lipid and protein (with or without conjugated carbohydrates); and in some insects, glycogen deposits are also found. In many cases, yolk is of an extraovarian origin and the fat body is the most common site of storage and synthesis of yolk components [1-3]. In addition, the nurse cells in meroistic ovarioles and follicle cells may contribute some yolk material. Nurse cells may be associated with each developing oocyte as in polytrophic ovarioles or housed exclusively in the germarium as in telotrophic ovarioles common to Hemiptera. The development of nutritive cords in the latter type has made this an interesting developmental system to study.

There have been a few histochemical studies of vitellogenesis in the Hemiptera (for example, *Acanthocephala*, Coreidae [4]; *Oncopeltus*, Lygaeidae [5-7]; *Gerris*, Gerridae [8]).

A recent study [9] showed that the gonotrophic cycle in *Lygus lineolaris* requires seven days to be completed. The current paper reports of observations on the histochemical changes during vitellogenesis in *L. lineolaris*.

MATERIALS AND METHODS

Insects were obtained and raised as described previously [9]. Virgin females aged 1-7 days were used throughout the study. Insects were anesthetized under CO₂ and dissected in insect Ringer [10]. Ovarioles with part of their associated lateral oviducts were removed, fixed and stored in 10% buffered formalin until use. Tissues used for detection of carbohydrate and protein were dehydrated through graded series of ethanol, passed successively through 1/2, 1/1, 2/1 Sorvall® embedding medium (E. I. Dupont Co. Newtown, Conn.)/absolute ethanol, infiltrated with three fresh changes of 12 hr each of embedding medium and embedded in the same at room temperature under nitrogen. Plastic sections (3-4 µm) were cut on a LKB ultratome using glass knives.

Periodic acid-Schiff (PAS) technique with and without periodic acid oxidation was employed as a general test for carbohydrate [11]. Dimedone was used as a free aldehyde blocking agent [12]. To demonstrate glycogen deposits, plastic sections

Accepted February 23, 1989

Received June 30, 1988

¹ Present address: Department of Entomology, Cornell University, Ithaca, NY 14853, USA.

were incubated in 0.5% diastase at 37°C for 30 min [13] followed by PAS staining. Control sections were similarly processed except for the enzyme incubation.

Treatment of sections with 0.1% bromphenol blue in 70% ethanol was used to demonstrate protein [13]. For detection of lipid, tissues previously fixed in 10% buffered formalin were washed overnight in water and passed through 5% and 10% gelatin for 2 hr each at 37°C in a vacuum oven. Tissues were then infiltrated with 25% gelatin overnight and embedded in the same at 4°C. Gelatin blocks with tissues were frozen with dry ice and 4 μ m cryosections were cut on an IEC cryostat (IEC Co. Ltd., Needham Heights, Mass.). Sections were picked up on a warm glass slide, stained with Sudan black B in propylene glycol [14] and mounted in glycerin jelly.

Tissue sections were examined under a Zeiss compound microscope and photographed with Panatomic X film (Kodak, 32 ASA).

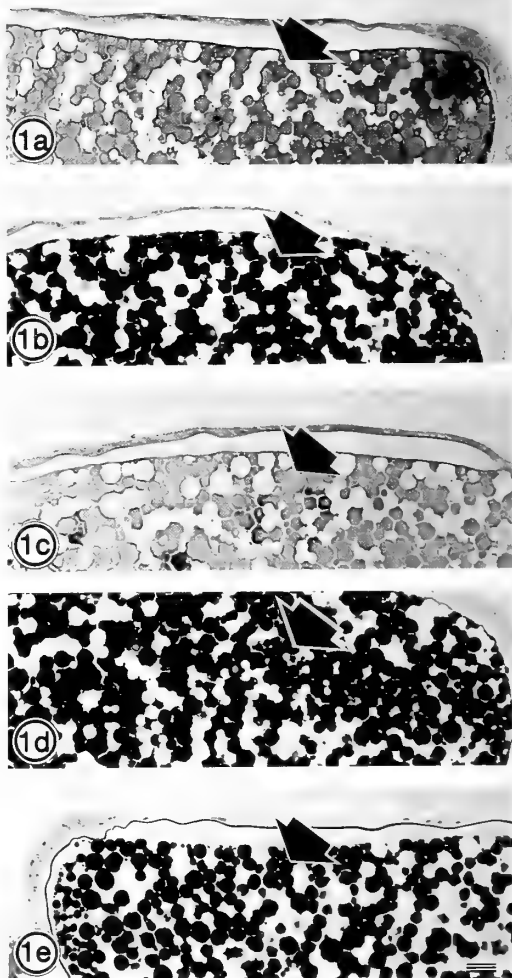
OBSERVATIONS

Three types of yolk bodies, YB I, II and III are distinguishable in vitellogenic oocytes in *L. lineolaris*. Results from bromphenol blue and PAS staining suggested that YB II and III are protein carbohydrate complexes (Figs. 1, 10, 11 and 12). Combination of PAS staining with diastase treatment further confirmed that the carbohydrate moiety of YB II and III is not glycogen (Fig. 1). YB II is more intensely stained (dark blue) with bromphenol blue and is relatively smaller (ca. 2–8 μ m) than YB III (pale blue and ca. 5–25 μ m) (Fig. 12). YB I is not preserved in plastic sections but is stained bluish black with sudan black B in cryosections suggesting its lipoidal nature (Figs. 2 and 3).

Throughout the gonotrophic cycle, neither nurse cells nor follicle cells were observed to have undergone any histochemical changes. PAS positive and bromphenol blue stained cellular inclusions were not observed in the trophic core and the nutritive cord (Figs. 4 and 5).

At early vitellogenesis, PAS positive flocculent material accumulates in the extraovarian space beneath the follicular epithelium (Fig. 6, 7 and 8). Small droplets of YB I and II appear at the

periphery of the oocyte and gradually proceed into the central region of the oocyte (Fig. 9). Later in



FIGS. 1. a-e. Sections of a mature egg of *L. lineolaris*. Arrow heads indicate protein/carbohydrate yolk stained by PAS (1b), bromphenol blue (1e), PAS treated with dimedone (1a), PAS without periodic acid oxidation (1c) and PAS with diastase digestion (1d). Clear areas between the protein/carbohydrate yolk are lipid yolk. Note the overall decrease in staining intensity of the section after blocking of free aldehyde groups with dimedone. Staining of protein/carbohydrate yolk in 1c is due to the counter stain picro-aniline blue, no PAS-positive reaction appears in these sections without going through periodic acid oxidation. Diastase treatment has no effect on PAS staining. All protein/carbohydrate yolk is stained with similar intensity by bromphenol blue. Plastic sections. (Bar = 10 μ m).

vitellogenesis, the relatively larger YB III begins to appear in the oocyte (Fig. 12). The end of vitellogenesis is indicated by the formation of a PAS positive vitelline membrane and the oocytes are filled up mainly with YB I and III (Fig. 1). This remains unchanged throughout choriogenesis and no histochemical changes are observed inside the mature oocytes even after ovulation.

DISCUSSION

The origin of lipid yolk in eggs of hemipteran

insects has been a controversial subject. Three different origins for lipid yolk have been reported i.e., extraovarian, trophic core and follicle cells [5, 7, 15]. Previously we showed in *Lygus* that minute amounts of lipid from the trophic core enter the developing oocyte during vitellogenesis [9]. Current observations suggest that part of the lipid yolk in vitellogenic oocytes of *Lygus* originates from the hemolymph while the follicle cells do not contribute any lipid to the oocytes.

As in other insects, large amounts of carbohydrate (in association with protein) are incorporated into the vitellogenic oocytes of *L. lineolaris*. The role(s) of the carbohydrate component(s) in the yolk precursor in insects is still unknown. Whether it is for maintenance of protein structure requisite for yolk precursor recognition or has additional nutritive value for the embryos remains to be determined [16].

In *L. lineolaris*, two types of protein/carbohydrate yolk spheres may be differentiated in vitellogenic oocytes by bromphenol blue staining. Since bromphenol blue staining intensity reflects the number of dye binding groups [17], it is possible that conversion of YB II into YB III is a result of molecular modification of the yolk precursor after incorporation into the oocytes similar to

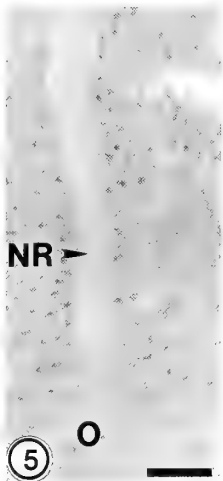
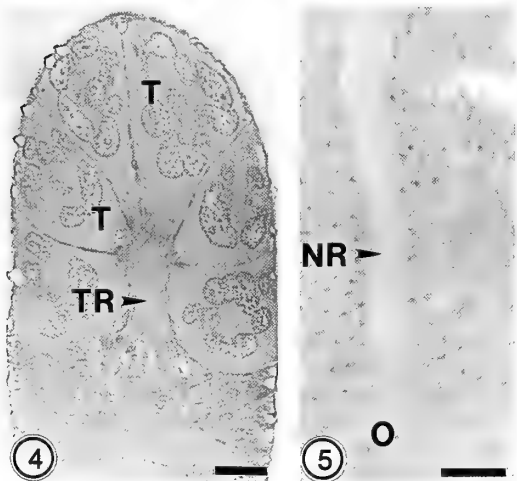
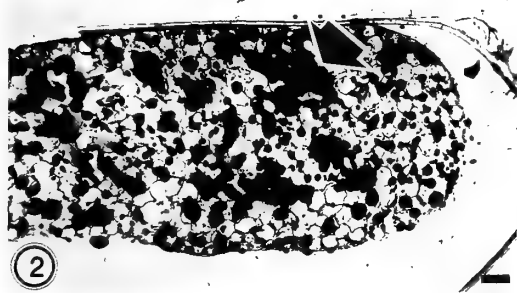
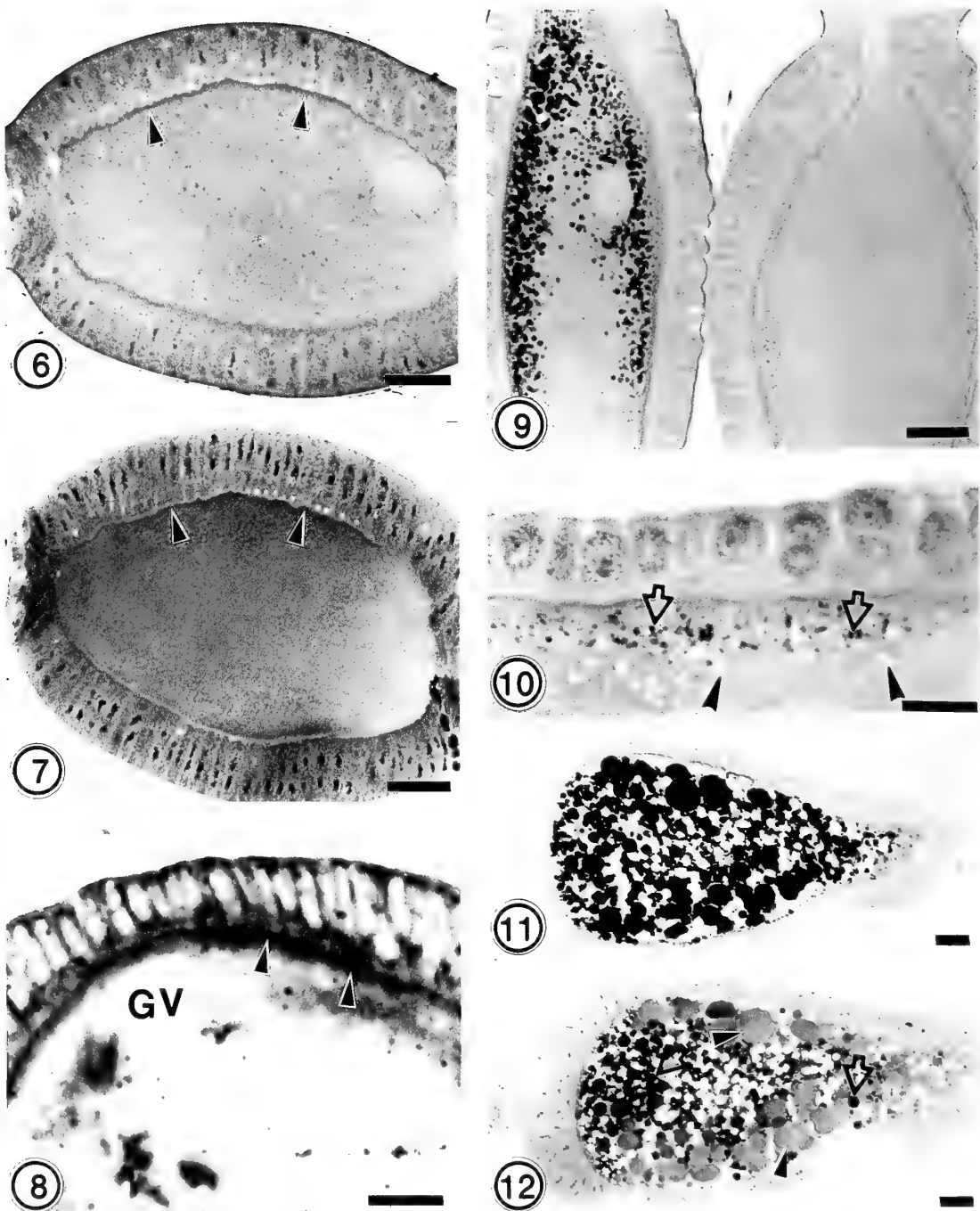


FIG. 2. Distribution of lipid yolk (arrow head) in a mature egg of *L. lineolaris*. Clear area around lipid yolk is due to protein/carbohydrate complexes which are very slightly stained. Cryosection, Sudan black B. (Bar = 10 μ m).

FIG. 3. Vitellogenic oocyte in *L. lineolaris* showing accumulation of lipid deposits on the oocyte surface (arrow) and also in the intercellular spaces (arrow heads) between follicle cells (FC). Cryosection, Sudan black B. (Bar = 10 μ m).

FIG. 4. Ovariole of *L. lineolaris* showing germarium that houses the nurse cells (T). Note the trophic core (TR) at the central region of the germarium which is bounded by nurse cells. The trophic core has a homogeneous overall staining and discrete cellular inclusions are not found. Plastic sections, PAS. (Bar = 10 μ m).

FIG. 5. The nutritive cord (NR) connects the trophic core (not shown) and the developing oocyte (O) throughout the gonotrophic cycle until chorion formation. Note the uniform staining of the nutritive cord and the oocyte and also the absence of inclusions in the former. Plastic section, PAS. (Bar = 5 μ m).



FIGS. 6-8. Terminal oocyte at early vitellogenesis showing accumulation of yolk precursor (arrow heads) in the space between follicular epithelium and oocyte. This yolk precursor is PAS-positive (Fig. 6) (Bar = 10 μ m) and stained dark blue by bromphenol blue (Fig. 7) (Bar = 10 μ m). In cryosection, the yolk precursor is stained bluish black by Sudan black B (Fig. 8) (Bar = 5 μ m). Note the large round germinal vesicle (GV) in the oocyte of Fig. 8.

FIG. 9. Terminal oocyte at early vitellogenesis (right) showing appearance of yolk droplets at the cortex of the oocyte. At later development, these yolk droplets coalesce and are seen to migrate into central core of the oocyte

that reported in cockroaches [18]. However, this is currently unknown in Hemiptera and further biochemical studies are necessary to validate the above hypothesis.

ACKNOWLEDGMENTS

We thank Dr. Gordon Snodgrass, USDA-ARS, Stoneville, Miss. for help in obtaining the insects used in this study and Drs. Erwin Huebner, Univ. of Manitoba, Gerald Baker, Howard Chambers and James Heitz for reviewing an earlier draft of this paper. This study was supported in part by a grant from Albany International (now Scentry, Inc., Buckeye, AZ). Miss. Agr. For. Exp. Stn. Paper No. 6333.

REFERENCES

- 1 Telfer, W. H. (1965) *Annu. Rev. Entomol.*, **10**: 161–184.
 - 2 Engelmann, F. (1968) *Annu. Rev. Entomol.*, **13**: 1–26.
 - 3 Kunkel, J. G. and Nordin, J. H. (1984) In "Comprehensive Insect Physiology, Biochemistry and Pharmacology". Vol.1. Ed. by G. A. Kerkert and L. I. Gilbert, Pergamon Press, New York, pp. 4 Schrader, F. and Leuchtenberger, C. (1952) *Exp. Cell Res.*, **3**: 136–146.
 - 5 Bonhag, P. F. (1955) *J. Morphol.*, **96**: 381–439.
 - 6 Bonhag, P. F. (1955) *J. Morphol.*, **97**: 283–311.
 - 7 Schreiner, B. (1977) *J. Morphol.*, **151**: 81–101.
 - 8 Eschenberg, K. M. and Dunlap, H. L. (1966) *J. Morphol.*, **118**: 297–316.
 - 9 Ma, W. K. and Ramaswamy, S. B. (1987) *Int. J. Insect Morphol. Embryol.*, **16**: 309–322.
 - 10 Pringle, J. W. S. (1938) *J. Exp. Biol.*, **15**: 101–113.
 - 11 Drury, R. A. B. and Wallington, E. A. (1976) *Carleton's Histological Technique*. (4ed). Oxford Univ. Press, London. pp. 204–206.
 - 12 Cannon, M. S., Kapes, E. D. and Cannon, A. M. (1982) *Lab. Med.*, **13**: 102–105.
 - 13 Klungness, L. M. and Peng, Y. S. (1984) *J. Insect Physiol.*, **30**: 511–521.
 - 14 Culling, C. F. A. (1975) *Handbook of Histopathological and Histochemical Techniques*. (3ed). Butterworths, London. pp. 360–361.
 - 15 Huebner, E. and Anderson, E. (1972) *J. Morphol.*, **138**: 1–40.
 - 16 Hagedorn, H. H. and Kunkel, J. G. (1979) *Annu. Rev. Entomol.*, **24**: 475–505.
 - 17 Mazia, D., Brewer, P. and Alfert, M. (1953) *Biol. Bull.*, **104**: 57–67.
 - 18 Brookes, V. J. and Dejmál, R. K. (1968) *Science*, **160**: 999–1001.
- (left). The PAS-positive flocculent material between follicular epithelium and oocyte is found to be more diffuse in oocyte at the right than the one at the left. Plastic section, PAS. (Bar=10 μ m).
- Fig. 10. Higher magnification of an early vitellogenic oocyte indicates that both protein/carbohydrate yolk (open arrows) and lipid yolk (arrow heads) appear on the periphery of the oocyte. Plastic section, PAS. (Bar=5 μ m).
- Figs. 11–12. Vitellogenic oocyte at later development is found to incorporate large amount of protein/carbohydrate yolk which is PAS-positive (Fig. 11). However, when stained with bromphenol blue (Fig. 12), this yolk can be distinguished into two types: YB II stained darker (open arrows) and ca. 2–8 μ m in size and YB III stained lighter (arrow heads) and ca. 5–25 μ m in size. Lipid yolk (YB I) is represented in these figures as clear areas around the protein/carbohydrate yolk. Plastic sections. (Bar=10 μ m).

[COMMUNICATION]

Effects of Puromycin and α -Amanitin on the Activity of Alkaline Phosphatase in Early Preimplantation Mouse Embryos

TOMOICHI ISHIKAWA¹

Department of Anatomy, Kochi Medical School,
Nankoku, Kochi 781-51, Japan

ABSTRACT—The activity of nonspecific alkaline phosphatase (ALPase) was cytochemically and biochemically investigated in early preimplantation mouse embryos. The ALPase activity was cytochemically detected in embryos from 2- to 8-cell stage. The activity was exclusively localized on the adjacent cell membranes of the two blastomeres. This activity was biochemically first detected at the very low level in the 2-cell embryos. Biochemical assay revealed that in 4- to 8-cell embryos the ALPase activity increased dramatically. In these embryos, intense activity of ALPase was also detected cytochemically. When 2-cell embryos were treated with puromycin (15 μ g/ml) in culture, the embryos could not develop to advanced stages and the expression of ALPase activity was inhibited. However, α -amanitin (2 and 10 μ g/ml) suppressed the further cleavage, although it did not interfere with the expression of ALPase activity. The results suggest that mRNA molecules for ALPase of maternal origin exist in 2-cell embryos.

INTRODUCTION

Non-specific alkaline phosphatase (ALPase, E.C.3.1.3.1) is one of the well-known enzymes in early mammalian embryos. Cytochemical studies have shown the presence of its activity in 8-cell and more advanced mouse embryos [1–5]. Most of these investigators could not detect ALPase activity in fertilized and 2-cell embryos, except Mulnard and Huygens [4] who succeeded in detecting its

activity in 2-cell embryos. They showed the precipitation of its reaction products in the adjacent cell membranes of the two blastomeres [4].

In the present study the expression of ALPase activity in the early mouse embryos was investigated in detail by employing both cytochemical and biochemical methods. Few information is available on the mechanism of ALPase expression except that concerning ascidian embryos, where ALPase has been employed as a histochemical marker for gut endodermal differentiation. This enzyme is considered to be maternal origin [6]. In the present investigation, inhibitors of transcription and translation were used to clarify whether the expression of ALPase activity in 2-cell embryos requires the *de novo* transcription and translation or not. The results suggest that the expression of ALPase activity requires *de novo* translation, but not transcription.

MATERIALS AND METHODS

Embryos

Female mice of strain 129/Sv were mated with male mice of the same strain after the superovulation by intraperitoneal injection of 5 i.u. pregnant mare serum gonadotropin (PMSG) followed by 5 i.u. human chorionic gonadotropin (hCG) 48 hr later. The 0 hr was defined as the time when hCG was injected. Two-cell stage and 4- to 8-cell stage embryos were flushed out from the oviduct 40–42 hr and 65–67 hr after hCG injection, respectively.

Accepted April 4, 1989

Received January 30, 1989

¹ Deceased on February 1, 1988. Reprint requests and correspondence should be addressed to Dr. T. Hirobe of National Institute of Radiological Sciences, Division of Biology, Anagawa, Chiba 260, Japan.

Embryos were cultured in the standard egg culture medium [7]. The embryos of the experimental groups were cultured with medium containing either 15 $\mu\text{g/ml}$ of puromycin or 2–10 $\mu\text{g/ml}$ of α -amanitin for 3–24 hr.

Cytochemistry of alkaline phosphatase

Embryos were prefixed with ice-cold 1% glutaraldehyde in 0.1 M cacodylate buffer (pH 7.3) for 20 min. They were then washed in the same buffer for more than 30 min. The lead citrate method [8] was used for the cytochemical demonstration of ALPase activity. The incubation was carried out at 37°C for 30–60 min in pH range of 9.2–9.3. No reaction was observed in control specimens which were incubated without substrate. After the incubation, specimens were washed with the buffer and embedded in agar blocks [9] and were fixed with ice-cold 1% OsO_4 solution for 60 min. They were dehydrated through a series of graded ethanols and embedded in epoxy resin.

For light microscopy, some of the specimens were washed with distilled water after the ALPase reaction and then dipped into diluted ammonium sulfide solution to detect the reaction products.

Biochemical assay of alkaline phosphatase

Fresh unfertilized eggs (>100), 2-cell embryos (>100) and 4- to 8-cell embryos (50–100) were collected for each assay. The blastomeres were broken by freezing and thawing. The ALPase

activity was assayed by using Chung's method [10]. The reaction was carried out at 37°C for 4 hr. The amount of p-nitrophenol released from p-nitrophenol phosphate by the enzyme reaction was determined by spectrophotometry at the wavelength of 410 nm. The specific activity of the enzyme was expressed in terms of nmol p-nitrophenol released in 1 hr per embryo. No enzyme activity was observed in the controls incubated in the same reaction mixture without the substrate.

RESULTS

Cytochemistry of alkaline phosphatase

ALPase activity was detected exclusively in the adjacent cell membranes of the two blastomeres in 2-cell embryos (Fig. 1a). Free cell surfaces of the blastomeres completely lacked ALPase activity. No ALPase activity was detected in the cell membranes of unfertilized eggs.

Biochemical assay of alkaline phosphatase activity

Embryos of 2-cell stage showed a weak ALPase activity (0.005 ± 0.007 nmol/hr/embryo, mean \pm standard deviation, Table 1). In contrast, unfertilized eggs completely lacked its activity. In 4- to 8-cell embryos, ALPase activity drastically increased. The enzyme activities (0.15 ± 0.070 nmol/hr/embryo, Table 1) in 4- to 8-cell embryos were

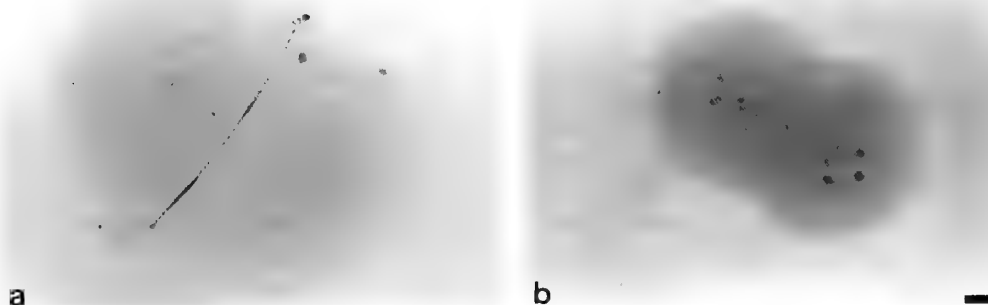


FIG. 1. Localization of ALPase activity in 2-cell mouse embryos and effects of puromycin on its activity. Mouse embryos were cultured with standard medium for 3 hr (a) and with medium containing 15 $\mu\text{g/ml}$ of puromycin (b). Alkaline phosphatase activity is shown on the adjacent cell membranes of the two blastomeres in 2-cell embryos of control (a). However, the enzyme activity was not observed when 15 $\mu\text{g/ml}$ of puromycin was added to the culture medium (b). Scale, 10 μm .

about 30 times higher than those in 2-cell embryos.

Effects of puromycin and α -amanitin on the development of 2-cell embryos in culture

When 2-cell embryos were cultured with standard medium for 24 hr, more than 50% embryos developed to advanced stages (Table 2). The effects of puromycin, an inhibitor of translation, on the development of 2-cell embryos were investigated. Puromycin added at a concentration of 15 μ g/ml completely blocked the development of

2-cell embryos in culture. Also, the effects of α -amanitin, an inhibitor of transcription, on the development of 2-cell embryos were investigated. When α -amanitin was added to the medium at the dose of 10 μ g/ml for 24 hr, most of embryos could not develop further (Table 2). However, more than 35% of the embryos could develop to advanced stages when 2-cell embryos were cultured with medium containing 2 μ g/ml of α -amanitin (Table 2).

TABLE 1. Biochemical assays of alkaline phosphatase activity in preimplantation mouse embryos

Developmental stage	No. of experiments	No. of eggs or embryos	Alkaline phosphatase activity*
Unfertilized eggs	2	130-150	0 \pm 0
2-cell embryos (41-43 hr after hCG)	5	70-130	0.005 \pm 0.007
4- to 8-cell embryos (65 hr after hCG)	3	15- 35	0.150 \pm 0.070

* nmol p-nitrophenol released/hr/embryo (mean \pm standard deviation)

TABLE 2. Effects of puromycin and α -amanitin on the development of 2-cell embryos cultured for 24 hr

Group	Dose	No. of embryos	2-cell	3-cell	4-cell	5- to 8-cell
Control	—	125	52 (41.6%)	12 (9.6%)	50 (40%)	11 (8.8%)
Puromycin	15 μ g/ml	64	64 (100%)	0 (0%)	0 (0%)	0 (0%)
α -amanitin	2 μ g/ml	53	34 (64.1%)	3 (5.7%)	12 (22.6%)	4 (7.6%)
α -amanitin	10 μ g/ml	60	56 (93.3%)	3 (5%)	1 (1.7%)	0 (0%)

TABLE 3. Effects of puromycin and α -amanitin on alkaline phosphatase activity in 2-cell embryos cultured for 24 hr

Group	Dose	No. of embryos	Alkaline phosphatase activity*		
			+	\pm	—
Control	—	15	12	2	1
Puromycin	15 μ g/ml	9	0	4	5
α -amanitin	2 μ g/ml	6	5	1	0
α -amanitin	10 μ g/ml	22	10	7	5

* +: positive reaction

\pm : weakly positive reaction

—: negative reaction

Effects of puromycin and α -amanitin on alkaline phosphatase activity

Most of the 2-cell embryos cultured with normal medium for 24 hr expressed ALPase activity (Table 3). When 2-cell embryos were treated in culture with 15 μ g/ml of puromycin for 24 hr, most of the embryos showed a very weak or no ALPase activity (Fig. 1b and Table 3). In contrast to puromycin, α -amanitin (2 and 10 μ g/ml) did not inhibit the expression of ALPase activity (Table 3). Although 10 μ g/ml of α -amanitin blocked the development of 2-cell embryos in culture, it did not suppress ALPase activity.

DISCUSSION

In the present study, ALPase activity was demonstrated in 2-cell mouse embryos both cytochemically and biochemically. Although ALPase activity was detected cytochemically in 2-cell mouse embryos by Mulnard and Huygens [4], their observations have not been supported by the biochemical analysis [5]. The present report, for the first time, describes the presence of ALPase activity in 2-cell embryos as demonstrated by biochemical means. The reason for the success in the detection of ALPase activity in 2-cell embryos probably due to the fact that the author used more than 100 fresh embryos for the assay.

When 2-cell embryos were treated with puromycin (15 μ g/ml) for 24 hr, they could neither undergo further cleavage nor express ALPase activity. It is probable that the suppression of ALPase activity is due to the inhibition of *de novo* synthesis of ALPase molecules, since puromycin is known to inhibit translation. It has been known that puromycin inhibits in the concentration ranges of 4.7–94 μ g/ml, the protein synthesis in rabbit reticulocyte [11]. When 2-cell embryos were treated with α -amanitin (2 or 10 μ g/ml) for 24 hr, the development was inhibited, but the expression of ALPase activity was not suppressed. From the results it was proposed that the ALPase activity in 2-cell embryos was expressed without *de novo* synthesis of mRNA, since α -amanitin is an inhibitor of RNA polymerase II. α -amanitin (0.4–40 μ g/ml) is known to completely inhibit RNA

polymerase II activity in calf thymocytes [12]. These results suggest that mRNA molecules for ALPase of maternal origin exists in 2-cell embryos. In contrast, the increase of ALPase activity in 4- to 8-cell embryos may be due to the embryonic transcription and translation, since ALPase activity increased drastically from 2-cell to 8-cell stage.

The 1- and 2-cell stages of development of a mouse embryo are thought to be dependent on the use of inherited maternal mRNA and on the operation of post-transcriptional regulators [13]. It is suggested that changes in the protein synthetic profile occur between the early 2-cell stage and the late 2-cell stage, and much of the maternally inherited mRNA is inactivated rapidly [14]. The stage of the 2-cell embryos used in the present study corresponds to the late 2-cell stage, since the embryos were collected from the oviduct 40–42 hr after hCG injection. Therefore, it is conceivable that the changes in the ALPase synthesis occur between the late 2-cell stage and the 4-cell stage. Although the difference between their results and the present findings cannot be fully explained, they might be attributed to difference in kind of proteins used. Molecular analyses of mRNA for ALPase in the mouse embryos at the late 2-cell stage remain to be investigated in a future study.

ACKNOWLEDGMENTS

The author expresses his thanks to Dr. T. Hirobe of National Institute of Radiological Sciences for his help in preparing the manuscript.

REFERENCES

- 1 Izquierdo, L. and Marticorena, P. (1975) Alkaline phosphatase in preimplantation mouse embryos. *Exp. Cell Res.*, **92**: 399–402.
- 2 Johnson, L. V., Calarco, P. G. and Siebert, M. L. (1977) Alkaline phosphatase activity in the preimplantation mouse embryo. *J. Embryol. Exp. Morph.*, **40**: 83–89.
- 3 Vorbrodt, A., Konwinski, M., Solter, D. and Koproski, H. (1977) Ultrastructural cytochemistry of membrane-bound phosphate in preimplantation mouse embryos. *Dev. Biol.*, **55**: 117–134.
- 4 Mulnard, J. and Huygens, R. (1978) Ultracytochemical localization of nonspecific alkaline phosphatase during cleavage and blastocyst formation in the

- mouse. *J. Embryol. Exp. Morphol.*, **44**: 121–131.
- 5 Izquierdo, L., Lopez, T. and Marticorena, P. (1980) Cell membrane regions in preimplantation mouse embryos. *J. Embryol. Exp. Morph.*, **59**: 89–102.
- 6 Whittaker, J. R. (1977) Segregation during cleavage of a factor determining endodermal alkaline phosphatase development in ascidian embryos. *J. Exp. Zool.*, **202**: 139–154.
- 7 Biggers, J. D., Whitten, W. K. and Whittingham, D. G. (1971) The culture of mouse embryos *in vitro*. In "Methods in Mammalian Embryology". Ed. by J. C. Daniel, Jr., Freeman, Co., San Francisco, pp. 86–116.
- 8 Mayahara, H., Hirano, H., Saito, T. and Ogawa, K. (1967) The new lead citrate method for the ultracytochemical demonstration of activity of non-specific alkaline phosphatase (orthophosphoric monoester phosphohydrazase). *Histochemie*, **11**: 88–96.
- 9 Ishikawa, T. and Seguchi, H. (1984) Mg^{++} -dependent adenosine triphosphatase activity in preimplantation mouse embryos. *Acta Histochem. Cytochem.*, **17**: 269–278.
- 10 Chung, A. E., Esters, L. E., Shinozuka, H., Braginsky, J., Lorz, C. and Chung, C. A. (1977) Morphological and biochemical observations on cells derived from the *in vitro* differentiation of the embryonal carcinoma cell line PCC4-F. *Cancer Res.*, **37**: 2072–2081.
- 11 Allen, D. W. and Zamecnik, P. C. (1962) The effect of puromycin on rabbit reticulocyte ribosomes. *Biochim. Biophys. Acta*, **55**: 865–874.
- 12 Keding, C., Gniazdowski, M., Mandel, J. L. Jr., Gissinger, F. and Chambon, P. (1970) α -Amanitin: a specific inhibitor of one of two DNA-dependent RNA polymerase activities from calf thymus. *Biochem. Biophys. Res. Commun.*, **38**: 165–171.
- 13 Davidson, E. H. (1986) *Gene Activity in Early Development*. 3rd ed. Academic Press, New York.
- 14 Johnson, M. H. (1981) The molecular and cellular basis of preimplantation mouse development. *Biol. Rev.*, **56**: 463–498.

INSTRUCTIONS TO AUTHORS

ZOOLOGICAL SCIENCE publishes contributions, written in English, in the form of (1) Reviews, (2) Articles, and (3) Communications of material requiring prompt publication. A *Review* is usually invited by the Editors. Those who submit reviews should consult with the Editor-in-Chief or the Managing Editor in advance. *Articles* of less than 6 printed pages and *Communications* less than 3 printed pages will be published free of charge. Charges will be made for extra pages (10,000 yen/page). A *Communication* cannot exceed 4 printed pages. No charge will be imposed for invited reviews up to 15 printed pages. No free reprints of Articles and Communications are available. To the author of an invited review 50 reprints are provided gratis. Submission of papers from nonmembers of the Society is welcome. However, page charges (10,000 yen/page) will be made to nonmembers.

A. SUBMISSION OF MANUSCRIPT

The manuscript should be submitted in triplicate, one original and two copies, each including all illustrations. Rough copies of line drawings and graphs may accompany the manuscript copies, but the two copies of continuous-tone prints (photomicrographs, etc.) should be as informative as the original. The manuscript should be sent to:

Dr. CHITARU OGURO, Managing Editor,
ZOOLOGICAL SCIENCE, Department of Biology,
Faculty of Science, Toyama University,
Toyama 930, Japan.

B. CONDITIONS

All manuscripts are subjected to editorial review. A manuscript which has been published or of which a substantial portion has been published elsewhere will not be accepted. It is the author's responsibility to obtain permission to reproduce illustrations, tables, etc. from other publications. Accepted papers become the permanent property of ZOOLOGICAL SCIENCE and may not be reproduced by any means, in whole or in part, without the written consent of both the Zoological

Society of Japan and the author(s) of the article in question.

C. ORGANIZATION OF MANUSCRIPT

The desirable style of the organization of an original paper is as follows: (1) Title, Author(s) and Affiliation (2) Abstract (3) Introduction (4) Materials and Methods (5) Results (6) Discussion (7) Acknowledgments (8) References (9) Tables (10) Illustrations and Legends (11) Footnotes. The author is not obliged to adhere rigidly to this organization. He or she may modify the style when such modification makes the presentation clearer and more effective. In a Communication, combination of some of these sections is recommended. There is no restriction on the style of review articles.

D. FORM OF MANUSCRIPT

Manuscripts should be typewritten and double spaced throughout on one side of white type-writing paper with 2.5 cm margins on all sides. Abstract not exceeding 250 words, tables, figure legends and footnotes should be typed on separate sheets. All manuscript sheets must be numbered successively. The use of footnotes to the text is not recommended.

1. Title page

The first page of manuscript should contain title, authors' names and addresses of university or institution, abbreviated form of title (40 characters or less, including spaces), and name and address for correspondence. Authors with different affiliations should be identified by the use of the same superscript on name and affiliation. If one or more of the authors has changed his or her address since the work was carried out, the present address(es) to be published should be indicated in a footnote. In addition, a sub-field of submitted papers to be used as heading of an issue may be indicated in the first page. Authors are encouraged to choose one of the following: physiology, cell biology, molecular biology, genetics, immunology, biochemistry, developmental biology, reproductive biology,

endocrinology, behavior biology, ecology, phylogeny, taxonomy, or others (specify). However, the Editors are responsible for the choice and arrangement of headings.

2. Introduction

This section should clearly describe the objectives of the study, and provide enough background information to make it clear why the study was undertaken. Lengthy reviews of past literature are discouraged.

3. Materials and Methods

This section should provide the reader with all the information that will make it possible to repeat the work. For modification of published methodology, only the modification needs to be described with reference to the source of the method.

4. Results

Results should be presented referring to tables and figures, without discussion.

5. Discussion

The Discussion should include a concise statement of the principal findings, a discussion of the validity of the observations, a discussion of the findings in the light of other published works dealing with the same subject, and a discussion of the significance of the work. Redundant repetition of material in Introduction and Results, and extensive discussion of the literature are discouraged.

6. Statistical analysis

Statistical analysis of the data using appropriate methods is mandatory and the method(s) used must be cited.

7. References

References should be cited in the text by an Arabic numeral in square parentheses and listed at the end of the paper in numerical order. For example:

- 1 Takewaki, K. (1931) Oestrus cycle of female rat in parabiotic union with male. *J. Fac. Sci. Imp. Univ. Tokyo, Sec. IV*, **2**: 353–356.
- 2 Shima, A., Ikenaga, M., Nikaido, O., Takabe, H. and Egami, N. (1981) Photoreactivation of ultraviolet light-induced damage in cultured fish cells as revealed by increased colony forming ability and decreased content of pyrimidine dimers. *Photochem. Photobiol.*, **33**: 313–316.
- 3 Hubel, O. and Wiesel, T. N. (1986) The

functional architecture of the striated cortex. In "Physiological and Biochemical Aspects of Nervous Integration". Ed. by F. D. Carlson, Prentice-Hall, New Jersey, pp. 153–161.

- 4 Campbell, R. C. (1974) *Statistics for Biologists*. Cambridge Univ. Press, London, 2nd ed., pp. 59–61.

Titles of cited papers may be omitted in Reviews and Communications. The source of reference should be given following the commonly accepted abbreviations for journal titles (e.g., refer to 'International List of Periodical Title Abbreviations'). The use of "in preparation", "submitted for publication" or "personal communication" is not allowed in the reference list. "Unpublished data" and "Personal communication" should appear parenthetically following the name(s) in the text. Text citations to references with three or more authors should be styled as, e.g., Everett *et al.* [7].

E. ABBREVIATIONS

Abbreviations of measurement units, quantity units, chemical names and other technical terms in the body of the paper should be used after they are defined clearly in the place they first appear in the text. However, abbreviations that would be recognized by scientists outside the author's field may be used without definition, such as SD, SE, DNA, RNA, ATP, ADP, AMP, EDTA, UV, and CoA. The metric system should be used for all measurements, and metric abbreviations (Table)

Table. Abbreviations for units of measure which may be used without definition

Length:	km, m, cm, mm, μm , nm, pm, etc.
Area:	km^2 , m^2 , cm^2 , mm^2 , μm^2 , nm^2 , pm^2 , etc.
Volume:	km^3 , m^3 , cm^3 , mm^3 , μm^3 , nm^3 , pm^3 , kl, liter (always spellout), ml, μl , nl, etc.
Weight:	kg, g, mg, μg , ng, pg, etc.
Concentration:	M, mM, μM , nM, %, g/l, mg/l, $\mu\text{g/l}$, etc.
Time:	hr, min, sec, msec, μsec , etc.
Other units:	A, W, C, atm, cal, kcal, R, Ci, cpm, dB, v, Hz, lx, $\times\text{g}$, rpm, S, J, IU, etc.

should, in general, be expressed in lower case without periods.

F. PREPARATIONS OF TABLES

Tables should only include essential data needed to show important points in the text. Each table should be typed on a separate sheet of paper and must have an explanatory title and sufficient explanatory material. All tables should be referred to in the text, and their approximate position indicated in the margin of manuscript.

G. PREPARATION OF ILLUSTRATIONS

All figures should be appropriately lettered and labelled with letters and numbers that will be at least 1.5 mm high in the final reproduction. Note the conventions for abbreviations used in the journal so that usage in illustrations and text is consistent. All figures should be referred to in the text and numbered consecutively (Fig. 1, Fig. 2, etc.). The figures must be identified on the reverse side with the author's name, the figure number and the orientation of the figure (top and bottom). The preferred location of the figures should be indicated in the margin of the manuscript. Illustrations that are substandard will be returned, delaying publication. Illustrations in color may be published at the author's expense.

1. Line drawings and graphs

Original artwork of high quality, glossy prints mounted on appropriate mounting card (**less than 25×38 cm**) should be submitted for reproduction. Author(s) may indicate size preference by making on the back of figures, such as "Do not reduce", "Two-column width" (**no wider than 14 cm**), or "One-column width" (**no wider than 7 cm**). Lines must be dark and sharply drawn. Solid black, white, or bold designs should be used for histograms. Xerox or any other copying mean may be used for the two review copies.

2. Continuous-tone prints

Three sets of continuous-tone prints (photomicrographs, etc.) must be submitted. One set for reproduction should be mounted on appropriate mounting card, and the other two for reviewers may be unmounted prints. Xerox or similar copies of photomicrographs are not acceptable for review purposes. The continuous-tone prints should be submitted preferably at the exact magnification which is to be used in the published papers and trimmed to conform to the page size (**in no case should it exceed 14×20 cm**). Press-on numbers should be applied to the lower right corner of individual prints. Letters (a, b, c, etc.) should be used for multiple parts of a single figure. If important structures will be covered by use of the lower right corner, identification may be applied in the lower left corner.

Reproduction of color photographs will have to be approved by the Editors. The extra costs of color reproduction will be charged to the authors.

3. Figure legends

Each figure should be accompanied by a title and an explanatory legend. The legends for several figures may be typed on the same sheet of paper. Sufficient detail should be given in the legend to make it intelligible without reference to the text.

H. PROOF AND REPRINTS

A galley proof and reprint order will be sent to the submitting author. The first proofreading is the author's responsibility, and the proof should be returned within 72 hours from the date of receipt (by air mail from outside Japan). The minimum quantity for a reprint order is fifty. Manuscript, tables and illustrations will be discarded after the editorial use unless their return is requested when the manuscript is accepted for publication.

Development Growth & Differentiation

Published Bimonthly by the Japanese Society of
Developmental Biologists
Distributed by Business Center for Academic
Societies Japan, Academic Press, Inc.

Papers in Vol. 32, No. 1. (February 1990)

1. **REVIEW:** H. Ide: Growth and differentiation of limb bud cells *in vitro*: Implications for limb pattern formation
2. K. Akasaka, T. Ueda, T. Higashinakagawa, K. Yamada and H. Shimada: Spatial patterns of arylsulfatase mRNA expression in sea urchin embryo
3. I. Kaneda, E. Kamitsubo and Y. Hiramoto: The mechanical structure of the cytoplasm of the echinoderm egg determined by "Gold Particle Method" using a centrifuge microscope
4. P. D. Nieuwkoop and B. Albers: The role of competence in the cranio-caudal segregation of the central nervous system
5. H. Katow: A new technique for introducing antifibronectin antibodies and fibronectin-related synthetic peptides into the blastulae of the sea urchin, *Clypeaster japonicus*
6. K. H. Kato, S. Washitani-Nemoto, A. Hino and S. Nemoto: Ultrastructural studies on the behavior of centrioles during meiosis of starfish oocytes
7. M. Fukumoto: The acrosome reaction in *Ciona intestinalis* (Ascidia, Tunicata)
8. R. Masho: Close correlation between the first cleavage and the body axis in early *Xenopus* embryos
9. H. Yamasaki, C. Katagiri and N. Yoshizaki: Selective degradation of specific components of fertilization coat and differentiation of hatching gland cells during the two phase hatching of *Bufo japonicus* embryos
10. Y. K. Maruyama and M. Shinoda: Archenteron-forming capacity in blastomeres isolated from eight-cell stage embryos of the starfish, *Asterina pectinifera*
11. H. Ohtsuki: Statocyte and ocellar pigment cell in embryos and larvae of the Ascidian, *Styela plicata* (Lesueur)
12. K. Asamoto, Y. Nojyo and H. Aoyama: Do peanut agglutinin receptors on somites control the behavior of neural cells?

Development, Growth and Differentiation (ISSN 0012-1592) is published bimonthly by The Japanese Society of Developmental Biologists, Department of Developmental Biology, Mitsubishi Kasei Institute of Life Science, Minami-ootani 11, Machida, Tokyo 194, Japan. 1989: Volume 31. Annual subscription for Vol. 32, 1990: U. S. \$ 148.00, U. S. and Canada: U. S. \$ 163.00, all other countries except Japan. All prices include postage, handling and air speed delivery except Japan. Second class postage paid at Jamaica, N.Y. 11431, U. S. A.

Outside Japan: Send subscription orders and notices of change of address to Academic Press, Inc., Journal Subscription Fulfillment Department, 1 East First Street, Duluth, MN 55802, U. S. A. Send notices of change of address at least 6-8 weeks in advance. Please include both old and new addresses. U. S. A. POSTMASTER: Send changes of address to *Development, Growth and Differentiation*, Academic Press, Inc., Journal Subscription Fulfillment Department, 1 East First Street, Duluth, MN 55802, U. S. A.

In Japan: Send nonmember subscription orders and notices of change of address to Business Center for Academic Societies Japan, 16-3, Hongo 6-chome, Bunkyo-ku, Tokyo 113, Japan. Send inquiries about membership to Business Center for Academic Societies Japan, 4-16, Yayoi 2-chome, Bunkyo-ku, Tokyo 113, Japan.

Air freight and mailing in the U. S. A. by Publications Expediting, Inc., 200 Meacham Avenue, Elmont, NY 11003, U. S. A.

NARISHIGE

THE ULTIMATE NAME IN MICROMANIPULATION

OUR NEW MODELS **WR-88** and **MO-102M**
MAKE PRECISION MICROMANIPULATION SO EASY!



SOME FEATURES of THE WR-88 WATER ROBOT MICROMANIPULATOR (3-DIMENSIONAL)

- * Drift-free, the new WR-88 has a DRIFT movement of less than 2 microns.
- * The new WR-88 has a SMOOTH MICRODRIVE MECHANISM.
- * An Aqua Purificate remote control ensures totally vibration-free operation.



NARISHIGE SCIENTIFIC INSTRUMENT LAB.

9-28 KASUYA 4-CHOME SETAGAYA-KU, TOKYO 157, JAPAN
PHONE (INT-L) 81-308-8233, FAX (INT-L) 81-3-308-2005
CABLE : NARISHIGE LABO, TELEX, NARISHIGE J27781

(Contents continued from back cover)

Taxonomy and Systematics

Abe, H.: Two species of the genus *Actacarus*
(Acari, Halacaridae) from Japan 111

Yunxia, T. and Y. Shaoyi: Comparative
study on LDH isozymes in different subfam-
ily of teleost fish - grass carp (*Ctenophryngo-*
don idellus) and blunt snout-bream (*Mega-*
lobrama amblycephala) 127

Watabe, H., X. C. Liang and W. X. Zhang:

The *Drosophila robusta* species-group (Dip-
tera: Drosophilidae) from Yunnan Province,
southern China, with the revision of its geo-
graphic distribution 133

Ando, A., S. Shiraishi and T. A. Uchida:
Reexamination on the taxonomic position of
two intraspecific taxa in Japanese *Eothe-*
nomys: evidence from crossbreeding experi-
ments (Mammalia: Rodentia) 141

Instructions to authors 159

ZOOLOGICAL SCIENCE

VOLUME 7 NUMBER 1

FEBRUARY 1990

CONTENTS

REVIEWS

- Gotoh, T. and T. Suzuki: Molecular assembly and evolution of multi-subunit extracellular annelidhemoglobins 1

- Lawrence, J. M.: The effect of stress and disturbance on echinoderms 17

ORIGINAL PAPERS

Cell Biology and Morphology

- Low, W. P., Y. K. Ip and D. J. W. Lane: A comparative study of the gill morphology in the mudskippers - *Periophthalmus chrysospilos*, *Boleophthalmus boddarti* and *Periophthalmodon schlosseri* 29

- Kondo, H., Y. Yonezawa and T. A. Nomaguchi: Difference in migratory ability between human lung and skin fibroblasts 39

Immunology

- Kono, H., A. Mizoguchi, H. Nagasawa, H. Ishizaki, H. Fugo and A. Suzuki: A monoclonal antibody against a synthetic carboxyl-terminal fragment of the eclosion hormone of the silkworm, *Bombyx mori*: characterization and application to immunohistochemistry and affinity chromatography .. 47

Biochemistry

- Michibata, H., T. Uyama and J. Hirata: Vanadium-containing blood cells (vanadocytes) show no fluorescence due to the tunichrome in the ascidian, *Ascidia sydneiensis samea* 55

Developmental Biology

- Ma, Y. K. and S. B. Ramaswamy: Histochemistry of yolk formation in the ovaries of the tarnished plant bug, *Lygus lineolaris* (Palisot

- de Beauvois) (Hemiptera: Miridae) (COMMUNICATION) 147

- Kamishima, Y.: Organization and development of reflecting platelets in iridophores of the giant clam, *Tridacna crocea* Lamarck 63

- Ishikawa, T.: Effects of puromycin and α -amanitin on the activity of alkaline phosphatase in early preimplantation mouse embryos (COMMUNICATION) 153

- Uchiyama, M., T. Murakami and H. Yoshizawa: Notes on the development of the crab-eating frog, *Rana cancrivora* 73

Reproductive Biology

- Asada, N. and T. Fukumitsu: Reaction mass formation in *Drosophila*, with notes on a phenoloxidase activation 79

- Jarosz, S. J. and W. R. Dukelow: Embryo transfer and pregnancy rate in the golden hamster (*Mesocricetus auratus*) 85

Endocrinology

- Tagawa, M., S. Miwa, Y. Inui, E. G. de Jesus and T. Hirano: Changes in thyroid hormone concentrations during early development and metamorphosis of the flounder, *Paralichthys olivaceus* 93

- Tasaki, Y. and S. Ishii: Effects of thyroidectomy, hypophysectomy, temperature and humidity on the occurrence of nocturnal locomotor activity in the toad, *Bufo japonicus*, during the breeding season 97

- Uchiyama, M. and T. Murakami: Effects of hypophysectomy and replacement therapy with several hormones on plasma sodium concentrations in bullfrog tadpoles 105

(Contents continued on inside back cover)

INDEXED IN:

Current Contents/LS and AB & ES,
Science Citation Index,
ISI Online Database,
CABS Database, INFOBIB

Issued on February 15

Printed by Daigaku Letterpress Co., Ltd.,
Hiroshima, Japan

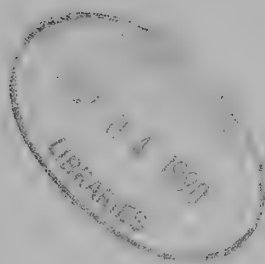
L
864
H
7 No. 2

April 1990

ZOOLOGICAL SCIENCE

An International Journal

PHYSIOLOGY
CELL and MOLECULAR BIOLOGY
GENETICS
IMMUNOLOGY
BIOCHEMISTRY
DEVELOPMENTAL BIOLOGY
REPRODUCTIVE BIOLOGY
ENDOCRINOLOGY
BEHAVIOR BIOLOGY
ENVIRONMENTAL BIOLOGY
ECOLOGY and TAXONOMY



published by **Zoological Society of Japan**

distributed by **Business Center for Academic Societies Japan**
VSP, Zeist, The Netherlands

ISSN 0289-0003

ZOOLOGICAL SCIENCE

The Official Journal of the Zoological Society of Japan

Editors-in-Chief:

Seiichiro Kawashima (Tokyo)

Hideshi Kobayashi (Tokyo)

Managing Editor:

Chitaru Oguro (Toyama)

Assistant Editors:

Yuichi Sasayama (Toyama)

Hitoshi Michibata (Toyama)

Miéko Komatsu (Toyama)

The Zoological Society of Japan:

Toshin-building, Hongo 2-27-2, Bunkyo-ku,
Tokyo 113, Japan. Tel. (03) 814-5675

Officers:

President: Hiromichi Morita (Fukuoka)

Secretary: Hideo Namiki (Tokyo)

Treasurer: Tadakazu Ohoka (Tokyo)

Librarian: Masatsune Takeda (Tokyo)

Editorial Board:

Howard A. Bern (Berkeley)

Horst Grunz (Essen)

Susumu Ishii (Tokyo)

Koscak Maruyama (Chiba)

Tokindo S. Okada (Okazaki)

Hiroshi Watanabe (Tokyo)

Walter Bock (New York)

Robert B. Hill (Kingston)

Yukiaki Kuroda (Mishima)

Roger Milkman (Okazaki)

Andreas Oksche (Giessen)

Mayumi Yamada (Sapporo)

Aubrey Gorbman (Seattle)

Yukio Hiramoto (Chiba)

John M. Lawrence (Tampa)

Kazuo Moriwaki (Mishima)

Hidemi Sato (Nagoya)

Ryuzo Yanagimachi (Honolulu)

ZOOLOGICAL SCIENCE is devoted to publication of original articles, reviews and communications in the broad field of Zoology. The journal was founded in 1984 as a result of unification of Zoological Magazine (1888-1983) and Annotationes Zoologicae Japonenses (1897-1983), the former official journals of the Zoological Society of Japan. ZOOLOGICAL SCIENCE appears bimonthly. An annual volume consists of six numbers of more than 1200 pages including an issue containing abstracts of papers presented at the annual meeting of the Zoological Society of Japan.

MANUSCRIPTS OFFERED FOR CONSIDERATION AND CORRESPONDENCE CONCERNING EDITORIAL MATTERS should be sent to:

Dr. Chitaru Oguro, Managing Editor, Zoological Science, Department of Biology, Faculty of Science, Toyama University, Toyama 930, Japan, in accordance with the instructions to authors which appear in the first issue of each volume. Copies of instructions to authors will be sent upon request.

SUBSCRIPTIONS. ZOOLOGICAL SCIENCE is distributed free of charge to the members, both domestic and foreign, of the Zoological Society of Japan. To non-member subscribers within Japan, it is distributed by Business Center for Academic Societies Japan, 6-16-3 Hongo, Bunkyo-ku, Tokyo 113. Subscriptions outside Japan should be ordered from the sole agent, VSP, Utrechtseweg 62, 3704 HE Zeist (postal address: P. O. Box 346, 3700 AH Zeist), The Netherlands. Subscription rates will be provided on request to these agents. New subscriptions and renewals begin with the first issue of the current volume.

All rights reserved. No part of this publication may be reproduced or stored in a retrieval system in any form or by any means, without permission in writing from the copyright holder.

© Copyright 1990, The Zoological Society of Japan

[Publication of Zoological Science has been supported in part by a Grant-in-Aid for
Publication of Scientific Research Results from the Ministry of Education, Science
and Culture, Japan.]

REVIEW

Mesenchymal-Epithelial Interactions in the Organogenesis of Digestive TractSADAO YASUGI¹ and TAKEO MIZUNO²¹*Zoological Institute, Faculty of Science, University of Tokyo, Tokyo 113,*²*Faculty of Pharmaceutical Sciences, Teikyo University,
Kanagawa 199-01, Japan*

ABSTRACT—It is now well established that the mesenchymal-epithelial interactions are essential in the spacio-temporally regulated differentiation processes in organogenesis of higher vertebrates. The mesenchymal-epithelial interactions in the digestive tract (DT) in avian and mammalian embryos have presented precious information on the nature of interaction, because the endoderm that later gives rise to the DT epithelium is a simple sheet consisted of undifferentiated cells at the early stages and with the development of DT the epithelium gradually acquires region-specific morphology and cytodifferentiation under the influence of the underlying mesenchyme. The studies carried out have demonstrated that the mesenchyme is dominant over the epithelium in determining the morphology of the latter and that the morphogenesis and cytodifferentiation are not always associated. Also the importance of epithelial competence against mesenchymal inductive influence has been repeatedly stressed. In this article we summarize these results and our recent findings to clarify the present status of the problem and to suggest the direction of further investigations.

INTRODUCTION

Regional differentiation of tissues in the animal development has been shown to be often brought about by the influences generated by other tissues within the embryo and transmission of signals between tissues which evoke specific response in the target tissue has been called 'induction' [1–3]. Induction has been postulated to work on the levels of morphology and cytodifferentiation, but the experimental dissociation of the two levels has been by no means easy. Moreover, studies have revealed that the induction processes are reciprocal in many systems, and that we can distinguish 'instructive' and 'permissive' inductions experimentally [4]. The nature of inductive process, however, has been not fully elucidated so far, partly because of time-consuming experimental systems and partly because of our lack of know-

ledge of events evoked in responding tissues. Recently more refined experimental systems have been developed as to the mesodermal induction in amphibian embryos with using the specific gene transcripts as a differentiation marker of responding tissue [5, 6]. However, the epithelial-mesenchymal interactions working in the organogenesis of many organs are still in the vague, although their importance is fully recognized.

The developing digestive tract (DT) of higher vertebrates such as mammals and birds provides us the opportunity to distinguish morphological and functional differentiation and offers us definitive markers of epithelial differentiation such as pepsinogens for the stomach and disaccharidases for the intestine. From these reasons, the DT is among the well-studied organ systems in the field of research on tissue interactions.

In this article, we will confine ourselves to the problems of effects of DT mesenchymes on the morphogenesis and cytodifferentiation of DT

epithelia, not dealing with the accessory glands of DT, i.e. the salivary glands, liver and pancreas, although our laboratory has been deeply concerned in studies of development of these organs [7-10].

THE DEVELOPMENT OF DIGESTIVE TRACT IN AVIAN AND MAMMALIAN EMBRYOS

The chicken DT consists of esophagus, proventriculus (glandular stomach), gizzard (muscular stomach), small and large intestines. Anatomically these organs can be recognized from day 3 to 4 of incubation [11]. The epithelial tissue is composed of simple columnar cells throughout the DT at this stage, and no organ-specific structures such as stomach glands or intestinal villi are seen.

In the chicken, the invagination of proventricular glands into the surrounding mesenchyme begins at day 6 [12]. Glands penetrate deep into the mesenchyme and repeat branching, forming the complex glands [13]. At day 13-15, the epithelial cells in the glands become cuboidal, while the luminal mucous epithelial cells and duct cells remain columnar. The embryonic pepsinogen, the zymogen of embryonic pepsin, appears first at day 9 [14-18]. The production of pepsinogen reaches maximum at day 15, and ceases to almost zero level in the latest period of embryonic life. The adult-type pepsinogens appear just after the hatching.

The epithelium of embryonic chicken gizzard does not form any complex glands. The cells are high columnar in form, contain many glycogen particles and actively secrete mucus. After day 12 of incubation, proliferation of epithelial cells become active and at the same time there occur the vertical striations of the epithelium. As a result of these changes, gizzard epithelium comes to possess finger-like projections in the later period of embryonic life. The cells still actively secrete mucus and secreted substances form a horny layer at the luminal surface. In the gizzard mesenchyme the muscle develops well [12].

The avian intestine can be divided into duodenum, small intestine, caecum and large intestine. At day 4 of incubation, the intestine is a very

simple tube, but in the following days, it elongates rapidly and form loops at duodenum level and small intestine. Large intestine can be recognized from day 5 on and always shorter and thicker than other part of intestine. The histological examination revealed that the villi formation begins at day 9 to 12, depending on the level of intestine, first at duodenum and later in more caudal parts. The brush border can be observed from day 12 and alkaline phosphatase activity from day 9-17 [19]. Disaccharidase (sucrase) can be detected by immunoelectron microscopy from day 8-10, histochemically and biochemically from day 14 [20-22].

The stomach of mouse and rat consists of two parts: the forestomach and glandular stomach. In the forestomach, epithelium has 2 to 3 layers of cells till the day 17 of gestation, becomes pluristratified at day 18, and first keratinization can be observed on day 19. In glandular part, pluristratification occurs at day 15-16, and intraepithelial vacuoles communicate with stomach lumen and become primitive pits of the stomach. At day 18, the epithelium becomes simple columnar, and villus-like structures develop. Morphologically identifiable parietal cells appear just before birth, while chief cells can be distinguished before weaning [23, 24]. In the mouse stomach a pepsinogen can be detected biochemically from day 16 of gestation. In the period just before birth another pepsinogen appears and the ratio of the two pepsinogens varies as the development proceeds [25].

The intestinal epithelium of the rat and mouse is pluristratified until day 15-18 of gestation, but from day 19 onward the formation of villi begins and the epithelium becomes simple columnar. Disaccharidases in the mouse intestine are low in activity before birth and become active after various periods depending on the kind of enzymes [26].

From this brief description of development of stomach and intestine of bird and mammal, it is obvious that these organs have their specific morphologies and functional specificities even in embryonic and fetal period. Considering that these organs are derived from a single, continuous tube, it is easily conceivable that the differentiation of these organs provides us very suitable model for the analysis of tissue interactions.

DETERMINATION OF MORPHOLOGICAL FEATURES OF EPITHELIUM BY ASSOCIATED MESENCHYME

Balinsky first studied the experimental alteration of developmental fate of DT epithelium by the mesenchyme: He transplanted the presumptive stomach region of axolotl to the presumptive region of liver of *Triton* and found that the stomach epithelium became liver parenchymal cells [27]. Okada [28] also analyzed the developmental fate of presumptive digestive organ epithelium transplanted heterotopically in the amphibian embryos and reported the presence in mesoderm of anteriorizing effect against endoderm, and stated that the developmental fate of endoderm is determined by both mesodermal factors and endodermal reactivity.

After these pioneering works, the studies of epithelial-mesenchymal interactions in the DT development have been carried out mainly in two groups, one in France led by Etienne Wolff and another in Japan led by one of the present authors (T.M.).

The exact location of fate map of DT is prerequisite for the experimental studies. This was achieved in chicken with the use of carbon marking method and X-ray-induced lesion [29] and with the use of ^3H -labelled tissues [30]. In the mammals the presumptive fate of the endodermal cells was not studied systematically, because of the difficulty in treating early embryos, and almost all the experiments were carried out on the DT of fetuses of latter half of gestation period.

Until about the mid 1970s, the experiments on the epithelial-mesenchymal interaction in DT were dependent exclusively on the morphological criteria. The situation was the same in other systems such as skin [31], tooth [4], kidney [32] and so on. Such morphological studies indefinitely showed the dominance of mesenchymal tissue over epithelial tissue in the determination of morphological traits of epithelial tissue in many instances. We will describe some examples below.

When the chicken epidermis was associated and cultured with mesenchyme of chicken gizzard, epidermal cells, which are determined to keratinize in the normal development, showed mucous

metaplasia [33], thus showing the inducing effect of gizzard mesenchyme. In the chicken stomach, the epithelial-mesenchymal interaction between proventriculus and gizzard was first studied by Sigot [34, 35]. He demonstrated that proventricular epithelium of 5- to 6-day embryos differentiates into gizzard-type epithelium when it was cultivated *in vitro* alone or with gizzard mesenchyme. On the other hand, proventricular mesenchyme induces gland formation in associated gizzard and intestinal epithelia, and the inductive ability of proventricular mesenchyme is highest on day 5 and disappears at day 7. David [36–38], who carried out the similar experiments with fetal rabbit stomach, concluded that there exist two inducing factors in the mesenchyme; first one is highly diffusible and induces epithelial morphogenesis, the second one is lightly diffusible and evokes cytodifferentiation. Naturally the second factor is produced in the later stage of development.

These studies demonstrated that the developmental fate of DT epithelium can be changed in some cases by the association of heterologous mesenchymes. But in the mouse DT, Soriano [39] and Fukamachi *et al.* [40, 41] reported the early determination of developmental fate of the DT epithelium. Fukamachi *et al.* carried out extensive tissue-recombination experiments *in vitro* using forestomachs and glandular stomachs and concluded that the developmental fate of the epithelium was not affected by the associated heterotypic and heterochronic mesenchymes, but the degree of differentiation was affected by the type of mesenchyme.

A group of researchers led by Mizuno studied extensively the inductive ability of DT mesenchyme on the epithelia of DT and embryonic membranes in the chicken embryos. Yasugi and Mizuno [42] associated the allantoic endoderm of 3- to 4-day embryos with various mesenchymes of DT of day 6 and older [43] and cultivated *in vitro* [44] or on the chorio-allantoic membrane (CAM) of 9-day embryos [45]. They demonstrated that morphological characters of allantoic endoderm were largely determined by the mesenchyme: when it was associated with esophageal mesenchyme it differentiated into pluristratified epithelium; with proventricular mesenchyme, it formed very com-

plex glands; with gizzard mesenchyme, it differentiated into highly columnar epithelium with high glycogen content; with intestinal mesenchyme it formed villus-like structures with simple columnar cells. Also, when the allantoic endoderm was implanted into the presumptive digestive area of young chicken embryos and hosts were kept alive until the latter half of the embryonic period or even after hatching, the endoderm differentiated heterotypically under the influence of surrounding mesenchymes [46, 47].

The inductive influence of DT mesenchyme seemed not restricted against allantoic endoderm. The DT epithelium could also more or less respond to the influence of DT mesenchyme [48](Table 1). Most remarkably, gizzard epithelium differentiated into proventricular epithelium and formed complex proventricular glands when it was associated with proventricular mesenchyme. In contrast, in the association of proventricular epithelium and gizzard mesenchyme, the epithelium never formed glands found in the normal

proventriculus, but is differentiated into the epithelium rather similar to the gizzard epithelium. Moreover, intestinal mesenchyme showed strong inductive influence against gizzard epithelium [48, 49].

Masui [50, 51] and Yasugi and Mizuno [52] respectively demonstrated the flexibility of differentiation potency of yolk sac endoderm and hypoblast of young chicken embryos under the influence of DT mesenchymes.

As to self-differentiation potency of the DT epithelium, studies of *in vitro* cultivation of isolated fragments of the endoderm have been performed extensively at Mizuno's laboratory, and we found that region-specific self-differentiation potency appears in young presumptive endoderms of DT epithelium [53–57]. Based on these and the above-mentioned results, Mizuno [58] postulated a hypothesis that the developmental fate of DT epithelium may be determined by both self-differentiation potency of the endoderm and the inductive influences of the mesenchyme.

Epithelial-mesenchymal interactions were demonstrated also with isolated and cultured cells. Fukamachi *et al.* [59, 60] showed the gland formation of human colon cancer cells (LS174T) maintained *in vitro* when the cells were recombined with fetal rat mesenchyme. They concluded that the desmosome formation in epithelial cells is important for the establishment of epithelial polarity and gland formation [61].

In France, Haffen and her colleagues studied actively the differentiation of intestinal epithelial cells and have demonstrated that fetal rat intestinal mesenchyme could permit the normal differentiation of cultured rat intestinal epithelial cells so that the latter formed villus-like structures, and that fibroblasts obtained from suckling rat duodenum could induce intestinal differentiation in embryonic chicken gizzard epithelium [62–65]. Also, epithelioid cultures derived from rat and quail intestine were able to differentiate into intestinal epithelium when they were associated with chicken embryonic intestinal mesenchyme [66].

These results mentioned above unequivocally demonstrate the importance of mesenchymal influence in determining the epithelial morphology in the development of avian and mammalian DT

TABLE 1. Homotypic and heterotypic differentiation of epithelia associated with various mesenchymes and cultivated on the chorio-allantoic membrane. Upper figure in each combination represents the percentage of homotypic differentiation, lower figure heterotypic differentiation. The sum of upper and lower figures is not necessarily 100 because some explants underwent both homotypic and heterotypic differentiation and some others remained undifferentiated. From Yasugi and Mizuno [48]

Epithelium	Mesenchyme associated			
	ES	PV	GZ	SI
ES	86	50	88	100
	0	100	24	0
PV	0	100	0	0
	25	0	100	50
GZ	100	0	100	0
	0	100	0	71
SI	75	100	100	100
	34	0	0	0

ES: Esophagus, PV: Proventriculus, GZ: Gizzard, SI: Small intestine.

on one hand, and that of the endodermal epithelium as a responding tissue on the other hand.

REGULATION OF ORGAN-SPECIFIC GENE EXPRESSION AND PROTEIN SYNTHESIS BY ASSOCIATED MESENCHYME

The most important aim of the current developmental biology is to clarify the mechanisms regulating the differential expression of genes during the course of development. Although the morphological differentiation of an organ is based on the local expression or suppression of sets of genes, we have at present no valid information about the genes involved in the morphogenesis. The role of mesenchyme in the epithelial differentiation must also be analyzed from the view point of its effects on the expression of specific genes. As stated above, digestive organs have advantage in that they possess many organ-specific marker proteins. The use of these markers as criteria of epithelial cell differentiation, that began at mid 1970s, brought about fruitful information.

It was already mentioned that the allantoic endoderm can differentiate morphologically into the epithelia of organs from which associated mesenchymes were derived. Yasugi [10] made use of anti-glucagon antibody to examine whether the allantoic endodermal cells can synthesize glucagon under the influence of pancreatic or intestinal mesenchyme after the recombinants were cultivated on the CAM. He obtained the positive results: both mesenchymes induced the anti-glucagon antibody-positive cells in the epithelium.

As for the induction of endocrine cells in the epithelium, Andrew and Rawdon carried out various recombination experiments and reported that the chicken mesenchymes of DT often induce ectopic endocrine cells in associated epithelia. For example, a wide variety of endocrine cell types differentiated in the gizzard and allantoic epithelia which are normally devoid of such cells [67–69].

The intestinal epithelial cells are characterized by the presence of brush border on the apical cell surface and the presence of disaccharidases on the brush border membrane. Among various disaccharidases, sucrase was purified and antibodies were raised by several workers, mainly because of

the abundance and ease of purification procedure of this enzyme.

In Japan, Matsushita studied the ontogeny of sucrase in chicken embryo and purified it and obtained the polyclonal antibody [21]. Using this antibody, he could show that the allantoic endoderm expresses sucrase in recombination with DT mesenchyme including non-intestinal ones. So it was concluded that the allantoic endoderm has an intrinsic tendency to differentiate into intestinal epithelium [70].

In France, Haffen and coworkers used wide range of brush border enzymes as markers (sucrase-isomaltase, maltase-glucoamylase, lactase, aminopeptidase, alkaline phosphatase and so on) that can be detected by monoclonal antibodies raised against each enzyme. Also they measured enzymatic activity of the recombinants biochemically. These experiments confirmed the results obtained in morphological studies. For example, when chicken embryonic gizzard epithelium was associated with duodenal fibroblasts derived from newborn rat, the epithelium differentiated into typical intestinal epithelium with brush border detected by electron microscopy, and the biochemical analysis showed the sucrase, maltase and alkaline phosphatase activity comparable to those of intact chicken intestine [65].

Pepsinogens, zymogens of pepsins, are proteins specifically synthesized in stomach gland cells, and have been most extensively studied in relation to epithelial-mesenchymal interactions. Yasugi and Mizuno [15–18] have investigated first the normal development of pepsinogen in chicken and quail proventriculus and demonstrated that embryonic proventriculus synthesizes embryo-specific pepsinogen (EPg) which is no longer expressed at the end of the embryonic life. Later the study was extended to ontogeny and phylogeny of pepsinogens among vertebrates and even among protochordates [71–74].

The use of antibody to ECPg [75] stimulated much the studies of tissue interaction in the avian DT (Table 2), and revealed some unexpected results: In some instances where the mesenchyme seemed to exert instructive induction on the associated epithelium, the cytodifferentiation was found not to be accompanied. For example, intestinal

and allantoic epithelia formed very complex glands that were never observed in the normal development of these epithelia when they were associated with proventricular mesenchyme and cultivated on the CAM. Nevertheless the application of monoclonal and polyclonal antibodies to EPg clearly demonstrated that those epithelia never express EPg. Biochemical analysis with specific inhibitor of pepsin also supported the results [76]. The allantoic endoderm implanted into the presumptive proventricular area of young chicken embryo formed complex glands, as stated above, but it never expressed EPg and made a quite clear contrast to the host proventricular glands which actively synthesized EPg, although the grafted allantoic endoderm and host gland cells were separated by only 50 μ m of mesenchymal cell layers [47].

These facts are very important in considering the relationship between morphogenesis and cytodifferentiation. Many workers in this field generally believed that the morphological differentiation is always accompanied by the biochemical differentiation. The results obtained from the association of intestinal and allantoic epithelia and proventricular mesenchyme clearly showed that morphogenesis and cytodifferentiation are separable events and achievement of morphological differentiation is not necessarily accompanied by cytodifferentiation. So far a few examples of separation of morphological and cytochemical differentiation have been reported: In recombinants of salivary gland mesenchyme and mammary gland epithelium [77], of adult rat urinary bladder epithelium and fetal urogenital sinus mesenchyme [78], of fetal urogenital sinus epithelium and glandular stomach mesenchyme (Mizuno *et al.*, Roux's Arch. Develop. Biol., in press), and others. The significance of these phenomena will be discussed in detail in another review paper (Mizuno and Yasugi, Cell Differ. Develop., in preparation).

Then a question arose whether the inability of intestinal and allantoic epithelia to synthesize EPg protein under the influence of proventricular mesenchyme is due to the lack of EPg gene transcription or due to the defects in posttranscriptional or translational processing. To answer this

question, Hayashi *et al.* [79–81] obtained cDNA of EPg and examined the expression of EPg gene transcripts in recombinants consisted of esophageal, proventricular, gizzard, intestinal or allantoic epithelia with proventricular mesenchyme, with cDNA of EPg as a probe. The Northern blot analysis after gel electrophoresis of mRNA extracted from recombinants clearly demonstrated that intestinal and allantoic epithelia could not express EPg gene while other epithelia synthesized mRNA of EPg the length of which was exactly the same as in normal embryonic proventriculus [81]. So we can now affirm that the inductive influence generated by proventricular mesenchyme could not evoke EPg gene transcription in intestinal and allantoic epithelia. This may be an important clue in analyzing the molecular basis of induction.

The appearance of EPg in various recombinants of chicken DT epithelia and mesenchymes derived from 6-day embryos is summarized in Table 2. From this it is obvious that proventricular and gizzard epithelia respond in just the same manner against the mesenchymal influences. Thus they synthesize small amount of EPg on the esophageal and intestinal mesenchymes, synthesize EPg very actively on the proventricular mesenchyme, and EPg synthesis was completely inhibited on the gizzard mesenchyme. This fact led Takiguchi *et al.* to analyze precisely the chronological changes of reactivity of gizzard epithelium to proventricular

TABLE 2. The expression of embryonic chicken pepsinogen (EPg) in various associations cultivated on the chorio-allantoic membrane (% of explants possessing EPg-positive gland cells)

Epithelium	Mesenchyme associated			
	ES	PV	GZ	SI
ES	0	100	0	63
PV	75	100	0	77
GZ	22	100	0	71
SI	0	0	0	71
AL	0	0	0	0

ES: Esophagus, PV: Proventriculus, GZ: Gizzard, SI: Small intestine AL: Allantois.

mesenchymal influence [82, 83]. The reactivity decreased rapidly after day 7 of incubation onward but still remained at very low level at day 12. The result indicates that gizzard epithelium does not express EPg in normal development because of both a decrease in ability to express the enzyme in the course of development and a suppressive influence of gizzard mesenchyme.

The induction of EPg in gizzard epithelium by proventricular mesenchyme was confirmed also in *in vitro* system, and the dissociated and reaggregated mesenchymal cells are also effective [84]. This opens the way to analyze the nature of induction by proventricular mesenchyme in *in vitro* culture system.

THE MEDIATOR SYSTEM OF INDUCTIVE INFORMATION IN THE DEVELOPMENT OF DIGESTIVE TRACT

The results described so far strongly suggest the transfer of some inductive information from mesenchyme to epithelium. Generally speaking, quite many factors may be involved in the transfer of informations. Among them are: informative substances emitted from mesenchymal cells, extracellular substances of mesenchyme, basement membrane, cell adhesion molecules, receptor of epithelial cells, intracellular information transfer systems, and so on. In the epithelial-mesenchymal interactions of DT development, some progresses have been made recently.

Structural organization of mesenchyme and the inductive action

First, whether the structural organization of mesenchyme is required for its inductive action was tested with using the isolation and cultivation *in vitro* of mesenchymal cells. As already mentioned, in the case of recombination of chicken gizzard epithelium and rat intestinal fibroblasts, fibroblastic cells cultivated *in vitro* still maintain inducing activity [65]. Dissociated and instantly reaggregated proventricular mesenchymal cells could elicit proventricular epithelial differentiation in associated proventricular and gizzard epithelia [84]. These studies showed that the structural integrity *in situ* is not necessary for the inductive

ability although there is a possibility that these mesenchymal cells reconstituted the normal structural integrity soon after the onset of cultivation with epithelium.

Quite unexpected results were obtained when proventricular epithelium of 6-day embryos was associated with cultured rat intestinal mesenchymal cells or cultured human or rat skin fibroblasts and recombinants were implanted into coelomic cavity of chicken embryo [85] (Table 3). These cells supported full differentiation of epithelium toward proventricular epithelium. The epithelium formed complex glands the cells of which synthesized EPg very actively. Under the same conditions, the intact chicken and rat intestinal mesenchymes suppressed the proventricular differentiation both morphologically and functionally. One can explain the results as these mesenchymal cells cultivated *in vitro* acted as dedifferentiated, 'neutral' cells lacking organ-specific inducing ability, and permitted the development of intrinsic tendency toward the proventricular epithelium.

The molecular differences of mesenchymes

The mesenchymes of proventriculus and gizzard exert contradictory effect on the proventricular and gizzard epithelia (see above). The elucidation of molecular difference between the two mesenchymes will be an important step for the understanding of inductive influence of mesenchyme. To detect the molecular difference, Takiguchi and Yasugi (unpublished result) used monoclonal antibody technique. The crude extract of embryonic chicken gizzard was injected into mouse and antibodies were screened with attention to the tissue distribution of antigen. Among many clones, we picked up an antibody designated as GM-1. The localization of GM-1 antigen varies between proventriculus and gizzard at day 6 of incubation when these mesenchymes show differential effect on the epithelium. GM-1 antigen was scarcely detected in 6-day proventriculus except the very weak signal in basement membrane, whereas in the gizzard GM-1 antigen localized in the mesenchymal layer just underneath the epithelium. The molecular weight of GM-1 antigen calculated from immunoblotting after SDS-PAGE was about 42 kDa and immunolocalization was quite different

TABLE 3. Differentiation of proventricular epithelium associated with mesenchyme or cultivated mesenchymal cells, derived from digestive organs, or with skin fibroblasts. From Yasugi *et al.* [85]

Type of associated mesenchyme or cells	No. of living grafts	No. of grafts showing		No. of grafts expressing	
		Complex glands	Simple glands	Pepsinogen	Sucrase
cPV mesenchyme	8	8	0	8	0
cPV mes cells	5	0	11	11	0
cSI mesenchyme	11	0	11	11	0
rSI mesenchyme	6	0	0	0	0
rSI mes cells	4	4	0	4	0
r skin fibrobl	5	5	0	5	1
h skin fibrobl	4	4	0	4	1

c: Chicken, r: Rat, h: Human, PV: Proventriculus, SI: Small intestine, mes: Mesenchymal, fibrobl: Fibroblasts.

from those of well-known ECM, such as fibronectin, laminin, and tenascin. By the way, the distribution of these common ECM was almost the same in proventriculus and gizzard.

GM-1 antigen represents one of organ-specific substances and may be thought to be involved in the establishment of regionality of mesenchyme, although we do not know the exact biological significance of it which is to be elucidated in the near future.

In mouse small intestine, tenascin appears in mesenchyme when epithelial cell differentiation begins and its expression is dependent on the epithelial-mesenchymal interactions [86].

The diffusibility of inductive action of mesenchyme

It is now well established that in many systems of tissue interactions the direct contact of inducer cells and responding cells is necessary [87, 88]. Takiguchi and Yasugi (Roux's Arch. Develop. Biol., in press) examined the diffusibility of inducing effect of proventricular mesenchyme with Nuclepore filter interposed between mesenchyme and epithelium. With Nuclepore filter of pore size less than $0.4\ \mu\text{m}$, the induction never occurred, while with filter of pore size larger than $0.6\ \mu\text{m}$ the epithelium expressed EPg and the amount of EPg expressed increased as the pore size became larger. It must be noted that mesenchymal cells can pass through the Nuclepore filter of pore size

larger than $0.6\ \mu\text{m}$, and even in case of $0.2\ \mu\text{m}$ filter the cell processes of mesenchyme reached the epithelial surface of filter. So we suppose that the direct contact of epithelial cells with mesenchymal cells or with mesenchymal extracellular substances is necessary also in the induction in these cases, although it must be confirmed by electron microscopic study.

Basement membrane

The important role of basement membrane (basal lamina) can be easily understood since basement membrane not only mechanically separates epithelium and mesenchyme but also regulates the flow of substances between these two tissues. In developing DT, the thinning of basement membrane was reported. In the proventriculus and intestine, cytoplasmic processes of epithelial cells penetrate the gaps made in basal lamina and make direct contact with mesenchymal cells [12, 89, 90]. Also basement membrane components (laminin, nidogen, type IV-collagen) are present at the epithelial-mesenchymal interface early in development and the spatial distribution of some extracellular matrix proteins is closely associated with morphogenesis [91]. Moreover, the production of basement membrane is thought to require epithelial-mesenchymal interaction, at least in experimental *in vitro* system [92].

Cytoskeletal system of epithelial cells and the expression of organ-specific proteins

Cytoskeletal systems are involved in the morphogenesis of cells, in intracellular transmission of information received at cell surface, and in physiological functions such as secretion. However, the studies on the relations of cytoskeletal systems and organ-specific gene expression in the organogenesis are very limited [93].

Epithelial cells contain cytokeratins as intermediate filaments, and the cytokeratins of chicken DT epithelial cells are partially characterized with antibodies [94].

Takiguchi *et al.* (unpublished results) studied the expression of cytokeratin immunoreactive to an antibody PKK-1 which is reactive to human cytokeratins 8, 18, and 19 and recognizes 52kDa protein in chicken DT. Interestingly enough, there is an inverse correlation between expression of PKK-1 antigen and of EPg in chicken proventriculus: In EPg-producing gland cells PKK-1 antigen disappears, while EPg-non producing luminal epithelial cells and duct cells are always PKK-1-positive. Epithelial cells of DT except the proventricular gland cells are also positive to PKK-1, and in the stomach of all vertebrates so far examined except mammals, the pepsinogen-producing gland cells are negative to PKK-1 [95]. Although the precise relation between pepsinogen expression and disappearance of PKK-1 antigen is not clear at present, disappearance of PKK-1 antigen is a very specific marker of appearance of pepsinogen-producing cells in the developing stomach.

Various epithelia were associated with proventricular mesenchyme and cultivated on the CAM to see whether the disappearance of PKK-1 antigen is also regulated by the mesenchymal influences. The results clearly indicated that esophageal, proventricular and gizzard epithelia, which expressed EPg, lost PKK-1 antigen without exception, while intestinal epithelium, which could not synthesize EPg, continuously expressed PKK-1 antigen. So the expression of PKK-1 antigen is also under the control of mesenchyme and the disappearance of PKK-1 antigen is well linked to EPg expression.

This raises very interesting questions: does the

proventricular mesenchyme emit two independent factors, one for the suppression of PKK-1 antigen and another for the induction of EPg? or does the mesenchyme release only one sort of signal that evokes at the same time the two events independently? or does the mesenchyme release a signal that induces EPg expression via the suppression of PKK-1 antigen expression? The fact that the intestinal epithelium did not lose the PKK-1 antigen in the presence of proventricular mesenchyme seems to exclude the first hypothesis.

PERSPECTIVES

We reviewed here various aspects of epithelial-mesenchymal interactions working in the organogenesis of DT in avian and mammalian embryos and fetuses. Although we are still far from the complete understanding of the nature of the processes, we have now ample clue to pursue the molecular basis of tissue interactions.

First and most important subject is to identify directly the substances that are responsible for the organ-specific inducing influence of mesenchyme. Evidence suggests that the inducing substances are not freely diffusible ones, and may be sought among extracellular or basement membrane components. There is a possibility, however, that some kinds of growth factors or their derivatives are involved in the process, since in some instances they act as potent inducing factors [96-98].

Next problem is to find out the nature of reactivity of epithelial cells in relation to the activation of specific gene expression. To approach the problem, it is necessary to elucidate the control mechanisms of expression of relevant genes such as EPg, sucrase or cytokeratin genes. The finding of trans-acting factors for these genes will provide much information of signal transfer routes in tissue interactions. As for the reactivity of various epithelia against the influence of the same mesenchyme, i. e., the reactivity of gizzard and intestinal epithelia against proventricular mesenchyme, it is prerequisite to know the structural differences of genes that are induced or not induced to be transcribed by the mesenchymal influence. One possibility is a methylated state of the genes, since the methylation of the genes often brought about the inactivation of them. In fact, in mammals,

pepsinogen genes are hypermethylated when they are out of work and become hypomethylated when they are transcribed [99]. This problem is currently under investigation with EPg gene in the laboratory of one of the present authors (S.Y.).

ACKNOWLEDGMENTS

We wish to express our deepest gratitude to Emeritus Professor Takashi Fujii, University of Tokyo, and Emeritus Professor Etienne Wolff, Collège de France, for introducing us to this problem and for their encouragement during the course of the studies.

REFERENCES

- Wessells, N. K. (1977) Tissue Interactions and Development. W. A. Benjamin, Inc., California/Massachusetts/London/Amsterdam/Ontario/Sydney.
- Nieuwkoop, P. D., Johnen, A. G. and Albers, B. (1985) The Epigenetic Nature of Early Chordate Development. Inductive Interaction and Competence. Cambridge University Press, Cambridge/London/New York/Rochelle/Mellbourne/Sydney.
- Raff, R. A. and Kaufman, T. C. (1983) Embryos, Genes, and Evolution. Macmillan Company, New York.
- Saxén, L., Karikinen-Jääskeläinen, M., Lehtonen, E., Nordling, S. and Wartiovaara, J. (1976) Inductive tissue interactions. In "The Cell Surface in Animal Embryogenesis and Development". Ed. by G. Poste and G. L. Nicolson, North-Holland Publ. Comp., Amsterdam/New York/Oxford, pp. 331-407.
- Gurdon, J. B., Fairman, S., Mohun, T. J. and Brennan, S. (1985) Cell, **41**: 913-922.
- Gurdon, J. B. (1987) Development, **99**: 285-306.
- Nogawa, H. (1981) J. Embryol. Exp. Morphol., **62**: 229-239.
- Fukuda-Taira, S. (1981) J. Embryol. Exp. Morphol., **63**: 111-125.
- Shiojiri, N. (1984) J. Embryol. Exp. Morphol., **79**: 24-39.
- Yasugi, S. (1976) C.R.Acad.Sci., Paris, **283**: 383-385.
- Romanoff, A. L. (1960) The Avian Embryo, The Macmillan Company, New York.
- Hayashi, K. (1987) Develop. Growth Differ., **29**: 285-295.
- Calhoun, M. L. (1954) Microscopic Anatomy of the Digestive System of the Chicken. Iowa State University Press, Ames.
- Yasugi, S., Mizuno, T. and Esumi, H. (1979) Experientia, **35**: 814-815.
- Yasugi, S. and Mizuno, T. (1979) C.R.Soc. Biol., **173**: 973-978.
- Yasugi, S. and Mizuno, T. (1981) J. Exp. Zool., **216**: 331-335.
- Yasugi, S. and Mizuno, T. (1981) J. Biochem., **89**: 311-315.
- Yasugi, S. and Mizuno, T. (1982) C.R.Soc. Biol., **176**: 575-579.
- Moog, F. (1950) J. Exp. Zool., **115**: 109-129.
- Matsushita, S. (1981) J. Fac. Sci., Univ. Tokyo, Sect. IV, **15**: 81-92.
- Matsushita, S. (1983) Comp. Biochem. Physiol., **76B**: 365-470.
- Matsushita, S. (1985) J. Exp. Zool., **233**: 377-383.
- Hellander, H. F. (1969) Gastroenterology, **56**: 53-70.
- Fukamachi, H. (1978) J. Fac. Sci., Univ. Tokyo, Sect. IV, **14**: 85-94.
- Yasugi, S., Matsumoto, F. and Mizuno, T. (1987) C. R. Soc. Biol., **181**: 450-453.
- Moog, F., Denes, A. E. and Powell, P. M. (1973) Develop. Biol., **35**: 143-159.
- Balinsky, B. I., (1948) Roux' Arch. Entwicklungsmech. Organ., **143**: 365-395.
- Okada, T. S. (1960) Roux' Arch. Entwicklungsmech. Organ., **152**: 1-21.
- Le Douarin, N. (1964) Bull. Biol. France Belg., **98**: 543-676.
- Rosenquist, G. C. (1971) Develop. Biol., **26**: 323-335.
- Sengel, P. (1971) Adv. Morphol., **9**: 181-230.
- Eklom, P. (1981) Medical Biol., **59**: 139-160.
- McLoughlin, C. B. (1960) Xe Congrès International. Biol. Cell., Paris, pp. 38-39.
- Sigot, M. and Marin, L. (1970) J. Embryol. Exp. Morphol., **24**: 43-63.
- Sigot, M. (1971) Arch. Anat. Microsc. Morphol. Exp., **60**: 169-204.
- David, D. (1971) Roux' Arch. Entwicklungsmech. Organ., **168**: 304-319.
- David D. (1972) J. Embryol. Exp. Morphol., **27**: 177-197.
- David, D. (1972) Roux' Arch. Entwicklungsmech. Organ., **170**: 1-12.
- Soriano, L. (1965) J. Embryol. Exp. Morphol., **14**: 119-128.
- Fukamachi, H., Mizuno, T. and Takayama, S. (1979) Anat. Embryol., **157**: 151-160.
- Fukamachi, H. and Takayama, S. (1980) Experientia, **36**: 335-336.
- Yasugi, S. and Mizuno, T. (1974) Roux' Arch. Entwicklungsmech. Organ., **174**: 107-116.
- Yasugi, S. (1979) Develop. Growth Differ., **21**: 343-348.
- Wolff, Et. and Haffen, K. (1952) Texas Rep. Biol.

- Med., **10**: 463–472.
- 45 Yasugi, S. (1976) C.R.Acad. Sci., Paris, **283**: 179–183.
 - 46 Gumpel-Piot, M., Yasugi, S. and Mizuno, T. (1978) C.R.Acad.Sci., Paris, **286**: 117–120.
 - 47 Yasugi, S. (1984) J. Embryol. Exp. Morphol., **80**: 137–153.
 - 48 Yasugi, S. and Mizuno, T. (1978) Develop. Growth Differ., **20**: 261–267.
 - 49 Ishizuya-Oka, A. and Mizuno, T. (1984) J. Embryol. Exp. Morphol., **82**: 163–176.
 - 50 Masui, T. (1981) J. Embryol. Exp. Morphol., **62**: 277–289.
 - 51 Masui, T. (1982) J. Embryol. Exp. Morphol., **72**: 117–124.
 - 52 Yasugi, S. and Mizuno, T. (1984) C. R. Soc. Biol., **178**: 580–583.
 - 53 Sumiya, M. and Mizuno, T. (1974) C.R. Acad.Sci., Paris, **278**: 1529–1532.
 - 54 Sumiya, M. (1976) J. Fac. Sci., Univ. Tokyo, Sect. IV, **13**: 363–381.
 - 55 Sumiya, M. (1976) Roux's Arch. develop. Biol., **179**: 1–18.
 - 56 Sumiya, M. and Mizuno, T. (1976) Proc. Japan Acad., **52**: 587–590.
 - 57 Ishizuya-Oka, A. (1983) Roux's Arch. Develop. Biol., **192**: 171–178.
 - 58 Mizuno, T. (1975) C. R. Soc. Biol., **169**: 1096–1098.
 - 59 Fukamachi, H., Mizuno, T. and Kim, Y. S. (1986) Experientia, **42**: 312–315.
 - 60 Fukamachi, H., Mizuno, T. and Kim, Y. S. (1987) J. Cell Sci., **87**: 615–621.
 - 61 Fukamachi, H. and Kim, Y.S. (1989) Develop. Growth Differ., **31**: 307–313.
 - 62 Keding, M., Haffen, K. and Simon-Assmann, P. (1987) Differentiation, **36**: 71–85.
 - 63 Keding, M., Simon-Assmann, P., Bouziges, F. and Haffen, K. (1988) Scand. J. Gastroenterol., **23**, Suppl. **151**: 62–69.
 - 64 Keding, M., Simon-Assmann, P.M., Lacroix, B., Marxer, A., Hauri, H.P. and Haffen, K. (1986) Develop. Biol., **113**: 474–483.
 - 65 Haffen, K., Lacroix, B., Keding, M. and Simon-Assmann, P. M. (1983) Differentiation, **23**: 226–233.
 - 66 Haffen, K., Keding, M., Simon, P. M. and Raul, F. (1981) Differentiation, **18**: 97–103.
 - 67 Kramer, B., Andrew, A. Rawdon, B. B. and Becker, P. (1987) Development, **100**: 661–671.
 - 68 Rawdon, B. B. (1988) Inaugural Lecture of University of Cape Town, **138**: 1–16.
 - 69 Rawdon, B. B. and Andrew, A. (1988) Cell Differ. Develop., **25**: 135–144.
 - 70 Matsushita, S. (1984) Roux's Arch. Develop. Biol., **193**: 211–218.
 - 71 Yasugi, S. and Mizuno, T. (1982) C. R. Soc. Biol., **176**: 880–884.
 - 72 Yasugi, S. (1987) Comp. Biochem. Physiol., **86B**: 675–680.
 - 73 Yasugi, S., Matsunaga, T. and Mizuno, T. (1988) Comp. Biochem. Physiol., **91A**: 564–569.
 - 74 Yasugi, S., Matsunaga, T. and Mizuno, T. (1989) Zool. Sci., **6**: 283–288.
 - 75 Yasugi, S., Hayashi, K., Takiguchi, K., Mizuno, T., Mochii, M., Kodama, R., Agata, K. and Eguchi, G. (1987) Develop. Growth Differ., **29**: 85–91.
 - 76 Yasugi, S., Matsushita, S. and Mizuno, T. (1985) Differentiation, **30**: 47–52.
 - 77 Sakakura, T., Nishizuka, Y. and Dawe, C. J. (1976) Science, **194**: 1439–1441.
 - 78 Suematsu, N., Takeda, H. and Mizuno, T. (1988) Zool. Sci., **5**: 385–395.
 - 79 Hayashi, K., Agata, K., Mochii, M., Yasugi, S., Eguchi, G. and Mizuno, T. (1988) J. Biochem., **103**: 290–296.
 - 80 Hayashi, K., Yasugi, S. and Mizuno, T. (1988) Biochem. Biophys. Res. Commun., **152**: 776–782.
 - 81 Hayashi, K., Yasugi, S. and Mizuno, T. (1988) Development, **103**: 725–731.
 - 82 Takiguchi, K., Yasugi, S. and Mizuno, T. (1986) Roux's Arch. Develop. Biol., **195**: 475–483.
 - 83 Takiguchi, K., Yasugi, S. and Mizuno, T. (1988) Roux's Arch. Develop. Biol., **197**: 56–62.
 - 84 Takiguchi, K., Yasugi, S. and Mizuno, T. (1988) Develop. Growth Differ., **30**, 241–250.
 - 85 Yasugi, S., Keding, M., Simon-Assmann, P., Bouziges, F. and Haffen, K. (1989) Roux's Arch. Develop. Biol., **198**: 114–117.
 - 86 Aufderheide, E. and Ekblom, P. (1988) J. Cell Biol., **107**: 2341–2349.
 - 87 Slavkin, H. C. and Bringas, P., Jr. (1976) Develop. Biol., **50**: 428–442.
 - 88 Lehtonen, E., Wartiovaara, J., Nordling, S. and Saxén, L. (1975) J. Embryol. Exp. Morphol., **33**: 187–203.
 - 89 Mathan, M., Hermos, J. A. and Trier, J. S. (1972) J. Cell Biol., **52**: 577–588.
 - 90 Ishizuya-Oka, A. and Mizuno, T. (1985) Roux's Arch. Develop. Biol., **194**: 301–305.
 - 91 Simon-Assmann, P., Keding, M. and Haffen, K. (1986) Differentiation, **32**: 59–66.
 - 92 Simon-Assmann, P., Bouziges, F., Arnold, C., Haffen, K. and Keding, M. (1988) Development, **102**: 339–347.
 - 93 Lesot, H., Karcher-Djuricic, V., Kubler, M. D. and Ruch, J. V. (1988) Differentiation, **37**: 62–72.
 - 94 O'Guin, W. M., Galvin, S., Schermer, A. and Sun, T.-T. (1987) Curr. Topics Develop. Biol., **22**: 97–125.
 - 95 Takiguchi-Hayashi, K. and Yasugi, S. (1988) C.R.

- Soc. Biol., **182**: 445–448.
- 96 Slack, J. M. W., Isaacs, H. V. and Darlington, B. G. (1988) *Development*, **103**: 581–590.
- 97 Ekblom, P., Thesleff, I., Saxén, L., Miettinen, A. and Timpl, R. (1983) *Proc. Natl. Acad. Sci., USA*, **80**: 2651–2655.
- 98 Partanen, A.-M. and Thesleff, I. (1987) *Differentiation*, **34**: 18–24.
- 99 Ichinose, M., Miki, K., Furihata, C., Tatematsu, M., Ichihara, Y., Ishihara, T., Katsura, I., Soga, K., Fujii-Kuriyama, Y., Tanji, M., Oka, H., Matsushima, T. and Takahashi, K. (1988) *Cancer Res.*, **48**: 1603–1609.

REVIEW

**Cellular and Molecular Aspects of
Embryonic Induction**

HEINZ TIEDEMANN

*Institut für Molekularbiologie und Biochemie, Freie Universität Berlin,
Arnimallee 22, D-1000 Berlin (West)33,
Federal Republic of Germany*

ABSTRACT—A homogeneous protein, which induces mesodermal and endodermal tissues in amphibian gastrula ectoderm (“vegetalizing factor”) has been isolated from chicken embryos. Inducing factors with similar chemical properties have been found in the *Xenopus* XTC-cell line and in calf kidney. The factors belong to evolutionary conserved proteins, which may also have regulatory functions in later differentiation processes or the maintenance of differentiation. They are related to the TGF- β protein superfamily. Members of this and of the FGF protein family induce mesodermal tissues. In early embryos mesoderm inducing factors show a graded distribution. Masked maternal neural inducing factors are in part activated after the cleavage stages. They have been partially purified from *Xenopus* embryos. We could show that phorbol ester evokes neural differentiation, suggesting a signal transduction mechanism which may include phospholipases and protein kinases.

INTRODUCTION

Amphibian eggs and embryos have been widely used to study the development of vertebrates. Early stages which can be handled with relative ease, are endowed with a high regulatory capacity. They are favorite objects for the study of tissue determination and induction. Determination has been defined as a process which initiates a specific pathway of development by singling it out from various possibilities for which the system is competent [1]. In very early stages determination is not yet definitive (except for endoderm) and can be changed by inductive tissue interactions. Dorsal ectoderm isolated before gastrulation forms epidermis like cells as does ventral ectoderm [2]. In 1924 Spemann and Hilde Mangold discovered that the ectoderm can be induced by the presumptive mesoderm [3]. When the induced dorsal ectoderm is isolated after gastrulation it forms the different parts of the nervous system. The induc-

tion of the nervous system is not an all or none, but a progressive process. Isolation experiments [4] and grafting experiments [5] have shown that at successive stages of gastrulation neural differentiations are obtained in the following order: Neural crest derivatives, archencephalic (forehead) and deuterocephalic (hindhead) structures.

**Test of inducing activity on omnipotent
gastrula ectoderm**

The inducing activity of tissues or isolated factors can be tested on omnipotent gastrula ectoderm. The differentiation of ectoderm can up to the early gastrula stage still be channelled into other pathways by the addition of inducers. In the implantation method devised by Mangold [6, 7] a piece of tissue or a pellet which contains inducing factors is implanted through a slit in the ectoderm into the blastocoelic cavity of an early gastrula of *Triturus* or *Ambystoma*. By the gastrulation movements the implanted tissue is brought into contact with the ventral ectoderm (Fig. 1). Purified factors

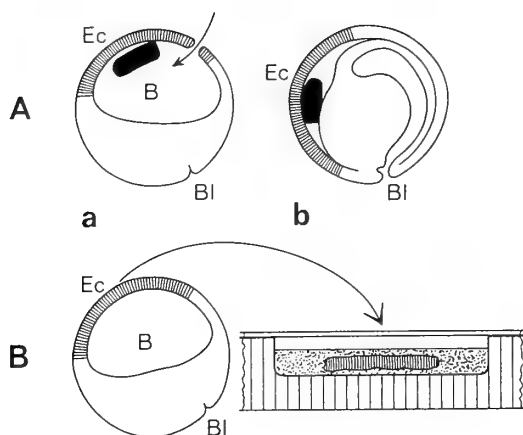


FIG. 1. Test of inducing factors. A. Implantation method a) Insertion of the implant into the blastocoelic cavity of an early gastrula, b) Position of the graft after gastrulation, facing the ventral ectoderm. B. Test on isolated ectoderm in solution. Ec = ectoderm; B = blastocoelic cavity; BI = blastopore. From Knöchel *et al.*, Blut, 59: 208 (1989), Springer-Verlag, Berlin.

can be tested by the implantation method in different dilutions, if the inducing substance is mixed with a non-inducing protein (i.e. γ -globulin) before the pellet for implantation is prepared. *Xenopus* gastrulae cannot be used for the implantation method [8] due to the different architecture of *Xenopus* embryos. Inducing factors can be tested in solution on isolated ectoderm of *Xenopus*, *Triturus* or *Ambystoma* embryos [7, 9, 10]. Bovine serum albumin is added to the solution to prevent the adsorption of the small amount of highly purified inducing factors to glass or plastic surfaces [11]. The test on isolated ectoderm has the advantage that *Triturus* and *Ambystoma* as well as *Xenopus* embryos which are available all the year round can be used, but the disadvantage that all induced explants must be examined histologically. Biochemical markers are at present only available for a limited number of tissues.

The response of ectoderm from different species especially to neural inducers is different. *Ambystoma* ectoderm is most susceptible to neural induction. Isolated ectoderm cultivated in a physiological salt solution forms neural tissue without the addition of an inducing factor (so called autoneuralization). *Triturus alpestris* ectoderm does on

the contrary not form any neural tissue at physiological salt concentration, but forms neural tissues when the Na^+ ion concentration is increased 1.5 fold [7]. *Xenopus* ectoderm is the least susceptible and does not form neural tissues at an 1.5 fold increased salt concentration. A strong autoneuralization, however, has been observed if the *Xenopus* ectoderm is dissociated into single cells and reassociated after a lag period [12].

Neural induction and neural inducing factors

The temporal changes of the neural inducing capacity of the presumptive dorsal mesoderm as well differences in the regional inductive capacity of the invaginated mesoderm (the archenteron roof) have been extensively investigated. The experiments have been carried out on *Triturus* and *Ambystoma* embryos which are more suitable for this type of investigation than the smaller and more rapidly developing *Xenopus* embryos [review 14]. The presumptive dorsal mesoderm of early cleavage stages induces neural tissues at a very low rate. The inducing activity starts at the morula stage [13]. Saxén and Toivonen [15] discovered that the simultaneous implantation of a mostly forehead inducing heterologous tissue (guinea pig liver) and a mostly mesoderm inducing tissue (guinea pig bone marrow) induced preferentially forehead, hindhead or neural tube depending on the proportions of neural and mesodermal inducers. This did lead to the theory that a double gradient of a neuralizing and a mesodermalizing agent are in the embryo responsible for the induction of the different regions of the nervous system. By other experiments ("the fold method") Nieuwkoop *et al.* [16] came to the conclusion that in neural induction a wave of activation (resulting in archencephalic structures) is followed by a wave of transformation (resulting in deuterocephalic structures). Attempts by Tiedemann *et al.* [17] to purify a deuterocephalic (hindhead) inducer led to the separation of a neural-archencephalic (forehead) and a mesoderm inducing fraction. Combination of the two fractions in different proportions did lead to hindhead and neural tube induction [18]. Toivonen and Saxén combined dispersed cells of the mesoderm and the forebrain anlage of

gastrulae in different ratios [19, 20]. They observed that a larger proportion of mesodermal cells causes formation of more caudal parts of the central nervous system. The ability of cells of the forebrain anlage to be transformed to more caudal parts of the brain is lost after about 10-12 hr, the transforming ability of the mesoderm lasts somewhat longer [21]. Isolated dorsal ectoderm of early *Triturus* gastrulae (which in normal development is induced to the nervous system) as well isolated ventral ectoderm can be induced to neural structures [22, 23]. In *Xenopus* the ventral ectoderm is, however, induced less frequently. This could be due to an earlier loss of competence in the ventral ectoderm but can not be considered as neural "predetermination" of dorsal ectoderm, which as ventral ectoderm forms neural tissues only after a neuralizing stimulus. The homeotic gene *XHox 6* which is expressed early in the development of the neural plate and restricted to the middle and posterior part of the neural axis was used as a marker for neural induction in these experiments [24]. An antigen related to the *Drosophila* homeotic gene *invected* (which is involved in segmentation) is expressed in the anterior neural plate [25].

The experiments on the transmission of the neural stimulus and the chemical nature of neural inducing agents are described in an excellent review by Saxén [26] and will only briefly be mentioned. Saxén and Toivonen have shown that the separation of the inducing mesoderm and the reacting ectoderm by nucleopore filters with pore diameters down to $0.05\ \mu$ did not prevent neural induction. Cytoplasmic bridges were not observed by electronmicroscopy, so that direct cell contacts in the transfilter experiments can be ruled out [27, 28]. The induction depends on short range interactions. Tacke and Grunz [29] observed that a close juxtaposition of the ectoderm and the inducing chorda mesoderm (distance of plasma membranes of opposite cells less than 50 nm) is needed for neural induction. This is correlated with an increase of the number of coated pits, a feature of receptor-mediated endocytosis, in the ectoderm. Connecting cell projections between ectoderm and mesoderm but no cytoplasmic bridges, which could allow a free transfer of inducing factors through intercellular channels, are formed during the mid-

gastrula stage [30].

The neural inducing activity of the blastoporal lip is diminished when the secretion of the factor from the blastoporal lip is impaired by treatment with actinomycin D or cycloheximide, substances which could inhibit the synthesis of components of the export system [31]. The factor may be secreted by a mechanism similar to that found in oocytes. Oocytes can secrete proteins which are injected or synthesized on foreign m-RNA. The proteins are probably sequestered into vesicles and exported by exocytosis [review: 32].

A small amount of neural inducing protein was isolated from the extracellular space between mesoderm and the neural plate, whereas proteoglycans from the extracellular space, isolated from the aqueous phase after phenol extraction, did not induce [33]. The proteoglycans did on the contrary prevent the autoneuralization of *Triturus alpestris* ectoderm cultured in Flickinger salt solution with 1.5 fold Na^+ ion concentration (Hildegard Tiedemann, unpublished experiments). The extracellular material did not contain RNA indicating little contamination from damaged cells. Duprat and Gualandris have shown that the extracellular material on the inner surface of the ectoderm is not implicated in neural determination [34]. The electric coupling of ectoderm and mesoderm which occurs 3-6 hr after combination of the two tissues [35] as well as the change of Na^+ and K^+ ion concentrations in induced ectoderm [36] may not be a prerequisite but a consequence of induction.

The induction of kidney tubules in meta-nephric mesenchyme in transfilter experiments depends on the other hand on direct cell to cell contact by cell processes penetrating the filter [37]. The cell to cell interaction leading to induction is dependent on protein glycosylation [38] and may be due to factors which are integrated into the plasma membrane or extracellular matrix proteins [for an example, 39]. Neural inducing protein factors have been separated from the soluble fraction of chicken embryo brain and retina by electrophoresis and isoelectric focusing [40] or by chromatography on DEAE-cellulose [15].

From *Xenopus* embryos neural inducing factors have been partially purified by Janeczek *et al.* [31, 41, 45 and unpublished experiments]. The factors

are found in oocytes and in gastrula stages in ribonucleoprotein particles of about 110 Å diameter, which are different from ribosomes or their subunits, in the high speed supernatant and in small vesicles. In addition a very small mesoderm inducing activity (as shown by the induction of hindheads; 15, 18) was found in these fractions. A forehead (archencephalic) induction is shown in Fig. 2. The factors are inactivated by proteolytic enzymes. The neural inducing factor in the RNP-particles is a basic protein with an apparent molecular weight >70,000 for the undegraded factor. Smaller proteins with neural inducing activity arise probably by enzymatic cleavage of the larger ones.

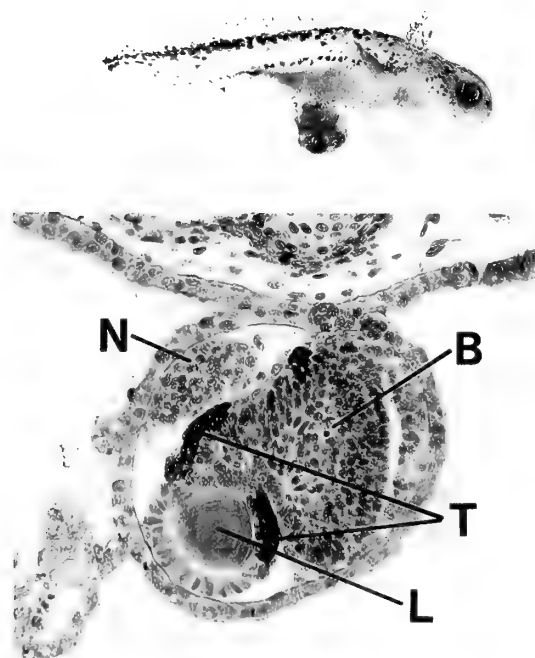


FIG. 2. A (upper). Forehead with eye induced on the ventral side of a *Triturus alpestris* larva by the implantation method. B (lower). Section through the forehead induction. L=lens; T=tapetum; B=brain; N=nose. The lumen of the induced nose is found in other serial sections of this induction.

The neural inducing factor in the supernatant has been partially purified by DEAE-cellulose

chromatography [53] or by size exclusion HPLC [41]. The factor from gastrulae elutes at several size classes (Mr 16,000, Mr 35–50,000 and Mr 130,000–150,000) whereas the factor from oocytes is preferentially found in the largest size class. The factor is not inactivated after reduction with mercaptoethanol. Its molecular weight is not changed after reduction, but many contaminating proteins are shifted to smaller size. To take advantage of this fact the high speed supernatant from gastrulae was prepared in the presence of the protease inhibitors α_2 -macroglobulin and leupeptin, reduced by mercaptoethanol and subjected to size exclusion HPLC. About 80–90% of the factor is then eluted at an apparent Mr of 100,000–150,000. When this protein fraction was subjected to SDS-polyacrylamide gel electrophoresis besides large proteins with an apparent Mr up to 150,000 also molecules of much smaller size were found. They obviously constitute a complex which is stable in 50% formic acid. Proteins of different size were then electroeluted from the gel and tested. About 20–30% of the neural inducing activity is found in proteins of an apparent molecular weight of 100,000–90,000, 70–80% of the activity in smaller proteins of Mr 15,000–25,000. Up to this step the smaller factor is purified about 800–1,000 fold. The experiments suggest that the larger factor could be a precursor of the smaller ones. The complex is not artificially formed in 50% formic acid. When the high speed supernatant was centrifuged on a sucrose gradient, most of the neural inducing activity was found in proteins larger than 100,000 Dalton.

It is possible, but has not been proven, that the factor in the RNP-particles is related to the supernatant factor. The factor in the ribonucleoprotein particles is, as was already mentioned, a basic protein, the factor complex in the supernatant, as the factor extracted from a fraction of small vesicles, an acidic protein (isoelectric point pH 5.5). Incubation with neuraminidase, hydrolysis with sulfuric acid under conditions where neuraminic acid is completely split from glycoproteins [44] or chemical deglycosylation with fluoromethansulfonic acid [Hoppe *et al.* unpublished experiments] did not change the isoelectric point. Treatment with phenol at 60°C does, however, convert a part

of the acidic neural inducing protein to a basic neural inducing protein perhaps by partially dissociating protein complexes.

Previous experiments have shown that the neuralizing factor is a maternal protein which is present in oocytes in ribonucleoprotein particles as well as in the supernatant in a masked biologically not active state [31, 44]. The neural inducing activity of the presumptive dorsal mesoderm increases from the morula stage onward [13, 46, 47]. This could depend on a partial activation of a maternal factor. The dorsal cortex has no inducing capacity [46]. The masked factors can artificially be activated by precipitation with ethanol, which denatures large protein complexes or by treatment with dissociating agents as urea, SDS or formic acid [31]. Whether the proteolytic cleavage of the precursor is related to the activation of the neuralizing factor is, however, not known. The precursor could be biologically inactive in the native state and treatment with dissociating agents like formic acid or SDS could lead to its activation. It is well known that for instance in enzymes regulatory domains can maintain a catalytic domain in an inactive state within a single peptide chain. In such molecules partial denaturation under dissociating conditions can have a similar effect as limited proteolysis (which eliminates the regulatory domain). Whether such an interaction between different domains of a single peptide chain exists in the large sized neural inducing factor is, however, not known. It is on the other hand not excluded (and may even be more likely) that other proteins which are associated with the factor keep the factor in a masked state and that the dissociation of the complex leads to its activation. The physiological process of demasking the factor(s) is unknown.

A small neural inducing activity has been found in germinal vesicles and in nuclei from later stages after activation with ethanol. Whether the factor in the nuclei differs from the factor(s) in the cytosolic fractions is not known [48]. Inducing factors are not integral proteins of plasma membranes [49].

Neural plates of *Triturus alpestris* induced by the underlying mesoderm acquire in turn neural inducing activity (homoio-genetic induction). This is correlated with the activation (and release) of a

neuralizing factor from the neural plate and may suggest an autocrine mechanism. It has, however, to be proven whether the neuralizing factor from mesoderm is identical with the releasing factor or whether special releasing (and demasking) factors exist [50].

Both the factors from RNP-particles and from the cytosol remain fully active when they are covalently bound to bromocyno-Sepharose or bromocyno-Sephadex particles, which cannot be taken up by the ectoderm cells. Control experiments have shown that the inducing activity is not due to a release of the bound factors [51]. This suggested that a signal transduction mechanism is involved in neural induction. We could show that neural tissues are formed in isolated ectoderm of *Triturus alpestris* [52] and to a lesser extent in *Xenopus* ectoderm which in addition differentiates also to mesodermal tissues [53], when phorbol ester (PMA=phorbolmyristate-acetate; TPA=tumor promoting agent) is added [52]. Phorbol ester activates protein kinase C (PKC), which is assumed to be involved in the transduction of signals from the plasma membrane to the nucleus. The activity of protein kinases has therefore been measured in isolated gastrula ectoderm induced with a neuralizing factor. Davids [53] has shown that the activities of protein kinase C (or a related enzyme), which was measured with an enzyme-specific peptide substrate, as well as of c-AMP/c-GMP dependent kinases increase after induction. Addition of c-AMP or c-GMP or their mono- and dibutyl derivatives to ectoderm does, however, not evoke neural differentiation [54]. It is therefore unlikely that the activation of c-AMP/c-GMP dependent kinases is the primary event in neural induction. Several proteins are more strongly phosphorylated in homogenates of induced ectoderm [53]. These proteins are also phosphorylated in homogenates of neural plates isolated from early neurula stages. The phosphorylation of 31 kD and 15 kD proteins seems to depend on PKC or a related enzyme. These phosphoproteins have first been detected 60 min after induction of isolated ectoderm with neuralizing factor. [Davids, unpublished experiments]. Their phosphorylation may not be the first event in neural induction, but may rather be part of a phosphory-

lation cascade. Otte *et al.* [55] have shown that protein kinase C is translocated to the plasma membrane after induction. Whereas phorbol esters are artificial activators of PKC's, the physiological activators are diacylglycerols or unsaturated fatty acids depending on the subspecies of the PKC's [review 56]. This may suggest that the breakdown of membrane phospholipids is involved in signal transduction after induction. Diacylglycerols and Inosin triphosphate are generated by phosphoinositide-specific phospholipase C (PLC), arachidonic acid is generated by phospholipase A₂. Experiments on signal transduction by adenylate cyclase have shown that the coupling of adenylate cyclase to effector occupied receptors is mediated by G- (GTP-binding) proteins. Adenylate cyclase activity is then terminated by GTP-ase activity intrinsic to the G-proteins. Non-hydrolyzable GTP-analogues as GTP_γS (guanosine-5'-O-thiotriphosphate) has therefore an intensifying effect. The finding that GTP_γS stimulates PLC activity have led to the assumption that the control of PLC occurs in a way analogous to adenylate cyclase [57, 58 review 59].

GTP_γS (1 μM) can evoke neural differentiation in gastrula ectoderm of *Triturus alpestris* (but not of *Xenopus laevis*; Loppnow-Blinde and Tiedemann, unpublished experiments). Li⁺ ions which are known for many years [60, 61] to evoke neural and mesodermal differentiation in amphibian gastrula ectoderm have also been shown to interfere with the phosphoinositide cycle [62, 63]. This could suggest that phospholipase C is involved in the induction mechanism. The other enzyme of the phospholipid metabolism which could be involved, phospholipase A₂, is easily activated by disturbances of plasma membrane conformation. It is possible that such processes could be related to the so called "autoneuralization" effect.

It has to be stressed that absolutely no autoneuralization occurred under the conditions for the test of neuralizing factors.

Phorbol ester can activate the Na⁺/H⁺ antiport system [64, 65]. Ectoderm from early gastrula stages of *Triturus alpestris* (but at the concentrations employed not ectoderm of *Xenopus*) forms neural tissues when N-(2-hydroxyethyl) piperazine-N-ethansulphonic acid (Hepes) in its proto-

nated form is added to the medium as a buffer substance [66]. These and other observations led to the consideration that Hepes could lead to an export of H⁺ from the ectoderm cells by an activation of the Na⁺/H⁺ antiport system. Ethylisopropyl-amiloride (100 μM) a potent and specific inhibitor of the Na⁺/H⁺ antiport [67], does, however, not inhibit the induction of *Triturus alpestris* ectoderm by the neuralizing factor. [Cragoe and Hildegard Tiedemann, unpublished experiments]. Similarly the action of growth factors is not inhibited by Amiloride derivatives in physiological bicarbonate buffer. These and other observations [reviewed in 68] suggest that a change of pH is probably not an intracellular messenger for neural induction or growth stimulation.

Concanavalin A, a lectin which binds especially to mannose residues in glycoproteins and Concanavalin A coupled to Sepharose evoke neural differentiation in gastrula ectoderm of *Triturus pyrrhogaster* [69] as well of *Xenopus laevis* [70] and of *Rana temporaria* [71, 71a]. The latter is only weakly induced by Con A-Sepharose [71]. Concanavalin could either bind to a cell surface receptor for the neuralizing factor or it could change the conformation of the plasma membrane after binding to distinct sites. Other lectins lead to a loss of neural competence [72]. Retinoic acid does not induce neural differentiation in gastrula ectoderm [Hildegard Tiedemann, unpublished experiments, 73]. The substance causes, however, microcephaly. It has been suggested that retinoic acid specifies regional differentiation of the central nervous system in amphibians [73] and in chicken the anterior-posterior axis during limb development [74]. The identification of nuclear receptors for retinoic acid in several tissues speaks strongly for its function as a physiological regulator, but its many teratogenic actions at a low concentration make it somewhat difficult to discriminate between these two possibilities.

A neural cell adhesion molecule [N-CAM, 75] is expressed during early neurogenesis in *Xenopus* [76]. Other neural specific proteins expressed after induction are neurofilaments and tetanus-toxin binding sites [77].

Induction of mesoderm and endoderm and the factors involved

The presumptive dorsal mesoderm has been regarded as the "organizer" of embryonic development. This should imply that this region is already determined to its fate in the fertilized egg. But when in 1962 Nakamura [78] isolated the presumptive mesoderm (the marginal zone) from different developmental stages of *Triturus pyrrhogaster*, the isolated mesoderm from very early stages did not differentiate into mesodermal tissues, its prospective fate. The marginal zone acquires its differentiation capacity in the morula stage. This demonstrated the epigenetic development of the "organizer" [79]. Hildegard Tiedemann [80] in 1965 observed that gastrula endoderm of *Triturus alpestris* when implanted into the blastocoel of early gastrula hosts induced in the ventral ectoderm mesenchymatic tails in about 20% of the cases. In 1967 Ogi [81, 82] combined isolated endoderm and ectoderm and obtained the induction of mesodermal tissues. He explained the formation of mesoderm as a result of regulation on the basis of two opposite animal-vegetal and vegetal-animal physiological gradients. The induction of mesodermal tissues in ectoderm explants which were combined with endoderm has been investigated in detail by Nieuwkoop and collaborators [83, 84] and Nakamura and collaborators [85]. Nakamura emphasized the importance of an animal-vegetal gradient, Nieuwkoop the induction of mesodermal tissues in ectoderm by the endoderm [86, 87]. Both views are certainly not mutually exclusive. Grunz and Tacke [88] have shown that the induction of mesoderm is not prevented by placing a Nucleopore filter between endoderm and ectoderm. Electronmicroscopy did rule out cell processes traversing the filter. The inducing effect is obviously mediated by diffusible factor(s). Dawid *et al.* [89] came to a similar conclusion. They observed that the appearance of a muscle specific marker was prevented by completely dissociating and dispersing *Xenopus* embryos during the period from early cleavage to early gastrula, a procedure that would dilute secreted inducing factors. Gurdon *et al.* [90] have concluded from dissection experiments that the "subequatorial"

zone of the fertilized *Xenopus* egg contains all components for muscle gene activation. Because the boundaries of the subequatorial zone are not exactly defined, the zone could include some presumptive endoderm. It is, however, not excluded that active factors which are needed for the differentiation of mesodermal tissues are in the fertilized egg already localized in the vegetal most part of the marginal zone. Asashima [91] has investigated the inducing capacity of endoderm from different stages of *Triturus alpestris*. Endoderm taken from uncleaved eggs induces mesothel and blood cells in a low percentage, whereas endoderm from later stages in addition induced muscle, notochord and pronephric tubules. Blastula endoderm has the highest inducing activity. Thereafter the inducing activity declines. The increase may depend on the activation and release of masked factor(s). *Xenopus* endoderm induces mesoderm from the cleavage to the early gastrula stage [92].

The inducing capacities of the dorsal and the ventral endoderm differ. Boterenbrood and Nieuwkoop [93] have shown that the dorsal endoderm induces dorsal mesodermal tissues (notochord and somites) whereas the ventral endoderm induces more ventral mesodermal tissues (absence of notochord, no well arranged somites, blood cells). Experiments with cell lineage labels and region specific markers confirmed that the dorsovegetal material induces dorsal type mesoderm and ventrovegetal material ventral type mesoderm [94]. Yamada has already shown in 1940 [95] that organs which are formed from different presumptive mesodermal regions change to a more dorsal type (i.e. blood cells to nephric tubules or nephric tubules to somites) when the notochord anlage is added to the explants. This suggests that within the presumptive mesoderm a dorso-ventral gradient of (still unknown) regulatory factor(s) is established, which in addition to factors from the ventral and dorsal endoderm is involved in the subdivision of the mesoderm. Gurdon *et al.* have shown that in embryos which have just completed gastrulation α -skeletal and α -cardiac actin genes start to be transcribed in the somite region of the mesoderm and to a lesser extent in the ventral mesoderm, which possibly

gives rise to the heart [96]. Actin c-DNA probes have been used as mesoderm markers. The ability to react to inducing factors, the competence of the ectoderm, is limited to certain stages. The reason for this temporal limitation is not yet known. In *Triturus alpestris* [97] and to a lesser extent in *Xenopus laevis* [98], the loss of competence is delayed when the protein synthesis in the ectoderm is inhibited.

A factor which induces mesoderm and endoderm has been isolated from 9–11 days old chicken embryos by Tiedemann *et al.* [99–102]. The factor is protein in nature. The most efficient way for its separation from nucleic acids is the extraction with phenol [103]. The phenol procedure was developed because at that time it was thought that the factor could be RNA in nature. The phenol procedure has then been widely used for the preparation of RNA. The RNA did, however, not show inducing activity. The final purification of the factor was achieved by size exclusion and reversed phase HPLC. The acid stable factor, which is enriched about 10^6 times, has been called vegetalizing factor, because the tissues which are induced constitute the vegetal half of the embryo. On the basis of our earlier investigations the factor has recently been isolated in higher yield [Tiedemann *et al.* unpublished results]. The method employs extraction with acid ethanol, the final purification is achieved by four consecutive steps of reversed phase HPLC. The factor induces at a concentration of 0.5–1.0 ng/ml in about 50% of the cases mesoderm, including muscle. The apparent molecular mass of the factor determined by SDS-polyacrylamide-electrophoresis is about 25,000 Dalton and that of the biologically inactive subunits after reduction of disulfide bridges 13,000 Dalton, the isoelectric point about pH 8.0. By size exclusion chromatography in 50% formic acid an apparent molecular mass of 13,000 was found [102]. The dissociation into subunits may be caused by reduction of interchain or intrachain disulfide bonds by formic acid and conformational changes. The inducing activity is diminished after size exclusion HPLC in 50% formic acid. It is only partially restored after the removal of formic acid. The inducing activity is not diminished when the partially purified factor was incu-

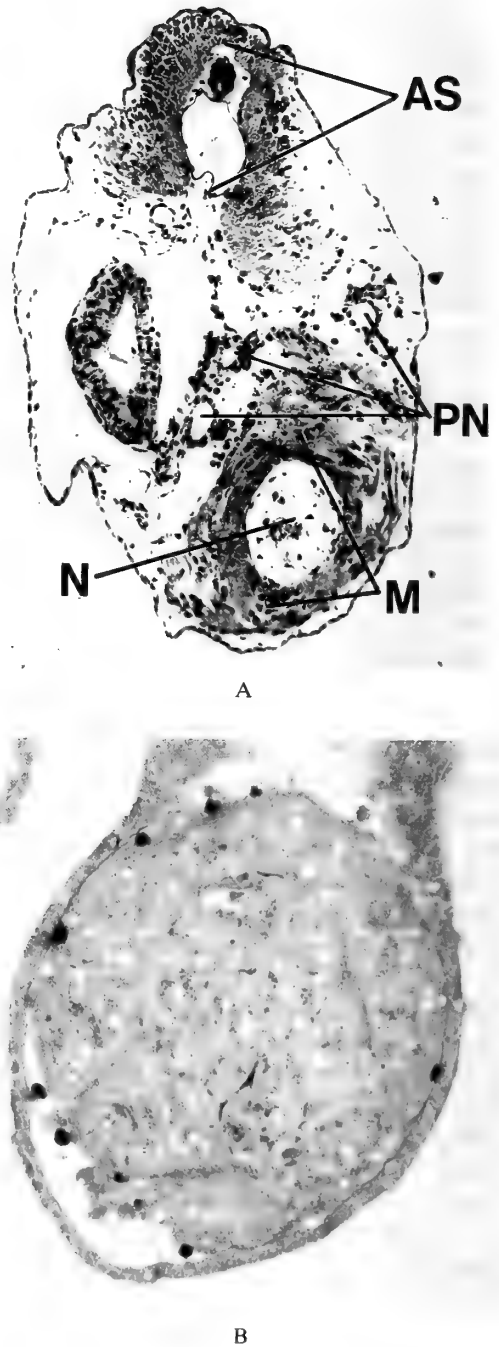


FIG. 3. A. Mesoderm induced in a *Triturus alpestris* larva by the implantation method. Induced tissues: N=notochord; M=muscle; PN=pronephric tubules. AS=Axis system of the host larva. B. Section through a *Xenopus* explant with induced somites.

bated with formic acid. A mesoderm inducing factor (Mr 23,500) which was isolated by Smith *et al.* from the XTC (fibroblast) cell line of *Xenopus laevis* [105] has similar properties [104]. Another factor which has similar properties as the factor from chicken embryos has recently been isolated from calf kidney (Plessow and Davids, unpublished experiments). This suggests that the factor is an evolutionary conserved protein which may also have regulatory functions in later stages of embryogenesis, in adult differentiation processes such as erythrocyte or cartilage differentiation or in regeneration processes. Asashima and coworkers have made the interesting observation that activin A, which is identical with the erythroid differentiation factor (EDF), has mesoderm inducing activity at a low concentration [106].

The vegetalizing factor induces, depending on its concentration all kinds of mesodermal tissues. Endoderm seems preferentially to be induced at a very high concentration. At gradually lower concentrations pronephros, somites (Fig. 3), notochord and mesothelia are induced [107]. In addition to mesodermal and endodermal tissues cells with the typical appearance of primordial germ cells were observed in explants which were cultured for at least 20 days [108].

When tested at a very high concentration by the implantation method the vegetalizing factor causes an exovagination (not exogastrulation) of the gastrula (Fig. 4). Endoderm which had invaginated during gastrulation, reappears in the blastopore and spreads over the induced ectoderm. The exovagination is caused by a change of cell affinities [109] of the gastrula ectoderm induced to endoderm and mesoderm. A similar effect has been observed after injection of XTC-cell factor into the blastocoel of *Xenopus embryos* [110].

The vegetalizing factor is in contrast to the neural inducing factor inactivated after covalent coupling to BrCN-sepharose or BrCN-sephadex [111]. The activity is completely recovered after degradation of the sephadex matrix with dextranase [112]. This suggests that the factor must be taken up by the cells to become biologically active. It does not exclude that cell surface receptors are involved.

A factor from guinea pig bone marrow which was partially purified by Yamada and Takata induces as the vegetalizing factor besides mesodermal also endodermal tissues [10, 113]. The histological identification of endodermal tissues is, however, difficult because endoderm differentiates late. The availability of endodermal

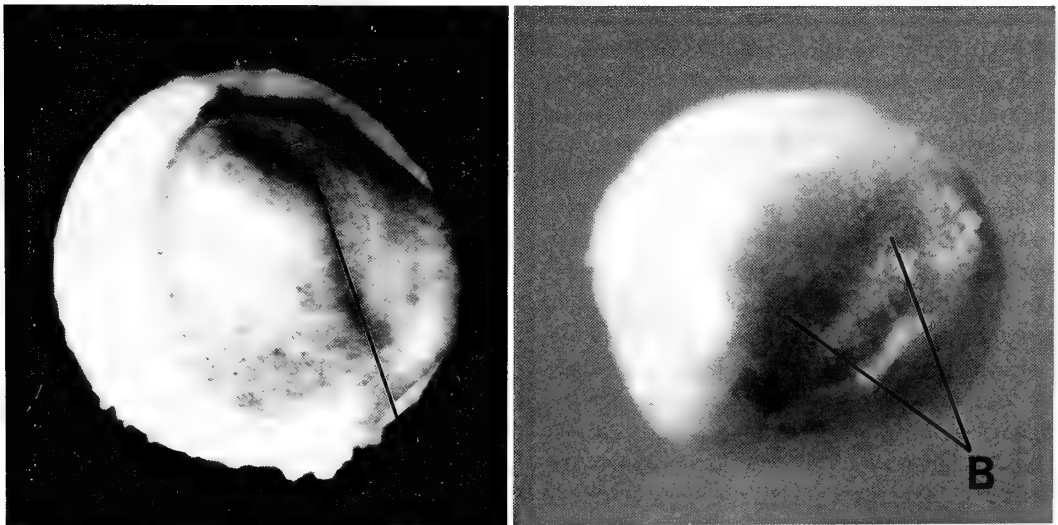


FIG. 4. Exovagination of *Triturus alpestris* embryos produced by the implantation of vegetalizing factor in high concentration into the blastocoel. The embryos are partially overspread by white migrating yolk-rich endoderm. A. N=small neural plate. From Kocher-Becker and Tiedemann, Science, 147: 167 (1965). Copyright 1965 by the AAAS. B. =rudiment of epidermis. A small rudimental neural plate was found in histological sections.

markers will therefore facilitate the detection of endoderm. Recently Rosa [114] has isolated mRNA's induced in *Xenopus* ectoderm by a partially purified XTC-cell factor. One of these RNA's encoding a homeodomain containing protein (Mix 1), which is expressed 20' after the addition of an inducing factor (XTC-cell factor or bFGF and TGF- β in combination) to ectoderm, is found in the embryo mostly in the future endoderm. Jones *et al.* [115] have prepared a monoclonal antibody which reacts with tail-bud endodermal tissues to identify endoderm induced in ectoderm explants.

Besides from guinea pig bone marrow mesoderm inducing factors have been extracted and partially purified from liver [116] and from the carp swim bladder [117].

The vegetalizing factor is *in vivo* in part bound to an acidic proteoglycan [118] and *in vitro* binds to heparin-sepharose which was used by Born *et al.* for affinity chromatography of the factor [119]. It was therefore tempting to investigate whether heparin binding growth factors of the FGF (fibroblast growth factor) protein family induce mesodermal tissues. It could indeed be shown that a-(acidic) as well as b-(basic) FGF induce the formation of mesodermal tissues [120–123]. Like the vegetalizing factor from chicken embryos both FGF's induce at a high concentration somites and at lower concentrations endothelium lined vesicles which contain, besides some pycnotic cells, single cells with the typical appearance of immature blood cells [123]. Recombinant human b-FGF induces at higher concentrations besides skeletal muscle also heart muscle with its typical honeycomb like appearance, surrounded by a mesothelium lined pericardial cavity [124].

In *Xenopus* the determination of heart mesoderm occurs prior to the end of gastrulation. The heart mesoderm is located in the gastrula in the deep zone lateral to the head mesoderm and migrates laterally and ventrally to fuse in the ventral midline during the late neurula stage [review 125]. The deep dorsal endoderm seems to contribute to the specification of heart mesoderm, whereas the superficial pharyngeal endoderm may enhance heart morphogenesis during later stages [126]. It is possible that in *Xenopus* ectoderm

explants endoderm, which is induced by b-FGF, undergoes regional differentiation and specifies the heart anlage. In urodeles (*Triturus alpestris*) no heart is formed when the endoderm is removed at the neural plate stage [127].

Notochord is not or very seldom induced by the FGF's in *Xenopus* ectoderm. The notochord anlage is the dorsal most part of the mesoderm. It has been suggested that FGF's induce preferentially ventral mesoderm [120]. The spectrum of tissues, which are induced depends also on the concentration of the factors, the species, and the test methods which are used. Recombinant b-FGF induces besides other mesodermal tissues also notochord in ectoderm explants of *Triturus alpestris*. Notochord is very rarely induced by the vegetalizing factor from chicken embryos in *Xenopus* ectoderm explants, but is induced at higher frequency when tested by the implantation method on *Triturus alpestris* gastrulae. Acidic and basic fibroblast growth factors show an amino acid sequence homology of 57%. To the FGF protein family belong also oncogene products and interleukins [review 128]. The protein products of the oncogenes int-2 and hst/ks (kfgf) have been shown to induce mesoderm with different potencies [129].

The vegetalizing and the fibroblast growth factors share heparin affinity but differ in other properties such as hydrophobicity, inactivation after reduction of disulfide bonds and molecular mass. In these properties the vegetalizing factor and the XTC-cell factor are more closely related to the transforming growth factors β . The transforming growth factors β stimulate phenotypic transformation (anchorage independent growth) of two cell lines, but their preferential action seems to be growth inhibition. Whether TGF- β stimulates or inhibits cell growth seems to depend on the entire set of growth factors acting on a cell [130, 131]. The promotion of angiogenesis by TGF- β seems to be mediated by monocytes which are attracted and stimulated to synthesize interleukin 1 [132]. The TGF- β family comprises genes with regulatory properties in embryogenesis, the β subunits of inhibin and the activins, substances which regulate the release of the follicle stimulating hormone [review 128]. The erythroid differentiation factor [EDF; 133] is identical to activin A, a homodimer

consisting of two β_A subunits [134]. The TGF- β family includes also the Vg1 gene, which was discovered by Weeks and Melton [135]. The m-RNA transcribed from this gene is uniformly distributed in the cytoplasm of immature *Xenopus* oocytes, but is then translocated to the vegetal half where it is localized as a crescent at the vegetal pole of mature oocytes [136].

Rosa *et al.* and Knöchel *et al.* have shown that transforming growth factors induce mesodermal tissues [122, 137, 138]. TGF- β_1 and β_2 induce at a concentration of 1 $\mu\text{g/ml}$ in *Triturus alpestris* ectoderm in about 60% of the cases small endothelium lined cavities which contain immature blood cells as well mesenchyme and in elongated explants at one pole a dense blastema tissue and metameric strands of cells like lateral plate mesoderm, which in the distal part of the explant form large masses of endothelial (mesothelial) networks. The networks can form capillary like structures. Muscle and notochord are induced in *Xenopus* and *Triturus* ectoderm only by TGF- β_2 . *Xenopus* explants were not induced by TGF- β_1 [137]. The TGF's or closely related factors induce in mammalian cell culture cartilage [139]. Asashima *et al.* [117] have recently shown that activin A (EDF) induces mesoderm at a low concentration. Activin A has a 40% sequence homology to TGF- β . Activins and inhibins bind as the vegetalizing factor to heparin-Sepharose [140]. The affinity of these factors to heparin is, however, lower as compared to the fibroblast growth factors. Binding to heparin depends on the native protein structure. Because the TGF's are extracted under dissociating conditions which change their protein conformation, it is not known whether the TGF's bind also to heparin.

The transforming growth factors are probably not identical with, but related to the vegetalizing factor and the XTC-cell factor. TGF- β and a mesoderm inducing factor in human blood platelets can be separated by size exclusion chromatography [Dau *et al.* unpublished experiments]. The growth factors must be applied to gastrula ectoderm in higher concentrations than the inducing factors for mesoderm induction.

The factors which determine endoderm and induce mesoderm in the embryo have not yet been

definitively identified. Kirschner *et al.* [141] have found that a m-RNA which is present in *Xenopus* oocytes and newly transcribed in the neurula stage, codes for a protein that is 84% identical to human b-FGF. The recombinant protein which was expressed from the c-DNA, induces at 20–50 ng/ml muscle specific actin m-RNA. This protein may be a natural inducer. b-FGF like proteins have been enriched from *Xenopus* eggs and embryos by heparin-Sepharose affinity chromatography [141, 142]. The factor is extracted in higher yield in the presence of Chaps, a zwitterionic detergent [Tiedemann *et al.*, unpublished experiments] and may in part be bound to particulate structures. Slack *et al.* [143] have identified receptors for the fibroblast growth factor in *Xenopus* blastula ectoderm. Besides the 4.2 kb transcript coding for the b-FGF like protein, a smaller transcript of 1 kb has been found which represents an antisense transcript to part of the FGF gene. It codes for an evolutionary conserved protein with a hitherto unknown function [144]. In addition to a b-FGF-like factor mesoderm inducing factors which are not bound to heparin-sepharose are present in *Xenopus* embryos. So far we could not extract with acid ethanol from the early stages of amphibian embryos a mesoderm inducing factor with properties similar to the vegetalizing or the XTC-cell factor. This could be due to the low solubility of the crude proteins, or sequences homologous to these factors could be integrated into larger proteins with other properties.

That different factors induce mesoderm is not unexpected. The factors could either induce more dorsal or more ventral regions of the mesoderm. They may also interfere with different targets in signal transduction chains from the cell surface to the chromatin.

Gene activation and pattern formation in early embryogenesis

In experiments with the vegetalizing factor from chicken embryos Minuth and Grunz [145] have shown that the differentiation of liver is enhanced by preventing interactions between the induced cells by dissociation of the induced *Triturus* ectoderm for 20 hr before reassociation.

Mesodermal tissues were induced at a high percentage if the ectoderm was not dissociated. This suggests that not different threshold concentrations of one factor, but cell interactions, in which additional factors are involved, are needed for the induction of different mesodermal tissues. Other experiments support this view. A shift in the quality of the induced tissues from mostly endoderm (induced at a high concentration of vegetalizing factor) to muscle and notochord was observed when a protein fraction, which was separated during the purification of the factor, was added to the highly purified factor. The added protein fraction alone had no mesoderm inducing activity [146]. Additional factors seem also to be involved in the induction of mesoderm by TGF- β . Medium which was conditioned by TGF- β induced ectoderm enhances the inducing activity [138]. This suggests that additional factors are secreted, which are either synthesized or activated in gastrula ectoderm treated with TGF β .

This does, however, not imply that endoderm is generally induced first and that factors generated in the endoderm then induce mesodermal tissues. A gene or genes activated by an inducer could activate other genes in the same cell or in neighboring cells, so that a network of genes would be generated. In induced ectoderm explants a large variety of interactions would be possible depending on inducer concentration, time of inducer action and of geometry. This can explain that in explants a variety of tissues in different proportions are induced.

The factors for determination of the axis system of the embryo and for the induction of the neural anlage are at least in part of maternal origin. The position of the factors which determine endoderm and mesoderm in the oocyte depends on cytoplasmic movements after fertilization [147]. The vegetal most blastomeres play an important part in axis formation. Gimlich and Gerhart [149] have shown that after UV-irradiation of the egg, which impairs the formation of axial mesodermal and of neural structures, one to three cells of the vegetal most octet of blastomeres from non-irradiated embryos of the 64 cell stage can partially or completely reconstitute axis formation. The inducing factors have probably their highest concen-

tration in these cells. Whether the maternal factor(s) which determine the endoderm act within the cell in which they are located, or by an autocrine mechanism on neighboring cells remains to be shown.

The mesoderm inducing factors are located in fertilized eggs and early embryos in a graded distribution [review 80, 87]. The precise localization of the factors and their mRNA's will, however, only be known when the genes coding for the factors have been isolated. It will then be possible to synthesize c-DNA's and after insertion into expression vectors the proteins, so that the distribution of the factors and their mRNA's can be measured by immunofluorescence or hybridization methods. So far only a *Xenopus* b-FGF related gene has been isolated [141].

The areas in which the factors are located in the embryo are probably larger than the areas of the tissues which are determined by these factors. A small amount of a mesoderm inducer is found in the animal (ectodermal) cap [150]. It is likely that not only a vegetal-animal graded distribution of factors, but also an animal-vegetal distribution of so far unknown factors exists. Animal pole explants of *Xenopus* express epidermis specific antigens which are not expressed in the vegetal half. The information to express one of these antigens is present in the animal half before cleavage [151, 152].

It should be borne in mind that the factors can be masked so that their total concentration is not equal to the concentration of the biologically active factor(s) or that other substances could counteract the inducing factors. Furthermore as in *Drosophila*, factors which repress gene activities [153] could be involved. Thus the ratio of two factors could decide whether a gene is activated in a certain position in the embryo. One factor in a graded distribution could on the other hand activate more than one gene depending on different threshold concentrations of the factor. A concentration dependent activation of different genes has been observed for the *Drosophila* bicoid protein [154–157]. It is, however, unlikely that one and the same factor directly induces different tissues at different threshold concentrations. A number of evolutionary conserved genes including homologs

of *Drosophila* regulatory genes are transcribed in *Xenopus* oocytes and embryos. Their differential expression in the embryo is one of the earliest events leading to tissue differentiation. The distribution of regulatory gene products seems not to be confined to the borders of the germ layers which in later stages reflect the tissue borders [114, 158].

These regulatory genes include genes which specify proteins with homeotic domains [review 159; 24, 25, 114, 160, 161] as well proteins with finger domains [162–164]. Both domains bind to DNA sequences and are thought to act as transcription factors.

Differential cell affinities which develop in the embryo [165] and the differential distribution of molecules of the extracellular matrix will then guide the morphogenetic process.

ACKNOWLEDGMENTS

Our own investigations which are included in this review were supported by the Deutsche Forschungsgemeinschaft and Fonds der Chemischen Industrie.

REFERENCES

- Hadorn, E. (1965) Brookhaven Symposium on Biology, **18**: 148–161.
- Grunz, H., Multier-Lajous, A.-M., Herbst, R. and Arkenberg, G. (1975) Wilhelm Roux's Arch. Dev. Biol., **178**: 277–284.
- Spemann, H. and Mangold, H. (1924) Wilhelm Roux's Arch. Entwicklungsmech. Org., **100**: 599–638.
- v. Woellwarth, C. (1952) Roux's Arch. Dev. Biol., **145**: 582–668.
- Eyal-Giladi, H. (1954) Arch. Biol., **65**: 179–259.
- Mangold, O. (1923) Wilhelm Roux's Arch. Entwicklungsmech., **100**: 198–301.
- Tiedemann, Hildegard (1986) In "Cellular Endocrinology: Hormonal Control of Embryonic and Cellular Differentiation" Ed. by G. Serrero and J. Hayashi, Alan R. Liss Inc., New York, pp. 25–34.
- Grunz, H. (1987) Zool. Sci., **4**: 579–591.
- Becker, U., Tiedemann, H. and Tiedemann, H. (1959) Z. Naturforsch., **14b**: 608–609.
- Yamada, T. and Takata, K. (1961) Dev. Biol., **3**: 411–423.
- Roberts, A. B., Anzano, M. A., Myers, Ch. A., Wideman, J., Blacher, R., Pan Yu-Ch. E., Stein, St., Lehrman, S. R., Smith, J. M., Lamb, L. C. and Sporn, M. (1983) Biochemistry, **22**: 5692–5698.
- Grunz, H. and Tacke, L. (1989) Cell Differ. Develop., **28**: 211–218.
- Asashima, M. (1980) Roux's Arch. Dev. Biol., **188**: 123–126.
- Saxén, L. and Toivonen, S. (1962) Primary Embryonic Induction. Logos Press-Academic Press, London.
- Saxén, L. and Toivonen, S. (1961) J. Embryol. exp. Morphol., **9**: 514–533.
- Nieuwkoop, P. D. (1952) J. exp. Zool., **120**: 1–108.
- Tiedemann, H., Becker, U. and Tiedemann, H. (1963) Biochim. Biophys. Acta, **74**: 557–560.
- Tiedemann, H. and Tiedemann, H. (1964) Rev. Suisse de Zool., **71**: 117–137.
- Saxén, L., Toivonen, S. and Vainio, T. (1964) J. Embryol. exp. Morph., **12**: 333–338.
- Toivonen, S. and Saxén, L. (1968) Science, **159**: 539–540.
- Toivonen, S. (1967) Exp. Biol. Med., **1**: 1–7.
- Holtfreter, J. (1933) Roux's Arch. Dev. Biol., **127**: 591–618.
- Holtfreter, J. (1933) Roux's Arch. Dev. Biol., **127**: 619–775.
- Sharpe, C. R., Fritz, A., De Robertis, E. M., and Gurdon, L. B. (1987) Cell, **50**: 749–758.
- Brivanlou, A. H. and Harland, R. M. (1989) Development, **106**: 611–617.
- Saxén, L. (1989) Int. J. Dev. Biol., **33**: 21–48.
- Saxén, L. (1961) Dev. Biol., **3**: 140–152.
- Toivonen, S., Tarin, D., and Saxén, L. (1976) Differentiation, **5**: 49–55.
- Tacke, L. and Grunz, H. (1988) Cell Differentiation, **24**: 33–44.
- Grunz, H. and Staubach, J. (1979) Differentiation, **14**: 59–65.
- Born, J., Janeczke, J., Schwarz, W., Tiedemann, H. and Tiedemann, H. (1989) Cell Differ. Develop., **27**: 1–7.
- Lane, Ch. D. (1983) Current Topics in Develop. Biol., **18**: 89–116.
- John, M., Janeczke, J., Born, J., Hoppe, P., Tiedemann, H. and Tiedemann, H. (1983) Roux's Arch. Dev. Biol., **192**: 45–47.
- Duprat, A. M., and Gualandris, L. (1984) Cell Differentiation, **14**: 105–112.
- Suzuki, A. S., Nakatake, H. and Hidaka, T. (1984) Differentiation, **28**: 73–77.
- Siegel, G., Grunz, H., Grundmann, U., Tiedemann, H. and Tiedemann, H. (1985) Cell Differentiation, **17**: 209–219.
- Saxén, L. and Lehtonen, E. (1978) J. Embryol. exp. Morph., **47**: 97–109.
- Eklblom, P., Nordling, S., Saxén, L., Rasilo, M.-L.

- and Reukonen, O. (1979) *Cell Differentiation*, **8**: 347–352.
- 39 Engel, J. (1989) *Febs Letters*, **251**: 1–7.
 - 40 Mikhailov, A. T., Gorgolyuk, N. A., Virtanen, I. and Lehto, V.-P. (1984) *Ontogenez*, **15**: 137–145.
 - 41 Janeczczek, J., Born, J., Hoppe, P., Schwarz, W., Tiedemann, H. and Tiedemann, H. (1986) In “Cellular Endocrinology: Hormonal Control of Embryonic and Cellular Differentiation” Ed. by G. Serrero and J. Hayashi, Alan R. Liss, New York, pp. 11–24.
 - 42 Janeczczek, J., John, M., Born, J., Tiedemann, H. and Tiedemann, H. (1984) *Roux's Arch. Dev. Biol.*, **193**: 1–12.
 - 43 Janeczczek, J., Born, J., Scharschmidt, M., Tiedemann, H. and Tiedemann, H. (1984) *Eur. J. Biochem.*, **140**: 257–264.
 - 44 Janeczczek, J., Tiedemann, H. and Tiedemann, H. (1986) *Progress in Developmental Biology*, B. Alan R. Liss, New York, pp. 357–360.
 - 45 Tiedemann, H. (1984) In “The Role of Cell Interactions in Early Neurogenesis”. Ed. by A.-M. Duprat, A. C. Kato and M. Weber, Plenum Press, New York, pp. 89–105.
 - 46 Malacinski, G. M., Chung, H.-M. and Asashima, M. (1980) *Dev. Biol.*, **77**: 449–462.
 - 47 Nakamura, O., Takasaki, H., Okumoto, T. and Iida, H. (1971) *Proc. Japan Acad.*, **47**: 203–208.
 - 48 Bretzel, G. and Tiedemann, H. (1986) *Roux's Arch. Dev. Biol.*, **195**: 123–127.
 - 49 Bretzel, G., Janeczczek, J., Born, J., John, M., Tiedemann, H. and Tiedemann, H. (1986) *Roux's Arch. Dev. Biol.*, **195**: 117–122.
 - 50 Grunz, H., Born, J., Tiedemann, H. and Tiedemann, H. (1986) *Roux's Arch. Dev. Biol.*, **195**: 464–466.
 - 51 Born, J., Hoppe, P., Janeczczek, J., Tiedemann, H. and Tiedemann, H. (1986) *Cell Differ.*, **19**: 97–101.
 - 52 Davids, M., Loppnow, B., Tiedemann, H. and Tiedemann, H. (1987) *Roux's Arch. Dev. Biol.*, **196**: 137–140.
 - 53 Davids, M. (1988) *Roux's Arch. Dev. Biol.*, **197**: 339–344.
 - 54 Grunz, H. and Tiedemann, Hildegard (1977) *Roux's Arch. Dev. Biol.*, **181**: 261–265.
 - 55 Otte, P. A., Koster, C. H., Snoek, G. T. and Durston, A. J. (1988) *Nature*, **334**: 618–620.
 - 56 Kikhawa, U., Kishimoto, A. and Nishizuka, Y. (1989) *Ann. Rev. Biochem.*, **58**: 31–44.
 - 57 Wallace, M. A. and Fain, J. N. (1985) *J. biol. Chem.*, **260**: 9527–9530.
 - 58 Cockcroft, S. and Gomperts, B.D. (1985) *Nature*, **314**: 534–536.
 - 59 Majerus, Ph. W., Connolly, Th. M., Deckmyn, H., Ross, Th. S., Bross, T. E., Ishii, H., Bansal, V. S. and Wilson, D. B. (1986) *Science*, **234**: 1519–1526.
 - 60 Masui, Y. (1960) *Mem. Konan Univ.*, **4**: 79–102.
 - 61 Grunz, H. (1968) *Roux's Arch. Dev. Biol.*, **160**: 344–347.
 - 62 Berridge, M. J., Downes C. P. and Hanley, M. R. (1982) *Biochem. J.*, **206**: 587–595.
 - 63 Busa, W. B. and Gimlich, R. L. (1989) *Dev. Biol.*, **132**: 315–324.
 - 64 Burns, C. P. and Rozengurt, E. (1983) *Biochem. Biophys. Res. Commun.*, **116**: 931–938.
 - 65 Rosoff, P. M., Stein, L., Cantley, L. C. (1984) *J. Biol. Chem.*, **259**: 7056–7060.
 - 66 Tiedemann, Hildegard (1986) *Roux's Arch. Dev. Biol.*, **195**: 399–402.
 - 67 Vigne, P., Ferlin, C., Cragoe, E. J. Jr. and Lazdunski, M. (1984) *Molecular Pharmacol.*, **25**: 131–136.
 - 68 Thomas, R. C. (1989) *Nature*, **337**: 601.
 - 69 Takata, K., Yamamoto, K. Y. and Ozawa, R. (1981) *Roux's Arch. Dev. Biol.*, **190**: 92–96.
 - 70 Grunz, H. (1985) *Cell Differentiation*, **16**: 82–92.
 - 71 Mikhailov, A. T., Gorgolyuk, N. A. and Bibikova (1989) *Ontogenez*, **20**: 507–515.
 - 71a Mikhailov, A. T., and Gorgolyuk, N. A. (1987) *Cell Differentiation*, **22**: 145–154.
 - 72 Duprat, A.-M., Gualandris, L., Kan, P. and Foulquier, F. (1984) In “The Role of Cell Interactions in Early Neurogenesis”. Ed. by A.-M. Duprat, A. C. Kato and M. Weber, Plenum Press, New York, pp. 3–20.
 - 73 Durston, A. J., Timmermans, J. P. M., Hage, W. J., Hendriks, H. F. J., de Vries, N. J., Heidewald, M. and Nieuwkoop, P. D. (1989) *Nature*, **340**: 140–144.
 - 74 Thaliel, C. and Eichele, G. (1987) *Nature*, **327**: 625–628.
 - 75 Thiery, J. P., Dubaud, S. L., Rutishauser, V., and Edelman, G. M. (1982) *Proc. Natl. Acad. Sci. USA*, **79**: 6737–6741.
 - 75a Edelman, G. M. (1986) *Ann. Rev. Cell. Biol.*, **2**: 81–96.
 - 76 Kintner, G. R. and Melton, D. A. (1987) *Development*, **99**: 311–325.
 - 77 Duprat, A. M., Gualandris, L., Foulquier, F., Paulin, D. and Bizzini, B. (1986) *Cell Differentiation*, **18**: 57–64.
 - 78 Nakamura, O. (1962) *Japn. J. Exp. Morph.*, **15**: 61–62.
 - 79 Nakamura, O. (1967) *Japn. J. Exp. Morph.*, **21**: 256–275.
 - 80 Tiedemann, H. (1975) In “The Biochemistry of Animal Development”. Vol. III Ed. by R. Weber, Academic Press, New York, p. 276.
 - 81 Ogi, K. (1967) *Sci. Rep. Tokoku Univ., Biol.*, **33**:

- 239-247.
- 82 Ogi, K. (1969) *Res. Bull. Gen. Educ. Nagoya Univ.*, **13**: 31-40.
- 83 Nieuwkoop, P. D. (1969) *Roux's Arch. Dev. Biol.*, **162**: 341-373.
- 84 Nieuwkoop, P. D. and Ubbels, G. A. (1972) *Roux's Arch. Dev. Biol.*, **169**: 185-199.
- 85 Nakamura, O., Takasaki, H. and Ishihara, M. (1971) *Proc. Japan Acad.*, **47**: 313-318.
- 86 Nakamura, O. and Takasaki, H. (1970) *Proc. Japan Acad.*, **46**: 546-551.
- 87 Nakamura, O., Hayashi, J. and Asashima, M. (1978) In "Organizer". Ed. by O. Nakamura and S. Toivonen, Elsevier-North Holland, Amsterdam, New York, pp. 1-47.
- 88 Grunz, H. and Tacke, L. (1986) *Roux's Arch. Dev. Biol.*, **195**: 467-473.
- 89 Sargent, T. D., Jamrich, M. and Dawid, I. B. (1986) *Dev. Biol.*, **114**: 238-246.
- 90 Gurdon, J. B., Mohun, T. J., Fairman, Sh. and Brennan, S. (1985) *Proc. Natl. Acad. Sci. USA*, **82**: 139-143.
- 91 Asashima, M. (1975) *Roux's Arch. Dev. Biol.*, **177**: 301-308.
- 92 Jones, E. A. and Woodland, H. R. (1987) *Development*, **101**: 557-563.
- 93 Boterenbrood, E. C. and Nieuwkoop, P. D. (1973) *Roux's Arch. Dev. Biol.*, **173**: 319-332.
- 94 Smith, J. C., Dale, L. and Slack, J. M. W. (1985) *J. Embryol. Exp. Morphol.* **89** (Suppl.): 317-331.
- 95 Yamada, T. (1940) *Okajimas Fol. anat. Jap.*, **19**: 131-197.
- 96 Mohun, T. J., Brennan, S., Dathan, N., Fairman, S. and Gurdon, J. B. (1983) *Nature*, **311**: 716-721.
- 97 Grunz, H. (1970) *Roux's Arch. Dev. Biol.*, **165**: 91-102.
- 98 Grainger, R. M. and Gurdon, J. B. (1989) *Proc. Natl. Acad. Sci. USA*, **86**: 1900-1904.
- 99 Tiedemann, H. and Tiedemann, H. (1959) *Hoppe-Seyler's Z. physiol. Chem.*, **306**: 7-32.
- 100 Born, J., Geithe, H.-P., Tiedemann, H., Tiedemann, H. and Kocher-Becker, U. (1972) *Hoppe-Seyler's Z. physiol. Chem.*, **353**: 1075-1084.
- 101 Geithe, H.-P., Asashima, M., Asahi, K.-I., Born, J., Tiedemann, H. and Tiedemann, H. (1981) *Biochim. Biophys. Acta*, **676**: 350-356.
- 102 Born, J., Hoppe, P., Schwarz, W., Tiedemann, H., Tiedemann, H. and Wittmann-Leibold, B. (1985) *Biol. Chem. Hoppe-Seyler*, **366**: 729-735.
- 103 Tiedemann, H. and Tiedemann, H. (1956) *Hoppe-Seyler's Z. physiol. Chem.*, **306**: 132-142.
- 104 Grunz, H., Born, J., Davids, M., Hoppe, P., Loppnow-Blinde, B., Tacke, L., Tiedemann, H. and Tiedemann, H. (1989) *Roux's Arch. Dev. Biol.*, **198**: 8-13.
- 105 Smith, J. C., Yaqoob, M., and Symes, K. (1988) *Development*, **103**: 591-600.
- 106 Asashima, M., Nakano, H., Shimada, K., Kinoshita, K., Ishii, K., Shibai, H. and Ueno, N. (1990) *Roux's Arch. Dev. Biol.*, **198**: 330-335.
- 107 Grunz, H. (1983) *Roux's Arch. Dev. Biol.*, **192**: 130-137.
- 108 Kocher-Becker, U. and Tiedemann, H. (1971) *Nature*, **233**: 65-66.
- 109 Kocher-Becker, U., Tiedemann, H. and Tiedemann, H. (1964) *Science*, **147**: 167-169.
- 110 Cooke, J. and Smith, J.C. (1989) *Dev. Biol.*, **131**: 383-400.
- 111 Tiedemann, H. and Born, J. (1978) *Roux's Arch. Dev. Biol.*, **184**: 285-299.
- 112 Born, J., Grunz, H., Tiedemann, H. and Tiedemann, H. (1980) *Roux's Arch. Dev. Biol.*, **189**: 47-56.
- 113 Takata, C. and Yamada, T. (1960) *Embryologia*, **5**: 8-20.
- 114 Rosa, F. M. (1989) *Cell*, **57**: 965-974.
- 115 Jones, E. A., Abel, M. H. and Woodland, H. R. (1989) *Abstract XI Congr. Int. Soc. Dev. Biol.*, Utrecht, The Netherlands.
- 116 Ya-Huei, W., Hui-yin, M. and Jie-Yi, S. (1963) *Acta Biol. Exp. Sinica*, **8**: 370-386.
- 117 Asashima, M., Nakano, H., Matsunaga, T., Sugimoto, M. and Takano, H. (1987) *Develop. Growth Differ.*, **29**: 221-227.
- 118 Niebel, J., Tiedemann, H. and Tiedemann, H. (1973) *Eur. J. Biochem.*, **32**: 242-246.
- 119 Born, J., Davids, M. and Tiedemann, H. (1987) *Cell Differentiation*, **21**: 131-136.
- 120 Slack, J. M. W., Darlington, B. G., Heath, J. K. and Goodsave, S. F. (1987) *Nature*, **326**: 197-200.
- 121 Kimelman, D. and Kirschner, M. (1987) *Cell*, **51**: 869-877.
- 122 Knöchel, W., Born, J., Loppnow-Blinde, B., Tiedemann, H., Tiedemann H., McKeehan, W. L. and Grunz, H. (1987) *Naturwissenschaften*, **74**: 604-606.
- 123 Grunz, H., McKeehan, W. L., Knöchel, W., Born, J., Tiedemann, H. and Tiedemann, H. (1988) *Cell Differ.*, **22**: 183-190.
- 124 Knöchel, W., Grunz, H., Loppnow-Blinde, B., Tiedemann, H. and Tiedemann, H. (1989) *Blut*, **59**: 207-213.
- 125 Jacobson, A. G. and Sater, A. K. (1988) *Development*, **104**: 341-359.
- 126 Sater, A. K. and Jacobson, A. G. (1989) *Development*, **105**: 821-830.
- 127 Mangold, O. (1957) *Naturwissenschaften*, **44**: 289-290.
- 128 Knöchel, W. and Tiedemann, H. (1989) *Cell Differ. Develop.*, **26**: 163-171.

- 129 Paterno, G. D., Gillespie, L. L., Dixon, M. S., Slack, S. M. W. and Heath, J. K. (1989) *Development*, **106**: 79–83.
- 130 Sporn, M. B., Roberts, A. B., Wakefield, L. M., and Assoian, R. K. (1986) *Science*, **233**: 532–534.
- 131 Roberts, A. B. and Sporn, M. (1990) In "Peptide Growth Factors and Their Receptors". Handbook of Experimental Pharmacology Vol. 95 I. Ed. by M. B. Sporn and A. R. Roberts. Springer, Heidelberg pp. 419–472.
- 132 Wahl, Sh. M., Hunt, D. A., Wakefield, L. M., McCartney-Francis, N., Wahl, L. M. Roberts, A. B. and Sporn, M. (1987) *Proc. Natl. Acad. Sci. USA*, **84**: 5788–5792.
- 133 Murata, M., Eto, Y., Shibai, H., Sakai, M. and Muramatsu, M. (1988) *Proc. Natl. Acad. Sci. USA*, **85**: 2434–2438.
- 134 Vale, W., Rivier, J., Vaughan, J., McClintock, R., Corrigan, A., Woo, W., Karr, D. and Spiess, S. (1986) *Nature*, **321**: 776–779.
- 135 Weeks, D. L., and Melton, D. A. (1987) *Cell*, **51**: 861–867.
- 136 Melton, D. A. (1987) *Nature*, **328**: 80–82.
- 137 Rosa, F., Roberts, A. B., Danielpour, L. L., Sporn, M. B. and Dawid, I. (1988) *Science*, **239**: 783–785.
- 138 Knöchel, W., Tiedemann, H. and Tiedemann, H. (1989) *Naturwissenschaften*, **76**: 270–272.
- 139 Seyedin, S. M., Segarini, P. R., Rosen, D. M., Thompson, A. Y., Bentz, H. and Graycar, J. (1987) *J. Biol. Chem.*, **262**: 1946–1949.
- 140 Ling, N., Ying, Sh.-Y., Ueno, N., Shimasaki, Sh., Esch, F., Hotta, M. and Guillemin, R. (1986) *Nature*, **321**: 779–782.
- 141 Kimelman, D., Abraham, J. A., Haaparanta, T., Palisi, Th. M. and Kirschner, M. W. (1988) *Science*, **242**: 1053–1056.
- 142 Slack, S. M. W. and Isaacs, H. V. (1989) *Development*, **105**: 147–153.
- 143 Gillespie, L. L., Paterno, G. D. and Slack, J. M. W. (1989) *Development*, **106**: 203–208.
- 144 Volk, R., Köster, M., Pötting, A., Hartmann, L. and Knöchel, W. (1989) *Embo J.*, **8**: 2983–2988.
- 145 Minuth, M. and Grunz, H. (1980) *Cell Differentiation*, **9**: 229–238.
- 146 Asahi, K.-i., Born, J., Tiedemann, H. and Tiedemann, H. (1979) *Roux's Arch. Dev. Biol.*, **187**: 231–244.
- 147 Vincent, J.-P. and Gerhart, J. C. (1984) *Dev. Biol.*, **123**: 526–539.
- 148 Gerhart, J., Ubbels, G., Black, S., Hara, K. and Kirschner, M. (1981) *Nature (London)*, **292**: 511–516.
- 149 Gimlich, R. L. and Gerhart, J. C. (1984) *Dev. Biol.*, **104**: 117–130.
- 150 Tiedemann, H., Becker, U., and Tiedemann, H. (1961) *Embryologia*, **6**: 204–218.
- 151 Jones, E. A. and Woodland, H. R. (1986) *Cell*, **44**: 345–355.
- 152 London, Ch., Akers, R. and Philips, C. (1988) *Dev. Biol.*, **129**: 380–389.
- 153 Gaul, U. and Jäckle, H. (1987) *Cell*, **51**: 549–555.
- 154 Struhl, G., Struhl, K. and Macdonald, P. M. (1989) *Cell*, **57**: 1259–1273.
- 155 Driever, W. and Nüsslein-Volhard, C. (1988) *Cell*, **54**: 95–104.
- 156 Driver, W. and Nüsslein-Volhard, C. (1989) *Nature*, **337**: 138–143.
- 157 Schröder, C., Tautz, D., Seifert, E. and Jäckle, H. (1988) *Embo. J.*, **7**: 2882–2887.
- 158 Wright, C. V. E., Cho, K. W. Y., Hardwicke, J., Collins, R. H. and De Robertis, E. M. (1989) *Cell*, **59**: 81–93.
- 159 Gehring, W. J. (1987) *Science*, **236**: 1245–1252.
- 160 Müller, M. M., Carrasco, A. E. and De Robertis, E. M. (1984) *Cell*, **39**: 157–162.
- 161 Ruiz i Altaba, A. and Melton, D. A. (1989) *Development*, **106**: 173–183.
- 162 Tautz, D., Lehmann, R., Schnurch, H., Schulz, R., Seifert, E., Kienlin, K. and Jäckle, H. (1987) *Nature*, **327**: 383–389.
- 163 Köster, M., Pieler, T., Pötting, A. and Knöchel, W. (1988) *EMBO J.*, **7**: 1735–1741.
- 164 Nietfeld, W., El Baradi, T., Mentzel, H., Pieler, T., Köster, M., Pötting, A. and Knöchel, W. (1989) *J. Mol. Biol.*, **208**: 639–659.
- 165 Townes, P. I. and Holtfreter, J. (1955) *J. exp. Zool.*, **128**: 53–120.

Ammoniogenesis in the Mudskipper, *Periophthalmus chrysospilos*

YUEN K. IP, SHIT F. CHEW and RITA W. L. LIM

*Department of Zoology, National University of Singapore,
Kent Ridge, Singapore 0511*

ABSTRACT—Enzymes associated with nitrogen metabolism were determined in the gill, liver and muscle tissues of *Periophthalmus chrysospilos*. Glutamate dehydrogenase, alanine transaminase and aspartate transaminase were detected in all tissues studied. A complete purine nucleotide cycle was not present. Glutamine synthetase was not detectable, suggesting that this enzyme was not responsible for detoxification of intra-mitochondrially generated ammonia. Glutamine was the most effective substrate for *in vitro* ammoniogenesis in the isolated muscle mitochondria. The possible role of glutamate dehydrogenase in mitochondrial ammoniogenesis in this mudskipper is discussed.

INTRODUCTION

In teleostan fishes, ammonia is the major nitrogenous endproduct while urea and trimethylamine oxide serve mainly for the maintenance of osmotic equilibria in species that synthesize them in significant quantities [1, 2]. Available data indicate that the sites of ammonia production in fish occur mainly in the liver and kidney [3]. The ammonia formed is then transported *via* the blood and excreted through the gills. However, gills without being surrounded by water are not efficient excretory organs. It, therefore, intrigues biologists to study the mechanisms by which amphibious fishes solve their problem of terrestrial nitrogenous waste excretion.

Mudskippers fascinate scientists for they enjoy an amphibious mode of life that is unparalleled among fishes. They resemble anuran amphibians in many aspects of their behaviour and ecology [4]. Gregory [5] found both ammonia and urea but no uric acid in the tissues of mudskippers. Except for arginase and carbamoyl transferase, other enzymes involved in the ornithine-urea cycle are either not detectable in the mudskippers *Periophthalmus expeditionium* and *P. gracilis* or have activities too low to account for the possibility of a

shift towards ureotelism when they are on land. Several studies on ammonia and urea excretion by mudskippers in aquatic and terrestrial environments have been performed [6–9]. Ammonia is mainly accumulated in the body of the fish during terrestrial exposure. Conversion of accumulated ammonia to urea is hardly performed. For this to be possible, the mudskipper must have a great tolerance to ammonia. Indeed, *P. cantonensis* can survive in 15 mM NH_4Cl for more than 7 days [10].

Chew and Ip [11] reported that transdeamination is the major pathway for ammoniogenesis in the mudskippers *Boleophthalmus boddarti* and *Periophthalmodon schlosseri*. Aspartate was found to be the major substrate for *in vivo* mitochondria ammonia production. However, aspartate transaminase activities in the muscle and hepatic mitochondria presented in the same report cannot account for such a high rate of ammoniogenesis from this substrate. Moreover, if ammonia production from aspartate involved transdeamination and occurred at such high rate, it is difficult to understand why then *in vitro* respiration of the isolated mudskipper muscle mitochondria in the presence of adenosine diphosphate (ADP) was stimulated by externally added glutamine and glutamate but not aspartate. In order to shed light on this matter, the present studies were undertaken to confirm the pathways of molecular ammonia production in another local mudskipper

P. chrysopilos. Also, during the course of the investigation, it was found necessary to re-examine the *in vitro* production of ammonia by the mitochondria of *B. boddaerti* and *P. schlosseri* in the presence of glutamine, glutamate and aspartate by the more advanced and selective ammonia assay method adopted in the present studies.

MATERIALS AND METHODS

Field collection and fish maintenance

P. chrysopilos of both sexes, weighing 2 to 12 g, were collected along the shores of West Coast and Pasir Ris, Singapore. *B. boddaerti* (8–17 g body weight) and *P. schlosseri* (70–80 g body weight) of both sexes were caught at the estuary at Pasir Ris. They were maintained in 50% seawater (18‰ salinity) in the laboratory for at least one day before being sacrificed for the experiments.

Preparation of sample for enzyme activity determinations

The lateral muscle, liver and gills of freshly killed *P. chrysopilos* were excised, blotted dry and weighed. Due to the small size of the fish, each gill sample contained tissues pooled from 7–8 fish while liver and muscle from 4–5 and 2 fish respectively constituted a sample. Samples were homogenized in ice-cold buffers (0–4°C) and fractionated according to the procedure of Iwata *et al.* [12]. The resulting mitochondrial and cytosolic fractions were used for glutamate dehydrogenase (GDH, EC 1.4.1.2), aspartate transaminase (EC 2.6.1.1), alanine transaminase (EC 2.6.1.2), glutamine synthetase (EC 6.3.1.2) and phosphate-dependent glutaminase (EC 3.5.1.2) activities determination.

For the preparation of adenosine monophosphate deaminase (AMP deaminase, EC 3.5.4.6), adenylosuccinate lyase (sAMP lyase, EC 4.3.2.2) and adenylosuccinate synthetase (sAMP synthetase, EC 6.3.4.4), the homogenized samples were centrifuged at $40,000 \times g$ for 1 hr. The resulting supernatant fluid was used for enzyme assays. Buffer used for AMP deaminase contained 50 mM Tris cacodylate (pH 7.1) and 2 mM dithiothreitol. For the extraction of sAMP lyase, buffer contain-

ing 0.25 M sucrose, 5 mM Hepes (pH 7.4) and 5 mM EDTA was used. The buffer used for sAMP synthetase extraction contained 0.25 M sucrose, 5 mM Hepes (pH 7.2), 1 mM EDTA and 1 mM dithiothreitol.

Enzyme assays

Spectrophotometric measurements were made at 25°C with a Shimadzu UV 260 double beam spectrophotometer. Specific activities were expressed as enzyme activity per mg protein.

Glutamate dehydrogenase was determined in the mitochondrial fraction according to Iwata *et al.* [12]. For the reductive amination direction, one unit of enzyme activity is defined as that amount which oxidised one μmol of NADH per min. In the oxidative deamination direction, one unit of enzyme activity is defined as one μmol of NAD reduced per min.

Transaminases were measured in both the cytosolic and mitochondrial fractions. For alanine transaminase, the assay procedure was based on the method of Wroblewski and LaDue [13]. Aspartate transaminase was measured with a Sigma aspartate aminotransferase assay kit no. 56-UV (Sigma Chemical Co.). For both transaminases, one unit of enzyme is defined as one μmol of NADH oxidized per min.

Glutamine synthetase was determined colorimetrically by the method of Pamiliijans *et al.* [14], using creatine phosphate and creatine kinase as the ATP regenerating system. It was also assayed according to Rowe *et al.* [15] where ATP was added to the reaction mixture. Phosphate-dependent glutaminase was determined by the method of Curthoys and Weiss [16] in both the cytosolic and mitochondrial fractions. For glutaminase, one unit of enzyme is defined as one μmol of NAD reduced per min.

AMP deaminase was assayed by the method of Gibbs and Bishop [17]. One unit of enzyme is defined as the amount that produces one μmol of ammonia per min. sAMP lyase was determined spectrophotometrically at 280 nm according to Campbell and Vorhaben [18]. One unit of enzyme is defined as the disappearance of one μmol of adenylosuccinate per min. For sAMP synthetase, both spectrophotometric and radiometric assays

were also performed according to Campbell and Vorhaben [18].

Preparation of muscle mitochondria for in vitro ammonia production and oxidative phosphorylation studies

The lateral muscle of freshly killed *P. chrysopilos*, *B. boddaerti* and *P. schlosseri* were excised, blotted dry and weighed. They were put into 10 volumes of ice-cold (0–4°C) extraction buffer containing 305 mM sucrose, 3 mM Tris-HCl (pH 7.2), 3 mM EDTA and 0.1% bovine serum albumin (BSA, Sigma Chemical Co.) with a final osmolality of 330 mosmo/kg. Homogenization was carried out once by using an Ikawerk Staufen Ultra-Turrax (Janke and Kunke Co.) homogenizer at 16,500 rpm for 10 sec. The homogenized samples were centrifuged at 4°C and $1,200\times g$ for 10 min (Kokusan model H-103N). The supernatant fluid was carefully drained and further centrifuged at $7,000\times g$ for 15 min (Kokusan model H-251CS) to obtain the mitochondria. The mitochondrial pellets were pooled together in extraction buffer and gently homogenized once with a Wheaton Teflon-pestle homogenizer. This sample was centrifuged at $1,200\times g$ for 10 min again to remove any contaminating muscle tissue. Mitochondria were obtained by resedimentation for 15 min at $7,000\times g$, washed one more time with extraction buffer and centrifuged again at the same gravitational force for the same duration. The washed mitochondria were finally resuspended in a small volume of extraction buffer by gently homogenizing once as stated before. Normally each gram of muscle produced approximately 0.18 mg of purified mitochondrial protein with minimum contamination of cytosolic lactate dehydrogenase.

In vitro ammonia production studies

To determine ammonia production from the isolated mitochondria of *P. chrysopilos*, 0.1 ml of the mitochondrial preparation (0.2–0.3 mg of muscle mitochondrial protein) was added to 1 ml of extraction buffer which was supplemented with 10 mM final concentration of the desired substrates with or without inhibitors. An aliquot of the sample was immediately assayed for ammonia by a Tecator Aquatec 5200 Analyzer equipped with the

^NRED cassette and interfaced with a Tecator FIA Star 5032 Detector Controller. Ammonium chloride solution was used as standard. The principle of this application is that the aqueous sample containing ammonium ions is mixed with sodium hydroxide. The ammonia released is allowed to diffuse through a gas permeable membrane to react with the indicator. The resulting colour shift was then measured spectrophotometrically. After 1 hr of incubation at 25°C, the ammonia content of the same sample was analyzed again. Such procedure allowed for the differentiation of ammonia originally present in the mitochondrial preparation or present in the amino acid substrate and that being produced by the mitochondria during the course of incubation. Normally, no attempt was made to differentiate between intra- and extra-mitochondrial ammonia. Ammonia production was reported as μmol ammonia produced per mg protein per hr.

In order to find out if the ammonia produced can exit the muscle mitochondria of *P. chrysopilos*, samples were incubated in the presence of 10 mM of glutamine for 1 hr at 25°C. The incubated samples were then centrifuged at $10,000\times g$ for 5 min. The ammonia content of the supernatant fluid was analysed. Precipitated mitochondria were lysed by the addition of 1 ml of 0.4 M perchloric acid followed by neutralization with 30% KOH. After the removal of potassium perchlorate by centrifugation, mitochondrial ammonia content was determined.

In vitro oxidative phosphorylation studies

Preliminary studies in our laboratory showed that ADP:O ratios could not be used as a good indicator of the satisfactory coupling condition of the mudskipper mitochondria due to the presence of high level of phosphatase activities. Therefore, oxidative phosphorylation by isolated *P. chrysopilos* muscle mitochondria was measured directly by determining the incorporation of radioactive inorganic phosphate (³²Pi) into the organic fraction according to the procedure of Grunberg-Manago *et al.* [19]. Mitochondria obtained in extraction buffer were suspended in respiratory medium (0.16 mg mitochondrial protein/ml) of 330 mosmol consisting of 40 mM Hepes (pH 7.2), 70 mM

sucrose, 90 mM D-mannitol, 5 mM $MgCl_2$, 3 mM EDTA, 4 mM KH_2PO_4 containing $0.2 \mu Ci/\mu mol$ of ^{32}P i (NEN), 0.1% BSA, 30 mM glucose, 2.5 mM ADP and 60 IU/ml of hexokinase (Sigma Chemical Co.). Reactions were started by the addition of 1 ml of the mitochondrial suspension into test tubes containing 10 mM final concentration of substrate. After 20 min of incubation at $25^\circ C$, the reaction was terminated by the addition of 0.1 ml of 40% trichloroacetic acid. Precipitated protein was removed by centrifugation. Radioactivity incorporated into glucose-6-phosphate was separated from ^{32}P i by conversion of the latter to ammonium phosphomolybdate which was extracted by isobutanol and ether [19, 20]. Radioactivity was determined by using Aquasol II (NEN) and a Kontron Betamatic scintillation spectrometer. Samples of the initial ^{32}P i were counted at the same time as the incubated samples to circumvent corrections for isotopic decay. Quenching effects were monitored and rectified by the sample channel ratio method.

Protein assay

Protein was measured using the method of Bradford [21] Bovine serum albumin (Sigma Chemical Co.) was used as standard for comparison.

RESULTS

Determination of enzymes associated with transdeamination and the purine nucleotide cycle in P. chrysospilos

The enzymes associated with transdeamination and the purine nucleotide cycle were assayed in the liver, gill and muscle tissues of *P. chrysospilos*. The activities of these enzymes were presented in Table 1. GDH was detected in all tissues examined. Similar to reports for other teleosts [22, 23], the liver mitochondria of *P. chrysospilos* showed the highest activities of GDH in both directions; the oxidative deamination rate being approximately 4.4% of that of reductive amination.

Alanine transaminase and aspartate transaminase were detected in all tissues studied with greater activities in the cytosolic than mitochondrial fractions. The activity of the former was higher than that of the latter in all tissues.

Glutamine synthetase was not detectable in *P. chrysospilos* by the two methods used in the present studies. Phosphate-dependent glutaminase, however, was detected only in the mitochondrial fractions of all the tissues.

Both sAMP lyase and AMP deaminase were present in all the tissues studied. The activity of sAMP lyase in the muscle was approximately 5 times greater than those in the liver and the gills.

TABLE 1. Specific activities of enzymes involved in ammoniogenesis in the tissues of *P. chrysospilos**

Enzymes	Gill		Liver		Muscle	
	Cytosol	Mitochondria	Cytosol	Mitochondria	Cytosol	Mitochondria
Glutamate dehydrogenase						
reductive amination	—	0.288 ± 0.087	—	1.913 ± 0.049	—	0.036 ± 0.003
oxidative deamination	—	0.015 ± 0.003	—	0.084 ± 0.005	—	0.004 ± 0.003
Aspartate transaminase	3.680 ± 0.482	0.107 ± 0.013	7.114 ± 2.950	1.423 ± 0.441	3.895 ± 0.128	0.085 ± 0.040
Alanine transaminase	0.516 ± 0.012	0.007 ± 0.002	1.562 ± 0.677	0.033 ± 0.008	0.597 ± 0.087	0.004 ± 0.002
AMP deaminase	0.227 ± 0.126	—	0.050 ± 0.001	—	0.054 ± 0.007	—
sAMP lyase	0.032 ± 0.006	—	0.047	—	0.183 ± 0.053	—
Phosphate-dependent glutaminase	n.d.	0.079 ± 0.034	n.d.	0.085 ± 0.062	n.d.	0.016 ± 0.009

*The values given are the means \pm SD of enzyme specific activities (refer to Materials and Methods) from three different samples except for sAMP lyase of the liver ($n=1$) and sAMP lyase of the muscle and gill ($n=2$); — = not determined; n.d. = not detectable.

The greatest AMP deaminase activity was however recorded in the gill tissue. sAMP synthetase was at first assayed spectrophotometrically. No activity was detected although the sample had been dialysed overnight to remove the interfering sAMP lyase. When the more sensitive radiometric method was employed, results were still negative.

In vitro ammonia production from the muscle mitochondria of P. chrysopilos in the presence of various L-amino acids

The muscle mitochondria of *P. chrysopilos* was able to deaminate all amino acids tested except serine (Table 2). The order of effectiveness in stimulating ammonia production was glutamine > glutamate > arginine > proline > lysine > alanine > aspartate.

The effects of various inhibitors on mitochondrial ammonia production were also examined (Table 2). Aminoxyacetate inhibited ammonia production from aspartate completely and significantly reduced ammonia production from glutamine. When aminoxyacetate was included in the incubation medium, it gave a higher than normal blank absorbance value; 0.042 ± 0.001 ($n=5$) as compare to zero for distilled water. However, it did not interfere with the ammonia assay process as the corrected absorbance values for 0.5, 2 and 5 mg/l of ammonium chloride standard in 2 mM aminoxyacetate were 0.029 ± 0.001 ($n=5$), 0.118 ± 0.003 ($n=5$) and 0.291 ± 0.007 ($n=5$) respectively, which were not significantly different ($P>0.05$) from the control values of 0.027 ± 0.002 ($n=5$), 0.119 ± 0.002 ($n=5$) and 0.287 ± 0.002 ($n=5$) in

TABLE 2. *In vitro* ammonia production ($\mu\text{mol NH}_3/\text{mg}$ protein per hr \pm SD) from various L-amino acids (10 mM) in the absence or presence of either 12 mM bromofuroate or 2 mM aminoxyacetate at 25°C by isolated muscle mitochondria of *P. chrysopilos*

Condition	n	Ammonia produced
Glutamine	12	0.119 ± 0.013
Glutamine + bromofuroate	5	0.025 ± 0.006
Glutamine + aminoxyacetate	3	0.038 ± 0.002
Glutamate	9	0.039 ± 0.017
Glutamate + bromofuroate	3	0
Arginine	3	0.027 ± 0.010
Proline	3	0.018 ± 0.004
Lysine	6	0.010 ± 0.004
Alanine	5	0.009 ± 0.003
Aspartate	6	0.003 ± 0.001
Aspartate + bromofuroate	3	0
Aspartate + aminoxyacetate	3	0
Serine	3	0

the absence of the inhibitor.

Bromofuroate, an inhibitor of glutamate dehydrogenase, decreased significantly ($p<0.01$) the ammonia production from glutamine and stopped ammonia release from glutamate and aspartate.

When glutamine was used as the substrate, 69.45 ± 7.31 ($n=5$) % of the ammonia produced was found in the incubation medium and 32.29 ± 6.79 ($n=5$) % was located within the mitochondria.

In vitro oxidative phosphorylation by muscle mitochondria of P. chrysopilos

Mitochondria isolated from the muscle of *P.*

TABLE 3. *In vitro* ammonia production ($\mu\text{mol NH}_3/\text{mg}$ protein per hr \pm SD, $n=4$) from 10 mM of glutamine or glutamate or aspartate in the absence or presence of either 12 mM bromofuroate or 2 mM aminoxyacetate at 25°C by isolated muscle mitochondria of *B. boddaerti* and *P. schlosseri*

Condition	Ammonia produced	
	<i>B. boddaerti</i>	<i>P. schlosseri</i>
Glutamine	0.225 ± 0.011	0.106 ± 0.060
Glutamate	0.026 ± 0.001	0.027 ± 0.010
Aspartate	0.009 ± 0.003	0.007 ± 0.003
Glutamine + bromofuroate	0.019 ± 0.007	0.040 ± 0.009
Glutamate + bromofuroate	0	0
Aspartate + bromofuroate	0	0
Aspartate + aminoxyacetate	0	0

chrysopilos could readily undergo oxidative phosphorylation in the presence of externally added substrate and ADP. Rate of phosphorylation obtained in the presence of glutamine, glutamate and aspartate, after correction for intrinsic phosphorylation in the presence of 2.5 mM ADP only, were 2.432 ± 0.254 (n=7), 0.520 ± 0.059 (n=3) and 0.056 ± 0.011 $\mu\text{mol } ^{32}\text{Pi}$ incorporated per mg mitochondrial protein per 20 min respectively.

In vitro ammonia production from the muscle mitochondria of B. boddaerti and P. schlosseri in the presence of either glutamine, glutamate or aspartate

Mitochondria isolated from the muscle of *B. boddaerti* and *P. schlosseri* were able to produce ammonia *in vitro* in the presence of the three substrates tested (Table 3). The order of effectiveness in stimulating ammonia production was glutamine > glutamate > aspartate. Bromofuroate also decreased significantly the ammonia production from glutamine and stopped ammonia release from glutamate and aspartate. Aminooxyacetate inhibited mitochondrial ammonia production from aspartate totally.

DISCUSSION

The deamination of amino acids through the purine nucleotide cycle proposed by Braunstein [24] and Lowenstein [25] has been suggested to occur in fish [26]. Similar to the other mudskippers, *B. boddaerti* and *P. schlosseri* [11], AMP deaminase and sAMP lyase were present in the tissues of *P. chrysopilos*. However, sAMP synthetase was not detectable by the two methods employed, thus rendering it improbable for this cycle to play a significant role in ammoniogenesis in this mudskipper. Janicki and Lingis [27] demonstrated that the liberation of ammonia from aspartate in teleost liver required both the mitochondrial and cytosolic fractions, a result which would not be expected if purine nucleotide cycle were solely responsible for ammoniogenesis. Casey *et al.* [22] also showed that the purine nucleotide cycle was not responsible for ammoniogenesis in the catfish, *I. punctatus* L. as the heavy nitrogen of ^{15}N -alanine was not incorporated into AMP in

isolated hepatocytes.

The activities of the mitochondrial GDH in *P. chrysopilos* were slightly lower (10%) than those obtained for the rat mitochondria [28] but much higher than the value reported previously by Iwata *et al.* [12] for another mudskipper *P. cantonensis* in the direction of reductive amination. Thermodynamically, GDH reaction favours reductive amination of α -ketoglutarate rather than oxidative deamination of glutamate [29]. In *P. chrysopilos*, the activities of GDH determined *in vitro* in the reductive amination direction were indeed greater than those in the oxidative deamination direction. However, the activities *in vivo* might in fact favour glutamate oxidation and ammonia release owing to factors such as relative levels of nucleotides and removal of reaction products [29]. When the GDH reaction is operated in conjunction with other transaminases present, transdeamination would be an avenue of ammonia production from various amino acids in the mudskipper.

Similar to mammalian [30] and channel catfish [31] hepatic mitochondria, the mechanism for aspartate deamination in isolated *P. chrysopilos* muscle mitochondria is transdeamination as it can be inhibited totally by either aminooxyacetate, a transaminase inhibitor, or bromofuroate, an inhibitor of GDH. However, contrary to the report on *B. boddaerti* and *P. schlosseri* [11], aspartate was not an effective substrate for *in vitro* mitochondrial ammonia production in *P. chrysopilos*. By re-examining the *in vitro* ammoniogenesis in the muscle mitochondria of the former two mudskippers by the ammonia assay methods described herein, it was confirmed that aspartate was not as efficient a substrate as compared to glutamine and glutamate for ammonia production (Table 3). Since aspartate normally is a non-penetrant anion in the absence of glutamate [32, 33] and the aspartate transaminase activity in the mitochondria of both *B. boddaerti* and *P. schlosseri* were not high enough to account for the fast rate of ammonia production [11], it is possible that the previous observations were results of interference of the enzyme coupled ammonia assay procedure used due to the presence of small amount of contaminating cytosolic aspartate transaminase and malate dehydrogenase. However, the results

obtained in the present studies (Table 3) verified the important role of GDH in mitochondrial ammoniogenesis in *B. boddaerti* and *P. schlosseri* as reported by Chew and Ip [11].

In agreement with the present studies, Campbell *et al.* [31] also demonstrated that glutamine was more effective as a substrate than glutamate for ammonia production in isolated channel catfish hepatic mitochondria. Such phenomenon can be explained by a restricted permeability of the inner mitochondria membrane to glutamate. When glutamine is a substrate, the permeability of the mitochondria membrane is not the rate-limiting step, and glutamate is produced inside the mitochondria. Glutaminase present inside the mitochondria can release the amide nitrogen to form ammonia and glutamate which can in turn be deaminated. The fact that bromofuroate completely inhibited the release of ammonia from glutamate and significantly reduced ammonia production from glutamine verified the important role of GDH in ammoniogenesis in the muscle mitochondria of *P. chrysopilos*.

Aminoxycetate, significantly reduced the *in vitro* mitochondrial ammonia production from glutamine in *P. chrysopilos* indicating that another enzyme, glutamine transaminase [34] may also be involved in the muscle mitochondrial glutamine metabolism. Although the present investigation did not examine the presence of this enzyme in *P. chrysopilos*, it has been found in both the cytosolic and mitochondrial compartments of the catfish liver. The normal products of such enzymatic reaction are α -ketoglutarate and ammonia. In order to accommodate the involvement of GDH in the metabolism of glutamine by the muscle mitochondria of *P. chrysopilos*, glutamine transaminase must therefore function in conjunction with some other enzymes. A combination of glutamine-phenylpyruvate transaminase, ω -amidase and phenylalanine- α -ketoglutarate transaminase catalyzes a net phenylpyruvate-stimulated glutaminase reaction producing glutamate and ammonia. Such pathway has indeed been discovered in the rat kidney. In the presence of bromofuroate, ammoniogenesis from glutamine was reduced to such an extent as though deamidation was also affected. Such observation might not be a direct

effect of bromofuroate on the deamidation process, but the inhibitory effect of the accumulating glutamate on both glutaminase and phenylalanine- α -ketoglutarate transaminase.

The isolated mitochondria used in these studies were in the coupling state as they could readily undergo oxidative phosphorylation in the presence of externally added substrate and ADP. In agreement with the ammonia studies, glutamine was a more effective substrate for oxidative phosphorylation than glutamate and aspartate. The fact that the ammonia produced could exit the coupling mitochondria indicates that exiting ammonia must be accompanied by a proton so that the hydrogen gradient generated by the electron transport system was not disrupted. The absence of glutamine synthetase suggested that this enzyme was not responsible for the detoxification of intramitochondrially generated ammonia in this mudskipper.

ACKNOWLEDGMENTS

This project was supported by grants RP70/85 from the National University of Singapore and GR05690J from the Singapore Turf Club.

REFERENCES

- 1 Goldstein, L. and Forster, R. P. (1970) Nitrogen metabolism in fishes. In "Comparative Biochemistry of Nitrogen Metabolism, vol. 2". Ed. by J. W. Campbell, Academic Press, New York, pp. 495–518.
- 2 Wood, J. D. (1958) Nitrogen excretion in some marine teleosts. *Can. J. Biochem. Physiol.*, **36**: 1237–1242.
- 3 Pequin, L. and Serfaty, A. (1963) L'Excretion ammoniacale chez un teleosteen dulcicole: *Cyprinus carpio* L. *Comp. Biochem. Physiol.*, **10**: 315–324.
- 4 Stebbins, R. C. and Kalk, M. (1961) Observations on the natural history of the mudskipper *Periophthalmus sobrinus*. *Copeia*, **1**: 18–27.
- 5 Gregory, R. B. (1977) Synthesis and total excretion of waste nitrogen by fish of the *Periophthalmus* (mudskipper) and *Scartelaos* Families. *Comp. Biochem. Physiol.*, **57A**: 33–36.
- 6 Gordon, M. S., Boetius, J., Boetius, I., Evan, D. H., McCarthy, R. and Oglesby, L. C. (1965) Salinity adaptation in the mudskipper fish (*Periophthalmus sobrinus*). *Hvalrad. Skr.*, **48**: 85–93.

- 7 Morii, H., Nishikata, K. and Tamura, O. (1978) Nitrogen excretion of mudskipper fish *Periophthalmus cantonensis* and *Boleophthalmus pectinirostris* in water and on land. *Comp. Biochem. Physiol.*, **60A**: 189–193.
- 8 Morii, H., Nishikata, K. and Tamura, O. (1979) Ammonia and urea excretion from mudskipper fish *Periophthalmus cantonensis* and *Boleophthalmus pectinirostris* transferred from land to water. *Comp. Biochem. Physiol.*, **63A**: 23–28.
- 9 Morii, H., (1979) Changes with time of ammonia and urea concentration in the blood and tissue of mudskipper fish, *Periophthalmus cantonensis* and *Boleophthalmus pectinirostris* kept in water and on land. *Comp. Biochem. Physiol.*, **64A**: 235–243.
- 10 Iwata, K. (1984) A high ammonia tolerance in the mudskipper *Periophthalmus cantonensis*. *Zool. Sci.*, **1**: 877.
- 11 Chew, S. F. and Ip, Y. K. (1987) Ammoniogenesis in mudskippers *Boleophthalmus boddaerti* and *Periophthalmodon schlosseri*. *Comp. Biochem. Physiol.*, **87B**: 941–948.
- 12 Iwata, K., Kakuta, I., Ikeda, M., Kimoto, S. and Nada, N. (1981) Nitrogen metabolism in the mudskipper, *Periophthalmus cantonensis*: A role of free amino acids in detoxification of ammonia produced during its terrestrial life. *Comp. Biochem. Physiol.*, **68A**: 589–596.
- 13 Wroblewski, F. and LaDue, J.S. (1956) Serum glutamic pyruvate transaminase in cardiac and hepatic disease. *Proc. Soc. Exp. Biol. Med.*, **91**: 569.
- 14 Pamiljans, V., Krishnaswamy, P. R., Dumville, G. and Meister, A. (1962) Studies on the mechanism of glutamine synthetase: isolation and properties of the enzyme from sheep brain. *Biochemistry*, **1**: 153–158.
- 15 Rowe, W. B., Ronzio, R. A., Wellner, V. P. and Meister, A. (1970) Glutamine Synthetase (sheep brain). In "Method Enzymol., vol. XVIIIA". Ed. by H. Tabor and C. W. Tabor, Academic Press, New York, pp. 900–910.
- 16 Curthoys, N. P. and Weiss, R. F. (1974) Regulation of renal ammoniogenesis. Subcellular localization of rat kidney glutaminase isoenzymes. *J. Biol. Chem.*, **249**: 3261–3266.
- 17 Gibbs, K. L. and Bishop, S. H. (1977) ATP-activated adenylate deaminase from marine invertebrate animals: properties of the enzyme from lugworm (*Arenicola cristata*) body wall muscle. *Biochem. J.*, **163**: 511–516.
- 18 Campbell, J. W. and Vorhaben, J. E. (1979) The purine nucleotide cycle in helix hepatopancreas. *J. Comp. Physiol.*, **129**: 137–144.
- 19 Grunberg-Manago, M., Ortiz, P. J. and Ochoa, S. (1956) Enzyme synthesis of polynucleotides I. Polynucleotide phosphorylase of *Azotobacter virlandii*. *Biochim. Biophys. Acta*, **20**: 269–285.
- 20 Berenblum, I. and Chain, E. (1938) An improved method for the colorimetric determination of phosphate. *Biochem. J.*, **32**: 295–298.
- 21 Braford, M. M. (1976) A rapid and sensitive method for the quantitation of microgram quantities of protein utilizing the principle of protein-dye binding. *Anal. Biochem.*, **72**: 248–254.
- 22 Casey, C. A., Perlman, D. F., Vorhaben, J. E., and Campbell, J. W. (1983) Hepatic ammoniogenesis in the channel catfish, *Ictalurus punctatus*. *Mol. Physiol.*, **3**: 107–126.
- 23 Waarde, A. V. (1980) Nitrogen metabolism in goldfish, *Carassius auratus* L.: Activities of transamination reactions, purine nucleotide cycle and glutamate dehydrogenase in goldfish tissues. *Comp. Biochem. Physiol.*, **68B**: 407–413.
- 24 Braunstein, A. E. (1957) Les voies principales de l'assimilation et dissimulation de l'azote chez les animaux. *Adv. Enzymol.*, **19**: 335–377.
- 25 Lowenstein J. M. (1972) Ammonia production in muscle and other tissues: the purine nucleotide cycle. *Physiol. Rev.*, **52**: 382–414.
- 26 Makarewicz, W. and Zydowo, M. (1962) Comparative studies on some ammonia producing enzymes in the excretory organs of vertebrates. *Comp. Biochem. Physiol.*, **6**: 269–275.
- 27 Janicki, R. and Lingis, J. (1970) Mechanism of ammonia production from aspartate in teleost liver. *Comp. Biochem. Physiol.*, **37**: 101–105.
- 28 Arnold, H. and Maier, K. P. (1971) Crystallization and some properties of glutamate dehydrogenase from rat liver. *Biochim. Biophys. Acta*, **251**: 133–140.
- 29 Krebs, H. A. and Veech, R. L. (1969) Pyridine nucleotide interrelationships. In "The Energy Level and Metabolic Control in Mitochondria". Ed. by S. Papa, J. M. Tager, E. Quagliariello and E. C. Slater, Adriatica Edice, Bari, pp. 329–382.
- 30 Hird, F. J. R. and Marginson, M. A. (1966) Oxidative deamination of glutamate and transdeamination through glutamate. *Arch. Biochem. Biophys.*, **115**: 247–256.
- 31 Campbell, J. W., Aster, P. L. and Vorhaben, J. E. (1983) Mitochondrial ammoniogenesis in liver of the channel catfish *Ictalurus punctatus*. *Am. J. Physiol.*, **244**: R709–R717.30.
- 32 Chappell, J. B. (1968) Systems used for the transport of substrates into mitochondria. *Br. Med. Bull.*, **24**: 150–157.
- 33 Klingenberg, M. (1979) ADP/ATP shuttle of mitochondria. *Trends Biochem. Sci.*, **5**: 1–4.
- 34 Cooper, A. J. L. and Meister, A. (1972) Isolation and properties of highly purified glutamine transaminase. *Biochemistry*, **11**: 661–671.

Expression of Circular Plasmids Which Contain Bacterial Chloramphenicol Acetyltransferase Gene Connected to the Promoter of Polypeptide IX Gene of Human Adenovirus Type 12 in Oocytes, Eggs and Embryos of *Xenopus laevis*

YUCHANG FU, KENZO SATO¹, KEIICHI HOSOKAWA¹
and KOICHIRO SHIOKAWA^{2,3}

Department of Biology, Faculty of Science, Kyushu University, Fukuoka 812, and

¹Department of biochemistry, Kawasaki Medical College,
Kurashiki 701-01, Japan

ABSTRACT—Polypeptide IX gene of adenovirus type 12 is unique in that it is expressed intermediately inbetween early and late genes, but the structure and function of its 5'-upstream promoter region have not been well characterized. In the present experiment, fertilized eggs as well as oocytes and unfertilized eggs of *Xenopus laevis* were injected with circular plasmid, pAd12.IXCAT, which contains bacterial chloramphenicol acetyltransferase (CAT) gene fused to the promoter of polypeptide IX gene of adenovirus type 12, and the activity of this plasmid to promote CAT enzyme expression in *Xenopus* embryonic cells was examined. For comparison, pAd12.ElaCAT which contains the promoter of Ela protein of adenovirus type 12, pSV2CAT which contains SV40 early promoter, and pSV0CAT and pA10CAT3m which do not contain promoter were also tested. In the oocyte nucleus, all these circular plasmids were expressed similarly actively. In embryos and unfertilized eggs, however, while pAd12.ElaCAT and pSV2CAT were strongly expressed, level of the expression of pAd12.IXCAT was as low as those of pSV0CAT and pA10CAT3m. These results show that the promoter of polypeptide IX gene of adenovirus type 12 is very weak as compared with that of Ela protein.

INTRODUCTION

The polypeptide IX is associated with the group of nine hexons of adenovirus virion, and may play a cementing role in the assemblage of virus particle [1, 2]. Polypeptide IX is expressed intermediately inbetween the early and late phases of adenovirus infection, and the regulation of its synthesis appears to differ from that of other structural polypeptides of the virus particle [3]. Polypeptide IX is unique in that it is encoded by a relatively small mRNA of about 9S (ca. 485 b), and unlike

other adenovirus mRNAs, the formation of polypeptide IX mRNA does not involve splicing [4]. To characterize the promoter function, Kruczek and Doerfler [5] isolated polypeptide IX gene from adenovirus type 12 genome, and after connecting its promoter to CAT gene, studied the effect of methylation on the promoter function. However, the expression of CAT enzyme activity from the fusion gene has not yet been studied in other eukaryotic cell system. In the present experiment, fertilized eggs as well as oocyte nuclei and unfertilized eggs of *Xenopus laevis* were injected with pAd12.IXCAT, a plasmid which contains the promoter of polypeptide IX of adenovirus type 12 [5] and the activity of the plasmid to promote CAT enzyme expression was compared with those of other CAT-containing plasmids.

Accepted May 2, 1989

Received March 29, 1989

² To whom all correspondence should be addressed.

³ Present address: Laboratory of Molecular Embryology, Zoological Institute, Faculty of Science, University of Tokyo, Tokyo 113, Japan.

MATERIALS AND METHODS

Plasmid DNAs

Five different plasmids, pSV0CAT, pAd12.IXCAT, pAd12.E1aCAT, pA10CAT3m, and pSV2CAT were used throughout the experiments. pSV0CAT contains CAT gene and has a Hind III site in front of the CAT gene for experimental promoter insertion [6]. pAd12.IXCAT was constructed by inserting the promoter region (1.2 Kb) of polypeptide IX gene into Hind III site of pSV0CAT (Fig. 1) [5]. pAd12.E1aCAT was produced by inserting the promoter of E1a early gene of adenovirus type 12 into pSV0CAT (Fig. 1) [5]. pSV2CAT contains a CAT gene fused to a relatively strong promoter of SV40 early gene (Fig. 1) [6]. pA10CAT3m is a derivative of pSV0CAT, into which a polylinker was inserted [7].

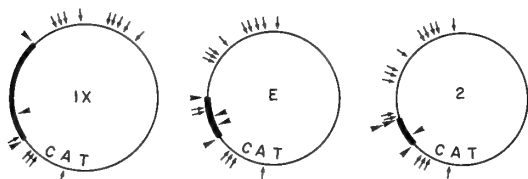


FIG. 1. Maps of pAd12.IXCAT as compared with pAd12.E1aCAT and pSV2CAT. Thick lines indicate promoter inserted. IX, E, and 2 corresponds to pAd12.IXCAT, pAd12.E1aCAT, and pSV2CAT, respectively. Arrowheads outside circles denote Hind III sites, and those inside circles indicate approximate TATA box positions. Small arrows denote Hpa II sites. CAT denotes the site of CAT gene. These figures were drawn according to Kruczek and Doerfler (5).

Plasmids were propagated, and DNAs were extracted as described previously by Tashiro *et al.* [8, 9]. Agarose gel electrophoresis showed that all the plasmid DNAs before injection consisted mainly of closed circular (c.c.) DNA, with little open circular (o.c.) DNA (Fig. 2).

Microinjection

Ovaries were digested for 3–4 hr with 500 $\mu\text{g}/\text{ml}$ of collagenase in Barth's solution (88 mM NaCl, 10 mM Hepes, pH 7.4, 1.0 mM KCl, 0.82 mM MgSO_4 , 0.33 mM $\text{Ca}(\text{NO}_3)_2$, 0.41 mM CaCl_2) which contained 50 units/ml of penicillin and 50

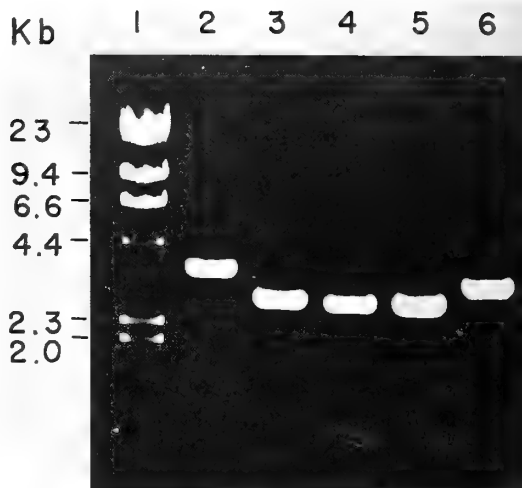


FIG. 2. Gel electrophoretic profiles of plasmid DNAs before injection. The main band shown is c.c. form for all the DNA preparations. Lane 1 (Marker Hind III-digest of lambda DNA), lane 2 (pAd12.IXCAT), lane 3 (pSV2CAT), lane 4 (pSV0CAT), lane 5 (pA10CAT3m) and lane 6 (pAd12.E1aCAT).

$\mu\text{g}/\text{ml}$ of streptomycin. Defolliculated oocytes at the stage 6 [10] were collected, and injected with ca. 20 nl of 100 $\mu\text{g}/\text{ml}$ of DNA solutions. All oocyte injections were aimed at the germinal vesicle. Samples for CAT assay and DNA extraction were prepared from pools of 40 oocytes.

Fertilized eggs were obtained by artificial insemination [11], and after being dejellied in 2.5% thioglycollate (pH 8.0) [12], injected into the cytoplasm with ca. 20 nl of 100 $\mu\text{g}/\text{ml}$ of DNA solutions in $1\times\text{MMR}$ (0.1 M NaCl, 2 mM KCl, 1 mM MgSO_4 , 2 mM CaCl_2 , 5 mM Hepes, pH 7.4, 0.1 mM EDTA) that contained 5% Ficoll [8]. After injection, embryos were left in $1\times\text{MMR}$ with 5% Ficoll, and transferred to $0.5\times\text{MMR}$ when they reached the stage 6 [13]. Embryos were incubated until the blastula (stage 8.5), gastrula (stage 11) and neurula (stage 18–19) stages at 20–21°C. Ten embryos were used for a sample.

Unfertilized eggs were manually stripped out from the gravid female, dejellied, then incubated in modified Barths' saline (88 mM NaCl, 1.0 mM KCl, 0.83 mM MgSO_4 , 0.34 mM $\text{Ca}(\text{NO}_3)_2$, 0.41 mM CaCl_2 , 7.5 mM Tris-HCl (pH 7.6), 2.4 mM NaHCO_3). Eggs were injected into the cytoplasm with DNA as above [14], and left in the modified

Barths' saline at 20–21°C for either 12 or 24 hr. About 20 eggs were collected as a sample.

CAT enzyme assay

Oocytes, unfertilized eggs, and embryos were homogenized in 0.25 M Tris-HCl (pH 8.0), and supernatants equivalent to 10 eggs were mixed with 1 μ Ci of (14 C)chloramphenicol (Amersham Corp.) and acetyl CoA. The mixture was incubated at 37°C for 2 hr, and was extracted twice with ethyl acetate [15]. The extracts were spotted onto a thin layer plate with silica gel, and chromatographed for ca. 30 min in 95% chloroform-5% methanol. Gels were dried and autoradiographed usually for 3–5 days (for oocytes and embryos) or 1–2 months (for unfertilized eggs).

RESULTS AND DISCUSSION

Circular pAd12.IXCAT and other plasmids (pAd12.E1aCAT, pSV2CAT, pSV0CAT, pA10CAT3m) were injected into the oocyte nucleus at 2 ng/oocyte, and CAT enzyme activity was assayed after different periods of time. Southern blot analysis carried out with pSV2CAT as a probe showed that injected plasmids were stably preserved after 24 hr of incubation (data not shown).

CAT enzyme expression with pAd12.IXCAT was not greatly different from that with other four plasmids (pAd12.E1aCAT, pSV2CAT, pSV0CAT, and pA10CAT3m) at 7 (lanes 1 to 3), 20 (lanes 4 to 9) and 24 hr (lanes 10 to 12) (Fig. 3). Thus, as in the previous data which were obtained with chicken ovalbumin genes [16], all the circular genes were expressed equally actively.

Fertilized eggs were then injected with pAd12.IXCAT and four other circular plasmids at 2 ng/egg, and CAT enzyme activity was tested at different stages of development (Fig. 4). Under the conditions used, CAT enzyme activity was not detected at the blastula stage with plasmids that carried adenovirus promoters (lanes 10, 13), although pSV2CAT was expressed weakly as Etkin and Balcells [15] recently showed (lane 7). At the gastrula stage, however, all the plasmids were expressed at widely differing extents. Thus, pSV2CAT (lane 8) and pAd12.E1aCAT (lane 14) were strongly expressed, whereas pAd12.IXCAT was expressed only at a low level (lane 11), which was close to those of pSV0CAT (lane 2) and pA10CAT3m (lane 6). The results were essentially the same also at the neurula stage (Fig. 4).

DNAs were extracted from the above DNA-injected embryos at the blastula, gastrula and

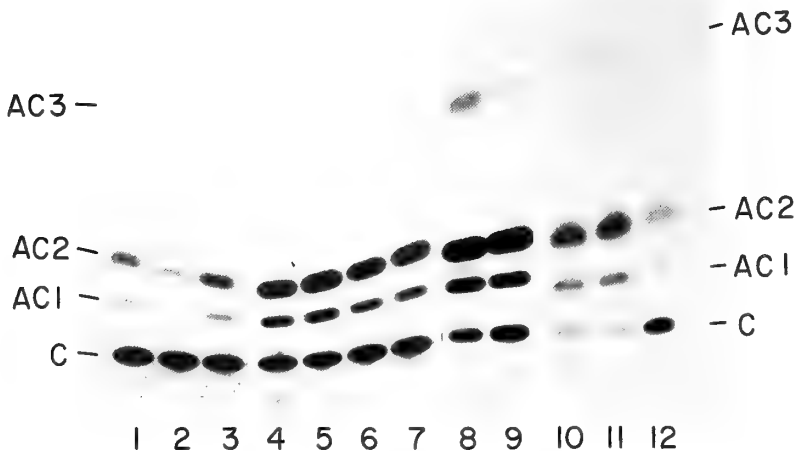


FIG. 3. CAT enzyme assay in oocytes injected with circular plasmids. Oocytes were injected with 2 ng of circular plasmids and harvested at 7 hr (lanes 1 to 3), 20 hr (lanes 4 to 9) and 24 hr (lanes 10 to 12). Lanes 1, 8 and 10 (pSV0CAT); lanes 2, 4, 11 (pAd12.IXCAT); lanes 3, 5, 9, and 12 (pSV2CAT); lane 6 (pAd10CAT3m); and lane 7 (pAd12.E1aCAT). C, AC1, AC2, and AC3 are for chloramphenicol, 1-acetylated chloramphenicol, 2-acetylated chloramphenicol, and 3-acetylated chloramphenicol, respectively.

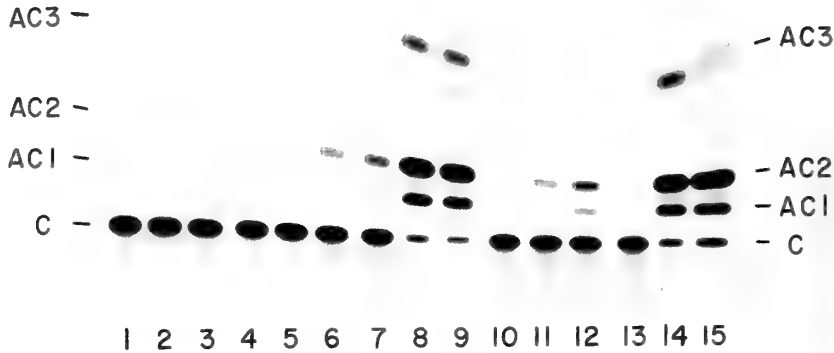


FIG. 4. CAT enzyme assay in developing embryos injected with circular plasmids. Fertilized eggs were injected with 2 ng of circular plasmids, and embryos were collected at the late blastula (lanes 1, 4, 7, 10 and 13), gastrula (lanes 2, 5, 8, 11, and 14), and neurula (lanes 3, 6, 9, 12, and 15) stages. Lanes 1 to 3 (pSV0CAT), lanes 4 to 6 (pA10CAT3m), lanes 7 to 9 (pSV2CAT), lane 10 to 12 (pAd12.IXCAT), and lanes 13 to 15 (pAd12.E1aCAT). For C, AC1, AC2 and AC3, see the legend to Fig. 3.

neurula stages, and Southern blot analysis was carried out using pSV2CAT as a probe. The results showed that injected pAd12.IXCAT as well as pSV0CAT and pA10CAT3m was not degraded, but copy number of the injected DNAs increased by several fold. Therefore, the low activity of pAd12.IXCAT (Fig. 4) may not be due to the instability of this plasmid after injection.

Expression of CAT enzyme activity from circular pAd12.IXCAT and other plasmids was also tested after injection into unfertilized eggs at 2 ng/egg. As shown in Figure 5, very weak, but distinct CAT enzyme activity was observed at 12 hr only with pAd12.E1aCAT (lane 5) and pSV2CAT (lane 3), and the activity of other plasmids was either very faint (pAd12.IXCAT) (lane 2) or negligible (pSV0CAT, lane 1 and pA10CAT3m, lane 4). Thus, results obtained with unfertilized eggs were quite similar to those obtained with embryos, although the extent of the expression was quite low.

Circular plasmids were injected into fertilized eggs and RNAs were extracted from embryos at the gastrula stage to compare the level of CAT mRNA by Northern blot analysis [17] using CAT antisense RNA [18] as a probe. The results obtained showed that the level of the mRNA which migrated at 1.6 Kb CAT antisense RNA was roughly comparable to the CAT enzyme level

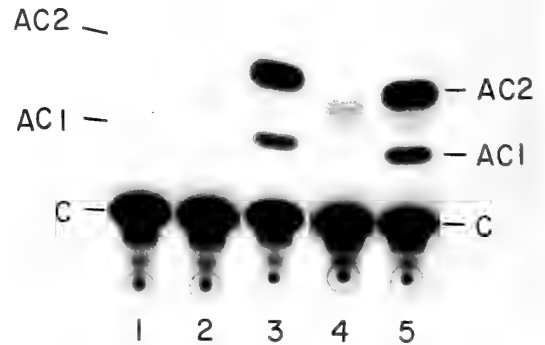


FIG. 5. CAT enzyme assay in unfertilized eggs injected with circular plasmids. Unfertilized eggs were injected with 2 ng of circular plasmids and harvested at 12 hr after the injection. Lane 1 (pSV0CAT), lane 2 (pAd12.IXCAT), lane 3 (pSV2CAT), lane 4 (pA10CAT3m) and lane 5 (pAd12.E1aCAT). For C, AC1, and AC2, see the legend to Fig. 3. Since this autoradiogram was obtained after autoradiographic exposure for 2 months, there appeared a faint band between AC1 and AC2 in all the lanes. However, this is not due to the CAT enzyme activity, because the same spot was obtained also with sample which had not been injected with CAT gene-containing plasmid (data not shown).

(data omitted). Therefore, we assume that CAT enzyme activity may be roughly correlated to the activity of transcription of CAT genes in

embryonic cells.

As shown in Figure 1, the size of the promoter region of polypeptide IX gene used is almost twice as large as those of E1a protein and SV40 early genes. Nevertheless, the activity of CAT enzyme expression with pAd12.IXCAT that carried the promoter of polypeptide IX gene was as low as those of pSV0CAT and pA10CAT3m which do not contain the promoter.

pSV2CAT and pAd12.E1aCAT were known to contain a relatively strong enhancer element within their promoter region [5, 6]. However, the 5'-upstream region of the polypeptide IX gene of adenovirus has not been shown to contain an enhancer element [1, 2, 4], although the promoter of protein IX gene of adenovirus type 12 is known to contain TATA box and GC-rich region [4, 19]. The low activity of pAd12.IXCAT observed here in *Xenopus* embryos and unfertilized eggs suggests that the promoter of the protein IX gene of adenovirus type 12 may not contain an enhancer element.

ACKNOWLEDGMENTS

We thank Professor K. Yamana for his warm encouragement throughout the experiments. We also thank Dr. W. Doerfler for kind supply of CAT gene-containing plasmids. The present study was supported in part by a Grant-in-Aid for Scientific Research to K. S. (No. 61540523), a Grant-in-Aid for Cancer Research to K. H. (No. 62010095) from the Ministry of Education, Science and Culture of Japan, and grants from Takeda Science Foundation (1986) and The Naito Foundation (1987) to K. S.

REFERENCES

- 1 Everitt, E., Lutter, L. and Philipson, L. (1975) Structural proteins of adenoviruses. XII. Location and neighbor relationship among proteins of adenovirus type 2 as revealed by enzymatic iodination, immunoprecipitation and chemical cross-linking. *Virology*, **67**: 197-208.
- 2 Everitt, E., Sundquist, B., Pettersson, U. and Philipson, L. (1973) Structural proteins of adenoviruses X. Isolation and topography of low molecular weight antigens from the virion of adenovirus type 2. *Virology*, **52**: 130-147.
- 3 Persson, H., Pettersson, U. and Mathews, M. B. (1978) Synthesis of a structural adenovirus polypeptide in the absence of viral DNA replication. *Virology*, **90**: 67-79.
- 4 Alestrom, P., Akusjarvi, G., Perricaudet, M., Mathews, M. B., Klessig, D. F. and Pettersson, U. (1980) The gene for polypeptide IX of adenovirus type 2 and its unspliced messenger RNA. *Cell*, **19**: 671-681.
- 5 Kruczek, I. and Doerfler, W. (1983) Expression of the chloramphenicol acetyltransferase gene in mammalian cells under the control of adenovirus type 12 promoters: Effect of promoter methylation on gene expression. *Proc. Natl. Acad. Sci. USA*, **80**: 7586-7590.
- 6 Gorman, C. M., Moffat, L. F., and Howard, B. H. (1982) Recombinant genomes which express chloramphenicol acetyltransferase in mammalian cells. *Mol. Cell. Biol.*, **2**: 1044-1051.
- 7 Laimins, L. A., Gruss, P., Pozzatti R. and Khoury, G. (1984) Characterization of enhancer elements in the long terminal repeat of Moloney murine sarcoma virus. *J. Virol.*, **49**: 193-189.
- 8 Tashiro, K., Inoue, M., Sakaki, Y. and Shiokawa, K. (1986) Preservation of *Xenopus laevis* rDNA-containing plasmid, pX1r101A, injected into the fertilized egg of *Xenopus laevis*. *Cell Struct. Func.*, **11**: 109-114.
- 9 Tashiro, K., Shiokawa, K., Yamana K. and Sakaki, Y. (1986) Structural analysis of ribosomal DNA homologues in nucleolus-less mutant of *Xenopus laevis*. *Gene* **44**: 299-306.
- 10 Dumont, J. N. (1972) Oogenesis in *Xenopus laevis* (Daudin) 1. Stages of oocyte development in laboratory maintained animals. *J. Morph.*, **136**: 153-180.
- 11 Tashiro, K., Misumi, Y., Shiokawa, K. and Yamana, K. (1983) Determination of the rate of rRNA synthesis in *Xenopus laevis* triploid embryos produced by low-temperature treatment. *J. Exp. Zool.*, **225**: 489-495.
- 12 Shiokawa, K. and Yamana, K. (1976) Pattern of RNA synthesis in isolated cells of *Xenopus laevis* embryos. *Dev. Biol.*, **16**: 368-388.
- 13 Nieuwkoop, P. D. and Faber, J. (1956) Normal Table of *Xenopus laevis* Daudin. Norht-Holland Publ. Co.
- 14 Berg, C. A. and Gall, J. G. (1986) Microinjected *Tetrahymena* rDNA ends are not recognized as telomers in *Xenopus* eggs. *J. Cell Biol.*, **103**: 691-698.
- 15 Etkin, L. D. and Balcells, S. (1985) Transformed *Xenopus* embryos as a transient expression system to analyze gene expression at the midblastula transition. *Dev. Biol.*, **108**: 173-178.
- 16 Wickens, M. P., Woo, S., O'Malley, B. W. and Gurdon, J. B. (1980) Expression of a chicken chromosomal ovalbumin gene injected into frog oocyte nuclei. *Nature*, **285**: 628-634.
- 17 Atsuchi, Y., Tashiro, K., Yamana, K. and Shioka-

- wa, K. (1986) Level of histone H4 mRNA in *Xenopus laevis* embryonic cells cultured in the absence of cell adhesion. *J. Embryol. exp. Morph.*, **98**: 175–185.
- 18 Melton, D. A., Krieg, P. A., Rebagliati, M. R., Maniatis, T., Zinn, K. and Green M. R. (1984) Efficient in vitro synthesis of biologically active RNA and RNA hybridization probes from plasmids containing a bacteriophage SP6 promoter. *Nucl. Acids Res.*, **12**: 7035–7056.
- 19 Berk, A. J. (1986) Adenovirus promoters and E1a transactivation. *Ann. Rev. Genet.*, **20**: 45–79.

Ultrastructural Studies of the Carotid Labyrinth in the Newt *Cynops pyrrhogaster*

TATSUMI KUSAKABE

*Department of Anatomy, Yokohama City University School
of Medicine, Yokohama 236, Japan*

ABSTRACT—Fluorescence, light, and electron microscopic observations of the carotid labyrinth of the newt *Cynops pyrrhogaster* showed the presence of glomus cells in the intervascular stroma of the labyrinth. These cells contain many dense-cored vesicles (60 nm–100 nm in diameter) and their ultrastructure was similar to that of glomus cells reported in many other animal species. In some glomus cells, there were intranuclear inclusion bodies (0.1–0.3 μ m in diameter), and long processes were in close contact with endothelial cells or with pericytes, which have not been reported in the carotid labyrinth so far. Two types of synapses (efferent and afferent) were found on the glomus cell surfaces. So-called reciprocal synapses were also found. On the basis of these findings, I conclude that the newt glomus cells may have a secretory as well as a chemoreceptor function.

INTRODUCTION

Amphibian carotid labyrinths have been morphologically studied by many workers (see Adams)[1]. Ishii *et al.* [2] confirmed in physiological experiments that they have an arterial chemoreceptor function analogous to that of the mammalian carotid body. The anuran carotid labyrinth contains glomus cells similar to those in mammalian carotid bodies and is innervated by glossopharyngeal and sympathetic nerves [3, 4]. It has been thought that the glomus cell functions as an element of the arterial chemoreceptor. In electron microscopy of the *Xenopus* carotid labyrinth, close contact of glomus cells with smooth muscle cells was reported, suggesting that the labyrinth might have another function other than chemoreception [5]. Most of the ultrastructural and physiological studies of the carotid labyrinth have been performed on anurans, and there are only a few morphological reports on the carotid labyrinth in urodela [6, 7]. In the present study, some ultrastructural characteristics of the newt glomus cell which are different from those pre-

viously described in other amphibia are reported.

MATERIALS AND METHODS

Fifteen Japanese newts, *Cynops pyrrhogaster*, of both sexes weighing 8–10 g were used. The animals were anesthetized with urethane (5 mg/g body weight), and the region of the carotid labyrinth was exposed on both sides. Through a thin nylon tube inserted into the aortic trunk, the labyrinth was washed with Ringer solution and perfused with fixatives, then removed from the body. For fluorescence microscopy, specimens were immersed in Grillo's fixative [8] at 4°C for 20 hr. They were sectioned transversely at 60 μ m. Observations were made with a fluorescence microscope (Olympus BHF) equipped with a HBO 200 high pressure mercury lamp, UG-5 and BG excitor filters, and a Y-475 barrier filter. For electron microscopy, the labyrinth was immersed in 2.5% glutaraldehyde in 0.1 M cacodylate buffer (pH 7.3) at 4°C for 3 hr. After being washed in buffer solution, the specimens were divided into small blocks and postfixed in 1% osmium tetroxide buffered with 0.1 M cacodylate for 1 hr. After dehydration in a graded ethanol series, the specimens were embedded in Epon-alardite mixture. Sections of 1 μ m were stained with toluidine blue

for light microscopy. Ultrathin sections were cut serially and double-stained with saturated uranyl acetate and Reynold's lead solution. electron micrographs were taken with a JEM 200-CX electron microscope at 80 kv.

RESULTS

Light and fluorescence microscopy

The carotid labyrinth had a maze-like structure consisting of the sinusoidal plexus and intervascular stroma. The stroma contained 6 main types of cells: glomus cells, smooth muscle cells, pericytes, fibroblasts, mast cells, and endothelial cells. The

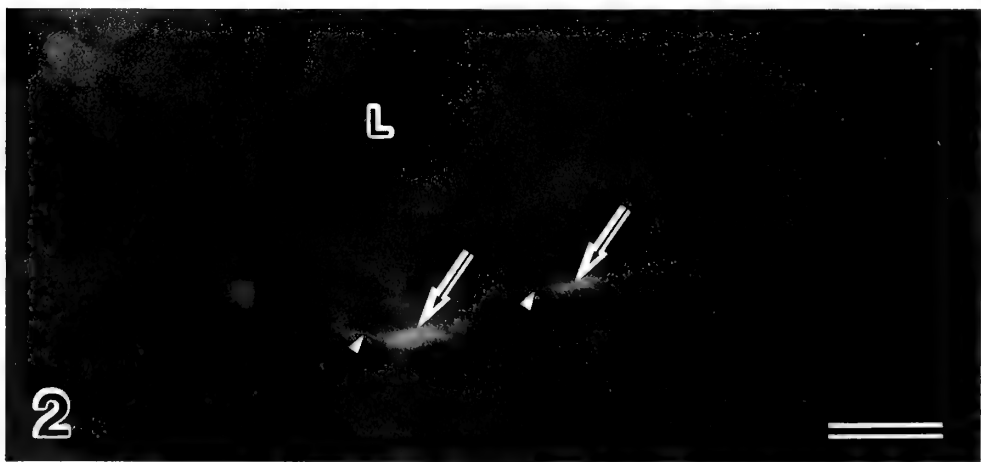
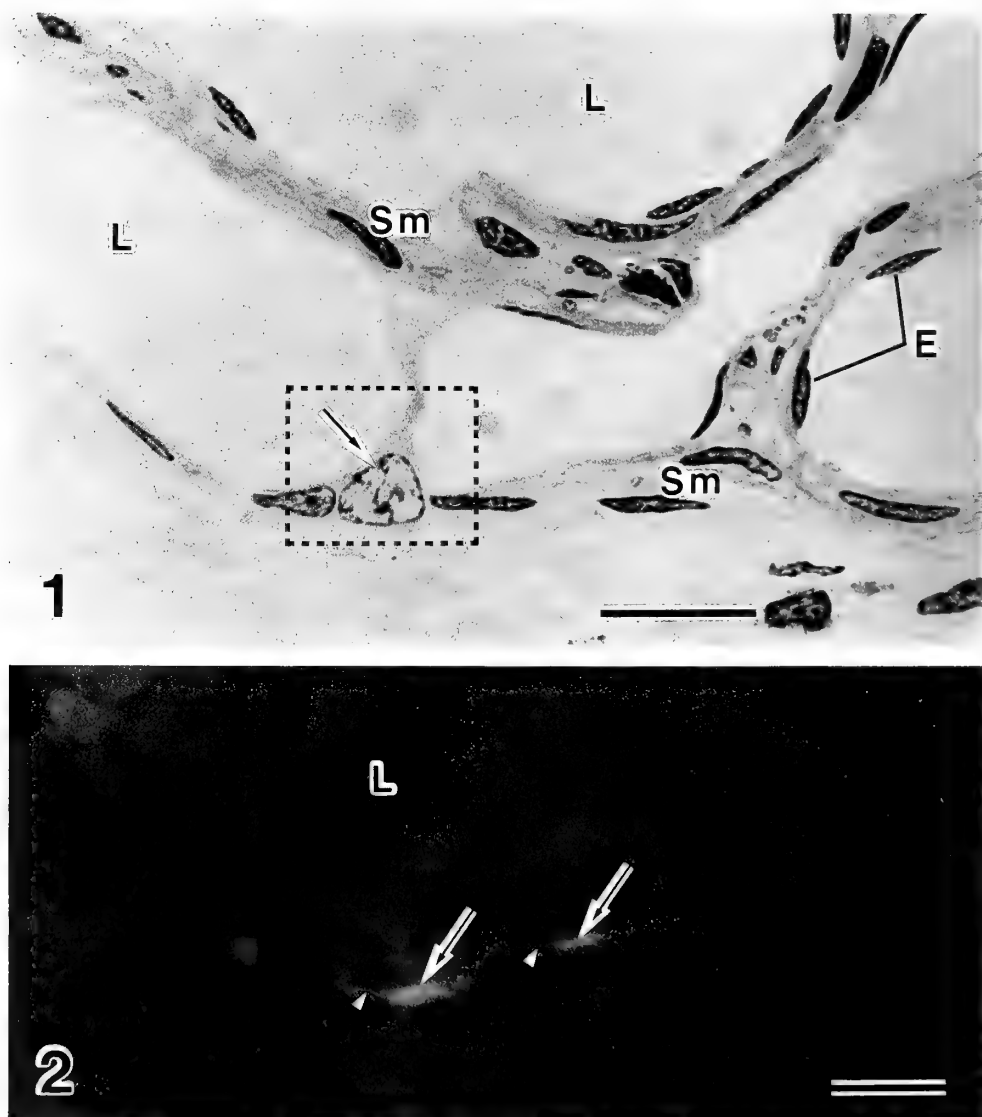


FIG. 1. Light micrograph of a toluidine blue-stained section of the carotid labyrinth. A glomus cell (arrow) is located near the lumen of a sinusoid (L). E, endothelial cells; Sm, smooth muscle cells. Scale bar, 20 μ m.

FIG. 2. Fluorescence micrograph of the carotid labyrinth. Two greenish-yellow fluorescent cells (arrows) with long processes (arrowheads). L, lumen of sinusoid. Scale bar, 50 μ m.

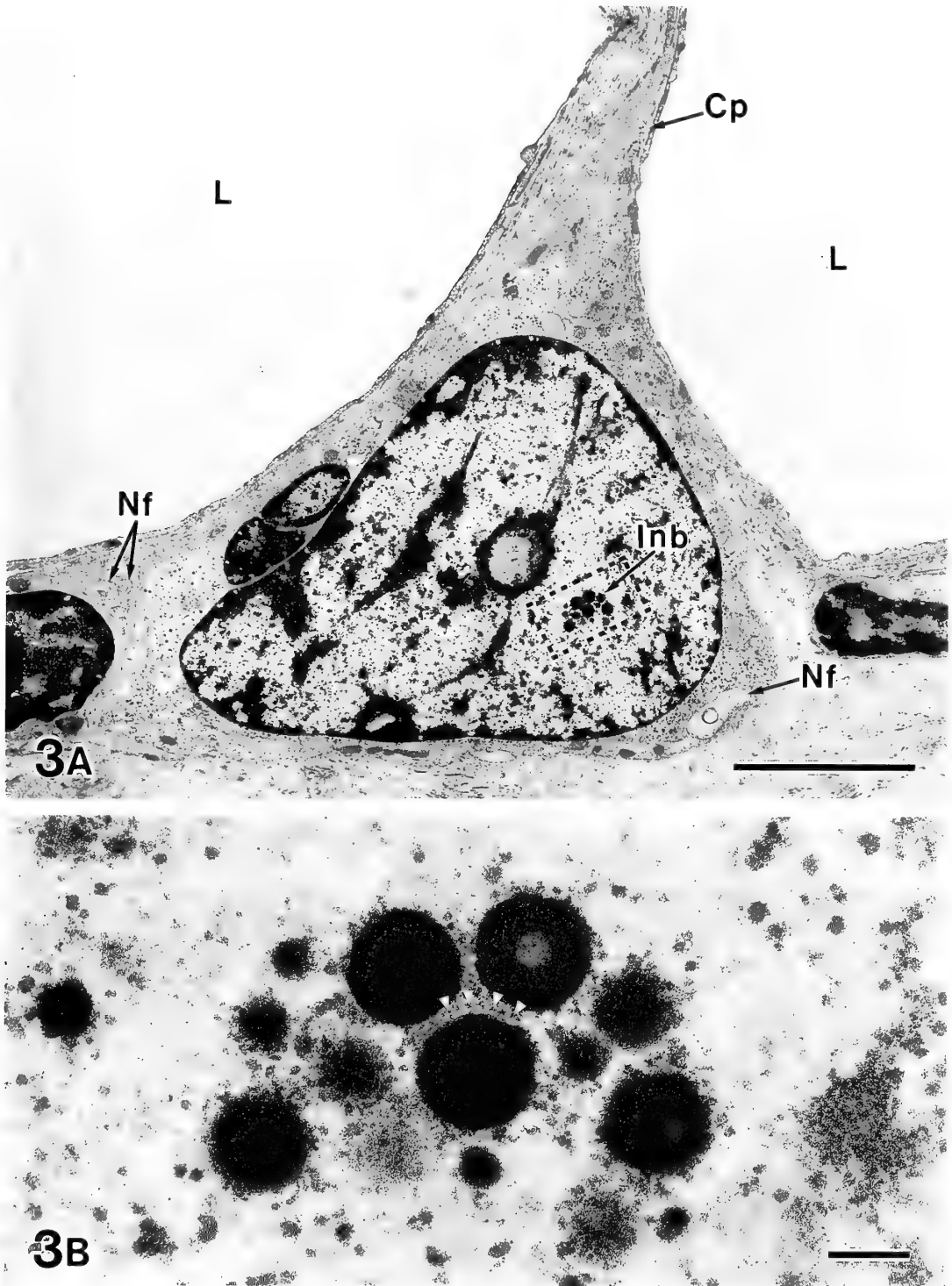


FIG. 3. A) Electron micrograph in low magnification of the glomus cell. The glomus cell (the boxed area in Figure 1) contains numerous cytoplasmic granules. Cp, cytoplasmic projection. Inb, intranuclear inclusion bodies; L, lumen of sinusoid; Nf, nerve fiber. Scale bar, 5 μm . B) High magnification of the intranuclear inclusion bodies. Between bodies small dense materials lie in a uniform array at regular intervals (arrowheads). Scale bar, 0.2 μm .

glomus cells had pale cytoplasm and a large oval nucleus, and were located singly or in clusters (50–60 μm in diameter) of 3–4 cells between connective tissues and smooth muscle cells (Fig. 1). In fluorescence microscopy, the glomus cells were identified as small, intensely fluorescent (greenish yellow) cells with long processes (Fig. 2).

Electron microscopy

The sinusoidal wall was composed of extremely thin endothelial cells. In the subendothelial stroma, several cellular elements and extracellular components such as collagenous fibers and amorphous ground substance were located. Enveloped by thin processes of supporting cells, the glomus cells were located in the vascular stroma singly or in clusters (Fig. 3A). Occasionally, a part of cell surface was directly in contact with the connective

tissue, losing its covering of supporting cells. Between the clustered cells desmosome-like junctions were often observed. The cells were usually oval. A single oval nucleus contained dispersed clumps of heterochromatin. Near the nucleolus, a group of electron-dense inclusion bodies of various sizes (0.1–0.3 μm in diameter) was sometimes observed (Fig. 3A). At high magnification, many small dense particles were attached to the surface of intranuclear inclusion bodies (Fig. 3B).

Numerous dense-cored vesicles (60–100 nm in diameter) were scattered throughout the cytoplasm. Coated pits were often found on the surface of the cell body and its processes (Fig. 4). A well-developed Golgi complex was found in the perinuclear area, and in its vesicles small newly synthesized low-density granules were seen. A relatively small amount of granulated endoplasmic

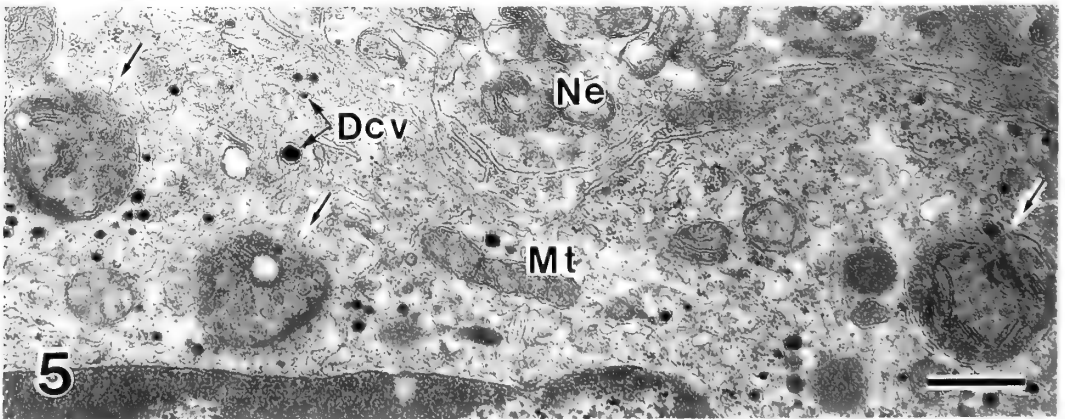
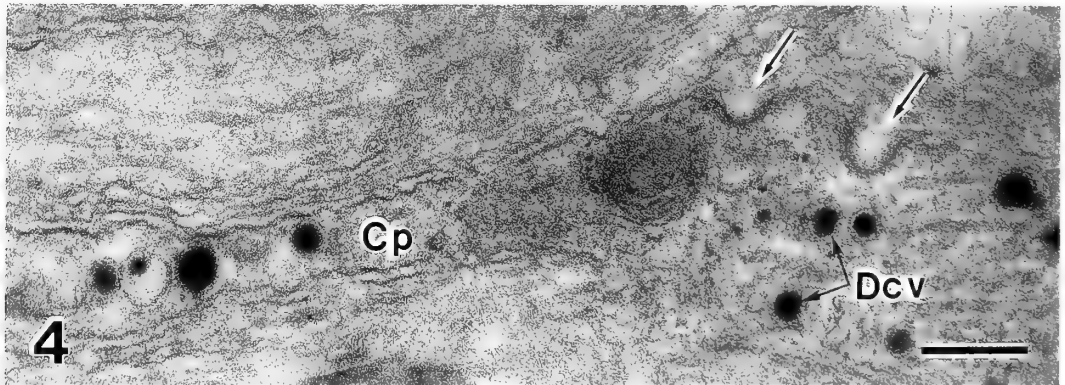


FIG. 4. Two membrane invaginations of the cytoplasmic processes (CP) of the glomus cell. Extruded content has almost dissolved. Arrows indicate membrane invaginations. Dcv, dense-cored vesicles. Scale bar, 0.2 μm .

FIG. 5. Residual bodies (arrows) in the glomus cell. Myelinated inclusions, small vesicles and a small vacuole can be seen. Dcv, dense-cored vesicles; Mt, mitochondria. Ne, nerve ending. Scale bar, 0.5 μm .

reticulum, numerous free ribosomes and oval elongated mitochondria were dispersed throughout the cytoplasm. Centrioles were located near the nucleus. Large residual bodies, a kind of lysosome, were also observed. They were round and about $0.7\ \mu\text{m}$ in diameter with myelinated inclusions and small vesicles (Fig. 5). Losing their covering of supporting cells, long thin cytoplasmic projections of the glomus cells extended toward the endothelium. Some of them were longer than $20\ \mu\text{m}$ and closely associated with the endothelial cells (g-e connection) (Fig. 6A) or with the pericytes (g-p connection) (Fig. 6B) without visible

intervening substances.

Enclosed by supporting cells, nerve endings lay close to the glomus cells to make synapses. Two types of synapses were distinguished on the glomus cell. Most of the large synapses were morphologically efferent and were characterized by the accumulation of clear vesicles (40–60 nm in diameter). At the junction the membrane of the nerve ending was thicker than the cell membrane (Fig. 7A). Small afferent type synapses were sometimes observed; specialized membrane thickenings were conspicuous on the cell membrane where dense-cored vesicles were aggregated (Fig. 7A). So-

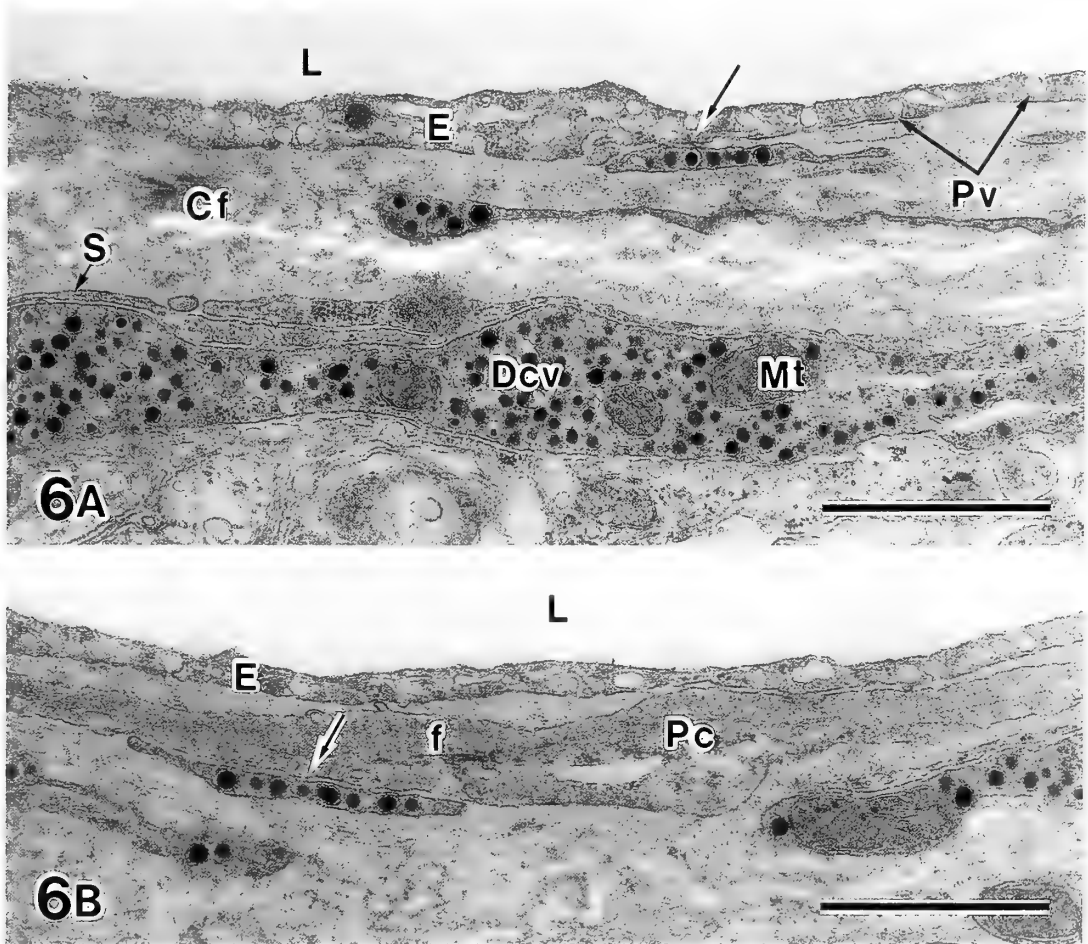


FIG. 6. A) Three cytoplasmic processes extend into the intervacular stroma. The inner two processes lose the covering of supporting cell cytoplasm (S), and luminal one makes g-e connection (arrow). Cf, collagenous fiber; Dcv, dense-cored vesicles; E, endothelial cell; L, lumen of sinusoid; Mt, mitochondria; Pv, plasmalemmal vesicles. Scale bar, $1\ \mu\text{m}$. B) A pericyte (Pc) directly connect with the process of a glomus cell (arrow). E, endothelial cell; f, filaments; L, lumen of sinusoid. Scale bar, $1\ \mu\text{m}$.

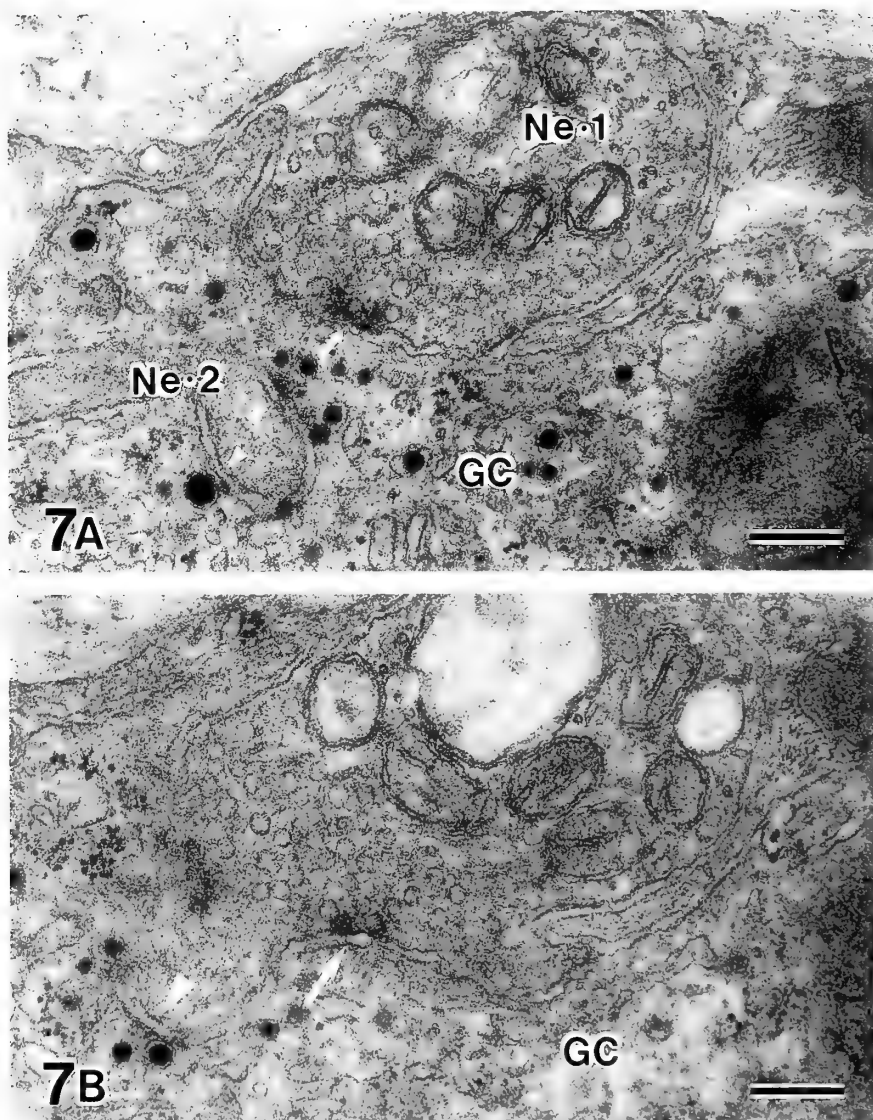


FIG. 7. A) Synaptic junctions between the glomus cell and nerve ending. The arrow and arrowheads indicate efferent and afferent type synapses, respectively. One nerve ending (Ne-1) which contains numerous clear vesicles and some mitochondria synapses with the glomus cell (Gc). The synapse shows asymmetrical membrane thickening on the Ne-1 side. Many synaptic vesicles accumulate at this junctional region (arrow). Another nerve ending (Ne-2) without clear vesicles synapses with the same glomus cell (Gc). Asymmetrical membrane thickenings are found on the glomus cell side. A few dense-cored vesicles aggregate at this synaptic region (arrowheads). Scale bar, $0.2 \mu\text{m}$. B) So-called reciprocal synapses between the glomus cell and nerve ending. The arrow and arrowhead show efferent and afferent type synapses, respectively. A and B are semi serial sections. Scale bar, $0.2 \mu\text{m}$.

called reciprocal synapses consisting of efferent and afferent type synapses on the same nerve ending were also observed (Fig. 7B).

DISCUSSION

The carotid labyrinth of the urodeles consists of a vascular maze [1, 9] and contains cells with many

dense-cored vesicles [6]. The present electron microscopic study in the newt *Cynops pyrrhogaster* showed that these cells (glomus cells) are situated in the vascular stroma as isolated cells or in clusters of 3 or 4 cells, and their ultrastructure is similar to that of glomus cells observed in arterial chemoreceptor regions of anurans [4, 10]. In the toad *Bufo vulgaris*, the carotid labyrinth has been physiologically confirmed to have an arterial chemoreceptor function similar to that of the mammalian carotid body [2]. The glomus cell has long been known to be a chemoreceptor, but in recent years it has been postulated to have a secretory function as well [5, 11]. Although there is no direct evidence, the structural characteristics of the newt carotid labyrinth point to a chemoreceptor function, in which the glomus cells play the main role.

In the present paper, I have reported for the first time the presence of intranuclear inclusion bodies in the glomus cell nucleus. Intranuclear inclusion bodies have been observed only in clearly defined secretory cells: in the intestine [12] and in the colon [13] of the horse, in the epididymis of the dog [14], and in the adenohypophysis of the rabbit [15]. Although their origin and role are as yet unknown, they may be considered a characteristic feature of the secretory function. This finding may indicate a secretory function of the glomus cell as stated above, or it may show that intranuclear inclusion bodies exist in more extensive cell domains than so far accepted.

In addition, the g-e connection was observed for the first time in amphibian glomus cells. Kondo [16] and Ookawara *et al.* [17] observed close contact of granule-containing cells with endothelial cells in the domestic fowl, and Kondo [16] proposed a secretory function for the granule-containing cells there. Since the vesicles in the endothelial cells are commonly accepted to be involved in intracellular transport [18, 19], catecholamines contained in dense-cored vesicles might be released into the blood vessels. However these might also be structures facilitating blood gas uptake by glomus cells for chemoreception. On the other hand, the g-p connection suggests that the vascular tone might be modified by catecholamine in glomus cell granules, if catecholamine releasing occurs in this region.

Two types of synapses, efferent and afferent, were reported in toad carotid labyrinth [4] and in tortoise carotid artery [20]. Also in this study, afferent and efferent synapses were observed between the nerve endings and glomus cells as described by Kobayashi [6]. Furthermore Yamauchi [21] reported reciprocal synapses in the toad carotid labyrinth. Serial sections suggested that all nerve endings may be reciprocal in the newt carotid labyrinth.

In conclusion, the newt glomus cells may have a secretory function in addition to their chemoreceptor function.

ACKNOWLEDGMENTS

I wish to thank Prof. M. Asashima of the Department of Biology for kindly supplying animals, Dr. R. C. Goris of Department of Anatomy, Yokohama City University for his help in preparing the manuscript and Drs. Kosei Ishii and Kazuko Ishii for their critical reading of the manuscript. This work was supported by Grants-in-Aid (No. 63770024) from the Ministry of Education, Science and Culture, Japan.

REFERENCES

- 1 Adams, W. E. (1958) The comparative morphology of the carotid body and carotid sinus. Charles C. Thomas, Springfield, pp. 202-214.
- 2 Ishii, K., Honda, K. and Ishii, K. (1966) The function of the carotid labyrinth in the toad. *Tohoku J. exp. Med.*, **88**: 103-116.
- 3 Rogers, D. C. (1963) Distinct cell types in the carotid labyrinth. *Nature*, **200**: 492-493.
- 4 Ishii, K. and Oosaki, T. (1969) Fine structure of the chemoreceptor cell in the amphibian carotid labyrinth. *J. Anat. (Lond)*, **104**: 263-280.
- 5 Ishii, K. and Kusakabe, T. (1982) The glomus cell of the carotid labyrinth of *Xenopus laevis*. *Cell Tissue Res.*, **224**: 459-463.
- 6 Kobayashi, S. (1971) Comparative cytological studies of the carotid body. 2. Ultrastructure of the synapse on the chief cell. *Arch. histol. jap.*, **33**: 397-420.
- 7 Wislang, M. R. (1965) The carotid labyrinth in two species of urodeles. *J. Anat. (Lond)*, **99**: 949.
- 8 Grillo, M. A., Jacobs, L. and Comroe, Jr. J. H. (1974) A combined fluorescence histochemical and electron microscopic method for studying special monoaminecontaining cells (SIF cells). *J. Comp. Neurol.*, **153**: 1-14.
- 9 Ishida, S. (1954) So-called carotic body of the

- amphibia. *Igaku Kenkyu* (Fukuoka), **24**: 1024–1050.
- 10 Ishii, K. Ishii, K. and Kusakabe, T. (1985) Chemo- and baroreceptor innervation of the aortic trunk of the toad *Bufo vulgaris*. *Respir. Physiol.*, **60**: 365–375.
 - 11 Kusakabe, T., Ishii, K. and Ishii, K. (1987) A possible role of the glomus cell in controlling vascular tone of the carotid labyrinth of *Xenopus laevis*. *Tohoku J. exp. Med.*, **151**: 395–408.
 - 12 Dual, D. E. (1980) The origin of nuclear bodies: A study of the undifferentiated epithelial cells of the equine small intestine. *Am. J. Anat.*, **157**: 61–70.
 - 13 Pfeiffer, C. J., Marry, M. J. and Legends, L. (1987) The equine colonic mucosal granular cell: Identification and X-ray microanalysis of apical granules and nuclear bodies. *Anat. Rec.*, **219**: 258–267.
 - 14 Nicander, L. (1964) Fine structure and cytochemistry of nuclear inclusions in the dog epididymis. *Exp. Cell Res.*, **34**: 533–541.
 - 15 Foster, C. L., Young, B. A., Allanson, M. and Cameron, E. (1965) Nuclear inclusions in the adenohypophysis of the rabbit. *J. Endocrinol.*, **33**: 159–160.
 - 16 Kondo, H. (1974) On the granule-containing cells in the aortic wall of the young chick. *Anat. Rec.*, **178**: 253–266.
 - 17 Ookawara, S., Suzuki K., Yoshida, Y. and Ooneda, G. (1974) Monoamine-storing cells in the media of the thoracic aorta of *Gullus domesticus*. *Cell Tiss. Res.*, **151**: 309–316.
 - 18 Palade, G. E. (1953) Fine structure of blood capillaries. *J. appl. Physics*, **24**: 1424.
 - 19 Simionescu, N., Simionescu, M. and Palade, G. E. (1975) Permeability of muscle capillaries to small heme-peptides. Evidence for the existence of patent transendothelial channels. *J. Cell Biol.*, **64**: 586–607.
 - 20 Kusakabe, T., Ishii, K. and Ishii, K. (1988) Dense granule-containing cells in the arterial chemoreceptor area of the tortoise (*Testudo hermanni*). *J. Morphol.*, **197**: 183–191.
 - 21 Yamauchi, A. (1977) On the recepto-endocrine property of granule-containing (GC) cells in the autonomic nervous system. *Arch. histol. jap.*, **40**, Suppl: 147–161.

Abnormal Development of Preimplantation Embryos Derived from Intersubspecific Hybrids between *Mus musculus molossinus* and *M. m. domesticus*

MICHIKO NIWA and NOBORU WAKASUGI

*Laboratory of Animal Genetics, Faculty of Agriculture,
Nagoya University, Chikusa-ku, Nagoya 464, Japan*

ABSTRACT—Japanese wild mice, *Mus musculus molossinus*, are genetically remote from laboratory mice which are derived predominantly from European wild mice *M. m. domesticus*. Our previous study demonstrated that F2 progeny between these two mouse subspecies show low fertility, even though F1 hybrids are fully fertile. In fact about half of the F2 females fail to become pregnant. We examined the *in vitro* development of preimplantation embryos from F2 progeny between MOM (one of the inbred strains derived from Japanese wild mice) and C57BL/6 (B6, an inbred strain of laboratory mice). We found that the low pregnancy rate of F2 females results from a high embryonic mortality: only 58.4% (66/113) of embryos developed to the blastocyst stage in the F2×F2 cross, whereas in the B6×B6 cross the corresponding figure was 100.0% (23/23). The mortality was not due to defects in sperm from F2 males but rather to defects in the eggs from F2 females: the survival rate of embryos up to the blastocyst stage was 52.2% (82/157) in the F2♀×B6♂ cross, whereas it was 94.9% (74/78) in the B6♀×F2♂ cross. The factors responsible for this mortality are attributable to nucleus, not to maternally inherited cytoplasm: more than 10% of N2 females derived from backcrossing either F1 females to B6 males or F1 males to B6 females showed the higher embryonic mortality. This finding suggests that intersubspecific genic combinations, either intragenic or intergenic, give rise to some deleterious effects on the oocytes during oogenesis.

INTRODUCTION

The species *Mus musculus* can be classified into several groups (subspecies) from a genetic perspective [1, 2]. It has been demonstrated that common laboratory mice originate predominantly from a European subspecies, *Mus musculus domesticus*, by the analysis of mitochondrial and nuclear genomes [3, 4]. Japanese wild mice, *M. m. molossinus*, are very different from *M. m. domesticus* and are closely related to *M. m. musculus* and *M. m. castaneus* [2, 3]. The evolutionary divergence of *M. m. molossinus* from *M. m. domesticus* is estimated to have occurred about one million years ago [3, 5, 6].

There appears to exist a severe restriction of the gene flow in the contact zone between *M. m. domesticus* and *M. m. musculus* in Europe [7]. It

can be inferred, therefore, that there is an incompatibility between the genomes of the two subspecies. Male sterility is suspected of being one manifestation of the incompatibility that is responsible for restriction of the gene flow in this area [7, 8].

Several inbred strains derived from Japanese wild mice, *Mus musculus molossinus*, have been established in our laboratory to provide us with a wide variety of experimental material. When we attempted to generate recombinant inbred strains from F1 hybrids between *molossinus* and laboratory strains, a serious depression in fertility was observed in the subsequent generations, despite the fact that both parental strains had been bred for more than 20 generations by brother-sister matings. So far, no evidence has been reported that there is a serious reproductive disturbance in the F2 females derived from inter-strain crosses among laboratory strains of inbred mice. We previously reported details of the reproductive

preformance of F1 and F2 generations from crosses between molossinus and laboratory strains [9]. Such F1 hybrids are fully fertile, but in the F2 generation, about half of the F2 females fail to become pregnant. Since the F2 progeny copulated normally, it appeared possible that preimplantation loss of embryos may be responsible for the infertility observed in half of the F2 females.

In the present study, we examined the development *in vitro* of preimplantation embryos obtained from F2 and backcross (N2) generations between molossinus and laboratory mice.

MATERIALS AND METHODS

Animals

C57BL/6 (B6) and MOM strains were used. The MOM strain is derived from Japanese wild mice (*Mus musculus molossinus*), whose ancestors were captured at Nagoya in Japan. The number of inbreeding generations was 46 at the time when the present study was undertaken. F1 and F2 generations were produced through reciprocal matings between B6 and MOM. Since there were no differences in the fertility between members of the F2 generations derived from (B6 ♀ × MOM ♂) F1 and from (MOM ♀ × B6 ♂) F1, they were pooled in the present study. Backcross progeny (N2) were produced from the crossing of either F1 ♀ × B6 ♂ or B6 ♀ × F1 ♂.

Observation of embryos

Two- to twelve-month-old females were mated with males and checked daily for vaginal plugs. The day on which a plug was found to be present was designated as Day 0 of pregnancy. The embryos were recovered by flushing oviducts with Medium 2 (M2) [10] from plug-positive females on Day 1 or Day 2, and they were examined with reference to developmental stage and morphology under a dissecting microscope. Subsequently, the embryos were cultured in pre-equilibrated Medium 16 (M16) [11] under paraffin oil in an atmosphere of 5% CO₂ in air at 37°C. Embryos were examined at intervals of 24 hr and the number of embryos that developed to the blastocyst stage was recorded.

RESULTS

Our of a total of 21 embryos obtained from three MOM females mated with MOM males, 18 (85.7%) developed into expanded blastocysts. Most embryos from F1 females which had been mated with B6, MOM, or F1 males also developed to the blastocyst stage: out of 103 morphologically normal embryos collected from 13 females, 95 (92.2%) developed into blastocysts. In these crosses, embryos were obtained on Day 1 and Day 2. As summarized in Table 1, ovulation and fertilization occurred normally in the F2 females.

All fertilized eggs were cultured *in vitro* and the number of embryos that developed to the blasto-

TABLE 1. Developmental ability of embryos obtained on Day 1 of pregnancy from F2 females between B6 and MOM strains and B6 females

Crosses ♀ × ♂	No. of ♀ ♀ examined	No. of eggs collected (mean ± sem)	No. of normal embryos ^{a)}	No. of embryos that developed to blastocysts during 4 days in culture
F2 × F2	16	114 (71. ± 0.5)	113 (99.1%)	66 (58.4) ^{b)}
F2 × B6	24	166 (6.9 ± 0.4)	157 (94.6)	82 (52.2)
B6 × F2	9	80 (8.9 ± 0.5)	78 (97.5)	74 (94.9)
B6 × B6	3	23 (7.7 ± 0.3)	23 (100.0)	23 (100.0)

^{a)} Morphologically normal 2- to 6-cell embryos were counted.

^{b)} Percentage was computed from the number of normal embryos.

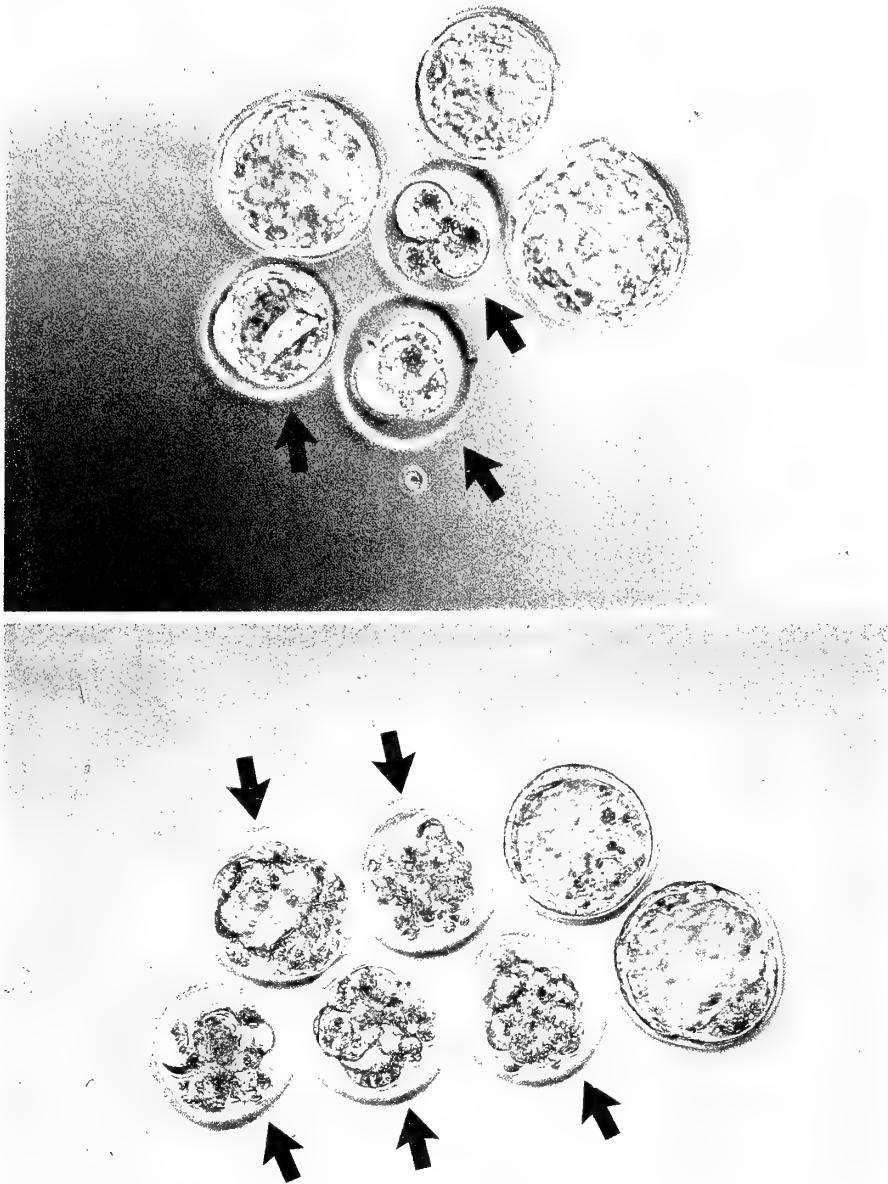


FIG. 1. Morphological appearance after culture *in vitro* of embryos from F2 ♀ × B6 ♂ cross, including degenerated or retarded embryos. Embryos were collected on Day 1 of pregnancy and photographed after 72 hr in culture. Arrows indicate the abnormal embryos that are developmentally retarded or have degenerated.

TABLE 2. Proportion of normal embryos on Day 2 of pregnancy from F2 and B6 females mated with B6 males, and their developmental ability in culture

Crosses $\text{♀} \times \text{♂}$	No. of ♀ examined	No. of embryos obtained ^{a)}	No. of normal embryos ^{a)}	No. of embryos that developed to blastocysts during 3 days in culture
F2 \times B6	22	161	118 (73.3%)	95 (59.0% ^{c)})
B6 \times B6	7	53	53 (100.0)	50 (94.3)

^{a)} Embryos, and not unfertilized eggs, were counted.

^{b)} Morphologically normal embryos at the 6-cell to the morula stage were counted.

^{c)} No. of blastocysts/No. of embryos obtained.

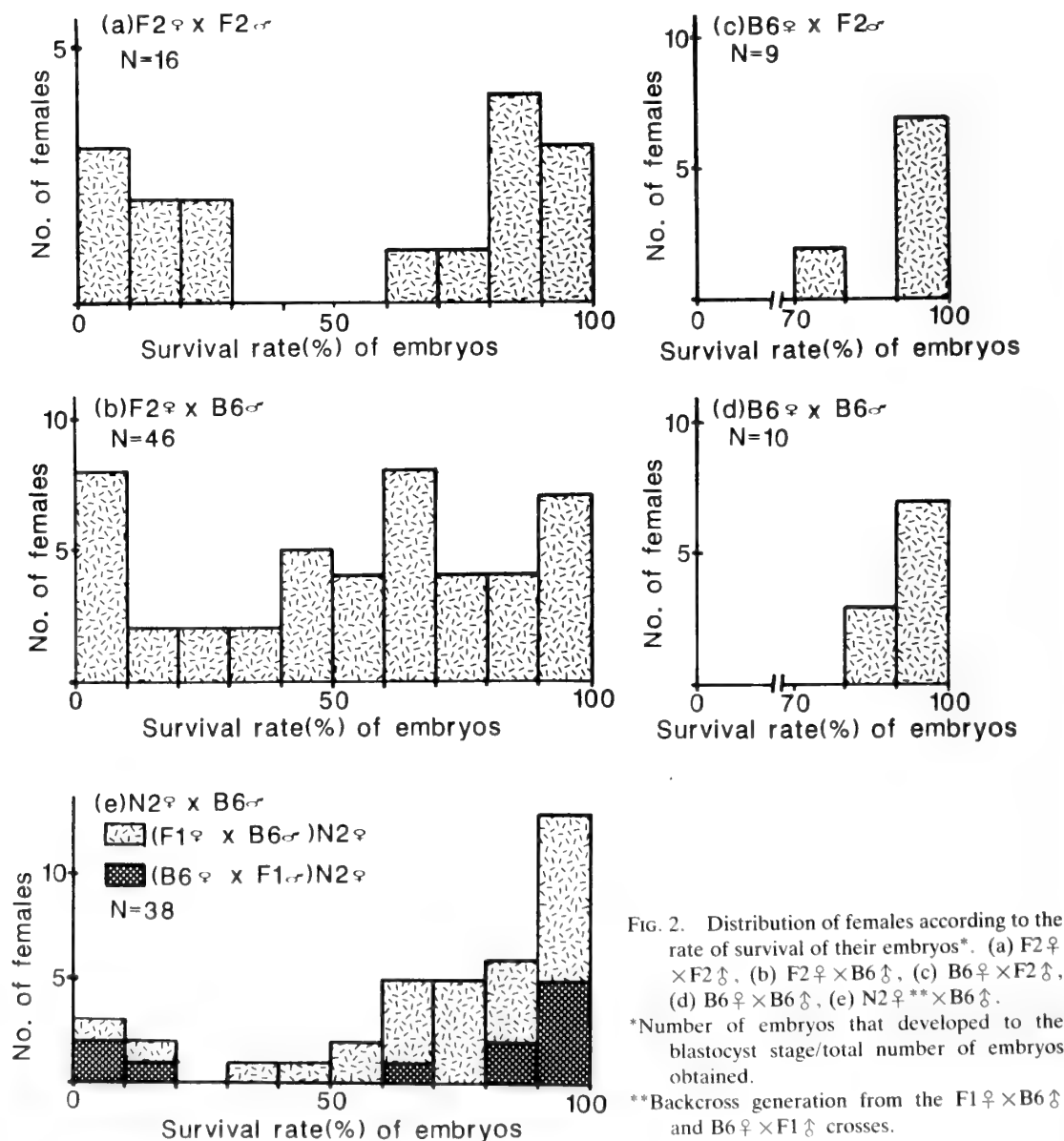


FIG. 2. Distribution of females according to the rate of survival of their embryos*. (a) F2♀ \times F2♂, (b) F2♀ \times B6♂, (c) B6♀ \times F2♂, (d) B6♀ \times B6♂, (e) N2♀ \times B6♂.

*Number of embryos that developed to the blastocyst stage/total number of embryos obtained.

**Backcross generation from the F1♀ \times B6♂ and B6♀ \times F1♂ crosses.

cyst stage was counted. In the crosses of $F2 \times F2$ and $F2 \text{♀} \times B6 \text{♂}$, the proportion of embryos that developed to the blastocyst stage, including unexpanded embryos, was very small (Table 1). Many embryos from $F2$ females exhibited morphological alterations or developmental arrest at various stages from the 2- to the 6-cell stage as far as blastulation. Figure 1 shows embryos from $F2$ females during culture. They were all morphologically normal, 2- to 4-cell embryos when collected on Day 1. In the case of the $B6 \text{♀} \times F2 \text{♂}$ and $B6 \times B6$ crosses, almost all embryos developed into normal, expanded blastocysts. These results suggest that the abnormality in development can be attributed to some disturbance in the eggs from $F2$ females.

Next we examined the embryos on Day 2 of pregnancy from $F2$ and $B6$ females mated with $B6$ males. As shown in Table 2, more than 70% of embryos collected from $F2 \text{♀} \times B6 \text{♂}$ crosses were morphologically normal at the 6-cell to the morula stage while the others were abnormal or had degenerated. During culture, about 60% of embryos survived to form blastocysts. This result confirmed the findings shown in Table 1: about half of the embryos from $F2$ females died around the morula stage both *in vivo* and *in vitro*. In the control cross, $B6 \times B6$, morphologically normal embryos were obtained and most of them developed to form expanded blastocysts.

Figure 2 shows the distribution of females according to the proportion of embryos that developed to the blastocyst stage. The results of $F2 \text{♀} \times F2 \text{♂}$ and $F2 \text{♀} \times B6 \text{♂}$ crosses (Fig. 2a, b) demonstrated that there are two types of female: one showing a higher rate of survival of embryos and the other showing a lower rate. In the crosses of $B6 \text{♀} \times F2 \text{♂}$ and $B6 \text{♀} \times B6 \text{♂}$, the rate of survival of embryos that developed to the blastocyst stage for each female was greater than 70% (Fig. 2c, d). This result demonstrates that the $F2$ sperm does not negatively influence the developmental abnormality of the embryos. Figure 2e shows the distribution of the survival rates of embryos obtained from $N2$ females, progeny of the $F1 \text{♀} \times B6 \text{♀}$ and $B6 \text{♀} \times F1 \text{♂}$ crosses, when they were mated with $B6$ males. The mean number of embryos obtained on Day 2 was 8.2 ± 0.3 . Ex-

tremely poor rates of survival of embryos, lower than 20%, were observed in the case of 5 $N2$ females out of 38 (13.2%); 3 of these females being from the $B6 \text{♀} \times F1 \text{♂}$ cross, and 2 from the $F1 \text{♀} \times B6 \text{♂}$ cross. The higher rates of embryonic mortality observed in the case of these $N2$ females demonstrate that the abnormality is inherited from both $F1$ females and $F1$ males.

DISCUSSION

In order to investigate the infertility of about half of the $F2$ females between the two subspecies *Mus musculus domesticus* and *M. m. molossinus*, we examined the preimplantation development of their embryos. Our data indicate that a higher frequency of embryonic mortality during preimplantation development is responsible for the infertility observed in the $F2$ females. We confirmed our previous observation that there is segregation of fertile and infertile $F2$ females. Some $F2$ females showed higher rates of survival of their embryos and others showed lower rates. This embryonic death can be attributed to defects in the eggs, not in the sperm, from the $F2$ generation. $F2$ males are fertile when they mate with $B6$ females [9]. The factors that cause the embryonic death which occurs around the morula stage are inherited from both $F1$ males and $F1$ females (Fig. 2e). It has been reported that embryonic genes are transcribed and expressed soon after fertilization [12, 13]. Such a conclusion implies the possible switching of the information for development from maternal to embryonic [12]. The early expression of embryonic genes is necessary for compaction of 8-cell mouse embryos [13]. Therefore, the mortality at the early developmental stage observed in our study may possibly be due to some abnormality in the embryonic genome and not in the maternally inherited cytoplasm which functions in the early stages of development. In addition, the factors that cause this abnormality appear to be autosomal. Some of the $N2$ females that showed lower rates of survival of embryos were derived from the $B6 \text{♀} \times (B6 \text{♀} \times \text{MOM} \text{♂}) F1 \text{♂}$ cross, having two $B6$ X-chromosomes.

The reproductive abnormality in the $F2$ generation observed in this study is presumably related to

a genetic incompatibility that arises from the combination of genes (chromosomes) from different subspecies. Such an incompatibility is observed in the contact zone between *Mus musculus domesticus* and *M. m. musculus* in Europe, where a restriction of the gene flow is observed [7, 14, 15]. Hybrid male sterility has been considered to be responsible for this restriction. Recently Vanlerberghe *et al.* [15] reported that the limitation of Y-chromosome introgression in the contact zone is not attributable to the sterility in F1 males between the two subspecies. The developmental abnormalities in the preimplantation embryos from F2 females of the intersubspecific crosses observed in this study provide one possible explanation. From an analysis of restriction patterns of mitochondrial DNA, it has been shown that *M. m. molossinus* is related to *M. m. musculus* and to *M. m. castaneus*, both of which are quite remote from *M. m. domesticus* [2, 4, 5, 16]. It has been proposed that *M. m. molossinus* originated from the hybridization of *M. m. musculus* and *M. m. castaneus* [17]. If this was indeed the case, it can be inferred that hybrids between *domesticus* and *musculus* in the contact zone in Europe could show reproductive defects in the same way as the intersubspecific hybrids described in this report. At investigation of this interpretation should prove interesting.

ACKNOWLEDGMENTS

We thank Drs. K. Kondo, T. Tomita, T. Namikawa, Y. Kawamoto, and other members of our laboratory for their helpful discussions. We also thank Dr. K. Moriwaki for his critical reading of the manuscript. We are also grateful to Ms. S. Narita for her help in taking care of our experimental animals.

REFERENCES

- Bonhomme, F., Catalan, J., Britton-Davidian, J., Chapman, V. M., Moriwaki, K., Nevo, E. and Thaler, L. (1984) Biochemical diversity and evolution in the genus *Mus*. *Biochem. Genet.*, **22**: 275–303.
- Moriwaki, K., Miyashita, N., Suzuki, H., Kurihara, Y. and Yonekawa, H. (1986) Genetic features of major geographical isolates of *Mus musculus*. In "Current Topics in Microbiology and Immunology, Vol. 127". Ed. by M. Potter, J. H. Nadeau and M. P. Cancro, Springer-Verlag, Berlin Heidelberg, pp. 55–61.
- Moriwaki, K., Shiroishi, T., Minezawa, M., Aotsuka, T. and Kondo, K. (1979) Frequency distribution of histocompatibility-2 antigenic specificities in the Japanese wild mouse genetically remote from the European subspecies. *J. immunogenet.*, **6**, 99–113.
- Yonekawa, H., Moriwaki, K., Gotoh, O., Miyashita, N., Migita, S., Bonhomme, F., Hjorth, J. P., Petras, M. L. and Tagashira, Y. (1982) Origins of laboratory mice deduced from restriction patterns of mitochondrial DNA. *Differentiation* **22**, 222–226.
- Ferris, S. D., Sage, R. D., Prager, E. M., Ritte, U. and Wilson, A. C. (1983) Mitochondrial DNA evolution in mice. *Genetics*, **105**, 681–721.
- Yonekawa, H., Moriwaki, K., Gotoh, O., Hayashi, J.-I., Watanabe, J., Miyashita, N., Petras, M. L. and Tagashira, Y. (1981) Evolutionary relationships among five subspecies of *Mus musculus* based on restriction enzyme cleavage patterns of mitochondrial DNA. *Genetics*, **98**: 801–816.
- Sage, R. D., Whitney, J. B. and Wilson, A. C. (1986) Genetic analysis of a hybrid zone between *domesticus* and *musculus* mice (*Mus musculus* complex): hemoglobin polymorphisms. In "Current Topics in Microbiology and Immunology, Vol. 127". Ed. by M. Potter, J. H. Nadeau and M. P. Cancro, Springer-Verlag, Berlin Heidelberg, pp. 75–85.
- Forejt, J. and Iványi, P. (1975) Genetic studies on male sterility of hybrids between laboratory and wild mice. *Genet. Res.*, **24**: 189–206.
- Niwa, M. and Wakasugi, N. (1988) Fertility in intersubspecific hybrids of laboratory mice (*Mus musculus domesticus*) and molossinus mice (*M. m. molossinus*). *Exp. Anim.*, **37**: 387–392.
- Quinn, P., Barros, C. and Whittingham, D. G. (1982) Preservation of hamster to assay the fertilizing capacity of human spermatozoa. *J. Reprod. Fert.*, **66**: 161–168.
- Whittingham, D. G. (1971) Culture of mouse ova. *J. Reprod. Fert. (suppl.)*, **14**: 7–21.
- Petzoldt, U. and Muggleton-Harris, A. (1987) The effect of the nucleocytoplasmic ratio on protein synthesis and expression of a stage-specific antigen in early cleaving mouse embryos. *Development*, **99**: 481–491.
- Smith, R. K. W. and Johnson, M. H. (1985) DNA replication and compaction in the cleaving embryo of the mouse. *J. Embryol. exp. Morph.*, **89**: 133–148.
- Hunt, W. G. and Selander, R. K. (1973) Biochemical genetics of hybridisation in European house mice. *Heredity*, **31**, 11–33.
- Vanlerberghe, F., Dod, B., Boursot, P., Ballis, M. and Bonhomme, F. (1986) Absence of Y-chromosome introgression across the hybrid zone between *Mus musculus domesticus* and *Mus musculus muscu-*

- lus*. Genet. Res., **48**: 191–197.
- 16 Moriwaki, K., Yonekawa, H., Gotoh, O., Minezawa, M., Winking, H. and Gropp, A. (1984) Implications of the genetic divergence between European wild mice with Robertsonian translocations from the viewpoint of mitochondrial DNA. Genet. Res., **43**:277–287.
- 17 Yonekawa, H., Moriwaki, K., Gotoh, O., Miyashita, N., Matsushima, Y., Shi, L., Cho, W. S., Zhen, X. L. and Tagashira, Y. (1988) Hybrid origin of Japanese mice “*Mus musculus molossinus*”: evidence from restriction analysis of mitochondrial DNA. Mol. Biol. Evol., **5**: 63–78.

Evidence for a Thy-1-Like Molecule Expressed on Earthworm Leucocytes

ABDEL HAKIM SAAD¹ and EDWIN COOPER²

¹Department of Zoology, Faculty of Science, Cairo University, Cairo, Egypt, and ²Department of Anatomy, University of California, Los Angeles, CA, U.S.A.

ABSTRACT—In this study, we analyzed the presence of a Thy-1 homolog in the earthworm, *Lumbricus terrestris*, using several monoclonal and xenoantisera in indirect immunofluorescence (IF) assay. The reactivity of monoclonal antibodies Thy-1.1 and Thy-1.2 proved specificities to the Thy-1.1 determinant. A rabbit anti-rat Thy-1 (Thy-1.1) antiserum was further investigated in IF assay by *in vitro* quantitative absorption. In all assays, earthworm leucocytes inhibited reactivity of antiserum as effectively as rat thymocytes in contrast to BALB/c (Thy-1.2) thymocytes. Thus, a Thy-1.1 cross-reacting determinant is probably expressed by a Thy-1 homolog on leucocytes of earthworms. The serological similarity between the earthworm Thy-1 homolog and the Thy-1 molecule in vertebrates will be strengthened by future immunochemical data.

INTRODUCTION

Coelomic fluid of earthworms contains several morphological categories of leucocytes which have been shown to play prominent role in allogeneic and xenogeneic graft rejection; the case of certain leucocytes associated with class I antigen in mammals [cf. in 1]. But until now, no attempts has been made to elucidate the nature of leucocyte membrane structures involved in such phenomena. Recently, Roch *et al.* [2] succeeded in demonstrating serological evidence for a membrane structure related to human β_2 -microglobulin expressed by certain earthworm leucocytes. In searching for the origin of Thy-1, Shalev *et al.* [3] have demonstrated Thy-1-like molecule in total extracts of earthworms and several other invertebrates by using radioimmunoassays. Their analysis did not involve, however, a search for a Thy-1-like molecule in association with certain earthworm leucocyte membranes, which we have demonstrated in the present study. The phylogenetic studies of a molecule may contribute to increased understanding of its function and significance. The function of

Thy-1 is still unknown but several lines of evidence suggest that the molecule is involved in T cell activation [4]. Recent reports strongly suggest that Thy-1 shares amino acid homolog with the constant and variable regions of immunoglobulins (Ig), with beta-2-microglobulin and major histocompatibility complex (MHC) encoded antigens [5, 6]. The hypothesis that either the Thy-1 or the β_2 -microglobulin gene are representatives of the ancestral gene must be supported by evidence of high evolutionary conservation of these genes or molecules [7]. Thus, it is of vital importance to reveal more concerning the Thy-1 molecule in invertebrates and to trace its evolutionary origin and function.

In this study, we analyzed the presence of the Thy-1 homolog on earthworms (*Lumbricus terrestris*) utilizing several monoclonal and xenoantisera in indirect immunofluorescence assay. We observed a strong cross-reaction in which both anti-rat Thy-1.1 and anti-mouse Thy-2 monoclonal antibodies detected a molecule, on the cell surface of earthworm leucocytes suggesting the occurrence of cell surface-bound forms of a putative Thy-1 homolog at this level of evolution.

MATERIALS AND METHODS

Animals

About 200 earthworms, *Lumbricus terrestris* (Lumbricidae, Annelida) exhibiting secondary sexual characteristics were purchased from Sure-Live Meal Worm Co., Torrance, CA, and maintained at 12°C in natural soil in the laboratory. Male and female, 5 to 7 weeks old, BALB/c mice, Wistar rats and New Zealand white rabbits were obtained from the United State Naval Medical Research Unit No. 3, Cairo.

Cell suspensions

L. terrestris leucocytes were harvested by submerging worms in 10% alcohol solution as described previously [1]. After worms shed leucocytes through integumentary pores at room temperature (22°C) the leucocytes were decanted into fresh Ca^{2+} , Mg^{2+} free buffered saline solution (BSS: 10 mM KH_2PO_4 , 10 mM K_2HPO_4 , 0.11 M NaCl, 10 mM HEPES; pH 7.2) through a stainless steel screen to remove debris. Pools of leucocytes from at least 30 worms were used, washed by centrifugation at $450\times g$ for 5 min at 4°C, and their viability assessed by trypan blue exclusion [8]. Suspensions of rat and BALB/c mouse thymocytes were prepared by teasing the thymus in PBS, pH 7.2. After washing 3 times each for 5 min by centrifugation at $600\times g$, thymocytes were counted and their viability assessed by trypan blue exclusion.

Reagents

Rabbit anti-purified rat Thy-1 antiserum were kindly provided by Dr. M. H. Mansour (University of California, Los Angeles). Previous findings indicate that rabbit-anti-rat Thy-1 antiserum recognizes three antigenic determinants: the rat-specific Thy-1 xenoantigen, the rat-mouse cross-reacting xenoantigen, and the Thy-1.1 determinant [9]. BALB/c mouse anti-rat Thy-1 (ascites fluid, IgG MRCOX-7 anti-rat Thy-1.1 mAb) was purchased from Accurate Chemical Scientific Corporation, Westbury, NY. BALB/c mouse anti-AKR/J mouse thymocytes (ascites fluid, 7S IgG anti-mouse Thy-1.1 mAb) and AKR/J mouse anti-C3H

thymocytes (19S IbM anti-mouse Thy-1.2 mAb) were purchased from New England Nuclear, Boston, MA. Rabbit anti-BALB/c mouse brain serum and rabbit anti-C3H mouse brain serum were purchased from Bionetics Laboratory Products, Kensington, MD and absorbed locally with crude liver cell-membranes from BALB/c and C3H mice. Normal rabbit and rat sera were collected in the laboratory from unimmunized animals. Fluorescein isothiocyanate (FITC-) labelled goat Ig, anti-rabbit globulins were purchased from Behring Institute, Marburg, West Germany and FITC-labelled rabbit anti-mouse Ig from GIBCO, Grand Island, NY.

Indirect immunofluorescence (IF) assays

Analysis of different specificities in the anti-sera against target earthworm leucocytes and/or rat and BALB/c mouse thymocytes was measured in indirect immunofluorescence assay by quantitative absorption. Preliminary experiments, performed to define optimal labelling conditions for our system, indicated that fluorescent antibodies must be used at a dilution of 1:20 for the anti-mouse Ig and 1:25 for the anti-rabbit globulins. Apart from appropriate changes in target cells, antisera and anti-serum dilutions (details are further elaborated in the Result Section), the standard assay involved absorption of the first-step antibody (200 μl) with increasing numbers of earthworm leucocytes and/or rodent thymocytes for 16 hr at 4°C, followed by incubation with $1-2\times 10^6$ freshly-prepared target earthworm leucocytes and/or rodent thymocytes for 45 min at 4°C. After 3-4 washings in PBS, target cells were reincubated with 100 μl of fluorescent conjugate for an additional 45 min at 4°C. After 3-4 washings, cells were finally mounted on microscope slides, scored alternately in phase contrast and fluorescence microscopy. Percentage of positive labelled cells were determined by counting a minimum of 200 cells. Positive as well as negative controls, explained in the results, were included in each experiment.

Iodination of cell surface and indirect immunoprecipitation of Thy-1 homolog

Aliquots of 10^7 viable earthworm leucocytes were surface labelled with 300 μCi Na^{125}I by the

lactoperoxidase-catalyzed reaction [10]. Washed labelled cells were solubilized with 200 μ l of 0.5% (w/v) Nonidet-P 40 in 0.15 M NaCl-0.02% NaN₃ (w/v-0.01 M Tris-HCl, pH=7.4), by incubation on ice for 1/2 hr. The cell particulates insoluble in NP-40 (nuclei and cellular debris) were removed by centrifugation at 1200 \times g for 35 min at 4°C. The supernatant containing solubilized cell surface components was used for indirect immunoprecipitation. To 10⁷ labelled cells (200 μ l), 50 μ l of monoclonal anti-mouse Thy-1 were added. After incubation with antiserum for 45 min at 4°C, 100 μ l of a 10% protein A bound to Sepharose 4 B (Pharmacia Fine Chemicals, Uppsala, Sweden) were added and incubated for an additional 45 min at room temperature. The precipitates were washed thrice with 0.2 M PBS, pH=7.2. Immunoprecipitates were dissolved in 2.2% SDS, 5% 2-mercaptoethanol, 0.1 mM EDTA in SDS-buffer

and boiled for 3 min at 100°C. Sodium dodecyl sulfate polyacrylamide gel electrophoresis (SDS-PAGE) was performed on 10% polyacrylamide gels. After electrophoresis, the gels were sliced (2 mm in length) and radioactivity counted in each slice by gamma counter [12].

RESULTS

The reactivity of both anti-Thy-1.1 monoclonal antibodies (mAbs Thy-1.1) and anti-Thy-1.2 monoclonal antibodies (mAbs Thy-1.2) was titrated in IF against earthworm leucocytes. The mAb Thy-1.1 showed a strong binding reactivity to earthworm leucocytes in contrast to mAb Thy-1.2 which was completely negative (data not shown). These results suggest that probably earthworm leucocytes are bearers of the Thy-1.1 determinant but lack the presence of the Thy-1.2 antigen.

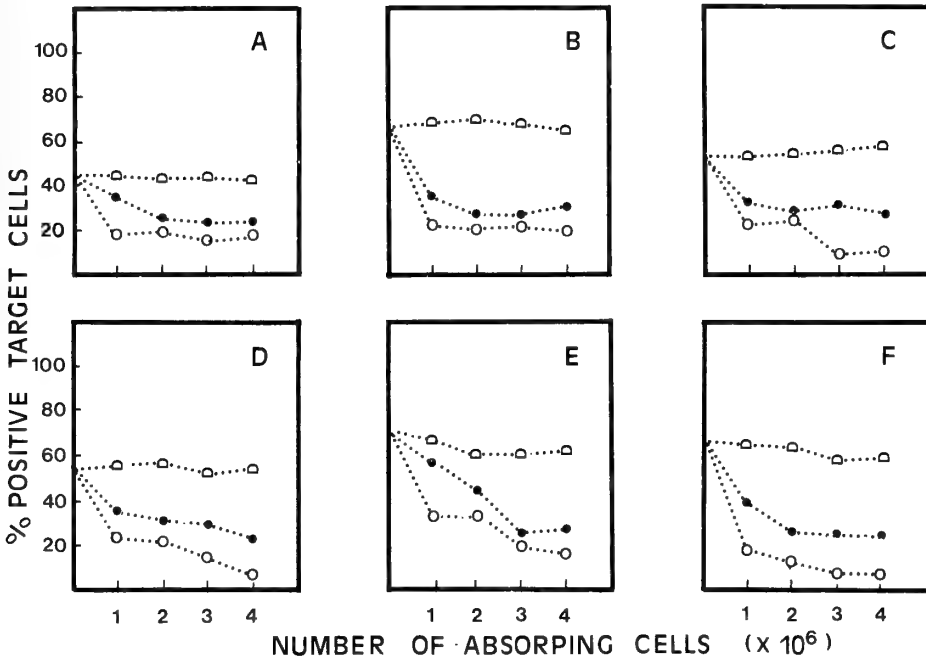


FIG. 1. Demonstration of a Thy-1 homolog on earthworm leucocytes using rodent Thy-1 antibodies in quantitative absorption assays. Numbers of absorbing cells are shown on the abscissae. Aliquots of earthworm leucocytes (●) and rat (○) and BALB/c mouse (◻) thymocytes were used as absorbents to assay the activity of anti-rat Thy-1.1 mAb (diluted 1:1500 in the absorbing assay) to rat thymocytes (A) and earthworm leucocytes (B), the activity of anti-mouse Thy-1.1 mAb (diluted 1:1800 in the absorbing assay) to rat thymocytes (C) and earthworm leucocytes (D) and the reactivity of rabbit anti-rat Thy-1 antiserum (diluted 1:100 in the absorbing assay) to earthworm leucocytes (E) and rat thymocytes (F). Each point in the curves represents the mean value of two separate experiments.

Recent amino acid sequence data of murine brain derived Thy-1 molecules have demonstrated that protein encoded by the alleles Thy-1.1 and Thy-1.2 differ by one amino acid residue, therefore antibodies are directed exclusively to one allelic Thy-1 product. Bearing this in mind, it was necessary to perform a set of quantitative absorptions to be certain that anti-Thy-1.1 mAb indeed detects the earthworm putative Thy-1 homolog. The absorptive capacity of worm leucocytes, rat and BALB/c mouse thymocytes to reduce the activity of BALB/c anti rat Thy-1 mAb towards rat thymocytes and earthworm leucocytes is depicted in Figure 1A and B, respectively. Within the given range of absorbents, earthworm leucocytes reduced detectable reactivities of mAb Thy-1.1 determinants as effectively as did the absorption of rat thymocytes (Thy-1.1 strain). In contrast, the binding capacity of mAb was not completely abolished by BALB/c mouse thymocytes (Thy-1.2 strain). Significant absorptions were further confirmed in quantitative absorption assays using BALB/c mouse anti-AKR/J mouse thymocyte mAb with target rat thymocytes (Fig. 1C) and earthworm leucocytes (Fig. 1D). This resulting pattern of reactivity was similar to that observed using anti-rat mAb, confirming the detectability of a Thy-1.1 cross-reacting determinant, by a putative Thy-1.1 homolog on earthworm leucocytes.

Although results from quantitative absorption assays suggest that the Thy-1.1 epitope is shared between rat Thy-1 molecules and a putative Thy-1 homolog on earthworm leucocytes, there is no evidence that the molecule(s) are serologically identical or not. In order to further map the difference between rodent and earthworm Thy-1, rabbit anti-rat Thy-1 antiserum was absorbed with rat and BALB/c mouse thymocytes and assayed with rat thymocytes (Fig. 1F) and earthworm leucocytes (Fig. 1E) as target cells. While rat thymocytes are capable of absorbing nearly all the binding reactivity, BALB/c mouse thymocytes absorbed only 30% and earthworm leucocytes absorbed 70% of the reactivity. Specific absorption occurred using the same number of earthworm leucocytes and rat thymocytes which indicates two main antibody specificities: a specificity directed to the antigenic determinants shared by

earthworm and rat (mouse), the earthworm-rat (-mouse) cross reacting xenoantigenic determinant and a specificity directed to an antigenic determinant selectively absorbed by rat, the Thy-1.1 antigenic determinant. In contrast, reactivity of rabbit anti-rat Thy-1 against BALB/c mouse thymocytes as targets was completely diminished by BALB/c mouse thymocytes and earthworm leucocytes, (data not shown); rat thymocytes absorbed only about 28% of the antibody specificities.

Immunoprecipitates of earthworm 125 I-labelled, solubilized leucocytes were obtained by anti-mouse Thy-1.1 mAb and subjected to SDS-PAGE analysis using 10% gels under reducing conditions. The results indicate an apparent molecular weight of 28.2 KD for the Thy-1 homolog (Fig. 2).

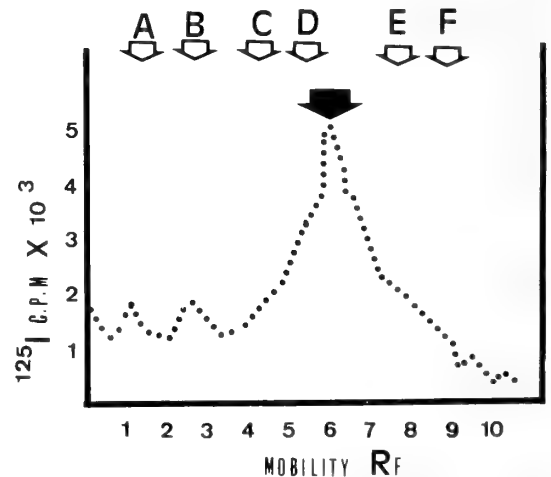


Fig. 2. Polyacrylamide gel electrophoresis (PAGE) analysis of immunoprecipitated earthworm leucocytes. The position of protein markers that we run simultaneously and stained with Coomassie Blue is indicated by arrows (A, phosphorylase b (94.0); B, BSA (67.0); C, ovalbumin (43.0); D, carbonic anhydrase (30.0); E, Soybean trypsin inhibitor (20.0) and F, Lactalbumin (14.0). This indicates an apparent molecular weight of 28.2 KD for the Thy-1 homolog.

DISCUSSION

Although Thy-1 has been used as a T-cell marker, there is no definite resolution as to its role in T-cell functions. Recently, it has been postulated that Thy-1 may be ancestral molecule from which

all members of the Ig superfamily might have evolved [11–13]. To follow up this ancestral molecule, studies in invertebrates, seemed to us, to be highly warranted. Although, invertebrates leucocytes have long been overlooked with respect to cell markers, they might prove to be the most suitable substrate for defining the roots of Thy-1 homolog from an evolutionary viewpoint.

In our approach to search for a Thy-1 homolog on earthworm leucocytes, the reactivity of two mAbs or proven specificities to the Thy-1.1 determinant of rat and AKR/J mouse Thy-1 molecule [14] and rabbit anti-rat Thy-1 antiserum [9] towards earthworm leucocytes was investigated in IF assays by quantitative absorption. Although, neither reagents generated a response the putative earthworm Thy-1 antigen, both were depleted of anti-Thy-1.1 reactivity by absorption with earthworm leucocytes to the same degree as rat thymocytes (Thy-1.1 strain). Due to the specificity of the antisera and the sensitivity of our assay, the membrane determinant revealed on earthworm leucocytes seemed to be related to the Thy-1 molecule. Two antibody specificities in the antisera were recognized and found to be directed towards two antigenic determinants expressed on earthworm leucocytes. These were referred to as: the earthworm-rat (mouse) cross reacting xenoantigenic determinants and the Thy-1.1 antigenic determinant. This observation substantiates the occurrence of a Thy-1 homolog on earthworm leucocytes, which in terms of structure, might share a common pattern with rodent Thy-1 molecule, manifested by the expression of Thy-1.1 determinant.

The similarity of Thy-1.1 determinant in earthworm and rat, in particular, may be strengthened by results from immunoprecipitation assays. The estimated molecular weight was in striking agreement with values obtained for rat [9], mouse [15], human [16], dog [16], frog [17] and tunicate [18] Thy-1 glycoprotein. However, the ultimate proof for this assumption would be obtained by biochemical characterization, purification and amino acid sequence studies on earthworm Thy-1 epitope which are in progress. The presence of another vertebrate-like molecule, within the Ig superfamily such as Thy-1, among

earthworms may not seem surprising since our results add to a growing list of such shared molecules, including for example, β_2 -microglobulin [4]. In terms of similarities in antigenicity, it is conceivable that the earthworm leucocytes Thy-1 homolog represents an ancestral Thy-1 molecule that underwent diversification. Vertebrates are assumed to have evolved from the chordate line represented by tunicates which are deuterostomes. That a putative Thy-1 homolog exists in earthworm which belongs to the protostome line, supports the view that Thy-1, a component of the Ig superfamily, is present universally. Moreover, this argues for later diversification of the terminal gene during evolution of other members of the superfamily such as Ig which is up to now not demonstrable in invertebrates and only present in all vertebrates [6, 7]. Such information may provide essential clues to our understanding of fundamental events concerning the evolution of the immune system.

REFERENCES

- 1 Cooper, E. L. (1976) The earthworm coelomocytes. A mediator of cellular immunity. In "Phylogeny of Thymus Bone Marrow Cells". Ed. by R. K. Wright and E. L. Cooper, Elsevier, Amsterdam, pp. 9–42.
- 2 Roch, P. Cooper, E. L. and Eskinazi, D. P. (1983) Surgical evidence for a membrane structure related to human beta-2-microglobulin expressed by certain earthworm leucocytes. *Eur. J. Immunol.*, **13**: 1037–1046.
- 3 Shalev, A., Segal, S. and Bar Eli, M. (1985) Evolutionary conservation of brain Thy-1 glycoprotein in vertebrates and invertebrates. *Dev. Comp. Immunol.*, **9**: 497–506.
- 4 Growford, J. M. and Goldschneider, I. (1980) Thy-1 antigen and B lymphocyte differentiation in the rat. *J. Immunol.*, **124**: 969–976.
- 5 Seki, T., Change, H. C., Moriuchi, T., Denome, R. and Silver, J. (1985) Thy-1 a hydrophobic transmembrane segment at the carboxyl terminus. *Fed. Proc.*, **44**: 2865–2869.
- 6 Williams, A. F. and Gagnon, J. (1982) Neuronal cell Thy-1 glycoprotein: Homolog with immunoglobulin. *Science*, **216**: 696–703.
- 7 Williams, A. F. (1984) The immunoglobulin superfamily takes shape. *Nature*, **308**: 12–18.
- 8 Cooper, E. L., McDonald, H. R. and Sordat, B. (1979) Separation of earthworm coelomocytes by velocity sedimentation. In "Function and Structure of the Immune System". Ed. by Plenum Press, New

- York, pp. 101-104.
- 9 Barclay, A., Letarte-Muirhead, M. and Williams, A. F. (1975) Purification of the Thy-1 molecule from rat brain. *Biochem. J.*, **151**: 699-707.
 - 10 Ades, E. W., Zwerner, R. K., Acton, R. T. and Balch, C. C. (1980) Isolation and partial characterization of the human homolog of Thy-1. *J. Exp. Med.*, **151**: 400-409.
 - 11 Kaufman, J. E. and Strominger, J. L. (1982) HLA-DR Light chain has a polymorphic N-terminal region and conserved immunoglobulin-like C-terminal region. *Nature*, **279**: 694-697.
 - 12 Parnes, J. K. and Seidman, J. G. (1982) Structure of wild-type and mutant mouse beta-2-microglobulin genes. *Cell*, **29**: 661-667.
 - 13 Cushley, W. and Owen, M. J. (1983) Structural and genetic similarities between immunoglobulins and class-I histocompatibility antigens. *Immunol. Today*, **4**: 87-92.
 - 14 Mason, D. W. and Williams, A. F. (1980) The kinetics of antibody binding to membrane antigens in solution and at the cell surface. *Biochem. J.*, **187**: 1-9.
 - 15 Zwerner, R. K., Barstad, P. A. and Acton, R. T. (1977) Isolation and characterization of murine cell surface components. I. Purification of milligram quantities of Thy-1.1. *J. Exp. Med.*, **146**: 986-995.
 - 16 McKenzie, J. L., Allen, A. K. and Fabre, J. W. (1981) Biochemical characterization including amino acid and carbohydrate composition of canine and human brain Thy-1 antigen. *Biochem. J.*, **197**: 629-637.
 - 17 Mansour, M. H. and Cooper, E. L. (1984) Purification and characterization of *Rana pipiens* brain Thy-1 glycoprotein. *J. Immunol.*, **132**: 2515-2525.
 - 18 Mansour, M. H. and Cooper, E. L. (1984) Serological and partial molecular characterization of Thy-1 homolog in tunicates. *Eur. J. Immunol.*, **14**: 1031-1042.

Neural Control of Flight Muscle Differentiation in the Fly, *Sarcophaga bullata*

PAKKIRISAMY SIVASUBRAMANIAN and DICK R. NÄSSEL¹

*Department of Biology, University of New Brunswick, Fredericton,
New Brunswick, Canada E3B 6E1, and ¹Department of Zoology,
University of Stockholm, Svante Arrhenius väg 16,
S-10691 Stockholm, Sweden*

ABSTRACT—Myoblasts derived from imaginal discs together with the degenerating larval muscles contribute to the formation of flight muscles in adult flies. Severance of the mesothoracic larval nerve in the freshly formed prepupa results in the absence of entire flight musculature on the operated side of the adult fly. Histological observations reveal very early stages of muscle differentiation in the form of association of myoblasts with degenerating larval muscle around day 3 of pupal development. Further differentiation is inhibited by nerve transection leading to the eventual degeneration of all muscles on the operated side. These results indicate that insect flight muscles are dependent on nerves from the early stages of their differentiation.

INTRODUCTION

Although the importance of innervation in the differentiation of vertebrate muscle has been established by several investigations [1–6], insects that undergo complete metamorphosis are better suited for such studies because of precise timing in the differentiation of adult muscles. When a crawling maggot such as that of a fly, metamorphoses into a flying insect there is a considerable reorganization of its locomotor apparatus. The larval muscles are histolysed and replaced by imaginal muscles. The nervous system too is remodelled accordingly. Such a metamorphosing system is very convenient for the study of neural control of muscle differentiation.

In one of his pioneering studies on the influence of nerves on muscle differentiation Kopeć [7] removed the thoracic ganglia from gypsy moth caterpillars. This resulted in the development of adults without thoracic muscles. Similar results were also obtained for silkmths by Williams and Schneiderman [8]. Nüesch extended these studies to single nerves innervating specific muscles of the

moth, *Antheraea pernyi* and concluded that innervation is essential for the completion of muscle differentiation [9]. We have studied the influence of nerves in the differentiation of muscles in a different order of insects namely, Dipera. As in other flies of Diptera, the adult *Sarcophaga bullata* has six pairs of dorsal longitudinal muscles (DLM), part of the indirect flight musculature, that increase the height of the thoracic box during flight and thus depress the wings. These muscles are innervated by the posterior dorsal mesothoracic nerve (PDMN) from the thoracic ganglion [10]. In this report we have examined the role of PDMN in the differentiation of DLM.

MATERIALS AND METHODS

The fleshfly *Sarcophaga bullata* was reared in the laboratory under constant conditions of temperature (25°C) and photoperiod (16L:8D). The adult flies were fed with sugar and water *ad libitum*. The larvae were raised in fresh beef liver. Post-feeding mature third instar larvae were collected and used for experiments within two hr after pupariation.

Denervation In the mature larva there are groups of embryonic cells enclosed within non-cellular peripodial membranes. These are called

imaginal discs which differentiate into adult structures during metamorphosis. Each disc is connected terminally to the larval epidermis via slender epithelial stalk. Most of the discs also have a basal stalk connecting them to the larval central nervous system. This stalk also contains a larval nerve [11]. Thus the pro- and mesothoracic leg discs are connected to the ventral side of the ganglion by pro- and mesothoracic larval nerves which also send off branches to innervate the larval thoracic muscles [12]. Since it has been known that (a) some larval thoracic muscles contribute to the formation of adult DLM [13], (b) larval neurons are remodelled into adult nerve cells [14], and (c) the PDMN innervating the DLM of the adult originates in the mesothoracic neuromere [15], we hypothesised that the nerve branch of the larval

mesothoracic nerve is transformed into PDMN of the adult and is essential for the differentiation of adult DLM. This larval nerve was transected as follows: a triangular cut was made in the puparium on the anterior ventral side (segments 4–5) of the 1–2 hr old prepupa. While lifting the puparial flap, a fine iridectomy scissors was introduced inside and the basal disc stalk along with its nerve branch of the mesothoracic leg disc was severed (Fig. 1A, top). The epithelial stalk was left intact. The window was closed back with the triangular flap and the drying of the hemolymph sealed the wound. In the sham operated controls, the entire mesothoracic leg disc was extirpated (Fig. 1A, bottom) leaving the larval nerve connection intact as described by Nässel *et al.* [16]. A single oblique cut was made on the anterior ventral (segments 3–

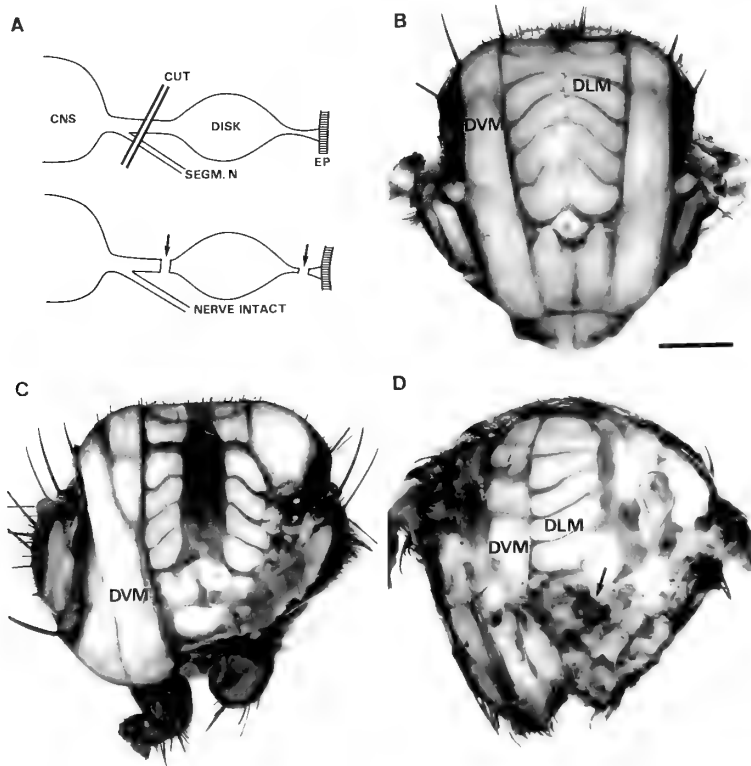


FIG. 1. Nerve transection procedure and its effects on adult flies. Abbreviations: DVM: Dorsoventral flight muscles; DLM: Dorsal longitudinal muscles; EP: Epithelium; Segm. N: Segmental nerve. Scale bar in B, C and D is the same = 1 mm. A. Top: Transection of mesothoracic leg disc stalk along with the larval mesothoracic nerve. Bottom: Extirpation of mesothoracic leg disc (sham-operation). B. Cross section of a thorax from an unoperated control fly. C. Cross section of a thorax from sham operated (mesothoracic leg disc extirpated) fly. D: Cross section of a thorax from nerve transected fly. Note the absence of flight muscles on the right side.

4) side of the freshly formed prepupa. Gentle pressure on one side externalized the mesothoracic leg disc which was then detached from its attachments on both ends. The mesothoracic larval nerve branch that innervates the larval muscles was left intact. Upon completion of metamorphosis (about 12 days at 25°C) the condition of their flight muscles was examined by simply slicing the thoraces as well as after histological staining of 8

μm thick serial paraffin sections.

RESULTS

Control 1 (unoperated flies)

Figure 1B is a cross section of a thorax from an unoperated adult fly. As in other cyclorrhaphous diptera it contains six pairs of DLM which are the main depressors of the wings during flight. These

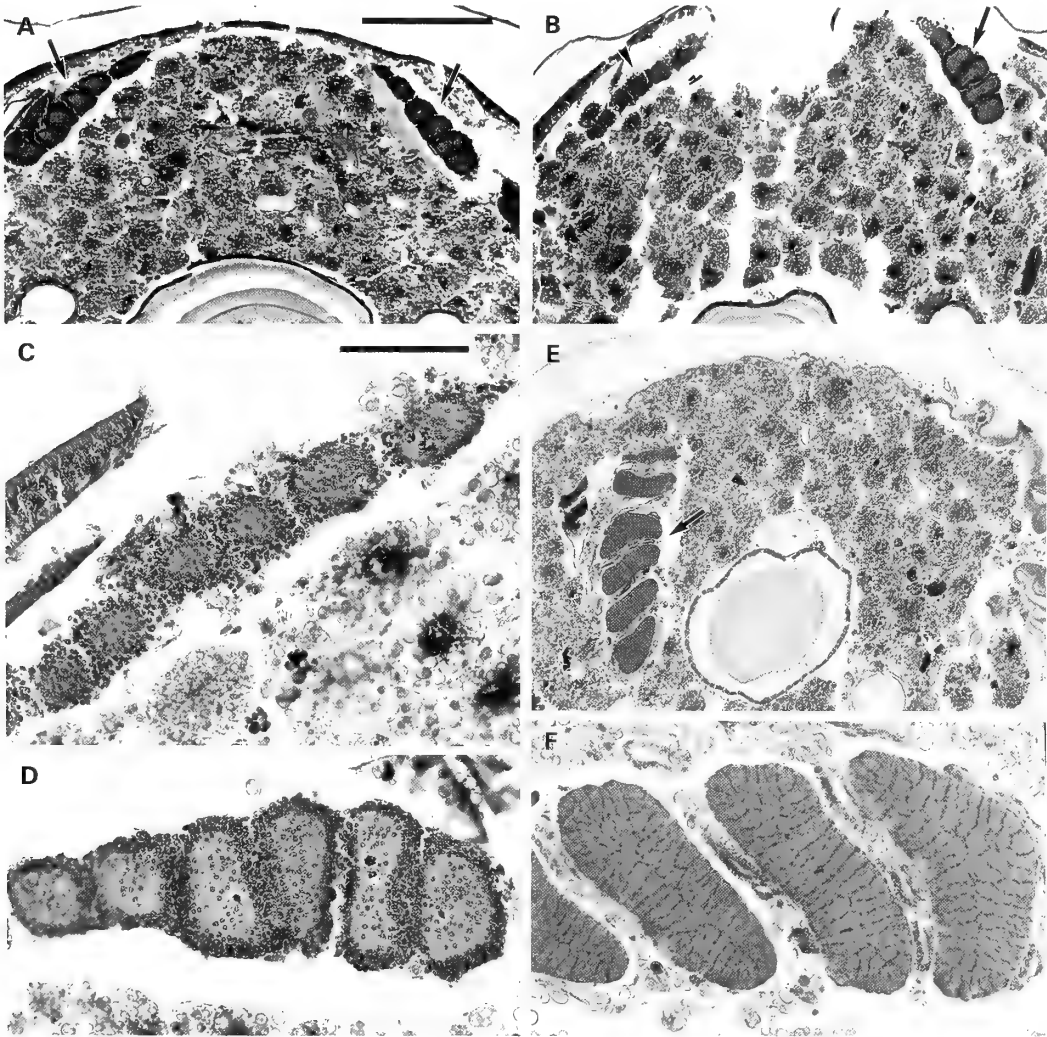


FIG. 2. Chronological stages of muscle degeneration after nerve transection. Magnification in A, B and E is the same. (scale bar = 400 μm). C, D and F are of same magnification (scale bar = 100 μm). A. 3 day old pupa showing DLM on both sides (arrows). B. 3.5 to 4 day old pupa. Note degenerating DLM on left side (arrow head). C. Enlarged view of degenerating DLM from 2B. D. Enlarged view of normal DLM from 2B. E. 7 day old pupa operated on the right side showing the DLM on left side only (arrow). F. Enlarged view of normal DLM from 2E.

muscles extend from the anterior half of alinotum to the post notum and second phragma.

Control II (sham operated flies)

The mesothoracic leg extirpated prepupae metamorphose into five-legged flies. Besides the mesothoracic leg, these flies also lack certain sclerites on the operated side such as the mesosternum. Nevertheless, all six pairs of DLM develop quite normally (Fig. 1C). However, the dorso-ventral muscles (DVM) are absent on the operated side.

Experimental flies

More than 75% of the pupae survive the operation and at least 35 flies that completed metamorphosis were used for examination. Upon transection of the basal stalk along with the attached larval nerve of the mesothoracic leg disc the pupae metamorphosed quite normally with all six legs and associated sclerites. However, they invariably failed to eclose unaided. When the flies were taken out of their puparia one could notice some external color difference between the right and left halves of the dorsal thorax. One half was paler than the other half. This was due to the complete absence of the entire set of fibrillar flight muscles on the operated side which could be seen through the as yet untanned cuticle. The muscleless half of the thoracic box was filled with fat body (Fig. 1D). The thoracic ganglion too was slightly abnormal in such flies and the PDMN was absent on the left side.

At what time during the course of development do muscles need innervation? In the experimental flies do the muscles differentiate first and then degenerate or they fail to differentiate altogether due to lack of innervation? To answer these questions, nerve transected pupae (10 per stage) were histologically examined at different stages of development. Three days after pupariation the larval mesothoracic muscles had cleaved longitudinally into six bundles on either (right and left) side of the thorax with the myoblasts lined up around them. In a cross section one can see these bundles just beneath the dorsal epidermis (Fig. 2A). Within the next 12–24 hr (3–4 day old pupa) these incipient muscle bundles start to degenerate on the operated side (Fig. 2B and 2C) and by the next day they have completely disappeared from the nerve

transected side. Figure 2E is a 7 day old pupa showing the flight muscles on the unoperated side.

DISCUSSION

By selective transection of larval mesothoracic nerve the present study confirms the earlier reports on moths by Kopeć [7] and Williams and Schneiderman [8] and demonstrates the importance of innervation for the differentiation of thoracic flight muscles in the fleshfly, *Sarcophaga bullata*. However, our results are slightly different from those obtained by Nüesch [9] after denervation of developing muscles in diapausing pupae of saturniid moth *Antheraea pernyi* where the nerve transection resulted in retardation of muscle differentiation with fewer nuclei and thinner, shorter muscle fibers. This difference in nerve influence may be due to the timing of denervation. In the moth the operation was performed in the pupal stage, whereas in the fly it was done much earlier in the freshly formed prepupa.

The indirect flight muscles of holometabolous insects develop from myoblasts derived from leg imaginal discs [17, 18] in association with degenerating larval intersegmental muscles [19, 20]. The residual larval intersegmental muscles of the mesothorax form a scaffolding around which the myoblasts line up in the form of compact columns and subsequently differentiate into myofibrils [21]. Upon nerve transection in the prepupa the adult thorax is completely devoid of flight muscles on the denervated side. Our histological preparations indicate that from the moment the myoblasts associate with the longitudinally cleaved larval muscles their further differentiation is dependent on innervation because, on the nerve transected side the muscles seem to start degenerating soon after this stage (Fig. 2B). The precise nature of degeneration is difficult to discern from the current histological observations. Only future studies using ultrastructural and immunocytochemical techniques will shed more light in this regard.

The importance of motor innervation during early stages of muscle differentiation is well documented for vertebrate embryos [1]. In chick embryos motor neuron growth cones associate with muscle forming mesodermal cells even before

myotube formation [22]. Destruction of motor neurons by bungarotoxin inhibits myotube formation in rat skeletal muscles [2]. It was suggested that motor neuron terminals have some trophic or inductive influence on myogenic cells [4, 5]. Accumulation of myosin in developing limb bud musculature of quail embryos is nerve dependent [23]. In grasshopper embryos too the motor neurons contact muscle pioneers very early in development [24] and may start influencing them from the very beginning.

The indirect flight muscles of the adult fleshfly *Sarcophaga bullata* are innervated by PDMN [10]. It is interesting to note that this nerve is missing on the operated side. The absence of muscles could not have caused the degeneration of PDMN because insect motor neurons are able to survive in the absence of their targets [25] and innervate inappropriate muscles [16, 26]. Therefore, it is tempting to suggest that the larval nerve which innervates the mesothoracic muscles of the larva perhaps becomes transformed into PDMN of the adult. Thus, the PDMN has a dual role; first, during metamorphosis it influences the flight muscle differentiation and then, in the adult fly it controls the function of these muscles. Transection of the larval mesothoracic nerve results in the absence of PDMN in the adult. Such a transformation of larval nerve innervating the dorsal musculature of the larva into adult nerve innervating the DLM of the adult is well established for the tobacco hornworm, *Manduca sexta* [14].

The absence of dorsoventral muscles (DVM) in the sham-operated (mesothoracic leg disc extirpated) controls needs some explanation. In this group of control flies there is an intact larval mesothoracic nerve and therefore the DLM differentiate. However, the DVM fail to form. Similar results have also been reported earlier for *Drosophila melanogaster* [27] and *Sarcophaga bullata* [28]. We can suggest two possible explanations. (a) Since mesothoracic leg discs also contribute to the adult epidermis of ventral mesothoracic segment [29] the DVM of disc extirpated animals would have degenerated secondarily due to lack of ventral attachment sites (sclerites). Studies with *Sarcophaga bullata* [30] and *Drosophila melanogaster* [31] support this possibility. (b) The source

of myoblasts for DVM and DLM may be different. Investigations with *Drosophila* wing mutants support this view. In the mutant *wingless* development of DVM is affected while DLM are normally formed. In *erect wing* mutants, on the other hand, DLM are completely absent while DVM are normal [31].

ACKNOWLEDGMENTS

This research was supported by grants from the Natural Sciences and Engineering Research Council of Canada and the Swedish Natural Sciences Research Council (NFR 1820-103).

REFERENCES

- 1 Bonner, P. H. and Adams, T. R. (1982) Neural induction of chick myoblast differentiation in culture. *Develop. Biol.*, **90**: 174-184.
- 2 Harris, A. J. (1981) Embryonic growth and innervation of rat skeletal muscles. I. Neural regulation of muscle fiber numbers. *Phil. Trans. Roy. Soc. Lond., Ser. B.* **293**: 257-277.
- 3 McLennan, I. S. (1983) Neural dependence and independence of myotube production in chicken hindlimb muscles. *Develop. Biol.*, **98**: 287-294.
- 4 Popiela, H. (1978) Trophic effects of adult peripheral nerve extract on muscle cell growth and differentiation in vitro. *Exp. Neurol.*, **62**: 405-416.
- 5 Popiela, H. and Ellis, S. (1981) Neurotrophic factor: Characterization and partial purification. *Develop. Biol.*, **83**: 266-277.
- 6 Sohla, G. S. and Holt, R. K. (1980) Role of innervation on the embryonic development of skeletal muscle. *Cell Tiss. Res.*, **210**: 383-393.
- 7 Kopeć, S. (1923) The influence of the nervous system on the development and regeneration of muscles and integument in insects. *J. Exp. Zool.*, **37**: 15-25.
- 8 Williams, C. M. and Schneiderman, H. A. (1952) The necessity of motor innervation for the development of insect muscles. *Anat. Rec.*, **113**: 560-561.
- 9 Nüesch, H. (1985) Control of muscle development. In "Comprehensive Insect Physiology, Biochemistry and Pharmacology" Vol. 2. Ed. by G. Kerkut, and L. I. Gilbert, Pergamon Press, pp. 425-452.
- 10 Ikeda, K. (1977) Flight motor innervation of a fleshfly. In "Identified Neurons and Behavior of Arthropods" Ed. by G. Hoyle, Plenum press, New York, pp. 357-368.
- 11 Auerbach, C. (1936) The development of the legs, wings and halteres in the wild type and some mutant strains of *Drosophila melanogaster*. *Trans. Roy.*

- Soc. Edin., **58**: 787–815.
- 12 Hertweck, H. (1931) Anatomie und Variabilität des Nervensystem und der Sinnesorgane von *Drosophila melanogaster*. Zeits. wiss. Zool., **139**: 559–563.
 - 13 Beinbrech, G. (1968) Elektronenmikroskopische Untersuchungen über die Differenzierung von Insektenmuskeln während der Metamorphose. Z. Zellforsch., **90**: 463–494.
 - 14 Casaday, G. B. and Camhi, J. M. (1976) Metamorphosis of flight motor neurons in the moth *Manduca sexta*. J. Comp. Physiol., **112**: 143–158.
 - 15 Power, M. E. (1948) The thoracic abdominal nervous system of an adult insect, *Drosophila melanogaster*. J. Comp. Neuro., **88**: 347–401.
 - 16 Nässel, D. R., Helgee, A. and Sivasubramanian, P. (1986) Development of axon paths of motoneurons after removal of target muscles in a holometabolous insect. Devel. Brain Res., **26**: 211–219.
 - 17 Poodry, C. A. and Schneiderman, H. A. (1970) Ultrastructure of the developing leg of *Drosophila melanogaster*. Roux's Arch. Dev. Biol., **166**: 1–44.
 - 18 Shatoury, H. H. El. (1956) Developmental interactions in the development of imaginal muscles of *Drosophila*. J. Embryol. exp. Morphol., **4**: 228–239.
 - 19 Reed, C. T., Murphy, C. and Fristrom, D. (1975) The ultrastructure of the differentiating pupal leg of *Drosophila melanogaster*. Roux's Arch. Dev. Biol., **178**: 285–302.
 - 20 Tiegs, O. W. (1955) The flight muscles of insects. Phil. Trans. Roy. Soc. Lond. (Biol.), **238**: 221–348.
 - 21 Peristianis, G. C. and Gregory, D. W. (1971) Early stages of flight muscle development in the blowfly *Lucilia cuprina*: A light and electron microscopic study. J. Insect Physiol., **17**: 1005–1022.
 - 22 Lance-Jones, C. and Landmesser, L. (1981) Pathway selection by chick lumbosacral motoneurons during normal development. Proc. Roy. Soc. Lond. (Biol.), **214**: 1–18.
 - 23 Merrifield, P. A. and Konigsberg, I. R. (1987) Nerve dependent accumulation of myosin light chain 3 in developing limb musculature. Development, **101**: 673–684.
 - 24 Ball, E. E., Ho, R. K. and Goodman, C. S. (1985) Development of neuromuscular specificity in the grasshopper embryo: Guidance of motoneuron growth cones by muscle pioneers. J. Neurosci., **5**: 1808–1819.
 - 25 Whittington, P. M., Bate, M., Seifert, E., Ridge, K. and Goodman, C. S. (1982) Survival and differentiation of identified embryonic neurons in the absence of their target muscles. Science, **215**: 973–975.
 - 26 Whittington, P. M. (1985) Functional connections with foreign muscles made by a target deprived insect motor neuron. Develop. Biol., **107**: 537–540.
 - 27 Zalokar, M. (1947) Anatomie du thorax de *Drosophila melanogaster*. Rev. Suisse Zool. **54**: 17–53.
 - 28 Sivasubramanian, P. and Nässel, D. R. (1985) Development of thoracic musculature after leg imaginal disc extirpation in the fly, *Sarcophaga bullata* (Parker) (Diptera: Sarcophagidae). Int. J. Insect Morphol. Embryol., **15**: 463–464.
 - 29 Bryant, P. J. (1978) Pattern formation in imaginal discs. In "The genetics and Biology of *Drosophila*" Vol. 2c, Ed. by M. Ashburner and T. R. F. Wright, Acad. Press, New York/London. pp. 230–335.
 - 30 Chiarodo, A. J. (1963) The effects of mesothoracic leg disc extirpation on the nervous system of the blowfly, *Sarcophaga bullata*. J. Exp. Zool., **153**: 263–277.
 - 31 Deak, I. I. (1978) Thoracic duplications in the mutant *wingless* of *Drosophila* and their effect on muscles and nerves. Develop. Biol., **66**: 422–441.

Effect of pH on the Participation of Calcium Ion in the Cell Aggregation of Sea Urchin Embryos

YASUTO TONEGAWA¹, EIICHI HOJIRO² and KAZUhide TAKAHASHI³

*Department of Regulation Biology, Faculty of Science,
Saitama University, Urawa 338, Japan*

ABSTRACT—The effect of pH on the cell aggregation of sea urchin embryos was investigated to demonstrate the involvement of Ca^{2+} in cell aggregation. The cell aggregation was maximum at pH 8, decreased gradually at lower pHs and the aggregation did not occur below pH 4. On further examination, the pH profile of $^{45}\text{Ca}^{2+}$ -binding to the aggregation factor was found to be almost identical with that of cell aggregation. The similarity of these pH profiles suggested the involvement of electrostatic interaction between Ca^{2+} and negatively charged groups of the aggregation factor in the cell aggregation of sea urchin embryos.

INTRODUCTION

The success in immunochemistry stimulated hypotheses involving antigen-antibody like reactions and sugar-lectin type reactions as the specific motive forces of cell aggregation. This line of research has advanced so far to propose the molecular mechanism for the interaction of aggregation factor and cell surface receptor [1-4]. On the other hand, biophysical approach has suggested the participation of electrostatic forces and van der Waals forces. Ca bridge hypothesis is most well known among them [5-7].

The cell aggregation factor of sea urchin embryos was shown to be a highly negatively charged sugar-protein complex extracted with Ca^{2+} -g, Mg^{2+} -free artificial sea water (CMF-SW). However, it has not yet been well characterized because of its instability [8]. The surface charge of dissociated cells is known to be negative at the pH of sea water [9]. Ca ion is indispensable for cell

aggregation and the rate of cell aggregation is dependent on Ca^{2+} concentrations [8]. Hence it is reasonable to assume that the electrostatic forces may play some substantial role in the cell aggregation of sea urchin embryos.

Following experiments were designed to examine this possibility. The cell aggregation was significantly affected by pH with a maximum aggregation at pH 8. The binding of $^{45}\text{Ca}^{2+}$ to the aggregation factor showed almost the same pH profile as that of cell aggregation. These results are discussed with special reference to the mode of Ca^{2+} involvement in cell aggregation.

MATERIALS AND METHODS

A Japanese sea urchin, *Hemicentrotus pulcherrimus*, was mostly used for the following experiments.

Preparation of aggregation factor and hyaline layer substance

Aggregation factor was prepared from swimming blastula embryos following the method previously described [8]. Hatched blastulae were washed twice with Ca^{2+} -, Mg^{2+} -free artificial sea water (CMF-SW) and gently stirred in ice-chilled CMF-SW for 60 min until embryos were dissociated into constituent cells. After removing dissoci-

Accepted December 5, 1989

Received October 9, 1989

¹ Deceased on October 8, 1989.

² Present address: Chiyoda Dames and Moor Co, LTD., 1-4-28 Mita, Minato-ku, Tokyo 108.

³ Present address: Clinical Research Institute, Kanagawa Cancer Center, 54-2 Nakao-cho, Asahi-ku, Yokohama 241.

ated cells with low-speed centrifugation ($3000\times g$, 5 min), the supernatant was subjected to high-speed centrifugation ($10,000\times g$, 20 min) at 4°C . The clear extract obtained was used as the cell aggregation factor.

To prepare [^{35}S]-labeled aggregation factor ([^{35}S]-AF), fertilized eggs were raised in [^{35}S]- MgSO_4 -containing artificial sea water ($5\text{ }\mu\text{Ci}/200\text{ ml}$). At blastula stage, metabolically labeled aggregation factor was extracted with CMF-SW according to the same method as that to prepare unlabeled aggregation factor.

Hyaline layer substance was extracted from fertilized eggs with CMF-SW and purified by precipitation with Ca^{2+} as was described previously [8].

Assay of cell aggregating activity

Dissociated blastula cells after the extraction of the aggregation factor were washed twice with CMF-SW, filtered through nylon mesh (380 mesh) and the cell numbers were counted with hemocytometer. Cell aggregation assay was performed on a zyratory shaker at 4°C . One ml of cell suspension (10^7 cells) and 1 ml of aggregation factor ($100\text{ }\mu\text{g}$ protein) were added to a 30 ml Erlenmeyer flask containing 3 ml of Herbt's artificial sea water buffered with citrate (5 mM) for pH 3–6 or with Na-barbiturate (5 mM) for pH 7–9. After rotation (80 rpm, 10 mm rad.) for 60 min, the average number of cells in an aggregate was determined as was described before [8].

To change the pH of the medium in the course of experiment, 1 ml of 50 mM buffer of different pH was added to the flask after 60 min of rotation in the first medium. Rotation was continued for further 60 min and the cell aggregation was scored. To prepare the fixed cells, dissociated cells were fixed with cold glutaraldehyde (1% in CMF-SW, buffered to pH 8 with Tris-HCl for 3 hr and dialyzed thoroughly to remove excess glutaraldehyde. The fixed cells were filtered through nylon mesh (380 mesh) to remove small aggregates formed during fixation.

Preparation of cell surface glycopeptide

Dissociated blastula cells were treated with 0.1% trypsin in buffered CMF-SW (10 mM Tris-

HCl, pH 8.0) at 20°C for 1 hour. After removing the cells by low speed centrifugation ($1000\times g$, 5 min), the extract was spun at $10,000\times g$ for 20 min and the supernatant was concentrated by ultrafiltration (Amicon PM-30). The concentrated trypsin extract was fractionated by gel filtration through Sephadex G-50 column ($2\times 100\text{ cm}$). The first fraction containing most of the sugar was pooled, lyophilized and used as cell surface glycopeptide.

Estimation of $^{45}\text{Ca}^{2+}$ -binding

To estimate the binding of $^{45}\text{Ca}^{2+}$ to the cells, 1 ml of cell suspension (10^7 cells) and 1 ml of CMF-SW or aggregation factor ($100\text{ }\mu\text{g}/\text{ml}$) were added to 3 ml of buffered artificial sea water containing $2\text{ }\mu\text{Ci}$ of [$^{45}\text{Ca}^{2+}$]- CaCl_2 . After rotation for 30 min in the cold (80 rpm, 20 mm rad.), the cells were separated from the supernatant by centrifugation ($1000\times g$, 5 min) and suspended in 5 ml of the same buffer. After standing for 10 min, the cells were spun down and transferred into scintillation vials, and the radioactivity was counted with a scintillation counter following addition of 10 ml of Triton-toluene scintillator. Additive washing of the cells did not affect the counting.

The binding of $^{45}\text{Ca}^{2+}$ to cell surface glycopeptide and to the aggregation factor was estimated by gel filtration. Small columns of Sephadex G-50 ($6\times 400\text{ mm}$) were equilibrated with buffered CMF-SW of different pHs. One hundred microliters of sample solution (cell surface glycopeptide, $100\text{ }\mu\text{g}$; aggregation factor, $500\text{ }\mu\text{g}$ protein) were mixed with $100\text{ }\mu\text{l}$ of CMF-SW containing $1\text{ }\mu\text{Ci}$ of $^{45}\text{Ca}^{2+}$. After incubation for 15 min at 0°C , the mixture was applied on the top of the column and eluted with the same buffer. Ten drop fractions were collected in each scintillation vial and the radioactivity was counted after addition of Triton-toluene scintillator. The peak appeared in the void volume was separated from the later peak retarded by the gel. The counts of the former peak were summed and estimated as bound $^{45}\text{Ca}^{2+}$ to macromolecular components.

Estimation of [^{35}S]-AF binding

The binding of [^{35}S]-AF to the cell was determined with the same procedure as that for $^{45}\text{Ca}^{2+}$

-binding, except for the use of [³⁵S]-AF (45,000 cpm/100 μ g protein/ml) instead of ⁴⁵Ca²⁺.

RESULTS

Effect of pH on cell aggregation

The cell aggregation induced by the aggregation factor was examined in artificial sea water of various pHs. As is shown in Figure 1, cell aggregation was dependent significantly on pH and was maximal at pH 8. The sizes of cell aggregates decreased gradually at lower pHs and no aggregates formed below pH 4. Cell aggregation did not occur at any pHs in the absence of divalent cations and also without the aggregation factor.

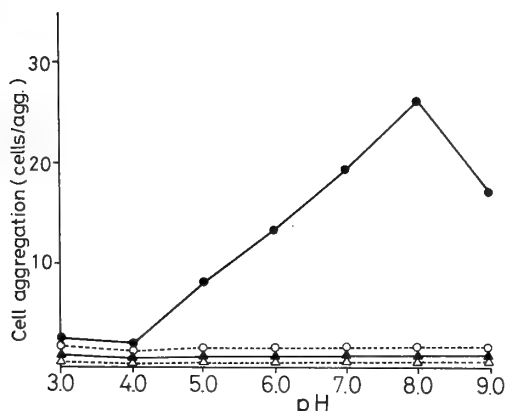


FIG. 1. Effect of pH on the cell aggregation of sea urchin embryos. Cell aggregation in the presence of the aggregation factor in artificial sea water (●—●), the same in CMF-SW (○---○); cell aggregation in the absence of the aggregation factor in artificial sea water (▲—▲), the same in CMF-SW (△---△).

A similar experiment was done with fixed cells to examine the possibility that the effect of pH on cell aggregation might be due to its effect on cell metabolism. The general pH profile of cell aggregation with fixed cells was similar to that of intact cells, although the extent of cell aggregation was markedly reduced (Fig. 2).

When pH was changed in the course of experiment (60 min) and the cells were kept at the second pH for further 60 min, the size of cell aggregates shifted close to that kept at the second

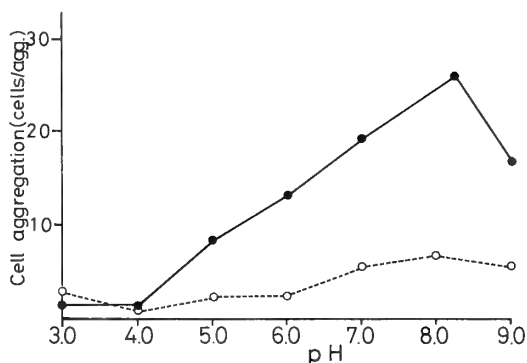


FIG. 2. Effect of pH on the aggregation of fixed cells of sea urchin embryos. Aggregation of fixed cells in the presence of the aggregation factor in artificial sea water (●—●) and aggregation of living cells under the same conditions (○---○).

pH from the beginning. When pH was changed from 4 to 8, the cells started to aggregate to reach the similar size to that of the aggregates formed on incubation at pH 8 (cells/aggregate, from 1.0 to 17.3). When pH was changed from 8 to 4, the cell aggregates began to dissociate but they were not completely dissociated after 60 min (cell/aggregate, from 24.5 to 11.6).

Effect of pH on the binding of ³⁵S-labeled aggregation factor to the cells

The binding of ³⁵S-labeled aggregation factor ([³⁵S]-AF) to the cells was examined in normal and CMF-SW (Fig. 3). The binding of [³⁵S]-AF in normal sea water was the highest at pH 8–9 and decreased as pH was lowered to 6, but increased again at pH 5–3. On the other hand, its binding in CMF-SW was low and did not change significantly from pH 9 to 5 but increased at pH 4–3. When the [³⁵S]-AF binding value in CMF-SW was subtracted from its binding value in normal sea water, the resulting pH profile (divalent cation-dependent binding) turned out to be similar to that of cell aggregation (Fig. 3).

Effect of pH on the binding of ⁴⁵Ca²⁺ to the cells and to cell surface glycopeptide

The binding of ⁴⁵Ca²⁺ to dissociated cells was examined in the absence and presence of the aggregation factor. The binding of ⁴⁵Ca²⁺ to the cells was the highest at pH 9 within the pH range

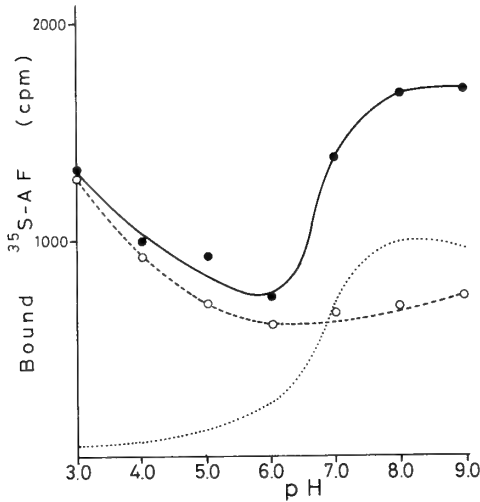


FIG. 3. Effect of pH on the binding of ^{35}S -labeled aggregation factor (^{35}S -AF) to the cells in artificial sea water (●—●) and in CMF-SW (○---○). Dotted line indicates the difference between the values.

examined and decreased continuously to pH 6 and retained half the maximal level at lower pHs (Fig. 4). The presence of aggregation factor at the concentration enough to cause cell aggregation did not alter this profile. In addition, the binding of $^{45}\text{Ca}^{2+}$ to cell surface glycopeptide showed a similar profile (Fig. 4).

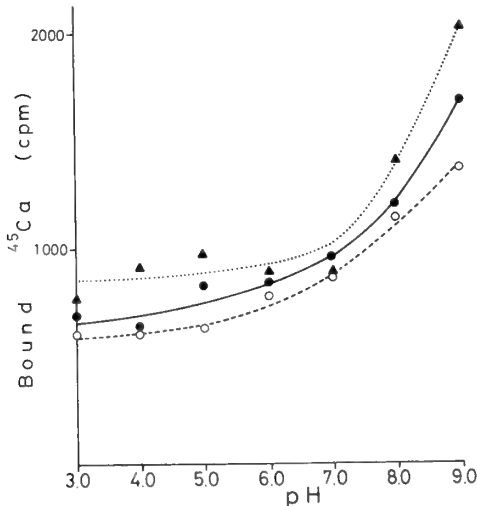


FIG. 4. Effect of pH on the binding of $^{45}\text{Ca}^{2+}$ to the sea urchin embryo cells in CMF-SW in the presence (---○---) and absence (●—●) of the aggregation factor, and the effect of pH on the binding of $^{45}\text{Ca}^{2+}$ to cell surface glycopeptide in CMF-SW (▲—▲).

Effect of pH on the binding of $^{45}\text{Ca}^{2+}$ to the aggregation factor

The binding of $^{45}\text{Ca}^{2+}$ to the aggregation factor was analyzed by gel filtration. $^{45}\text{Ca}^{2+}$ was bound to the aggregation factor maximally at pH 7–9, and its binding was also dependent on pH. It decreased continuously at lower pHs, and no significant binding occurred below pH 4 (Fig. 5). This pH profile of $^{45}\text{Ca}^{2+}$ binding to the aggregation factor was almost identical to that of cell aggregation and to that of divalent cation-dependent ^{35}S -AF binding to the cells.

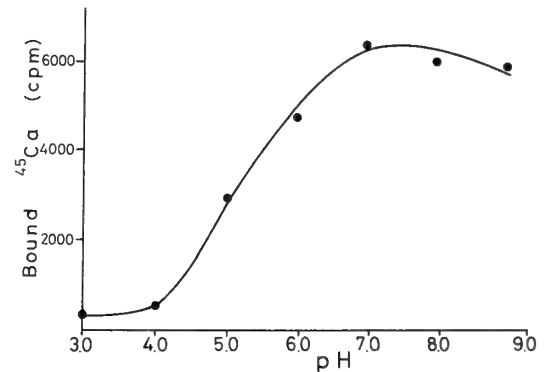


FIG. 5. Effect of pH on the binding of $^{45}\text{Ca}^{2+}$ to the aggregation factor of sea urchin embryos in CMF-SW.

Cell aggregation induced by the hyaline layer substance

The hyaline layer substance manifested cell aggregating activity at all pHs tested in the pre-

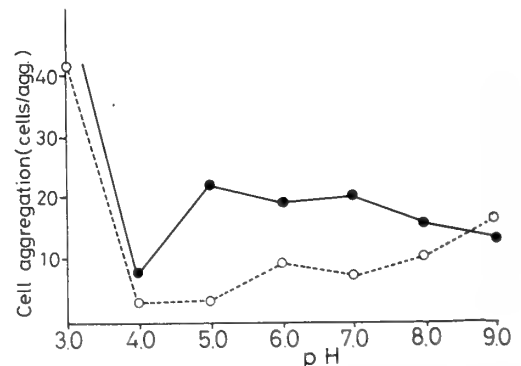


FIG. 6. Effect of pH on the cell aggregation induced by hyaline layer substance. Cell aggregation in the presence of hyaline layer substance in artificial sea water (●—●), the same in CMF-SW (○---○).

sence of Ca²⁺. The rate of cell aggregation did not change significantly between pH 9 and 5. It was reduced at pH 4 but large cell clumps were formed at pH 3 (Fig. 6). Cell aggregating activity was also observed in the absence of divalent cations at higher pHs. These pH profiles were quite different from those by the aggregation factor.

DISCUSSION

There has been a number of reports on the effects of pH on cell aggregation [7, 10, 11]. These authors showed pronounced cell aggregation at physiological pHs and reduced aggregation at lower pHs. In the present study, cell aggregation, induced by the aggregation factor of sea urchin embryos, was examined at a wide range of pHs and the extent of cell aggregation was shown to be remarkably influenced by pH. This pH dependency suggested the participation of electrostatic forces in cell aggregation. The change of pH would influence the ionization of charged groups of cell aggregation-related molecules and consequently the electrostatic interaction among them.

When one considers the necessity of Ca²⁺ in cell aggregation, it would be natural to take account of the electrostatic interactions among positively charged Ca²⁺ and negatively charged groups of the cell surface and those of the aggregation factor. These negatively charged groups, when not ionized at lower pHs, would not interact with Ca²⁺. At higher pHs, on the contrary, they would be ionized and accordingly be ready to interact electrostatically with Ca²⁺. Thus pH dependent ionization of the negatively charged groups appears to be the cause of pH dependent cell aggregation.

There is a possibility that the pH dependency of cell aggregation is due to indirect effect of pH through cell metabolism. However, cell aggregation with fixed cells showed almost a similar pH profile to that with live cells and the effect of pH on cell aggregation was reversible. These results favor the view that cell aggregation is influenced by pH through reversible ionization of the charged groups.

Previous experiments with labeled aggregation factor [12], have shown that [³⁵S]-AF bound to the

cells and the binding was quantitatively proportional to the rate of cell aggregation. They suggested actual involvement of the aggregation factor in cell aggregation as an essential constituent. Accordingly, the effect of pH on [³⁵S]-AF binding to the cells was examined in the present experiments. Unexpectedly, its pH profile was not similar to that of cell aggregation, and a considerable extent of binding was detected at lower pHs. However, when the value of [³⁵S]-AF binding in CMF-SW was subtracted from that in normal sea water, the value of divalent cation-dependent binding manifested the same pH profile as that of cell aggregation.

When one assumes that the aggregation factor and Ca²⁺ constitute the intercellular bridges in cell aggregation, two sites are possible to be influenced by pH; one between Ca²⁺ and the negatively charged groups of the cell surface and the other between Ca²⁺ and those of the aggregation factor. The binding of ⁴⁵Ca²⁺ to the cells was shown to be independent of pH at lower pHs and the general profiles was quite different from that of cell aggregation. On the contrary, the pH profile of ⁴⁵Ca²⁺-binding to the aggregation factor was almost identical to that of cell aggregation. Therefore, it would be reasonable to conclude that the linkage between Ca²⁺ and the aggregation factor constitutes the rate limiting step in the effect of pH on cell aggregation. It is assumed that the binding of Ca²⁺ and the aggregation factor forms an essential link in the cell aggregation.

When one admit this assumption, the linkage of aggregation factor to the cell surface still remains to be elucidated. In our experiments, pH-dependent binding of [³⁵S]-AF to the cells needed Ca²⁺, but it was also true that some significant portion of [³⁵S]-AF bound to the cells without Ca²⁺. As was reported in other systems [13–16], it would be also possible that the aggregation factor binds the cell surface by another mechanism without the participation of Ca²⁺. Calcium ion might just enhance the cooperation among the aggregation factors to stabilize the intercellular bridges. Further studies to identify the mode of binding of the aggregation factor and to elucidate the mechanism of its binding to the cell surface are needed to settle this problem.

The pH profile of cell aggregation induced by the hyaline layer substance turned out to be entirely different from that by the aggregation factor. Hyaline layer substance is a different cell aggregating agent from the so called aggregation factor [8]. Present result has added another proof to distinguish them.

ACKNOWLEDGMENTS

We thank to the staffs of Misaki Marine Biological Station for their kind supply of sea urchins and the offer of space and facilities. Thanks are also due to Dr. M. Hozumi for his generous offer to use the liquid scintillation spectrometer at the Saitama Cancer Research Center. We are also indebted to Prof. K. Ishihara for his kind assistance in the preparation of the manuscript. This work is partly supported by the grant in aid from the Ministry of Education, Science and Culture, Japan.

REFERENCES

- 1 Balsamo, J. and Lilien, J. (1975) The binding of tissue-specific adhesive molecules to the cell surface. A molecular basis for specificity. *Biochemistry*, **14**: 167-171.
- 2 Edelman, G. M. (1983) Cell adhesion molecules. *Science*, **219**: 450-457.
- 3 Müller, W. E. G. and Müller, I. (1980) Sponge cell aggregation. *Mol. Cell. Biochem.*, **29**: 131-143.
- 4 Turner, R. S. and Burger, M. M. (1973) Involvement of carbohydrate group in the active site for surface guided reassociation of animal cells. *Nature*, **244**: 509-510.
- 5 Curtis, A. S. G. (1967) *The Cell Surface: Its Molecular Role in Morphogenesis*. Logos Press, London.
- 6 Pethica, B. A. (1961) The physical chemistry of cell adhesion. *Exp. Cell Res. Suppl.*, **8**: 123-140.
- 7 Steinberg, M. S. (1958) On the chemical bonds between animal cells, A mechanism for type-specific association. *Amer. Nat.*, **92**: 65-81.
- 8 Tonegawa, Y. (1973a) Isolation and characterization of a particulate cell-aggregation factor from sea urchin embryos. *Dev. Growth Differ.*, **14**: 337-352.
- 9 Sano, K. (1977) Changes in cell surface charges during differentiation of isolated micromeres and mesomeres from sea urchin embryos. *Dev. Biol.*, **60**: 404-415.
- 10 Balsamo, J. and Lilien, J. (1974) Embryonic cell aggregation: Kinetics and specificity of binding of enhancing factors. *Proc. Natl. Acad. Sci. USA*, **71**: 727-731.
- 11 Müller, W. E. G., Müller, I. and Zahn, R. K. (1974) Two different aggregation principles in reaggregation process of dissociated sponge cells (*Geodia cydonium*). *Experientia*, **30**: 899-902.
- 12 Tonegawa, Y. (1973b) On the role of aggregation factor in the reaggregation of dissociated cells. *Zool. Mag.*, **82**: 254 (In Japanese).
- 13 Brackenbury, R., Rutishauser, U. and Edelman, G. M. (1981) Distinct calcium-independent and calcium-dependent adhesion systems of chicken embryo cells. *Proc. Natl. Acad. Sci. USA*, **78**: 387-391.
- 14 Jumblatt, J. E., Schlup, V. and Burger, M. M. (1980) Cell-cell recognition: Specific binding of *Microciona* sponge aggregation factor to homotypic cells and the role of calcium ions. *Biochemistry*, **19**: 1038-1042.
- 15 Magnani, J. L., Thomas, W. A. and Steinberg, M. S. (1981) Two distinct adhesion mechanisms in embryonic neural retina cells I. A kinetic analysis. *Dev. Biol.*, **81**: 96-105.
- 16 Takeichi, M. (1977) Functional correlation between cell adhesive properties and some cell surface proteins. *J. Cell Biol.*, **75**: 464-474.

**Mechanisms Underlying Regulation of Local Immune Responses
in the Uterus during Early Gestation of Eutherian
Mammals. III. Possible Functional Differentiation of
Macrophages Cultured Together with Blastocyst
in vitro, with Special Reference to the
Cellular Shape and Production of
Leukotriene C₄**

CHIKASHI TACHI and SUMIE TACHI¹

Zoological Institute, Faculty of Science, University of Tokyo, Tokyo 113, and

¹*Department of Anatomy, Tokyo Women's Medical
College, Tokyo 162, Japan*

ABSTRACT—In the blastocyst-macrophage co-culture of the mouse, we found two major groups of macrophages which were different in the morphology, i.e., the rounded cells, and the elongated cells. The macrophages in direct contact with the embryonic cells, regardless of whether they were trophoblast or ICM cells, assumed invariably rounded cellular shape. Colchicine, cytochalasin B and D induced strong rounding of the macrophage. The rate of synthesis of leukotriene C₄ in those rounded macrophages remained at a low level of the unstimulated cells. Therefore, it was tentatively proposed that in the blastocyst-macrophage co-culture, the rate of production of LTC₄ in the rounded macrophages, might remain at a low level, while in the elongated ones the rate might be enhanced [C. Tachi and U. Zor, *Zool. Sci.*, in press]. On the other hand, tuftsin, a naturally occurring tetrapeptide known to augment phagocytosis as well as capability of antigen presentation in macrophages, raised slightly the rate of LTC₄ synthesis around the concentration of 60 nM or above. Recently Gupta presented evidence indicating that LTC₄ mediates the initial estrogen-dependent phase of endometrial modification during nidation in mice. While it is strongly suspected that the major source of LTC₄ produced during that period, might be one of the functionally differentiated groups of macrophages in the endometrium, further work is needed to corroborate the view.

INTRODUCTION

We proposed [1–3], on the basis of the observations made in the rat and the mouse, that macrophages are probably involved in the local immune responses elicited in the endometrium by implanting blastocysts during early gestation of eutherian mammals. We suggested [1–3], furthermore, that the decidua might function to limit the access of macrophages to the embryonic antigens, regulating the afferent flow of immunological information to the maternal immune system during the initial phase of the recognition of the concep-

tuses. However, the precise role played by the endometrial macrophages during implantation and/or nidation that is one of most critical episodes in the true viviparity of mammals, remains yet to be clarified.

As an approach to the problem, we analyzed, at ultrastructural levels, the mode of cell-to-cell interactions between the blastocysts and macrophages cultured together *in vitro* [4]. During the course of experiments, it came to our notice that the macrophages in the co-culture assumed, as will be described in this report in detail, mainly two distinctly different cellular shapes, i.e., they were either rounded or elongated.

Macrophages have been known to change their shape according to their functional states or to the

changes in their environmental conditions [5–10]. In turn, it is possible to bring about functional transformation of the macrophages cultured *in vitro* by exposing them to compounds which affect the cytoskeletal organization of the cells. Thus, colchicine, cytochalasin B and vinblastin stimulate the release of neutral peptidases, including elastase [11, 12], collagenase [11], gelatinase [11], azocaseinase [11] from the cultured peritoneal [11] as well as alveolar [12] macrophages of the mouse. Colchicine stimulates also the rate of production of interleukin-1 [13], in the irradiated peritoneal macrophages of the rat. Calcium ionophore A23187 added to the cultured peritoneal macrophages of the mouse [Tachi and Zor, Zool. Sci., in press] induced at alkaline pH's of the medium, strong elongation of the cellular shape, accompanied by the highly accelerated rate of leukotriene C₄ (LTC₄ in the following) production; stimulation of the Ca⁺⁺-dependent synthesis of LTC₄ [14] by A23187 in macrophages has been reported earlier in the literature [15–17].

Leukotrienes, as termed by Samuelsson *et al.* [18], are a family of metabolites of arachidonic acid, and produced via 5-lipoxygenase pathway. Leukotriene C₄ is the first peptidolipid to be synthesized in the family and held responsible for mediating inflammation, asthma and many other functions of leukocytes and/or macrophages [for review see, 19–25] which are the major source of LTC₄ in the mammalian body. Recently, in 1989, Gupta *et al.* [26] proposed that LTC₄ might be one of the mediators of the endometrial changes elicited during the estrogen-dependent early phase of implantation in the mouse, although the exact source of LTC₄ produced during the period is yet to be determined.

In order to examine the possibility that the morphological difference of the macrophages in the blastocyst-macrophage co-culture might reflect the underlying functional difference which, in turn, might be correlated with the rate of LTC₄ synthesis in the phagocytes, we analyzed the distribution of macrophages according to their morphology in the co-culture, and at the same time, we assayed the rate of LTC₄ production in the macrophages under the influence of the compounds which affect the cytoskeletal organization of the

cells. It was hoped that such analyses will provide us clues to understand the mechanisms underlying the blastocyst-endometrial interactions during implantation and/or nidation in eutherian mammals.

Part of the results has been presented in abstract form [27–29].

MATERIALS AND METHODS

Animals

Specific pathogen free (SPF) mice of BALB/c (H-2^d) and C3H/HeJ (H-2^k) strains were used throughout the experiments. They were purchased from a local dealer (Nippon Clea & Co., Ltd., Tokyo, Japan), and had been kept in the animal room of our laboratory under regulated temperature (25°C) and illumination cycles (12 hr dark and 12 hr light per day), until they were used for the experiments. Female BALB/c mice were mated on the day of proestrus with fertile BALB/c males, and if the vaginal plugs were found next morning, the day was counted as Day 1 of pregnancy.

Drugs and reagents

Unlabelled LTC₄ was purchased from Wako Pure Chemical Industries & Co., Ltd. (Osaka, Japan). Calcium ionophore A23187, cytochalasin B and D were obtained from Sigma Chemical & Co., Ltd. (St. Louis, Mo, USA); each of the three compounds was dissolved in dimethyl sulfoxide (DMSO; Wako Pure Chemical Industries) at a concentration of 500 µg/ml. Colchicine (Merck, Darmstadt, West Germany) and Tuftsin (Wako Pure Chemical Industries), a polypeptide known to be an activator of macrophages, were dissolved in glass distilled water at a concentration of 500 µg/ml. Sterilized Ficoll-Hypaque solution (d = 1.090 ± 0.001) was purchased from Otsuka Assay Laboratories (Tokushima-shi, Japan).

Radioactive LTC₄

Aqueous solution of tritium-labeled leukotriene C₄ (specific activity, 39 Ci/mMol, Amersham Japan & Co., Ltd., Tokyo, Japan), as supplied by its manufacturer, was diluted with 50% ethanol to give a final concentration of 1.0 µCi/ml.

Macrophages

The macrophages were collected from peritoneal exudate of C3H/HeJ mice by injecting 60 units of heparin dissolved in Earl's minimum essential medium (MEM) at a concentration of 30 units/ml under ether anesthesia. After 3–5 min, the animals were killed by cervical dislocation and the peritoneal fluid was gently aspirated into a glass syringe.

For the co-culture experiments, the procedures previously described were essentially followed [4]. The macrophages were collected by centrifugation at approximately 1000 rpm for 5 min, and washed three times with phosphate-buffered saline (PBS) and added to the culture medium which is known to favor the trophoblast spreading [30].

For the assay of LTC₄, and the examination of the effects of various compounds which affect the cytoskeletal organization of the cells, highly purified peritoneal macrophages were prepared as described previously [28, C. Tachi and U. Zor, *Zool. Sci.*, in press].

Blastocysts

Blastocysts were collected from BALB/c mice as described before [4] by flushing the uterine lumen with the standard egg culture medium (SECM) [31] on Day 4 of pregnancy. The collected embryos were washed twice in SECM and introduced into the culture of macrophages.

Co-culture of blastocysts and macrophages

The zona-encased blastocysts (BALB/c) collected in the afternoon of Day 4 from the uterine lumen were introduced to the culture of macrophages (C3H/HeJ); usually 5 blastocysts were added to a single Falcon dish (diameter of the dish, 34.5 mm) which contained macrophages allogeneic to the embryos at an approximate concentration of $1-3 \times 10^6$ cells per dish. The co-cultures were incubated at 37°C under the atmosphere of 5% CO₂ and 95% air.

Determination of the rate of LTC₄ production

The rate of LTC₄ production was determined, as will be described elsewhere [C. Tachi and U. Zor, *Zool. Sci.*, in press], by assaying the total amount

of the cysteinyl leukotrienes released into the medium from the macrophages during 1.5–2.0 hr of the culture period. The radioimmunoassay of the cysteinyl leukotrienes were done essentially following the procedures described by Danzlinger *et al.* [32] with minor modifications; the monoclonal antibodies against cysteinyl leukotrienes were generous gift of Dr F. Kohen, Department of Hormone Research, Weizmann Institute of Science, Rehovot, Israel. The antibodies reacted with LTC₄ (100%), LTD₄ (105%), and LTE₄ (77%) at a 50% saturation level of binding [F. Kohen, personal communication].

One tenth ml of the sample solution to be assayed was mixed with an equal amount of the antibody solution and incubated at 0°C for 30 min. Then, 0.1 ml of ³H-LTC₄ solution containing 7 nCi of the isotope, was added to the mixture, and had been stood at 4°C overnight. Free LTC₄ was removed by adding 0.2 ml of dextran-charcoal, and by centrifugation at 15,000 rpm for 3 min. The radioactivity was measured by liquid scintillation counting.

Differential counting of macrophages according to their cell shape

The photomicrographs of the co-cultures were taken using a phase contrast microscope (Model CK, Olympus & Co., Tokyo, Japan), approximately 72 hr after the initiation of the culture. For histological examination, the cells were fixed with 3.5% formaldehyde solution and stained with Giemsa's. The number of the cells of the elongated, or the rounded cellular shape were differentially counted on the photomicrographs, by using a microcomputer-based graphic analysis system (TACSYS/G) previously described by C. Tachi [2].

RESULTS

1. Cellular shape of the macrophages cultured together with blastocysts in vitro

Microscopic appearance of macrophages adhered to the zona pellucida or the blastocysts following the co-culture of the phagocytes with the zona-encased embryos, is shown in Figure 1A.

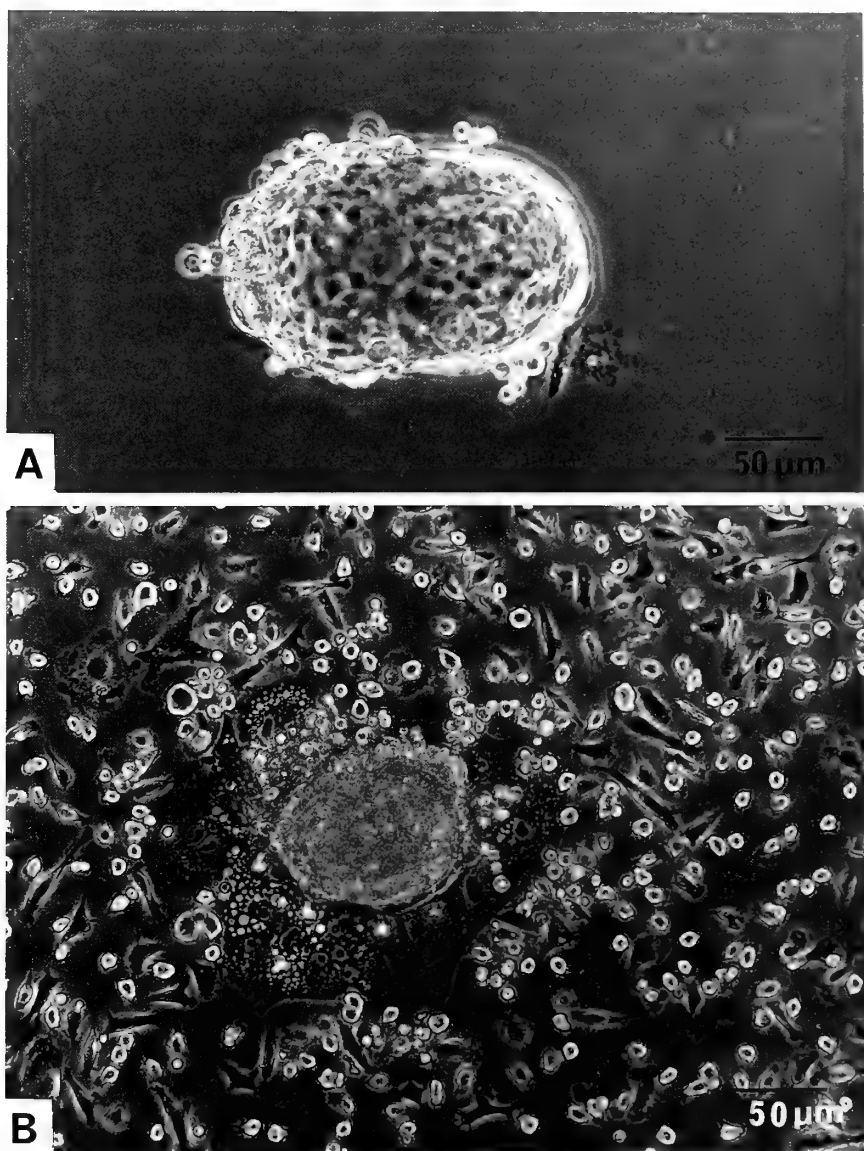


FIG. 1. Photomicrographs of blastocyst-macrophage co-culture. A) The blastocyst (BALB/c) is encased in zona pellucida onto which numerous macrophages (C3H/HeJ) are firmly adhered. Approximately 6 hr after the initiation of co-culture. B) The blastocyst is undergoing trophoblast spreading. Approximately 72 hr after the initiation of co-culture.

The macrophages which were tightly bound to the zona, assumed strongly rounded cellular shape without exception; none of the zona-bound phagocytes observed was of elongated morphology.

In Figure 1B, representative photomicrograph of the blastocyst-macrophage co-cultures approximately 48 hr after the initiation, is presented. The

blastocyst was undergoing trophoblast spreading and numerous macrophages were found in contact with the periphery of the trophoblast cell layer. Some of the macrophages were located within the embryos (Fig. 1B).

In the co-culture, two groups of macrophages of distinctly different morphology were discernible,

i.e., those which were rounded and the others which were either elongated or spread (Fig. 1B). The macrophages with spread morphology, however, were only rarely observed under the conditions we employed. We counted the number of macrophages according to their cellular shape, and the distance from the periphery of the trophoblast spread. The results are presented in Table 1. Almost all the macrophages in contact with the spreading trophoblast cells, were rounded (Table 1); no elongated macrophages were found inside the blastocysts. While the macrophages lying in close vicinity of the embryos (less than 20 μm from the edge of the trophoblast spread) tended to assume the rounded morphology, the difference in the relative frequencies of the rounded cells, from those in other areas was not statistically significant.

2. Drug-induced rounding of macrophages and production of LTC_4 in vitro

In order to understand the mechanisms underlying the rounding of the macrophages, induced when they are in contact with the embryonic cells, we tested the effect of various compounds which are known to affect the cytoskeletal organization of the cells. Furthermore, the rate of production of LTC_4 in the phagocytes under the influence of those compounds was examined.

In Figure 2A-D, the photomicrographs show the effects of colchicine, cytochalasin B and D upon the cellular shape of highly purified peritoneal macrophages of the mouse. All the three compounds induced strong rounding of the cells at the concentrations indicated in the legends to the figures. Tuftsin, an activator of macrophages, had little effects upon the morphology of the cells (Fig. 2E).

In Figure 3A, the relative contents of the macrophages of the rounded and the elongated morphology in the culture, are presented according to the concentrations of colchicine added. At the concentrations above 5 $\mu\text{g}/\text{ml}$, all the macrophages were seen rounded. The rates of LTC_4 production in the same cell populations are shown in Figure 3B. Colchicine affected little the rates which remained unchanged after the addition of the compound to the cells, and stayed at a low level throughout the range of the colchicine concentrations examined.

Cytochalasins, both B and D, at sufficiently high concentrations, resulted in the complete rounding of the phagocytes in the culture (Fig. 4A, 5A). The rate of production of LTC_4 , however, remained at the control level throughout the range of concentrations of the compounds examined (4B, 5B).

TABLE 1. Distribution of macrophages with either elongated or rounded cellular shape in blastocyst-macrophage co-culture of allongeneic combinations¹⁾

Location of Macrophages	No. of Experiments	Rounded Macrophages		Elongated Macrophages	
		No. of Cells	Relative Frequency	No. of Cells	Relative Frequency
		cells/embryo ²⁾	%	cells/embryo	%
On the Zona Pellucida	6	54.0 \pm 13.7	100.0	0.0 \pm 0.0	0.0
		cells/embryo	%	cells/embryo	%
Within 20 μm from Edge of Trophoblast Spread	12	39.5 \pm 9.6	75.8	12.6 \pm 3.9	24.2
		cells/0.1 mm^2	%	cells/0.1 mm^2	%
Areas Surrounding the Embryo (Further than 20 μm from the Edge)	12	78.8 \pm 25.0	61.5	49.0 \pm 11.2	38.5

¹⁾ Blastocysts were obtained from BALB/c mice, and macrophages were collected from C3H/HeJ mice.

²⁾ Only the number of macrophages on a hemisphere of the zona facing toward the observed through the lenses, was actually counted. The values obtained for the hemisphere were multiplied by a factor of 2, and presented as number of cells per embryo.



FIG. 2. Photomicrographs showing the effects of drugs which affect the cytoskeletal organization of cells, upon the morphology of macrophages *in vitro*. A) Control with no additions; B) colchicine (500 µg/ml); C) cytochalasin B (500 ng/ml); D) cytochalasin D (500 ng/ml); E) Tuftsin (60 nM/ml).

3. Effects of tuftsin upon the cellular morphology and the rate of production of LTC₄

Tuftsin, a polypeptide known to be a stimulator of macrophage activities [33–41], did not induce

noticeable changes in the morphology of these cells (Fig. 6A). It did not cause significant changes in the rate of LTC₄ production, except at 60 nM where slight but significant elevation in the rate was observed (Fig. 6B).

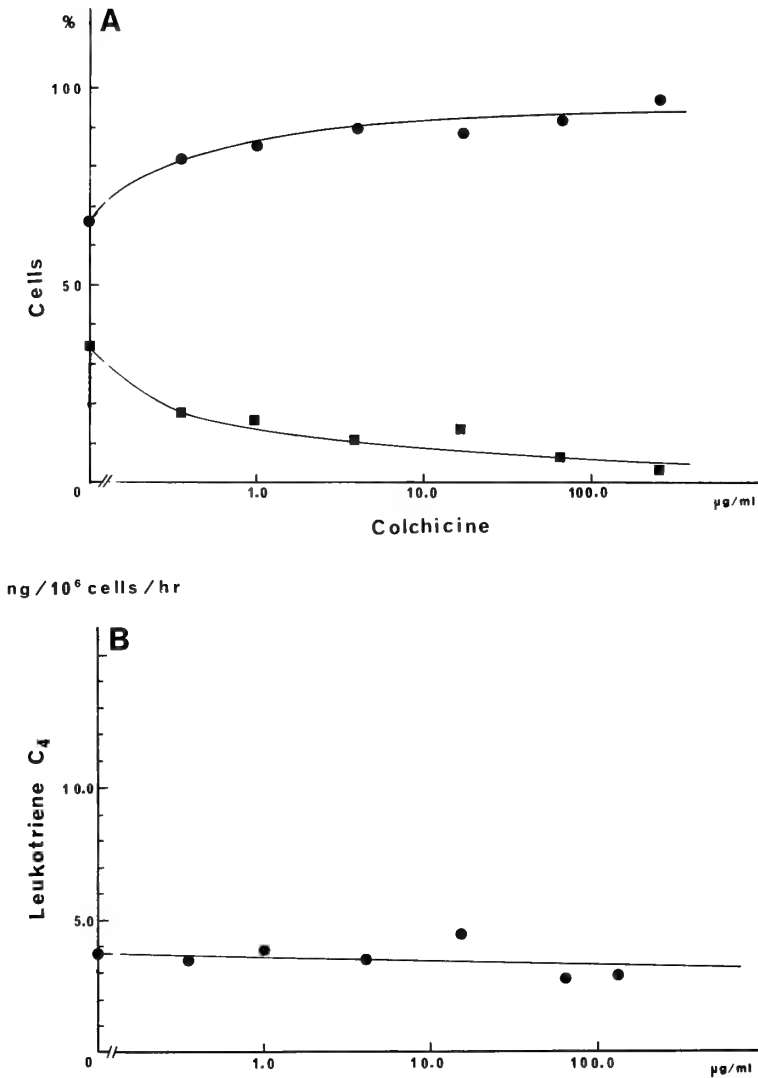


FIG. 3. Effects of colchicine upon the macrophages cultured *in vitro*. A) Morphology. ●, rounded cells; ■, elongated cells. B) The rate of production of leukotriene C_4 assayed as the total amount of cysteinyl leukotrienes released into the medium (see Materials and Methods).

DISCUSSION

Present report demonstrated that in the blastocyst-macrophage co-culture of the mouse, two major morphologically distinct groups of macrophages, i.e., those which were rounded, and the others which were elongated, are present, and that the phagocytes in direct contact with the

embryonic cells, regardless of whether they were trophoblast or ICM cells, assumed invariably rounded cellular shape. Evidence was presented, furthermore, indicating that the rate of synthesis of cysteinyl leukotrienes in the rounded macrophages is probably low, and remains at the level of unstimulated macrophages.

Fauve *et al.* [42], as a part of their studies upon

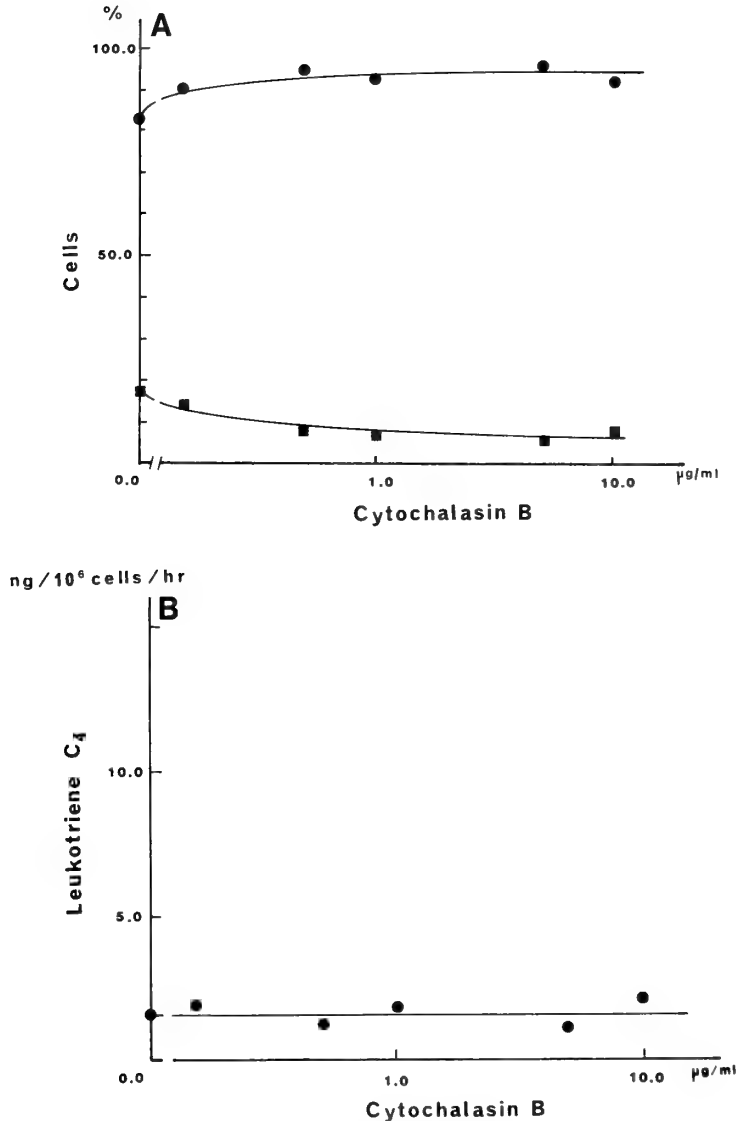


FIG. 4. Effects of cytochalasin B upon the macrophages cultured *in vitro*. A) Morphology. ●, rounded cells; ■, elongated cells. B) The rate of production of leukotriene C₄ assayed as the total amount of cysteinyl leukotrienes released into the medium (see Materials and Methods).

the anti-inflammatory effects of murine malignant teratocarcinoma cells, examined the interactions between the trophoblast cells and the macrophages cultured together *in vitro*. They noted [42] that in the vicinity of the trophoblast cells, the macrophages were unable to spread but became necrotic. They suggested that the trophoblast cells, like the teratocarcinoma cells, might escape the immunological surveillance of the host by exerting a

direct cytotoxic effect on macrophages, and by releasing a hypothetical inhibitor of inflammatory reactions.

We could not convincingly observe, however, the evidence for explicit cytotoxic influence of the trophoblast cells upon the macrophages.

The peritoneal macrophages used by Fauve *et al.* [42] were of considerably high purity [43]. However, possibility cannot be entirely excluded that the

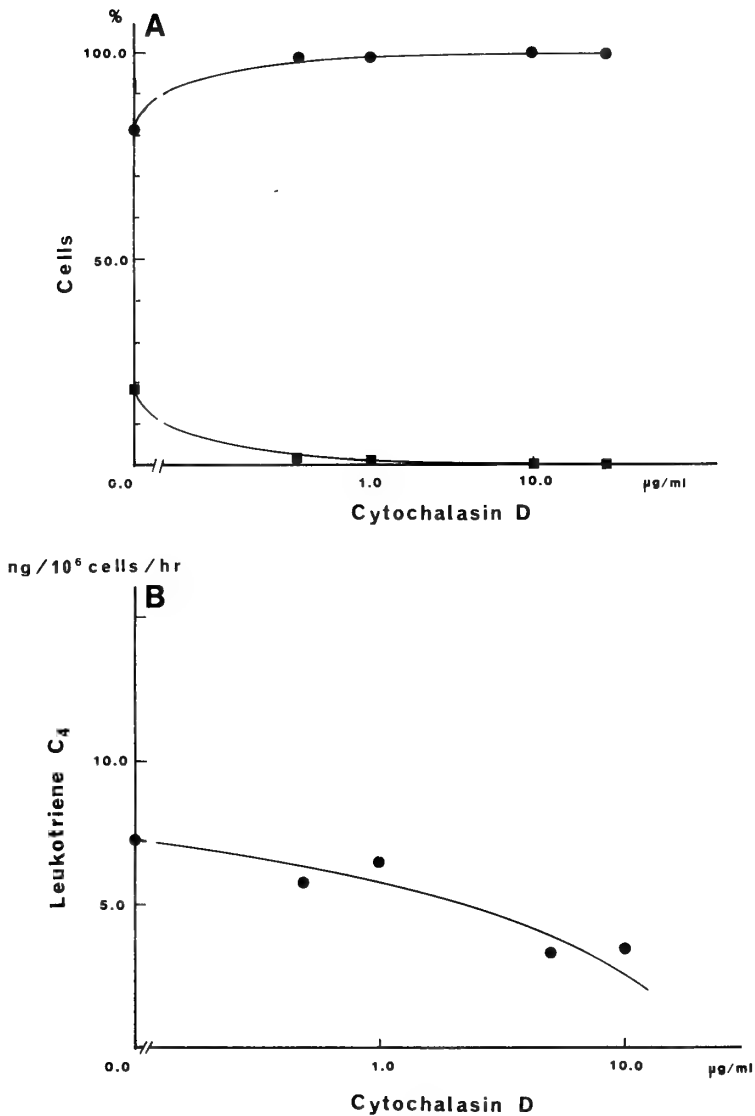


FIG. 5. Effects of cytochalasin D upon the macrophages cultured *in vitro*. A) Morphology. ●, rounded cells; ■, elongated cells. B) The rate of production of leukotriene C₄ assayed as the total amount of cysteinyl leukotrienes released into the medium (see Materials and Methods).

necrotic cells were not macrophages but lymphocytes which adhered non-specifically to the culture dishes, and contaminated the macrophage preparation.

We, too, occasionally observed in the blastocyst-macrophage co-culture, cells which resembled dead macrophages and were ingested by the trophoblast cells [4]. Although we could not definitely identify the type of the ingested cells, we

considered it rather unlikely that these cells represented the macrophages actively killed and ingested by the trophoblast cells [4].

Under the experimental conditions we employed, colchicine, cytochalasin B and D induced strong rounding of the cellular shape in the macrophages.

According to the observations reported earlier by White *et al.* [12], while colchicine caused round-

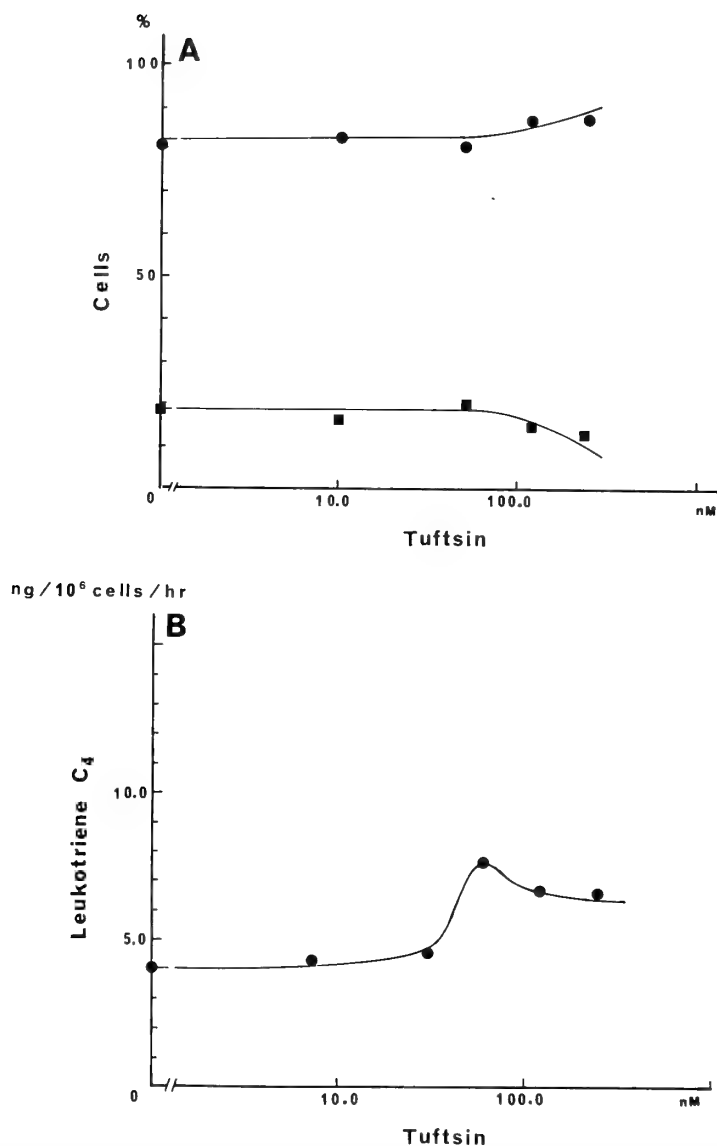


FIG. 6. Effects of tuftsin upon the macrophages cultured *in vitro*. A) Morphology. ●, rounded cells; ■, elongated cells. B) The rate of production of leukotriene C₄ assayed as the total amount of cysteinyl leukotrienes released into the medium (see Materials and Methods).

ing of the cultured macrophages, cytochalasin B had little effect upon the morphology of the phagocytes; both of the drugs were added to the cells at a concentration of 10^{-6} M. The cause for the discrepancy between our results and those described by White *et al.*, is not clear.

Macrophages are one of the major sources of leukotrienes in the mammalian body, and these

metabolites of arachidonic acid are known to mediate variety of pathological conditions, including inflammation, allergy, asthma etc. (for reviews see [20–25]). While the production of LTC₄ is dependent upon the increased intracellular levels of calcium, macrophages contain a cytoskeletal protein, gelsolin, the activity of which is regulated by calcium [44–46]. Indeed, Ca ionophore added

to macrophages at alkaline pH's of the medium, induced strong elongation of the macrophages, while the rate of leukotriene C₄ production increased approximately 100-fold [C. Tachi and Zor, Zool. Sci., in press].

Since, as stated in Introduction, the disturbance of cytoskeletal organization in the phagocytes by drugs, results in the increased rate of release of various molecules of biological activity from the cells, it is pertinent to ask if the morphological changes of macrophages induced by the contact with the embryos, or by the drugs, might results in the modified rate of synthesis of leukotrienes.

Our results presently described, however, clearly demonstrated that the macrophages of the rounded morphology induced by the compounds which affect the cytoskeletal organization of the cells, were inactive with regard to the release of the cysteinyl leukotrienes.

On the basis of those findings, we would like to tentatively propose, as a working hypothesis, that in the blastocyst-macrophage co-culture, the rate of production of LTC₄ in the rounded macrophages, may remain at a low level, while in the elongated ones the rate might be enhanced [C. Tachi and U. Zor, Zool. Sci., in press].

However, the drug-induced transformations of the cellular morphology may not be immediately comparable to those caused in the co-culture, under the influence of the embryos. Therefore, it remains to be investigated, if the elongated and the rounded macrophages in the co-culture, are in fact synthesizing LTC₄ at different rates.

Tufts, a naturally occurring tetrapeptide derived from Fc segment of IgG [33–36], has been shown to specifically bind to macrophages [38], augment phagocytosis [35, 36, 38] and triggers the antigen-specific, macrophage-dependent education of T-cells [37]. The peptide appeared to raise slightly the rate of LTC₄ synthesis around the concentration of 60 nM or above.

Gupta *et al.* [26] proposed that LTC₄ might mediate the initial estrogen-dependent phase (phase I) of peri-nidatory changes of the endometrium in the mouse. Experimental evidence in support of the hypothesis implicating the role of prostaglandins [47–51] and/or leukotrienes [52–55] in the process of decidualization, has been re-

ported in the literature.

While it is tempting to propose that the major source of LTC₄ might be one of the functionally differentiated groups of macrophages which abundantly emerge, as described originally by ourselves [1, 3], in the endometrium during the early phase of implantation, further analytical work on the functional as well as the morphological aspects of the blastocyst-macrophage interactions *in vitro* is necessary to corroborate the view.

ACKNOWLEDGMENTS

The authors would like to thank Prof. U. Zor and Dr F. Kohen, Dept. Hormone Research, Weizmann Institute of Science, Rehovot, Israel, for valuable discussions and for the generous gift of the monoclonal antibodies against cysteinyl leukotrienes.

The work is supported in part by a grant-in aid (No. 63640004) to C. Tachi, for scientific research on priority areas "Molecular Mechanisms Underlying the Maintenance of Germ-Lines in Animals and Man", from the Ministry of Education, Science, Culture, Japan.

REFERENCES

- 1 Tachi, C., Tachi, S., Knyszynski, A. and Lindner, H. R. (1981) Possible involvement of macrophages in embryo-maternal relationships during ovum implantation in the rat. *J. Exp. Zool.*, **217**: 81–92.
- 2 Tachi, C. (1985) Mechanisms underlying regulation of local immune responses in the uterus during early gestation of eutherian mammals. I. Distribution of immuno-competent cells which bind anti-IgG antibodies in the post-nidatory uterus of the mouse. *Zool. Sci.*, **2**: 341–348.
- 3 Tachi, C. and Tachi, S. (1986) Macrophages and implantation. *Ann. New York Acad. Sci.*, **476**: 158–182.
- 4 Tachi, S., Tachi, C. and Knyszynski, A. (1985) Mechanisms underlying regulation of local immune responses in the uterus during early gestation of eutherian mammals. II. Electron microscopic studies in the interactions between blastocysts and macrophages cultured together *in vitro*. *Zool. Sci.*, **2**: 671–680.
- 5 Carr, K. and Carr, I. (1970) How cells settle on glass: a study by light and scanning electron microscopy of some properties of normal and stimulated macrophages. *Z. Zellforsch.*, **105**: 234–241.
- 6 Carr, I. (1973) *The Macrophage. A Review of Ultrastructure and Function.* Academic Press, New York.
- 7 Rabinovitch, M. and DeStephano, M. J. (1973)

- Macrophage spreading *in vitro*. I. Inducers of spreading. *Exptl Cell Res.*, **77**: 323–334.
- 8 Rabinovitch, M. and DeStephano, M. J. (1973) Macrophage spreading *in vitro*. II. Manganese and other metals as inducers or as co-factors for induced spreading. *Exptl Cell Res.*, **79**: 423–430.
 - 9 Cohn, Z. A. (1975) Macrophage physiology. *Fed. Proc.*, **34**: 1725–1729.
 - 10 Onozaki, K., Homma, Y., Miura, K. and Hashimoto, T. (1981) Scanning electron microscopic study of changes in the surfaces of lymphokine-treated guinea pig macrophages. *J. Reticuloendoth. Soc.*, **30**: 471–481.
 - 11 Gordon, S. and Werb, Z. (1976) Secretion of macrophage neutral proteinase is enhanced by colchicine. *Proc. Natl. Acad. Sci. U.S.A.*, **73**: 872–876.
 - 12 White, R. R., Leon, I. and Kuhn, C., III. (1981) Effect of colchicine, vinblastin, D₂O and cytochalasin B on elastase secretion, protein synthesis and fine structure of mouse alveolar macrophages. *J. Reticuloendoth. Soc.*, **29**: 295–305.
 - 13 Stolic-Grujicic, S. and Simic, M. M. (1982) Modulation of interleukin 1 production by activated macrophages: *in vitro* action of hydrocortisone, colchicine, and cytochalasin B. *Cell. Immunol.*, **69**: 235–247.
 - 14 Zor, U., Her, E., Talmon, J., Kohen, F., Harell, T., Moshonov, S. and Rivnay, B. (1987) Hydrocortisone inhibits antigen-induced rise in intracellular free calcium concentration and abolishes leukotriene C₄ production in leukemic basophils. *Prostaglandins*, **34**: 29–40.
 - 15 Bach, M. K. and Brashler, J. R. (1978) Ionophore A23187-induced production of slow reacting substance of anaphylaxis (SRS-A) by rat peritoneal cells *in vitro*: evidence for production by mononuclear cells. *J. Immunol.*, **120**: 998–1005.
 - 16 Bach, M. K., Brashler, J. R., Brooks, C. D. and Neerken, A. J. (1979) Slow reacting substances: comparison of some properties of human lung SRS-A and two distinct fractions from ionophore-induced rat mononuclear cell SRS. *J. Immunol.*, **122**: 160–165.
 - 17 Rankin, J. A., Hitchcock, M., Merrill, W., Bach, M. K., Brashler, J. R. and Askenase, P. W. (1982) IgE-dependent release of leukotriene C₄ from alveolar macrophages. *Nature*, **297**: 329–331.
 - 18 Samuelsson, B., Borgeat, P., Hammerstrom, S. and Murphy, R. C. (1979) Introduction of a nomenclature: leukotrienes. *Prostaglandins*, **17**: 785–787.
 - 19 Samuelsson, B. and Hammerstrom, S. (1982) Leukotrienes: a novel group of biologically active compounds. *Vitam. Horm.*, **39**: 1–30.
 - 20 Piper, P. J. (1983) Pharmacology of leukotrienes. *Brit. Med. Bull.*, **39**: 255–259.
 - 21 Piper, P. J. (1984) Formation and actions of leukotrienes. *Physiol. Rev.*, **64**: 744–761.
 - 22 Lewis, R. A. and Austen, K. F. (1984) The biologically active leukotrienes. *J. Clin. Invest.*, **73**: 889–897.
 - 23 Ford-Hutchinson, A. W. (1985) Leukotrienes: their formation and role as inflammatory mediators. *Fed. Proc.*, **44**: 25–29.
 - 24 Salmon, J. A. and Higgs, G. A. (1987) Prostaglandins and leukotrienes as inflammatory mediators. *Brit. Med. Bull.*, **43**: 285–296.
 - 25 Piper, P. J. and Samhoun, M. W. (1987) Leukotrienes. *Brit. Med. Bull.*, **43**: 445–459.
 - 26 Gupta, A., Huet, Y. M. and Dey, S. K. (1989) Evidence for prostaglandins and leukotrienes as mediators of phase I of estrogen action in implantation in the mouse. *Endocrinology*, **124**: 546–548.
 - 27 Tachi, C. and Zor, U. (1986) Possible correlation between the production of leukotriene C₄ and cytoskeletal organization in mouse peritoneal macrophages cultured *in vitro*. *Zool. Sci.*, **3**: 1011.
 - 28 Tachi, C. (1988) Cellular mechanisms of the interactions between blastocysts and macrophages co-cultured *in vitro*. *Proc. 2nd Annual Meeting, Japan Society for Basic Reproductive Immunology*. Ed. by O. Tanizawa, pp. 71–75.
 - 29 Tachi, C., Tachi, S. and Zor, U. (1988) Role of macrophages in local immune responses elicited by implanting blastocysts during early gestation in the endometrium of muridae rodents. In "Human Reproduction, Current Status/Future Prospect". Ed. by R. Iizuka and K. Semm, Elsevier Science Publ. B. V., Amsterdam, pp. 519–521.
 - 30 Spindle, A. I. and Pedersen, R. A. (1973) Hatching, attachment, and outgrowth of mouse blastocysts *in vitro*: fixed nitrogen requirements. *J. Exp. Zool.*, **186**: 305–318.
 - 31 Biggers, J. D., Whitten, W. K. and Whittingham, D. G. (1971) The culture of mouse embryos *in vitro*. In "Methods in Mammalian Embryology". Ed. by J. C. Daniel, Jr, W. H. Freeman & Co., San Francisco, pp. 86–116.
 - 32 Danzlinger, C., Guhlmann, A., Scheuber, P. H., Wilker, D., Hammer, D. K. and Keppler, D. (1986) Metabolism and analysis of cysteinyl leukotrienes in the monkey. *J. Biol. Chem.*, **261**: 15601–15606.
 - 33 Fidalgo, B. V. and Najjar, V. A. (1967) The physiological role of the lymphoid system. III. leucophilic-globulin and the phagocytic activity of the polymorphonuclear leucocytes. *Proc. Natl. Acad. Sci. U.S.A.*, **57**: 957–964.
 - 34 Fidalgo, B. V., Katayama, Y. and Najjar, V. A. (1967) The physiological role of the lymphoid system. V. The binding of autologous (erythrophilic)-globulin to human red blood cells. *Biochemistry*, **6**: 3378–3385.

- 35 Najjar, V. A. and Nishioka, K. (1970) 'Tuftsin': a natural phagocytosis stimulating peptides. *Nature*, **228**: 672-673.
- 36 Nishioka, K., Constantopoulos, A., Satoh, P. S. and Najjar, V. A. (1972) The characterization, isolation and synthesis of the phagocytosis stimulating peptide tuftsin. *Biochem. Biophys. Res. Commun.*, **47**: 172-179.
- 37 Tzeheval, E., Segal, S., Stabinsky, Y., Fridkin, M., Spierer, Z. and Feldman, M. (1978) Tuftsin (and Ig-associated tetrapeptide) triggers the immunogenic function of macrophages: implications for activation of programmed cells. *Proc. Natl. Acad. Sci. U.S.A.*, **75**: 3400-3404.
- 38 Bar-Shavitt, Z., Stabinsky, Y., Fridkin, M. and Goldman, R. (1979) Tuftsin-macrophage interaction: specific binding and augmentation of phagocytosis. *J. Cell. Physiol.*, **100**: 55-62.
- 39 Nishioka, K., Amoscato, A. A. and Babcock, G. F. (1981) Tuftsin: a hormone-like tetrapeptide with antimicrobial and antitumor activities. *Life Sciences*, **28**: 1081-1090.
- 40 Fridkin, M. and Gottlieb, P. (1981) Tuftsin, Thr-Lys-Pro-Arg. *Mol. Cell. Biochem.*, **41**: 73-97.
- 41 Gottlieb, P., Tzeheval, E., Feldman, M., Segal, S. and Fridkin, M. (1983) Peptide fragments from the tuftsin containing domain of immunoglobulin G synthesis and biological activity. *Biochem. Biophys. Res. Commun.*, **115**: 193-200.
- 42 Fauve, R. M., Hevin, B., Jacob, H., Gaillard, J. A. and Jacob, F. (1974) Anti-inflammatory effects of murine malignant cells. *Proc. Natl. Acad. Sci. U.S.A.*, **71**: 4052-4056.
- 43 Fauve, R. M. (1964) Resistance cellulaire à l'infection bacterienne. *Ann. Inst. Pasteur*, **107**: 472-483.
- 44 Stossel, T. P. and Hartwig, J. H. (1976) Interactions of actin, myosin, and a new actin-binding protein of rabbit pulmonary macrophage. *J. Cell Biol.*, **68**: 602-612.
- 45 Yin, H. L. and Stossel, T. P. (1979) Control of cytoplasmic actin gel-sol transformation by gelsolin, a calcium dependent regulatory protein. *Nature (Lond.)*, **281**: 583-586.
- 46 Stossel, T. P., Hartwig, J. H., Yin, H. C. Davies, W. A. (1979) Actin-binding protein. In "Cell Motility". Ed. by S. Hatano, H. Ishikawa and H. Sato. Univ. Tokyo Press, Tokyo, pp. 189-210.
- 47 Tachi, C. and Tachi, S. (1974) Cellular aspects of ovum implantation and decidualization in the rat. In "Physiology and Genetics of Reproduction", Part B. Ed. by E. M. Coutinho and F. Fuchs. Plenum Press, New York, pp. 263-286.
- 48 Sananes, N., Baulieu, E. E. and Gascogne, C. (1976) Prostaglandin(s) as inductive factor of decidualization in the rat uterus. *Mol. Cell. Endocrinol.*, **6**: 153-158.
- 49 Rankin, J. C., Ledford, B. E., Jonsson, H. T., Jr. and Baggett, B. (1979) Prostaglandins, indomethacin and the decidual cell reaction in the mouse uterus. *Biol. Reprod.*, **20**: 399-404.
- 50 Kennedy, T. G. (1977) Evidence of a role for prostaglandins in the initiation of blastocyst implantation in the rat. *Biol. Reprod.*, **16**: 286-291.
- 51 Kennedy, T. G. (1986) Prostaglandins and uterine sensitization for the decidual cell reaction. *Ann. N. Y. Acad. Sci.*, **476**: 43-48.
- 52 Pakrasi, P. L., Becka, R. and Dey, S. K. (1985) Cyclooxygenase and lipoxygenase pathways in the preimplantation rabbit uterus and blastocyst. *Prostaglandins*, **29**: 481-495.
- 53 Holmes, P. V., Lindenberg, S., Hellberg, P. and Janson, P. O. (1987) Evidence for the involvement of lipoxygenase products during blastocyst implantation in the mouse. (Abstract). Human Reproduction, special issue, Abstracts from the 3rd Meeting of the European Society of Human Reproduction and Embryology, p. 87.
- 54 Malathy, P. V., Cheng, H. C. and Dey, S. K. (1986) Production of leukotrienes and prostaglandins in the rat uterus during peri-implantation period. *Prostaglandins*, **32**: 605-604.
- 55 Tawfik, O. W., Sagrillo, C., Johnson, D. C. and Dey, S. K. (1987) Decidualization in the rat: role of leukotrienes and prostaglandins. *Prostaglandins Leukotrienes and Medicine*, **29**: 221-228.

Note added in proof. The paper cited in the text as C. Tachi & U. Zor in press, has since been published as follows;
 Tachi, C. and Tachi, S. (1989) Effect of calcium ionophore A23187 upon the rate of leukotriene C₄ production and the cellular morphology in highly purified mouse peritoneal macrophages cultured *in vitro*. *Zool. Sci.*, **6**: 251-257.

Effects of Thyroxine on Locomotor Activity and Carbon Dioxide Release in the Toad, *Bufo japonicus*

YOKO TASAKI and SUSUMU ISHII

*Department of Biology, School of Education, Waseda University,
Tokyo 169, Japan*

ABSTRACT—To elucidate a role of thyroxine (T_4) in toad migration during the breeding season, we studied effects of administration of T_4 on locomotor activity and CO_2 release using normal and thyroidectomized adults of both sexes which were captured before hibernation. All the experiments were performed during the breeding season under laboratory conditions. Locomotor activity was estimated by passage of infrared beams in an activity box and CO_2 release was estimated comparing CO_2 contents in inflow air to the activity box and outflow air from the activity box. Locomotor activity was significantly suppressed (to 9%) by T_4 treatment ($10 \mu\text{g/day}$ for 2 weeks) in intact males. T_4 also suppressed CO_2 release in intact males at moving states, while T_4 enhanced CO_2 release at resting states. T_4 had no effect on either locomotor activity or CO_2 release in female toads. Thyroidectomy in males resulted in a 3-fold increase in locomotor activity and T_4 administration suppressed activity in dose-dependent fashion (1 to 100 ng/g BW/day for 3 weeks). Neither thyroidectomy nor T_4 administration had any effect in females. These results suggest that thyroxine can not be the factor which induces breeding migration to the pond in the toad. If the sedative effect of thyroxine is physiological, it is probable that thyroxine initiates the post-breeding inactive stage.

INTRODUCTION

Thyroxine has been shown to play some role in the migration of lower vertebrates as reported in sticklebacks [1], young salmonids [1–4], tiger salamanders [5] and red-spotted newts [6]. Dent [6] provided evidence suggesting that thyroxine initiates the migration of post-breeding adult newts from water to land. One of the other proposed major roles of thyroxine is control of energy metabolism. In adult anurans, thyroid hormone administration stimulated the O_2 consumption of the animal [7–10] and glycogen metabolism in the liver [7, 11, 12].

We surveyed the annual cycles of plasma thyroid hormone levels in the toad, *Bufo japonicus*, and theorized two possible roles of thyroid hormone in the toad in winter and early spring [13]. They are initiation of migratory movement to and/or from the pond and regulation of energy metabolism at low temperatures during the breeding season.

In the present experiment, we observed effects of administration of thyroxine on locomotor activity and CO_2 release to examine a relation between circulating thyroxine and breeding migration.

MATERIALS AND METHODS

Material

Adult male and female toads (*Bufo japonicus*) were captured in the suburbs of Tokyo in October and November, 1984 (Experiment I) and 1986 (Experiment II). The mean of their body weights and standard error was $203.8 \pm 9.5 \text{ g}$ in Exp. I, and $127.4 \pm 6.2 \text{ g}$ in Exp. II. Males and females were put in separate plastic boxes ($55 \times 40 \times 43 \text{ cm}$) with loose fitting tops and kept outdoors. Wet pieces of plastic sponge were put in the boxes with the toads to maintain humidity. No feeding took place, since toads abstain from food during winter and spring.

Design of Experiment I

Seven females and nine males were used. Ten μg of L-thyroxine (SIGMA) suspended in saline

was injected daily for two weeks into the dorsal lymphsacs of four males and four females. The remaining three females and five males received injections of saline alone and served as controls. All the injections were performed between 0900 and 1100 hr. Locomotor activity and CO_2 release were measured for 18 hr from 1500 to 0900 hr the next morning during the period between March 3rd and 28th, 1985.

Design of Experiment II

Twenty-nine female and twenty-four male toads were used. Twenty-three females and nineteen males were thyroidectomized under anesthetization with MS-222 two weeks before the start of thyroxine treatments. A part of the hyoid cartilage was also removed with the thyroid. The remaining six females and five males were sham-operated. The thyroidectomized females were divided into four groups of 5, 6, 6, and 6, and received daily injections of 0, 0.001, 0.01, and $0.1 \mu\text{g/g}$ body weight/day of L-thyroxine in 0.1 ml of saline, into the dorsal lymphsac. The injections were performed once a day between 1000 and 1200 hr for three weeks until the day before the locomotor activity measurement. Thyroidectomized males were also divided into four groups of 5, 5, 4, and 5, and received the same injections as females. Locomotor activity of each toad was measured for 20 hr from 1200 to 0800 hr the next morning during the period between February 9th and March 2nd, 1987.

Recording of locomotor activity and CO_2 release in Experiment I

A small plastic chamber, 42 cm long, 20 cm wide and 15 cm deep (Fig. 1) was used to measure both the locomotor activity and CO_2 release of a toad simultaneously and automatically. Each toad was kept in the chamber for 21 hr (1200 to 0900 hr the next morning). After an initial three-hour acclimation, the locomotor activity and CO_2 release were continuously recorded for 18 hr. The temperature of the chamber was regulated at $10 \pm 1^\circ\text{C}$. The chamber was illuminated from 0600 to 1800 hr, and kept in darkness the remaining hours. To quantify the locomotor activity of the toad in the chamber, seven pairs of photosensor units

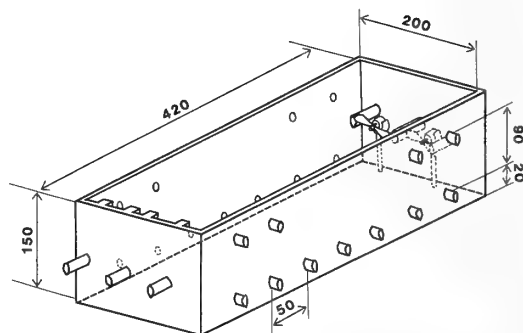


Fig. 1. The chamber used in Experiment I in order to record both the locomotor activity and the CO_2 release of a toad simultaneously and automatically. See text for details.

were mounted on the longitudinal side walls of the chamber at 5 cm intervals, 2 cm from the floor (Fig. 1). Each photosensor unit consisted of an infrared LED lamp (TLN 110, Toshiba) and a photodiode (TPS 703A, Toshiba). Interruption of the infrared light was recorded for each photosensor unit separately at 5 second intervals, and the records were stored in the memory of an 8 bit personal computer (NEC PC-8001, Fig. 2). Thus, the longitudinal position of the toad was recorded every 5 sec with the precision of ± 2.5 cm. At the end of each experiment, data in the memory were transferred to a floppy disk. The total distance of locomotion was calculated later by the same computer.

Carbon dioxide released from a toad placed in the chamber was quantified as follows. The inflow air tube was divided into three parts and had 1.0 cm openings on the wall of one of the longitudinal ends of the chamber. The outflow air tube was connected similarly to the openings on the wall of the other end. Inflow air, which had been collected from the outdoors and stored in a balloon, was pumped into the chamber at the flow rate of 5.0 l per min. It was humidified by being passed through a water filter inserted between the balloon and the chamber. Air in the chamber was circulated by two small, slowly-rotating electric fans (RF-510T, Mabuchi) which were installed on a wall of the chamber (Fig. 1). The outflow air was channeled into an open-flow infrared gas analyzer (VIA-300, Horiba), and the CO_2 concentration was determined (Fig. 2). At the same time, part of

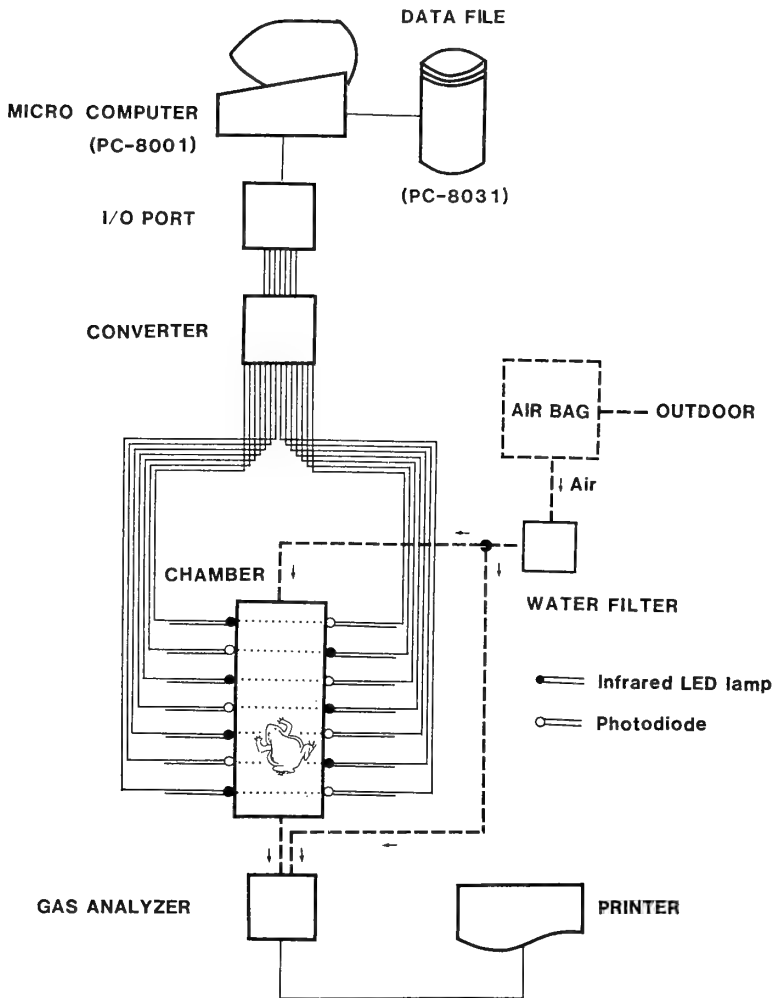


FIG. 2. Diagram showing the recording system in Experiment I.

the inflow air was introduced into the analyzer through a bypass, and its CO_2 concentration was also determined. From the difference in CO_2 concentration between the inflow and outflow air and the flow rate, the release of CO_2 from the toad was calculated. The mean CO_2 release when the toad stayed immobile at least one hour was referred to as the basal CO_2 release (Fig. 5). The mean difference between the active phase CO_2 release, which is the CO_2 release when the toad is moving, and the basal CO_2 release was referred to the activated CO_2 release (Fig. 5). The activated CO_2 release can be regarded as the rise in CO_2 release caused by locomotion.

Recording of locomotor activity in Experiment II

In this experiment, only the locomotor activity was measured. The chamber used had dimensions of $30 \times 30 \times 15$ cm (Fig. 3). The position of the toad in the chamber was recorded two-dimensionally by eight photosensor units. Each of the four walls was mounted with two infrared LED lamps and two photodiodes which were arranged reciprocally at 6 cm intervals. Their height from the floor was 2 cm on two opposing walls, and 4 cm on the other two. The air temperature and humidity of the chamber were regulated at $9.3 \pm 0.7^\circ\text{C}$ and $54 \pm 3\%$, respectively. The chamber was illuminated

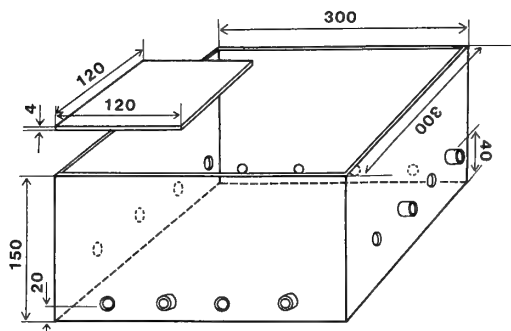


FIG. 3. The chamber used for recording the locomotor activity of a toad in Experiment II. The position of the toad in the chamber is recorded two dimensionally. See text for details.

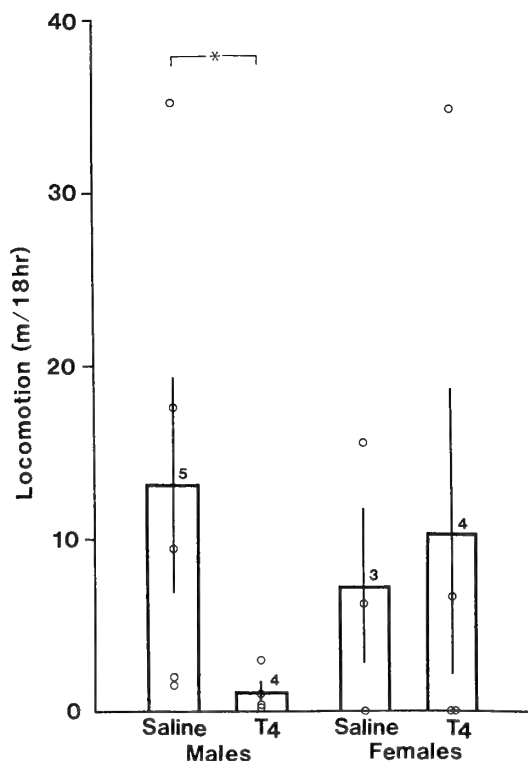


FIG. 4. Total locomotion distances (open circles) of thyroxine and saline-injected normal toads of both sexes for 18 hr. The column and vertical bar indicate the mean and standard error of each group, respectively. The mean of the thyroxine injected male group is significantly lower than that of the control group. No significant difference was observed between the female groups ($p > 0.05$) when given the randomization test (* $p = 0.0317$ by the randomization test).

from 0630 to 1730 hr, and kept in darkness the remaining hours. Data were recorded and analyzed as in Experiment I.

Statistical methods The significant difference between the means of the two groups was determined by the randomization test in Experiment I. The one-way matrix analysis of variance followed by Duncan's multiple range test was used in Experiment II. For these tests, computer programs [14] were employed.

RESULTS

Experiment I

The locomotor activity (total distance of

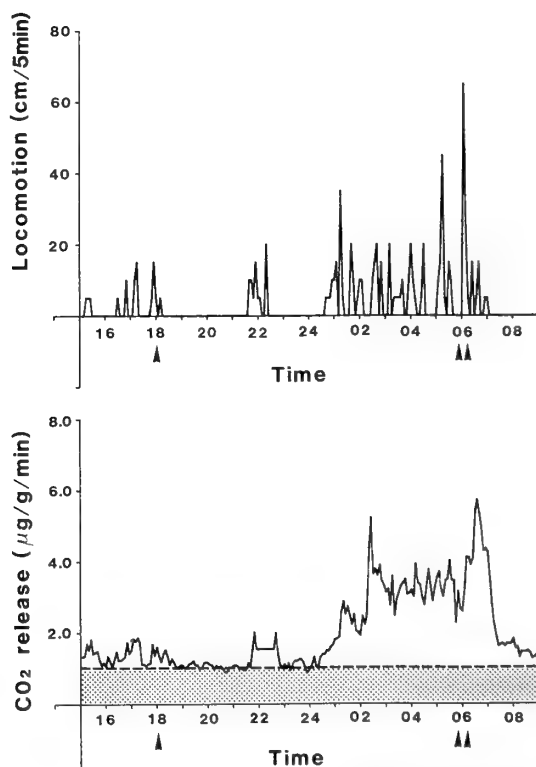


FIG. 5. Record of the locomotion distance (upper) and CO_2 release (lower) of a thyroxine-injected female toad (a typical case). Lights were turned on at 0600 hr (double arrow heads) and off at 1800 hr (single arrow head). Note that the CO_2 release is synchronized with the locomotion. In the lower figure, the dotted area corresponds to the basal CO_2 release and the area above the dotted line corresponds to the activated CO_2 release.

locomotion) of toads varied individually over a wide range (Fig. 4). Treatment with thyroxine seemed to have no effect on the mean locomotor activity of female toads, as the difference between the means of the control and treated groups (7.22 ± 4.52 m and 10.36 ± 8.28 m, respectively) was not significant ($p > 0.05$). However, in males, thyroxine suppressed activity, as the difference between the means of the control and treated groups (13.16 ± 6.24 m and 1.14 ± 1.61 m, respectively) was significant ($p < 0.05$).

The change in CO_2 release faithfully coincided with changes in locomotor activity (Fig. 5). In females, there was no significant difference between activated CO_2 release of the control (377 ± 277 ng/g B.W./min) and treated (259 ± 170 ng/g B.W./min) groups (Fig. 6). In males, the activated

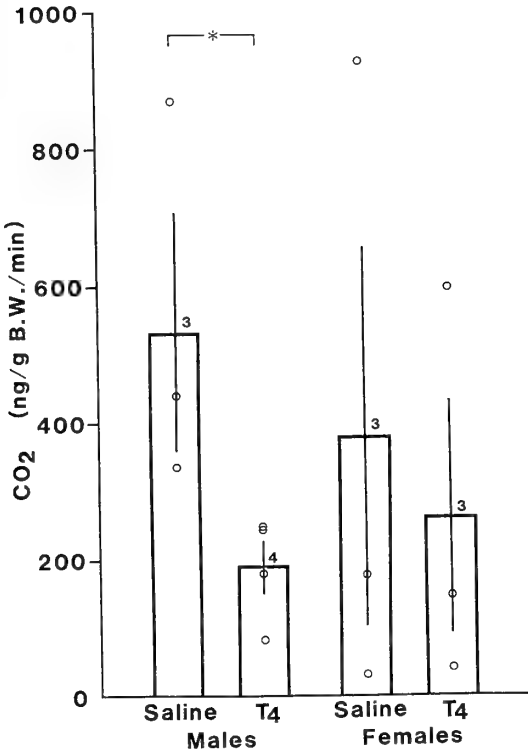


FIG. 6. The activated CO_2 release (open circles) of male and female toads. The column and vertical bar indicate the mean and standard error of each group, respectively. The mean of the thyroxine-injected male group is significantly lower than that of the control group ($*p = 0.0286$ by the randomization test).

CO_2 release in the control and treated groups was 532 ± 175 ng/g B.W./min and 188 ± 39 ng/g B.W./min, respectively, and the difference was significant ($p < 0.05$, Fig. 6).

The basal CO_2 release was higher in females than in males. In females, it was not significantly changed by thyroxine treatment (Fig. 7). In males, however, the basal CO_2 release was significantly increased by thyroxine treatment, up to or over the levels of female toads ($p < 0.05$, Fig. 7).

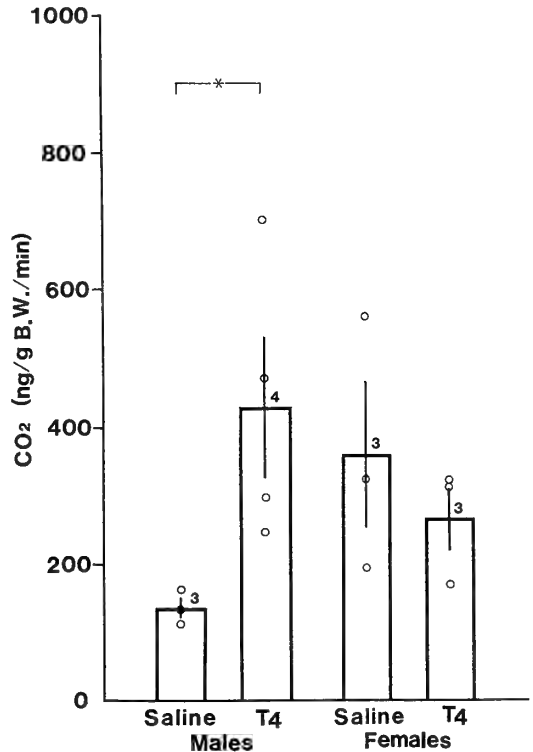
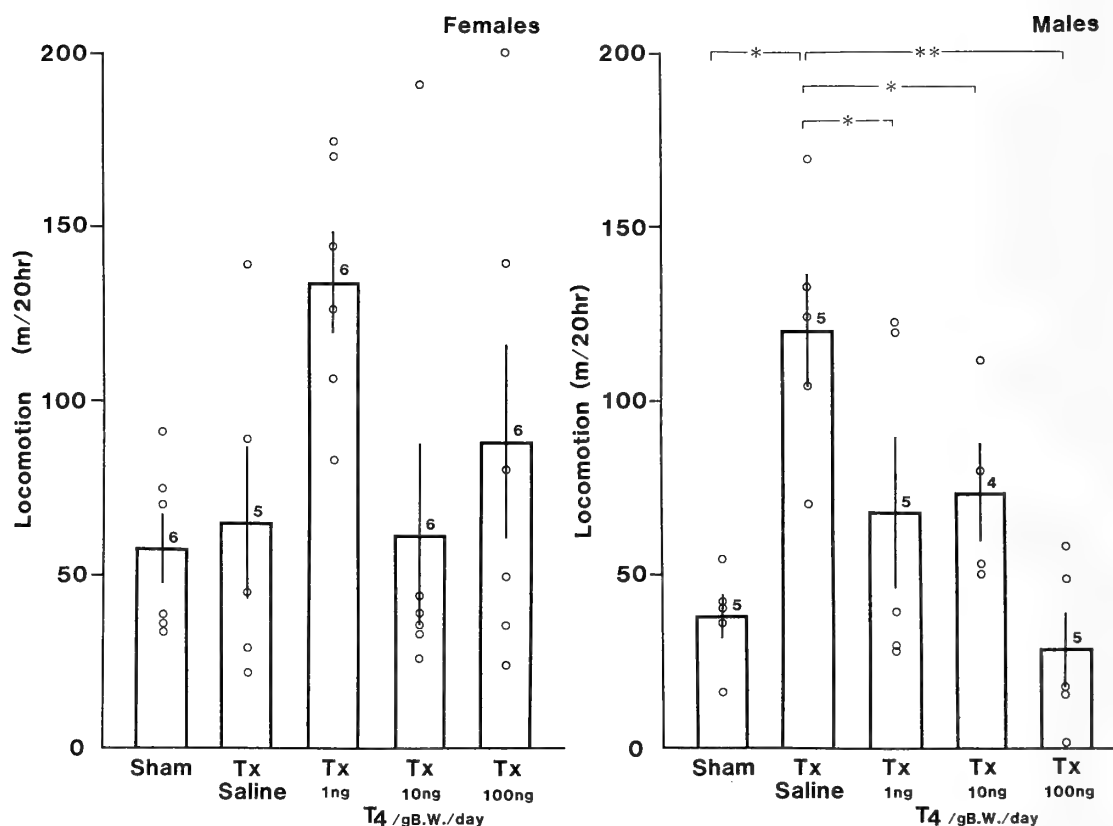


FIG. 7. The basal CO_2 release of male and female toads. The column and vertical bar indicate the mean and standard error of each group, respectively. The mean of the thyroxine-injected male group was significantly higher than that of its control group ($*p = 0.0286$ by the randomization test).

Experiment II

In females, neither thyroidectomy nor thyroxine administrations seemed to influence locomotor activity, as the difference in mean activity among the five groups was not significant when tested by analysis of variance ($p > 0.05$, Fig. 8). The group



FIGS. 8 and 9. Total locomotion distances (open circles) of sham-operated, thyroidectomized, and thyroidectomized and thyroxine-treated female (Fig. 8, Left) and male (Fig. 9, Right) toads. The column and vertical bar indicate the mean and standard error of each group, respectively. Thyroidectomized males showed a significantly higher ($p < 0.01$ when given Duncan's multiple range test) locomotor activity than the shamoperated males. Replacement therapy suppressed the activity significantly ($p < 0.01$ for the highest dose and $p < 0.05$ for the lowest and middle doses when given Duncan's multiple range test).

receiving the lowest doses of thyroxine had a higher mean activity level than the other groups, but this could be within the range of random fluctuation.

In contrast to females, thyroidectomized males showed significantly higher ($p < 0.01$ by Duncan's multiple range test) locomotor activity than the sham-operated males, increase being about three-fold (Fig. 9). Replacement therapy suppressed the activity to some extent or even to a subnormal level depending upon the dose levels.

DISCUSSION

It is well known that prolactin is a factor which induces migration of newts and salamanders from

land to water for breeding [15–20]. Recently however, Yoneyama *et al.* [21], Ishii *et al.* [22] and Yamamoto *et al.* [23] presented evidence showing that prolactin can not be the factor inducing migration to the breeding pond, at least in *Bufo*. Our survey of the annual cycle of plasma thyroid hormone levels in the toad, *Bufo japonicus*, revealed that the plasma thyroxine level increased gradually during the inactive winter period and reached a relatively high level at the commencement of the breeding migration. From this observation, we previously postulated that thyroxine, instead of prolactin, is the factor which induces breeding migration. However, in the present study, we found that both endogenous and

exogenous thyroxine suppressed the locomotor activity of male toads in spring, but we failed to show that effect in female toads. In either case, it is difficult to suggest that thyroxine is a suitable candidate for the migration inducing factor in the toad.

Dent [6] proposed the hypothesis that thyroxine causes the movement of terrestrial species of amphibians from water to land after breeding. Our recent finding [13] that the plasma thyroid hormone level in the toad is remarkably elevated when they arrive at the breeding pond strongly supports Dent's hypothesis. However, our present finding showing the sedative effect of thyroxine on locomotor activity is neutral to or may contradict Dent's hypothesis. This effect of thyroxine can however, explain the commencement of the post-breeding inactive period of the toad which lasts until May or June. Recently, Kubokawa and Ishii [24], surveying the annual cycle of various endocrine and metabolic parameters of the toad, pointed out that among various hormones, only thyroxine is secreted in the post-breeding inactive period. Further study is needed to elucidate the hormonal mechanism controlling the migration of toads to and from the breeding pond.

From many years past, it has been repeatedly reported that thyroxine stimulates O_2 consumption in whole animals [7, 8, 25] or liver slices in amphibians [9, 10, 26] as well as in higher vertebrates. In the present study, we observed that the basal CO_2 release in the male toad was elevated by thyroxine injection. This result coincides well with previous reports on O_2 consumption [7-9, 24, 25]. In contrast, the activated CO_2 release in the thyroxine-treated male toad was lower than in the normal male toad. This may be due to decreased intensity of locomotor activity caused by thyroxine.

The basal CO_2 release reflects the basal metabolism. Accordingly, our results on basal CO_2 release suggest that the enhancement of basal metabolism by thyroxine is accompanied by a decrease of muscular activity in male toads. This reminds us of the old work that thyroxine leads to the uncoupling of oxidative phosphorylation [27], although this effect was shown to be nonphysiological [28].

ACKNOWLEDGMENTS

The authors are grateful to Prof. Yasuyuki Oshima for his valuable advice and suggestions and to Mr. Taroh Ishii, Mitsubishi Kasei Co. Ltd for his assistance in designing the recording system. This study was supported by a Grant-in-Aid from the Japanese Ministry of Education, Science and Culture.

REFERENCES

- 1 Baggerman, B. (1962) Some endocrine aspects of fish migration. *Gen. Comp. Endocrinol. Suppl.*, **1**: 188-205.
- 2 Baggerman, B. (1963) The effect of TSH and antithyroid substances on salinity preference and thyroid activity in juvenile Pacific salmon. *Can. J. Zool.*, **41**: 307-319.
- 3 Nishioka, R. S., Young, G., Bern, H. A., Jochimsen, W., and Hiser, C. (1985) Attempts to intensify the thyroxin surge in coho and king salmon by chemical stimulation. *Aquaculture*, **45**: 215-225.
- 4 Yamauchi, K., Ban, M., Kasahara, N., Izumi, T., Kojima, H., and Harako, T. (1985) Physiological and behavioral changes occurring during smoltification in the masu salmon, *Oncorhynchus masou*. *Aquaculture*, **45**: 227-235.
- 5 Norris, D. O., Duvall, D., Greendale, K., and Gern, W. A. (1977) Thyroid function in pre- and postspawning neotenic tiger salamanders (*Ambystoma tigrinum*). *Gen. Comp. Endocrinol.*, **33**: 512-517.
- 6 Dent, J. N. (1985) Hormonal interaction in the regulation of migratory movements in urodele amphibians. "The endocrine system and the environment", ed. B.K. Follet, S. Ishii, and A. Chandola, Japan Sci. Soc. Press. Tokyo/Springer-Verlag, Berlin. pp. 79-84.
- 7 Warren, M. R. (1940) Studies on the effect of experimental hyperthyroidism on the adult frog, *Rana pipiens*, Schreber. *J. Exp. Zool.*, **83**: 127-159.
- 8 Maher, M. J. (1967) Response to thyroxine as a function of environmental temperature in the toad, *Bufo woodhousii*, and the frog, *Rana pipiens*. *Copeia*, **2**: 361-365.
- 9 Packard, G. C., Packard, M. J., and Stiverson, R. K. (1974) The influence of thyroxine on oxygen consumption of tissues from the frog *Rana pipiens*. *Gen. Comp. Endocrinol.*, **22**: 195-198.
- 10 Packard, G. C. and Packard, M. J. (1975) The influence of acclimation temperature on the metabolic response of frog tissue to thyroxine administered *in vivo*. *Gen Comp. Endocrinol.*, **27**: 162-168.
- 11 Lagerspetz, K. Y. H., Harri, M. N. E., and Oklahti, R. (1974) The role of the thyroid in the temperature acclimation of the oxidative metabo-

- lism in the frog, *Rana temporaria*. Gen. Comp. Endocrinol., **22**: 169–176.
- 12 Kasprzyk, A. and Obuchowicz, L. (1980) The effect of thyroxine and triiodothyronine on glucose-6-phosphate and 6-phosphogluconate dehydrogenase activity in liver and fat body of the frog, *Rana esculenta*. Gen. Comp. Endocrinol., **42**: 384–388.
- 13 Tasaki, Y., Inoue, M., and Ishii, S. (1986) Annual cycle of plasma thyroid hormone levels in the toad, *Bufo japonicus*. Gen. Comp. Endocrinol., **62**: 404–410.
- 14 Ishii, S. (1983) "Programs of statistical methods for biologists by N88-BASIC." Baifukan, Tokyo.
- 15 Reinke, E. E. and Chadwick, C. S. (1940) The origin of the water drive in *Triturus viridescens*. J. Exp. Zool., **83**: 223–233.
- 16 Chadwick, C. S. (1944) Further observations on the water drive in *Triturus viridescens*. J. Exp. Zool., **86**: 175–187.
- 17 Crim, J. W. (1975) Prolactin-induced modification of visual pigments in the eastern red-spotted newt, *Notophthalmus viridescens*. Gen. Comp. Endocrinol., **26**: 233–242.
- 18 Duvall, D. and Norris, D. O. (1977) Prolactin and substrate stimulation of locomotor activity in adult tiger salamanders (*Ambystoma tigrinum*). J. Exp. Zool., **200**: 103–106.
- 19 Duvall, D. and Norris, D. O. (1980) Stimulation of terrestrial substrate preferences and locomotor activity in newly transformed tiger salamanders (*Ambystoma tigrinum*) by exogenous or endogenous thyroxine. Anim. Behav., **28**: 116–123.
- 20 Moriya, T. (1982) Prolactin induces increase in the specific gravity of salamander, *Hynobius retardatus*, that raises adaptability to water. J. Exp. Zool., **223**: 83–88.
- 21 Yoneyama, H., Ishii, S., Yamamoto, K. and Kikuyama, S. (1984) Plasma prolactin levels of *Bufo japonicus* before, during and after breeding in the pond. Zool. Sci., **1**: 969.
- 22 Ishii, S., Yoneyama, H., Inoue, M., Yamamoto, K., and Kikuyama, S. (1989) Changes in plasma and pituitary levels of prolactin in the toad, *Bufo japonicus*, throughout the year with special reference to the breeding migration. Gen. Comp. Endocrinol., **74**: 365–372.
- 23 Yamamoto, K., Kikuyama, S., and Ishii, S. (1989) Homologous radioimmunoassay for plasma and pituitary prolactin in the toad, *Bufo japonicus* Gen. Comp. Endocrinol., **74**: 373–376.
- 24 Kubokawa, K. and Ishii, S. (1989) Annual cycles in various hormones in the toad, *Bufo japonicus*. Proceedings of the Japan Society for Comparative Endocrinology, No. 3 (In press)
- 25 May, T. W. and Packer, R. K. (1976) Thyroid hormones stimulate *in vivo* oxygen consumption of adult *Rana pipiens berlandieri* at high environmental temperatures. Gen. Comp. Endocrinol., **30**: 525–527.
- 26 Packard, G. C. and Packard, M. J. (1973) Preliminary study of the influence of thyroxine, temperature, and sex on oxygen uptake by tissues from the spadefoot toad *Scaphiopus bombifrons*. Gen. Comp. Endocrinol., **20**: 530–533.
- 27 Martius, C. and Hess, B. (1951) The mode of action of thyroxine. Arch. Biochem. Biophys., **33**: 486–487.
- 28 Tata, J. R., Ernster, L., Lindberg, O., Arrhenius, E., Pedersen, S., and Hedman, R. (1963) The action of thyroid hormones at the cell level. Biochem. J., **86**: 408–428.

Intragranular Colocalization of Arginine Vasopressin- and Angiotensin II-Like Immunoreactivity in the Hypothalamo-Neurohypophysial System of the Goldfish, *Carassius auratus*

CHIFUMI YAMADA¹, SHINOBU NOJI^{2,3}, SEIJI SHIODA⁴,
YASUMITSU NAKAI⁴ and HIDESHI KOBAYASHI

Research Laboratory, Zenyaku Kogyo Co., Ltd., Tokyo 178, ²Department of Biology, Faculty of Science, Toho University, Chiba 274, ⁴Department of Anatomy, Showa University School of Medicine, Tokyo 142, Japan

ABSTRACT—In the preoptic nucleus (PON) of the goldfish, *Carassius auratus*, four types of cells were observed under a light microscope: cells showing colocalization of immunoreactive angiotensin II (ANG II) and immunoreactive arginine vasopressin (AVP), cells with only ANG II-like immunoreactivity, cells with only AVP-like immunoreactivity and cells with neither immunoreactivity. Under an electron microscope, only two types of nerve terminals were found in the neurohypophysis: those showing immunoreactivity of both antisera and those with neither immunoreactivity. No terminals showing alternative immunoreactivity could be found. The discrepancy in these findings obtained by light and electron microscopes is discussed. In nerve terminals reactive to both antisera, an immunogold technique indicated the presence of neurosecretory granules with colocalization of immunoreactive ANG II and AVP, granules with only ANG II-like immunoreactivity and granules showing only AVP-like immunoreactivity. The AVP-like immunoreactivity observed in the PON and the neurohypophysis is considered due to arginine vasotocin.

INTRODUCTION

A renin-angiotensin system in the brain has been demonstrated biochemically and pharmacologically in mammals [1]. Immunohistochemically, angiotensin II (ANG II) and arginine vasopressin (AVP) have been shown to be present in the same neurons of the supraoptic, paraventricular and suprachiasmatic nuclei of the rat [2–4]. However, intragranular colocalization of these peptides in these neurons has not been studied.

In the present study, the colocalization of immunoreactive ANG II and immunoreactive AVP was examined in neurosecretory cells of the preop-

tic nucleus (PON) of the goldfish, *Carassius auratus*. Further, intragranular colocalization of these substances was electron microscopically examined in axon terminals in the neurohypophysis.

MATERIALS AND METHODS

Antisera

The following antisera were used for light microscopy. Antiserum to ANG II was raised in rabbit against synthetic Asp¹-Ileu⁵-ANG II (Protein Research Foundation, Osaka) by Yamaguchi [5]. The complete cross-reactivities of this antiserum with Asp¹-Val⁵-ANG II [5] and Asn¹-Val⁵-ANG II (unpublished data) were demonstrated by radioimmunoassay. Antiserum to arginine AVP was raised in rabbit against synthetic AVP (Protein Research Foundation, Osaka) and cross-reacted with arginine vasotocin (AVT) at 42% and with

Accepted May 11, 1989

Received April 27, 1989

¹ Present address: Department of Physiology, National Defense Medical College, Tokorozawa 359, Japan

³ Present address: Department of Clinical Laboratories, Keio University Hospital, Tokyo 160, Japan

oxytocin (OXT) at only 3.5% [6].

For electron microscopy, the ANG II antiserum was the same as that used for the light microscopic experiment. AVP antiserum raised against synthetic AVP in rabbit (UCB Bioproducts, Belgium) and having complete cross-reactivity with AVT and less than 0.003% cross reactivity with oxytocin or mesotocin was used.

Light microscopy

Twenty five goldfish, *Carassius auratus* (about 10 cm in total length) were obtained commercially. After decapitation, brains with the pituitary or brains alone were quickly removed and fixed in Bouin's solution overnight. Tissue was dehydrated through a series of ethanol, cleared in xylol and embedded in paraffin. Four μm thick sagittal sections were made and mounted on slides. To examine the colocalization of immunoreactive ANG II and AVP, two consecutive sections were immunostained, one with ANG II and the other with AVP antiserum.

Deparaffinized preparations were immunostained by the peroxidase-anti-peroxidase (PAP) method of Sternberger *et al.* [7]. Incubation was performed as follows: (1) in 0.3% H_2O_2 for 30 min at room temperature (RT), (2) in ANG II antiserum (1:1000) or AVP antiserum (1:2000) overnight at 4°C, (3) in goat anti-rabbit IgG (GAR; Polysciences Inc., Warrington, Pennsylvania; 1:200) for 90 min at RT, (4) in peroxidase-anti-peroxidase (PAP; Dako Corp., Copenhagen or Cappel Laboratories, West Chester, Pennsylvania; 1:200) for 90 min at RT, and (5) in 0.02% 3,3'-diaminobenzidine in 0.05 M Tris buffer (pH 7.6) containing 0.006% H_2O_2 for 10–15 min at RT. To rinse the preparations and dilute the antisera, 0.1 M phosphate buffer saline (pH 7.2) containing 0.3% Triton X-100 was used.

For the control, immunostaining was conducted using the following sera instead of the primary antisera: normal rabbit serum (NRS; Polysciences Inc., Warrington, Pennsylvania; 1:1600), ANG II antiserum preabsorbed with Asn¹-Val⁵-ANG II (Hypertensin, Ciba; 20, 100 $\mu\text{g}/\text{ml}$ diluted antiserum), ANG II antiserum preabsorbed with AVT (Protein Research Foundation, Osaka; 20 $\mu\text{g}/\text{ml}$ diluted antiserum), AVP antiserum preabsorbed

with Asn¹-Val⁵-ANG II (20 $\mu\text{g}/\text{ml}$ diluted antiserum), the primary antisera preincubated with 1% bovine serum albumin (BSA) and AVP antiserum preabsorbed with AVT (20, 100 $\mu\text{g}/\text{ml}$ diluted antiserum). AVP antiserum was preabsorbed with AVT but not AVP, since, as is well known, neurosecretory cells produce AVT but not AVP in teleosts.

Electron microscopy

Ten goldfish (each about 8 cm in total length) were obtained from a commercial source. They were anesthetized with 0.01% ethyl m-aminobenzoate methanesulfonate (MS222) and perfused with a mixture of paraformaldehyde (4%) and glutaraldehyde (0.4%) in 0.05 M phosphate buffer (PB; pH 7.2). The pituitary of each specimen was removed and fixed in the same fixative for 2–3 hr at 4°C. This was followed by rinsing in 0.1 M Millonig PB and postfixation in 2% OsO_4 in 0.1 M Millonig PB for 1.5 hr at 4°C. All tissue was subsequently dehydrated through a series of ethanol, transferred to propylene oxide and embedded in an Epon-Araldite mixture. Ultrathin sections were cut and mounted on 200-mesh nickel grids.

Ultrathin sections were stained by a double immunogold technique. First, one face of a section was incubated in (1) saturated sodium metaperiodate for 30 min at RT, (2) 1% egg albumin in 0.01 M PBS (pH 7.2) for 10 min at RT, (3) AVP antiserum (1:16000) overnight at 4°C, and (4) colloidal gold labeled GAR (1:20; gold particles of about 5 nm in diameter) for 90 min at RT. Next, another face was incubated in the same way, but immunostained with ANG II antiserum (1:1000) overnight at 4°C, and colloidal gold labeled GAR (1:10; gold particles of about 15 nm in diameter) for 90 min at RT. Immunostained sections were stained further with both uranyl acetate and lead citrate, and examined with Hitachi HS-9 and HU-12A electron microscopes.

For the control, ANG II antiserum preabsorbed with either Asn¹-Val⁵-ANG II or AVT (each 10 $\mu\text{g}/\text{ml}$ diluted antiserum), and AVP antiserum preabsorbed with AVT, ANG II or isotocin (Protein Research Foundation, Osaka) (each 10 $\mu\text{g}/\text{ml}$ diluted antiserum) were used as primary antisera.

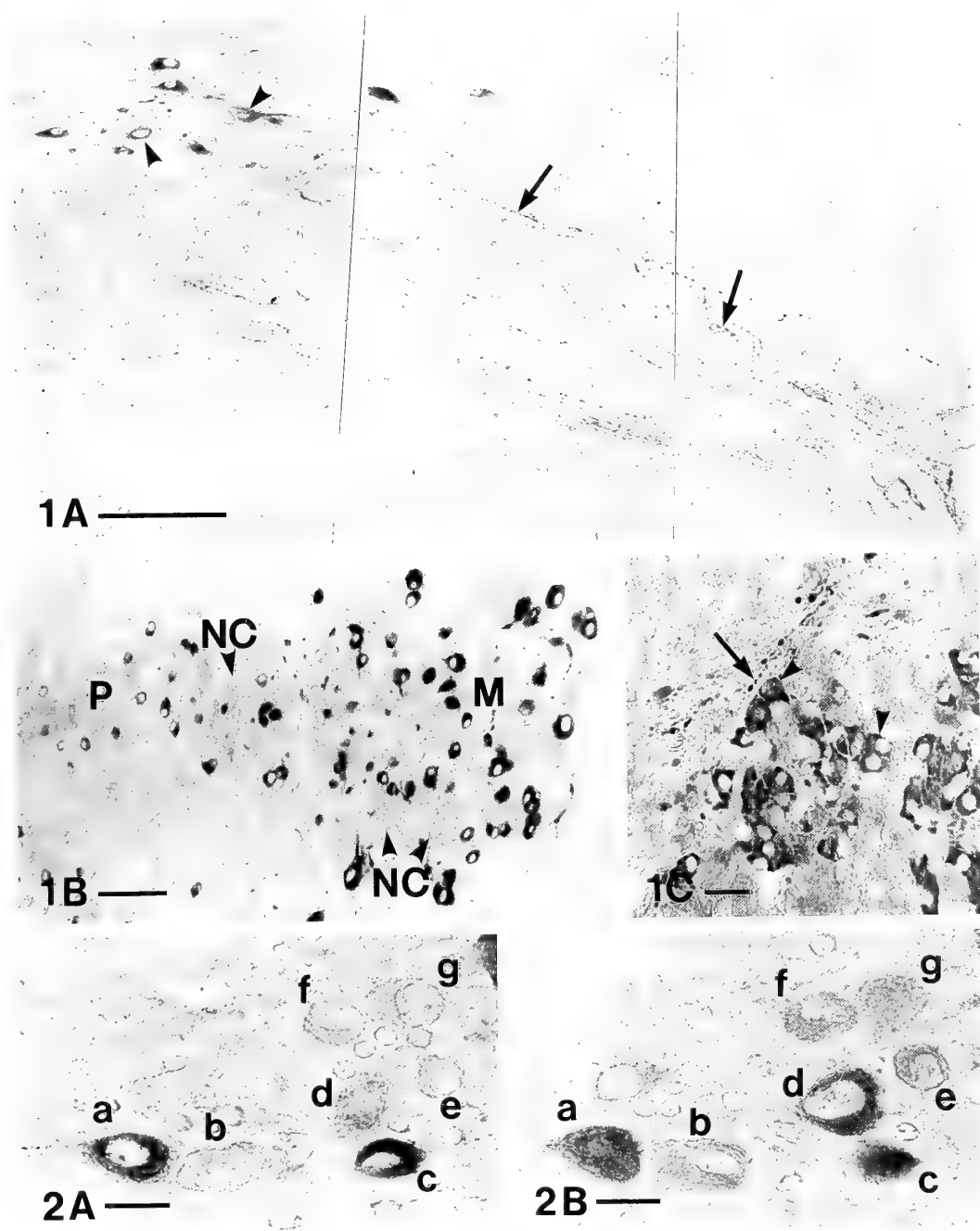


FIG. 1. A: ANG II-like immunoreactive cells in the PON (arrow-heads) and their fibers (arrows) extending to the neurohypophysis in the hypothalamus of the goldfish, *Carassius auratus*. Bar=100 μ m. B: ANG II-like immunoreactive cells in magnocellular (M) and parvocellular groups (P) of the PON. In both groups, many non-immunoreactive cells (NC) were found. Bar=50 μ m. C: ANG II-like immunoreactive cells (arrowheads) in the pars distalis and immunoreactive fibers (arrow) extending to the pars distalis from the PON. Reaction of fibers to ANG II antiserum was abolished by preabsorption of the serum with ANG II, but not that of the cells. Bar=20 μ m.

FIG. 2. Two consecutive sections of a PON region of the goldfish. Immunostaining with ANG II (A) and AVP (B) antisera. Cells a, c and d were reactive to both antisera; cells b, e, f and g were reactive only to AVP antiserum. Bar=20 μ m.

RESULTS

Light microscopy

ANG II and AVP antisera, preabsorbed with synthetic ANG II and AVT, respectively, showed no indication of immunoreaction. However, ANG II immunoreaction in the cells of the pars distalis was not abolished by ANG II antiserum preabsorbed with ANG II. Immunoreaction of these cells is considered nonspecific. Immunostaining by NRS also failed to indicate immunoreaction. Other control sera used did not abolish immunoreactions. Immunoreaction to ANG II antiserum in the brain may thus be considered specific

to ANG II and the immunoreaction to AVP antiserum observed in the brain is considered due not to AVP but to AVT. That teleostean neurosecretory neurons produce AVT but not AVP supports these considerations.

Immunoreactivity to ANG II antiserum was observed in the cells of the magnocellular and parvocellular groups of the preoptic nucleus (PON) (Figs. 1A, B, 2A) as well as to AVP antiserum (Fig. 2B). The colocalization of ANG II- and AVP-like immunoreactivity was evident in many neurons (Fig. 2). Certain neurons possessed only AVP-like immunoreactivity (Fig. 2), while others, only ANG II-like immunoreactivity; the number of the latter was very small. Neurons

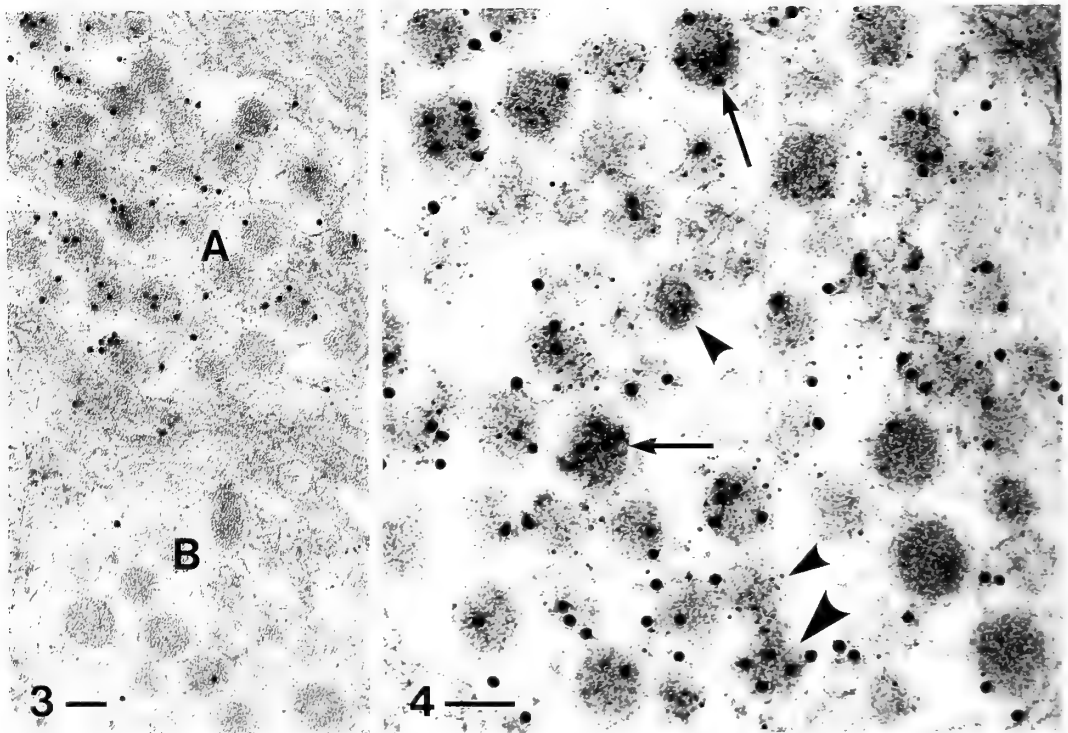


FIG. 3. Ultrastructural localization of ANG II- and AVP-like immunoreactivity in the neurohypophysis of a goldfish. Large colloidal gold particles (diameter, about 15 nm) and small colloidal gold particles (diameter, about 5 nm) demonstrate ANG II- and AVP-like immunoreactivity, respectively. A nerve terminal (A) contained both immunoreactivities while another, (B), neither. Bar=100 nm.

FIG. 4. Intragranular localization of ANG II- and AVP-like immunoreactivity in the same nerve terminal of the neurohypophysis of a goldfish. Large colloidal gold particles (diameter, about 15 nm) and small colloidal gold particles (diameter, about 5 nm) demonstrate ANG II- and AVP-like immunoreactivity, respectively. In some neurosecretory granules, both immunoreactivities could be detected (arrows). Some granules show only ANG II-like immunoreactivity (large arrowheads) while others, only AVP-like immunoreactivity (small arrowheads). Bar=100 nm.

showing no immunoreaction to either antiserum were also present. The fibers with either ANG II- or AVP-like immunoreactivity extended as far as to the neurohypophysis (Fig. 1A) and pars distalis (Fig. 1C). In the pars distalis, immunoreaction to ANG II antiserum was observed in the cells and fibers (Fig. 1C). The reaction of the fibers in the pars distalis was abolished by ANG II antiserum preabsorbed with ANG II, but that of the cells was not abolished because of its nonspecificity. The cells of the pars intermedia were not stained by either antiserum.

Electron microscopy

In control experiments, immunoreaction was abolished by preabsorption of ANG II and AVP antisera with Asn¹-Val⁵-ANG II and AVT, respectively. Immunoreaction to ANG II antiserum was not abolished by preabsorption of ANG II antiserum with AVT, nor was that to AVP antiserum preabsorbed with ANG II or isotocin.

Electron microscopy indicated a number of granules and synaptic vesicle-like structures to be present in nerve terminals in the neurohypophysis. Two types of axon terminals were observed, those with both ANG II- and AVP-like immunoreactivity and those with neither immunoreactivity (Fig. 3). In the former terminals, the three following kinds of granules (about 80 nm in diameter) were detected: 1) granules showing both ANG II- and AVP-like immunoreactivity, indicated by large and small gold particles, respectively, 2) granules showing only ANG II-like immunoreactivity and 3) granules showing only AVP-like immunoreactivity (Fig. 4). The ratio of these kinds of granules differed for each terminal. Some granules in the terminals with both immunoreactivities showed greater ANG II-like immunoreactivity than AVP-like immunoreactivity or visa versa.

DISCUSSION

In the present study, immunoreaction to AVP antiserum was frequently observed in the cells of the magnocellular and parvocellular groups of the PON and in the neurohypophysis. This reaction may possibly be due to AVT, since the AVP antiserum used in the present experiment was

demonstrated to cross-react with AVT, and also, it is known that one of the neurohypophysial hormones in teleosts is AVT but not AVP. Thus, in the following description, AVT was used instead of AVP.

Most fibers of ANG II-like immunoreactive neurons in the magnocellular and parvocellular groups extended as far as to the neurohypophysis, as in the case of the rat [8, 9]. Some invaded the pars distalis of the adenohypophysis, as well as AVT fibers. It would thus seem that the hypothalamo-hypophysial nervous system of ANG II is present in the goldfish, although its function has yet to be clarified.

The colocalization of ANG II- and AVT-like immunoreactivity was observed in the perikarya of many neurosecretory neurons of the PON. It has also been demonstrated that immunoreactive ANG II and AVP colocalized in the neurons of the paraventricular, supraoptic and suprachiasmatic nuclei in the rat [2, 4]. Further, the intragranular colocalization of immunoreactive ANG II and immunoreactive AVT in some axon terminals of the neurohypophysis was found in the present study. It would appear that both peptides are simultaneously released from these terminals into the capillaries. In the rat, ANG II has been shown to stimulate ACTH release from the adenohypophysis as well as AVP [10] and ANG II and AVP to potentiate the ACTH-releasing activity of corticotropin-releasing factor (CRF) [11 for ANG II, 12 for AVP]. In the goldfish, ANG II and AVT stimulate the release of ACTH [13]. It should thus be reasonable to conclude that ANG II and AVT, following their simultaneous release from the same terminal, may potentiate the ACTH-releasing activity of CRF in this fish.

The colocalization of AVP and CRF in the neurons of the paraventricular nucleus and in the fibers in the median eminence has been reported in mammals [14–17]. In teleosts, this has also been shown in some neurons of the PON [13, 18, 19]. The present authors noted ANG II-, AVT- and CRF-like immunoreactivity in the same neurons in the PON of the goldfish (unpublished data). Thus, ANG II, AVT and CRF may be released simultaneously from the same neurons. These peptides possibly exert a synergistical effect on the release

of ACTH from the adenohypophysis or ANG II and AVT may modulate the release of CRF.

By light microscope, four types of the nerve cells were observed in the PON: 1) cells with both immunoreactive ANG II and AVT, 2) cells with only immunoreactive AVT, 3) cells with only immunoreactive ANG II, and 4) cells without any immunoreaction. By electron microscope, however, only two types of nerve terminals were found in the neurohypophysis: 1) terminals showing immunoreactive ANG II and AVT, and 2) terminals showing no immunoreactivity. The discrepancy with respect to cell type number as determined using these different microscopes may be due to variation in the amount of storage of these peptides in the cell bodies and in the terminals. Immunoreactivity in cells containing the peptides in very small amounts would not be detected by light microscopy, leading to the erroneous conclusion that there are four cell types. However, both light and electron microscopy also indicate the presence of cells and nerve terminals containing neither ANG II- nor AVT-like immunoreactivity. These neurons may contain neuropeptides other than ANG II or AVT.

ACKNOWLEDGMENTS

We are grateful to Dr. Ken-ichi Yamaguchi, Department of Physiology, Niigata University School of Medicine, for kindly providing the ANG II antiserum, and to Professor Seiichiro Kawashima, Zoological Institute, Faculty of Science, University of Tokyo, and Dr. Keiichi Kawamoto, Zoological Institute, Faculty of Science, Hiroshima University, for giving us the AVP antiserum.

REFERENCES

- Printz, P., Ganten, D., Unger, T. and Phillips, M. I. (1982) The brain renin angiotensin system. In "Experimental Brain Research Suppl. 4, The Renin-Angiotensin System in the Brain". Ed. by D. Ganten, M. Printz, M. I. Phillips, and B. A. Scholkens, Springer-Verlag, Berlin Heidelberg New York, pp. 5-52.
- Kilcoyne, M. M., Hoffman, D. L. and Zimmerman, E. A. (1980) Immunocytochemical localization of angiotensin II and vasopressin in rat hypothalamus: evidence for production in the same neuron. *Clinical Sci.*, **59**: 57s-60s.
- Fuxe, K., Ganten, D., Anderson, K., Calza, L., Agnati, L. F., Lang, R. E., Poulsen, K., Hökfelt, T. and Bernardi, P. (1982) Immunocytochemical demonstration of angiotensin II- and renin-like immunoreactive nerve cells in the hypothalamus. Angiotensin peptides as comodulators in vasopressin and oxytocin neurons and their regulation of various types of central catecholamine nerve terminal systems. *Exp. Brain Res., Suppl.*, **4**: 208-232.
- Hoffman, D. L., Krupp, L., Schrag, D., Nilaver, G., Valiquette, G., Kilcoyne, M. M. and Zimmerman, E. A. (1982) Angiotensin immunoreactivity in vasopressin cells in rat hypothalamus and its relative deficiency in homozygous Brattleboro rats. *Ann. New York Acad. Sci.*, **394**: 135-141.
- Yamaguchi, K. (1981) Effect of water deprivation on immunoreactive angiotensin II levels in plasma, cerebroventricular perfusate and hypothalamus of the rat. *Acta Endocrinol.*, **97**: 137-144.
- Kawamoto, K. (1985) Immunohistochemical study of vasopressin and oxytocin in the neurosecretory system during reorganization of the neural lobe in mice. *Zool. Sci.*, **2**: 371-380.
- Sternberger, L. A., Hardy, P. H. Jr., Cuculis, J. J. Jr. and Meyer, H. G. (1970) The unlabeled antibody enzyme method of immunohistochemistry: preparation and properties of soluble antigen-antibody complex (horseradish peroxidase-anti-horseradish peroxidase) and its use in identification of spirochetes. *J. Histochem. Cytochem.*, **18**: 315-333.
- Brownfield, M. S., Reid, I. A., Ganten, D. and Ganong, W. F. (1982) Differential distribution of immunoreactive angiotensin and angiotensin-converting enzyme in rat brain. *Neurosci.*, **7**: 1759-1769.
- Lind, R. W., Swanson, L. W. and Ganten, D. (1985) Organization of angiotensin II immunoreactive cells and fibers in the rat central nervous system. An immunohistochemical study. *Neuroendocrinology*, **40**: 2-24.
- Spinedi, E. and Negro-Vilar, A. (1983) Angiotensin II and ACTH release: site of action and potency relative to corticotropin releasing factor and vasopressin. *Neuroendocrinology*, **37**: 446-453.
- Schoenberg, P., Kehre, P., Muller, A. F. and Gailard, R. C. (1987) Angiotensin II potentiates corticotropin-releasing activity of CRF41 in rat anterior pituitary cells: mechanism of action. *Neuroendocrinology*, **45**: 86-90.
- Gillies, G. E., Linton, E. A. and Lowry, P. J. (1982) Corticotropin releasing activity of the new CRF is potentiated several times by vasopressin. *Nature*, **229**: 355-357.
- Fryer, J. N. (1988) Neuropeptides regulating the secretory activity of goldfish corticotropes and melanotropes. Program and Abstracts, 1st Intern. Symp. on Fish Endocrinology, Univ. of Alberta, Edmonton, Canada, p. 19.

- 14 Tramu, G. Croix, C. and Pillez, C. A. (1983) Ability of the CRF immunoreactive neurons of the paraventricular nucleus to produce a vasopressin-like material. *Neuroendocrinology.*, **37**: 467–469.
- 15 Kiss, J. Z., Mezey, E. and Skirboll, L. (1984) Corticotropin-releasing factor-immunoreactive neurons of the paraventricular nucleus become vasopressin positive after adrenalectomy. *Proc. Natl. Acad. Sci. USA*, **81**: 1854–1858.
- 16 Whitnall, M. H., Mezey, E. and Gainer, H. (1985) Co-localization of corticotropin-releasing factor and vasopressin in median eminence neurosecretory vesicles. *Nature*, **317**: 248–250.
- 17 Hisano, S., Tsuruo, Y., Katoh, S., Daikoku, S., Yanaihara, N. and Shibasaki, T. (1987) Intragranular colocalization of arginine vasopressin and methionine-enkephalin-octapeptide in CRF axons in the rat median eminence. *Cell Tissue Res.*, **249**: 497–507.
- 18 Olivereau, M., Moons, L., Olivereau, J. and Vandesande, F. (1988) Coexistence of corticotropin-releasing factor-like immunoreactivity and vasotocin in perikarya of the preoptic nucleus in the eel. *Gen. Com. Endocrinol.*, **70**: 41–48.
- 19 Yulis, C. R. and Lederis, K. (1987) Co-localization of the immunoreactivities of corticotropin-releasing factor and arginine vasotocin in the brain and pituitary system of the teleost *Catostomus commersoni*. *Cell Tissue Res.*, **247**: 267–273.

Ovarian Development and Sex Steroid Hormones during the Reproductive Cycle of *Rana esculenta* Complex

ALBERTA MARIA POLZONETTI-MAGNI, ROBERTA CURINI¹, OLIANA CARNEVALI,
CLAUDIO NOVARA, MASSIMO ZERANI and ANNA GOBBETTI

*Dipartimento di Biologia Cellulare, Università di Camerino,
Via Camerini 1, 62032 Camerino, and ¹Dipartimento
di Scienze Chimiche, Università di Camerino,
Via S. Agostino 1, 62032 Camerino, Italy.*

ABSTRACT—The aim of this work is to investigate the ovarian development of *Rana esculenta* living in Colfiorito pond (820 m a. s.l.). This process depends on a complex interplay between the estradiol-induced hepatic vitellogenin and the uptake of vitellogenin by the ovary. In order to establish whether the ovarian growth may depend on hydration process as well, the ovaries have been analyzed—during the annual cycle—by thermo-analysis. As far as we know, this method has been employed for the first time to lower vertebrate tissues with the present work. Vitellogenin titre varies according to a temporal pattern which is characteristic of this mountain population and is well correlated with plasma estradiol concentration. Samples of ovarian tissues, monitored by thermal analysis, show that, in the pre-spawning period three different kinds of water are bonded to the tissues with different energies of interaction. In the ovulatory period, the water is released in one process only. Samples of the post-ovulatory period give the curves, which can be plotted in-between the pre-spawning and ovulatory ones. In conclusion, the present results describe how two different kinds of water are released during the ovarian development. The low weight ovaries, with small oocytes, show a high water percentage which is lost in only one step; the high weight ovaries show a low water percentage, that is lost in three steps. Therefore, in the recovery phase, the ovarian growth, seems mainly due to yolk storage and only partly to the hydration process which, moreover, is closely related with plasma sex steroid concentration.

INTRODUCTION

The ovarian development in anuran amphibian *Rana esculenta* is cyclical: the growth starts in September (recovery phase), stops temporarily during winter stasis and resumes just before ovulation (April-May). This development is regulated by several environmental cues (temperature and photoperiod) and endocrine mechanisms.

Previous studies [1] have shown that the length of the recovery phase depends mainly on temperature. In fact the recovery phase in the population of green frogs living in the mountains is shorter than that in the population living at sea level. Such a difference depends on an early drop of mountain

temperature in autumn. The ovarian growth is essentially due to the storage of vitellogenin, synthesized by the liver and then released in the blood. Moreover, also hydration process—not yet well known—plays a part in ovary weight increase [2].

The vitellogenesis occurs under hormonal control: in fact, as in other amphibian species [3–5], also in *Rana esculenta* [6, 7], estradiol is the hormone most responsible for the vitellogenin synthesis, while the gonadotropins support the ovarian uptake. Nevertheless, Gobbetti *et al.* [8] pointed out a significant intervention of gonadotropins in inducing hepatic vitellogenin synthesis. It is certain, however, which is the role of hydration in ovarian growth and how it is regulated by sex steroid hormones. Therefore it seemed a good opportunity to investigate these aspects by thermal

analysis; as far as we know, this was the first application to lower vertebrate tissues. At the same time, the plasma vitellogenin and sex hormone titre were monitored during the reproductive cycle of *Rana esculenta*. All samples were taken in the field to avoid the stress of captivity on plasma steroid concentration [9].

MATERIALS AND METHODS

Animals and tissues

Ten female frogs, *Rana esculenta* complex, were monthly captured in the mountain pond of Colfiorito (820 m above sea level) and anesthetized with MS 222 (Sandoz). Previous data indicate that MS 222 does not affect the hormone profiles in *Rana esculenta* [10, 11]. Blood was collected into heparinized centrifuge tubes by a heparinized glass capillary which was inserted into the *conus arteriosus*. After centrifugation, individual plasma samples were stored at -20°C until hormonal determinations. Ovaries taken from these animals were removed and weighed. One of these was kept at -20°C until thermal analysis and the other one was placed in amphibian Krebs-Ringer solution. The latter was opened carefully and dissected in order to separate follicular oocytes, as previously described [1]. The dissected oocytes were screened by granulometric sieves into three classes: black atretic follicles (ϕ : 0.4–0.69 mm), previtellogenic follicles (ϕ : 0.70–1.2 mm), and vitellogenic follicles (ϕ : 1.21–2.0 mm).

Thermal analysis

The water interactions, in the biological systems, are in function of the hydrogen bonds, of the Van der Waals forces and the London forces etc.; so the water in the biological systems is bound to the matrix by different energies, also in relation to the different kinds of molecules present in the matrix. When a biological system is heated, the water is released in different successive steps in function of the necessary activation energy to be obtained in the break of each different bond from its water-matrix. Each step will thus represent a particular onertype of water characterized by one particular value of the interaction energy with the

matrix.

The different kinds of water and their percentage were determined by thermal analysis (TG) as described by Wendlandt [12], using a Perkin Elmer TG-S2 thermobalance equipped with a data station. The operational atmosphere was air or oxygen at a flow of 150 ml min^{-1} . An inert atmosphere was also used in the preliminary phase to check whether oxidation phenomena may anticipate the decomposition of the organic matter which would interfere with the water percentage determination. The temperature program chosen was $10^{\circ}\text{C min}^{-1}$ and the sample weight ranged between 20 and 50 mg.

Vitellogenin assay

Male frogs were estrogenized with estradiol silastic tubes implanted into the ventral cavity and were kept in water tanks on a diet of mealworms. After 20 days, the estrogenized males were anaesthetized on MS 222 and blood samples were collected as previously described. Vitellogenin was purified from estrogenized serum by the EDTA-MgCl₂ method [13] and then chromatographed on DEAE cellulose (Whatman).

Using a protocol developed in our laboratory, purified vitellogenin has been used to raise antibodies. When antiserum was tested by immunoblotting, strong reactivity was observed vs. isolated vitellogenin. Control experiments were made with preimmune serum. The antibodies recognized a protein present in estrogenized frog serum but failed to react against control serum. The data lead us to conclude that i) the antiserum is specific for vitellogenin and ii) the antigen was purified to a high extent. So the α -VTG Abs were used to determine the plasma vitellogenin titre by enzyme-linked assay (ELISA). The serum of ten female frog, used as antigen, was absorbed on polystyrene microplates. Rabbit vitellogenin antiserum was diluted 1:1000 and was incubated for 2 hr at room temperature. The conjugate was alkaline-phosphatase goat antirabbit immunoglobulin, diluted 1/1000 and incubated for 2 hr at room temperature. P-nitrophenyl-phosphate was employed as enzyme substrate for 60 min, the results were expressed in absorbance units at 405 nm. The calibration curve shown in Figure 1 enables

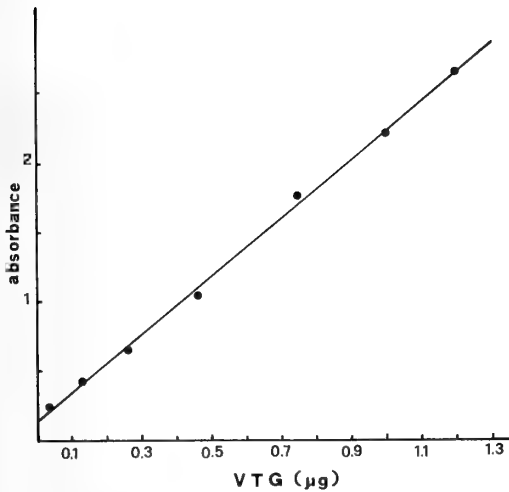


FIG. 1. Calibration curve of *Rana esculenta* plasma vitellogenin as determined by enzyme-linked immunosorbent assay. The absorbance was plotted versus the relative amount of antigen placed in the hole. Each point represents the mean of three independent measurements.

the antigen titre to be measured in all the sera collected.

The sensitivity of the ELISA method was 3 ng (intraassay 6%; interassay 11%).

Protein concentration was determined by the procedure which uses bovine serum albumin as standard.

Plasma hormone determinations

Plasma samples, taken monthly from ten females, were extracted with ether; subsequently radioimmunological analyses (RIA) of estradiol- 17β (E), progesterone (P) and androgens (A), were carried out as previously described [15].

The following sensitivities were observed: testosterone 5 pg (intraassay, 7%; interassay, 13%; progesterone, 7 pg (intraassay, 4%; interassay, 8%). Testosterone was not separated from dihydrotestosterone and therefore, since its antibody reacts with dihydrotestosterone, the data are expressed as "androgen". The antisera were provided by Dr G. Bolelli, Centro di Fisiopatologia della Riproduzione, C. N. R., Bologna.

All numerical data of the present experiments were analyzed using an ANOVA method.

RESULTS

The ovarian growth, during the reproductive period, has been evaluated considering the oocytes diameter. During the ovulatory period (May), the ovary comprises mainly full-growth oocytes (1.21–2.0 mm). In the post-reproductive period (July), the number of full-growth oocytes decreases and the smallest oocytes look atretic as in the previtellogenic stage. During the recovery phase (September), the number of oocytes entering the vitellogenic cycle increases and the cells continue their growth and gradually accumulate in the later stages.

The plasma vitellogenin profile is correlated with ovarian composition. The ovary weight presents its main peak in winter (stasis period), before ovulation (April). In the post-reproductive period, because the oocytes are ovulated, the ovary weight is very low, and begins to grow during the recovery phase (autumn), to reach its maximum the next winter, as can be seen in Figure 2.

These modifications, when submitted to analysis of variance, were statistically significant ($p < 0.001$).

Also the variations of plasma vitellogenin titre were statistically significant ($p < 0.001$). The high vitellogenin levels both in stasis and in the recovery period are correlated with the ovary weight. On the contrary, in the reproductive and post-reproductive period, the ovary weight is low because the ovulation and vitellogenin accumulates in the plasma. The estradiol profile agrees with our previous data [15]. The significant increase ($p < 0.001$) of plasma estradiol levels in July is responsible for the induction of hepatic vitellogenin synthesis which in turn allows recovery of the ovarian weight [8].

Samples of ovarian tissues, corresponding to the different periods of the ovarian cycle, were analysed by TG to assay the hydration process. The curves obtained show three types of behavior, each characteristic of a specific period of the cycle. Figure 3 shows a characteristic trend of water percentage in the fullgrowth oocytes (pre-reproductive period). In fact the water is released through three different processes occurring within

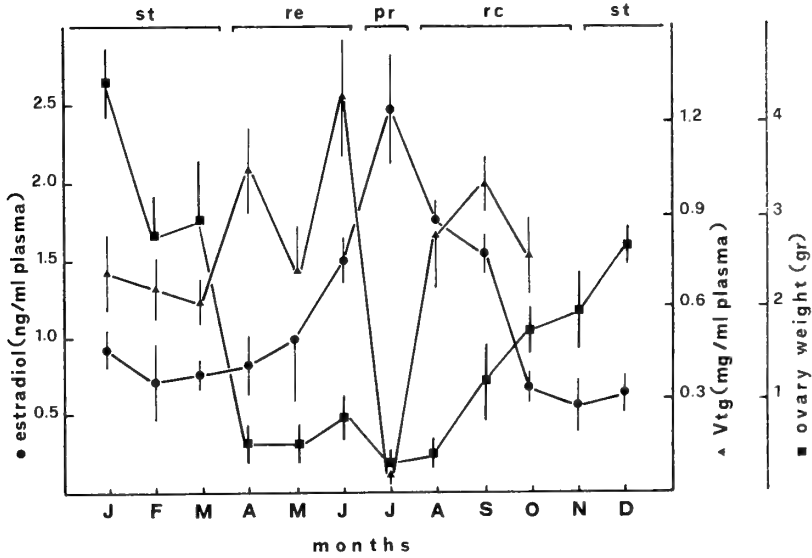


FIG. 2. Time course of vitellogenin and estradiol titre in the plasma of *Rana esculenta* cycle includes four periods: reproductive period (re), post-reproductive (pr), recovery (rc) and stasis (st). Number of frogs used is shown in the text.

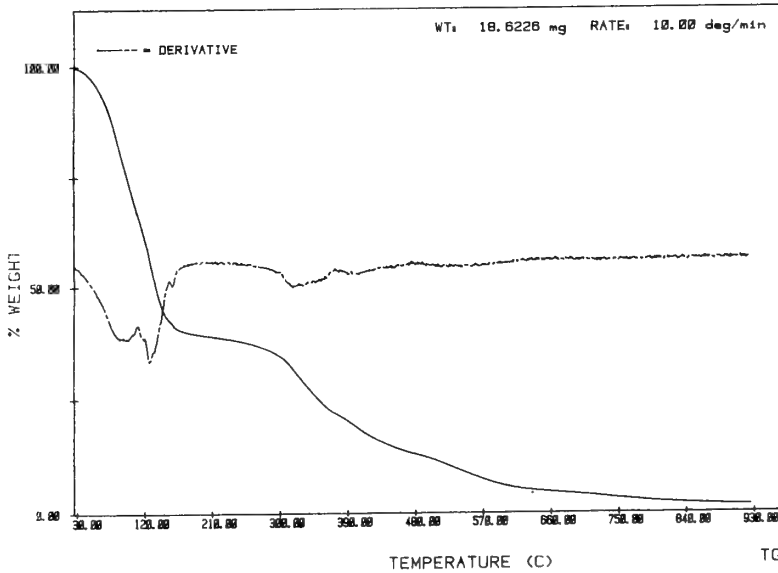


FIG. 3. Thermogravimetric analysis (TG) of *Rana esculenta* ovaries during the pre-ovulatory period.

the temperature intervals of 25–105°C (1st process), 105–155°C (2nd process) and 155–210°C (3rd process). They suggest that three different kinds of water are bonded to the tissues with different energies of interaction.

The thermal behavior is surprisingly constant during a very long interval of time, especially in

consideration of the fact that such samples were obtained from 10 different animals. The percentage of total water contained in the examined tissues ranged between 45 and 55%. The curves corresponding to the ovulatory period samples (low weight ovaries) show that the water is lost in one process only, occurring in the temperature

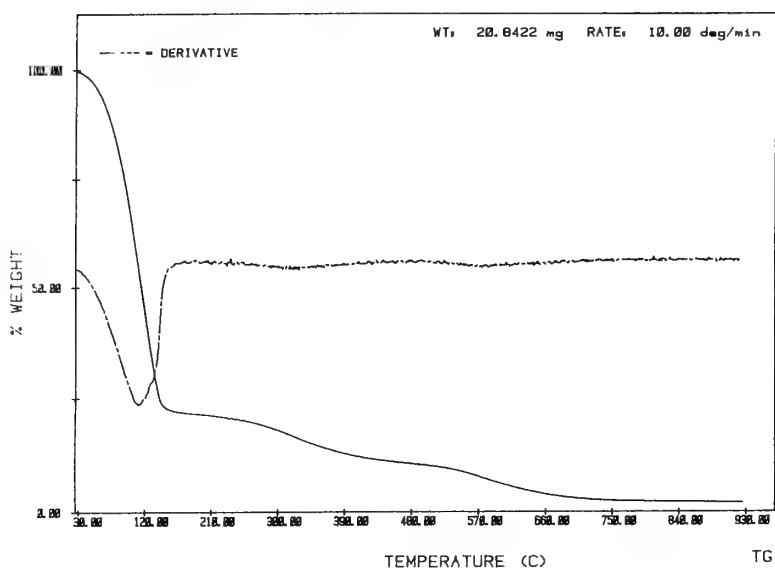


FIG. 4. Thermogravimetric analysis (TG) of *Rana esculenta* ovaries during the ovulatory period.

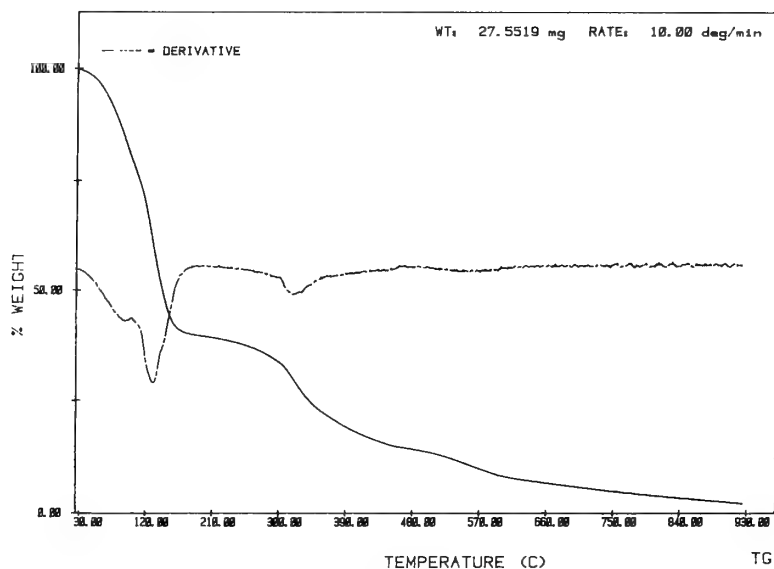


FIG. 5. Thermogravimetric analysis (TG) of *Rana esculenta* ovaries during the post-reproduction period.

interval of 25–180°C with a fluctuation as described above. The thermal behavior is quite constant and only rarely is the peak split in two different tips. The percentage of total water contained in the examined tissues ranged between 65 and 75% (Fig. 4). Samples of the post-ovulatory period originate TG curves, that are plotted in between those for the ovulatory and

pre-spawning period. Figure 5 depicts an example of typical intermediate TG behavior.

DISCUSSION

Ovarian development in non-mammalian vertebrates entails a complex interplay between the ovary and various other organs [16]. A high

molecular weight yolk precursor (vitellogenin) is synthesized and secreted by the liver and subsequently transferred to the ovary by endocytic uptake. Since synthesis and uptake of vitellogenin are both hormone-dependent, the turn-over of vitellogenin in the blood appears to be a function of the hormonal balance influencing both processes. In *Rana esculenta*, Gobbetti *et al.* [17] found that estradiol-17 β induces vitellogenin synthesis, as in other amphibian species. Recent results also suggest that the availability of specific liver receptors is strongly related to vitellogenin hormonal regulation [18].

The present data show a strict relationship between vitellogenin titre and ovarian behavior as witnessed by ovary weight during stasis and the recovery phase. On the contrary, when the ovary weight is very low in May (full-growth oocytes are ovulated), high concentrations of vitellogenin accumulate in the plasma.

The results obtained on ovarian tissue checked by TG at the different periods of the cycle support the hypothesis that the determination of water content could be important in the explanation of ovarian growth. In fact, our results indicate that two different kinds of water are released during ovarian development. The low weight ovaries with small oocytes show a high water percentage, which

is lost in only one step. In contrast, high weight ovaries (full-growth oocytes) show a low water percentage, that is lost in three steps. In the high weight ovaries, therefore, the water percentage is lower than in small ovaries. The water of the full growth oocytes, released at high temperature (210°C), is probably connected with yolk macromolecules. On the contrary, the high water percentage of small oocytes is released at low temperature. Therefore, the increase of ovarian weight during the recovery period of *Rana esculenta* seems mainly due to the storage of yolk and only partly to hydration processes [19].

The water percentage is well related with the plasmatic sex steroid concentrations. In *Rana esculenta* the main peak of plasma androgen levels was found in the reproductive period [20]. Also in these experiments the androgen titre is higher when the water percentage is about 50% (Fig. 6). During the post-reproductive period the high titre of plasmatic estradiol agrees with the high percentage of water in low weight ovaries. It is already known that steroid hormones in fish and in mammals are involved in tissues hydration process [21, 22]; while, as far as amphibians are concerned, other hormones, such as prolactin in urodeles, may play an important role. It is therefore worthwhile studying more in depth in anurans the implication

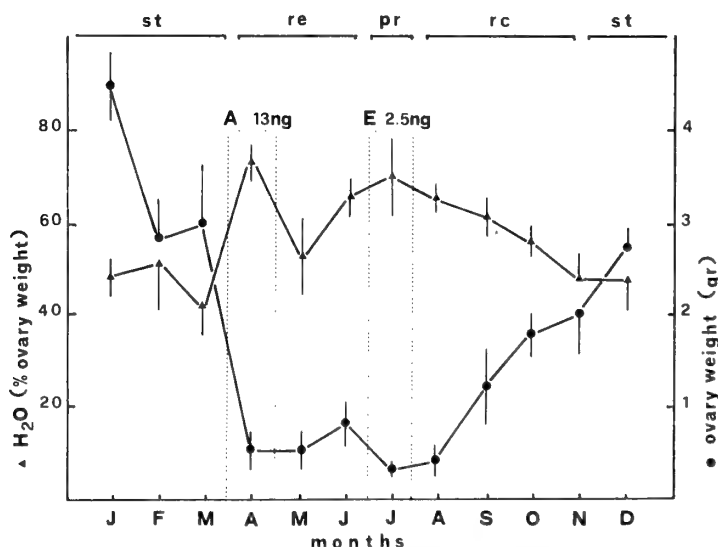


FIG. 6. Relationship between ovary weight, ovary water percentage and plasma sex steroid levels (A = androgens; E = estradiol-17 β), in the different phases of female *Rana esculenta* reproductive cycle.

of other hormones in the hydration process.

ACKNOWLEDGMENTS

Financially aided by the Italian Ministry of Education (40 and 60%) and CNR.

REFERENCES

- Polzonetti-Magni, A., Pagano, M., Gobbetti, A., Bellini-Cardellini, L. and Botte, V. (1984) Accrescimento annuale dell'ovario in popolazioni di *Rana esculenta*, viventi in località con differente andamento climatico. *Riv. Biol.*, **77**: 97-103.
- Pierantoni, R., Varriale, B., Simeoli, C., Di Matteo, L., Milone, M., Rastogi, R. K. and Chieffi, G. (1983) Fat body and autumn recrudescence of the ovary in *Rana esculenta*. *Comp. Biochem. Physiol.*, **76A**: 31-35.
- Wallace, R. A. and Jared, D. W. (1969) Studies on amphibian yolk. VIII. The estrogen-induced hepatic synthesis of a serum lipophosphoprotein and its selective uptake by the ovary and transformation into yolk platelet proteins in *Xenopus laevis*. *Dev. Biol.*, **19**: 498-526.
- Wallace, R. A. (1978) Oocyte growth: non mammalian vertebrates. In "Evolution of the Vertebrate Ovary". Ed. by R. E. Jones, Plenum Press, New York, pp. 469-502.
- Searle, P. F. and Tata, J. R. (1981) Vitellogenin gene expression in male *Xenopus* hepatocytes during primary and secondary stimulation with estrogen in cell cultures. *Cell*, **23**: 741-746.
- Giorgi, F., Gobbetti, A. and Polzonetti-Magni, A. (1982) Variations in the vitellogenin titre during the reproductive cycle of *Rana esculenta* L. *Comp. Biochem. Physiol.*, **72B**: 501-506.
- Varriale, B., Pierantoni, R., Di Matteo, L., Minucci, S., Milone, M. and Chieffi, G. (1988) Relationship between estradiol-17 β seasonal profile and annual vitellogenin content of liver, fat body, plasma, and ovary in the frog (*Rana esculenta*). *Gen. Comp. Endocrinol.*, **69**: 328-334.
- Gobbetti, A., Polzonetti-Magni, A., Zerani, M., Carnevali, O. and Botte, V. (1985) Vitellogenin hormonal control in the green frog, *Rana esculenta*. Interplay between estradiol and pituitary hormones. *Comp. Biochem. Physiol.*, **82A**: 855-858.
- Licht, P., Mc Creery, B. R., Barnes, R. and Pang, R. (1983) Seasonal and stress related changes in plasma gonadotropins, sex steroids and corticosterone in the bullfrog, *Rana catesbeiana*. *Gen. Comp. Endocrinol.*, **50**: 124-145.
- D'Istria, M., Delrio, G., Botte, V. and Chieffi, G. (1974) Radioimmunoassay of testosterone, 17 β -oestradiol and oestrone in the male and female plasma of *Rana esculenta* during sexual cycle. *Steroids Lipids Res.*, **5**: 42-48.
- Pierantoni, R., Iela, L., Delrio, G. and Rastogi, R. K. (1984) Seasonal plasma sex steroid levels in the female *Rana esculenta*. *Gen. Comp. Endocrinol.*, **53**: 126-134.
- Wendlandt, W. W. (1986) Thermal analysis. *Anal. Chem.*, **58**: 1R-6R.
- Wiley, H. S. and Dumont, J. N. (1978) Stimulation of vitellogenin uptake in stage. IV. *Xenopus* oocytes by treatment with chorionic gonadotropin *in vivo*. *Bio. Reprod.*, **18**: 762-771.
- Lowry, O. H., Rosebrough, N. J., Farr, A. L. and Randall, R. J. (1951) Protein measurement with Folin phenol reagent. *J. Biol. Chem.*, **193**: 265-275.
- Polzonetti-Magni, A., Botte, V., Bellini-Cardellini, L., Gobbetti, A., Crasto, A. (1984) Plasma sex hormones and post-reproductive period in the green frog, *Rana esculenta* complex. *Gen. Comp. Endocrinol.*, **54**: 372-377.
- Follett, B. K., Redshaw, M. R. (1974) The physiology of vitellogenesis. In "Physiology of Amphibia". vol. 2, Ed. by B. Lofts, Academic Press, New York, pp. 219-308.
- Gobbetti, A., Polzonetti-Magni, A., Zrani, M. and Paolucci, M. (1983) Vitellogenin synthesis induced by estradiol-17 β in the green frog, *Rana esculenta* complex. *Rend. Acc. Sci. Fis. Mat.*, **4**: 60.
- Paolucci, M. and Botte, V. (1988) Estradiol-binding molecules in the hepatocytes of the female water frog, *Rana esculenta*, and plasma estradiol and vitellogenin levels during the reproductive cycle. *Gen. Comp. Endocrinol.*, **70**: 466-476.
- Rastogi, R. K., Izzo-Vitiello, I., Di Meglio, M., Di Matteo, L., Franzese, R., Di Costanzo, M. G., Minucci, S., Iela, L. and Chieffi, G. (1983) Ovarian activity and reproduction in the frog, *Rana esculenta*. *J. Zool. Lond.*, **200**: 233-247.
- Lupo, C., Zerani, M., Carnevali, O., Gobbetti, A. and Polzonetti-Magni, A. (1988) Testosterone binding protein in the encephalon and plasma sex hormones during the annual cycle in *Rana esculenta* complex (Amphibia Ranidae). *Monitore Zool. Ital. (N. S.)*, **22**: 133-144.
- Babiker, M. M. and Ibrahim, H. (1979) Studies on the biology of reproduction in the cichlid *Tilapia nilotica* (L.): effects of steroid and trophic hormones on ovulation and ovarian hydration. *J. Fish Biol.*, **15**: 21-30.
- Warren, J. C. and Crist, R. D. (1973) Effects of ovarian steroids on uterine metabolism. In "Handbook of Physiology", Ed. by R. O. Greep and E. B. Aswood, publ. pp. 49-67.

Long-Term Effects of Hypophysectomy on the Growth and Calcification of Otoliths and Scales in the Goldfish, *Carassius auratus*

YASUO MUGIYA

*Department of Biology and Aquaculture, Faculty of Fisheries,
Hokkaido University, Hakodate 041, Japan*

ABSTRACT—Goldfish (*Carassius auratus*) were given tetracycline for time-marking, followed by hypophysectomy. They were kept at 0.25% NaCl-tap water for 32 weeks and then sacrificed to examine long-term effects of hypophysectomy on the accretive growth and calcification of otoliths and scales. Plasma was also analysed for calcium and sodium concentrations.

Hypophysectomy resulted in cessation of somatic growth in length. Hypercalcemia and hyponatremia were induced by hypophysectomy. Tetracycline-induced bands indicated that scale growth almost ceased after operation, while otoliths continued to grow at a rate reduced to approximately half. The marginal osteoid of scales was poorly developed in hypophysectomized fish. X-ray energy spectra revealed no difference in elemental constituents of the newly formed regions of these tissues between the experimental and control groups: major elements were phosphorus and/or calcium, suggesting that these regions are fully calcified. These results were discussed with the allometric growth of otoliths to somatic growth.

INTRODUCTION

Teleost otoliths and scales are mainly composed of calcium salts, and are used for age determination. They grow by the deposition of calcium carbonate or phosphate on the non-collagenous or collagenous matrix. Their growth has been considered to be isometric to somatic growth, at least before the somatic growth becomes asymptotic. However, Secor and Dean [1] have recently indicated the presence of two components in otolith growth: one is an endogenously defined incremental growth, which can occur during periods of decreased or arrested somatic growth, and the other is a continuous growth within a day in some proportion to daily somatic growth. They have proposed a daily increment packing (DIP) model for such a mode of otolith growth. The DIP model suggests that somatic and otolith growth is not necessarily isometric in detail.

Somatic growth is under endocrine control, and

it has repeatedly been reported that the removal of the pituitary gland results in cessation of fish growth in length [2–4]. Pickford [2] examined otoliths and scales from hypophysectomized killifish and found no new circulus formation in the scales and no new deposition on the otoliths. Her findings came from a morphological comparison of the outermost margin of these tissue between hypophysectomized and control fish. Therefore, it remains uncertain how, quantitatively, hypophysectomy affects the growth rate of otoliths and scales.

The present study was undertaken to examine quantitatively long-term effects of hypophysectomy on the growth and calcification of otoliths and scales using tetracycline-labeled goldfish.

MATERIALS AND METHODS

The goldfish, *Carassius auratus*, weighing approximately 21.7 g were obtained from a commercial dealer and acclimated to experimental conditions for at least 2 weeks before use. They were maintained at $23 \pm 1^\circ\text{C}$ and fed carp pellets once a

day throughout the acclimation and experimental periods.

Twenty fish were given a single intraperitoneal injection of tetracycline (Takeda Chemical Ind.) at a dose of 0.1 mg/g body weight and allowed to recover for 4 days. Then, they were randomly divided into 2 groups and one group was hypophysectomized by the opercular approach technique [5]. The other group was subjected to drilling of the prootic bone only, and used as sham-operated control.

Hypophysectomized and sham-operated fish were separately placed into one of the two compartments halved by a wire-netting in a 120 l tank containing aerated and filtrated 0.25% NaCl tap water (Na conc. 43.1 mM and Ca conc. 0.2 mM). They were taken out for measurement of body size twice a month and returned to the other compartment each time. This replacement made their environmental conditions as even as possible. No individual discrimination was made. The dividing netting was removed after about 3 months and both groups were maintained in the same compartment from then on. Nevertheless, it was easy to distinguish the experimental fish from the control, because the red body color had faded to almost white in the hypophysectomized fish. They were sacrificed 32 weeks after operation.

Blood was collected from the caudal vessels by cutting the tail of the fish and draining it into heparinized (as Li salt) capillary tubes. After centrifugation, the separated plasma was stored at -40°C for 1 day and analysed for calcium and sodium concentrations by emission spectrophotometry (Hitachi, 518).

Somatic growth was expressed as a relative growth rate (RGR) after Ricker [6].

$$\text{RGR} = \frac{B-A}{T-t} \times \frac{1000}{A}$$

where A and B represent initial and final sizes, respectively, and T-t is the change in time (32 weeks). RGR in scales and otoliths was calculated in the same manner.

After blood collection, 6 scales were removed with forceps from the antero-dorsal part of each fish. Special attention was paid not to include regenerating scales. They were carefully rinsed

several times with distilled water and examined for tetracycline-induced fluorescence under ultraviolet illumination (Nikon, EFD). The distance of accretive growth during the experiment was measured with a calibrated eye-piece to the nearest μm in the anterior part of scales and RGR was calculated. After measurement, scales were stained with 1% silver nitrate [7] for calcium detection.

Otoliths (asterisci and lapilli) were dissected, rinsed with distilled water and dried. After measurements of weight and length in the dorso-ventral axis, asterisci were embedded within a mass of methacrylate of suitable hardness and ground down to approximately 100 μm in thickness so that the polished plane was parallel to the axis accross the center. Ground otoliths were subjected to microscopic examination for fluorescence. The distance of accretive growth was measured in the dorsal and ventral directions. Only weight and length in the antero-posterior axis were measured in lapilli.

Student's t-test for unpaired observations was applied to assess statistical significance of differences between mean values. Significance was accepted at a P-value of <0.05 .

The degree of calcification of the newly formed regions of scales and otoliths was estimated by X-ray microanalyses. Scales and ground otoliths were ultrasonically cleaned in xylene and/or distilled water and mounted on a carbon holder with a carbon tape. After being coated with carbon, they were examined for elemental constituents at 20 kV by spot analyses using a Horiba EMAX-2000 energy-dispersive X-ray microanalysis system. Spectrum collection time was 100 sec.

RESULTS

Hypophysectomy resulted in a marked reduction in somatic growth (Table 1). Relative growth in weight gain was reduced by 70% in hypophysectomized fish compared to the sham-operated control. No increase in length was found in the experimental fish in spite of their active feeding.

Plasma sodium and calcium were significantly affected by hypophysectomy (Table 2). Although fish were maintained in 0.25% NaCl throughout the course of the experiment, sodium concentra-

TABLE 1. Somatic growth in hypophysectomized and sham-operated goldfish

	Sham-operated	Hypophysectomized
Body weight (g)		
Initial	21.0±1.0 (8)*	22.4±1.0 (9)
Final	33.6±3.0 (7)	26.2±1.6 (8)
RGR**	18.8	5.3
Standard length (cm)		
Initial	8.3±0.1 (8)	8.4±0.2 (9)
Final	9.3±0.3 (7)	8.3±0.1 (8)
RGR	3.77	-0.38

* Mean±SE (No. of fish examined).

** Relative growth rate.

TABLE 2. Plasma calcium and sodium concentrations (mEq/l) in hypophysectomized and sham-operated goldfish

	Sham-operated	Hypophysectomized	Significance
Ca	4.7±0.1 (7)*	5.2±0.2 (6)	P<0.05
Na	135.2±1.1 (7)	129.9±0.7 (6)	P<0.01

* Mean±SE (No. of fish examined).

TABLE 3. Otolith sizes in hypophysectomized and sham-operated goldfish

	Sham-operated	Hypophysectomized	Significance
Length (μm)			
Asteriscus	2988±64 (10)*	2605±22 (12)	P<0.001
Lapillus	1957±31 (12)	1879±22 (12)	
Weight (mg)			
Asteriscus	7.9±0.3 (10)	6.7±0.3 (12)	P<0.01
Lapillus**	8.0±0.4 (6)	6.4±0.2 (6)	P<0.01

* Mean±SE (No. of otoliths examined).

** A pair of lapilli were pooled for weighing.

tions decreased in hypophysectomized fish ($p<0.01$). On the other hand, hypophysectomy resulted in an increase in plasma calcium concentrations at the end of the experiment ($p<0.05$).

Measurements of whole otoliths showed that otolith growth was inhibited by hypophysectomy (Table 3). Asterisci of hypophysectomized fish gained significantly less ($p<0.01$), 13% and 15% less in length and weight respectively, than those of the control, while a significant ($p<0.01$) effect of hypophysectomy on lapillus growth was found

only in weight, showing a 20%-reduced gain. Tetracycline-induced bands visually confirmed the inhibitory effects of hypophysectomy on otolith growth in length (Fig. 1). Otolith growth toward the dorso-ventral directions is presented as a relative growth rate (Table 4). Hypophysectomy reduced the rates by half in both directions ($p<0.001$). The pattern of X-ray energy spectra was almost the same between the experimental and control otoliths. The heavy presence of calcium with a trace of phosphorus was confirmed in the

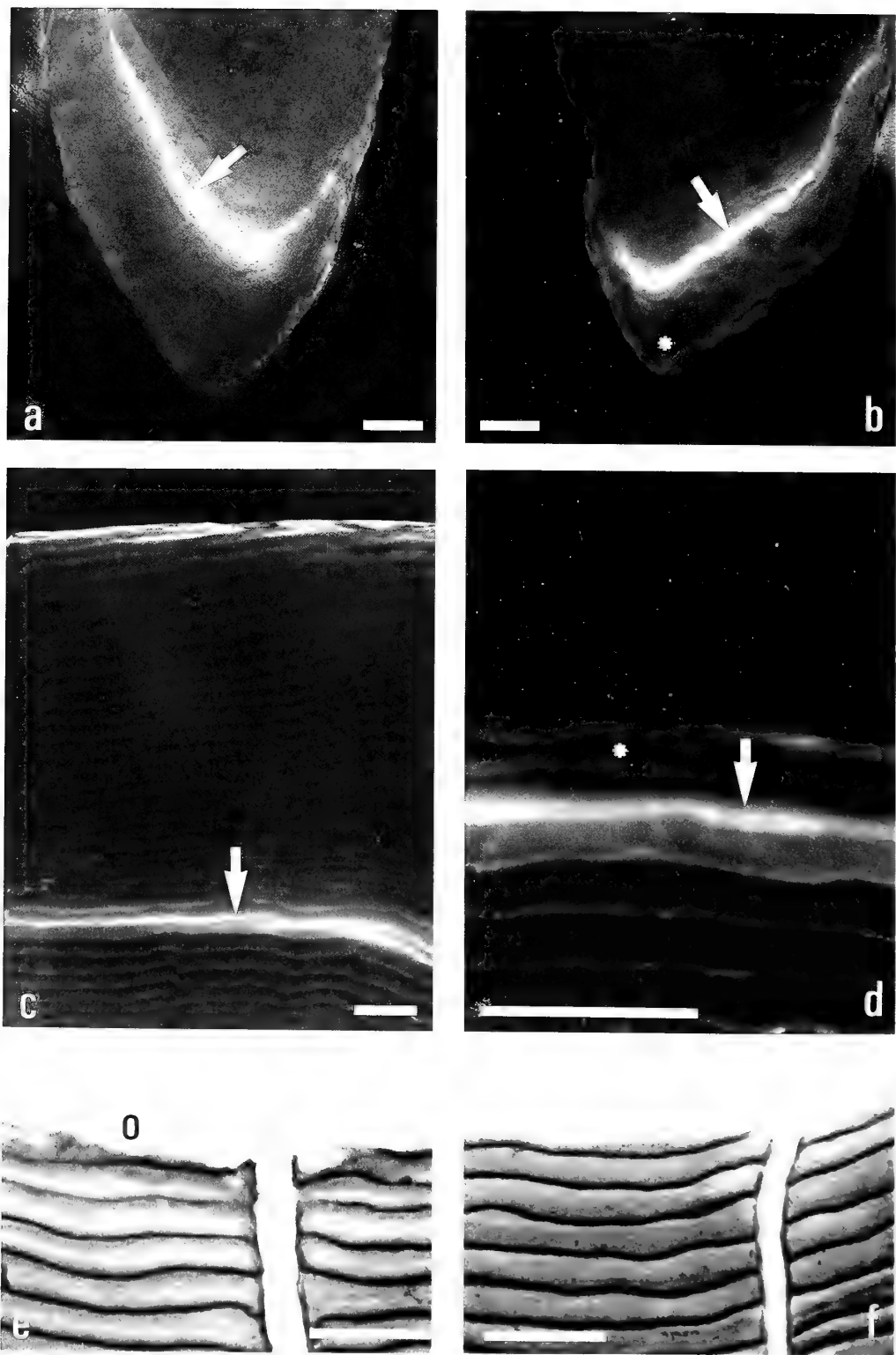


TABLE 4. Relative growth rates in otoliths and scales in hypophysectomized and sham-operated goldfish

	Sham-operated	Hypophysectomized	Significance
Otolith (asteriscus)			
Dorsal	5.91 ± 0.38 (10)*	3.05 ± 0.19 (14)	$P < 0.001$
Ventral	4.93 ± 0.33 (10)	2.44 ± 0.20 (14)	$P < 0.001$
Scale	6.43 ± 0.76 (18)	0.62 ± 0.06 (20)	$P < 0.001$

* Mean \pm SE (No. of samples examined).

newly formed region following hypophysectomy (Fig. 2). Therefore this region should be calcified.

Scale growth was markedly reduced by hypophysectomy. Only 1 or 2 ridges were added to the hypophysectomized fish scales during the experiment, while 16–30 ridges were newly formed in the control (Fig. 1). Relative growth rates showed that hypophysectomy reduced scale growth to about one-tenth of the control (Table 4). Therefore, it is evident that scale growth was more severely affected by hypophysectomy than otolith growth. The newly formed region of scales following hypophysectomy was positively stained by sil-

ver nitrate. The marginal osteoid was poorly developed in the scales (Fig. 1). X-ray microanalyses revealed no essential difference in the energy spectra between experimental and control scales. Major elemental constituents in the newly formed region were calcium and phosphorus (Fig. 3), which are probably present in apatite. No spectrum difference was found between the ridge and inter-ridge regions.

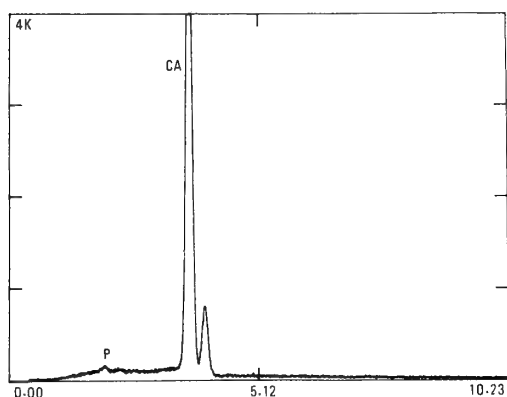


FIG. 2. X-ray energy spectrum from the newly formed region (cf. Fig. 1b) of an otolith after hypophysectomy. The major elemental constituent is Ca.

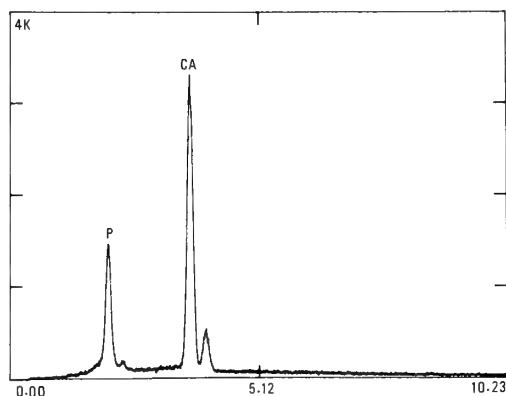


FIG. 3. X-ray energy spectrum from the newly formed region (cf. Fig. 1d) of a scale after hypophysectomy. The major elemental constituents are Ca and P.

DISCUSSION

The pituitary secretes various kinds of hor-

FIG. 1. Otoliths (asterisci) and scales of goldfish at the dorsal and anterior margins, respectively. Arrows represent tetracycline-induced fluorescent bands. White asterisks indicate the spots when X-ray microanalyses were performed (Figs. 2 and 3). Scale bars are 0.1 mm. (a) and (b) Fluorescent images of vertically ground otoliths from sham-operated (a) and hypophysectomized (b) fish. (c) and (d) Fluorescent images of scales from sham-operated (c) and hypophysectomized (d) fish. (e) and (f) Scales stained with silver nitrate. The osteoid (o) is well developed in sham-operated fish (e), but hypophysectomized fish (f) lack the osteoid.

mones. Therefore, the removal of the gland severely affects the fish: cessation in somatic growth [2], disturbances in ion and water balance [8], and arrest in sexual development [9]. The present results of the removal of the pituitary induced cessation in somatic growth in the length of goldfish, which agrees with earlier reports in other fish species [2, 4]. Scale growth was markedly inhibited by hypophysectomy, while otoliths continued to grow at a reduced rate after hypophysectomy, showing an allometric relationship to somatic growth. Outgrowth and calcification in scales are preceded by the formation of marginal osteoid [10], which is collagenous in nature. In hypophysectomized fish, little or no osteoid was found at the scale margin. Therefore, hypophysectomy appears to affect scale growth by retarding osteoid formation. Retardation in osteoid formation probably resulted from the lack of somatotropin, which stimulates the synthesis of proteins and other matrix-related macromolecules via somatomedin [11]. Replacement therapy with somatotropin was effective in restoring hypophysectomy-induced cessation in somatic growth in killifish [3] and bullhead [12].

The above-mentioned interpretation is fundamentally applicable to the effect on otolith growth. However, since otoliths are a highly calcified tissue and the amount of organic matrix is much less than that of scales [13], the relative contribution of the matrix to accretive growth may be not so critical as in scales. According to Degens *et al.* [14], otoliths grow by two processes: the new deposition of calcium as carbonate on non-collagenous matrix and successive growth of the crystals by epitaxy. The latter is a physicochemical process and therefore may be less affected by hypophysectomy. Even if the former phase of matrix formation is reduced to some extent, otoliths could continue to grow at a reduced rate through the process of crystal growth, because the endolymph bathing otoliths are considered to be highly supersaturated to the otolith mineral, calcium carbonate, in goldfish [15].

Allometric growth of otoliths to somatic growth has been reported especially in suboptimal environmental conditions such as low temperatures and food deprivation [16, 17]. Secor and Dean [1]

were the first to explain the allometry by daily increment formation in otoliths. They deduced that a range of somatic growth effects on otolith allometry can be explained by two associated processes: incremental growth of otoliths during periods of arrested somatic growth and continuous growth in some proportion to somatic growth. They have proposed to call such otolith growth pattern the daily increment packing model. Although the DIP model cannot be directly applied to the hypophysectomy-induced asynchronous relationship, it will be necessary to examine incremental microstructures in the newly formed region of otoliths in hypophysectomized fish.

Hypophysectomy induced hypocalcemia in killifish [18, 19] and goldfish [5]. One possible cause for this is a reduction in branchial uptake of calcium [5]. However, hypercalcemia was the case with the present study which focused on long-term effects of hypophysectomy. Since the experimental fish showed no gain in length during the experiment, an increase in bone mass is not expected. Since most calcium (more than 80%) taken up by goldfish is distributed in bone and scales [13], cessation in new skeletal formation would result in an excess of plasma calcium even at a reduced rate of branchial calcium uptake. Therefore, the present increase in plasma calcium concentrations following hypophysectomy can be attributed to the secondary effect of reduced skeletal tissue growth.

Then, why did hypophysectomy induce hypocalcemia and hypercalcemia? Mugiya and Odawara [5] showed that calcium incorporation into scales was not affected by hypophysectomy 2 weeks after operation. This is supported by the present result that 1 or 2 ridges were newly added to scales after hypophysectomy. Therefore, it is reasonable to suppose that inhibitory effects of hypophysectomy on skeletal tissue growth become effective with a lagged period of a few weeks after operation. This would partially explain the conflicting effects of hypophysectomy on plasma calcium concentrations in goldfish in the short-term and long-term experiments.

ACKNOWLEDGMENTS

The author is grateful to Professor N. Watabe, University of South Carolina for a critical reading of the manuscript. Thanks are also due to Messrs. F. Odawara and T. Hakomori for their technical assistance during the experiment.

REFERENCES

- 1 Secor, D. H. and Dean, J. M. (1989) Somatic growth effects on the otolith-fish size relationship in young pond-reared striped bass, *Morone saxatilis*. Can. J. Fish. Aquat. Sci., **46**: 113–121.
- 2 Pickford, G. E. (1953) A study of the hypophysectomized male Killifish, *Fundulus heteroclitus* (Linn.). Bull. Bingham Oceanogra. Coll., **14**: 5–41.
- 3 Pickford, G. E. (1954) The response of hypophysectomized male killifish to purified fish growth hormone, as compared with the response to purified beef growth hormone. Endocrinology, **55**: 274–287.
- 4 Ball, J. N. (1965) Partial hypophysectomy in the teleost Poecilia: Separate identities of teleostean growth hormone and teleostean prolactin-like hormone. Gen. Comp. Endocrinol., **5**: 654–661.
- 5 Mugiya, Y. and Odawara, F. (1988) Effects of hypophysectomy and replacement therapy with ovine prolactin on serum calcium levels, and calcification in otoliths and scales in goldfish. Nippon Suisan Gakkaishi, **54**: 2079–2083.
- 6 Ricker, W. E. (1979) Growth rates and models. In "Fish Physiology, Vol. 8". Ed. by W. S. Hoar, D. J. Randall and J. R. Brett, Academic Press, New York, pp. 677–743.
- 7 McManus, J. F. A. and Mowry, R. W. (1960) Staining Methods. Harper & Row Pub., New York, pp. 191–222.
- 8 Griffith, R. W. (1794) Pituitary control of adaptation to fresh water in the teleost genus *Fundulus*. Biol. Bull., **146**: 357–376.
- 9 Yamazaki, F. (1965) Endocrinological studies on the reproduction of the female goldfish, *Carassius auratus* L., with special reference to the function of the pituitary gland. Mem. Fac. Fish. Hokkaido Univ., **13**: 1–64.
- 10 Kobayashi, S., Yamada, J., Maekawa, K. and Ouchi, K. (1972) Calcification and nucleation in fish-scales. Biomineralisation, **6**: 84–90.
- 11 Nasu, N., Kato, Y. and Suzuki, F. (1980) Bioassay of somatomedin activity by cultured rabbit chondrocytes. Bone Metab., **13**: 294–299, (In Japanese).
- 12 Kayes, T. (1977) Effects of hypophysectomy, beef growth hormone replacement therapy, pituitary autotransplantation, and environmental salinity on growth in the black bullhead (*Ictalurus melas*). Gen. Comp. Endocrinol., **33**: 371–381.
- 13 Ichii, T. and Mugiya, Y. (1983) Comparative aspects of calcium dynamics in calcified tissues in the goldfish, *Carassius auratus*. Bull. Japan. Soc. Sci. Fish., **49**: 1039–1044.
- 14 Degens, E. T., Deuser, W. G. and Haedrich, R. L. (1969) Molecular structure and composition of fish otoliths. Mar. Biol., **2**: 105–113.
- 15 Shichiri, T. (1985) Growth of statolith. J. Japan. Assoc. Cryst. Growth, **12**: 42–56.
- 16 Marshall, S. L. and Parker, S. S. (1982) Pattern identification in the microstructure of sockeye salmon (*Oncorhynchus nerka*) otoliths. Can. J. Fish. Aquat. Sci., **39**: 542–547.
- 17 Campana, S. E. and Neilson, J. D. (1985) Microstructure of fish otoliths. Can. J. Fish. Aquat. Sci., **42**: 1014–1032.
- 18 Pang, P. K. T., Schreibman, M. P. and Griffith, R. W. (1973) Pituitary regulation of serum calcium levels in the killifish, *Fundulus heteroclitus* L. Gen. Comp. Endocrinol., **21**: 536–542.
- 19 Pang, P. K. T., Schreibman, M. P., Balbontin, F. and Pang, R. K. (1978) Prolactin and pituitary control of calcium regulation in the killifish, *Fundulus heteroclitus*. Gen. Comp. Endocrinol., **36**: 306–316.



Urea Stimulation of Pituitary Pars Intermedia Cells of Suckling Mice under Copious Drinking

YASUO KOBAYASHI and MANABU OKADA

*Department of Biology, Faculty of Science, Okayama University,
Okayama 700, Japan*

ABSTRACT—Ultrastructural alterations in cells of the pars intermedia (PI) of the pituitary gland were investigated morphometrically in suckling mice being fed with the pelleted food (Group I), in suckling dams given a liquid diet containing 11.5% milk powder (Group II) and in those received a 11.5% liquid milk diet supplemented with 1% urea (Group III) for 5 days from day 13 to day 17 of lactation. The percent area of the cytoplasm occupied by the rough endoplasmic reticulum increased from $11.9 \pm 1.0\%$ (Group I) through $17.9 \pm 1.0\%$ (Group II) to $36.9 \pm 1.1\%$ (Group III). The numerical density of immature Golgi granules also increased from 0.9 ± 0.06 (Group I) through 1.2 ± 0.09 (Group II) to 1.5 ± 0.09 (Group III). Whereas the numerical density of secretory granules decreased from 2.3 ± 0.11 (Group I) through 1.9 ± 0.07 (Group II) to 1.0 ± 0.05 (Group III). These results indicated that the release of secretory granules and the protein synthesis increased significantly in PI cells of suckling mice fed a liquid milk diet and, further, the urea supplement to the liquid milk diet elicited the secretion activity of PI cells more significantly than those of animals received the liquid milk diet only.

INTRODUCTION

Our previous electron microscopic and morphometric studies have demonstrated marked hypersecretion in cells of the pars intermedia (PI) of the mouse pituitary gland in response to dietary sodium restriction [1-3] suggesting a new role for the PI hormone(s) as a major pituitary factor in the regulation of aldosterone secretion by the adrenals [4, 5]. This new proposition has now been supported and confirmed by *in vitro* studies indicating that pro-opiomelanocortin-derived peptides such as α -MSH, β -MSH and γ -MSH are involved in the control of aldosterone secretion by the adrenals from rats and human beings with idiopathic hyperaldosteronism [6, see also references]. However, several lines of evidence have shown that the renin-angiotensin system is a prime regulator of aldosterone secretion [7, 8]. Thus, the physiological interrelationship between the pro-opiomelanocortin-derived PI peptides and the renin-angiotensin system in the regulation of aldosterone secretion has not yet been settled.

Our recent morphometric studies have also demonstrated that experimental copious drinking has an effect to cause marked hypersecretion in PI cells of the mouse pituitary [9] and that the PI cells of new-born mice indicate structural hypersecretion when, after 5 hr of separation, pups are reunited with their mother and allowed to suck their mother's breast for 1 hr [10]. These results suggest another new role of PI peptides in the regulation of hydro-mineral metabolism in mice.

On the other hand, one of the interesting behaviours of mice observed during lactation is a kind of coprophagy [11]. The suckling mice used to lick pups' urine and stools off their rump during nursing. In addition, there is a parallelism between a high blood urea concentration and the enlarged pars intermedia in mice with hereditary nephrogenic diabetes insipidus [12, 13]. Then the present study was designed to investigate the effects of experimental polydipsia [9] and of combined urea and polydipsia on pituitary PI cells of suckling dams whose water consumption is about 4 times as much as that of age matched nulliparous mice. Plasma osmolality and hematocrit were also evaluated since the specificity of the effect of osmolality on aldosterone secretion has been re-

cently reported [14, 15].

MATERIALS AND METHODS

Albino mice of the ICR/Jcl strain were housed at a temperature of $22 \pm 1^\circ\text{C}$ and 12 hr-periods of light and darkness (7.00–19.00 light on). Primigravid mice were isolated single in a cage provided with a pelleted mouse food and tap water. One day after the parturition, the number of siblings was reduced and adjusted to 6 pups. On day 12 of lactation, suckling dams were divided into three groups, and the following experiments were undertaken during the period from day 13 to day 17 of lactation. The first group served as controls receiving a pelleted food and distilled water. The second group was subjected to copious drinking; animals were deprived of a pelleted food and water and, instead, were fed with a liquid diet consisting of powdered milk (Yuki-zirushi Neomilk, Yukizirushi, Tokyo) at the concentration of 11.5%, the same concentration used in nursing a human baby. The third group also received a liquid diet of 11.5% powdered milk supplemented with 1% urea. The final concentration of urea used was determined in a way to keep the consumption of a urea plus milk liquid diet on a level with that of a milk liquid diet. Oral intake of a liquid diet was measured daily and the body weight of both suckling dams and pups was weighed. On day 17 of lactation, the suckling mice were killed by decapitation and the blood was collected from trunk vessels into heparinized capillary tubes. The hematocrit value was obtained after centrifugation of the blood samples for 10 min at a speed of 9,500

rpm. Plasma osmolality (mOsm/kg) was measured using Shimazu OSM-1 osmometer. The pituitaries were removed immediately after the sacrifice and small pieces of parasagittal slices of specimens were fixed in the solution of 1% glutaraldehyde and 1% paraformaldehyde with phosphate buffer at pH 7.4 for 1 hr followed by 1% OsO_4 (pH 7.4) for another 1 hr. After dehydration specimens were embedded in Quetol 812. Ultrathin sections were stained with uranyl acetate and lead citrate and examined with an H-11E Hitachi Electron Microscope. Electron micrographs were taken at original magnification of 2,500 and enlarged optically at 10,000 times.

In each group approximately 50 PI cells of electron micrographs were chosen at random for morphometric analysis. The area of the cytoplasm, nucleus and Golgi region was measured

TABLE 2. Hematocrit and osmolality of suckling mice given a pelleted food and distilled water (Group I), a 11.5% milk diet (Group II) and a 11.5% milk diet added with 1% urea (Group III) on day 17 of lactation

	Hematocrit (%)	Osmolality (mOsm/kg)
Pellet + D.W. (Group I)	48.7 ± 0.6^a	305 ± 2.2 (3)
Milk diet (Group II)	$57.4 \pm 0.6^*$	309 ± 2.2 (6)
Milk + Urea (Group III)	$56.5 \pm 0.5^*$	308 ± 1.3 (8)

^a) Mean \pm S.E.M., * Group I vs. Group II and Group III, $p < 0.01$. No. of animals is shown in parentheses.

TABLE 1. Water (D.W.) and liquid diet consumption (ml/10 g b.w./day) by suckling mice being fed with a pelleted food (Group I), with a 11.5% milk diet (Group II) and with a 11.5% milk diet added with 1% urea (Group III) from day 13 to day 17 of lactation

Day of lactation	13	14	15	16	17
Pellet + D.W. (Group I)	7.5 ± 0.8^a	7.8 ± 0.7	7.5 ± 0.5	6.4 ± 0.3	8.5 ± 0.6 (3)
Milk diet (Group II)	$13.6 \pm 0.9^*$	$13.8 \pm 1.0^*$	$14.3 \pm 0.7^*$	$17.0 \pm 1.5^*$	$16.4 \pm 1.2^*$ (6)
Milk + Urea (Group III)	$12.8 \pm 0.6^*$	$14.0 \pm 0.7^*$	$16.6 \pm 1.0^*$	$17.0 \pm 1.1^*$	$18.4 \pm 1.3^*$ (8)

^a) Mean \pm S.E.M., * Group I vs. Group II and Group III, $p < 0.01$. No. of animals is shown in parentheses.

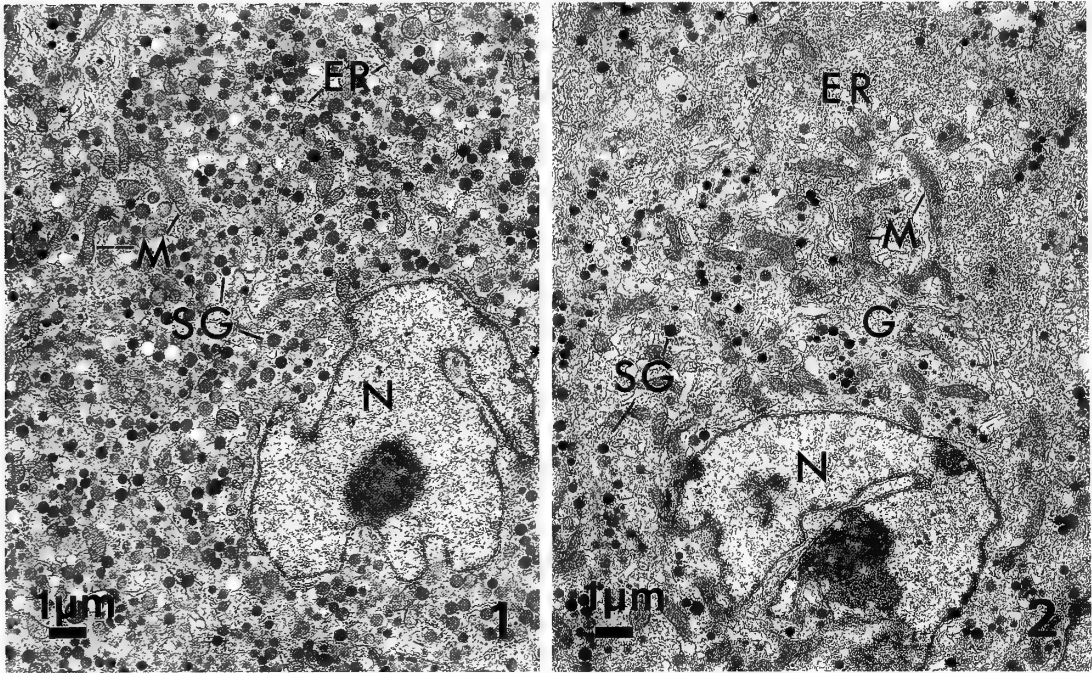


FIG. 1. Part of pituitary pars intermedia cells of the suckling mouse received pelleted food and distilled water. Note numerous secretory granules (SG), scanty rough endoplasmic reticulum (ER) and rod shaped mitochondria (M) in the cytoplasm. The nucleus (N) shows marked indentation with a prominent nucleolus.

FIG. 2. Part of pituitary pars intermedia cells of the suckling dam fed a liquid diet containing 11.5% milk powder and 1% urea. Note well developed rough endoplasmic reticulum (ER), extensive Golgi apparatus (G), sparse secretory granules (SG) and scattering mitochondria (M). The nucleus (N) is irregular in shape.

TABLE 3. The percent area of the rough endoplasmic reticulum (% r-ER), the numerical density of secretory granules (Secretory G./ μm^2) and of immature Golgi granules (Golgi G./ μm^2) in the Golgi region, and the total number of Golgi granules in the median of Golgi area (Golgi G./Med.) in suckling dams fed with a pelleted food and distilled water (Group I), with a 11.5% milk diet (Group II) and with a 11.5% milk diet supplemented with 1% urea (Group III) from day 13 to day 17 of lactation

	% r-ER	Secretory G./ μm^2	Golgi G./ μm^2	Golgi G./Med. ^{a)}
Pellet. + D.W. (Group I)	11.9 \pm 1.0 ^{b)}	2.3 \pm 0.11	0.9 \pm 0.06	9.0 (3)
Milk diet (Group II)	17.9 \pm 1.0**	1.9 \pm 0.07*	1.2 \pm 0.09°	12.6 (6)
Milk + Urea (Group III)	36.9 \pm 1.1**,*†	1.0 \pm 0.05**,*†	1.5 \pm 0.09**,*†	25.5 (6)

^{a)} Total number of Golgi granules in the median of the Golgi area was obtained multiplying the number of Golgi granules per unit area by the median of the Golgi area. ^{b)} Mean \pm S.E.M., Group I vs. Group II and Group III; * $p < 0.01$ ** $p < 0.001$. Group II vs. Group III; † $p < 0.01$ †† $p < 0.001$. No. of animals is shown in parentheses.

with a planimeter (X-PLAN 360, Ushikata, Tokyo). The number of secretory granules and of Golgi immature granules was counted in each cell. The numerical density of secretory granules and of Golgi immature granules was calculated, in which the cytoplasmic area for secretory granules was estimated subtracting the Golgi area from the whole cytoplasm of the cell. The percent area of the cytoplasm occupied by the r-ER was obtained with a Planimex 25 (Nihon Regulator, Japan). Statistical significance was assessed with Student's t-test.

RESULTS

1. Oral intake of distilled water and of liquid milk diet supplemented with or without urea

During the experimental period of lactation from day 13 to day 17, suckling dams (Group I) drank distilled water in the mean of 7.5 ± 1.5 ml/10 g b.w./day (Table 1). This water consumption of lactating mice was about 4 times as much as that of age matched unliparous female mice (1.8 ± 0.3 ml/10 g b.w./day, data not presented). When suckling mice were deprived of a pelleted food and, instead, given a 11.5% milk diet (Group II) their daily liquid consumption increased to 181%, 177%, 191%, 266% and 193% of the each corresponding control value (Group I), respectively, from day 13 to day 17 of lactation (Table 1). Likewise, lactating mice given a 11.5% milk diet plus 1% urea (Group III) showed copious drinking in a range of 171%, 179%, 221% 266% and 216% of the each control value (Group I) during the same period from day 13 to day 17 of lactation (Table 1).

2. Hematocrit and plasma osmolality

Hematocrit of the blood increased to 118% in suckling mice given a liquid milk diet (Group II) and to 116% in those fed a milk plus urea diet (Group III) when compared to that of the control (Table 2). Plasma osmolality in the Group II and Group III was not significantly different from that of the control Group I (Table 2).

3. Electron microscopy and morphometry of PI cells of the pituitary gland

In the control suckling mice (Group I) PI cells of the pituitary appeared to contain numerous secretory granules in the cytoplasm. The rough endoplasmic reticulum (r-ER) was poorly developed (Fig. 1). Whereas PI cells of the suckling dams given milk plus urea liquid regimen showed a cellular sign of hypersecretion; well developed r-ER, extensive Golgi apparatus and sparse secretory granules in the cytoplasm (Fig. 2).

The percent area of the cytoplasm occupied by the r-ER in suckling mice given liquid milk diet (Group II) and in those fed milk plus urea diet (Group III) increased to 150% and 310% of the control value, respectively (Table 3). The numerical density of immature Golgi granules in the Group II and Group III increased to 133% and 167% of the control value, respectively. In this case, however, the Golgi apparatus showed marked hypertrophy especially in those of the Group III. Thus the theoretical number of Golgi granules per the median of Golgi area was calculated. The total Golgi granules of the median Golgi area increased to 140% and 283% of the control value in the Group II and Group III, respectively (Table 3). On the contrary, the numerical density of secretory granules in the cytoplasm decreased to 83% and to 43% of the control value in the Group II and Group III, respectively.

DISCUSSION

The present study demonstrated an enhanced activity in cells of the pars intermedia (PI) of the pituitary in suckling mice given either a 11.5% liquid milk diet or a 11.5% milk diet supplemented with 1% urea for 5 days from day 13 to day 17 of lactation. It is of interest to describe here that oral intake of a urea plus milk diet resulted in marked hypersecretion in PI cells of suckling dams more significantly than that of a milk diet only.

The development of polydipsia and polyurea in old male rats of the Wistar/Tw strain at the age of 16 months has been reported [16–18], but the studies have not focused on the cytology of pituit-

ary PI cells. Polydipsia (137% v/w/day) in mice with hereditary nephrogenic diabetes insipidus (DI) associated with marked hypertrophic and hyperplastic PI has been well documented [12, 13, 19]. Further, electron microscopic observations have revealed that predominant light PI cells contain many electron dense core granules and the sparse endoplasmic reticulum [20]. Thus, polydipsia in DI mice exerts also little effects on the synthesis and release of hormones of PI cells in fine structure. Therefore, it seems reasonable to assume that these polydipsic animals including DI mice as well as normal suckling dams (ca. 75% v/w/day) are in a condition under which hydro-mineral metabolism is regulated within a physiological range. What is the exact meaning of a physiological range in polydipsia remains to be disclosed.

When the pelleted food is absent, suckling dams drink a large amount of liquid milk (164% v/w/day) during the test period, and their pituitary PI cells show small but significant hypersecretion in fine structure (Table 3). In this case animals are considered to be in a nutritionally balanced condition since they are fed with a 11.5% milk diet that is the same concentration used in a human baby. Thus this small change in the PI cell morphology despite copious drinking may be due to either a supply of minerals from a milk diet or less amount of water intake than that of the case of a 5% glucose regimen (oral intake ca. 200% v/w/day) [9].

An interesting new finding in the present study is unexpected hypersecretion in PI cells of suckling dams given a 11.5% milk plus 1% urea diet. Morphometric data in two dimensional analysis clearly indicate the significance of hypersecretion of PI cells. The percent area of the cytoplasm occupied by r-ER, a parameter of protein synthesis, is 2.06 times; and the number of Golgi immature granules, a capacity of granule formation, is 2.02 times; whereas the numerical density of secretory granules reflecting the release of secretory granules is 0.53 times, respectively, when compared to those of suckling mice given a milk diet only (Table 3). These results imply that the rate of degranulation exceeded the rate of both increased protein synthesis and granule formation in PI cells

by twice in magnitude in suckling dams fed a urea plus milk diet. This urea-induced activation of PI cells in mice during lactation is the first report in the present study.

An abnormally high blood urea concentration and increased serum osmolality are apparently associated with the hypertrophy (but not with the hypersecretion) of the pars intermedia of mice with hereditary nephrogenic diabetes insipidus [12, 24]. In their studies, however, causative relationships between the hypertrophy of the PI and the high blood urea concentration in DI mice are not explained. Although it is generally assumed that the cell membranes are freely permeable to urea this assumption has met the conflicting data [21–23]. A high blood urea nitrogen (BUN) concentration is associated with a shift of water from the cells into the extracellular water and blood. Therefore, when the blood urea nitrogen is high, there is variable lowering of the serum sodium concentration due to dilution of the extracellular water [23]. It is uncertain in the present study whether the same mechanism of lowering sodium concentration by a high blood urea nitrogen is involved. Alternatitvely, PI peptides(s) being released by oral intake of excessive urea plus milk diet may have some pivotal functions other than the stimulation of aldosterone secretion by the adrenals as reported before [4, 5]. Further studies on urea mediated activation of PI cells in mice are in progress.

ACKNOWLEDGMENTS

This work was supported in part by a Grant-in-Aid for Scientific Research to Y. K. from the Ministry of Education, Science and Culture of Japan (No. 62540568).

REFERENCES

- 1 Kobayashi, Y. (1974) Quantitative and microscopic studies on the pars intermedia of the hypophysis. I. Dietary effect of brown rice on the kindey, adrenal and pituitary of C57BL/6 mouse. *J. Electron Microscopy*, **23**: 107–115.
- 2 Kobayashi, Y. (1974) Quantitative and microscopic studies on the pars intermedia of the hypophysis. II. Alteration of the pars intermedia and adrenal zona glomerulosa of albino mice following sodium restriction. *Annot. Zool. Japon.*, **47**: 221–231.

- 3 Kobayashi, Y. (1974) Quantitative and microscopic studies on the pars intermedia of the hypophysis. III. Effect of short-term administration of a sodium deficient diet on the pars intermedia of mice. *Cell Tissue Res.*, **154**: 321-327.
- 4 Kobayashi, Y. and Takema, M. (1976) A morphometric study on the pars intermedia of the hypophysis during impairment of the renin-angiotensin-aldosterone system in sodium depleted mice. *Cell Tissue Res.*, **168**: 153-159.
- 5 Kobayashi, Y. (1977) Morphological evidence for a pituitary factor, the pars intermedia hormone, that may stimulate aldosterone secretion by adrenals in sodium depleted mice. In "Hormonal Regulation of Body Fluid." Ed. by H. Oide and Y. Kondo, Proc. 14th Gunma Symp. Endocrinol., pp. 61-74.
- 6 Brownie, A. C. and Pedersen, R. C. (1986) Control of aldosterone secretion by pituitary hormones. *J. Hypertension*, **4**(suppl. 5): s72-s75.
- 7 Davis, J. O. (1962) The control of aldosterone secretion. *The Physiologist*, **5**: 65-86.
- 8 Swartz, S. L., William, G. H. Hollenberg, N. K. Dluhy, R. G. and Moor, T. J. (1980) Primacy of the renin-angiotensin system in mediating the aldosterone response to sodium restriction. *J. Clin. Endocrinol.*, **50**: 1071-1074.
- 9 Kobayashi, Y., Kumazawa, T. and Takeuchi, M. (1984) A new method for inducing copious drinking and the accompanying stimulation of the pars intermedia of the mouse pituitary gland. *Arch. Histol. Japon.*, **47**: 71-77.
- 10 Kobayashi, Y. and Takeuchi, M. (1985) Postnatal development of inhibitory control and suckling-induced activation of pituitary pars intermedia in infant mice. *Proc. Japan Acad.*, **61**(B): 37-40.
- 11 Ebino, K. Y., Yoshinaga, K., Saito, T. R. and Takahashi, K. W. (1988) Coprophagy as an innate behavior in the mouse. *Zool. Sci.*, **5**: 863-868.
- 12 Naik, D. V. and Sokol, H. W. (1970) The hypothalamo-hypophyseal neurosecretory system in mice with vasopressin-resistant urinary concentrating defects. *Gen. Comp. Endocrinol.*, **15**: 59-69.
- 13 Naik, D. V. (1970) Pituitary-adrenal relationships in mice with hereditary nephrogenic diabetes insipidus, with special emphasis on the neurohypophysis and pars intermedia. *Z. Zellforsch.*, **107**: 317-342.
- 14 Schneider, E. G., Radke, K. J., Ulderich, D. A. and Taylor, Jr., R. E. (1985) Effect of osmolality on aldosterone secretion. *Endocrinology*, **166**: 1621-1626.
- 15 Taylor, Jr., R. E., Glass, J. T., Radke, K. J. and Schneider, E. G. (1987) Specificity of effect of osmolality on aldosterone secretion. *Am. J. Physiol.*, **252**: E118-E123.
- 16 Kobayashi, Y. and Kawashima, S. (1980) Polydipsia and polyurea in aged male rats of the Wistar/Tw strain. *Proc. Japan. Acad., Ser. B.*, **56**: 643-648.
- 17 Kobayashi, Y. and Kawashima, S. (1984) Age-related changes in the water and electrolyte metabolism in male rats of the Wistar/Tw strain. *Exp. Gerontol.*, **129**: 107-113.
- 18 Kawashima, S., Kawamoto, K. and Kobayashi, Y. (1986) Aging of the hypothalamo-neurohypophyseal system and water metabolism in rats. *Zool. Sci.*, **3**: 227-244.
- 19 Naik, D. V. (1972) Salt and water metabolism and neurohypophyseal vasopressor activity in mice with hereditary nephrogenic diabetes insipidus. *Acta Endocrinol.*, **69**: 227-244.
- 20 Naik, D. V. (1972) Electron microscopic studies on the pars intermedia in normal and in mice with hereditary nephrogenic diabetes insipidus. *Z. Zellforsch.*, **133**: 415-434.
- 21 Bozler, E. (1961) Distribution of non-electrolytes in muscle. *Am. J. Physiol.*, **200**: 651-655.
- 22 Bradbury, M. W. B. and Coxon, R. V. (1962) The penetration of urea into the central nervous system at high blood levels. *J. Physiol.*, **163**: 423-435.
- 23 Goldberger, E. (1980) A primer of water, electrolyte and acid-base syndromes. Les and Febiger, Philadelphia, 6th ed., pp. 460-462.
- 24 Naik, D. V. and Valtin, H. (1969) Hereditary vasopressin resistant urinary concentration defects in mice. *Am. J. Physiol.*, **217**: 1183-1189.

Formation of Ganglions and Stomodaeum in Normal and Separate Embryos of Horseshoe Crab, *Tachypleus tridentatus*

TOMIO ITOW, TATSUYA MASUDA and KOICHI SEKIGUCHI¹

Department of Biology, Faculty of Education, Shizuoka University,
Shizuoka 422, and ¹Jobu University, Shin-Machi,
Gunma 370-13, Japan

ABSTRACT—The process of formation of ganglions and stomodaeum was examined in normal embryos and separate embryos whose stomodaea did not pass through the middle of the nervous system. The following facts were established. 1) The structure of the stomodaeum is recognizable after stage 14. 2) The cell masses of ganglions are observed clearly after stage 16; the commissures are stained by eosin after stage 19. 3) The final number of ganglions is settled by stage 19; this means that the formation of segment primordia is settled by stage 19. 4) The stomodaeum passes through the area between the commissure of the first prosomatic ganglions (chelicera segment) and that of the second ganglions. 5) The crossing of the stomodaeum and the nervous system is thought to be formed at stage 18–19. 6) The crossing is constructed during the clustering of the cells composing the brain; the stomodaeum does not determine the pathway for the clustering of these cells. 7) The position of the mouth is not appropriate as an indicator for determination of homologous segments among arthropodan species. 8) The crossing does not constitute a valid reason for rejecting the idea that Deuterostomia have originated from Protostomia.

INTRODUCTION

The morphology and embryology of the horseshoe crab have been described by many authors [*Tachypleus tridentatus*: 1–3; *Limulus polyphemus*: 4–7]. However, not all structures and processes have yet been clarified. Study of the formation of ganglions and stomodaeum, especially the crossing between the nervous system and the stomodaeum, remains incomplete. The present study tries to make this process clear for the Japanese horseshoe crab, *Tachypleus tridentatus*. For this purpose, we examined the formation of ganglions and the stomodaeum in normal embryos. We also examined the process in separate embryos whose stomodaea did not pass through the middle of the nervous system. Such embryos are formed by treatment with calcium-free seawater or DNA synthesis inhibitors [8, 9].

The cause of release of the crossing of the nervous system and stomodaeum is discussed in

the light of cell construction during the process of embryonic development. As the crossing is a remarkable characteristic of Protostomia, the possibility for change of form and structure in macroevolution is also considered.

MATERIALS AND METHODS

Adult Japanese horseshoe crabs, *Tachypleus tridentatus* (Chelicerata, Arthropoda), collected in north Kyushu, Japan, were brought to Shizuoka University, where eggs were inseminated artificially. The developmental stages of the embryos were determined from Sekiguchi's normal table [2].

The separate embryos were obtained by 24-hr treatment with calcium-free seawater, 10^{-1} M NaHCO_3 or inhibitors of DNA synthesis (10^{-2} and 5×10^{-2} M hydroxyurea and 10–25 $\mu\text{g}/\text{ml}$ azaserine). The treatment stages are described in the results.

Normal embryos and ones given these chemical treatments were stained vitally with neutral red and observed under a stereomicroscope. Normal and treated embryos were also fixed in Bouin's,

Carnoy's, or FAA (formalin-70% ethanol-acetic acid, 5:15:1) solutions, embedded in celloidin and paraffin, and sectioned at 5–20 μm . The sections were stained with Mayer's hematoxylin and eosin. Some normal embryos and larvae were dissected for an examination of the nervous system and alimentary canal.

RESULTS

Formation of ganglions and stomodaeum in normal embryos

In this paper, the ganglions in the front area of the 1st prosomatic segment (except for ganglions of the 1st segment) are called the brain.

Enlargement of the germ disc of the horseshoe crab finished at stage 10 (stage of completion of germ disc). Obvious morphogenetic movement started at stage 10. Observation with time-lapse cinemicrography in the previous study [10] had shown that the formation of the stomodaeum begins at the stage of morphogenetic movement (stage 11). The stomodaeum appeared at the anterior margin of the embryonic area. The position of the stomodaeum differed from that of the blastopore. In this process, two narrow bands are formed along the median body axis; these narrow bands may be early nervous systems.

At the stage of the appearance of prosomatic appendages (stage 14), the stomodaeum was observed as a tubular structure. The existence of neuroblasts which would become the brain was

recognized, but construction of the brain was not yet complete (Fig. 1).

Ganglions could be observed in embryos fixed at the stage of development of prosomatic appendages (stage 16). The opening of the stomodaeum (mouth) could be observed clearly at the area in front of the 1st prosomatic segment (segment with chelicera = 1st prosomatic appendages). However the development of the brain and other ganglions was incomplete, the commissures of ganglions in particular being under-developed. The formation of the epithelium of the stomodaeum proceeded further at stage 16.

When embryos at the stage after the 1st embryonic moulting (stage 18) were stained with neutral red, nervous systems were stained clearly. A brain and 9 pairs of ganglions could be observed. The commissures of the ganglions were not clear in the stained embryos or sectioned specimens, although they were recognized in fixed embryos. The mouth began to migrate posteriorly at stage 18; it was situated in the region of the 1st prosomatic segment at this stage.

At the stage after the 2nd embryonic moulting (stage 19), the commissures became clear. The neurofibers developed and were stained easily with eosin. The mouth migrated to the region of the 3rd prosomatic segment. The stomodaeum passed through the area between the commissure of the 1st prosomatic segment and that of the 2nd one.

All the ganglions were formed by stage 19; that is, the formation of all segment primordia was complete at this stage. The mouth was situated in

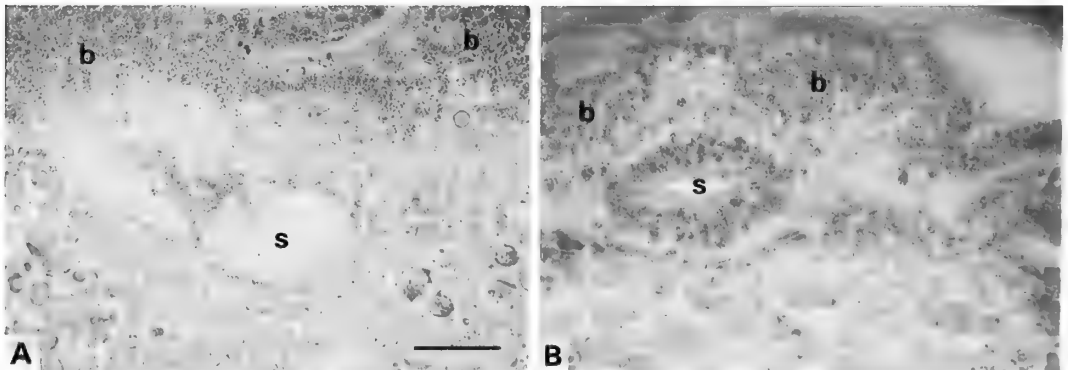


FIG. 1. The histological features in the neighboring region of the stomodaeum. A. Stage 14. B. Stage 16. b; prospective region of the brain, s; stomodaea. The bar shows 0.05 mm.

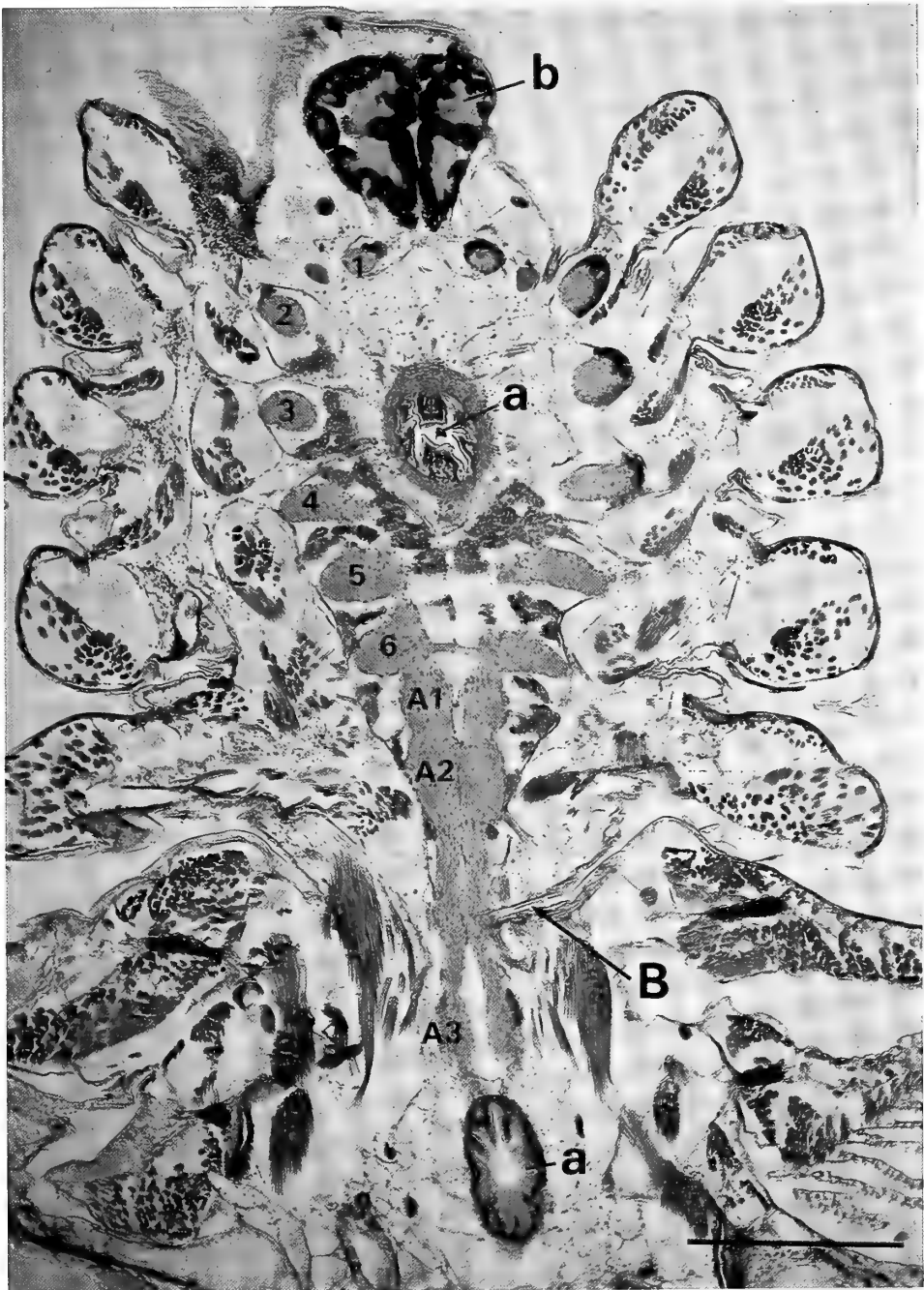


FIG. 2. The horizontal section of a 2nd instar larva. a; alimentary canal, b; brain, 1-6; each cephalothoracic ganglion, A1-A3; each abdominal ganglion, B; border between prosome and opisthosome. The number of pairs of prosomatic ganglions except for the brain is eight. The bar shows 0.5 mm.

the region between the 3rd and 4th prosomatic segments. The position was the same as that in the adults.

The embryos at stage 21 (the stage after the 4th embryonic moulting) have the same form and structure as the 1st instar larvae. At this stage the

circumbuccal part (the structure of the peristome) was formed completely. The stomodaeum was well developed and differentiated. As a result, the proventriculus (fore-gut) and intestine (mid-gut) were also differentiated. However, there was yolk in the intestine, and the formation of the

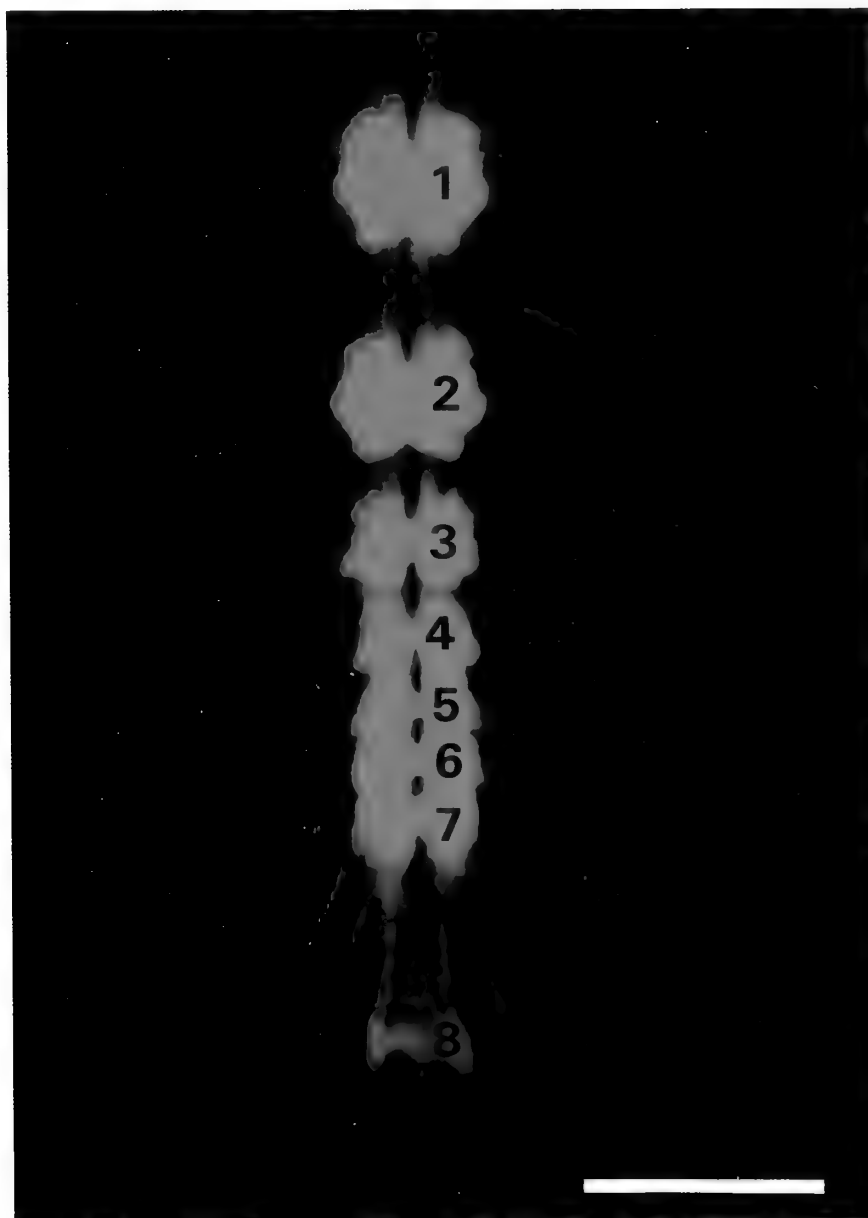


FIG. 3. The opisthosomatic nervous system of the 2nd instar larva. 1-8: each opisthosomatic ganglion. The 1st and 2nd abdominal ganglions belong to the prosome. The 1st opisthosomatic ganglion is equal to the 3rd abdominal one. The bar shows 0.5 mm.

alimentary canal was not complete.

The condition and position of the brain and other ganglions of the 1st instar larvae were similar to those of the 2nd instar larvae. In these larvae all the prosomatic ganglions had commissures. In the border area between the prosome and opisthosome there were no ganglions without appendages (Fig. 2). The prosome had a brain and 8 pairs of prosomatic ganglions. The prosomatic ganglions consisted of 6 pairs of cephalothoracic ganglions and 2 pairs of abdominal ganglions (ganglions of chilaria and operculum). The shape of the cephalothoracic ganglions differed from that of the abdominal ones. The opisthosome had 8 pairs of ganglions (the rest were abdominal ganglions) (Fig. 3). The shapes of the opisthosomatic ganglions were similar to those of the abdominal ganglions in the prosome.

The alimentary canal of the 2nd instar larva was complete. At this stage, formation of intestine was finished and the larvae began to eat.

Release of the crossing of the nervous system and stomodaeum in separate embryos

Calcium-free seawater, NaHCO_3 and inhibitors of DNA synthesis induced the separate embryo (Table 1, Fig. 4). The ventral plate of the separate embryo was divided into an anterior region and a posterior region.

The conditions of induction were as follows. When embryos were treated for 24 hr with calcium-free seawater or NaHCO_3 at stages 7, 8 and 9 (stage of enlargement of the germ disc, the gastru-

la stage), they developed into the separate embryos whose ventral plates were separated mainly at the region between the 3rd and 5th prosomatic segments. When treated for 24 hr at stages 10 and 11 (stages of obvious morphogenetic movement), the ventral plates of the treated embryos were separated mainly at the 2nd and 3rd prosomatic segments. Following treatment for 24 hr with an inhibitor of DNA synthesis at the stage of enlargement of germ disc, the treated embryos developed into separate embryos, whose ventral plates were separated mainly at the 2nd and 3rd prosomatic segments.

When embryos at the stage of enlargement of the germ disc were treated with calcium-free seawater or NaHCO_3 , the connection between cells composing the germ disc was weakened. Their ventral plates were separated mainly at the region between the 3rd and 5th segments of the cephalothorax, which was formed in the process of enlargement of the germ disc. When embryos at the stage of enlargement of the germ disc were treated by inhibitors of DNA synthesis, cell proliferation of germ disc became incomplete and the cell density of the germ disc became low in spite of normal spreading of the germ disc. The incomplete germ disc was separated mainly at the 2nd and 3rd prosomatic segments in the process of obvious morphogenetic movement. During the movement, the embryonic area elongated anteriorly and posteriorly at the region where the 2nd and 3rd prosomatic segments had recently been formed. Calcium-free seawater and NaHCO_3

TABLE 1. The frequency of formation of separate embryos. The embryos were treated for 24 hr either at the stage of enlargement of the germ disc (I) or at the stage of obvious morphogenetic movement (II)

		Separate embryo Number (%)	Developed embryo Number (%)
[I]	Hydroxyurea 5×10^{-2} M	134 (32.1)	318 (74.2)
	Azaserine 25 $\mu\text{g}/\text{ml}$	73 (16.7)	436 (68.4)
[II]	NaHCO_3 10^{-1} M	20 (19.2)	104 (13.4)
	Ca^{2+} -free seawater	57 (29.2)	192 (43.3)
	Normal seawater	6 (0.1)	6,829 (100.0)

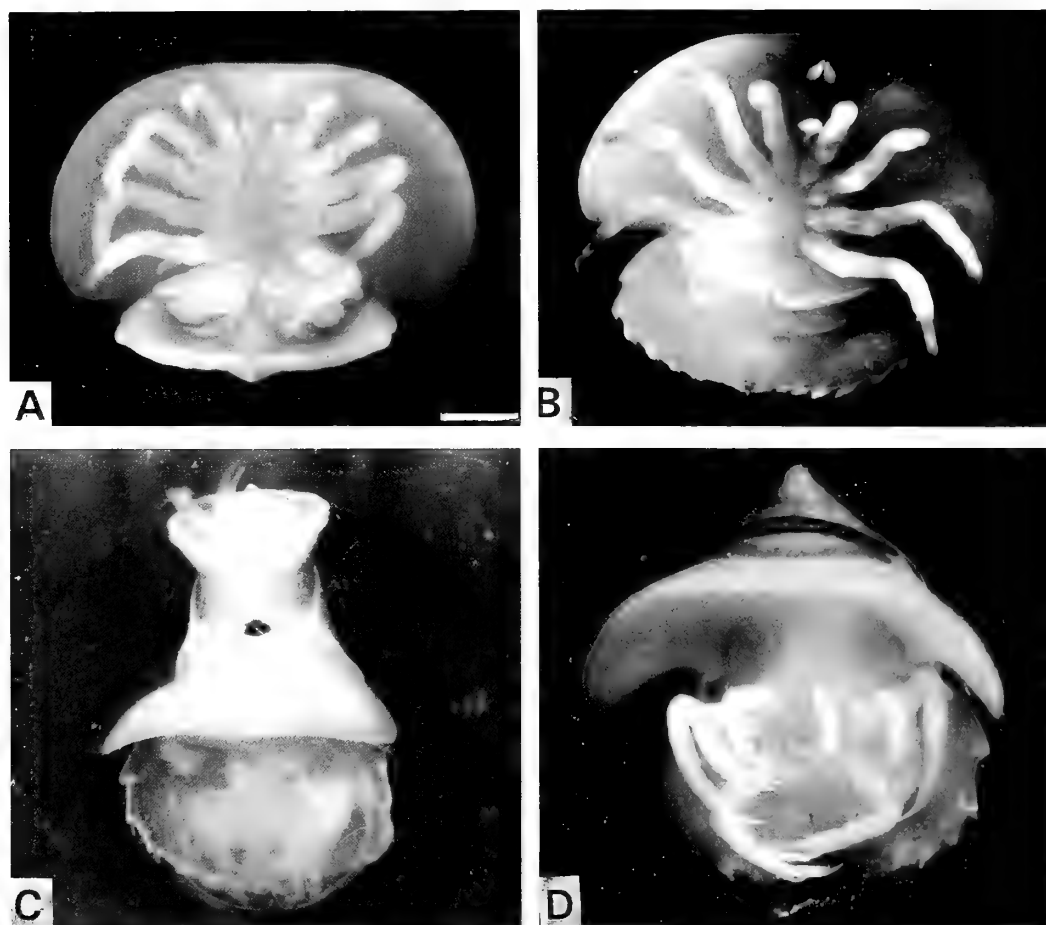


FIG. 4. Examples of a normal embryo and separate embryos. A: A normal embryo (stage 20). B: An incomplete separate embryo (stage 20) whose ventral plate is separated at the point between the 1st prosomatic segment and the 2nd one. C: A complete separate embryo (stage 21) whose ventral plate is separated at the point between the 3rd prosomatic segment and the 4th one. D: A complete separate embryo (stage 21) whose ventral plate is separated at the 2nd prosomatic segment. The 2nd appendages are lost. The bar shows 0.5 mm.

directly affected the central region of elongation at the stage of obvious morphogenetic movement. The ventral plates of the treated embryos were separated mainly at the 2nd and 3rd prosomatic segments.

The form and structure of the separate embryos depended on the position of separation. It was impossible to recognize any difference between embryos induced by different reagents, if the position of separation was the same. In addition the separate embryos obtained in normal seawater had the same characteristics as those of the separate embryos obtained by treatment with chemical reagents.

The separate embryos could be classified into the complete and incomplete separate ones. The ventral plate of the complete separate embryo was separated completely, but that of the incomplete one was not. The central nervous systems of both types of separate embryos were separated at the position of separation of the ventral plate, although light microscopy did not reveal clearly the very fine nervous fibers. On the other hand, alimentary canals were not separated in any type of embryo.

In some of the separate embryos, the stomodaea passed through the middle of the brain. The crossing of the nervous system and stomodaeum

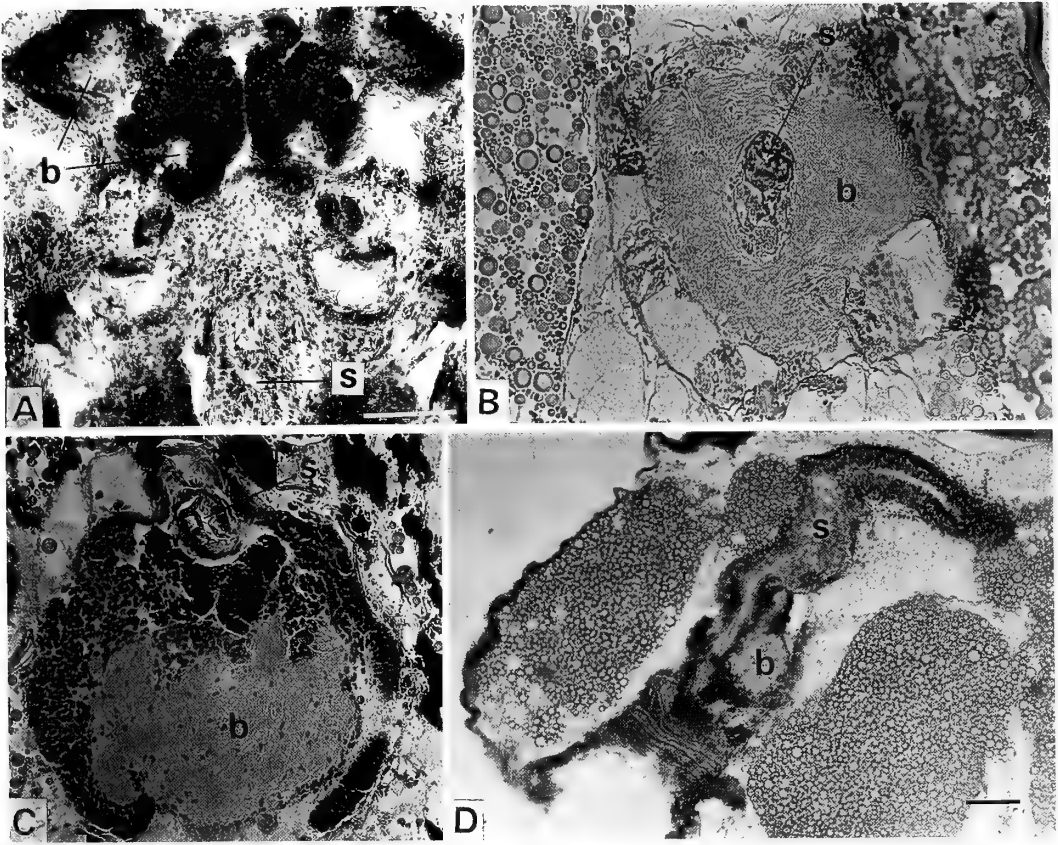


FIG. 5. The brains and stomodaeum in a normal embryo and in separate ones at stage 20. A: A horizontal section of a normal embryo. B: A horizontal section of a separate embryo whose ventral plate is separated at the 2nd prosomatic segment. The stomodaeum passes through the middle of the brain. C: A horizontal section of a separate embryo whose ventral plate is separated at the region between the 1st prosomatic segment and the 2nd one. The stomodaeum and the nervous system do not cross each other. D: A longitudinal section of a separate embryo whose ventral plate is separated at the same region as in "C". "B" and "C" were taken at the same magnification. The bars indicate 0.1 mm.

was released in some of the separate embryos (Fig. 5). Release of the crossing was observed in both types of separate embryo, the complete separate embryos and the incomplete ones. This means that the release of the crossing was not related directly to the degree of separation, but it was related closely with the position of separation, that is, the extent of the anterior region of the separate ventral plate (Fig. 6). When the anterior region had more than three pairs of appendages, the stomodaeum passed behind the brain and both structures crossed each other. When it was moderate, the stomodaeum passed the middle of the brain. When the anterior ventral plate of the separate

embryos had no or only one pair of cephalothoracic appendages, the crossing was released. The size of the posterior region of the separate ventral plate was not related directly to the release of the crossing of the nervous system and stomodaeum.

In embryos which had lost the anterior ventral plates (no-anterior embryos), there was no brain or stomodaeum. In the separate embryos whose ventral plates were separated at the 1st prosomatic segment, the neuroblasts of the brain were clustered behind the stomodaeum and formed the brain at this position. Crossign of the nervous system and stomodaeum did not occur (Fig. 7).

Anterior piece \ Posterior piece				
	behind 5th prosomatic segment	behind 4th prosomatic segment	behind 3rd prosomatic segment	behind 2nd prosomatic segment
Nothing*	X	XX	X	
Only embryonic area (No appendages)		●	●	●●●●
Only 1st appendages	●	●	●● △△	●● △△
1st & 2nd appendages	△△ △△	△△△ △△△ △△△	△△△△△ △△△△△ △△△△△ △△△△△ △△△△△	—
3 pairs of appendages	△ ○	△△△ ○○	—	—

FIG. 6. Release of the crossing of the stomodaeum and nervous system. The schematic diagrams show the features of each piece of the separate ventral plates. Each mark indicates an embryo. X: Embryos having no brains or stomodaea. ●: Nervous systems and stomodaea do not cross each other. △: Embryos whose stomodaea pass through the middle of the brain. ○: Embryos whose stomodaea pass behind the brain (normal position). *: Embryos without anterior pieces of separated ventral plates (=no-anterior embryos).

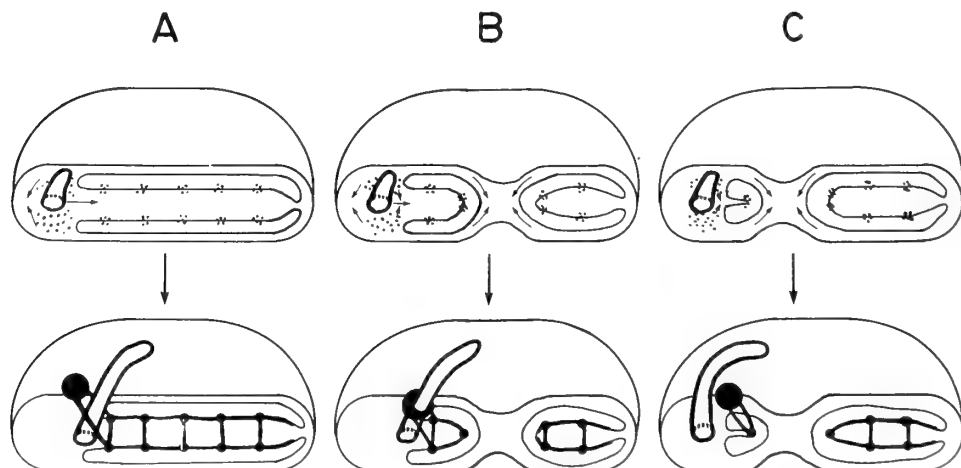


FIG. 7. Diagrammatic representations of development of normal embryos and separate embryos. A: A normal embryo. B: A separate embryo whose ventral plate is separated at the 2nd and the 3rd prosomatic segment. C: A separate embryo whose embryonic area is separated at the 1st prosomatic segment.

DISCUSSION

Several facts about normal embryos are recorded for the first time here. We consider the crossing of the nervous system and stomodaeum.

The tubular structure of the stomodaeum was formed at stage 14. The commissures of the ganglions were not formed at this stage. Remarkably developed commissures were recognizable at stage 19. The opening of the stomodaeum (mouth) first appeared in front of the 1st prosomatic segment. The mouth began to migrate posteriorly at stage 18. These results and the fact that the stomodaeum passed through the area between the commissure of the ganglions of the 1st and 2nd prosomatic segment indicate that the crossing of the nervous system and stomodaeum occurs at stage 18–19.

Prospective cells of the stomodaea and brains were determined before the time of separation of the ventral plates, because regulation did not occur after separation. The prospective cells of the brain were moved by the separation (Fig. 7). When the anterior part of the separate ventral plates was very small, the prospective cells of the brain were situated behind the stomodaeum. As a result the crossing of the nervous system and stomodaeum did not occur.

The release of crossing reveals the following four points. (1) The crossing is constructed through the process of clustering of brain cells. (2) It is not determined that the cells of the brain cluster anterior to the stomodaeum; that is, the stomodaeum does not determine the clustering point of the brain. Further the brain does not determine the pathway of elongation of the stomodaeum. (3) As the position of the mouth is changed easily, it is not appropriate as an indicator of determination of homologous segments among arthropod species [11, 12]. (4) The crossing is susceptible to modification in at least one repre-

sentative Protostomia, the horseshoe crab. Attempts to derive Deuterostomia from Protostomia cannot be rejected because of the crossing of the alimentary canal and central nervous system.

REFERENCES

- 1 Shoji, K. (1929) The horseshoe crab. In "The Anatomy of the Animal III" Ed. by Y. Okada, Kyoritsu, Tokyo, pp. 109–160. (in Japanese)
- 2 Sekiguchi, K. (1973) A normal plate of the development of the horseshoe crab, *Tachypleus tridentatus*. Sci. Rep. Tokyo Kyoiku Daigaku B., **15**: 1253–162.
- 3 Sekiguchi, K. (Ed.) (1984) The Biology of Horseshoe Crabs. Science House, Tokyo. (in Japanese)
- 4 Kigsley, J. S. (1893) Embryology of *Limulus* (part II). J. Morphol., **8**: 195–268.
- 5 Packard, A. S. (1893) Further studies on the brain of *Limulus polyphemus*, with notes on its embryology. Mem. Nat. Acad. Sci., **6**: 289–331.
- 6 Patten, W. (1896) Variations in the development of *Limulus polyphemus*. J. Morphol., **12**: 17–148.
- 7 Scholl, G. (1977) Beitrage zur Embryonalentwicklung von *Limulus polyphemus* L. (Chelicerata, Xiphosura). Zoomorphologie, **86**: 99–154.
- 8 Itow, T. (1979) Experimentally induced separation of embryonic area in the eggs of the horseshoe crab. Bull. Edu. Shizuoka Univ., Nat. Sci., **30**: 5–14.
- 9 Itow, T. (1982) Effect of the glutamine-analogue "azaserine" on embryonic development of the horseshoe crab. Develop. Growth and Differ., **24**: 295–303.
- 10 Itow, T. and Sekiguchi, K. (1980) Morphogenic movement and experimentally induced decrease in number of embryonic segments in the Japanese horseshoe crab, *Tachypleus tridentatus*. Biol. Bull., **158**: 324–338.
- 11 Savory, T. (1977) Arachnida, Academic press, London, 2nd ed., pp 3–6.
- 12 Weycoldt, P. (1979) Significance of later embryonic stages and head development in arthropod phylogeny. In "Arthropod Phylogeny". Ed. by A. P. Gupta, Van Nostrand Reinhold Co., New York, pp. 107–135.

The Genus *Phorticella* Duda (Diptera: Drosophilidae) from Burma and Southern China¹

SOE WYNN², MASANORI J. TODA³ and TONG XU PENG⁴

Laboratory of Genetics, Department of Biology, Tokyo Metropolitan University,
Setagaya, Tokyo 158, Japan, ³Institute of Low Temperature

Science, Hokkaido University, Sapporo 060, Japan, and

⁴Guangdong Institute
of Entomology, Guangzhou, China

ABSTRACT—Three new species of the genus *Phorticella* Duda are reported from Burma and southern China, along with collection records of two known species from Burma.

INTRODUCTION

Okada and Carson [1] resolved the taxonomical confusion among the genera *Phorticella* Duda, *Zaprionus* Coquillett, and the *Drosophila lineosa* subgroup of the *D. immigrans* species-group, all of which are characterized by silvery or chalky white longitudinal stripes on frons and mesoscutum. They included six Oriental, New Guinean and/or Australian species in the genus *Phorticella*, and classified those species into two subgenera, *Phorticella* Duda and *Xenophorticella* Okada et Carson. On the other hand, Okada and Carson [1] and Bock [2] pointed out some affinities between the subgenus *Phorticella* and the subgenus *Scaptodrosophila* Duda of the genus *Drosophila* Fallén. However, taxonomical revision of these subgenera awaits comprehensive phylogenetical analyses including the whole subgenus *Scaptodrosophila*, which is a quite large subgenus including a total of 229 species.

The present paper deals with 3 new species of the genus *Phorticella* from Burma and southern China, along with collection records of 2 known species from Burma.

Genus *Phorticella* Duda

Phorticella Duda, 1923, Ann. Hist.-nat. Mus. Natn. Hung., 20: 36.—Okada and Carson [1], 540. Type species: *Drosophila bistriata* de Meijere, 1911.

Diagnosis. Anterior reclinate orbital usually fine, posterior reclinate near to proclinate than to inner vertical. Epandrium truncate below. Novasternum with 2 or 3 pairs of long submedian spines.

Subgenus *Phorticella* Duda

Phorticella: Okada and Carson [1], 540.

Diagnosis. Frons laterally with broad, silvery white, longitudinal stripes, but without median stripe. Third antennal joint white, except for Australian *Ph. albostrata* (Malloch, 1924) [3]. Tarsi of mid and hind legs without minute cuneiform bristles. Prescutellars absent. Mid sternopleural minute. Male genitalia closely resemble those of *D. (Scaptodrosophila)* species [2].

Other characters commonly seen in the following 3 new species are first described below.

Head: Eye with pile. Second antennal joint brown. Arista with *ca.* 4 upper and *ca.* 2 lower branches in addition to terminal fork. Frons slightly broader than long, with some frontal hairs. Carina low, narrow. Cheek narrow.

Legs: Preapicals on all tibiae; apicals on fore and mid tibiae.

Accepted April 28, 1989

Received March 31, 1989

¹ Drosophilidae (Diptera) in Burma, V.

² Present address: 554 (c), Nei-bain-da road, Nan-tha-gone quarter, Insein township, Insein post office, Yangon Division (Rangoon), Union of Myanmar (Burma).

Wing: R_{2+3} straight; R_{4+5} and M nearly parallel. Haltere white.

Periphallic organs: Epandrial heel prominently protruded; toe round. Cercus separated from epandrium, nearly entirely pubescent. Surstylus somewhat semicircular in caudal view.

Phallic organs: Posterior parameres(?) medially fused to each other.

Phorticella (Phorticella) tortia Wynn

et Toda, sp. nov.

(Fig. 1)

♂, ♀. Body length, ♂ *ca.* 2.2 mm, ♀ *ca.* 2.3 mm. Thorax length (including scutellum) *ca.* 1.1 mm in both sexes.

Head: Eye brownish red. Frons yellowish brown; periorbit dark brown, narrow, restricted to upper half of frons; ocellar triangle dark brown. Anterior reclinate orbital *ca.* 1/3 length of posterior reclinate; proclinate slightly longer than posterior reclinate. Face and cheek yellowish brown; carina brown. Clypeus brown. Cheek *ca.* 1/10 as broad as maximum diameter of eye. Second oral weak, *ca.* 1/2 length of vibrissa. Palpus yellowish white, with *ca.* 5 bristles aligned laterally; terminal bristle longest.

Thorax: Mesoscutum brownish yellow, medially with broad, dark brown, longitudinal stripe which is laterally bordered by slightly silvery yellow stripe from anterior margin to level of anterior dorsocentrals and is broadened between dorsocentrals. Scutellum dark brown, antero-laterally yellowish, apically white. Thoracic pleura brown. Humerals 2. Acrostichal hairs in 6 rows. Anterior dorsocentral *ca.* 3/5 length of posterior; cross distance of dorsocentrals *ca.* 3 times length distance. Anterior/posterior scutellar *ca.* 7/10. Distance from posterior scutellar to anterior almost equal to distance between posteriors. Sterno-index *ca.* 0.8.

Legs brownish yellow; coxae and fore femur darker. Fore metatarsus slightly longer than 2 succeeding tarsal joints together; mid and hind metatarsi as long as 3 succeeding together.

Wing hyaline. Veins brownish yellow; costa slightly clouded at 2nd break; crossveins clear. C1-bristles 2; ventral one weak. Wing indices: C

ca. 1.8, 4V *ca.* 2.6, 4C *ca.* 1.7, 5x *ca.* 2.0, Ac *ca.* 2.4, C3-fringe *ca.* 0.6.

Abdomen: First tergite entirely pale yellow; 2nd laterally with 1 pair of dark brown patches; 3rd and 4th in ♂ and 3rd to 5th in ♀ with broad, dark brown, caudal band medially and laterally protruded; 5th and 6th in ♂ and 6th in ♀ entirely dark brown. Sternites yellowish white.

Periphallic organs (Figs. 1A, D): Epandrium pubescent except anterior and ventral marginal portions, with *ca.* 16–20 bristles; caudoventral part lobular. Surstylus with *ca.* 13 primary teeth on concave distal margin, several small bristles on caudoventral portion and many long spines on inner surface. Cercus narrow, with *ca.* 25 bristles. Decasternum rhomboidal, medially sparsely pubescent (Fig. 1D).

Phallic organs (Figs. 1B, C): Aedeagus laterally hirsute, shaped like torch in lateral view (thus the species name), dorsally bilobed and with 1 pair of small, triangular, marginally serrate flaps; apodeme broad, slightly longer than aedeagus. Anterior paramere long, curved ventrad, apically slightly expanded and round, dorsomedially sparsely hirsute, with *ca.* 9 sensilla aligned along nearly entire length on outer surface. Novasternum somewhat quadrate, broader than long, concave on anterior margin, with 3 pairs of submedian spines on caudal margin; base of submedian spines expanded, forming small lobe.

♀ reproductive organs: Ovipositor (Fig. 1E) apically blunt, with *ca.* 1 bristle-like discal, *ca.* 5 somewhat long apical and *ca.* 16 marginal teeth, and 1 long subterminal and 3 small terminal hairs. Spermatheca (Fig. 1F) broader than long, somewhat quadrangular in lateral view; duct slightly constricted medially in introvert.

Holotype ♂, Burma: Pyin Oo Lwin, 30.XII.1981–6.I.1982, ex trap (Toda); deposited in Entomological Institute, Hokkaido University, Sapporo, Japan (EHU). Paratypes, Burma: 7 ♂, 17 ♀, same data as holotype; in EHU and the collection of senior author (S.W.).

Distribution. Burma (Pyin Oo Lwin).

Relationship. This species is somewhat similar to *Ph. singularis* (Duda, 1924) in having 6 rows of acrostichal hairs, but clearly distinguishable from the latter by color patterns on thorax and legs [1,

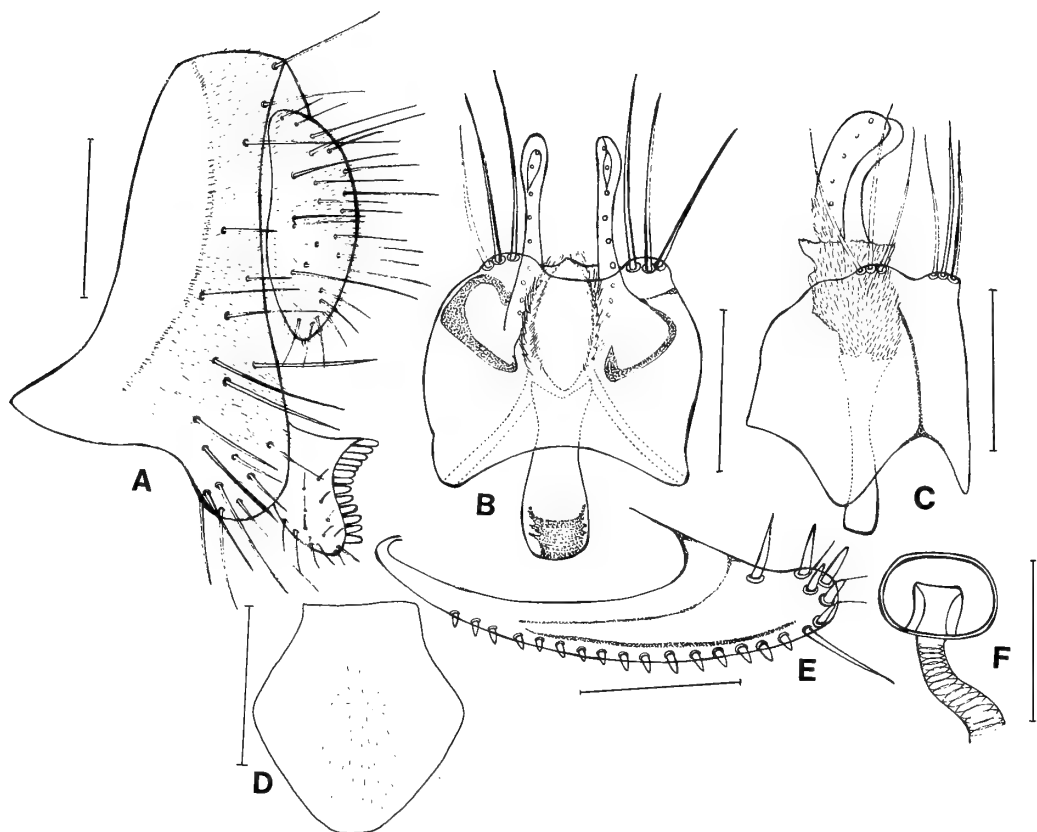


FIG. 1. *Phorticella (Phorticella) tortia* Wynn et Toda, sp. nov. A: Periphallic organs, B: phallic organs (ventral view), C: ditto (lateral view), D: decasternum, E: ovipositor, F: spermatheca. (Scale-line=0.1 mm.)

Fig. 1E] and having 3 pairs of submedian spines on novasternum (2 pairs in *Ph. singularis*).

***Phorticella (Phorticella) htunmaungi* sp. nov.**
(Fig. 2)

This species is very close to the foregoing species, *Ph. tortia*. The following description is made referring only to the differences from the latter.

♂, ♀. Body length, ♂ *ca.* 2.2–2.3 mm, ♀ *ca.* 2.3–2.8 mm. Thorax length, ♂ *ca.* 1.0 mm, ♀ *ca.* 1.1 mm.

Head: Anterior reclinate orbital *ca.* 1/4–1/3 length of posterior reclinate; proclinate as long as posterior reclinate. Carina pale yellow. Cheek width *ca.* 1/10 maximum diameter of eye. Second oral *ca.* 1/3–1/2 length of vibrissa.

Thorax: Mesoscutum dark brown, patterned

as follows: 1 pair of broad, slightly silvery shining pale brown stripes appearing to continue from frontal white stripes and extending posteriorly to level of anterior dorsocentrals; narrow yellowish stripes present medially and along dorsocentral lines; yellowish patches present laterally. Scutellum dark brown, laterally black. Thoracic pleura dark brown. Anterior dorsocentral *ca.* 7/10 length of posterior; cross distance of dorsocentrals *ca.* 2.5–3.3 times length distance. Anterior/posterior scutellar *ca.* 7/10–4/5; posteriors slightly more distant from each other than from anterior. Sterno-index *ca.* 0.7.

Wing indices: C *ca.* 1.7–2.0, 4V *ca.* 2.4–2.9, 4C *ca.* 1.4–1.8, 5x *ca.* 1.9–2.3, Ac *ca.* 2.0–2.3, C3-fringe *ca.* 0.5–0.6.

Abdomen: Second to 4th tergites pale yellow, sublaterally with 1 pair of large or small, dark

brown patches; 5th in ♀ with 3 dark brown patches.

Periphallic organs (Figs. 2A, D): Epandrium with *ca.* 18–20 bristles. Cercus with *ca.* 20 bristles. Decasternum medially densely haired (Fig. 2D).

Phallic organs (Figs. 2B, C): Aedeagus dorsally with small, marginally serrate flap somewhat variable in shape; apodeme as long as aedeagus. Anterior paramere heavily hirsute medially to subapically on dorsal margin, with *ca.* 12 sensilla. Novasternum medially slightly notched and sublaterally with 3 pairs of submedian spines on caudal margin; base of submedian spines not so expanded.

♀ reproductive organs: Ovipositor (Fig. 2E) with *ca.* 5–6 apical and *ca.* 15–18 marginal teeth. Spermatheca (Fig. 2F) hemispherical; introvert slightly annulate.

Holotype ♂, Burma: Pyin Oo Lwin, 30.XII.1981–6.I.1982, ex trap (Toda); in EHU. Paratypes, Burma: 9♂, 4♀, same data as holotype;

pe; in EHU and S.W. China: 1♂, 1♀, Conghua, Guangdong Province, 27.I.1987, by sweeping on tree trunks and forest floor (Toda); Dinghushan, Guangdong Province, 1♀, 5–13.VII.1986, 1♀, 21–27.VII.1986, 1♀, 20–25.II.1987, 2♀, 14–23.V.1987, ex traps (Peng); in the Guangdong Institute of Entomology, Guangzhou, China (GIE) and EHU.

Distribution. Burma (Pyin Oo Lwin), China (Guangdong).

Relationship. As mentioned above, this species is closely related to the foregoing species, *Ph. tortia*, but can be distinguished from the latter by color patterns on thorax and abdomen, denser hairs on anterior paramere and decasternum, and unexpanded base of submedian spines.

Remarks. This species is named in honor of Dr. Htun Maung, the Emeritus Professor of Zoological Department and the Rector of Mandalay University.

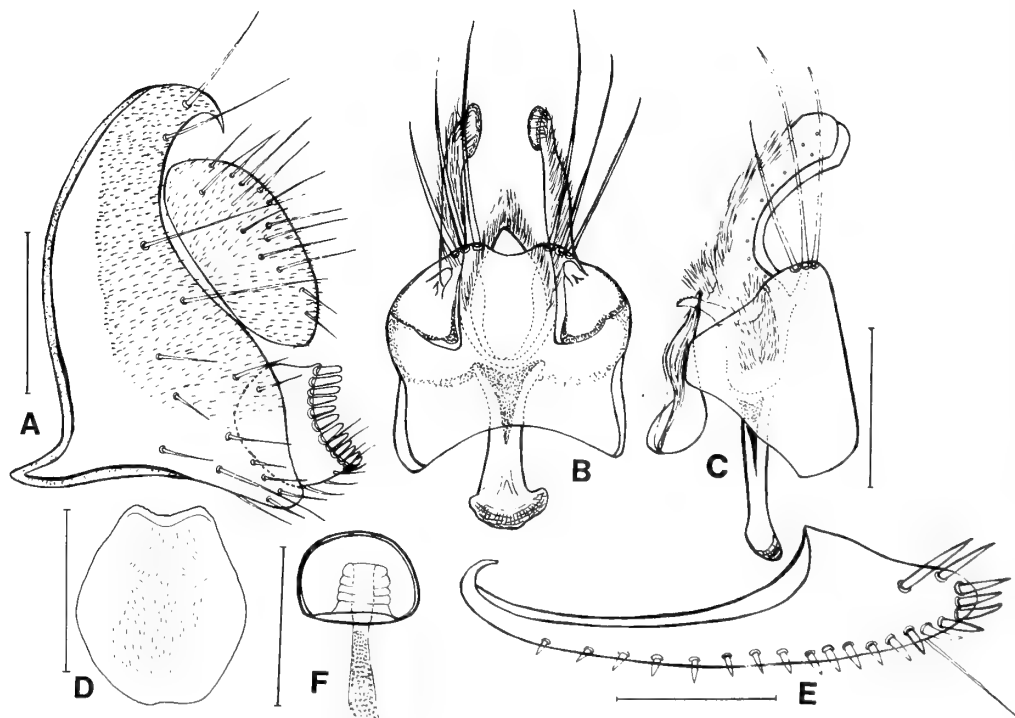


FIG. 2. *Phorticella* (*Phorticella*) *htunmaungi* sp. nov. A: Periphallic organs, B: phallic organs (ventral view), C: ditto (lateral view), D: decasternum, E: ovipositor, F: spermatheca. (Scale-line=0.1 mm.)

***Phorticella (Phorticella) nullistriata* sp. nov.**

(Fig. 3)

♂, ♀. Body length, ♂ *ca.* 2.25 mm, ♀ *ca.* 2.5 mm.

Head: Eye dark red. Frons brown. Carina brown. Clypeus black. Cheek *ca.* 1/20 as broad as maximum diameter of eye. Second oral *ca.* 1/3 length of vibrissa. Palpus grayish white, with *ca.* 3 bristles aligned laterally; terminal bristle longest.

Thorax black, shiny. Mesoscutum without whitish longitudinal stripes (thus the species name). Scutellum laterally dark, apically milky white. Humerals 2, unequal. Acrostichal hairs in 8 rows. Cross distance of dorsocentrals *ca.* 2.4–3.7 times length distance. Anterior/posterior scutellar *ca.* 9/10; posteriors slightly more distant from each other than from anterior. Sterno-index *ca.* 0.8.

Legs: All femora blackish brown, tibiae and tarsi whitish yellow.

Wing somewhat fuscous. C1-bristle 1. Wing indices: C *ca.* 1.6–2.0, 4V *ca.* 2.7–3.0, 4C *ca.* 1.5–1.7, 5x *ca.* 2.5–3.5, Ac *ca.* 2.1–2.5, C3-fringe *ca.* 0.5.

Abdomen: First tergite yellow; 2nd and 3rd in

♂ and 2nd to 5th in ♀ medially yellow, laterally black; 4th to 6th in ♂ entirely black and subshining. First to 3rd sternites yellowish white, 4th to 6th gray or black in ♂; 1st to 6th yellowish white, 7th black in ♀.

Periphallic organs (Figs. 3A, D): Epandrium pubescent except anteroventral portion, with *ca.* 3 bristles on upper part and *ca.* 14 on lower part; anterior and posterior margins nearly parallel. Surstylus with *ca.* 12 primary teeth (upper *ca.* 5 blunt and slightly longer than rest), *ca.* 3 minute bristles at ventral corner and *ca.* 4 minute ones on inner surface. Cercus somewhat oblong, with *ca.* 13 bristles. Decasternum consisting of 2 parts; ventral plate rectangular; dorsal part shirt-like in ventral view (Fig. 3D).

Phallic organs (Figs. 3B, C): Aedeagus hairy, pointed in both ventral and lateral views. Anterior paramere finger like, with a few sensilla aligned in oblique row basally on outer surface. Novasternum hexagonal, with 2 pairs of submedian spines; inner pair much longer than outer pair.

♀ reproductive organs: Ovipositor (Fig. 3E) grayish, apically round, with *ca.* 1 discal, *ca.* 6 apical (ultimate one especially long), *ca.* 10 mar-

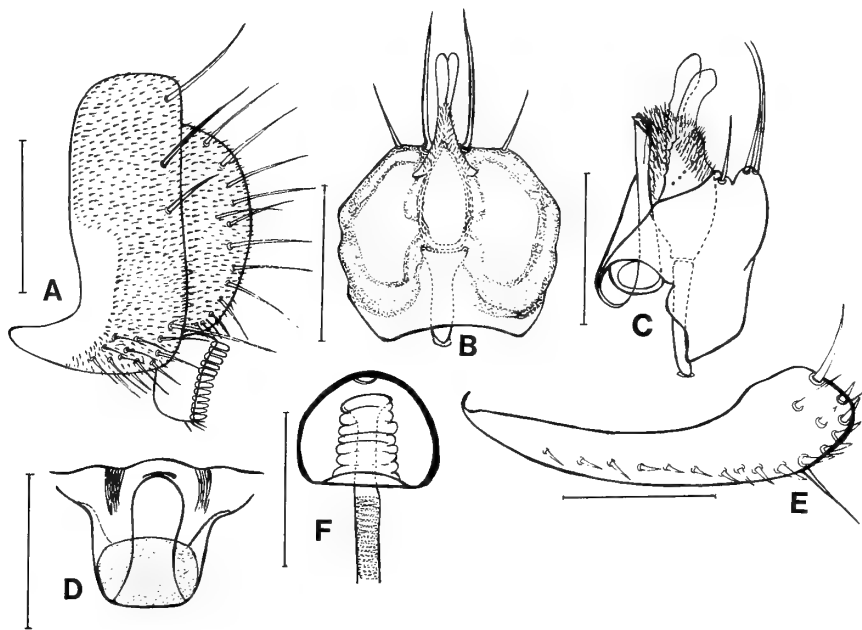


FIG. 3. *Phorticella (Phorticella) nullistriata* sp. nov. A: Periphallic organs, B: phallic organs (ventral view), C: ditto (lateral view), D: decasternum, E: ovipositor, F: spermatheca. (Scale-line=0.1 mm.)

ginal teeth, and 1 long subterminal and *ca.* 2 small terminal hairs. Spermatheca (Fig. 3F) black, umbrella-shaped, apically slightly indented; introvert deep, annulate.

Holotype ♂, China: Guanzhou, Guangdong Province, 23.IX.1986 (Peng); in GIE. Paratypes, China: 3♂, 7♀, same data as holotype; 1♀, same data as holotype except 21–29.XI.1985; 1♀, Dinghushan, Guangdong Province, 24.XI–1.XII.1986 (Peng); in GIE and EHU.

Distribution. China (Guangdong).

Relationship. This species certainly belongs to the subgenus *Phorticella*, because of having white 3rd antennal joint and lateral silvery white longitudinal stripes on frons, but is unique in having no whitish longitudinal stripes on mesoscutum.

Phorticella (Phorticella) bistriata (de Meijere)

Drosophila bistriata de Meijere, 1911, Tijdschr. Ent., **54**: 397 (Java).

Phorticella bistriata: Duda, 1924, Arch. Naturg., **90**(A): 182 (Java).

Phorticella (Phorticella) bistriata: Okada and Carson [1], 540 (Sumatra, Burma).

Zaprionus albicornis Enderlein, 1922, Deutsch. ent. Zeitschr., **1922**: 295 (syn. by Duda, 1926, Suppl. Ent., **14**: 45) (Taiwan).

Drosophila albicornis: Lin and Tseng, 1973, Bull. Inst. Zool. Acad. Sinica, **12**: 22 (Taiwan).

Phorticella fenestrata Duda, 1923, Ann. Hist.-nat. Mus. Natn. Hung., **20**: 36 (as var. of *bistriata*) (Taiwan).

Specimens examined. Burma: 1♀, Pyin Oo Lwin, 30.XII.1981–6.I.1982, ex trap (Toda); 5♂, 2♀, Mandalay, 26.XII.1981–4.I.1982, ex traps (Toda); 1♂, 1♀, Mandalay, 31.XII.1981, by sweeping on tree trunks (Toda); 2♂, Shwebo, 2, 3.I.1982, by sweeping on tree trunks (Toda); 13♂, 8♀, Rangoon, 18, 22.XII.1981, 9, 10, 13, 14.I.1982, by sweeping at ditches and on tree trunks (Toda).

Distribution. China (Taiwan, Guangdong), Java, Sumatra, Burma (Pyin Oo Lwin, Mandalay, Shwebo, Rangoon).

Subgenus *Xenophorticella* Okada et Carson

Xenophorticella Okada et Carson [1], 542. Type species: *Zaprionus flavipennis* Duda, 1929.

Diagnosis. Frons with median, longitudinal, whitish stripe in addition to lateral ones. Third antennal joint gray. Tarsi of mid and hind legs with minute cuneiform bristles.

Phorticella (Xenophorticella) flavipennis (Duda)

Zaprionus flavipennis Duda, 1929, Treubia, **7**: 416 (Buru Is.).

Phorticella flavipennis: Wheeler, 1981, Genetics and Biology of *Drosophila*, **3a**: 73.

Phorticella (Xenophorticella) flavipennis: Okada and Carson [1], 543 (Ryukyu Is., India, Singapore, New Guinea).

Drosophila (Hirtodrosophila) bicolorvittata Singh, 1974, Zool. J. Linn. Soc., **54**: 162 (India).

Phorticella striata Sajjan et Krishnamurthy, 1975, Orient. Ins., **9**: 118 (India).

Phorticella carinata Takada, in Takada and Maki-no, 1981, J. Fac. General Educ. Sapporo Univ., (19): 31 (Ryukyu Is.).

Specimens examined. Burma: 1♂, 1♀, Pyin Oo Lwin, 30.XII.1981–6.I.1982, ex trap (Toda); 8♂, 1♀, Mandalay, 26.XII.1981–6.I.1982, ex traps (Toda).

Distribution. Ryukyu Is., China (Taiwan, Guangdong), Singapore, Burma (Pyin Oo Lwin, Mandalay), India, New Guinea, Moluccas (Buru Is.).

ACKNOWLEDGMENTS

This work was supported by a Grant-in-Aid for Overseas Scientific Survey from the Ministry of Education, Science and Culture, Japan (Nos. 56041049, 57043044, 60041061, 61043056, 62041085).

REFERENCES

- Okada, T. and Carson, H. L. (1983) The genera *Phorticella* Duda and *Zaprionus* Coquillett (Diptera, Drosophilidae) of the Oriental Region and New Guinea. Kontyû, Tokyo, **51**: 539–553.
- Bock, I. R. (1982) Drosophilidae of Australia. V. Remaining genera and synopsis (Insecta: Diptera). Aust. J. Zool., Suppl. **89**: 1–164.
- Bock, I. R. (1976) Drosophilidae of Australia. I. *Drosophila* (Insecta: Diptera). Aust. J. Zool., Suppl. **40**: 1–105.

Early Larval and Postlarval Morphology of the Soldier Crab, *Mictyris brevidactylus* Stimpson (Crustacea: Brachyura: Mictyridae)

YASUSHI FUKUDA

Biological Laboratory, Faculty of Education, Kumamoto University,
Kumamoto 860, Japan

ABSTRACT—The first zoea and megalopa of *Mictyris brevidactylus* are described and illustrated. Their relationships with those of *M. longicarpus* are discussed. The megalopa is unique in having a whorl-like arrangement of setae on the top of the antenna which possibly represents one of the diagnostic characters of either *Mictyris* or Mictyridae.

INTRODUCTION

The soldier crabs, familiar to us especially because of their habits of aggregation on sandy mud flats during low tide, belong to the genus *Mictyris* which is now known to accommodate four species [1, 2]. A Japanese species, *Mictyris brevidactylus*, was first described by Stimpson [3] based upon materials collected from the Ryukyu Islands and Hong Kong, but it has long been considered identical with *M. longicarpus* from Australia [4]. Yamaguchi [5] suggested that there may be ecological, and therefore taxonomic differences between Australian and Japanese populations. Most recently, in his revisionary work of the genus *Mictyris*, Takeda [2] concluded that the Japanese and the Australian forms were specifically different.

The purpose of this study is to provide detailed descriptions of larval and postlarval morphology of *M. brevidactylus*, and to discuss the taxonomic status of the Japanese soldier crab from the viewpoints of larval and postlarval morphology.

MATERIALS AND METHODS

Ovigerous females of *M. brevidactylus*, collected on Amamin-ōshima of the Ryukyu Islands, Febru-

ary 22, 1978, were transported to Kumamoto and reared under laboratory conditions. First zoeas hatched on March 11; but all of them died during the preparation of food supply; the first zoeas were fixed with 50% ethylene glycol for examination. The megalopas here used were collected from the same locality by Dr. T. Yamaguchi on March 1, 1973, and by myself on February 22, 1978. The collected samples of the megalopas are referable to *M. brevidactylus* because of their habitat, and morphology, particularly of the whorl-like arrangement of setae on the top of the antenna as displayed by the Australian *M. longicarpus* [7]. All the specimens were preserved in 75% (ethyl) alcohol. The setation of each appendage is presented from proximal to distal.

Description of first zoea

Size.—Carapace length (distance between tip of rostral spine and posterior margin of carapace) 0.71–0.73 mm (average 0.72 mm); 10 specimens examined.

Carapace (Fig. 1A, B).—Smooth, inflated and globose; lateral and dorsal spines absent; rostral spine overreaching antenna, bearing row of fine setae distolaterally; eyes immovable.

Abdomen (Fig. 1A).—Five somites and telson; somite 1 completely concealed beneath carapace; somite 2 with anteriorly directed lateral process; remaining somites each with small posterolateral

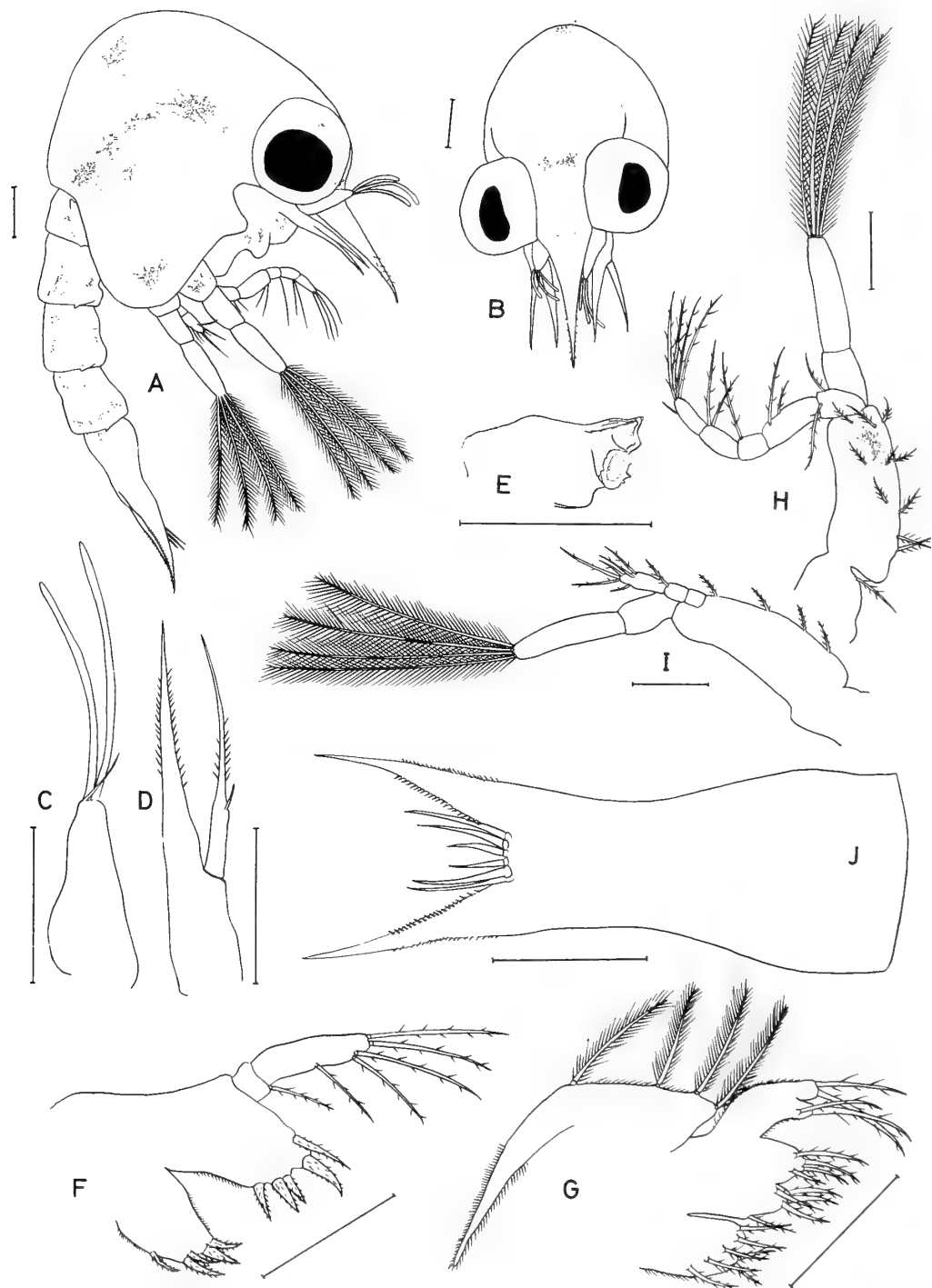


FIG. 1. First zoea of *Mictyris brevidactylus* Stimpson. A, lateral view; B, frontal view; C, antennule; D, antenna; E, mandible; F, maxillae; G, maxilla; H, first amxilliped; I, second maxilliped; J, telson. Scales, 0.1 mm.

spine.

Telson (Fig. 1A, J).—Elongate, medially constricted; furcae slightly curving dorsal, bearing numerous tiny spines on mesial margin and fine setae on lateral margin; posterior margin bearing 6 simple elongate setae.

Antennule (Fig. 1C).—Rod-like, somewhat inflated basally; 2 long aesthetascs and 1 short seta.

Antenna (Fig. 1D).—Protopodal process elongate, bearing a row of spinules on mesial and lateral margin; exopod falling short of end of protopodal process, with 1 spinule at 1/3 of length from proximal end; plus numerous setae mesially and laterally.

Mandible (Fig. 1E).—Molar process short and subcylindrical, with denticles of irregular size; incisor process bluntly bidentate.

Maxillule (Fig. 1F).—Endopod 2-segmented, proximal segment short, 1/4 as long as distal segment, with 1 distolateral seta; distal segment with 1 midlateral, 2 subterminal, 2 terminal setae; coxal and basal endites bearing 5 setose spines each; other pubescence as illustrated.

Maxilla (Fig. 1G).—Endopod distally bifurcate with 2 terminal, 2 subterminal setae; distal and proximal lobes of basal and coxal endites, bearing 4, 5 and 2, 5 setae respectively; scaphognathite with 4 soft plumose setae plus 1 stout, apical plumose projection; fine hairs on margins of endopod, coxal endite and scaphognathite, as illustrated.

First maxilliped (Fig. 1H).—Endopod 5-segmented, with setation of 2, 2, 1, 2, 4+1; exopod 2-segmented, with 4 natatory setae; basis elongate, subcylindrical, bearing 4 groups of setae (2, 2, 3, 3), progressing distally 10 in all as illustrated; coxa with 1 seta.

Second maxilliped (Fig. 1I).—Three-segmented endopod relatively short, about half as long as exopod, with setation of 0, 1, 2+3+1; exopod 2-segmented, with 4 natatory setae; basis elongate and subcylindrical with 4 equidistant setae; coxa naked.

Chromatophores (Fig. 1A, B).—Located at base of rostrum, between eyes, carapacial center, cardiac and postcardiac regions, labrum, mandible, basis of first maxilliped, second through fifth abdominal somites and telson. Color not noted.

Description of megalopa

Size.—Carapace length 1.72–1.81 mm (average 1.77 mm); carapace width 1.41–1.48 mm (average 1.45 mm); 5 specimens examined.

Carapace (Fig. 2A–B).—Posteriorly widened, dorsally convex; 2 tubercular processes on gastric region, each fringed with setae posteriorly; median rostral process very short and strongly deflexed, lateral processes small, directed upward, each with one terminal seta; postero-lateral margin of carapace setiferous; orbit rather shallow; buccal cavern large, nearly trapezoidal.

Thorax and pereopods (Fig. 2A, C, E, F).—Sixth and seventh sternal segments with tubercular process near lateral margin. Pereopods sparsely setose; chelipeds relatively slender, stouter but distinctly shorter than the three walking legs; walking legs somewhat compressed laterally, first leg longest, fourth leg reduced in size, with 5 long branchyuran feelers.

Abdomen (Fig. 2B, D).—Six somites and telson; dorsal surface sparsely setose as illustrated; somites 2–4 with 2 small posterolateral spines on each pleuron; pleuron of somite 5 with single large, acute, posteriorly directed spine; somite 6 unarmed, about half as long as telson.

Pleopods (Fig. 2B, D).—Decreasing in size on somites 2–6; exopods of somites 2, 3, 4 and 5 bearing 18, 18, 18, and 15 natatory setae, respectively; endopods each with 3 small terminal hooks; uropod with 5 long plumose setae.

Antennule (Fig. 3A).—Four-segmented; proximal segment markedly inflated, with 2 lateral spine-like setae; second segment with 1 short lateral seta; third segment with 2 setae at articulation; 6 aesthetascs, 1 subterminal seta on fourth segment.

Antenna (Fig. 3B).—Five-segmented; penultimate segment bearing whorl of 16–18 long setae as illustrated.

Mandible (Fig. 3C).—Incisor process with dentate cutting edge; molar process smooth, not toothed; mandibular palp 3-segmented, ultimate segment with 9 short setose spines on distal half.

Maxillule (Fig. 3D).—Endopod unsegmented with 1 terminal and 2 lateral setae; basal and coxal endites with numerous spines and setae; a long plumose seta at base of endopod.

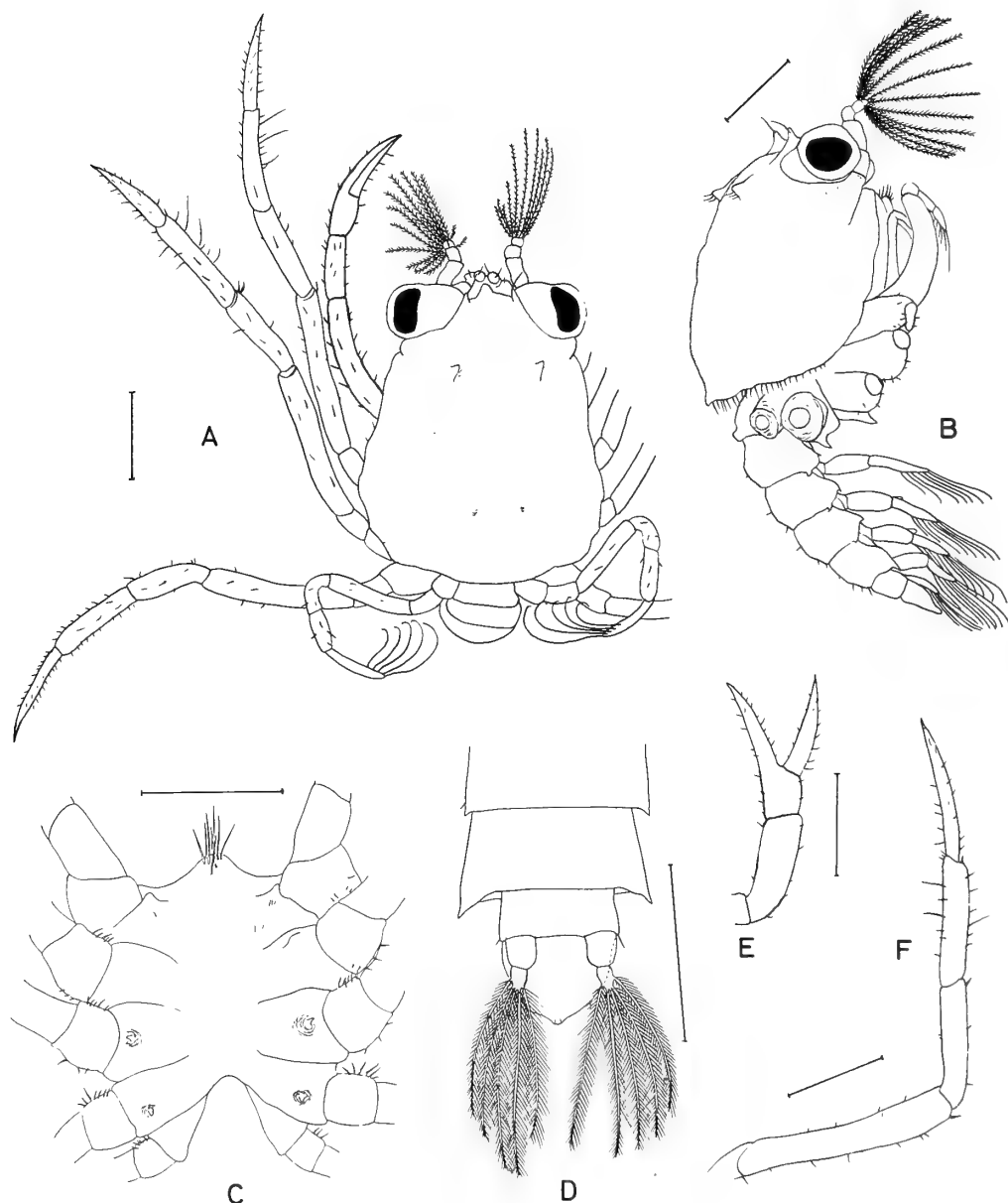


FIG. 2. Megalopa of *Mictyris brevidactylus* Stimpson. A, dorsal view; B, lateral view; C, thoracic sternum; D, posterior half of abdomen and tail fan; E, right chela, interior view; F, right second walking leg, interior view. Scales, 0.5 mm.

Maxilla (Fig. 3E).—Endopod unsegmented, bearing 3 proximal marginal setae; scaphognathite well developed, fringed with 58–62 plumose setae; basal and coxal endites bilobed, distal and proximal lobes bearing 12, 9 and 9, 23–24 spine-like setae respectively.

First maxilliped (Fig. 3F).—Exopod and endopod apparently unsegmented: exopod with 2 long plumose setae at 1/3 of length from distal end, terminal margin with 1 setal nub; endopod without setae but with 2 setal nubs at distal end; epipod roughly triangular, bearing a total of 5 plumodenticulate

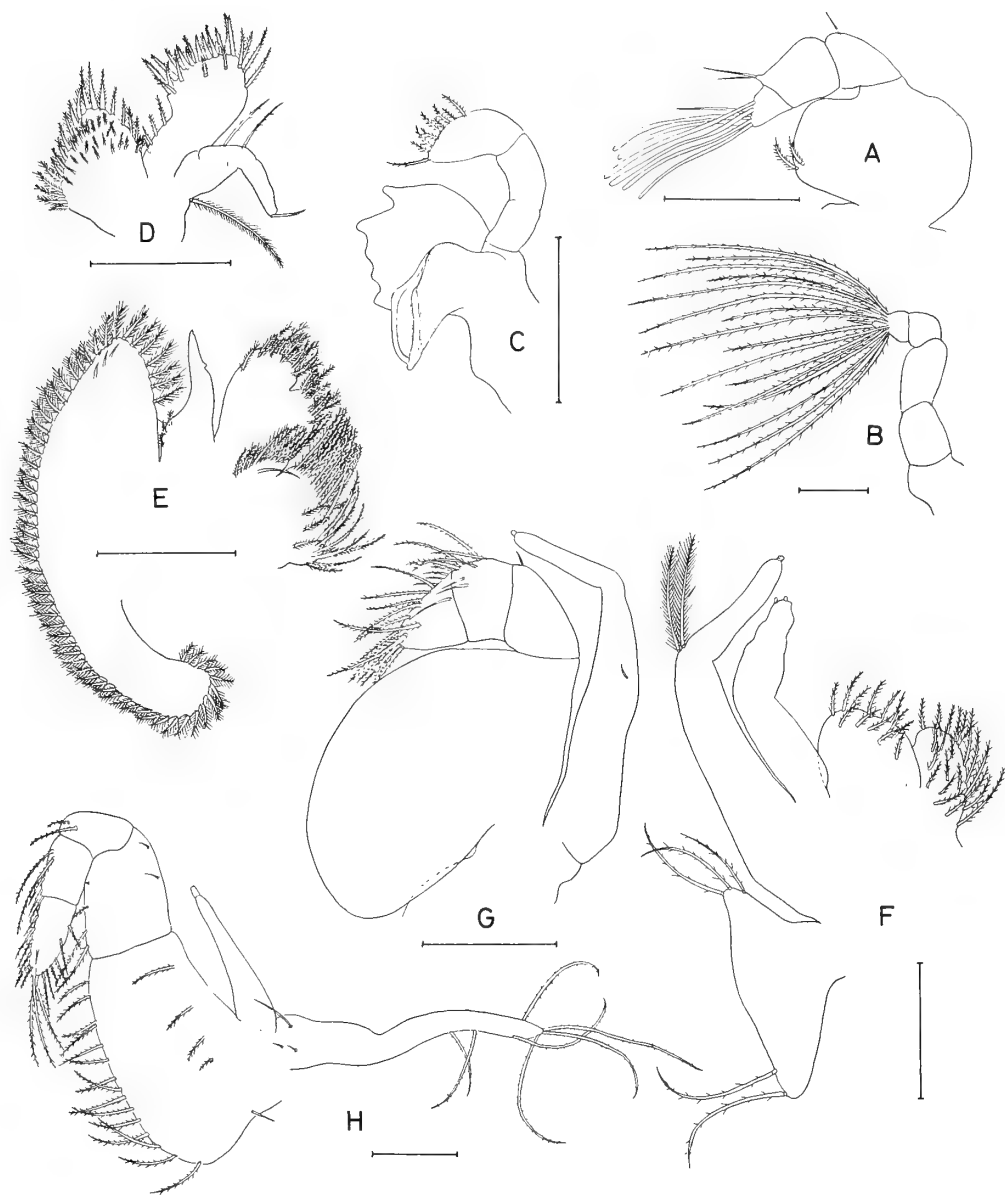


FIG. 3. Megalopa of *Mictyris brevidactylus* Stimpson. A, antennule; B, antenna; C, mandible; D, maxillule; E, maxilla; F, first maxilliped; G, second maxilliped; H, third maxilliped. Scales, 0.2 mm.

setae at corners, as illustrated.

Second maxilliped (Fig. 3G).—Exopod unsegmented with 1 setal nub at distal end; endopod 4-segmented, segment 1 (proximal) very broad and foliaceous naked; segments 2, 3, 4 bearing 1, 8, 15–17 spine-like setae respectively; epipod absent.

Third maxilliped (Fig. 3H).—Exopod reduced in size, terminal margin with 1 setal nub; endopod 5-segmented, with setae as shown; narrowed distally, ischial segment elongate, fully twice as long as meral segment; epipod well developed with several long setae on distal 1/3 of length.

DISCUSSION

Based upon adult morphology, Takeda [2] revised the genus *Mictyris* and concluded that the Japanese and Australian soldier crabs, both previously merged with *Mictyris longicarpus*, are specifically distinct and that the Japanese species should be called *M. brevidactylus* Stimpson. These two species, however, are not remote in distribution. The southern limits of their ranges are rather close, the boundary being placed roughly between the vicinity of the Sulu Sea and the south of the Philippines [1]. Notwithstanding their close range, ecological differences, especially in tunnel feeding habits and wandering activity patterns, have been noted [5]. In addition to these data, the differences between *M. longicarpus* and *M. brevidactylus* are also distinct from the viewpoint of larval and postlarval morphology.

Cameron [6] briefly described the first zoea of *M. longicarpus* obtained from females collected from Moreton Bay, Southern Queensland. Fielder *et al.* [7] provided definitive descriptions of the 5 zoeal stages of that species obtained by rearing, and of megalopas collected on the same shore of Moreton Bay, and thus modified Cameron's definition of the larvae of the species in several respects.

The present data are compared with those of Fielder *et al.* Listed below are the morphological differences in the first zoeas and megalopas between *M. longicarpus* and *M. brevidactylus*.

	<i>M. longicarpus</i>	<i>M. brevidactylus</i>
FIRST ZOEAE		
Exopod of antenna	1 short seta at midlength	without seta
Coxal endite of maxilla	7 spines	6 spines
Basis of first maxilliped	9 spines	10 spines
MEGALOPA		
Molar process of mandible	absent	present
Distal segment	8 spines	9 spines

of mandibular palp

Endopod of maxilla	without seta	3 proximal marginal setae
Exopod of third maxilliped	1 plumodenticulate seta	without seta
Hair formula of uropod	0-6	0-5

These differences are sufficient to warrant the Australian and Japanese populations to be regarded as distinct species. Thus, zoeal and megalopal morphology fully complements the work by Takeda [2] on adults.

The oval, dorsally rounded carapace, the strongly deflexed rostrum, and the very wide buccal cavern containing largely foliaceous endopods of the second and third maxillipeds and slenderly reduced exopods of three pairs of maxillipeds, are very characteristic of megalopa in the genus *Mictyris*. The last two of these seem to be related to the feeding habits, *i.e.* the making of sand pellets during feeding. A similar situation is seen in the megalopa of the ocyrodid crab *Scopimera globosa* [8].

The exopod of the third maxilliped in *M. brevidactylus* lacks a flagellum, whereas that in *M. longicarpus* has a distinct plumodenticulate seta which, however, is possibly lost in the next juvenile stage, for the absence of the flagellum represents one of the familial characteristics of the Micytridae [4, 8].

The antennal whorl of setae, which is shared by the megalopas of both the Japanese and the Australian species of *Mictyris*, has not been recorded in postlarvae of other brachyuran crabs. Very possibly it represents either a generic or a familial characteristic, though no information is available on the two other known species of this genus.

ACKNOWLEDGMENTS

I thank Dr. K. Baba of Kumamoto University and Dr. R. H. Gore, Bio-Econ, Incorporated, Naples, Florida, for reviewing a draft of the manuscript. Thanks are also due to Dr. M. Takeda of the National Science Museum, Tokyo, for his advice regarding systema-

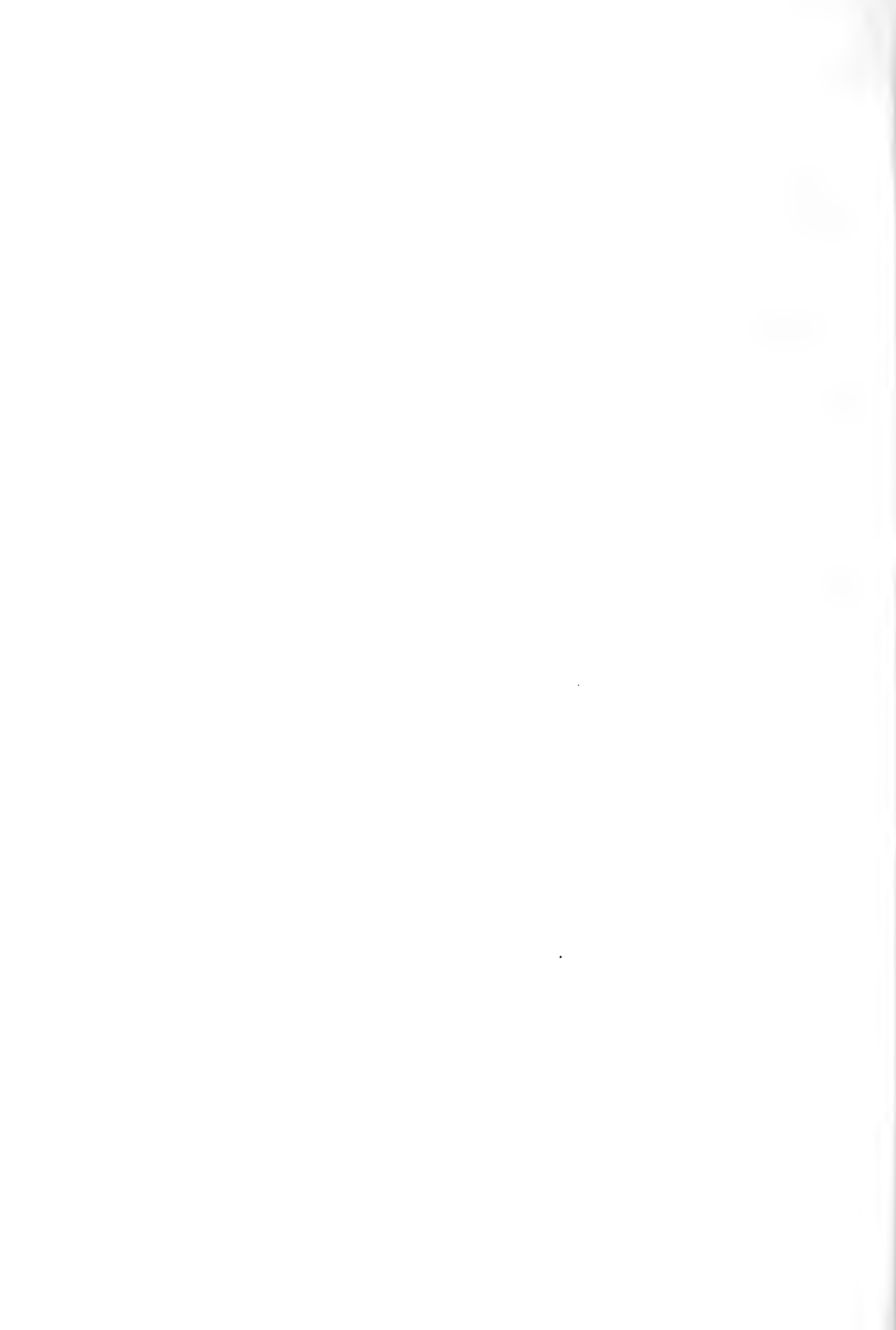
tic treatment of *Mictyris*. I am obliged to Dr. T. Yamaguchi of the Aitsu Marine Biological Station, Kumamoto University, for making specimens of *M. breavidactylus* available for study. I acknowledge Dr. Y. Miya of Nagasaki University and Dr. Y. Nakasone of the University of the Ryukyus, for preparing copies of references at my request. I am also grateful to the anonymous reviewers for making helpful comments on the manuscript.

This study was supported in part by a grant-in-aid from the Ministry of Education, Science and Culture of Japan, No. 57340036.

Contribution No. 52 from the Aitsu Marine Biological Station, Kumamoto University.

REFERENCES

- 1 McNeill, F. A. (1926) Studies in Australian carcinology. No. 2. Rec. Aust. Mus., **15**: 100–131, pls. 9–10.
- 2 Takeda, M. (1978) Soldier crabs from Australia and Japan. Bull. Natn. Sci. Mus., Ser. A (Zool.), **4**: 31–38.
- 3 Stimpson, W. (1858) Prodromus descriptionis animalium evertibratorum, quae in Expeditione ad Oceanum Pacificum Septentrionalem, a Republica Federata missa, Cadwaladaro Ringgold et Johanne Rodgers Ducibus, observavit et descripsit. Pars V. Crustacea Ocypodidea. Proc. Acad. Natl. Sci. Phila., **10**: 93–110.
- 4 Sakai, T. (1976) Crabs of Japan and the adjacent seas. Kodansha, Tokyo. (In 3 volumes: (1) English text, xxix+773 pp. (2) Plates volume, 16 pp., 251 pls. (3) Japanese text, 461 pp.)
- 5 Yamaguchi, T. (1976) A preliminary report on the ecology of the sand bubbler crab, *Mictyris longicarpus* Latreille. Benthos Res. Jap., **11/12**: 1–13. (In Japanese with English abstract)
- 6 Cameron, A. M. (1965) The first zoea of the soldier crab *Mictyris longicarpus* (Grapsoidea: Mictyridae). Proc. Linn. Soc. N. S. W., **90**: 222–224.
- 7 Fielder, D. R., Greenwood, J. G. and Quinn, R. H. (1984) Zoal stages, reared in the laboratory, and megalopa of the soldier crab *Mictyris longicarpus* Latreille, 1806 (Decapoda, Mictyridae). Bull. Mar. Sci., **35**: 20–31.
- 8 Ono, Y. (1965) On the ecological distribution of ocypodid crabs in the estuary. Mem. Fac. Sci., Kyushu Univ., Ser. E (Biol.), **4**: 1–60.



Some *Nesothrips* (Insecta, Thysanoptera, Phlaeothripidae) from East Asia

SHÛJI OKAJIMA

*Laboratory of Entomology, Tokyo University of Agriculture,
Setagaya, Tokyo 156, Japan*

ABSTRACT—Four East Asian species of the genus *Nesothrips* Kirkaldy are reported. *N. brevicollis* sensu Mound (1974) is divided into two species, *N. brevicollis* (Bagnall) and *N. minor* (Bagnall). *N. malacca* Mound is additionally recorded from West Malaysia, Indonesia and the Philippines. An additional new species, *N. yasumatsui* Okajima, is described from Thailand. These thrips are usually found on grass tussocks, dead branches or leaves, and may be fungus-feeders.

The genus *Nesothrips* Kirkaldy belongs to the tribe Pygothripini of the subfamily Idolothripinae, and was revised by Mound in 1974 [1]. In 1983, the related genus *Rhaebothrips* Karny was synonymized with this genus by Mound and Palmer [2]. According to these publications, 22 *Nesothrips* species have been known from the world, and three of them have been known from eastern Asia (exclusive of Oceanic islands). *N. brevicollis* (Bagnall) and *N. lativentris* (Karny) are widespread in the tropical and subtropical regions of eastern Asia, and another species, *N. malacca* Mound, is distributed to West Malaysia and Sumatra.

Two widespread species, *brevicollis* sensu Mound, 1974, and *lativentris*, show intraspecific variation between local populations in colour and structure. It is therefore very difficult to know if two or more species are involved under the respective names. Recently, I had an opportunity to examine a long series of *brevicollis* sensu Mound, 1974, from many localities. After a careful examination, it became clear that two distinct species were involved in the lot. The other species, *lativentris*, is excluded from the present paper, since the material at hand is still insufficient to clarify its status.

In this paper, four *Nesothrips* species from eastern Asia are dealt with; they are: *N. brevicollis*, *N.*

malacca, *N. minor* (Bagnall) which is revived from a synonym of *brevicollis*, and an additional new species from Thailand.

The holotype and most of the paratypes of the new species described hereinafter will be preserved in the Laboratory of Entomology, Tokyo University of Agriculture.

The following abbreviations are used for the five pairs of prothoracic setae: aa, antero-angulars; am, antero-marginals; ml, mid-laterals; pa, postero-angulars; epim, epimerals.

Nesothrips brevicollis (Bagnall, 1914)
(Figs. 1–6, 11–13, 16–17, 19 and 20)

Oedemothrips (?) *brevicollis* Bagnall, 1914 [3], 29–30.

Neosmerinthothrips formosensis Priesner, 1935 [4], 368–372. [Synonymized by Mound, 1974 [1], 162]. *Nesothrips brevicollis*: Mound, 1974 [1], 162–163 (in part).

[*Nesothrips fulviceps*: Kudô, 1974 [5], 115; misidentification].

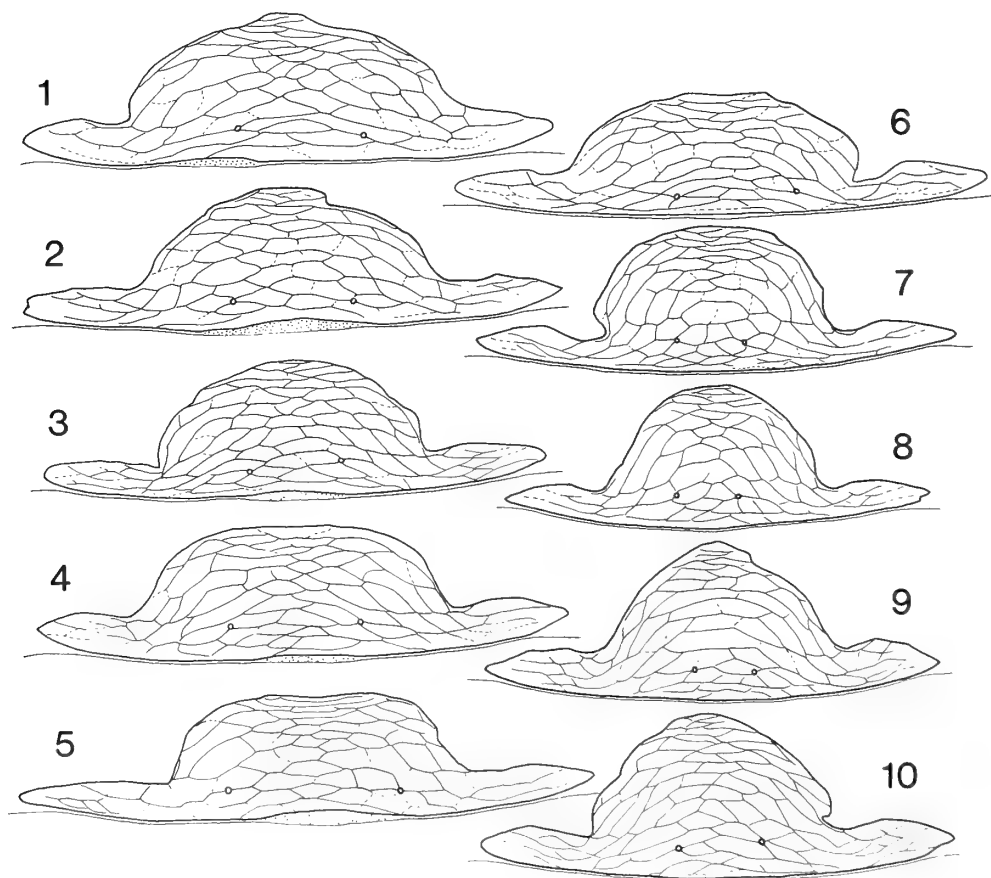
Bagnall [3] described this species only from the apterous form. Recently, Mound [1] treated *Nesothrips minor* (Bagnall), which was described only from the macropterous form, as a synonym of this species. He considered that the two are different morphs of the same species. More recently, however, I studied more than 200 recently collected specimens of *brevicollis* sensu Mound,

1974, from many localities in East Asia and the Hawaiian Islands, and after carefully examining them, came to the conclusion that they included two distinct species. In the present paper, I regard one of them as *brevicollis* (Bagnall) and the other as *minor* (Bagnall).

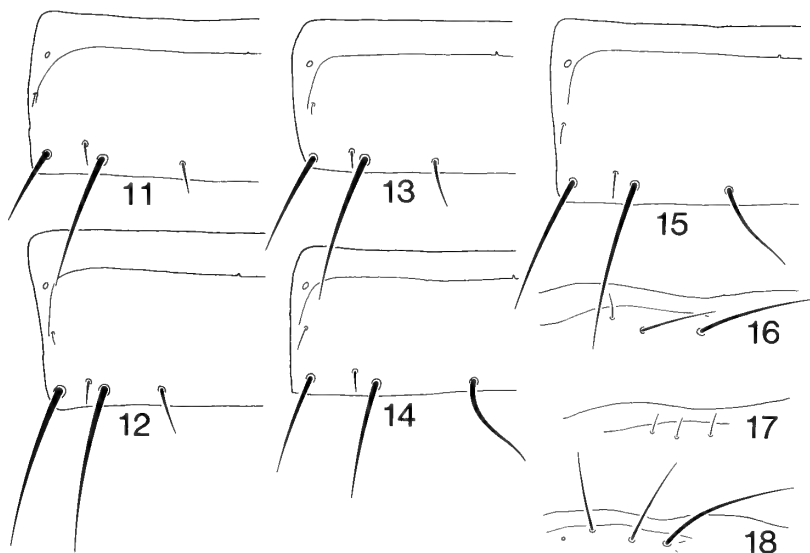
There are some differences between them, which are probably not related to the presence or absence of wings. Relative length of the tube is shorter than the head with rounded sides in *brevicollis*, but longer than the head with rather straight sides in *minor*. The pelta of *brevicollis* is sometimes eroded in median portion of the posterior margin and with somewhat wide median lobe (Figs. 1–6), though that of *minor* is not eroded and

with narrower median lobe (Figs. 7–10), in both macropterae and micropterae. Moreover, the wing retaining setae of *brevicollis* are short and straight (Figs. 11–13), while those of *minor* are long and curved (Figs. 14–15) also in both macropterae and micropterae. In macropterae, only two subbasal wing setae are developed in *brevicollis* (Fig. 16), but three of them are developed in *minor* (Fig. 18). Finally, these two forms show sympatric distribution in the Ogasawara (Bonin) Islands, northwestern end of Micronesia. Judging from these characters and distribution, I consider *brevicollis* and *minor* to be specifically different.

Thus redefined, *N. brevicollis* is distributed to Japan, including the Ryukyu and the Ogasawara



FIGS. 1–10. Female pelta of *Nesothrips* species—1–6, *N. brevicollis*, macroptera from Honshu, Japan (1), macroptera from Ishigaki Is., Ryukyus (2), macroptera from Taiwan (3), microptera from Honshu, Japan (4), aptera from the Ogasawara Isls. (5) and microptera from Okinawa Is., the Ryukyus (6); 7–10, *N. minor*, macroptera from the Ogasawara Isls. (7), macroptera from Hawaii (8), macroptera from Thailand (9) and microptera from Java (10).



FIGS. 11–15. Left half of female abdominal tergite VI of *Nesothrips* species—11–13, *N. brevicollis*, aptera from the Ogasawara Isls. (11), macroptera from Ishigaki Is., the Ryukyus (12) and microptera from Yonaguni Is., the Ryukyus (13); 14–15, *N. minor*, macroptera from the Ogasawara Isls. (14) and microptera from Java (15). FIGS. 16–18. Subbasal wing setae of *Nesothrips* species—16–17, *N. brevicollis* from Honshu, Japan (16) and from Taiwan (17); 18, *N. minor* from the Ogasawara Isls.

Islands, and Taiwan. It is common at certain localities, and is found mainly on grass tussocks. Micropterous (rarely apterous) females and males are usually found but macropterous females are collected only occasionally.

There are some differences between local populations in colour and structure. Specimens from the Ryukyus and Taiwan have somewhat smaller body and paler head, in contrast with specimens from Honshu, mainland of Japan, which have larger body and darker head. Moreover, macropterous females from Taiwan have reduced subbasal wing setae (Fig. 17), and two apterous females from the Ogasawara Islands have somewhat small compound eyes. However, there are some intermediate specimens from the Ryukyus, and there is no evidence that more than one species is involved.

The macropterous female (Figs. 19 and 20) and micropterous male are briefly described below.

Female (macroptera). General structure almost as in micropterous female: Forewings each with 6–11 duplicated cilia; subbasal wing setae B_1 reduced, B_2 and B_3 distinct, B_3 the longest, but they

are reduced in material from Taiwan; wing retaining setae short and rather straight.

Male (microptera). Some of the structures show extreme allometry: Prominent setae of head and prothorax well developed in large male; prothorax and forefemora well developed in large male; foretarsus with a tooth which is variable in shape and size; prothorax with a strong median longitudinal line in large male, without in small male.

Measurements of large (small) males in μm . Total distended body length 1900 (1500). Head length 175 (150), maximum width across cheeks 192 (185); eye length 65 (55). Pronotum median length 175 (110), width 260 (210); forefemur length 230 (130). Abdominal tergites median length/width as follows: II 65 (55)/370 (330); IV 80 (65)/400 (350); VI 110 (90)/405 (340); VIII 95 (85)/280 (255); IX 75 (65)/170 (160). Tube length 145 (125), basal width 90 (78), apical width 44 (40). Antennal segments I to VIII length/width as follows: 38 (37)/40 (35); 50 (48)/34 (31); 63 (57)/30 (30); 65 (55)/31 (30); 68 (58)/32 (30); 57 (48)/33 (30); 43 (38)/26 (25); 30 (25)/13 (13).

Length of setae. Postocellars 60–65 (32–40);

postoculars 98–102 (68–70). Prothoracic aa 35–45 (less than 20), am 28–35 (25), ml 85–105 (43–45), pa 85–98 (48–50), epim 75–77 (60–65). B₁ on tergite IX 80–82 (75–80), B₂ 100–105 (85–88); anals 110–120 (90–95).

Material examined. Taiwan: Makoo, Hookotoo Is., lectotype ♀ (mic.) and 1 paralectotype ♀ (mic.) of *Neosmerinthothrips formosensis*, 5-vi-1930, S. Minowa (in coll. Senckenberg Museum, Frankfurt); Pintung Hsien, Kenting National Park, on grass, 1 ♀ (mic.) 25-v-1972, 2 ♀ 1 ♂ (mic.) and 1 ♀ (mac.) 18-iii-1984, 2 ♀ 3 ♂ (mic.) and 2 ♀ (mac.) 19-iii-1984, S. Okajima; Kaohsiung Hsien, Liukuei, 2 ♀ (mic.) on bush, 22-iii-1984, S. Okajima; Nantou Hsien, Nanshanchi, on grass 3 ♀ 1 ♂ (mic.) 25-iii-1984, 2 ♀ (mic.) 30-iii-1984, S. Okajima; Nantou Hsien, foot of Mt. Nonkao, nr. Wanta, 1 ♀ (mic.) on grass, 1-iv-1984, S. Okajima; Taipei Hsien, Mt. Tatung-shan, 2 ♀ 1 ♂ (mic.) on grass, 4-iv-1984, S. Okajima; Lan-Yu, 2 ♀ (mic.) 6-vi-1980, H. Makihara. Japan, the Ryukyus (including Satsunan Is.): Yonaguni Is., Mt. Urabu, 2 ♀ (mic.), 19-iii-1977, W. Suzuki; Yonaguni Is., Sonai, 1 ♀ (mic.) on dead oak, 29-iii-1975, S. Saito; Ishigaki Is., 1 ♀ (mac.), 6-vi-1971, S. Okajima; Ishigaki Is., Mt. Omoto, 1 ♀ (mic.) 12-vi-1972, 1 ♀ (mic.) 14-vi-1972, S. Okajima; Ishigaki Is., Hirakubo, 3 ♀ (mic.) on *Miscanthus*, 15-vi-1972, S. Okajima; Iriomote Is., Sonai, 2 ♀ (mic.) on dry twigs, 19-vi-1972, S. Okajima; Iriomote Is., Mt. Tedou, 1 ♀ (mic.) on dead Palmae, 19-vi-1972, S. Okajima; Okinawa Is., Nago, 2 ♀ 1 ♂ (mic.) on dead leaves, 13-v-1972, S. Okajima; Okinawa Is., Katsuyama, 2 ♀ (mic.) on dead leaves, 2-viii-1973, S. Okajima; Yuku Is., Onoaida, 9 ♀ 2 ♂ (mic.) on *Miscanthus*, 6-i-1972, K. Haga. Japan, Honshu: Kyoto Pref., nr. Shizuhara, 1 ♀ (mic.) and 1 ♀ (mac.) on grass, 6-viii-1980, S. Okajima; Aichi Pref., Nisshin Nokata, 1 ♀ (mic.) in soil, 13-i-1986, T. Kato; Fukui Pref., Tsuruga, Shiraki, 4 ♀ (mic.) on dead branches, 7-vii-1978, S. Okajima; Kanagawa Pref., nr. Tsukui, 2 ♀ 1 ♂ (mic.) on grass, 10-x-1982, S. Okajima; Yamanashi Pref., nr. Fujiyoshida, 1 ♀ 1 ♂ (mic.) on grass, 30-vii-1981, S. Okajima; Chiba Pref., Ichikawa-shi, lower reaches of Riv. Tonegawa 10 ♀ 1 ♂ (mic.) and 5 ♀ (mac.) on grass, vi-1983, R. Terakoshi; Akita Pref., Honjoh-shi,

lower reaches of Riv. Koyoshi-gawa, 15 ♀ 8 ♂ (mic.) and 4 ♀ (mac.) on grass, 9-vii-1988, S. Okajima. Japan, Ogasawara Islands: Chichi-jima Is., Mt. Asahi-yama, 1 ♀ (apt.) on dead branches, 11-iii-1988, S. Okajima; Haha-jima Is., nr. Minami-zaki, 1 ♀ (apt.) on grass, 5-iii-1988, S. Okajima.

Nesothrips malacciae Mound, 1974

(Fig. 21)

Nesothrips malacciae Mound, 1974 [1], 164–166.

This species was described by Mound [1] based on three females from West Malaysia and Sumatra. Recently, additional females and males were collected from West Malaysia, Indonesia (Sulawesi and Bali) and the Philippines (Luzon and Mindanao). These records suggest its wide distribution in Southeast Asia.

All females and males of this species are macropterae, micropterae still having been unknown. There are some differences between local populations in colour of the legs and antennae. Specimens from West Malaysia have the third antennal segment largely brown and all femora brown with distal third yellow, but specimens from southern Sulawesi have the third antennal segment yellow to brownish yellow and all femora brown with distal half yellow. However, those from central Sulawesi, Bali and the Philippines are something intermediate between them.

The males are recorded for the first time, and a brief description is given below based on a male from West Malaysia.

Male (macroptera). Colour almost as in female. Head (Fig. 21) 0.88 times as long as broad; postocular setae longer than half the length of head, postocular and middorsal (vertexal) setae well developed; prothorax well developed, pronotum with a strong median longitudinal line, ml well developed, much longer than pa; forefemora enlarged, foretarsus with a strong tooth; B₂ and B₃ of subbasal wing setae long; tube 1.17 times as long as head.

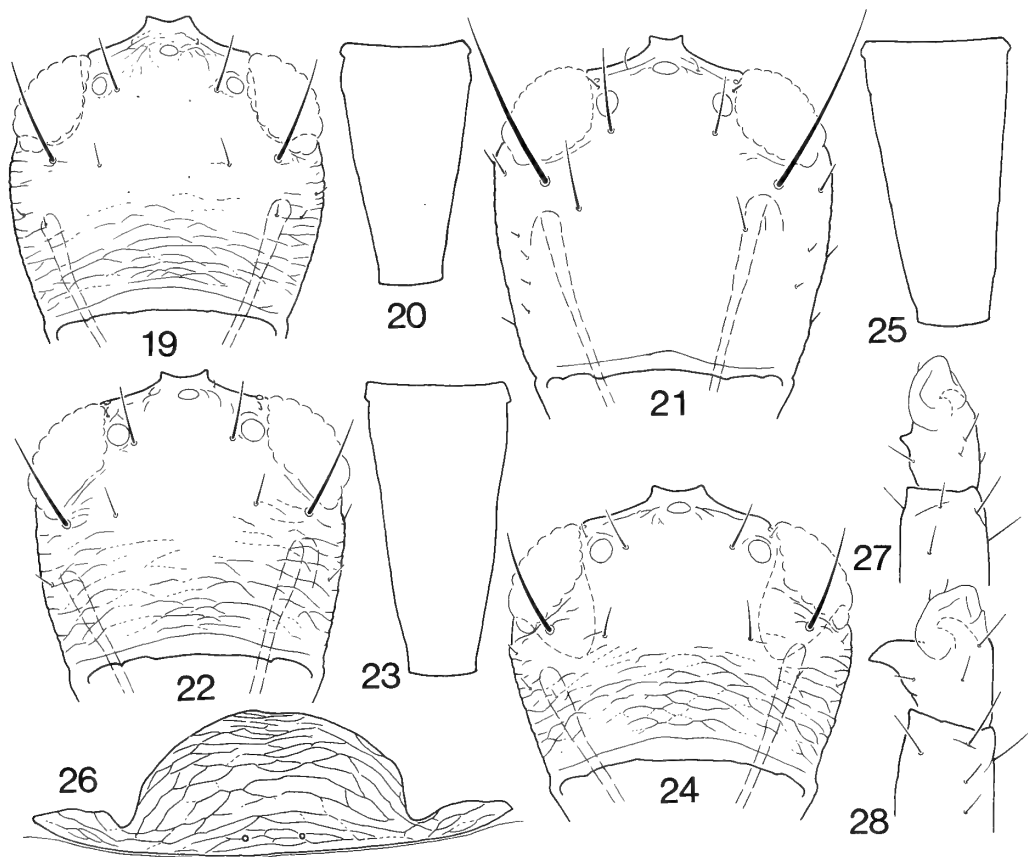
Measurements of male in µm. Total distended body length 2220. Head length 210, width across cheeks 240; eye length 70. Pronotum median length 184, width 290; forewing length 890. Pelta

median length 100, width 305. Tube length 245, basal width 107, apical width 49. Antennal segments I to VIII length (width) as follows: 55 (46); 56 (34); 87 (32); 79 (36.5); 76 (34.5); 69 (31); 45 (26); 20 (16.5).

Length of setae. Postocellars 40–61, postoculars 137–140, middorsals (vertexals) 24–50. Prothoracic aa 60–70, am 25–55, ml 170, pa 122, epim 140–150. Forewing subbasals B₁ 45–103, B₂ 175–200, B₃ 217–227. B₁ on tergite IX 180–185, B₂ on IX 121–148; anals 172–190.

Material examined. West Malaysia: Cameron Highlands, Tanah Rata, 2 ♀ 1 ♂ (mac.) on dead leaves, 2-iii-1976, 1 ♀ (mac.) 5-iii-1976, W. Suzuki, 1 ♀ (mac.) on dead branches, 24-vii-1976, S. Okajima; Genting Highlands, 30 ml E of Kuala Lumpur, 4,500', 1 ♀ (mac.) on dead wood with leaves,

28-ix-1973, L. A. Mound. Indonesia: South Sulawesi, Malino, alt. about 900 m, 3 ♀ (mac.) on dead Palmae, 3-viii-1984, S. Okajima; South Sulawesi, Karaenta Forest Res., Maros to Camba, alt. about 400 m, on dead branches, 3 ♀ (mac.) 5-viii-1984, 4 ♀ 2 ♂ (mac.) 6-viii-1984, S. Okajima; Central Sulawesi, nr. Rantepao, Pedamaran, alt. about 1,000 m, on dead leaves and branches, 1 ♀ (mac.) 8-viii-1984, 1 ♀ (mac.) 12-viii-1984, 1 ♀ 1 ♂ (mac.) 13-viii-1984, 1 ♀ (mac.) 14-viii-1984, S. Okajima; Central Sulawesi, 31 km W from Palopo, Puncak, alt. about 1,300 m, 2 ♀ 1 ♂ (mac.) on dead leaves and branches, 19-viii-1984, S. Okajima; Bali Is., Candi Kuning, alt. about 1,200 m, 4 ♀ (mac.) on dead branches, 26-vii-1984, S. Okajima. Philippines: Luzon Is., Quezon National Forest Park, 1 ♀ (mac.) on dead Palmae, 20-vii-



FIGS. 19–23. Head and tube of *Nesothrips* species—19–20, *N. brevicollis*, female, head (19) and tube (20); 21, *N. malacca*, male, head; 22–23, *N. minor*, female, head (22) and tube (23). FIGS. 24–28. *N. yasumatsui* sp. nov.—24, female, head; 25, female, tube; 26, female, pelta; 27, small male, foretarsus; 28, large male, foretarsus.

1979, S. Okajima; Mindanao Is., Mt. Apo, Agko, alt. about 1,300 m, 1 ♀ (mac.) on dead leaves, 3-viii-1979, S. Okajima; Mindanao Is., Mt. Apo, Agko, alt. about 1,100 m, 1 ♀ (mac.) 5-viii-1979, W. Suzuki.

Nesothrips minor (Bagnall, 1921), sp. rev.
(Figs. 7–10, 14–15, 18, 22 and 23)

Coenurothrips minor Bagnall, 1921 [6], 287–288.
Neosmerinthothrips formosensis var. *karnyi* Priesner, 1935 [4], 368–370.

Nesothrips minor: Mound, 1968 [7], 141.

Nesothrips brevicollis: Mound, 1974 [1], 162–163 (in part).

This species was described by Bagnall [6] based on a macropterous female from Rodrigues. Recently, Mound [1] treated it as a junior synonym of *brevicollis*. However, the specific name *minor* is now revived from a synonym of *brevicollis*, the reason for which is given under *brevicollis*. Mound [1] also treated *N. formosensis* var. *karnyi*, described on macropterous females from Java, as a synonym of *brevicollis*. However, it has the long wing retaining setae and tube, which are typical of *minor* but not found in *brevicollis*. Moreover, recently collected material from India, West Malaysia, Thailand, Indonesia (Java and Bali), Ogasawara Isls. and Hawaiian Isls. could well be determined as *minor*. These suggest its widespread distribution in tropical and subtropical Asia.

Contrary to the fact that the micropterous form is common in *brevicollis*, the macropterous form is prevalent in this species and the micropterous form is only rarely collected. However, I have examined some micropterous females and males from Thailand and Indonesia (Java and Sulawesi), which have well developed, long and curved wing retaining setae as in macropterae without exception.

Mound [1] regarded the Australian species *rhizophorae* possibly as a mere local colour variant of *brevicollis*. At present, *rhizophorae* is possibly only a colour variant of *minor*.

Material examined. Rodrigues: Holotype ♀ (mac.) of *Coenurothrips minor*, vii to xi-1918, H. J. Snell and H. P. Thomasset (in coll. British

Museum (Natural History), London). Indonesia: Java, Tjibodas, 1,400 m, lectotype ♀ (mac.) of *Neosmerinthothrips formosensis* var. *karnyi*, 1923, H. Karny (in coll. Senckenberg Museum, Frankfurt); Java, Mt. Tengger, 5 ♀ (mic.) on dead leaves, 14-iv-1981, T. Senoh; Bali Is., Kuta, Sea level, 1 ♀ (mac.) on dead leaves and branches, 30-viii-1984, S. Okajima; South Sulawesi, Malino, alt. about 900 m, 1 ♀ (mac.) on grass, 3-viii-1984, S. Okajima; South Sulawesi, 11 km E from Malino, Kanreapia, alt. about 1,500 m; 1 ♀ 1 ♂ (mic.) on grass, 2-viii-1984, S. Okajima. India: Aryankavu, 1 ♀ (mac.) on dry twing, 19-vii-1969, T. N. Ananthakrishnan. West Malaysia: Genting Highlands, 5,000', 4 ♀ (mac.) and 4 ♂ (hemimac.), 8-x-1973, L. A. Mound. Thailand: Phuket Is., 5 ♀ 5 ♂ (mac.) on dead leaves, 20-viii-1976, 20 ♀ 15 ♂ (mac.) on dead Banana leaves, 17-viii-1976, S. Okajima; Bangkok, Bangkokhen, Campus of Kasetsart University, NBCRC, on dead branches of *Casuarina equisetifolia*, 2 ♂ (hemimac.) 13-i-1988, 1 ♂ (hemimac.) 18-i-1988, S. Okajima; same locality as above, 1 ♀ (mac.) and 1 ♀ (mic.) on *Bougainvillea* ? *glabra*, 28-xii-1987, S. Okajima; nr. Chiang Mai, Mt. Doi Suthep, alt. about 500 m, 16 ♀ 10 ♂ (mac.) on grass, 8-viii-1976, S. Okajima. Hawaiian Isls.: Hawaii, Pupukeya, 1 ♀ (mac.) on *Leucaena glauca*, 16-xii-1969, F. Andre; Hawaii, Barber's Point, 16-xii-1969, 1 ♀ (mac.) by sweeping, F. Andre, 1 ♂ (hemimac.) on *Desmanthus*, K. Sakimura; Oahu, Honolulu, 1 ♀ (hemimac.) on *Cyperus rotundus*, 11-xii-1960, K. Sakimura. Japan, Ogasawara Isls.: Haha-jima Is., Okimura, 3 ♀ (mac.) on dead leaves, 13-vi-1972, Y. Watanabe; Haha-jima Is., 1 ♂ (mac.) on dead leaves and branches, 18-v-1984, M. Hasegawa; Haha-jima Is., nr. Okimura, Mt. Chibusa-yama, 1 ♀ (mac.) on dead leaves, 9-iii-1988, S. Okajima; Chichi-jima Is., Mt. Asahi-yama, 1 ♀ (mac.) on bamboo (*Pseudosasa japonica*), 11-iii-1988, S. Okajima; Chichi-jima Is., nr. Tokoyonotaki, 2 ♀ (mac.) and 1 ♂ (hemimac.) on dead branches, 11-iii-1988, S. Okajima.

Nesothrips yasumatsui sp. nov.
(Figs. 24–28)

Female (macroptera). Head yellow to brownish

yellow; thorax brown, in contrast with yellowish head; abdomen brown to dark brown, segments II and IX somewhat paler than intermediate segments; tube blackish brown. Antennal segments I to VI yellow, almost concolorous with head or a little paler, sometimes apex of segment VI shaded with brown, segment VII yellowish brown, segment VIII brown. Legs yellow to brownish yellow, almost concolorous with head. Postocular and postocellar setae yellowish, all other major setae on thorax and abdomen brownish.

Head (Fig. 24) much broader than long, broadest across cheeks, very weakly projecting in front of eyes, dorsal surface weakly sculptured posteriorly; cheeks rounded; postocular setae acute; postocellar setae usually a little longer than half the length of postocular setae, situated just inside posterior ocelli. Eyes prolonged ventrally. Ocelli small, about 13 μm in diameter. Antennae about 2.7 times as long as head; segments III and IV with two and four sense cones respectively. Maxillary stylets typical of the genus.

Pronotum weakly sculptured posteriorly, with a weak short median line; major setae acute, am reduced to a short and slender hair. Metanotum sculptured with polygonal reticulation, but weak medially; median pair of setae slender, about 35 μm long. Forefemora not enlarged, foretarsi unarmed. Forewings each with 7 duplicated cilia; only two subbasal wing setae developed, B_1 reduced.

Pelta (Fig. 26) with a pair of micro-pores; median lobe broad, lateral wings not separated from median lobe, but somewhat constricted at base; posterior margin not eroded. Tergal wing retaining setae well developed, long and curved, but reduced on tergite II; B_1 and B_2 setae on tergite IX acute, much shorter than tube, B_2 longer than B_1 . Tube (Fig. 25) about 1.2 times as long as head (excluding preocular part), sides almost straight; anal setae much shorter than tube.

Measurements of holotype female (mac.) in μm . Total distended body length 1940. Head length from anterior margin of eyes to base at middle 153, width across cheeks 220; eye dorsal length 66, ventral length 87. Pronotum median length 132, width 244; forewing length about 800. Pelta median length 81, width 271. Abdominal tergites

median length (width) as follows: II 66 (406); IV 84 (464); VI 127 (472); VIII 107 (362); IX 78 (214). Tube length 184, basal width 91, apical width 46. Antenna total length 413, segments I to VIII length (width) as follows: 47.5 (46); 50 (36); 63 (32); 60 (32); 58 (33); 56 (31.5); 39.5 (24); 29 (15).

Length of setae. Postocellars about ?40, postoculars 70. Prothoracic aa 37–40, am 32–40, ml 40–44, pa 55–58, epim 80–85. Forewing subbasals B_2 71–72, B_3 82–84. B_1 on tergite IX 76–80, B_2 on IX 97–100; anals 105–116.

Female (microptera). Colour and general structure almost as in macropterous female. Antenna about 2.7 times as long as head; metanotum a little shorter than that of macroptera; tube 1.05–1.16 times as long as head (excluding preocular projection); size of ocelli and shape of pelta very similar to those of macroptera.

Measurements of female (mic.) in μm . Total distended body length 2020. Head length from anterior margin of eyes to base at middle 158, width across cheeks 220; eye dorsal length 71, ventral length 84–87. Pronotum median length 143, width 256. Pelta median length 82, width 277. Abdominal tergites median length (width) as follows: II 71 (372); IV 92 (470); VI 131 (484); VIII 111 (344); IX 78 (209). Tube length 183, basal width 91, apical width 48. Antenna total length 402, segments I to VIII length (width) as follows: 47 (46.5); 52 (36); 60 (31); 59.5 (33.5); 55 (32.5); 52 (31); 38 (20); 28.5 (14).

Length of setae. Postocellars 42–45, postoculars 74–76. Prothoracic aa 38–40, am 25–28, ml 48–52, pa 50–55, epim 95–105. B_1 on tergite IX 82–85, B_2 on IX 110–116; anals 92–116.

Male (microptera). Colour almost as in female. Large male: prothorax well developed, pronotum with a strong median longitudinal line, forefemora enlarged, foretarsi each with a strong tooth (Fig. 28). Small male: Prothorax almost as in female or smaller, pronotum with or without a weak median longitudinal line, forefemora not enlarged, foretarsi each with a small tooth (Fig. 27).

Measurements of large (small) males in μm . Total distended body length 1500 (1200). Head length from anterior margin of eyes to base at middle 146 (128), width across cheeks 179 (163); eye dorsal length 60 (51), ventral length 62 (62).

Pronotum median length 152 (96), width 219 (168); forefemur length 220 (118). Pelta median length 51 (44), width 214 (143). Abdominal tergites median length/ width as follows: II 46 (40)/ 311 (229); IV 66 (50)/ 335 (253); VI 96 (76)/ 331 (252); VIII 81 (68)/ 228 (190); IX 66 (61)/ 146 (128). Tube length 148 (120), basal width 81 (66), apical width 40 (38). Antennal segments I to VIII length/ width as follows: 42 (34.5)/ 39.5 (32.5); 45 (39)/ 31.5 (30); 55 (46)/ 27 (24); 53 (43)/ 29 (27); 50 (42)/ 28 (28); 47.5 (43)/ 29 (28); 36 (29)/ 23 (20.5); 25 (24)/ 13 (13).

Length of setae. Postocellars 32–36 (26–29), postoculars 70–80 (45–54). Prothoracic aa 44–48 (20–30), am 30–34 (20–25), ml more than 70 (?40), pa 72 (37–40), epim 87 (58–60). Metanotal medians 40–45 (22–24). B₁ on tergite IX 74 (61–66), B₂ on IX 88 (about 80); anals 90–95 (75–80).

Holotype ♀ (mac.). Thailand: Kamphaeng Saen Campus of Kasetsart University, on grass, 22-xii-1987, S. Okajima.

Paratypes (42 ♀ 12 ♂ in total). Thailand: 3 ♀ (mic.), data almost the same as for holotype, but 12-i-1988; Chiang Mai, 26 ♀ 8 ♂ (mic.) on grass in rice field, 4-v-1978, K. Yasumatsu; 13 ♀ 4 ♂ (mic.), data very similar to above, but 7-v-1978.

Comments. This species is somewhat similar in appearance to *propinquus* (Bagnall) and *fodinae* Mound. The pelta of *propinquus* is eroded posteriorly and the lateral wings are separated from the median lobe, but the former is not eroded in this species and the lateral wings are widely fused to the median lobe. Moreover, the pedicel of the seventh antennal segment of this species is more or less broader than that of *propinquus*. From *fodinae*, it can easily be distinguished by the paler head and longer tube.

ACKNOWLEDGMENTS

I wish to express my gratitude to Prof. T. N. Ananthakrishnan, Loyola College, Madras, Dr. L. A. Mound, Keeper of Entomology, British Museum (Natural History), London, and Dr. R. zur Strassen, Senckenberg Museum, Frankfurt, for loan of specimens and other ways. I am much indebted to Dr. Shun-Ichi Uéno, National Science Museum, Tokyo, for kindly reading the original manuscript. My thanks are also due to the late Prof. K. Yasumatsu, Drs. K. Haga, T. Senoh and W. Suzuki, Messrs. M. Hasegawa, T. Kato, H. Makihara, K. Sakimura, R. Terakoshi and Y. Watanabe for their kindness in offering specimens.

REFERENCES

- 1 Mound, L. A. (1974) The *Nesothrips* complex of spore-feeding Thysanoptera (Phlaeothripidae: Idolothripinae). Bull. Br. Mus. nat. Hist., (Ent.), **31**: 110–188.
- 2 Mound, L. A. and J. M. Palmer (1983) The generic and tribal classification of spore-feeding Thysanoptera (Phlaeothripidae: Idolothripinae). Bull. Br. Mus. nat. Hist., (Ent.), **46**: 1–174.
- 3 Bagnall, R. S. (1914) Brief descriptions of new Thysanoptera III. Annls. Mag. nat. Hist., (8), **13**: 287–297.
- 4 Priesner, H. (1935) New or little known oriental Thysanoptera. Philip. J. Sci., **57**: 351–375.
- 5 Kudô, I. (1974) Some graminivorous and gall forming Thysanoptera of Taiwan. Kontyû, Tokyo, **42**: 110–116.
- 6 Bagnall, R. S. (1921) On Thysanoptera from the Seychelles Islands and Rodrigues. Annls. Mag. nat. Hist., (9), **7**: 257–293.
- 7 Mound, L. A. (1968) A revision of R. S. Bagnall's Thysanoptera collection. Bull. Br. Mus. nat. Hist., (Ent.), Suppl. **11**: 1–181.

Nautiliniellid Polychaetes Collected from the Hatsushima Cold-Seep Site in Sagami Bay, with Descriptions of New Genera and Species

TOMOYUKI MIURA¹ and LUCIEN LAUBIER²

Faculty of Fisheries, Kagoshima University, Kagoshima 890, Japan, and

²IFREMER, 66 avenue d'Iéna, 75116 Paris, France

ABSTRACT—Polychaete species belonging to the family Nautiliniellidae were found in the mantle cavities of two bivalve species collected from the Hatsushima cold-seep site in Sagami Bay at a depth of 1170 m. As a result of the comparison with *Nautiliniella calyptogenicola*, new combination, two new genera and two new species are described. The new genus *Shinkai* differs from the type genus of the family in having only one pair of prostomial antennae instead of two pairs. *Shinkai sagamiensis* new species is parasitic on *Calyptogena soyae*. *Natsushima bifurcata*, new genus and species, differs from all other species of the family by the presence of additional numerous bifurcate setae on each parapodium instead of the exclusive presence of simple hooks in the others. This species is parasitic in the mantle cavity of an undescribed bivalve species of the genus *Solemya*. The position of the family Nautiliniellidae is discussed, after a reexamination of the type specimens of *Antonbruunia viridis*.

The polychaete family Nautiliniellidae characterized by simple ventral hooks, was proposed with the description of a single representative species, *Nautilina calyptogenicola* Miura & Laubier, 1989 [1]. However, the classification of the family has not been deeply discussed because of the scarcity of the knowledge on the Japanese cold-seep community and on the parasitic polychaetes on bivalves. In the course of the serial dives of the deep-sea submersible "Shinkai 2000" of the Japan Marine Science and Technology Center, the first author (T.M.) could dive at the *Calyptogena soyae*-dominant community of the Hatsushima cold-seep site [2] which may be comparable to the *Calyptogena phaseoliformis*-dominant sites of the Japan Trench [3, 4]. During Dives 315, 316 and 381 of the submersible "Shinkai 2000" at depths of 1100 to 1200 m, many specimens of cold-seep bivalves and vestimentiferans were collected. The parasites and associated invertebrates living on these cold-seep animals were removed from their hosts on the mother ship, "Natsushima" and two

polychaete species of the family Nautiliniellidae, a species of the family Phyllodocidae and a species of poecilostomatoid copepod were found [5, 6]. In this paper, these two new species and new genera of the nautiliniellid polychaetes parasitic in the mantle cavity of cold-seep bivalves are described and a new name is also proposed for the previously described genus for reason of the preoccupation.

The types are deposited in the National Science Museum, Tokyo (NSMT) and the Japan Marine Science and Technology Center (JAMSTEC).

Nautiliniellidae

Type genus: *Nautiliniella*, new genus with the type species *Nautilina calyptogenicola* Miura and Laubier, 1989, by monotypy.

Nautiliniella new genus

Type species: *Nautilina calyptogenicola* Miura and Laubier, 1989, by monotypy.

Remarks: The generic name *Nautilina* is preoccupied in a molluscan species and in a protozoan species (after Nomenclator Zoologicus). The new generic name *Nautiliniella* is proposed here. A

Accepted June 28, 1989

Received May 29, 1989

¹ To whom all correspondence should be addressed.

newly combined name, *Nailiniella calyptogenicola* is also proposed for the previously described species, *Nautilina calyptogenicola*.

Shinkai new genus

Type species: *Shinkai sagamiensis*, new species, by monotypy. Gender feminine.

Diagnosis: Body long, vermiform, tapering posteriorly with numerous setigerous segments; body in cross-section flattened ventrally and more or less arched dorsally. Prostomium short with a pair of antennae, without eyes. Muscular proventriculus present. Achaetous peristomial ring absent. First setiger more or less fused with prostomium. Parapodia subbiramous with dorsal and ventral cirri; dorsal cirri well developed; ventral cirri very short; neuropodia with a single embedded acicula and a few simple stout hooks. Pygidium cylindrical without appendage.

Etymology: The genus is named in the honor of the submersible "Shinkai 2000" of the JAMSTEC with which the host bivalves of the parasitic polychaetes were collected during Dives 315 and 381.

Remarks: Species of the new genus *Shinkai* resemble *Nautiliniella calyptogenicola* in having a dorsally arched body in cross-section, a muscular proventriculus and ventral simple hooks. However they differ from the latter in having only one pair of prostomial antennae instead of two pairs.

Shinkai sagamiensis, new species

(Fig. 1)

Materials: Holotype (NSMT-Pol. H-293), complete with regenerated posterior segments, off Hatsushima, Sagami Bay 34°00.0'N, 139°13.8'E, 1170 meters, 19 November 1987, deep-sea submersible "Shinkai-2000" Dive 315, collected from the mantle cavity of *Calyptogena soyoe*. Paratypes (JAMSTEC), one anterior fragment, same station as the holotype, from washings and sievings of sediment with *C. soyoe* collected by a power-driven grab; one complete, same site, 5 November, 1988, Dive 381, washings.

Measurements: Holotype, 14 mm long, 1.0 mm wide including parapodia, with 65 setigers (38

anterior segments and 27 regenerated segments). Larger fragmental paratype, 8.0 mm long, 1.2 mm wide, with 32 anterior setigers.

Description: Body vermiform, flattened ventrally and slightly arched dorsally. Integument smooth. Specimens preserved in alcohol pale or colorless.

Prostomium very short, anteriorly incised, with a pair of very short cirriform antennae, without eyes or other appendages (Fig. 1a, b). Achaetous peristomial ring absent. Mouth opening situated ventrally, between prostomium and first setiger. Ventral cirri of first setiger larger than followings, inserted in front of neuropodia (Fig. 1f). Foregut with well-developed muscular part (may be proventriculus).

Pygidium cylindrical, without anal cirri (Fig. 1c).

Parapodia subbiramous, with well-developed dorsal cirri and much reduced ventral cirri; first dorsal cirrus greatly reduced; first ventral cirrus located in front of neuropodial fascicle; bases of dorsal cirri swollen, forming globular pads with embedded slender notoacacula; dorsal cirri five times as long as ventral ones; neuropodia globular (Fig. 1d).

Setae consisting of simple ventral hooks only; several hooks projected from each neuropodium on anterior parapodia, e.g. 3–4 on parapodium 1, 5–8 on parapodia 2–6, 1–3 on parapodia 7–20, and 1 on posterior parapodia; several developing hooks embedded around acicula. Hooks simple, stout and strongly curved on very short distal end with remarkable knob (Fig. 1e).

Etymology: The specific name is derived from the type locality, Sagami Bay.

Natsushima new genus

Type species: *Natsushima bifurcata*, new species, by monotypy. Gender feminine.

Diagnosis: Body long, vermiform, tapering posteriorly with numerous setigerous segments; body in cross-section flattened ventrally and slightly arched dorsally. Prostomium short with a pair of antennae, without eyes. Muscular proventriculus present. Achaetous peristomial ring absent. Parapodia subbiramous with dorsal and ventral cirri;

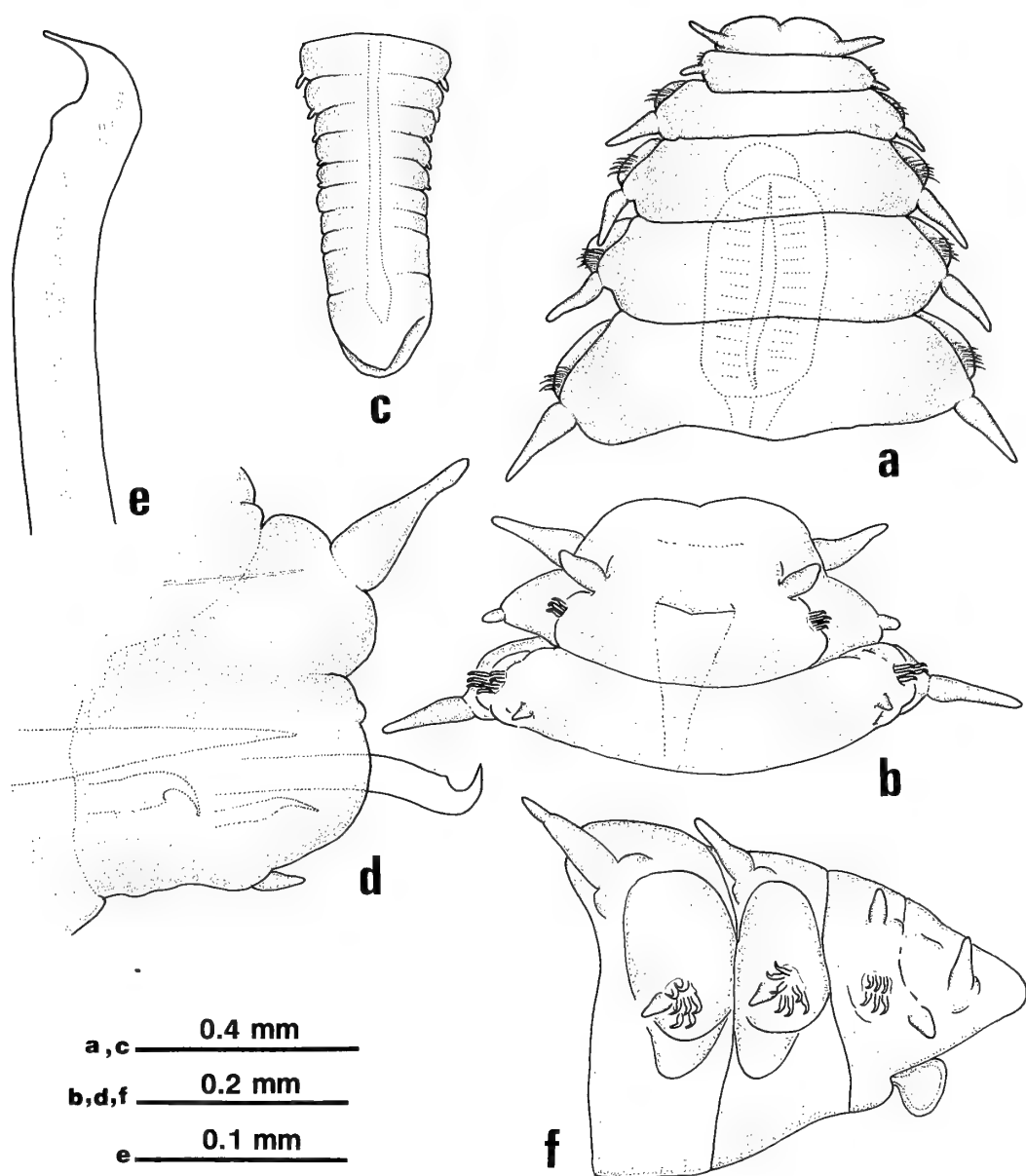


FIG. 1. *Shinkai sagamiensis* g. sp. n.: a, Anterior end, dorsal view (holotype); b, Same, ventral view; c, Pygidium, dorsal view; d, Parapodium 19, anterior view; e, Hook; f, Anterior end, lateral view (paratype).

dorsal cirri longer than ventral ones; neuropodium with a single embedded acicula, a few simple stout hooks and many bifurcate simple setae. Pygidium simple without appendage.

Etymology: The genus is named in the honor of the research vessel "Natsushima" of the JAM-STEAC, the mother ship of the submersible "Shink-

ai 2000".

Remarks: The new genus belongs to the family Nautiliniellidae in having subbiramous parapodia with characteristic simple ventral hooks, however the single species of this genus differs from those of other genera in having additional numerous smaller bifurcate setae on each parapodium instead of

exclusive presence of simple hooks.

Natsushima bifurcata, new species
(Fig. 2)

Material: Holotype (NSMT-Pol. H-294), complete, off Hatsushima, Sagami Bay, 34°00.0'N, 139°13.8'E, 1170 meters, 19 November 1987, deep-sea submersible "Shinkai-2000" Dive 315, collected from the mantle cavity of *Solemya* sp.

Measurements: Holotype 5.0 mm long, 0.6 mm wide including parapodia, with 47 setigers.

Description: Body vermiform, flattened ventrally and slightly arched dorsally. Integument

smooth. Specimens preserved in alcohol pale or colorless.

Prostomium very short, anteriorly slightly incised, with a pair of short cirriform antennae, without eyes or other appendages (Fig. 2a, b). Achaetous peristomial ring absent. Mouth opening situated between prostomium and first setiger, without jaws or paragnaths. First segment partially fused with prostomium. Foregut with well-developed muscular part, without tubiform pharynx.

Pygidium simple, rounded, without anal cirri (Fig. 2c).

Parapodia subbiramous throughout body, with

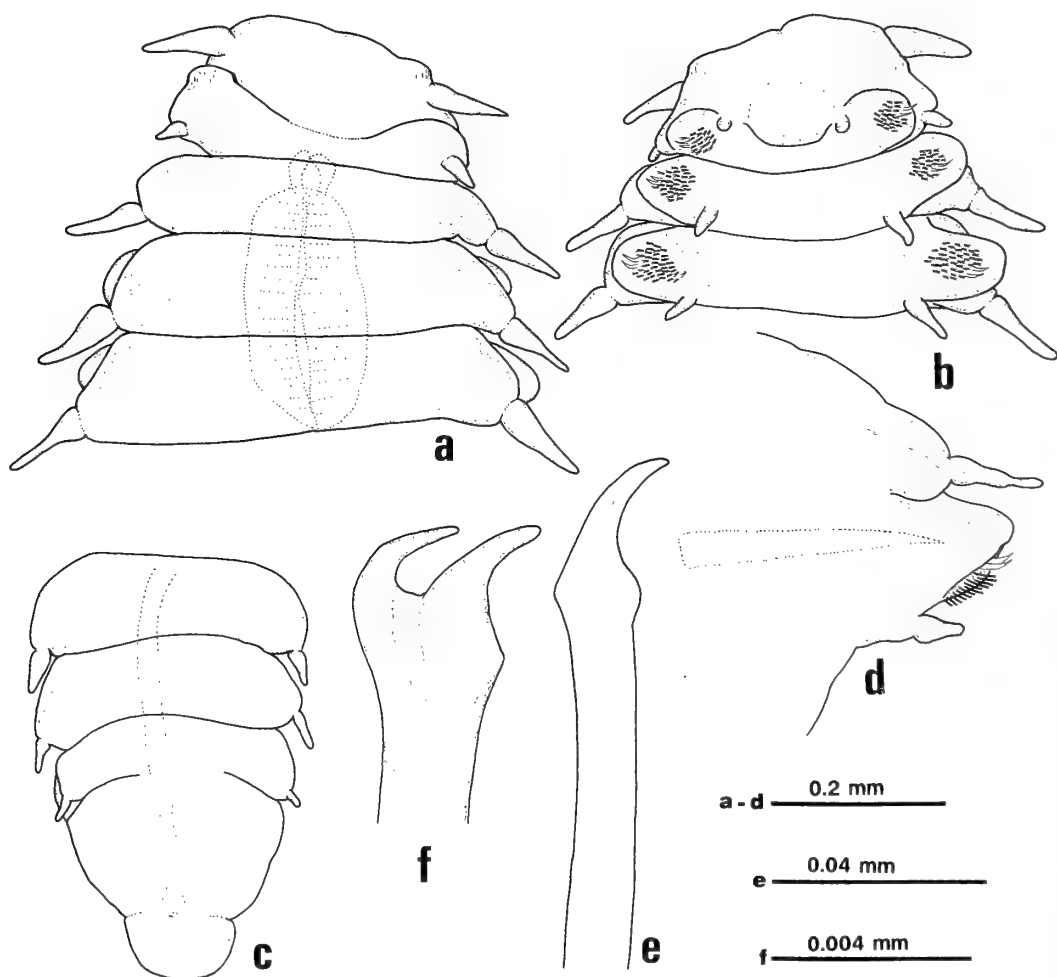


FIG. 2. *Natsushima bifurcata* g. sp. n. (holotype): a, Anterior end, dorsal view; b, Same, ventral view; c, Pygidium; d, Parapodium 16, anterior view; e, Hook; f, Bifurcate seta.

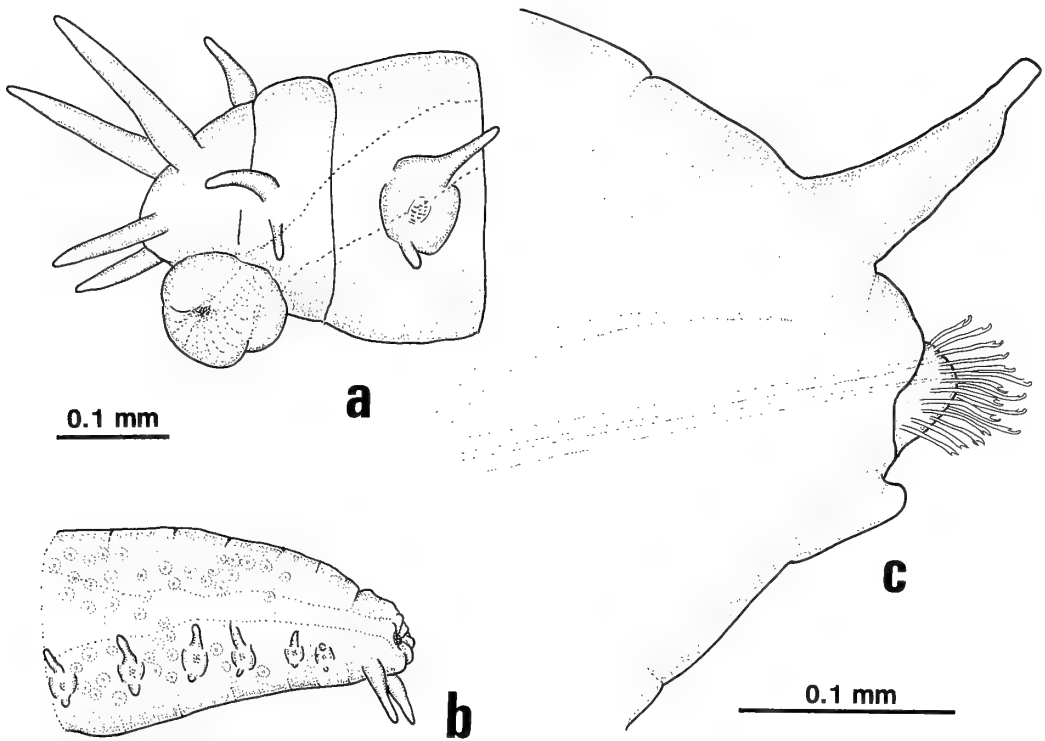


FIG. 3. *Antonbruunia viridis* Hartman and Boss, 1965 (Paratypes: USNM 56718): a, Anterior end, lateral view; b, Posterior end, lateral view; c, Posterior parapodium, anterior view.

well-developed dorsal and short ventral cirri; bases of dorsal cirri swollen, with very fine embedded notoacacula; dorsal and ventral cirri of first setiger reduced; neuropodia cylindrical (Fig. 2d).

Setae consisting of stout simple hooks and smaller bifurcate simple setae; a few hooks (2–4) projected from each setal lobe; several developing hooks embedded around acicula. Hooks simple, stout and slightly curved on distal end (Fig. 2e). Numerous smaller bifurcate setae situated below stout hooks. Distal teeth of bifurcate setae separated each other, strongly curved (Fig. 2f).

Etymology: The specific name is derived from the presence of bifurcate setae.

DISCUSSION

The single representative species of the family Antonbruuniidae Fauchald, 1977 [7], *Antonbruunia viridis* Hartman and Boss, 1965, is known as living in the mantle cavity of the bivalve *Lucina*

fosteri Hartman and Boss, 1965 [8]. This species resembles the nautiliniellid species in having simple body with subbiramous parapodia and commensal life. However, several important morphological differences between these two families were found from the original description of *A. viridis* and after the reexamination of four paratypes (USNM 56718) of this species. *A. viridis* has five occipital antennae including central unpaired one, while nautiliniellid species have one or two pairs of lateral antennae and lack the central one. There are a distinct achaetous periostomial ring with tow pairs of cirri and a pair of cylindrical anal cirri in the former (Fig. 3a, b), while those are absent in the latters. In *A. viridis*, each parapodium is supported by three similar acicula with bases adjoining or contacted one another. Two neuropodial acicula are directed to the setal fascicle and a single notopodial one to the base of dorsal cirrus but not penetrating inside the cirrus (Fig. 3c). The appearance of acicula in nautiliniellid species

completely differs from that of *A. viridis*. In nautiliniellid species, there are a single slender notoaciculum and a single thick neuroaciculum. The notoacacula of nautiliniellids are always situated apart from the neuroacacula and often embedded in the dorsal cirri. They are very thin compared with the neuroacacula. The setal composition is also different in these two families. Simple stout hooks are present in all nautiliniellid species but do not occur in *A. viridis*. *A. viridis* also exhibits clear sexual dimorphism, with dwarf males. This biological adaptation was not encountered in nautiliniellid species, which could be due to the small number of specimens collected.

The discovery of two new species enables to establish the morphological features of the family Nautiliniellidae on a more definitive basis. The major characters of the family are the presence of a muscular proventriculus, subbiramous parapodia and ventral simple hooks, and the absence of achaetous peristomial ring. Some pilargid polychaetes resemble the species of the family Nautiliniellidae in the characters mentioned above, with the exception of the typical pilargid notopodial acicular spines. The species of the genus *Litocorsa* have stout neuropodial spines [9–11]. Although the simplified nautiliniellid body recalls the species of the families Calamyzidae and Levidoridae as mentioned in our previous paper [1], the compound setal structure in these families was not found in the nautiliniellid species. The simple setae of the family Levidoridae are thought to be derived from compound setae by fusion of shafts and blades [12], while the typical ventral simple hooks of nautiliniellids may have originated from simple ventral spines or setae, like the neuropodial spines of *Litocorsa*. The simple structure of typical nautiliniellid ventral hooks may be an important character supporting a hypothetical relation of the family Nautiliniellidae with the Pilargidae.

It was clarified above that the nautiliniellid polychaetes may have another type of setae beside the ventral simple hooks. The simple bifurcate setae of *Natsushima bifurcata* rather recall those of the family Oweniidae than the others. Nilsen and Holthe discussed the phylogenetical development of the typical oweniid uncini with two equal teeth

and considered that they might have derived from the typical long-shafted uncini found in several sedentary families [13]. The shafts of these uncini are long and curved with distinct narrow parts called "neak" [13, 14], and completely separated from the nautiliniellid straight setae without neck. The nautiliniellid bifurcate setae may have independently evolved in the pathway to the parasitic life.

As a conclusion, even if there may still be some doubt, the family Nautiliniellidae should be placed in the order Phyllodocida, near the family Pilargidae.

ACKNOWLEDGMENTS

The authors wish to thank Dr. Suguru Ohta of Ocean Research Institute, University of Tokyo for his identification of the host vibalves and the staff of JAMSTEC for their assistance in sampling the materials available for study at "Shinkai 2000" Dives 315 and 381. We also express our thanks to Dr. Kristian Fauchald and Dr. Linda Ward of the Smithsonian Institution for their kind arrangement of the loan of type material examined here. Part of this study was supported by the grant-in-aid from Itoh Science Foundation.

REFERENCES

- 1 Miura, T. and L. Laubier (1989) *Nautilina calyp-togenicola*, a new genus and species of parasitic polychaete on a vesicomid bivalve from the Japan Trench, representative of a new family Nautilinidae. Zool. Sci., 6: 387–390.
- 2 Okutani, T. and K. Egawa (1985) The first underwater observation on living habit and thanatocoenoses of *Calypptogena soyoae* in bathyal depth of Sagami Bay. Venus (Japan. J. Malacol.), 44: 285–289.
- 3 Métivier, B., T. Okutani, and S. Ohta. (1986) *Calypptogena (Ectenagena) phaseoliformis* n. sp., an unusual vesicomid bivalve collected by the submersible Nautilite from abyssal depths of the Japan and Kurile Trenches. Venus (Japan. J. Malacol.), 45: 161–168.
- 4 Ohta, S. and L. Laubier (1987) Deep biological communities in the subduction zone of Japan from bottom photographs taken during "nautilite" dives in the Kaiko project. Earth Planet. Sci. Lett., 83: 329–342.
- 5 Miura, T. (1988) Parasitic animals collected in a *Calypptogena*-dominant community developing off Hatsushima, Sagami Bay. JAMSTECTR Deepsea

- Res., 4: 239–244. (In Japanese).
- 6 Miura, T. (1988) A new species of the genus *Protomystides* (Annelida, Polychaeta) associated with a vestimentiferan worm from the Hatsushima cold-seep site. Proc. Japan. Soc. Syst. Zool., 38: 10–14.
 - 7 Fauchald, K. (1977) The polychaete worms. Definitions and keys to the orders, families and genera. Nat. Hist. Mus. Los Angeles Cty., Sci. Ser., 28: 1–190.
 - 8 Hartman, O. and K. J. Boss (1965) *Antonbruunia viridis*, a new inquiline annelid with dwarf males, inhabiting a new species of pelecypod, *Lucina fosteri*, in the Mozambique Channel. Ann. Mag. Nat. Hist., ser. 13, 8: 177–186.
 - 9 Pearson, T. H. (1970) *Litocorsa stremma* a new genus and species of pilargid (Polychaeta: Annelida) from the west coast of Scotland, with notes on two other pilargid species. J. Nat. Hist., 4: 69–77.
 - 10 Wolf, P. S. (1986) Three new species of Pilargidae (Annelida: Polychaeta) from the east coast of Florida, Puerto Rico, and the Gulf of Mexico. Proc. Biol. Soc. Wash., 99: 464–471.
 - 11 Imajima, M. (1987) Pilargidae (Annelida, Polychaeta) from Japan (Part 1). Bull. Natn. Sci. Mus., Tokyo, Ser. A, 13: 151–164.
 - 12 Perkins, T. H. (1987) Levidoridae (polychaeta), new family, with descriptions of two new species of *Levidorum* from Florida. Bull. Biol. Soc. Wash., 7: 162–168.
 - 13 Nilsen, R. and T. Holthe (1985) Arctic and Scandinavian Oweniidae (polychaeta) with a description of *Myriochele fragilis* sp. n., and comments on the phylogeny of the family. Sarsia, 70: 17–32.
 - 14 Imajima, M. and Y. Morita (1987) Oweniidae (Annelida, Polychaeta) from Japan. Bull. Natn. Sci. Mus., Tokyo, Ser. A, 13: 85–102.

[COMMUNICATION]

**Tectal Visual Afferents from Fish
Dorsolateral Tegmental Cells**

AKIYOSHI NIIDA and TAKASHI OHONO

*Department of Biology, Faculty of Science, Okayama University,
Okayama 700, Japan*

ABSTRACT—The cells of the nucleus dorsolateralis tegmenti (NDT) in the crucian carp were physiologically identified and marked with Lucifer dye. The Lucifer dye filled axons projected into the tectum, where their main axons extended into the deep tectal layer. All the identified NDT cells responded to both optic nerve and rhombencephalic electrical stimulation. Out of 40 such NDT cells, 24 cells were visual and/or tactile. The remaining cells were unresponsive. However, some of the unresponsive cells were visually driven in conjunction with rhombencephalic electrical stimulation.

INTRODUCTION

The nucleus dorsolateralis tegmenti (NDT) in fish is located ventrolaterally to the torus semicircularis, which is considered to be a recipient of visual, auditory and lateral line inputs [1-3]. The dorsolateral tegmental area, including the NDT or deep tectum has been found to be reciprocally connected with the optic tectum by degeneration and HRP-labelling studies [4-9]. In a previous study [10] by means of intra-axonal dye marking and intracellular recordings we obtained the following results: (1) wide distribution of axonal branching of the NDT cells in the deep layer of the ipsilateral tectum; (2) further projection of the axon described in (1) to the contralateral tectum via the tectal commissure; (3) responses of the NDT cells to three set of electrical stimulation, optic nerve, rhombencephalon and tectal commissure. These results strongly indicate that there

exist, in the tectum, afferents with various kinds of response modalities from the tectum. The goal of this study is thus to show the presence of visual or other sensory related responses of the NDT cells, which were identified by physiological criteria combined with cell morphology.

MATERIALS AND METHODS

Experiments were performed on 50 crucian carp (*Carassius carassius*), 15-20 cm in overall length. The surgical procedure, methods for electrical and sensory stimulation, the recording apparatus and histological procedures have been described in detail elsewhere [10, 11]. The fish were initially anesthetized with MS-222 and immobilized with an intraperitoneal injection of Flexedil. The gills were kept out of water, and perfused with aerated water through a tube inserted into the oral cavity. Beveled glass micropipettes, filled with 4% Lucifer Yellow CH (Sigma) in distilled water [12], were used for potential recording and markings. A hyperpolarizing DC current of 2 nA for 2-5 min gave good marking of the cells. The brain was removed 3-5 hr after the injection of dye and fixed for 13-15 hr with formalin acidified to pH 4.0 with acetate buffer.

The criteria for physiological identification of the NDT have been established in a previous study [10] by a combination of intra-axonal recording and Lucifer dye marking. The criteria were: 1) antidromic response of the axon, running through the stratum album centrale (SAC), to electrical stimulation (300 Hz) of the tectal commissure and

2) orthodromic response of the same axon described in (1) to electrical stimulation of both the rhombencephalon and the optic nerve. In addition to such criteria, based on a previous experiment

[10], the following latency values were used for the identification of the NDT cell: 0.4–0.8 ms for the tectal commissure, 5–10 ms for the optic nerve and 1.2–1.6 ms for the rhombencephalon.

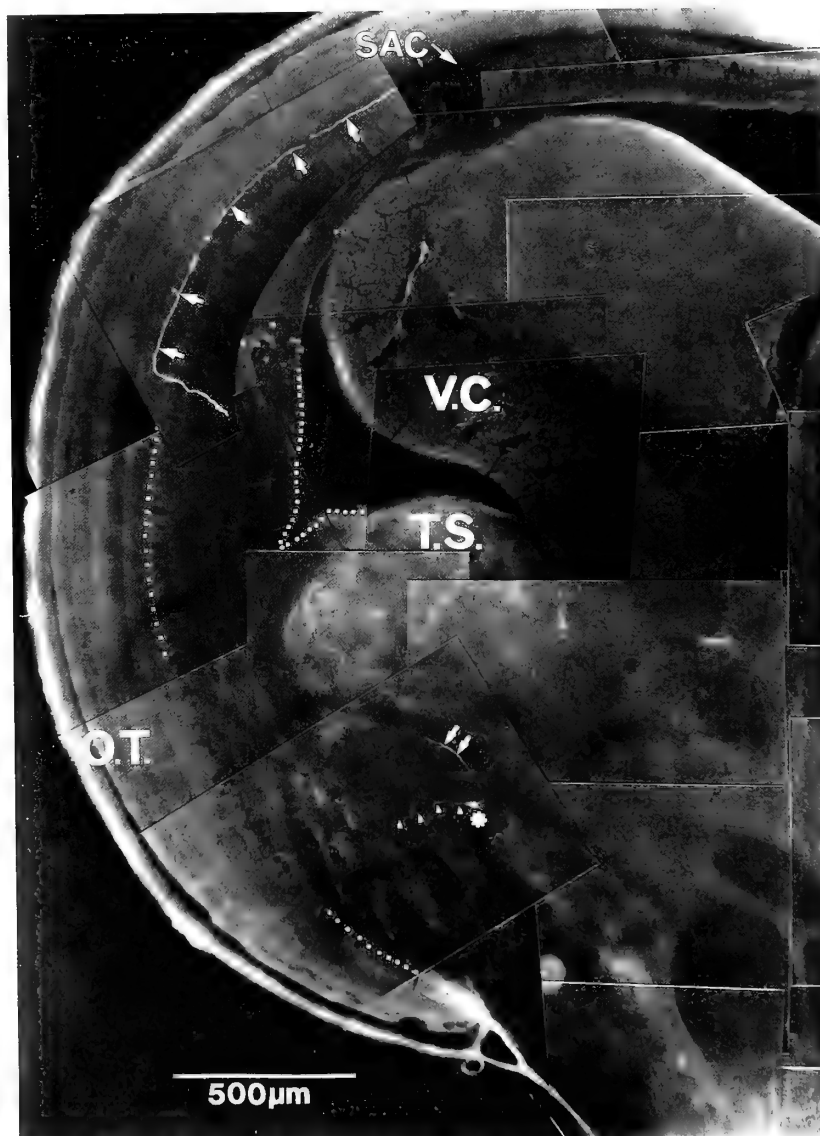


FIG. 1. Fluorescence photomicrograph of a NDT cell filled with Lucifer dye. This montage photograph was prepared by two serial coronal sections. The NDT cell is located ventrolaterally to the torus semicircularis. Dendrites (arrow heads) extend toward the tectobulbar pathway and the axon (thin arrows) arising from the soma (asterisk) ascends toward the ipsilateral tectum. The axon (thick arrows) running through SAC, the deep tectal layer could be further traced to the contralateral tectum by observing serial sections. The overall morphology of this cell is shown in Figure 2Bb. Lines of squares lateral and medial to the midline show a lower boundary of SAC and a part of the wall of the optic ventricle, respectively. The tectobulbar pathway courses downward along the line of squares lateral to the midline. Abbreviation: O.T., optic tectum; SAC, stratum album centrale; T.S., torus semicircularis; V.C., valvula cerebelli.

RESULTS AND DISCUSSION

Using above-mentioned criteria, we observed the responses of 40 NDT cells. Twenty-one of these cells, in which Lucifer dye had been injected, were well-stained (as seen from Fig. 1) and permitted tracing of the axon to the contralateral tectum. Seven of the 40 cells identified as NDT were visuo-tactile, 16 cells were visual, 1 cell was tactile and 16 cells were unresponsive.

Visuo-tactile cells

Figure 2Aa and 2Ab show one example of recordings from the bimodal NDT cells. These responses were obtained from the cell illustrated in Figure 2Ba: A spot of light (0.5 subtense angle) induced a transient response and subsequent stimuli gave a reduced number of spikes (Fig. 2Aa), indicating remarkable habituation. Simultaneously, this cell also responded to the tactile stimuli delivered by touching the facial part (stippled area in the inserted drawing) with a writing brush (Fig. 2Ab). Another example from the visuo-tactile cell following morphological identification is shown in Figure 2Ac, where normally occurring spontaneous discharges notably increased by touching the facial part. This cell responded to moving objects as well (not shown here). Bimodal units obtained by extracellular recordings have been reported by Page and Sutterlin [1] in the dorsolateral tegmentum of goldfish that are closely related to the present material. Unlike our results, they were all acoustico-visual units. This discrepancy is possibly due to differences in their topographical positions where visuo-acoustic and visuo-tactile cells are located: the recording sites shown by Page and Sutterlin [1] lie more anterior to those of our cells.

Visual cells

Besides visual NDT cells coupled with tactile input, we encountered visual NDT cells with rhombencephalic inputs, which were not ascertained in response modality. They were mostly on-transient or sensitive to moving objects. As seen from Figure 2Ad, the exemplified NDT cell was directionally selective: the leading edge of a black rectangular stripe (subtense angle: 8°), mov-

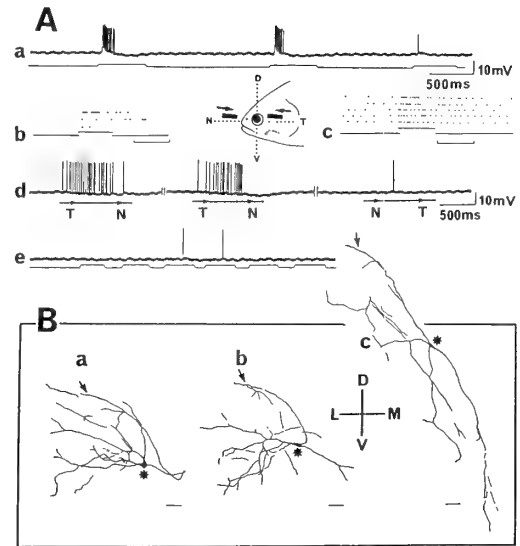


FIG. 2. A: responses of NDT cells to visual and/or tactile stimuli. (Aa) responses of the bimodal cell to a 0.5° spot of light, and (Ab) responses of the same cell to touching of the facial part (inserted drawing). Dot pattern representation of spike discharges, together with (Ac). These responses (Aa and Ab) were recorded from the cell shown in Figure 2Ba. In both responses (Aa and Ab), remarkable habituation occurs, whereas another bimodal cell (Ac) shows much less habituation with the responses induced by tactile stimuli. Their tactile receptive fields were on the facial part (stippled area in the inserted drawing). Upward deflection in each trace shows light-on for Aa and Ae, and touch for Ab and Ac. In Ab and Ac, time scale represents 1 sec. (Ad) responses of NDT cell to moving edge. When a leading edge of a black rectangular stripe moved in the temporal to nasal direction (as seen from the inserted drawing), a response was vigorously induced. A stationary spot of light to this cell was almost ineffective (Ae). These responses were recorded from the cell shown in Figure 2Bb. Calibration in (Ad) also serves for (Ae). B: composite drawings of NDT cells marked with Lucifer dye. Explanation of each cell's morphology is given in the text. Each arrow indicates axon and asterisks position of soma. Calibration bars: $50\ \mu\text{m}$. Abbreviation: D, dorsal; L, lateral; M, medial; N, nasal; T, temporal; V, ventral.

ing ($40^\circ/\text{sec}$) in the temporal to nasal direction through the receptive field, produced spike discharges, whereas motion in the reverse direction (nasal to temporal direction) gave a much weak response. In this example, the slightly deviated

orientation of the edge from naso-temporal axis, as seen in the inserted drawing, was the most effective in the initiation of spike discharges. A moving spot of light gave no response (not shown), and a stationary spot of light was also not effective in this cell (Fig. 2Ae). The response characteristics mentioned above were obtained from the cell in Figure 2Bb, where the axon (thin arrow) filled with Lucifer dye projected into the ipsilateral optic tectum, and the dendritic field of this cell expanded in a fan-like manner toward the tectobulbar pathway (see also Fig. 1). Unlike the cell illustrated in Figure 2Ba and 2Bb, in Figure 2Bc the ventral dendrite of the NDT cell, which was sensitive to moving objects, extended toward the F.L.L. (fasciculus longitudinalis lateralis). All the identified visual cells, except for the bimodal cells, were unresponsive to acoustic and/or tactile stimuli. However, they responded to rhombencephalic electrical stimulation, indicating that these cells receive rhombencephalic inputs, such as lateral line, vestibular, and possibly proprioceptive informations.

Unresponsive cells

Among NDT cells there were some unresponsive cells in a slightly greater frequency (about 40%). They did not respond to visual, acoustic or tactile stimuli, although these cells were responsive to both optic nerve and rhombencephalic electrical stimulation. Some of these cells, however, like some of tectal efferent cells [11], which normally failed to respond to acoustic, tactile, or visual stimuli, responded to light stimuli under specific conditions: when continuing the rhombencephalic electrical stimulation, simultaneously applied visual stimuli induced visual responses. One of the possible interpretations for this, is that summation of visual input and heterosynaptic sensory inputs might activate responsiveness of the NDT cell. As yet neural mechanisms responsible for the unresponsiveness of these cells remain to be studied in

detail. Morphological features of the unresponsive cells were substantially similar to those of visual or bimodal cells: the wide distribution of the axonal branching in the tectum, the dendritic profile extending toward the tectobulbar pathway, and the cell locations similar to those of responsive cell of the NDT.

The present study raised a crucial problem that the responses, in the deep tectum, derived from the NDT cells may be erroneously identified as intrinsic tectal unitary responses, unless we use well-defined criteria for determining whether the responses recorded in the tectum originate from the intrinsic tectal cells or from the tegmental cells. The same appears to be the case in tectal afferents from the pretectal area and the nucleus isthmi. This situation will be overcome by a combination of more sophisticated electrical stimulation and recording techniques by which cell identification can be made.

REFERENCES

- 1 Page, C. H. and Sutterlin, A. M. (1970) *J. Neurophysiol.*, **33**: 129-136.
- 2 Knudson, E. I. (1977) *J. comp. Neurol.*, **173**: 417-432.
- 3 Schellart, N. A. M. (1983) *Neurosci. Lett.*, **42**: 39-44.
- 4 Ebbesson, S. O. E. and Vanegas, H. (1976) , **184**: 435-454.
- 6 Grover, B. G. and Sharma, S. C. (1981) *J. comp. Neurol.*, **196**: 471-488.
- 7 Luiten, P. G. M. (1981) *Brain Res.*, **220**: 51-65.
- 8 Wolf, F. A. De., Schellart, N. A. M. and Hoogland, P. V. (1983) *Neurosci Lett.*, **38**: 209-213.
- 9 Echter, S. M. (1984) *J. comp. Neurol.*, **230**: 536-551.
- 10 Niida, A. and Ohono, T. (1984) *Neurosci. Lett.*, **48**: 261-266.
- 11 Niida, A., Ohono, T. and Iwata, K. S. (1989) *Brain Res. Bull.*, **22**: 389-398.
- 12 Stewart, W. W. (1978) *Cell*, **14**: 741-759.

[COMMUNICATION]

Morphological and Physiological Characterization of the Para-Ocellar Nerve of the Cockroach, *Periplaneta americana*

AKIKO MIZUTANI and YOSHIHIRO TOH

*Department of Biology, Faculty of Science, Kyushu University,
Fukuoka 812, Japan*

ABSTRACT—The structure and physiological properties of the para-ocellar nerve have been examined in American cockroaches. The para-ocellar nerve contains 120–200 fibers, originating from several bundles around the ocellus. The fibers project into the deutocerebrum and descent to terminate in the suboesophageal ganglion. Spike discharges were recorded in the para-ocellar nerve in response to air puffs directed towards the ocellar cornea, indicating that the para-ocellar nerve contains axons of mechanosensory sensilla surrounding the ocellus. It was previously assumed that the para-ocellar nerve coupled ocellar photoreception with neurosecretion of the corpora cardiaca. However, our data could not confirm this assumption, since we could not find responses of the para-ocellar nerve to ocellar illumination.

INTRODUCTION

The dorsal ocellus of insects is usually connected with the protocerebrum by a single ocellar nerve [1]. In cockroaches, however, the ocellus is connected with the brain by two nerves: the ocellar nerve and the para-ocellar nerve. Structure of the ocellus and ocellar nerve has been well documented in cockroaches [1–6], but only little is known about the para-ocellar nerve [7]. Silver impregnation showed two courses of para-ocellar nerve fibers in the deutocerebrum. Some fibers terminated with arborizations in the superior internal cortical area of olfactory lobe, where they keep close proximity to the neurons projecting

their axons into para-cardiac nerve. Other fibers further descend to the circumoesophageal connectives [7]. Based upon this morphology the para-ocellar nerve was assumed to couple ocellar photoreception with the neurosecretion of the corpora cardiaca [7]. However, this assumption has not been examined electrophysiologically or anatomically using electron microscopy.

In the present study, the para-ocellar nerve fibers of American cockroaches *Periplaneta americana* have been examined using cobalt backfills, electron microscopy and electrophysiological techniques.

MATERIALS AND METHODS

Morphology

The para-ocellar nerves of the cockroaches *P. americana* were prepared for scanning and transmission electron microscopy through the same procedures previously reported for the ocellus and ocellar nerve of the same species [4, 5, 8]. The projections of the para-ocellar nerve fibers in the brain were studied by backfilling the fibers from the ocellus with cobalt chloride. Backfilled fibers were examined by light microscopy using the same procedure previously described for the ocellar nerve fibers in the same species [4, 5, 8].

Physiology

The cockroach was fixed on an acrylic platform

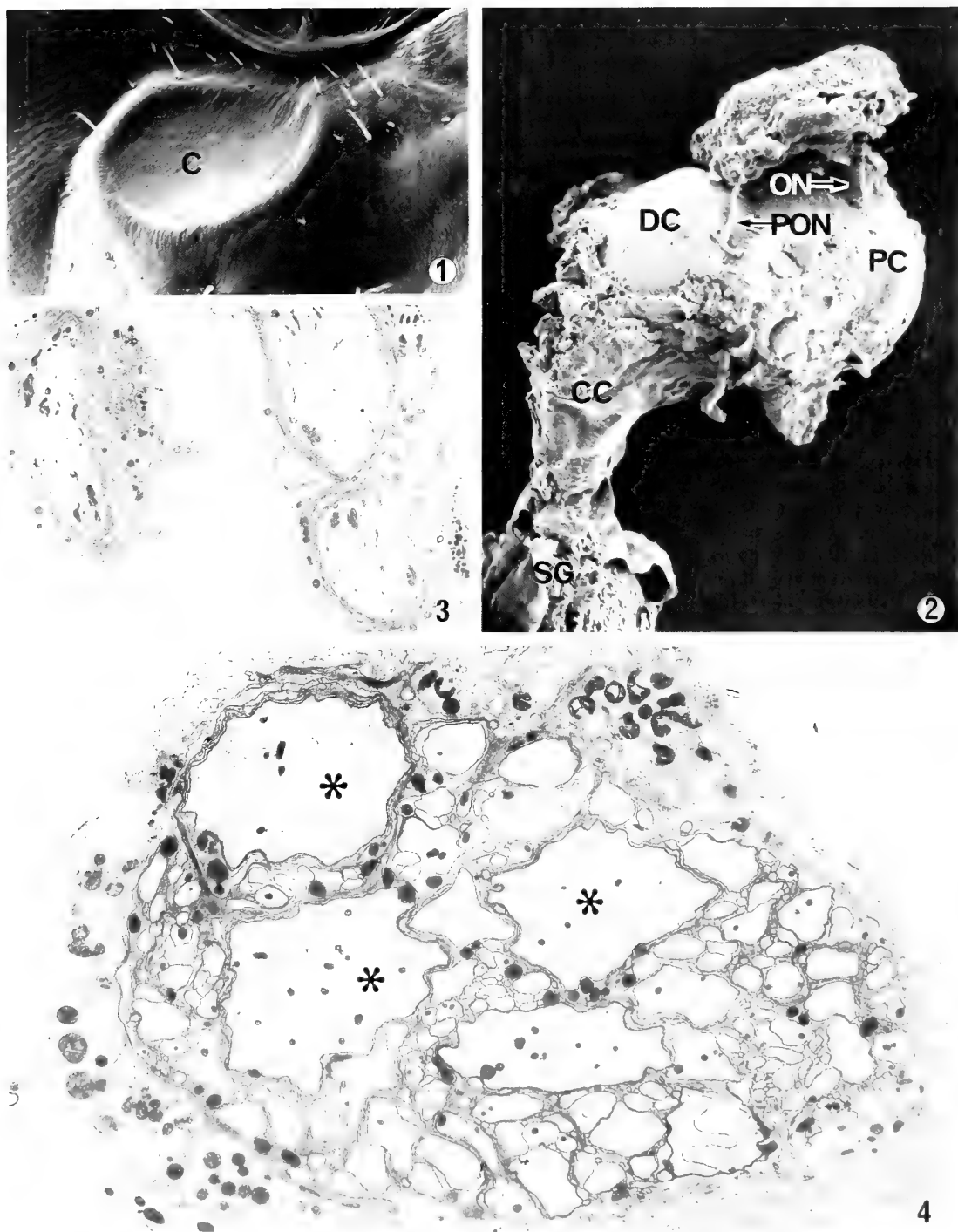


FIG. 1. A surface view of the ocellar region. Chaetic hairs occur around the ocellus. C, ocellus. $\times 68$.

FIG. 2. A bivalved brain viewed from the median plane. The para-ocellar nerve (PON) enters the deutocerebrum (DC). CC, circumoesophageal connective; ON, ocellar nerve; PC, protocerebrum; SG, suboesophageal ganglion. $\times 65$

with bees wax, and the para-ocellar nerve was exposed by partial removal of the cuticular integument. A suction electrode filled with physiological saline [9] was attached to the mid-region of the para-ocellar nerve, an indifferent electrode being inserted into the apex of the head. Two different stimuli were presented. Light from a tungsten lamp was focused upon the ocellus, its intensity being high enough to produce maximal ocellar ERG. Air puffs derived from an air compressor were directed towards the ocellar cornea through silicon tubes (2mm in diameter). The outlet of the tube was 10 mm apart from the head, and the velocity of the air stream was about 4 m/sec. Responses of the para-ocellar nerve were AC-amplified and photographed. Moreover, responses of chaetic sensilla located around the ocellar cornea to air puffs were extracellularly recorded by a sharpened tungsten electrode inserted into the base of the sensillum.

RESULTS AND DISCUSSION

The cockroach *P. americana* possesses a pair of ocelli: each ocellus ($400 \times 500 \mu\text{m}$) is located near the base of the antenna. The ocellar cornea is externally depressed, and sensory hairs occur around and on the cornea (Fig. 1). The ocellus is connected to the brain by two nerves. The ocellar nerve ($50 \mu\text{m}$ in thickness, $500 \mu\text{m}$ in length) originates in the posterior part of the ocellus, and enters the protocerebrum, whereas the para-ocellar nerve ($25 \mu\text{m}$ in thickness, $250 \mu\text{m}$ in length) originates in the anterior part of the ocellus and enters the deutocerebrum (Fig. 2). The para-ocellar nerve, viewed in cross sections through the mid-region, contains 130–200 fibers, about ten of them ranging between $1\text{--}5 \mu\text{m}$ (Fig. 4). The fibers contain many microtubules and mitochondria and only few vesicles. Adjacent fibers are separated from each other by thin glial cell envelopes, but no synaptic specializations occur among them. The para-ocellar nerve appears to be divided distally

into several bundles near the ocellus (Fig. 3).

The distribution of the para-ocellar nerve fibers within the CNS can be seen with cobalt backfills from the ocellus. The cobalt backfills show quite different courses of the ocellar nerve fibers and para-ocellar nerve fibers in the brain (Fig. 5). Usually several para-ocellar nerve fibers were stained. They descend through the ipsilateral circumoesophageal connective, and terminate in the suboesophageal ganglion. On their descending way they project lateral branches (up to $50\text{--}80 \mu\text{m}$ in length) in the mid-region of the circumoesophageal connective and into the anterior part of the suboesophageal ganglion (Fig. 6). They change their course in the suboesophageal ganglion towards the median plane, and terminate there with many branches (Fig. 7). Unlike the data obtained by silver impregnation [7], fibers, which were arborized and terminated around the olfactory lobe could not be cobalt-backfilled in the present study.

The distribution of the para-ocellar nerve fibers in the CNS, as was shown in the present study, is similar to previously reported mechanoreceptor axons: some examples are antennal mechanoreceptors of the locust which also terminate in the suboesophageal ganglion [10, 11]. In accordance with these anatomical findings it is assumed that the para-ocellar nerve may consist of primary axons of mechanoreceptive sensilla around the ocellar cornea: these axons must be backfilled by cobalt chloride which diffused out from the ocellus to the surrounding region. This assumption was physiologically confirmed. We found that the sensilla surrounding the ocellus responded to air puffs, and spike discharges were also recorded from the para-ocellar nerve in response to air puffs directed towards to ocellar cornea (Fig. 8).

These data suggest that the para-ocellar nerve contains axons transmitting mechanosensory information to the CNS. Whether the para-ocellar nerve is also involved in transmitting ocellar information remains unresolved, since we could

FIG. 3. Bundles of axons near the ocellar capsule. These bundles come together on their way to the brain to form the para-ocellar nerve shown in Fig. 4. $\times 2,200$.

FIG. 4. A cross section of the para-ocellar nerve near the deutocerebrum. Of about 200 fibers included three (asterisks) are more than $5 \mu\text{m}$ thick. $\times 5,200$.

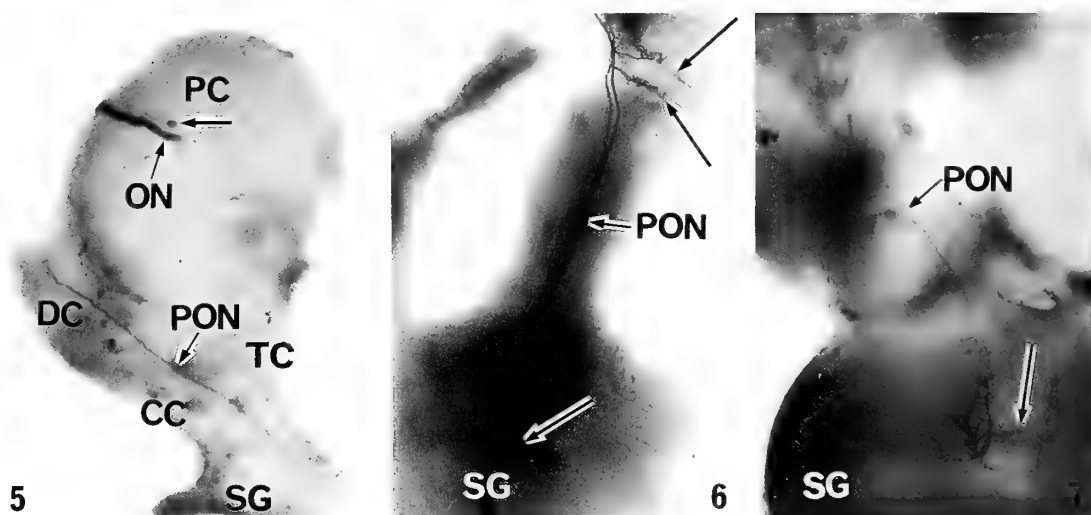


FIG. 5. Cobalt backfilled para-ocular nerve fibers (PON) and ocellar nerve fibers (ON) in a lateral view of the bivalved brain. Arrow, a cell body of the ocellar nerve fiber; CC, circumoesophageal connective; DC, duetocerebrum; PC, protocerebrum; TC, tritocerebrum; SG, suboesophageal ganglion. $\times 30$.

FIGS. 6 and 7. Cobalt backfilled para-ocular nerve fibers (PON) in frontal view of the brain. Note side branches (arrows) in Fig. 6, and terminal arborizations (arrow) in Fig. 7. CC, circumoesophageal connective; SG, suboesophageal ganglion. $\times 75$ in Fig. 6; $\times 94$ in Fig. 7.

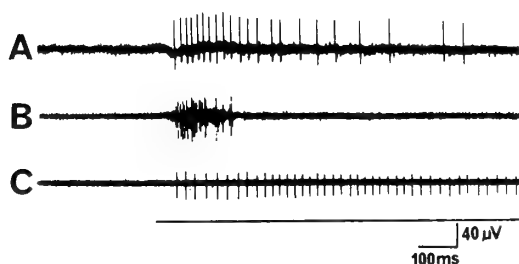


FIG. 8. Responses of the chaetic sensillum (A) and para-ocular nerve fibers (B, C) to air puffs to the ocellar cornea. The response of the para-ocular nerve fibers is phasic (B) or tonic (C). Multiple units were usually recorded (B). Bottom bar indicates the stimulus duration.

not find any responses to ocellar illumination. More elaborate studies are required to answer this question, because only several, probably thick, fibers were stained and their activities were recorded in the present study, and morphology and physiology of remaining fibers are still problematic.

ACKNOWLEDGMENTS

This work was supported in part by a grant-in-aid for Special Project Research on Molecular Mechanism of

Bioelectrical Response 60123002 from Japanese Ministry of Education, Science and Culture. The authors express their thanks to Dr. J. M. Ramirez, Department of Physiology, University of Alberta, Edmonton, Canada for critical reading of the manuscript.

REFERENCES

- 1 Goodman, L. J. (1981) In "Handbook of Sensory Physiology". Ed. by H. Autrum, Springer, Berlin, Vol. VII/6C, pp. 201–286.
- 2 Cooter, R. J. (1975) *Int. J. Insect Morphol. Embryol.*, **4**: 273–288.
- 3 Weber, G. and Renner, M. (1976) *Cell Tissue Res.*, **168**: 209–222.
- 4 Toh, Y. and Hara, S. (1984) *J. Ultrastruct. Res.*, **86**: 135–148.
- 5 Toh, Y. and Sagara, H. (1984) *J. Ultrastruct. Res.*, **86**: 119–134.
- 6 Koontz, M. A. and Edwards, J. S. (1984) *Cell Tissue Res.*, **236**: 133–146.
- 7 Brousse-Gaury, P. (1964) *C. R. Acad. Sci. (Paris)*, **267**: 649–650.
- 8 Toh, Y. and Yokohari, F. (1988) *J. Comp. Neurol.*, **269**: 157–167.
- 9 Yamasaki, T. and Narahashi, T. (1959) *J. Insect Physiol.*, **3**: 146–158.
- 10 Aubele, E. and Klemm, N. (1977) *Cell Tissue Res.*, **178**: 199–219.
- 11 Gewecke, M. (1979) *Entomol. Gen.*, **5**: 317–320.

Development

Growth & Differentiation

Published Bimonthly by the Japanese Society of
Developmental Biologists
Distributed by Business Center for Academic
Societies Japan, Academic Press, Inc.

Papers in Vol. 32, No. 2. (April 1990)

- J. D. Ebert: Yoshihiro Kato (1924–1988)—A celebration of a life in science
13. L. E. Stephens, G. W. Shiflet and F. Wilt: Gene expression, DNA synthesis and protein synthesis in cells from dissociated sea urchin embryos
 14. H. Urushihara, T. Saigo and K. Yanagisawa: Cell fusion promoting factor common to homothallic and heterothallic mating system in *Dictyostelium discoideum*
 15. M. R. Diaz, T. C. Takahashi and K. Takata: Concanavalin A acts as a factor in establishing the dorso-ventral gradient in the ventral mesoderm of newt gastrula embryo
 16. H. Kondoh: The mechanism of $\delta 1$ -crystallin gene regulation: cooperation of lense-specific and non-specific elements
 17. Y.-C. Hsu: Heterogenous macromolecular contributions to early mouse embryo development
 18. M. Ito, T. Kaneko-Ishino, F. Ishino, M. Mitsuhashi, M. Yokoyama and M. Katsuki: Developmental potential of haploid-derived parthenogenic cells in mouse chimeric embryos
 19. S. Tanaka and K. Dan: Study of lineage and cell cycle of small micromeres in embryos of the sea urchin, *Hemicentrotus pulcherrimus*
 20. K. Kitamura, M. Sezaki and M. Yanazawa: Analysis of embryonic chick periderm by monoclonal antibody against periderm
 21. H. Nakano, K. Kin Shita, K. Ishii, H. Shibai and M. Asashima: Activities of mesoderm-inducing factors secreted by mammalian cells in culture
 22. T. Mizuno, K. Kitamura, M. Saito and S. Tanemura: Epidermal metaplasia induced on amniotic ectoderm by the dermis of chicken embryos
 23. Y. Suzuki, T. Obara, S. Takiya, C.-C. Hui, K. Matsuno, T. Suzuki, E. Suzuki, M. Ohkubo, and T. Tamura: Differential transcription of the fibroin and sericin-1 genes in cell-free extracts
 24. R.-P. Huang, H. Muramatsu, and T. Muramatsu: Effect of different conditions of retinoic acid treatment on expression of MK genes, which is transiently activated during differentiation of embryonal carcinoma cells
 25. N. Hashimoto, S. Iwashita, Y. Shoji-Kasai, T. Kishimoto and K. Imahori: Thiol protease inhibitor, E-64-d, prevents spindle formation during mouse oocyte maturation
 26. Papaconstantinou, J., J. P. Rabek and Dong-er Zhang: Molecular mechanisms of liver-specific albumin and α -fetoprotein gene regulation: A review
 27. Sawyer, R. H.: Avian scale development XV: A study of cell proliferation in the epidermis of the scaleless, sc/sc, mutant
 28. H. Asaka, T. Inoue, and K. Mikoshiba: Two dimensional polypeptide mapping of the cerebella from neuropathological mutant mice, weaver, nervous and staggerer
 29. DeHaan, R. L., S. Fujii and J. Satin: Cell interactions in cardiac development

Development, Growth and Differentiation (ISSN 0012-1592) is published bimonthly by The Japanese Society of Developmental Biologists, Department of Developmental Biology, Mitsubishi Kasei Institute of Life Science, Minami-ootani 11, Machida, Tokyo 194, Japan. 1989: Volume 31. Annual subscription for Vol. 32, 1990: U. S. \$ 148.00, U. S. and Canada: U. S. \$ 163.00, all other countries except Japan. All prices include postage, handling and air speed delivery except Japan. Second class postage paid at Jamaica, N.Y. 11431, U. S. A.

Outside Japan: Send subscription orders and notices of change of address to Academic Press, Inc., Journal Subscription Fulfillment Department, 1 East First Street, Duluth, MN 55802, U. S. A. Send notices of change of address at least 6–8 weeks in advance. Please include both old and new addresses. U. S. A. POSTMASTER: Send changes of address to *Development, Growth and Differentiation*, Academic Press, Inc., Journal Subscription Fulfillment Department, 1 East First Street, Duluth, MN 55802, U. S. A.

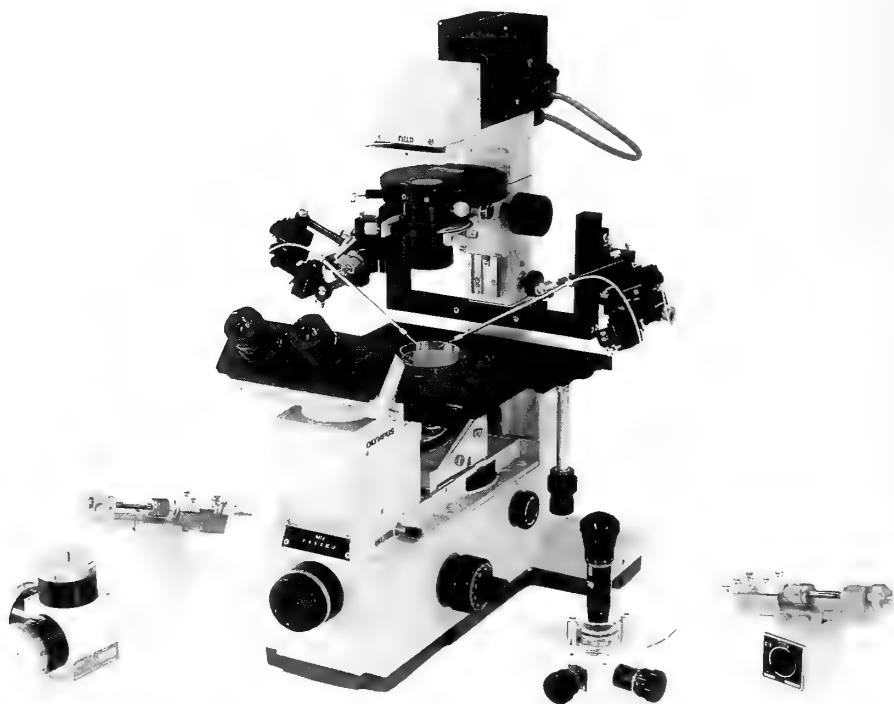
In Japan: Send nonmember subscription orders and notices of change of address to Business Center for Academic Societies Japan, 16-3, Hongo 6-chome, Bunkyo-ku, Tokyo 113, Japan. Send inquiries about membership to Business Center for Academic Societies Japan, 4-16, Yayoi 2-chome, Bunkyo-ku, Tokyo 113, Japan.

Air freight and mailing in the U. S. A. by Publications Expediting, Inc., 200 Meacham Avenue, Elmont, NY 11003, U. S. A.

NARISHIGE

THE ULTIMATE NAME IN MICROMANIPULATION

OUR NEW MODELS **WR-88** and **MO-102M**
MAKE PRECISION MICROMANIPULATION SO EASY!



SOME FEATURES of THE WR-88 WATER ROBOT MICROMANIPULATOR (3-DIMENSIONAL)

- * Drift-free, the new WR-88 has a DRIFT movement of less than 2 microns.
- * The new WR-88 has a SMOOTH MICRODRIVE MECHANISM.
- * An Aqua Purificate remote control ensures totally vibration-free operation.



NARISHIGE SCIENTIFIC INSTRUMENT LAB.

9-28 KASUYA 4-CHOME SETAGAYA-KU, TOKYO 157, JAPAN
PHONE (INT-L) 81-308-8233, FAX (INT-L) 81-3-308-2005
CABLE : NARISHIGE LABO, TELEX, NARISHIGE J27781

Sophisticated Balance between Safety and Centrifugation Capability without Compromise.

**Centrifuge in
Integrated with A
Refrigerator**

**Extra-Quiet
Operation**

**Ease of Loading/
Unloading
The Rotors**

**Quick Start/
Quick Stop**

High Quality

**Triple Safety
Design**

**Corrosion
Resistance**



**HIGH SPEED
REFRIGERATED
MICRO CENTRIFUGE**

MODEL MR-150

TOMY CORPORATION

SOLE AGENT

1002 SOLEIL NARIMASU BLDG., 31-8, NARIMASU 1-CHOME,
ITABASHI-KU, TOKYO 175 JAPAN
TEL:(03)976-3411 TLX: 02723111 TOMYCO J
CABLE: TOMYSHO TOKYO FAX: (GIII GII) (03)930-7010

TOMY SEIKO CO., LTD.

MANUFACTURER

2-2-12, ASAHICHO NERIMA-KU, TOKYO 176 JAPAN
TEL:(03)976-3111

(Contents continued from back cover)

Ovarian development and sex steroid hormones during the reproductive cycle of *Rana esculenta* complex 265

Mugiya, Y.: Long-term effects of hypophysectomy on the growth and calcification of otoliths and scales in the goldfish, *Carassius auratus* 273

Kobayashi, Y. and M. Okada: Urea stimulation of pituitary pars intermedia cells of suckling mice under copious drinking 281

Morphology

Itow, T., T. Masuda and K. Sekiguchi: Formation of ganglions and stomodaeum in normal and separate embryos of horseshoe crab, *Tachypleus tridentatus* 287

Taxonomy

Wynn, S., M. J. Toda and T. X. Peng: The genus *Phorticella* Duda (Diptera: Drosophilidae) from Burma and southern China .. 297

Fukuda, Y.: Early larval and postlarval morphology of the soldier crab, *Mictyris brev-dactylus* Stimpson (Crustacea: Brachyura: Mictyridae) 303

Okajima, S.: Some *Nesothrips* (Insecta, Thysanoptera, Phlaeothripidae) from east Asia 311

Miura, T. and L. Laubier: Nautiliniellid polychaetes collected from the Hatsushima cold-seep site in Sagami Bay, with descriptions of new genera and species 319

ZOOLOGICAL SCIENCE

VOLUME 7 NUMBER 2

APRIL 1990

CONTENTS

REVIEWS

- Yasugi, S. and T. Mizuno: Mesenchymal-epithelial interactions in the organogenesis of digestive tract 159
- Tiedemann, H.: Cellular and molecular aspects of embryonic induction 171

ORIGINAL PAPERS

Physiology

- Ip, Y. K., S. F. Chew and R. W. L. Lim: Ammoniogenesis in the mudskipper, *Periophthalmus chrysospilos* 187
- Niida, A. and T. Ohono: Tectal visual afferents from fish dorsolateral tegmental cells (COMMUNICATION) 327
- Mizutani, A. and Y. Toh: Morphological and physiological characterization of the paracellular nerve of the cockroach, *Periplaneta americana* (COMMUNICATION) 331

Cell Biology

- Fu, Y., S. Sato, K. Hosokawa and K. Shiokawa: Expression of circular plasmids which contain bacterial chloramphenicol acetyltransferase gene connected to the promoter of polypeptide IX gene of human adenovirus type 12 in oocytes, eggs and embryos of *Xenopus laevis* 195
- Kusakabe, T.: Ultrastructural studies of the carotid labyrinth in the newt, *Cynops pyrrhogaster* 201

Genetics

- Niwa, M. and N. Wakasugi: Abnormal development of preimplantation embryos derived from intersubspecific hybrids between *Mus musculus molossinus* and *M. m. domesticus* 209

Immunology

- Saad, A. H. and E. Cooper: Evidence for a Thy-1-like molecule expressed on earthworm leucocytes 217

Developmental Biology

- Sivasubramanian, P. and D. R. Nässel: Neural control of flight muscle differentiation in the fly, *Sarcophaga bullata* 223
- Tonegawa, Y., E. Hojiro and K. Takahashi: Effect of pH on the participation of calcium ion in the cell aggregation of sea urchin embryos 229

Reproductive Biology

- Tachi, C. and S. Tachi: Mechanisms underlying regulation of local immune responses in the uterus during early gestation of eutherian mammals. III. Possible functional differentiation of macrophages cultured together with blastocyst *in vitro*, with special reference to the cellular shape and production of leukotriene C₄ 235

Endocrinology

- Tasaki, Y. and S. Ishii: Effects of thyroxine on locomotor activity and carbon dioxide release in the toad, *Bufo japonicus* 249
- Yamada, C., S. Noji, S. Shioda, Y. Nakai and H. Kobayashi: Intragranular colocalization of arginine vasopressin- and angiotensin II-like immunoreactivity in the hypothalamo-neurohypophysial system of the goldfish, *Carassius auratus* 257
- Polzonetti-Magni, A. M., R. Curini, O. Carnevali, C. Novara, M. Zerani and A. Gobbetti:

(Contents continued on inside back cover)

INDEXED IN:

Current Contents/LS and AB & ES,
Science Citation Index,
ISI Online Database,
CABS Database, INFOBIB

Issued on April 15

Printed by Daigaku Letterpress Co., Ltd.,
Hiroshima, Japan

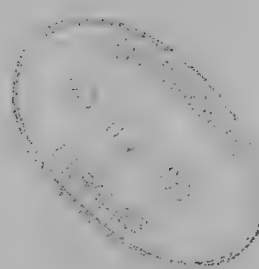
Vol. 7 No. 3

June 1990

ZOOLOGICAL SCIENCE

An International Journal

PHYSIOLOGY
CELL and MOLECULAR BIOLOGY
GENETICS
IMMUNOLOGY
BIOCHEMISTRY
DEVELOPMENTAL BIOLOGY
REPRODUCTIVE BIOLOGY
ENDOCRINOLOGY
BEHAVIOR BIOLOGY
ENVIRONMENTAL BIOLOGY
ECOLOGY and TAXONOMY



published by **Zoological Society of Japan**

distributed by **Business Center for Academic Societies Japan**
VSP, Zeist, The Netherlands

ISSN 0289-0003

ZOOLOGICAL SCIENCE

The Official Journal of the Zoological Society of Japan

Editors-in-Chief:

Seiichiro Kawashima (Tokyo)

Hideshi Kobayashi (Tokyo)

Managing Editor:

Chitaru Oguro (Toyama)

Assistant Editors:

Yuichi Sasayama (Toyama)

Hitoshi Michibata (Toyama)

Miëko Komatsu (Toyama)

The Zoological Society of Japan:

Toshin-building, Hongo 2-27-2, Bunkyo-ku,
Tokyo 113, Japan. Tel. (03) 814-5675

Officers:

President: Hiromichi Morita (Fukuoka)

Secretary: Hideo Namiki (Tokyo)

Treasurer: Tadakazu Ohoka (Tokyo)

Librarian: Masatsune Takeda (Tokyo)

Editorial Board:

Howard A. Bern (Berkeley)

Horst Grunz (Essen)

Susumu Ishii (Tokyo)

Koscak Maruyama (Chiba)

Tokindo S. Okada (Okazaki)

Hiroshi Watanabe (Tokyo)

Walter Bock (New York)

Robert B. Hill (Kingston)

Yukiaki Kuroda (Mishima)

Roger Milkman (Iowa)

Andreas Oksche (Giessen)

Mayumi Yamada (Sapporo)

Aubrey Gorbman (Seattle)

Yukio Hiramoto (Chiba)

John M. Lawrence (Tampa)

Kazuo Moriwaki (Mishima)

Hidemi Sato (Nagano)

Ryuzo Yanagimachi (Honolulu)

ZOOLOGICAL SCIENCE is devoted to publication of original articles, reviews and communications in the broad field of Zoology. The journal was founded in 1984 as a result of unification of Zoological Magazine (1888-1983) and *Annotationes Zoologicae Japonenses* (1897-1983), the former official journals of the Zoological Society of Japan. ZOOLOGICAL SCIENCE appears bimonthly. An annual volume consists of six numbers of more than 1200 pages including an issue containing abstracts of papers presented at the annual meeting of the Zoological Society of Japan.

MANUSCRIPTS OFFERED FOR CONSIDERATION AND CORRESPONDENCE CONCERNING EDITORIAL MATTERS should be sent to:

Dr. Chitaru Oguro, Managing Editor, Zoological Science, Department of Biology, Faculty of Science, Toyama University, Toyama 930, Japan, in accordance with the instructions to authors which appear in the first issue of each volume. Copies of instructions to authors will be sent upon request.

SUBSCRIPTIONS. ZOOLOGICAL SCIENCE is distributed free of charge to the members, both domestic and foreign, of the Zoological Society of Japan. To non-member subscribers within Japan, it is distributed by Business Center for Academic Societies Japan, 6-16-3 Hongo, Bunkyo-ku, Tokyo 113. Subscriptions outside Japan should be ordered from the sole agent, VSP, Utrechtseweg 62, 3704 HE Zeist (postal address: P. O. Box 346, 3700 AH Zeist), The Netherlands. Subscription rates will be provided on request to these agents. New subscriptions and renewals begin with the first issue of the current volume.

All rights reserved. No part of this publication may be reproduced or stored in a retrieval system in any form or by any means, without permission in writing from the copyright holder.

© Copyright 1990, The Zoological Society of Japan

[Publication of Zoological Science has been supported in part by a Grant-in-Aid for
Publication of Scientific Research Results from the Ministry of Education, Science
and Culture, Japan.]

REVIEW

Recent Studies of Fish Pancreatic Hormones: Selected Topics

ERIKA M. PLISETSKAYA

*School of Fisheries, HF-15, University of Washington,
Seattle, Washington 98195, U.S.A.*



Contents

Introduction
Immunocytochemical and structural studies of pancreatic hormones
Circulating levels of pancreatic hormones and their biological activity
Hormone-receptor interactions
Pancreatic hormones in fish under various physiological conditions
a) Smoltification
b) Spawning migration
c) Experimental fasting <i>versus</i> feeding in teleost fishes
Conclusion
References

INTRODUCTION

Interest in fish pancreatic hormones has grown substantially during recent years. This interest stems not only from the fact that Brockmann bodies of fish provide a useful model for the processing and secretion of peptide hormones, but also from the conviction among biologists that fish research promises both theoretical and practical benefits [1].

Various aspects of progress in the field of fish pancreatic hormones and their roles in regulation of metabolism in cyclostomes and fishes have been reviewed recently [2-7]. Epple and Brinn's [8] book "The Comparative Physiology of the Pancreatic Islets", an encyclopedic source of information, deals with most aspects of the structure of the vertebrate pancreas and the functions of its active peptides. Specific details of the amino acid sequences of pancreatic hormones and their biosynthetic pathways in fish, as compared to other vertebrates, have been thoroughly covered by

Conlon [9]. Nevertheless, new information in this field is accumulating so rapidly that it seems worthwhile at this time to summarize the latest trends and findings in the studies of the fish endocrine pancreas. Most references to the actions of mammalian pancreatic hormones on fish were deliberately omitted because these topics have been repeatedly and adequately discussed in the literature [3, 8, 10].

List of abbreviations used

aPY or YG-anglerfish pancreatic peptide Y
CCK-cholecystokinin
EGF-epidermal growth factor
ELISA-enzyme linked immunoassay for soluble antigens
GLP-glucagon-like peptide
GLU-glucagon
GH-growth hormone
IGF-1, IGF-2-insulin-like growth factors 1 and 2
INS-insulin
NPY-neuropeptide Y
PP-pancreatic polypeptide
RIA-radioimmunoassay
sPP-salmon pancreatic polypeptide
SST-somatostatin
YY-peptide YY

IMMUNOCYTOCHEMICAL AND STRUCTURAL STUDIES OF PANCREATIC HORMONES

Reports of basic immunocytochemical investigations, as well as correlative immunocytochemical and electron microscopical studies, continue to be numerous [11–20]. A typical pattern of recent research of this type is the use of several mono- or polyclonal antisera (instead of one), raised against the same antigen, but recognizing different oligopeptide or polypeptide fragments of hormone molecule.

Employing this approach McDonald *et al.* [21], discovered that two peptides of the somatostatin (SST) family, SST-14 and SST-28, which in the anglerfish (*Lophius americanus*) are the products of two separate genes (gene I and gene II), are expressed in different types of pancreatic cells. Moreover, the islet cells that process the product of gene II, (so called SST-28-II) were localized in close association with glucagon-immunopositive (GLU-immunopositive) cells. This observation was extended by Nozaki *et al.* [17] who found that, in salmon and trout Brockmann bodies, the cells producing SST-25-II were in close topographical association with GLU-immunopositive cells, while the cells producing SST-14-I, were located more centrally, in association with insulin-immunopositive (INS-immunopositive) cells (Fig. 1). This finding suggests that, in teleostean fish, such as catfish (*Ictalurus* sp.), eel (*Anguilla anguilla*), sculpin (*Cottus scorpius*) and probably many others, which, in contrast to mammals, possess two separate sets of genes for SSTs [3, 4, 9, 22], these SSTs will also be found in different types of cells. Indeed, Abad *et al.* [13] reported recently that, in the Brockmann body of gilthead sea bream (*Sparus auratus*), from which the gene II SST has not been yet isolated, immunostaining with antibodies against SST-25-II from salmon and against mammalian SST-14-I, follows a pattern similar to that in the anglerfish, salmon and trout. These observations lead, naturally, to several questions that need to be addressed. First, why is there such a specific separation of anatomical sites of production of the two SSTs, since some other peptides, even if they belong to different families, such as

GLU and pancreatic polypeptide (PP), often co-exist in the same cells and, moreover, in the same secretory granules [reviewed in 12, 18]? Second, does the close topographical association between cells that produce SST-25-II with GLU cells and between cells that produce SST-14-I with INS cells, imply an as yet unknown functional relationship between these pancreatic peptides in fish? Yet another enigma to be resolved is the distribution in the brain of some “big” SSTs, which are either the products of gene II (e.g., in salmonids, catfish, sculpin, anglerfish and eel), or truncated products of gene I [lamprey, 23; hagfish, 24]. Morel *et al.* [25], came to the conclusion that processing of two distinct precursors of SSTs in the teleostean fish operates “in a fixed pattern rather than in a tissue-specific manner”, however, they found that in the pancreas of anglerfish the product of gene II (SST-28-II) prevails while in the brain the level of SST-28-II is very low. In the gut cells only traces of SST-28-II could be detected. Nozaki *et al.* [17] failed to find any cells that were immunopositive for SST-25-II in the neurohypophysis or hypothalamus of either Pacific salmon or trout, while cells positive for SST-14-I were abundant. It is noteworthy that Marchant *et al.* [26] and Marchant and Peter [27] found that neither catfish SST-22-II, nor salmon SST-25-II inhibited the release of growth hormone (GH), while SST-14-I retained its full inhibitory potency. Therefore, the abbreviation SRIF (somatotropin release inhibiting factor) does not seem to be applicable to the SSTs encoded by the gene II family. SST-14-I was the only SST that has been found in the pancreas and in the gut of cartilaginous fishes [28]. In these fishes, the distribution of SST and GLU-immunoreactivities suggests a possible regulatory role of both peptides in gastric secretion and/or cell proliferation. Moreover, paracrine interrelationships between GLU and SST-14-I have been suggested both in the pancreas and in the gut [29, 30].

In dogs, only SST-28-I (the amino-terminal extension of SST-14-I) from the stomach and intestine seems to respond to physiological stimuli. The pancreatic SST-14-I, by contrast, is believed to have mainly a nonhormonal, local paracrine function [31–35]. What then is the situation in lam-



FIG. 1. Four successive sections of a rainbow trout pancreas stained differentially with antibodies against salmon SST-25-II, preabsorbed with SST-14-I (a); antibodies against mammalian-type SST-14-I (b); antibodies against salmon insulin (c) and antibodies against salmon glucagon (d). Note the topographical differences in the distribution of cells that contain SST-25-II-like (a) and SST-14-I-like (b) immunoreactivities. Note also topographical associations between the cells containing sSST-25-I-like and glucagon-like immunoreactivities (a, d) and SST-14-I-like and insulin-like immunoreactivities (b, c) respectively. From reference [17] (Gen. Comp. Endocrinol., with permission).

preys and teleost fish, in which the pancreatic cells that express gene I SST-34 (lamprey) or one of gene II SSTs (teleosts) are either present in equal numbers or are more abundant than any other types of cells, and "big" SSTs are the major peptides processed in the islet organ [16, 17, 23, 36, 37]? Is the role of these pancreatic SSTs confined to paracrine effects on adjacent GLU/GLP cells (in teleost fish) or upon INS-secreting cells (in lampreys)? Do these SSTs also have metabolic or still other potencies, as has been reported by Sheridan *et al.* [38]? Is there any functional difference between SSTs of the gut and those of pancreatic origin in lampreys, which have abundant SST-immunopositive cells located both in the gut and in the pancreatic islets [16, 36]?

In 1988 much progress was made in the elucidation of the primary structures of pancreatic hormones of agnathans (hagfish and lamprey), the only two current representatives of the most primitive vertebrates. Pancreatic SSTs of hagfish (*Myxine glutinosa*) and lamprey (*Petromyzon marinus*) were isolated and their amino acids sequenced [23, 24]. SSTs of lamprey are peptides of 34–37 amino acids with SST-34-I, as the predominant form. Hagfish SST is also a peptide of 34 amino acids and it is strikingly similar to lamprey SST at the carboxyl end, where 17 of the amino acids are identical. By contrast, 16 other amino acids in the hagfish and lamprey SST-34 are completely different, and only 2 of them are in identical positions [23] (Fig. 2). Agnathan SSTs are the result of significant differences in the processing of proSSTs (precursors to SSTs) as compared to the processing of SSTs in either teleost fish or mammals: in both hagfish and lamprey, a series of

amino-terminally truncated peptides is processed proteolytically at a single Arg residue, as well as at adjacent basic residues [23, 24].

Lamprey INS, also isolated in 1988 [39], differs from both teleostean and mammalian INSs to the same extent as the latter differ from one another. For example, lamprey INS has 14 amino acid substitutions at the variant positions when compared to porcine INS, and the same number of substitutions when compared to salmon INS. The primary structures of agnathan insulins seem to confirm that hagfishes and lampreys, have followed markedly independent routes of evolution [40]. Lamprey (*Petromyzon marinus*), as compared to hagfish (*Myxine glutinosa*), has 17 substitutions among 52 amino acids in the A- and B-chains of INS [39, 41]. These differences contrast with the known similarities in the structures of INS from related species of fish. For example, three species of Pacific salmon (*Oncorhynchus kisutch*, *O. keta* and *O. gorbuscha*) and three species of holocephalan fish, belonging to each of three existing families, namely, *Hydrolagus colliei*, *Chimaera monstrosa* and *Callorhynchus milii*, are 96–100% identical in terms of their INS structures [42–48]. Even more striking is the result, that the ray (*Torpedo marmorata*) and the shark (*Squalus acanthias*), despite the divergence in their evolution about 200 million years ago, still retain more than 90% homology in their INS structures [49, 50]. It would be worthwhile to determine whether the INS structures of various species of lamprey (or hagfish) show as much similarity within the respective groups as do the structures of salmonid or holocephalan insulins.

The amino acid sequences of several C-peptides

Somatostatins



Fig. 2. Comparison of amino acid sequence of somatostatins from the lamprey (*Petromyzon marinus*) and the hagfish (*Myxine glutinosa*). From references [23 and 24]. The vertical lines indicate putative sites of processing for production of SST-14-I and SST-34-I.

from fish have been deduced from nucleotide sequences of clones of cDNA for preproinsulin [reviewed in 51]. However, only one C-peptide of fish (European eel, *Anguilla anguilla*) has actually been isolated [51]. A comparison of its structure with the predicted structures of C-peptides from hagfish, ray, anglerfish, salmon and carp has revealed that, unlike the insulins, the structural similarity among C-peptides is weak, with the exception of several amino acids in the central region of the polypeptide chain.

Information of considerable interest has appeared concerning another family of pancreatic hormones, namely glucagon (GLU) and its related peptides. This information followed the discovery of the so-called glucagon-like peptides (GLPs), the sequences of 31–34 amino acids located at the carboxyl end of the preproglucagon molecule. In contrast to the mammalian species, in which two GLPs, organized in tandem, are encoded in the same preproglucagon sequence [52], only one GLP has been isolated from teleostean fishes [anglerfish, catfish, salmon and sculpin, 3]. The same is true for the primitive holostean garfish, *Lepisosteus spatula* [53], and for a holocephalan fish, *Hydrolagus colliei* [54]. To date no GLP has been found in agnathans. However, the above mentioned studies do not exclude the possibility that piscine proglucagons may still contain more than one GLP sequence. Thus far, both GLPs (GLP-1 and GLP-2) have been found only at the evolutionary stage of amphibia: two GLPs are expressed, in the endocrine pancreas of the bullfrog, *Rana catesbeiana* just as they are in mammals [55].

Multiple, often truncated, molecular forms of SST, INS, GLU and GLP, each encoded in the same preprohormone, seem to be the rule rather than the exception in fish. Recent examples have been provided by Andrews *et al.* [23] and Conlon *et al.* [24, 54] who found multiple molecular forms of SST in the lamprey, and multiple forms of INS and GLP in the ratfish. Each of these groups of peptides probably contains the products of the same gene. By contrast, salmon may contain two preproinsulin genes that encode for two different preproinsulins, one of which is present at much higher levels [42] than the other [48, 56]. Two

different insulins were discovered about thirty years ago in bonito fish [57] and quite recently in an amphibia, *Xenopus laevis* [58, 59].

The pancreatic polypeptides (PP) and their expression in fish have also been the focus of substantial attention during the recent years. Anglerfish (*Lophius americanus*) PP, named YG (glycine-extended form) or aPY, resembles neuropeptide Y (NPY) from porcine brain and the peptide YY from intestine more closely than it resembles any mammalian PP [60]. The same is true for PP from salmon [61], sculpin [22, 62] and garfish [63]. It is remarkable that such similarities seem to be confined to fish, while amphibian (bullfrog) PP is a typical bird- or mammalian-type peptide, being similar to the human PP sequence [55].

More detailed studies on anglerfish have revealed that there is more than one molecular form of NPY-like peptide in their islet organ. The majority of NPY-like peptides appear to be the YG-peptide that is expressed in a subset of islet cells, while the minor form of NPY-like peptide, closely resembling porcine or human NPY, is localized in the neurons of anglerfish brain and in islet nerves [64, 65]. It has been suggested that peptide YG is a precursor of biologically active peptide [Des³⁷-Gly]-aPY-amide [65a].

As far as we know, there are no reports of the identification of a novel peptide, pancreastatin, in fish endocrine islets. This peptide of 49 amino acids was recently purified from extracts of the porcine pancreas by Tatamoto *et al.* [66] and was demonstrated to be important in the regulation of pancreatic exocrine and endocrine secretions in mammals [67, 68].

CIRCULATING LEVELS OF PANCREATIC HORMONES AND THEIR BIOLOGICAL ACTIVITIES

The major technique used for the measurement of circulating levels of pancreatic hormones in fish has been the radioimmunoassay (RIA), although it is now evident that the enzyme-linked immunosorbent assay (ELISA) should be considered seriously as a future substitute for RIAs. It was anticipated in 1979 that non-radiometric, ELISA methods could be developed that would be as

sensitive as or even more sensitive than existing RIAs [69, 70]. Such methods are less hazardous since they do not involve the use of radiolabeled hormones and they eliminate the problem of radioactive-waste disposal.

Assays for specific measurements of pancreatic hormones in fish systems are still not common. However, assessment of INS by RIAs using piscine components are already performed in scientific laboratories in Canada, Israel, Japan, Norway, Spain, the United Kingdom, the USA and the USSR. The main obstacle for much of the potentially important fish-related research remains the lack of homologous fish hormones and antisera, although heterologous antibodies raised against insulins from scorpion fish, bonito, cod and anglerfish and their respective [125 I] derivatives as tracers, have been used satisfactorily in RIAs of insulins from other species of teleosts [71–78]. The need to develop more assays for teleost INS has increased since the initiation of projects directed towards the transplantation of the Brockmann bodies of fish into diabetic mammals [79] which made necessary measurements of the hormones released from the transplants.

A fully homologous RIA for fish (salmon) INS [80] has been used extensively. The results of assays of plasma INS in juvenile salmonids, in a wild population of pink salmon (*O. gorbuscha*) during their spawning migration, and in domesticated fish starved or fed specially designed diets, were reported recently [3–5, 80–86]. These results are described in more detail below.

As is now the case in mammalian studies, the regulatory effects of the novel peptides galanin and pancreastatin [66, 87] on the secretion of INS in fish and the mechanisms of their actions will probably become the focus of numerous studies as soon as these peptides are isolated from fish gut and pancreas.

Another breakthrough can be expected in the measurement of circulating levels of the second most abundant fish pancreatic hormone, a gene II SST. A fully homologous assay system for coho salmon (*O. kisutch*) SST-25-II, which has proved to be suitable for measurements in a variety of other salmonid species, was recently developed by Sheridan *et al.* [88]. Since the structure of second

SST from fish, SST-14-I, is identical in fish and homeothermal vertebrates, the mammalian RIA systems should suffice for the measurement of this peptide in fish.

Unlike INS and SST-25-II, circulating levels of GLU can be assayed by mammalian RIA [77], although such assays are still rarely used. Only two groups of researchers have employed either catfish [89] or salmon [90] homologous RIA systems to measure GLU in the Brockmann body and plasma of the respective species of fish.

RIAs for mammalian glucagon-like peptide (GLP) have been described by Ørskov and Holst [91] and Oshima *et al.* [92] but we not know of any application of these RIAs to fish. It seems that antibodies raised against piscine GLP do not cross-react with mammalian GLP (Plisetskaya, unpubl.). The only published data on levels of circulating GLP in fish have been obtained by homologous salmon RIAs [85, 86, 90, 93]. Under non of the experimental conditions studied were the titres of GLU and GLP in plasma of salmonids higher than the INS titres [90]. Plasma levels of GLP were usually higher than plasma levels of GLU. The same pattern was observed after extraction of the principal islets of the fish [94, 95]. Several hypotheses have been suggested to explain the discrepancy in the yields of the two peptides that are part of the same prohormone. None has been proven. However, the differences in circulating levels of GLU and GLP have, seemingly, been provided with a logical explanation: Oshima *et al.* [92] reported that, in mammals, GLP *in vivo* is degraded more slowly than GLU. Our preliminary results from studies of incubation of isolated salmon hepatocytes in the presence of salmon GLP and GLU (Mommensen and Plisetskaya, unpubl.) suggest the same trend in fish.

While the data concerning the biological activities of INS and SST in fish continue to accumulate steadily [reviewed in 90, 96, 97], explorations into the role of GLU and, in particular, GLP in both mammals and fish made the very rapid progress during the last three years [90, 93, 96, 98–100]. The most unexpected finding was the apparently strong glycogenolytic, gluconeogenic and lipolytic effects of teleost GLP in fish [90, 101], while all attempts of find similar effects in the mammalian

liver have failed [102–105]. It was even suggested that GLP, although a member of the GLU-family, has no metabolic activity [102]. Part of the solution to this problem may have been found recently, when several research groups [106–108] reported simultaneously that the biologically active form of mammalian GLP-1 consists, not of 37 amino acids, but of 31 (sequence 7–37) which correspond to the amino acid sequence of GLP from salmon and anglerfish [94, 95].

The biological activities of GLP 7–37 (or GLP 7–36-amide) in mammals were tested primarily to determine the relation of these peptide to other pancreatic hormones, and GLP emerged as the most potent stimulator of the release of INS [106–110]. In addition GLP 7–36-amide enhances the release of SST and inhibits the release of GLU [110–111]. To reveal any insulinotropic effect of salmon GLP on perfused Brockmann bodies from fish of the same species, this peptide should be applied at concentrations at least 100-fold higher than those reported for mammals [97]. In experiments *in vivo*, the insulinotropic action of the GLP is barely detectable [90]. Teleost fishes still remain the only vertebrate group in which glycolytic and gluconeogenic fluxes are influenced by GLP [100]. By contrast, a fragment of GLU (GLU 19–29), which exhibits a potent metabolic action that is mediated by calcium ions in the mammalian liver [99, 112], seems to be without effect in piscine liver, supposedly because of the absence of analogous calcium-dependent systems [100].

Although GLPs from salmon, anglerfish and catfish all activate the production of glucose in teleosts, notable differences exist between fish species. Moreover, the actions of GLP, as is also true for GLU, are strongly dependent on the season and, probably, on the stage of the fish life cycle [100]. Both GLU and GLP seem to affect identical targets in the liver. However, the mechanisms of their action may differ: Mommsen and Moon [100] reported that no direct relationship exists between the amount of intracellular cAMP and either the metabolic action of GLU, or, in particular, of GLP. (Fig. 3). Once again, the differences between fish species are substantial [93, 101].

In this field of research more questions remain

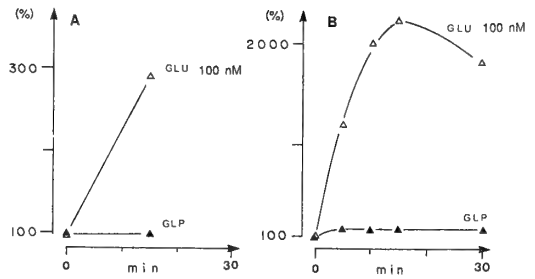


Fig. 3. Time course of intrahepatic accumulation of cAMP after application of GLU and GLP to hepatocytes from (A) trout (*O. mykiss*) and (B) eel (*Anguilla rostrata*). Values are expressed in terms of the percentage increase over vehicle-treated controls. Control levels of cAMP in salmon and eel, respectively, were 386 and 533 pmoles/g fresh weight of cells. Both bovine glucagon and salmon GLP were applied at concentrations of 10^{-7} M. \triangle glucagon; \blacktriangle glucagon-like peptide. From reference [100] (Fish. Biochem. Physiol., with permission).

to be addressed than have been answered. The first among them is: why does the metabolic action of GLP seem to be confined to fish? Does this unique property of GLP have any special physiological meaning? Can the preproglucagon be expressed in piscine organs, other than the pancreas and gut, for example, in the brain, as it is in mammals [113]?

Diurnal oscillations in piscine plasma levels of INS have been reported [83, 114] but it remains to be determined whether INS, GLU and SSTs in fish are secreted steadily or in pulses, as they are in mammals [115].

The study of the fourth group of fish pancreatic hormones, the pancreatic polypeptides (PP) has also progressed substantially during the recent years, mostly due to efforts of B. D. Noe, P. C. Andrews, A. Balasubramanian and their associates. Radioimmunoassays for anglerfish peptide YG (glycin-extended form) and for NPY-amide have been developed and aPY-like peptides in the anglerfish brain and pancreas were characterized [65, 115a]. The next logical step will probably be an attempt to assess levels of these peptides in plasma, followed by an evaluation of changes in these levels under various physiological conditions.

Anglerfish peptides belonging to the PP-family,

namely, YG and APY-NH₂, and salmon PP (NPY-NH₂) have been synthesized and tested for their biological activity in mammals. Bolus doses of natural and synthetic salmon PP and synthetic anglerfish aPY-NH₂ increased the blood pressure and decreased the heart rate in anesthetized rats in a dose-dependent manner; aPY-NH₂ diminished the volume and bicarbonate content of pancreatic juice during secretin-stimulated, exocrine pancreatic secretion in conscious dogs [116–117].

These results demonstrate that teleost PPs are not only structurally similar to mammalian NPY and PYY, but also that they can mimic NPY- and PYY-like activities in mammals [116, 117]. Of additional interest are the pilot data (Balasubramaniam, personal communication) from the direct injection of fish PP into the rat hypothalamus. This treatment enhanced the feeding behavior of the experimental animals, as does mammalian NPY [118, 119]. Consequently, we can hypothesize that PP plays a similar role in teleost fish during naturally occurring periods of either fasting or restoration of feeding. Moreover, these data appear to support the hypothesis [61] that a very low number of PP (NPY) cells and a low content of the peptide in the Brockmann body of spawning coho salmon are the correlates of a particular period in the life cycle, when the fish is naturally fasting.

In comparison to efforts in previous years, less time is now being devoted to experiments *in vitro* and *in situ* on fish Brockmann bodies and/or principal islets. Ronner and Scarpa [89], using their experimental model, which consists of a perfused isolated Brockmann body from the channel catfish (*Ictalurus punctatus*), reported a striking similarity in the responses of the catfish and higher vertebrates to hexoses. However, the catfish Brockmann body seemed to be sensitive to fewer of the common stimuli for the release of pancreatic hormones than is the mammalian pancreas.

One observation which clearly deserves more attention is that the D-cells of the catfish Brockmann body, which produce SST-14-I, are more sensitive to glucose (but not to amino acids) than INS cells [89]. This finding was confirmed by Sheridan *et al.* [88] in experiments *in vivo*. We can speculate that this particular pattern may be re-

sponsible for the comparatively low, and sometimes delayed, glucose-stimulated release of INS in teleost fish, as compared to the amino acid-stimulated release of INS. If, in addition, it is confirmed, in the future, that GLP in fish is not as potent a stimulator of the secretion of INS as it is in mammals [5] we will be closer to an understanding of the intolerance to carbohydrates of apparently INS-nondeficient fish.

No reports of studies *in vitro* of agnathans' pancreatic islets have appeared during the past few years.

The average plasma levels of INS, SST, GLU and GLP in the peripheral blood of teleosts are usually higher than those in mammals (cf., for example, Table 1 and 4). It is known, however, that the high levels of immunoreactive INS, observed in mammals under certain conditions, such as in cases of INS-resistant *diabetes mellitus*, are in fact caused by an increase in levels of proinsulin in the immunoreactive pool, measured as INS [120]. Conlon and Thim [51] recently isolated the first teleostean (eel) C-peptide of proinsulin. It is to be hoped that this accomplishment will provide researchers with a tool for the assessment of levels of proinsulin in fish, so that the question of the contribution by proinsulin to plasma levels of INS in fish and to binding to receptors can finally be addressed.

Our knowledge of plasma levels of pancreatic hormones in fish has resulted in a clear change in the attitudes of comparative physiologists and biochemists: most of them are turning now to usage of "physiological doses" of hormones for experiments both *in vivo* and *in vitro*. However, the question remains as to whether the levels of hormones that are routinely measured in the peripheral blood correspond to those that the liver cells actually "see".

As in mammals, the fish liver is the major organ for glucose homeostasis, the primary target for pancreatic peptides and an important site for their degradation [121]. Consequently, it is logical to expect that in fish, as in mammals, the liver is exposed, through the hepatic portal vein, to much higher levels of pancreatic peptides than is any other organ. However, until 1989 no actual values for levels of pancreatic peptides circulating in

TABLE 1. Titres of some pancreatic hormones in the peripheral blood of various salmonids

Species	(ng/ml)*				References
	Insulin	Glucagon	GLP	SST-25-II	
<i>O. kisutch</i>	0.9–15.0	0.01–2.00	0.10–2.30	0.15–1.20	<i>INS, GLU, GLP</i>
<i>O. tshawytscha</i>	1.5–9.1	0.05–0.06	0.20–2.80	0.15–1.20	[3, 4, 80, 83]
<i>O. gorbuscha</i> (wild population)	0.2–3.0				[85, 86, 90, 17] <i>SST-25-II</i>
<i>O. mykiss</i>	1.7–48.0	0.01–2.00	0.10–2.10	0.15–1.20	[88]
<i>S. salar</i>	2.0–40.0	0.01–1.60	0.05–1.90		
<i>S. gairdneri</i> ** (steelhead, wild population)	0.1–4.2				

* The values represent a summary of results of many different assays of fish of a particular species (60–200 fish per group), but of different age, sex and feeding conditions, maintained on various diets and at various water temperatures. For variations in levels of hormones in uniform groups of fish see the original publications.

** New species name for *Salmo gairdneri* is *Oncorhynchus mykiss*.

various blood vessels of the same fish could be found in the literature. Such values were obtained from an adult trout and published recently [122]. As could have been expected, levels of INS, GLU and GLP in peripheral blood constituted only 20–30% of those in the hepatic portal vein (Table 1). There is no doubt that differential blood sampling from various vessels, if continued in studies on fish, will provide us with new insights into the uptake and processing of biologically active peptides by their target tissues.

Precise information about the concentrations of pancreatic hormones at the “entrance” to and “exit” from the liver will be of benefit to several groups of researchers who are experimenting with slices of fish liver or isolated hepatocytes [93, 100, 121, 123]. These studies have become even more challenging since the publication of the new concepts that have been introduced into investigations on mammalian liver. The idea [124] that the liver acinus is a unit of hepatic microcirculation seems to be generally accepted by mammalian physiologists [125]. Three distinct metabolic zones in liver acini, namely, the periportal, perivenous (or pericentral) and intermediate zones have been proposed. Morphological, histochemical and biochemical differences between these zones [125, 126] and some differences in the hormonal regulation of gluconeogenesis and ketogenesis in periportal and perivenous rat hepatocytes have been

reported [127]. Methods have been developed for the separation of so-called periportal and perivenous liver cells from mammals [128–131]. Whether this idea of metabolic zonation can be applied to the piscine liver, microstructure of which differs in many ways from that of the mammalian liver [132–134], remains controversial. The first studies on two populations of hepatocytes separated from the same liver of trout and catfish by pulses of digitonin that were followed by digestion with collagenase and Percoll-gradient centrifugation, were undertaken by Mommsen *et al.* [135] and Ottolenghi *et al.* [136]. Although some metabolic differences between “periportal” and “perivenous” pools of cells were found, both studies failed to reveal either a real “metabolic zonation” or different responsiveness to glucagon, in terms of carbohydrate fluxes, in these cells. Improved methods for the separation of cells may be needed for future research in this field.

HORMONE-RECEPTOR INTERACTIONS

In sharp contrast to extensive investigations in mammalian systems the receptors for pancreatic hormones in fish tissues remain almost completely unexplored [2], although the cyclostome and fish hormones, in particular INS, have been tested for their binding to mammalian plasma membranes. These studies have concentrated mostly on evalua-

tions of the potency of newly isolated piscine hormones, as compared to their mammalian counterparts. Fish pancreatic peptides either do not bind to mammalian receptors or have much lower binding affinities than do the mammalian peptides [42, 54, 105, 137–140]. The same pattern (lower binding affinity as compared to mammalian INS) has been found when agnathan or piscine insulins are bound to the receptors in homologous tissues [141–144]. Report on the structure of the INS receptor in the plasma membranes of the hagfish (*Myxine glutinosa*) liver [145] supports an earlier conclusion that the receptor protein has been much better conserved in the course of vertebrate evolution than the ligand [141, 142, 146]. The partial amino acid sequence of the INS receptor from coho salmon (S. Chan, personal communication) lends further support to this hypothesis. However, an INS receptor from the stingray (*Dasyatis americana*) liver [147] seems to display some peculiar features in its structure. It has been reported to be a dimer, consisting of two identical subunits, each with a binding (alpha) and a tyrosine kinase (beta) domain. Stuart [147] suggested that the stingray receptor is not completely cleaved. This stands in marked contrast to all other (mammalian, avian, reptilian and amphibian) receptors for INS, which are tetramers, built from two extracellular alpha subunits and two transmembrane/intracellular beta subunits. The alpha subunits are connected to one another and to the beta subunits by disulfide bonds [148–151]. The same description seems to be applicable to the INS receptor from *Drosophila melanogaster* [152] which has a subunit structure similar to that of the mammalian INS receptor. By contrast, the proposed structure of the stingray INS receptor [147] more closely resembles that of receptors for IGF II and for EGF.

Competitive binding of INS and IGF to the INS receptor of the stingray led Stuart [147] to the conclusion that, at the phylogenetic stage of the elasmobranch fish, both INS and IGF may transduce their signals through the same receptor. Some overlap in structure, specificity and function between receptors for IGF-I, IGF-II and INS has been reported recently in the early chick embryo and in the lizard brain [151, 153]. Nevertheless,

recent studies of Gutiérrez and Plisetskaya [154] on liver plasma membranes from salmon demonstrated binding with much higher affinity for INS than for either mammalian IGF-I or IGF-II. Similar studies should be undertaken with a wider range of lower vertebrates and lower chordates. Such investigations appear especially relevant since the report by Chan *et al.* [155] that the overall organization of the preproinsulin gene of an amphioxus (*Branchiostoma lanceolatum*) indicates close relation to both INS and IGF-I.

It is widely accepted, that, in mammalian INS-sensitive tissues, the numbers of receptors for INS on the plasma membrane are regulated by the circulating levels of INS [156–158], so that elevation in levels of INS causes a decline in the number of receptors. This assumption has been extrapolated to the properties of the INS receptors in fish. Therefore, when Ablett *et al.* [159] found that isolated hepatocyte from trout reared on a high-carbohydrate diet had more specific binding sites for INS than those from control fish, it was concluded that the plasma INS levels in this fish were low. Developing this idea still further, Christiansen and Klungsøyr [160] suggested that, because of the strictly reciprocal relationship between the concentration of receptors and plasma levels of INS, the assessment of receptor binding can provide an estimate of INS levels in the course of the nutritional studies on fish. Since the high-carbohydrate diet resulted in an increase of the numbers of specific binding sites for INS in trout liver [159], it was concluded that glucose does not stimulate the secretion of INS in the rainbow trout.

Such a conclusion from the abovementioned experiment is difficult to accept. First of all, glucose does indeed stimulate the secretion of INS in agnathans and in teleost fishes [71, 143, 161], including the rainbow trout [81], though it is not as potent in this respect as amino acids. Secondly, the question should be addressed as to whether the reciprocity between plasma levels of INS and number of receptors, as reported in mammals, should be applied to fish. Two recent publications [162, 163] provide some evidence that, at least in the Baltic lamprey (*Lampetra fluviatilis*), neither natural INS deficiency, caused by prolonged pre-spawning anorexia, nor hyperinsulinemia induced

by injection of insulin, changes the binding parameters of INS in the liver, heart muscle or brain. Moreover, the data obtained from mammals [164] indicate that, at least, receptors for INS from brains of adult animals are unaffected by alterations in the levels of circulating INS. In primary cultures of cortical cells from fetal mice, elevated concentrations of INS in the media cause "up-regulation" of INS receptors [165].

Leibush [144] commented that since the "down-regulation" phenomenon is related, most probably, to the internalization of the receptors for INS, a process that does not take place at low temperatures, this phenomenon could hardly be expected to occur in either agnathans or fish that are maintained at low water temperatures. It is likely that the problem is even more complicated, since Gutierrez *et al.* [166] and Gutierrez and Plisetskaya [154] found either the presence or the absence of down-regulation, dependent not only on environmental temperature but on some unidentified physiological conditions of fish. Whatever may be the mechanism that governs the number of the receptors for INS in fish, it is clear that the time has come to examine it in more detail. The same is true for other pancreatic peptides, such as GLU and GLP. While the receptors for GLU and the transduction of signals from the cell surface to the intracellular targets have been analyzed in great detail in mammals [99, 112, 167, 168] no similar studies have been undertaken in fish. However, some indirect information about receptors and post-receptor events is available. Clear differences are already apparent at the level of binding of GLU to its receptor. For example, catfish glucagon, although very close in terms of structure to mammalian GLU, does not bind to GLU receptors in the liver, pituitary or hypothalamus of the rat. It does not activate adenylate cyclase in any of these tissues, while its porcine counterpart strongly activates this enzyme. By contrast, catfish GLP does stimulate the activity of hypothalamic and pituitary adenylate cyclase in rats [105]. Postreceptor transduction of signals also seems to differ between fish and mammals, especially in regard to the stimulation of adenylyl cyclase activity, which can be achieved only after treatment with pharmacological concentrations of GLU (see above and

Fig. 3).

As far as we know, there is at present no available information about hormone-receptor interaction of peptides that belong to the gene II SST- or to PP families in fish.

PANCREATIC HORMONES IN FISH UNDER VARIOUS PHYSIOLOGICAL CONDITIONS

a) *Smoltification*

Smoltification or the parr-to smolt-transformation in salmonids involves profound morphological and physiological changes. This crucial period prepares juvenile salmon for downstream migration as well as for survival at sea. Smoltification includes changes, mostly increases, in the titres of many hormones, such as thyroxine, GH, prolactin, catecholamines, sex steroids, cortisol and some others [169–171]. It is surprising that pancreatic hormones have received only scant attention in this regard [169]. The first pancreatic hormone measured during the entire period of the parr-to-smolt transformation was INS [83]. In experiments continued from 1984 to 1989, the plasma profiles of this hormone revealed an annual peak at a specific time, namely at the very beginning of the transformation of parr to the transitional stage (Table 3). The annual peak was followed by a rapid or gradual decline in levels of INS. It is noteworthy

TABLE 2. Circulating levels of insulin in plasma of juvenile coho salmon, *Oncorhynchus kisutch*, in 1985; According to Plisetskaya *et al.* [83]

Date	Insulin (ng/ml)	Stage
February 1	2.0±0.2 (9)*	Parr
February 15	1.1±0.1 (9)	Parr
March 15	1.0±0.1 (8)	Parr
March 29	7.7±1.7 (6)	Parr-transitional
April 6	1.9±0.4 (7)	Parr-transitional
April 12	0.8±0.1 (7)	Transitional-smolt
May 3	0.8±0.1 (8)	Smolt
May 17	0.6±0.1 (7)	Smolt
May 24	1.1±0.2 (7)	Smolt
June 21	2.4±1.0 (8)	Smolt transferred to seawater

* In parentheses: number of samples.

TABLE 3. Circulating levels of glucagon and glucagon-like peptide in plasma of juvenile coho salmon, *Oncorhynchus kisutch*, in 1989

Date	Glucagon (ng/ml)	Glucagon-like peptide (ng/ml)	Stage
February 22	0.40±0.08 (4)*	1.60±0.20 (4)	Parr
March 8	1.00±0.04 (4)	1.10±0.04 (4)	Parr
March 21	0.50±0.06 (7)	1.00±0.10 (7)	Parr-transitional**
April 3	0.60±0.06 (8)	1.70±0.26 (8)	Parr-transitional
April 17	0.50±0.02 (5)	0.80±0.17 (5)	Smolt
April 26	0.70±0.06 (4)	2.00±0.32 (4)	Smolt
May 5	2.30±0.40 (6)	1.10±0.18 (6)	Smolt

* Each sample of plasma represents a pool from 2–3 fish.

** Insulin levels rise to a maximum of 7–10 ng/ml; data for insulin are not shown but the profiles are similar to those presented in Table 2.

TABLE 4. Titres of pancreatic hormones (ng/ml±S.E.M.) in salmonids that were either fed or fasted

Hormone	Fed	Fasted	Species	Details	Reference ²
<i>Insulin</i>	6.8±0.60 (10) ¹	1.6 ±0.30 (10)	<i>S. gairdneri</i>	Fasted 1 week	[73*]
	4.2±0.30 (10)	2.2 ±0.30 (10)		Fasted 1 week	
	4.5±0.80 (10)	1.4 ±0.20 (10)	<i>O. kisutch</i>	Fasted 1 week	[80**]
	4.3±0.80 (9)	0.9 ±0.10 (9)		Fasted 2 weeks	
	12.1±1.10 (10)	2.0 ±0.10 (10)	<i>O. mykiss</i> 1986	Fasted 6 weeks	[85**]
	13.0±1.70 (15)	2.2 ±0.10 (15)	<i>O. mykiss</i> 1988	Fasted 6 weeks	[86**]
	10.9±0.70 (30)	3.0 ±0.10 (26)	<i>O. mykiss</i> 1989	Fasted 6 weeks	[191**]
<i>Glucagon</i>	0.80±0.10 (10)	0.20±0.10 (10)	<i>O. mykiss</i>	Fasted 6 weeks	[85**]
	0.12±0.05 (15)	0.08±0.03 (15)	<i>O. mykiss</i>	Fasted 6 weeks	[86**]
	1.60±0.10 (29)	1.20±0.20 (25)	<i>O. mykiss</i>	Fasted 6 weeks	Plisetskaya, (unpublished)**
<i>GLP</i>	0.60±0.10 (10)	0.30±0.04 (10)	<i>O. mykiss</i>	Fasted 6 weeks	[85**]
	1.10±0.04 (10)	0.80±0.01 (10)	<i>O. mykiss</i>	Fasted 6 weeks	[86**]
	1.90±0.30 (28)	0.40±0.02 (25)	<i>O. mykiss</i>	Fasted 6 weeks	Plisetskaya (unpublished)**

¹ In parentheses: numbers of fish assayed. ² Radioimmunoassay with * cod components; ** coho salmon components

that neither the maximum number of the receptors for INS in the liver nor the maximum binding of INS to the liver plasma membrane, were coincident with this surge in levels of INS [154]. The titres of members of the glucagon family peptides, namely GLU and GLP, assessed during smoltification in 1989, fluctuated without any particular periods of significant elevation or decline (Table 4).

The surge of levels of INS seems to be consistent with a switch in metabolic conditions, as the clearly anabolic parrs become catabolic smolts [172, 173].

Changes in the secretion of INS evidently play a major role in these metabolic shifts, as was demonstrated in model experiments that included either inactivation of INS in parr by injection of INS-specific anti-serum or administration of INS to smolts. After these experimental treatments, parrs acquired some metabolic features of smolts and *vice versa*.

Within several weeks after entering the sea water, smolts of Pacific salmon usually regain high plasma levels of INS which are favourable for a rebuilding of stores of lipid and glycogen. In

juvenile fish that reach the sea prematurely and cease their normal growth ("stunting" phenomenon), levels of INS remain low [83, 169].

b) *Spawning migration*

Profiles of plasma INS were assessed in wild population of Pacific salmon (*O. gorbuscha*) along their way to the spawning grounds [82, 174] and in reproductively maturing Atlantic salmon, *S. salar* [175]. Fish of both species, although anorexic during the spawning period, maintain relatively high levels of plasma INS. Metabolic studies on the liver cells isolated from anorexic *O. keta*, at four sampling sites along their 1150-km migration route, led French *et al.* [176] to the conclusion that spawning of sockeye salmon is apparently supported by the catabolism of carbohydrates. The final depletion of carbohydrate reserves from both muscles and liver of Pacific salmon occurs during or immediately after spawning. In maturing salmon, INS may participate in the preservation of these carbohydrate reserves, accumulated mostly *via* gluconeogenesis, from premature exhaustion. It is remarkable, that relatively high levels of INS during spawning migration in anorexic fish coincide with enhanced gluconeogenesis while, in normally feeding fish, INS is believed to act to reduce gluconeogenesis [177]. Therefore, the interaction between INS and gluconeogenic fluxes in anorexic fish should be reevaluated and studied in greater detail.

In Atlantic salmon, the elevation in levels of INS, GLU and GLP is observed in spring prior to the onset of maturation, when the fish continue to feed extensively [175, 178]. Similar changes have previously been described for the scorpion fish, *Scorpaena porcus* [161], and for the sea bass, *Dicentrarchus labrax* [179]. Although some involvement of INS in the regulation of the uptake of vitellogenin has been reported [180] and binding sites for INS have been found on the plasma membrane of the ovaries of *S. salar* (Gutiérrez, personal communication), details of the role of INS in the maturation process await further investigation. Another possibility that deserves to be explored is the direct transfer of INS from the blood of females into the eggs prior to spawning.

The spring elevation in plasma levels of INS in

Atlantic salmon seems to coincide with an increase in levels of GLU and GLP, an observation that again contradicts the relationship between these hormones in mammals. The surge in levels of INS in the spring may enable the maturing fish to increase their stores of protein, lipids and carbohydrates in somatic tissues, in anticipation of maturation. It is possible that, when these metabolic stores reach some particular level, they may signal the readiness of fish for sexual maturation and for the switch from somatic to gonadal growth. After feeding has ceased, the gonads, and in particular the ovaries, continue to incorporate proteins and lipids stored in the somatic tissues [175].

In both Pacific and Atlantic salmon at the time of spawning, males have higher plasma levels of INS than do females [82, 178]. This difference may be caused by the necessity of meeting an increased demand for energy, since the males arrive at the spawning grounds before the females so that they can defend their territory, and the males remain there for a longer time to engage in multiple spawnings [175]. An alternative explanation for the difference in INS levels is that, in females, some INS is transferred from the circulation to the eggs.

Is the hormonal regulation of metabolism in fasting fish similar (albeit slow because of their natural heterothermic conditions) to the regulation of metabolic fluxes in other vertebrates? Such a comparison is difficult to make because the fish that have been studied are mostly carnivorous, while common laboratory mammals and birds are omnivorous. Fortunately, in this regard, a group of French scientists has conducted a thorough study of the physiology and biochemistry of the long-term, natural fasting in penguins. Their study included measurements of metabolic indices and the regulation of these indices by pancreatic hormones [181–183]. The experimental subjects, chicks of the king penguin (*Aptenodytes patagonica*), experience a natural 4-to-6 month fast during the subantarctic winter. These birds are strictly carnivorous. Therefore, the results accumulated by the French group should be suitable for comparisons with the data obtained from fish. The researches distinguish two phases of the natural

fast: the first is accompanied by the early metabolic adjustments that are characterized by a decline in the plasma levels of hormones (including INS) and a decline in the utilization of energy sources. During the next, long-term phase of the fast, the levels of INS and GLU remain stable [182, 183], a situation that resembles conditions in migrating fish.

c) *Experimental fasting versus feeding in teleost fishes*

Because of their remarkable ability to tolerate long non-feeding periods, fish are becoming valuable experimental models for studies of the metabolic patterns of fasting conditions. The metabolic strategies of previously actively feeding fish, which are then experimentally deprived of food, seem to differ from those described above for upstream-migrating anorexic fish. At the same time they bear some similarity to the early period of fasting in penguins [182].

The elevation of plasma levels of GLU observed in the sea bass by Gutierrez *et al.* [184] and in the juvenile Atlantic salmon by Sundby (personal communication), is not easily detectable. Even if such an elevation occurs it lasts for only a short period of time (usually during fourth and fifth days after withdrawal of food). Moreover, in contrast with the situation in mammals [85], in fish plasma the molar ratios of GLU to INS never reach, not to mention never exceed, 1.0, with levels of GLU always remaining lower than those of INS. After this initial period, experimental fasting leads to a decline in plasma levels of INS, GLU and GLP (Table 4). This decline is, however, not uniform: levels of INS drop more rapidly than levels of GLU and GLP. As a result, the molar ratios of GLU and, especially, of GLP to INS tend to increase during the course of starvation, and this increase favours an enhancement of the activities of gluconeogenic enzymes and, consequently, the gluconeogenic potential of the liver [85, 86]. At the same time, as has been demonstrated in experiments on chinook salmon *in vitro*, fasting for three weeks sharply diminishes the responsiveness of the liver slices to the glycolytic action of GLU [185].

We have not discussed the role of hormones in fish growth in this survey. The subject was well presented in both 1986 and 1987 [186, 187]. De-

ciphering of the structure of the first identified piscine IGF [188], as well as the findings that the expression of IGF in piscine liver is regulated by the GH [188] and that an injection of GH elevates levels of immunoreactive IGF in fish plasma [189] open new and fertile areas for exploration of the mutual interrelationships between GH, IGF and INS in the regulation of fish growth and metabolism. There is no doubt that stunted fish, which possess high levels of plasma GH [187, 190], coincidental with low levels of INS [83], may be considered an ideal model for these studies.

CONCLUSION

The divergent life cycles and feeding habits of fish, their consistent growth, and amazing tolerance of long periods of food deprivation are characteristics that keep fishes in a central position in studies of the adaptive evolution of metabolism and its regulatory mechanisms in vertebrates.

Pancreatic hormones play the pivotal role in these regulatory mechanisms, and an overview of the recent literature demonstrates the growing importance of fish as an experimental model for studies of the structure and functions of these hormones. There is no doubt that, if the pace of studies of pancreatic hormones in fish remains the same as it has been during the past several years, answers to the majority of the questions addressed in this review will soon become available.

ACKNOWLEDGMENTS

The author's research was supported by grants from the U. S. National Science Foundation (DCB 8615551 and DCB 8915935) and a Washington Sea Grant (R/A-54). The author is indebted to Dr. Aubrey Gorbman and Steven Duguay for critical reading of the manuscript.

REFERENCES

- 1 Powers, D. A. (1989) *Science*, **246**: 352–358.
- 2 Plisetskaya, E. M. (1985) In "Evolutionary Biology of Primitive Fishes". Ed. by R. E. Foreman, A. Gorbman, J. M. Dodd and R. Olsson, Plenum Publ. Corp., New York, pp. 339–361.
- 3 Plisetskaya, E. M. (1989) In "Comparative Physiology of Regulatory Peptides". Ed. by S. Holmgren. Chapman and Hall, London/New York, pp. 174–

- 202.
- 4 Plisetskaya, E. M. (1989) *Fish. Physiol. Biochem.*, **7**: 39–48.
- 5 Plisetskaya, E. M. (1990) In "Progress in Comparative Endocrinology". Ed. by A. Eppler, C. S. Scanes and M. H. Stetson, Wiley-Liss, Inc., New York, pp. 67–72.
- 6 Conlon, J. M., Reinecke, M., Thorndyke, M. C. and Falkmer, S. (1988) *Horm. Metab. Res.*, **20**: 406–410.
- 7 Steiner, D. F. and Chan, S. J. (1988) *Horm. Metab. Res.*, **20**: 443–444.
- 8 Eppler, A. and Brinn, J. E. (1987) *The Comparative Physiology of the Pancreatic Islets*. Zoophysiology, vol. 21, Springer Verlag, Berlin.
- 9 Conlon, J. M. (1989) In "The Comparative Physiology of Regulatory Peptides". Ed. by S. Holmgren, Chapman and Hall, London/New York, pp. 344–369.
- 10 Plisetskaya, E. M. (1975) *Hormonal Regulation of Carbohydrate Metabolism in Lower Vertebrates*. Nauka, Leningrad (In Russian), 215 pp.
- 11 Abad, M. E., Peeze Binkhorst, F. M., Elbal, M. T. and Rombout, J. H. W. M. (1987) *Gen. Comp. Endocrinol.*, **66**: 123–136.
- 12 Abad, M. E., Taverne-Thiele, J. J. and Rombout, J. H. W. M. (1988) *Gen. Comp. Endocrinol.*, **70**: 9–19.
- 13 Abad, M. E., Lozano, M. T., Taverne-Thiele, J. J. and Rombout, J. H. W. M. (1990) *Gen. Comp. Endocrinol.*, **77**: 1–8.
- 14 Avala, A. G., Lozano, M. T. and Agulleiro, B. (1987) *Gen. Comp. Endocrinol.*, **68**: 235–248.
- 15 Elliott, W. M. and Youson, J. H. (1987) *Cell Tiss. Res.*, **247**: 351–357.
- 16 Elliott, W. M. and Youson, J. H. (1988) *Amer. J. Anat.*, **182**: 73–83.
- 17 Nozaki, M., Miyata, K., Oota, Y., Gorbman, A. and Plisetskaya, E. M. (1988) *Gen. Comp. Endocrinol.*, **69**: 271–280.
- 18 Nozaki, M., Miyata, K., Oota, Y., Gorbman, A. and Plisetskaya, E. M. (1988) *Cell Tiss. Res.*, **253**: 371–375.
- 19 Yui, R., Nagata, Y. and Fujita, T. (1988) *Arch. Histol. Cytol.*, **51**: 109–119.
- 20 Cheung, R., Andrews, P. C., Plisetskaya, E. M. and Youson, J. H. (1990) *Gen. Comp. Endocrinol.*, In press.
- 21 McDonald, J. K., Greiner, F., Bauer, G. E., Elde, R. P. and Noe, B. D. (1987) *J. Histochem. Cytochem.*, **35**: 155–162.
- 22 Cutfield, S. M., Carne, A. and Cutfield, J. F. (1987) *FEBS Lett.*, **214**: 57–61.
- 23 Andrews, P. C., Pollock, H. G., Elliott, W. M., Youson, J. H. and Plisetskaya, E. M. (1988) *J. Biol. Chem.*, **263**: 15809–15814.
- 24 Conlon, J. M., Åskensten, U., Falkmer, S. and Thim, L. (1988) *Endocrinology*, **122**: 1855–1859.
- 25 Morel, A., Kuks, P. F. M., Bourdais, J. and Cohen, P. (1988) *Biochem. Biophys. Res. Comm.*, **151**: 347–354.
- 26 Marchant, T. A., Fraser, R. A., Andrews, P. C. and Peter, R. E. (1987) *Reg. Pept.*, **17**: 41–52.
- 27 Marchant, T. A. and Peter, R. E. (1989) *Fish Physiol. Biochem.*, **7**: 133–139.
- 28 Conlon, J. M., Agoston, D. V. and Thim, L. (1985) *Gen. Comp. Endocrinol.*, **60**: 406–413.
- 29 Tagliaferro, G., Faraldi, G. and Pesarino, M. (1985) *Cell. Mol. Biol.*, **31**: 201–207.
- 30 Tagliaferro, G., Farina, L., Faraldi, G., Rossi, G. G. and Vacchi, M. (1989) *Gen. Comp. Endocrinol.*, **75**: 1–9.
- 31 Klaff, L. J. and Taborsky, G. J., Jr. (1987) *Amer. J. Physiol.*, **252** (Endocrinol. Metab. 15): E 751–E 755.
- 32 Klaff, L. J. and Taborsky, G. J., Jr. (1987) *Diabetes*, **36**: 592–596.
- 33 Klaff, L. J., Dunnung, B. E. and Taborsky, G. J. Jr. (1988) *Endocrinology*, **123**: 2668–2674.
- 34 D'Alessio, D. A., Sieber, C., Beglinger, C. and Ensinn, J. W. (1989) *J. Clin. Invest.*, **84**: 857–862.
- 35 Ensinn, J. W., Laschansky, E. C., Vogel, R. E., Simonowitz, D. A., Roos, B. A. and Francis, B. H. (1989) *J. Clin. Invest.*, **83**: 1580–1589.
- 36 Elliott, W. M. and Youson, J. H. (1986) *Cell Tiss. Res.*, **243**: 629–634.
- 37 Plisetskaya, E. M., Pollock, H. G., Rouse, J. B., Hamilton, J. W., Kimmel, J. R., Andrews, P. C. and Gorbman, A. (1986) *Gen. Comp. Endocrinol.*, **63**: 252–263.
- 38 Sheridan, M. A., Plisetskaya, E. M., Bern, H. A. and Gorbman, A. (1987) *Gen. Comp. Endocrinol.*, **66**: 405–414.
- 39 Plisetskaya, E. M., Pollock, H. G., Elliott, W. M., Youson, J. H. and Andrews, P. C. (1988) *Gen. Comp. Endocrinol.*, **69**: 46–55.
- 40 Hardisty, M. W. (1982) In "The Biology of Lampreys". Ed. by M. W. Hardisty and I. C. Potter Vol. 4B, Academic Press, London, pp. 165–259.
- 41 Peterson, J. D., Steiner, D. F., Emdin, S. O. and Falkmer, S. (1974) *J. Biol. Chem.*, **250**: 5183–5191.
- 42 Plisetskaya, E. M., Pollock, H. G., Rouse, J. B., Hamilton, J. W., Kimmel, J. R. and Gorbman, A. (1985) *Reg. Peptides*, **11**: 105–116.
- 43 Conlon, J. M. and Thim, L. (1987) In "Protein Purification: Micro to Macro". Ed. by R. Burgess, UCLA Symposia on Molecular and Cellular Biology. Vol. 68, New Series, A. R. Liss, New York, pp. 255–261.

- 44 Rusacov, Yu. I., Karasev, V. S., Pertseva, M. N. and Pankov, Yu. A. (1987) *Biokhimiya*, **52**: 211–217. Plenum Press. (In Russian, English translation)
- 45 Rusacov, Yu. I., Karasev, V. S., Pertseva, M. N. and Pankov, Yu. A. (1987) *Zh. Evol. Biokhim. Fiziol.*, **23**: 473–480. (In Russian)
- 46 Conlon, J. M., Andrews, P. C., Falkmer, S. and Thim, L. (1988) *Gen. Comp. Endocrinol.*, **72**: 154–160.
- 47 Berks, B. C., Marshall, C. J., Carne, A., Gallo-way, S. M. and Cutfield, J. F. (1989) *Biochem. J.*, **263**: 261–266.
- 48 Koval, A. P., Petrenko, A. I., Dmitrenko, V. V. and Kavsan, V. M. (1989) *Mol. Biol.*, **23**: 473–480.
- 49 Bajaj, M., Blundell, T. L., Pitts, J. E., Wood, C. P., Tatnell, M. A., Falkmer, S., Emdin, S. O., Gowan, L. K., Crow, H., Schwabe, S., Wollmer, A. and Strassburger, W. (1983) *Eur. J. Biochem.*, **135**: 535–542.
- 50 Conlon, J. M. and Thim, L. (1986) *Gen. Comp. Endocrinol.*, **64**: 199–205.
- 51 Conlon, J. M. and Thim, L. (1989) *Comp. Biochem. Physiol.*, **93B**: 359–362.
- 52 Bell, G. I., Santerre, R. F. and Mullenbach, G. T. (1983) *Nature*, **302**: 716–718.
- 53 Pollock, H. G., Kimmel, J. R., Ebner, K. E., Hamilton, J. W., Rouse, J. B., Lance, V. and Rawitch, A. B. (1988) *Gen. Comp. Endocrinol.*, **69**: 133–140.
- 54 Conlon, M. J., Göke, R., Andrews, P. C. and Thim, L. (1989) *Gen. Comp. Endocrinol.*, **73**: 136–146.
- 55 Pollock, H. G., Hamilton, J. W., Rouse, J. B., Ebner, K. E. and Rawitch, A. B. (1988) *J. Biol. Chem.*, **263**: 9746–9751.
- 56 Sorokin, A. V., Petrenko, O. I., Kavsan, V. M., Koslov, Y. I., Debabov, V. G. and Zlochevskij, M. L. (1982) *Gene*, **20**: 367–376.
- 57 Yamamoto, M., Kotaki, A., Okuyama, T. and Satake, K. (1960) *J. Biochem. (Tokyo)*, **48**: 84–92.
- 58 Shuldiner, A. R., Bennett, C., Robinson, E. A. and Roth, J. (1989) *Endocrinology*, **125**: 469–477.
- 59 Shuldiner, A. R., Phillips, S., Roberts, C. T., Jr., LeRoith, D. and Roth, J. (1989) *J. Biol. Chem.*, **264**: 9428–9432.
- 60 Andrews, P. C., Hawke, D., Shively, J. E. and Dixon, J. E. (1985) *Endocrinology*, **116**: 2677–2681.
- 61 Kimmel, J. R., Plisetskaya, E. M., Pollock, H. G., Hamilton, J. W., Rouse, J. B., Ebner, K. E. and Rawitch, A. B. (1986) *Biochem. Biophys. Res. Comm.*, **141**: 1084–1091.
- 62 Conlon, J. M., Schmidt, W. E., Gallwitz, B., Falkmer, S. and Thim, L. (1986) *Regul. Pept.*, **16**: 261–268.
- 63 Pollock, H. G., Kimmel, J. R., Hamilton, J. W., Rouse, J. B., Ebner, K. E., Lance, V. and Rawitch, A. B. (1987) *Gen. Comp. Endocrinol.*, **67**: 375–382.
- 64 Noe, B. D., McDonald, J. K., Greiner, F., Wood, J. G. and Andrews, P. C. (1986) *Peptides*, **7**: 147–154.
- 65 Noe, B. D., Milgram, S. L., Balasubramaniam, A., Andrews, P. C., Calka, J. and McDonald, J. K. (1989) *Cell Tiss. Res.*, **257**: 303–311.
- 65a Balasubramaniam, A., Andrews, P. C., Renugopalakrishnan, V. and Rigel, D. F. (1989) *Peptides*, **10**: 581–585.
- 66 Tatemoto, K., Efendic, S., Mutt, G., Makk, G., Feistner, G. J. and Barchas, J. D. (1986) *Nature*, **324**: 476–478.
- 67 Ahrén, B., Lindskog, S., Tatemoto, K. and Efendic, S. (1988) *Diabetes*, **37**: 281–285.
- 68 Ishizuka, J., Asada, I., Poston, G. J., Lluís, F., Tatemoto, K., Greeley, G. H., Jr. and Thompson, J. C. (1989) *Pancreas*, **4**: 277–281.
- 69 Voller, A., Bidwell, D. E. and Bartlett, A. (1979) *The Enzyme-Linked Immunosorbent Assay (ELISA)*. Dynatech Laboratories, Inc. pp. 3–67.
- 70 Albertson, B. D. and Haseltine, F. P. (Eds.) (1988) *Non-Radiometric Assays. Technology and Application in Polypeptide and Steroid Hormone Detection*. Alan R. Liss, New York.
- 71 Patent, G. J. and Foá, P. P. (1971) *Gen. Comp. Endocrinol.*, **6**: 41–46.
- 72 Plisetskaya, E. M. and Leibush, B. N. (1974) *Z. evol. Biokhim. Physiol.*, **10**: 623–625. (In Russian)
- 73 Thorpe, A. and Ince, B. W. (1976) *Gen. Comp. Endocrinol.*, **30**: 332–339.
- 74 Furuichi, M., Nakamura, Y. and Yone, Y. (1980) *Bull. Jap. Soc. Sci. Fish.*, **46**: 1177–1181.
- 75 Wagner, G. F. and McKeown, B. A. (1982) *Can. J. Zool.*, **60**: 2079–2084.
- 76 Tilzey, J. F., Waights, V. and Holmes, R. (1985) *Comp. Biochem. Physiol.*, **81A**: 821–825.
- 77 Gutiérrez, J., Fernandez, J., Blasco, J., Gesse, J. M. and Planas, J. (1986) *Gen. Comp. Endocrinol.*, **63**: 328–333.
- 78 Hertz, Y., Epstein, N., Abraham, M., Madar, Z., Hopher, B. and Gertler, A. (1989) *Aquaculture*, **80**: 175–187.
- 79 Schrezenmeir, J., Laue, Ch., Faust, P., Kirschgessner, J., Boddin, J., Liao, E., Lassak, D., Stallmach, Th., Muntefering, H. and Beyer, J. (1989) *Acta Endocrinol. Suppl.*, **1**: 1. (Abstract)
- 80 Plisetskaya, E. M., Dickhoff, W. W., Paquette, T. L. and Gorbman, A. (1986) *Fish. Physiol. Biochem.*, **1**: 37–43.
- 81 Hilton, J. W., Leatherland, J. F. and Plisetskaya,

- E. M. (1987) *Physiol. Biochem. Fish.*, **4**: 113–120.
- 82 Plisetskaya, E. M., Donaldson, E. M. and Due, H. M. (1987) *J. Fish. Biol.*, **30**: 21–26.
- 83 Plisetskaya, E. M., Swanson, P., Bernard, M. G. and Dickhoff, W. W. (1988) *Aquaculture*, **72**: 251–264.
- 84 Sheridan, M. A. and Plisetskaya, E. M. (1988) *Amer. Zool.*, **28**: 56A. (Abstract)
- 85 Moon, T. W., Foster, G. D. and Plisetskaya, E. M. (1989) *Can. J. Zool.*, **67**: 2189–2193.
- 86 Storebakken, T., Hung, S. S. O., Calvert, C. C. and Plisetskaya, E. M. (1990) *J. Nutrition*. (In preparation)
- 87 Tatemoto, K., Rökæus, Å., Jörnvall, H., McDonald, T. J. and Mutt, V. (1986) *FEBS Letters*, **164**: 124–128.
- 88 Sheridan, M. A., Eilertson, C. D. and Plisetskaya, E. M. (1990) *Gen. Comp. Endocrinol.* In Press.
- 89 Ronner, P. and Scarpa, A. (1987) *Gen. Comp. Endocrinol.*, **65**: 354–362.
- 90 Plisetskaya, E. M., Ottolenghi, C., Sheridan, M. A., Mommsen, T. P. and Gorbman, A. (1989) *Gen. Comp. Endocrinol.*, **73**: 205–216.
- 91 Ørskov, C. and Holst, J. J. (1987) *Scand. J. Clin. Invest.*, **47**: 165–174.
- 92 Oshima, I., Hirota, M., Ohboshi, C. and Shima, K. (1988) *Reg. Pept.*, **21**: 85–93.
- 93 Ottolenghi, C., Puviani, A. C., Gavioli, M. E., Fabbri, E., Brighenti, L. and Plisetskaya, E. M. (1989) *Fish. Physiol. Biochem.*, **6**: 387–394.
- 94 Andrews, P. C. and Ronner, P. (1985) *J. Biol. Chem.*, **260**: 3910–3914.
- 95 Plisetskaya, E. M., Pollock, H. G., Rouse, J. B., Hamilton, J. W., Kimmel, J. R. and Gorbman, A. (1986) *Reg. Pept.*, **14**: 57–67.
- 96 Plisetskaya, E. M., Sheridan, M. A. and Mommsen, T. P. (1989) *J. Exp. Zool.*, **249**: 158–164.
- 97 Plisetskaya, E. M. (1990) *J. Exp. Zool.* (In press)
- 98 Conlon, J. M. (1988) *Diabetologia*, **31**: 563–566.
- 99 Blache, P., Kervran, A., Dufour, M., Martinez, J., Le-Nguyen, D., Lotersztajn, S., Pavoine, C., Pecker, F. and Bataille, D. (1989) *C. R. Acad. Sci. Paris*, **308**, Ser. III: 467–472.
- 100 Mommsen, T. P. and Moon, T. W. (1989) *Fish Physiol. Biochem.*, **7**: 279–288.
- 101 Mommsen, T. P., Andrews, P. C. and Plisetskaya, E. M. (1987) *FEBS Letters*, **219**: 227–232.
- 102 Ghigione, M., Blazquez, E., Uttenthal, L. O., de Diego, J. G., Alvarez, E., George, S. K. and Bloom, S. R. (1985) *Diabetologia*, **28**: 920–921.
- 103 Ghigione, M., Uttenthal, L. O., George, S. K. and Bloom, S. R. (1984) *Diabetologia*, **27**: 599–600.
- 104 Shimizu, I., Hirota, M., Ohboshi, C. and Shima, K. (1986) *Biomed. Res.*, **7**: 431–436.
- 105 Hoosein, N. M., Marenholz, A. M., Andrews, P. C. and Gurd, R. S. (1987) *Bioch. Biophys. Res. Comm.*, **143**: 87–92.
- 106 Holst, J. J., Ørskov, C., Vagn-Nielsen, O. and Schwartz, T. W. (1987) *FEBS Letters*, **211**: 169–174.
- 107 Mojsos, S., Weir, G. C. and Habener, J. F. (1987) *J. Clin. Invest.*, **79**: 616–619.
- 108 Shima, K., Hirota, M. and Ohboshi, C. (1988) *Regulatory Peptides*, **22**: 245–252.
- 109 Weir, G. C., Mojsos, S., Hendrick, G. K. and Habener, J. F. (1989) *Diabetes*, **38**: 338–342.
- 110 Komatsu, R., Matsuyama, T., Namba, M., Watanabe, N., Itoh, H., Kono, N. and Tarui, S. (1989) *Diabetes*, **38**: 902–905.
- 111 Ørskov, C., Holst, J. J. and Nielsen, O. V. (1988) *Endocrinology*, **123**: 2009–2013.
- 112 Mallat, A., Pavione, C., Dufour, M., Lotersztajn, S., Bataille, D. and Pecker, F. (1987) *Nature*, **325**: 620–622.
- 113 Drucker, D. J. and Asa, S. (1988) *J. Biol. Chem.*, **263**: 13475–13478.
- 114 Perez, J., Zanuy, S. and Carillo, M. (1988) *Fish Physiol. Biochem.*, **5**: 191–197.
- 115 Weigle, D. S. (1987) *Diabetes*, **36**: 764–775.
- 115a Milgram, S. L., Balasubramaniam, A., Andrews, P. C., McDonald, J. K. and Noe, V. D. (1989) *Peptides*, **10**: 1013–1017.
- 116 Rudnicki, M., Balasubramaniam, A., McFadden, D. W., Rigel, D. F., Nussbaum, M., Andrews, P. C. and Fischer, J. E. (1989) *American Endocrine Society Meeting*. Seattle. (Abstract)
- 117 Balasubramaniam, A., Rigel, D. F., Chance, W. T., Stein, M., Fischer, J. E., King, D. and Plisetskaya, E. M. (1990) *Peptides*, In press.
- 118 Clark, J. T., Kalra, P. S. and Kalra, S. P. (1985) *Endocrinology*, **117**: 2435–2442.
- 119 Morley, J. E. (1987) *Endocrinol. Rev.*, **8**: 256–287.
- 120 Porte, D., Jr. and Kahn, S. E. (1989) *Diabetes*, **38**: 1333–1336.
- 121 Suarez, R. K. and Mommsen, T. P. (1987) *Can. J. Zool.*, **65**: 1869–1882.
- 122 Plisetskaya, E. M. and Sullivan, C. W. (1989) *Gen. Comp. Endocrinol.*, **75**: 310–315.
- 123 Janssens, P. A. and Waterman, J. (1988) *Comp. Biochem. Physiol.*, **91B**: 451–456.
- 124 Rappaport, A. M. (1958) *Anat. Rec.*, **130**: 637–686.
- 125 Jungermann, K. and Katz, N. (1989) *Physiol. Rev.*, **69**: 708–764.
- 126 Gumucio, J. J. (1989) *Hepatology*, **9**: 154–160.
- 127 Tosh, D., George, K., Alberti, M. M. and Agius, L. (1988) *Biochem. J.*, **256**: 197–204.
- 128 Lindros, K. O. and Penttillä, K. E. (1985)

- Biochem. J., **228**: 757–760.
- 129 Quistorff, B. and Grunnet, N. (1985) *Biochem. J.*, **226**: 289–297.
 - 130 Quistorff, B. and Grunnet, N. (1987) *Biochem. J.*, **243**: 87–95.
 - 131 Misra, U. K., Yamanaka, H., Kizaki, Z., Kauffman, F. C. and Thurman, R. G. (1988) *Biochem. Biophys. Res. Comm.*, **155**: 455–462.
 - 132 Hampton, J. A., McCuskey, P. A., McCuskey, R. S. and Hinton, D. E. (1985) *Anat. Rec.*, **213**: 166–175.
 - 133 Hinton, D. E., Walker, E. R., Pinkstaff, C. A. and Zuchelkowski, E. M. (1984) In "Use of Small Fish Species in Carcinogenicity Testing". National Cancer Institute Monograph #65. Ed. by G. L. Hoover. NCI, Bethesda.
 - 134 Diaz, J. P. and Connes, R. (1988) *Ann. Sci. Nat. Zool.*, **9**: 123–141.
 - 135 Mommsen, T. P., Danulat, E., Gavioli, M. E., Foster, G. D. and Moon, T. W. (1990) *Can. J. Zool.*, In press.
 - 136 Ottolenghi, C., Ricci, D., Gavioli, M. E., Puviani, A. C., Fabbri, E., Capuzzo, A., Brighenti, L. and Plisetskaya, E. M. (1990) *Can. J. Zool.*, In press.
 - 137 Emdin, S. O., Gammeltoft, S. and Gliemann, J. (1977) *J. Biol. Chem.*, **252**: 602–608.
 - 138 Emdin, S. O., Steiner, D. F., Chan, S. J. and Falkmer (1985) In "Evolutionary Biology of Primitive Fishes". Ed. by R. E. Foreman, A. Gorbman, J. M. Dodd and R. Olsson. Plenum Press, New York, pp. 363–378.
 - 139 Makower, A., Dettmer, R., Rapoport, T. A., Knospe, S., Behlke, J., Prehn, S., Franke, P., Etzoldt, J. and Rosenthal, S. (1982) *Eur. J. Biochem.*, **122**: 339–345.
 - 140 Leibush, B. N. (1981) *Z. evol. Biokhim. Fiziol.*, **17**: 141–147. (In Russian)
 - 141 Muggeo, M., Van Obberghen, E., Kahn, C. R., Roth, J., Ginsberg, B. H., De Meyts, P., Emdin, S. O. and Falkmer, S. (1979) *Diabetes*, **28**: 175–181.
 - 142 Muggeo, M., Ginsberg, B. H., Roth, J., Neville, D. M., De Meyts, P. and Kahn, C. R. (1979) *Endocrinology*, **104**: 1393–1402.
 - 143 Emdin, S. O. (1981) Myxine insulin. Amino acid sequence, three dimensional structure, biosynthesis, release, physiological role, receptor binding affinity, and biological activity. Umeå University Medical Dissertations, New Series #66, Umeå, pp. 1–158.
 - 144 Leibush, B. N. (1989) Insulin receptor interactions in vertebrate evolution. D. Sc. Thesis, Leningrad, USSR. (In Russian)
 - 145 Czech, M. P. and Massague, J. (1982) *Fed. Proc.*, **41**: 2719–2723.
 - 146 Le Roith, D., Lowe, W. L., Jr. and Roberts, C. T., Jr. (1989) In "Molecular and Cellular Biology of Diabetes Mellitus". Ed. by B. Draznin, S. Melmed and D. LeRoith, Vol. 2, pp. 1–9.
 - 147 Stuart, C. A. (1988) *J. Biol. Chem.*, **263**: 7881–7886.
 - 148 Foty, R. A. and Liversage, R. A. (1989) *Amer. Zool.*, **29**: 20A.
 - 149 Simon, J. and LeRoith, D. (1986) *Eur. J. Biochem.*, **158**: 125–132.
 - 150 Simon, J., Rosebrough, R. W., McMurtry, J. P., Steele, N. C., Roth, J., Adamo, M. and LeRoith, D. (1986) *J. Biol. Chem.*, **261**: 17081–17088.
 - 151 Shemer, J., Perrotti, N., Roth, J. and LeRoith, D. (1987) *J. Biol. Chem.*, **262**: 3436–3439.
 - 152 Rosen, O. M. (1987) *Science*, **237**: 1452–1458.
 - 153 Bassas, L. L., De Pablo, F., Lesniak, M. A. and Roth, J. (1987) *Endocrinology*, **121**: 1468–1476.
 - 154 Gutiérrez, J. and Plisetskaya, E. M. (1989) Insulin binding to the liver membranes: teleost model. XI Intern. Symp. Comp. Endocrinol., Malaga, Spain, Thomas Jefferson University Printing Center, Philadelphia, p. 146.
 - 155 Chan, S. J., Cao, Q-P. and Steiner, D. F. (1989) Conference on Insulin. Structure, Chemistry and Biology, University of York, England, p. 48. (Abstract)
 - 156 Gavin, J. R., III, Roth, J., Neville, D. M., Jr., De Meyts, P. and Buell, D. N. (1974) *Proc. Natl. Acad. Sci. U.S.A.*, **71**: 84–88.
 - 157 Bar, R. S., Gorden, P., Roth, J., Kahn, C. R. and de Meyts, P. (1976) *J. Clin. Invest.*, **58**: 1123–1135.
 - 158 Kahn, C. R. (1979) *Proc. Soc. Exper. Biol. Med.*, **162**: 13–21.
 - 159 Ablett, R. F., Taylor, M. J. and Selivonchick, D. P. (1983) *Br. J. Nutr.*, **50**: 129–140.
 - 160 Christiansen, D. S. and Klingsøyr, L. (1987) *Comp. Biochem. Physiol.*, **88B**: 701–711.
 - 161 Plisetskaya, E. M., Leibush, B. N. and Bondareva, V. M. (1976) In "The Evolution of Pancreatic Islets". Ed. by T. A. I. Grillo, L. Leibson and A. Eppe, Pergamon Press, Oxford, pp. 251–269.
 - 162 Leibush, B. N. and Bondareva, V. M. (1987) *Z. Evol. Biokhim. Fiziol.*, **23**: 193–198. (In Russian)
 - 163 Leibush, B. N., Soltitskaya, L. M. and Ukhanova, M. V. (1987) *Z. Evol. Biokhim. Fiziol.*, **23**: 468–472. (In Russian)
 - 164 LeRoith, D., Lowe, W. L., Jr., Shemer, J., Raizada, M. K. and Ota, A. (1988) *Int. J. Biochem.*, **20**: 225–230.
 - 165 Van Schravendijk, F. H., Hooghe-Peters, E. L., De Meyts, P. and Pipeleer, D. G. (1984) *Biochem. J.*, **220**: 165–172.
 - 166 Gutiérrez, J., Åsgård, T., Fabbri, E. and

- Plisetskaya, E. M. (1989) *Amer. Zool.*, **29**: 19A. (Abstract)
- 167 Shimizu, I., Hirota, M., Ohboshi, C. and Shima, K. (1987) *Endocrinology*, **121**: 1076–1082.
- 168 Horwitz, E. M. and Gurd, R. S. (1988) *Arch. Biochem. Biophys.*, **267**: 758–769.
- 169 Bern, H. A. (1978) In "Comparative Endocrinology". Ed. by P. J. Gaillard and H. H. Boer., Elsevier/North Holland Biomedical Press, Amsterdam, pp. 97–100.
- 170 Barron, M. G. (1986) *J. Endocrinol.*, **108**: 313–319.
- 171 Hoar, W. S. (1988) In "Fish Physiology". Ed. by W. S. Hoar and D. J. Randall. Acad. Press. San Diego, vol. 11B, pp. 273–343.
- 172 Woo, N. Y. S., Bern, H. A. and Nishioka, R. S. (1978) *J. Fish. Biol.*, **23**: 625–639.
- 173 Sheridan, M. A., Woo, N. Y. S. and Bern, H. A. (1985) *J. Exper. Zool.*, **236**: 35–44.
- 174 Bondareva, V. M., Soltitskaya, L. P. and Rusacov, Ju. I. (1980) *Z. Evol. Biokhim. Fiziol.*, **16**: 518–521. (In Russian)
- 175 Dickhoff, W. W., Yan, L., Plisetskaya, E. M., Sullivan, C. V., Swanson, P., Hara, A. and Bernard, M. G. (1989) *Fish Physiol. Biochem.*, **7**: 147–155.
- 176 French, C. J., Hochachka, P. W. and Mommsen, T. P. (1983) *Am. J. Physiol.*, **245**, Reg. Integr. Comp. Physiol., **14**: R827–R830.
- 177 Cowey, C. B., Knox, C., Walton, M. J. and Andron, J. W. (1977) *Brit. J. Nutr.*, **38**: 463–470.
- 178 Yan, L. (1988) Profiles of seasonal change in plasma sex steroids, thyroid hormones, pancreatic hormones and vitellogenin in Atlantic salmon (*Salmo salar*). Ph. D. Thesis, University of Washington, Seattle.
- 179 Gutierrez, J., Fernandez, J., Carillo, M., Zanuy, S. and Planas, J. (1987) *Fish Physiol. Biochem.*, **4**: 137–141.
- 180 Tyler, C., Sumpter, J. and Bromage, N. (1987) Third Intern. Symp. Reprod. Physiol. of Fish., p. 142. St. John's, Canada. (Abstract)
- 181 Cherel, Y., Robin, J. P., Walch, O., Karmann, H., Netchitailo, P., and LeMaho, Y. (1988) *Amer. J. Physiol.*, **254**, Regul. Integr. Comp. Physiol., **23**: R170–R177.
- 182 LeNinan, F., Cherel, Y., Robin, J.-P. Leloup, J. and LeMaho, Y. (1988) *J. Comp. Physiol.*, **B. 158**: 395–401.
- 183 LeNinan, F., Cherel, Y., Sardet, C. and LeMaho, Y. (1988) *Gen. Comp. Endocrinol.*, **71**: 331–337.
- 184 Gutierrez, J., Perez, J., Navarro, I., Zanuy, S. and Carillo, M. (1989) XI Intern. Symp. Comp. Endocrinol., Malaga, Spain, Thomas Jefferson University Printing Center, Philadelphia, p. 147.
- 185 Klee, M., Eilertson, C. and Sheridan, M. A. (1990) *J. Exp. Zool.*, **254**: 202–206.
- 186 Matty, A. J. (1986) *Fish Physiol. Biochem.*, **2**: 141–150.
- 187 Bolton, J. P., Young, G., Nishioka, R. S., Hirano, T. and Bern, H. A. (1987) *J. Exp. Zool.*, **242**: 379–382.
- 188 Cao, Q-P., Duguay, S. J., Plisetskaya, E. M., Steiner, D. and Chan, S. J. (1989) *Molec. Endocrinol.*, **3**: 2005–2010.
- 189 Funkenstein, B., Sibergeld, A., Cavari, B. and Laron, Z. (1989) *J. Endocrinol.*, **120**: R19–R21.
- 190 Gray, E. S., Young, G. and Bern, H. (1989) *Amer. Zool.*, **29**: 46A. (Abstract)
- 191 Gutiérrez, J. and Plisetskaya, E. M. (1990) In preparation.

REVIEW

Structure and Function of Sea Urchin Egg Jelly Molecules

NORIO SUZUKI

*Noto Marine Laboratory, Kanazawa University, Ogi, Uchiura,
Ishikawa 927-05, Japan*

ABSTRACT—Sea urchin egg jelly consists of a fucose sulfate glycoconjugate, a sialoglycoprotein and sperm-activating peptides. The fucose sulfate glycoconjugate isolated from the solubilized jelly layer of *Hemicentrotus pulcherrimus* is composed of several proteins (a sugar-containing core protein, a 258 kDa protein, a 237 kDa protein and a 120 kDa protein); the substance plays a major role in the induction of the acrosome reaction in *Hemicentrotus pulcherrimus* spermatozoa. The protein components of the fucose sulfate glycoconjugate seem to be associated with one another through disulfide bonds. Sixty-three sperm-activating peptides have been isolated from the solubilized jelly layers of fifteen sea urchin species distributed over four taxonomic orders. Sperm-activating peptides stimulate sperm respiration and motility, increase the levels of both cAMP and cGMP in sea urchin sperm cells, induce net H^+ efflux from sea urchin spermatozoa and cause a shift in the mobility of guanylate cyclase, a major sperm plasma protein, on an SDS-polyacrylamide gel. These peptides are specific at the ordinal level and are classified into four groups, i.e., sperm-activating peptide I (SAP-I), sperm-activating peptide II (SAP-II), sperm-activating peptide III (SAP-III) and sperm-activating peptide IV (SAP-IV). SAP-I (Gly-Phe-Asp-Leu-Asn-Gly-Gly-Gly-Val-Gly) promotes the induction of the acrosome reaction in *Hemicentrotus pulcherrimus* spermatozoa by acting as a specific co-factor of the fucose sulfate glycoconjugate.

INTRODUCTION

Sea urchin eggs are surrounded by a transparent, gelatinous matrix called the jelly layer, through which spermatozoa must pass before reaching the plasma membrane of the egg during fertilization. The jelly layer has been shown to induce the acrosome reaction, which was first described in detail by Dan [1–14]. The jelly layer of sea urchins mainly consists of polysaccharide-protein complexes which can be separated into a fucose sulfate glycoconjugate and a sialoglycoprotein [13, 15–22]. The latter is considered to cause sperm-isoagglutination and the former to be responsible for the induction of the acrosome reaction. The acrosome reaction in spermatozoa is an essential requirement for fertilization of eggs in many animals [23–43]. In sea urchins, the acrosome reaction occurs within seconds after sperma-

tozoa have come into contact with the egg jelly layer [4, 9–14, 43] or the egg surface component, a sperm-binding factor on the vitelline membrane [45].

Considering the large number of acidic groups belonging to the ester-linked sulfate in the fucose sulfate glycoconjugate and carboxyl residues in the bound sialic acids of the sialoglycoprotein, it follows that the pH values within the jelly layer would be lower than the pH of normal sea water [46–47]. At low pH values, the respiration and motility of sea urchin spermatozoa are markedly reduced and their movements in the jelly layer, therefore, are slower than those that prevail in sea water [48–51]. Thus, one can surmise that the egg jelly is provided with a system of controlling motility and respiration, because the spermatozoa need to maintain their activity at the initial high level attained in sea water during their passage through the acidic environment of the jelly layer to reach the egg surface.

It has been known for over 70 years that the jelly layers of certain species of sea urchins, dissolved in sea water, are able to cause a transient activation of sperm motility and sperm agglutination [52]. Since then many investigators have shown that soluble factors associated with sea urchin eggs stimulate the motility and respiration of sea urchin spermatozoa [53–58]. However, such stimulation has only been seen on occasion and has been difficult to reproduce. In 1976, Ohtake demonstrated that the respiration of sea urchin spermatozoa could be reproducibly stimulated by jelly layer factors obtained from the sea urchin *Pseudocentrotus depressus* if the extracellular pH was maintained at acidic values [50–51]. Thereafter, Kopf *et al.* and Hansbrough and Garbers reported that the jelly layer of the sea urchin *Strongylocentrotus purpuratus* contains a substance which elevates the respiration rates and cyclic nucleotide concentrations in *Strongylocentrotus purpuratus* spermatozoa [59–61]. Hansbrough and Garbers named the substance speract which stands for sperm-activating peptide. In 1981, my collaborators and I first purified a substance from the solubilized jelly

layer of the sea urchin *Hemicentrotus pulcherrimus* and demonstrated that the substance is a decapeptide whose structure is Gly-Phe-Asp-Leu-Asn-Gly-Gly-Gly-Val-Gly and stimulates the respiration and motility of *Hemicentrotus pulcherrimus* spermatozoa [62]. The same peptide has also been purified from the solubilized jelly layer of *Strongylocentrotus purpuratus* [63].

PURIFICATION OF EGG JELLY MOLECULES

Since the jelly layer of sea urchin mainly consists of highly viscous large molecular weight polysaccharide-protein complexes, it is quite difficult to deal with an intact jelly layer using common biochemical methods. In preparation for analysis of the jelly layer, it must first be dissolved, which is accomplished by treating eggs with sea water adjusted to pH 5.0 or 5.5 (Fig. 1). The centrifuged supernatant (solubilized jelly layer) is used for the purification of jelly molecules.

To purify sperm-activating peptides, the solubilized jelly layer is mixed with a 2-fold volume of

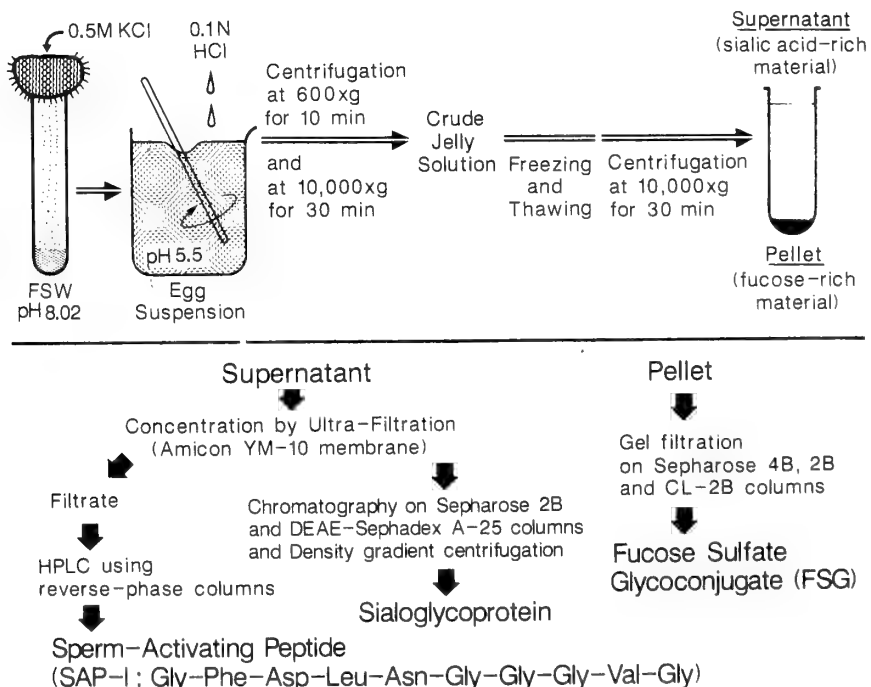


FIG. 1. Schematic drawing of the purification procedure for sea urchin egg jelly molecules.

99% ethanol and then centrifuged. The resulting supernatant is concentrated under reduced pressure at 50°C and lipids are removed by chloroform extraction. The water layer is then lyophilized and the residue, dissolved in deionized and distilled water (DDW), is used for peptide purification. When my collaborators and I first isolated sperm-activating peptides from the solubilized jelly layer of *Hemicentrotus pulcherrimus*, we used sequential chromatographies on Sephadex G-25, DEAE-Sephadex A-25, Sephadex G-15 and Avicell SF thin layer plate [62]. At that time we used about 20 liters of solubilized jelly layer prepared from 5,000 female sea urchins. This procedure, however, was time-consuming and required a large amount of solubilized jelly layer to obtain pure peptides. We then modified the purification procedure and we now use sequential high performance liquid chromatography (HPLC) on a reverse-phase column to purify the peptides [64]. In general, separations are carried out using a combination of the following programs. Program I: Flow rate is 9.9 ml/min, the column (Shimpack C-8 Prep, particle size 5 μ m, 20 \times 250 mm) is equilibrated with 5% acetonitrile (ACN) in 0.1% trifluoroacetic acid (TFA) in DDW and eluted 15 min with equilibration solvent, followed by elution with 60% ACN in TFA in DDW for the next 15 min. Program II: Flow rate is 1.0 ml/min, the column (Unisil C-8, particle size 5 μ m, 4.6 \times 250 mm) is equilibrated with 10% ACN in 0.1% TFA in DDW and eluted for 10 min with equilibration solvent, followed by a linear gradient of ACN from 10% to 50% in 0.1% TFA in DDW over a 50 min time period. Program III: Flow rate is 1.0 ml/min, the same column used in Program II is equilibrated with 5% ACN in 5 mM sodium phosphate (pH 5.7) and eluted for 20 min with the equilibration solvent, followed by a linear gradient of ACN from 5% to 30% in 5 mM sodium phosphate (pH 5.7) over a 40 min time period. By using this modified procedure, we purified three new sperm-activating peptides from solubilized jelly layer obtained from 150 female *Hemicentrotus pulcherrimus* sea urchins.

For purification of the large molecular weight components of the jelly layer, solubilized jelly layer is dialyzed against 0.1 M NaCl and then applied to a Sepharose 2B column equilibrated

with 0.1 M NaCl at 4°C [17–18, 65]. Fucose-containing material is eluted earlier than the material containing sialic acid. To purify a fucose sulfate glycoconjugate, fractions containing fucose are subjected to chromatography on a Sepharose CL-2B column with 7 M urea containing 10 mM HEPES (pH 7.0) [18, 65]. The purified fucose sulfate glycoconjugate which contains one mol sulfate/mol fucose possesses 2.0 times the amount of protein to fucose by weight. When further purification is needed, a fucose sulfate glycoconjugate containing-fraction obtained from Sepharose CL-2B gel filtration is subjected to HPLC on a TSK G-6000 PW column equilibrated with 0.1 M sodium phosphate (pH 6.8) containing 0.1% SDS.

Fractions containing sialic acid obtained from chromatography of solubilized jelly layer on a Sepharose 2B column are pooled and then dialyzed against 10 mM sodium acetate (pH 5.0) containing 0.1 M NaCl and chromatographed on a DEAE-Sephadex A-25 column with a linear gradient of NaCl from 0.1 M to 1.2 M in sodium acetate (pH 5.0) [65]. Fraction containing sialic acid are pooled and dialyzed against DDW. Solid guanidine hydrochloride, CsCl and 1 M sodium acetate (pH 5.0) are added to the dialysate at final concentrations of 4 M, 0.47 g/ml and 10 mM, respectively. The solution is centrifuged at 100,000 $\times g$ for 48 hr in a Hitachi RPS 50 rotor at 4°C. A sialoglycoprotein is obtained from the clear, bottom fraction with a density of 1.47 g/ml. The sialoglycoprotein consists of sialic acid (90%, w/w) and protein (10%, w/w).

It should be noted that in the case of *Hemicentrotus pulcherrimus*, the fucose-containing material becomes insoluble in a 1 M NaCl solution upon freeze-thawing. About 80% of the fucose in the original solubilized jelly layer is recovered in the precipitate fraction by centrifugation at 10,000 $\times g$ for 30 min (Fig. 1) [65]. The precipitate thus obtained dissolves easily in DDW but not in artificial sea water (ASW) or even in 4 M guanidine hydrochloride solution. The supernatant fraction contains about 76% of the sialic acid present in the original solubilized jelly layer. Thus, we sometimes use the precipitate or the supernatant fraction for the purification of a fucose sulfate glycoconjugate or a sialoglycoprotein. However, this

works only with solubilized jelly layer prepared from *Hemicentrotus pulcherrimus* eggs. The solubilized jelly layer obtained from *Anthocardis cras-*

sispina, *Strongylocentrotus nudus*, *Pseudocentrotus depressus* or *Clypeaster japonicus* does not precipitate upon freeze-thawing [66].

TABLE 1. Sperm-activating peptides from the egg jelly of various species of sea urchins*

Subclass Regularia
Order Diadematoidea
Suborder Diademina
Family Diadematoidea
<i>Diadema setosum</i>
GCPWGGAVC (SAP-IV, Mw 847)
Order Arbacioidea
Suborder Phymosomatina
Family Phymosomatidae
<i>Glyptocidaris crenularis</i>
SAKLCPGGNCV (Ser, Ala-SAP-IIB, Mw 1048)
KLCPGGNCV (SAP-IIB, Mw 890)
LCPGGNCV (Des-Lys ¹ -SAP-IIB, Mw 762)
SFKLCPGGQCV (ser, Phe-[Gln ⁷]-SAP-IIB, Mw 1138)
KLCPGGQCV ([Gln ⁷]-SAP-IIB, Mw 904)
LCPGGQCV (Des-Lys ¹ -[Gln ⁷]-SAP-IIB, Mw 776)
Suborder Arbacina
Family Arbaciidae
CVTGAPGCVGGGRL-NH ₂ (SAP-IIA, Mw 1245)
Order Echinoida
Suborder Temnopleurina
Family Toxopneustidae
<i>Lytechinus pictus</i>
GFDLTGGGVQ ([Thr ⁵ , Gln ¹⁰]-SAP-I, Mw 950)
FDLTGGGVQ (Des-Gly ¹ -[Thr ⁵ , Gln ¹⁰]-SAP-I, Mw 893)
<i>Tripneustes gratilla</i>
GFDLNGGGVG (SAP-I, 892)
GFNLNGGGVG (Asn ³]-SAP-I, Mw 891)
GFSIGGGVG ([Ser ³ , Ile ⁴ , Gly ⁵]-SAP-I, Mw 807)
GFDLGGGGVG ([Gly ⁵]-SAP-I, Mw 835)
GFSLGGGGVG ([Ser ³ , Gly ⁵]-SAP-I, Mw 807)
GFGLGGGGVG ([Gly ^{3,5}]-SAP-I, Mw 777)
G(Br-F)NLNGGGVG ([Br-Phe ² , Asn ³]-SAP-I, Mw 971)
G(Br-F)DLNGGGVG ([Br-Phe ²]-SAP-I, Mw 972)
<i>Pseudoboletia maculata</i>
GFALDGVN (Des-Gly ^{6,7} -[Ala ³ , Asp ⁵ , Asn ¹⁰]-SAP-I, Mw 792)
GFALDGVG (Des-Gly ^{6,7} -[Ala ³ , Asp ⁵]-SAP-I, Mw 735)
<i>Pseudocentrotus depressus</i>
GFDLNGGGVG (SAP-I, Mw 892)
GFDLTGGGVG (Thr ⁵]-SAP-I, Mw 879)
GFALGGGGVG (Ala ³ , Gly ⁵]-SAP-I, Mw 791)
Suborder Echinina
Family Strongylocentrotidae
<i>Strongylocentrotus nudus</i>
GFDLNGGGVG (SAP-I, Mw 892)
GFSLSGGGVG ([Ser ^{3,5}]-SAP-I, Mw 837)
GFALGGGGVG ([Ala ³ , Gly ⁵]-SAP-I, Mw 791)
GFSLGGGGVG ([Ser ³ , Gly ⁵]-SAP-I, Mw 807)
GFDLTGGGVG ([Thr ⁵]-SAP-I, Mw 879)

(continued Table 1)

<i>Strongylocentrotus purpuratus</i>	
GFDLNGGGVG	(SAP-I, Mw 892)
GFALGGGGVG	([Ala ³ , Gly ⁵]-SAP-I, Mw 791)
GFSLTGGGVG	([Ser ³ , Thr ⁵]-SAP-I, Mw 851)
<i>Hemicentrotus pulcherrimus</i>	
GFDLNGGGVG	(SAP-I, Mw 892)
GFDLTGGGVG	([Thr ⁵]-SAP-I, Mw 879)
GFSLNGGGVS	([Ser ^{3,10}]-SAP-I, Mw 894)
SFALGGGGVG	([Ser ¹ , Ala ³ , Gly ⁵]-SAP-I, Mw 821)
GFSLSGSGVD	([Ser ^{3,5,7} , Asp ¹⁰]-SAP-I, Mw 925)
Family Echinometridae	
<i>Echinometra mathaei</i> (type A)	
GYSLSGGAVD	([Tyr ² , Ser ^{3,5} , Ala ⁸ , Asp ¹⁰]-SAP-I, Mw 925)
GFALSGGGVG	([Ala ³ , Ser ⁵]-SAP-I, Mw 821)
GFSLSGGGVG	([Ser ^{3,5}]-SAP-I, Mw 837)
GFDLTGGGVG	([Thr ⁵]-SAP-I, Mw 879)
<i>Echinometra mathaei</i> (type B)	
GYSLSGGAVD	([Tyr ² , Ser ^{3,5} , Ala ⁸ , Asp ¹⁰]-SAP-I, Mw 925)
GYNLNGDRID	([Try ² , Asn ³ , Asp ^{7,10} , Arg ⁸ , Ile ⁹]-SAP-I, Mw 1136)
GFSLSGGGVG	([Ser ^{3,5}]-SAP-I, Mw 837)
GFDLTGGGVG	([Thr ⁵]-SAP-I, Mw 879)
<i>Anthocidaris crassispina</i>	
GFDLTGGGVG	([Thr ⁵]-SAP-I, Mw 879)
GFDLSGGGVG	([Ser ⁵]-SAP-I, Mw 865)
GFSLSGSGVG	(Ser ^{3,5,7}]-SAP-I, 867)
<i>Heterocentrotus mammillatus</i>	
GTLP TGSGVS	([Thr ^{2,5} , Leu ³ , Pro ⁴ , Ser ^{7,10}]-SAP-I, Mw 875)
GFEMGGTGVG	([Glu ³ , Met ⁴ , Gly ⁵ , Thr ⁷]-SAP-I, Mw 911)
GYNLGGGGID	([Tyr ² , Asn ³ , Gly ⁵ , Ile ⁹ , Asp ¹⁰]-SAP-I, Mw 922)
GFGLSGGGIG	([Gly ³ , Ser ⁵ , Ile ⁹]-SAP-I, Mw 821)
Subclass Irregularia	
Order Clypeasteroida	
Suborder Clypeasterina	
Family Clypeasteroidae	
<i>Clypeaster japonicus</i>	
DSDSAQNLI	(SAP-III, Mw 1019)
GTDSAQNLI	([Gly ¹ , Thr ²]-SAP-III, Mw 975)
SDSAQNLI	(Des-Asp ¹ -SAP-III, Mw 904)
SDSAHLI	(Des-Asn ⁷ -[His ⁶]-SAP-III, Mw 914)
DTDSAHLI	(Des-Asn ⁷ -[Thr ² , His ⁶]-SAP-III, Mw 928)
NTDSAHLI	(Des-Asn ⁷ -[Asn ¹ , Thr ² , His ⁶]-SAP-III, Mw 928)
GTDSAHLI	(Des-Asn ⁷ -[Gly ¹ , Thr ² , His ⁶]-SAP-III, Mw 870)
SDSAHLI	(Des-Asp ¹ , Asn ⁷ -[His ⁶]-SAP-III, Mw 799)
SDSAFLI	(Des-Asn ⁷ -[Phe ⁶]-SAP-III, Mw 924)
Suborder Laganina	
Family Astriclypeidae	
<i>Astriclypeus manni</i>	
SDSAHLI	(Des-Asn ⁷ -[His ⁶]-SAP-III, Mw 914)
DTDSAHLI	(Des-Asn ⁷ -[Thr ² , His ⁶]-SAP-III, Mw 928)
TDSAHLI	(Des-Asp ¹ , Asn ⁷ -[Thr ² , His ⁶]-SAP-III, Mw 813)

* Amino acids in the sequences are given a one-letter abbreviation: asparagine (N), aspartic acid (D), alanine (A), arginine (R), isoleucine (I), glycine (G), glutamine (Q), glutamic acid (E), cystine ($\bar{C}\bar{C}$), cysteine (C), serine (S), tyrosine (Y), tryptophan (W), valine (V), histidine (H), phenylalanine (F), proline (P), methionine (M), lysine (K) and leucine (L).

TABLE 2. Respiratory stimulating effect of sperm-activating peptides on sea urchin spermatozoa

	Spermatozoa used			
	<i>Diadema setosum</i>	<i>Glyptocidaris crenularis</i>	<i>Hemicentrotus pulcherrimus</i>	<i>Clypeaster japonicus</i>
SAP-IV	+	—	—	—
SAP-IIB	—	+	—	—
SAP-IIA	—	±	—	—
SAP-I	—	—	+	—
SAP-III	—	—	—	+

The respiratory-stimulating activity of a sperm-activating peptide is expressed as a plus sign (+) when the peptide stimulated sperm respiration one half-maximally less than 5 nM. When the half-maximal respiratory stimulation was induced by a peptide concentration between 5 and 500 nM, the plus-minus sign (±) was used. Practically no respiratory stimulation was depicted by a minus sign (—).

SPERM-ACTIVATING PEPTIDES

During the last ten years, my collaborators and I purified sixty-three sperm-activating peptides from the solubilized jelly layer obtained from eggs of fifteen sea urchin species distributed over four taxonomic orders (Table 1) [62, 67–75]. These peptides essentially demonstrate the same biological activity toward a given sea urchin spermatozoa although the biological activities of the peptides are specific at the ordinal level (Table 2) [76–77]. Considering structure and biological specificity, the peptides can be classified into four groups, i.e., sperm-activating peptide I from the species in the order Echinoidea, sperm-activating peptide II (subclass A and B) from the species in the order Arbacioida, sperm-activating peptide III from the species in the order Clypeasteroida and sperm-activating peptide IV from the species in the order Diadematoida. These groups of peptides may be abbreviated as SAP-I, SAP-II, SAP-III and SAP-IV [64].

The peptides stimulate the decreased respiration rates of sea urchin spermatozoa due to the acidification of sea water, back to the level of respiration rates in normal sea water [68]. The stimulated respiration rate does not exceed that of spermatozoa in normal sea water even if large amounts of peptides are added to the sperm suspension medium. The respiratory stimulation induced by the peptide continues for a few minutes and then sperm respiration rates usually decline to the basal

rate normally observed at that particular pH. After reaching the basal state, spermatozoa can again be stimulated by the addition of peptide. This is also true when respiratory stimulation is induced by solubilized jelly layer. When a limited concentration of peptide is used for respiratory stimulation of spermatozoa and the sperm suspending medium is centrifuged before the second addition of peptide, the resultant supernatant fluid, upon examination for respiration-stimulating activity toward spermatozoa, does not stimulate sperm respiration [78]. This suggests that the peptide binds tightly to the spermatozoa. Smith and Garbers reported that *Strongylocentrotus purpuratus* spermatozoa had approximately 6,000–8,000 binding sites (receptors)/cell specific for SAP-I [79]. We suggested that in *Hemicentrotus pulcherrimus* spermatozoa, the receptors exclusively localize on the sperm tail [78].

Monensin, an ionophore that catalyzes an electro-neutral Na^+/H^+ exchange across the cell membrane stimulates sea urchin sperm respiration and motility one half-maximally at about 1–10 μM , and induces a Na^+ -dependent net proton efflux as well as an increased flux of Na^+ in both directions across the cell membrane [61, 68, 80–82]. Sperm-activating peptide stimulate sperm respiration one half-maximally at about 10–100 pM. The respiratory stimulation induced by SAP-I or monensin is dependent on the concentration of external Na^+ [61, 68, 80, 82]. Approximately 50 mM Na^+ is required for half-maximal respiratory responses to

peptides or monensin. There seem to be similarities between the effects of SAP-I and monensin. It is well known that many types of metabolic activation in cells are induced by intracellular alkalinization [83]. Thus, induction of respiratory stimulation by sperm-activating peptides may be explained by the hypothesis that the peptides trigger Na^+/H^+ exchange across sperm plasma membrane and raise the intracellular pH [43, 84].

It has been known that spermatozoa from various species including sea urchin spermatozoa possess enzymes such as adenylate cyclase, guanylate cyclase, cyclic nucleotide phosphodiesterase, cyclic nucleotide-dependent protein kinases and phosphoprotein phosphatases which are involved in cyclic nucleotide metabolism [84–97]. In many instances, these enzymes possess higher specific activity in spermatozoa than in other tissues.

Sperm-activating peptides cause transient increases in sea urchin sperm cGMP concentrations as well as cAMP concentrations in both acidic and normal sea water [63, 69, 73]. Half-maximal elevations of cGMP are 2×10^{-9} M and half-maximal elevations of cAMP are 2×10^{-8} M peptide (Fig. 2). The increases in cGMP concentrations are explained by transient activation of the membrane form of guanylate cyclase, which is a major protein of sperm tail plasma membrane [43, 88, 98–102].

Ward and Vacquier reported that within seconds after addition of solubilized jelly layer prepared from *Arbacia punctulata* to an *Arbacia punctulata* sperm suspension, a 160 kDa sperm protein disappeared and a new protein appeared at 150 kDa on an SDS-polyacrylamide gel [103–105]. The extent to the change was a function of jelly concentration but, at a given jelly concentration, was independent of incubation time. The change is specific for *Arbacia punctulata* jelly. Thereafter, we demonstrated that the factor responsible for the change is a sperm-activating peptide whose sequence is Cys-Val-Thr-Gly-Pro-Gly-Gys-Val-Gly-Gly-Gly-Arg-Leu-NH₂ (SAP-IIA) [69]. Similar changes are commonly observed in sea urchin spermatozoa of many species treated with a specific sperm-activating peptide [70–76]. *Hemicentrotus pulcherrimus* spermatozoa possess several major proteins and one of them, which was recently identified as guanylate cyclase, changes its relative mobility on SDS-polyacrylamide gels from 131 kDa to 128 kDa upon treatment with SAP-I (Fig. 3) [106]. The 160 kDa protein of *Arbacia punctulata* spermatozoa can be labeled with ³²P-orthophosphate when intact *Arbacia punctulata* spermatozoa are incubated in sea water containing ³²P-orthophosphate. The label which is in the form [³²P]-phosphoserine, disappears completely after exposure by the spermatozoa to the solubilized

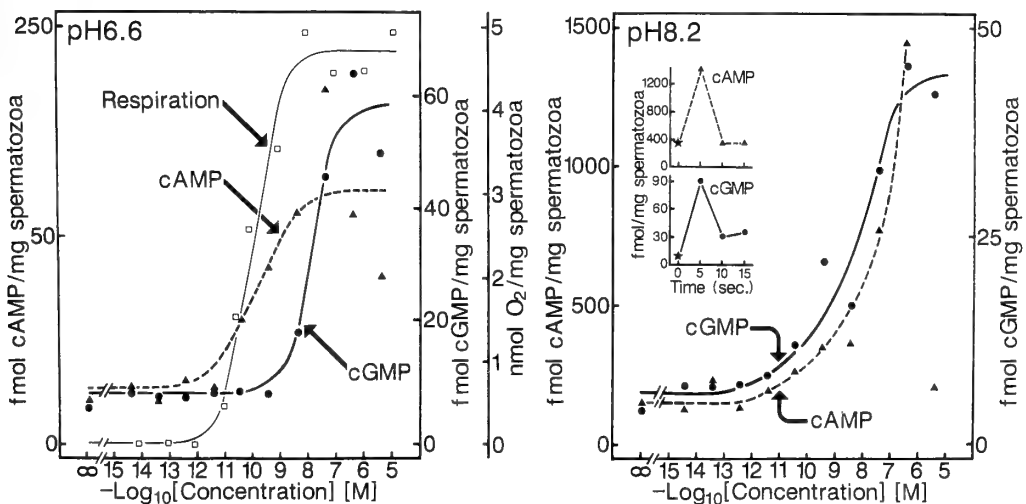


FIG. 2. Concentration-dependent effect of SAP-I on cAMP and cGMP concentrations and respiration of *Hemicentrotus pulcherrimus* spermatozoa. See [ref. 73] for experimental details.

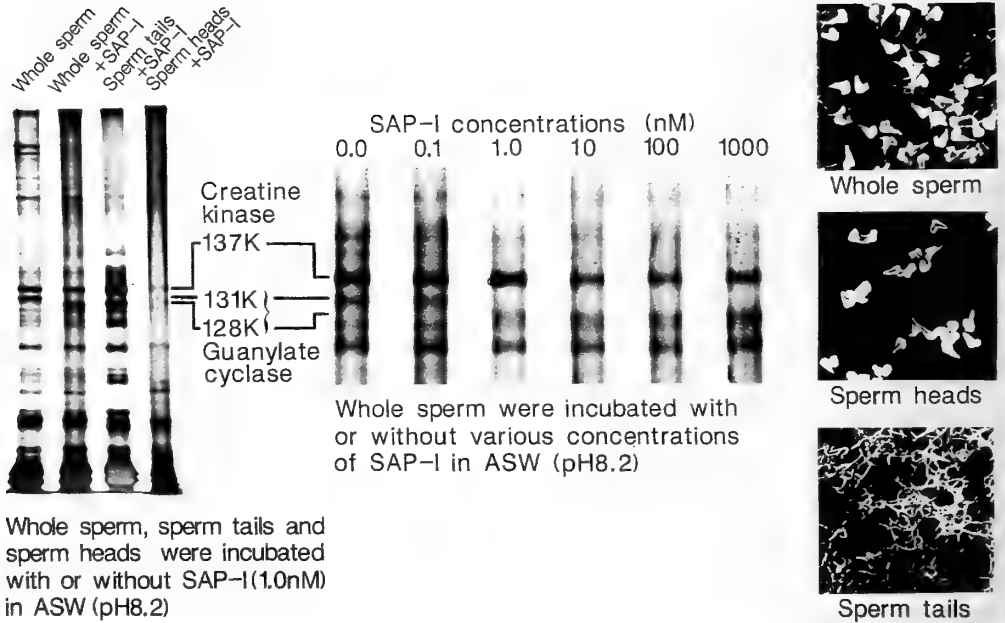


FIG. 3. Effect of SAP-I on the electrophoretic mobility of a high molecular weight protein of *Hemicentrotus pulcherrimus* spermatozoa. See [ref. 78] for experimental details.

jelly layer of *Arbacia punctulata* or SAP-IIA, without the corresponding appearance of radioactivity at 150 kDa [103, 107–108]. The 160 kDa and 150 kDa proteins have proven to be two forms of the same protein and identified as guanylate cyclase [104]. Loss of phosphate from guanylate cyclase and change in the molecular form which is dependent upon external Na^+ and Ca^{2+} concentrations result in a large decrease in the specific activity of the enzyme [95–96]. Therefore, sperm-activating peptides appear to cause an initial transient activation and subsequent inactivation of guanylate cyclase [102]. The mechanism in detail, however, remains to be elucidated.

Guanylate cyclase of *Arbacia punctulata* spermatozoa has been proven to be the receptor for SAP-IIA but not for SAP-I [98–101, 109]. Dangott and Garbers reported that the receptor for SAP-I on *Strongylocentrotus purpuratus* spermatozoa is a 77 kDa protein which has no known enzyme activity [110–112]. Receptors for SAP-IIB, SAP-III and SAP-IV have yet to be identified.

FUCOSE SULFATE GLYCOCONJUGATE

It has long been believed that a fucose sulfate polysaccharide or a fucose-sulfate-rich complex in the jelly layer of sea urchins is the only substance responsible for the induction of the acrosome reaction in sea urchin spermatozoa [9, 11–16]. Recently, my collaborators and I demonstrated that full induction of the acrosome reaction in *Hemicentrotus pulcherrimus* spermatozoa with a fucose sulfate glycoconjugate requires a specific co-factor, i.e., sperm-activating peptide I (Gly-Phe-Asp-Leu-Asn-Gly-Gly-Gly-Val-Gly) [17–18, 65]. The acrosome reaction of sea urchin spermatozoa is accompanied by Na^+ and Ca^{2+} influx, and H^+ and K^+ efflux [44, 113–128]. Activation of sea urchin spermatozoa by sperm-activating peptides is also accompanied by these ionic changes which cause an increased intracellular pH and trigger sperm plasma membrane depolarization [82, 129–130].

In 1952, Dan first discovered using sea urchin gametes that the acrosome reaction is essential for fertilization and that the factor responsible for the

acrosome reaction exists in an extracellular matrix called the jelly layer [1]. Since then many investigators have made tremendous efforts to identify this factor and to clarify the mechanism of the reaction [2–16]. Ishihara and Dan reported that treatment of the solubilized jelly layer of *Hemicentrotus pulcherrimus* with trypsin and pronase results in a reduction of the acrosome reaction-inducing ability to about half of that with the untreated jelly [5]. SeGall and Lennarz isolated a fucose sulfate-containing substance containing less than 30% protein from the solubilized jelly layer of four species of sea urchin by gel filtration and ion-exchange chromatography [13]. They demonstrated that the acrosome reaction-inducing capacity of the substance resides solely in the fucose sulfate polysaccharide, although the inducing activity decreases during purification. They concluded that this decrease in activity is due to the loss of Ca^{2+} during purification. Garbers *et al.* reported that a fucose-sulfate-rich complex purified from the solubilized jelly layer of *Strongylocentrotus purpuratus* is capable of elevating sperm cAMP concentrations and inducing the

acrosome reaction [16]. They also demonstrated that NaOH or pronase treatment of the complex results in significant reductions in both acrosome reaction-inducing potency and maximal ability of the complexes to elevate cAMP concentrations.

The fucose sulfate glycoconjugate purified from the solubilized jelly layer of *Hemicentrotus pulcherrimus* induces the acrosome reaction in *Hemicentrotus pulcherrimus* spermatozoa, but the potency is about half that of the unfractionated jelly (Table 3) [18, 65]. When a sperm-activating peptide-free macromolecular fraction is prepared from the solubilized jelly layer of *Hemicentrotus pulcherrimus* which is composed of a sialoglycoprotein and a fucose sulfate glycoconjugate, the rates of the acrosome reaction induced by the fraction are also about half that of the original unfractionated jelly [17]. The addition of synthetic SAP-I to the fraction or the fucose sulfate glycoconjugate increases the rate of the acrosome reaction to a level comparable with that of the unfractionated jelly at all pHs tested. SAP-I promotes the acrosome reaction with fucose sulfate glycoconjugate in *Hemicentrotus pulcherrimus* sperma-

TABLE 3. The rate of acrosome reaction in *Hemicentrotus pulcherrimus* spermatozoa in the presence or absence of SAP-I treated with crude jelly, sialoglycoprotein, FSG, pronase-digested FSG and carboxymethylated FSG

	Percentage of Reacting Spermatozoa	
	Exp. 1	Exp. 2
Crude jelly	90%	87%
FSG + none	32	45
+ SAP-I	75	81
Pronase-digested FSG		
+ none	15	
+ SAP-I	49	
Carboxymethylated FSG		
+ none		24
+ SAP-I		54
Sialoglycoprotein		
+ none		3
+ SAP-I		5
ASW alone	3	2

Spermatozoa were incubated in 0.5 ml of ASW or ASW containing crude jelly [62.5 (Exp. 1) or 100 (Exp. 2) nmol fucose/ml], sialoglycoprotein (100 nmol sialic acid/ml), fucose sulfate glycoconjugate (FSG) [62.5 (Exp. 1) or 100 (Exp. 2) nmol fucose/ml], pronase-digested FSG (62.5 nmol fucose/ml), and carboxymethylated FSG (100 nmol fucose/ml) with or without SAP-I (0.5 μM).

tozoa in a concentration-dependent manner with a half-maximal rate of 4×10^{-10} M which is almost the same concentration of peptide needed to cause half-maximal stimulation of sperm respiration [18]. Since SAP-I alone does not induce the acrosome reaction and sialoglycoprotein, another large molecular weight component of the jelly layer, also does not show any appreciable potency for induction of the acrosome reaction, we think that

the major substance responsible for induction of the acrosome reaction is the fucose sulfate glycoconjugate and SAP-I promotes the induction of the acrosome reaction by acting as a co-factor [65].

The fucose sulfate glycoconjugate isolated from the solubilized jelly layer of *Hemicentrotus pulcherrimus* contains a large amount of protein [65]. The proteins associated with fucose sulfate can not be removed even when the glycoconjugate is dis-

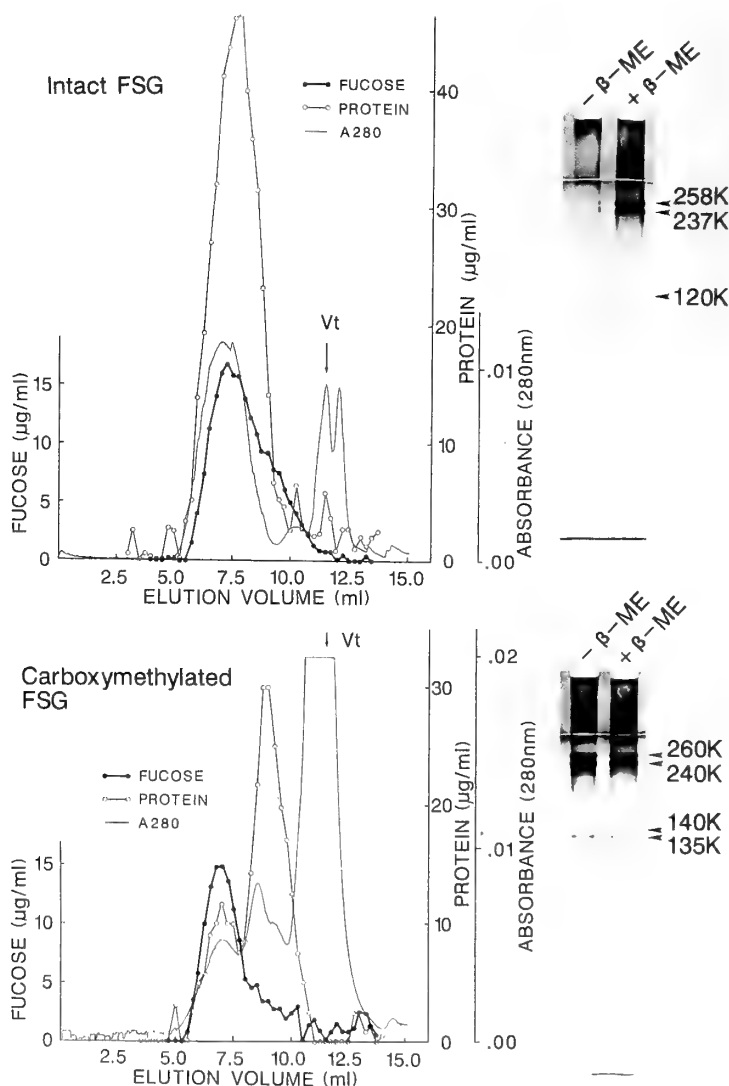


FIG. 4. HPLC and SDS-PAGE of intact and carboxymethylated fucose sulfate glycoconjugate isolated from the solubilized jelly layer of *Hemicentrotus pulcherrimus*. Fucose sulfate glycoconjugate is abbreviated as FSG in the figure. See [ref. 65] for experimental details.

solved in 7 M urea or 0.1% SDS and chromatographed on a Sepharose CL-2B or a TSK G-6000 PW column (Fig. 4). Furthermore, no protein band is detectable on the electrophoretogram of SDS-polyacrylamide gel electrophoresis (SDS-PAGE) of the intact fucose sulfate glycoconjugate without a reducing agent such as 2-mercaptoethanol. These results suggest that the protein may be covalently bound to the polysaccharide portions of the glycoconjugate. When the glycoconjugate is dissolved in an SDS solution containing 2-mercaptoethanol and subjected to SDS-PAGE in the presence of 2-mercaptoethanol, two major (258 kDa and 238 kDa) and one minor (120 kDa) protein bands appeared. A reduced and carboxymethylated fucose sulfate glycoconjugate (CmFSG) separated into two major (260 kDa and 240 kDa) and two minor (140 kDa and 135 kDa) protein bands on an SDS-gel despite the absence of 2-mercaptoethanol (Fig. 4). When CmFSG was subjected to HPLC on a TSK G-6000 PW column, a fucose-containing material, which possesses about 30% of the protein originally associated with the fucose sulfate glycoconjugate, was separated from the rest of the proteins. These proteins separated into 260 kDa, 240 kDa, 140 kDa and 135 kDa components by SDS-PAGE. This indicates that the fucose sulfate glycoconjugate consists of fucose sulfate polymers bound to a core protein and several other protein components associated with each other through disulfide bounds. In order to confirm the presence of disulfide bonds in the fucose sulfate glycoconjugate, free sulfhydryl groups in the fucose sulfate glycoconjugate are first treated with non-radioactive iodoacetic acid, which results in the carboxymethylation of about half of the cysteine residues present in the original glycoconjugate, and they are then reduced and carboxymethylated with [^{14}C] iodoacetic acid. The resulting labeled carboxymethylated glycoconjugate was analyzed by SDS-PAGE, and showed that protein bands corresponding to 140 kDa and 135 kDa proteins have strong radioactivity although weaker radioactivity was detected in the 260 kDa, 240 kDa, 110 kDa and 87 kDa protein bands. In amino acid analyses of protein components isolated from CmFSG, a 140 kDa and 135 kDa protein fraction contained the largest mol%

of carboxymethylated cysteine. These results suggest that 140 kDa and 135 kDa proteins, which are probably the same protein(s) detected in a 120 kDa protein band in SDS-PAGE of the intact fucose sulfate glycoconjugate with 2-mercaptoethanol have more sulfhydryl groups than other protein components available for disulfide bond formation and may serve to make bridge between the polysaccharide bound core protein and other protein components.

Complete carboxymethylation of cysteine residues in the major acrosome reaction-inducing jelly molecules, the fucose sulfate glycoconjugate, results in the release of most of the constituent proteins from the glycoconjugate and about a 50% decrease in the acrosome reaction-inducing capacity of the glycoconjugate [65]. When about 70% of the constituent proteins is removed from the fucose sulfate glycoconjugate by pronase digestion, the resulting fucose-rich glycoconjugate loses more than 50% of the acrosome reaction-inducing activity of the original untreated glycoconjugate (Table 3) [18]. In both cases, the decreased potency could be partially restored by the addition of SAP-I, monensin, 3-isobutyl-1-methylxanthine (IBMX) which is an inhibitor for cyclic nucleotide phosphodiesterase or a Ca^{2+} -ionophore, A23187 [18]. Fucoidan, a polymer of L-fucose-4-sulfate which is a major sugar component in the fucan sulfate isolated from the solubilized jelly layer of *Hemicentrotus pulcherrimus*, does not appreciably induce the acrosome reaction of *Hemicentrotus pulcherrimus* spermatozoa [65]. These results suggest that the protein moiety of fucose sulfate glycoconjugate is involved in the acrosome reaction although the mechanism remains unclear.

FUTURE PROSPECTS

It is known that the acrosome reaction is dependent on increased intracellular pH [29–30]. SAP-I increases an intracellular Ca^{2+} which is coupled to Na^{+} entry and induces a rise in intracellular pH in *Strongylocentrotus purpuratus* spermatozoa [129–130]. Thus, we may presume that SAP-I promotes an acrosome reaction with fucose sulfate glycoconjugate by increasing intracellular pH in sperm cells.

A fucose-sulfate-rich complex obtained from the solubilized jelly layer of *Strongylocentrotus purpuratus* causes Ca^{2+} -accumulation, elevates cAMP and induces the acrosome reaction [16, 44, 114, 131-134]. In connection with this, it should be noted that monoclonal antibodies against a 210 kDa glycoprotein purified from *Strongylocentrotus purpuratus* sperm plasma membrane cause an increase in intracellular Ca^{2+} of *Strongylocentrotus purpuratus* spermatozoa and induce the acrosome reaction when intracellular pH is increased with NH_4Cl [118, 135-139]. Antibodies induce the cAMP-dependent phosphorylation of sperm histone H1 as occurs upon treatment of spermatozoa with the solubilized jelly layer of *Strongylocentrotus purpuratus* [91-93]. Similar results are presented by Sendai *et al.* using sea urchin gametes of *Strongylocentrotus intermedius* [38-39]. However, an ionophore A23187 which is known to induce the acrosome reaction and acts as a co-factor of a pronase-digested fucose sulfate glycoconjugate for induction of the acrosome reaction neither induces histone H1 phosphorylation nor increases cAMP concentrations in sea urchin spermatozoa [9, 18, 92, 140]. This supports the idea which suggests that cAMP is not directly involved in the acrosome reaction. Since a fucose-sulfate-rich complex obtained from *Strongylocentrotus purpuratus* jelly induces the elevation of inositol trisphosphate and the elevation is dependent on external Ca^{2+} , the products generated from stimulated PI turnover in sea urchin spermatozoa may be potential second messengers in induction of the acrosome reaction [141].

Sea urchin gametes have long been used for studying fertilization and development [3, 29, 43, 64, 84, 127, 142-152]. It is not an exaggeration to say that sea urchin are one of the most extensively used experimental animals in basic biology. However, we must realize that we do not know much about the substances involved in sea urchin gamete interaction. An understanding of this would not only lead to an understanding of fertilization in mammals and other animals, but it would serve as a valuable indicator of mechanisms which can be anticipated in cells other than gametes. Sperm-activating peptides cause many biochemical responses in sea urchin spermatozoa

such as increases in cGMP and cAMP concentrations, induction of ionic exchanges across the plasma membrane and increases in intracellular pH. The mechanism of action of the peptides resembles in many aspects that of the atrial natriuretic peptides, although the mechanism has yet to be described in detail [153-156]. Since de Bold *et al.* suggested that a factor released from the atria of the heart evokes a variety of physiological responses affecting cardiovascular homeostasis, intensive studies have been carried out in an attempt to identify the factor and a receptor(s) for the factor [153-159]. Recently, the structure of a receptor for atrial natriuretic peptides was determined by Chinkers *et al.* as a result of advanced research on a sperm-activating peptide receptor [160]. This serves as an excellent example for demonstrating that the results of research in one field can be applied to solving the problems in other fields.

The receptor for the fucose sulfate glycoconjugate, which is the major substance responsible for induction of the acrosome reaction has yet to be isolated. Study of the receptor protein appears to have great significance because questions have arisen as to whether or not this protein could also represent a calcium channel. Parallel to the isolation and characterization of the receptor, the function of primary and secondary messengers will be an important future area of research, much as in other cells.

ACKNOWLEDGMENTS

The research described in this article was conducted at Teikyo University School of Medicine and Noto Marine Laboratory, Kanazawa University with the financial support of the Ministry of Education, Science and Culture of Japan (Nos. 57540425, 58540474, 59540471, 60480022, 62540458 and 63480021). The author would like to thank Drs. Kohji Nomura, Masaaki Yamaguchi, Saburo Isaka, Toshifumi Takao and Yasutsugu Shimonishi for their kind and helpful collaboration. He wishes to express his appreciation to graduate students in his laboratory for their hard work and assistance, and to Miss Hiroko Kajiura of the National Institute for Basic Biology who performed the sequencing with an automated sequencer. He is also indebted to Prof. Chitaru Oguro of Toyama University for help with scanning electron microscopy, Prof. Yoshitaka Nagahama of the National Institute for Basic Biology and the staff of the Radioisotope Center, Kanazawa University, for facilitating the use of equip-

ment for determining cyclic nucleotide concentrations. He is grateful to the staff members of the Sesoko Marine Science Center of the University of Ryukyus and of the Asamushi Marine Biological Station of Tohoku University for the time and energy they spent collecting sea urchins for this research.

REFERENCES

- Dan, J. C. (1952) *Biol. Bull.*, **103**: 43–66.
- Dan, J. C. (1954) *Biol. Bull.*, **107**: 335–349.
- Dan, J. C. (1956) *Int. Rev. Cytol.*, **5**: 365–393.
- Dan, J. C., Ohori, Y. and Kushida, H. (1964) *J. Ultrastruct. Res.*, **11**: 508–524.
- Ishihara, K. and Dan, J. C. (1970) *Develop. Growth and Differ.*, **12**: 179–188.
- Tilney, L. G., Hatano, S., Ishikawa, H. and Mooseker, M. S. (1973) *J. Cell Biol.*, **59**: 109–126.
- Summers, R. G. and Hylander, B. L. (1975) *Exp. Cell Res.*, **93**: 63–68.
- Summers, R. G., Hylander, B. L., Colwin, L. H. and Colwin, A. L. (1975) *Am. Zool.*, **15**: 523–551.
- Decker, G. L., Joseph, D. B. and Lennarz, W. J. (1976) *Develop. Biol.*, **53**: 115–125.
- Collins, F. and Epel, D. (1977) *Exp. Cell Res.*, **106**: 211–222.
- Kinsey, W. H., SeGall, G. K. and Lennarz, W. J. (1979) *Develop. Biol.*, **71**: 49–59.
- Kinsey, W. H., Rubin, J. A. and Lennarz, W. J. (1980) *Develop. Biol.*, **74**: 245–250.
- SeGall, G. K. and Lennarz, W. J. (1979) *Develop. Biol.*, **71**: 33–49.
- SeGall, G. K. and Lennarz, W. J. (1981) *Develop. Biol.*, **86**: 87–93.
- Ishihara, K., Oguri, K. and Taniguchi, H. (1973) *Biochim. Biophys. Acta*, **320**: 628–634.
- Garbers, D. L., Kopf, G. S., Tubb, D. J. and Olson, G. (1983) *Biol. Reprod.*, **29**: 1211–1220.
- Yamaguchi, M., Niwa, T., Kurita, M. and Suzuki, N. (1988) *Develop. Growth and Differ.*, **30**: 159–167.
- Yamaguchi, M., Kurita, M. and Suzuki, N. (1989) *Develop. Growth and Differ.*, **31**: 233–239.
- Isaka, S., Akino, M., Hotta, K. and Kurokawa, M. (1968) *Exp. Cell Res.*, **54**: 247–249.
- Hotta, K., Hamazaki, H., Kurokawa, M. and Isaka, S. (1970) *J. Biol. Chem.*, **245**: 5434–5440.
- Hotta, K., Kurokawa, M. and Isaka, S. (1970) *J. Biol. Chem.*, **245**: 6307–6311.
- Isaka, S., Hotta, K. and Kurokawa, M. (1970) *Exp. Cell Res.*, **59**: 37–42.
- Bedford, J. M. (1976) *Adv. Biosci.*, **4**: 35–50.
- Yanagimachi, R. and Usui, N. (1974) *Exp. Cell Res.*, **89**: 161–174.
- Baccitti, B. and Afzelius, B. A. (1976) *The Biology of the Sperm Cell*. In "Monographs in Developmental Biology". Ed. by A. Wolsky, vol. 10, S. Karger, Basel and New York.
- Cornett, L. E. and Meizel, S. (1978) *Proc. Natl. Acad. Sci. USA*, **75**: 4954–4958.
- Saling, P. M., Sowinski, J. and Storey, B. T. (1979) *J. Exp. Zool.*, **209**: 229–238.
- Uno, Y. and Hoshi, M. (1978) *Science*, **200**: 58–59.
- Shapiro, B. M. and Eddy, E. M. (1980) *Int. Rev. Cytol.*, **66**: 257–302.
- Shapiro, B. M., Shackmann, R. W. and Gabel, C. A. (1981) *Ann. Rev. Biochem.*, **50**: 815–843.
- Nishiyama, I., Sasaki, H., Matsui, T. and Hoshi, M. (1985) *Develop. Growth and Differ.*, **27**: 461–468.
- Matsui, T., Nishiyama, I., Hino, A. and Hoshi, M. (1986) *Develop. Growth and Differ.*, **28**: 339–348.
- Matsui, T., Nishiyama, I., Hino, A. and Hoshi, M. (1986) *Develop. Growth and Differ.*, **28**: 349–357.
- Matsui, T., Nishiyama, I., Hino, A. and Hoshi, M. (1986) *Develop. Growth and Differ.*, **28**: 359–368.
- Nishiyama, I., Matsui, T., Yasumoto, T., Oshio, S. and Hoshi, M. (1986) *Develop. Growth and Differ.*, **28**: 443–448.
- Hoshi, M., Matsui, T., Nishiyama, I., Fujimoto, Y. and Ikekawa, N. (1986) *Adv. Invertebrate Reprod.*, **4**: 275–282.
- Nishiyama, I., Matsui, T. and Hoshi, M. (1987) *Develop. Growth and Differ.*, **29**: 161–169.
- Nishiyama, I., Matsui, T., Fujimoto, Y., Ikekawa, N. and Hoshi, M. (1987) *Develop. Growth and Differ.*, **29**: 171–176.
- Fujimoto, Y., Yamada, T., Ikekawa, N., Nishiyama, I., Matsui, T. and Hoshi, M. (1987) *Chem. Pharm. Bull.*, **35**: 1829–1832.
- Wasserman, P. M. (1987) *Ann. Rev. Cell Biol.*, **3**: 109–142.
- Wasserman, P. M. (1987) *Science*, **235**: 553–560.
- Wasserman, P. M. (1988) *Ann. Rev. Biochem.*, **57**: 415–442.
- Garbers, D. L. (1989) *Ann. Rev. Biochem.*, **58**: 719–742.
- Kopf, G. S. and Garbers, D. L. (1980) *Biol. Reprod.*, **22**: 1118–1126.
- Aketa, K., Yoshida, M., Miyazaki, S. and Ohta, T. (1979) *Exp. Cell Res.*, **123**: 281–284.
- Levin, Y., Pecht, M., Goldstein, L. and Katchalski, E. (1964) *Biochemistry*, **3**: 1905–1913.
- Goldstein, L., Levin, Y. and Katchalski, E. (1964) *Biochemistry*, **3**: 1913–1919.
- Vasseur, E. and Hagstrom, B. (1946) *Ark. Zool.*, **37A**, **17**: 1–17.
- Rothschild, Lord (1958) *J. Exp. Biol.*, **33**: 155–

- 173.
- 50 Ohtake, H. (1976) *J. Exp. Zool.*, **198**: 303–312.
- 51 Ohtake, H. (1976) *J. Exp. Zool.*, **198**: 313–322.
- 52 Lillie, F. R. (1913) *J. Exp. Zool.*, **14**: 515–574.
- 53 Carter, G. S. (1931) *J. Exp. Biol.*, **8**: 176–193.
- 54 Cohn, E. J. (1918) *Biol. Bull.*, **34**: 167–218.
- 55 Gray, J. (1928) *J. Exp. Biol.*, **5**: 337–344.
- 56 Gray, J. (1928) *J. Exp. Biol.*, **5**: 362–365.
- 57 Rothschild, Lord (1956) *Vie Milieu*, **7**: 405–412.
- 58 Hathaway, R. R. (1963) *Biol. Bull.*, **125**: 486–498.
- 59 Kopf, G. S., Tubb, D. J. and Garbers, D. L. (1979) *J. Biol. Chem.*, **254**: 8554–8560.
- 60 Hansbrough, J. R. and Garbers, D. L. (1981) *J. Biol. Chem.*, **256**: 1447–1452.
- 61 Hansbrough, J. R. and Garbers, D. L. (1981) *J. Biol. Chem.*, **256**: 2235–2241.
- 62 Suzuki, N., Nomura, K., Ohtake, H. and Isaka, S. (1981) *Biochem. Biophys. Res. Commun.*, **99**: 1238–1244.
- 63 Garbers, D. L., Watkins, H. D., Tubb, D. J., Smith, A. C. and Misono, K. S. (1982) *J. Biol. Chem.*, **257**: 2734–2737.
- 64 Suzuki, N. (1989) In "Bioorganic Marine Chemistry". vol. 3, Ed. by P. J. Scheuer, Springer-Verlag, Berlin, pp. 47–70.
- 65 Shimizu, T., Kinoh, H., Yamaguchi, M. and Suzuki, N. (1990) *Develop. Growth and Differ.*, in press.
- 66 Shimizu, T. and Suzuki, N. unpublished data.
- 67 Nomura, K., Suzuki, N., Ohtake, H. and Isaka, S. (1983) *Biochem. Biophys. Res. Commun.*, **117**: 147–153.
- 68 Suzuki, N., Ohizumi, Y., Yasumasu, I. and Isaka, S. (1984) *Develop. Growth and Differ.*, **26**: 17–24.
- 69 Suzuki, N., Shimonura, H., Radany, E. W., Ramarao, C. S., Bentley, J. K. and Garbers, D. L. (1984) *J. Biol. Chem.*, **259**: 14874–14879.
- 70 Shimomura, H., Suzuki, N. and Garbers, D. L. (1986) *Peptides*, **7**: 491–495.
- 71 Suzuki, N., Kurita, M., Yoshino, K., Nomura, K. and Yamaguchi, M. (1987) *Zool. Sci.*, **4**: 649–657.
- 72 Suzuki, N., Kajiura, H., Nomura, K., Garbers, D. L., Yoshino, K., Kurita, M., Tanaka, H. and Yamaguchi, M. (1988) *Comp. Biochem. Physiol.*, **89B**: 687–693.
- 73 Suzuki, N., Yoshino, K., Kurita, M., Nomura, K. and Yamaguchi, M. (1988) *Comp. Biochem. Physiol.*, **90C**: 305–311.
- 74 Yoshino, K., Kajiura, H., Nomura, K., Takao, T., Shimonishi, Y., Kurita, M., Yamaguchi, M. and Suzuki, N. (1989) *Comp. Biochem. Physiol.*, **94B**: 739–751.
- 75 Yoshino, K., Kurita, M., Yamaguchi, M., Nomura, K., Takao, T., Shimonishi, Y. and Suzuki, N. (1990) *Comp. Biochem. Physiol.*, **95B**: 423–429.
- 76 Suzuki, N., Hoshi, M., Nomura, K. and Isaka, N. (1982) *Comp. Biochem. Physiol.*, **72A**: 489–495.
- 77 Suzuki, N., Yoshino, K., Kurita, M., Yamaguchi, M. and Amemiya, S. (1988) In "Echinoderm Biology". Ed. by R. D. Burke, P. V. Mladenov, P. Lambert and R. D. Parsley, A. A. Balkema, Rotterdam, pp. 213–218.
- 78 Suzuki, N., Kurita, M., Yoshino, K. and Yamaguchi, M. (1987) *Zool. Sci.*, **4**: 641–648.
- 79 Smith, A. C. and Garbers, D. L. (1984) In "Biochemistry of Metabolic Processes". Ed. by D. L. F. Lennon, F. W. Stratman and R. N. Zhaltan, Elsevier/North-Holland, New York, pp. 15–28.
- 80 Hansbrough, J. R. and Garbers, D. L. (1981) In "Adv. Enzyme Regulation". vol. 19, Ed. by G. Weber, Pergamon Press, New York, pp. 351–376.
- 81 Ovchinnikov, Yu. A., Ivanov, V. T. and Shkrob, A. M. (1974) In "Membrane-Active Complexones". B. B. A. Library, vol. 12, Elsevier Scientific Publ. Co., Amsterdam/Oxford/New York, pp. 331–405.
- 82 Repaske, D. L. and Garbers, D. L. (1983) *J. Biol. Chem.*, **258**: 6025–6029.
- 83 Nuccitelli, R. and Deamer, D. W. (eds.) (1982) *Intracellular pH: Its Measurement, Regulation, and Utilization in Cellular Functions*. Alan R. Liss, Inc., New York.
- 84 Trimmer, J. S. and Vacquier, V. D. (1986) *Ann. Rev. Cell Biol.*, **2**: 1–26.
- 85 Garbers, D. L. and Hardman, J. G. (1975) *Nature*, **257**: 677–678.
- 86 Garbers, D. L., Hardman, J. G. and Rudolph, F. G. (1974) *Biochemistry*, **13**: 4166–4171.
- 87 Garbers, D. L., Watkins, H. D., Tubb, D. J. and Kopf, G. S. (1978) *Adv. Cyclic Nucleotide Res.*, **9**: 583–595.
- 88 Sano, M. (1976) *Biochim. Biophys. Acta*, **172**: 20–30.
- 89 Swarup, G. and Garbers, D. L. (1982) *Biol. Reprod.*, **2**: 953–960.
- 90 Wells, J. N. and Garbers, D. L. (1976) *Biol. Reprod.*, **15**: 46–53.
- 91 Green, G. R. and Poccia, D. L. (1985) *Develop. Biol.*, **108**: 235–245.
- 92 Porter, D. C. and Vacquier, V. D. (1986) *Develop. Biol.*, **116**: 203–212.
- 93 Porter, D. C., Moy, G. W. and Vacquier, V. D. (1988) *J. Biol. Chem.*, **263**: 2750–2755.
- 94 Radany, E. W., Gerzer, R. and Garbers, D. L. (1983) *J. Biol. Chem.*, **258**: 8346–8351.
- 95 Ramarao, C. S. and Garbers, D. L. (1985) *J. Biol. Chem.*, **260**: 8390–8396.
- 96 Ramarao, C. S. and Garbers, D. L. (1988) *J. Biol. Chem.*, **263**: 1524–1529.

- 97 Thorpe, D. S. and Garbers, D. L. (1989) *J. Biol. Chem.*, **264**: 6545–6549.
- 98 Bentley, J. K. and Garbers, D. L. (1986) *Biol. Reprod.*, **34**: 413–421.
- 99 Bentley, J. K. and Garbers, D. L. (1986) *Biol. Reprod.*, **35**: 1249–1259.
- 100 Bentley, J. K., Shimonura, H. and Garbers, D. L. (1986) *Cell*, **45**: 281–288.
- 101 Bentley, J. K., Tubb, D. J. and Garbers, D. L. (1986) *J. Biol. Chem.*, **262**: 14859–14862.
- 102 Garbers, D. L. (1988) In "ISI Atlas of Science: Biochemistry/1988". pp. 120–126.
- 103 Ward, G. E. and Vacquier, V. D. (1983) *Proc. Natl. Acad. Sci. USA.*, **80**: 5578–5582.
- 104 Ward, G. E., Garbers, D. L. and Vacquier, V. D. (1985) *Science*, **227**: 768–770.
- 105 Ward, G. E., Moy, G. W. and Vacquier, V. D. (1986) *J. Cell Biol.*, **103**: 95–101.
- 106 Harumi, T., Kurita, M., Yamaguchi, M. and Suzuki, N. unpublished data.
- 107 Vacquier, V. D. and Moy, G. W. (1986) *Biochem. Biophys. Res. Commun.*, **137**: 1148–1152.
- 108 Vacquier, V. D. (1986) *TIBS.*, **11**: 77–81.
- 109 Shimomura, H., Dangott, L. J. and Garbers, D. L. (1986) *J. Biol. Chem.*, **261**: 8719–8728.
- 110 Dangott, L. J. and Garbers, D. L. (1984) *J. Biol. Chem.*, **259**: 13712–13716.
- 111 Dangott, L. J. and Garbers, D. L. (1987) *Ann. N. Y. Acad. Sci.*, **513**: 274–283.
- 112 Dangott, L. J., Jordan, J. E., Bellet, R. A. and Garbers, D. L. (1989) *Proc. Natl. Acad. Sci. USA.*, **86**: 2128–2132.
- 113 Schackmann, R. W., Eddy, E. M. and Shapiro, B. M. (1978) *Develop. Biol.*, **65**: 483–495.
- 114 Garbers, D. L. and Kopf, G. S. (1980) *Adv. Cyclic Nucleotide Res.*, **13**: 251–306.
- 115 Schackmann, R. W. and Shapiro, B. M. (1981) *Develop. Biol.*, **81**: 145–154.
- 116 Schackmann, R. W., Christen, R. and Shapiro, B. M. (1981) *Proc. Natl. Acad. Sci. USA.*, **78**: 6066–6070.
- 117 Garcia-Soto, J. and Darszon, A. (1985) *Develop. Biol.*, **110**: 338–345.
- 118 Trimmer, J. S., Trowbridge, I. S. and Vacquier, V. D. (1985) *Cell*, **40**: 697–703.
- 119 Garcia-Soto, J., Gonzalez-Marinez, N., Torre, L. de De la and Darszon, A. *Develop. Biol.*, **120**: 112–120.
- 120 Towicharanont, P. and Shapiro, B. M. (1988) *J. Biol. Chem.*, **263**: 6877–6883.
- 121 Sendai, Y., Ohta, T. and Aketa, K. (1989) *Develop. Growth and Differ.*, **31**: 459–466.
- 122 Sendai, Y. and Aketa, K. (1989) *Develop. Growth and Differ.*, **31**: 467–473.
- 123 Gurrero, A. and Darszon, A. (1989) *Biochim. Biophys. Acta*, **980**: 109–116.
- 124 Lee, H. C., Johnson, C. and Epel, D. (1983) *Develop. Biol.*, **72**: 126–137.
- 125 Schackmann, R. W., Christen, R. and Shapiro, B. M. (1984) *J. Biol. Chem.*, **259**: 13914–13922.
- 126 Darszon, A., Garcia-Soto, J., Lievano, A., Sanchez, J. A. and Islas-Trejo, A. D. (1986) In "Ionic Channels in Cells and Model Syatem". Ed. by R. Latorre, Plenum Press, New York, pp. 291–305.
- 127 Epel, D. (1978) *Curr. Top. Develop. Biol.*, **12**: 185–246.
- 128 Christen, R., Schackmann, R. W. and Shapiro, B. M. (1983) *Develop. Biol.*, **98**: 1–14.
- 129 Schackmann, R. W. and Chock, P. B. (1986) *J. Biol. Chem.*, **261**: 8719–8728.
- 130 Lee, H. C. and Garbers, D. L. (1986) *J. Biol. Chem.*, **261**: 16026–16032.
- 131 Tubb, D. J., Kopf, G. S. and Garbers, D. L. (1978) *Biol. Reprod.*, **18**: 181–185.
- 132 Watkins, H. D., Kopf, G. S. and Garbers, D. L. (1978) *Biol. Reprod.*, **18**: 890–894.
- 133 Garbers, D. L., Tubb, D. J. and Kopf, G. S. (1980) *Biol. Reprod.*, **22**: 526–532.
- 134 Garbers, D. L. (1981) *J. Biol. Chem.*, **256**: 620–624.
- 135 Lopo, A. C. and Vacquier, V. D. (1980) *Develop. Biol.*, **79**: 325–333.
- 136 Podell, S. B. and Vacquier, V. D. (1984) *Exp. Cell Res.*, **155**: 467–476.
- 137 Podell, S. B. and Vacquier, V. D. (1985) *J. Biol. Chem.*, **260**: 2715–2718.
- 138 Trimmer, J. S., Schackmann, R. W. and Vacquier, V. D. (1986) *Proc. Natl. Acad. Sci. USA.*, **83**: 9055–9059.
- 139 Trimmer, J. S., Ebina, Y., Schackmann, R. W., Meinhof, C-G. and Vacquier, V. D. (1987) *J. Cell Biol.*, **105**: 1121–1128.
- 140 Summers, R. G., Talbot, P., Keough, E. M., Hylander, B. L. and Franklin, L. E. (1976) *J. Exp. Zool.*, **196**: 381–385.
- 141 Domino, S. E. and Garbers, D. L. (1988) *J. Biol. Chem.*, **263**: 690–695.
- 142 Metze, C. B. (1967) In "Fertilization: Comparative Morphology, Biochemistry and Immunology". vol. 1, Ed. by C. B. Metze and A. Monroy, Academic Press, New York, pp. 163–236.
- 143 Longo, F. G. (1973) *Biol. Reprod.*, **9**: 149–215.
- 144 Guidice, G. (1973) *Developmental Biology of the Sea Urchin Embryo*. Academic Press, New York.
- 145 Horstadius, S. (1973) *Experimental Embryology of Echinoderms*. Oxford Univ. Press, London/New York.
- 146 Stearns, L. W. (1974) *Sea Urchin Development, Cellular and Molecular Aspects*. Dowden, Hutchinson & Ross, Stroudsville.

- 147 Czihak, G. (1975) *The Sea Urchin Embryo: Biochemistry and Morphogenesis*. Springer-Verlag, Berlin.
- 148 Shapiro, B. M. (1977) *Horizons Biochem. Biophys.*, **4**: 201–243.
- 149 Poste, G. and Nicolson, G. L. (eds.) (1978) *Cell Surface Rev.*, vol. 5, North Holland, Amsterdam.
- 150 Dirksen, E. R., Prescott, D. and Fox, C. H. (eds.) (1978) *Cell Reproduction*. Academic Press, New York.
- 151 Schatten, G. (1982) *Int. Rev. Cytol.*, **79**: 59–163.
- 152 Guidice, G. (1985) *The Sea Urchin Embryo. A Developmental Biology System*. Springer-Verlag, Berlin.
- 153 Kuno, T., Andresen, J. W., Kamisaki, Y., Waldman, S. A., Chang, L. Y., Saheki, S., Leitman, D. C., Nakane, M. and Murad, F. (1986) *J. Biol. Chem.*, **261**: 5817–5823.
- 154 Paul, A. K., Marala, R. B., Jaiswal, P. K. and Sharna, P. K. (1987) *Science*, **235**: 1224–1226.
- 155 Takayanagi, R., Snajdar, R. M., Imada, T., Tamura, M., Pandey, K. N., Misono, K. S. and Inagami, T. (1987) *Biochem. Biophys. Res. Commun.*, **144**: 244–250.
- 156 Hamet, P., Trembly, J., Pang, S. C., Garcia, R., Thibault, G., Gutkowska, J., Cantin, M. and Genest, J. (1984) *Biochem. Biophys. Res. Commun.*, **123**: 515–527.
- 157 de Bold, A. J., Borenstein, H. B., Veress, A. T. and Sonnenberg, H. (1981) *Life Sci.*, **28**: 89–94.
- 158 Mittal, C. K. and Murad, F. (1982) In "Handbook of Experimental Pharmacology". Ed. by J. A. Nathanson and J. W. Kebabian, vol. 58, pp. 225–260, Springer-Verlag, Berlin.
- 159 Kangawa, K. and Matsuo, H. (1984) *Biochem. Biophys. Res. Commun.*, **118**: 131–139.
- 160 Chinkers, M., Garbers, D. L., Chang, M.-S., Lowe, D. G., Chin, H., Goeddel, D. V. and Shultz, S. (1989) *Nature*, **338**: 78–83.

Regulation of Water Permeability of the Skin of the Treefrog, *Hyla arborea japonica*

HIROSHI NAKASHIMA and YOSHIHISA KAMISHIMA¹

Department of Biology, Faculty of Science, Okayama University,
Okayama 700, Japan

ABSTRACT—Water permeability of excised skin was investigated in Japanese treefrogs during the non-breeding season. In normal frogs, water flowed inward across the ventral skin at a rate of $0.30 \mu\text{l}/\text{cm}^2/\text{min}$, and outward at a rate of $0.0015 \mu\text{l}/\text{cm}^2/\text{min}$ across the dorsal skin. The water flux across the ventral skin was greatly stimulated when frogs were submitted to dehydration. The sympathomimetic agent noradrenaline and the beta-adrenergic receptor agonist isoproterenol (IP) greatly increased the water flux across the ventral skin, but these had no effect on the dorsal skin. The beta-receptor antagonist propranolol (PP) suppressed the enhanced water influx by dehydration or IP treatment. However, PP had no effect on normal water permeation across the ventral skin. Ouabain, a specific inhibitor of Na^+ , K^+ -ATPase, also suppressed the stimulatory effect of IP, whereas this inhibitor again had no effect in normal water flux of the ventral skin. The adrenergic alpha-receptor agonist phenylephrine had no effects on water permeation in either ventral or dorsal skin. Prolactin administration for one week prior to the experimentation decreased water permeability significantly across the ventral skin in both normal and stimulated preparations. These results all argue for the presence of two types of water transport system in the ventral skin of the Japanese treefrog. The first is mediated by the adrenergic beta-receptor and by Na^+ , K^+ -ATPase activity and may be activated by dehydration. The second is not mediated by the adrenergic receptor and may function as the normal, basal water permeation.

INTRODUCTION

Anuran amphibians are known not to take water orally. They take the most of their water through the skin [1–6]. Water permeation through the skin is mainly confined to the pelvic patch [7–9] and can be modified by various factors, including sympathomimetic agents [10–15] and neurohypophyseal hormones [1, 2, 5, 7, 15]. Water permeation in the skin is stimulated by dehydration [4, 11]. Water permeability differs according to both species and season. Generally, terrestrially-adopted species have more permeable skin than do aquatic species [8, 9]. Water also evaporates readily from normal frog skin [1, 3]. This evaporation helps to cool the animal, and is known to be less in terrestrially-adopted anurans such as toads and treefrogs [16, 17]. These findings raise the para-

doxical question of how these anurans manage to survive in hot and dry environments, where they cool themselves at the cost of water which is already scarce in their habitats.

The Japanese treefrogs are known to have survived long periods of drought, and have been reported to accumulate glycosaminoglycans in their epidermis following dehydration treatment. The glycosaminoglycans might cause retardation of water movement across the skin [18]. Prolactin administration brought similar morphological changes in the skin of these frogs. In the present experiment we intended to find out regulating factors of water permeation in the Japanese treefrogs, especially in terms of neural and hormonal control under the dehydrated condition.

MATERIALS AND METHODS

Japanese treefrogs, *Hyla arborea japonica*, were collected from fields and kept for at least one week in a terrarium in the laboratory prior to the

Accepted September 8, 1989

Received May 8, 1989

¹ To whom all correspondence should be addressed.

experiments. The terrarium was maintained at 24°C under 12L-12D photoperiod. Frogs were fed periodically with crickets and allowed access to water *adlibitum*. Young adults weighing 1 ± 0.3 g were used. In these specimens no sexual difference was observed in water permeation between the period November through February during which time the present experiment was performed.

Water permeation of the skin was measured by recording water movement between two small chambers partitioned with an experimental skin. Both chambers were connected with a filter holder (Swinnex sx00 013 00, Millipore Corp.), on which excised skin was mounted in the position of a filter. The chamber facing the dermal side (the inside) of the skin was filled with an airated, modified Ringer solution (230 mOsM) [19] and attached with a graded pipette. The chamber facing the epidermal side was filled with distilled water (DW). Net water movement across the partitioned skin was measured by recording changes of the meniscus in the pipette. Dilute Ringer solution (20 mOsM) was substituted for the DW in the outside bath, but significant difference in water movement was not detected. Thus, DW was used in all experiments for the outside bath. The osmotic difference between the two chambers was maintained at approximately 230 mOsM throughout the experiments.

To dehydrate frogs, they were kept in a chamber in which relative humidity was maintained at 90%. The formation of water droplets in the chamber was carefully prevented. Frogs were neither fed nor allowed to access to water during this treatment. Dehydration treatment ended after approximately 40 hr when the animal lost 30% of its initial weight.

In the prolactin treatment, frogs were injected daily with ovine prolactin (Sigma, 0.25 IU (8.1 μ g)/gbw/day) in 2 ml of Ringer solution intraperitoneally for 7 days. During this treatment they were kept under the normal conditions and fed as per usual. As a control, another group of frogs were injected with egg albumin (Nakarai Chem. LTD) in the same protein concentration as prolactin.

Five animals were used in each experiment and the experiment was repeated three times. Since

the available filtrating area of the apparatus was 0.75 cm², direct reading of the pipette was calibrated as a net water movement in μ l/cm² and plotted in 10 min intervals for 100 min. In order to compare water permeability of the experiments, an average water flux (Jw) was calculated and expressed in μ l/cm²/min. Positive value in Jw shows water movement from the epidermal side to the dermal side and a negative value indicates the reverse.

RESULTS

Hyla arborea japonica exhibited a fundamental difference between water permeation of the dorsal and ventral sides of their isolated skin (Fig. 1). Under normal conditions, that is, immersing the dermal side of the excised skin in Ringer solution (230 mOsM) and the epidermal side in distilled water, water flowed inwardly across the ventral skin at a constant rate of 0.29 μ l per cm² per min, or $Jw = +0.29$. In the dorsal skin, however, water permeation took place at a lower rate of $Jw = -0.015$, which meant water movement from the inside to the outside. The movement was against the osmotic gradient.

When frogs were kept in the dehydration chamber (24°C, 90% relative humidity) for approximately 40 hr and had lost nearly 30% of their initial weight, the ventral skin enhanced water permeability (Fig. 1). The water flux was not constant throughout the experiment. It lessened over time, but the average rate over 100 min was as high as $Jw = +0.91$, four times greater than that in the control group. In dorsal skin, however, no such change in water permeability was observed during dehydration treatment.

When noradrenalin, one of the sympathomimetic agents, was added to the inside bath of the normal preparation, the water flux increased to $Jw = 1.52$ in ventral skin, five times the control rate (Fig. 2). Daily administration of prolactin for 7 days caused a significant decrease in water permeation across the ventral skin (Fig. 2). The water flux, $Jw = +0.08$, was only one-fourth the control value. Dehydration had a less pronounced effect in the frogs pre-treated with prolactin. The rate of water flux ($Jw = +0.51$) was less than 60% of that

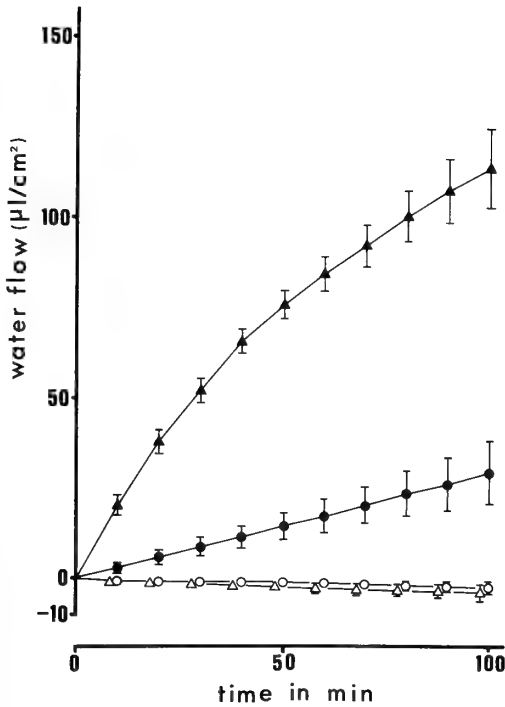


FIG. 1. Rates of the water permeation across the excised skin of the treefrog. Water flowed from mucousa to serosa at a rate of $29 \mu\text{l}/100 \text{ min}$ across the normal ventral skin (filled circle) and at a rate of $-1.5 \mu\text{l}/100 \text{ min}$ across the dorsal skin, which showed a net water movement from the inside to the outside (open circle). Dehydration of the frogs caused a marked increase in the water flow across the ventral skin, to a rate of $112 \mu\text{l}/100 \text{ min}$ (filled triangle), but dehydration had no effects on the dorsal skin (open triangle). The vertical bar shows the standard margin of error.

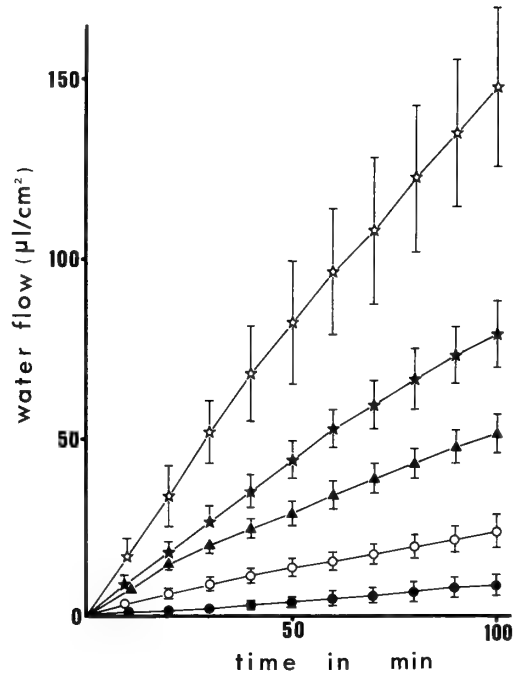


FIG. 2. Hormonal effects on water permeation across the excised ventral skin of the treefrog. The sympathomimetic agent noradrenalin (10^{-5} M) added to the inner experimental medium caused an enhancement on the water flow (open star). Daily administration of prolactin ($8.1 \mu\text{g}/\text{day}$) for a week decreased the water flow (filled circle). Prolactin pretreatment also suppressed the water flow which had previously been stimulated by dehydration (filled triangle) and by noradrenalin administration (filled star). Albumin administration serving as the control for prolactin-treated group, caused no effects on water flow (open circle). The vertical bar shows the standard margin of error.

of dehydrated normal frogs (Fig. 2). Stimulation of water flux by noradrenalin was also significantly depressed in the prolactin-treated frogs. The water flux ($J_w = +0.78$) was one-half of the normal skin treated with noradrenalin. When egg albumin at the same protein concentration as the prolactin was injected for the same term, no significant change was observed (Fig. 2).

An adrenergic beta-receptor agonist, isoproterenol (IP, 10^{-5} M), enhanced the water flux ($J_w = +1.6$) similarly to the noradrenalin treatment. Propranolol (PP, 10^{-5} M), an adrenergic beta-receptor antagonist, not only counteracted isoproterenol, but also depressed the water flux induced by the

dehydration significantly to $J_w = +0.61$, two-thirds the rate of dehydrated frogs (Fig. 3). However, propranolol did not affect the water flux in normal frogs at all. Isoproterenol administration to the normal preparation caused an instantaneous rise of the water flux to $J_w = +1.6$ (Fig. 3). However, replacement of this medium by one containing propranolol caused slow and gradual depression of the water flux, which finally reached the normal rate, $J_w = +0.35$, in 40 min (Fig. 3). Alpha-adrenergic agents such as phenylephrine (alpha-receptor agonist) or dibenamine (alpha-receptor

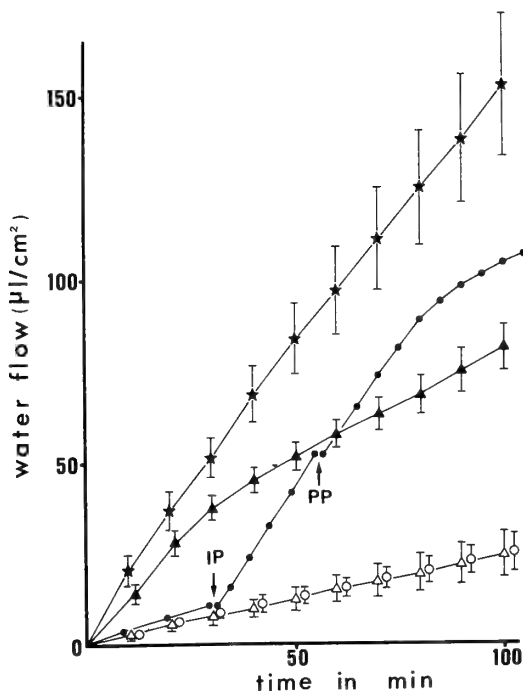


FIG. 3. Effects of adrenergic agents on water permeation across the ventral skin of the treefrog. When the adrenergic beta-receptor agonist isoproterenol (10^{-5} M) was added to the experimental medium, the water flux increased markedly (filled star), while the addition of the alpha-agonist phenylephrine (10^{-5} M) had no effect at all (open circle). An adrenergic beta-antagonist propranolol (PP, 10^{-5} M) counteracted the isoproterenol stimulation (IP). Propranolol suppressed the enhancement induced by dehydration (filled triangle). Propranolol, however, had no effect on normal skin (open triangle). The vertical bar indicates the standard margin of error.

antagonist) had no effect on the water flow across the skin of either dehydrated or normal frogs.

Stimulation of the water flux by isoproterenol was very strong. It persisted continuously for 60 min or more even after the agent had been washed out from the medium (Fig. 4). However, pretreatment of the skin with ouabain, a specific Na^+ , K^+ -ATPase inhibitor, obstructed the stimulating effect of isoproterenol completely. Ouabain, however, did not affect the basal water flux in the normal

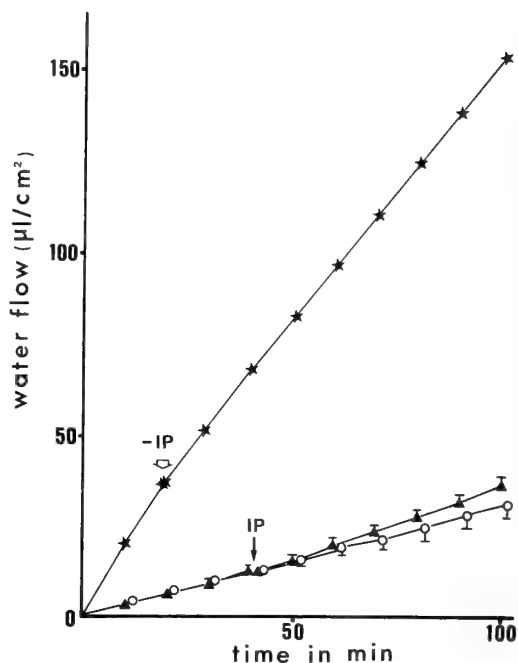


FIG. 4. Effect of ouabain on the isoproterenol-stimulated water flow across the ventral skin of the treefrog. Stimulation by isoproterenol for 20 min caused a prolonged increase in the water flow (filled star) even after the agent had been removed (-IP). However, pretreatment with ouabain (10^{-5} M) for 40 min completely counteracted the stimulatory effect of isoproterenol (filled triangle). Ouabain treatment, however, did not have any effect on normal skin (open circle).

DISCUSSION

It has previously been reported in American treefrogs that water flux in the ventral skin is 10 to 20 times greater than that of the dorsal skin [8]. The present study shows an even more remarkable dorso-ventral difference in water permeation across the skin of Japanese treefrogs. When excised skin was examined, water normally flowed inwardly in great quantities across the ventral skin, while it flowed outwardly in a small amount across the dorsal skin. When the treefrogs were kept in dehydrated conditions, water flux increased markedly in the ventral skin, but no significant change was observed in the dorsal skin. Similar increase in water flux can be induced by adrenergic beta-stimulation in various anurans [10-15].

When dehydrated treefrogs, which had lost 30% of their body weight, were allowed to take water, they recovered 90% of their previous weight within 10 min by absorbing the water across the ventral skin (unpublished data). This rapid water absorption across the ventral skin seems to be regulated by the adrenergic beta-receptor, since propranolol, a beta-receptor antagonist, depressed enhancement of the water flux caused by dehydration. In the present experiment, the propranolol depressed only the stimulated water flux across ventral skin, and did not affect normal water flux across either side of the skin. Thus, it is probable that there are two types of water pathways in the ventral side of the treefrog skin. The first pathway is mediated by beta-receptor stimulation that begins to function in cases of urgent water requirement, such as dehydration, and is ouabain sensitive. The second pathway is the basal one which functions under the normal condition and is not affected by beta-adrenoceptor stimulation. Similarly, two water transport systems have also been reported in toads [10, 14]. In one of these studies [14] alpha-receptors have been reported to inhibit water flux. However, no effects of alpha-agents on the water flow across the ventral skin of Japanese treefrogs were observed in this study.

De Sousa *et al.* reported that ouabain did not have any effect on the isoproterenol-stimulated water flow in toad skin [10]. In the present experiment, concomitant administration of ouabain and isoproterenol also failed to produce any clear suppressive effect. This may be due to the difference in modes of action of the two agents. As mentioned above, the stimulating effect of isoproterenol appears instantaneously and persists for a certain period even after it has been washed out, while ouabain takes 30 to 40 min to produce the suppressive effect. Therefore, it is likely that the Na^+ , K^+ -ATPase activity is necessary for the attainment of the beta-action.

Pretreatment with prolactin for one week reduced the water flux approximately 50% in the ventral skin. Suppression by prolactin occurred not only in the stimulated water flow but also with the basal flow in the normal frogs. This prolactin suppression seems to be caused by a mechanism different from that of the suppressive agents men-

tioned above. Prolactin is generally known to prevent osmotic water permeation in adult urodiles [5, 20], as well as in larval anurans [20] and fresh water fish [19]. This is primarily due to the mucous secretion on the integument under the hormonal stimulation. The mucous not only functions as the water-resistant coating of the skin, but may also produce certain osmotic effects itself by retaining electrolytes in the coating, resulting in a lesser osmotic gradient between inside and outside of the animal body [18]. Indeed, frogs have been reported to have increasing amount of prolactin receptor in the skin during the breeding season when they become aquatic [21]. Suppression of water flux by prolactin pretreatment in the present experiment also seems to be related to the mucous secretion, which has previously been observed histochemically in those frogs (not published). On the other hand, extirpation of pars distalis or removal of the whole pituitary in the toad *Bufo bufo* depressed water flux which had been stimulated by dehydration [22]. This, in a sense, conflicts with the present findings that administration of prolactin depressed the stimulated water flow. However, the hypophysectomy does not indicate disappearance of prolactin alone in the animals.

In summary, the following results are characteristic of this species: marked difference in dorsal and ventral water permeation, particularly, reverse-directional water movement in ventral and dorsal skin under normal conditions, and two water pathways in the ventral skin, including a regulatory system mediated by adrenergic beta-receptor and Na^+ , K^+ -ATPase, and a basal system indifferent to these mediators. Both pathways are regulated by prolactin.

REFERENCES

- 1 Deyrup, I. J. (1964) Water balance and kidney. In "Physiology of the Amphibia". Ed. by J. A. Moor, Academic Press, New York, pp. 251-328.
- 2 Shoemaker, V. H. and Nagy, K. A. (1977) Osmoregulation in amphibians and reptiles. *Ann. Rev. Physiol.*, **39**: 449-471.
- 3 Deullman, W. E. and Trueb, L. (1986) *Biology of Amphibians*. McGraw-Hill, New York, pp. 197-228.
- 4 Bentley, P. J. and Yorio, T. (1979) Do frogs drink?

- J. Exp. Biol., **79**: 41-46.
- 5 Lorenz, C. A. and Bern, H. A. (1982) Prolactin and osmoregulation in vertebrates. *Neuroendocrinology*, **35**: 292-304.
 - 6 Bentley, P. J. (1982) *Comparative Vertebrate Endocrinology*. 2nd. Ed., Cambridge Univ. Press, Cambridge, pp. 303-337.
 - 7 Hillyard, S. D. (1976) Variation in the effects of antidiuretic hormone on the isolated skin of the toad, *Scaphiopus couchi*. *J. Exp. Zool.*, **195**: 199-206.
 - 8 Yorio, T. and Bentley, P. J. (1977) Asymmetrical permeability of the integument of treefrogs (*Hylidae*). *J. Exp. Biol.*, **67**: 197-204.
 - 9 McClanahan, L. and Baldwin, R. (1969) Rate of water uptake through the integument of the desert toad, *Bufo punctatus*. *Comp. Biochem. Physiol.*, **28**: 381-389.
 - 10 De Sousa, R. C. and Grosso, A. (1982) Osmotic water flow across the abdominal skin of the toad *Bufo marinus*: effect of vasopressin and isoprenaline. *J. Physiol.*, **329**: 281-296.
 - 11 Yokota, S. D. and Hillman, S. S. (1984) Adrenergic control of the anuran cutaneous hydroosmotic response. *Gen. Comp. Endocrinol.*, **53**: 309-314.
 - 12 Brown, D., Grosso, A. and de Sousa, R. C. (1980) Isoproterenol-induced intramembrane particle aggregation and water flux in toad epidermis. *Biochem. Biophys. Acta*, **595**: 158-164.
 - 13 Hyllard, S. D. (1979) The effect of isoproterenol on the anuran water balance response. *Comp. Biochem. Physiol.*, **62C**: 93-95.
 - 14 Gamundi, S. S., Scheucher, A. and Coviello, A. (1986) Alpha-2 adrenergic agonists inhibit basal and stimulated osmotic water permeability in toad skin. *Comp. Biochem. Physiol.*, **84C**: 199-203.
 - 15 Elliot, A. B. (1968) Effect of adrenaline on water uptake in *Bufo*. *J. Physiol.*, **197**: 87-88.
 - 16 Wygoda, M. L. (1984) Low cutaneous evaporative water loss in arboreal frogs. *Physiol. Zool.*, **57**: 329-337.
 - 17 Withers, P. C., Hillman, S. S., Drewes, and Sokol, O. M. (1982) Nitrogen excretion in sharp-nosed reed frogs (*Hyperolius nasutus*: Anura, Hyperoliidae). *J. Exp. Biol.*, **97**: 335-343.
 - 18 Shephard, K. I. (1981) The influence of mucus on the diffusion of water across fish epidermis. *Physiol. Zool.*, **54**: 224-229.
 - 19 Johnsen, A. H. and Nielsen, R. (1984) Correlation between cAMP in isolated frog skin epithelium and stimulation of sodium transport and osmotic water flow by antidiuretic hormone and phosphodiesterase inhibitor. *Gen. Comp. Endocrinol.*, **54**: 144-153.
 - 20 Loudi, B., Biciotti, M. and Viotto, B. (1982) Cutaneous osmoregulation in *Triturus cristatus carnifex* (Laur.) (Urodela). *Gen. Comp. Endocrinol.*, **46**: 452-457.
 - 21 D'Istria, Fasano, S. and Delrio, G. (1987) Prolactin receptors in the male *Rana esculenta*. *Gen. Comp. Endocrinol.*, **68**: 6-11.
 - 22 Cristensen, C. U. and Jorgensen, C. B. (1972) Role of pars distalis and pars nervosa of the hypophysis in the water economy of the toad. *Gen. Comp. Endocrinol.*, **18**: 169-174.

Regulatory Actions of 5-Hydroxytryptamine and Some Neuropeptides on the Heart of the African Giant Snail, *Achatina fulica* Férussac

KATSUHIKO HORI¹, YASUO FURUKAWA² and MAKOTO KOBAYASHI³

*Physiological Laboratory, Faculty of Integrated Arts and Sciences,
Hiroshima University, Hiroshima 730, Japan*

ABSTRACT—Effects of putative neurotransmitters and modulators on the atrium preparation of the African giant snail, *Achatina fulica* were observed to investigate the regulatory mechanisms of these substances on the heart beat. Application of 5-hydroxytryptamine (5-HT) as well as stimulation of a heart excitatory neuron, PON, resulted in the enhancement of the heart beat. The enhancement of the beat was blocked by a 5-HT blocker, methysergide. A neuropeptide FMRFamide potentiated the excitatory responses of the atrium to both PON stimulation and 5-HT application, whereas small cardioactive peptide B (SCP_B) depressed them.

A burst of impulses in the cerebral neuron, d-RCDN or d-LCDN, evoked excitatory response in the heart excitatory neurons, TAN, TAN-2 and TAN-3, as well as in PON. It depolarized the membrane and increased the frequency and duration of spikes in three TANs. Similar responses were elicited by 5-HT application. On the contrary, FMRFamide hyperpolarized the membrane and shortened the spike duration in three TANs and PON. The experiment of current measurement showed that 5-HT and FMRFamide act antagonistically in the heart excitatory neurons.

INTRODUCTION

It has been known that several neurotransmitters, such as acetylcholine (ACh) and 5-hydroxytryptamine (5-HT), are involved in the control of the molluscan heart beat, and that some invertebrate neuropeptides show powerful modulatory actions in the synaptic transmission [1, 2]. The modes of action of the transmitters as well as the modulators are not uniform in general but quite variable depending on species and organs [3–5].

In the African giant snail, *Achatina fulica*, several heart regulatory neurons have been identified in the central nervous system [6, 7]. Among them,

two cerebral ganglion cells, the dorsal right cerebral distinct neuron (d-RCDN) and the dorsal left cerebral distinct neuron (d-LCDN), produce a slow depolarization and prolong the duration of action potential in the periodically oscillating neuron (PON), which is the most effective heart excitor. The transmitter of the two cerebral neurons is suggested to be 5-HT [8]. The direct action of 5-HT on the heart has also been examined by using the isolated ventricle and dual effects, enhancing and arresting, on the beat have been demonstrated [9]. However, in *Achatina* heart, responses to putative neurotransmitters and modulators are not always similar between the ventricle and atrium [10].

In the present study, to demonstrate the regulatory mechanisms on the heart beat, the effects of application of several putative neurotransmitters including neuropeptides and stimulation of heart excitatory neurons on the isolated atrium preparation were observed. In addition, the mode of action of the cerebral neurons (d-RCDN and d-LCDN) on the heart excitors were also investigated.

Accepted September 11, 1989

Received August 11, 1989

¹ Present address: Biological Science Research Institute, Mitsui-Seiyaku, Mobara 297, Japan.

² Present address: Center for Neurobiology and Behavior, Columbia University, 722 West 168th Street, New York, NY 10032, U.S.A.

³ To whom all correspondence should be addressed.

MATERIALS AND METHODS

The African giant snail, *Achatina fulica* Férusac, which was captured in Okinawa, transported by air to Hiroshima and bred in our laboratory at 24°C, was used. Circumoesophageal ganglia and heart connected with the intestinal nerve were dissected from the animal. The connective capsule and the inner sheath covering the dorsal surface of the cerebral ganglia and the right parietal ganglion were completely removed by dissection. Most of the ventricle was cut off leaving the atrium intact. The preparation was pinned to the bottom of an experimental chamber coated with silicone resin. The chamber consisted of two compartments (ganglia compartment and heart compartment) which could be perfused separately [6].

The composition of normal physiological solution was as follows (mM/l): NaCl, 61.0; KCl, 3.3; CaCl₂, 10.7; MgCl₂, 13.0; glucose, 5.0; and Hepes, 10.0 (pH adjusted to 7.5 by titration with NaOH). High magnesium solution was prepared by merely adding extra MgCl₂ to normal saline.

For the application of 5-HT to the preparation a definite volume of the drug was introduced into the solution in the chamber through a small pipette, which was rapidly spread throughout the solution by means of air bubbles released from the bottom of the chamber. The concentration of the drug was stated as final concentration in the solution. Duration of 5-HT application was usually less than 2 min, except for cases stated otherwise, during which perfusion of the solution was stopped, and interval of at least 20 min was allowed between the two applications. The application of 5-HT antagonist, methysergide, and several neuropeptides for a longer period was made by perfusing the solution containing the chemical at a given concentration.

The following drugs were used: 5-hydroxytryptamine creatinine sulfate (5-HT, Sigma), methysergide-hydrogenmaleinate (methysergide, Sandoz), 3-hydroxytyramine hydrochloride (dopamine, Katayama), DL-octopamine hydrochloride (octopamine, Nakarai), FMRFamide, YGGFMRFamide, pQDPFLRFamide, small cardioactive peptide A (SCP_A) and SCP_B (Peninsula Laboratories Inc.), and FLRFamide (Cambridge Research Biochemicals).

Intracellular recording and stimulation of neurons were carried out using glass microelectrodes filled with 3 M potassium acetate, having a resistance of 5–10 MΩ. Heart beat was recorded by a strain gauge. In a few experiments, the intestinal nerve was cut off from the ganglia and it was stimulated by an Ag-AgCl bipolar electrode at the point just before entering the pericardium.

When interconnections between two neurons or effects of chemicals on neurons were investigated, only the preparation of circumoesophageal ganglia was used. Membrane current was measured using a voltage-clamping method by two microelectrodes as described previously [8].

The data were stored in an FM tape recorder (Sony, DFR3515) for later analysis and redisplayed on an ink-writing pen-recorder (Nihon Kohden, RJG 4024).

All the experiments were carried out at room temperature of 23–25°C.

RESULTS

Effects of 5-HT application and nerve stimulation on heart beat

Isolated atrium usually repeats regular beating in the experimental chamber. When 5-HT at concentrations above 10⁻⁸ M was applied to the atrium, the frequency and amplitude of heart beat were enhanced. Stimulation of the intestinal nerve produced potentiation of heart beat similar to that obtained by 5-HT application (Fig. 1). The potentiation by nerve stimulation was abolished when the preparation was perfused with high magnesium (3×Mg²⁺) solution which may block the neuromuscular synapses. The enhancement of heart beat by 5-HT application, however, was not blocked in 3×Mg²⁺ solution, suggesting that 5-HT acts postsynaptically. Dopamine exhibited effects similar to 5-HT on the atrium, but the threshold concentration was 10⁻⁶ M. Octopamine showed no significant effects at concentrations up to 10⁻⁵ M.

The action of heart excitatory neurons

A neuron in the right parietal ganglion, PON, has been shown to be the most potent heart excitor

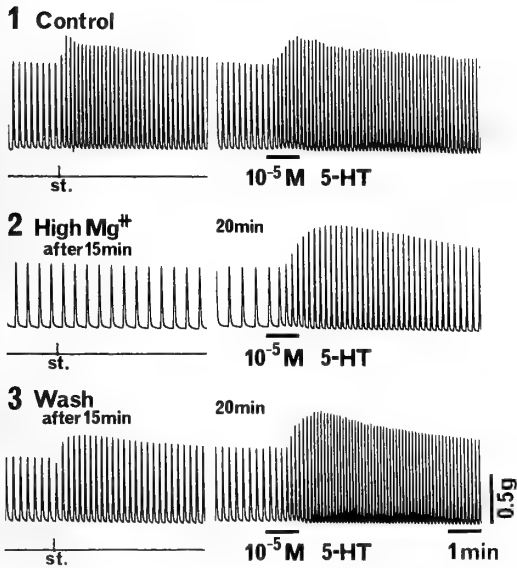


FIG. 1. Effects of high- Mg^{2+} in solution on the excitatory responses of the atrium to nerve stimulation (st.) and 5-HT application. The intestinal nerve was stimulated with electrical pulses of 3 V, 1 msec at 5 Hz for 1 sec. 5-HT was applied during the period shown by the horizontal line under each record.

extending axons directly to the heart [6]. In the experiments illustrated in Figure 2, the effects of methysergide, a potent blocker of 5-HT receptor in the gastropod heart muscles, on the action of PON stimulation and 5-HT application were examined. The intracellular stimulation of PON evoked impulses in PON, which, in turn, enhanced the frequency and amplitude of heart beat. This enhancement of the beat was almost completely blocked by perfusing the atrium preparation with methysergide (Fig. 2A). Similarly, the potentiation of heart beat by 5-HT application was blocked by methysergide, although methysergide showed no significant direct effects on the beat (Fig. 2B). These results suggest that the potentiation of heart beat by PON stimulation may be mediated by 5-HT.

To obtain a better understanding on the mode of action of PON, modulatory effects of several neuropeptides on the heart excitatory action of this neuron as well as direct effects of those substances on the heart beat were examined. Of six neuropeptides (FMRFamide, FLRFamide, YGGFMRFamide, pQDPFLRFamide, SCP_A and

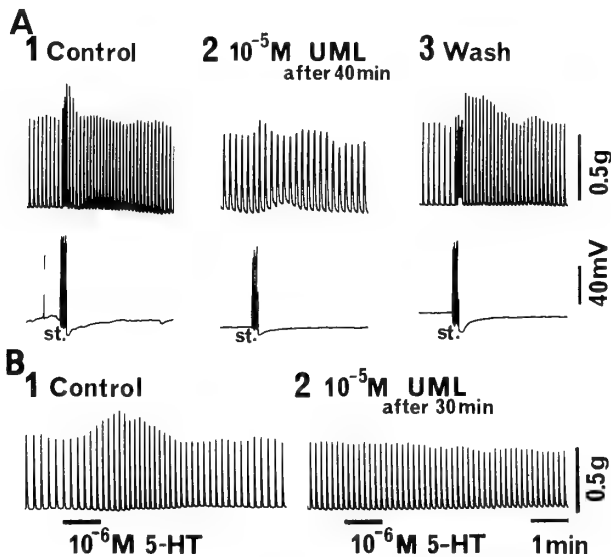


FIG. 2. Effects of a 5-HT blocker, methysergide (UML), on responses of the atrium to PON-stimulation (A) and 5-HT application (B). A and B are records from different preparations. In A, the heart beat (upper tracings) induced by the spikes of PON (lower tracings) are recorded simultaneously. PON was made to fire by current injection (st.) at 5 Hz for 10 sec. In B, 5-HT was applied during the period shown by the horizontal line under each record.

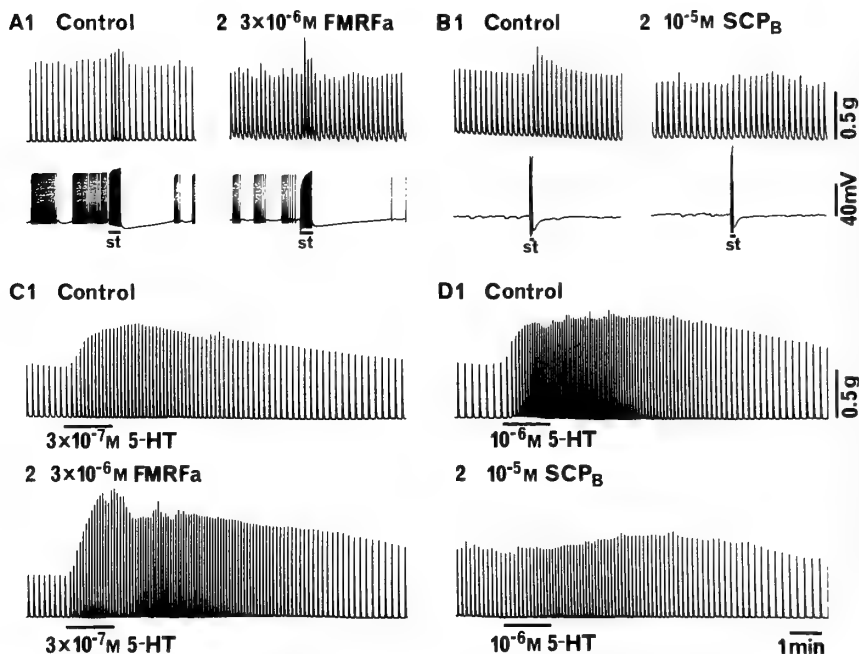


FIG. 3. Effects of neuropeptides on the enhancement of heart beat induced by the spikes of PON (A and B) and 5-HT application (C and D). A, B, C and D are records from different preparations. In A and B, PON was stimulated (st) at 5 Hz for 20 sec and 10 sec, respectively. A₂ was recorded 20 min after application of FMRFamide (FMRFa), and B₂ was 30 min after application of SCP_B. In C and D, 5-HT was applied during the period shown by the horizontal line under each record. C₂ and D₂ were recorded 20 min after application of FMRFa and SCP_B, respectively.

SCP_B) tested, FMRFamide and FLRFamide showed slight enhancing effects on the heart beat with the threshold concentration at $10^{-6} \sim 3 \times 10^{-6}$ M. SCP_B had no effects on the most preparations but exhibited potentiation in a few. YGGFMRFamide, pQDPFLRFamide and SCP_A showed neither direct effects on the heart beat nor modulatory effects on the action of PON. Thus, the modulatory effects of FMRFamide and SCP_B on the heart excitatory action of PON were further investigated. The preparation used in the experiment with the results being illustrated in Figure 3 showed no significant direct responses to FMRFamide at 3×10^{-6} M nor to SCP_B at 10^{-5} M. However, when the atrium preparation was perfused with FMRFamide for more than 20 min, the excitatory action of PON was enhanced and the response to 5-HT was also potentiated (Fig. 3A, C). On the contrary, perfusion with SCP_B resulted in depression of the excitatory responses to both PON stimulation and 5-HT application (Fig. 3B,

D). The effects of FMRFamide and SCP_B were reversible (not shown).

The mode of action of the other heart excitors named tonically autoactive neurons, TAN, TAN-2 and TAN-3 [6, 11] was also examined. However, the heart excitatory action of these neurons was not modulated by perfusing the atrium preparation with any of the foregoing six kinds of neuropeptides.

The action of d-RCDN and d-LCDN on heart excitors

When the cerebral neuron, d-RCDN or d-LCDN, was stimulated intracellularly to evoke a burst of impulses, excitatory responses were produced in TAN, TAN-2 and TAN-3. These three TANs behaved similarly with no different properties. Figure 4A shows an example in the case between d-RCDN and TAN-2. By the stimulation of d-RCDN at 10 Hz, TAN-2 which had previously been hyperpolarized to stop firing was depolarized

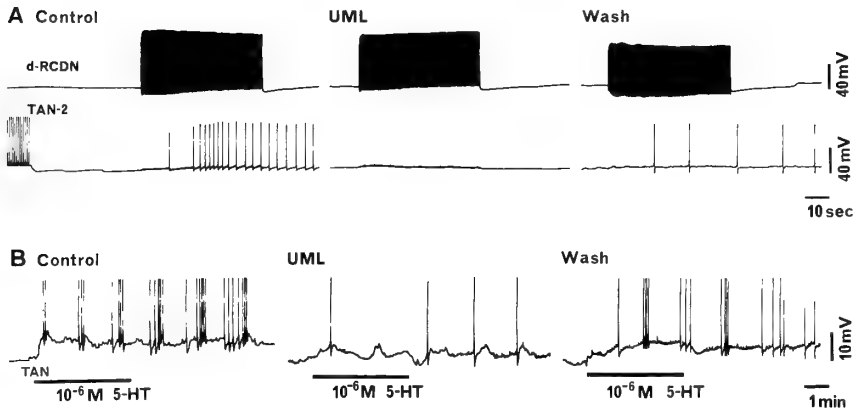


FIG. 4. Blocking action of methysergide (UML) on the depolarizing responses of TAN induced by a burst of impulses in d-RCDN (A) and 5-HT application (B). A. TAN-2 was hyperpolarized by 10 mV. d-RCDN was stimulated at 10 Hz for 50 sec. Middle record (UML) was obtained 60 min after application of methysergide. B. TAN was hyperpolarized by 30 mV. The top of action potentials was cut off. 5-HT was applied during the period shown by the horizontal line under each record. Middle record (UML) was obtained 30 min after application of methysergide.

and began to fire. These excitatory responses were found to be depressed reversibly by 5-HT antagonist, methysergide. Similarly, as shown in Figure 4B, application of 5-HT produced spikes superimposed on a slow depolarization in TAN, which were also depressed by methysergide. These results are essentially the same as those obtained in PON [8], suggesting that the neurotransmitter of

the two cerebral neurons is 5-HT.

In the experiments shown in Figure 5, the effects of a burst of impulses in the cerebral neuron or the application of putative neurotransmitters on the activities of three TANs were examined. A burst of impulses in d-LCDN increased the spike frequency in TAN-2 and produced a broadening of the spikes (Fig. 5A). The application of 5-HT also

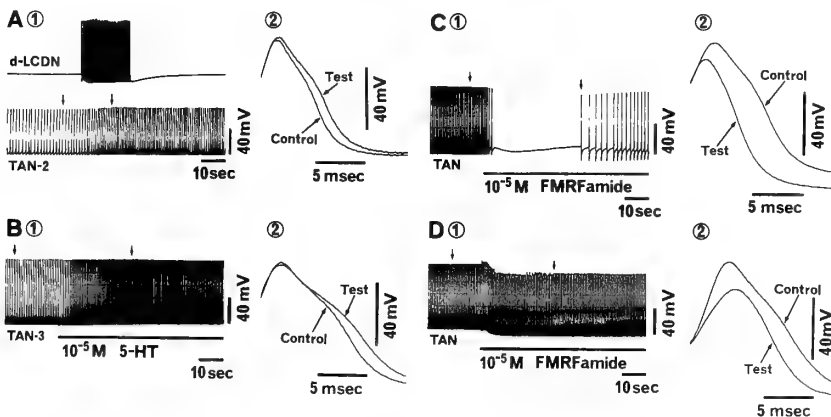


FIG. 5. Change in spike duration of TAN produced by a burst of impulses in d-LCDN (A), application of 5-HT (B) and FMRFamide (C and D). In A~C, spontaneous activities of TAN-2 (A), TAN-3 (B) and TAN (C) were recorded. In D, TAN was driven to fire by a depolarizing current injection at 2 Hz. In A, d-LCDN was stimulated at 10 Hz for 20 sec. In B~D, 5-HT (B) or FMRFamide (C and D) was applied during the period shown by the horizontal line under each record. Arrows in A₁, B₁, C₁ and D₁ indicate selected spikes which are displayed at expanded time scale in A₂, B₂, C₂ and D₂.

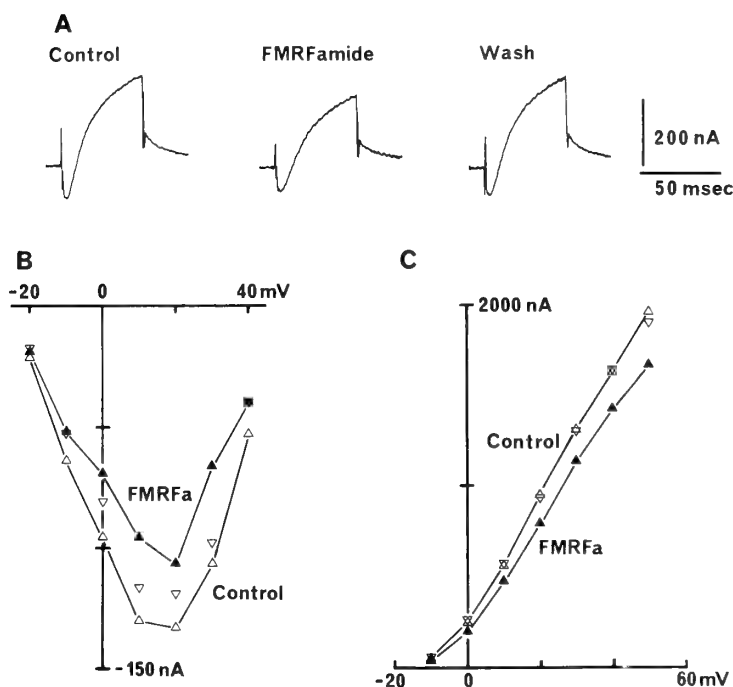


FIG. 6. Effects of FMRFamide on the membrane currents of TAN. A. Membrane currents with and without 1.25×10^{-5} M FMRFamide. Holding potential was -40 mV. The command pulse was 50 msec in duration and depolarized to 0 mV. B. I-V relationships of peak inward currents with (closed triangles) and without (open triangles) FMRFamide (FMRFa). Open upright (\triangle) and upside-down (∇) triangles denote values before application of FMRFamide (Control) and after wash (Wash), respectively. C. I-V relationships of outward currents measured at the end of the pulse with and without FMRFamide. Symbols mean the same with B.

elicited similar responses (Fig. 5B). On the contrary, by the application of FMRFamide to TAN a tentative cessation of spontaneous firings and remarkable shortening of recovered spikes were demonstrated (Fig. 5C). Even when TAN was driven to fire by current injection at 2 Hz, FMRFamide produced a slight hyperpolarization and shortened the spike duration (Fig. 5D). These inhibitory actions of FMRFamide were also demonstrated in PON, results of which were reported in part previously [5]. Further, FMRFamide-related peptides such as FLRFamide and pQDPFLRFamide were found to cause similar responses in TANs.

Finally, the effects of FMRFamide on the membrane currents were examined in TAN, which was axotomized to get better conditions for space-clamp. Holding potential was set at -40 mV. The membrane currents measured using depolarizing

command pulses consisted of a transient inward current and slowly developing outward current (Fig. 6A). Application of FMRFamide remarkably reduced both the peak inward current and delayed outward current. In Figures 6B and C, I-V relationships with and without FMRFamide are illustrated. These results are in contrast to those obtained by applying 5-HT to PON [8].

It is concluded that 5-HT and FMRFamide act antagonistically in the heart excitatory neurons, PON and TANs.

DISCUSSION

The present study demonstrated that application of 5-HT produced potentiation of the beat in the atrium preparation like stimulation of a heart excitatory neuron, PON. The potentiation of heart beat by both 5-HT application and PON

stimulation was blocked by a 5-HT blocker, methysergide, suggesting that potentiation by PON stimulation may be mediated by 5-HT.

A neuropeptide FMRFamide usually showed direct enhancing effects slightly on the beat of *Achatina* atrium. However, since the threshold was quite high and the effects were variable depending on preparations, it may be difficult to consider this peptide acts physiologically directly to *Achatina* atrium. On the other hand, the modulatory action of FMRFamide on the effects of PON stimulation or 5-HT application was effective at relatively low concentrations with little variability. FMRFamide is known to show powerful modulatory effects on the synaptic transmission in molluscs [12, 13]. In the cerebral and suboesophageal ganglia of *Achatina* there have been shown a number of FMRFamide immunoreactive neurons [14]. By using an immunohistochemical method, we have also observed FMRFamide-containing nerve terminals in the atrium as well as FMRFaminergic neurons in the ganglia (unpublished data). Thus, the excitatory modulation by FMRFamide (or FMRFamide-related peptide) at the synapse from PON to the heart seems to be probable physiologically.

In the present experiment, the activity of two cerebral neurons, d-RCDN and d-LCDN, produced excitatory responses in three TANs, which were depressed by a 5-HT blocker like those to 5-HT application. Moreover, both the activity of the cerebral neurons and 5-HT application produced the spike broadening in TANs. These results are consistent with our previous results [8] that d-RCDN and d-LCDN may be serotonergic neurons. However, the results conflict with those by Croll [15], who showed using histochemical methods that these cerebral neurons do not contain significant amounts of 5-HT. One possible explanation for this disagreement would be, as Croll has suggested (personal communication), that d-RCDN and d-LCDN may exert their effects upon PON and TANs via a polysynaptic pathway with the last cell in the chain being serotonergic. However, we have considered that the pathway could be monosynaptic from our results of physiological experiments [7]. The second possibility would be that the specificity of methysergide to the

receptor of *Achatina* neurons might not be so strict and it may block the receptor of the other transmitters rather than serotonin. The third possibility would be that the cell bodies of d-RCDN and d-LCDN do not contain or less synthesize 5-HT, which may be synthesized during axonal transport and will be released from the axonal terminals. This seems likely to us but it remains to be examined further.

5-HT and FMRFamide showed antagonistic actions to the heart excitatory neurons, PON and three TANs. 5-HT depolarized the membrane of PON, closed 5-HT-sensitive K channels, increased the voltage-dependent Ca^{2+} current and produced spike broadening [8, 16]. The present experiment showed that spike broadening by 5-HT also occurred in TANs. Contrary to these, FMRFamide hyperpolarized TAN membrane, produced spike shortening and decreased inward current possibly by increasing background K^{+} current. These antagonistic actions between 5-HT and FMRFamide are similar to those found in *Aplysia* sensory neurons [17–20].

It is well known that actions of FMRFamide are variable on the same organ in different species as well as on different organs in one species [5, 12]. Thus, it may not be surprising that in *Achatina* FMRFamide inhibited the action of heart excitatory neurons in the ganglia and enhanced the effect of excitatory substances released from the neurons at the peripheries. It is postulated that FMRFamide causes spike shortening in PON and TANs, possibly resulting in the decrease of the transmitter release, and promotes the efficacy of the substance to the heart, i.e. FMRFamide may contribute to the efficient use of the transmitter.

ACKNOWLEDGMENTS

The authors are very grateful to Dr. Yojiro Muneoka for his helpful suggestions and discussion. The authors also thank Sandoz Ltd. for a sample of methysergide. This research was supported in part by Grant-in-Aid (No. 63540575) from the Ministry of Education, Science and Culture, Japan.

REFERENCES

- 1 Leake, L. D. and Walker, R. J. (1980) "Inverte-

- brate Neuropharmacology". Blackie & Son Ltd., Glasgow, p. 358.
- 2 Jones, H. D. (1983) The circulatory systems of gastropods and bivalves. In "The Mollusca". Vol. 5, Physiology, Part 2. Ed. by A. S. M. Saleuddin and K. M. Wilbur, Academic Press, New York, pp. 189–238.
- 3 Painter, S. D. and Greenberg, M. J. (1982) A survey of the responses of bivalve hearts to the molluscan neuropeptide FMRFamide and to 5-hydroxytryptamine. *Biol. Bull.*, **162**: 311–332.
- 4 Walker, R. J. (1986) Transmitters and modulators. In "The Mollusca". Vol. 9, Neurobiology and Behavior, Part 2. Ed. by A. O. D. Willows, Academic Press, New York, pp. 279–485.
- 5 Kobayashi, M. and Muneoka, Y. (1989) Functions, receptors, and mechanisms of the FMRFamide-related peptides. *Biol. Bull.*, **177**: 206–209.
- 6 Furukawa, Y. and Kobayashi, M. (1987) Neural control of heart beat in the African giant snail, *Achatina fulica* Férussac. I. Identification of the heart regulatory neurones. *J. exp. Biol.*, **129**: 279–293.
- 7 Furukawa, Y. and Kobayashi, M. (1987) Neural control of heart beat in the African giant snail, *Achatina fulica* Férussac. II. Interconnections among the heart regulatory neurones. *J. exp. Biol.*, **129**: 295–307.
- 8 Furukawa, Y. and Kobayashi, M. (1988) Modulation of ionic currents by synaptic action and 5-HT application in the identified heart excitatory neurone of the African giant snail, *Achatina fulica* Férussac. *J. exp. Biol.*, **137**: 319–339.
- 9 Akagawa, M., Furukawa, Y. and Kobayashi, M. (1988) Dual effects of 5-hydroxytryptamine on the heart of a pulmonate, *Achatina fulica* Férussac. *Comp. Biochem. Physiol.*, **89C**: 327–331.
- 10 Hori, K., Akagawa, M., Furukawa, Y. and Kobayashi, M. (1987) Actions of putative neurotransmitters on the heart beat of a mollusc, *Achatina fulica* Férussac. *Dobutsu seiri*, **4**: 148.
- 11 Matsuoka, T., Goto, T., Watanabe, K. and Takeuchi, H. (1986) Presence of TAN (tonically autoactive neuron) and its two analogous neurons, located in the right parietal ganglion of the suboesophageal ganglia of an African giant snail (*Achatina fulica* Férussac). Morphological and electrophysiological studies. *Comp. Biochem. Physiol.*, **83C**: 345–351.
- 12 Greenberg, M. J., Payza, K., Nachman, R. J., Holman, G. M. and Price, D. A. (1988) Relationships between the FMRFamide-related peptides and other peptide families. *Peptides*, **9** (Suppl. 1): 125–135.
- 13 Bulloch, A. G. M., Price, D. A., Murphy, A. D., Lee, T. D. and Bowes, H. N. (1988) FMRFamide peptides in *Helisoma*: Identification and physiological actions at a peripheral synapse. *J. Neurosci.*, **8**: 3459–3469.
- 14 Takayanagi, H. and Takeda, N. (1987) FMRFamide immunoreactive neurons in the central nervous system of the snail, *Achatina fulica*. *Comp. Biochem. Physiol.*, **88A**: 263–268.
- 15 Croll, R. P. (1988) Distribution of monoamines within the central nervous system of the juvenile pulmonate snail, *Achatina fulica*. *Brain Res.*, **460**: 29–49.
- 16 Furukawa, Y. and Kobayashi, M. (1988) Two serotonin-sensitive potassium channels in the identified heart excitatory neurone of the African giant snail, *Achatina fulica* Férussac. *Experientia*, **44**: 738–740.
- 17 Siegelbaum, S. A., Belardetti, F., Camardo, J. S. and Shuster, M. J. (1986) Modulation of the serotonin-sensitive potassium channel in *Aplysia* sensory neurone cell body and growth cone. *J. exp. Biol.*, **124**: 287–306.
- 18 Siegelbaum, S. A., Camardo, J. S. and Kandel, E. R. (1982) Serotonin and cyclic AMP close single K^+ channels in *Aplysia* sensory neurones. *Nature*, **299**: 413–417.
- 19 Belardetti, F., Kandel, E. R. and Siegelbaum, S. A. (1987) Neuronal inhibition by the peptide FMRFamide involves opening of $S K^+$ channels. *Nature*, **325**: 153–156.
- 20 Brezina, V., Eckert, R. and Erxleben, C. (1987) Modulation of potassium conductances by an endogenous neuropeptide in neurones of *Aplysia californica*. *J. Physiol., Lond.*, **382**: 267–290.

Evidence for the Phagocytotic Removal of Photoreceptive Membrane by Pigment Cells in the Eye of the Planarian, *Dugesia japonica*

NOBUAKI TAMAMAKI^{1,2}

Department of Anatomy, Fukui Medical School, Matsuoka, Fukui 910-11 Japan

ABSTRACT—Fine structural changes induced by daily cycles and dark adaptation were investigated in the eye of *Dugesia japonica*. During the daily cycle, an irregular arrangement of microvilli and an accumulation of vesicles in the microvillar area were often observed in animals fixed before dawn. The changes before dawn were enhanced as the period of dark adaptation was prolonged. Pigment cells, which surround the microvillar area, are shown to serve much the same function as the vertebrate pigment epithelium. The pigment cells phagocytose the accumulated vesicles and ingested debris is degraded further into granules and membrane whorls. Internalization by the pigment cells is regarded as one of the mechanisms for the photoreceptive membrane removal in the planarian, *Dugesia japonica*.

INTRODUCTION

The eye of the planarian *Dugesia* is composed of a pigment cup formed by pigment granule-containing cells (pigment cells) and photoreceptor cells whose apical microvilli-bearing processes are enclosed in the pigment cup [1–3]. The fine structure of other planarian eyes has also been well described [4–7]. According to the results of the following studies [4, 8–10], the eye structures are thought not to be stationary, but to change constantly during the normal daily cycle and in conditions of abnormal light- or dark-adaptation. The structural changes may be due to the turnover of the photoreceptive membrane, i.e. addition and removal, as reviewed by Schwemer [11].

Concerning the mechanism of the removal of the photoreceptive membrane, it is well known that the rhabdomic membrane in the compound eye of many arthropods is internalized by photoreceptor cells via the formation of coated vesicles [12–15]. Also in the planarian *Dalyellia*, Bedini *et al.*

[10] postulated an internalization of receptive membrane into the photoreceptor cells, in addition to the drastic changes in the eye structure in daily cycles.

On the other hand, Carpenter *et al.* [3] discussed the possibility that cytoplasmic extensions of the pigment cells, which cover the pupillary opening of the pigment cup, may phagocytose photoreceptive membrane in the eye of the planarian *Dugesia dorotocephala*. Glial cells such as pigment epithelium are known to serve as a removal system in vertebrate eyes [16–18]. Removal of the photoreceptive membrane by surrounding glial cells has also been reported in annelid eyes [19] and in arthropod eyes [20, 21], but generally such the removal is unusual in invertebrate eyes. Therefore, it is interesting to investigate how the pigment cells in the *Dugesia* eye may participate in the membrane turnover system.

I report in this paper that the pigment cells phagocytose remnants of shed photoreceptive membrane in the eye of the *Dugesia japonica*.

MATERIALS AND METHODS

Specimens of *Dugesia japonica* were collected at Takeda river in the vicinity of Fukui in May and June. The animals live on the underside of rocks which are half buried in the sand. Since it was

Accepted July 5, 1989

Received March 6, 1989

¹ Present address: Department of Neurobiology and Behavior, State University of New York at Stony Brook, Stony Brook, New York 11794, U.S.A.

² Reprint requests should be addressed to the address in Japan.

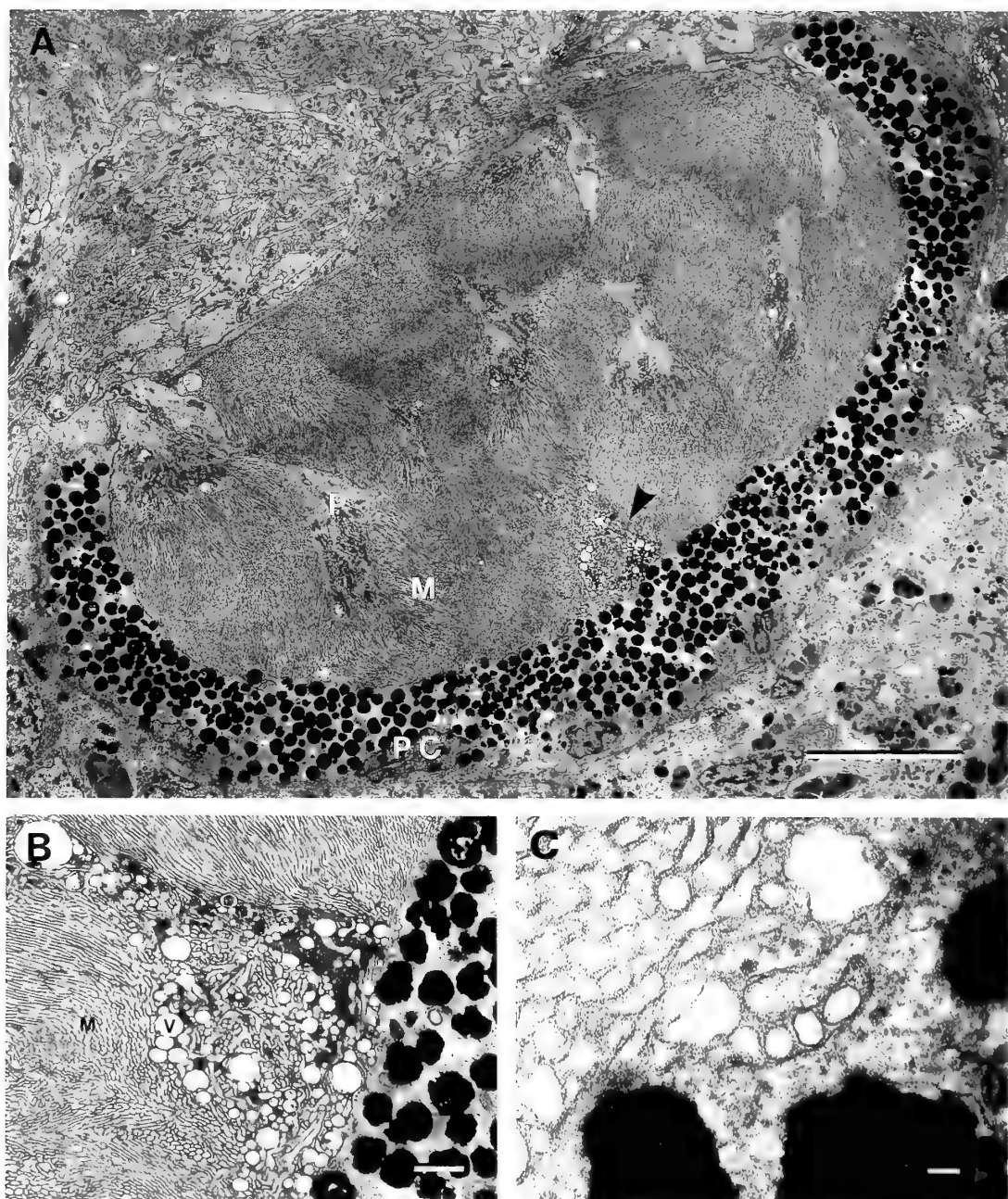


FIG. 1. A: Section through an eye of an animal fixed at 4:00 showing the pigmented eye cup surrounding the microvillar area. (M) microvilli; (PC) pigment cells; (P) microvilli-bearing process of receptor cell. Arrow head indicates the accumulation of vesicles between rhabdomeres and pigment cells. Bar = $10\ \mu\text{m}$. B: Accumulation of vesicles between rhabdomeres fixed at 4:00. The tips of some microvilli were swollen. (M) microvilli; (V) vesicles; Bar = $1\ \mu\text{m}$. C: Higher magnification electron micrograph of the boundary between the microvillar area and the pigment cells fixed at 4:00. The pigment cells seemed to phagocytose the vesicles. Bar = $0.1\ \mu\text{m}$.

impossible to perform an accurate measurement of luminous intensity at the places where the animals live, the animals were not maintained in the laboratory but collected at each time they were required for use. Morphological changes depending on daily cycles were investigated in groups of 5 animals, collected under a dim red light and fixed immediately, at 0:00, 4:00, 8:00, 12:00, 16:00 and 20:00 hr. Further groups of five animals collected at 20:00 were dark-adapted for 1 day, 2 days, 4 days, 6 days, 8 days, and 10 days at the same temperature as that of river water, and fixed. All the animals were fixed in 2.5% glutaraldehyde and 0.1 M phosphate buffer (pH 7.4) for 2 hr at 4°C. After trimming the specimens, tissue blocks containing the eyes were postfixed in 1% OsO₄ and 0.1 M phosphate buffer (pH 7.4) for 2 hr at 4°C. The tissue blocks were dehydrated with alcohol series and embedded in Epon 812. Silver thin sections were contrasted with uranyl acetate and lead citrate, and observed with an electron microscope (Hitachi H600).

RESULTS

Morphological changes in the normal daily cycle

The morphology of *Dugesia* eyes has already been described well by MacRae [1], Kishida [2] and Carpenter *et al.* [3]. The eye of *Dugesia japonica* is composed of rhabdomeric photoreceptor cells and pigment cells (Fig. 1A). The pigment cells form a pigmented eye cup surrounding photoreceptive parts of the photoreceptor cells (microvillar area). Microvilli of the photoreceptor cells present an orderly appearance. The microvilli belonging to one cell form a rhabdomere. In the section shown in Figure 1A about 14 rhabdomeres were observed. The microvilli-bearing process contains much smooth endoplasmic reticulum and many mitochondria. Multivesicular bodies smaller than 1 μ m in diameter were sometimes observed in the stalk region [3] of the photoreceptor cells. The pigment cup is formed by a single layer of pigment cells. Inner concave surface of the pigment cup possesses few microvilli and is rather flat. Most of spaces in the pigment cell are occupied by membrane bound pigment granules and nucleus.

TABLE 1. Eye volume changes induced by dark adaptation. Area occupied by pigment cells and microvillar area, and their ratios to the total area (pigment cells+microvillar area) were measured on photographs of sections which appropriately contain the optical axis of eyes fixed at 16:00 and eyes dark adapted for 10 days. Volume changes were estimated from these values

	Eyes at 16:00				
	Total (μ m ²)	Microvillar area (μ m ²)	(/total)	Pigment cells (μ m ²)	(/total)
1	3,430	2,270	66.2%	1,160	33.8%
2	3,230	2,180	67.3%	1,060	32.7%
3	2,550	1,590	62.4%	726	37.6%
4	2,740	1,780	64.9%	961	35.1%
Mean	2,990	1,950	65.4%	1,030	34.6%
	Eyes of 10 days dark adaptation				
	Total (μ m ²)	Microvillar area (μ m ²)	(/total)	Pigment cells (μ m ²)	(/total)
1	2,310	989	42.8%	1,320	57.2%
2	1,700	839	49.3%	862	50.7%
3	2,460	1,390	56.4%	1,070	43.6%
4	2,110	1,075	50.9%	1,035	49.1%
Mean	2,150	1,070	50.0%	1,070	50.0%

Investigation of eye structures fixed at 4 hr intervals revealed that some structural changes occur in daily cycles. The rhabdomeric microvilli commonly present an orderly appearance. However, in the eye fixed at 4:00 the microvilli were often irregularly arranged, especially in the area facing the inner concave surface of the pigment cup (Fig. 1A, B). In addition, the tips of some microvilli were swollen (Fig. 1B). Accumulations of vesicles were sometimes observed in extracellular spaces, i.e. between rhabdomeres, in the eyes fixed at 4:00

(arrow head in Fig. 1A, B). The inner concave surface of nearby pigment cells possessed some cytoplasmic extensions extending into the accumulation of vesicles, and the pigment cells seemed to phagocytose the vesicles (Fig. 1C). These structural changes were sometimes observed in the eyes fixed at times other than 4:00, but on a smaller scale.

Morphological changes in dark-adapted condition

After 10 days of dark adaptation, the diameters

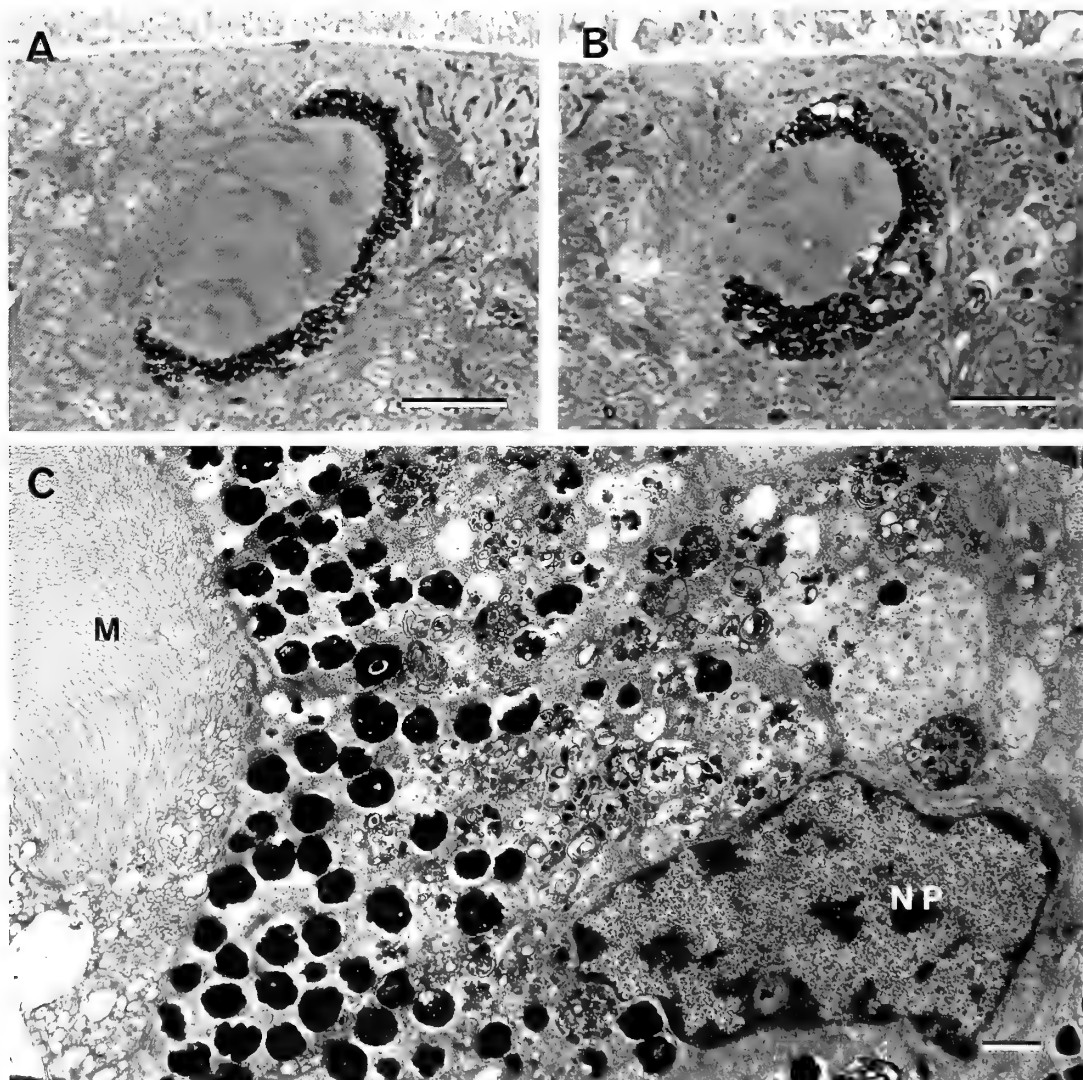


FIG. 2. A: Cross-section showing an eye of an animal fixed at 4:00. Bar=50 µm B: Cross-section showing an eye after 10 days' dark adaptation. Bar=50 µm C: Electron micrograph of pigment cells of an eye fixed after 10 days' dark adaptation. (M) microvilli; (NP) nucleus of pigment cell. Bar=1 µm.

of most eyes became smaller than those of animals maintained in the normal daily cycle (Fig. 2A, B). The dark-adapted eyes had a smaller microvillar area, while the pigment cells were thicker than in normal eyes. In order to make a comparison between the 10 days dark-adapted eyes and the eyes fixed at 16:00, semithin sections containing optical axes of these eyes were made carefully, and the microvillar area and the area occupied by pigment cells were measured (Table 1). During

the dark adaptation, microvillar area decreased more than 40%, but the area of pigment cells seemed to increase by a few percent. The pigment cells of dark-adapted eyes contain areas devoid of pigment granules (Fig. 2B), in addition to the perinuclear region. The cellular regions lacking pigment granules contain many vacuoles, which in turn contain membrane debris (Fig. 2C). In normal eyes, pigment granules are lacking only in the perinuclear region (Fig. 2A).

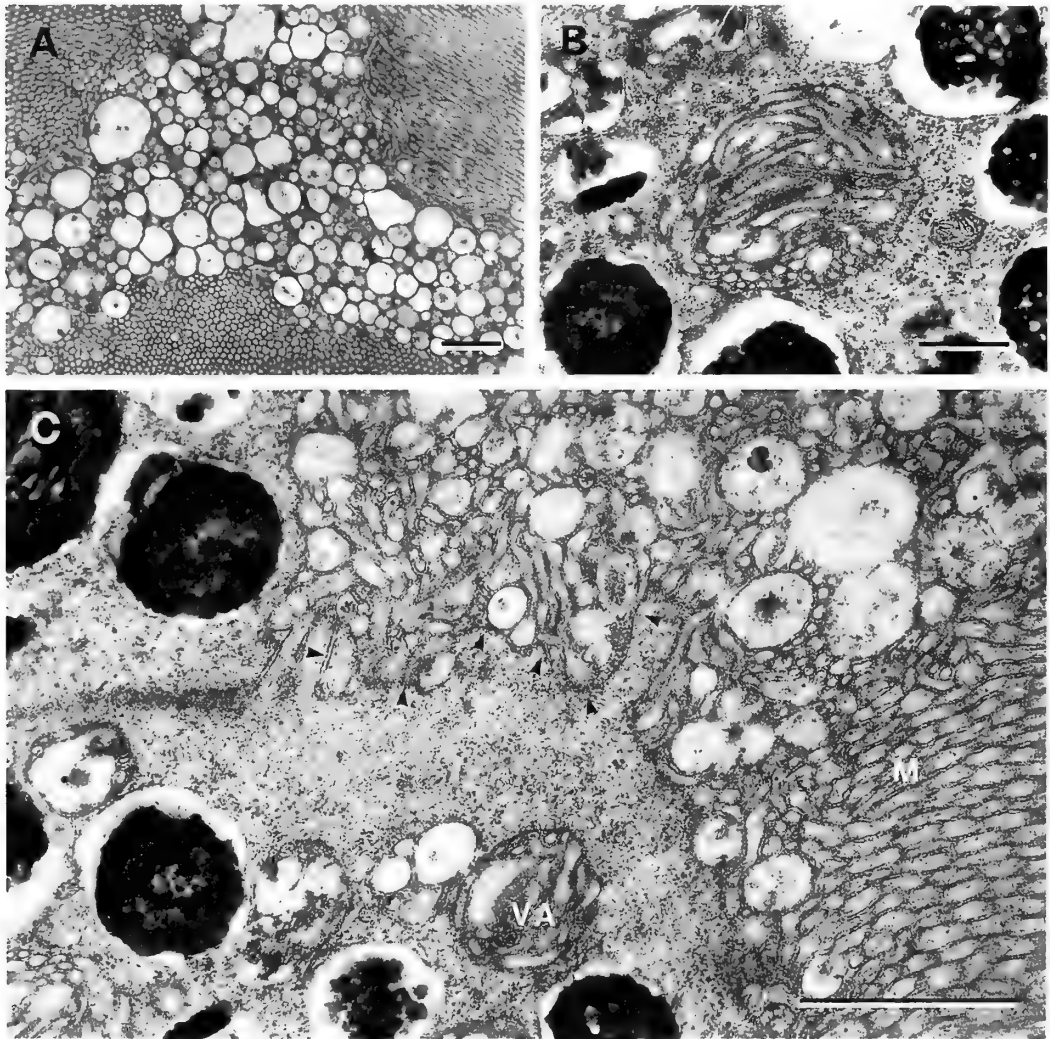


FIG. 3. A: Accumulation of vesicles between rhabdomeres fixed after 8 days' dark adaptation. Bar = $1\ \mu\text{m}$. B: Vacuole containing tubular membrane debris observed in the apical portion of a pigment cell fixed after 6 days' dark adaptation. Bar = $0.5\ \mu\text{m}$. C: Boundary region between the accumulated vesicles and the pigment cells fixed after 6 days' dark adaptation. Arrow heads indicate the cytoplasmic extensions surrounding the accumulated vesicles. (M) microvilli; (VA) vacuole containing tubular membrane debris. Bar = $1\ \mu\text{m}$.

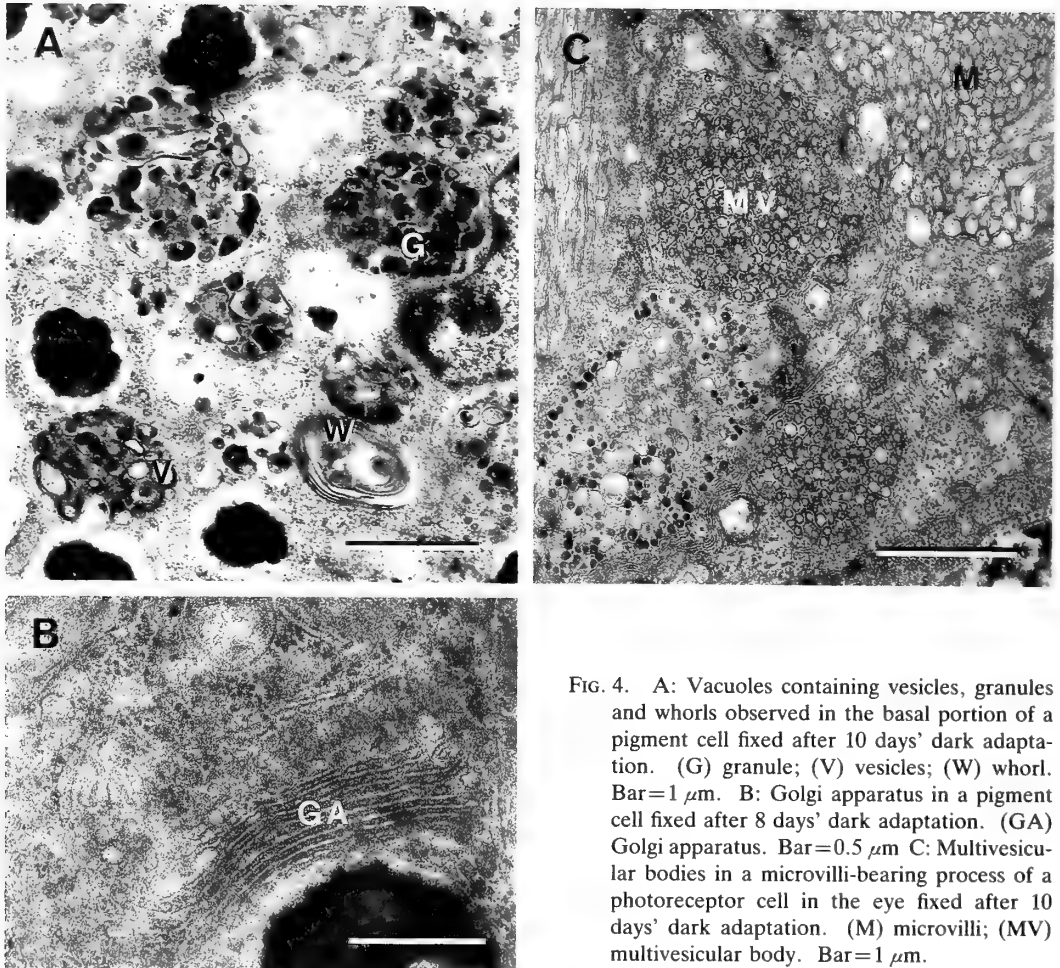


FIG. 4. A: Vacuoles containing vesicles, granules and whorls observed in the basal portion of a pigment cell fixed after 10 days' dark adaptation. (G) granule; (V) vesicles; (W) whorl. Bar = $1\ \mu\text{m}$. B: Golgi apparatus in a pigment cell fixed after 8 days' dark adaptation. (GA) Golgi apparatus. Bar = $0.5\ \mu\text{m}$. C: Multivesicular bodies in a microvilli-bearing process of a photoreceptor cell in the eye fixed after 10 days' dark adaptation. (M) microvilli; (MV) multivesicular body. Bar = $1\ \mu\text{m}$.

After longer dark-adaptation, many more microvilli appeared to be irregularly arranged and a considerable number of vesicles were accumulated between the rhabdomeres and pigment cells (Fig. 2C) or between adjacent rhabdomeres (Fig. 3A). The inner surface of the pigment cell, which is ordinarily concave, became convex in the region facing the accumulation of vesicles and possessed cytoplasmic extensions extending into the accumulation of vesicles (arrow heads in Fig. 3C). Vacuoles containing vesicles were often observed in a part of the pigment cells closest to the accumulation of vesicles. Tubular membrane debris, which seem similar to the microvilli of the photoreceptor cells, were also observed in these vacuoles (Fig. 3B and VA in Fig. 3C). The vacuoles observed in that region of the pigment cells closest

to the outer surface of the pigment cup contained mainly vesicles, granules and membrane whorls (Fig. 4A). The pigment cells of dark-adapted eyes had Golgi apparatus as shown in figure 4B (Fig. 4B). As one more additional feature of dark-adapted eyes, photoreceptor cells often contained multivesicular bodies larger than $1\ \mu\text{m}$ in diameter, in their microvilli-bearing processes as well as in their stalk region (Fig. 4C).

DISCUSSION

In the eyes of the planarian *Dugesia japonica*, morphological changes in daily cycles and in dark adaptation were investigated with special attention to the pigment cup and microvillar area. An irregular arrangement of photoreceptive microvilli

and an accumulation of vesicles in the perimicrovillar extracellular space were often found in animals fixed before dawn. The eye morphology of the animals used in this study did not show rhythmic circadian changes in total darkness. The morphological changes observed before dawn were enhanced as the period of dark adaptation was prolonged. Therefore, as reported by others [4, 8, 10], light conditions actually have significant effects on photoreceptive membrane structures in the planarian eyes.

Formation of vesicles in the perimicrovillar extracellular space was sometimes regarded as an artifact caused by an inadequate fixation. However, the formation of vesicles is now known to be prevalent in some animals [19, 21, 22], and is regarded as one mechanism of the photoreceptive membrane turnover [11]. In the planarian eye, it is believed that dark adaptation caused a swelling [4] and an irregular wavy appearance in the microvilli [9] as the result of decreased membrane stability and eventual photoreceptor atrophy [8]. Therefore, in the eyes of the planarian *Dugesia japonica*, the accumulation of vesicles which follows the decrease in microvilli is unlikely to be an artifact rather than the result of a biological mechanism. Shedding of microvilli may be initiated by a swelling of the apical edge, leading to an accumulation of vesicles in the perimicrovillar extracellular space.

When the animals are dark-adapted, the decrease in the size of the microvillar area was accompanied by a certain increase in the volume of the pigment cells (Table 1). Such a correlation between the decrease in the microvillar area and the increase in the volume of pigment cells may imply that some amounts of substances are transferred from the microvillar area to the pigment cells. Up until now, the possible phagocytotic activity of pigment cells has been discussed once with respect to the *Dugesia eyes* [3]. The accumulated vesicles in the microvillar area of the dark-adapted eyes seem to be taken up into the pigment cells by phagocytosis (Fig. 3C). Sometimes microvilli may also be taken up into the pigment cells by direct phagocytosis (Fig. 3B). The cellular regions lacking pigment granules contain many vacuoles containing membrane debris (Fig. 2C). These

ultrastructural observation undoubtedly support the notion that the substances transferred from the microvillar area to the pigment cells are the vesicles produced by the shedding of microvilli and the microvilli themselves.

Granules and membrane whorls are observed in the vacuoles of the basal half of the pigment cells. Similar particles are observed in the accessory eye of a giant snail *Achatina fulica* and are thought to be made from shed microvilli membrane [23]. The work of Chamberlain and Barlow [24] supports the idea that membrane whorls are normal breakdown products within the *Limulus* retina. The granules and membrane whorls in the *Dugesia* eye may also be changed from the phagocytosed vesicles.

The process of degradation of the vesicles taken into the pigment cells may be carried out by the action of lysosomal enzymes, such as acid phosphatase (AcPh) [25, 26]. Up to now, I have not seen precisely localized AcPh-deposits within the phagocytic vacuoles and the Golgi apparatus. However, Golgi apparatus may produce this kind of enzyme to degrade the debris of photoreceptive membrane [20]. The reuse of photoreceptive membrane taken into pigment cells has also been discussed by Brandenburger and Eakin [25–27].

After the dark adaptation, multivesicular bodies in the photoreceptor cells increase in number and size. Multivesicular bodies larger than 1 μm were often observed not only in the stalk region but also in the microvilli-bearing processes of the dark adapted photoreceptor cells. The increase in number and size of the multivesicular bodies is also correlated with the decrease in microvillar area. Multivesicular bodies can contribute to that decrease by a resorbence of microvilli membrane, and the multivesicular bodies will be transported from the microvillar area to the perinuclear region of sensory cell. This correlation may imply that the formation of multivesicular bodies is one of the mechanisms of the photoreceptive membrane removal in the eyes of *Dugesia japonica*.

Bedini *et al.* [10] attributed the drastic decrease in microvilli induced by darkness in the *Dalyellia* eye to the resorbence of microvilli into the sensory cells. The resorbence of microvilli into the sensory cells in the planarian *Dalyellia* reminded us of the resorbence of microvilli by the formation of mul-

tivesicular bodies in arthropoda eyes [12–15]. On the other hand, the phagocytosis of pigment cells to remove shed photoreceptive membrane in *Dugesia japonica* reminded us of the phagocytosis of pigment epithelium to remove tips of rod and cone outer segments in vertebrate eyes [16–18]. There may be two mechanisms by which the photoreceptive membrane is removed from the eye of *Dugesia japonica*. One is the phagocytosis of the pigment cell, i.e. removal by phagocytosis of surrounding glial cells, and the other is the formation of multivesicular bodies in the sensory cells, i.e. removal by resorbence of sensory cells. Swelling of the pigment cells after dark adaptation is induced by the phagocytosis of shed photoreceptive membrane in the microvillar area. Although the increase in the volume of pigment cells was small and did not completely compensate the decrease in the microvillar area, the greater volume of membrane debris would be phagocytosed and digested by the pigment cells. Therefore, even if the formation of multivesicular bodies may be a potential explanation for the decrease of the microvillar area, the phagocytosis by pigment cells must be also regarded as one of the mechanisms for the photoreceptive membrane removal in the planarian *Dugesia japonica*. It is very interesting to know that the two mechanisms for photoreceptive membrane removal prevailing in vertebrate and invertebrate coexist in planarian eyes.

ACKNOWLEDGMENTS

The author thank Mrs. Yayoi Asamoto for her skilled technical help.

REFERENCES

- MacRae, E. K. (1964) Observations on the fine structure of photoreceptor cells in the planarian *Dugesia tigrina*. J. Ultrastruct. Res., **10**: 334–349.
- Kishida, Y. (1965) The ultrastructure of the eyes in *Dugesia japonica*. I. The distal portion of the visual cell. Zool. Mag. (Tokyo), **74**: 149–155.
- Carpenter, K. S., Morita, M. and Best, J. B. (1974) Ultrastructure of the photoreceptor of the planarian *Dugesia dorotocephala*. I. Normal eye. Cell Tissue Res., **148**: 143–158.
- MacRae, E. K. (1966) The fine structure of photoreceptors in a marine flatworm. Z. Zellforsch., **75**: 469–484.
- Eakin, R. M. and Brandenburger, J. L. (1981) Fine structure of the eye of *Pseudoceros canadensis* (Turbellaria, Polycladida). Zoomorphology, **98**: 1–16.
- Lanfranchi, A. and Bedini, C. (1982) The ultrastructure of the sense organs of some Turbellaria rhabdocoela. I. The eyes of *Polycystis naegelii* Kolliker (Eukalyptorhynchia Polycystididae). Zoomorphology, **101**: 95–102.
- Fournier, A. (1984) Photoreceptors and photosensitivity in platyhelminthes. In "Photoreception and Vision in Invertebrates", Plenum, Ed. by Al: Ma, Plenum, New York, pp. 217–239.
- Röhlich, P. and Tar, E. (1968) The effect of prolonged light-deprivation on the fine structure of planarian photoreceptors. Z. Zellforsch., **90**: 507–518.
- Carpenter, K. S., Morita, M. and Best, J. B. (1974) Ultrastructure of the photoreceptor of the planarian *Dugesia dorotocephala*. II. Changes induced by darkness and light. Cytobiologie, **8**: 320–338.
- Bedini, C., Ferrero, E. and Lanfranchi, A. (1977) Fine structural changes induced by circadian light-dark cycles in photoreceptors of Dalyelliidae (*Turbellaria: Rhabdocoela*). J. Ultrastr. Res., **58**: 66–77.
- Schwemer, J. (1985) Turnover of photoreceptive membrane and Visual Pigment in Invertebrates. In "The molecular mechanism of photoreception". Ed. by H. Stieve, Springer, pp. 303–326.
- White, R. H. (1964) The effect of light upon the ultrastructure of the mosquito eye. Am Zool., **4**: 433.
- White, R. H. (1967) The effect of light and light deprivation upon the structure of the larval mosquito eye, II. The rhabdom. J. Exp. Zool., **166**: 405–425.
- White, R. H. (1968) The effect of light and light deprivation upon the structure of the larval mosquito eye, III. Multivesicular bodies and protein uptake. J. Exp. Zool., **169**: 261–268.
- Eguchi, E. and Waterman, T. H. (1967) Changes in retinal fine structure induced in the crab *Libinia* by light and dark adaptation. Z. Zellforsch., **79**: 209–229.
- Young, R. W. and Bok, D. (1969) Participation of the retinal pigment epithelium in the rod outer segment renewal process. J. Cell Biol., **42**: 392–403.
- Young, R. W. (1971) Shedding of discs from rod outer segments in the rhesus monkey. J. Ultrastruct. Res., **34**: 190–203.
- Young, R. W. (1977) The daily rhythm of shedding and degradation of cone outer segment membranes in the lizard retina. J. Ultrastruct. Res., **61**: 172–185.
- Eakin, R. M. and Brandenburger, J. L. (1985) Effects of light and dark on photoreceptors in the

- polychaete annelid *Nereis limnicola*. Cell Tissue Res., **242**: 613–622.
- 20 Piekos, W. B. (1986) The role of reflecting pigment cells in the turnover of crayfish photoreceptors. Cell Tissue Res., **244**: 645–654.
- 21 Blest, A. D. and Maples, J. (1979) Exocytotic shedding and glial uptake of photoreceptor membrane by a salticid spider. Proc. Roy. Soc. Lond. B., **204**: 105–112.
- 22 Williams, D. S. and Blest, A. D. (1980) Extracellular shedding of photoreceptor membrane in the open rhabdom of a tipulid fly. Cell Tissue Res., **205**: 423–438.
- 23 Tamamaki, N. and Kawai, K. (1983) Ultrastructure of the accessory eye of the giant snail, *Achatina fulica* (Gastropoda, Pulmonata). Zoomorphology, **102**: 205–213.
- 24 Chamberlain, S. C. and Barlow, R. B. Jr. (1984) Transient membrane shedding in *Limulus* photoreceptors: Control mechanisms under natural lighting. J. Neurosci., **4**: 2794–2810.
- 25 Brandenburger, J. L. and Eakin, R. M. (1980) Cytochemical localization of acid phosphatase in ocelli of the seastar *Patiria miniata* during recycling of photoreceptor membranes. J. Exp. Zool., **214**: 127–140.
- 26 Brandenburger, J. L. and Eakin, R. M. (1985) Cytochemical localization of acid phosphatase in light- and dark-adapted eyes of a polychaete worm, *Nereis limnicola*. Cell Tissue Res., **242**: 623–628.

Eurythermic Growth and Synthesis of Heat Shock Proteins of Primary Cultured Goldfish Cells

MAKI SATO, HIROSHI MITANI and AKIHIRO SHIMA

*Zoological Institute, Faculty of Science, University of Tokyo,
Bunkyo-ku, Tokyo 113, Japan*

ABSTRACT—Cells derived from the tail fin of goldfish (*Carassius auratus*) are cultured at 37°C (GTF e-2) and 27°C (GTF e-3). It is observed that the doubling times of GTF e-2 cells and that of GTF e-3 cells depend solely on the incubation temperature, irrespective of difference in the temperature at which the primary culture is started. It has been reported previously that some goldfish cell lines cultured *in vitro* for a long time grew stenothermally. The present study indicated that cells derived from the primary culture retained their ability to grow eurythermally at least in the early passages.

The relationship of protein synthesis as to incubation temperature was studied empirically. When GTF e-3 cells were exposed to 37°C, four major heat shock proteins were induced. Their molecular weights were 90 K dalton (hsp 90), 70 K dalton (hsp 70), 42 K dalton (hsp 42) and 30 K dalton (hsp 30). In GTF e-2 cells these proteins were synthesized constitutively at 37°C. The levels of synthesis of these proteins were much higher than those observed when the cells were incubated at 27°C. At 40°C, hsp 70 and hsp 30 were the dominantly synthesized proteins of GTF e-2 and e-3 cells.

INTRODUCTION

Cells derived from fish and those derived from mammals can be cultured using the same medium and the same serum, but the incubation temperature is usually different. For the cultured mammalian cells, the range of permissive growth temperature is 36–39°C with an optimal at 37°C [1]. For most fish cell lines the optimal growth temperature is 20–25°C and upper limit temperature for growth is about 30°C [2]. In general, the suitable temperature for cultured fish cells correlates with the temperature of the animals natural habitat; the cultured cells derived from cold-water fish grow most rapidly at low temperature (about 20°C), while those from some tropical fish could be kept at 37°C [2 and 3 for review]. Cell lines derived from different species of fish have different optimal growth temperatures [4–6]. The RBCF-1 cells derived from the caudal fin of the goldfish grow most rapidly at 37°C. They also can grow continuously at 20°C [6]. Recently, we isolated from RBCF-1 cells two cell clones which grow only in a

narrow range of temperatures (stenothermic growth), the optimal growth temperature being 37°C and 27°C. It has been shown that cell hybrids of two stenothermic clones with different optimal growth temperature could continue to grow in a wide range of temperatures (the eurythermic growth) [7]. These results suggest that the eurythermic or stenothermic characteristics of growth of goldfish cells in culture may be modified during a prolonged *in vitro* cultivation. In this report, we investigated the growth temperature for primary cultured goldfish cells, and the effects of incubation temperature on the protein synthesis of the cells.

MATERIALS AND METHODS

Primary culture

The tail fin about 1 cm² of an adult goldfish with about 5 cm body length was cut off. It was soaked in 0.4% NaClO, washed in Ca²⁺- and Mg²⁺-free phosphate-buffered saline (PBS(–)), and cut into pieces in trypsin-EDTA (0.1% trypsin and 0.02% EDTA in PBS(–)). The small tissue pieces were gently stirred in the presence of trypsin-EDTA at

room temperature for about 60 min. The tissue pieces and dispersed cells were collected by centrifugation and seeded into two 25 cm² plastic flasks (Corning Glass Works, Corning, N.Y.). Each flask was incubated at 37°C (GTF e-2) or 27°C (GTF e-3). The medium used was Leibovitz's L-15 medium (GIBCO, Grand Island, N.Y.), containing 15% fetal bovine serum (Hyclone Laboratories, Logan) and the antibiotics (50 µg/ml streptomycin and kanamycin, 60 µg/ml). A half volume of the medium was renewed every 3 days. The primary culture was harvested 18 days after the inoculation, and 1×10^6 cells were inoculated into the fresh dishes with 10 ml of the medium. Both cell lines were subcultured every 3 days. The population doubling number (PDN) was calculated from the day of first subcultivation by $\log(\text{cumulative growth ratio})/\log 2$.

Growth curve

Cells were seeded in culture petri dishes at 2.0×10^5 cells/dish. For each cell line half the dishes were incubated at 27°C, half at 37°C. Each 3 days 3 dishes were counted for the number of cells. This was continued for 12 days. The population doubling number (PDN) of the GTF e-2 was 3.2. The PDN of the GTF e-3 was 1.3.

Protein analysis

To analyze the protein synthesis of GTF cells at various temperatures, each flask was inoculated with 5×10^5 cells (GTF e-2 at PDN 10.8, and GTF e-3 at PDN 4.2) and incubated for 10 hr at 37°C or

27°C, respectively. Before starting labeling, cells were cultured for 2 hr in methionine-free Dulbecco's modified Eagle medium with 10% FBS. Then, Tran ³⁵S-label™, *E. coli* hydrolysate labeling reagent, containing ³⁵S-methionine (ICN Biomedicals, Irvine: specific activity >1000 Ci/mmol) was added to the medium to a final concentration of 10 µCi/ml and transferred to desired temperatures and incubated for additional 2 hr. Subsequently, the medium was removed and the cells were washed with PBS(-), harvested by a small rubber policeman. The cells were suspended in Laemmli's buffer [8], and boiled for 3 min.

The protein was analyzed on 10% polyacrylamide-SDS slab gels with 2.5% stacking gel using the discontinuous buffer system of Laemmli [8]. Protein samples with approximately the same ³⁵S counts (about 30,000 cpm) were used for analysis. Slab gels (5 cm × 8.5 cm) were run at 15 mA for about 110 min, and stained with silver stain (2D-Silver Stain Kit 'DPC'; Daiichi Pure Chemical, Tokyo). The gels were dried and autoradiographed using Kodak X-Omat R5 film.

RESULTS

The cells dispersed from caudal fin of the goldfish and the remaining tissue pieces attached to the plastic substratum. Many cells migrated from tissue pieces and continued to proliferate both at 37°C and 27°C. After 18 days of incubation, GTF e-2 and GTF e-3 cells reached confluency. At that time the total cell numbers were 5×10^6

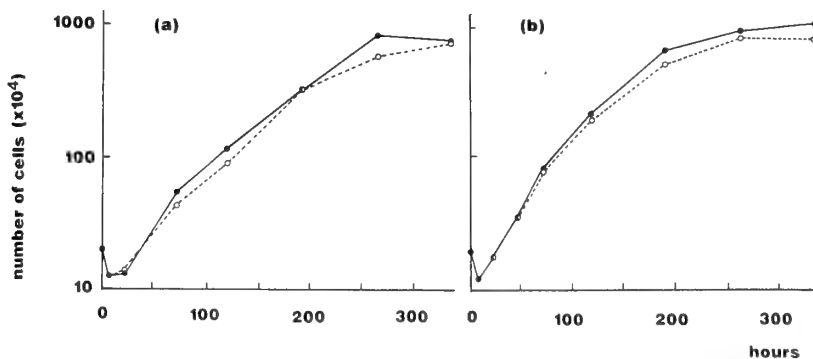


FIG. 1. Growth curve of GTF e-2 and e-3 cells at 27°C (a) and 37°C (b). The ordinate is the average number of cells recovered from a dish, and the abscissa is time in hours after inoculation. ●—●: GTF e-2, primary culture was started at 37°C. ○—○: GTF e-3, primary culture was started at 27°C.

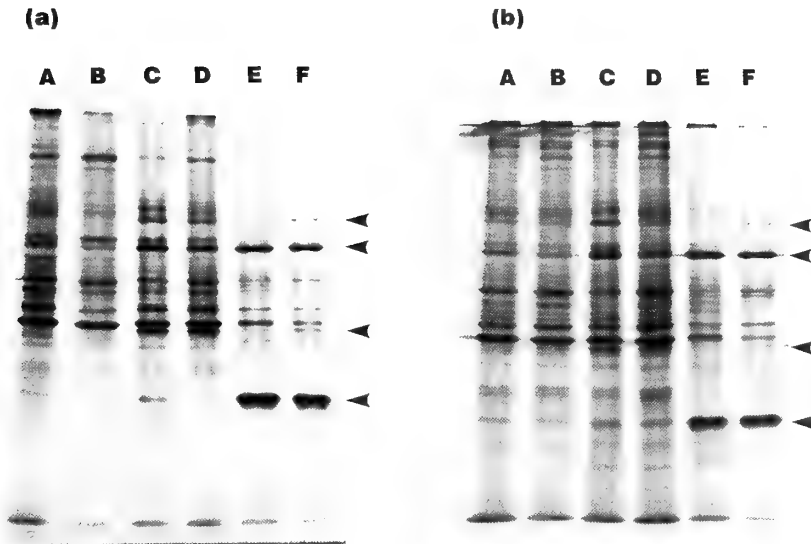


FIG. 2. The autoradiograph of heat shock proteins in (a) GTF e-3, and (b) GTF e-2. The temperature was shifted as shown below:

lane A: 27°C (12 hr)–27°C (labeled for 2 hr)

lane B: 37°C (12 hr)–27°C (labeled for 2 hr)

lane C: 27°C (12 hr)–37°C (labeled for 2 hr)

lane D: 37°C (12 hr)–37°C (labeled for 2 hr)

lane E: 27°C (12 hr)–40°C (labeled for 2 hr)

lane F: 37°C (12 hr)–40°C (labeled for 2 hr)

The cells were labeled with ^{35}S -methionine at the corresponding times. The arrows indicate hsp 90, hsp 70, hsp 42 and hsp 30 (from top to bottom), respectively.

for GTF e-2 and 4×10^5 for GTF e-3, and the morphology of the cells did not show any observable difference between the two cell strains. Both cell strains continued to grow without any sign of crisis of growth. This is one of the notable characteristics of cultured fish cells reported previously [4, 9, 10]. Figure 1 shows growth curves of GTF cells at early passages (PDN < 11). The doubling time of GTF e-2 cells calculated from the slope of the initial straight line portion of the growth curve was 35 hr at 27°C, and 25 hr at 37°C. The doubling time for GTF e-3 cells was 36 hr at 27°C, and 25 hr at 37°C. Thus, the doubling time of cultured goldfish cells at early passages did not depend on the temperature at which the primary culture was started, but depended only on the incubation temperature.

Figure 2 shows the autoradiographs of newly synthesized proteins. The four major proteins were identified when the cells were transferred to

higher incubation temperature. The molecular weights of hsps observed in the present study were 90, 70, 42 and 30-kD, and would correspond respectively to hsp 90, hsp 70, hsp 42 and hsp 30 of RBCF-1 cells [7]. The synthesis of these proteins was markedly increased when the GTF e-2 and GTF e-3 cells were incubated first at 27°C for 12 hr and then transferred to 37°C or after a long incubation at 37°C. At higher temperature (40°C) the hsp 70 and hsp 30 became dominant newly synthesized protein, and relative amount of hsp 90 and hsp 42 synthesis decreased in both cell strains.

DISCUSSION

It is generally accepted that cultured cells grow optimally when the incubation temperature is slightly higher than that preferred by the intact animal. For example, in case of cold-water fish like rainbow trout (*Salmo gairdnerii*), the cultured

cells grow most rapidly at temperature from 8 to 12°C [3]. As to goldfish cell lines, the optimal growth temperature reported has not been consistent. Rio *et al.* [4] reported 20°C for SJU-1 cell line, while 33°C was reported for CAF cell line by Etoh and Suyama [5]. Shima *et al.* established the RBCF-1 cell line which was initially cultured at 37°C and could grow at a wide range of temperatures from 20°C to 37°C (eurythermic growth) [6]. Recently, after a long term cultivation at 27°C or 37°C, clones of RBCF-1 line which could grow only at a narrow range of temperatures (stenothermic growth) were isolated [7].

In this study, we found that both GTF e-2 and e-3 cells which were derived from a goldfish tail fin, retained eurythermic growth properties at early passages (PDN < 11), in spite of 10°C difference in primary culture. A probable cause for difference between eurythermic and stenothermic growth may be the difference in the length of their subcultivation time. SJU-1 cell line was at 110th passage after 39 months of subcultivation during which periods the cells were cultured at 20°C. RBCF-1 cells have been subcultured for more than 10 years. GTF cells were at only 2nd passage (the PDN is 3.2 for GTF e-2, and 1.3 for GTF e-3) after 4 days of subcultivation when they were used for the experiments. The intact goldfish as individuals can survive both at 27°C and 37°C, and this fact seems to correlate with the growth properties of GTF cells. So the cells *in vivo* may have the eurythermic growth properties. SJU-1 and RBCF-1 cells, which have been cultured for a long time at a constant temperature, may have lost their ability to grow eurythermically.

The molecular weights of major heat shock proteins synthesized by GTF cells were almost the same as those synthesized by cells of *Drosophila* [11, 12], mammals [13] and rainbow trout [14]. The hsp 90 of GTF cells may correspond to hsp 83 of *Drosophila* in the manner of response to the change of temperature; hsp 83 was not induced at a higher temperature (38°C) in *Drosophila* [11], and in GTF cells hsp 90 was not induced at 40°C.

The hsp 42 was induced in GTF cells when the cells were transferred from 27°C to 37°C, and also when they had been kept at 37°C. This response to temperature shift was similar to that of hsp 90.

The cells of *Drosophila* do not synthesize hsp 42 [11, 12]. Rainbow trout cells (hsp 42) [14], chicken embryo fibroblasts (hsp 47) [15] as well as HeLa cells (hsp 43) [13] synthesize this class of hsp, all of which may correspond to hsp 42 of GTF cells. Therefore, hsp 42 may be the common heat shock protein in the cells of vertebrates so far examined.

The cells of *Drosophila* synthesize hsp 70 and hsp 26 which correspond to hsp 70 and hsp 30 of GTF cells. The hasps 70 and 26 are reported to be induced at a higher temperature than the temperature which induced hsp 90 [12]. This was also observed in GTF cells.

The relationships between the range of growth temperatures of cells and the temperature which can induce heat shock proteins in the cells have been reported for only a few species [11–14]. However, it may generally be said that hsps syntheses are induced when cells are transferred to a temperature which is a few degrees higher than their optimal growth temperature. Furthermore, the heat shock proteins may be synthesized as a consequence of environmental stress. In this study, we found that GTF cells do not follow this pattern, at 37°C hsps seem to be induced continuously, although the cells could grow actively at that temperature. This is quite different from RBCF-1 cells. When RBCF-1 cells were transferred from 26°C to 37°C, four major heat shock proteins were induced, but after 12 hr incubation synthesis of heat shock proteins decreased [7].

To summarize, in this study we found that cultured fish cells in the very early passages (PDN < 3.2) can grow actively at both 27°C and 37°C. This eurythermic growth may reflect a growth characteristic of goldfish cells *in vivo*. It was also observed that in the cultured goldfish cells at early passages, four major hsps were induced at 37°C in spite of continued growth at this temperature for a long time. These results indicate that primary cultured goldfish cells are quite useful for investigating factors that determine the optimal growth temperature of cells, and the function of hsps in eurythermic animals.

ACKNOWLEDGMENTS

This research was supported by a grant from Fisheries Agency, Japan to A. Shima.

REFERENCES

- 1 Sisken, J. K., Morasca, L. and Kibby, S. (1965) Effects of temperature on the kinetics of the mitotic cycle of mammalian cells in culture. *Exp. Cell Res.*, **39**: 103–116.
- 2 Wolf, K. and Ahne, W. (1982) Fish cell culture. *Advances in Cell Culture*, **2**: 305–328.
- 3 Wolf, K. (1979) Cold-blooded vertebrate cell and tissue culture. *Methods in Enzymology*, **58**: 466–477.
- 4 Rio, G. J., Magnavita, F. J., Rubin, J. A. and Beckert, Wm. H. (1973) Characteristics of an established goldfish *Carassius auratus* (L.) cell line. *J. Fish Biol.*, **5**: 315–321.
- 5 Suyama, I. and Etoh, H. (1977) A cell line derived from the fin of the goldfish, *Carassius auratus*. *Zool. Mag.*, **88**: 321–324.
- 6 Shima, A., Nikaido, O., Shinohara, S. and Egami, N. (1980) Continued *in vitro* growth of fibroblast-like cells (RBCF-1) derived from caudal fin of the fish, *Carassius auratus*. *Exp. Gerontol.*, **15**: 305–314.
- 7 Mitani, H., Naruse, K. and Shima, A. (1989) Eurythermic and stenothermic growth of cultured fish cells and their. *J. Cell Sci.*, **93**: 731–737.
- 8 Laemmli, U. K. (1970) Cleavage of structure proteins during the assembly of the head of bacteriophage T4. *Nature*, **227**: 680–685.
- 9 Komura, J., Mitani, H. and Shima, A. (1988) Fish cell culture: Establishment of two fibroblast-like cell lines (OL-17 and OL-32) from fins of the medaka, *Oryzias latipes*. *In Vitro*, **24**: 294–298.
- 10 Shima, A. and Setlow, R. B. (1985) Establishment of a cell line (PF line) from a gynogenetic teleost, *Poecilia formosa* (Girard) and characterization of its repair ability of UV-induced DNA damage. *Zool. Sci.*, **2**: 477–483.
- 11 Lindquist, S. (1986) The heat shock response. *Ann. Rev. Biochem.*, **55**: 1151–1191.
- 12 Lindquist, S. (1980) Varying patterns of protein synthesis in *Drosophila* during heat shock: Implication for regulation. *Develop. Biol.*, **77**: 463–479.
- 13 Hickey, E. D. and Weber, L. A. (1982) Modulation of heat-shock polypeptide synthesis in HeLa cell during hyperthermia and recovery. *Biochemistry*, **21**: 1513–1521.
- 14 Kothary, R. K. and Candid, E. P. M. (1981) Induction of a normal set of polypeptides by heat shock or sodium arsenite in cultured cells of rainbow trout, *Salmo gairdnerii*. *Can. J. Biochem.*, **60**: 347–355.
- 15 Nagata, K., Hirayoshi, K., Obara, M., Suga, S. and Yamada, K. M. (1988) Biosynthesis of a novel transformation-sensitive heat shock protein that binds to collagen. *J. Biol. Chem.* **263**: 8344–8349.

Motility of Cultured Iridophores from the Freshwater Goby *Odontobutis obscura*

TETSURO IGA, JIRO KINUTANI and NAOMI MAENO

Department of Biology, Faculty of Science, Shimane University, Matsue 690, Japan

ABSTRACT—Iridophores in the integument of the freshwater goby, *Odontobutis obscura*, are motile. Iridophores isolated from scales of the goby were cultured in L-15 medium. The primary cultured cells were motile. Their movements involved aggregation and dispersion of platelets within the cells, which were not caused by a reversible retraction of cellular processes. Alpha-MSH induced aggregation of platelets, while melatonin and norepinephrine, separately, induced dispersion of the platelets. These responses of the cultured iridophores to drugs were the same with as those of iridophores in preparations of isolated scales. The speed of migration of platelets in cultured iridophores was very slow, and it appeared to be the same as that in iridophores in intact scales. Most of the cultured iridophores exhibited sensitivity to light; they assumed a dispersed state in the light and an aggregated state in darkness.

INTRODUCTION

Iridophores are light-reflecting chromatophores commonly found in the dermis of many poikilothermal vertebrates, and they are known to play a predominant role in the generation of skin coloration [1]. Electron-microscopic observations have revealed that iridophores in fishes contain a large number of platelets, which run parallel to each other and form stacks [2-5]. These platelets are mainly composed of guanine and have a very high reflective index, so that, when stacked, they generate various colors. The phenomenon is called physical or structural coloration [6, 7]. Until recently, these iridophores in fishes were not thought to play an active part in changes of color via phenomena that involved motility.

Quite recently, we found that iridophores in the integument of the freshwater goby, *Odontobutis obscura*, respond to neural and hormonal stimulation via changes in the reflective surface of the cells [8]. Light- and electron-microscopic observation suggested that the motility of the iridophores involved the translocation of reflecting platelets within the cells [8, 9]. At present, however, information on the movements of the reflecting

platelets within the iridophores is very scanty. Studies with cultured iridophores may provide us with much useful information about such movements.

The purpose of the present experiments was to present the motility of cultured iridophores from the freshwater goby, *Odontobutis obscura*.

MATERIALS AND METHODS

Culture of iridophores

Scales isolated from the dorso-lateral side of the freshwater goby, *Odontobutis obscura*, were immersed in a solution composed of a mixture of equal volumes of physiological saline (128 mM NaCl, 2.6 mM KCl, 1.8 mM CaCl₂, 5 mM HEPES-NaOH buffer, pH 7.2) and an isotonic solution of KCl for 40 min. This solution, with in its high level of K⁺, induced dispersion of platelets in the iridophores [8]. The epidermis was removed with fine forceps from the scales, after they had been immersed in physiological saline supplemented with 2.5 mg/ml collagenase (Type II, Worthington Biochemical Co., Freehold) for 20 min. The epidermis-free scales were then transferred into a vial filled with a dissociation medium which consisted of 2.5 mg/ml collagenase and 1.5 mg/ml trypsin (Sigma Chemical Co., St Louis). The vials

were gently stirred for 40–60 min at room temperature. Dissociated cells were collected with a fine pipette under a dissecting microscope and cultured in plastic dishes coated with collagen (Type A,

Nitta Gelatin, Osaka). The culture medium was Leibovitz L-15 medium (Gibco Lab., New York) supplemented with 10% fetal calf serum, 100 IU/ml penicillin, 100 μ g/ml streptomycin (Gibco

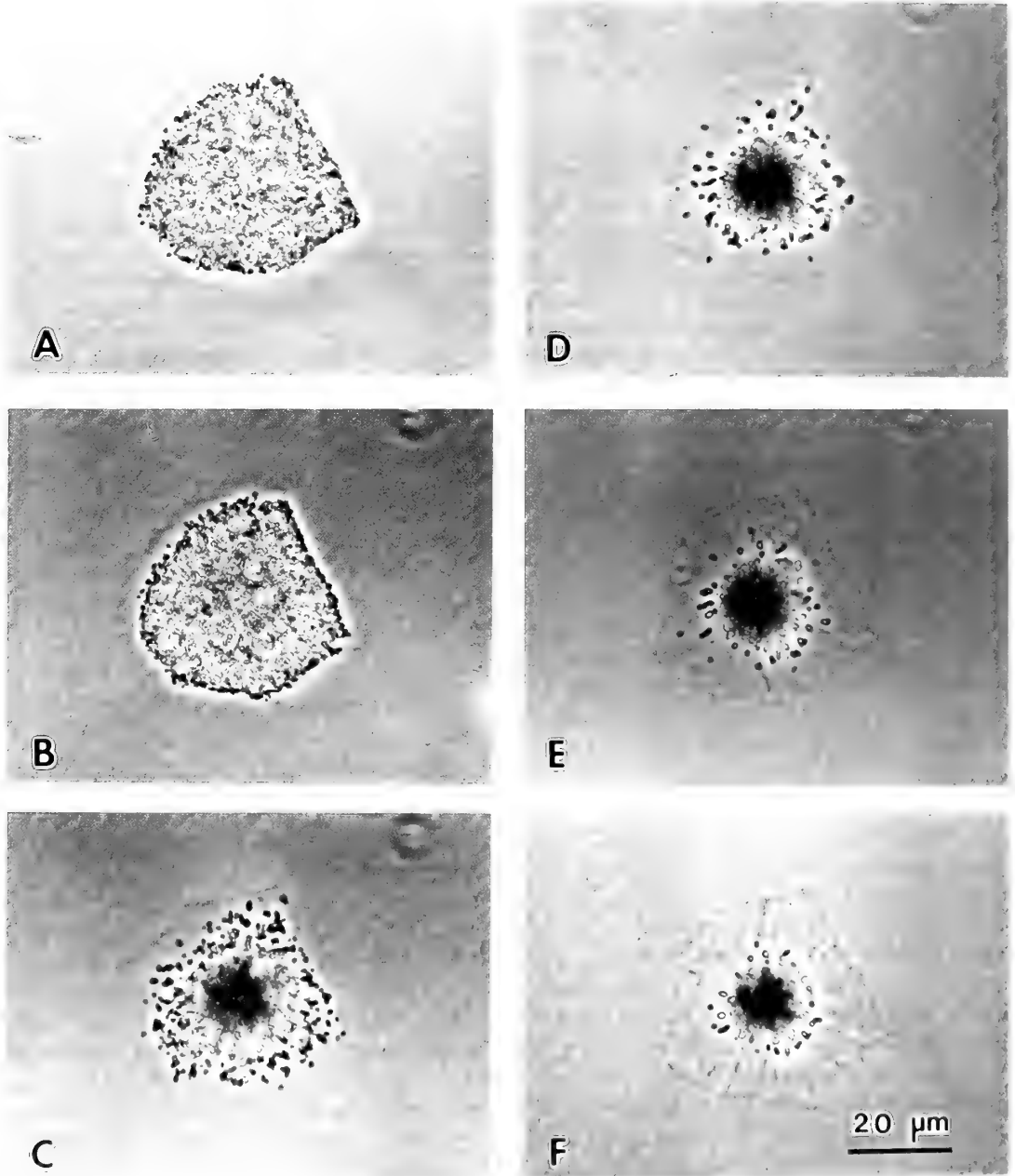


FIG. 1. Micrographs showing responses of cultured iridophores from *Odontobutis obscura* to alpha-MSH and melatonin. A, In culture medium. B, In saline. C, D, E, F and G, 10, 30, 60, 90 and 120 min, respectively, after treatment with 100 nM alpha-MSH. H, I, J, K and L, 20, 40, 60, 90 and 180 min, respectively, after treatment with 1 μ M melatonin.

Lab.), and 10% DW. The dishes were incubated at 26°C in air.

Recording of responses of cultured iridophores

Cultures were observed under an inverted phase-contrast microscope (Olympus CK-2) and their responses were photographed for analysis of

cellular motility.

Drugs

Alpha-MSH, melatonin and norepinephrine hydrochloride were obtained from Sigma Chemical Co. These drugs were dissolved in physiological saline.

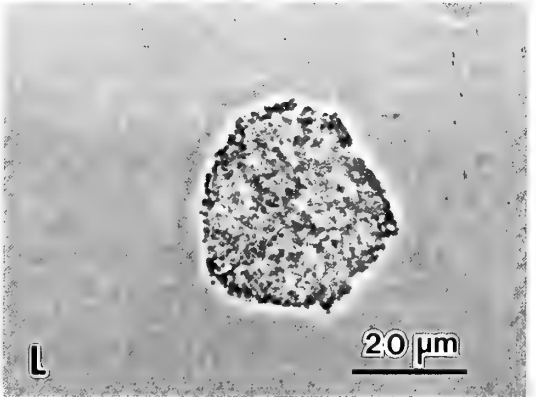
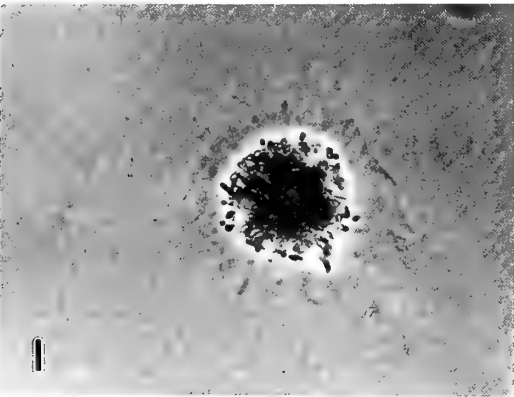
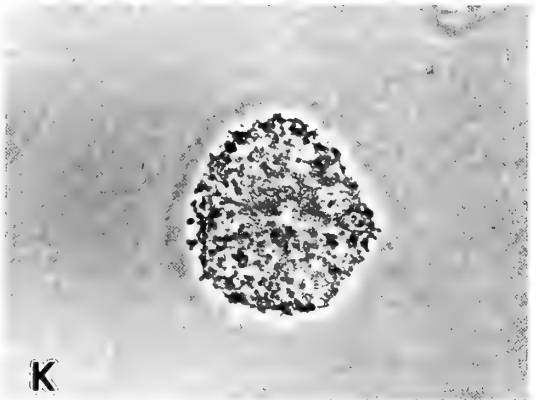
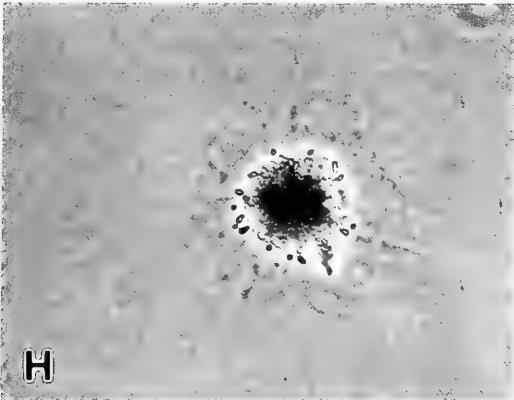
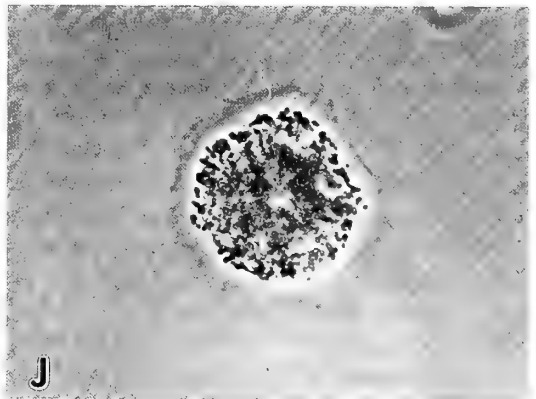
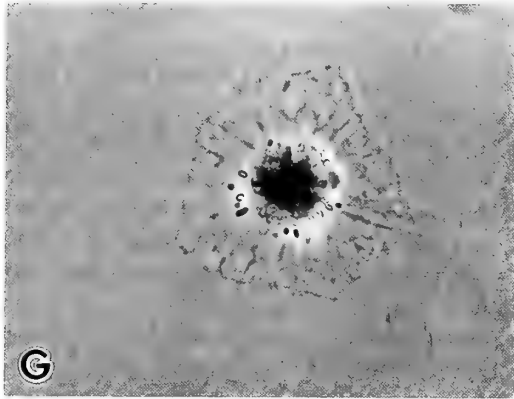


FIG. 1. —Cont.

All experiments were performed at room temperature (22.0–25.0°C).

RESULTS

Cultured iridophores

After inoculation, the iridophores attached to the substratum and began to spread within a day. After 2 to 3 days in culture most iridophores were fully spread and platelets were evenly dispersed throughout the cells. The shapes of iridophores were variable, with rod-like, dendritic, and discoidal iridophores being observed. The diameters ranged from 20 to 50 μm , like those of iridophores in intact scales.

The platelets in these iridophores assumed a dispersed state within the cells in the light. After being kept overnight in darkness, aggregation of platelets in the cell centers occurred in most of the iridophores, while some remained in the dispersed state. If the cultures were transferred to the light, iridophores with aggregated platelets returned to the dispersed state within 3 hr. Thus, the cultured iridophores appear to be sensitive to light.

Responses of cultured iridophores

Iridophores fully spread after 2 to 3 days in culture were used for experiments. Alpha-MSH (100 nM) induced aggregation of platelets into the central regions of the iridophores. The platelets began simultaneously to move centripetally and became aggregated in the central region of each cell after 90 to 120 min of the treatment (Fig. 1A-G).

During this time, the cell membranes attaching to the substratum remained in their original state without retraction. When melatonin (1 μM) was applied to iridophores with platelets in an aggregated state, the platelets began to disperse centrifugally from the aggregates and returned to their original dispersed state after 90 to 180 min (Fig. 1H-L). Norepinephrine (1 μM) also induced dispersion of platelets with the same time course as that observed with melatonin. If the solution of alpha-MSH was changed to physiological saline, the platelets remained aggregated for at least 60 min without any sign of dispersion.

Requirement for Ca^{++} in the action of MSH

The action of MSH was inhibited in Ca^{++} -free saline that contained 1 mM EDTA. If the vehicle for the peptide was changed to the standard saline, aggregation of the platelets was induced in standard fashion. It is noteworthy that a similar aggregation of platelets occurred when iridophores that had been exposed to a prolonged treatment with MSH, in an absence of Ca^{++} , were immersed in the standard saline.

Migration of reflecting platelets

For analysis of the migration of reflecting platelets within the iridophores during the course of the aggregation response, the results of the application of 100 nM alpha-MSH to cultured iridophores were followed by photographing them at intervals of 10 min, and the migration of platelets was traced from the micrographs.

A typical example, indicating the migration of platelets within a cell, is shown in Figure 2. The platelets did not always appear to move linearly. The profile of their velocity was also not linear. Among the bulk of platelets that were moving

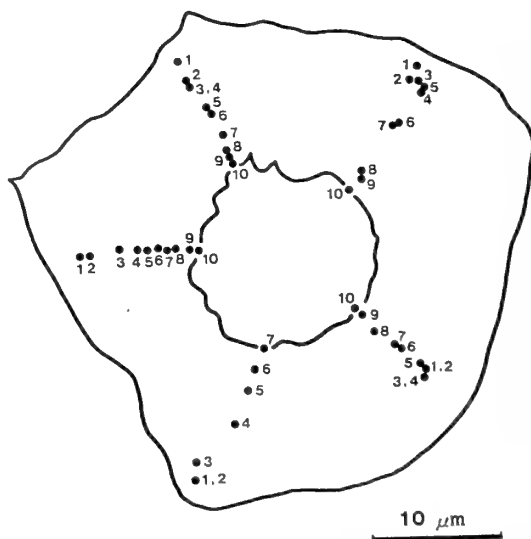


FIG. 2. A typical example of recordings that show the centripetal migration of platelets in a cultured iridophore from *Odontobutis obscura*. Each point with a number shows, in order, the position of an individual platelet at intervals of 10 min.

centripetally, there were some that were stationary and other that even moved in the reversal direction. From the distance of platelet migration measured every 10 min with 35 of platelets in 7 cells, the velocity of platelet migration was calculated. The maximum velocity of platelet migration was calculated as $0.5 \mu\text{m}/\text{min}$, with a mean value of $0.1 \mu\text{m}/\text{min}$.

DISCUSSION

Iridophores with platelets in a dispersed state were used for isolation of cells, because they gave well-spread cultured cells. Iridophores with platelets in the dispersed state may be more resistant to the isolation treatment than those with platelets in the aggregated state, which did not give such well-spread cells in culture. Iridophores of *Odontobutis obscura* appeared dendritic *in vivo*. In culture, however, most of the cells assumed a discoidal shape. Iwata *et al.* [10] reported that the shapes of cultured cells may be influenced by various factors, especially by the properties of the substratum in the case of melanophores from the medaka, *Oryzias latipes*, and that melanophores cultured on a collagen-coated substratum had complex shapes. In the present case, better adhesion and spreading of the cells were obtained on a collagen-coated substratum than on uncoated plastic. There were no observable differences in the shapes of cells in the well-spread state between cells on the two substrata.

The cultured iridophores were responsive to α -MSH, melatonin and norepinephrine. The responses were same as those of iridophores in the preparations of intact scales. Properties of hormone receptors appeared to be unchanged by culture *in vitro*.

The present experiments clearly showed that motility of the iridophores involves centripetal or centrifugal migration of the platelets within the cells, but no retraction or elongation of cellular processes. Most of the cultured cells did not change their contours during their responses to the agents applied. Some cells did change their shapes during their responses, perhaps as a result of a weakness of adhesion of the cells to the substratum. Responses of such cells were not so clear-cut.

In iridophores in preparations of isolated scales, the shapes of cells were unchanged after repeated responses. Electron-microscopic observations have suggested that dendrites of the iridophores are firmly anchored in the connective tissues and that the platelets move within the cells [9].

The iridophores of the integument of some species of amphibian undergo conspicuous changes in shape, from a dendritic to a punctate appearance, and such changes are regulated by MSH from the hypophysis [11, 12]. However, whether movement of platelets results passively from dendritic retraction, or whether it is a selective movement independent of changes in dendritic morphology remains to be determined [13]. Cultured iridophores from the tail skin of tadpoles of the bullfrog, *Rana catesbeiana*, have been shown to attach to dishes and form dendritic structures; such iridophores respond to ACTH with contraction of cells [14]. Recently, Butman *et al.* [15] studied responses to hormones of cultured iridophores from the integument of the Mexican leaf frog, *Pachymedusa dacnicolor*. These iridophores were of two distinct types which differed with respect to both morphological and physiological features. One type (type I) of iridophore responded to some hormones by a reversible retraction of cellular processes and rounding up of cells.

Physiologically active iridophores are also known to be present in the integument of some species of fish, namely the neon tetra, *Paracheirodon innesi* [16], and the blue damselfish, *Chrysiptera cyanea* [17]. In iridophores of the damselfish, the motility is assumed to involve simultaneous changes in the distance between contiguous platelets in all the piles of platelets within the cells, and such changes cause a shift in the spectral reflectance from the cells [18]. The situation may be similar to that in iridophores of the neon tetra.

Thus, motile iridophores in fishes can be classified into two types, in terms of motility: the damselfish type, where changes occur in the distance between adjoining platelets; and the goby type, where the intracellular migration of platelets occurs. Quite recently, we found that iridophores in the integument of some species of Gobiidae are motile. The motility appears to be of the goby type [19, Honma and Iga, unpubl.].

In the centripetal migration of platelets, the course and the velocity of the migration are not always linear. The movement is very slow, as in iridophores in preparations of scales [8, 20]. As far as we know, the movements may be the slowest of those examined in fish chromatophores [21–25]. The present findings are important for elucidation of the mechanisms of movement of the iridophores.

MSH possesses strong pigment-dispersing action in melanophores of poikilothermal vertebrates [1, 26], and Ca^{++} is indispensable for its action [27–29]. Such a dependence of the action of MSH on Ca^{++} was also shown in some non-melanophoral, motile chromatophores of fishes, namely in platyfish erythrophores, and in xanthophores as well as leucophores of the medaka, *Oryzias latipes* [30]. The involvement of Ca^{++} may be important for signal transduction from the receptor to the catalytic unit of adenylate cyclase and/or for the activation of the catalytic unit [31–33]. MSH acts to induce "aggregation" of platelets in the iridophores of *Odontobutis obscura*, as it does in preparations of isolated scales [8], and Ca^{++} is indispensable for its action. Upon subsequent application of standard saline, in the absence of the peptide, after prolonged treatment with MSH in a Ca^{++} -free medium, the platelets in the iridophores began to aggregate. This result suggests a role for Ca^{++} in transduction of signal generated by MSH.

Iridophores in the integument of the neon tetra were light-sensitive and changed in color from deep violet to blue-green in response to illumination [16]. Most of the cultured iridophores from the integument of the *Odontobutis* goby appear to be light-sensitive. Studies on the light sensitivity of chromatophores in fishes are now in progress.

REFERENCES

- Bagnara, J. T. and Hadley, M. E. (1973) Chromatophores and Color Change. Prentice-Hall, New Jersey.
- Kawaguti, S. and Kamishima, Y. (1964) Electron microscopic study on the iridophore of the Japanese porgy. Biol. J. Okayama Univ., **10**: 75–81.
- Kawaguti, S. (1965) Electron microscopy on iridophores in the scale of the blue wrasse. Proc. Japn. Acad., **41**: 610–613.
- Harris, J. E. and Hunt, S. (1973) The fine structure of iridophores in the skin of the Atlantic salmon (*Salmo salar* L.) Tiss. Cell, **5**: 479–488.
- Hawkes, J. W. (1974) The structure of fish skin II. The chromatophore unit. Cell Tiss. Res., **149**: 159–172.
- Fox, D. L. (1976) Animal Biochromes and Structural Colours. Univ. of California Press, Berkeley, Los Angeles.
- Land, M. F. (1972) The physics and biology of animal reflectors. Prog. Biophys. Molec. Biol., **24**: 75–106.
- Iga, T. and Matsuno, A. (1986) Motile iridophores of a freshwater goby, *Odontobutis obscura*. Cell Tissue Res., **244**: 165–171.
- Matsuno, A. and Iga, T. (1989) Ultrastructural observations of motile iridophores from the freshwater goby, *Odontobutis obscura*. Pigment Cell Res., **2**: 431–438.
- Iwata, A., Iwata, M. and Nakano, E. (1986) Changes in the shape of melanophores of the medaka, *Oryzias latipes*, cultured on collagen and fibronectin-coated substrata. Zool. Sci., **3**: 73–81.
- Bagnara, J. T., Hadley, M. E. and Taylor, J. D. (1969) Regulation of bright-colored pigmentation of amphibians. Gen. Comp. Endocrinol., suppl. **2**: 425–438.
- Hadley, M. E. and Goldman, J. M. (1972) The physiological regulation of the amphibian iridophores. In "Pigmentation: Its Genesis and Biologic Control". Ed. by V. Riley, Appleton-Century-Crofts, New York, pp. 225–245.
- Taylor, J. D. and Bagnara, J. T. (1972) Dermal chromatophores. Am. Zool. **12**: 43–62.
- Ide, H. (1973) Effects of ACTH on melanophores and iridophores isolated from bullfrog tadpoles. Gen. Comp. Endocrinol., **21**: 390–397.
- Butman, B. T., Obika, M., Tchen, T. T. and Taylor, J. D. (1979) Hormone-induced pigment translocations in amphibian dermal iridophores, *in vitro*: Changes in cell shape. J. Exp. Zool., **208**: 17–34.
- Lythgoe, J. N. and Shand, J. (1982) Changes in spectral reflexions from the iridophores of the neon tetra. J. Physiol., **325**: 23–34.
- Oshima, N., Sato, M., Kumazawa, T., Okeda, N., Kasukawa, H. and Fujii, R. (1985) Motile iridophores play the leading role in damselfish coloration. In "Pigment Cell 1985: Biological, Molecular and Clinical Aspects of Pigmentation". Ed. by J. Bagnara, S. N. Klaus, E. Paul, and M. Scharlt, Univ. of Tokyo Press, Tokyo, pp. 241–246.
- Kasukawa, H., Oshima, N. and Fujii, R. (1987) Mechanism of light reflection in blue damselfish motile iridophores. Zool. Sci., **4**: 243–257.

- 19 Iga, T., Maeno, N. and Asari, T. (1988) Receptor mechanisms of motile iridophores of the floating goby, *Chaenogobius annularis*. Zool. Sci., **5**: 1211.
- 20 Iga, T., Takabatake, I. and Watanabe, S. (1987) Nervous regulation of motile iridophores of a freshwater goby, *Odontobutis obscura*. Comp. Biochem. Physiol., **88C**: 319–324.
- 21 Green, L. (1968) Mechanism of movements of granules in melanocytes of *Fundulus heteroclitus*. Proc. Natl. Acad. Sci. USA, **59**: 1179–1186.
- 22 Iga, T. (1978) The mode of action of potassium ions on the leukophores of a freshwater teleost, *Oryzias latipes*. J. Exp. Zool., **205**: 413–422.
- 23 Schliwa, M. and Euteneuer, U. (1978) Quantitative analysis of the microtubule system in isolated fish melanophores. J. Supramol. Struct., **8**: 177–190.
- 24 Matsumoto, J., Akiyama, T. and Nakahari, M. (1984) Surface morphology of fish pigment cells: its roles in analyses of their motility and functional differentiation. In "Scanning Electron Microscopy III", Ed. by A. M. F. O'Hare, SEM Inc., Chicago, pp. 1279–1288.
- 25 Obika, M. (1986) Intracellular transport of pigment granules in fish chromatophores. Zool. Sci., **3**: 1–11.
- 26 Fujii, R. and Oshima, N. (1986) Control of chromatophore movements in teleost fishes. Zool. Sci., **3**: 13–47.
- 27 Vesely, D. L. and Hadley, M. E. (1979) Ionic requirements for melanophore stimulating hormone (MSH) action on melanophores. Comp. Biochem. Physiol., **62A**: 501–508.
- 28 Van de Veerdonk, F. C. G., Worm, R. A. A., Seldenrijk, R. and Heussen, A. A. (1979) The role of calcium in hormone-controlled pigment migration in *Xenopus laevis*. In "Pigment Cell". Ed. by S. N. Klaus, Karger, Basel, pp. 72–78.
- 29 Iga, T. and Takabatake, I. (1982) Action of melanophore-stimulating hormone on melanophores of the cyprinid fish *Zacco temminckii*. Comp. Biochem. Physiol., **73C**: 51–55.
- 30 Oshima, N. and Fujii, R. (1985) Calcium requirement for MSH action on non-melanophoral chromatophores of some teleosts. Zool. Sci., **2**: 127–129.
- 31 De Graan, P. N. E., Eberle, A. N. and van de Veerdonk, F. C. G. (1982) Calcium sites in MSH stimulation of *Xenopus* melanophores: studies with photoreactive α -MSH. Mol. Cell. Endocrinol., **26**: 327–339.
- 32 Sawyer, T. K., Hraby, V. J., Hadley, M. E. and Engel, M. H. (1983) α -melanocyte stimulating hormone: chemical nature and mechanism of actions. Amer. Zool., **23**: 529–540.
- 33 De Graan, P. N. E., van de Kamp, A. J., Hup, D. R. W., Gispen, W. H. and van de Veerdonk, F. C. G. (1984) Calcium requirement for α -MSH action on melanophores: studies with forskolin. J. Receptor Res., **4**: 521–536.

Changes in Lipid Composition in the Tail of *Rana catesbeiana* Larvae during Metamorphosis

MASASHI RYUZAKI¹ and MAKOTO OONUKE

Department of Biology and Department of Physiology, Kitasato
University School of Medicine, Sagamihara 228, Japan

ABSTRACT—The composition of simple lipids and phospholipids obtained from the larval tails in *Rana catesbeiana* at Taylor and Kollros (TK) stage V, X, XX, XXI, and XXII–XXIII were analyzed to clarify their relationship with the regressive process of tails during metamorphosis in this frog. The weight percentage of total simple lipid to total lipid (TL) was about 33% at TK stages V and X and increased gradually to about 70% at TK stages XXII–XXIII. That of total phospholipid to TL was about 66% at TK stages V and X decreased gradually to about 28% at TK stages XXII–XXIII. The weight percentage of free fatty acid (FFA) and triglyceride (TG) to TL were about 12–15% and 4% at TK stages V and X, and increased gradually to about 38% and 13% at TK stages XXII–XXIII, respectively. Those of the other simple lipids, i.e., cholesterol and cholesterol ester did not change much during metamorphosis. The weight percentage of phospholipid classes, i.e., phosphatidylethanolamine, phosphatidylcholine, phosphatidylserine, phosphatidylinositol, sphingomyelin and lysophosphatidylcholine to total phospholipid also did not significantly change throughout metamorphosis. The resulting increase in the weight percentage of total simple lipid to TL was due primarily to increase in FFA and TG during the metamorphic climax.

INTRODUCTION

Biochemical changes occurring during anuran metamorphosis have been reviewed by Bennett and Frieden [1], Brown [2], Frieden [3], Weber [4], Fox [5] and Yoshizato [6]. A critical review of these studies shows that although remarkable changes have been described in the ornithine-urea cycle enzymes [7], haemoglobin [8, 9], serum protein [9, 10], visual pigments [11], nucleic acids especially of liver [12] and lysosomal acid hydrolases such as acid phosphatase [13–15], comparatively very little is known of the alternations in the lipids of the anuran tadpoles during metamorphosis.

Whatever information is available on the lipids during anuran metamorphosis comes from the work of Camerio, Italian group, reviewed by Urbani [16], regarding changes during metamorphosis of *Bufo vulgaris* and *Rana esculenta*.

Urbani [17] found an approximate fourfold decrease in the total body lipid of *Bufo vulgaris* during the metamorphosis period. Light and Waschek [18] studied the liver fatty acids of the tadpole and adult *Rana grylio* and reported no appreciable difference in them. Sawant and Varute [19] have reported on the lipid changes; that is, total lipids, neutral lipids and phospholipids, in the tadpole *Rana tigrina* during development. Recently Okamura and Kishimoto [20] have reported on qualitative and quantitative changes in the nervous system glycolipids during metamorphosis of *Xenopus laevis*, and Yates *et al.* [21] studied the patterns of brain gangliosides of *Rana catesbeiana* during metamorphosis and in the adult frog.

Lipids have the potential of serving as a source of biochemical intermediates for the tricarboxylic acid cycle. Their rapid utilization during a period of starvation usually follows when the glycogen reserves are almost depleted. Lipids have also long been recognized as important membrane constituents playing a significant role in various cellular phenomena [22–24]. Striking differences have also been reported in the fatty acids of aquatic and

Accepted September 20, 1989

Received January 20, 1989

¹ To whom reprints request should be addressed.

terrestrial animals [25]. Metamorphosis is a picturesque even in the life cycle of anurans involving biochemical, physiological, and anatomical alternations, which have an adaptive value in the transition from one environment to another. It follows therefore that an insight into the alternations, if any, in the lipids during metamorphosis will be interesting and hence desirable. As a first step with this view, the present author analyzed two kinds of lipids; that is, neutral lipids and phospholipids, contained in the larval tail of *Rana catesbeiana* in order to clarify the relationship between these lipid compositions and the regression of the larval tail during metamorphosis.

MATERIALS AND METHODS

Animals

Rana catesbeiana tadpoles were collected from their natural habitats in the suburbs of Ryugasaki City, Ibaragi Prefecture. The animals fed on boiled spinach in tubs in the laboratory at ca. 18–22°C. Extraction and analysis of lipids from the larval tails were made at five developmental stages of Taylor and Kollros (TK) [26]; that is, V (the length of the limb bud is twice its diameter), X (the margin of the foot paddle is indented between all five toes), XX (one or both fore-legs have protruded), XXI (the angle of the mouth has reached a point midway between the nostril and the anterior margin of the eye) and XXII–XXIII (XXII: the angle of the mouth has reached the level of the middle of the eye, XXIII: the angle of the mouth has reached the level of the posterior margin of the eyeball). Extraction and analysis of lipids from the fat bodies were made at four developmental stages of TK; that is, XV (the proximal toe pads appear), XX, XXI and XXII–XXIII. Extraction and analysis of lipids from the fat body were also made on the adult female frog. The fat bodies of tadpoles and adult frogs, as well as the whole larval tails, were subjected to chemical analysis. After the animals were pithed, samples were removed from the body, washed in saline, and analyzed immediately.

Lipid extraction

The total lipids were extracted by our modification [27] of the Folch method [28]. The samples were homogenized with 20 volumes of chloroform/methanol (2:1 or 1:2, v/v) by the use of an ultrahomogenizer, UH-1 type, Nissei, Tokyo. The extracts were filtered through a Büchner funnel. The residues were again homogenized with 20 volumes of chloroform/methanol (2:1 or 1:2, v/v). The extracts were combined and concentrated to dryness in a rotary evaporator under nitrogen. The residue obtained was dissolved in chloroform/methanol (2:1, v/v) and was filtered through a glass filter (GA-100, Toyoroshi, Tokyo). The soluble material was concentrated to dryness in a rotary evaporator under nitrogen and then the dry lipid samples were weighed. The total lipids in the samples were determined gravimetrically. The dry lipid samples were dissolved in 25 ml of chloroform/methanol (2:1, v/v), flushed with nitrogen and stored at –20°C for lipid analysis.

Separation of simple lipids and phospholipids

Thin-layer plates of Silica Gel HR (Merk, Darmstadt, West Germany) were prepared according to routine procedure. Sodium carbonate impregnated plates were made by the method of Skipski *et al.* [29]. The lipid samples dissolved in chloroform/methanol (2:1, v/v) were applied with a Terumo microsyringe (MS-N25) on the activated plates. Simple lipids were separated by one-dimensional thin-layer chromatography (TLC) on layers of Silica Gel HR using hexane/diethyl ether/acetic acid (85:15:2, v/v/v) as developing solvent. Phospholipids were separated by one-dimensional TLC on layers of Silica Gel HR impregnated with sodium carbonate using chloroform/methanol/acetic acid/water (50:25:8:4 or 25:15:4:2, v/v/v/v) [29] as developing solvent. Authentic standards of the simple lipids and phospholipids (Sigma) were cochromatographed in each respective run.

Identification of simple lipids and phospholipids on the dried plates was made by exposing the plate to iodine vapour. The phospholipid spots were further identified by employing the following sprays: Dittmer and Lester's reagent [30] and Vaskovsky's modified spray [31] for general phos-

pholipids, ninhydrin (0.2% in butanol) for phospholipids containing free amino groups, Dragendroff reagent [32] for choline phospholipids, p-benzoquinone for ethanolamine, ammonium silver nitrate for inositol and mercuric oxide barium acetate for inositol. Details of these sprays and their diagnostic importance in thin-layer chromatography are critically described by Marinetti [33]. The simple lipids were identified by employing a dichromate sulfuric acid spray [34]. The detection of cholesterol and cholesterol ester was further confirmed by employing antimony trichloride spray [35].

Infrared spectra of the simple lipids and phospholipids were measured by pressing a film between NaCl plates.

Separation of phospholipid spots and estimation of phospholipids

Phospholipids were fractionated by one-dimensional TLC as described above. Segments of the plate containing each phospholipid were scraped off and the amount of each phospholipid was determined by measuring the phosphorus content, according to the method of Bartlett [36].

Separation of simple lipid spots and estimation of simple lipids

Simple lipids were separated by one-dimensional TLC as described above. The segment of the Silica Gel HR layer containing each simple lipid was scraped off and the amount was measured. The amount of triglyceride was estimated according to the method of Snyder and Stephens [37]. The free fatty acid isolated by the preparative Silica Gel HR layer was esterified with 3% hydrogen chloride-methanol at 100°C for three

hours. The fatty acid methyl esters were analyzed and estimated at 160°C by a Shimadzu GC-5A unit equipped with a 1.5 m × 3 mm glass column packed with 15% ethylene glycol succinate on Celite 545 HMDS. Methyl heptadecanoate (Applied Science Laboratories Inc., Lot 1933, Penna.) was used as the internal standard. The amount of cholesterol and cholesterol ester was estimated according to the method of Zak [38].

For confirmation of results, the thin-layer chromatographic separations and the assays of phospholipids and simple lipids were carried out in triplicate sets of tadpoles in batches as described above.

RESULTS

Lipid content in larval tail

The lipid content from the whole tail of each specimen at various stages of metamorphosis (TK stage XX to XXII-XXIII) of tadpoles is recorded in Table 1. The total lipid content at TK stage XX was about 5.44 of wet tissue and 52.05 mg/g of tissue residue after lipid extraction, and gradually increased during metamorphosis. The content was found to be about 11.13 mg/g wet tissue and 77.02 mg/g residue at TK stages XXII-XXIII.

Thin-layer chromatograms of total lipid from larval tail

Thin-layer chromatographic patterns of total lipid from the whole tails of each specimens at the various stages of premetamorphic stage (TK stages V and X) and metamorphic climax stage (TK stage XX to XXII-XXIII) of tadpoles, as shown in Figure 1, quantitatively indicate that the total

TABLE 1. The content of total lipids from the metamorphosing tadpole tail of *Rana catesbeiana*

	Developmental stages of Taylor and Kollros		
	X	XXI	XXII
Total lipid			
mg/g of wet tissue weight	5.44 ± 0.10	6.88 ± 1.22	11.13 ± 0.46
mg/g of residue of the tissue after lipid extraction	52.05 ± 1.11	67.20 ± 7.65	77.02 ± 5.60

The data are expressed as mg of lipid per g of wet tissue and per g of residue of the tissue after lipid extraction. The values are the mean ± SD of triplicate specimens.

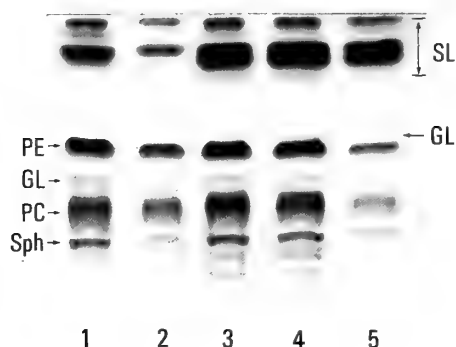


FIG. 1. Thin-layer chromatograms of total lipids from the tadpole tail of *Rana catesbeiana* at the following five developmental stages of Taylor and Kollros (TK); i.e. 1(V), 2(X), 3(XX), 4(XXI) and 5(XXII-XXIII). Total lipids were separated by one-dimensional thin-layer chromatography (TLC) on a layer of Silica Gel HR using chloroform/methanol/water (65:25:4, v/v/v) as developing solvent. The bands are the lipids, visualized by spray application of anthrone-sulfuric acid. SL, simple lipid; PE, phosphatidylethanolamine; PC, phosphatidylcholine; Sph, sphingomyelin; GL, glycolipid.

lipids consist mainly of simple lipids and phospholipids as the major component, and glycolipids which were positively visualized by spraying with anthrone-sulfuric acid. By comparing these chromatographic patterns, it was found that the simple lipid fraction which contains free fatty acid (FFA) and triglyceride (TG) was quantitatively different at TK stage XX to XXII-XXIII than those at TK stages V and X.

Thin-layer chromatograms of phospholipids from larval tail

Thin-layer chromatographic separation of the phospholipids at the various stages of development of tadpoles, as shown in Figure 2, quantitatively indicates that the total phospholipids consist mainly of phosphatidylethanolamine (PE), phosphatidylcholine (PC), phosphatidylserine (PS), phosphatidylinositol (PI), sphingomyelin (Sph), as the major components and lysophosphatidylcholine (LysoPC). A quantitative comparison shows that PC and PE were predominant, whereas PS, Sph and PI were present in lesser concentrations and LysoPC occurred in trace amount. Except for the minor quantitative changes, the gross patterns of

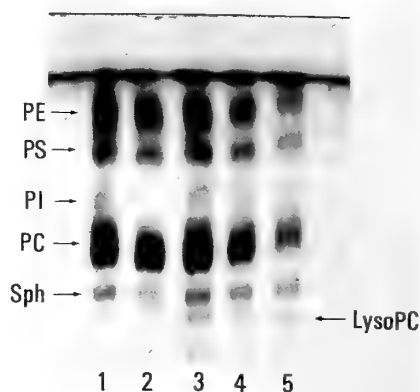


FIG. 2. Thin-layer chromatograms of total phospholipids from the tadpole tail of *Rana catesbeiana* at the following five developmental stages of TK; i.e. 1(V), 2(X), 3(XX), 4(XXI) and 5(XXII-XXIII). Total phospholipids were separated by one-dimensional TLC on a layer of Silica Gel HR impregnated with sodium carbonate using chloroform/methanol/acetic acid/water (50:25:8:4 or 25:15:4:2, v/v/v/v) [29] as developing solvent. The phospholipids are visualized by spray application of 50% aqueous sulfuric acid. PE, phosphatidylethanolamine; PS, phosphatidylserine; PI, phosphatidylinositol; PC, phosphatidylcholine; Sph, sphingomyelin; LysoPC, lysophosphatidylcholine.

the phospholipids did not show any significant changes during the various developmental stages of the tadpoles.

Thin-layer chromatograms of simple lipids from larval tail

Thin-layer chromatographic separation of the simple lipids of the various developmental stages of the tadpoles, as shown in Figure 3, indicates that the total simple lipids consist mainly of TG, FFA, cholesterol (Chol) and cholesterol ester (Chol.E). By comparing each chromatographic patterns, it was found that the gross patterns of Chol and Chol.E did not show any significant changes at the various developmental stages. However, FFA and TG did show a qualitative change. Comparing gross patterns of FFA; qualitatively FFA was predominant at TK stage XX to XXII-XXIII, although FFA occurred in relatively low concentration at TK stages V and X.

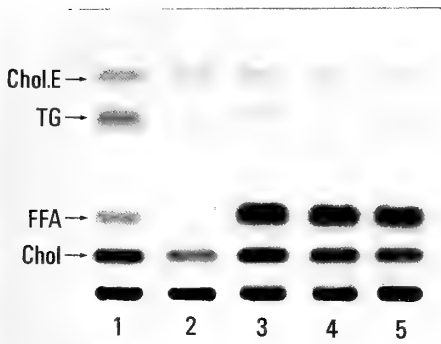


FIG. 3. Thin-layer chromatograms of total simple lipids from the tadpole tail of *Rana catesbeiana* at the following five developmental stages of TK; i.e. 1(V), 2(X), 3(XX), 4(XXI) and 5(XXII-XXIII). Total simple lipids were separated by one-dimensional TLC on a layer of Silica Gel HR using hexane/diethyl ether/acetic acid (85:15:2, v/v/v) as developing solvent. The bands are the lipids, visualized by spray application of 50% aqueous sulfuric acid. Chol. E, cholesterol ester; TG, triglyceride; FFA, free fatty acid; Chol, cholesterol.

Thin-layer chromatograms of simple lipids from blood, liver and muscle of larvae and adult frogs

Thin-layer chromatographic separation of the simple lipids from the blood, liver and muscle of the metamorphic climax stage (TK stage XXI) of tadpoles and adult frog in *Rana catesbeiana* qualitatively indicates that total simple lipids consist mainly of TG, FFA, Chol and Chol.E (Fig. 4). In liver and muscle tissue, TG and FFA qualitatively were predominant in metamorphic climax stage (TK stage XXI) of tadpoles, whereas they present in lesser concentration in the adult frog. FFA occurred in trace amount in the blood at both animal stages.

Thin-layer chromatograms of simple lipids from fat bodies of tadpoles

Thin-layer chromatographic patterns of total simple lipids from a whole fat body during a period when the growth rate was reduced and metamorphic change accelerated to give rise to the metamorphic climax stage (TK stage XX, XXI and XXII-XXIII) of the tadpoles indicate that a large TG fraction is present in total simple lipids at each stage (Fig. 5).

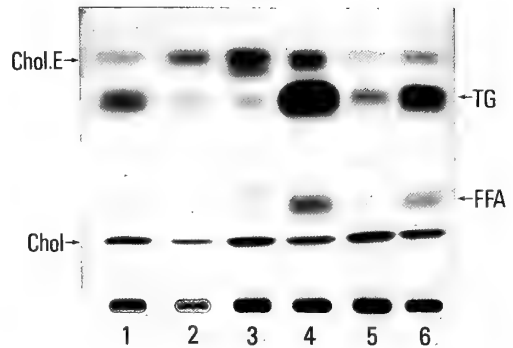


FIG. 4. Thin-layer chromatograms of total simple lipids from the blood, liver and muscle in metamorphosing tadpoles at TK stage XXI and in the adult frog of *Rana catesbeiana*. Total simple lipids were separated by one-dimensional TLC on a layer of Silica Gel HR using hexane/diethyl ether/acetic acid (85:15:2, v/v/v) as developing solvent. The bands are the lipids, visualized by spray application of 50% aqueous sulfuric acid. 1, adult frog blood; 2, tadpole blood; 3, adult frog liver; 4, tadpole liver; 5, adult frog muscle; 6, tadpole muscle. Abbreviations are described in Fig. 3.

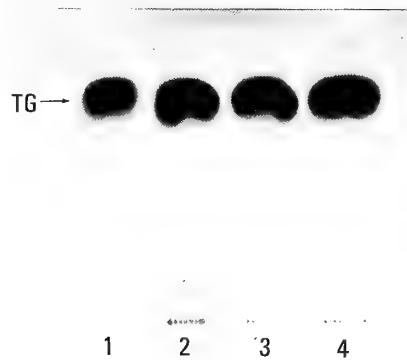


FIG. 5. Thin-layer chromatograms of total simple lipids from the fat body of *Rana catesbeiana* at following four developmental stages of TK; i.e. 1(XV), 2(XX), 3(XXI) and 4(XXII-XXIII). Total simple lipids were separated by one-dimensional TLC on a layer of Silica Gel HR using hexane/diethyl ether/acetic acid (85:15:2, v/v/v) as developing solvent. The bands are the lipids, visualized by spray application of 50% aqueous sulfuric acid. TG, triglyceride.

Thin-layer chromatograms of simple lipids from fat bodies of adult females

Thin-layer chromatographic patterns of total



FIG. 6. Thin-layer chromatograms of total simple lipids from the fat body in duplicate mature female specimens (1, 2) of *Rana catesbeiana*. Total simple lipids were separated by one-dimensional TLC on a layer of Silica Gel HR using hexane/diethyl ether/acetic acid (85:15:2, v/v/v) as developing solvent. The bands are the lipids, visualized by spray application of 50% aqueous sulfuric acid. TG, triglyceride.

simple lipids from the whole fat body of the mature female *Rana catesbeiana* qualitatively indicate that a relatively large amount of TG is present at each of various stages of development, as described above (Fig. 6).

Quantitative data of lipid classes

The alternations in various components of phospholipids and simple lipids are shown in Table 2. The quantitative data of phospholipid classes, PE, PS, PI, PC, Sph and LysoPC, at the 5 developmental stages of Taylor and Kollros (TK), V, X, XX, XXI and XXII-XXIII, were obtained by the routine method previously described. The quantitative data of simple lipid classes, FFA, TG, Chol and Chol.E, at the same five developmental stages were also obtained following the same routine method.

The total simple lipid content of total lipid remained essentially unchanged between TK stages V and X at ca. 33% during development. It gradually increased during metamorphic climax stage, becoming about 70% at TK stages XXII-XXIII.

The quantitative data for the total phospholipid amount in total lipid also remained unchanged between TK stages V and X, at ca. 66%, during development. However, in contrast with the quantitative data for the simple lipid fraction, the data for total phospholipid gradually decreased during metamorphosis and the content was found to be ca. 29% at TK stages XXII-XXIII. During meta-

TABLE 2. Analysis of the lipid composition from the tadpole tail during metamorphosis of *Rana catesbeiana*

	Developmental stages of Taylor and Kollros				
	V	X	XX	XXI	XXII-XXIII
Total simple lipid (% total lipid)	32.6±2.8	33.0±3.1	55.4±3.4	60.3±2.3	70.1±3.1
Total phospholipid (% total lipid)	66.6±3.4	66.1±2.3	43.3±1.5	38.5±1.2	28.7±1.9
<i>Simple lipid classes (% total lipid)</i>					
Free fatty acid	15.1±0.6	12.3±0.5	30.4±1.6	29.8±1.3	38.3±1.4
Cholesterol	10.1±0.4	12.8±0.7	11.8±0.6	14.2±0.5	13.1±0.5
Triglyceride	3.5±0.2	4.2±0.2	9.2±0.6	11.7±0.6	13.2±0.7
Cholesterol ester	3.9±0.3	3.7±0.2	4.0±0.3	4.6±0.4	5.5±0.4
<i>Phospholipid classes (% total phospholipid)</i>					
Phosphatidylcholine	45.6±0.5	48.2±1.2	45.1±2.1	43.7±0.8	41.2±1.8
Phosphatidylethanolamine	33.2±0.9	30.0±1.3	33.8±1.4	31.3±0.5	28.3±1.4
Phosphatidylserine	7.9±0.7	5.0±0.2	4.3±0.8	5.5±0.6	5.0±0.7
Phosphatidylinositol	2.7±0.6	4.0±0.5	4.0±0.6	4.6±0.4	4.2±0.5
Sphingomyelin	7.6±0.5	7.3±0.4	8.1±0.8	9.8±0.6	13.7±0.9
Lysophosphatidylcholine	3.0±0.3	5.5±0.2	4.7±0.5	5.2±0.5	7.6±0.8

The data are expressed as the weight percentage. The values are mean±SD of triplicate specimens.

morphosis, there was a compensatory relationship in amount between the simple lipid and phospholipid fraction.

As shown in Table 2, a large amount of free fatty acid was detected. The weight percentage of free fatty acid in total lipid was about 12 to 15% during the premetamorphic stage from TK stages V and X increased dramatically to about 30 to 38% during the metamorphic climax stage from TK stage XX to XXII-XXIII. The weight percentage of triglyceride was about 4% at the premetamorphic stage from stage TK V to X. Though the ratio of triglyceride in total lipid was not as large as that of free fatty acid, the relative percentage of both substances dramatically increased after TK stage XX. The ratio of cholesterol to total lipid was approximately 10 to 13% at TK stages V and X, and did not significantly change at TK stage XX to XXII-XXIII. Cholesterol ester was detected at each TK stage from V to XXII-XXIII: the ratio of cholesterol ester to total lipid was about 4 to 6%, and significant changes were not detected throughout the metamorphosis. Phosphatidylcholine and phosphatidylethanolamine were the major components of phospholipid classes. Phosphatidylcholine occupied about 41 to 48% of total phospholipids, while phosphatidylethanolamine occupied about 28 to 34% throughout TK stage V to XXII-XXIII. The ratio of phosphatidylcholine and phosphatidylethanolamine to total phospholipids was relatively stable. The ratio of sphingomyelin to total phospholipids did not change during TK stage V to X, while afterward it increased slightly until TK stages XXII-XXIII. The ratio of phosphatidylserine, phosphatidylinositol and lysophosphatidylcholine did not significantly change from TK stage V to XXII-XXIII.

DISCUSSION

From the present study, it is evident that glycerol-based phospholipids including phosphatidylcholine, phosphatidylethanolamine, phosphatidylserine and phosphatidylinositol are predominantly present among the lipids in larval tissues and in eucaryotic cell membranes [24, 39] (Fig. 2, Table 2). Sphingomyelin (sphingosine-based lipids) and cholesterol are also major components

of the cell membrane. In this animal, triglycerides may also play roles in energy storage as described for other animals [40] in whose adipose tissue they are present (Figs. 4, 5, 6). Since many biochemical alternations that occur during the metamorphosis of anuran tadpoles have been shown to be influenced by thyroxine [1, 3, 5, 6, 41], significant alternations in lipids during growth and metamorphosis may also be reasonably considered to take place under its influence. Thyroid hormone acts directly on each type of cell to induce two different events; death of epidermal cells, mesenchymal fibroblasts and probably muscle cells, and activation of macrophages during metamorphosis [5, 6].

Lipid seems to be an important constituent of the tadpole body and the values for percentage total lipids and neutral lipids also increase during pre- and prometamorphosis; this is followed by significant decrease during the metamorphic climax. Phospholipids, on the other hand, apparently do not undergo significant variation on a percentage body weight basis, though during larval development, increase in their amounts is discernible [19]. Urbani [17] observed a fourfold decrease in total lipid content during metamorphosis. Sawant and Varute [19] showed such decrease to be due to that in various constituents of neutral lipids and phospholipids.

During the climax period, when tadpoles do not feed and histolytic events such as degeneration of internal gills, skin degeneration in fore limb window formation and tail regression occur maximally, lipid content decrease sharply, especially that of neutral lipids such as triglycerides that accumulate during development and endogenous energy alone is available.

The decrease in total phospholipids during metamorphosis may quite likely be due to the breakdown of tail cell membranes whose phospholipids form integral components in the histolytic events of metamorphosis. This is supported by the fact that fatty acids are not present in the early stages of metamorphosis. The catabolic breakdown of phospholipids leads to the formation of fatty acids and nitrogenous bases [23]. Phospholipid degradation in *E. coli* has been summarized by Rock and Cronan [42] as follows. Phospholipid

degradation, i.e., the hydrolysis of fatty acids from the 1-position and 2-position of phospholipids, is hydrolyzed by phospholipase A, and in particular, the hydrolysis of fatty acids from the 1-position occurs most rapidly in the cells of *E. coli*. Phospholipase A is located in the soluble fraction (cytoplasm) and outer cell membranes of *E. coli*. Lysophospholipase is located in the soluble fraction and inner cell membranes of *E. coli*. The biochemical and physiological functions of these degradative enzymes remain unknown in amphibian cells during development and metamorphosis. However, a similar phenomenon of phospholipid degradation by these enzyme in macrophages may possibly occur during the regression of tadpole tails in *Rana catesbeiana*.

The present study demonstrates that there may possibly be a correlation between the regressive process of this tadpole tail and the presence of relatively large amounts of free fatty acids during metamorphosis. It would thus follow these free fatty acids may mainly be those hydrolyzed from the 1-position and 2-position of phospholipids during metamorphosis. It is generally known that the transport of fatty acids is a major function of triglycerides in mammals [40]. In this animals, free fatty acids may be stabilized by association with albumin or similar proteins, and albumin or similar proteins may carry fatty acids from the tail to the liver or fat body. These fatty acids may be regarded as triglyceride components in a fat body which is produced in this tadpole during metamorphosis. Triglycerides may play major roles in energy storage as deposits of adipose tissue. Additional research should be conducted for greater clarification of the functions of phospholipid degradative enzymes in the regressive process of tadpole tails during metamorphosis.

Quantitative and qualitative data on glycolipids in the tadpole tail during metamorphosis in *Rana catesbeiana* will be reported in the next publication.

ACKNOWLEDGMENTS

The author is especially indebted to M. S. Ralph Johnston for his critical review of the manuscript.

REFERENCES

- 1 Bennett, T. P. and Frieden, E. (1962) Metamorphosis and biochemical adaptations in amphibia. In "Comparative Biochemistry". Vol. 1VB, Ed. by M. Florkin and H. S. Mason, Academic Press, New York, pp. 483-556.
- 2 Brown, G. W. Jr. (1964) The metabolism of amphibia, In "Physiology of Amphibia". Ed. by J. H. Moore, Academic Press, New York, pp. 1-98.
- 3 Frieden, E. (1968) Biochemistry of amphibian metamorphosis. In "Metamorphosis: A Problem in Developmental Biology". Ed. by W. Etkin and L. I. Gilbert, North-Holland, Amsterdam, pp. 349-398.
- 4 Weber, R. (1967) Biochemistry of amphibian metamorphosis. In "The Biochemistry of Animal Development". Vol. II, Academic Press, New York, pp. 227-252.
- 5 Fox, H. (1984) Metamorphosis in anurans. In "Amphibian Morphogenesis". Ed. by H. Fox, Human Press Inc., Clifton, pp. 9-16.
- 6 Yoshizato, K. (1986) How do tadpoles lose their tails during metamorphosis? Zool. Sci., **3**: 219-226.
- 7 Brown, G. W. Jr., Brown, W. R. and Cohen, P. P. (1959) Comparative biochemistry of urea cycle enzymes in metamorphosing *Rana catesbeiana* tadpoles. J. Biol. Chem., **191**: 377-378.
- 8 Trader, C. D., Wortham, J. S. and Frieden, E. (1963) Haemoglobin: molecular changes during metamorphosis. Science, **139**: 918-919.
- 9 Manwell, C. (1966) Metamorphosis and gene action-I. Electrophoresis of dehydrogenases, esterases, phosphatases, haemoglobin and other soluble proteins of tadpoles and adults of bull frog. Comp. Biochem. Physiol., **17**: 805-825.
- 10 Herner, A. E. and Frieden, E. (1960) Biochemistry of anuran metamorphosis-VII. Changes in serum proteins during spontaneous and induced metamorphosis. J. Biol. Chem., **235**: 2845-2851.
- 11 Wald, G. (1960) The distribution and evolution of visual pigments. In "Comparative Biochemistry". Vol. I, Ed. by M. Florkin and H. S. Mason, Academic Press, New York, pp. 311-345.
- 12 Tata, J. R. (1966) Requirement for RNA and protein synthesis for induced regression of the tadpole tail in organ culture. Devel. Biol., **13**: 77-94.
- 13 Weber, R. (1964) Ultrastructural changes in regressing tail muscles of *Xenopus* larvae at metamorphosis, J. Cell Biol., **22**: 481-487.
- 14 Varute, A. T. and More, N. K. (1971) β -Glucuronidase in alimentary canal of tadpoles of *Rana tigrina* in growth and metamorphosis. Comp. Biochem. Physiol., **38B**: 225-233.
- 15 Varute, A. T. (1972) Histochemical of β -glucuronidase in the resorbing tails of tadpoles of *Rana tigrina* at metamorphosis. Acta Histochem.,

- 41: 306-324.
- 16 Urbani, E. (1962) Comparative biochemical studies on amphibian and invertebrate development. In "Advances in Morphogenesis". Vol. II, Ed. by M. Ambercombie and J. Brachet, Academic Press, New York, pp. 61-108.
 - 17 Urbani, E. (1956) Lipases and lipids in the embryonic and larval developments of *Bufo vulgaris* and *Rana esculenta*. Atti Acad. Nazl. Lincei, **21**: 498-503.
 - 18 Light, R. L. and Waschek, C. C. (1965) Liver fatty acids of *Rana grylio* tadpoles and frogs. Comp. Biochem. Physiol., **15**: 167-173.
 - 19 Sawant, V. A. and Varute, A. T. (1973) Lipid changes in the tadpoles of *Rana tigrina* during growth and metamorphosis. Comp. Biochem. Physiol., **44B**: 729-750.
 - 20 Okamura, N. and Kishimoto, Y. (1983) Changes in nervous system glycolipids during metamorphosis of *Xenopus laevis*. J. Biol. Chem., **258**: 12243-12246.
 - 21 Yates, A. J., McGill, J. M., Markowitz, D. L. and Tassava, R. A. (1985) The patterns of brain gangliosides of *Rana catesbeiana* during metamorphosis and in adult. Devel. Biol., **110**: 255-258.
 - 22 Ansell, G. B. and Howthorne, J. N. (1964) Phospholipids-Chemistry, Metabolism and Function. Elsevier Scientific Publ. Co., London, pp. 1-427.
 - 23 Dawson, R. M. C. (1966) The metabolism of animal phospholipids and their turnover in cell membranes. In "Essays in Biochemistry". Vol. II, Ed. by C. Chapman, Academic Press, New York, pp. 59-115.
 - 24 Ansell, G. B., Dawson, R. M. C. and Howthorne, J. N. (1973) Form and Function of Phospholipids. Elsevier Scientific Publ. Co., Amsterdam, pp. 1-494.
 - 25 Hilditch, T. P. (1956) The Chemical Constitution of Natural Fats. 3rd Edition, Ed. by T. P. Hilditch, John Wiley, New York, pp. 25-145.
 - 26 Taylor, A. C. and Kollros, J. J. (1946) Stages in the normal development of *Rana pipiens* larvae. Anat. Rec., **94**: 7-24.
 - 27 Ryuzaki, M., Kojima, H. and Tamai, Y. (1975) Study on amphibian lipids II. Characteristic constituent of monoglycosylceramides from the skin of three frog species. Comp. Biochem. Physiol., **52C**: 81-84.
 - 28 Folch, J., Lee, M. and Sloane-Stanley, G. H. (1957) A simple method for the isolation and purification of total lipids from animal tissues. J. Biol. Chem., **226**: 497-509.
 - 29 Skipski, V. P., Peterson, R. M. and Barvlog, M. (1964) Quantitative analysis of phospholipids by thin-layer chromatography. Biochem. J., **90**: 374-378.
 - 30 Dittmer, J. C. and Lester, R. L. (1964) A simple, specific spray for the detection of phospholipids on thin-layer chromatograms. J. Lipid Res., **5**: 126-127.
 - 31 Vaskovsky, V. E. and Kostatsky, E. Y. (1968) Modified spray for the detection of phospholipids on thin-layer chromatograms. J. Lipid Res., **9**: 396-401.
 - 32 Waldi, D. (1965) Spray reagents for thin-layer chromatography. In "Thin-Layer Chromatography". Ed. by E. Stahl, Academic Press, New York, pp. 483-484.
 - 33 Marinetti, A. V. (1966) Chromatographic separation, identification and analysis of phosphatides. J. Lipid Res., **3**: 1-20.
 - 34 Mangold, H. K. and Kammereck, R. (1962) Thin-layer chromatography of lipids. J. Am. Oil Chem. Soc., **39**: 201-205.
 - 35 Weicker, H. (1959) Specific detection tests for neutral lipids. Klin. Wochscur., **37**: 763-765.
 - 36 Bartlett, G. R. (1957) Phosphorus assay in column chromatography. J. Biol. Chem., **234**: 466-468.
 - 37 Snyder, F. and Stephens, N. (1959) A simplified spectrophotometric determination of ester groups in lipids. Biochim. Biophys. Acta, **34**: 244-245.
 - 38 Zak, B. (1957) Simple rapid microtechnic for serum total cholesterol. Am. J. Clin. Path., **27**: 583-588.
 - 39 Law, J. H. and Snyder, W. R. (1972) Membrane lipids. In "Membrane Molecular Biology". Ed. by D. E. Vance and J. E. Vance, Benjamin/Cummings Publ. Co., Menlo Park, pp. 213-241.
 - 41 Etkin, W. (1968) Hormonal control of amphibian metamorphosis. In "Metamorphosis: A Problem in Developmental Biology". Ed. by W. Etkin and L. I. Gilbert, North-Holland, Amsterdam, pp. 313-438.
 - 42 Rock, C. O. and Cronan, J. E. (1985) Lipid metabolism in procaryotes. In "Biochemistry of Lipids and Membranes". Ed. by D. E. Vance and J. E. Vance, Benjamin/Cummings Publ. Co., Menlo Park, pp. 73-114.

Inheritance of the Color Patterns of the Blue Snakeskin and Red Snakeskin Varieties of the Guppy, *Poecilia reticulata*

V. P. E. PHANG, A. A. FERNANDO¹ and E. W. K. CHIA

Department of Zoology, National University of Singapore, Kent Ridge,
Singapore 0511, and ¹Freshwater Fisheries Section, Primary Production
Department, Sembawang Road 17 km, Singapore 2776

ABSTRACT—The Blue Snakeskin (BSS) and Red Snakeskin (RSS) varieties are popular strains commercially cultured in Singapore. The blue-black tail color of BSS guppies is determined by a dominant X-linked gene (*Blt*) and the silvery snakeskin pattern on the body of males is under the control of a Y-linked gene (*Ssb*). The Y-linked snakeskin tail pattern gene (*Sst*) though present in BSS males is masked by the blue-black tail color gene (*Blt*). The putative genotypes for males and females of the BSS variety are $X_{Blt}Y_{Ssb,Sst}$ and $X_{Blt}X_{Blt}$, respectively. The red tail color of the RSS variety is due to an X-linked dominant gene (*Rdt*). The snakeskin body pattern of RSS males is under the control of the Y-linked *Ssb* gene while the black reticulations on the tail is due to interaction between the snakeskin tail pattern gene (*Sst*) and the red tail gene (*Rdt*). The proposed genotypes for males and females of the RSS variety are $X_{Rdt}Y_{Ssb,Sst}$ and $X_{Rdt}X_{Rdt}$, respectively. An estimate of 0.9% crossover frequency was obtained between the Y-linked *Ssb* and *Sst* genes and a 2.7 % crossover rate of the *Blt* gene from the X- to the Y-chromosome.

INTRODUCTION

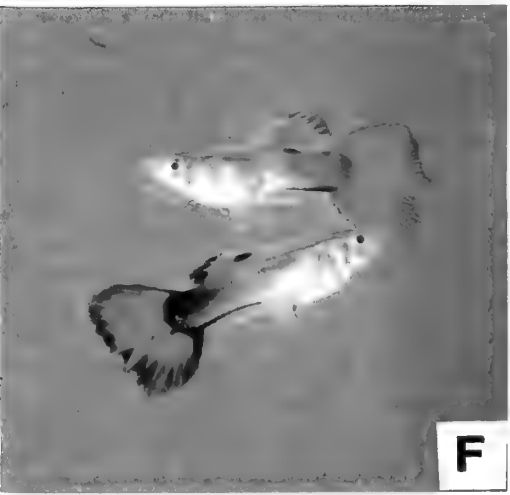
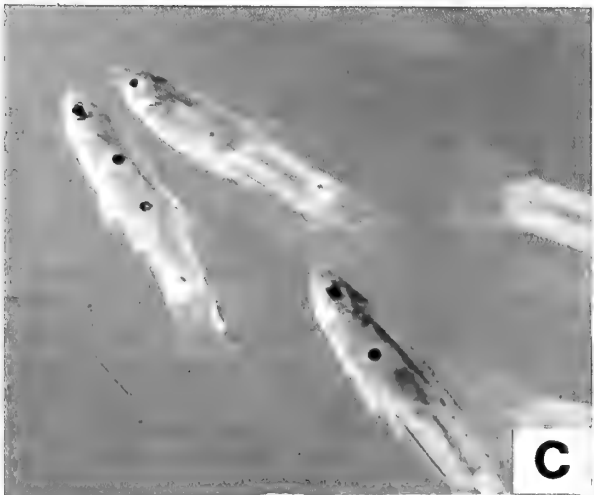
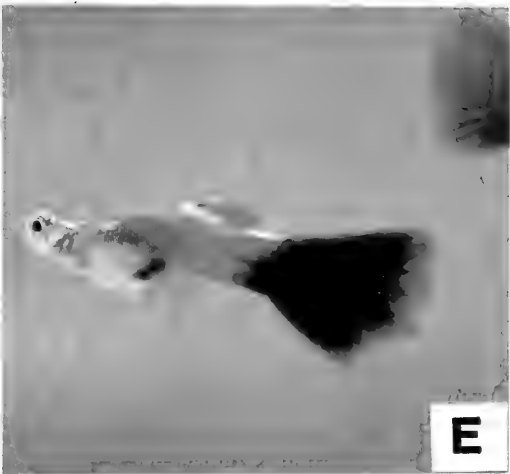
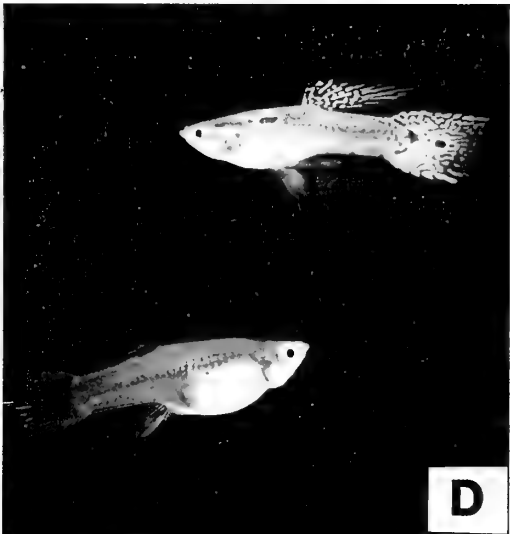
The guppy, *Poecilia reticulata* being a voracious omnivorous feeder and tolerant of polluted waters was introduced to Singapore and other parts Asia for mosquito control [1]. It has been commercially cultured in Singapore since the 1950's and is economically the most important species of freshwater ornamental fish produced almost exclusively for the export market. The wide variation of brilliant and beautiful colors on the body, tail and dorsal fin of male guppies makes it one of the most popular and ubiquitous ornamental fish. About 30 domesticated varieties of guppies are produced on monoculture farms in Singapore. Each farm specialises in 8–12 varieties [2]. Guppy farmers continuously strive to improve the quality of the fish and to breed new varieties with novel color patterns. To do so it is important to understand the gene control of the color phenotypes of domesticated guppies. So far there are few reports on the

inheritance of color patterns of domesticated varieties of the guppy [3–7]. The objective of this study is to elucidate the gene control of the color phenotype of the Blue Snakeskin and Red Snakeskin varieties of *P. reticulata* cultured in Singapore.

MATERIALS AND METHODS

Source of the fish

Two- to three-weeks old fry of the Blue Snakeskin (BSS) and Red Snakeskin (RSS) varieties were obtained from the Lim Chin Lam Guppy Farm in Singapore. Wild-type (WT) fry were collected from a stream in a rural area of Singapore. Since virgin females were required for the reciprocal crosses, fry were raised in 33 liter clear plastic tanks (20 fish/tank) in the aquarium area of the Department of Zoology, National University of Singapore, at temperatures of 26–28°C. Sexual differentiation takes place at 4–6 weeks of age under laboratory conditions. The young fish were checked daily for developing



males which are recognized by the modification of the anal fin into the gonopodium. Males when spotted were immediately removed and raised separately from females.

Description of the varieties

Adult males and females of the BSS and RSS varieties have total length of 4–5 cm. Adult RSS males have iridescent snakeskin-like reticulations on the olive-brown body and an orange-red colored tail with black reticulations (Fig. 1A). BSS males are also characterized by silvery snakeskin-like pattern on the body but the tails are blue-black in color (Fig. 1B). Both RSS and BSS females lack the snakeskin patterns. RSS females have the normal wild-type olive brown body coloration with tinges of red and opaque white on the tail. BSS females have the WT body coloration and partial expression of the blue-black tail color.

Wild-type guppies are smaller than the domesticated varieties, with marked size differences between males and females. Adult WT females are 3.0–3.5 cm long while adult males are about 2 cm long. WT males have highly polymorphic color patterns, consisting of spots or patches of various colors on the body, tail and sometimes the dorsal fin while the females lack color patterns (Fig. 1C).

Reciprocal crosses

The inheritance of the color phenotypes of the BSS and RSS varieties were elucidated by performing single-pair reciprocal crosses between each of them and the wild-type stock, using 3-month old sexually mature virgin fish. The pairs were kept in eight liter breeding tanks. The following notations were used for the crosses:

- Cross 1A: BSS male \times WT female, Cross
1B: WT male \times BSS female
Cross 2A: RSS male \times WT female, Cross
2B: WT male \times RSS female

Broods were usually produced 4–6 weeks after mating. F_2 broods were obtained from single-pair matings between full-sib F_1 fish. Phenotypic proportions among the F_1 and F_2 progeny were subjected to chi-square tests.

Twenty adult females of the BSS and RSS parental stocks and all the F_1 and F_2 female progeny that were not required for breeding were fed with the androgen, methyl testosterone, to express any inherent color genes [8, 9].

RESULTS

Androgen treatment of BSS and RSS females

When androgen treated the tail color of BSS females deepened to a dark blue no snakeskin pattern was manifested on the body. Androgen treated RSS females developed red color on the tail but not the iridescent snakeskin body pattern or the black reticulations on the tail. These results showed that the BSS and RSS females carried the genes for the blue tail color and red tail color, respectively, but not the genes determining the snakeskin pattern.

Cross between the BSS variety and WT stock

Twelve matings between BSS males and WT females (Cross 1A) gave a total of 120 male and 150 female F_1 progeny (Table 1). The F_1 males had the hyaline tail color of WT guppies and a delicate, silvery snakeskin pattern on the body and tail (Fig. 1D). We called the color phenotype of these F_1 males wild-type snakeskin (WTSS). The F_1 females had blue tinges on the tail which on androgen treatment deepened in color but no snakeskin pattern developed the body or tail. These females were considered to have the blue tail phenotype (BT). Since only the male progeny inherited the snakeskin pattern from the BSS male

FIG. 1.A. Adult male (upper) and female (lower) of the Red Snakeskin variety of the guppy.

FIG. 1.B. Adult female (left) and male (right) of the Blue Snakeskin variety of the guppy.

FIG. 1.C. Three adult male wild-type guppies.

FIG. 1.D. A F_1 male of the cross between BSS males and WT females showing delicate iridescent snakeskin pattern on the body and tail and hyaline wild-type tail (wild-type snakeskin phenotype) (upper). A F_1 female of this cross (lower).

FIG. 1.E. A F_1 male of the cross between WT males and BSS females showing blue tail (BT) phenotype.

FIG. 1.F. Two F_1 male of the cross between WT males and RSS females showing the red tail (RT) phenotype.

TABLE 1. F₁ and F₂ segregation data of reciprocal crosses between the Blue Snakeskin variety and the wild type stock

Cross (Cross No.)	Gen.	No. matings (No. broods)	No. & Phenotypes Males	of Progeny Females	Exp. ratio	χ^2
BSS ♂ × WT ♀ (Cross 1A)	F ₁	12 (12)	120 WTSS	150 BT	1:1	3.33
	F ₂	10 (15)	46 WISS	51 BT	1:1:1:1	1.92
			60 BSS	53 WT		
			[§] 2 WISST			
WT ♂ × BSS ♀ (Cross 1B)	F ₁	12 (12)	97 BT	108 BT	1:1	0.59
	F ₂	12 (15)	76 BT	178 BT	*1:1:2	2.86
			72 WT	[#] 5 WT		

[§] Exceptional F₁ males with wild type body and snakeskin tail pattern (*Sst*).

[#] Exceptional F₂ females (Cross 1B) with hyaline tail color.

* Exp. ratio for the typical F₂ offspring of Cross 1B.

parent, it showed Y-linkage of the genes determining the snakeskin pattern. The presence of snakeskin reticulations on the tail of F₁ males showed that the BSS male parents were carrying the gene for snakeskin tail pattern which was masked by the blue-black tail color. The snakeskin body and tail patterns of another guppy variety, the Green Snakeskin, are controlled by two closely linked genes (*Ssb* and *Sst*) on the Y-chromosome [10]. Absence of the blue tail color of the BSS male parents in F₁ males and presence in all F₁ females gave evidence of X-linkage and dominance of the gene determining the blue tail coloration which has been designated as *Blt* [11]. The recessive allele, *Blt*⁺, present in WT guppies gives the hyaline tail color.

The F₂ generation of Cross 1A consisted of BSS males, WTSS males, BT females and WT females with observed numbers conforming to the 1:1:1:1 expected ratio (Table 1). These results gave evidence that the putative color genotype of BSS males is $X_{Blt}Y_{Ssb,Sst}$ and that for WTSS males is $X_{Blt}+Y_{Ssb,Sst}$. A genetic model is proposed to show segregation of the color genes in Cross 1A (Fig. 2).

However, there were two exceptional F₂ males with WT body color and snakeskin pattern on the tail giving further evidence that the snakeskin body and tail patterns are determined by two Y-linked genes, *Ssb* and *Sst*, respectively. The absence of the expected snakeskin body pattern in these two

males is probably due to crossing-over of the *Ssb* gene from the Y- to the X-chromosome. The crossover frequency between the *Ssb* and *Sst* genes calculated from the F₂ offspring of Cross 1A is 0.9%, two crossovers out of a total of 212 F₂ individuals.

Twelve matings of the reciprocal cross (Cross 1B) between WT males and BSS females gave 12 F₁ broods consisting of 97 males and 108 females, all with blue tails (BT phenotype) and without any snakeskin pattern (Fig. 1E). With the exception of five females with the WT phenotype, the F₂ progeny of this cross segregated into BT males, WT males and BT females according to the 1:1:2 hypothetical ratio. Thus the F₁ and F₂ results gave evidence that the BSS parental females were homozygous for the X-linked dominant blue tail gene (*Blt*) with the genotype being $X_{Blt}X_{Blt}$. Figure 2 shows the proposed genetic model for the segregation of color genes in Cross 1B.

The occurrence of five exceptional F₂ females of Cross 1B, with hyaline tails instead of the expected blue tail color of the typical F₂ females could be due to crossing over of the X-linked *Blt* gene to the Y-chromosome in the F₁ male parents of these individuals. Since there were five crossover females out of a total of 183 F₂ females of Cross 1B, the crossover frequency of the *Blt* gene from the X- to the Y-chromosome in the F₁ females of this cross is 2.7%. Crossovers among the F₂ males cannot be detected (Fig. 2).

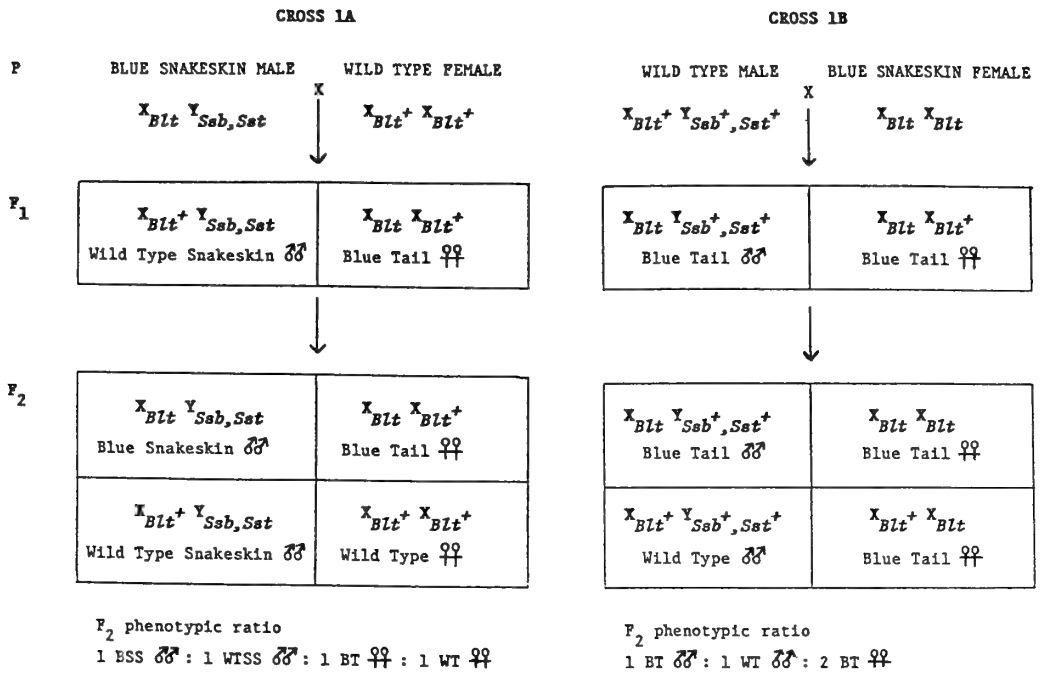


FIG. 2. Schematic diagram of the proposed genetic model for the segregation of color genes in the F₁ and F₂ generations of reciprocal crosses between the Blue Snakeskin variety and wild-type guppies.

TABLE 2. F₁ and F₂ segregation data of reciprocal crosses between the Red Snakeskin variety and the wild type stock

Cross (Cross No.)	Gen.	No. matings (No. broods)	No. & Phenotypes of Progeny		Exp. ratio	χ ²
BSS ♂ × WT ♀ (Cross 2A)	F ₁	6 (12)	117	WTSS	135	1:1
	F ₂	5 (13)	74	RSS	98	1:1:1:1
			76	WTSS	80	
WT ♂ × BSS ♀ (Cross 2B)	F ₁	5 (10)	94	RT	122	1:1
	F ₂	6 (12)	56	RT	140	1:2:1
			70	WT		
*WT ♂ × RSS ♀ (Cross 2B)	F ₁	1 (3)	16	RT	22	1:1:1:1
			10	WTSS	12	

* Exceptional mating between a RSS ♀ producing three exceptional broods, giving evidence that the RSS female parent was heterozygous for the *Ssb* and *Sst* genes.

Cross between the RSS variety and WT stock

Six matings between RSS males and WT females (Cross 2A) produced 12 F₁ broods (Table 2). The 117 F₁ males had hyaline tails and iridescent snakeskin pattern on the body and tail (WTSS phenotype) like the F₁ males of Cross 1A. The 135 F₁ females showed pink tinges on the tail which deepened to red after androgen treatment (RT

phenotype). The pooled F₁ data conformed to the 1 WTSS male: 1 RT female. Thus, results showed that the RSS parental males carried the dominant X-linked red tail gene (designated as *Rdt*) which they passed to their daughters and the Y-linked snakeskin body (*Ssb*) and snakeskin tail (*Sst*) genes which were transmitted to their sons. The recessive tail color allele, *Rdt*⁺ gives the hyaline tail color. The F₂ progeny of this cross segregated into

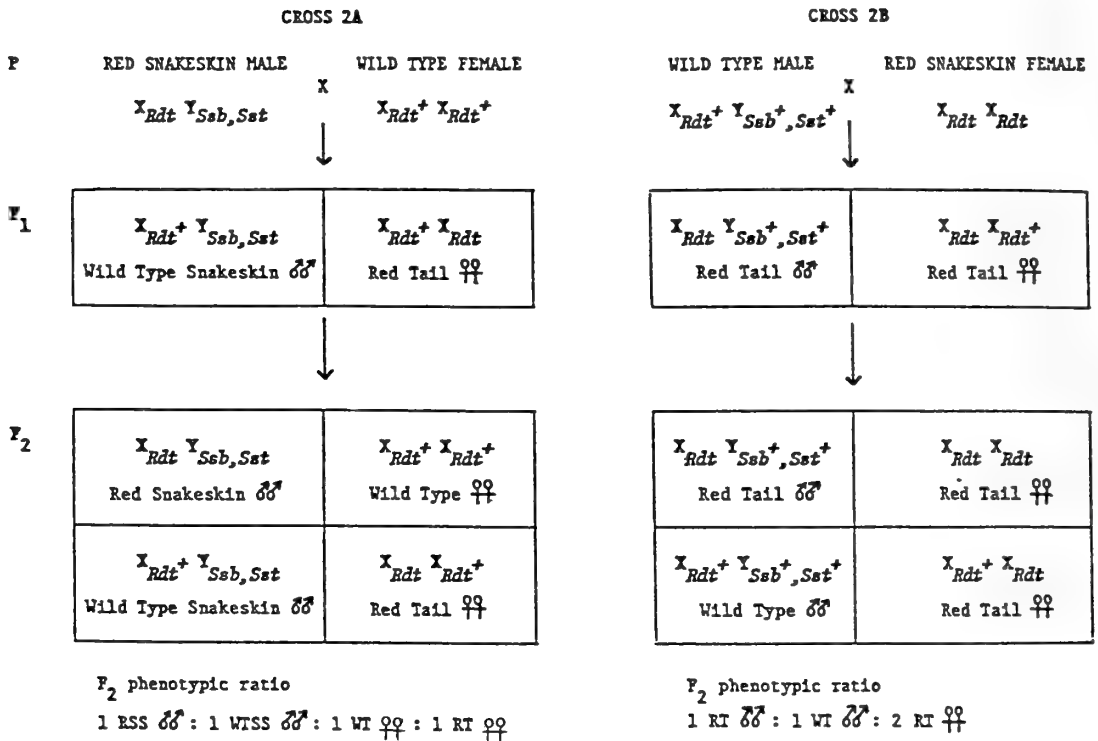


FIG. 3. Schematic diagram of the proposed genetic model for the segregation of color genes in the F₁ and F₂ generations of reciprocal crosses between the Red Snakeskin variety and wild-type guppies.

four phenotypic classes: red snakeskin males (RSS), wild-type snakeskin males (WTSS), red tail females (RT) and WT females with observed numbers conforming to the expected 1:1:1:1 ratio. The putative genotype of RSS males is $X_{Rdt} Y_{Ssb, Sst}$ and that for WTSS males is $X_{Rdt}^+ Y_{Ssb, Sst}$. A genetic model is proposed to show the segregation of color genes in Cross 2A (Fig. 3).

Five matings of the reciprocal cross of WT males with RSS females (Cross 2B) gave 10 typical F₁ broods consisting of red tail (RT) males and females with numbers conforming to the expected 1:1 segregation ratio (Fig. 1F). The phenotypes of the females were expressed after androgen treatment. The 12 F₂ broods consisted of 56 RT, 70 WT males and 140 RT females. These observed numbers fit an expected segregation ratio of 1:1:2 and provided evidence that the RSS parental females were homozygous for the X-linked dominant red tail gene, Rdt ($X_{Rdt} X_{Rdt}$ genotype).

A single atypical mating of Cross 2B gave three exceptional F₁ broods consisting of four phenotypic classes: expected RT males, unexpected WTSS males, expected RT females and unexpected WTSS females. The observed numbers segregated according to the hypothetical 1:1:1:1 ratio (Table 2). These results give evidence that the exceptional RSS female parent of this mating carried the *Ssb* and *Sst* genes on one of the X-chromosomes.

DISCUSSION

The blue-black tail color of the BSS variety is found to be controlled by the X-linked *Blt* gene and the red tail color of RSS guppies by the X-linked *Rdt* gene. There is similar evidence of X-linkage of the blue tail and red tail color tail genes present in the domesticated Blue Tail variety and Red Tail variety, respectively [6]. Fernando *et*

al. [11] also reported Y-linkage of these genes in domesticated varieties from one farm in Singapore. In this study 2.7% of crossing over of the *Blt* gene from the X- to the Y-chromosome was found, while no crossovers were observed for the *Rdt* gene. Crossing over of genes from the X- to the Y-chromosome and *vice versa* in the guppy was first documented by Winge [12] and the crossover data have been used to map the sex chromosomes [3, 5, 13, 14]

In male guppies with wild-type hyaline tails (*Blt*+ and *Rdt*+) the snakeskin tail pattern gene (*Sst*) is expressed as iridescent delicate reticulations. The *Sst* gene in males carrying the red tail gene (*Rdt*) is manifested as black reticulations on the orange-red tail. However, in males carrying the *Blt* gene which gives the blue-black tail color, the *Sst* gene when present is completely masked. Outcrosses with WT females showed that the BSS male guppies are carrying the *Sst* gene.

The 0.9% recombination frequency between the Y-linked *Ssb* and *Sst* genes found among the F₂ progeny of Cross 1A is in close agreement with the 1% reported in another domesticated guppy variety, the Green Snakeskin [10]. No crossovers were found among the progeny of Cross 1A showing that the *Ssb* and *Sst* genes tend to behave as a supergene and are transmitted as a single unit on the Y-chromosome through the male line. The single RSS female parent of Cross 2B heterozygous for the *Ssb* and *Sst* genes, gave evidence that one or both these normally Y-linked genes could be found on the X-chromosome due to crossing-over. Our results also showed that the *Blt*, *Ssb* and *Sst* genes are found on the homologous segments of the sex chromosomes. Currently experiments are being conducted to test for possible allelism of the blue tail (*Blt*) and red tail (*Rdt*) color genes.

ACKNOWLEDGMENTS

This work was supported by a grant from the National University of Singapore. We would like to thank Mr. K. J. Goh and Mr. H. K. Yip for photography of the guppies and Mrs. J. Mui for typing the tables.

REFERENCES

- 1 Herre, A. W. C. T. (1940) Additions to the fish fauna of Malaya and notes on rare and little known Malayan and Bornean fishes. *Bull. Raffles Mus. Sing.*, **16**: 27–61.
- 2 Fernando, A. A. and Phang, V. P. E. (1985) Culture of the guppy, *Poecilia reticulata* in Singapore. *Aquaculture*, **51**: 49–63.
- 3 Dzwillo, M. (1959) Genetische Untersuchungen an domestizierten Stämmen von *Lebistes reticulatus* (Peters). *Mitt. Hamburg Zool. Mus. Inst.*, **57**: 143–186.
- 4 Dzwillo, M. (1962) Über künstliche erzeugung funktioneller Männchen weiblichen Genotyp bei *Lebistes reticulatus*. *Biol. Zentrabl.*, **81**: 575–584.
- 5 Nayudu, P. L. (1979) Genetic studies of melanic color patterns and atypical sex determination in the guppy, *Poecilia reticulata*. *Copeia*, **2**: 225–231.
- 6 Phang, V. P. E., Chow, O. K. and Fernando, A. A. (1985) Genetic analysis of scale chromatophores of two domesticated varieties of the guppy, *Poecilia reticulata*. *J. Sing. Nat. Acad. Sci.*, **14**: 1–5.
- 7 Phang, V. P. E., Fernando, A. A. and Chow, O. K. (1986) Inheritance of body and tail coloration in two domesticated varieties of the guppy. In "Genetics in Aquaculture II". Ed. by G. A. E. Gall and C. A. Busack, Elsevier, Amsterdam, p. 372.
- 8 Hildemann, W. (1954) The effects of sex hormones on secondary sex characters of *Labistes reticulatus*. *J. Exp. Zool.*, **121**: 1–5.
- 9 Fernando, A. A. and Phang, V. P. E. (1985) Expression of sex-limited color pattern genes in selected strains of female guppies *Poecilia reticulata* with androgen treatment. *Sing. Nat. Acad. Sci.*, **14**: 157–159.
- 10 Phang, V. P. E., Ng, L. N. and Fernando, A. A. (1989) Inheritance of the snakeskin pattern in the guppy. *J. Hered.* (In press)
- 11 Fernando, A. A. and Phang, V. P. E. (1988) Evidence for X- and Y-linkage of a tail colour gene in a domesticated variety of the guppy, *Poecilia reticulata*. *J. Sing. Nat. Acad. Sci.* (In press)
- 12 Winge, O. (1923) Crossing over between the X- and Y-chromosome in *Lebistes*. *C. R. T. Lab. Carlsberg*, **14**: 1–19.
- 13 Winge, O. (1934) The experimental alteration of sex chromosomes into autosomes and vice versa, as illustrated by *Lebistes*. *C. R. T. Lab. Carlsberg*, **21**: 1–49.
- 14 Winge, O. and Ditlevsen, E. (1947) Color inheritance and sex determination in *Lebistes*. *Heredity* **1**: 65–83.

Distribution of Immunoreactive Thyrotropin-Releasing Hormone in the Brain and Hypophysis of Larval Bullfrogs with Special Reference to Nerve Fibers in the Pars Distalis

YUTAKA TANIGUCHI¹, SHIGEYASU TANAKA²
and KAZUMASA KUROSUMI

*Department of Morphology, Institute of Endocrinology,
Gunma University, Maebashi 371, Japan*

ABSTRACT—Thyrotropin-releasing hormone (TRH) was immunohistochemically detected in the brain and hypophysis of bullfrog larvae. At embryonic stage 24 (Shumway's classification), immunoreactive TRH was first detected in some fibers and perikarya in the hypothalamus, pars nervosa and pars intermedia. As metamorphosis proceeded, TRH-immunoreactive perikarya as well as fibers become conspicuous in several regions such as preoptic nucleus, infundibular nucleus, septum, amygdala and diagonal band of Broca. Appearance of immunoreactive TRH fibers in the pars distalis exclusively at Taylor-Korllos stage XIII-XVII was noted. The significance of this finding is discussed in relation to metamorphosis.

INTRODUCTION

Although thyrotropin-releasing hormone (TRH) has been purified and characterized early in the 1970's [1, 2], it was rather recent that the precise distribution of this peptide within the brain was elucidated. Leechan and Jackson [3] have succeeded in demonstrating TRH in the histological sections of the rat brain using acrolein as the fixative, and their protocol was applied to the tadpole brain by Mimmagh *et al.* [4]. We have investigated the development and localization of immunoreactive TRH neurons in the brain and hypophysis of larval bullfrogs, and found that a few immunoreactive TRH fibers appear in the pars distalis during a limited period of prometamorphosis. Significance of the temporal existence of the immunoreactive TRH fibers in the pars distalis will be discussed.

MATERIALS AND METHODS

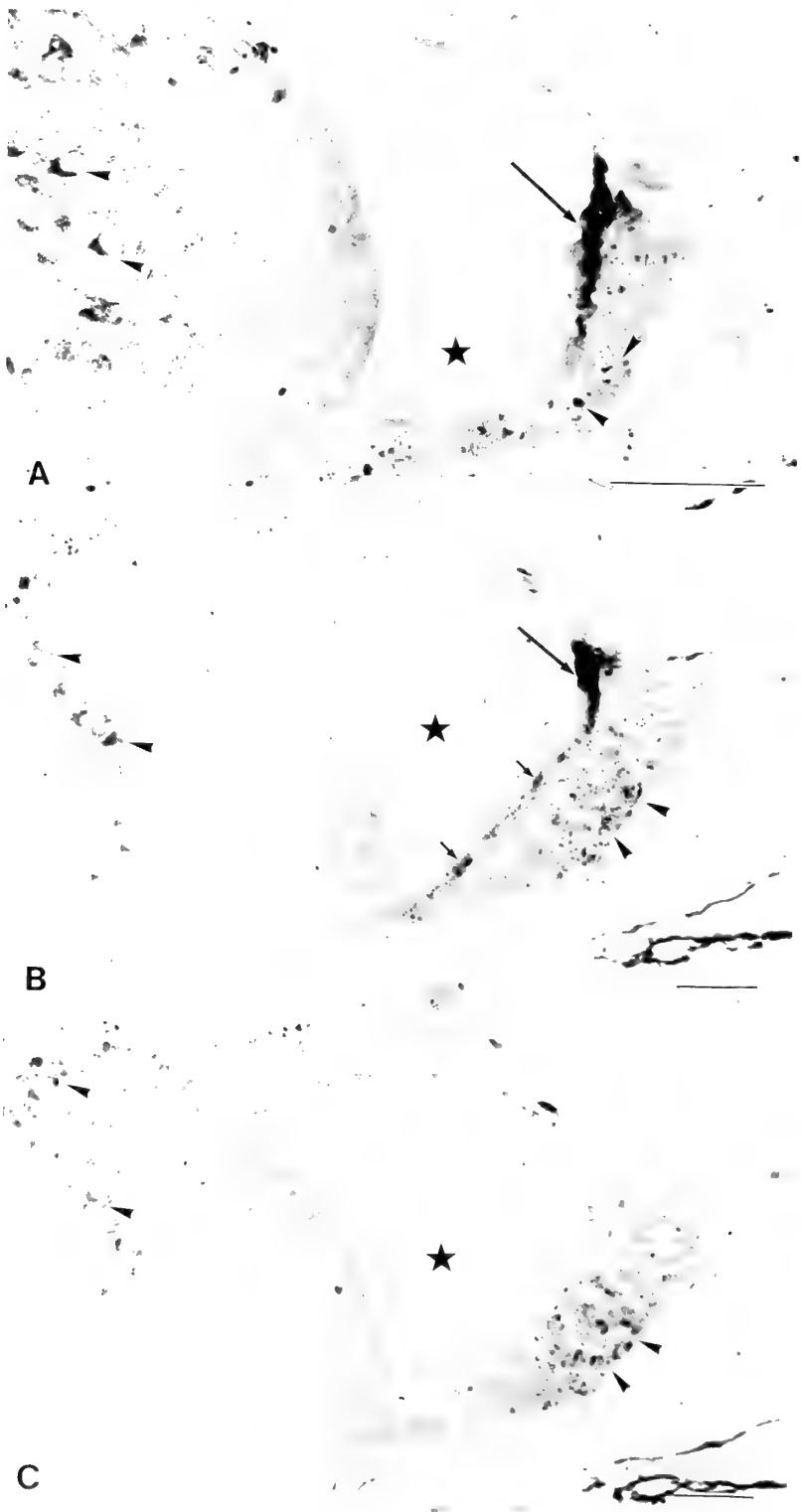
Larvae of the bullfrog (*Rana catesbeiana*) at various developmental stages were collected from the fields in the vicinity of Maebashi city. The animals were staged according to Shumway [5] for embryonic stages and Taylor and Kollros [6] for metamorphic stages. After acclimatization in a laboratory condition for 20 days, the animals were decapitated and the brain with hypophysis was carefully removed from the skull and fixed in 5% acrolein in 1/15 M phosphate buffer (pH 7.4) for 3 hr at room temperature. The tissue was embedded in paraplast after the dehydration with ethanol series. Serial sagittal 4 μ m-thick sections were cut and immunohistochemically stained according to the method of Leechan and Jackson [3] with minor modifications. The deparaffinized sections were treated first with 10 mM sodium metaperiodate in phosphate-buffered saline (PBS) for 1.5 min, followed by PBS wash. Then they were treated with 1% sodium borohydride in PBS for 1.5 min, followed by thorough wash with PBS. Then the sections were stained by the peroxidase-anti-peroxidase (PAP) method: normal goat serum

Accepted August 28, 1989

Received July 26, 1989

¹ Present address: Department of Anatomy, Wakayama Medical College, Wakayama 640, Japan.

² To whom all correspondence should be addressed.



(1:20) for 2 hr, rabbit anti-TRH serum (1:3000) for 14–18 hr, PBS wash, goat anti-rabbit γ -globulin (1:200) for 2 hr, PBS wash, PAP complex (1:200) for 2 hr, PBS wash. The reaction product was visualized with 0.02% 3,3'-diaminobenzidine tetrahydrochloride and 0.005% H_2O_2 for 5–10 min. After washing with distilled water, the sections were stained with Methyl green, dehydrated with an ethanol series, and mounted with Eukitt.

To check the specificity of the immunostaining, the diluted anti-TRH serum was preabsorbed with TRH at a final concentration of 10 μ g/ml overnight at 4° C prior to its use in the immunohistochemistry. The anti-TRH serum was a kind gift from Dr. M. Mori, School of Medicine, Gunma University [7], and PAP complex was purchased from Dakko-pats, Denmark.

RESULTS

No immunoreactive TRH was detected in the

brain of the specimens at earlier stages than embryonic stage 24 (body length ca. 8 mm). TRH immunoreactivity was first demonstrable in the brain and pars nervosa at stage 24 (Fig. 1A). In the brain, immunoreactive TRH nerve fibers were found in the medial preoptic area and in the region of infundibular nucleus. Some neuronal perikarya in the region of putative preoptic nucleus were also TRH-positive at this stage. In the hypophysis only the putative pars nervosa was immunostained with anti-TRH serum. At stage 25 (body length ca. 13 mm), immunoreactive TRH fibers ascending from the ventral hypothalamus to the pars nervosa were observed (Fig. 1B). The pars nervosa was diffusely immunostained with anti-TRH serum from this stage onwards. As metamorphosis proceeds, the immunoreactive TRH structures became more widely distributed in the brain, including preoptic nucleus, infundibular nucleus, septum, amygdala and diagonal band of Broca, and the intensity of the staining was increased (Fig. 2). Similarly, in

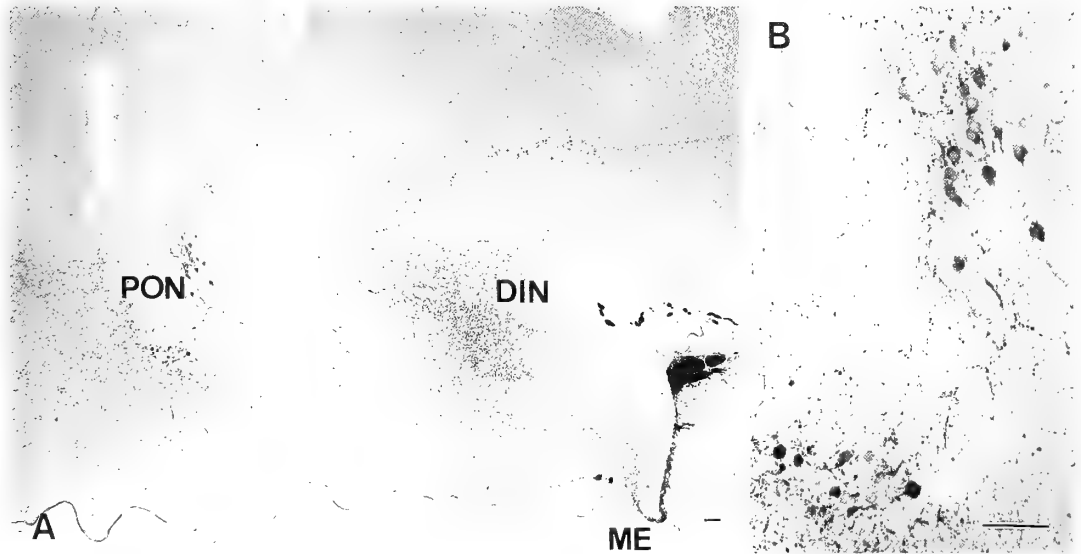


FIG. 2. Sagittal section of brain in bullfrog tadpoles at stage XIII immunostained with anti-TRH serum. Many perikarya and fibers were observed in the dorsal portion of preoptic nucleus (PON) (Fig. 2B). In the dorsal infundibular nucleus (DIN), a dense fiber network were found. ME: Median eminence. Bar: 50 μ m.

FIG. 1. Sagittal sections of embryonic brain and hypophysis in bullfrogs immunostained with anti-TRH serum. The star indicates the third ventricle. The putative pars nervosa (arrow) was first stained at stage 24 (A). At stage 25 (B), in addition to the pars nervosa (arrow), some fibers are observed to ascent the future median eminence and infundibular floor (short arrows). When adjacent section of B was immunostained with the preabsorbed anti-TRH serum, immunoreactivity was completely abolished (C). Note that embryonic cells contain much melanin pigment (arrowhead). Bar: 50 μ m.

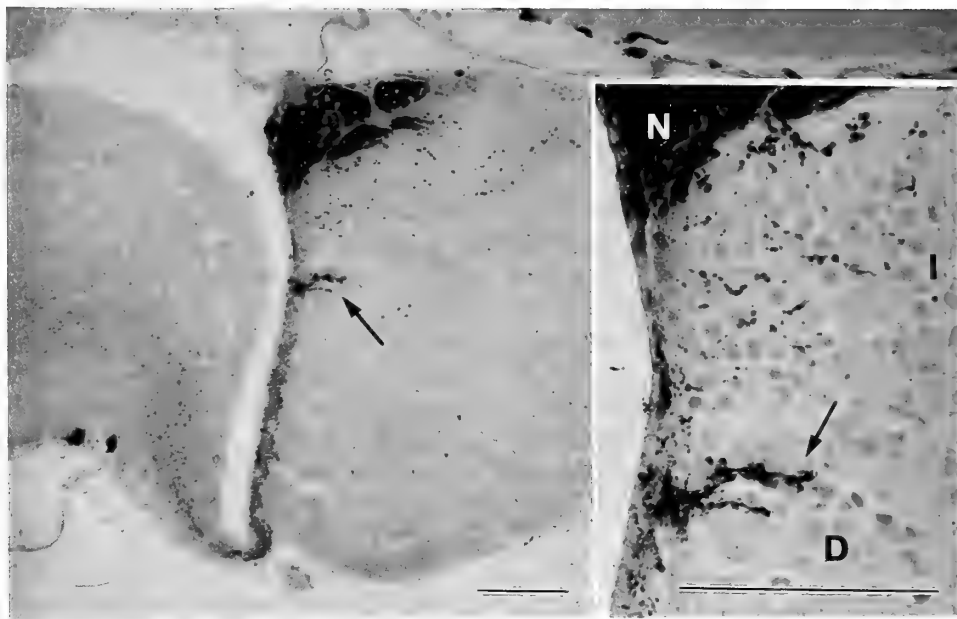


FIG. 3. Sagittal sections of hypophysis in bullfrog tadpoles at stage XIII immunostained with anti-TRH serum. The fibers are sometimes found to penetrate into the pars distalis (arrow) as shown in the inset. D: Pars distalis; I: Pars intermedia; N: Pars nervosa. Bar: 50 μ m.

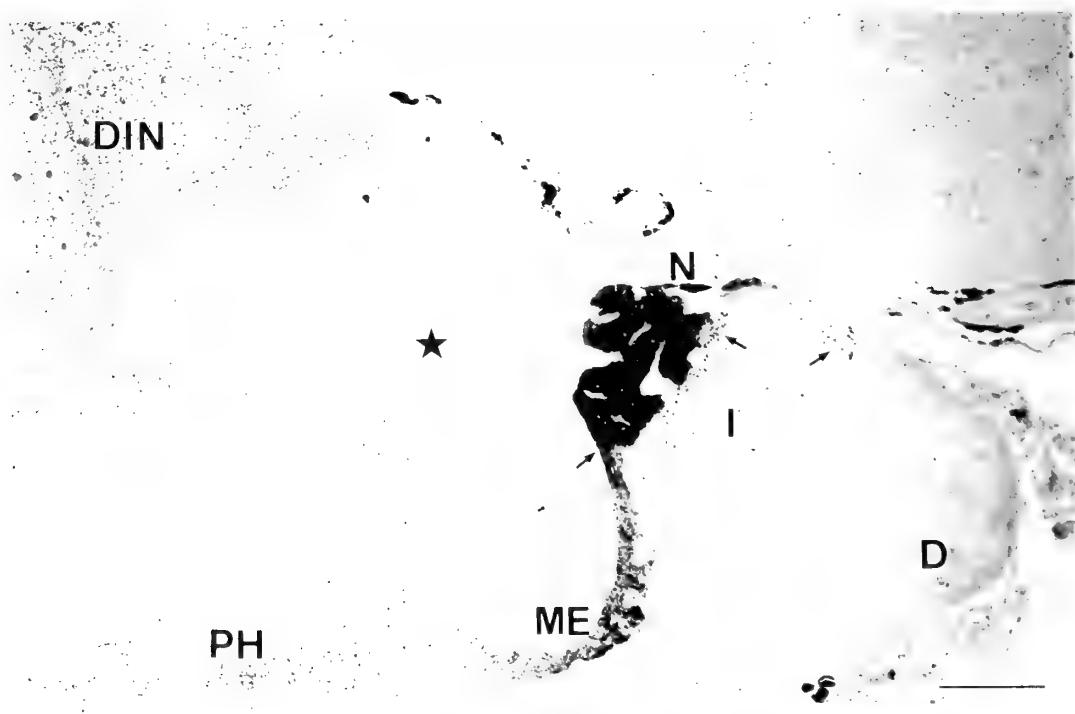


FIG. 4. A sagittal section of bullfrog hypophysis after metamorphosis completed (stage XXV). No TRH-fibers are observed in the pars distalis (D), though in the pars intermedia (I) and in the pars nervosa (N) the immunostaining remains as before (arrow). DIN: Dorsal infundibular nucleus; ME: Median eminence; PH: Preoptic-hypophysial tract. Bar: 100 μ m.

the pars nervosa the immunoreactivity became intense. In the pars intermedia, numerous immunoreactive TRH fibers were observed from stage 24 throughout the process of metamorphosis. Although embryonic cells contained much melanin pigment, the reaction product of immunostaining was easily distinguishable from the melanin granules by the difference in their colors. Moreover, as shown in Figure 1C, these immunoreactions were completely abolished after preabsorption of the anti-TRH serum. Careful observations revealed that at stages XIII-XVII in prometamorphosis, a few immunoreactive TRH fibers penetrated into the pars distalis from the median eminence as well as from the pars intermedia (Fig. 3). These immunoreactive TRH fibers in the pars distalis disappeared at the onset of metamorphic climax (stage XX). In the larvae beyond stage XX, TRH-immunoreactivity in the hypophysis was confined to the pars nervosa and pars intermedia (Fig. 4).

DISCUSSION

The present study demonstrated the localization of immunoreactive TRH in the brain and hypophysis of larval bullfrog during metamorphosis. During metamorphosis, immunoreactive TRH was found in the pars nervosa and pars intermedia, and in some brain areas including preoptic nucleus, infundibular nucleus, septum, amygdala and diagonal band of Broca. This histological distribution of immunoreactive TRH was essentially similar to that reported previously [4, 8, 9]. Moreover, the present study demonstrated clearly that immunoreactive TRH fibers penetrate into the pars distalis at prometamorphic stage. To our knowledge, the presence of TRH fibers in the pars distalis has not been described in the bullfrog or other vertebrates throughout larva and adult. The discrepancy between the present study and others may be ascribed to the technical differences. Previous investigators used the mixture of formaldehyde and glutaraldehyde as the fixative and thick frozen sections, while we used acrolein fixative and thin-paraplast sections. Leechan and Jackson [3] have reported that TRH in the tissue is well preserved only with acrolein. Moreover, the

employment of thick frozen sections may get into difficulty to reveal the precise distribution of immunoreactive TRH fibers in the hypophysis.

Aronsson [10] has demonstrated monoaminergic nerve fibers in the pars distalis of *Rana temporaria* by Falck-Hillarp method and stated that the presence of these fibers was confined to the stages from prometamorphosis to just before the climax. Kawakami-Kondo *et al.* [11] have reported the tyrosine hydroxylase-positive nerve fibers in the pars distalis which was confined to the Gosner's stage 31 to 40. The time of appearance and disappearance of these monoaminergic or dopaminergic fibers in the pars distalis was nearly identical to those of the immunoreactive TRH fibers in the present study.

In the teleost hypophysis, some nerve endings exist in the pars distalis [12]. In higher vertebrates, indirect connection by way of the hypophysial portal vessels was predominantly seen, although nerve fibers were occasionally observed in the pars distalis in rats [13]. The immunoreactive TRH- and monoamine-containing fibers in the pars distalis during metamorphosis might be considered as an intermediate type between the teleost and the higher vertebrate.

In amphibian larvae at premetamorphic and early prometamorphic stages, the pars distalis is in close contact with the median eminence where the capillary loop is poorly developed. Penetration of the capillary into the median eminence takes place as metamorphosis progresses. At climax, development of the median eminence is completed and the pars distalis almost detaches from the median eminence, being connected with it by the portal vessel at the rostral region [14]. This morphological change in the hypothalamus-hypophysial complex, which also observed in the present experiment, may have something to do with the disappearance of the immunoreactive TRH fibers from the pars distalis. Considering that the hypophysial portal vessels are still in the process of formation during the period of the existence of the immunoreactive TRH fibers in the pars distalis, the immunoreactive TRH may temporally function as a controlling factor of secretion of a certain hypophysial hormone(s) by "paracrine mechanism" which is involved in metamorphosis [see, 15,

16]. However, no definite conclusion can be drawn since physiological role of TRH in controlling hypophysial function in amphibian larvae is not clear.

The effect of mammalian TRH on hypophysis-thyroid axis in the amphibians has been controversial. It has been generally thought that TRH has no thyrotropin-releasing effect both *in vivo* and *in vitro* [17–21]. However, recent reports indicate that TRH increases thyroxine levels in the frog [22, 23]. Therefore, a direct evidence that TRH induces thyrotropin release is awaited. On the other hand, it is evident that TRH stimulates the release of prolactin from the pars distalis *in vitro* [24–26] and *in vivo* [27]. Further studies on the identification of cell type(s) of the pars distalis around which the immunoreactive TRH fibers terminate may give on insight into the physiological role of TRH in the regulation of hypophysial hormone secretion during metamorphosis.

ACKNOWLEDGMENTS

We are grateful to Professor S. Kikuyama, Department of Biology, School of Education, Waseda University for stimulating and helpful discussion, and Dr. M. Mori, School of Medicine, Gunma University for supplying anti-TRH serum.

REFERENCES

- Burgus, R., Dunn, T. F., Desiderio, D., Ward, D. N., Vale, W. and Guillemin, R. (1970) Characterization of ovine hypothalamic hypophysiotropic TSH-releasing factor. *Nature*, **226**: 321–325.
- Nair, R. M. G., Barrett, J. F., Bowers, C. Y. and Schally, A. V. (1970) Structure of porcine thyrotropin releasing hormone. *Biochemistry*, **9**: 1103–1106.
- Leechan, R. M. and Jackson, I. M. D. (1982) Immunohistochemical localization of thyrotropin-releasing hormone in the rat hypothalamus and pituitary. *Endocrinology*, **111**: 55–65.
- Mimnagh, K. M., Bolaffi, J. L., Montgomery, N. M. and Kaltenbach, J. C. (1987) Thyrotropin-releasing hormone (TRH): Immunohistochemical distribution in tadpole and frog brain. *Gen. Comp. Endocrinol.*, **66**: 394–404.
- Shumway, W. (1942) Stages in the normal development of *Rana pipiens* larvae. *Anat. Rec.*, **78**: 139–147.
- Taylor, A. C. and Kollros, J. J. (1946) Stages in the normal development of *Rana pipiens* larvae. *Anat. Rec.*, **94**: 7–23.
- Mori, M., Kobayashi, I. and Wakabayashi, K. (1978) Suppression of serum thyrotropin (TSH) concentrations following thyroidectomy and cold exposure by passive immunization with antiserum to thyrotropin-releasing hormone (TRH) in rats. *Metabolism*, **27**: 1485–1490.
- Seki, T., Nakai, Y., Shioda, S., Mitsuma, T. and Kikuyama, S. (1983) Distribution of immunoreactive thyrotropin-releasing hormone in the forebrain and hypophysis of the bullfrog, *Rana catesbeiana*. *Cell Tissue Res.*, **233**: 507–516.
- Stoeckel, M. E., Hindelang, C., Lamacz, M., Tonon, M. C. and Vaudry, H. (1987) Co-existence of TRH and mesotocin within nerve fibres in neurointermediate lobe of the frog pituitary. *Gen. Comp. Endocrinol.*, **66**: 16.
- Aronsson, S. (1976) The ontogenesis of monoaminergic fibers in the hypophysis of *Rana temporaria* with special reference to the pars distalis. *Cell Tissue Res.*, **171**: 437–448.
- Kawakami-Kondo, Y., Yoshida, M., Karasawa, N., Yamada, K., Takagi, I., Kondo, T. and Nagatsu, I. (1984) Ontogenetic study on the monoamine and peptide containing cells in the pituitary and hypothalamus of the bullfrog *Rana catesbeiana* by immunohistochemistry. *Acta Histochem. Cytochem.*, **17**: 387–397.
- Vollrath, L. (1967) Über die neurosekretorische Innervation der Adenohypophyse von Teleostern, insbesondere von *Hippocampus kuda* und *Tinca tinca*. *Z. Zellforsch.*, **78**: 234–260.
- Kurosumi, K. and Kobayashi, Y. (1980) Nerve fibers and terminals in the rat anterior pituitary gland as revealed by electron microscopy. *Arch. histol. jap.*, **43**: 141–155.
- Etkin, W., Kikuyama, S. and Rosenbluth, J. (1965) Thyroid feedback to the hypothalamic neurosecretory system in frog larvae. *Neuroendocrinology*, **1**: 45–64.
- White, B. A. and Nicoll, C. S. (1986) Hormone control of amphibian metamorphosis. In "Metamorphosis". Ed. by L. I. Gilbert and E. Frieden, Plenum Press, New York, pp. 363–396.
- Kikuyama, S., Yamamoto, K. and Kawamura, K. (1988) Hormonal regulation of amphibian metamorphosis. In "Regeneration and development". Ed. by S. Inoue *et al.*, Proc. 6th M. Singer Symposium, pp. 161–171.
- Etkin, W. and Gona, A. G. (1968) Failure of mammalian thyrotropin-releasing factor preparation to elicit metamorphic responses in tadpoles. *Endocrinology*, **82**: 1067–1068.
- Gona, A. G. and Gona, O. (1974) Failure of synthetic TRF to elicit metamorphosis in frog tadpoles or red-spotted newts. *Gen. Comp. Endocrinol.*

- nol., **24**: 223–225.
- 19 Taurog, A., Oliver, C., Eskay, R. L., Porter, J. C. and McKenzie, J. M. (1974) The role of TRH in the neoteny of the Mexican Axolotl (*Ambystoma mexicanum*). *Gen. Comp. Endocrinol.*, **24**: 267–279.
 - 20 Vandesande, F. and Aspeslagh, M-R. (1974) Failure of thyrotropin releasing hormone to increase ¹²⁵I uptake by the thyroid in *Rana temporaria*. *Gen. Comp. Endocrinol.*, **23**: 355–356.
 - 21 Millar, R. P., Nicolson, S., King, J. A. and Louw, G. N. (1983) Functional significance of TRH in metamorphosing and adult anurans. In "Thyrotropin-releasing Hormones". Ed. by E. C. Griffiths and G. W. Bennett, Raven Press, New York, pp. 217–227.
 - 22 Darras, V. M. and Kühn, E. R. (1982) Increased plasma levels of thyroid hormones in a frog *Rana ridibunda* following intravenous administration of TRH. *Gen. Comp. Endocrinol.*, **48**: 469–475.
 - 23 Denver, R. J. (1988) Several hypothalamic peptides stimulate *in vitro* thyrotropin secretion by pituitaries of anuran amphibians. *Gen. Comp. Endocrinol.*, **72**: 383–393.
 - 24 Clemons, G. K., Russell, S. M. and Nicoll, C. S. (1979) Effect of mammalian thyrotropin releasing hormone on prolactin secretion by bullfrog adenophyses *in vitro*. *Gen. Comp. Endocrinol.*, **38**: 62–67.
 - 25 Hall, T. R. and Chadwick, A. (1984) Effects of synthetic mammalian thyrotropin releasing hormone, somatostatin and dopamine on the secretion of prolactin and growth hormone from amphibian and reptilian glands incubated *in vitro*. *J. Endocrinol.*, **102**: 175–180.
 - 26 Seki, T. and Kikuyama, S. (1986) Effect of thyrotropin-releasing hormone and dopamine on the *in vitro* secretion of prolactin by the bullfrog pituitary gland. *Gen. Comp. Endocrinol.*, **61**: 197–202.
 - 27 Kühn, E. R., Kikuyama, S., Yamamoto, K. and Darras, V. M. (1985) *In vivo* release of prolactin in *Rana ribunda* following an intravenous injection of thyrotropin-releasing hormone. *Gen. Comp. Endocrinol.*, **60**: 86–89.

Vasodepressor Effect of Atrial Natriuretic Peptides in the Quail, *Coturnix coturnix japonica*

YOSHIO TAKEI and TAKUSHI X. WATANABE¹

Department of Physiology, Kitasato University School of Medicine,
Sagamihara 228, and ¹Peptide Institute, Protein Research
Foundation, Minoh 562, Japan

ABSTRACT—An intravenous injection of α -human atrial natriuretic peptide-(1-28) (α -hANP) caused dose-dependent decreases in both arterial pressure and heart rate in the urethane-anesthetized quail. The hypotension always preceded the bradycardia. The ED₅₀ for the vasodepressor effect (58.2 ± 4.6 pmol/100 g, $n=28$) was smaller than that for the bradycardial effect (107.2 ± 8.9 pmol/100 g, $n=23$). The hANP peptides with 3-6 amino acids removed from the NH₂-terminus were as potent as α -hANP, but the peptide with 4 amino acids removed from the COOH-terminus had only about half the vasodepressor potency of the parent molecule. Among the peptides of hANP in which an amino acid within the ring structure was modified, only des-Gly⁹ hANP, [(Met (O)¹²] hANP, and [Asn¹³] hANP had decreased the potency. Formation of the ring structure between the 7th and the 23rd position with an ethylene linkage instead of a disulfide bond did not change the potency. These results suggest that the amino acid residues at the COOH-terminus and some amino acids within the ring structure of hANP are important for the expression of its vasodepressor activity in the quail.

INTRODUCTION

Since the discovery of a potent diuretic and natriuretic substance in the rat atrium by de Bold *et al.* [1], a growing number of studies have been performed in mammals to elucidate the structure and biological actions of this substance. These studies have demonstrated that the stored form of the natriuretic factor has 126 amino acids in the rat and human, and is named cardiodilatin-126, γ -atrial natriuretic peptide (ANP) or pro-atrial natriuretic factor [see 2]. Later studies have shown that the circulating form of ANP has 28 amino acids that comprise the COOH-terminus of the propeptide, and that this (1-28) molecule, termed α -ANP by Kangawa and Matsuo [3], is most potent among the endogenous peptides of ANP. In addition to natriuretic and diuretic effects, ANP has been shown to exhibit a potent vasodepressor effect [1, 4, 5] and a cardiosuppressive effect [6-8] in several species of mammals. The mechanism

that causes hypotension could involve a decrease in total peripheral resistance, a decrease in cardiac output, and/or a decrease in blood volume via diuresis, but the actual mechanism has not yet been determined [2]. In nonmammalian vertebrates, the effect of ANP on blood pressure is still controversial. It has been shown that synthetic ANP peptides decrease arterial pressure in the chicken [9] and dogfish [10], while they have no effect on arterial pressure in the toadfish [11], and increase it in the rainbow trout [12].

In the present study, we attempted to examine the effects of α -human ANP (α -hANP) on arterial pressure and heart rate in the quail. We also examined structure-activity relationships of hANP peptides for the effect on blood pressure to examine the structural requirement of ANP molecules for quail vascular receptors. The results were compared with other *in vivo* studies on the natriuretic activity in the rat [13, 14] and antidiuretic activity in the rat [15], and *in vitro* studies on the spasmolytic activity of the rat and rabbit aortic strips [14, 16] and of the chick rectum [13, 14].

MATERIALS AND METHODS

Animals

Male Japanese quail, *Coturnix coturnix japonica*, were purchased from a local dealer at the age of 4 weeks. They were kept individually in wire cages ($21 \times 12 \times 17 \text{ cm}^3$) under a short daily photoperiod (8L:16D) at $25 \pm 1^\circ\text{C}$ for more than 2 weeks before use. Quail diet (Nippon Haigo shiryo, Yokohama) containing 150 meq/kg of Na and tap water were freely available until the day of experiment. The birds weighed $106 \pm 2 \text{ g}$ ($n=28$) at the time of experiments.

Surgery

The birds were lightly anesthetized by an intramuscular injection of urethane (2 g/kg) in the breast region and fixed on an operating board. It has been reported that urethane anesthesia is suitable for cardiovascular studies because of its little effects on cardiovascular reflexes [17]. After tracheotomy, a polyethylene tube (PE10, Clay Adams) was inserted into the right atrium through the right external jugular vein for injection of ANP, and a cannula assembly was inserted into the right common carotid artery for measurement of arterial pressure (Fig. 1). Care was taken not to damage the vagus nerve and other nerves that innervate the carotid sinus. Almost no bleeding was observed during surgery. The jugular cannula was filled with isotonic saline, and the arterial cannula was filled with isotonic saline which contained 100 units/ml of heparin.

Measurement of arterial pressure and heart rate

The cannula in the carotid artery was connected to a small semiconductor-type pressure transducer (PML-500GC, Kyowa Electric Instruments Co., Ltd., Tokyo) via a short silicone-rubber tube (Fig. 1). Since the transducer was connected to a carrier amplifier (Type 3126, Yokogawa Electric Works Ltd, Tokyo) by a long, flexible cord, the cannula would not slip out of the artery even when the fixed birds move slightly under anesthesia. The original pressure waves and the integrated waves (the mean pressure) were amplified and recorded with a recorder (Rectigraph-8K, NEC San-ei,

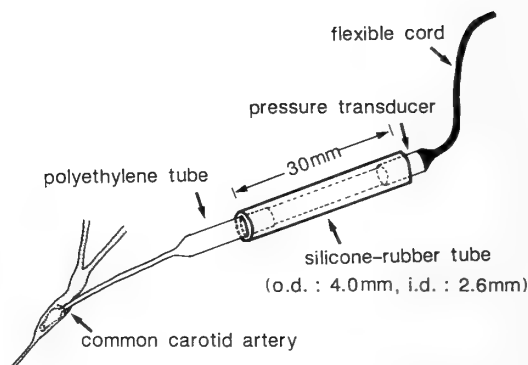


FIG. 1. Cannula assembly for the measurement of arterial pressure from the common carotid artery of the quail. The polyethylene tube (o.d.: 2.7 mm, i.d.: 1.8 mm) is narrowed to 0.6–0.8 mm by pulling the tube after heating, and then its tip is dilated by heating. The polyethylene tube and silicone-rubber tube (SH-3, Create Medic, Yokohama, Japan) are filled with heparinized saline (100 units/ml). The outer diameter of the transducer is 2.8 mm. Since the transducer is not fixed, the cannula does not escape from the artery even though the bird moves to some extent during the measurements. Another advantage of this system is that, because the cannula is rather thick and short, the pulse wave can be recorded with a small distortion.

Tokyo). The original waves after amplification were also introduced into a tachometer (#1322, NEC San-ei, Tokyo) for measurement of heart rate, and they were stored in a data recorder (R-260, TEAC, Tokyo) for further analyses.

Experimental protocol

In the first experimental group ($n=10$), the ED_{50} of α -hANP for its effects on arterial pressure and heart rate was determined. Intravenous injections of 0, 0.05, 0.1, 0.2, 0.5, 1 or $2 \mu\text{g}/100 \text{ g}$ body weight of α -hANP in 0.05 ml of 0.9% NaCl were given twice for each dose in random order. Each injection was followed by flushing of the cannula (dead space: 0.01 ml) with 0.03 ml of 0.9% NaCl. The injection was repeated after the arterial pressure returned to the level before injection, since it was shown in preliminary experiments that repeated injections of $0.5 \mu\text{g}$ of α -hANP given in this way generated reproducible effects.

In the second experimental group ($n=18$), the structure-activity relationship of the vasodepressor effect was examined using various analogs of

hANP. For this purpose, 0, 0.05, 0.1, 0.2, 0.5, 1 and 2 $\mu\text{g}/100\text{ g}$ of α -hANP (hANP-(1-28)) were first injected in that order, then three or four of the analogs were injected at the doses of 0.1, 0.3 and 1 $\mu\text{g}/100\text{ g}$ in that order. The analogs of hANP used were [Ile¹²] hANP-(1-28) (α -rat ANP), [Met(O)¹²] hANP-(1-28), hANP-(4-28), hANP-(5-28), hANP-(7-28), [Nle¹²] hANP-(7-28), [D-Ala⁹] hANP-(7-28), [Asn¹³] hANP-(7-28), des-Gly⁹ hANP-(7-28), hANP-(5-25), hANP-(7-23), and [Asu^{7,23}] hANP-(7-23). The order of injection of the analogs was random. After the last injection of the analogs, injections of 0.1, 0.3 and 1 $\mu\text{g}/100\text{ g}$ of α -hANP were repeated to confirm the reproducibility of results. All hANP-related peptides were synthesized by the liquid-phase method [18] at the Peptide Institute Inc. (Osaka, Japan).

Statistical analyses

Since it was found that decreases in arterial pressure and heart rate were greater when the pre-injection levels were higher, the decreases were expressed in terms of percentages from pre-injection levels. The ED₅₀ of α -hANP was calculated from all data of 28 birds used in this study. For calculation of the ED₅₀, changes in arterial pressure or heart rate at doses between 0.05 and 2 μg were fitted to a logistic curve by each bird, and the dose that produced a half-maximal response was obtained from the curve. The curve fitting was executed by the Newton-Raphson algorithm based on estimates of maximum likelihood [19]. The changes in arterial pressure and heart rate at each dose were compared with the changes observed after injection of saline by the paired t-test. In the experiment to examine the vasodepressor potency of analogs of hANP relative to α -hANP, the potency ratio was calculated from the ratio of the ED₅₀ of hANP to that of an analog. In this case, the ED₅₀ of α -hANP was calculated with data obtained at doses between 0.1 and 1 μg , as was done for each analog. The response to 2 μg of α -hANP was used only to assess the maximum response. All results are expressed as means \pm SE of the mean.

RESULTS

Dose-response relationship for α -hANP

The mean, resting arterial pressure of the quail before injection was $84.1 \pm 2.3\text{ mmHg}$ ($n=28$). The arterial pressure decreased immediately after injection of α -hANP, and the decreases become greater as the dose increased (Fig. 2). The largest decrease at high doses was about 50% of the level before injection. The ED₅₀ calculated by the logistic-log transformation was $179 \pm 14\text{ ng}$ ($58.2 \pm 4.6\text{ pmol}$)/100 g body weight ($n=28$) (Fig. 3). The significant decrease in arterial pressure was obtained at 100 ng/100 g, and 9 out of 28 birds decreased their arterial pressure at 50 ng/100 g (Fig. 2). The decreased pressure continued for longer as the dose increased (Fig. 2).

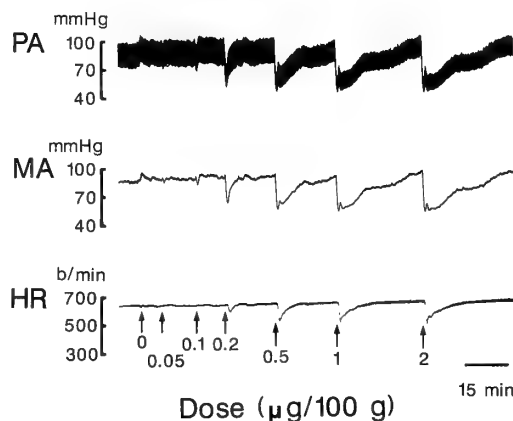


FIG. 2. Changes in arterial pressure (PA), mean PA (MA), and heart rate (HR) after injection of 0–2 $\mu\text{g}/100\text{ g}$ body weight of α -hANP into the jugular vein of a quail.

The mean heart rate of the quail before injection was $515 \pm 22\text{ beats/min}$ ($n=28$). The heart rate decreased after injection of α -hANP, and the decrease was greater as the dose increased (Fig. 2). The ED₅₀ was $330 \pm 27\text{ ng}$ ($107.2 \pm 8.9\text{ pmol}$)/100 g ($n=23$) (Fig. 4). The significant decrease was obtained at 100 ng/100 g. Compared to the vasodepressor effect, the bradycardia occurred a little more slowly and recovered more quickly, and the extent of the decrease was smaller. In 5 of 28 birds, injection of α -hANP caused tachycardia

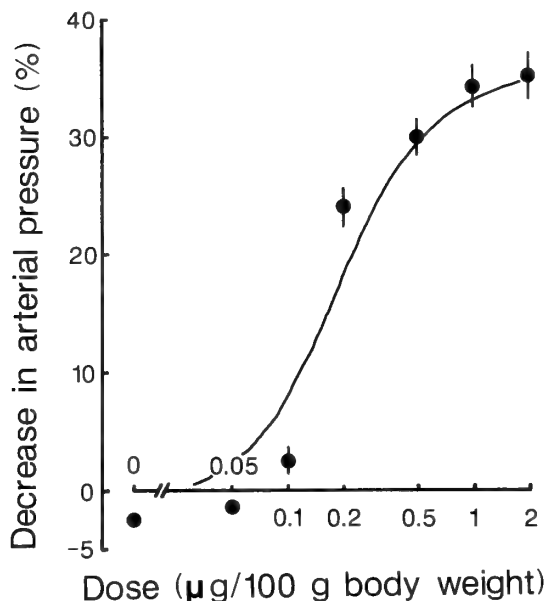


FIG. 3. Dose-response relationship for the vasodepressor effect of α -hANP in 28 quail. Doses are expressed in a log scale. The logistic curve that fitted best is shown in the figure. The calculated ED_{50} in 179 ± 14 ng (58.2 ± 4.6 pmol)/100 g body weight. The vertical bars represent standard errors of the mean.

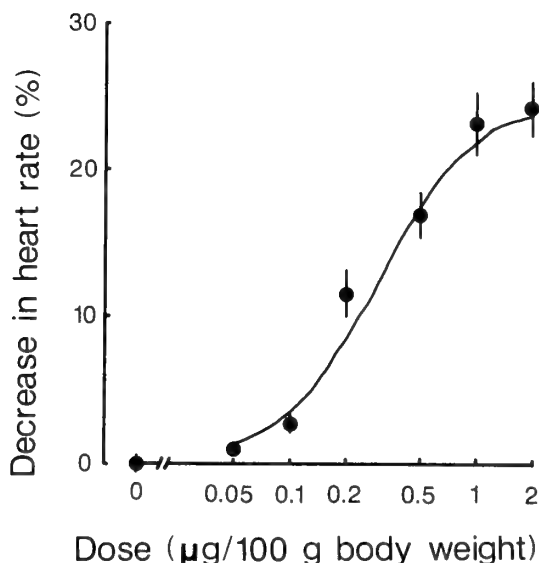


FIG. 4. Dose-response relationship for the bradycardial effect of α -hANP in 23 quail. Doses are expressed in a log scale. Among 28 quail examined, 5 quail showed tachycardia after injection of hANP. The logistic curve that fitted best is shown in the figure. The calculated ED_{50} is 330 ± 27 ng (107.2 ± 8.9 pmol)/100 g body weight. The vertical bars represent standard errors of the mean.

although hypotension was induced in the same birds. The basal heart rate of these birds (370 ± 45 beats/min, $n=5$) was smaller than that of the other birds in which bradycardia was induced (561 ± 19 beats/min, $n=23$).

Structure-activity relationships for analogs of hANP

As shown in Figure 5, sensitivity to hANP was well conserved and little tachyphylaxis was observed even after repetitive injections of α -hANP and its analogs. The hANP analogs with amino acids removed from the NH_2 -terminus, hANP-(4-28), hANP-(5-28) and hANP-(7-28) were almost as potent as α -hANP in terms of their vasodepressor activity (Table 1). However, the peptides with amino acids removed from the $COOH$ -terminus, hANP-(5-25) and hANP-(7-23), were less potent. No significant change in the vasodepressor potency was observed after the disulfide bond of hANP-(7-23) ([Cys^{7,23}] hANP-(7-23)) was replaced by the ethylene linkage ([Asu^{7,23}] hANP-(7-23)). The modification of amino acids within the ring structure had variable effects (Table 1). When Met at the 12th position was replaced by Ile (rat ANP) or Nle, or when Gly at the 9th position was replaced by D-Ala, the potency did not change from that of the parent molecule. However, replacement of Asp at the 13th position with Asn, oxidation of Met at the 12th position, or removal of Gly at the 9th position, greatly decreased the potency of the peptide.

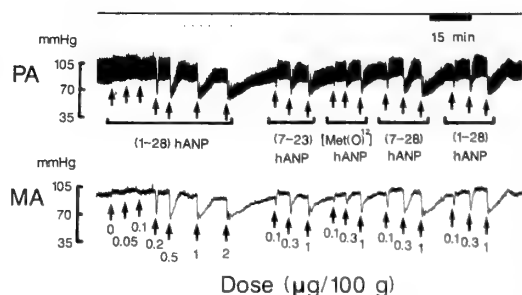


FIG. 5. Changes in arterial pressure (PA) and its mean (MA) after injection of hANP-(1-28) (α -hANP), hANP-(7-23), [Met(O)¹²] hANP-(1-28), and hANP-(7-28) into a quail. The injection of α -hANP was repeated at the end of the experiment to confirm the reproducibility of data.

TABLE 1. Relative vasodepressor potencies of hANP analogs in the quail (n=6). Relative potencies by the spasmytic activity in the chick rectum and rat aorta *in vitro* and by natriuretic activity in the rat *in vivo* are given for comparison. Values are means \pm SE of the mean. Amino acid sequence of hANP-(1-28) is:

1 5 10 15 20 25
S-L-R-R-S-S-C-F-G-G-R-M-D-R-I-G-A-Q-S-G-L-G-C-N-S-F-R-Y

Analog of hANP	Potencies (%)			
	quail depressor	chick* rectum	rat* aorta	rat* natriuresis
(1-28)				
hANP	100	100	100	100
[Ile ¹²]	83.2 \pm 9.7	122	226	236
[Met(O) ¹²]	15.8 \pm 4.0	2	4	13
(4-28)				
hANP	86.3 \pm 10.7	64	79	97
(5-28)				
hANP	77.9 \pm 15.1	67	96	73
(7-28)				
hANP	123.5 \pm 16.2	364	154	148
[Nle ¹²]	82.5 \pm 15.3	169	61	141
[D-Ala ⁹]	119.0 \pm 15.6	356	120	107
[Asn ¹³]	18.8 \pm 5.9	5	1	0
des-Gly ⁹	26.5 \pm 6.9	1	0	0
(5-25)				
hANP	63.7 \pm 14.7	31	5	82
(7-23)				
hANP	50.7 \pm 12.7	139	3	27
[Asu ^{7,23}]	60.3 \pm 7.7	77	1	6

*[14]

DISCUSSION

A moderate dose of α -hANP caused a profound hypotension in the quail, as has been reported to occur in the chicken after injection of α -rat ANP [9]. In the chicken, a crude heart extract also decreases arterial pressure. Thus, ANP-like material appears to be present in the chicken heart, as suggested by the results of immunohistochemical analysis [20]. The presence of ANP-like material was also reported in the quail by immunohistochemistry using antibodies to pig ANP [21]. We also observed in preliminary experiments that the quail heart contained substances that cross-react with antibodies raised against α -hANP, and that the

substance extracted had a potent vasodepressor effect in the quail (Takei and Ando, unpubl. data). However, the amino acid sequence of this immunoreactive ANP may differ from that of α -hANP, since the concentration in the heart extract determined by the quail vasodepressor bioassay was more than 10,000 times greater than the value measured by radioimmunoassay for hANP. Thus, hANP has a potent vasodepressor effect in the quail, although its molecule may be structurally different from quail ANP. Very recently, amino acid sequence of chicken ANP has been determined, whose sequence has only 52% homology to hANP [22].

In mammals, a bolus injection of α -hANP has

been shown to decrease arterial pressure in a linear fashion at doses between 33 and 333 pmol (0.1 and 1 μ g)/kg in anesthetized dogs [23], and at doses between 0.18 and 9 nmol/kg in conscious, spontaneously hypertensive rats [24]. Values of ED₅₀ were not calculated but dogs appear to be a little more sensitive to the vasodepressor effect of human (also native to dogs) ANP than are the rat and the quail. However, the maximal hypotension in birds (50%) was greater than that of mammals (10–20%).

It is known that, in mammals, an acute hypotension is usually followed by reflex tachycardia, which is mediated via sino-aortic baroreceptors [25]. Since profound hypotension was induced in all quail in the present study but bradycardia was induced in most birds after injection of hANP, hANP may have some inhibitory effect on heart rate. In guinea pigs, ANP also induces hypotension and bradycardia, but the effect of ANP on heart rate does not appear to be a direct action, since rat ANP-(5-28) did not change the frequency of spontaneously beating atrium *in vitro* [26].

For the expression of vasodepressor activity in the quail, amino acids at the COOH-terminus appear to be more important than those at the NH₂-terminus, and the modification of some amino acids within the ring structure, which may change the tertiary structure of the molecule, affects the potency. These results are similar to those obtained in the spasmolytic activity of the chick rectum and rat aorta, and in the natriuretic activity of rats (Table 1). However, some differences are observed in different preparations; in the chick rectum, removal of 6 amino acids from the NH₂-terminus increases the activity more than three folds, and in the rat preparations, the homologous rat peptide has more than two-fold activities than does the human peptide. Other major differences of the quail preparation from other preparations are that modifications of some amino acids within the ring structure cause smaller loss of activity, and that substitution of a disulfide bond with an ethylene linkage does not decrease the activity. Garcia *et al.* [16] showed that amino acids at the NH₂-terminus as well as those at the COOH-terminus are important for the spasmolytic activity in the rabbit aorta. For the antidiuretic

activity in the rat, the removal of amino acids from the NH₂-terminus does not change the activity, but the (7-23) peptide has no activity [15]. Collectively, it appears that quail vascular receptors can respond to a greater variety of ANP analogs than do other ANP receptors. Supporting this idea are our preliminary data which show that ANP-like substance extracted from carp hearts causes hypotension in the quail, but has no relaxant effect on the chick rectum (Uemura and Takei, unpubl. data). It appears that the quail vasodepressor effect is a useful assay system for nonmammalian ANPs whose molecular structures may be different from mammalian ANPs.

In summary, the quail exhibited high sensitivity to the vasodepressor effect of hANP, and because of their small size (100 g), they can respond to as little as 50 ng (16 pmol)/bird. The vasodepressor effect was profound (50%), and reproducible even after repeated injections (see Fig. 5). Thus, it seems that the quail vasodepressor bioassay is considered to be a useful *in vivo* assay system for the comparative study of ANP in nonmammalian vertebrates.

ACKNOWLEDGMENTS

This investigation was supported on part by a grant from the Ministry of Education, Science and Culture of Japan (62740449), and by the Kitasato Research Foundation under Grant No. 10.

REFERENCES

- 1 De Bold, A. J., Borenstein H. J., Veress, A. T. and Sonnenberg, H. (1981) A rapid and potent natriuretic response to intravenous injection of atrial myocardial extract in rats. *Life Sci.*, **28**: 89–94.
- 2 Genest, J. and Cantin, M. (1988) The atrial natriuretic factor: its physiology and biochemistry. *Rev. Physiol. Biochem. Pharmacol.*, **110**: 1–145.
- 3 Kangawa, K. and Matsuo, H. (1984) Purification and complete amino acid sequence of α -human atrial natriuretic polypeptide (α -hANP). *Biochem. Biophys. Res. Commun.*, **118**: 131–139.
- 4 Richards, A. M., Nicholls, M. G., Ikram, H., Webster, M. W., Yandle, T. G. and Espiner, E. A. (1985) Renal, hemodynamic, and hormonal effects of human alpha atrial natriuretic peptide in healthy volunteers. *Lancet*, **1**: 545–548.
- 5 Hirata, Y., Ishii, M., Sugimoto, T., Matsuoka, H.,

- Sugimoto, T., Kangawa, K. and Matsuo, H. (1985) The effects of atrial 28-amino acid peptide on systemic and renal hemodynamics in anesthetized rats. *Circ. Res.*, **57**: 634–639.
- 6 Ackermann, U., Irizawa, T. G., Milojevic S. and Sonnenberg, H. (1984) Cardiovascular effects of atrial extracts in anesthetized rats. *Can. J. Physiol. Pharmacol.*, **62**: 819–826.
 - 7 Breuhaus, B. A., Saneii, H. H., Brandt, M. A. and Chimoskey, J. E. (1985) Atriopeptin II lowers cardiac output in conscious sheep. *Am. J. Physiol.*, **249**: R776–R780.
 - 8 Cody, R. J., Atlas, S. A., Laragh, J. H., Kubo, S. H., Covit, A. B., Ryman, K. S., Shaknovich, A., Pondolfino, K., Clark, M., Camargo, M. J. F., Scarborough, R. M. and Lewicki, J. A. (1986) Atrial natriuretic factor in normal subjects and heart failure patients: plasma levels and renal, hormonal and hemodynamic responses to peptide infusion. *J. Clin. Invest.*, **78**: 1362–1372.
 - 9 Gregg, C. M. and Wideman, Jr. R. F. (1986) Effects of atriopeptin and chicken heart extract in *Gallus domesticus*. *Am. J. Physiol.*, **251**: R543–R551.
 - 10 Solomon, R., Taylor M., Dorsey, D., Silva, P. and Epstein, F. H. (1985) Atriopeptin stimulation of rectal gland function in *Squalus acanthias*. *Am. J. Physiol.*, **249**: R348–R354.
 - 11 Lee, J. and Malvin, R. L. (1987) Natriuretic response to homologous heart extract in aglomerular toadfish. *Am. J. Physiol.*, **252**: R1055–R1058.
 - 12 Duff, D. W. and Olson, K. R. (1986) Trout vascular and renal responses to atrial natriuretic factor and heart extract. *Am. J. Physiol.*, **251**: R639–R642.
 - 13 Thibault, G., Garcia, R., Carrier, F., Seidah, N. G., Lazure, C., Chétién, M., Cantin, M. and Genest, J. (1984) Structure-activity relationships of atrial natriuretic factor (ANF). I. Natriuretic activity and relaxation of intestinal smooth muscle. *Biochem. Biophys. Res. Commun.*, **125**: 938–946.
 - 14 Watanabe, T. X., Noda, Y., Chino, N., Nishiuchi, Y., Kimura, T., Sakakibara, S. and Imai, M. (1988) Structure-activity relationships of α -human atrial natriuretic peptide. *Europ. J. Pharmacol.*, **147**: 49–57.
 - 15 Ito, H., Nakao, K., Katsuura, G., Morii, N., Shiono, S., Yamada, T., Sugawara, A., Saito, Y., Watanabe, K., Igano, K., Inouye, K. and Imura, H. (1987) Atrial natriuretic polypeptide: structure-activity relationships in the central action—a comparison of their antidipsogenic actions. *Neurosci. Lett.*, **74**: 102–106.
 - 16 Garcia, R., Thibault, G., Seidah, N. G., Lazure, C., Cantin, M., Genest, J., and Chétién M. (1985) Structure-activity relationships of atrial natriuretic factor (ANF). II. Effect of chain-length modifications on vascular reactivity. *Biochem. Biophys. Res. Commun.*, **126**: 178–184.
 - 17 Maggi, C. A. and Meli, A. (1986) Suitability of urethane anesthesia for physiopharmacological investigations in various systems. Part 2: Cardiovascular system. *Experientia*, **42**: 292–297.
 - 18 Chino, N., Nishiuchi, Y., Masui, Y., Noda, Y., Watanabe, T. X., Kimura, T. and Sakakibara, S. (1985) Synthesis of α -human atrial natriuretic polypeptide (α -hANP) and its related peptides. In "Peptide Chemistry 1984". Ed. by N. Izumiya, Protein Research Foundation, Osaka, pp. 241–246.
 - 19 Cox, D. R. (1970) *The Analysis of Binary Data*. Chapman and Hall, London.
 - 20 Chapeau, C., Gutkawska, J., Schiller, P. W., Milne, R. W., Thibault, G., Garcia, R., Genest, J. and Cantin, M. (1985) Localization of immunoreactive synthetic atrial natriuretic factor (ANF) in the heart of various animal species. *J. Histochem. Cytochem.*, **33**: 541–550.
 - 21 Reinecke, M., Nehls, M. and Forssmann, W. G. (1985) Phylogenetic aspects of cardiac hormones as revealed by immunohistochemistry, electronmicroscopy, and bioassay. *Peptides*, **6**: 321–331.
 - 22 Miyaka, A., Minamino, A., Kangawa, K. and Matsuo, H. (1988) Identification of a 29-amino acid natriuretic peptide in chicken heart. *Biochem. Biophys. Res. Commun.*, **155**: 1330–1337.
 - 23 Ishihara, T., Aisaka, K., Hattori, K., Hamasaki, S., Morita, M., Noguchi, T., Kangawa, K. and Matsuo, H. (1988) Vasodilatory and diuretic actions of α -human natriuretic polypeptide (α -hANP). *Life Sci.*, **36**: 1205–1215.
 - 24 Lappe, R. W., Todt, J. A. and Wedt, O. L. (1986) Hemodynamic effects of infusion versus bolus administration of atrial natriuretic factor. *Hypertension*, **8**: 866–873.
 - 25 Heymans, C. and Neil, E. (1958) *Reflexogenic Areas of the Cardiovascular System*. Little, Brown and Company, Boston, pp. 45–55.
 - 26 Bergery, J. L. and Kotler, D. (1985) Effects of atriopeptins I, II and III on atrial contractility, sinus nodal rate (guinea pig) and agonist-induced tension in rabbit aortic strips. *Europ. J. Pharmacol.*, **110**: 277–281.

A New Milliped of the Genus *Riukiaria* from Is. Yaku-shima, Japan (Diplopoda: Polydesmida: Xystodesmidae)

TSUTOMU TANABE¹

*Zoological Institute, Faculty of Science, Hokkaido University,
Sapporo 060, Japan*

ABSTRACT—A new species of Xystodesmidae, *Riukiaria jamila*, is described and figured based on male and female adults from Is. Yaku-shima, off the southern coast of Kyūshū, Japan. This species is characterized by the gray tergites, the yellowish white paranota, and the acropodite of the male gonopod which is very wide from the base to the twisted portion.

INTRODUCTION

The genus *Riukiaria* of the family Xystodesmidae is currently represented by approximately 20 species from Japan [1–10], Korea [8, 11] and Taiwan [3, 8, 12, 13]. One species, *R. puella*

Tanabe, is known from Is. Yaku-shima, off the southern coast of Kyūshū, Japan.

In the present paper, I describe a new species of this genus as the second species from that island.

Terminology follows that of Shelley [14] except for parts of the acropodite of the male gonopod.



FIG. 1. *R. jamila* sp. nov., ♂ paratype, dorsal view.

Accepted July 11, 1989

Received April 12, 1989

¹ Present address: Tokushima Prefectural Museum, Tokushima 770, Japan.

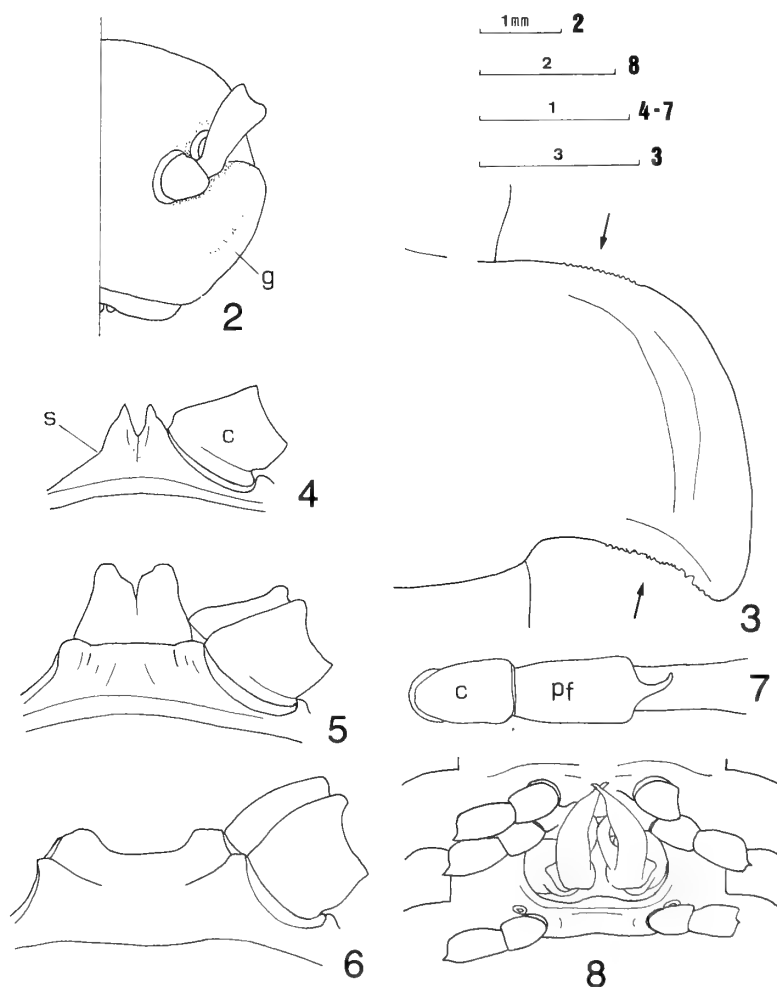
Riukiaria jamila sp. nov.
(Figs. 1–16)

Types: 15 ♂♂ (holotype and paratypes), 12 ♀♀ (paratypes) from the litter of *Ardisia quinquegona*, along Ôko-rindô mountain path, Kurio, Yaku-chô, Is. Yaku-shima, Kumage-gun, Kago-shima-ken, 12-V-1987, T. Tanabe leg. 1 ♂ (paratype), locality as above, 26-IV-1986. A. Moroto leg. The ♂ holotype and 1 ♀ paratype are deposited in the collection of the National Science Museum, Tokyo. 1 ♂ and 1 ♀ paratypes are to be deposited in the collection of the North Carolina

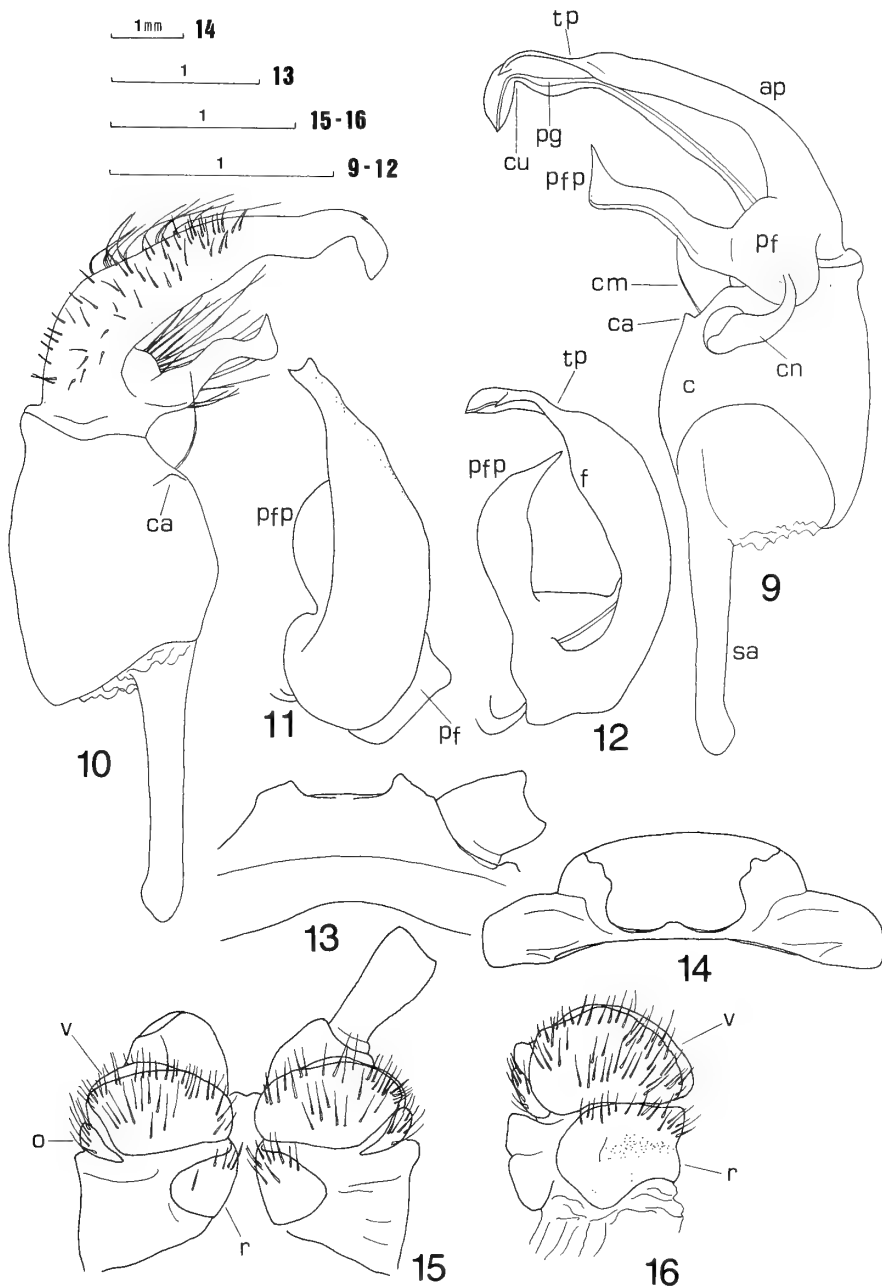
State Museum of Natural Science, Raleigh, NC, USA. 12 ♂♂ and 9 ♀♀ paratypes deposited in my private collection.

Diagnosis: Different from all other species of *Riukiaria* in having gray tergites and yellowish white paranota. The male with following diagnostic characters: Gonopod very wide from the base to the twisted portion, with a small coxal apophysis on anterior face of coxa and an acute medial process at curved portion of acropodite. Fifth sternite with high processes between 4th legs; prefemoral spines curved anterodorsally.

Description. ♂ holotype.



FIGS. 2–8. *R. jamila* sp. nov. 2–7, ♂ holotype: 2, head, anterior view, setae omitted. 3, right paranotum of 8th segment, dorsal view. 4–6, 4th–6th sternites, setae omitted: 4, 4th, posterior view; 5, 5th, posterior view; 6, 6th, posterior view. 7, coxa and prefemur of 10th left leg, ventral view, setae omitted. 8, Gonopods *in situ* of ♀ paratype, ventral view, setae omitted. c, coxa. g, gena. pf, prefemur. s, sternite.



FIGS. 9-16. *R. jamila* sp. nov. 9-12, left gonopod of holotype: 9, medial view, setae omitted except coxa; 10, lateral view, setae omitted; 11, dorsal view, setae omitted; 12, dorsomedial view, setae omitted. 13-15, ♀♀ paratypes: 13, 5th sternite, anterior view; 14, 4th segment, ventral view; 15, cyphopods, posterior view; 16, left cyphopod, anterior view. ap, acropodite. c, coxa. ca, coxal apophysis. cm, coxal macroseta. cn, cannula. cu, curve. f, flange. o, operculum. pf, prefemur. pfp, prefemoral process. pg, prostatic groove. r, receptacle. sa, sternal apodeme. tp, twisted portion. v, valve.

Head: Capsule smooth, polished. First antennomere subglobose, 2nd-6th clavate, 7th short and truncate; relative length of antennomeres $2=3=4=5=6>1>7$. Genae (Fig. 2) with distinct central impressions. Facial setae as follows: Epicranial 2 (left), 2 (right); inter antennal 1 (left), 1 (right); frontal+genal about 40; clypeal about 30; labral about 25.

Tergites without setae and tubercles, polished. Collum finely coriaceous, somewhat narrower than 2nd tergite. Protergites smooth. Metatergites finely coriaceous, without transverse medial depressions. Paranota (Fig. 3) finely serrate on both anterior and posterior margins; posterolateral corners rounded on segments 1-4, becoming progressively more acute posteriorly. Peritremata distinct. Ozopores located at about posterior 1/3, opening laterally.

Sternites smooth, without setae, polished: 4th sternite (Fig. 4) with a pair of small acuminate processes, about as long as width of adjacent coxae; 5th sternite (Fig. 5) with a pair of high coalesced projections between 4th legs, and a pair of small, flat, widely segregated elevations between 5th legs; 6th sternite (Fig. 6) with a pair of short, flat, widely segregated elevations between 6th legs, and convexly recessed between 7th legs. Postgonopodal sternites without distinct tubercle between any leg pair.

Pregonopodal legs densely hirsute; postgonopodal legs becoming progressively less hirsute posteriorly. Coxae with blunt, indistinct, distomedial projections, but those of 3rd and 4th legs with slightly rounded projection proximomedially. Prefemoral spine beginning on 4th segment, becoming progressively longer posteriorly, pointed bending anterodorsally on midbody (Fig. 7).

Gonopodal aperture elliptical, 2.1 mm wide and 1.1 mm long at midpoint; sides raised above metazonal surface. Gonopods *in situ* as in Fig. 8. Gonopod structure as follows (Figs. 9-12): Coxa with a small coxal apophysis near dorsal margin on anterior face and a macroseta between coxal apophysis and cannula. Sternal apodeme long, straight. Prefemur flat proximolaterally (Fig. 11). Prefemoral process flat, arcuate, tapering into acuminate tip, strongly reflexed in apical half; tip directed laterally. Acropodite thin, leaning antero-

medially, extending beyond level of prefemoral process, twisted at about 3/4 of length, curved dorsally near tip; very wide from base to twisted portion and tapering into acuminate tip, with inner surface broadly excavated from base to twisted portion and medial flange from 1/3 of length to twisted portion; flat from twisted portion to tip, with an acute medial process at curved portion; tip simple. Prostatic groove originating in pit at base of prefemur, running along lateral side of inner surface of acropodite to apical opening.

Color in life: Paranota yellowish white. Metatergites gray. Protergites yellowish white, with transverse gray stripes at midlength. Collum gray, with yellowish white stripes along both anterior and posterior margins. Epicranium pale gray. Face gray. Genae, clypeus, labrum and antennae all yellowish white. Venter and legs yellowish white. Paraprocts yellowish white; each with a central gray spot.

♂♂ paratypes: The ♂♂ paratypes agree with the ♂ holotype in most structural details, except numbers of the following facial setae ($n=5$): Frontal+genal about 25-50; clypeal about 25-30; labral 30-40.

♀♀ paratypes: Somatic features as in male, except numbers of the following features: Facial setae ($n=5$): Frontal+genal about 25-40; clypeal 25-40; labral 25-30. Body more arched, and generally larger. Paranota shorter. 5th sternite (Fig. 13) with a pair of short, flat separated elevations between 4th legs, without processes between 5th legs. 6th sternite without processes. Legs more slender. Coxae of 3rd and 4th legs with no projections proximomedially. Cyphopodal aperture (Fig. 14) with a slight anterior projection of caudal margin. Cyphopods as in Figs. 15 and 16. Valves subequal in size and shape; receptacle projecting at midwidth of dorsal margin and strongly depressed centrally on anterior side, and much smaller in size on posterior side. Coloration somewhat paler than in male.

Measurements: ♂ holotype. Body length 37 mm. Head width (across genal apices) 4.1 mm. Collum: Length/width ratio 47.3%. 10th segment: Protergal width/metatergal width ratio 66.9%. Metatergite of 10th segment: Length/width ratio 27.7%; depth/width ratio 68.3%. Segmental

widths as follows:

Collum 5.5 mm	13–4th 6.4
2nd 5.9	15th 6.2
3rd 6.1	16th 5.9
4th 6.2	17th 5.2
5th 6.3	18th 4.1
6th–12th 6.5	

Paratypes (8 ♂♂, 7 ♀♀ in parentheses). Body length 33–36 mm (34–40 mm). Head width (across genal apices) 3.8–4.1 mm (3.9–4.5 mm). Collum: Width 4.9–5.5 mm (5.0–5.8 mm); length/width ratio 37.5–50.0% (44.0–47.4%). 10th segment: Protergal width/metatergal width ratio 64.5–70.4% (70.5–73.5%). Metatergite of 10th segment: Width 5.9–6.5 mm (6.0–7.1 mm); length/width ratio 27.0–32.7% (26.5–28.6%); depth/width ratio 65.6–68.9% (70.5–74.6%).

Distribution: Known only from the type locality.

Remarks: This species is similar to *R. holstil* (Pocock) from Is. Okinawa-jima, the Ryukyu Islands, but can be distinguished in having gray colored tergites, a pair of high sternal projections between 4th legs of the male, and the acropodite of the male gonopod which is very wide from the base to the twisted portion.

ACKNOWLEDGMENTS

I wish to express my gratitude to Dr. Rowland M. Shelley (North Carolina State Museum of Natural Science) and Dr. H. Katakura (Hokkaido Univ.) for their critical reading of earlier drafts of the manuscript and valuable comments. I am also grateful to Dr. R. L. Hoffman (Virginia Museum of Natural History), Mr. Y. Murakami (Niihama) and Mr. K. Shinohara (Koiwa High School, Tokyo) for their valuable advice and encouragement. Mr. A. Moroto (Mie) kindly offered me a valuable material used in this paper.

REFERENCES

- 1 Pocock, R. I. (1895) Report upon Chilopoda and Diplopoda in the Chinese Seas. *Ann. Mag. Nat. Hist. Ser. 6*, **15**: 346–372.
- 2 Verhoeff, K. W. (1936) Zur Kenntniss ostasiatischer Strongylosomiden und Fontariiden. *Zool. Anz.*, **115**: 297–311.
- 3 Takakuwa, Y. (1942) Über weitere japanische *Rhyssodesmus* Arten. *Trans. Nat. Hist. Soc. Formosa*, **32**: 197–203.
- 4 Miyosi, Y. (1952) Beiträge zur Kenntniss japanischer Myriopoden 5. Aufsatz: Über zwei neue Arten von Diplopoda. *Zool. Mag. Tokyo*, **61**: 314–316. (In Japanese, with German résumé.)
- 5 Miyosi, Y. (1957) Beiträge zur Kenntniss japanischer Myriopoden 22. Aufsatz: Über zwei neue Arten von Diplopoda. *Zool. Mag. Tokyo*, **66**: 403–406. (In Japanese, with German résumé.)
- 6 Jeekel, C. A. W. (1952) Milliped Miscellany. *Ent. Berichten*, **14**: 71–77.
- 7 Haga, Y. (1968) [Millipeds of Japan 1], 1–11., pls. 1–6. The author. (In Japanese)
- 8 Shinohara, K. (1977) Reevaluation on *Riukiaria* (Diplopoda). *Acta Arachnol.*, **27**: 115–119. (In Japanese)
- 9 Tanabe, T. (1988) Two new species of the genus *Riukiaria* from Kyūshū and Is. Yaku-shima, Japan (Diplopoda: Polydesmida: Xystodesmidae). *Acta Arachnol.*, **37**: 37–45.
- 10 Golovatch, S. I. (1978) Some east Asian millipedes (Diplopoda) in the collection of the Zoological Institute, USSR Academy of Science. *Entomologicheskoe Obozr.*, **57**: 677–681. (In Russian)
- 11 Takakuwa, Y. (1941) *Rhyssodesmus* Arten aus Japan. *Trans. Nat. Hist. Soc. Formosa*, **31**: 413–415.
- 12 Wang, Y. M. (1956) *Serica* Ie: Records of myriapods on Formosa with description of new species (2). *Quart. Jour. Taiwan Mus.*, **9**: 157–158.
- 13 Wang, Y. M. (1957) *Serica* Ig: Records of myriapods on Taiwan Island (4) six new Polydesmids. *Quart. Jour. Taiwan Mus.*, **10**: 103–111.
- 14 Shelley, R. M. (1981) Revision of the milliped genus *Sigmoria* (Polydesmida: Xystodesmidae). *Mem. Amer. Entomol. Soc.*, No. 33: 140 pp.

Ciliated Protozoa in the Rumen of Holstein-Friesian Cattle (*Bos taurus taurus*) in Hokkaido, Japan, with the Description of Two New Species

AKIRA ITO and SOICHI IMAI¹

*Nishimon Agricultural and Mutual Aid Association, Okoppe Branch, Monbetsu-gun,
Hokkaido 098-15, and ¹Department of Parasitology, Nippon Veterinary
and Zootechnical College, Musashino, Tokyo 180, Japan*

ABSTRACT—The composition of rumen ciliates in the Holstein-Friesian cattle bred in Hokkaido, Japan was surveyed. Of 50 species with 19 formae under 15 genera identified, two new species were recognized, then described as *Entodinium okoppensis* and *Ostracodinium munham*. *Entodinium okoppensis* may be classified further into such four morphotypes as, *okoppensis*, *bispinosum*, *bifidum* and *monospinosum* on the basis of caudal processes. Thirteen species were the first record in Japanese cattle. The average number of individuals per 1 ml of rumen fluid was 5.4×10^5 , and that of species per head of host was 17.2.

INTRODUCTION

Rumen ciliate faunae would be different among the species of their hosts and/or among the hosts inhabiting separated areas [1, 2]. Surveys and comparisons of rumen ciliate faunae of various ruminants in different regions should provide informations about phylogenetic relationships among rumen ciliates, because it is suggested that the composition of rumen ciliates has peculiarly differentiated in relatively limited habitats since transfaunation has been assumed to occur only by direct contact between the hosts [3].

Various races of cattle including Japanese Black and Japanese Brown for beef, and Holstein-Friesian for milk have been kept in various localities in Japan [4, 5]. Holstein-Friesian which originated in the Netherlands and Germany were imported to Japan mainly through United States of America in the last part of the 19th century [5]. Since then, they have been kept as the most popular dairy cattle in Japan, especially in Hokkaido.

The rumen ciliate faunae of Japanese cattle in Honshu and Kyushu have been surveyed by Imai *et*

al. [6, 7], but not of those in Hokkaido. The present paper deals with the species composition of ciliates obtained from the Holstein-Friesian cattle in Hokkaido and includes descriptions of two new species with four new formae.

MATERIALS AND METHODS

Samples were collected from 71 Holstein-Friesian cattle bred in Okoppe, Hokkaido, Japan by means of rumen puncture from 1985 to 1988. They were immediately fixed and stained in methylgreen-formalin-saline (MFS) solution [3]. For close examination of nuclei and for type specimens, a part of the samples in which new species were recognized was stained with Mayer's hematoxylin and prepared as permanent slides. Identification was made followed by Ogimoto and Imai [3], Dogiel [8], Kofoed and MacLennan [9–11], and Imai [12]. Terminology of the morphology and orientation of ciliates for description of the new species conformed to our previous papers [1, 2, 3, 13]. The total ciliate number was calculated by means of Fuchs-Rosenthal haemocytometer. To obtain the average value for the ciliate density under normal distribution, it was computed from each value of ciliate number converted into logarithms. The generic composition is

shown as the percentage of each genus in about 300 individuals.

RESULTS

Entodinium okoppensis n. sp.

(Figs. 1 and 2)

Description: Body rectangular to nearly square. Ectoplasm forming one to three caudal spines or lobes with various size at the posterior end of body. Anterior end of body flattened or concave. Anterior lip hardly visible when adoral cilia retracted. Vestibulum fairly large and funnel-shaped extending vertically but slightly bending leftward. Rectum short and extending vertically to

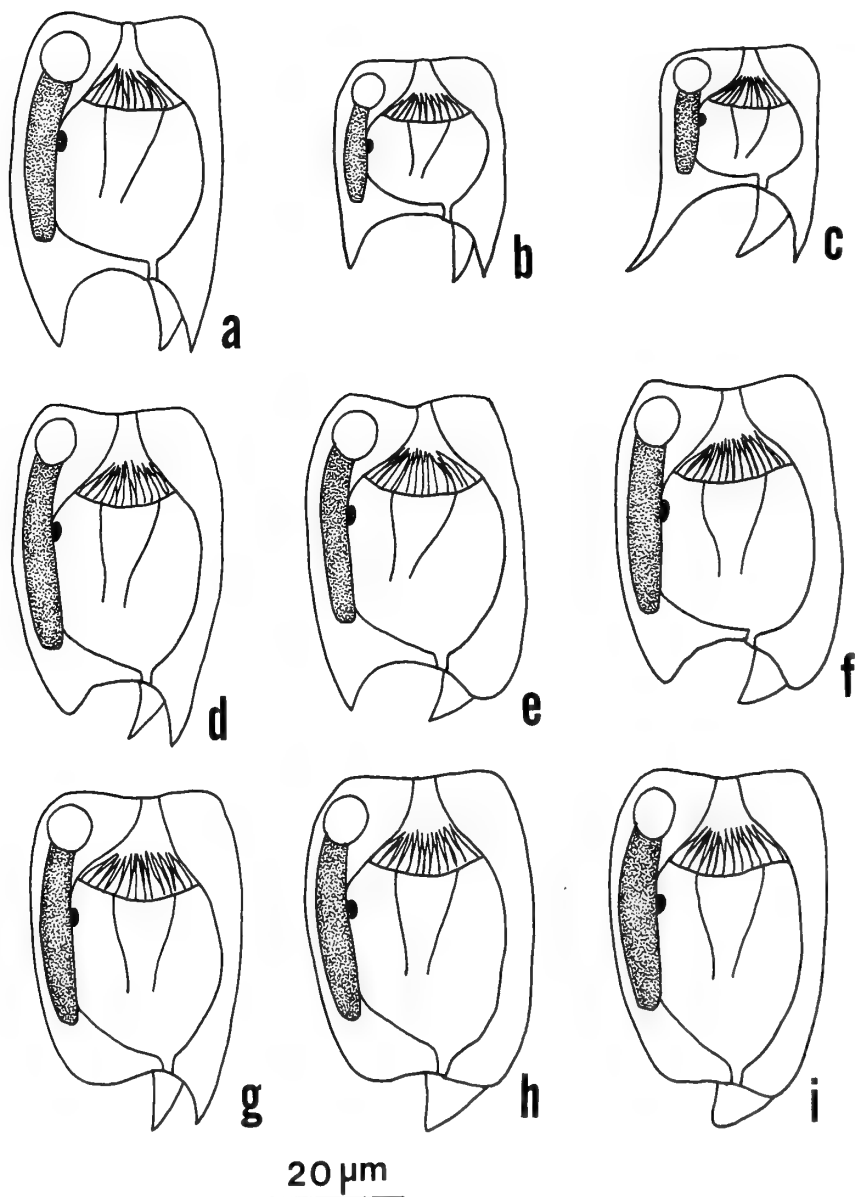


FIG. 1. *Entodinium okoppensis* n. sp. with its formae. a-d: forma *okoppensis*. e and f: forma *bispinosum*. g: forma *bifidum*. h and i: forma *monospinosum*.

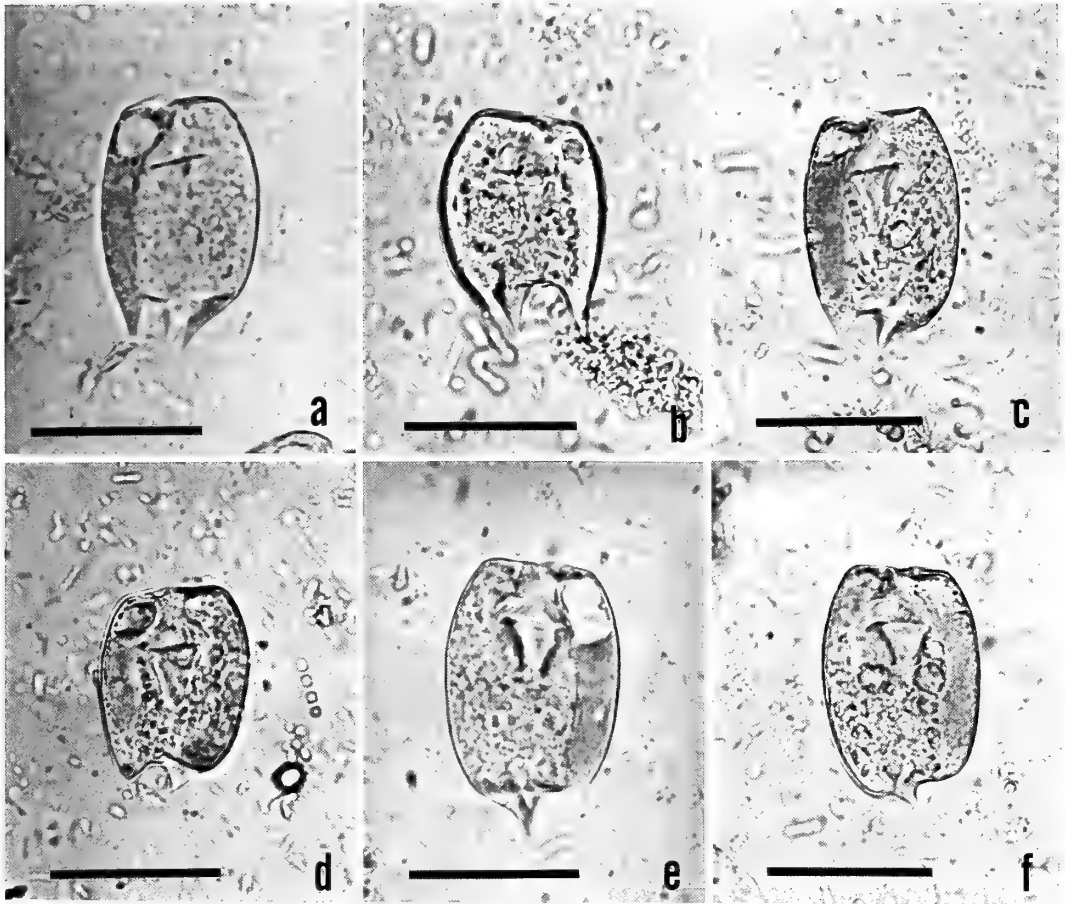


FIG. 2. Photomicrographs of *Entodinium okoppensis* n. sp. a and b: forma *okoppensis*. c and d: forma *bispinosum*. e: forma *bifidum*. f: forma *monospinosum*. All the specimens are fixed and stained with MFS solution. Bar in each figure indicates 30 μm .

cytoproct in the left side of median line. Macronucleus straight and slender rod shaped, four-fifths of body length, situated in the right periphery of body. Anterior end of macronucleus flattened, but posterior end rounded. An ovoidal micronucleus near left margin of middle of macronucleus. A contractile vacuole at just anterior and slightly upper to macronucleus.

Measurement: Body length 35.7 ± 6.3 (24–55), caudal process 4.2 ± 2.3 (1–10), width 26.2 ± 3.0 (21–42) μm , length/width ratio 1.36 ± 0.20 (0.9–1.7) ($n=60$).

Type specimens: Holotype, individual with retracted adoral cilia on microslide, No. 18901. Col. 5 MAR 1988, Ito, and 2 paratypes are deposited in

the Department of Parasitology, Nippon Veterinary and Zootechnical College, Musashino, Tokyo, Japan.

Type host and locality: Holstein-Friesian cattle, *Bos taurus taurus*, in Hokkaido, Japan.

Habitat: Rumen.

Frequency: In 53.5% of the cattle surveyed.

Etymology: *Entodinium okoppensis* is named after the place this new species was found.

Four formae may be distinguished based on the number and shape of caudal processes.

Entodinium okoppensis forma *okoppensis* n. f.
(Figs. 1-a, b, c, d and 2-a, b)

Diagnosis: Three caudal processes; right one pointed or dull spine and sometimes bends outward, left-lower and left-upper ones pointed spines.

Frequency: In 53.5 % of the cattle surveyed.

Entodinium okoppensis forma *bispinosum* n. f.
(Figs. 1-e, f and 2-c, d)

Diagnosis: Three caudal processes; right one pointed or dull spine, left-upper one pointed spine, left-lower one blunt lobe.

Frequency: In 5.6 % of the cattle surveyed.

Entodinium okoppensis forma *bifidum* n. f.
(Figs. 1-g and 2-e)

Diagnosis: Two caudal spines in the same length at left side only.

Frequency: In 5.6 % of the cattle surveyed.

Entodinium okoppensis forma *monospinosum* n. f.
(Figs. 1-h, i and 2-f)

Diagnosis: One pointed or dull caudal spine at left-upper side.

Frequency: In 5.6 % of the cattle surveyed.

Remarks: *Entodinium okoppensis* closely resembles *Entodinium indicum* Kofoed et MacLennan, 1930 [9] and *E. bubalum* Imai, 1981 [14] in the shape of body and macronucleus, and the position of contractile vacuole. It is, however, distinguished from both *E. indicum* and *E. bubalum* by the position of the cytoproct and of caudal spines; that is, the largest caudal spine of both species is situated at the center of body, and the cytoproct lies at the center of body within the central spine. The body shape of *E. okoppensis okoppensis* also resembles *E. triacum* Buisson, 1923 [8, 15, 16], especially *E. triacum dextrum* Dogiel, 1927 [8]. Unfortunately, none of descriptions on the position of contractile vacuole which is one of the most important taxonomic criteria were made in *E. triacum* [8, 15, 16]. However, anterior end of *E. triacum* is more rounded than *E. okoppensis*, and the adoral lips are visible in *E. triacum* when the ciliate contracts the adoral cilia [8] but not visible in *E. okoppensis*. *Entodinium okop-*

ensis bifidum resembles *E. bifidum* Dogiel, 1927 [8] in the possession of two caudal spines at the posterior left end, but it is easily distinguished from *E. bifidum* by the difference in body shape and the location of contractile vacuole.

Taxonomical comment: The caudal process is one of the most prominent features under the microscope. However, it is clearly shown that the variation of caudal processes is continuous [3, 17, 18], thus these features are considered to be not suitable as the taxonomical character for species at present. In addition, the variation of caudal processes is recognized within one and the same host as also shown in *E. okoppensis* in the present examination, so that it also may not be able to be established as the character for subspecies. Therefore, the features of caudal processes seem to be the most adequate when they are used as the classification of formae which are not prescribed by the International Code of Zoological Nomenclature. There are some opinions that the establishment of formae is not necessary. However, the caudal processes seem to be related to the differentiation of rumen ciliates within the hosts, since a peculiar spinated form, such as *Epidinium ecaudatum capricornisi* has been found from only one host, Japanese serow [19], in spite of very wide distribution of other formae of this species, such as *E. ecaudatum ecaudatum* and *E. ecaudatum caudatum* [3]. Thus, the authors consider that it is significant to create formae in a species of rumen ciliates.

Ostracodinium munham n. sp.
(Figs. 3 and 4)

Description: Body ovoid. An apparent round lobe to the right of cytoproct at posterior end of body. Lobe with some variations (Fig. 3-b, c). Left posterior end of body rounded and sometimes projecting (Fig. 3-d). Large, slightly flattened operculum at top of body. Clear lips surrounding peristome and left ciliary zone when the ciliate contracted. Rectum clear and forming a short slit. Macronucleus rod-shaped tapering posteriorly with bend some degree along the left periphery of ectoplasm. An elliptical micronucleus at lower side of the middle of macronucleus. Three con-

tractile vacuoles in tandem in ectoplasm at lower-left side of macronucleus. Most anterior and posterior vacuoles at same level as anterior and posterior ends of macronucleus. Broad skeletal plate over most of upper part of body forming a weak arc and running obliquely to long axis from just posterior of operculum to the level of the posterior contractile vacuole. Left edge of the plate turning inward and extending one-fifth of the width of plate.

Measurement: Body length 78.7 ± 7.5 (65–90), width 54.6 ± 4.3 (50–65) μm , length/width ratio 1.43 ± 0.08 (1.3–1.6) ($n=20$).

Type specimens: Holotype, individual with re-

tracted adoral cilia on microslide, No. 18902. Col. 18 JAN 1988, Ito, and 6 paratypes are deposited in the Department of Parasitology, Nippon Veterinary and Zootechnical College, Musashino, Tokyo, Japan.

Type host and locality: Holstein-Friesian cattle, *Bos taurus taurus*, in Hokkaido, Japan.

Habitat: Rumen.

Frequency: In 2.8% of the cattle surveyed.

Etymology: *Ostracodinium munham* is named after the possession of lobe. Munha means a lobe in Aino.

Remarks: This new species closely resembles *Ostracodinium iwawoi* Imai, 1988 [13], in size and shape of body and of skeletal plate, but *O. iwawoi* differs from *O. munham* in its four contractile vacuoles and a skeletal plate turning one-third of its width. It also resembles *O. trivesiculatum* Kofoed et MacLennan, 1932 [10], *O. rugoloricatum* Kofoed et MacLennan, 1932 [10] and *O. mammosum* (Railliet, 1890) [8, 10], in having three contractile vacuoles. However, it differs from *O. trivesiculatum* in the folded skeletal plate and the presence of posterior lobe, from *O. rugoloricatum* in possessing no skeletal plate turning toward the middle of body, and from *O. mammosum* in shape of skeletal plate, and shape and number of posterior lobe of ectoplasm. In the point of possession of a right posterior lobe, the present species is also common with *O. obtusum* f.

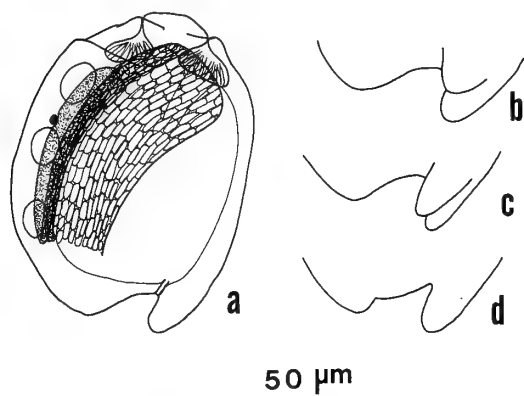


FIG. 3. *Ostracodinium munham* n. sp. a: Upper view of whole body. b-d: Variations in the caudal lobes.

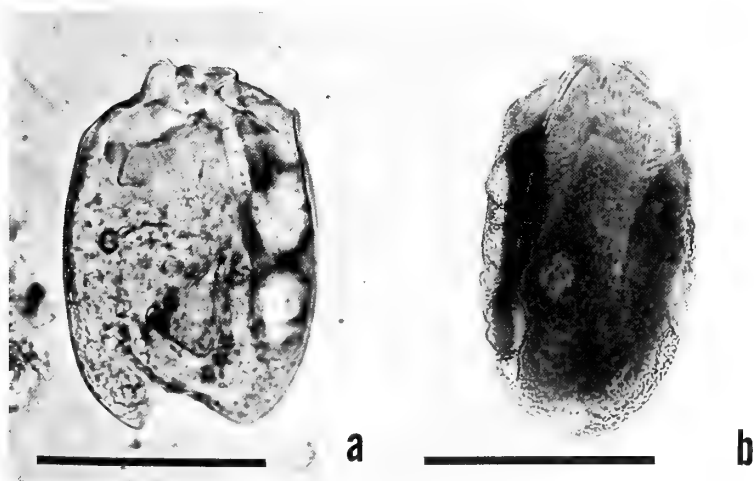


FIG. 4. Photomicrographs of *Ostracodinium munham* n. sp. a: Cell fixed and stained with MFS solution. b: Cell stained with Mayer's hematoxylin. Bar in each figure indicates 50 μm .

TABLE 1. Species composition and frequency of rumen ciliate protozoa found from the Holstein-Friesian cattle in Hokkaido

Family	Species	Frequency (%)
Isotrichidae	<i>Dasytricha</i>	
	<i>ruminantium</i> Schuberg	71.8
	<i>Isotricha</i>	
	<i>prostoma</i> Stein	66.2
	<i>intestinalis</i> Stein	33.8
	<i>Oligoisotricha</i>	
	<i>bubali</i> (Dogiel)	9.9
Blepharocorythidae	<i>Microcetus</i>	
	<i>lappus</i> Orpin et Mathiesen*	1.4
	<i>Charonina</i>	
Ophryoscolecidae	<i>ventriculi</i> (Jameson)	59.2
Entodiniinae	<i>Entodinium</i>	
	<i>nanellum</i> Dogiel	100.0
	<i>simplex</i> Dogiel	100.0
	<i>parvum</i> Buisson	95.8
	<i>longinucleatum</i> Dogiel	95.8
	<i>caudatum</i>	
	f. <i>caudatum</i> Stein	85.9
	f. <i>lobosopinosum</i> Dogiel	77.5
	<i>rostratum</i> Fiorentini	76.1
	<i>exiguum</i> Dogiel	60.6
	<i>dilobum</i> (Dogiel)	54.9
	<i>okoppensis</i> n. sp*	
	f. <i>okoppensis</i> n. f.	53.5
	f. <i>bispinosum</i> n. f.	5.6
	f. <i>bifidum</i> n. f.	5.6
	f. <i>monospinosum</i> n. f.	5.6
	<i>bursa</i> Stein	33.8
	<i>ovinum</i> Dogiel	19.7
	<i>bimastus</i> Dogiel	12.7
	<i>minimum</i> Schuberg	11.3
	<i>chatterjeei</i> Das-Gupta*	11.3
	<i>bovis</i> Wertheim*	5.6
	<i>rectangulatum</i> Kofoid et MacLennan*	4.2
	<i>simulans</i> Lubinsky*	2.8
	<i>dubardi</i> Buisson	1.4
	<i>quadricuspis</i> Dogiel*	1.4
Ophryoscolecidae	<i>Diplodinium</i>	
	<i>anisacanthum</i> Da Cunha	
	f. <i>anisacanthum</i> Da Cunha	50.7
	f. <i>monacanthum</i> Dogiel	19.7
	f. <i>anacanthum</i> Dogiel	16.9

	<i>f. diacanthum</i> Dogiel	7.0
	<i>f. triacanthum</i> Dogiel	7.0
	<i>f. tetracanthum</i> Dogiel	7.0
	<i>f. pentacanthum</i> Dogiel	5.6
	<i>dentatum</i> (Stein)	5.6
	<i>minor</i> (Dogiel)	4.2
	<i>Eodinium</i>	
	<i>lobatum</i> Kofoid et MacLennan	52.1
	<i>posterovesiculatum</i> (Dogiel)	46.5
	<i>monolobosum</i> (Hsiung)*	8.5
	<i>rectangulatum</i> Kofoid et MacLennan*	1.4
	<i>Eudiplodinium</i>	
	<i>rostratum</i> (Fiorentini)	84.5
	<i>dilobum</i> (Dogiel)	50.7
	<i>maggii</i> (Fiorentini)	42.3
	<i>bovis</i> (Dogiel)	19.7
	<i>monolobum</i> (Dogiel)	16.9
	<i>Polyplastron</i>	
	<i>multivesiculatum</i> (Dogiel et Fedorowa)	39.4
	<i>Metadinium</i>	
	<i>affine</i> Dogiel et Fedorowa	39.4
	<i>medium</i> Awerinzew et Mutafova	7.0
	<i>ypsilon</i> (Dogiel)*	7.0
	<i>Ostracodinium</i>	
	<i>mammosum</i> (Railliet)	45.1
	<i>gracile</i> Dogiel	39.4
	<i>trivesiculatum</i> Kofoid et MacLennan*	21.1
	<i>obtusum</i> (Dogiel et Fedorowa)	19.7
	<i>clipeolum</i> Kofoid et MacLennan	5.6
	<i>munham</i> n. sp.*	2.8
	<i>Enoploplastron</i>	
	<i>triloricatum</i> (Dogiel)*	1.4
Ophryoscolecidae		
Ophryoscolecinae	<i>Epidinium</i>	
	<i>ecaudatum</i> (Fiorentini)	
	<i>f. caudatum</i> Fiorentini	25.4
	<i>f. ecaudatum</i> Fiorentini	18.3
	<i>f. cattanei</i> Fiorentini	7.0
	<i>f. bulbiferum</i> Dogiel	4.2
	<i>f. quadricaudatum</i> Sharp	2.8
	<i>f. hamatum</i> Schulze	1.4
	<i>Ophryoscolex</i>	
	<i>purkynjei</i> Stein	14.1
		15 genera
Total genera, species and formae		50 species
		19 formae

* First record in Japanese cattle.

TABLE 2. Percentage generic composition of the rumen ciliate protozoa in the Holstein-Friesian cattle in Hokkaido*

Genus	Mean	Range
<i>Entodinium</i>	82.7	43.6–98.6
<i>Eudiplodinium</i>	4.6	0–17.7
<i>Diplodinium</i>	2.5	0–24.7
<i>Dasytricha</i>	2.0	0–8.0
<i>Epidinium</i>	2.0	0–26.7
<i>Ostracodinium</i>	1.7	0–6.7
<i>Eodinium</i>	1.5	0–6.7
<i>Isotricha</i>	1.2	0–9.3
<i>Charonina</i>	0.6	0–4.0
<i>Metadinium</i>	0.6	0–4.7
<i>Oligoisotricha</i>	0.2	0–4.7
<i>Polyplastron</i>	0.2	0–2.0
<i>Microcetus</i>	0.1	0–0.7
<i>Enoploplastron</i>	0.1	0–2.0
<i>Ophryoscolex</i>	0.1	0–2.3

* n=71.

monolobum Dogiel, 1927 [8], but it is easily discriminated from *O. munham* in different body size and number of contractile vacuoles.

Composition of rumen ciliates. Species and their frequency from 71 Holstein-Friesian examined are shown in Table 1. Fifty species with 19 formae under 15 genera were identified in all. Of them, 13 species were the first record in Japanese cattle. *Entodinium simplex* and *E. nanellum* occurred in all the hosts examined. Of the other ciliates, 6 species with 2 formae; *Entodinium parvum*, *E. longinucleatum*, *E. caudatum* f. *caudatum*, *E. caudatum* f. *lobosospinosum*, *E. rostratum*, *Eudiplodinium rostratum* and *Dasytricha ruminantium*, were predominant, and the frequencies of them were over 70% in the animals examined.

Table 2 shows the percentage compositions of

genera of the ciliates in this examination. The percentage occupied by the genus *Entodinium* was the highest, the ratio of which was 82.7% on average. Though average ratio of the genus *Eudiplodinium* was next highest in number, *Epidinium* and *Diplodinium* occasionally showed higher ratio depending on the host individual.

The average number of species per head of host and the total ciliate number per one milliliter of rumen fluid are shown in Table 3. The average number of ciliate species was 17.2, and the average ciliate density of 71 samples was $5.4 \times 10^5/\text{ml}$.

DISCUSSION

Rumen ciliate compositions of the cattle in Japan, mainly in Honshu were formerly surveyed on various races without distinction by Imai *et al.* [6, 7], and 42 species with 12 formae were identified. When the present results were compared to that by Imai *et al.* [6, 7], 37 species were common in both areas, and the prominent species almost coincided with each other; included are several species of the genus *Entodinium*, *E. nanellum*, *E. parvum*, *E. simplex* and *E. longinucleatum*.

Thirteen species with 7 formae including 2 new species were the first record in Japanese cattle. Of those, *Entodinium bovis*, *E. rectangulatum*, *E. simulans*, *E. quadricuspis*, *Microcetus lappus*, *Metadinium ypsilon* and *Enoploplastron trilorica-tum* have been already detected from the various races of humpless cattle (*Bos taurus taurus*) in various areas [8, 20–22]. *Microcetus lappus* was first described from the cattle in Norway [22], and the present detection places the second report of this species.

Entodinium chatterjeei, *Eodinium monolobosum*, *Eod. rectangulatum*, and *Ostracodinium trivesiculatum* have been found mainly from the

TABLE 3. Average number of species appeared and average ciliate density in the Holstein-Friesian cattle in Hokkaido*

Number of species		Ciliate density ($\times 10^4/\text{ml}$)	
Mean	Range	Mean	Range
17.2	5–30	53.7	14.5–168.2

* n=71.

domestic animals kept in tropical area [1, 2, 10, 13, 23, 24] but few from humpless cattle. There may be two possible reasons for this. One is that Holstein-Friesian cattle in Hokkaido might have an experience of contact with the cattle introduced from any tropical area, and the other is that these ciliate species are originally worldwide as well as *E. nanellum* and *E. simplex*. However, the former possibility seems to be low, because Holstein-Friesian cattle have been kept thoroughly in the temperate zones, and have had very few chances to contact with the tropical cattle. The high frequency of appearance of *E. okoppensis* was characteristic of the rumen ciliate fauna of the cattle in Hokkaido. The morphological features of the anterior end of body and macronucleus, and the position of contractile vacuole of *E. okoppensis* closely resemble those of *E. indicum* and *E. bubalum*. These two species have also been detected mainly from the animals inhabiting tropical areas [1, 2, 9, 13, 14], thus it seems to have a poor relationship to Holstein-Friesian. However, it will be interesting that *Campylodinium ovumrajae*, a closely related species to *Entodinium* and detected only from the forestomach of camels [8], has very similar morphological aspects on the anterior end of body, macronucleus and the position of contractile vacuole. Provided these species are assumed to reflect their phylogenetic relations in spite of their phylogenetically separated hosts, we can speculate that such morphotype is of primitive group and must have a wide distribution in various ruminants. This speculation would be supported by the fact that *E. triacum* with two formae which has been widely detected from the cattle in Europe [8, 25], Mexico [26] and China [23] also resembles *E. okoppensis*, although the description of *E. triacum* has been insufficient [8, 15, 16].

The average of the ciliate density and the average number of species per head of the host resembled those in the cattle in Honshu and Kyushu reported by Imai *et. al.* [6, 7]. The percentage composition of genera also almost coincided with the data from the Japanese cattle reported earlier by us [7]. It is known that the ciliate density and the composition of genera are strongly affected by the kinds and amounts of food taken by the host [27–29], and that when the host is fed with concen-

trates-rich ration, entodiniid ciliates rapidly grow, and the ratio of entodiniid ciliates and the total ciliate density become higher [29]. The similarity of ciliate percentage composition in various areas of Japan may be due to the similarity of feeding conditions. Frequent introduction of the Japanese dairy cattle from Hokkaido to Honshu may be another reason.

ACKNOWLEDGMENTS

The authors wish to thank Mr. Shinkichi Kakuta, owner of the Kakuta Farm, for cooperating in the collection of the samples. Thanks are also due to Miss. Kuniko Kitamura, of the Okoppe Library, Dr. Yoshikatsu Morikawa and his colleagues, of the Nishimon A. M. A. A., Okoppe Branch, for their helpful assistance in the present examination. The first author expresses his gratitude to his wife, Takako Ito, for her continuous help.

REFERENCES

- 1 Imai, S. (1985) Rumen ciliate protozoal faunae of Bali cattle (*Bos javanicus domesticus*) in Indonesia, with the description of a new species, *Entodinium javanicum* sp. nov. Zool. Sci., **2**: 591–600.
- 2 Imai, S. (1986) Rumen ciliate fauna of zebu cattle (*Bos taurus indicus*) in Sri Lanka, with the description of a new species, *Diplodinium sinhalicum* sp. nov. Zool. Sci., **3**: 699–706.
- 3 Ogimoto, K. and Imai, S. (1981) Atlas of Rumen Microbiology, Japan Scientific Societies Press, Tokyo, 231 pp.
- 4 Rouse, J. E. (1970) World Cattle, Vol. 2, University of Oklahoma Press, Norman, pp. 991–1001.
- 5 Shoda, Y. (1987) Domesticated Animals of The World, Kodansha, Tokyo, 223 pp. (In Japanese)
- 6 Imai, S., Katsuno, M. and Ogimoto, K. (1978) Distribution of rumen ciliate protozoa in cattle, sheep and goat and experimental transfaunation of them. Jpn. J. Zootech. Sci., **49**: 494–505. (In Japanese with English summary)
- 7 Imai, S., Shimizu, M., Kinoshita, M., Toguchi, M., Ishii, T. and Fujita, J. (1982) Rumen ciliate protozoal fauna and composition of the cattle in Japan. Bull. Nippon Vet. Zootech. Coll., **31**: 70–74. (In Japanese with English summary)
- 8 Dogiel, V. A. (1927) Monographie der Familie Ophryoscolecidae. Arch. Protistenkd., **59**: 1–288.
- 9 Kofoed, C. A. and MacLennan, R. F. (1930) Ciliates from *Bos indicus* Linn. 1. The genus *Entodinium* Stein. Univ. Calif. Publ. Zool., **33**: 471–544.
- 10 Kofoed, C. A. and MacLennan, R. F. (1932) Cili-

- ates from *Bos indicus* Linn. 2. A revision of *Diplodinium* Schuberg. Univ. Calif. Publ. Zool., **37**: 53–152.
- 11 Kofoed, C. A. and MacLennan, R. F. (1933) Ciliates from *Bos indicus* Linn. 3. *Epidinium* Crawley, *Epiplastron* gen. nov., and *Ophryoscolex* Stein. Univ. Calif. Publ. Zool., **39**: 1–33.
 - 12 Imai, S. (1988) Some progress in taxonomy and phylogeny of rumen ciliate protozoa. J. Jpn. Vet. Med. Assoc., **41**: 73–80. (In Japanese)
 - 13 Imai, S. (1988) Ciliate protozoa in the rumen of Kenyan zebu cattle, *Bos taurus indicus*, with the description of four new species. J. Protozool., **35**: 130–136.
 - 14 Imai, S. (1981) Four new rumen ciliates, *Entodinium ogimotoi*, sp. n., *E. bubalum* sp. n., *E. fujitai* sp. n. and *E. tsunodai* sp. n., and *Oligoisotricha bubali* (Dogiel, 1928) n. comb. Jpn. J. Vet. Sci., **43**: 201–209.
 - 15 Buisson, J. (1923) Infusoires nouveaux parasites d'antilopes Africaines. C. R. Soc. Biol., **89**: 1217–1219.
 - 16 Buisson, J. (1924) Quelques infusoires parasites d'antilopes Africaines. Ann. Parasitol. Hum. Comp., **2**: 155–160.
 - 17 Hempel-Zawitkowska, J. and Latteur, B. (1977) Quelques remarques sur la systematique du genre *Entodinium* Stein, 1858. Acta Zool. Pathol. Antverp., **69**: 189–202.
 - 18 Poljansky, G. and Strelkow, A. (1934) Beobachtungen über die Variabilität einiger Ophryoscolecidae (Infusoria, Entodiniomorpha) in Klonen. Zool. Anz., **107**: 215–220.
 - 19 Imai, S., Abe, M. and Ogimoto, K. (1981) Ciliate protozoa from the rumen of the Japanese serow, *Capricornis crispus* (Temminck). Jpn. J. Vet. Sci., **43**: 359–367.
 - 20 Wertheim, P. (1935) Infusorien aus dem Wiederkäuermagen von Gebiete Jugoslawiens nebst einer Übersicht dieser Tierchen von Balkanhalbinsel-Bereich und ein kurzer Bericht über die Pferdedarminfusorien, zugleich Revision der familie Ophryoscolecidae. Vet. Arh., **5**: 386–536.
 - 21 Lubinsky, G. (1957) Studies on the evolution of the Ophryoscolecidae (Ciliata : Oligotricha). 1. A new species of *Entodinium* with “*caudatum*”, “*lobosporinosum*” and “*dubardi*” forms and some evolutionary trends in the genus *Entodinium*. Can. J. Zool., **35**: 111–133.
 - 22 Orpin, C. G. and Mathiesen, S. D. (1986) *Microcetus lappus* gen. nov., sp. nov. : New species of ciliated protozoan from bovine rumen. Appl. Environm. Microbiol., **52**: 527–530.
 - 23 Hsiung, T.-S. (1932) A general survey of the protozoan fauna of the rumen of the Chinese cattle. Bull. Fan Mem. Inst. Biol., **3**: 87–107.
 - 24 Das-Gupta, M. (1935) Preliminary observations on the protozoan fauna of rumen of the Indian goat, *Capra hircus* Linn. Arch. Protistenkd., **85**: 153–172.
 - 25 Jirovec, O. (1933) Beobachtungen über die Fauna des Rinderpansens. Z. Parasitenkd., **5**: 584–591.
 - 26 Chavarria, M. (1933) Estudios protistologicos. 1. Fauna del tubo digestivo del toro (*Bos taurus* Linn.) de Mexico. Ann. Inst. Biol. Univ. Nac. Mexico, **3**: 109–142.
 - 27 Ferber, K. E. (1928) Die Zahl und Masse der Infusorien im Pansen und ihre Bedeutung für den Eiweissaufbau beim Wiederkäuer. Z. Tierzucht. Zuchtungsbiol., **12**: 31–63.
 - 28 Warner, A. C. I. (1962) Some factors influencing the rumen microbial population. J. Gen. Microbiol., **28**: 129–146.
 - 29 Hungate, R. E. (1966) Rumen and Its Microbes, Academic Press, New York, 533 pp.

The *Drosophila polychaeta* and the *D. quadrisetata* Species-Groups (Diptera: Drosophilidae) from Yunnan Province, Southern China

HIDE-AKI WATABE, XING CHAI LIANG¹

and WEN XIA ZHANG¹

Biological Laboratory, Sapporo College, Hokkaido University of Education,
Sapporo 002, Japan, and ¹Kunming Institute of Zoology,
Academia Sinica, Kunming, China

ABSTRACT—Three new and four known species of the *Drosophila polychaeta* and the *D. quadrisetata* species-groups are reported from Yunnan Province, southern China. An evolutionary process of the *virilis-repleta* Radiation is discussed on the basis of the recent information from southern China.

INTRODUCTION

The present paper deals with three new and four known species of the *Drosophila polychaeta* and the *D. quadrisetata* species-groups from Yunnan Province, southern China, both of which belong to the *virilis* section of the subgenus *Drosophila*.

Most of specimens described here were collected at watersides, by using traps baited with fermenting bananas. All the holotypes and a part of paratypes are deposited in the Kunming Institute of Zoology, Academia Sinica, Kunming, China, and the remaining paratypes in the Biological Laboratory, Hokkaido University of Education, Sapporo, Japan.

DROSOPHILA POLYCHAETA SPECIES-GROUP

D. polychaeta species-group, Sturtevant, 1942, Univ. of Texas Publ., 4213: 31.

Drosophila (Drosophila) daruma Okada

Drosophila (Drosophila) daruma Okada, 1956, Syst. Study, 155.

Specimens examined. China: 1 ♂, 1 ♀, Kunming, 11. X. 1988 (Collector: H. Watabe); 3 ♂, 1 ♀, Simao, 4. XI. 1987 (X. C. Liang); 2 ♂, Jinhong, Xishuang-banna district, 13. IX. 1985 (W. X. Zhang); 1 ♂, Menghan, Xishuang-banna district, 21. IX. 1985 (W. X. Zhang).

Distribution. Korea, Japan, Malaya, Borneo, India; China: Taiwan, Guangdong, Yunnan (n. loc.).

Remarks. This species is relatively common in southern and middle parts of Yunnan Province, but has not been collected in its northern districts.

Drosophila (Drosophila) latifshahi Gupta et Ray-Chaudhuri

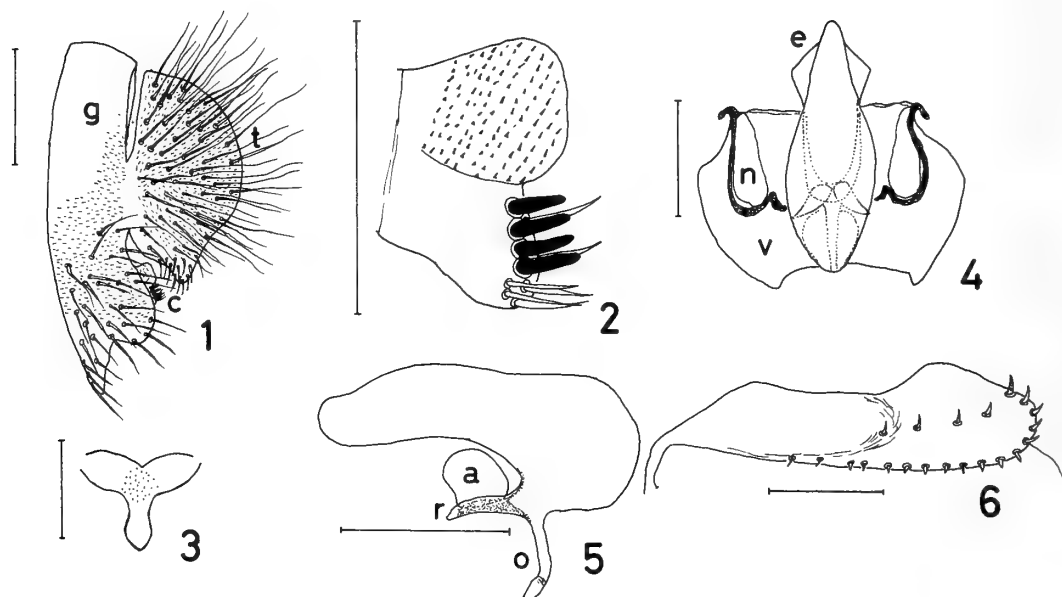
Drosophila (Scaptodrosophila) latifshahi Gupta et Ray-Chaudhuri, 1970 [1]: 67

Drosophila (Drosophila) latifshahi; Toda and Peng, 1989 [2]: 155.

Specimens examined. China: 31 ♂, 14 ♀, Simao, 4. XI. 1987 (X. C. Liang); 1 ♂, Menghan, 3. X. 1985 (W. X. Zhang).

Distribution. India, Bangladesh; China: Guangdong, Yunnan (n. loc.).

Remarks. *D. latifshahi* is a dominant species of waterside drosophilids, in Simao and Xishuang-banna districts.



FIGS. 1–6. *Drosophila (Drosophila) polychaeta* Patterson et Wheeler, 1942. 1: Periphallallic organs. 2: Surstylus. 3: Decasternum. 4: Phallic organs. 5: Aedeagus (lateral view). 6: Ovipositor. Signs: a, anterior paramere; c, surstylus; e, aedeagus; n, novasternum; o, aedeagal apodeme; r, vertical rod; t, cercus; v, ventral fragma. Scale-line=0.1 mm.

Drosophila (Drosophila) polychaeta
Patterson et Wheeler
(Figs. 1–6)

Drosophila (Drosophila) polychaeta Patterson et Wheeler, 1942 [3]: 102.

Patterson and Wheeler [3] described this species based on the laboratory strain from Texas, but did not refer to its genitalia. The present specimens are supposed to belong to a native population of *D. polychaeta*, and the description of the male and female genitalia is made below, together with its diagnostic characters.

Diagnosis. Brown species with 3 pairs of post-sutural dorsocentral bristles. Palpus with *ca.* 2 moderate and *ca.* 18 short bristles. C-index *ca.* 1.96, C3-fringe *ca.* 0.93. Epandrium fused to cercus at middle; anteroventral corner sharply pointed; caudoventral corner rounded (Fig. 1). Spermatheca unsclerotized.

Periphallallic organs (Figs. 1–3): Epandrium brown, darker on lower margin, pubescent except in upper portion and ventral margin, with *ca.* 30 bristles on lower half. Surstylus distally constricted into two parts; upper part flap-shaped, with tiny

thorn-like spines in somewhat regular rows; lower part nearly quadrate, with *ca.* 4 primary teeth and *ca.* 2 bristles on distal margin, and with *ca.* 5 bristles at caudoventral corner. Cercus oval, ventrally narrowing, entirely pubescent with *ca.* 53 long bristles and tuft of *ca.* 11 short bristles at lower apex. Decasternum pale brown, Y-shaped in ventral view, medially with small dark patches.

Phallic organs (Figs. 4, 5): Aedeagus T-shaped in lateral view, proximally broadened; aedeagal apodeme short, *ca.* 1/4 as long as aedeagus. Anterior paramere oval, without sensilla; posterior paramere absent. Vertical rod dark brown. Novasternum nearly triangular, without submedian spines. Ventral fragma laterally flattened, distally concaved in middle.

♀ reproductive organs (Fig. 6): Lobe of ovipositor pale orange, dorso-submedially expanded, with *ca.* 4 discal teeth, *ca.* 24 spine-like marginal teeth and 1 subterminal hair; ultimate marginal tooth darker than penultimate. Spermatheca very small, embedded in adipose tissue.

Specimens examined. China: 12 ♂, 13 ♀, Simao, 4. XI. 1987 (X. C. Liang).

Distribution. Neotropics, Micronesia, Hawaii,

North America, Europe; China (n. loc.): Yunnan.

Origin. *D. polychaeta* is cosmopolitan, but its extremely wide range of distribution is probably due to the propagation with man [4]. Fonseca [5] states that *D. polychaeta* is frequently collected on ships in British ports but does not establish its permanent population there. The origin of this species was unknown. The present collection was made in a natural subtropical forest remote from a human residence. This suggests that southern China might be the original distribution range of *D. polychaeta*.

DROSOPHILA QUADRISETATA SPECIES-GROUP

D. quadrisetata species-group: Toda and Peng, 1989 [2]: 158.

This group is very small, and consisted of only three species: *D. potamophila* Toda et Peng and *D. beppui* Toda et Peng from southern China, and *D. quadrisetata* Takada, Beppu et Toda from northern Japan. The last species was previously included in the *polychaeta* species-group [6]. Three new species are added in this article.

Drosophila (Drosophila) potamophila Toda et Peng

Drosophila (Drosophila) potamophila Toda et Peng, 1989 [2]: 159.

Specimens examined. China: 1 ♂, 1 ♀, Simao, Yunnan Province, 4. XI. 1987 (X. C. Liang).

Distribution. China: Guangdong, Yunnan (n. loc.).

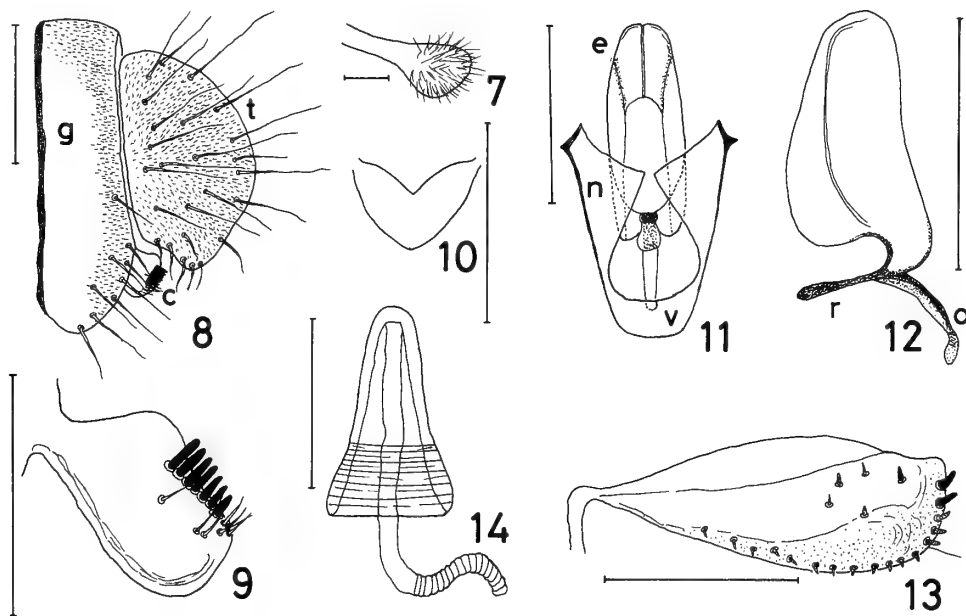
Remarks. This species is abundant in subtropical districts of Yunnan, but has not been collected in Kunming (center of Yunnan) and Dali (northern Yunnan) districts.

Drosophila (Drosophila) karakasa

Watabe et Liang, sp. nov.

(Figs. 7-14)

Diagnosis. Small and yellowish brown species with cercus separated from epandrium. Palpus short, with short hairs but without stout bristles (Fig. 7). 4C-index ca. 7/9 and C3-fringe ca. 3/5. Surstylus rectangular, distally with ca. 7 primary teeth and ca. 7 short bristles (Fig. 9). Lobe of ovipositor brown, much darker on ventral margin, roundish at tip (Fig. 13). Spermatheca cone-



FIGS. 7-14. *Drosophila (Drosophila) karakasa* Watabe et Liang, sp. nov. 7: Palpus. 8: Peripheral organs. 9: Surstylus. 10: Decasternum. 11: Phallic organs. 12: Aedeagus (lateral view). 13: Ovipositor. 14: Spermatheca. Signs and scales as in figs. 1-6.

shaped, with sparse horizontal stripes on basal half of outer capsule (Fig. 14).

♂, ♀. Body length, ♂ *ca.* 2.33 mm (range: 2.1–2.5), ♀ *ca.* 2.31 mm (2.1–2.5). Wing length, ♂ *ca.* 2.83 mm (2.6–3.0), ♀ *ca.* 2.73 mm (2.6–2.8).

Head: Eye red with thick piles. Second joint of antenna reddish brown; 3rd grayish brown. Arista with *ca.* 4 (4–6) upper and *ca.* 2 (2–3) lower short branches in addition to terminal fork. Frons dark brown, *ca.* 0.54 (0.43–0.65) as broad as head, anteriorly with a few frontal hairs. Anterior reclinate orbital (Orb 2) *ca.* 0.44 (0.33–0.56) length of posterior reclinate orbital (Orb 1); proclinate orbital (Orb 3) *ca.* 0.63 (0.56–0.78) length of Orb 1. Face brown; carina somewhat low, narrow. Clypeus reddish brown. Cheek tannish brown, *ca.* 0.25 (0.20–0.31) as broad as maximum diameter of eye, with *ca.* 3 long bristles along lower margin. Second oral (Or 2) minute, *ca.* 0.29 (0.23–0.36) length of vibrissa (Or 1). Palpus brown, club-shaped, basally baring (Fig. 7).

Thorax: Mesoscutum yellowish brown, medially with a darker longitudinal stripe running to scutellum. Scutellum brown, paler on lateral sides. Lower humeral *ca.* 0.70 (0.55–0.86) length of upper one. Two extra pairs of dorsocentrals present in front of usual ones. Anterior acrostichal bristles present between 1st (anteriormost) dorsocentrals; posterior ones between 2nds; length and location of acrostichal bristles more or less variable. Relative lengths of dorsocentrals and acrostichal bristles to 4th (posteriormost) dorsocentral: 1st dorsocentral *ca.* 0.57 (0.51–0.62), 2nd *ca.* 0.57 (0.49–0.62), 3rd *ca.* 0.71 (0.65–0.79), anterior acrostichal bristle *ca.* 0.35 (0.29–0.43), posterior one *ca.* 0.53 (0.46–0.68). Length distance from 1st dorsocentral to 2nd *ca.* 0.57 (0.52–0.68), distance from 2nd to 3rd *ca.* 0.48 (0.44–0.55), distance from 3rd to 4th *ca.* 0.56 (0.52–0.64) cross distance between 3rds. Acrostichal hairs (Ac) sparse, in 4 irregular rows. Anterior scutellars (SctA) nearly parallel and posterior ones (Sctp) convergent; SctA *ca.* 1.07 (0.88–1.17) length of SctP. Sterno-index *ca.* 0.72 (0.64–0.76).

Legs light brown; preapicals on all three tibiae; apicals on fore and mid tibiae.

Wing hyaline, slightly fuscous. Veins dark brown; crossveins clear. R_{2+3} straight; R_{4+5} and

M parallel. C_1 bristles 2, subequal. Number of small stout bristles on 3rd costa (3CFr) *ca.* 28 (24–33). Wing indices: C in ♂ *ca.* 3.10 (2.96–3.34) and in ♀ *ca.* 2.77 (2.50–3.11), 4V *ca.* 1.64 (1.54–1.87), 4C *ca.* 0.77 (0.70–0.86), 5X *ca.* 1.57 (1.33–1.73), Ac in ♂ *ca.* 2.26 (2.17–2.36) and in ♀ *ca.* 2.64 (2.14–3.00), C3-fringe *ca.* 0.61 (0.52–0.67). Haltere white, basally brown.

Abdomens: Tergites brown, darker on middle and paler on lateral margin. Sternites brown, darker on posterior margin, nearly quadrate.

Periphallal organs (Figs. 8–10): Epandrium yellowish brown, darker on anterior margin, pubescent on posterior half, with *ca.* 9 bristles on lower half. Surstylus pale brown, marginally darker, somewhat swollen at caudodorsal corner. Decasternum translucent, heart-shaped. Cercus brown, slightly projecting at ventral apex, entirely pubescent, with *ca.* 17 long bristles and tuft of *ca.* 5 short bristles along lower margin.

Phallic organs (Figs. 11, 12): Aedeagus yellow, bilobed, ventrally broadened; apodeme dark brown, *ca.* 3/8 as long as aedeagus. Anterior paramere small. Vertical rod black, plate-shaped in ventral view. Novasternum pale brown, without submedian spines; ventral fragma narrow.

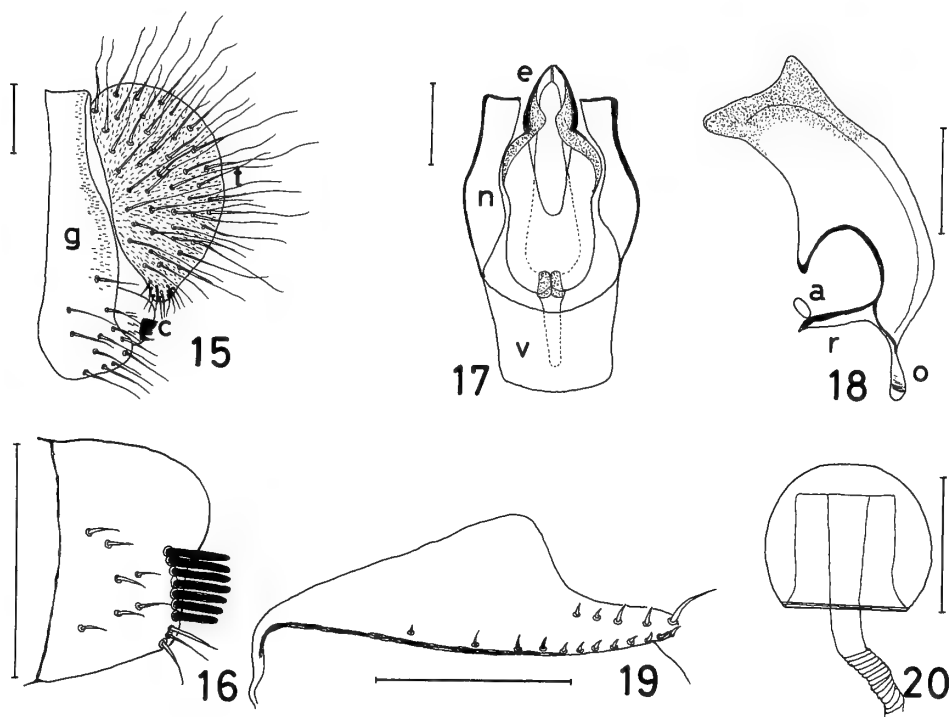
♀ reproductive organs (Figs. 13, 14): Lobe of ovipositor with *ca.* 3–5 discal teeth and *ca.* 17 short marginal teeth: first 2 marginal teeth darker and larger than others. Spermatheca grayish brown, slightly constricted in middle; introvert deep.

Holotype ♂, China: Xianguan, Dali district, Yunnan Province, 19. IX. 1988 (X. C. Liang).

Paratypes, China: 1 ♂, same data as holotype, 2 ♀, Dabochin, Dali district, Yunnan Province, 21. IX. 1988 (X.C. Liang).

Distribution. China: Yunnan; Dabochin, Xianguan.

Relationships. *D. karakasa* somewhat resembles the foregoing species, *D. potamophila*, in the general morphology and chaetotaxy, but clearly distinguishable from the latter by the diagnostic characters. The aedeagus of this species is very similar to that of four species of the *D. robusta* species-group: *D. okadai* Takada, *D. neokadai* Kaneko et Takada, *D. gani* Liang et Zhang and *D. unimaculata* Strobl [7].



Figs. 15–20. *Drosophila (Drosophila) barutani* Watabe et Liang, sp. nov. 15:Periphallallic organs. 16: Surstylus. 17: Phallic organs. 18: Aedeagus (lateral view). 19: Ovipositor. 20: Spermatheca. Signs and scales as in figs. 1–6.

Drosophila (Drosophila) barutani

Watabe et Liang, sp. nov.

(Figs. 15–20)

Diagnosis. Dull brown species with cercus close to epandrium at middle (Fig. 15). Third oral subequal to vibrissa. Palpus with ca. 3 moderate bristles. 4C-index ca. 5/9 and C3-fringe ca. 9/10. Surstylus arc-shaped, broadened at caudodorsal corner (Fig. 16). Lobe of ovipositor sharply pointed at tip; ultimate marginal tooth large, bristle-like (Fig. 19). Spermatheca hemispherical (Fig. 20).

♂, ♀. Body length, ca. 3.60 mm (3.4–3.8). Wing length, ca. 4.03 mm (3.9–4.1).

Head: Eye brownish red with thick piles. Second joint of antenna reddish brown; 3rd blackish brown. Arista ca. 4 (4–6) upper and ca. 2 (1–2) lower short branches in addition to terminal fork. Frons reddish brown, ca. 0.47 (0.46–0.48) as broad as head, anteriorly with a few frontal hairs. Orb 2 ca. 0.32 (0.31–0.34) length of Orb 1; Orb 3 ca. 0.40 (0.33–0.47) length of Orb 1. Face brown; carina

broad. Clypeus dark red. Cheek reddish brown, ca. 0.28 (0.24–0.33) as broad as maximum diameter of eye, with ca. 3 long bristles along lower margin. Or 2 thin, ca. 0.16 (0.14–0.17) length of Or 1; Or 3 ca. 0.99 (0.92–1.11) length of Or 1. Palpus grayish brown, laterally flattened.

Thorax: Mesoscutum brown, with 4 darker longitudinal stripes. Scutellum brown, lateral sides black. Lower humeral ca. 0.58 (0.55–0.59) length of upper one. Two extra pairs of dorsocentrals present. Anterior acrostichal bristles present between 1st dorsocentrals; posterior slightly below cross line between 2nds. Relative lengths of dorsocentrals and acrostichal bristles to 4th dorsocentral: 1st (anteriormost) dorsocentral ca. 0.66 (0.65–0.67), 2nd ca. 0.68 (0.62–0.74), 3rd ca. 0.86 (0.79–0.98), anterior acrostichal bristle ca. 0.58 (0.48–0.70), posterior one ca. 0.54 (0.52–0.57). Length distance from 1st dorsocentral to 2nd ca. 0.64 (0.60–0.71), distance from 2nd to 3rd ca. 0.55 (0.50–0.61), distance from 3rd to 4th ca. 0.58 (0.55–0.61) cross distance between 3rds. Ac

sparse, in 6 irregular rows. SctAs parallel and Sctps convergent; SctA *ca.* 0.97 (0.93–1.03) length of SctP. Sterno-index *ca.* 0.72 (0.52–0.84).

Legs dark brown; coxae and trochanters paler. Fore femur posteriorly with *ca.* 5 bristles. Preapicals on all three tibiae; apicals on fore and mid tibiae.

Wing hyaline, slightly fuscous. Veins dark brown; crossveins clear. R_{2+3} nearly straight; R_{4+5} and M parallel. C_1 bristles 2, inner bristle *ca.* 5/9 length of outer one. Number of 3CFr *ca.* 38 (35–40). Wing indices: C *ca.* 3.46 (3.04–3.70), 4V *ca.* 1.61 (1.56–1.70), 4C *ca.* 0.57 (0.53–0.62), 5X *ca.* 1.06 (1.00–1.17), Ac *ca.* 2.01 (1.82–2.20), C3-fringe *ca.* 0.90 (0.87–0.94). Haltere pale yellow; stalk anteriorly darker.

Abdomens: Tergites entirely dark brown. Sternites pale grayish brown, nearly quadrate; ♂ 5th slightly convexed posteriorly.

Periphallic organs (Figs. 15, 16): Epandrium brown, dorsally narrowing and ventrally broadened, posteriorly pubescent except lower portion, with *ca.* 12 bristles. Surstylus dark brown, distally with *ca.* 7 primary teeth on margin and *ca.* 3 bristles at caudoventral corner, medially with *ca.* 7 spine-like bristles on outer surface. Cercus dark brown, somewhat projecting ventrally, entirely pubescent, with *ca.* 38 long bristles and tuft of *ca.* 12 short bristles at lower apex.

Phallic organs (Figs. 17, 18): Aedeagus yellowish brown, much darker at distal portion, bilobed, concaved on distal margin; apodeme short, *ca.* 2/7 as long as aedeagus. Anterior paramere rudiment. Vertical rod brown, ventrally black. Novasternum narrow; ventral fragma handmill-shaped.

♀ reproductive organs (Figs. 19, 20): Lobe of ovipositor brown, marginally black, dorso-subapically swollen, with *ca.* 4 discal teeth and *ca.* 13 marginal teeth in regular row; ultimate marginal tooth prominent, *ca.* 3 times as long as penultimate. Spermatheca pale yellow, apically somewhat flattened, wrinkled on basal margin, without apical indentation; introvert deep, *ca.* 5/8 height of outer capsule.

Holotype ♂, China: Dabochin, Dali district, Yunnan Province, 21. IX. 1988 (X. C. Liang).

Paratypes, China: 1 ♂, Xianguan, Dali district, Yunnan Province, 21. IX. 1988, (X. C. Liang);

1 ♀, same data as holotype.

Distribution. China: Yunnan; Dabochin, Xianguan.

Relationships. *D. barutani* is somewhat similar to *D. potamophila* in the abdominal coloration and large value of C3-fringe, but easily distinguishable from the latter by the shapes of its aedeagus and ovipositor.

Drosophila (Drosophila) multidentata

Watabe et Zhang, sp. nov.

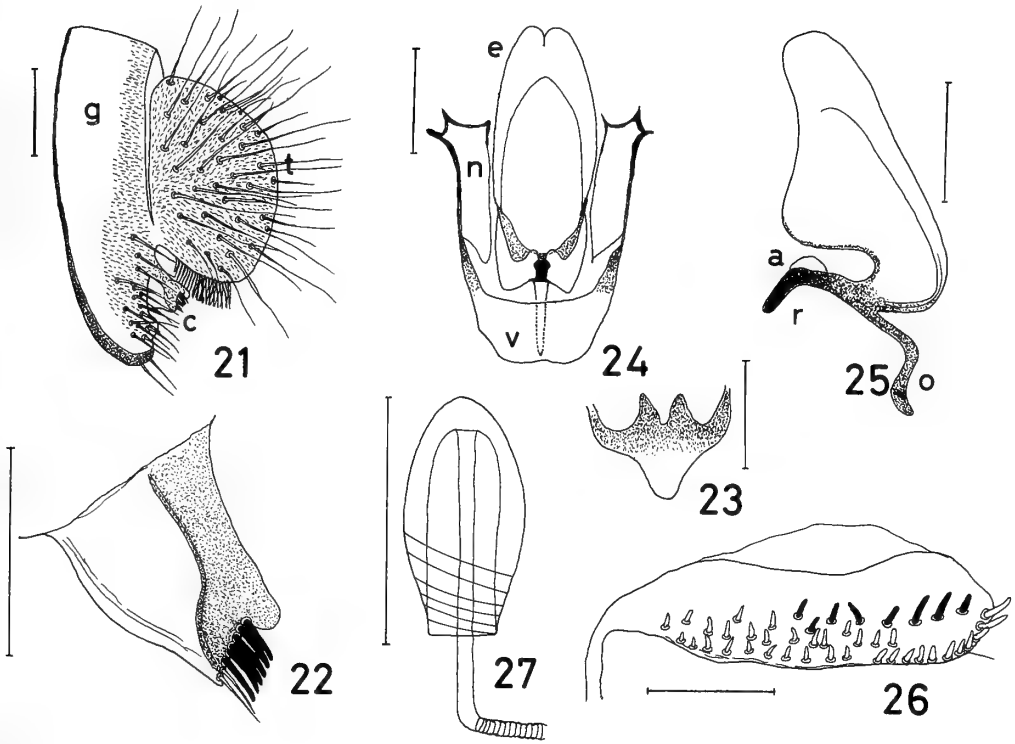
(Figs. 21–27)

Diagnosis. Dull brown species, with cercus fused to epandrium at submedian portion (Fig. 21). Or 2 *ca.* 4/9 length of Or 1. C3-fringe *ca.* 5/9. Lobe of ovipositor with many irregular teeth (Fig. 26). Spermatheca slender, with sparse oblique lines on basal 1/3 of outer capsule (Fig. 27).

♂, ♀. Body length, ♂ *ca.* 2.55 mm (2.4–2.8), ♀ *ca.* 2.85 mm (2.6–3.1). Wing length, ♂ *ca.* 3.18 mm (3.0–3.5), ♀ *ca.* 3.48 mm (3.2–3.8).

Head: Eye dark red with thick piles. Second joint of antenna dark brown; 3rd grayish brown. Arista with *ca.* 4 (3–4) upper and *ca.* 1 lower branches in addition to short terminal fork. Frons dark brown, *ca.* 0.46 (0.42–0.49) as broad as head, medially with black cuneiform line. Orb 2 *ca.* 0.36 (0.25–0.46) length of Orb 1; Orb 3 *ca.* 0.52 (0.42–0.79) length of Orb 1. Face reddish brown; carina very high, wider below. Clypeus blackish brown. Cheek brown, *ca.* 0.26 (0.23–0.31) as broad as maximum diameter of eye, with *ca.* 3 long and *ca.* 11 short bristles along lower margin. Or 2 thin, *ca.* 0.44 (0.23–0.61) length of Or 1; Or 3 minute. Palpus brown, small, club-shaped, with 1 somewhat long bristle at tip.

Thorax: Mesoscutum brown, medially darker; scutellum dark brown. Lower humeral *ca.* 0.61 (0.44–0.69) length of upper one. Anterior acrostichal bristles present below cross line between 1st dorsocentrals; posterior below cross line between 2nds. Relative lengths of dorsocentrals and acrostichal bristles to 4th dorsocentral: 1st dorsocentral (anteriormost) *ca.* 0.46 (0.39–0.52), 2nd *ca.* 0.51 (0.39–0.58), 3rd *ca.* 0.68 (0.60–0.79), anterior acrostichal bristle *ca.* 0.33 (0.24–0.44), posterior one *ca.* 0.42 (0.37–0.44). Length distance from 1st



FIGS. 21–27. *Drosophila (Drosophila) multidentata* Watabe et Zhang, sp. nov. 21: Periphallic organs. 22: Surstylus. 23: Decasternum. 24: Phallic organs. 25: Aedeagus (lateral view). 26: Ovipositor. 27: Spermatheca. Signs and scales as in figs. 1–6.

dorsocentral to 2nd *ca.* 0.55 (0.44–0.74), distance from 2nd to 3rd *ca.* 0.45 (0.39–0.48), distance from 3rd to 4th *ca.* 0.51 (0.46–0.56) cross distance between 3rds. Ac in 6 irregular rows; a few acrostichal hairs in rows of dorsocentrals somewhat longer than other hairs. SctAs slightly and SctPs heavily convergent; SctA *ca.* 0.96 (0.86–1.05) length of SctP. Sterno-index *ca.* 0.73 (0.52–0.96).

Legs brown; fore tarsi darker. Fore femur posteriorly with *ca.* 2–3 long bristles. Preapicals on all three tibiae; apicals on fore and mid tibiae.

Wing hyaline, slightly fuscous. Veins dark brown; crossveins clear. R_{2+3} nearly straight; R_{4+5} and M parallel. C_1 bristles 2, subequal. Number of 3CFr *ca.* 24 (17–28). Wing indices: C *ca.* 3.54 (3.12–4.20), 4V *ca.* 1.69 (1.52–1.78), 4C *ca.* 0.68 (0.60–0.77), 5X *ca.* 1.22 (1.00–1.50), Ac *ca.* 2.00 (1.67–2.13), C3-fringe *ca.* 0.56 (0.43–0.65). Haltere white; stalk grayish brown.

Abdomens: Tergites grayish brown, darker in middle; sternites brown, each with *ca.* 26–34 bristles.

Periphallic organs (Figs. 21–23): Epandrium brown, darker on anterior margin, posteriorly pubescent, with *ca.* 15 bristles on lower half and *ca.* 2 bristles along ventral margin. Surstylus brown, darker on upper half, distally narrowing, slightly projecting at caudodorsal corner, with *ca.* 6 primary teeth and *ca.* 2 bristles. Decasternum dark brown, paler on lower portion. Cercus blackish brown, with *ca.* 34 long bristles and tuft of *ca.* 23 pale yellow bristles along ventral margin.

Phallic organs (Figs. 24, 25): Aedeagus yellow, bilobed, submedially broadened; apodeme dark brown, *ca.* 1/3 as long as aedeagus. Anterior paramere pale yellow, hemispherical. Vertical rod black, recurved dorsally. Novasternum pale yellow, darker on lateral margin, without submedian spines; ventral fragma slightly concaved at middle.

♀ reproductive organs (Figs. 26, 27): Lobe of ovipositor dark brown, with *ca.* 45 stout teeth in irregular rows and 1 long subterminal hair; *ca.* 8 upper teeth much darker than others. Spermatheca grayish brown, slightly wrinkled basally; introvert deep; inner duct narrow.

Holotype ♂, China: Xianguan, Dali district, Yunnan Province, 19. IX. 1988 (X. C. Liang).

Paratypes, China: 2♂, 2♀, Dabochin, Dali district, Yunnan Province, 21. IX. 1988 (H. Watabe & X. C. Liang).

Distribution. Yunnan; Dabochin, Xianguan, Kunming.

Relationships. One of the diagnostic characters for the *D. quadrisetata* species-group described by Toda and Peng [2] is "cercus separated from epandrium". The cercus of *D. multidentata* fuses to epandrium at its lower portion. However, *D. multidentata* should be involved in the *quadrisetata* species-group by the following characters: 1) two extra pairs of dorsocentrals and prominent acrostichal bristles present, 2) C-index *ca.* 3.54, 3) 4V-index *ca.* 1.69, and 4) aedeagus large and curved ventrally.

Since the cercus in the *robusta* species-group fuses to epandrium, the same type cercus found in *D. multidentata*, as well as the large value of C-index and the shape of aedeagus, implies the phylogenetic relationship between this species and the *robusta* group [2, 7].

THE VIRILIS-REPLETA RADIATION IN THE OLD WORLD

The *virilis-repleta* Radiation, which might have occurred during the Oligocene to early Miocene, is one of main lineages in the evolution of the genus *Drosophila*. Throckmorton [4] considers that first the *polychaeta* group might have emerged in the Old World tropics and then several groups, e.g., the *robusta*, the *virilis* and the *melanica* species-groups, might have diverged adaptively in its temperate forest. However, the phylogenetic relationship among these species-groups, especially between the *polychaeta* group and other groups, was still open to question, mainly due to the insufficient information from China.

The recent *Drosophila*-survey in southern China

has resulted in the establishment of a new species-group, the *quadrisetata* group. This group is closely related to the *polychaeta* group in the external morphology and to the *robusta* group in the male genitalia. Toda and Peng [2] consider that the *quadrisetata* group occupies a systematic position between these two species-groups. Similarly, a geographical information on the distribution of these three groups has made it possible to trace the evolutionary process. Most of the *polychaeta* group flies are distributed from the tropics to the subtropics of the East Asia, whereas the *robusta* group flies in its temperate zone [1, 2, 4, 8]. The distribution range of the *quadrisetata* group overlaps with that of the *polychaeta* group and that of the *robusta* group. Of six *quadrisetata* group species, *D. potamophila* and *D. beppui* are distributed in the subtropics and the remaining four species in the temperate forest [2, 6, 8]. In particular, in northern Yunnan, the present three new species are sympatric to *D. neokadai* and *D. gani* of the *robusta* species-group [9].

These information from southern China, including the discovery of *D. polychaeta* in a natural forest of Simao, strongly supports the Throckmorton's hypothesis: the *polychaeta* group first emerged in the Old World tropics and then the *robusta* group in the temperate forest of the East Asia probably through the emergence of the *quadrisetata* group in its subtropics.

ACKNOWLEDGMENTS

The authors are grateful to Prof. Osamu Kitagawa (Tokyo Metropolitan University) and to Dr. Masanori J. Toda (Hokkaido University) for their interest and advice during this study. This work was supported by Grants-in Aid for Overseas Scientific Survey from the Ministry of Education, Science and Culture, Japan (Nos. 62041085, 63043060).

REFERENCES

- 1 Gupta, J. P. and Ray-Chaudhuri, S. P. (1970) Some new and unrecorded species of *Drosophila* (Diptera: Drosophilidae) from India. Proc. Roy. ent. Soc. Lond., (B) 39: 57-72.
- 2 Toda, M. J. and Peng, T. X. (1989) Eight species of the subgenus *Drosophila* (Diptera: Drosophilidae) from Guangdong Province, southern China. Zool. Sci., 6: 155-166.

- 3 Patterson, J. T. and Wheeler, M. R. (1942) Description of new species of the subgenus *Hirtodrosophila* and *Drosophila*. Univ. of Texas. Publ., **4213**: 67–109.
- 4 Throckmorton, L. H. (1975) The phylogeny, ecology, and geography of *Drosophila*. In "Handbook of Genetics, Vol. III". Ed. by R. C. King, Plenum Publ., New York, pp. 421–469.
- 5 Fonseca, E. C. M. d'A (1965) A short key to the British Drosophilidae (Diptera) including a new species of *Amiota*. Trans. Soc. Brit. Ent., **16**: 233–244.
- 6 Takada, H., Beppu, K. and Toda, M. J. (1979) *Drosophila* Survey of Hokkaido, XXXVI. New and unrecorded species of Drosophilidae. J. Fac. Gener. Edu., Sapporo Univ., **14**: 105–129.
- 7 Watabe, H. and Nakata, S. (1989) A comparative study of genitalia of the *Drosophila robusta* and *D. melanica* species-groups (Diptera: Drosophilidae). J. Hokkaido Univ. of Education, Ser. IIB, **40**: 1–18.
- 8 Beppu, K., Peng, T. X. and Xie, L. (1989) An ecological study on drosophilid flies (Diptera, Drosophilidae) living at watersides in southern China. Jpn. J. Ent. (Kontyû, Tokyo), **57**: 185–198.
- 9 Watabe, H., Liang, X. C. and Zhang, W. X. (1990) The *Drosophila robusta* species-group (Diptera: Drosophilidae) from Yunnan Province, southern China, with the revision of its geographic distribution. Zool. Sci., **7**: 133–140.

Cestodes of Field Micromammalians (Insectivora) from Central Honshu, Japan

ISAMU SAWADA and MASASHI HARADA¹

Biological Laboratory, Nara Sangyo University, Nara 636, and

¹*Laboratory of Experimental Animals, Osaka City
University Medical School, Osaka 545, Japan*

ABSTRACT—Two new species of hymenolepidid and one new species of dilepidid cestodes were obtained through the examination of 18 shrews belonging to three species of three genera, collected at Toyama and Nagano Prefectures from October 6 to November 15, 1988. *Staphylocystis* (*Staphylocystis*) *toyamaensis* sp. n. from *Crocidura dsinezumi chisai* is related to but differs from *S. (S.) solitaria* in the shape of rostellar hooks. *Ditestolepis longicirrosa* sp. n. from *Sorex shinto shinto* is related to but differs from *D. diaphona* in many morphological characters. *Amoebotaenia urotrichi* sp. n. from *Urotrichus talpoides hondonis* resembles four known species of *Amoebotaenia* in being armed with 10–12 rostellar hooks, but differs from all of them in the length and shape of rostellar hooks. This is the first record of the genus *Amoebotaenia* from wild animals.

INTRODUCTION

The cestode parasites of Insectivora in Japan have been unknown for the most part except two by Sawada and Harada [1], who described *Vampirolepis notoensis* from *Crocidura dsinezumi chisai* collected at Suzu-shi, Ishikawa Prefecture and *V. amamiensis* from *C. horsfield watasei* at Amami-ôshima, Kagoshima Prefecture.

Hymenolepidid cestodes collected from the dsinezumi-shrew, *C. dsinezumi chisai* Thomas at Asahi-machi and Tateyama-machi, Toyama Prefecture, the shinto-shrew, *Sorex shinto shinto* Thomas at Ina-shi, Nagano Prefecture, and dilepidid cestodes from the Japanese shrew-mole, *Urotrichus talpoides hondonis* Thomas at Ina-shi, Nagano Prefecture, are undescribed species of *Staphylocystis* Villot, 1877, *Ditestolepis* Stofsky, 1952 and *Amoebotaenia* Cohn, 1900, respectively.

MATERIALS AND METHODS

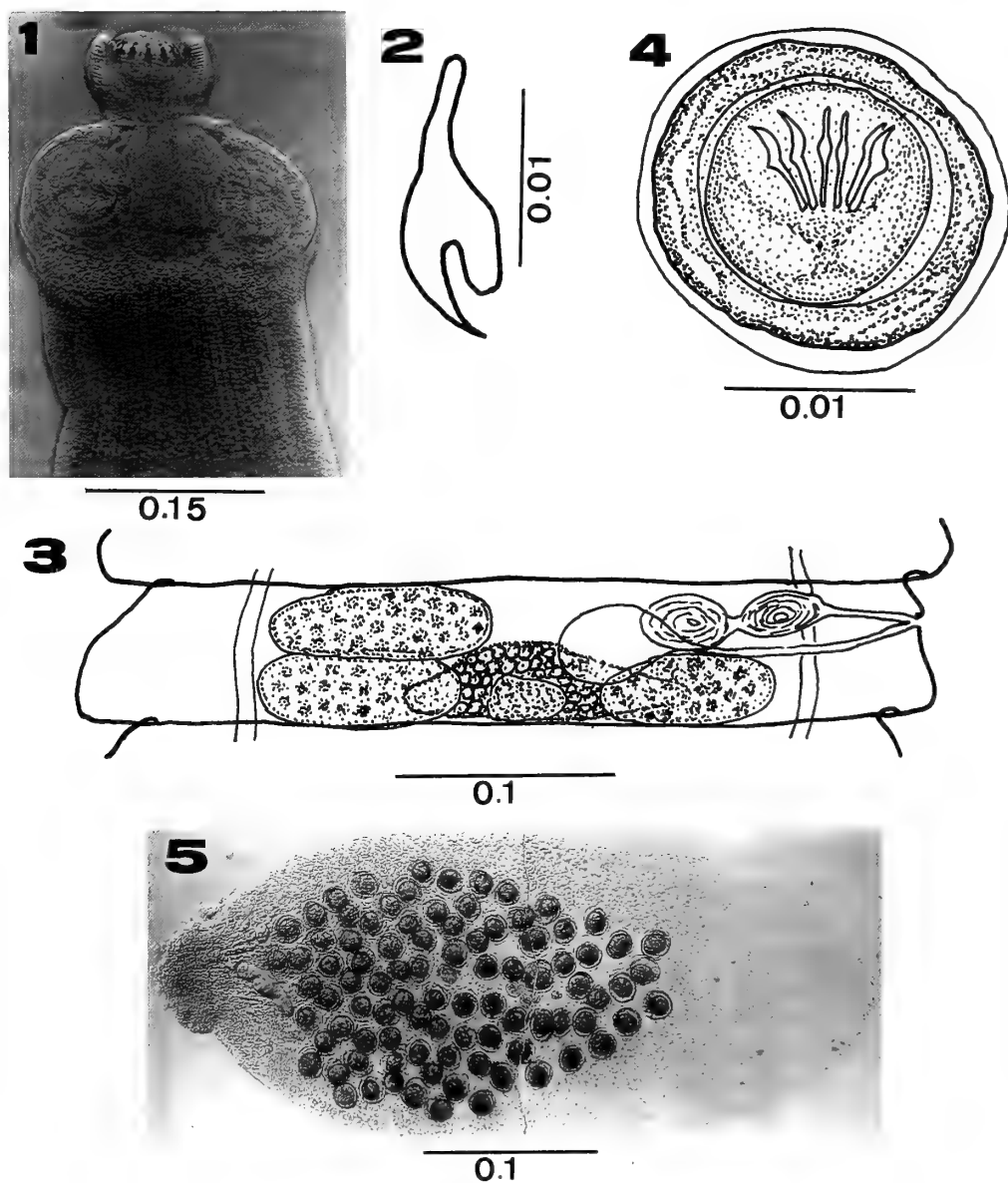
The shrews were autopsied immediately at the collecting sites and their intestinal tracts were fixed

in Carnoy's fluid and bought back to the laboratory. After being soaked in 45% acetic acid for five hr for expanding, they were cut open in 70% ethanol and examined for cestodes. The cestodes obtained were stored in 70% ethanol. The scoleces, eggs and a part of mature segments were unstained and observed under an interference contrast light microscope. The strobilae were stained with ethanol-hydrochloride-carmin, dehydrated in ethanol, cleared in xylene, and mounted in Canada balsam. Measurements are given in millimeters.

Staphylocystis (*Staphylocystis*) *toyamaensis* sp. n.
(Figs. 1–6)

From November 13 to 14, 1988, three specimens of *Crocidura dsinezumi chisai* Thomas were captured by trap at Asahi-machi, Shimoniikawa-gun and Tateyama-machi, Nakashinkawa-gun, Toyama Prefecture. On dissection, they were found infected with 1–48 mature cestodes.

Description: Small-sized hymenolepidid; mature strobila 3–4 in length and 0.4–0.5 in maximum width. Mature segments serrate. Scolex 0.210–0.224 long by 0.245–0.252 wide, not sharply from strobila. Suckers circular, 0.084–0.091 in



FIGS. 1-5. *Staphylocystis (Staphylocystis) toyamaensis* sp. n.

1: Scolex. 2: Rostellar hook. 3: Mature segment. 4: Egg. 5: Detached senile segment. Scale in mm.

diameter. Rostellum 0.042 long by 0.063 wide, armed with a crown of 16 thorn-shaped hooks measuring 0.014 long, blade long, slender and pointed, guard shorter and thick, and handle long. Rostellar sac elongated, 0.140 long by 0.112 wide, extending past posterior margin of sucker. Neck absent.

Genital pores unilateral, located slightly anter-

ior to middle of segment margin. Cirrus sac cylindrical, 0.084-0.140 long by 0.021-0.028 wide, extending beyond longitudinal osmoregulatory canals. Internal seminal vesicle 0.028 long by 0.021-0.035 wide, occupying almost whole of cirrus sac. External seminal vesicle 0.025-0.028 long by 0.021 wide. Testes three in number, ovoid, 0.126 by 0.035, arranged in a form of triangle, one

poral and two aporal. Testes not in contact with longitudinal osmoregulatory canals laterally. Ovary triangular, 0.105–0.140 across, located at posterior margin of two posterior testes. Vitelline gland compact, 0.049–0.056 long by 0.021–0.028 wide. Seminal receptacle well developed, 0.077 by 0.049. Gravid uterus sacculated, not filling whole of segment. Ripe eggs spherical, 0.042–0.053 in diameter; surrounded by four thin envelopes. Onchospheres spherical, 0.028–0.032 in diameter; embryonic hooks 0.014 long.

Host: *Crocidura dsinezumi chisai* Thomas, 1906.

Site of infection: Small intestine.

Locality and date: Ogawa'motoyu, Asahimachi, Shimoniikawa-gun and Senjugahara, Tateyama-machi Nakaniikawa-gun, Toyama Prefecture; November 13–14, 1988.

Type specimen: Holotype: NSU Lab. Coll. No. 9005; Paratypes: No. 9006.

Remarks: Yamaguti [2] divided the genus *Staphylocystis* Villot, 1877, into two subgenera: *S. (Staphylocystis)* Villot, 1877 and *S. (Staphylocystoides)* Yamaguti, 1959. The present new cestode finds its place in subgenus *Staphylocystis* on the base of a single row of rostellar hooks and disposition of testes. Seven species; *S. scalaris* (Dujardin, 1845) Villot, 1788, *S. tiara* (Dujardin, 1854) Spasskii, 1950, *S. furcata* (Stieda, 1862) Spasskii, 1950, *S. dodecantha* (Baer, 1952) Spasskii, 1950, *S. solitaria* (Meggitt, 1927) Yamaguti, 1959, *S. fuelleborni* (Hilmy, 1936) Spasskii, 1950, *S. loossi* (Hilmy, 1936) Spasskii, 1950, were described from the *Crocidura* (Yamaguti [2], Spasskii [3], Olsen and Kuntz [4], Schmidt [5]). The present new species closely resembles *S. solitaria* [6], of which the description is deficient in some details, in the

number and length of rostellar hooks. However, it differs from that species in the shape of rostellar hooks (Fig. 6).

Ditestolepis longicirrosa sp. n.
(Figs. 7–14)

A number of specimens of cestodes representing a species of *Ditestolepis* Stofsky, 1952, were found in one shinto-shrew, *Sorex shinto shinto* Thomas captured at October 8, 1988.



FIG. 7. *Ditestolepis longicirrosa* sp. n. Entire worm, Scale in mm.

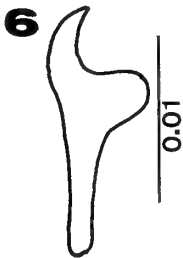
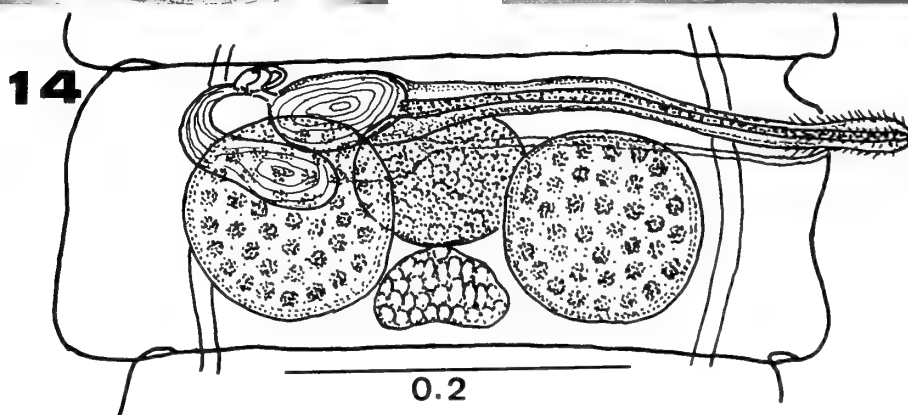
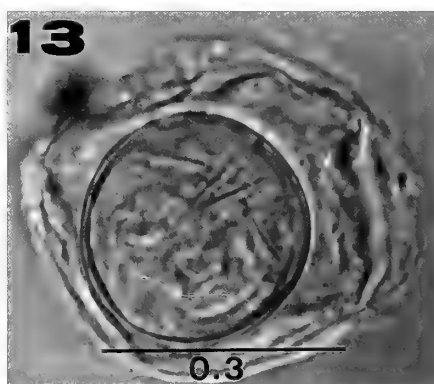
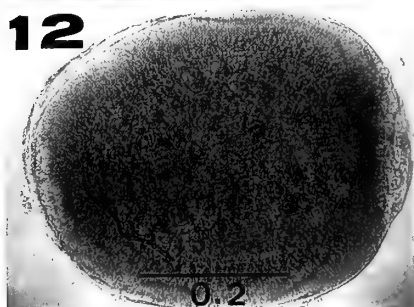
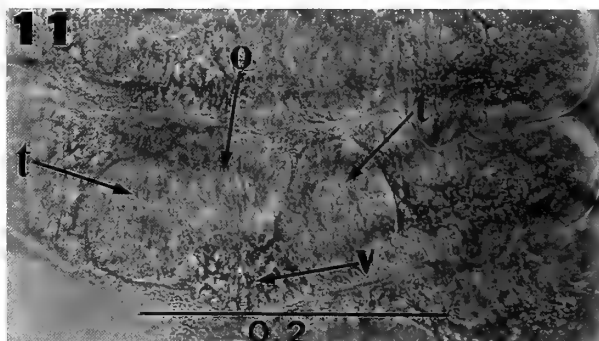
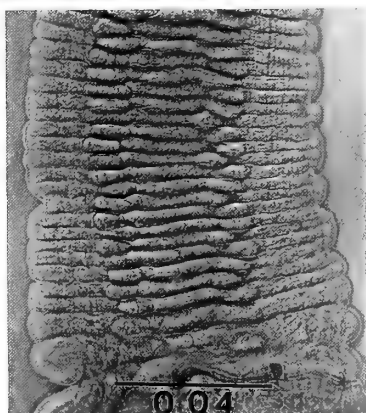
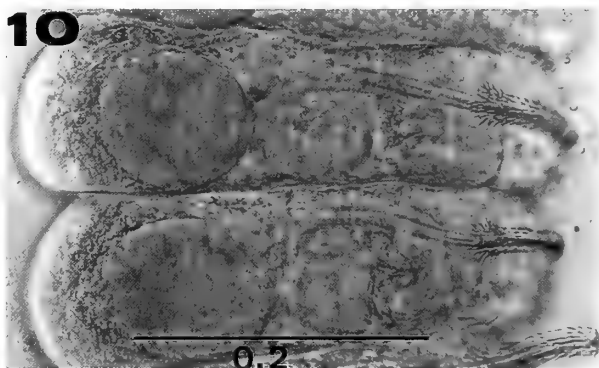
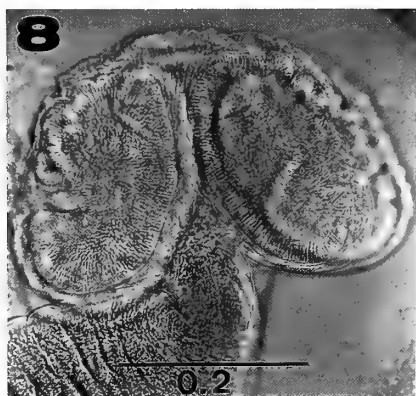
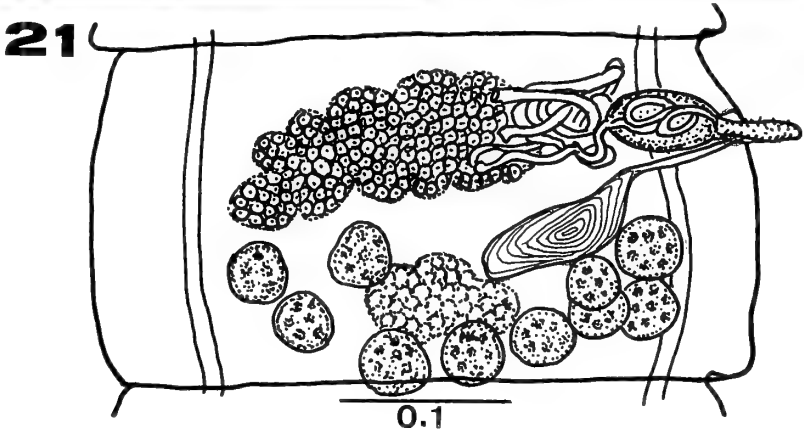
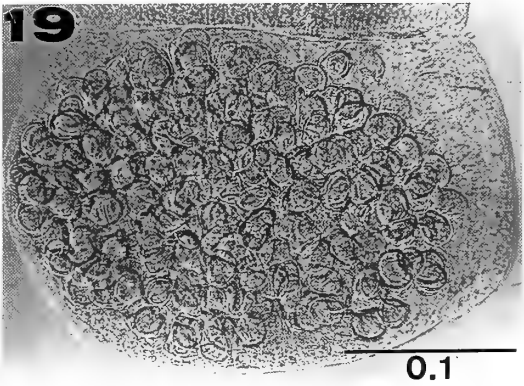
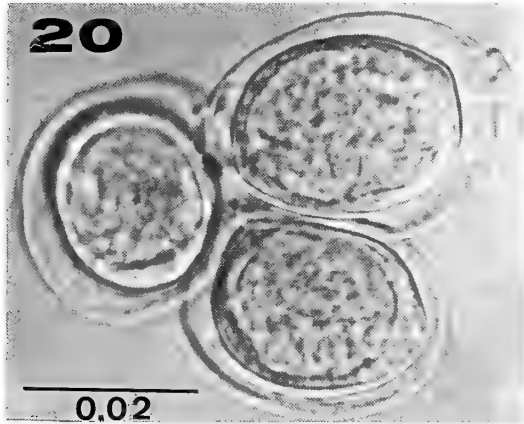
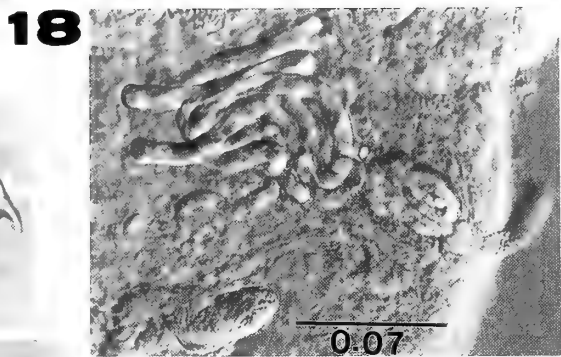
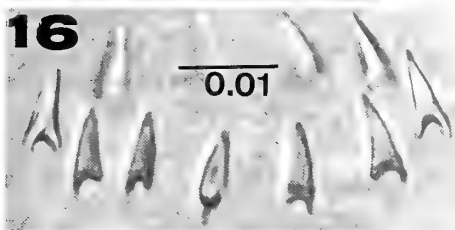
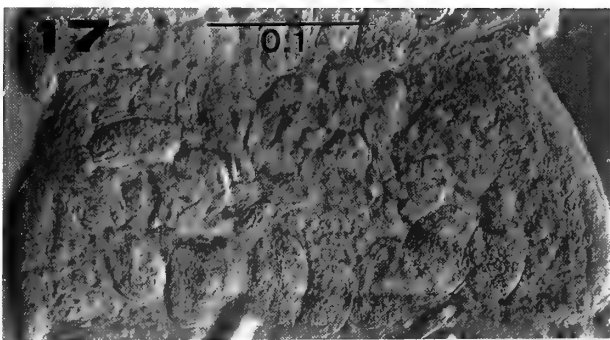


FIG. 6. Rostellar hook of *Staphylocystis* (*S.*) *solitaria*. Scale in mm.

Description: Small-sized hymenolepidid; worm length 2.1–2.6; maximum width 0.3–0.4. Metamerism distinct, margins not serrate. Strobila characterized by a distinctly marked subdivision into three series, each of which possessing segments uniformly advanced in development. First series containing 26–34 immature segments; its maximal width 0.19–0.22. Second series containing 9–13 segments with a mature reproductive apparatus; maximal width of this series 0.22–0.28. Third series comprising 16–19 immature uterine segments; maximum width 0.098–0.130. This latter series spilling off from strobila and maturing independently in host's intestine. Detached senile segment oval, 0.67–0.77 long by 0.46–0.53 wide. Scolex 0.245 long by 0.329–0.350 wide, sharply demarcated from short neck. Rostellum rudimentally. Suckers confluent, 0.217–0.231 long by





0.140–0.148 wide. Neck short, 0.11–0.18 long by 0.07 wide. Genital pores unilateral, located at anterior 1/3 of segment margins. Testes two in number, spherical, 0.056–0.070 by 0.046–0.063, one on each side of ovary. Ovary subspherical, 0.060–0.070 long by 0.049–0.056 wide. Vitelline gland compact, 0.053–0.070 by 0.035. Cirrus sac elongate, surpassing center of segment, 0.161–0.175 long by 0.028 wide. Cirrus covered with delicate spines, 0.147–0.154 long. Internal seminal vesicle, located at inner part of cirrus sac, 0.042–0.046 long by 0.028–0.032 wide. External seminal vesicle 0.085–0.095 long by 0.032–0.042 wide. Vagina opening in genital atrium, extending to aporal side, then enlarging forming seminal receptacle measuring 0.032–0.035 long by 0.021–0.028 wide. Eggs spherical, 0.046–0.049 by 0.039–0.046, surrounded by four thin envelopes, with smooth surface. Onchospheres spherical, 0.025–0.032 by 0.028; embryonic hooks 0.011 long.

Host: *Sorex shinto shinto* Thomas, 1905.

Site of infection: Small intestine.

Locality and date: Ogurogawa, Ina-shi, Nagano Prefecture; October 8, 1988.

Type specimen: Holotype: NSU Lab. Coll. No. 9007; Paratypes: No. 9008.

Remarks: At present, only one species, *Diaphona* (Cholodkovsky, 1906) belonging to the genus *Ditostolepis*, of which the descriptions are incomplete, has been recorded from shrews in Estonia and Poland [7–12]. The present new species differs from *D. diaphona* in many morphological characters.

Amoebotaenia urotrichi sp. n.
(Figs. 15–22)

Of 14 specimens of Japanese shrew-mole, *Urotrichus talpoides hondonis* Thomas, collected at Ogurogawa, Ina-shi, Nagano Prefecture from

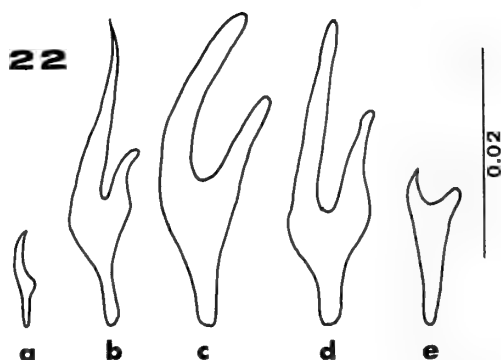


FIG. 22. Comparison of rostellar hooks of five related species. Scale in mm.

a; *A. fuhrmanni*, b; *A. oligorchis*, c; *A. longisacculus*, d; *A. spinosa*, e; *A. urotrichi* sp. n.

October 6 to November 15, three were found infected with a greater number of specimens of the present new cestodes.

Description: Small-sized dilepidid; strobila length 0.8–1.0 and maximum width 0.3–0.4, consisting of 8–9 segments. Metamerism distinct, margins not serrate, segments broader than long. Scolex square, 0.119–0.133 by 0.112–0.126, provided with four suckers and a well-developed protrusible rostellum. Rostellum 0.070–0.079 long by 0.042–0.063 wide, armed with a single row of 10–11 somewhat urench-shaped hooks, each measuring 0.014; guard and blade short, about equal in length, handle solid and longest. Rostellar sac muscular, 0.112–0.126 long by 0.042–0.070 wide. Sucker round, 0.119–0.133 by 0.112–0.126. Neck absent.

Genital pores alternating regularly, located slightly anterior to middle of segment margin. Testes roundish, 9–10 in number, 0.021–0.025 by 0.018–0.021, spreading posterodorsal part of segment between osmoregulatory canals. Cirrus sac oval, 0.070 long by 0.028–0.035 wide. Cirrus opening directly in front of vagina into genital

FIGS. 8–14. *Ditostolepis longicirrosa* sp. n.

8: Scolex. 9: Immature segments. 10: Mature segment, dorsal view. 11: Mature segment, ventral view; o: ovary. v: vitelline gland. t: testis. 12: Detached senile segment. 13: Egg. 14: Outline tracing of mature segment, dorsal view. Scale in mm.

FIGS. 15–21. *Amoebotaenia urotrichi* sp. n.

15: Scolex. 16: Rostellar hooks. 17: Mature segment. 18: Cirrus sac and vas deferens. 19: Senile segment. 20: Eggs. 21: Outline tracing of mature segment, dorsal view. Scale in mm.

TABLE 1. Species of *Amoebotaenia* armed with 10–12 mm long rostellar hooks from domestic and wild birds

Cestode species	Rostellar hooks		Host
	Number	Length	
<i>Amoebotaenia fuhrmanni</i> Tseng, 1932 [13]	10	0.007	<i>Gallinago</i> sp.
<i>A. oligorchis</i> Yamaguti, 1935 [14]	10	0.030–0.036	<i>Gallus gallus</i>
<i>A. longisacculus</i> Yamaguti, 1956 [15]	12	0.033	<i>Gallus domesticus</i>
<i>A. spinosa</i> Yamaguti, 1956 [15]	10–12	0.033–0.035	<i>Gallus gallus</i>

atrium. Cirrus covered with delicate spines. Vas deferens strongly coiled at proximal end of cirrus sac. Ovary transversely elongated and botryoidal, 0.140–0.175 across. Vitelline gland trilobate, 0.098 long by 0.049–0.056 wide, located ventral to testes at posterior field of segment. Seminal receptacle transversely elongate, 0.077 by 0.028, situated dorsal to ovary on poral side. Uterus occupying entire segment when fully developed. Eggs oval or spherical, 0.046–0.053 by 0.032; onchospheres spherical, 0.023–0.028 by 0.021; embryonal hooks 0.011 long.

Host: *Urotrichus talpoides hondnis* Thomas, 1908.

Site infection: Small intestine.

Locality and date: Ogurogawa, Ina-shi, Nagano Prefecture; October 8, 1988.

Type specimen: Holotype: NSU Lab. Coll. No. 9009; Paratypes: No. 9010.

Remarks: Out of known 24 species of the genus *Amoebotaenia* from domestic and wild birds, four have 10–12 rostellar hooks (Table 1) [2, 13–15]. *Amoebotaenia urotrichi* sp. n. differs from all of them in the length and shape of rostellar hooks (Fig. 22). This is the first record of the genus *Amoebotaenia* from wild animals.

REFERENCES

- 1 Sawada, I. and Harada, M. (1986) Two new species of the *Vampirolepis* (Cestoda: Hymenolepididae) from Japanese shrews. *Jpn. J. Parasitol.*, **35**: 171–174.
- 2 Yamaguti, S. (1959) *Systema Helminthum*. Vol. II The Cestodes of Vertebrates. Interscience Publ., New York, 860 pp.
- 3 Spasskii, A. A. (1950) A new approach to the structure and systematics of the hymenolepids (Cestoda: Hymenolepididae) (in Russian), *Dokl. Akad. Nauk SSSR*, **75**: 895–898.
- 4 Olsen, O. W. and Kuntz, R. E. (1978) *Staphylocystis* (*Staphylocystis*) *suncusensis* sp. n. (Cestoda: Hymenolepididae) from the musk shrew, *Suncus murinus* (Soricidae), from Taiwan, with a key to the known species of *Staphylocystis* Villot, 1877. *Proc. Helminth. Soc. Washing.*, **45**: 182–189.
- 5 Schmidt, G. D. (1986) *Handbook of Tapeworm Identification*. CRC Press, Florida, 675 pp.
- 6 Meggitt, F. J. (1927) On cestodes collected in Burma. *Parasitology*, **19**: 141–153.
- 7 Cholodkovsky, N. (1906) Cestodes nouveaux ou peu connus. *Arch. Parasitol.*, **10**: 332–347.
- 8 Stottys, A. (1952) The helminths of common shrew (*Sorex araneus* L.) of the National Park of Bialowieza (Poland). (in Polish) *Ann. Univ. M. Curie-Skeod. Sec. C*, **6**: 165–209.
- 9 Zarnowski, E. (1955) Parasitic worms of forest micromammals (Rodentia and Insectivora) of the environment of Pulawy (district Lubin). 1. Cestoda. (in Polish with English summary). *Acta Parasitol. Polo.*, **3**: 279–368.
- 10 Rybicka, K. (1959) Tapeworms of forest micromammals (Rodentia and Insectivora) from Kampinos Wilderness. *Acta Parasitol. Polo.*, **7**: 393–422.
- 11 Kisieleska, K. (1961) Circulation of tapeworms of *Sorex araneus araneus* L. in biocenosis of Białowieza National Park. *Acta Parasitol. Polon.*, **9**: 331–369.
- 12 Vaucher, C. (1971) Les Cestodes parasites des Soricidae d'Europe Etude anatomique, révision taxonomique et biologie. *Rev. Suisse Zool.*, **78**: 1–113.
- 13 Tseng, Shen. (1932) Studies on avian cestodes from China. Part 1. Cestodes from charadriiform birds. *Parasitology*, **24**: 87–106.
- 14 Yamaguti, S. (1935) Studies on the helminth fauna of Japan. Part 6. Cestodes of birds, 1. *Japan. J. Zool.*, **6**: 183–232.
- 15 Yamaguti, S. (1965) Parasitic worms mainly from Celebes. Part 11. Cestodes of birds. 41 pp., Publ. by author.

Crabs of the Genus *Calappa* from the Ryukyu Islands, with Description of a New Species

MASATSUNE TAKEDA and NORIKAZU SHIKATANI¹

Department of Zoology, National Science Museum, Shinjuku, Tokyo 169, and

¹Department of Marine Sciences, University of the Ryukyus,
Nishihara, Okinawa 903-01, Japan

ABSTRACT—Nine species of the genus *Calappa* (Crustacea, Decapoda, Calappidae) are recorded from the Ryukyu Islands based on the collections of the University of the Ryukyus. One of them is described as a new species under the name of *C. quadrimaculata*, being readily distinguished from the closest congener, *C. lophos* (Herbst), by having no striped markings on the carapace and chelipeds, and also by the different proportion and armature of the carapace. The new species is also known from Taiwan.

INTRODUCTION

The crabs of the genus *Calappa* (Family Calappidae) living in shallow-water of the Indo-Pacific and Atlantic Oceans are called the box crabs due to having the thin clypeiform expansion at each posterolateral side of the carapace, and well known by their peculiar habit of breaking the shell by the right chela to eat its soft part or hermit crab living in the empty shell [1, 2].

During the extensive survey of the shallow-water crab fauna of Nakagusuku Bay in southeastern Okinawa-jima Island, the Ryukyu Islands, we encountered five specimens referable to the species close to, but different from *C. lophos* (Herbst) which is one of the commonest *Calappa* species in Japanese waters. On a detailed comparative examination, they were proved to represent a new species which will be described in the present paper under the name of *C. quadrimaculata*, together with records of the known species from the Ryukyu Islands based on the collections of the Department of Marine Sciences, the University of the Ryukyus. During the recent field survey in Taiwan, the senior author found three specimens

of *Calappa* without doubt referable to the new species at the fish market together with *C. lophos* (Herbst) and *C. philargius* (Linnaeus), both of which are very common.

The *Calappa* species attract not only some biologists, but also certain collectors and aqualists, due to the big size and the beautiful coloration with spots and bands in addition to the peculiar shape and ecology. It is generally considered that the census has been made on rather thorough investigations, and thus the present discovery of a new species is remarkable and worth noting.

The bulk of the specimens examined is preserved in the University of the Ryukyus (URM) except for the holotype and one of the paratypes of the new species and a duplicate specimen of each species, which are deposited in the National Science Museum, Tokyo (NSMT). In the measurements of each species, the breadth and length of the carapace are abbreviated to cb and cl, respectively, with the greatest breadth including the clypeiform expansions of both sides.

SYSTEMATIC ACCOUNT

Family Calappidae

Genus *Calappa* Weber, 1795

Calappa bicornis Miers, 1884

OKINAWA. Nakagusuku Bay, 15-20 m

Accepted August 9, 1989

Received June 1, 1989

¹ Present address: Ocean Research Institute, University of Tokyo, Nakano, Tokyo 164, Japan.

deep.—1 ♀ (URM-CR 0075; cb 62.5 mm), 9-IX-1985; 1 ♀ (URM-CR 0081; cb 57.8 mm), 1 ♀ (UR M-CR 0082; cb 71.8 mm), 30-VII-1986; 1 ♂ (URM-CR 1103, NSMT-Cr 9620; cb 81.7 mm), 1 ♀ (URM-CR 1104; cb 65.5 mm), 10-VI-1987.

Remarks. This species is readily distinguished from *Calappa gallus* (Herbst) by having a tubercular tooth immediately behind the external orbital angle. *C. woodmasoni* Alcock based on a young specimen from off south coast of Sri Lanka was decidedly synonymized with this species by Rathbun [3]. *C. woodmasoni* was, however, resurrected by Ihle [4] who recorded a young female from Manipa Island in the Malay Archipelago. It is well known that the contour of the carapace is remarkably variable during development in the genus *Calappa*, and that the carapace is generally narrower and more quadrangular in the young. Based on the difference in the second peduncular segment of antenna, Ihle [4] distinguished both species, but this character is probably variable just like in the other groups of crabs, e.g., some genera of the family Xanthidae, in which the orbit completely closed by the well developed antennal peduncle is considered as one of the generic criteria, but the orbit is still incomplete, with a wide hiatus, in the young.

This species is known from the Providence Islands (type locality) and the Seychelles in the western Indian Ocean, and from Tosa Bay and several localities around the Kii Peninsula in central Japan. If *C. woodmasoni* is synonymized with this species, the records from Sri Lanka and Manipa Island will become the localities intervening between the western Indian Ocean and Japan.

Calappa calappa (Linnaeus, 1758)

OKINAWA. Nakagusuku Bay.—1 ♂ (URM-CR 0760; cb 120.2 mm), 1 ♀ (URM-CR 0761; cb 125.0 mm), 15-X-1985; 1 ♂ (URM-CR 0759, NSMT-Cr 9621; cb 117.8 mm), 1 ♂ (URM-CR 0757; cb 131.0 mm), 1 ♀ (URM-CR 0758; cb 141.2 mm), 4-V-1984.

Remarks. This species is uniformly yellowish brown or sometimes mottled with many purplish blotches on the carapace, being characterized by the unarmed clypeiform expansion at each side.

This species is widely distributed in the Indo-West Pacific from Sagami Bay in Japan and the Hawaiian Islands through New Caledonia and the Malay Archipelago to the east coast of Africa.

Calappa capellonis Laurie, 1906

OKINAWA. Nakagusuku Bay, 15–20 m deep.—1 ♀ (URM-CR 1105, NSMT-Cr 9622; cb 57.8 mm), 10-VI-1987.

Remarks. This species was originally described as the variety of *Calappa gallus* (Herbst) by Laurie [5], but the differences in armature of the carapacial dorsal surface and clypeiform expansions enumerated by Sakai [6, 7] and Takeda and Koyama [8] warrant its specific distinction from *C. gallus*.

This species is known only from Sri Lanka (type locality), and the Kii Peninsula, Kagoshima and Okinawa in Japan.

Calappa gallus (Herbst, 1803)

OKINAWA. Nakagusuku Bay.—1 ♀ (URM-CR 0083, NSMT-Cr 9623; cb 46.0 mm), 10-III-1986. Zampa-misaki.—1 ♀ (URM-CR 0080; cb 42.9 mm), VIII-1984. Yakata-katabaru.—1 ♂ (URM-CR 1429; cb 33.0 mm), 1987.

Remarks. This species is well figured by Klunzinger [9], Sakai [6, 7, 10], Rathbun [11], Barnard [12] and Monod [13].

This species is widely distributed in the whole Indo-West Pacific from Japan to the Red Sea and South Africa, the tropical Atlantic coast of Africa, and the western Atlantic from the Florida Keys to Bahia, Brazil. Such distribution pattern is quite unusual in the shallow-water crabs, so that the geographic speciation in these respective areas is to be confirmed with current knowledge of identification.

Calappa hepatica (Linnaeus, 1758)

OKINAWA. Manza beach.—1 ♀ (URM-CR 0076; cb 69.0 mm), 31-V-1985.

IRIOMOTE. Amitori Bay.—1 young ♂, 1 ♀ (URM-CR 0077; cb 30.3 and 55.3 mm), 1 young ♂ (URM-CR 0079; cb 32.5 mm), 16-VIII-1985.

Remarks. This is the most commonest species in the genus *Calappa* and well figured by Sakai [6, 7], being widely distributed in the whole Indo-West Pacific.

Calappa yamasitae Sakai from Japan described in 1980 [14] is the closest congener of this species, but according to the original description, distinguished by the following features: 1) Low protuberances of good size tipped each with a small tubercle are on the anterior two thirds of the carapacial dorsal surface, and the posterior third is tuberculate and granulated. 2) The front consists of two median obtuse teeth separated medially by an U-shaped sinus, each tooth bearing a subdistal tooth on its outer border. 3) The hepatic margin is gently turned into the clypeiform expansion of the branchial region without distinct constriction. 4) In both sexes the terminal abdominal tergum is broadly triangular in outline, not narrowed distally.

Calappa lophos (Herbst, 1782)

OKINAWA. Nakagusuku Bay.—1 ♂ (URM-CR 0754, NSMT-Cr 9624; cb 123.7 mm, cl 79.4 mm), 3-XII-1984; 1 ♀ (URM-CR 0073; cb 43.5 mm, cl 31.3 mm), 14-VI-1985; 1 ♀ (URM-CR 0071; cb 60.0 mm, cl 42.4 mm), 3-VII-1985; 1 ♀ (URM-CR 0072; cb 61.2 mm, cl 44.8 mm), 15-IV-1986; 1 ♀ (URM-CR 0070; cb 61.0 mm, cl 43.0 mm), 6-V-1986.

Remarks. This species is characteristic in its color pattern in the adult which is distinct even in spirit, being figured by de Haan [15], Sakai [6, 7, 10], Stephensen [16] and Barnard [12]. As mentioned by Alcock [17] and figured by Sakai [6], in the young the carapace is traversed by dark-colored longitudinal lines and marked with a pair of large ocelli in its posterior third.

This species is rather common in the sandy bottom, ranging from Japan through Sulawesi, India and the Persian Gulf to the east coast of Africa.

Calappa philargius (Linnaeus, 1758)

OKINAWA. Nakagusuku Bay, 15–20 m deep.—1 ♂ (URM-CR 0749, NSMT-Cr 9625; cb

112.0 mm), 12-XII-1984; 1 ♂ (URM-CR 0069; cb 58.8 mm), 13-V-1985; 1 ♂ (URM-CR 0068; cb 52.5 mm), 24-IX-1985; 1 ♂ (URM-CR 1161; cb 59.0 mm), 10-VI-1987.

Remarks. This species is characteristic in having a chocolate-brown band surrounding the orbit at each side, with a large spot each on the outer surface of the chelipedal carpus and palm. In its general shape it is close to *C. lophos* (Herbst), but the margin of the clypeiform expansions of both sides and the posterior border of the carapace are armed with much sharper teeth, as figured by de Haan [15], Shen [18], Sakai [6, 7, 10] and Guinot [19]. In *C. dumortieri* Guinot [19] from the Red Sea these teeth are further salient and rather tuberculated.

The geographical distribution is wide in the Indo-West Pacific from Japan through the Malay Archipelago and the Andaman Sea, Western Australia and the Persian Gulf to the Red Sea.

Calappa quadrimaculata sp. nov.

(Figs. 1–4)

OKINAWA. Nakagusuku Bay.—1 ♂, paratype (URM-CR 0751; cb 67.5 mm, cl 41.3 mm), 17-XII-1984; 1 ♂, paratype (URM-CR 0752; cb 76.3 mm, cl 48.0 mm), 1 ♂, holotype (URM-CR 0753, NSMT-Cr 9626; cb 76.6 mm, cl 47.4 mm), 11-XII-1984; 1 ♂, paratype (URM-CR 0074; cb 72.2 mm, cl 44.8 mm), 01-XI-1985; 1 ♂, paratype (URM-CR 0084, NSMT-Cr 9627; cb 70.4 mm, cl 43.5 mm), 25-XII-1985.

TAIWAN. Tong-Kang, Ping-Tong County.—3 ♂ ♂, paratypes (NSMT-Cr 9628; cb 72.0 mm, cl 45.8 mm—cb 73.6 mm, cl 46.4 mm—cb 78.0 mm, cl 48.2 mm), 15-VII-1989.

Description. Typical of *Calappa*, with well developed clypeiform expansion at each side. Carapace strongly convex fore and aft, especially for its posterior part; its dorsal surface shining, but uneven with a pair of submedian deep furrow bordering mesogastric, cardiac and intestinal regions and with several linear shallow furrows on each branchial region; protogastric regions of both sides with 2 transverse rows of 4 blunt protuberances, each hepatic region with 2 protuberances, mesogastric region with 1, and each branchial region with 1 in a

line with mesogastric protuberance and 2 behind hepatic protuberances; frontorbital region in front of hepatic and protogastric protuberances thickly covered with microscopical vesicular granules; posterior surface on and around intestinal region

sparsely covered with frosted minute granules along posterior margin of carapace. Front deeply cleft in a shape of V; lower and upper edges of lateral margin obtusely angulated. Supraorbital margin rather strongly raised, with 2 closed

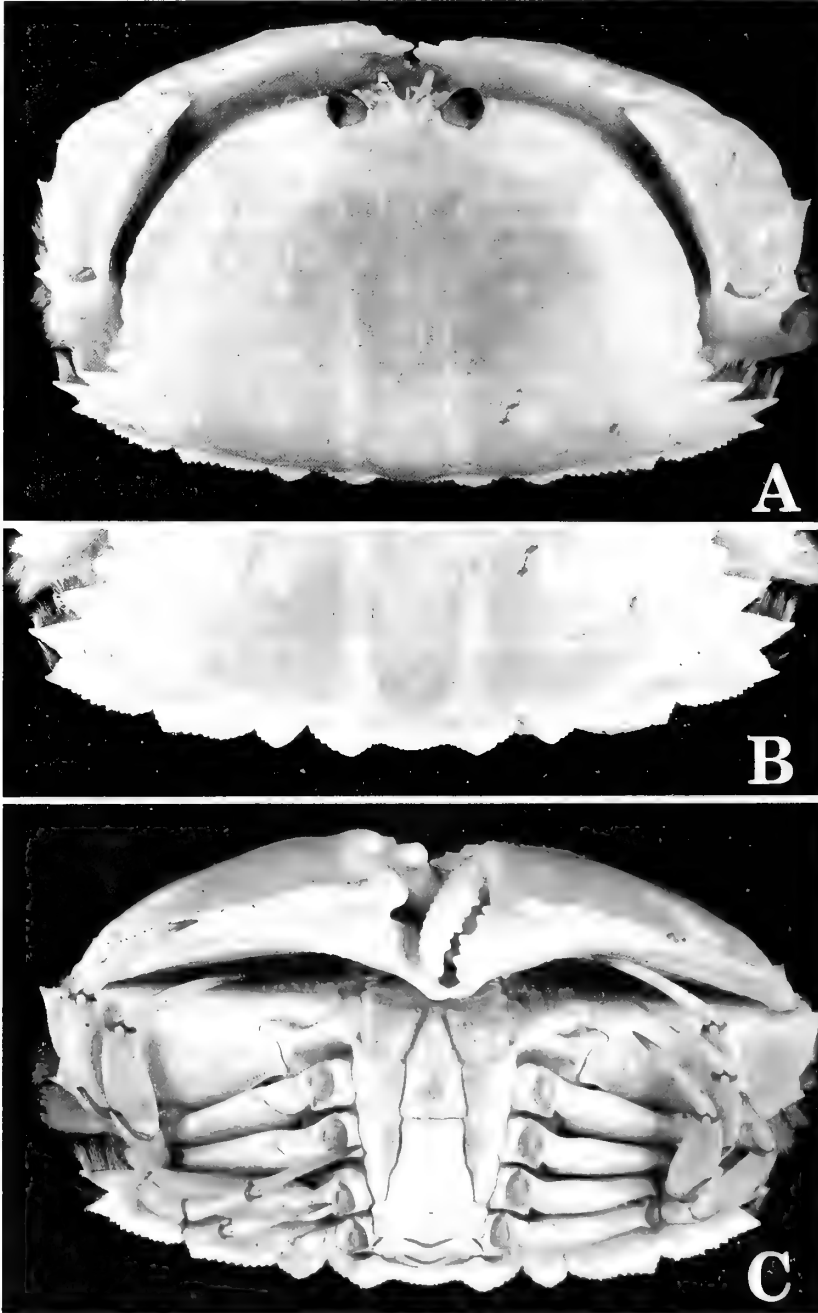


FIG. 1. *Calappa quadrimaculata* sp. nov., ♂, holotype (URM-CR 0753, NSMT-Cr 9626; cb 76.6 mm).

fissured on its outer half; its inner edge produced as a small tubercle separated from upper angle of front. Anterolateral margin of carapace gently convex, with 12 or 13 lobate teeth which are close together; first 4 or 5 teeth each with some minute granules of same size along margins, but posterior teeth except for the last with a median main granule and 2 accessory granules each on anterior and posterior slopes; clypeiform expansion well developed, with 4 strong teeth; first 2 obtusely angulated, and last 2 sharply pointed, end at same level; posterior margin of last tooth more or less serrulated with several granules, forming first lobe

of posterior margin of carapace; second lobe also serrulated along its whole margin, as wide as first lobe, obtusely angulated near lateral end; third lobe triangular, obtusely angulated at its apex, about half as wide as second lobe; median lobe weakly convex behind intestinal region along its central 1/3, with a triangular lobe at each side; apex of this lateral lobe obtuse, exceeding the level of median lobe and also that of third lobe.

Distal margin of chelipedal merus cut into 4 lobes, fringed with long hairs; median 2 lobes about 1/2 as wide as proximal and distal lobes; distal lobe sharply pointed distally, and subdistal



FIG. 2. *Calappa quadrimaculata* sp. nov., ♂, paratype (URM-CR 0074; cb 72.2 mm).

lobe with a spine at its median part; carpus and palm smooth and shining; upper margin of palm cut into 9 teeth, the first and the last of which are with pale brownish fringe.

Etymology. The species name, *quadrимaculata*, is referred to four ocelli of the carapace, which are somewhat variable in size, but always distinct.

Remarks. At a glance the new species is readily distinguished from the known species by the different color pattern. The basic color patterns of

the carapace and chelipeds are individually constant in the *Calappa* species and kept so long even in spirit, being one of the effective clues to distinguish the species.

The new species is without doubt most close to *Calappa lophos* (Herbst) in the general formation of the carapace and chelipeds, but distinguished from it by the proportional difference of the carapace and the morphological difference of the posterior lobes of the carapace. The carapace of the new species is seemingly, but apparently, wider than that of *C. lophos*.

This proportional difference is indicated with the measurements given to both species; in five specimens of *C. lophos* examined, the mean ratio of the carapace breadth to length is 1.43, while in eight specimens of the new species the ratio varies from 1.57 to 1.63 (mean 1.61). In addition, it is remarkable that in the new species the second posterior lobe of the carapace is almost equal to the first lobe in its width, but in *C. lophos* the second posterior lobe is at most $\frac{2}{3}$ as wide as the first lobe.

Alcock [17] doubtfully synonymized *Calappa guerini* de Brito Capello with *C. lophos*. According to its original description and figure [20], it differs from *C. lophos* by having the sharply toothed innermost pair of the posterior lobes of

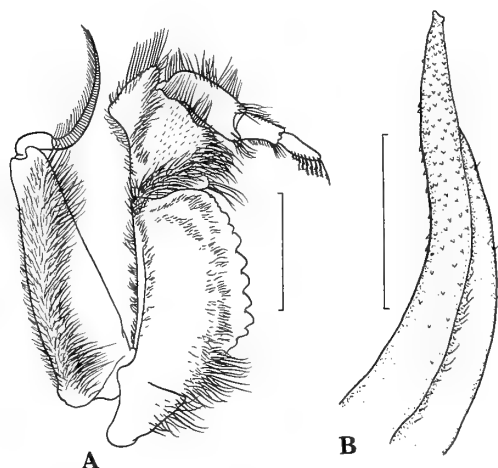


FIG. 3. *Calappa quadrimaculata* sp. nov., third maxilliped (A) and first pleopod (B) of ♂, paratype (URM-CR 0074). Scales=5 mm for A, 1 mm for B.

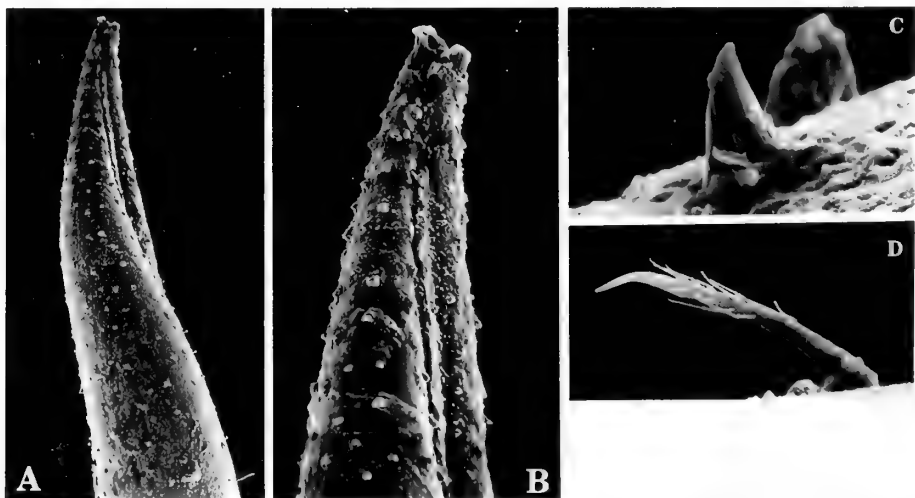


FIG. 4. *Calappa quatrimaculata* sp. nov., first pleopod of ♂, paratype (URM-CR 0074). A, distal fourth; B, distal part, further enlarged; C, one of tubercles dispersed on shaft; D, one of sensory hairs arranged in a line along seam.

TABLE 1. Japanese species of the genus *Calappa*

Species	Distribution	Foreign loc.
** <i>C. bicornis</i> Miers, 1884	Kii Penin. & Tosa Bay	W. Indian Ocean
* <i>C. calappa</i> (Linnaeus, 1758)	Sagami Bay to Ryukyus	Indo-W. Pacific
* <i>C. capellonis</i> Laurie, 1906	Kii Penin. to Ryukyus	Sri Lanka
* <i>C. gallus</i> (Herbst, 1785)	Sagami Bay to Ryukyus	Cosmopolitan
* <i>C. hepatica</i> (Linnaeus, 1758)	Sagami Bay to Ryukyus	Indo-W. Pacific
<i>C. japonica</i> Ortman, 1892	Sagami Bay to Kyushu	Indian Ocean
** <i>C. lophos</i> (Herbst, 1782)	Tokyo Bay to Kyushu	Indo-W. Pacific
** <i>C. philargius</i> (Linnaeus, 1758)	Tokyo Bay to Kyushu	Indo-W. Pacific
<i>C. pustulosa</i> Alcock, 1896	Sagami Bay to Tosa Bay	India
** <i>C. quadrimaculata</i> sp. nov.	Okinawa	Taiwan
** <i>C. terraereginae</i> Ward, 1936	Korean Channel	Australia
<i>C. yamasitae</i> Sakai, 1980	Kii Penin.	

Four species with an asterisk have hitherto been known not only from the Japanese mainland, but also from the Ryukyu Islands. Five species with two asterisks including a new species were newly added to the carcinological fauna of the Ryukyu Islands.

the carapace. There is no subsequent record of the species or discussion on its identity, and thus it is not always sure at present whether Alcock's synonymization is justified or not. However, at least, *C. guerini* is very close to and nearly identical with *C. lophos*, and the new species is separated from this doubtful species also by the different contour and armature of the carapace.

Calappa terraereginae Ward, 1936

OKINAWA. Nakagusuku Bay, 15–20 m deep.—1 ♂ (URM-CR 0088, NSMT-Cr 0629; cb 50.3 mm), 21-VI-1985; 1 ♂ (URM-CR 1162; cb 53.0 mm), 10-VI-1987.

Remarks. This species is only known by Ward [21], Sakai [6, 7] and Tyndale-Biscoe and George [22] from Lindeman Island off Queensland and Western Australia, and from off Cheju Island in the Korean Channel. The general formation of the carapace much resembles that of *C. lophos* (Herbst), but the carapace is slightly narrower, with more strongly arched anterolateral borders of the carapace, the teeth of the clypeiform expansion are rather triangular in dorsal view and not so sharp as in *C. lophos*, and the posterior border of the carapace is pronouncedly produced beyond the posterior border of the clypeiform expansion.

GEOGRAPHICAL NOTES

The genus *Calappa* is composed of 1 cosmopolitan, 15 Indo-West Pacific, 3 East Atlantic and 9 West Atlantic species. As enumerated in Table 1, the species known from Japanese waters are 12 including the new species described in the present paper. Four of them have hitherto been recorded not only from the Japanese mainland, but also from the Ryukyu Islands. In the present paper 4 known species were newly added to the carcinological fauna of the Ryukyu Islands.

Both of 2 species unrecorded from the Ryukyu Islands, *Calappa japonica* and *C. pustulosa*, are known from the Japanese mainland and Indian Ocean without the intervening localities. These two species are the deeper-water inhabitants than most of the other species, ranging bathymetrically from ca. 50 to 200 m. Therefore it may be possible to conclude that the absence of these two species from the Ryukyu Islands and the Southeast Asia is not due to the topographical condition, but to the insufficient operation of collecting the samples at the continental shelf.

Calappa bicornis, *C. capellonis* and *C. terraereginae* are also known only from Japan and the distant localities, viz., the western Indian Ocean, Sri Lanka and Australia, respectively, but it is reasonable that in due time they will be recorded

from the intervening localities. *C. gallus* is, as noted in the text, peculiar in its worldwide distribution.

ACKNOWLEDGMENTS

We wish to tender our cordial thanks to Dr. Shigemitsu Shokita, Associate Professor of the Department of Marine Sciences, University of the Ryukyus, who made the specimens collected by the students available to us for systematic study and gave the intensive guidance to the junior author. Thanks are also due to the Chinen and Tozoe Fishermen's Unions for providing us with the facilities to collect the specimens from gill-nets. Dr. Hsiang-Ping Yu, Professor of National Taiwan University of Marine Sciences, kindly arranged the field survey for the senior author and gave him the information about the crabs from Taiwan.

REFERENCES

- Shoup, J. E. (1958) Shell opening by crabs of the genus *Calappa*. Science, **160**: 887–888.
- Takeda, M. and Suga, H. (1979) Feeding habits of box crabs, *Calappa*. Res. Crust., **9**: 43–46, pl. 1.
- Rathbun, M. J. (1911) Marine Brachyura. The Percy Sladen Trust Expedition to the Indian Ocean in 1905. 3(11). Trans. Linn. Soc. London, (2), **14**: 191–261, pls. 15–20.
- Ihle, J. E. E. (1918) Die Decapoda Brachyura der Siboga-Expedition. III. Oxystomata: Calappidae, Leucosiidae, Raninidae. Siboga-Exped., **39b**: 155–322.
- Laurie, R. D. (1906) Report on the Brachyura collected by Professor Herdman, at Ceylon, in 1902. Ceylon Pearl Oyster Fish. Rep., **5** (Suppl.): 349–432, pls. 1, 2.
- Sakai, T. (1937) Studies on the crabs of Japan. II. Oxystomata. Sci. Rep. Tokyo Bunrika Daigaku, (B), **3** (Suppl.): 67–192, pls. 10–19.
- Sakai, T. (1976) Crabs of Japan and the Adjacent Seas. Kodansha Ltd., Tokyo, pp. xxix+773 (English); pp. 461 (Japanese); pp. 16+pls. 251 (plates).
- Takeda, M. and Koyama, Y. (1974) On some rare crabs from Kii Province. Res. Crust., **6**: 103–121.
- Klunzinger, C. B. (1906) Die Spitz- und Spitzmundkrabben (Oxyrhyncha und Oxystomata) des Roten Meeres. Stuttgart, pp. vii+88, pls. 2.
- Sakai, T. (1965) The Crabs of Sagami Bay collected by His Majesty the Emperor of Japan. Maruzen Co., Ltd., Tokyo, pp. xvi+206 (English part)+92 (Japanese part)+32 (bibliography and index), map 1, pls. 100.
- Rathbun, M. J. (1937) The oxystomatous and allied crabs of America. Bull., U. S. Natn. Mus., **166**: i-vi, 1–278, pls. 1–86.
- Barnard, K. H. (1950) Descriptive catalogue of South African decapod Crustacea. Ann. S. Afr. Mus., **38**: 1–837.
- Monod, T. (1956) Hippidea et Brachyura ouest-africains. Mém. I.F.A.N., **45**: 1–674.
- Sakai, T. (1980) New species of crabs of the families Lithodidae and Calappidae. Res. Crust., **10**: 1–11, pl. 1, frontispiece.
- Haan, W. de (1833–1849) Crustacea. In: Von Siebold, Fauna Japonica sive descriptio animalium, quae in itinere per Japoniam, jussu et auspiciis superiorum, qui summum in India Batava Imperium tenent, suscepto, annis 1823–1830 collegit, notis, observationibus et abumbrationibus illustravit. Pp. xvii+xxxi+244, pls. 55+A-Q+2.
- Stephensen, K. (1945) The Brachyura of the Iranian Gulf. Danish Sci. Invest. Iran, **4**: 57–237.
- Alcock, A. (1896) Materials for a carcinological fauna of India. No. 2. The Brachyura Oxystomata. J. Asiat. Soc. Bengal, **65**: 134–296, pls. 6–8.
- Shen, C. J. (1931) The crabs of Hong Kong. Part II. Hong Kong Nat., **2**: 185–197, pls. 12–14.
- Guinot, D. (1964) Sur une collection de crustacés décapodes brachyours de Mer Rouge et de Somalie. Remarques sur les genres *Calappa* Weber, *Menaethiops* Alcock, *Tyche* Bell, *Ophthalmias* Rathbun et *Stilbognathus* von Martens. Boll. Mus. Civ. Venezia, **15**: 7–63, pls. 1–4.
- de Brito Capello, F. (1870) Algumas especies novas ou pouco conhecidas de crustaceos pertencentes aos generos «*Calappa*» e «*Telphusa*». J. Sci. Math. Phys. Nat., Lisboa, **3**: 128–134, pl. 2.
- Ward, M. (1936) Crustacea Brachyura from the coasts of Queensland. Mem. Qld. Mus., **11**: 1–13, pls. 1–3.
- Tyndale-Biscoe, M. and George, R. W. (1962) The Oxystomata and Gymnopleura (Crustacea, Brachyura) of Western Australia with descriptions of two new species from Western Australia and one from India. J. Roy. Soc. W. Aust., **20**: 45–96.

Description and Complete Larval Development of a New Species of *Baccalaureus* (Crustacea: Ascothoracida) Parasitic in a Zoanthid from Tanabe Bay, Honshu, Japan

TATSUNORI ITÔ¹ and MARK J. GRYGIER²

¹ Seto Marine Biological Laboratory, Faculty of Science, Kyoto University, Shirahama, Wakayama 649-22, and ² Sesoko Marine Science Center, University of the Ryukyus, Sesoko, Okinawa 905-02, Japan

ABSTRACT—An unidentified species of *Zoanthus* from Tanabe Bay, Honshu, Japan, is the host of an endoparasitic ascothoracid crustacean, *Baccalaureus falsiramus*, new species. This is the first record of this zoanthid genus serving as the host of an ascothoracid and the second species of *Baccalaureus* from Japan. The morphology of the adult females, nauplii, and ascothoracid larva is described based upon a detailed study combining light microscopy and SEM. The female of this new species is characterized by a coiled carapace but very short, more or less distally upturned thoracic horns, and very long, ventrally directed papillae for seminal receptacle ducts lateral to thoracopods II–IV. Much variability is recognized in the antennule, thoracopods, penis, and abdominal ornamentation. Larval specimens were individually reared in the laboratory. Six lecithotrophic naupliar instars with rudimentary endites on the antennae and mandibles are present before the ascothoracid larva. The nauplii swam for about one month without feeding until the metamorphosis to the ascothoracid larva. Naupliar instars II–VI have a sculpture of concentric cuticular ridges on the marginal area of the dorsal shield. A nauplius eye is present through all naupliar instars as well as in the ascothoracid larva. Setae are gradually added to the antennules, but the antennae and mandibles remain essentially unchanged after instar III; rudimentary maxillules appear in instar II. The ascothoracid larva is a “Tessmann’s larva” similar to one recently described from Hawaiian plankton, but lacking central pores within the carapace reticulations. Morphological and developmental features of the nauplii and ascothoracid larva are discussed.

INTRODUCTION

One of us (T. I.) has been conducting an extensive parasitological survey in Tanabe Bay, Japan, to discover the adults of *Facetotecta* Grygier (Crustacea, Maxillopoda), which are currently known only from so-called y-larvae [1]. An unidentified *Zoanthus* (Hexacorallia) examined in this survey was infested by a previously unknown species of *Baccalaureus* Broch (Crustacea, Ascothoracida, Lauridae), which is described in this paper.

The present paper also reports the first successful study of a generalized larval history in an ascothoracid, based upon larvae of the new

species individually reared in the laboratory. The only other complete report is that of Brattström [2] on *Ulophysema oeresundense* Brattström, 1936, a species with abbreviated development. Wagin [3] and Karande and Oguro [4] gave more or less complete accounts of the larvae of *Ascothorax ophioctenis* Djakonov, 1914, and *Dendrogaster* (= *Myriocladus*) *astropectinis* Yosii, 1931, respectively, but in neither case were naupliar instars clearly determined, just arbitrary stages.

MATERIAL AND METHODS

Five adult females and one possible male of the new species were collected from a single colony of *Zoanthus* sp. (Japanese name: mame-sunagincha-ku) that was found on a rocky cliff on the north side of Toshima Rock in Tanabe Bay (33°41'N,

135°21'E), at a depth of 4 m. Parts of this zoanthid colony that yielded ascothoracidans were sampled on several occasions by one of us (T. I.) using SCUBA. Three females that were examined by light microscopy have been designated as the type series (data given later). The other two females and the possible male were examined by SEM. One of the females (SEM-1; collected 22-I-1989), which was accompanied by the possible male, was fixed with 10% Formalin-sea water solution; the other female (SEM-2; collected 5-II-1989) was pre-fixed with 2% glutaraldehyde (phosphate-buffered, with sucrose to adjust osmotic pressure) for 4 hr, treated with a mixture of 2% tannic acid and 2% guanidine hydrochloride solution for 8 hr, and then post-fixed with 2% osmic acid for 8 hr. An instar I nauplius collected from the brood chamber of SEM-2 was similarly treated for SEM study. Four instar II nauplii obtained from a paratype and two ascothoracid larvae metamorphosed in the laboratory were fixed with Formalin-sea water, and were also used for SEM study. After fixation, all the specimens used for SEM study were dehydrated through a graded series of ethanol, transferred into isoamyl acetate, and desiccated in a critical point dryer using CO₂. Dried specimens were sputter-coated with gold, and examined in a scanning electron microscope (JEOL, JSM T-220) at accelerating voltages of 5 to 15 kv.

Several instar I nauplii from the holotype and instar II nauplii from a paratype were dissected in glycerine for examination of appendages. Three nauplii obtained from the same paratype were reared in the laboratory. Initially, as shown later by examination of their exuviae, two were second instar and one was third. They were kept in small dishes individually at 19°C, with daily changes (twice a day) of sterilized dishes containing fresh, paper-filtered sea water until the metamorphosis to the ascothoracid larva. Exuviae were removed from the dishes when present, fixed in Formalin-sea water, and mounted on glass slides in glycerine for light microscopical examination. One of the resulting ascothoracid larvae was dissected and mounted first in glycerine, then in glycerine jelly for microscopical examination; the other two were prepared for SEM study as described above.

Due to the extensively modified body and

appendages in *Baccalaureus*, there has historically been considerable disagreement about the number of thoracic segments and the identity of most of the cephalic and anterior thoracic appendages and bodily projections. The morphological terminology adopted here is that of Brattström [5] as modified by Grygier [6].

Part 1. Taxonomy

Baccalaureus falsiramus sp. nov.

Diagnosis. Adult female: *Baccalaureus* round in side view, with coiled lateral carapace lobes making almost two full revolutions, and with spines on edges of coils. Anterior thoracic horns shorter than thorax, naked, either distally upturned or almost straight. All three pairs of mouthparts well developed. Small plate-like organ at base of first thoracopod, or just a swelling instead, barely or not extending dorsally over lateral chitinous ridge of thorax. Thoracopod 1 variform, represented by a papilla or cylindrical process, with 0–2 apical setae. Thoracopods 2–4 containing seminal receptacles, each limb flanked laterally by prominent, ventrally directed, conical papilla with apical opening. Thoracopod 5 variform. Thoracopod 6 variform, or absent. Dorsal setae only on last thoracomere and first abdominal segment. Penis uniramous, variform, often with distal spines. Furcal rami as long as first two abdominal segments combined, narrow, with 2–3 hirsute terminal setae, no medial setae or sensilla, lateral side partly bare of cuticular ctenae.

Nauplii: lecithotrophic, six instars, with bowl-shaped dorsal shield after instar I, four-segmented antennules at instar VI, vestigial protopodal endites on antennae and mandibles, caudal armament barely protruding beyond end of dorsal shield. Ascothoracid larva: a "Tessmann's larva", carapace valves without central pores in polygonal cells delineated by chitinous, mesh-like ridges.

Type series. Holotype: adult female, fully dissected, brooding eggs and nauplii, trunk and carapace lobes preserved in ethanol, dissected appendages and part of carapace mounted onto slide glasses with glycerine jelly. Paratype-1: adult female, brooding eggs, carapace partly torn, specimen otherwise intact, preserved in ethanol. The

holotype and paratype-1 were recovered by M. J. G. from host material that had been fixed (10-IX-1988) and preserved in 70% ethanol by T. I. after

being kept in an aquarium (Original collection date 26-VII-1988). Paratype-2: adult female (fully dissected), brooding eggs and nauplii, recovered

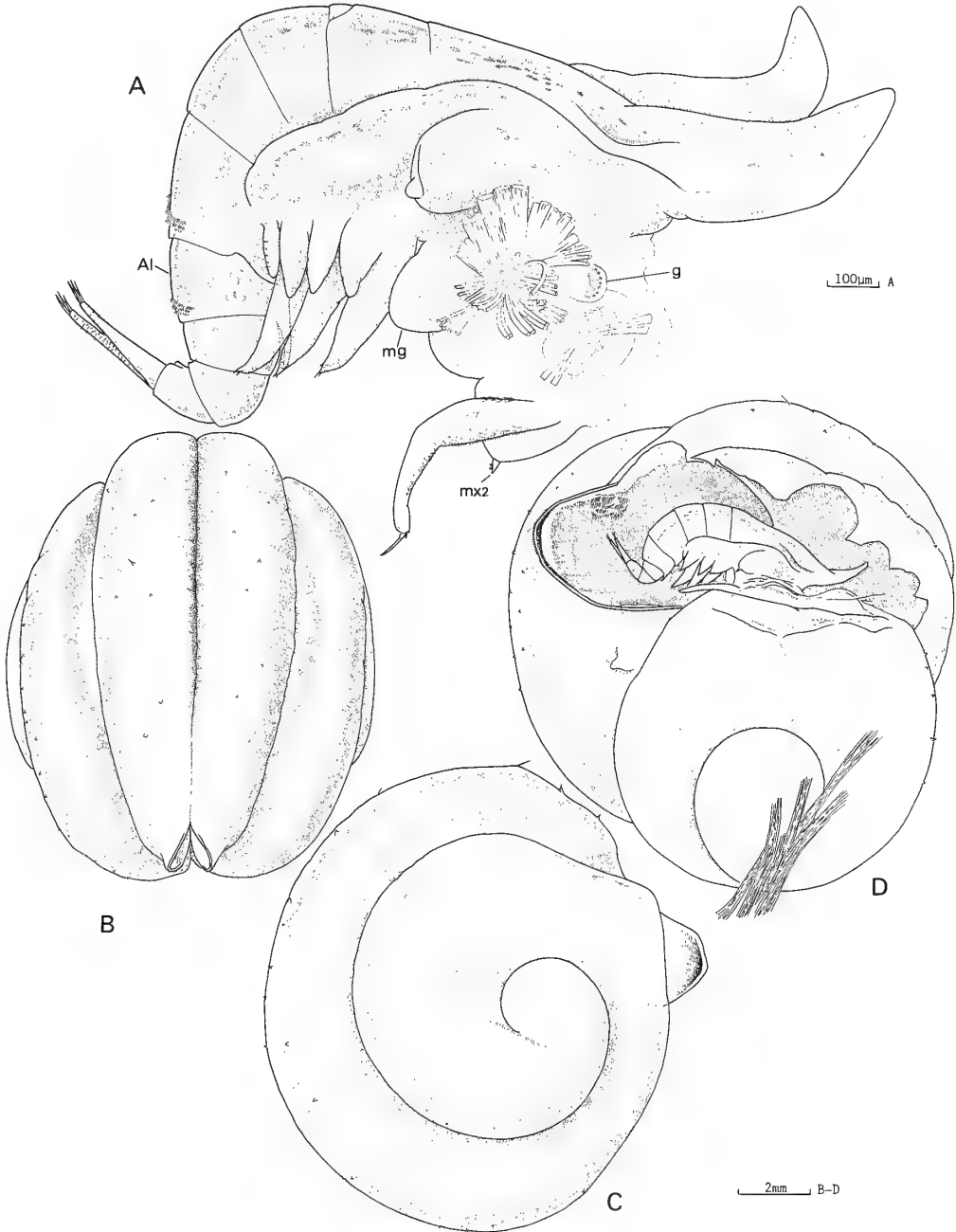


FIG. 1. *B. falsiramus* sp. nov. A, lateral view of holotype (carapace removed; AI, first abdominal segment; g, gut diverticulum; mg, maxillary gland; mx2, maxilla). B-D, paratype-1. B, dorsal view of carapace; C, lateral view of carapace; D, lateral view of habitus with partly torn carapace.

by T. I. from living host material (26-VII-1988), cephalic area and much of carapace missing, remainder of carapace removed from trunk, preserved in ethanol, dissected appendages mounted onto slide glass with glycerine jelly. Type locality: Tanabe Bay, Honshu, Japan. The type series is deposited in the Seto Marine Biological Laboratory, Kyoto University.

Etymology. The specific name (from Latin "*falsus*" = false plus Latin "*ramus*" = branch) refers to the extraordinarily large papillae at the bases of thoracopods 2–4.

1-1. DESCRIPTION OF HOLOTYPE

Carapace with small, medial body chamber connected to pair of large, coiled, lateral lobes serving as brood sacs (see Fig. 1B-C of paratype-1), tintured with reddish brown along aperture lips, other parts with very faint tinge of yellowish brown. Outer coils nearly circular in side view, 6.0 mm high, 5.1 mm long, subsequent coiling of diminishing radius, up to nearly two full revolutions altogether (± 675). Exposed lateral faces of coils with sparse, simple papillae, edges with widely spaced spines sometimes exceeding 0.15 mm long, outer part of hidden medial faces with similar but smaller tubercles (Fig. 3C). Gut diverticula and ovaries readily visible through carapace wall, with radially arranged side branches from main central coil, side branches dividing once or twice. Body chamber protruding beyond outer coil posteriorly, with vertical posterior aperture; aperture lips bearing adherent exuviae of four earlier instars (partially shown in Fig. 3A). Lips with short marginal spines, inner sculpturing of cuticular ridges forming hexagons, and dense interior lining of fine cuticular hairs (Fig. 3B). Ventral margins of lateral sides of body chamber adjoining but readily separable as far forward as oral cone; no special armament.

Body attitude as shown in Figure 1A; almost colorless but scattered spots of faint purple. Distance from tips of horns to tips of furcal rami 3.7 mm. Body cuticle loose, animal preparing to molt. Head bearing oral cone, posteriorly directed antennules, and pair of lobes representing maxillary glands. Thorax six-segmented, boundary of first and second segments not expressed externally,

that of second and third segments weakly expressed. Pair of anterior horns arising from first segment, parallel, shorter than thorax, laterally flattened, tapering to rounded, upturned tips, naked, semitransparent. Dorsoproximal part of each horn markedly swollen laterally in connection with anterior part of lateral chitinous ridge, latter present from basal part of horn to middle of sixth thoracomere, consisting of at least four or five separate, segmentally arranged thickenings and forming outer edge of trough along side of body, highest point near supposed boundary of first two thoracomeres. Transverse band of short rows of hairs on rear of sixth thoracomere and first abdominal segment. Five pairs of thoracopods present. Abdomen four-segmented, each segment narrower and less high than preceding one, ornamented with many small pores among sparse, delicate spinules (Fig. 3D). First abdominal segment with ventral penis.

Antennules (Fig. 4A, C) strap-like, about 0.9 mm long, curved or sharply bent, indistinctly divided into about four segments and apical process, hairy all over surface, transverse rows of longer hairs along anterior (ventral) face of proximal half. Terminal segment with two short, subapical setae, one medial and one anterior; medial seta apparently folded or bipartite (Fig. 4B, D). Apical process small, with trifurcate aesthetasc and short seta.

Labrum (Fig. 1A) deeper than long, short posterior edges adjoining behind other mouthparts but readily separable.

Mandible (Fig. 4E) narrow, distal half tapered with many short, basally directed spinules on proximal two-thirds of anteromedial margin, four arched rows of spinules posterolaterally.

Distal part of maxillule (Fig. 4F) represented by conical process with hairs of different lengths.

Maxillae (Fig. 4G) largely fused, their tips protruding through distal labral aperture; tips separate, bifid, each accompanied subterminally by basally bent, triangular, lateral plate.

Thoracopod 1 represented by a small papillary process arising from basal swelling, with no seta. Right one (Fig. 3E) shorter and wider than left one (Fig. 3F). Basal swelling hemispherical, somewhat inflated but not extending as "plate-like organ"

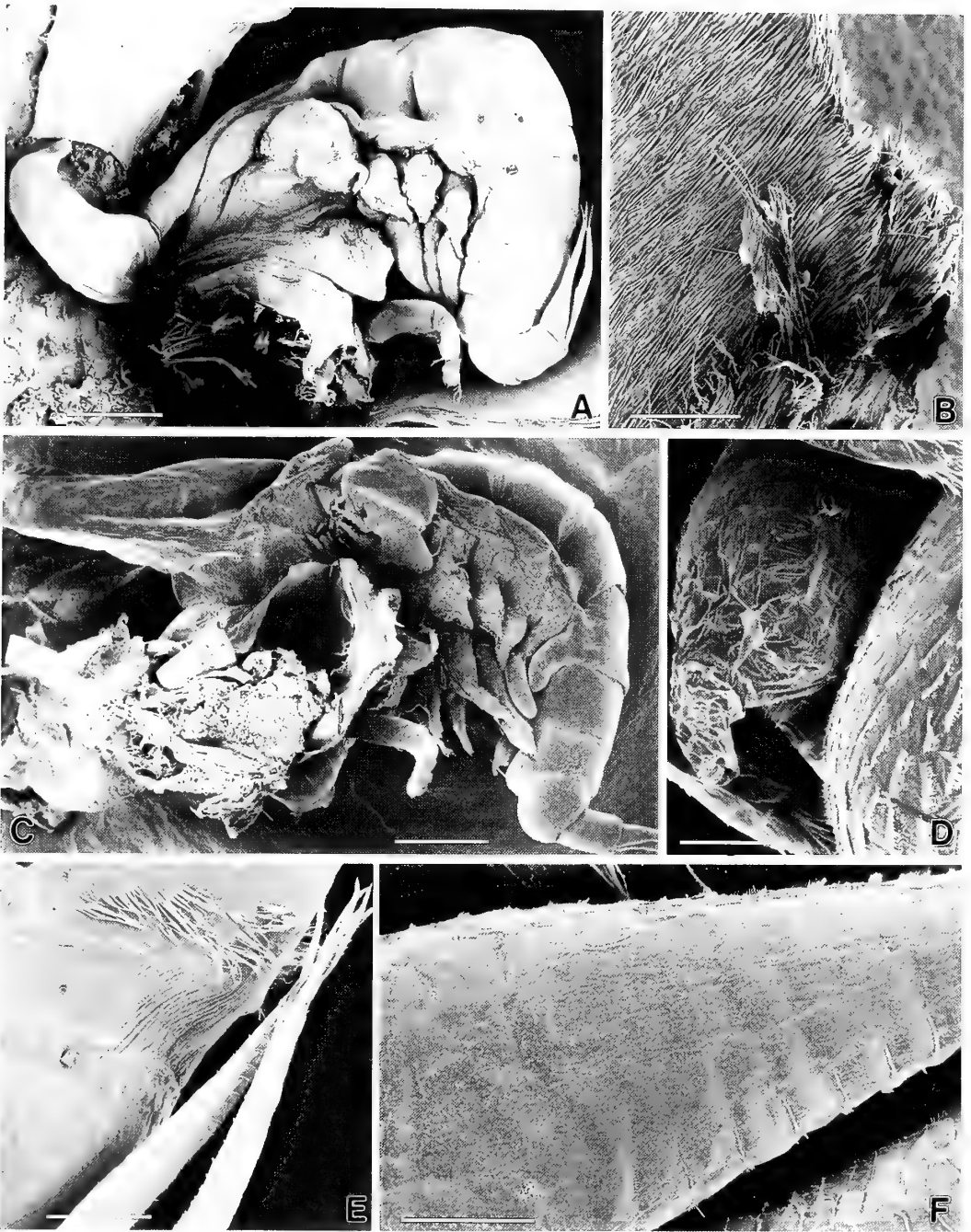


FIG. 2. SEM photomicrographs of *B. falsiramus* sp. nov. C-D SEM-2, otherwise SEM-1. A, habitus, lateral; B, internal side of carapace near aperture lip; C, habitus, lateral; D, penis and first abdominal segment; E, apical portion of furcal rami and first abdominal segment with hairs; F, furcal rami, lateral. Scales: A, C 500 μm ; B, E 100 μm ; D, F 50 μm .

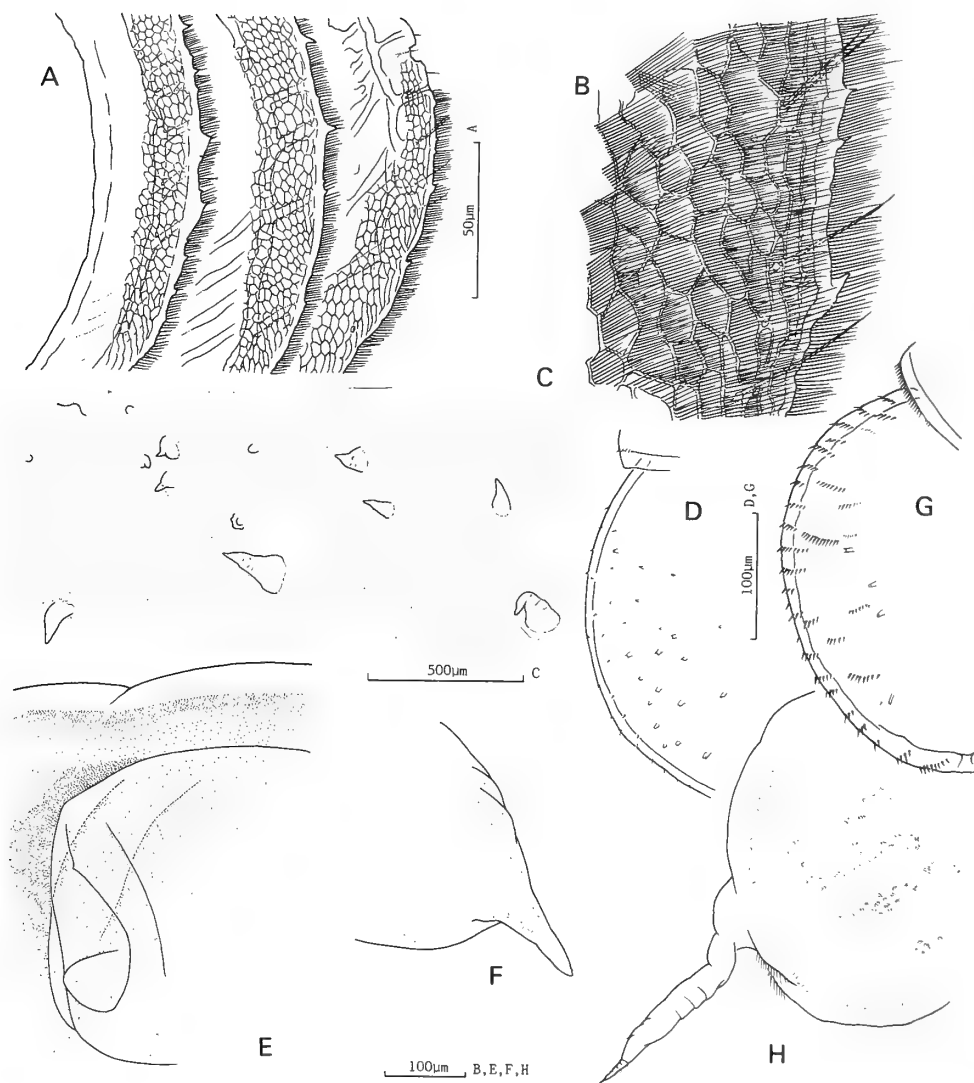


FIG. 3. *B. falsiramus* sp. nov. A-C, paratype 1. A, internal view of aperture lip, showing adherent exuvia; B, detail of marginal part of A; C, carapace spination, 3 large spines (below) on edge of coil, smaller ones (above) on inner face below edge. D-F, holotype. D, lateral view of third abdominal segment; E-F, right and left thoracopods 1 with basal swelling. G-H, paratype-2. G, lateral view of third abdominal segment; H, right thoracopod 1 with basal swelling.

dorsally over chitinous ridge.

Thoracopod 2 (Fig. 6A) large, well-developed, appearing biramous because of presence of prominent lateral papilla; leg itself unsegmented, but tiny distal, setose "ramus" distinguishable from "protopod" filled with seminal receptacles, "ramus" armed apically and laterally with four (right) or five (left) short setae or spiniform pro-

cesses together with cuticular ctenae and hairs (Fig. 6B, C). Lateral papilla conical, pointing ventrally, almost bare, extending to about middle of "protopod", terminating in relatively large opening (Fig. 6D), apparently many much smaller pores on sides of papilla, precise relationships to seminal receptacle ducts unclear. Seminal receptacles bottle-shaped, the number estimated at 14-17,

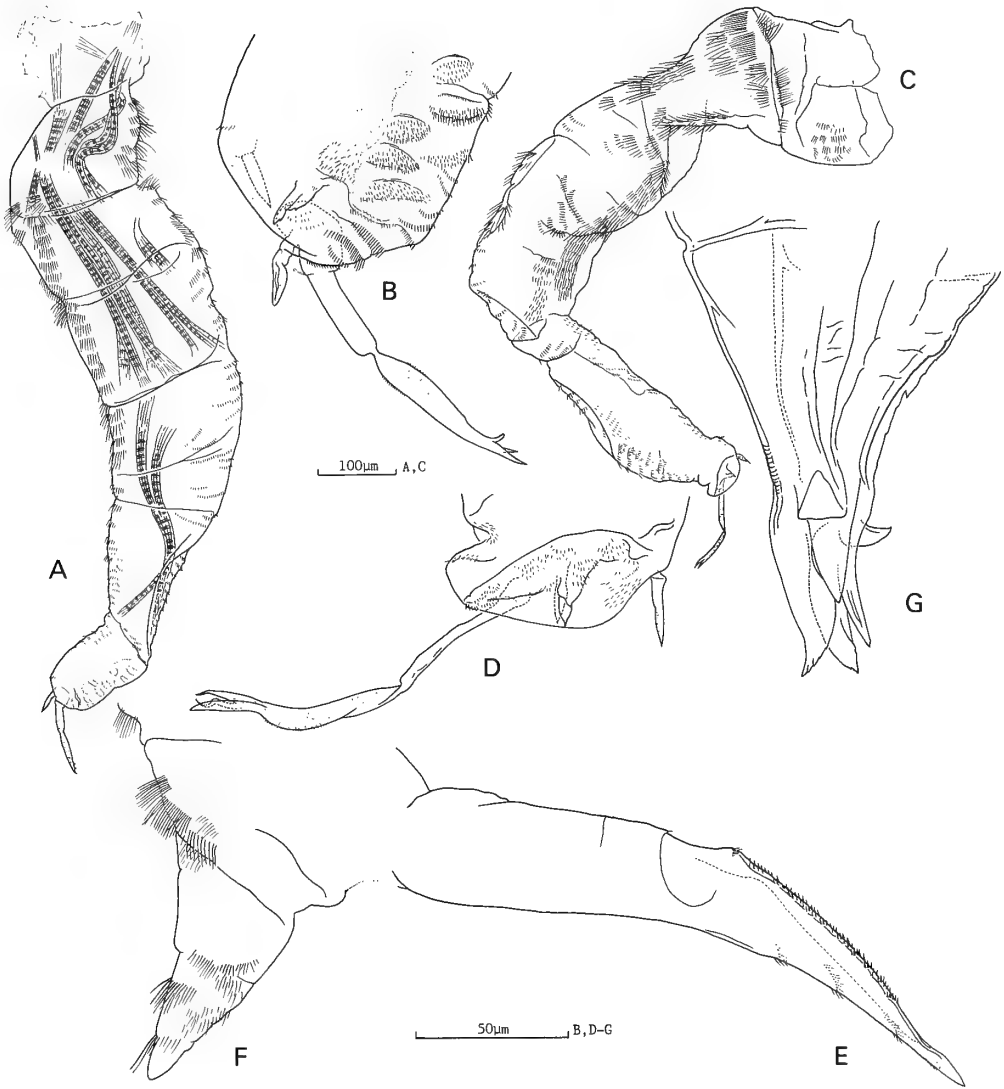


FIG. 4. *B. falsiramus* sp. nov. Holotype, A, right antennule, showing musculature; B, apical part of A; C, left antennule; D, apical part of C; E, mandible; F, maxillule; G, maxillae.

with long, extremely narrow ducts sheathed in cells. Within receptacles, sperm usually in small knot near duct entrance (see Fig. 6J, paratype), some sperms with elongate heads 42 μ m long expressed from them.

Thoracopods 3–4 similar to thoracopod 2. Thoracopod 3 armed with spiniform processes or short setae on each ramus, three lateral and two terminal on the left (Fig. 6E), five lateral, two terminal, and one medial on the right (Fig. 6F), each con-

taining 14–15 seminal receptacles. Right thoracopod 4 (Fig. 7A) armed with one terminal and three short lateral setae, left thoracopod 4 (Fig. 7B) armed apically with one strong spine and one seta, 8–11 seminal receptacles in each “protopod”.

Left thoracopod 5 (Fig. 7C) sausage-shaped, right one tapered, both same size, less than half as long as preceding three pairs, lacking seminal receptacles and lateral papilla, ornamented with delicate cuticular ctenae almost all over its surface,

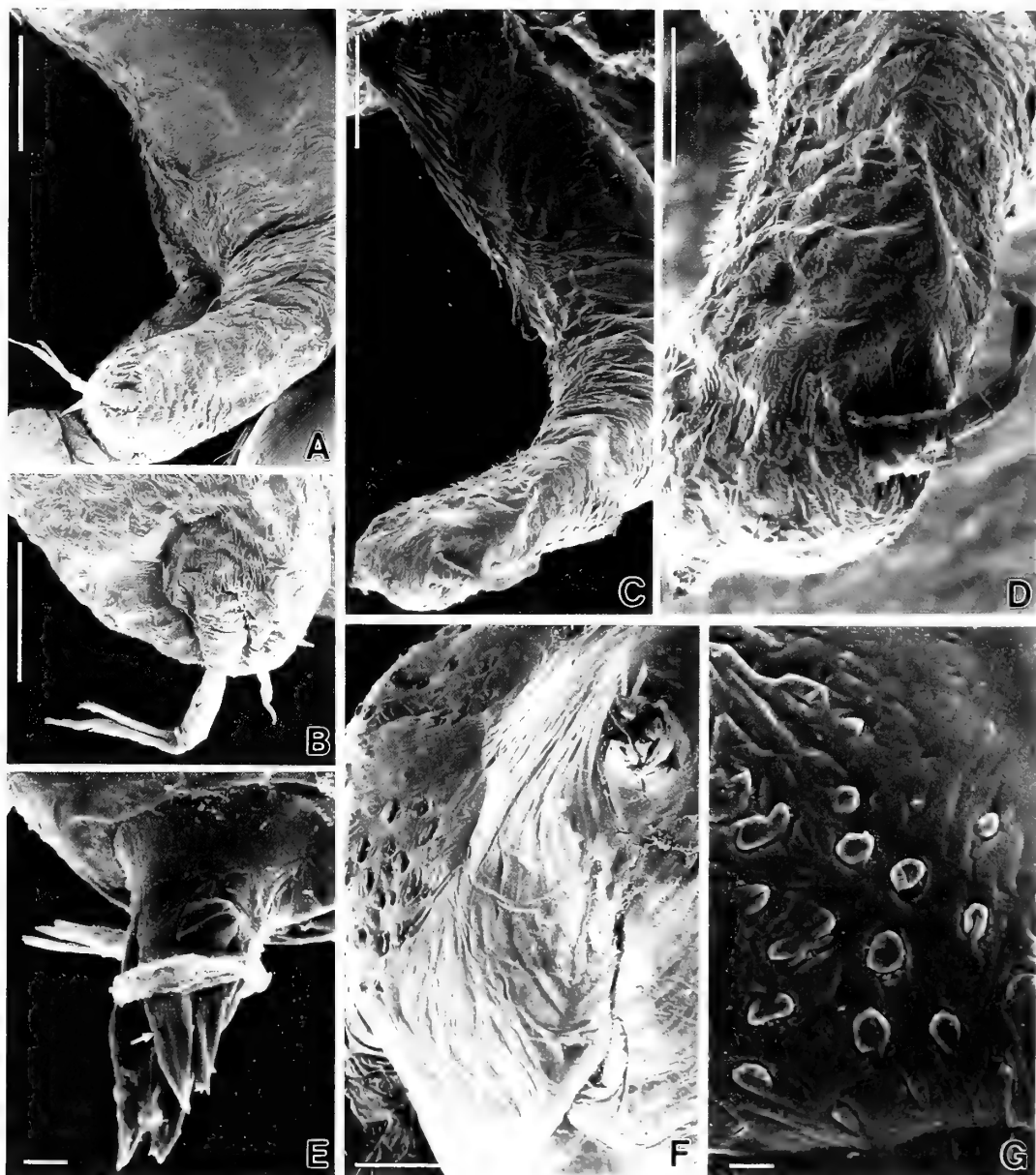


FIG. 5. SEM photomicrographs of *B. falsiramus* sp. nov. A-B SEM-1, otherwise SEM-2. A, left antennule; B, apical part of A; C, left antennule; D, apical part of C; E, tips of maxillae (arrow indicating duct opening); F, ventral view of labrum and maxillae; G, round papillae of labrum. Scales: A, C 100 μm ; B, D, F 50 μm ; E, G 10 μm .

with neither setae nor spines.

Thoracopod 6 absent, though ventral side of sixth thoracomere produced into transverse fold.

Penis (Fig. 7D) vermiform, reaching end of second abdominal segment, tapering toward two

sharp spines. Possible duct opening between spines.

Furcal rami (Fig. 7E) 0.50 mm long, basal height 0.13 mm, tapering and weakly sigmoidal. Three hirsute terminal setae, no medial setae or sensilla.

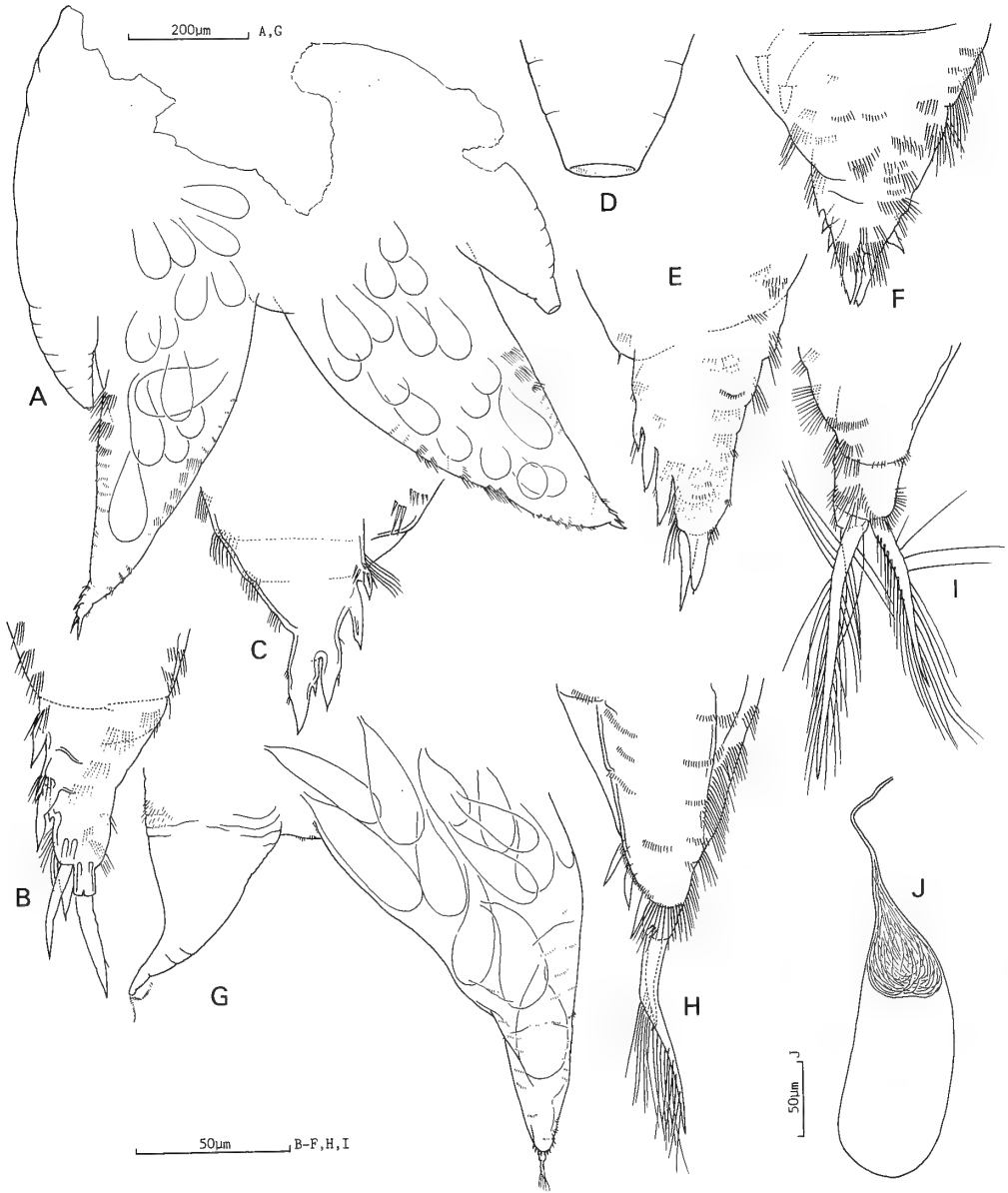


FIG. 6. *B. falsiramus* sp. nov. A-F, holotype. A, thoracopod 2; B, apex of right thoracopod 2; C, apex of left thoracopod 2; D, apex of lateral papilla of left thoracopod 2; E, left thoracopod 3, posterior; F, right thoracopod 3. G-J, paratype-2. G, thoracopod 2; H, apex of thoracopod 2; I, apex of thoracopod 3; J, seminal receptacle.

Short cuticular ctenae present on whole medial surface, distal quarter of lateral surface, and dorsal and ventral edges. Thickened dorsal and ventral margins appearing scalloped internally.

1-2. DESCRIPTION OF OTHER FEMALES

Outer coils of carapace of paratype-1 (Fig. 1B-D) 6.9 mm high, 6.2 mm long, paratype-2 indeterminate in this respect due to damage. Pair of dense patches of hairs dorsolaterally within body

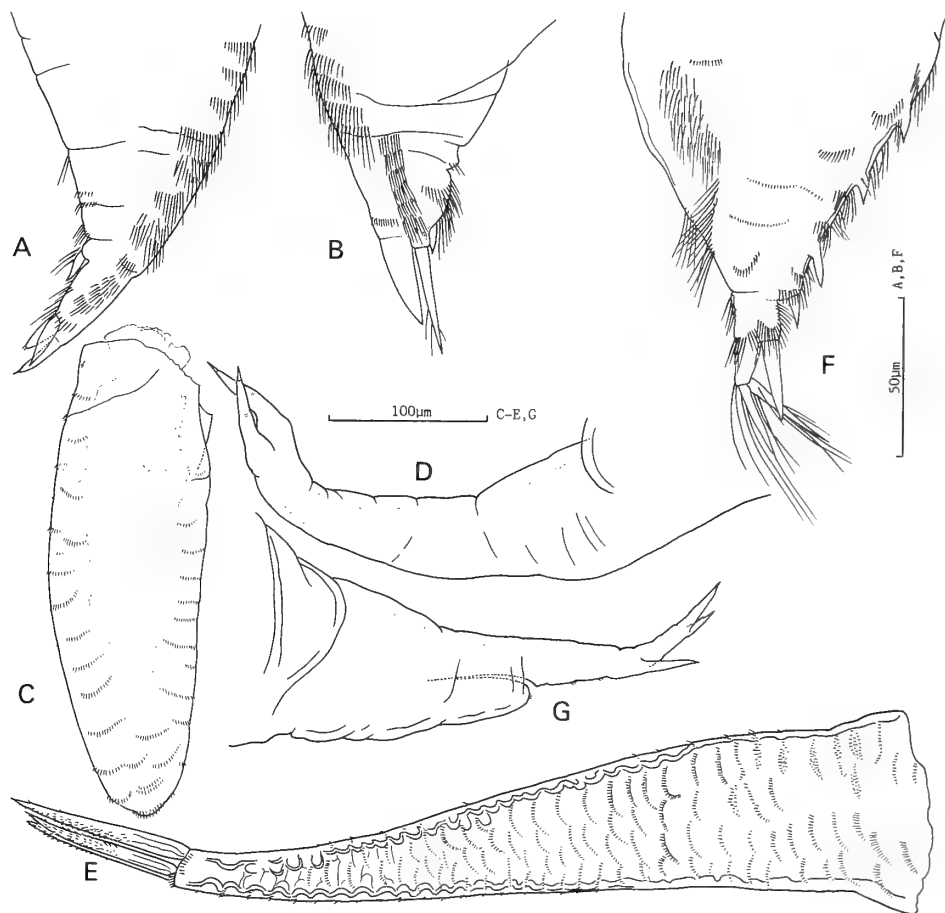


FIG. 7. *B. falsiramus* sp. nov. A-E, holotype. A, apex of right thoracopod 4; B, apex of left thoracopod 4; C, thoracopod 5; D, penis; E, medial view of furcal ramus. F-G, paratype-2. F, apex of left thoracopod 4; G, penis.

chamber (Fig. 1C; see also Fig. 2B). Bands of filamentous material firmly attached to a carapace coil of paratype-1 (Fig. 1C), probably pieces of host tissue.

Body attitude in all these females almost the same as in holotype, but horns of SEM-2 extending straight forward, not particularly upturned (cf. Fig. 2A and C). Distance from tips of horns to tips of furcal rami 3.9 mm in paratype-1, 4.2 mm in paratype-2, about 5 mm in SEM-1, 5.5 mm in SEM-2.

Thoracic segmentation of SEM-1 more obvious than in type specimens, evident as five tergites (thoracomeres 2-6) separated by wide areas of thinner cuticle (Fig. 2A). Wide band of thin cuti-

cle separating lateral chitinous ridge from bases of thoracopods (Fig. 2C), probably collapsed within longitudinal groove visible in SEM-1 (Fig. 2A). Paratype-2 and SEM-2 with prominent, dense cuticular ctenae on ventral half of abdomen (Figs. 3E, 2D), SEM-1 lacking such prominent ctenae but with many small pores instead (Fig. 8D, E), similar to holotype. In both specimens examined with SEM, dorsal setal patches on the last thoracic and first abdominal segments composed of many rows of hairs (Fig. 2E).

Antennules of SEM-1 similar to those of holotype in principal armature of apical segment and its process (Fig. 5A, B), though details of branching of terminal aesthetascs somewhat different. Apic-

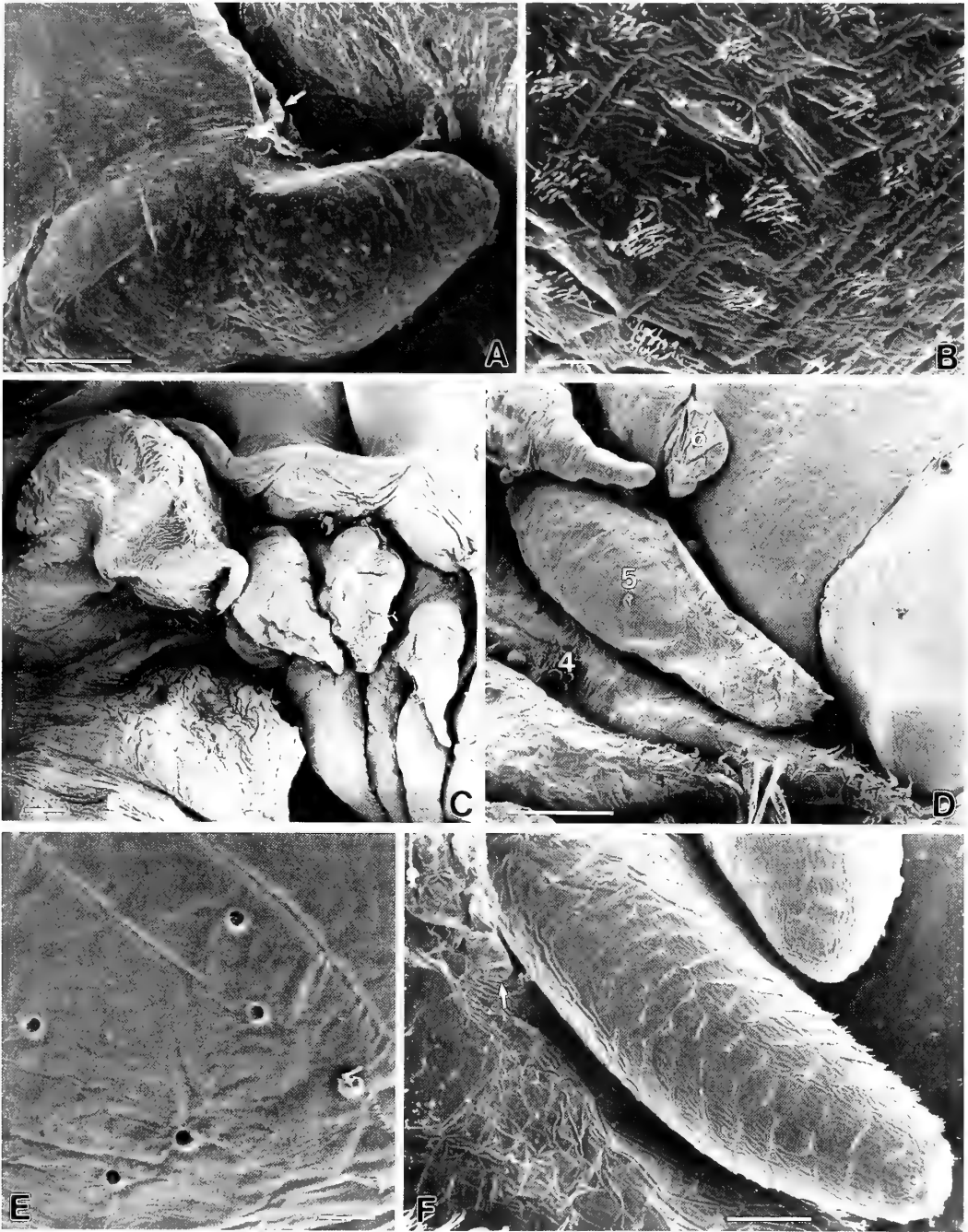


FIG. 8. SEM photomicrographs of *B. falsiramus* sp. nov. A, B and F SEM-2, otherwise SEM-1. A, thoracopod 1 with basal swelling (arrow indicating membranous structure with hairs); B, enlarged view of A, showing patches of hairs; C, thoracopods 1-4; D, thoracopods 4-6 (labeled as 4-6); E, pores on third abdominal segment; F, thoracopods 4-6 (arrow indicating apical opening of lateral papilla of thoracopod 4). Scales: A, C, D 100 μm ; B, E 10 μm ; F 50 μm .

al process clearly delimited from apical segment, but no other segmentation detected, at least externally. Apical process ornamented with cuticular ctenae as in apical segment. Left antennule of SEM-2 (right one lost) distinct in many respects (Fig. 5C, D), lacking distinct apical process but ending in rounded apex with delicate hairs and very small, closely set setae on frontal side. Unbranched aesthetasc arising from subapical, posterior side, small seta attached to thick basal part of aesthetasc.

Labrum bearing many flat, round, proximolateral papillae (Fig. 5F, G).

Apical part of maxillae protruding from labrum in SEM-2 with at least partial ring of unknown material distal to triangular lateral plates, and two closely set, spiniform structures extending anterior, that may be debris (Fig. 5E). Duct opening on anterior prong of bifid tip. Left triangular plate ending in two minute points.

Thoracopod 1, including its basal swelling, quite variform. In paratype-2, right one similar to holotype but left one a narrow, hairy, cylindrical process arising from semicircular swelling, armed with small apical seta (Fig. 3H). In paratype-1 (Fig. 1C), right one apparently similar to left one of paratype-2, but details not determined. Thoracopod 1 in SEM-1 similar to elongate ones in paratypes, but basal swelling more massive, reaching dorsal limit of lateral chitinous ridge of thorax and covered with long, dense hairs, especially abundant on dorsal edge (Figs. 2A, 8C). Basal swelling of this specimen apparently separated into two parts by shallow slit along dorsal edge (Fig. 8C). Left thoracopod 1 of SEM-2 represented by thick, papillary process arising from ventroposterior portion of discoidal plate (Fig. 2C) and armed with two dorsoapical setae (Fig. 8A); plate extending a little over dorsal limit of lateral chitinous ridge and equipped with numerous patches of short hairs (Fig. 8A, B). Membranous structure fringed with dense hairs (female gonopore ?) arising from dorsal gap between plate-like organ and trunk (Fig. 8A).

Terminal armament of thoracopods 2-4 variable. In paratype-2 thoracopods 2-4 bearing two or three prominent, apical setae in addition to lateral spines (Figs. 6H, I; 7F).

Lateral papillae of thoracopods 2-4 in SEM-1 almost naked (Fig. 8C), but those in SEM-2 ornamented with numerous patches of fine hairs. Papilla of right thoracopod 2 of paratype-2 with two cylindrical projections at tip rather than usual opening (Fig. 6G); each projection with internal duct and apparently extending from inside papilla, though its origin unclear. Apical opening of lateral papilla clearly seen in thoracopod 4 of SEM-2 (Fig. 8F).

In SEM-1, thoracopod 5 somewhat like thoracopods 2-4 except for absence of lateral papilla (Fig. 8C, D). This specimen with rudimentary thoracopod 6 (Fig. 8D). In SEM-2, thoracopod 5 represented by long, cylindrical process with round tip, ornamented with numerous cuticular ctenae (Fig. 8F). This specimen with prominent thoracopod 6 similar to thoracopod 5 in general appearance, including ornamentation, but shorter (Figs. 2C, 8F).

Penis of paratype-2 abruptly narrowing beyond duct opening at about middle of ventral side, terminating in two spiniform processes with single subapical spiniform process (Fig. 7G). Penis of paratype-1 also with spines but details unknown; penis of SEM-1 hidden in preparation. Penis of SEM-2 with narrow, nozzle-like apex with terminal opening and transversely arranged, fine spinules (Fig. 2D), short spine at least on right side proximal to nozzle.

Furcal rami examined with SEM ornamented with fine, longitudinal wrinkles (Fig. 2F). Furcal rami of SEM-2 slimmer than in SEM-1. Right ramus of paratype-1 with only two terminal setae.

1-3. POSSIBLE MALE

A possible male was found in association with a female (SEM-1), located near the aperture lips of the female, partially embedded in the host (Fig. 9A). This is similar to the positional relationship of males and females in *Baccalaureus japonicus* Broch, 1929 [7]. Since the main body was not visible, the possibility that this specimen is a settled ascothoracid larva cannot be wholly excluded.

Carapace apparently bivalved, about 0.60 mm long, surface ornamented with polygons delineated by chitinous ridges and lacking central pores

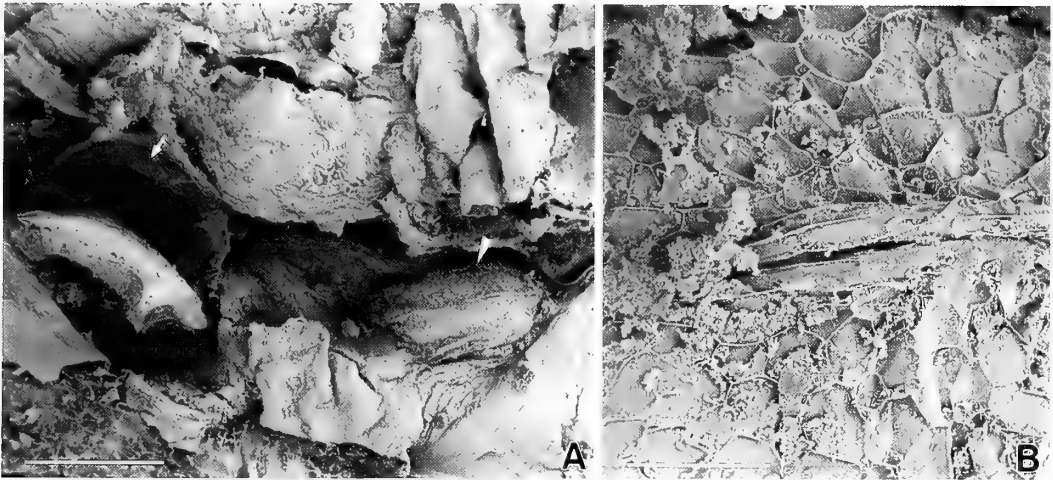


FIG. 9. SEM photomicrographs of *B. falsiramus* sp. nov. A, aperture lip of SEM-1 female (arrow) and possible male (arrowhead); B, enlarged view of carapace of possible male. Scales: A 500 μm ; B 50 μm .

(Fig. 9B).

1-4. COMMENTS ON HABITS

The adult females except for SEM-2 occurred individually in nodules at the bases of groups of 5-6 polyps, but each nodule's inner cavity seemed to be connected to only one or two polyps' gastro-vascular cavities. In one case, an external hole for the carapace aperture was evident between the bases of two nodule-associated polyps. SEM-2 occurred inside a spherical nodule formed of the basal portion of a single polyp, and the lips of its carapace aperture were clearly seen externally.

1-5. TAXONOMIC AND MORPHOLOGICAL REMARKS

The present new species, *Baccalaureus falsiramus*, is easily distinguished from the nine described species of the genus. None of the previous descriptions [5-14] mentions such enormous papillae lateral to the three major pairs of thoracopods, only sometimes small, nipple-like protrusions [e.g., 6]. Elsewhere in the Lauridae, *Laura bicornuta* Grygier, 1985 [6], as moderately large, laterally directed, conical papillae at the bases of thoracopods 2-5, and *Polymarsypus digitatus* (Pyefinch, 1939) [12] has flat lateral lobes at the bases of thoracopods 3 and 4; seminal receptacle ducts pass through both structures [6].

The coiled carapace lobes of *B. maldivensis* Pyefinch, 1934 [9], *B. hexapus* Pyefinch, 1936 [10], *B. torrensis* Pyefinch, 1937 [11], *B. argalicornis* Brattström, 1936 [14], and *B. durbanensis* Brattström, 1956 [5], all make over 1.5 turns like the present new species, but these species all also have long, downturned, coiled thoracic horns that wrap around the columellae of the carapace lobes and the horns are usually said to have short, retrorse hairs; in *B. falsiramus* the horns are short, more or less upturned, and naked. *B. verrucosus* Pyefinch, 1939, is the only species with horns as short as *B. falsiramus*, but they are still downturned and hirsute [12]. Carapace spines like those in the present new species have not been reported before.

The apical process or isolated aesthetasc on the antennules of *B. falsiramus* as well as the "terminal spine" in the unidentified specimen studied by Grygier [6], the "lobe" in *B. japonicus* [7], and the long, thin, spine-like tips observed by Pyefinch [12] in *B. pyefinchi* Brattström, 1956 [5], and *B. disparcaudatus* Pyefinch, 1939 [12], are probably homologous to the claw guard and/or proximal sensory complex of the distal antennular segment of other ascothoracids, including male laurids.

In the maxillae, the bent, triangular plates presumably correspond to the posterior, movable hooks of many other ascothoracids; if so, the bifid distal tip is unusual, and a duct has never

been observed there before.

The small, narrow furcal rami of *B. falsiramus* are most similar to those of *B. argalicornis* and *B. torrensis*, although in the last species they are terminally unarmed. There are apparently different kinds of furcal armament in *Baccalaureus*: terminal spines, terminal setae, tiny medial setae and sensilla, cuticular ctenae. The true distribution of these elements among the species is not clear from semantically ambiguous and incomplete descriptions, but true setae terminally, lack of medial armament aside from ctenae, and partial lack of lateral ctenae may be peculiar to the new species.

The variable structure of thoracopod 1 in *B. falsiramus* is problematic. The first thoracopod in *Baccalaureus* is usually accompanied by a "plate-like organ" (interpreted by Grygier as a form of filamentary appendage [6]). Only *B. pyefinchi*, which has little carapace coiling but long thoracic horns, has been previously known to have such small swellings hardly extending dorsally over the lateral chitinous ridge. However, the present material of *B. falsiramus* exhibits marked variability, and SEM-2 has a prominent structure that may be called a "plate-like organ". Thoracopod 1 proper in the present material appears as either a small papillary process, a cylindrical process with an apical seta, or a prominent papillary process with two setae. Hence, thoracopod 1 morphology might not be easily used as a diagnostic character within this genus.

The number of thoracopods has been one of the primary features used to diagnose species of *Baccalaureus* [e.g., 11], but since the sixth pair is not always present in *B. falsiramus*, this feature is actually not reliable at the species level.

The type specimens are smaller than the specimens examined by SEM. The largest one (SEM-2) has the best developed basal swelling (plate-like organ) of thoracopod 1 and the most prominent thoracopod 6. In SEM-1, the basal swelling is less developed than in the largest specimen but more so than in smaller specimens, and it has a rudimentary thoracopod 6 while the smaller specimens do not. These size-correlated morphological differences may reflect, at least in part, differences between adult instars.

Up to the present, most ascothoracidans have not been subjected to detailed studies of morphological variability. *Dendrogaster astropectinis* would be an exceptional case, in which variation of antennular morphology was studied by Karande and Oguro [15]. As mentioned above, the examined females of *B. falsiramus* show enormous variability, not only in the antennule but also in the thoracopods, penis, abdominal ornamentation, etc. Although this suggests that they may not all be conspecific, we treat them for the time being as conspecific because they share a characteristic thoracic horn morphology, their thoracopods 2–4 are always associated with prominent lateral papillae, and they lived in a single host colony.

Most of the identified hosts of *Baccalaureus* have been various species of *Palythoa*, but *B. japonicus* parasitizes a species of *Parazoanthus* and Muirhead and Ryland [16] recorded *Isaurus* as the host of an undescribed species. Hence the present report is the first confirmed occurrence of this parasite in a species of *Zoanthus*. The host of the type species, *B. japonicus*, has been recorded under several names in Japan, including *Zoanthus cnidosus* [7], but the name now used for this zoanthid is *Parazoanthus gracilis* (Lwowsky) [e.g., 17].

Baccalaureus is most widely recorded in the Indian Ocean [5, 9, 10, 12, 14, 18], with Pacific records limited to Japan [7, 8, 13, 17], Vietnam [19], northeastern Australia [11, 16], and French Polynesia [6]. The present finding adds a second species to the Japanese fauna of this genus and family.

Part 2. Larval Development

2-1. NAUPLII-GENERAL

Brood sizes are somewhat uncertain, but the holotype had over 375 brooded eggs and nauplii and paratype-1 had about 325 eggs in half of its carapace plus part of the other half, perhaps 550–600 in all.

There are six naupliar instars (one orthonauplius and five metanauplii) before the ascothoracid larva. In culture, the duration of instar I could not be determined. When one of us (T. I.) removed a

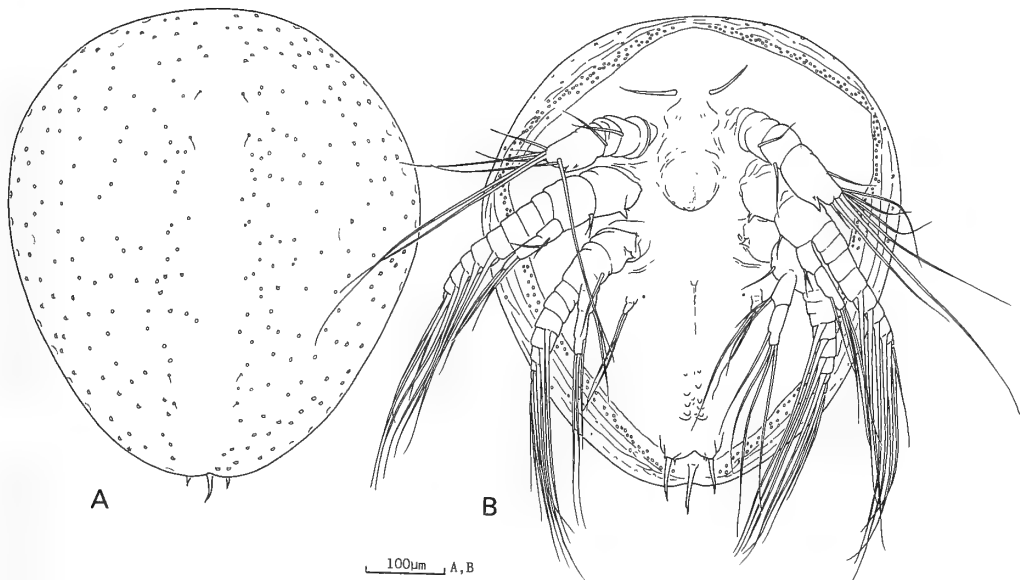


FIG. 10. *B. falsiramus* sp. nov. Exuvium of instar VI nauplius. A, dorsal view; B, ventral view.

female (paratype-2) from the host, it released a number of instar I nauplii together with eggs and possibly some instar II nauplii. The released nauplii immediately started to molt. None of the three nauplii isolated for individual culture from this batch of nauplii within 30 min. after release was still in the first instar. They were put in culture on 26 July, 1988, and metamorphosed into the ascothoracid larva on either 22 (one) or 23 (two) August, 1988. At 19°C, instar II lasted at least 3 days, and instars III–VI respectively 3, 2.5, 4, and 14–15 days. Molts were nearly synchronous, differing by at most one day. Thoracic limb buds of the ascothoracid larva were first recognized on the 8th–10th day of the last naupliar instar. The nauplii continued to swim during this period of about one month without feeding.

Eggs oval, 0.48 mm × 0.35 mm. Late instar I and newly molted instar II nauplii about 0.59 mm long (excluding caudal armament), 0.45 mm wide, 0.28 mm thick (excluding labrum). Instar VI nauplii 0.60 mm long, 0.52 mm wide.

Body of instar I oval, with no ventral depression where appendages occur, without distinct dorsal shield. Cuticle of instar I very delicate (Fig. 11E), with wrinkles, most likely separated from cuticle of internally formed, succeeding instar. Body of

instars II–VI with broad depression where appendages occur, and with bowl-shaped dorsal shield (Figs. 10, 11), broader in front, cuticle only significantly thickened in instar VI. Border of shield outlined by equatorial pores (sensu Grygier [6]) on inner “brim” of “bowl”. No equatorial pores in instar I (Fig. 11B, E). At each molt after instar II, cuticle splits ventrally along border of thin, ventral cuticle and innermost edge of “brim” of dorsal shield, except for short, caudal region (Fig. 15). Nauplii escape from exuvia through gap formed by widening of this fissure. Exuvia of instar I always crumpled, often torn into pieces, uncertain whether definite fissure line exists.

Dorsal shield of instars II–VI ornamented with about three concentric, cuticular ridges on ventral and outer face of “brim” (Figs. 10A, 11A, D), some ridges connected with each other. No such ridges in instar I (Fig. 11B, E). Instars II–VI with small dorsal pores except along midline (Fig. 10A). Four pairs of hairs on dorsum of instar VI, two anterior pairs in instar II. Instars III–V unknown in this respect. No such pores or hairs on dorsum of instar I.

Nauplius eye present in front of antennules in all instars, with two obvious, red pigment cups. Pair of simple frontal filaments 90–100 µm long in

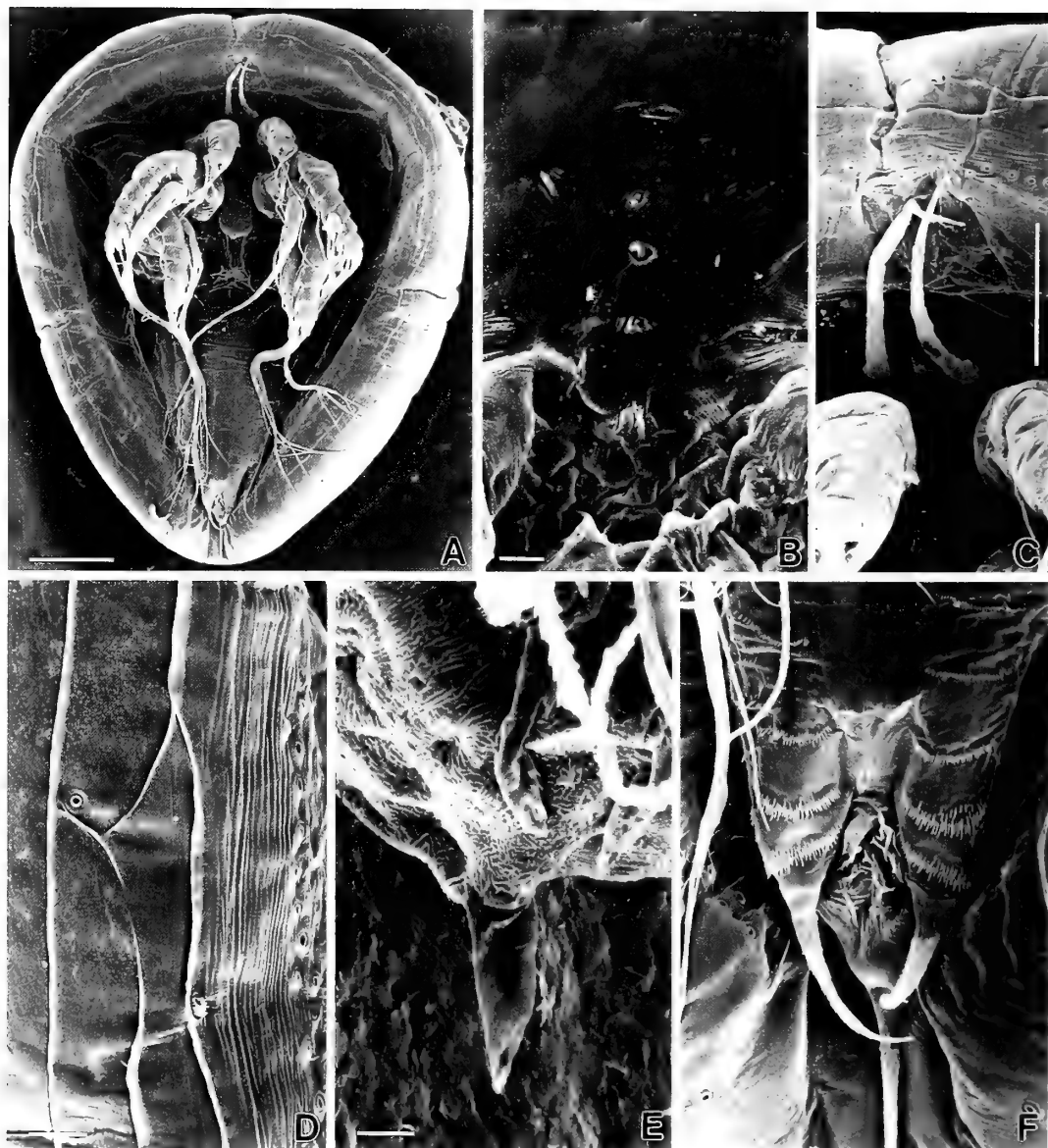


FIG. 11. *B. falsiramus* sp. nov. SEM photomicrographs of nauplii. A, ventral view of instar II; B, ventral surface between and anterior to antennules of instar I; C, frontal filaments of instar II; D, chitinous ridges of instar II; E, caudal region of instar I; F, caudal region of instar II. Scales: A 100 μ m; B, D-F 10 μ m; C 50 μ m.

instars II-VI (Figs. 10B, 11C). Cylindrical, internal "cord", possibly a sensory organ, extending dorsally from point under cuticle between frontal filaments in at least instar II. No frontal filaments in instar I (Fig. 11B), but longitudinal row of three pit-like, sensory structures at midline, at least frontal two with rod-like sensillum, possibly diffe-

rent manifestation of internal "cord" of instar II.

Labrum small and triangular in all instars, with two apical pores and two widely spaced pores on hind surface at least in instars III-VI (Fig. 10). Short, cuticle-lined duct extending anteriorly from hind base of labrum in at least instars II-VI, probably representing rudimentary mouth.

Relatively well-developed antennules, antennae, and mandibles present in all instars, rudimentary maxillules also present from instar II. Caudal armament terminal in instar I, subterminal on ventral side in instar II-VI (Fig. 15).

2-2. ANTENNULES

Instar I (Fig. 12A): Short apical segment defined, with patch of spinules, but otherwise segmentation indistinct, about five additional patches of spinules marking possible future segments. Setation matching Grygier's [22] basic pattern for brooded ascothoracid nauplii: two single median setae (a, b), grossly unequal pair of more distal median setae (long-d, short-e) opposite a lateral seta (f), and three unequal terminal setae (g). Except for seta "c", and shortest, medial "g" seta, these setae thick and spinulose.

Instar II (Fig. 12B): five-segmented, three basal segments subequal in length, next twice as long, last very small, setation 0-1-1-(2+1)-3, relative lengths of setae as in instar I but narrower; lateral "g" seta subterminal. Two setae, "d" longest "g",

plumose in this and later instars.

Instar III (Fig. 12C): Four-segmented due to fusion of distal two segments of previous instar, segments weakly marked, distal one spinulose, setation 0-1-1-7 with new setae (h_1) on lateral side, presumably the most proximal one there, a little shorter than seta "f". Medial "g" seta, formerly very short, now almost as long as "d" and setulose. Lateral "g" seta, now the shortest of the three, distally spinulose, perhaps in this instar only.

Instar IV (Fig. 12D): Similar to foregoing; segmentation less distinct, setation 0-1-1-8 with very short seta " h_2 " added proximal to " h_1 ".

Instar V (Fig. 12E): Unchanged except for addition of tiny lateral seta " h_3 " next to somewhat longer " h_2 ".

Instar VI (Fig. 12F, G): Clearly four-segmented, with unarmed basal segment, seta "a" on second, seta "b" on third, each accompanied by rudimentary new seta; fourth segment with subterminal claw rudiment (c) on medial side accompanied by small, anterior seta (i), three groups of distal setae: setae "d" and "e" medially terminal,

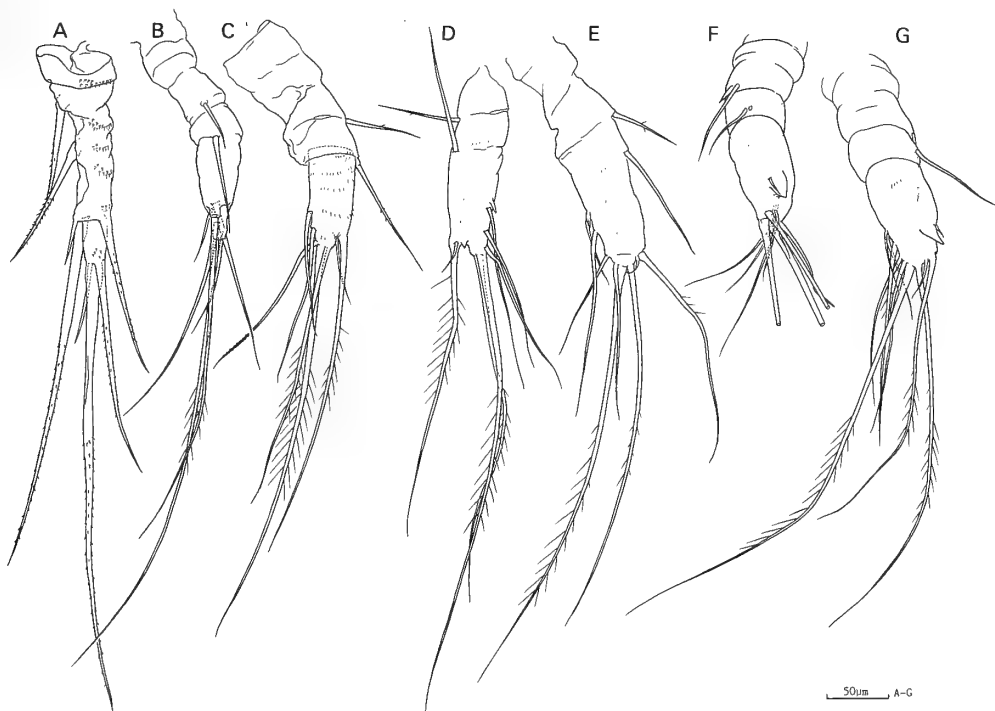


FIG. 12. *B. falsiramus* sp. nov. Antennules of naupliar exuvia. A-E, instars I-V; F-G, instar VI.

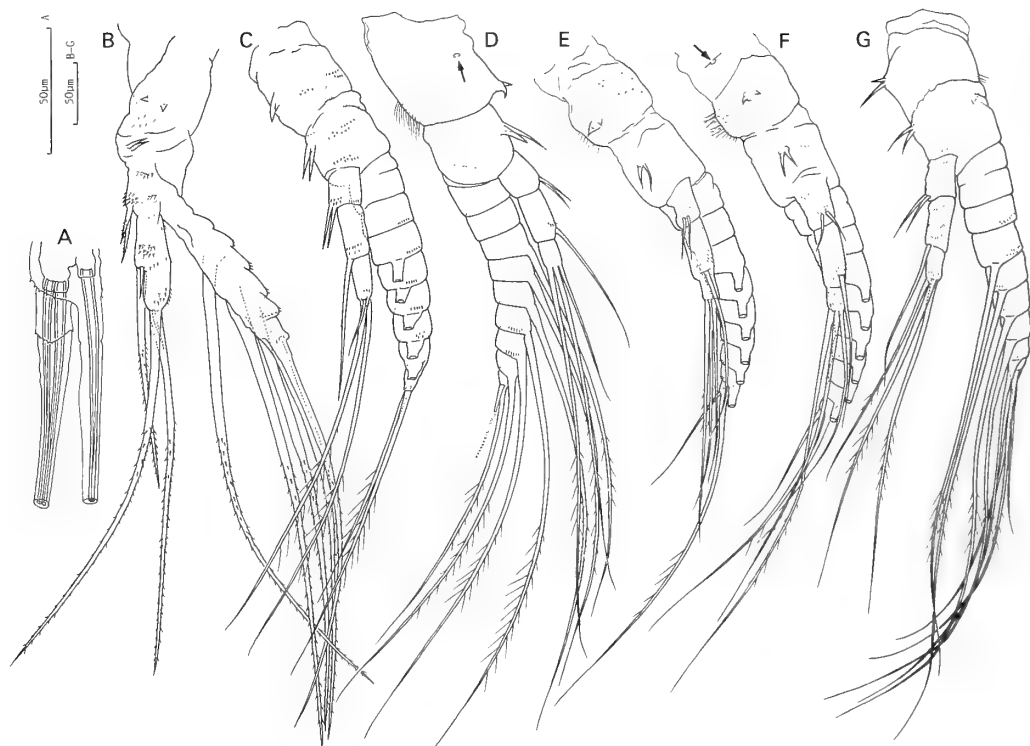


FIG. 13. *B. falsiramus* sp. nov. Naupliar antennae. A, apical part of exopod of instar I, showing two apical setae of instar II formed inside single terminal seta. B-G, exuvia of instars I-VI (some setae of C, E, and F omitted) (arrows indicating openings of possible antennal gland).

three "g" setae laterally terminal, setae "f" and "h₁₋₃" subterminolateral, none of these setae very short.

2-3. ANTENNAE

Instar I (Fig. 13B): Biramous, segmentation indistinct. Coxal area with two small, widely spaced, enditic spines and scattered spinules. Basal area with two closely set, enditic spines. Endopod as long as protopod, stepped at two points along medial edge; two subequal short setae on proximal step, thin seta on distal step; two long and one short, thin setae arising from apex; most setae spinulose but short, thin ones on distal step and apex simple; minute spinules occurring about stepped edges and apex. Exopod twice as long as endopod, indistinctly annulated, bearing from midlength five, thick spinulose setae up to 380 μm long. In individuals ready to molt to instar II, basal seta and distal seta of exopod each contain-

ing two setae of next instar (Fig. 13A).

Instar II (Fig. 13C): Boundary between coxa and basis clear. Coxa with two tiny, unequal, enditic spines, pore (? opening of antennal gland duct) on medioproximal edge, and fine hairs laterally. Basis with two equal, simple spines longer than coxal ones. Endopod equally three-segmented, first with two equal, simple setae, second with one narrow seta (clearly basally setulose only in this instar and one individual of instar VI), third with three apical setae, two of them well-developed and setulose. Exopod nine- or exceptionally ten-segmented, sometimes varying within a specimen, first segment short and indistinctly demarcated from second; segments 1-3 with no seta, segments 4-8 (5-9 on ten-segmented exopods) each with one seta, last segment with two apical setae; all setae well-developed and setulose.

Instar III (Fig. 13D): Unchanged except exopod ten-segmented due to splitting of terminal segment

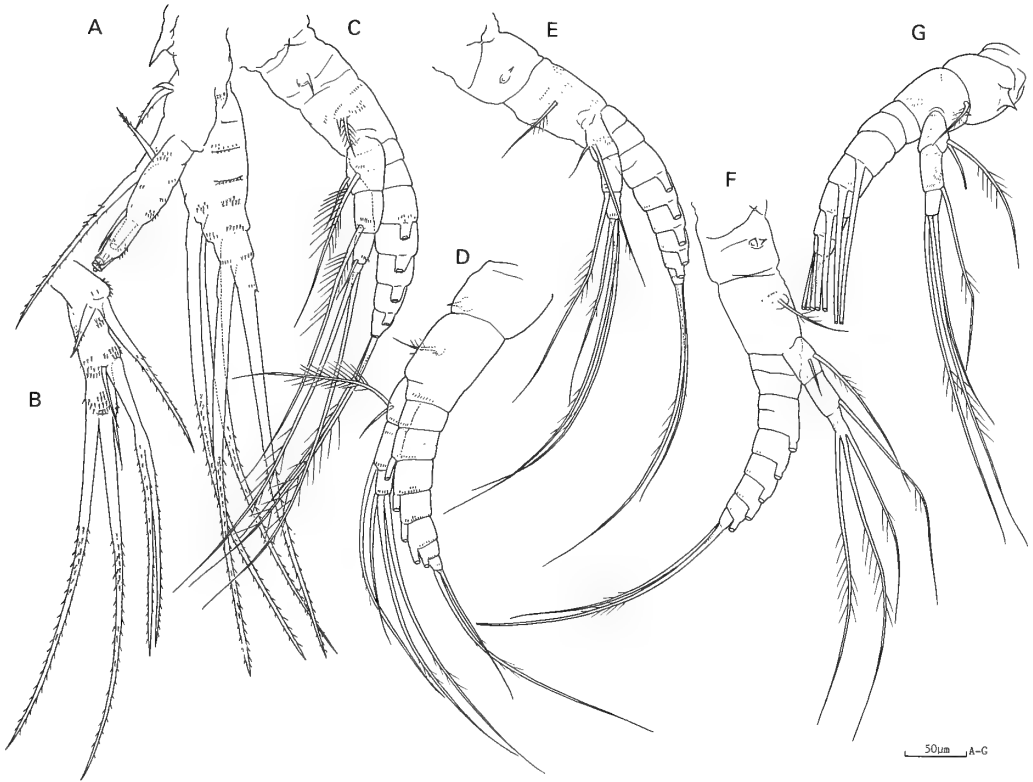


FIG. 14. *B. falsiramus* sp. nov. Naupliar mandible, exuviae. A, instar I (four endopodal setae omitted); B, endopod of instar I, with bifid aberrant seta; C-G, instars II-VI (some exopodal setae omitted).

and bearing eight setae, segments 4-9 with one each, terminal segment with two, including short, probably simple one; shortest apical endopod seta longer than before.

Instars IV-V (Fig. 13E, F): Unchanged from instar III in major ornamentation.

Instar VI (Fig. 13G): Coxal spines longer, one of them rather setiform, shortest terminal endopod seta setulose and grown to two-thirds length of other two, otherwise unchanged.

2-4. MANDIBLES

Instar I (Fig. 14A): Segmentation indistinct. Coxal region with thick enditic spine and much smaller one. Basis region with two short, enditic spines, longer one spinulose. Endopod stepped at two places along medial edge, two thick unequal setae on first step, one thin and one thick setae on second step, two thick setae and short, thin one apically; all thick setae spinulose, thin ones naked.

Abnormal, bifurcate setae seen on one endopod (Fig. 14B). Exopod a little longer than endopod, indistinctly annulated, with patches of fine spinules, bearing from midlength four thick, spinulose setae. In nauplii preparing to molt to instar II, basal seta and terminal seta of exopod each containing two setae of next instar.

Instar II (Fig. 14C): Segmentation clear. Coxa with distinct, medial, condylic articulation to ventral body surface, not seen in antennae. Coxal endite represented by low protuberance bearing spinule on anterior margin and, probably, very minute spinule posteriorly. Endite of basis represented by spine and short, setulose seta. Endopod three-segmented, first segment with two setae, longer one plumose, second segment with well-developed, plumose seta, third with two well-developed, plumose setae and hairlike seta. Exopod 1.5 times as long as endopod, seven-segmented; segments 1-2 short, with no seta;

segments 3–6 each with one well-developed seta; segment 7 with two well-developed apical setae; all setae setulose.

Instars III–V (Fig. 14D–F): Coxa as in instar II except enditic spine shorter. Enditic spine of basis reduced to spinule, seta unchanged. On endopod, hairlike apical seta of instar II now well-developed

and bearing some setules, though shorter than other two apical setae, otherwise unchanged. Exopod eight-segmented due to splitting of terminal segment and bearing seven setae, segments 3–7 with one each, terminal segment with two, including relatively short, simple one. Indistinct partial division of third segment.

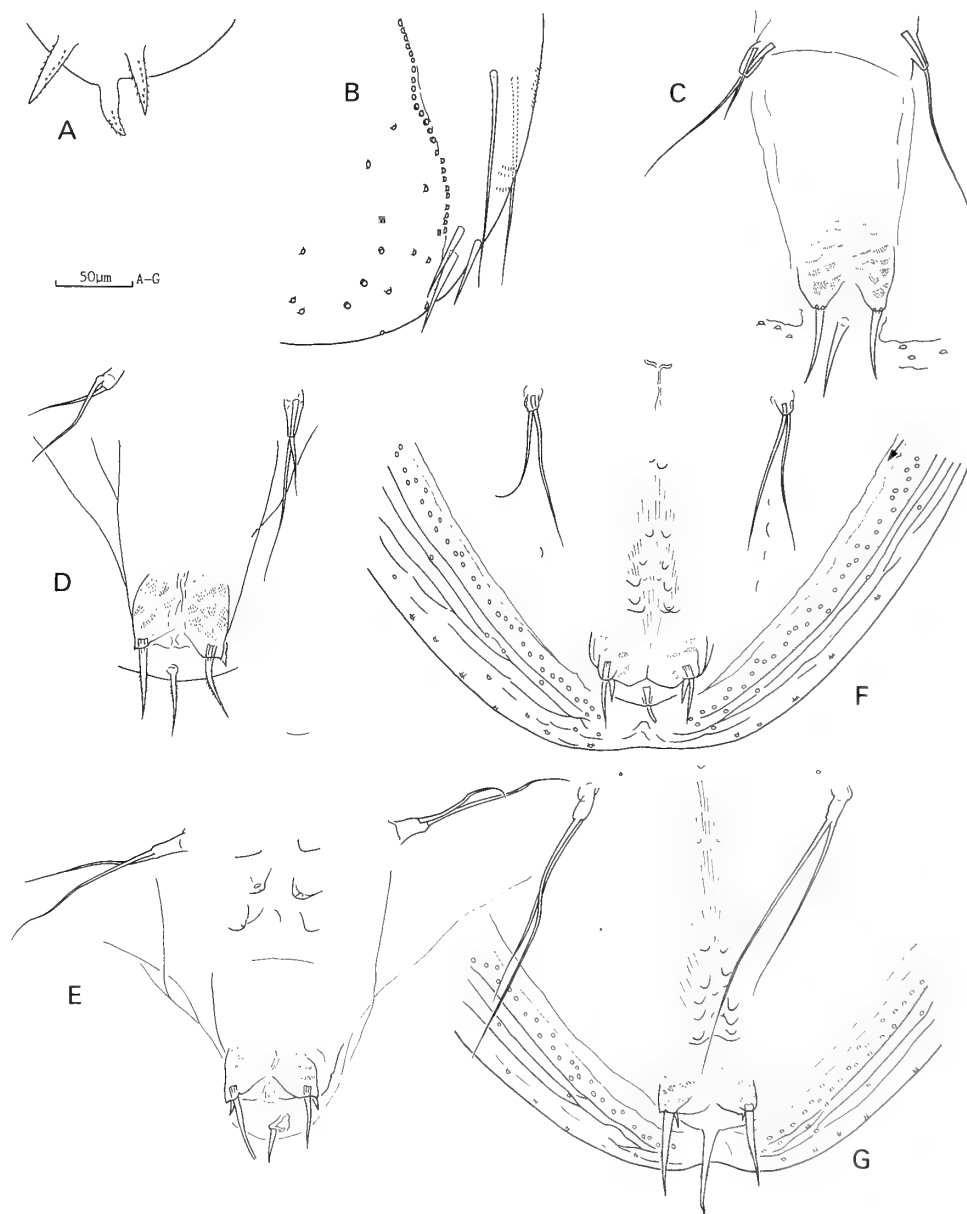


FIG. 15. *B. falsiramus* sp. nov. Caudal region and rudimentary maxillules of nauplii. A, instar I; B–E, exuvia of instars II–V with maxillules; F–G, exuvia of instar VI with maxillules and other rudimentary appendages (arrows indicating fissures).

Instar VI (Fig. 14G): Coxa with short, wide, enditic spine with two apical points. Otherwise unchanged.

2-5. MAXILLULES AND OTHER POSTERIOR APPENDAGES

Instar I: No maxillules.

Instar II (Fig. 15B): Maxillules represented by pair of long, simple setae. No sign of more posterior limbs, though seven or eight pairs of transverse rows of spinules or spinular bands between maxillular bases and furcal spines (Fig. 11F).

Instars III-IV (Fig. 15C, D): Maxillules represented by pair of small, papillary processes, each normally bearing two simple setae (only one seta on left in one of three instar series: see Fig. 15C). No sign of more posterior limbs.

Instar V (Fig. 15E): Maxillules unchanged, though setal lengths varying. Two or three pairs of conical, posteroventral bumps representing more posterior limbs.

Instar VI (Fig. 15F, G): Maxillules unchanged in principal structure, though setal lengths varying. In two cases formed as one-segmented rudiments on short, non-articulated bases. Five or six pairs of smaller and more posterior bumps than in instar V.

2-6. CAUDAL ARMAMENT

Instar I (Figs. 11E, 15A): Terminal spine and furcal setae equal in length (35 μ m), but terminal spine thicker, all more or less spinulose.

Instar II (Figs. 11F, 15B): Terminal spine extending slightly beyond rear of dorsal shield, usually longer than furcal setae, all thinner and more pointed than in instar I, with very delicate spinules.

Instars III-VI (Fig. 15C, D): Terminal spine and furcal setae as in instar II, length variable among specimens, patches of fine spinules anterior to furcal spines.

Instar V (Fig. 15E): Additional short spine or seta appearing dorsal to each furcal seta.

Instar VI (Figs. 10, 15F, G). Unchanged.

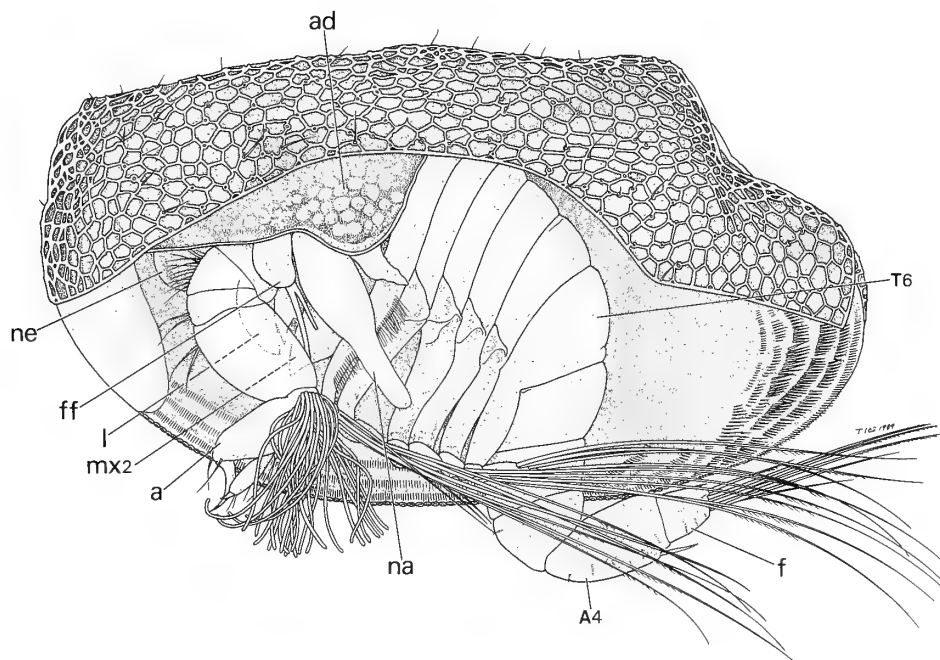


FIG. 16. *B. falsiramus* sp. nov. Scheme of ascothoracid larva, with carapace optically cut away. a, antennule; ad, adductor muscle; A4, fourth abdominal segment; f, furcal ramus; ff, frontal filament complex; mx2, maxilla; l, labrum; na, naupliar antenna; ne, nauplius eye; T6, sixth thoracic segment.

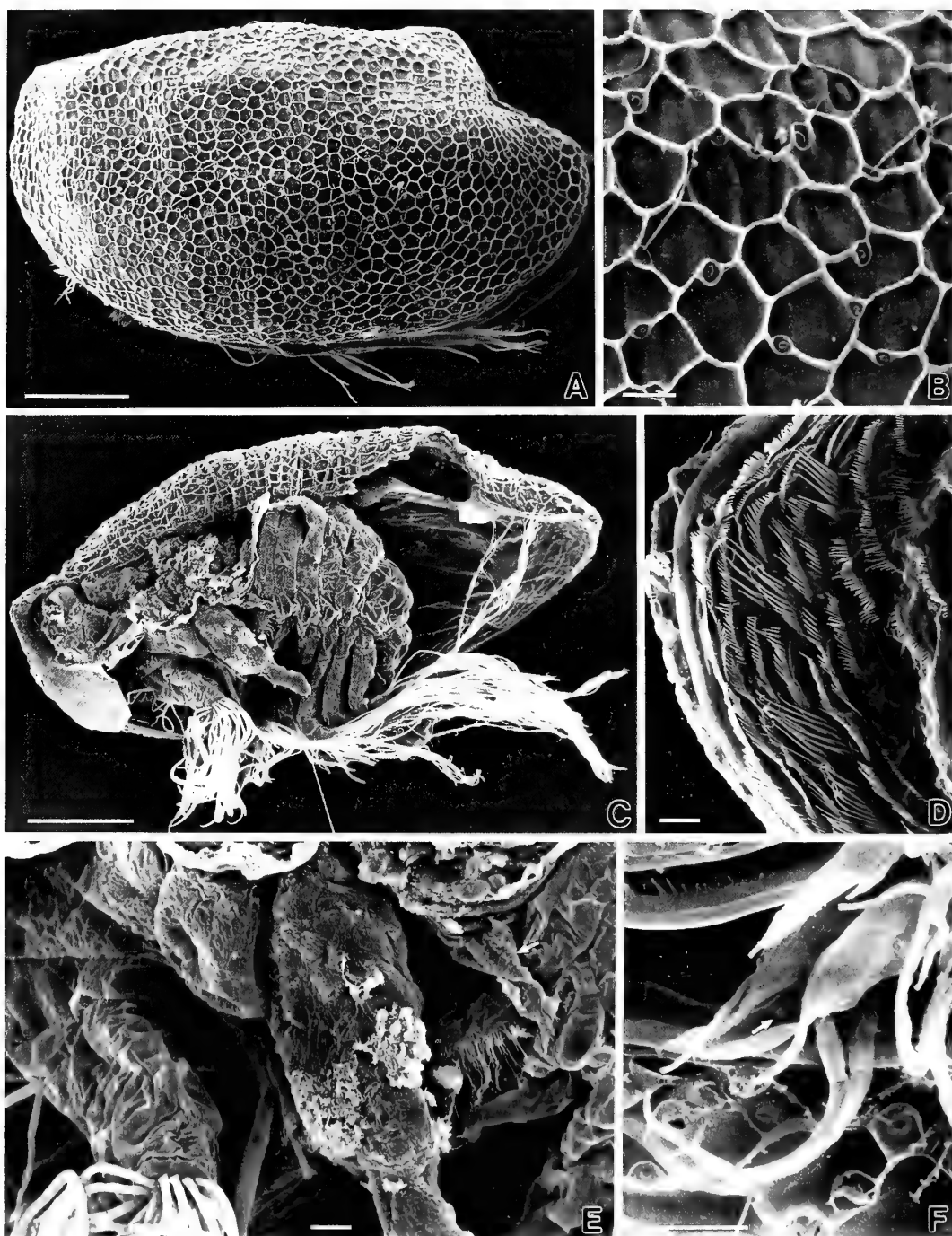


FIG. 17. *B. falsiramus* sp. nov. SEM photomicrographs of ascothoracid larva. A, habitus lateral; B, posterolateral portion of carapace; C, habitus (left carapace removed); D, internal view of posterior portion of carapace; E, antennule, frontal filament complex, and naupliar antenna (arrow indicating possible naupliar mandible); F, apical hood of antennular claw guard (arrow indicating possible gland opening). Scales: A, C 100 μm ; B, D-F 10 μm .

2-7. SUMMARY OF NAUPLIAR DEVELOPMENT

There are six naupliar instars. The greatest morphological changes take place at the molt from instar I to instar II: equatorial pores and frontal filaments appear, the dorsal shield takes form, the appendages become well segmented and set in a deep ventral depression, the exopods of the antennae and mandibles gain two setae each, the natatory setae become setulose, maxillular rudiments differentiate, and the caudal armament moves ventrally. At later molts there are only minor changes: addition of another segment and seta to

the antennal and mandibular exopods at instar III along with incorporation of the distal antennular segment into the penultimate one; gradual addition of lateral setae and a claw rudiment to the antennule (Fig. 20); appearance of postmaxillular limb buds and a second pair of furcal spines at instar V; thickening of the dorsal shield of instar VI.

2-8. ASCOTHORACID LARVA

The ascothoracid larvae (Fig. 16) are active swimmers. They open their carapace valves to extend their antennules and abdomen when swimming. The red nauplius eye was easily seen ven-

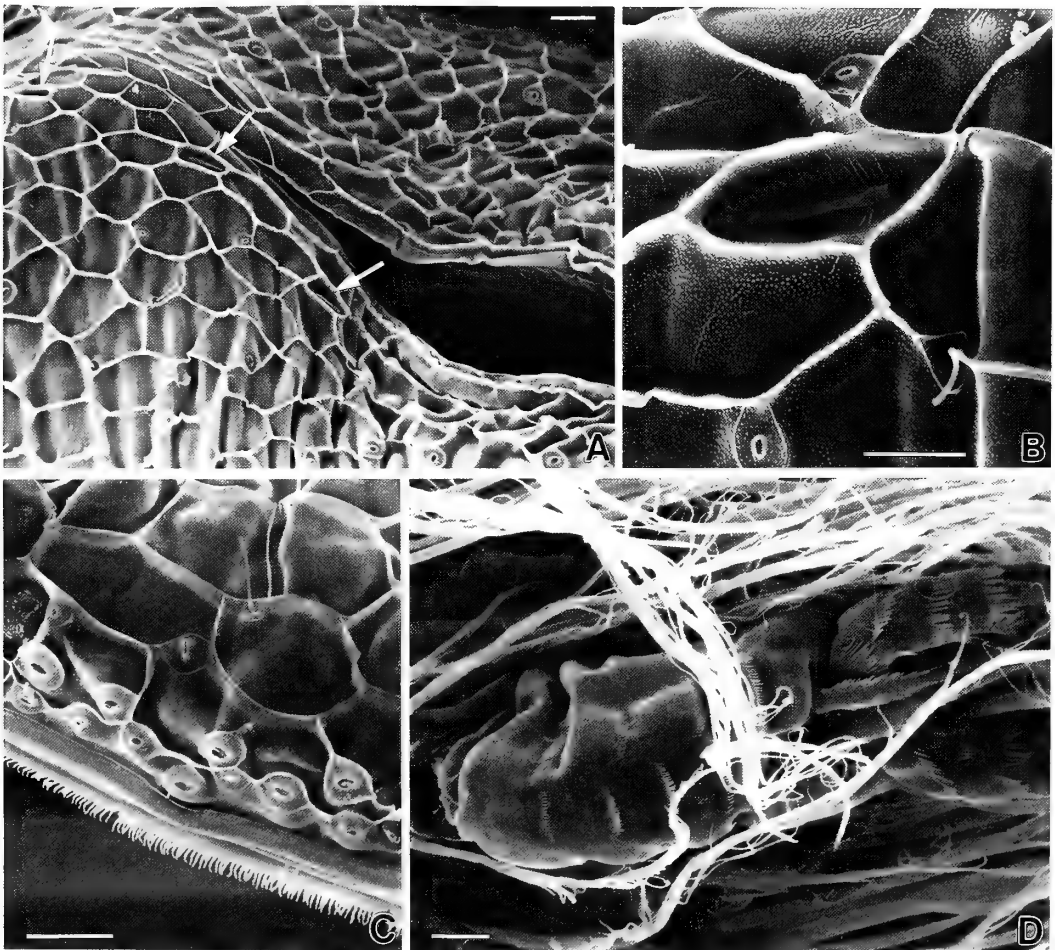


FIG. 18. *B. falsiramus* sp. nov. SEM photomicrographs of ascothoracid larva. A, dorsocaudal region of carapace, showing cardiac organs (arrows); B, enlarged view of cardiac organ; C, ventral margin of carapace; D, last abdominal segment and furcal rami. Scales: A, C, D 10 μ m; B 5 μ m.

trally while they were swimming. The furcal rami are movable, often splaying apart from each other laterally.

Carapace bivalved, 0.51 mm long, 0.31 mm high, 0.30 mm wide (Fig. 17A). Dorsal hinge line

thickened, somewhat interdigitated, recessed. In side view, valve outline slightly convex dorsally, rounded anteriorly and posteroventrally, almost straight mid-ventrally, concave posterodorsally below angle formed by protrusion above hinge line.

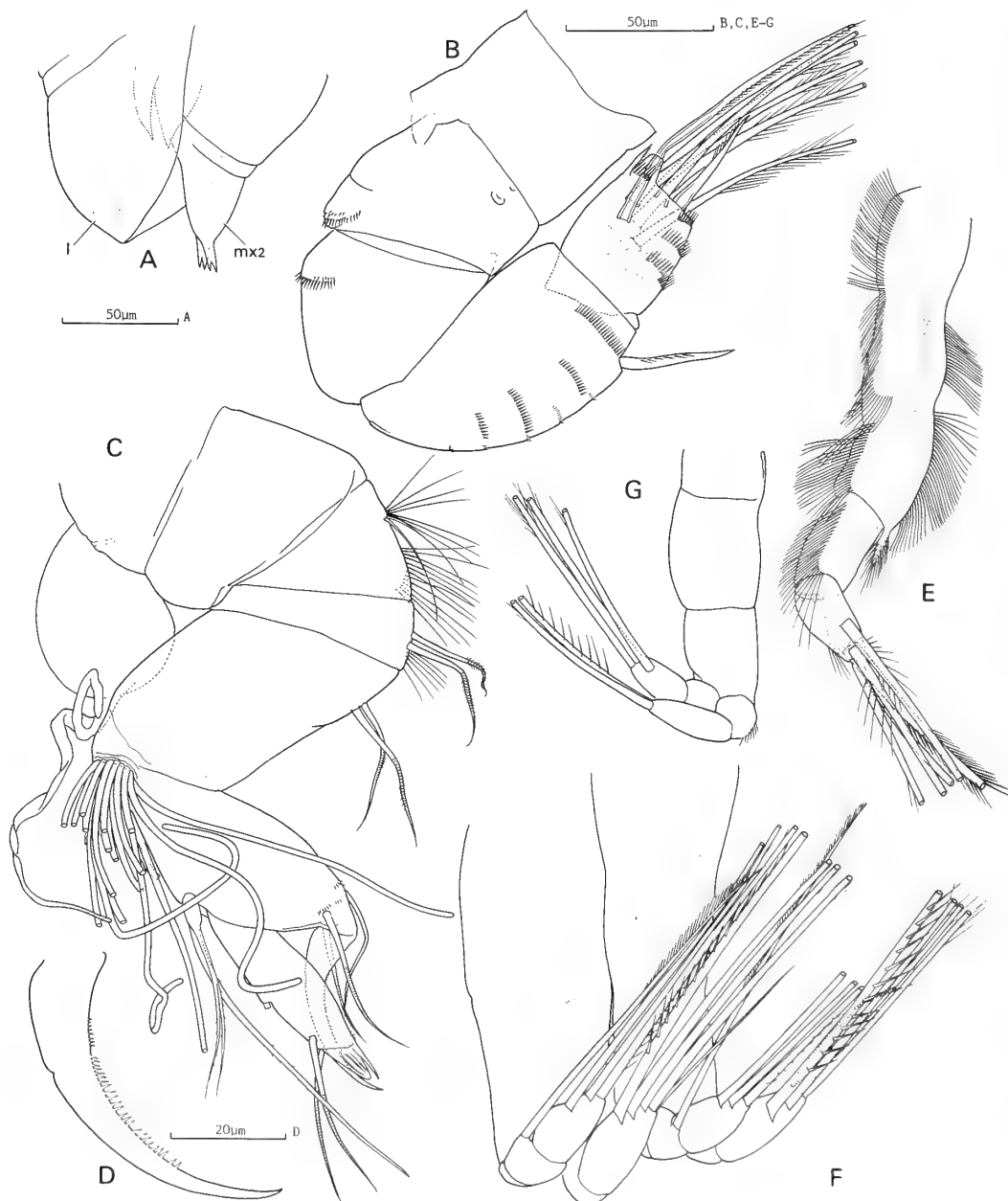


FIG. 19. *B. falsiramus* sp. nov. Ascothoracid larva. A, oral area (l, labrum; mx2, maxilla); B, abdomen (penis broken); C, antennule (most aesthetascs broken during dissection) and frontal filament complex; D, antennular claw; E, thoracopod 1; F, thoracopods 4-5; G, thoracopod 6.

Outer surface of valves with polygonal (principally hexagonal) meshes averaging $13\ \mu\text{m}$ across and outlined by low, cuticular ridges (Fig. 17B). No pits or pores in centers of meshes, but meshwork often interrupted or adjoined by small, rounded, ridge-bounded meshes $3\text{--}5\ \mu\text{m}$ across, with either central pore surrounded by elevated rim or seta about $25\ \mu\text{m}$ long; these features absent in area overlying adductor muscle attachment. Entire outer surface, except certain areas as described below, with very fine granulation (Fig. 18B). On each valve, five narrow, polygonal meshes equidistant from hinge line, three flanking front of hinge, two near its rear (Fig. 18A); each with tube arising from anterior pit, running longitudinally along bottom of mesh, and opening at posterior end (Fig. 18B). Bottoms of these five meshes with no granulation.

Band of prominent pores, derived from naupliar equatorial pores, along entire free margin of valves outside marginal cuticular ctenae (Fig. 18C). Inner surface of valves with several cuticular ridges parallel to edge, additional posterior armament of fine fringes of cuticular ctenae and several arrays of long guard spines (Fig. 17D).

Body completely enclosed by carapace when abdomen retracted, $0.40\ \text{mm}$ from antennule to tip of furcal rami in retracted position, with head, six-segmented thorax, and four-segmented abdomen with furca (Figs. 16, 17C). Large nauplius eye with two obvious red pigment cups in hemispherical ventral protrusion of "forehead" anterior to labrum.

Frontal filament complex hanging just lateral to rear base of antennule, with rounded, rather pyriform basal part ($42\ \mu\text{m}$ long, $32\ \mu\text{m}$ wide in SEM specimen) and biramous sensory process; branches unequal, main one about $100\ \mu\text{m}$ long, shorter, thinner one arising near its base (Figs. 17E, 19C).

Antennule composed of six major segments, Z-shaped (Fig. 19C). First segment short, next three together not much bigger than fifth, third one triangular with long hairs on anterior edge, fourth and fifth each with two nearly equal anterior setae. Sixth segment with thin, movable claw with bump on convex side and row of distally longer denticles on concave side (Fig. 19D); three long setae at base of claw. Laterally flanged claw guard

with one seta distal and two proximal to small apical hood, latter a membrane armed marginally and externally with many spinules and protecting short, protruding tubule on end of claw guard (Fig. 17F); shelf at mid-length of claw guard on free side, bearing short tubule (? broken seta) on one antennule of dissected specimen only. Proximal sensory process near base of claw guard short and cylindrical, with three setae, one long and thick, other two replaced by bifid seta in one case, all three setae with delicate spinules. Cluster of about 25 long aesthetascs arising on sixth segment from basolateral, oval region with thick, chitinous border (Figs. 17C, E; 19C).

Pair of vestigial but large naupliar antennae (Fig. 17C, E) posterior to frontal filament complexes; medial sides, including possible endopods, not clearly seen; internal musculature present; vestiges of 5–6 setae on narrow distal part, presumably representing exopod. Another, much smaller and badly shrunken structure apparent behind antenna in SEM specimen (Fig. 17E), possibly vestige of naupliar mandible.

Oral cone imperfectly formed (Fig. 19A). Labrum a rounded lobe partly enclosing other mouthparts. Mandibles and maxillules spiniform, but latter thicker. Maxillae relatively large, tips narrow and bifid.

Thorax demarcated from head by distinct suture (Fig. 17C), first segment shorter than segments 2–4, segments 5 and 6 much longer dorsally due to body curvature; segments 2–4 with small external swelling anteriorly above limb articulations.

Six pairs of thoracopods biramous. First limb narrower than others; coxa and basis lined on both sides by long hairs (Figs. 17E, 19E); exopod two-segmented, with hairs on lateral edge of first segment and medial edge of second one, armed with five setae, medialmost one thicker than others and with dense, fine spinules bilaterally, others more or less plumose; endopod represented by small, hairy, setiform process. Limbs 2–5 (Fig. 19F) similar to each other; posterior border between coxa and basis unclear; basis with shallow, lengthwise groove on at least distal half of anterior surface; exopod two-segmented, first segment with no seta, second one with five setae, lateralmost seta thin, short, and minutely spinulate, others

equally thick and long, medialmost one markedly spinulate while others plumose; endopod three-segmented, with no seta on first segment, markedly spinulate seta on second segment, three more or less plumose setae on third segment. Limb 6 (Fig. 19G) smaller than previous limbs; coxa and basis distinct, both naked; lengthwise, anterior groove of basis clear, reaching near coxa; rami two-segmented; exopod with no seta on first segment, three similar, more or less plumose setae on second segment; endopod with short spinules on medial edge of first segment, two terminal setae on second segment.

When observed in whole mount, first abdominal segment seemed to bear lobe-like penis, but penis lost from dissected abdomen so details unknown (Fig. 19B). Fourth abdominal segment longer than others, with ventral and ventrolateral cuticular ctenae and pair of lanceolate, movable, somewhat setiform telsonic spines (Figs. 18D, 19B).

Furcal rami (Fig. 19B) slightly longer than high in lateral view, flattened laterally, slightly curved with concave medial faces, closer together dorsally than ventrally. Armament consisting of transverse cuticular ctenae laterally; lanceolate, short spine on dorsal edge near posterior end; four apical and

three medial setae, dorsalmost seta inserted into short process, both it and ventral seta dorso-ventrally flattened and lanceolate, other setae setulose.

2-9. DISCUSSION

Nauplii. -The present study has demonstrated that lecithotrophic nauplii of ascothoracids can be raised at least to the ascothoracid larva in the laboratory by using the culturing method that was originally developed to raise y-larvae [20]. This kind of laboratory culture is essential for the identification of larval instars and for a precise analysis of their morphological changes. Although Grygier [21, 22] reported without full descriptions a minimum of five naupliar instars in *Gorgonolaureus muzikae* Grygier, 1981, and *Parascothorax* cf. *synagogoides* Wagin, 1964, and Wagin [3] described seven "stages", one hypothetical, in the naupliar development of *Ascothorax ophiocetis*, the present results are the first that shows conclusively that some ascothoracids have six naupliar instars. This number is generally regarded as plesiomorphic in at least some maxillopodan taxa, such as Copepoda and Cirripedia.

It is not clear when the nauplii in the present

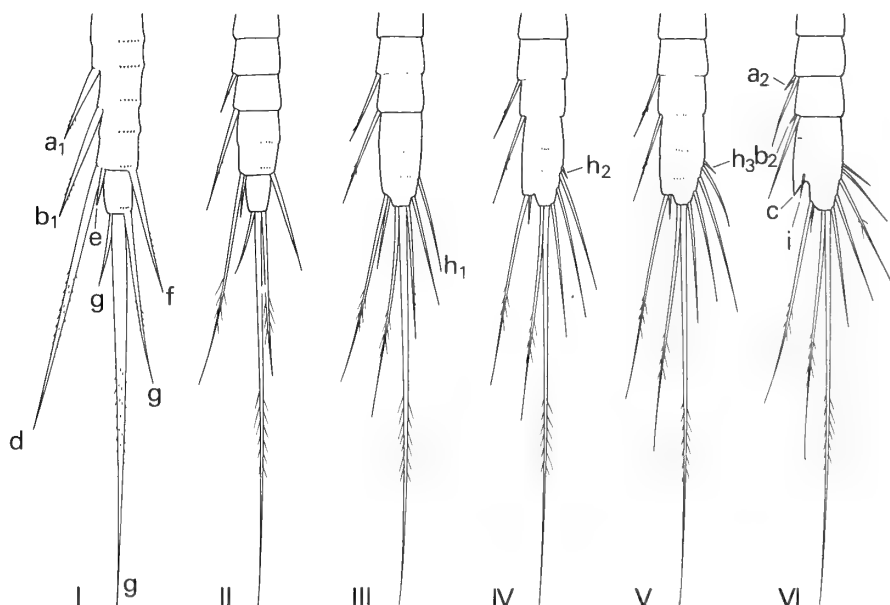


FIG. 20. *B. falsiramus* sp. nov. Schematic representation of antennular development through six naupliar instars (I-VI). Arrows indicating newly added setae and claw, other labels used for explanation in the text.

species normally leave the female's brood chambers. However, the cuticle of instar I nauplii is very thin and delicate and tore easily, and they immediately molted into the next instar after being released into sea-water. Instar I nauplii are not active swimmers, but instar II nauplii have setulose natatory setae and are good swimmers. These observations suggest that, like cirriped nauplii, they normally leave the female's brood chambers at the end of instar I, whereupon they may molt immediately to instar II and remain planktonic until the metamorphosis to the ascothoracid larva.

Early instar nauplii have been described in several laurids (list in [22]). Most have apparently planktotrophic nauplii with very strong antennal and mandibular endites. The present nauplii are considerably larger than those previously reported in *Baccalaureus*. Nauplii of *B. japonicus* are 0.4 mm long and 0.3 mm wide [7], and *B. pyefinchi* and *B. argalicornis* have nauplii only about 0.3 mm long [12, 14]. These might not all be the same instar. Nonetheless, the present nauplii differ additionally from those of *B. japonicus* in never developing large, enditic spines on the antennae and mandibles and in not having a long, protruding terminal spine flanked by three pairs of posterior dorsal shield papillae. Nauplii of *B. maldivensis* and *B. hexapus* seem to have weakly armed limbs according to schematic diagrams and a setation table [9, 10]. However, they differ from *B. falsiramus* by the large, pointed, rear end of their bodies and the much longer limbs relative to the body. Within the Lauridae, *Polymarsypus digitatus* has nauplii most similar to the present ones [6]; these are probably instar I ready to molt to instar II. They are nearly the same size as the equivalent stage in the present material (0.62×0.44 mm), have similar, weak armament of the antennae and mandibles, and a rounded rear end. However, they reportedly have frontal filaments and equatorial pores already, clear appendage segmentation, and somewhat different proportions of the protopods and rami. But the frontal filaments and equatorial pores might actually have belonged to the fully developed instar II within; their absence in the present instar I nauplii was only confirmed on the basis of exuviae and SEM. Such a misinterpretation may also explain the supposed presence

of these structure in some other first instar nauplii like those of *Laura bicornuta* [cf., 6].

In comparison to the few known planktonic ascothoracidan metanauplii tentatively attributed to the Lauridae [22, 23], the present sixth instar nauplii have less well-developed antennules (four segments instead of six), little development of complex appendage armament for feeding, and little elaboration of the furcal armament. The pattern of dorsal pores and setae on the last instar differs from that of Boxshall and Böttger-Schnack's [23] Red Sea metanauplius type I, which has three pairs of setae toward the rear instead of two pairs each at front and rear, and three longitudinal pore-free strips instead of one. In both, the pores are most dense in a row to either side of the central bare zone.

Development of naupliar antennules in *B. falsiramus* in summarized in Figure 20. The addition of several setae (h_{1-3}) proximal to the original lateral seta (f) of the penultimate antennular segment has not been observed in ascothoracidan development before. Its occurrence in *B. falsiramus* suggests that the lateral spine on the naupliar antennule of *Endaster hamatosculum* Grygier, 1985 [22, 24], which is not homologizable with any of the previously recognized setae in ascothoracidan antennules, might be an "h" seta. In the six-segmented antennules of the planktonic ascothoracidan metanauplii cited above, the fourth segment has a claw rudiment and two setae, one of which is probably equivalent to the small seta (i) next to the claw rudiment in the present species, and the other to an "h" seta.

The present study revealed that some ascothoracidan nauplii have cuticular ridges at least on the marginal area of their dorsal shield. More broadly developed, cuticular ridges have long been known to occur in so-called, nauplius y larvae [e.g., 25–27] and the possession of such prominent cuticular ridges has been believed to define, at least in part, the Facetotecta in which these larvae are accommodated [21]. Despite ignorance of the presence of such ridges in the Ascothoracida, Bresciani [28] suggested, and Itô [1] seconded, a possibility that y-larvae are the larval stages of certain ascothoracidans, but Grygier [22, 29] has disagreed. The present finding of cuticular ridges

in an ascothoracidan appears to bridge over one of the morphological gaps between these two thecos-tracan groups. However, it has recently been reported that the thoracican cirripede *Ibla* has marginal ridges on its nauplii [30]. Now it is apparent that variously developed, cuticular ridges are widely distributed within the Thecostraca.

Ascothoracid larva. Ascothoracid larvae similar to this species' have been reported several times before and tentatively assigned to the Lauridae, which is strongly supported by the present study. Tessmann [31] first described one from the Indian Ocean, and thus such larvae can be called "Tessmann's larvae" [32]. McKenzie [33] schematically illustrated a similar larva from the eastern Indian Ocean, and Bonaduce *et al.* ([34]: FIG. 2, fig. 4) found an isolated carapace valve in Red Sea sediments, which they mistakenly attributed to an ostracod. Grygier [6] found a single larval carapace valve together with adults of the laurid *Zoanthoeus cerebroides* Grygier, 1985, and later [32] gave a detailed, SEM-assisted description of a shallow-water, Hawaiian form. The carapaces all have a reticulate pattern of chitinous ridges and a posterodorsal emargination like the present examples, and the three forms with described appendages [31, 32; herein] have a proximal cluster of aesthetascs on the claw-bearing segment of antennules. Additional common features of the present larvae with Grygier's [32] Hawaiian form are the antennular claw with a comb-like row of spinules, an imperfectly formed oral cone, the thoracopodal setation, including a setiform endopod on the first limb, and the frontal filament complex with a bifid filament. Some of these features may eventually prove to be universally characteristic of Tessmann's larvae.

Tessmann's description of the distal antennular and thoracopodal structures [31] seems incomplete (thoracopodal rami uniformly two-segmented, exopods with two setae, endopods with one), and the supposedly four-segmented antennules and five-segmented abdomen (equivalent of first segment in other larvae drawn with discontinuous tergite) are at odds with the other descriptions. Grygier's Hawaiian larvae [32] are larger than the present ones (0.60×0.35 mm), their carapace meshes each have a deep pit with a pore instead of a flat surface,

and the polygons are smaller, about $11 \mu\text{m}$ across. On the antennule, the setae on segment 5 are unequal, the distal setae on segment 6 much shorter, the claw more deeply curved, and the claw denticles less numerous than in *B. falsiramus*; there are fewer proximal aesthetascs (only up to 13). There are no vestigial naupliar appendages, although this might not be a stable character because Tessmann's original larva might have such vestiges ([31]: "röhrenförmiges Gebilde") and reduction of vestigial naupliar appendages is known in facetotectan cyprids [20]. In the Hawaiian form the first thoracomere is not well delineated from the head, and the furcal rami are longer with supposedly non-setulate setae. Thus, Tessmann's larvae from Hawaii differ from the larvae of *B. falsiramus* in many morphological features, which may become taxonomically useful once more forms are linked to their adults.

In the echinoderm-infesting, ascothoracidan order Dendrogastrida, many species have two ascothoracid larval instars (e.g., [2, 35]; review in [21]). Such a relatively gradual transition from the nauplius to the adult has been assumed to be the plesiomorphic relative to the single cypris larva in the Cirripedia [21, 36], but it is important to be sure that it is not a secondary development in a single ascothoracidan clade. The dendrogastridan first instar is characterized by inflated, poorly hinged carapace valves; antennules in an intermediate state between the metanaupliar and adult conditions (e.g., [22]; Fig. 6a); the labrum not fully surrounding the other mouthparts; sometimes remnants of the naupliar antennae and mandibles; short, simple setae on the legs, usually only distally; and a four-segmented abdomen. The ascothoracid larva of *B. falsiramus* has an incompletely developed oral cone, a pair of naupliar appendages, and lacks protopodal setae on the legs, but in other respects it is as well developed as typical dendrogastridan late ascothoracid larvae (in this species the adults have four-segmented abdomens, so that is not significant in the larvae). This circumstantial evidence suggests, but certainly does not prove, that this species has a single ascothoracid larval instar.

The presence of a large nauplius eye in these ascothoracid larvae, as well as in the nauplii, is

significant because it confirms Tessmann's identification of a nauplius eye in his original larva [31] and because only previous record of an eye in an ascothoracid nauplius concerned the first recorded species, *Laura gerardiae* Lacaze-Duthiers, 1865 [37].

The presence of up to three setae proximal and one distal to a poorly understood apical structure (herein formally termed the apical hood) on generalized claw guards in the Ascothoracida has long been noted [e.g., 38]. There is a "spinulose tip" on the claw guard in *Isidascus bassindalei* Moyse, 1983 [39] and many short hairs on the "articulating tip" of the claw guard in *Cardomanica andersoni* Lowry, 1985 [40], but the microstructure of the apical hood has not previously been examined. In the present larva it proves to be a spinulose cloak around a previously unsuspected tubule. Grygier [32] may have seen the tubule in the Hawaiian Tessmann's larva, mistaking it for a sensillum on the "distal flange." The function of the tubule, whether chemosensory or a gland duct, is unclear.

The subterminal position of the antennular claw rudiment (c) in naupliar instar VI supports Grygier's assertion [22] that the claw-bearing segment (sixth segment in the present ascothoracid larva) is not really the most terminal one in ascothoracid antennules. Rather, at least the proximal sensory process on the claw-bearing segment is assumed to be equivalent to the palp (apical segments distal to the claw-bearing segment) in facetotectan antennules [22, 41].

The five pairs of peculiar organs near the carapace hinge line have been recorded in other ascothoracid, though usually only four pairs. We would like to formally call them "cardic organs" (from Latin *cardo*=hinge). The second ascothoracid larva of *Ascothorax gigas* Wagin, 1968, has two pairs of "slit-like pores or sensory organs" at either end of the hinge [35], and so does the last (second ?) instar ascothoracid larva of *Parascothorax ?synagogoides* [21] and an unidentified ascothoracid larva from the Virgin Islands, in which they are called "oval pits" [32]. Adult *Waginella sandersi* (Newman, 1974) have at least two pairs [38]. Due to their position near the hinge, the cardiac organs might be interpreted as proprioceptors. However, they may also be parts of

glands, because they involve an externally produced tube.

Cardic organs may be homologous to similarly placed, supposedly chemoreceptive "lattice organs" recently described in detail in a lepadomorph cirriped cyprid [42], and whose morphology has been summarized for 28 other cirriped species as well [43]. There are usually five pairs of these narrow, elongate structures symmetrically disposed near the carapace midline, two pairs anteriorly, three posteriorly. They have a porose floor ("sensory field") with a single large pore anteriorly in the front two pairs, posteriorly in the rear ones, and the sensory field is surrounded by a ring of non-porose, often thickened cuticle. The cardiac and lattice organs are also somewhat similar in form and especially position to the "dorsal compound organs" on the midline of the carapaces of pelagic eucarids and at both ends of the carapace midline in the leptostracan *Nebaliopsis typica* Sars, 1887, for which a photosensitive capacity has been postulated [44]. The malacostracan organs consist in part of paired pores and often slits, the latter at least superficially reminiscent of cardiac and lattice organs. The ultrastructure and neurology of all these organs need to be investigated.

ACKNOWLEDGMENTS

This study was supported by Grant-in-Aid for Scientific Research No. 62540567 from the Ministry of Education, Science and Culture of Japan to T. I., by a travel grant from the Seto Marine Biological Laboratory to M. J. G., and by the Sesoko Marine Science Center of the University of the Ryukyus, where M. J. G. was Visiting Foreign Researcher in 1988-89.

REFERENCES

- 1 Itô, T. (1987) Y-larvae - enigmatic crustacean larvae. Ann. Rep. Seto Mar. Biol. Lab., 1: 52-58. (In Japanese)
- 2 Brattström, H. (1948) Undersökningar över Öresund XXXIII. Studies on *Ulophysema öresundense* 2. On the larval development of the ascothoracid *Ulophysema öresundense* Brattström. Lunds Univ. Aarskr. N. Ser., Avd. 2, 44: 1-70.
- 3 Wagin, V. L. (1954) [On the structure, larval development and metamorphosis of dendrogasterids (parasitic crustaceans of the order Ascothoracida)]. Uch. Zap. Leningr. Gos. Univ. Ser. Biol. Nauk,

- 172: 42–89. (In Russian)
- 4 Karande, A. A. and Oguro, C. (1981) Larvae of *Myriocladus astropectinis* (Yosii 1931) (Ascothoracica) reared under laboratory conditions. *Proc. Ind. Acad. Sci., Anim. Sci.*, **90**: 23–31.
 - 5 Brattström, H. (1956) On the organization of the genus *Baccalaureus* with description of a new South African species. In "Bertil Hanström, Zoological Papers in Honour of his Sixty-fifth Birthday November 20, 1956". Ed. by K.G. Wingstrand, Zoological Institute, Lund, pp. 106–119.
 - 6 Grygier, M. J. (1985) Lauridae: taxonomy and morphology of ascothoracid crustacean parasites of zoanthids. *Bull. Mar. Sci.*, **36**: 278–303.
 - 7 Yosii, N. (1931) Note on the organisation of *Baccalaureus japonicus*. *Annot. Zool. Japon.*, **13**: 169–187.
 - 8 Broch, H. (1929) *Baccalaureus japonicus*, ein neuer Cirriped aus der Unterordnung der Ascothoracida. *Mitt. Zool. Mus. Berlin*, **15**: 237–244.
 - 9 Pyefinch, K. A. (1934) *Baccalaureus maldivensis*, a new species of ascothoracican. *Quart. J. Microsc. Sci.*, **77**: 223–242.
 - 10 Pyefinch, K. A. (1936) The internal anatomy of *Baccalaureus* with a description of a new species. *Quart. J. Microsc. Sci.*, **78**: 653–686.
 - 11 Pyefinch, K. A. (1937) The anatomy of *Baccalaureus torrensis*, sp. n. (Cirripedia Ascothoracica). *J. Linn. Soc. Lond. Zool.*, **40**: 347–371.
 - 12 Pyefinch, K. A. (1939) Ascothoracica (Crustacea, Cirripedia). *John Murray Exped. 1933–34 Scient. Rep.*, **5**: 247–262.
 - 13 Okada, Y. K. (1938) Les Cirripèdes Ascothoraciques. *Trav. Stat. Zool. Wimereux*, **13**: 489–514.
 - 14 Brattström, H. (1936) *Baccalaureus argalicornis* n. sp., eine neue Ascothoracide aus Madagascar. *Kungl. Fysiogr. Sällsk. Lund Förhandl.*, **6**(20): 1–14.
 - 15 Karande, A. A. and Oguro, C. (1981) Comments on taxonomic characters of *Myriocladus astropectinis* Yosii, 1931 (Ascothoracica). *Crustaceana*, **41**: 108–110.
 - 16 Muirhead, A. and Ryland, J. S. (1985) A review of the genus *Isaurus* Gray, 1828 (Zoanthidea), including new records from Fiji. *J. Nat. Hist.*, **19**: 323–335.
 - 17 Utinomi, H. and Kikuchi, T. (1966) Fauna and flora of the sea around the Amakusa Marine Biological Laboratory. Part IV. Cirriped Crustacea. *Contr. Amakusa Mar. Biol. Lab., Kyushu Univ.*, **195**: 1–11.
 - 18 Herberts, C. (1972) Étude systématique de quelques zoanthaires tempérés et tropicaux. *Tethys Suppl.*, **3**: 69–156.
 - 19 Dawydoff, C. (1952) Contribution à l'étude des invertébrés de la faune marine benthique de l'Indochine. *Bull. Biol. Fr. Belg. Suppl.*, **37**: 1–158.
 - 20 Itô, T. and Takenaka, M. (1988). Identification of bifurcate paraocular process and postocular filamentary tuft of facetotectan cyprids (Crustacea: Maxillopoda). *Publ. Seto Mar. Biol. Lab.*, **33**: 19–38.
 - 21 Grygier, M. J. (1984) Comparative morphology and ontogeny of the Ascothoracida, a step toward a phylogeny of the Maxillopoda. Ph. D. Thesis, University of California San Diego. 417 pp.
 - 22 Grygier, M. J. (1987) Nauplii, antennular ontogeny and the position of the Ascothoracida within the Maxillopoda. *J. Crust. Biol.*, **7**: 87–104.
 - 23 Boxshall, G. A. and Böttger-Schnack, R. (1988) Unusual ascothoracid nauplii from the Red Sea. *Bull. Br. Mus. Nat. Hist. (Zool.)*, **54**(6): 275–283.
 - 24 Grygier, M. J. (1985) Crustacea Ascothoracida. *Mém. Mus. Nat. Hist. Nat., Paris, Sér. A. Zool.*, **133**: 417–426.
 - 25 Hansen, H. J. (1899) Die Cladoceren und Cirripeden der Plankton-Expedition. *Ergeb. Plankt.-Exped. Humboldt-Stift.*, **2**(G, d): 1–58.
 - 26 Schram, T. A. (1972) Further records of nauplius y type IV Hansen from Scandinavian waters. *Sarsia*, **50**: 1–24.
 - 27 Itô, T. (1986) Three types of "nauplius y" (Maxillopoda: Facetotecta) from the North Pacific. *Publ. Seto Mar. Biol. Lab.*, **31**: 63–73.
 - 28 Bresciani, J. (1965) Nauplius "y" Hansen: its distribution and relationship with a new cypris larva. *Vidensk. Medd. Dansk Naturh. For.*, **128**: 245–258.
 - 29 Grygier, M. J. (1987) New records, external and internal anatomy, and systematic position of Hansen's y-larvae (Crustacea: Maxillopoda: Facetotecta). *Sarsia*, **72**: 261–278.
 - 30 Anderson, D. T. (1987) The larval musculature of the barnacle *Ibla quadrivalvis* Cuvier (Cirripedia, Lepadomorpha). *Proc. R. Soc. Lond., B*, **231**: 313–338.
 - 31 Tessmann, M. (1904) Beiträge zur Entwicklungsgeschichte der Cirripeden. Inaugural-Dissertation, Universität zu Leipzig. 38 pp.
 - 32 Grygier, M. J. (1988) Larval and juvenile Ascothoracida (Crustacea) from the plankton. *Publ. Seto Mar. Biol. Lab.*, **33**: 163–172.
 - 33 McKenzie, K. G. (1972) Contribution to the ontogeny and phylogeny of Ostracoda. In "Proc. IPU, XXIII Internat. Geol. Congr., Prague, 1968." pp. 165–188.
 - 34 Bonaduce, G., Ciliberto, B., Minichelli, G., Masoli, M. and Pugliese, N. (1983) The Red Sea benthic ostracodes and their geographical distribution. In "Applications of Ostracoda". Ed. by R. F. Madocks, University of Houston Department of Geosciences, Houston, pp. 472–491.
 - 35 Grygier, M. J. and Fratt, D. B. (1984) The ascothoracid crustacean *Ascothorax gigas*: rede-

- scription, larval development, and notes on its infestation of the Antarctic ophiuroid *Ophionotus victoriae*. *Antarct. Res. Ser.*, **41**: 43–58.
- 36 Boxshall, G. A. and Huys, R. (1989) New tantulocarid, *Stygotantulus stocki*, parasitic on harpacticoid copepods, with an analysis of the phylogenetic relationships within the Maxillopoda. *J. Crust. Biol.*, **9**: 126–140.
 - 37 Lacaze-Duthiers, H. de. (1880) Histoire de la *Laura gerardiae*: type nouveau de Crustacé parasite. *Arch. Zool. Exp. Gén.*, (1)**8**: 537–581.
 - 38 Grygier, M. J. (1983) Revision of *Synagoga* (Crustacea: Maxillopoda: Ascothoracid). *J. Nat. Hist.*, **17**: 213–239.
 - 39 Moyse, J. (1983) *Isidascus bassindalei* gen. nov., sp. nov. (Ascothoracida: Crustacea) from north-east Atlantic with a note on the origin of barnacles. *J. Mar. Biol. Ass. U. K.*, **63**: 161–180.
 - 40 Lowry, J. K. (1985) *Cardomanica andersoni* n. gen., n. sp. from the western Tasman sea with notes on species from the tropical western Atlantic Ocean (Crustacea: Ascothoracida: Synagogidae). *Rec. Austral. Mus.*, **37**: 317–323.
 - 41 Itô, T. (1989) A new species of *Hansenocaris* (Crustacea: Facetotecta) from Tanabe Bay, Japan. *Publ. Seto Mar. Biol. Lab.*, **34**: 55–72.
 - 42 Elfimov, A. S. (1986) Morphology of the carapace in the cypris larva of *Heteralepas mystacophora* Newman (Cirripedia, Thoracica). *Biologiya Morya* 1986(3): 30–34. (In Russian with English summary)
 - 43 Elfimov, A. S. (1989) [The cypris larvae of cirripedes and their significance in the formation of fouling]. *Avtoreferat of Candidate Thesis*, Moscow State Univ., pp. 1–22. (In Russian)
 - 44 Mauchline, J. (1977) The integumental sensilla and glands of pelagic Crustacea. *J. Mar. Biol. Ass. U. K.*, **57**: 973–994.

Three New Species of the Genus *Rhombognathus* (Acari, Halacaridae) from Japan

HIROSHI ABÉ

Department of Systematic Zoology, Division of Environmental Structure,
Graduate School of Environmental Science, Hokkaido
University, Sapporo 060, Japan.

ABSTRACT—Three new species of the genus *Rhombognathus* are described from Japan. *Rhombognathus atuy* sp. nov. and *Rhombognathus ezoensis* sp. nov. differ from their congeners in the chaetotaxies of the posterodorsal plate, genital region and legs, and from *Rhombognathus dissociatus* sp. nov. in having three ventral plates.

INTRODUCTION

The genus *Rhombognathus* was established by Trouessart [1]. Only two species of *Rhombognathus* have hitherto been known from waters adjacent to Japan, viz. *Rhombognathus terminalis* and *Rhombognathus denticulatus* described by Sokolov [2] from the Sea of Japan. The present paper describes three new species of this genus collected from marine algae at intertidal zones in Hokkaido, northern Japan.

The type-series is deposited in the collections of the National Science Museum, Tokyo, of the Zoological Institute, Faculty of Science, Hokkaido University, Sapporo, and of the National Museum of Natural History, Smithsonian Institution, Washington, DC, U.S.A., and in my private collection.

Terms and the systems of notation for numerical data follow Newell [3-5].

Abbreviations: AD, anterodorsal plate; PD, posterodorsal plate; OC, ocular plate; AE, anterior epimeral plate; PE, posterior epimeral plate; GA, genitoanal plate; ds, dorsal setae; aes-i, anterior epimeral setae; aes-ii-lat (-v, -adj), lateral (ventral, adjunctive) setae of coxae II; pes-iii-lat (-v, adj), lateral (ventral, adjunctive) setae of coxae III; pes-iv, setae of coxae IV; P-1 to P-4, first to fourth segment of palp.

In addition, the following abbreviations are used in the figure legends: Ds, dorsal view; Vr, ventral view; R, right appendage (or part); L, left appendage (or part).

Family **Halacaridae** Murray
Subfamily **Rhombognathinae** Viets
(Japanese name: *Kaisoudani*-aka, new)

Genus ***Rhombognathus*** Trouessart
(Japanese name: *Kaisoudani*-zoku, new)

Rhombognathus atuy sp. nov.
(Japanese name: *Umibe-kaisoudani*, new)
(Figs. 1-4)

Type-series. Holotype: Female, intertidal, on *Sargassum* at 0.5 m depth at low tide, Usu (42°31'N, 140°47'E), Hokkaido, Japan, 10. vii. 1986, H. Abé coll. Allotype: Male, data same as the holotype. Paratypes: 1 female, intertidal, on *Sargassum* at 0.5 m depth in tide pool, Usujiri (41°56'N, 140°57'E), Hokkaido, 12. vi. 1986, H. Abé coll.; 2 males, 1 female, intertidal, on *Corallina* at 0.1 m depth in tide pool, Mitsuishi (42°14'N, 142°36'E), Hokkaido, 8. xii. 1988, H. Abé coll.

Female (holotype). Idiosoma 364 μ m long, 240 μ m wide. Color in life dark green.

Dorsum (Fig. 1A): Dorsal plate ornamented with weak panels, and partly with fine canaliculi. AD and PD separated by interval of approximately PD length. AD 80 μ m long, 110 μ m wide,

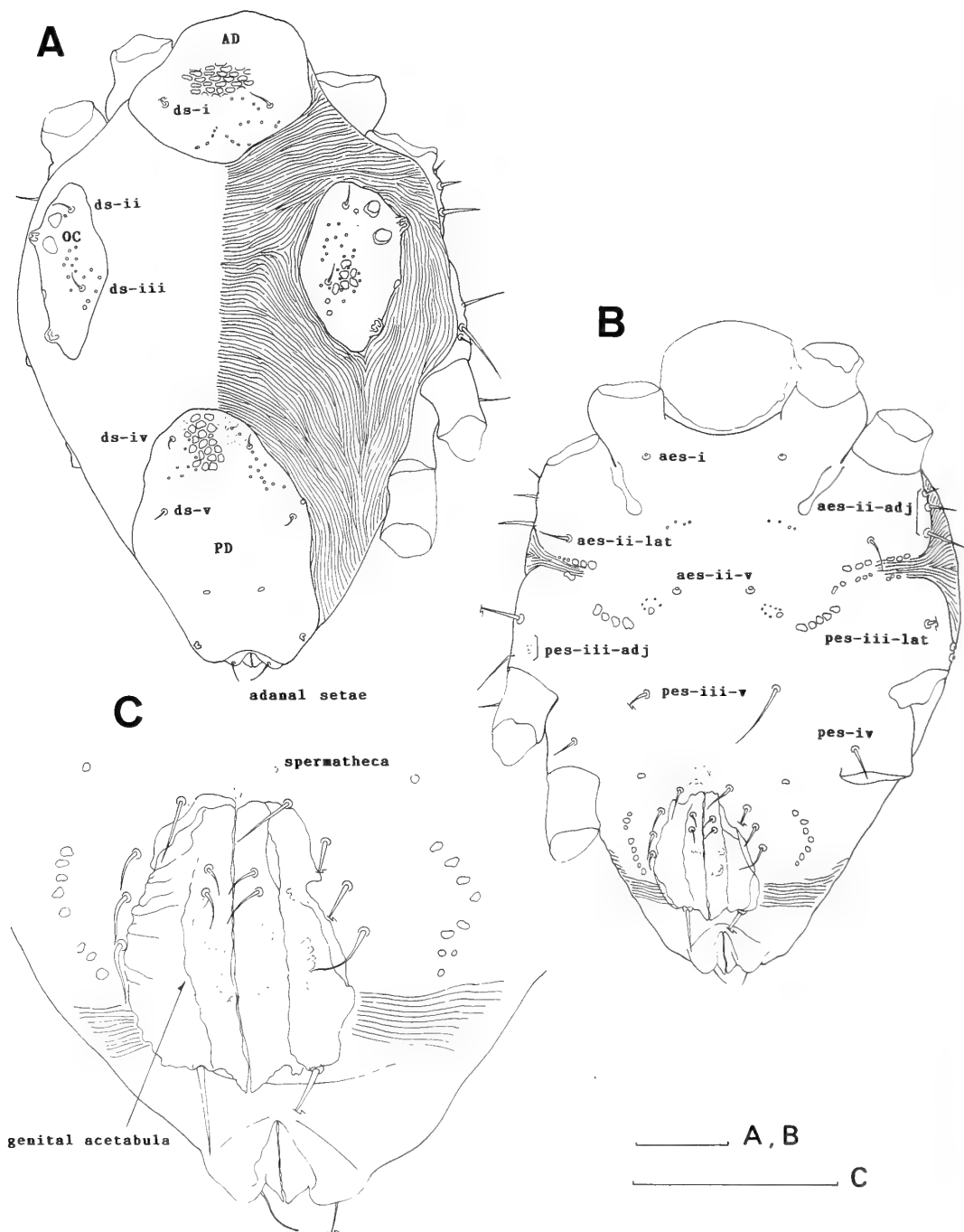


FIG. 1. *Rhombognathus atuy* sp. nov., Female (holotype). A, idiosoma (Ds); B, idiosoma (Vr); C, genitoanal region. Scale bars=50 μ m.

weakly convex anteriorly and weakly protruded posteriorly, ornamented with chevron-shaped areolation posteriorly, without distinct dorsal

pore. OC 92 μ m long, 50 μ m wide, extending anteriorly to level slightly posterior to posterior margin of AD, reaching posteriorly to level slightly

anterior to insertion of leg III, furnished with two large corneae and two large polygonal pores, bearing one tiny pore-like structure in the vicinity of lateral margin, one maze-like subsurface pore medially to anterior cornea, and two tiny subsurface pores near posteromedial margin. Areolation indistinct. PD 138 μm long, 82 μm wide, reaching anteriorly to level slightly posterior to insertion of leg III, furnished with small subsurface pore at 0.24, tiny areolation at 0.73, and dorsal pore on posterolateral margin on each side. Costae almost parallel, scattered with fine canaliculi. Paracosta lacking.

Chaetotaxy of dorsal region: Setae ds-i on AD, at 0.49, slightly longer and thicker than the others; ds-ii each on OC near anteromedial corner at 0.13; ds-iii each on OC near posteromedial margin at 0.61; ds-iv and ds-v on PD at 0.18 and 0.44, respectively.

Venter (Fig. 1B): Epimeral, genital and anal plates fused to form a single plate. Ornamentation indistinct, but very faintly reticulated in part. Epimeral region furnished with membranous collar anteriorly, several subsurface pores medially, and elongate subsurface structure between insertions of leg I and leg II on each side, incised laterally with membranous cuticle with bordering several subsurface pores at level midway between insertions of leg II and leg III.

Chaetotaxy of epimeral region: Setae aes-i at level slightly anterior to insertion of leg II; aes-ii-lat placed medially at level slightly anterior to lateral incision; aes-ii-v placed most medially at level slightly posterior to lateral incision; aes-ii-adj located on lateral margins, each consisting of three setae; pes-iii-lat placed near lateral margins, at level midway between lateral incision and insertion of leg III; pes-iii-v placed medially, at level of insertion of leg III; pes-iv located at level slightly anterior to insertion of leg IV; pes-iii-adj placed dorsolaterally, each consisting of two thick setae.

Genitoanal region (Fig. 1C): Genital region slightly incised laterally with membranous cuticle at level of posterior portion of genital foramen, furnished with a round subsurface pore, and a series of polygonal subsurface pores on each side of genital foramen. Genital foramen 70 μm long, 54 μm wide, oval, occupying from level slightly

posterior to insertion of leg IV to level anterior to anal papilla. Genital sclerites band-like, with membranous wide fringe. Genital acetabula internal, three pairs. Spermatheca bilobed, extending to level of insertion of leg IV. Ovipositor placed inside of genital foramen. Anal papilla somewhat swollen, placed terminally.

Chaetotaxy of genitoanal region: Five pairs of long thick filiform perigenital setae located around genital foramen as arranged in Figure 1C. Subgenital setae filiform; two setae on each genital sclerite, arrange 2-0. Adanal setae one pair, very fine, placed on anal papilla dorsoproximally.

Gnathosoma (Fig. 2A): 72 μm long, 72 μm wide, gnathosomal-length/idiosomal-length 0.20. Base, length/width 0.53, slightly expanded laterally, lacking seta, ornamented with fine punctations and a few round thin panels. Pharyngeal plate elongate, furnished with three longitudinal stems and double row of several minute filamentous subsurface structures. Anterior margin of tectum with three acute points. Rostrum approximately 34 μm long, 17 μm wide, nearly lanceolate, not reaching to level of distal end of palp. Rostral setae two pairs as follows: Proximal pair long and robust, at just anterior to swollen point; distal pair short, at just anterior to proximal pair. Rostral sulcus short, barely reaching to level of proximal rostral setae. Chelicera (Fig. 2B) elongate, with basal segment 68 μm long, 24 μm wide without clear ornamentation. Movable digit 16 μm long, with 11-12 minute denticles along dorsal edge. Fixed digit 13 μm long, extending distally to mid-level of movable digit. Palp (Fig. 2C), 30 μm long; P-1, length/width 0.38, short and cylindrical; P-2, length/width 0.42, longest and robust, very weakly reticulated, with a seta distidorsally; P-3, length/width 0.29, short and cylindrical; P-4, length/width 1.75, conical, with three short and thick filiform setae intermediately, and two appressed blunt spiniform projections terminally.

Legs (Fig. 3A-D): Length of legs I, II, III, IV = 240, 236, 236, 248 μm , respectively. Ornamentation indistinct. Each tarsus furnished with claw fossa, without ventral seta. Lateral claw with rake-like accessory process, bearing nine to twelve delicate teeth. Median claw and comb absent. Carpite short and rod-like. Cavity in claw present.

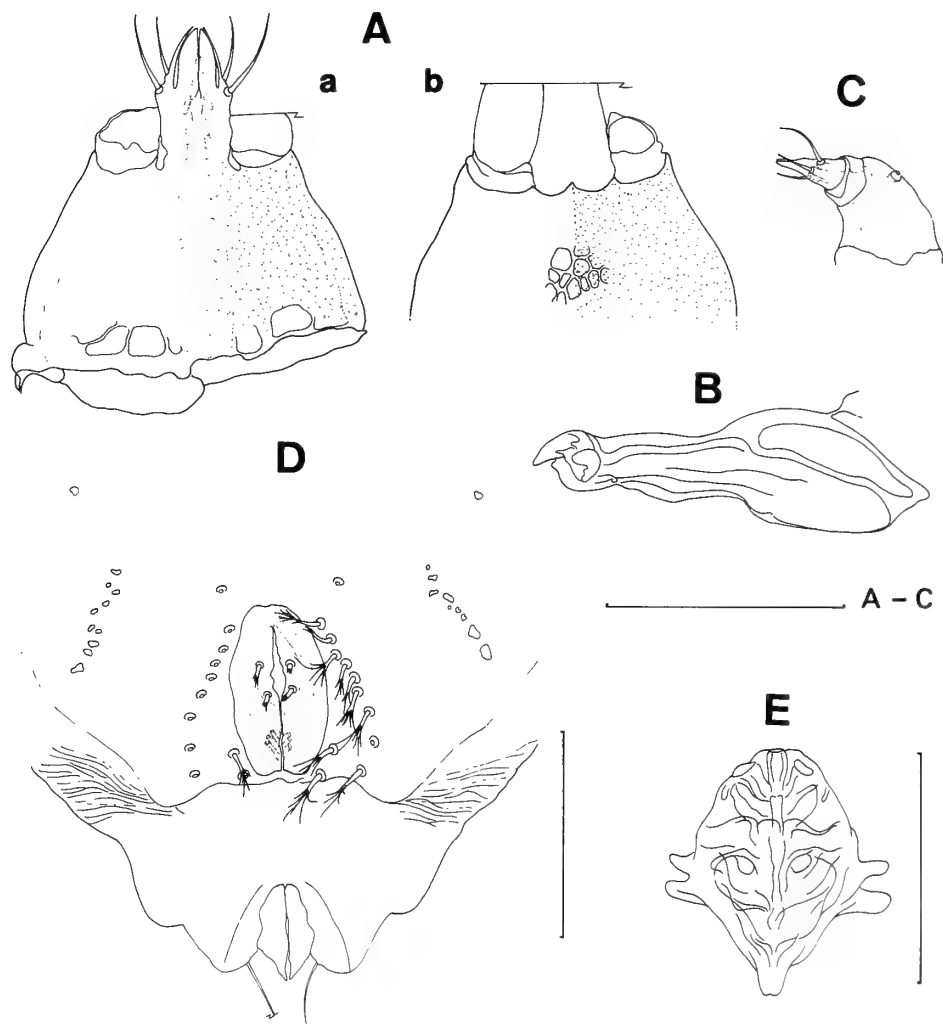


FIG. 2. *Rhombognathus atuy* sp. nov., Female (holotype). A, gnathosoma (a-Vr, b-Ds); B, chelicera (R); C, palp (R). Male (allotype). D, genitoanal region; E, spermatophorotype. Scale bars = 50 μ m.

Short seta usually faintly rough, long seta smooth.

Leg chaetotaxy as follows: Trochanters I-IV, 1-1-1-0; basifemora, 2-3-2-2; telofemora, 7-7-5-4; genua, 5-5-3-4; tibiae, 6-6-5-5. As for large bipectinate seta: Tibiae I-IV, 2-1-1-1. Tarsus I (Fig. 4A) with three dorsal setae, one solenidion, one famulus, and four parambulacral setae (paired doublet euphathidia). Solenidion long bacilliform on posterodorsal surface of claw fossa. Famulus papilliform with fine canaliculus at just ventroproximally to solenidion. Tarsus II (Fig. 4B) with three dorsal setae, one solenidion, and four parambulacral setae. Solenidion long bacilliform on

posterodorsal surface of claw fossa. Tarsus III (Fig. 4C) with four dorsal setae, and two parambulacral setae (one single euphathidium on posterior surface, one bud-shaped proeuphathidium on anterior surface). Tarsus IV (Fig. 4D) with three dorsal setae (one long thick filiform seta on basidorsal limb, one fronded seta on claw fossa, one fine filiform seta on anterodorsal surface), and two parambulacral setae (one single euphathidium on posterior surface, one bud-shaped proeuphathidium on anterior surface).

Male (allotype). Idiosoma 360 μ m long, 240 μ m wide, gnathosomal-length/idiosomal-length 0.19,

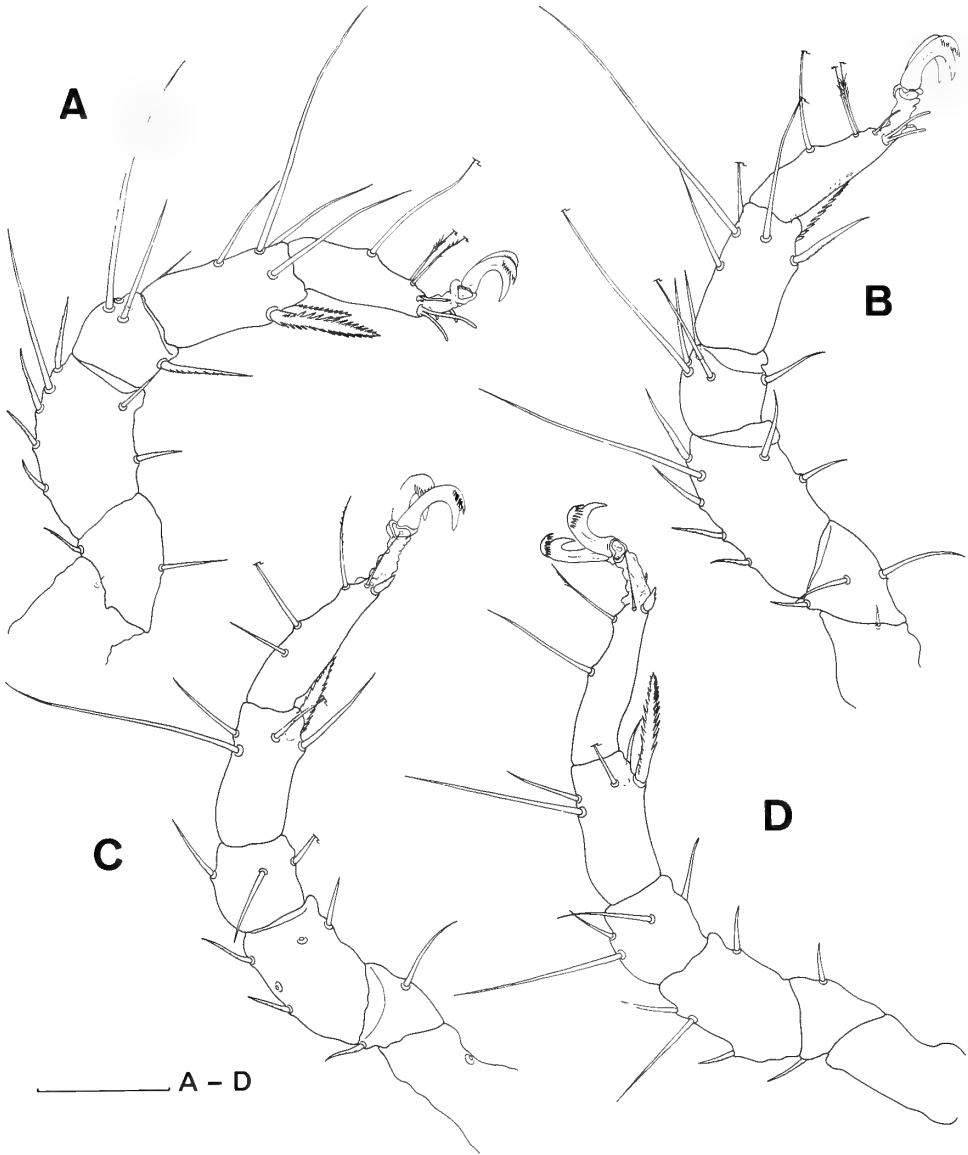


FIG. 3. *Rhombognathus atuy* sp. nov., Female (holotype). A, leg I (R); B, leg II (R); C, leg III (L), D, leg IV (L). Scale bar=50 μ m.

resembling the female in essential respects except for characters of genitoanal region, and chaetotaxy of tarsus IV.

Genitoanal region (Fig. 2D) furnished with a round subsurface pore, a series of polygonal subsurface pores, and very faint panels on each side of genital foramen, bearing terminally tufted 11 and 12 perigenital setae as arranged in Figure 2D. Genital foramen 50 μ m long, 24 μ m wide. Sub-

genital setae divided terminally; two setae on each genital sclerite, arranged 2-0. Genital acetabula internal, three pairs. Spermatophorotype (Fig. 2E) 62 μ m long, 50 μ m wide, massive and obovate.

Tarsus IV (Fig. 4E) furnished with three dorsal setae (one long thick filiform seta on basidorsal limb, one froned seta on claw fossa, one delicate branched seta on anterodorsal surface of claw

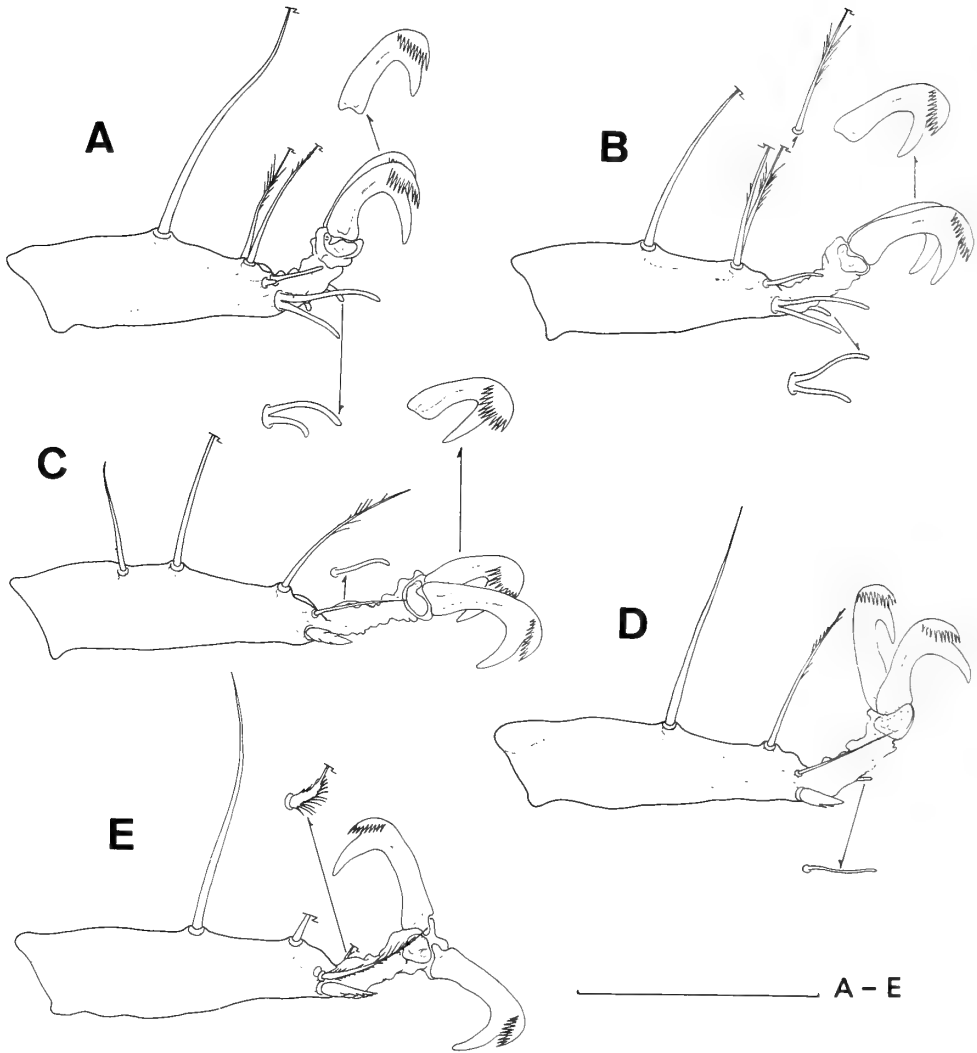


FIG. 4. *Rhombognathus atuy* sp. nov., Female (holotype). A, tarsus I (R); B, tarsus II (R); C, tarsus III (L); D, tarsus IV (L). Male (allotype). E, tarsus IV (L). Scale bar = 50 μ m.

fossa), two parambulacral setae (one long plumose proeuphathidium on posterior surface, one bud-shaped proeuphathidium on anterior surface).

Immatures: Not collected.

Morphological variation and abnormality: The number of setae aes-ii-adj and pes-iii-adj on each side of the idiosoma varies from two to three, and one to two, respectively. The number of the perigenital setae on each side of the genital foramen varies from 11 to 12 in the male, five to six in the female. The leg chaetotaxy varies among specimens as follows: Trochanters I-IV, (0,1)-

(0,1)-1-0; telofemora, 7-(6,7)-5-4; genua, 5-(4,5)-3-4; tibiae, 6-6-(5,6)-5. One specimen lacks the dorsoproximal seta on tarsus III.

Etymology: The specific epithet is derived from "Atuy" which means the sea in the language of the Ainu (native people in northern Japan).

Distribution: Pacific coast of Hokkaido, northern Japan.

Remarks: *Rhombognathus atuy* is distinguishable from other *Rhombognathus* species by the following characters: Separated dorsal plates, PD with two pairs of setae, arrangements of perigenit-

al setae in the both sexes (Figs. 1C, 2D), leg chaetotaxy, and rake-like accessory process.

Among the *Rhombognathus* species characterized by having five perigenital setae in the female, *Rhombognathus atuy* resembles *R. caudiculus* Bartsch, 1983 [6] in the arrangement of these setae. However, *R. atuy* is easily discernible from *caudiculus* by the following characters (corresponding condition in the latter species in parentheses): (1) Two pairs of dorsal setae on PD (one pair); (2) rostrum lanceolate and shorter than the length of the base of gnathosoma (elongate, longer than the length of the base of gnathosoma); (3) two pairs of basal perigenital setae located near the posterior site of genital foramen in the male (one pair); (4) tibiae I-IV with 2-1-1-1 large bipectinate setae (tibiae I-IV with 2-1-1-2); (5) accessory process rake-like (not developed).

Moreover, *Rhombognathus atuy* is similar to *R. robustus* Bartsch, 1977 [7] in the arrangement of the perigenital setae in the male. However, *R. atuy* differs from *robustus* in the arrangement of the perigenital setae in the female (four pairs anteriorly, one pair posteriorly to genital foramen in *atuy*; two pairs anteriorly, three pairs posteriorly in *robustus*), in the developed accessory process, and in having tibiae I-IV with 2-1-1-1 large bipectinate setae.

Rhombognathus sandwichi Newell, 1984 [5] also has two pairs of basal perigenital setae in the male as in *R. atuy*, although the arrangement of these setae is not clear because no illustration was given. However, the two species clearly differ from each other in the shape and arrangement of the dorsal plates and leg chaetotaxy.

***Rhombognathus dissociatus* sp. nov.**

(Japanese name: *Wakare-kaisoudani*, new)

(Figs. 5-8)

Type-series. Holotype: Female, intertidal, on *Sargassum* exposed on ledge at low tide, Shamodomari, Oshoro Bay (43°12', 140°51'E), Hokkaido, 21. ii. 1987, H. Abé coll. Allotype: Male, intertidal, on *Polysiphonia* at 0.3 m depth in tide pool Poromai, Oshoro Bay, 6. iii. 1989, H. Abé coll. Paratypes: 1 female, 4 males, data same as the allotype; 1 female, intertidal, among *Sargassum*

belt in crevice at low tide, Kabuto Rock, Oshoro Bay, 15. iv. 1986, H. Abé coll.; 1 female, intertidal, on *Rhodomela* at 0.3 m depth in tide pool, Kabuto Rock, Oshoro Bay, 21. ii. 1987, H. Abé coll.; 1 female, intertidal, on *Sargassum* exposed on ledge at low tide, Kikonai (41°42'N, 140°32'E), Hokkaido, 16. v. 1987, H. Abé coll.

Female (holotype). Idiosoma 472 μm long, 316 μm wide. Color in life dark green.

Dorsum (Fig. 5A): Dorsal plate ornamented with clear panels, and partly with fine canaliculi. AD and PD separated by interval of approximately PD length. AD 100 μm long, 116 μm wide, strongly protruded anteriorly, and truncated posteriorly, reaching posteriorly to level of insertion of leg II, ornamented with triangular areolation at posterior portion, with a large pore near each lateral margin at 0.44. OC 114 μm long, 60 μm wide, extending posteriorly to level slightly anterior to insertion of leg III, furnished with two large corneae, two large polygonal pores, bearing one maze-like subsurface pore just posteromedially to anterior cornea, one pore-like angular structure near lateral margin at 0.70, and two tiny subsurface pores near posteromedial margin. Areolation not seen. PD 176 μm long, 176 μm wide, protruded anteriorly, slightly concave posteriorly, reaching anteriorly to level of insertion of leg III, furnished with a large dorsal pore at 0.91, and a tiny areolation at 0.89 on each side. Costae almost parallel and scattered with fine canaliculi. Paracosta lacking.

Chaetotaxy of dorsal region: Setae ds-i on AD at 0.54, longer and thicker than the others; ds-ii each on OC near anteromedial corner at 0.11; ds-iii each on OC near medial margin at 0.49; ds-iv and ds-v on PD at 0.23 and 0.59, respectively.

Venter (Fig. 5B): Membranous cuticle clearly striated. Ventral plates three in number, completely separated, and entirely ornamented with porous panels. PE and genital plate fused to form a single middle plate. AE and middle plate separated from each other by a strip of membranous cuticle. AE 100 μm long, 276 μm wide, convex posteriorly, reaching posteriorly to level about midway between insertions of leg II and leg III, furnished with wide thin membranous collar anteriorly, several subsurface pores along post-

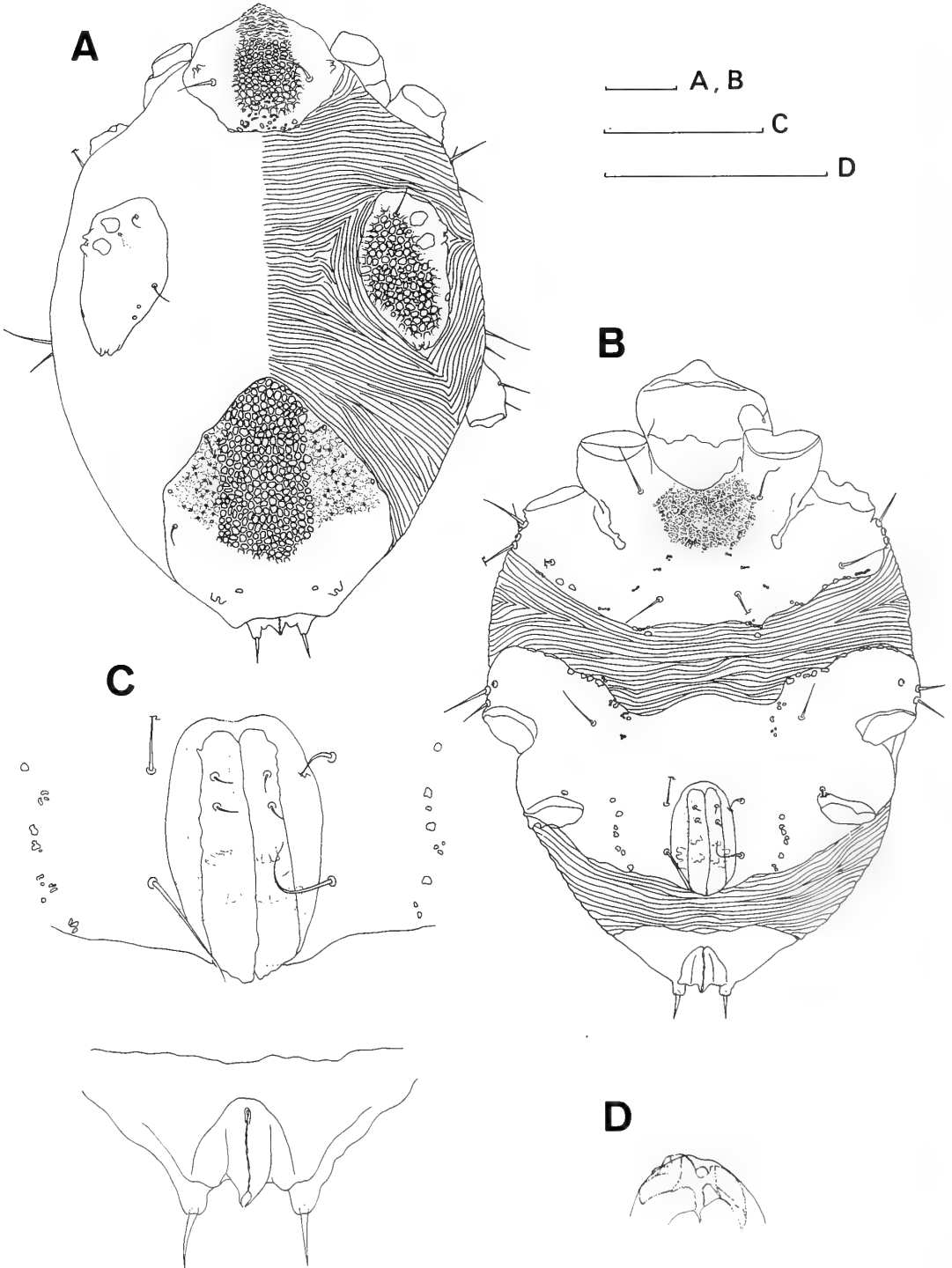


FIG. 5. *Rhombognathus dissociatus* sp. nov., Female (holotype). A, idiosoma (Ds); B, idiosoma (Vr); C, genitoanal region; D, spermatheca. Scale bars = 50 μ m.

erior margin, and elongate subsurface structure between insertions of leg I and leg II on each side. A round subsurface pore located on striated membranous cuticle medially on each side, at just posterior to posterior margin of AE. Middle plate 152 μm long, 316 μm wide, concave anteriorly, convex posteriorly, reaching posteriorly to about mid-level between insertion of leg IV and the end of idiosoma, ornamented with several subsurface pores along boundary between each posterior epimeral region and genital region. Anal plate 46 μm long, 122 μm wide, surrounding anal pailla, completely separated from genital region by a strip

of striated membranous cuticle.

Chaetotaxy of epimeral region: Setae aes-i on AE, at level slightly anterior to insertion of leg II; aes-ii-lat on AE, near posterolateral corners; aes-ii-v on AE, near posterior margin; aes-ii-adj placed on lateral margins (three setae on left side, four setae on right side); pes-iii-lat on middle plate, located near lateral margins, at mid-level between anterior margin of middle plate and insertion of leg III; pes-iii-v on middle plate, at level of insertion of leg III; pes-iv on middle plate, at level just anterior to insertion of leg IV; pes-iii-adj placed on lateral margins of middle plate, each

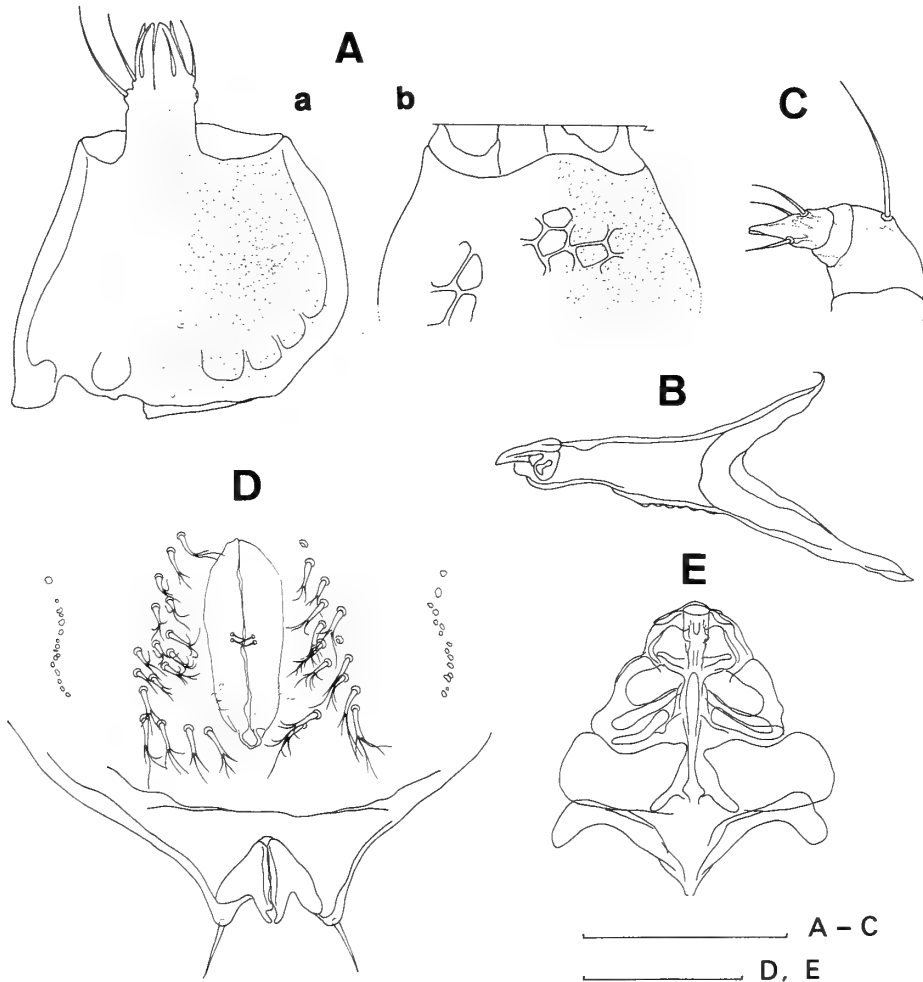


FIG. 6. *Rhombognathus dissociatus* sp. nov., Female (holotype). A, gnathosoma (a-Vr, b-Ds); B, chelicera (R) [broken basally]; C, palp (R). Male (allotype). D, genitoanal region; E, spermatophorotype. Scale bars=50 μm .

consisting of two thick setae.

Genitoanal region (Fig. 5C): Genital region occupying medial portion of middle plate, furnished with a round subsurface pore, and a series of polygonal subsurface pores on each side of genital foramen. Genital foramen $88\text{ }\mu\text{m}$ long, $48\text{ }\mu\text{m}$ wide, elliptical, located posteromedially on middle plate. Genital sclerites band-like, extending posteriorly somewhat beyond posterior margin of middle plate. Genital acetabula internal, three pairs. Spermatheca (Fig. 5D) bilobed, not extending anteriorly from anterior margin of genital foramen. Ovipositor placed inside of genital foramen. Anal papilla placed terminally on anal plate.

Chaetotaxy of genitoanal region: Two pairs of long filiform perigenital setae located near genital foramen as arranged in Figure 5C. Subgenital setae short, filiform; two setae on each genital sclerite, arranged 2-0. Adanal setae one pair, robust, placed dist dorsally.

Gnathosoma (Fig. 6A): $94\text{ }\mu\text{m}$ long, $88\text{ }\mu\text{m}$ wide, gnathosomal-length/ideosomal-length 0.20. Base, length/width 0.65, slightly expanded laterally, lacking seta, ornamented with fine punctations and several panels. Pharyngeal plate elongate, furnished with three longitudinal stems, and double row of several fine filamentous subsurface structures. Anterior margin of tectum weakly convex. Rostrum approximately $37\text{ }\mu\text{m}$ long, $20\text{ }\mu\text{m}$ wide, elongate, not reaching to level of distal end of palp. Rostral setae two pairs as follows: Proximal pair long and robust, at half level of rostrum; distal pair at just anterior to proximal pair, about $2/3$ length of proximal pair. Rostral sulcus short, barely reaching to level of proximal rostral setae. Chelicera (Fig. 6B) elongate, with basal segment $86\text{ }\mu\text{m}$ long, without clear ornamentation. Movable digit $18\text{ }\mu\text{m}$ long, with 12-13 minute denticles along dorsal edge. Fixed digit $15\text{ }\mu\text{m}$ long, extending distally to about midway of denticulate dorsal margin of movable digit. Palp (Fig. 6C) $38\text{ }\mu\text{m}$ long; P-1, length/width 0.33, short and cylindrical; P-2, length/width 0.50, longest and robust, weakly reticulated with porous panels, with long thick filiform seta dorsally; P-3, length/width 0.31, short and cylindrical; P-4, length/width 0.59, conical, with three short and thick filiform setae intermediately, and two appressed blunt

spiniform projection terminally.

Legs (Fig. 7A-D): Length of legs I, II, III, IV = 244, 246, 230, $236\text{ }\mu\text{m}$, respectively, ornamented with fine porous panels which are clear only on telofemora. Each Tarsus furnished with claw fossa, lacking ventral seta. Lateral claw with tiny rake-like accessory process bearing five to seven very minute and fine teeth. Median claw and comb absent. Carpite short and rod-like. Cavity in claw present. Short seta usually faintly rough, long seta smooth.

Leg chaetotaxy as follows: Trochanters I-IV, 1-1-2-0; basifemora, 2-3-2-2; telofemora, 7-7-5-6; genua, 6-6-4-5; tibiae, 6-6-5-5. As for large bipectinate seta: Genua I-IV, 1-0-0-0; tibiae, 2-2-2-2; each one bipectinate seta on tibia II and tibia III weakly pectinated. Tarsus I (Fig. 8A) with three dorsal setae, one solenidion, one famulus, and four parambulacral setae (paired doublet euphathidia). Solenidion long straight bacilliform, on posterodorsal surface of claw fossa. Famulus papilliform with fine canaliculus, at just ventrally to solenidion. Tarsus II (Fig. 8B) with three dorsal setae, one solenidion, and four parambulacral setae. Solenidion long bacilliform on posterodorsal surface of claw fossa. Tarsus III (Fig. 8C) with four dorsal setae, and two parambulacral setae (one single filiform proeuphathidium on posterior surface, one bud-shaped proeuphathidium on anterior surface). Tarsus IV (Fig. 8D) with three dorsal setae (one lone thick filiform seta on basidorsal limb, one long serrated seta on claw fossa, one straight fine filiform seta on anterodorsal surface), two parambulacral setae (one straight fine filiform proeuphathidium on posterior surface, one bud-shaped proeuphathidium on anterior surface).

Male (allotype). Idiosoma $400\text{ }\mu\text{m}$ long, $240\text{ }\mu\text{m}$ wide, gnathosomal-length/ideosomal-length 0.22, resembling the female in essential respects except for characters of body size, genitoanal region, and chaetotaxy of tarsus IV.

Body size somewhat smaller than that in the female.

Genitoanal region (Fig. 6D) furnished with a series of polygonal subsurface pores, and terminally tufted 15 and 17 perigenital setae as arranged in Figure 6D. Genital foramen $72\text{ }\mu\text{m}$ long, $26\text{ }\mu\text{m}$ wide. Subgenital setae short, filiform; two setae at

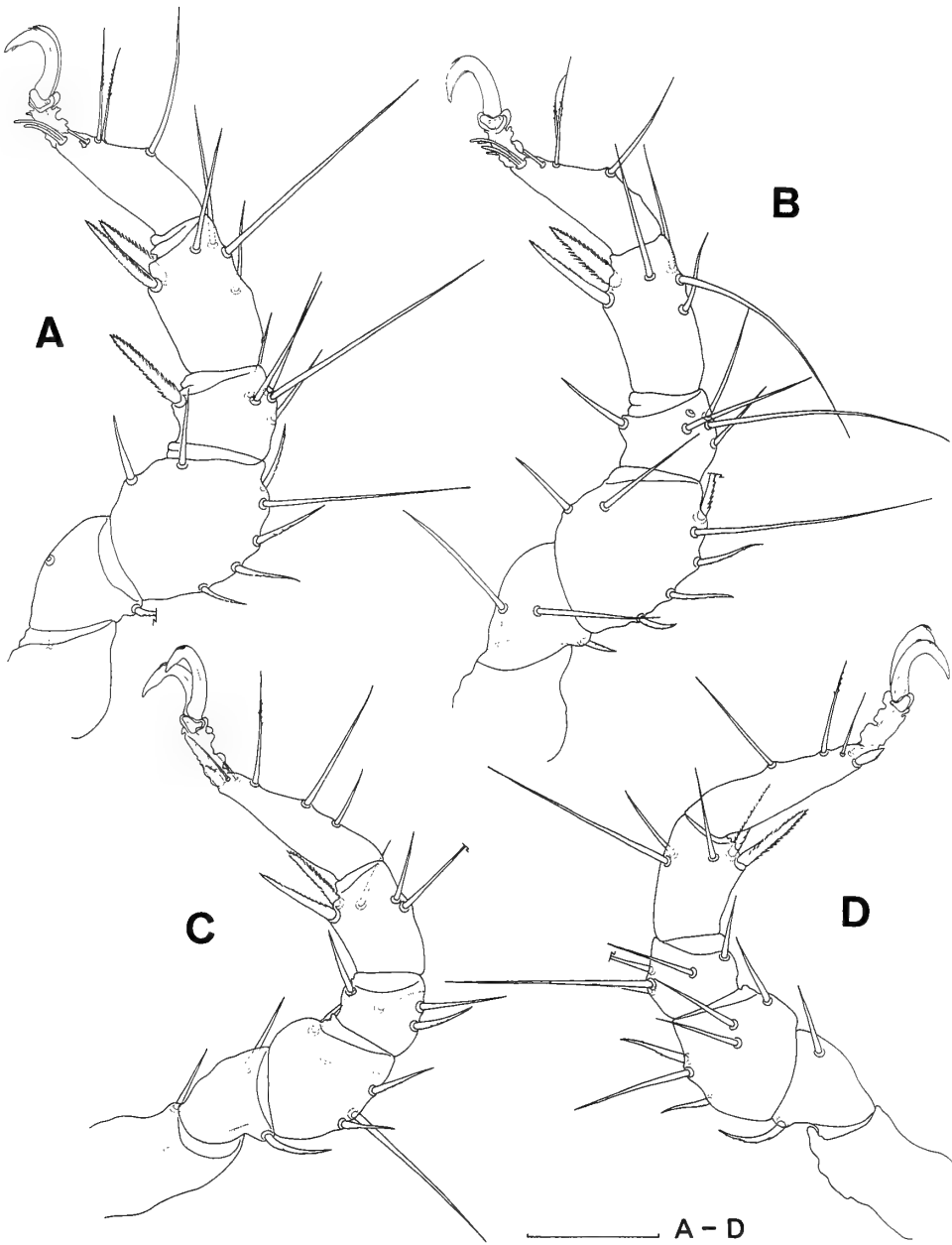


FIG. 7. *Rhombognathus dissociatus* sp. nov., Female (holotype). A, leg I (L); B, leg II (L); C, leg III (L); D, leg VI (L).

mid-level on each genital sclerite, arranged 2-0. Genital acetabula internal, three pairs. Anal plate not so clearly separated from middle plate as that in the female. Spermatophorotype (Fig. 6E) 88 μm long, 84 μm wide, very massive.

Tarsus IV (Fig. 8E) furnished with three dorsal setae (one long thick filiform seta on basidorsal limb, one fronded seta on claw fossa, one branched seta on anterodorsal surface of claw fossa), two parambulacral setae (one long branched

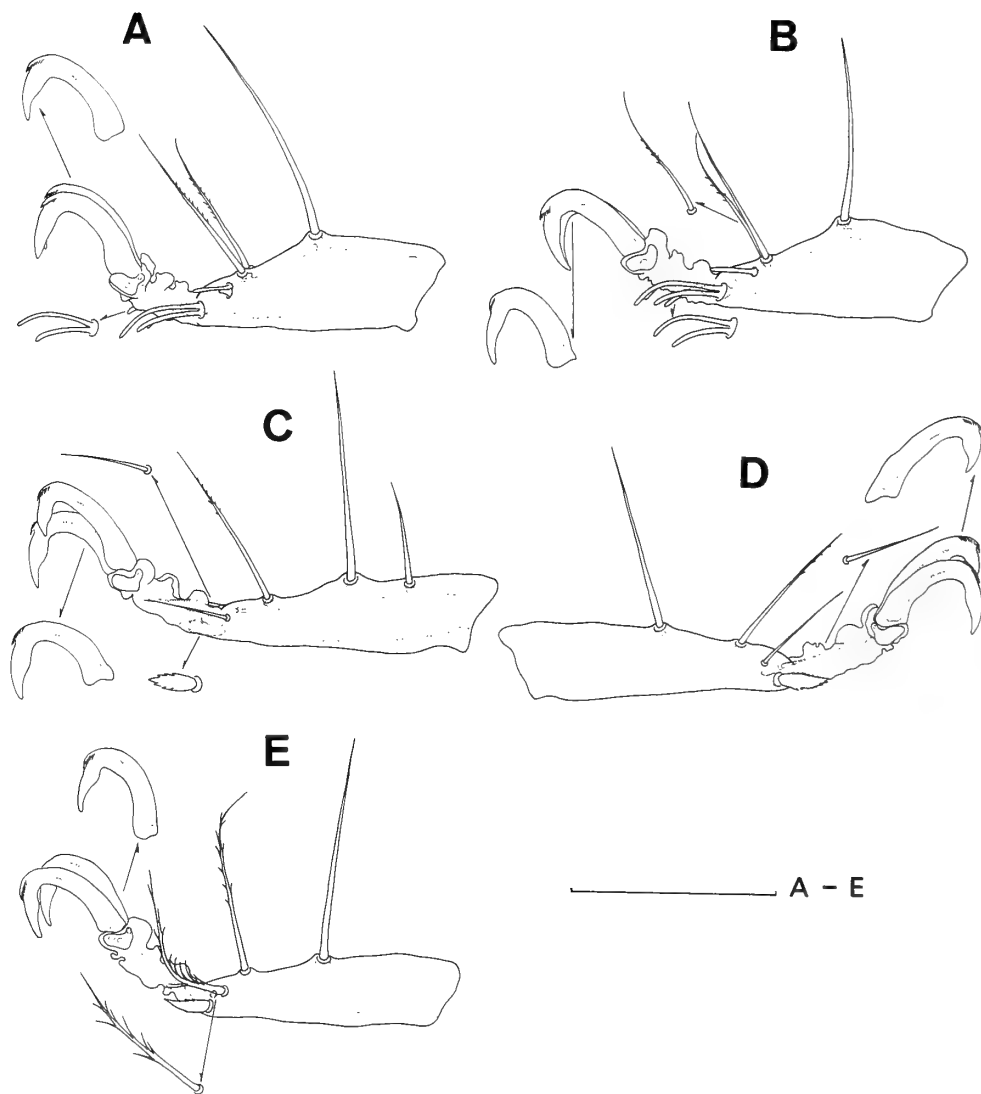


FIG. 8. *Rhombognathus dissociatus* sp. nov., Female (holotype). A, tarsus I (L); B, tarsus II (L); C, tarsus III (L); D, tarsus IV (L). Male (allotype). E, tarsus IV (R). Scale bar = 50 μ m.

proeuphathidium on posterior surface, one bud-shaped proeuphathidium on anterior surface).

Immatures: Not collected.

Morphological variation and abnormality: The holotype female specimen has four aes-ii-adj setae on right lateral margin of AE. However, all other specimens examined have three aes-ii-adj (the anteriormost seta shortest, the posteriormost longest) on each lateral side of AE. One specimen has two maze-like subsurface pores on left OC, and no ds-iii. The number of the perigenital setae

on each side of the genital foramen varies from 14 to 25 in the male; this number varies not only according to specimens, but also within one specimen. The leg chaetotaxy varies as follows: Trochanters I-IV, (6,7)-(7,8)-(5,6)-(4,5,6,7); genua, (5,6)-(5,6)-(3,4)-(4,5,6); tibiae, 6-6-5-(5,6). One specimen has only one large bipectinate seta on tibia III, and tibia IV, respectively.

Etymology: The specific epithet is derived from "the dissociated ventral plates".

Distribution: The Japan Sea coast of Hokkaido.

Remarks: This new species obviously belongs to the genus *Rhombognathus* on the grounds that (1) the genital foramen is placed ventrally (not terminally) and guarded by band-like (not cusp-like) genital sclerites, (2) each ocular plate has two setae, and (3) all legs have two claws. All the hitherto named species of *Rhombognathus* have one, two, or five ventral plates in the adult, and have more than three pairs of perigenital setae in the female. However, the species is unique in the following characters: (1) the venter is covered with three ventral plates (anterior epimeral plate, a middle plate consisting of posterior epimeral plates and a genital plate, and anal plate); (2) two pairs of perigenital setae in the female as shown in Figure 5 C; (3) the leg chaetotaxy is distinctive in having trochanters I-IV with 1-1-2-0 setae.

***Rhombognathus ezoensis* sp. nov.**

(Japanese name: *Ezo-kaisoudani*, new)

(Figs. 9-12)

Type-series. Holotype: Female, intertidal, on *Sargassum* on boulder at 0.2 m depth at high tide, Shamodomari, Oshoro Bay, Hokkaido, 23. vi. 1987, H. Abé coll. Allotype: Male, intertidal, on *Sargassum* on boulders at 0.3 m depth at low tide, Shamodomari, Oshoro Bay, 21. ii. 1987, H. Abé coll. Paratypes: 1 female, 2 tritonymphs, 2 deutonymphs, data same as the holotype; 1 male, 2 females intertidal, among *Sargassum* belt at 0.5 m depth at low tide, Ebisu Rock, Oshoro Bay, 15. iv. 1986, H. Abé coll.; 2 females, intertidal, on *Sargassum* at 0.3 m depth in tide pool, Kabuto Rock, Oshoro Bay, 21. ii. 1987, H. Abé coll.; 1 male, intertidal, on *Sargassum* at 0.5 m depth in tide pool, Usujiri, Hokkaido, 12. vi. 1986, H. Abé coll.; 1 female, intertidal, on *Sargassum* exposed on ledge at low tide, Kikonai, Hokkaido, 16. v. 1987, H. Abé coll.; 2 males, 2 females, intertidal, on *Corallina* at 0.1 m depth in tide pool, Mitsuishi, Hokkaido, 8. xii. 1988, H. Abé coll.

Female (holotype). Idiosoma 388 μm long, 256 μm wide. Color in life dark green with a fine dorsal semitransparent line longitudinally.

Dorsum (Fig. 9A): Dorsal plate uniformly ornamented with clear panels, and partly with fine canaliculi. Ad and PD separated by interval of

approximately two times as long as AD. AD 80 μm long, 100 μm wide, almost truncated anteriorly and posteriorly, ornamented with fine areolation at posterior portion, without clear dorsal pore. OC 96 μm long, 52 μm wide, extending anteriorly to level slightly posterior to posterior margin of AD, reaching posteriorly to level slightly anterior to insertion of leg III, furnished with two large corneae, two large polygonal pores, bearing one angular pore-like structure near lateral margin, one maze-like subsurface pore medially to corneae, and three tiny subsurface pores near posteromedial margin. Areolation not seen. PD 164 μm long, 120 μm wide, extending anteriorly to level of insertion of leg IV, furnished with a small subsurface pore at anterolateral corner, and a dorsal pore on posterolateral margin on each side. Areolation not clear. Costae almost parallel and scattered with fine canaliculi. Paracosta lacking.

Chaetotaxy of dorsal region: Setae ds-i on AD at 0.43, longer and thicker than the others; ds-ii each on OC near anterior margin at 0.08; ds-iii each on OC near medial margin at 0.52; ds-iv and ds-v on PD at 0.14 and 0.47, respectively.

Venter (Fig. 9B): Epimeral, genital, and anal plates fused to form a single plate which is entirely reticulated with faint panels. Epimeral region furnished with membranous collar anteriorly, several subsurface pores medially, and elongate subsurface structure between insertions of leg I and leg II on each side, incised laterally with membranous cuticle with bordering several subsurface pores at mid-level between insertions of leg II and leg III.

Chaetotaxy of epimeral region: Setae aes-i at level slightly anterior to insertion of leg II; aes-ii-lat placed medially at level slightly anterior to lateral incision; aes-ii-v located medially at level of anterior margin of lateral incision; aes-ii-adj placed near lateral margins, each consisting of three setae on left, whereas two setae on right; pes-iii-lat placed near lateral margins, at mid-level between lateral incision and insertion of leg III; pes-iii-v placed medially at level of insertion of leg III; pes-iv placed slightly anterior to insertion of leg IV; pes-iii-adj located dorsolaterally, each consisting of two setae.

Genitoanal region (Fig. 9C): Genital region

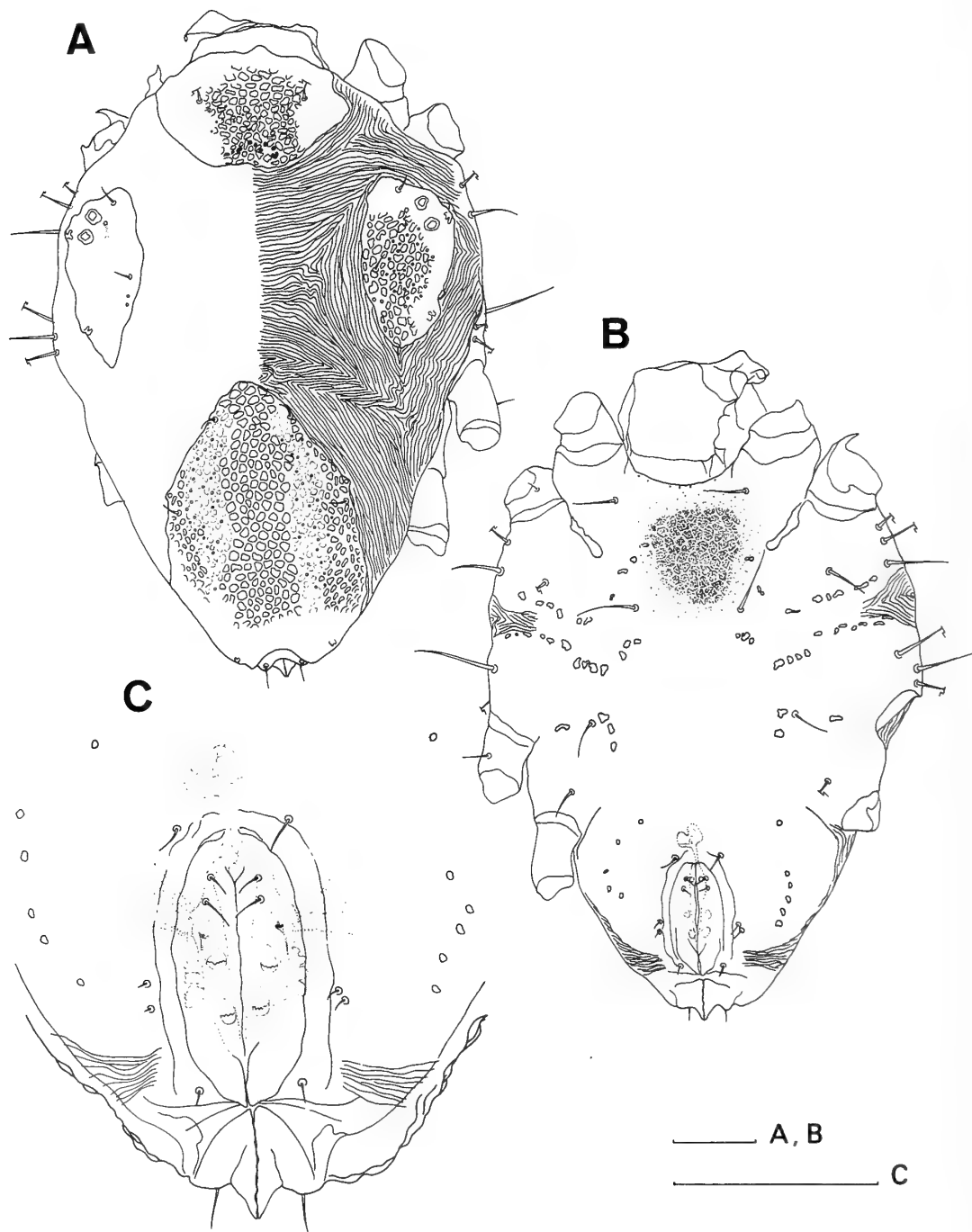


FIG. 9. *Rhombognathus ezoensis* sp. nov., Female (holotype). A, idiosoma (Ds); B, idiosoma (Vr); C, genitoanal region. Scale bars=50 μ m.

slightly incised laterally with membranous cuticle at level of posterior portion of genital foramen, furnished with a round subsurface pore, and a

series of several subsurface pores on each side of genital foramen. Genital foramen 66 μ m long, 40 μ m wide, subelliptical, reaching to level slightly

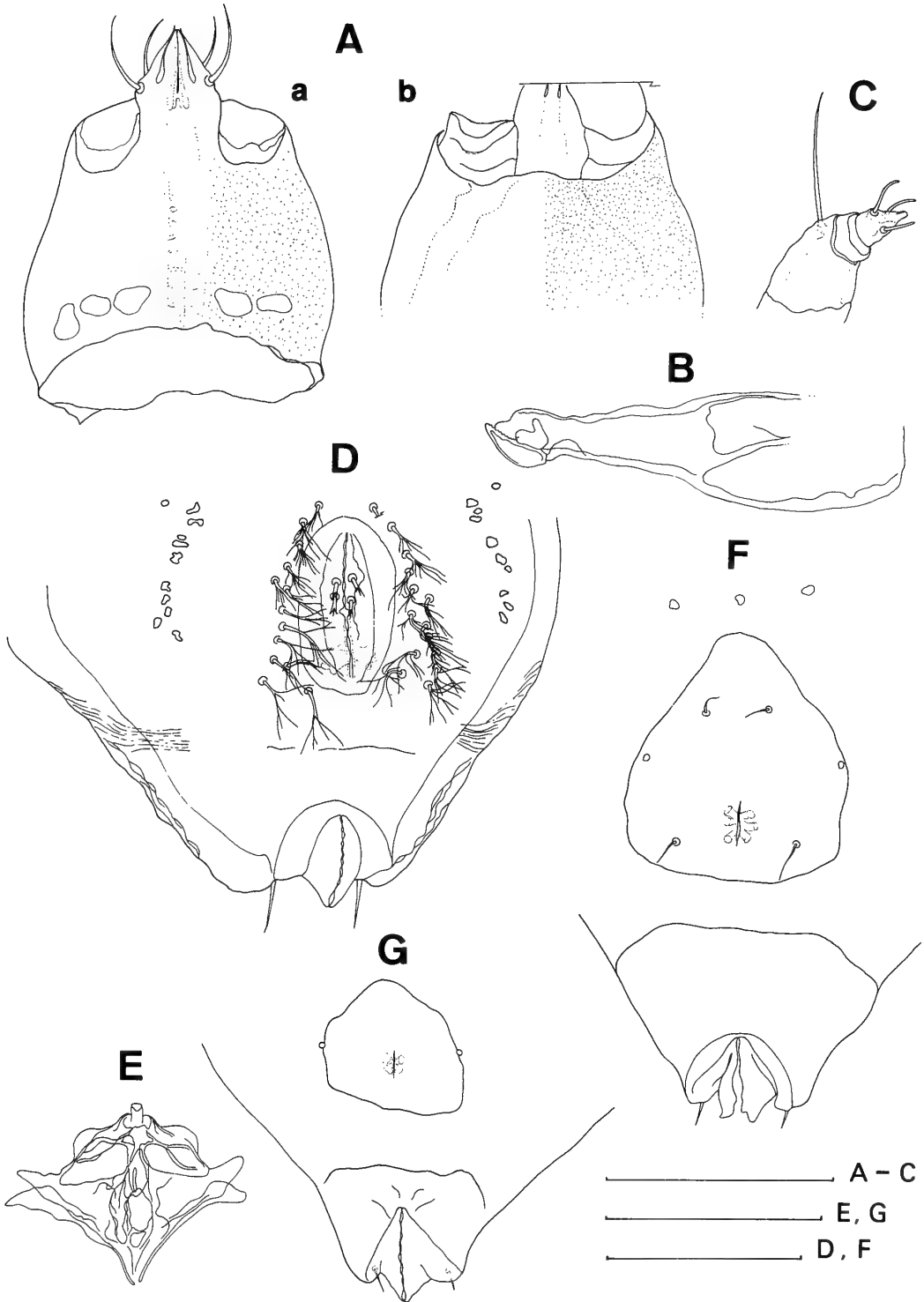


FIG. 10. *Rhombognathus ezoensis* sp. nov., Female (holotype). A, gnathosoma (a-Vr, b-Ds); B, chelicera (R); C, palp (R). Male (allotype). D, genitoanal region; E, spermatophorotype. Tritonymph (paratype). F, genitoanal region. Deutonymph (paratype). G, genitoanal region. Scale bars=50 μ m.

anterior to anal papilla, furnished with band-like genital sclerites and three pairs of internal genital acetabula. Spermatheca bilobed, extending to level of insertion of leg IV. Ovipositor placed inside of genital foramen. Anal papilla placed terminally.

Chaetotaxy of genitoanal region: Four pairs of short filiform perigenital setae located in the vicinity of genital foramen as arranged in Figure 9 C. Subgenital setae filiform; two setae on each genital sclerite, arranged 2-0. Adanal setae one pair, placed on anal papilla dorsoproximally.

Gnathosoma (Fig. 10A): 76 μm long, 70 μm wide, gnathosomal-length/idiosomal-length 0.20. Base, length/width 0.51, slightly expanded laterally, lacking seta, ornamented with fine punctations, and a few round panels on ventroproximal site. Pharyngeal plate elongate, furnished with three longitudinal stems, and double row of several minute filamentous subsurface structures. Anterior margin of tectum weakly convex and slightly waved. Rostrum 40 μm long, 22 μm wide, nearly lanceolate, not reaching to level of distal end of palp. Rostral setae two pairs as follows: Proximal pair long and thick at just anterior to swollen part of rostrum; distal pair short, at just anterior to proximal pair. Rostral sulcus short, barely reaching to level of proximal rostral setae. Chelicera (Fig. 10B) elongate, with basal segment 76 μm long, 24 μm wide, without clear ornamentation. Movable digit 15 μm long, with 11-12 minute denticles along dorsal edge. Fixed digit 13 μm long, extending slightly proximally to distal end of movable digit. Palp (Fig. 10C) 28 μm long; P-1, length/width 0.38, short and cylindrical; P-2, length/width 0.40, longest and robust, very faintly reticulated, with a long filiform seta distidorsally; P-3, length/width 0.25, short and cylindrical; P-4, length/width 1.75, conical, with three short and thick filiform setae intermediately, and two appressed blunt spiniform projection terminally.

Legs (Fig. 11A-D): Length of legs I, II, III, IV = 208, 208, 214, 214 μm , respectively. Ornamentation indistinct. Each tarsus furnished with claw fossa, without ventral seta. Lateral claw with rake-like accessory process bearing six to eight delicate teeth. Median claw and comb absent.

Carpite short and rod-like. Cavity in claw present. Short seta usually faintly rough, long seta smooth.

Leg chaetotaxy as follows: Trochanters I-IV, 1-1-1-0; basifemora, 2-3-2-2; telofemora, 7-7-5-4; genua, 6-6-3-4; tibiae, 7-7-5-6. As for large bipectinate seta: Genua I-IV, 1-0-0-1; tibiae, 2-1-1-1. Tarsus I (Fig. 12A) with three dorsal setae, one solenidion, one famulus, and four parambulacral setae (paired doublet euphathidia). Solenidion long bacilliform, on posterodorsal surface of claw fossa. Famulus papilliform with fine canaliculus, at just ventrally to solenidion. Tarsus II (Fig. 12B) with three dorsal setae, one solenidion, and four parambulacral setae. Solenidion long bacilliform on posterodorsal surface of claw fossa. Tarsus III (Fig. 12C) with four dorsal setae, and two parambulacral setae (one single euphathidium on posterior surface, one bud-shaped proeuphathidium on anterior surface). Tarsus IV (Fig. 12D) with three dorsal setae (one long robust filiform seta on basidorsal limb, one fronded seta on claw fossa, one fine filiform seta on anterodorsal surface), two parambulacral setae (one fine filiform proeuphathidium on posterior surface, one bud-shaped proeuphathidium on anterior surface).

Male (allotype). Idiosoma 332 μm long, 212 μm wide, gnathosomal-length/idiosomal-length 0.22; resembling the female in essential respects except for characters of body size, genitoanal region, and chaetotaxy of tarsus IV.

Body size somewhat smaller than that in the female.

Genitoanal region (Fig. 10D) furnished with a round subsurface pore, and a series of polygonal subsurface pores on each side of genital foramen, bearing terminally tufted 13 and 14 perigenital setae as arranged in Figure 10D. Genital foramen 46 μm long, 18 μm wide. Subgenital setae divided terminally; two setae on each genital sclerite, arranged 2-0. Genital acetabula internal, three pairs. Spermatophorotype (Fig. 10E) 48 μm long, 62 μm wide, massive and rhombic.

Tarsus IV (Fig. 12E) with three dorsal setae (one long robust filiform setae on basidorsal limb, one fronded seta on claw fossa, one branched seta on anterodorsal surface of claw fossa), two parambulacral setae (one long plumose proeuphathidium on posterior surface, one bud-shaped

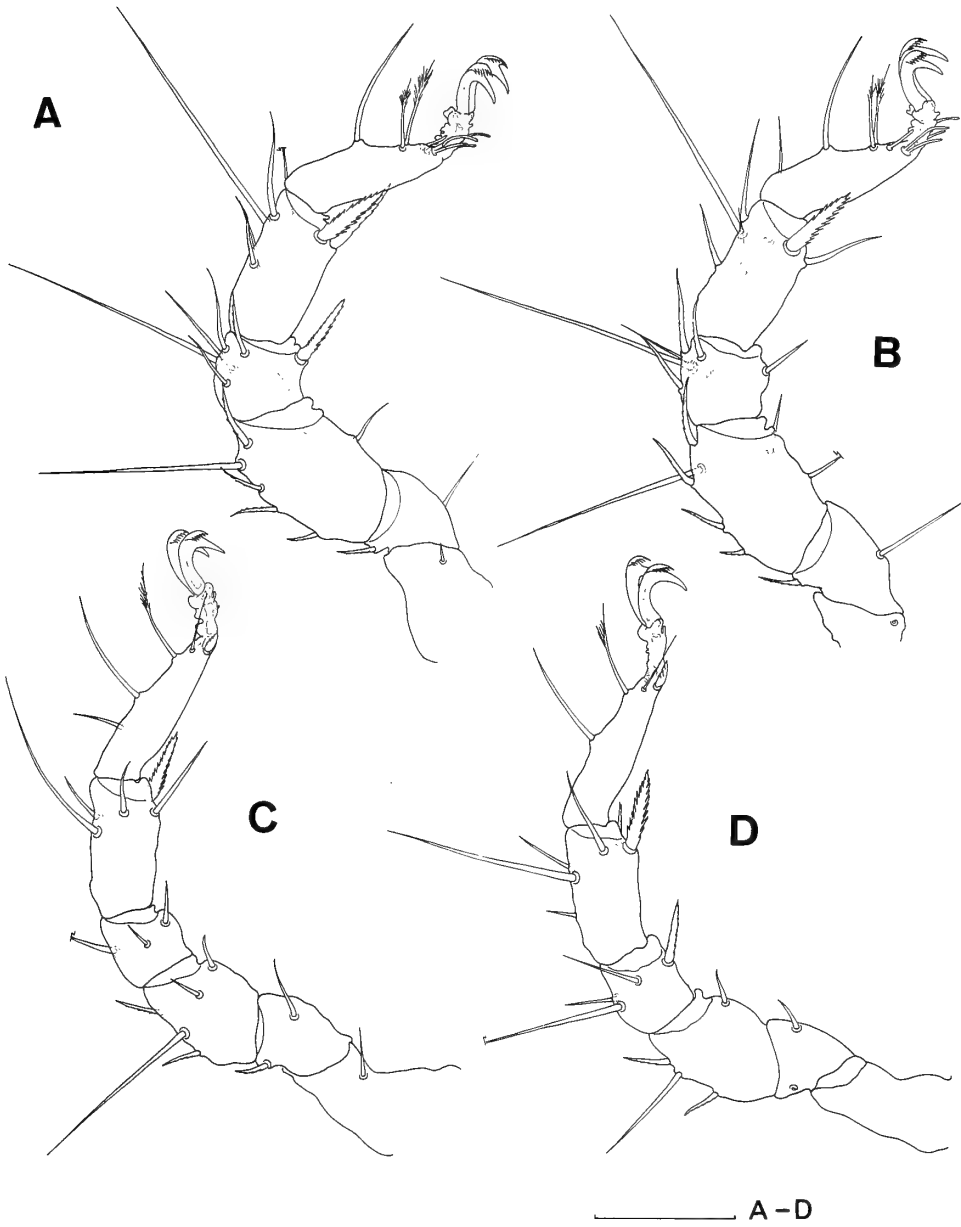


FIG. 11. *Rhombognathus ezoensis* sp. nov., Female (holotype). A, leg I (L); B, leg II (L); C, leg III (L); D, leg VI (L). Scale bar = 50 μm .

proeuphathidium on anterior surface).

Tritonymph (paratype). Idiosoma 332 μm long, 196 μm wide, gnathosomal-length/idiosomal-length 0.20.

Dorsum: AD concave posteriorly. PD convex anteriorly. AD and PD separated by interval

about two times as long as PD. OC with two subsurface pores at posteromedial margin.

Venter: AE furnished with a number of subsurface pores medially as well as along posterior margin, with two aes-ii-adj on each lateral margin. PE furnished with several subsurface pores along

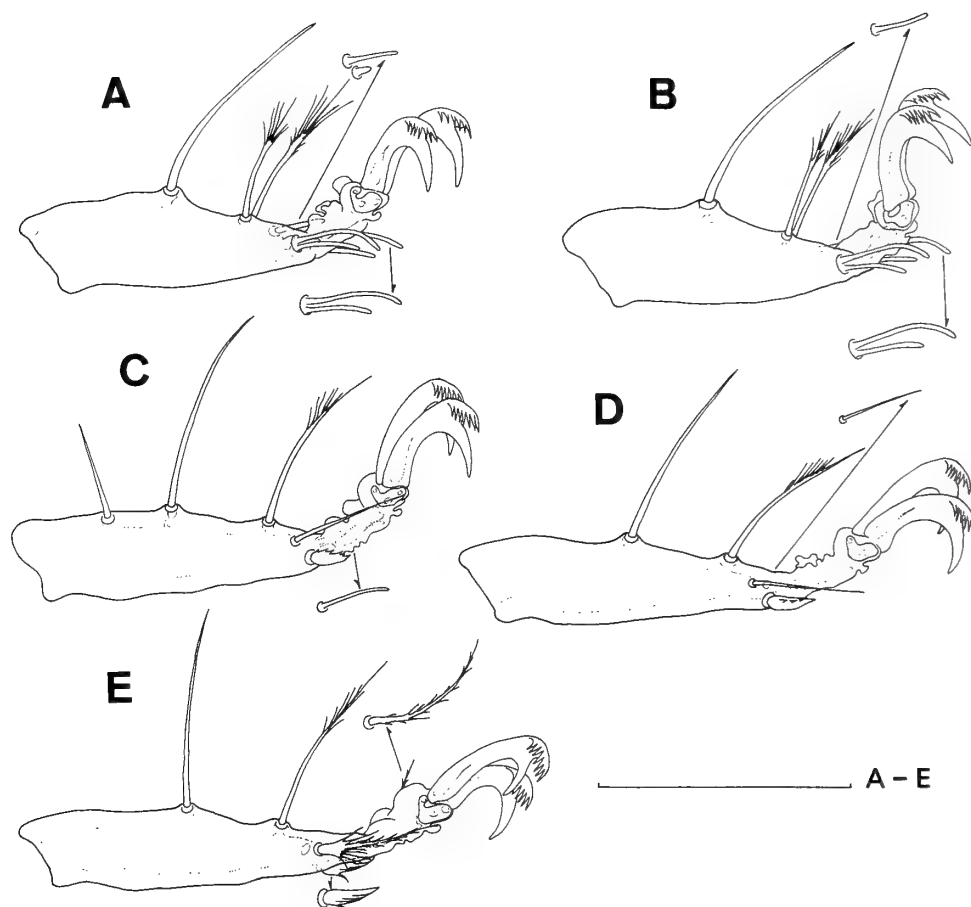


FIG. 12. *Rhombognathus ezoensis* sp. nov., Female (holotype). A, tarsus I (L); B, tarsus II (L); C, tarsus III (L); D, tarsus IV (L). Male (allotype). E, tarsus IV (R). Scale bar=50 μ m.

anteroventral margin. A small subsurface pore placed on membranous cuticle medially on each side, at level of anterior margin of PE.

Genitoanal region (Fig. 10F): Genital plate 64 μ m long, 52 μ m wide, bluntly protruded anteriorly, nearly truncated posteriorly, furnished with two short setae of which one is placed at 0.31, and another at 0.84 on each side, bearing a tiny subsurface pore at 0.43 on each lateral margin. Primordial genital slit occupied from 0.69 to 0.84, with three pairs of internal genital acetabula. Subgenital seta absent. Three minute subsurface pores placed on membranous cuticle slightly anterior to anterior margin of genital plate. Anal plate small, nearly truncated anteriorly.

Legs: Leg chaetotaxy of telofemora I-IV, 6-6-4-4; tibiae, 6-6-5-5. Tarsus with less fringed dorsal seta.

Deutonymph (paratype). Idiosoma 264 μ m long, 168 μ m wide, gnathosomal-length/idiosomal-length 0.19.

Dorsum: AD protruded posteriorly. PD small. Costa indistinct.

Venter: AE with one aes-ii-adj on each lateral margin. Left PE with two pes-iii-adj of which one very minute, whereas right PE with only one pes-iii-adj.

Genitoanal region (Fig. 10G): Genital plate 38 μ m long, 30 μ m wide, furnished with primordial genital slit, with two pairs of internal genital

acetabula. Genital seta absent.

Legs: leg chaetotaxy of basifemora I-IV, 2-3-2-1; telofemora, 4-4-3-2; genua, 5-5-3-4; tibiae, 5-6-5-5. Genu IV with one large but less pectinate seta.

Protonymph and larva: Not collected.

Morphological variation and abnormality: The number of the subsurface pores near the posterior margin of OC varies from two to four. The number of setae aes-ii-adj and pes-iii-adj on each side of the idiosoma in the adult varies from two to three, and one to two, respectively. The number of the perigenital setae on each side of the genital foramen varies from three to five in the female, and 12 to 14 in the male; this number varies according to specimens and even to each side of the genital foramen in one specimen. The leg chaetotaxy of the adult specimens varies as follows: Trochanters I-IV, (0,1)-(0,1)-1-0; basifemora, 2-(2,3)-2-(1,2); telofemora, (6,7)-7-(4,5,6)-(3,4,5); genua, (5,6)-(5,6)-3-4; tibiae, (6,7)-(6,7)-(5,6)-(5,6). One specimen lacks the dorsoproximal seta on tarsus III.

Etymology: The specific epithet is derived from "Ezo", the old Japanese name for Hokkaido.

Distribution: Widespread on the coast of Hokkaido.

Remarks: This new species is distinguishable from other *Rhombognathus* species by the following characters: Separated dorsal plates, two pairs of setae on PD, four pairs perigenital setae with characteristic arrangement (Fig. 9C) in the female, leg chaetotaxy and rake-like accessory process on lateral claw.

Rhombognathus ezoensis closely resembles *R. reticulatus* Krantz, 1976 [8] in the conformation of the dorsal plates and the idiosomal chaetotaxy of the dorsal and epimeral regions. However, *R. ezoensis* is distinctive from *reticulatus* in the follow-

ing characters (corresponding condition in the latter species in parentheses): (1) Perigenital filiform setae short (long); (2) four pairs of perigenital setae (three pairs); (3) leg chaetotaxy of telofemora I-IV, 7-7-5-4; genua, 6-6-3-4 (telofemora I-IV, 6-6-4-4; genua, 6-6-3-3); (4) genital plate completely separated from anal plate in the deutonymph (fused to form a single genitoanal plate).

ACKNOWLEDGMENTS

The author wishes to express his sincere thanks to Dr. H. Katakura (Hokkaido University) for his critical revision of the manuscript. Cordial thanks are also due to Professor G. W. Krantz (Oregon State University) for his valuable criticisms and suggestions in improving the manuscript.

REFERENCES

- 1 Trouessart, E. (1888) Note sur les Acariens marins recueillis par M. Giard au laboratoire maritime de Wimereux. C. R. Acad. Sci., **107**: 753-755.
- 2 Sokolov, I. (1952) Halacarae. Fauna S.S.S.R., **5**(5): 1-201.
- 3 Newell, I. (1947) A systematic and ecological study of the Halacaridae of eastern North America. Bull. Bingham Oceanogr. Coll., **10** (3): 1-232.
- 4 Newell, I. (1967) Abyssal Halacaridae (Acari) from the southeast Pacific. Pac. Insects, **9**: 693-708.
- 5 Newell, I. (1984) Antarctic Halacaroidae. Antarc. Res. Series, **40**: 1-284.
- 6 Bartsch, I. (1983) Zur Halacaridenfauna der Philippinen Beschreibung von fünf Arten der Gattung *Rhombognathus* (Acari, Halacaridae). Entomol. Mitt. zool. Mus. Hamburg, **7**: 399-416.
- 7 Bartsch, I. (1977) Interstitielle Fauna von Galapagos XX. Halacaridae (Acari). Mikrofauna Meeresbodens, **65**: 1-108.
- 8 Krantz, G. (1976) Arenicolous Halacaridae from the intertidal zone of Schooner Creek, Oregon (Acari: Prostigmata). Acarologia, **18**: 251-258.

[COMMUNICATION]

Nociception in Crocodiles: Capsaicin Instillation, Formalin and Hot Plate Tests

T. I. KANUI, K. HOLE¹ and J. O. MIARON

Department of Animal Physiology, University of Nairobi, Nairobi, Kenya, and

¹Department of Physiology, University of Bergen, Bergen, Norway

ABSTRACT—Three tests of nociception were adapted for the use in crocodiles (47.0–65.2 cm long). In the capsaicin instillation test, capsaicin in concentrations of 10^{-9} to 10^{-3} g/ml instilled in the eye induced concentration related protective reactions which were counted. In the formalin test, 150 μ l of 5% formalin was injected subcutaneously in the fore paw, and the time spent “lifting the foot” and “not using the foot” was recorded. In the hot plate test, the plate temperature was set at 55°C and the latency until the following behavioural categories occurred was recorded: “lifting toes”, “lifting foot”, and “attempt to escape”. This test could be repeated with similar results after an interval of 60 min.

It was concluded that the crocodile has a well developed nociceptive system, and it may be possible to study the function of this system using these modifications of well known tests of nociception.

INTRODUCTION

The physiology and anatomy of the nervous system of the crocodile is incompletely known. The embryonic development of crocodilian nervous system has been investigated [1]. Pain perception, and the regulation of pain sensitivity, are basic functions of the central nervous system, with a fundamental biological importance. Knowledge of the physiology of this sensory system and its regulation may be important for the understanding of the physiology and the behaviour of the animal.

MATERIALS AND METHODS

The crocodiles (*Crocodylus niloticus africana*)

weighed 231–1125 g, they were 47.0–65.2 cm long, and the abdominal circumference was 9–19 cm. They were estimated to be 4 to 10 months old. The animals were obtained from Mombasa (Kenya) and were transported to Nairobi for experimentation.

The animals were kept in a quiet room in an environment resembling their natural environment. Water was available, as well as stones and sand to lie on. The water temperature was $30.9 \pm 0.2^\circ\text{C}$ and the ambient temperature was $29.5 \pm 3.9^\circ\text{C}$. The dry surface temperature of the crocodiles was $31.3 \pm 0.2^\circ\text{C}$. Heating bulbs (250 W) were used for maintaining the temperature and evaporating water to maintain the humidity.

The experiments were started a month after the start of the acclimatization. During this period, the animals were handled daily.

Capsaicin instillation

Capsaicin (98%) was supplied by Sigma, U.S.A. A stock solution of capsaicin (1%) was prepared using a vehicle: 10% ethanol, 10% tween 80 and 80% of 0.9% NaCl. Further dilutions were made with 0.9% NaCl.

Capsaicin in concentrations between 10^{-9} g/ml and 10^{-2} g/ml were instilled into the eye according to Gamse *et al.* [2]. Two drops were instilled. The number of protective reactions such as blinking, wiping, blepharospasm, rubbing, head shaking and eyeball movements were counted using a manual counter, during the ensuing period. Blinking and blepharospasm were similar and were therefore scored together. The latency to the first reaction as well as the time-course of the reactions were determined.

In control experiments, the vehicle was instilled in the contralateral eye. The same eye was used more than once with at least 45 min intervals. Twelve crocodiles were used for the capsaicin experiment. Wire-mesh cages (60×40×27 cm) were used as observation cages.

Formalin test

The formalin test was adapted from that described in rats and mice [3, 4]. A volume of 150 μ l 5% formalin was injected subcutaneously in the left fore paw. Two categories of pain-induced behavior were scored: lifting the foot, and completely not using the foot. The crocodiles completely lifted the whole fore leg, from the surface of the observation cages, in the latter behaviour. The time spent in each behavioural category was recorded. Injection of 150 μ l 0.9% NaCl in the right fore paw was used as control. Five crocodiles were used. The sequence of saline or formalin injection was random, with an interval of at least 14 days.

The same observation cages were used as in the capsaicin instillation experiment.

Hotplate test

The apparatus used was an IITC Inc Model 35 D Analgesimeter, the temperature was set at 55°C.

Before testing on the hot plate, the animal was placed in a wiremesh cage for 60 min for drying of the skin. Three categories of pain related behaviour were scored: "lifting toes from the plate", "lifting foot", and "attempt to escape". The latency until the behaviour occurred was recorded.

Testing was repeated twice in the same animal with an interval of 60 min and the mean for the three trials was used as the response latency for the animal.

RESULTS

Instillation of capsaicin into the eye

Instillation of capsaicin into the eye produced a number of protective reactions. Blepharospasm was the most common response elicited. At the threshold dose (10^{-9} g/ml) blepharospasm persisted for 3.5 ± 0.5 min (mean \pm S.E.M). At a concentration of 10^{-3} g/ml, the highest dose studied, the duration of blepharospasm was $18.7 \pm$

1.0 min. A few trials at a concentration of 10^{-2} g/ml capsaicin resulted in closure of the eye for most of the observation period, and experiments using this concentration were discontinued.

The protective behaviour occurred immediately. There was a distinct dose-response relationship during the first 3 min when capsaicin was instilled at concentrations between 10^{-9} and 10^{-3} g/ml (Fig. 1). In this period the vehicle elicited 2.0 ± 0.3 protective reactions. The threshold concentration (10^{-9} g/ml) produced 5.5 ± 1.0 , while the highest concentration (10^{-3} g/ml) used produced 34.7 ± 5.0 protective reactions. Head shaking was observed 6 times: like wiping and eye-ball rolling, head shaking occurred at the highest concentration used (10^{-3} g/ml). These behaviours occurred during the first 2 min. The concentration (10^{-3} g/ml) produced 2.1 ± 0.8 wipings and 10.5 ± 5.2 eyeball movements. The head was raised and vigorously shaken from side to side. The ipsilateral hind paw was raised forwards and used to wipe the eye. Rubbing was scored together with wiping because of their similarity. The eyeball moved up and down its socket during rolling.

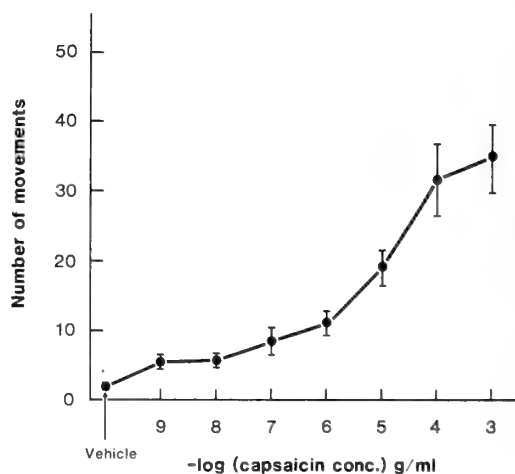


FIG. 1. Number of protective movements in the first 3 min after instillation of capsaicin (10^{-9} – 10^{-3} g/ml) or vehicle. Mean \pm S.E.M. $n=13$ for each concentration.

For all the concentrations of capsaicin used, most protective reactions occurred during the first 10 min (Fig. 2). No pain behaviour could be observed after the 40 min observation period. At a

concentration of 10^{-3} g/ml, repeated [5] instillation of capsaicin elicited 44.7 ± 4.5 , 51.2 ± 6.9 , 51.8 ± 6.7 , 50.3 ± 9.2 and 44.5 ± 5.3 protective reactions, during the first 3 min. No significant change in the response was observed at this and other concentrations used.

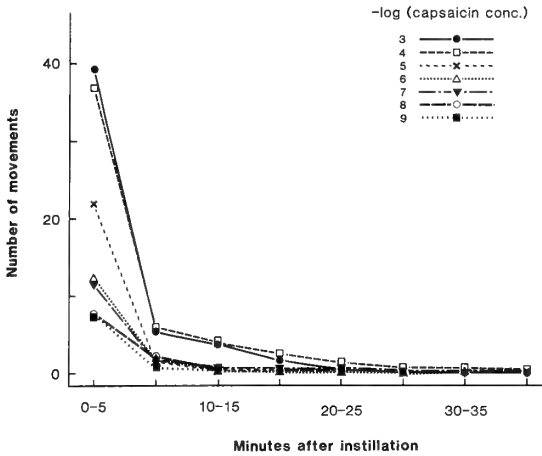


FIG. 2. Time-course of mean number of protective movements after instillation of capsaicin 10^{-9} – 10^{-3} g/ml. Blocks of 5 min. $n=13$ for each concentration.

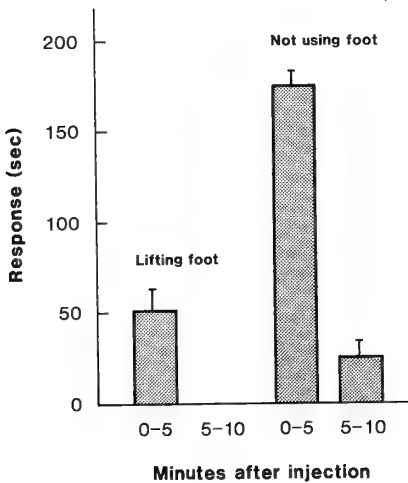


FIG. 3. Time spent "lifting the foot" and "not using the foot" in the formalin test. Blocks of 5 min observation periods. Mean \pm S.E.M. $n=5$.

The Formalin test

The formalin injection immediately induced pain related behavioural responses. "Lifting the foot" was observed only in the first 5 min period

after injection, while "not using the foot" was observed both in the first and the second 5 min period (Fig. 3). No pain behaviour was observed after 10 min.

Saline injections did not induce this pain behaviour.

The hot plate test

The response latencies for "lifting toes from the plate", "lifting foot", and "attempt to escape" are shown in Figure 4. There were only small and inconsistent differences in the results of the first, the second and the third trial, and no statistically significant difference when the response latencies for the second or the third trial were compared to the first trial ($P < 0.05$ for both comparisons for all three latencies, t-test).

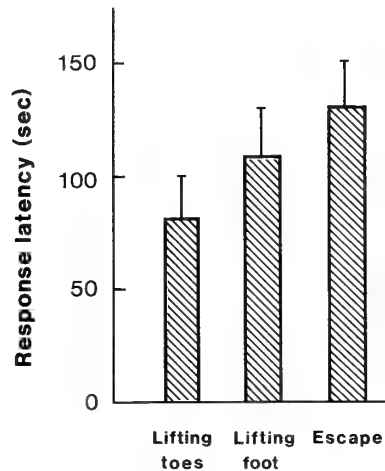


FIG. 4. Response latencies for "lifting toes", "lifting foot" and "attempt to escape" in the hot plate test. Mean \pm S.E.M. $n=5$ for animals ($n=15$ for trials).

DISCUSSION

Our observations indicate that crocodiles are very sensitive to capsaicin unlike amphibians [5] and birds [5–7]. In crocodiles, capsaicin instillation elicited behavioural responses similar to those reported in mammals [5, 8]. The threshold concentration of capsaicin (10^{-9} g/ml) that evoked protective reactions was considerably lower than that (10^{-6} g/ml) evoking responses in guinea pigs and rats [5, 8]. Surprisingly, although crocodiles were sensitive to capsaicin, repeated instillation of capsaicin did not produce any desensitizing effect.

Possibly, capsaicin in crocodiles does not cause a depletion of substance P which may be associated with desensitization [9, 10].

The formalin test in mammals (rat, mice, cat, monkey) elicits both acute and long-lasting pain [3, 4, 11]. The main behavioural responses in these animals are licking, scratching and not using the injected limb. Crocodiles were sensitive to 5% formalin and responded by lifting the foot and not using the foot. The crocodiles did not show a second phase of pain as reported in mammals [3, 4, 11]. The second phase is probably induced by inflammation [3, 4], and requires a stronger stimulus to be elicited than the first phase [Rosland *et al.*, unpubl. data]. The inflammatory stimulus is strong enough to induce licking and scratching in rats and mice, however, it may not be strong enough to induce "lifting the foot" and "not using the foot" in crocodiles.

In the hot plate test, the first response observed in the crocodile was the lifting of one or more toes. It seems that the latency until this response occurs, may be used as a measure of the pain threshold, and may be the response in the crocodile that is the closest to the hind paw lick response in mice and rats [12–15]. The escape response presumably occurs at a stimulus well above pain threshold. The skin temperature may be an important variable in test of nociception applying heat as the stimulus [16]. It is probably important therefore that the ambient temperature is kept constant and that the skin of the feet of the crocodiles is dried well before testing.

All the three tests described here seem to be suitable as tests of nociception in the crocodile. Comparing the three tests, the hot plate test has some advantages as in this test both threshold and suprathreshold responses can be easily and reliably scored, and the test may be repeated even after a rather short interval. We have found that the test is sensitive to morphine and other analgesic drugs [T. I. Kanui *et al.*, unpubl. data]. Since the stimulus as well as the response are different in the three tests, each may be useful for studying different aspects of the regulation of nociception. The tests may also be used to study the influence of drugs on this function of the nervous system in the crocodile.

It may be concluded that the crocodile has a well developed nociceptive system, and it may be possible to study the function of this system using modifications of well known tests of nociception. The nociceptive system is necessary for the survival of the crocodile in the wild. It is responsible for eliciting defense and protective reactions, when crocodiles are attacked by other wild animals or humans.

ACKNOWLEDGMENTS

This project was supported by the NORAD KEN 046 Project.

REFERENCES

- 1 Ferguson, M. W. J. (1985) In "Biology of the Reptilia". Ed. by C. Gans, F. Billet and P. F. A. Maderson, John Wiley and Sons, New York, pp. 329–492.
- 2 Gamse, R., Holzer, P. and Lembeck, F. (1980) *Brit. J. Pharmacol.*, **68**: 207–313.
- 3 Hunskaar, S., Fasmer, O. B. and Hole, K. (1985) *J. Neurosc. Meth.*, **14**: 69–76.
- 4 Dubuisson, D. and Dennis, S. G. (1977) *Pain*, **4**: 161–174.
- 5 Szolcsányi, J., Sann, H. and Pierau, F.-K. (1986) *Pain*, **27**: 247–260.
- 6 Mason, R. J. and Maruniak, J. A. (1983) *Pharmacol. Biochem. Behav.*, **19**: 857–862.
- 7 Geissthövel, E. and Simon, E. (1984) In "Thermal Physiology". Ed. by J. R. S. Hales, Raven Press, New York, pp. 29–32.
- 8 Makara, G. B. (1970) *Acta. Physiol. Acad. Sci. Hung.*, **38**: 393–399.
- 9 Jessel, T. M., Iversen, L. L. and Cuello, A. C. (1978) *Brain Res.*, **152**: 183–188.
- 10 Gamse, R., Leeman, S. E., Holzer, P. and Lembeck, F. (1981) *Naunyn-Schmiedeberg's Arch. Exp. Path. Pharmacol.*, **317**: 140–148.
- 11 Alreja, M., Mutalik, P., Nayar, U. and Manchada, S. K. (1984) *Pain*, **20**: 97–105.
- 12 Woolfe, G. and MacDonald, A. D. (1944) *J. Pharmacol. Exp. Therap.*, **80**: 300–307.
- 13 Eddy, N. B., Touchberry, C. F. and Lieberman, J. E. (1950) *J. Pharmacol. Exp. Therap.*, **98**: 121–137.
- 14 Kitchen, I. and Crowder, M. (1985) *J. Pharmacol. Meth.*, **13**: 1–7.
- 15 Ankier, S. I. (1974) *Eur. J. Pharmacol.*, **27**: 1–4.
- 16 Tjlosen, A., Berge, O.-G., Eide, P. K., Broch, O. J. and Hole, K. (1988) *Pain*, **33**: 225–231.

[COMMUNICATION]

Critical Period of Induction by Tamoxifen of Genital Organ Abnormalities in Male MiceSATOKO IRISAWA, TAISEN IGUCHI¹ and NOBORU TAKASUGI¹*Laboratory of Biology, Tokyo Kasei Gakuin University, Machida 194-02, and*¹ *Department of Biology, Yokohama City University,
Kanazawa-ku, Yokohama 236, Japan*

ABSTRACT—C57BL/Tw male mice given 5 daily injections of 100 μ g tamoxifen (Tx) starting on the day of birth (0 day) were examined at 5, 10, 15, 20 and 30 days of age. Body and organ weights and diameter of seminiferous tubules in Tx mice were significantly smaller than those of the age-matched controls. Spermatogenesis was found in 30-day-old control mice, but was completely suppressed in Tx mice at the same age. In addition, 60-day-old male mice given neonatal injections of 100 μ g clomiphene (Clm) or nafoxidine (Naf), and those given injections of 100 μ g Tx beginning at different early postnatal ages were also examined. Tx caused more damage to testis than did Clm and Naf. Mean spermatogenic index and diameters of seminiferous tubules in mice given Tx beginning at 0 day were significantly smaller than those in mice given Tx starting at 5 days. These findings suggest that the critical period of producing the deleterious effects of Tx on the genital organs is present within 3 days after birth.

mammals [15–23]. In male mice, neonatal exposure to Tx resulted in permanent suppression of spermatogenesis and atrophy of genital organs [24] as reported in mice treated neonatally with estrogenic hormones [3–6]. Recently, various abnormalities of pelvis [25, 26] and os penis [27] were found in male mice treated neonatally with Tx. Other antiestrogens, clomiphene (Clm) and nafoxidine (Naf) also caused various abnormalities in genital organs of mammals [28]. However, none of the previous studies examined the responsiveness of mouse genital organs to administration of Tx starting at different early postnatal ages. The present study was aimed at examining the Tx-induced sequential changes in genital organs and their responsiveness to Tx in neonatal and early-postnatal male mice.

INTRODUCTION

Perinatal treatment with natural and synthetic estrogens including diethylstilbestrol (DES) induces permanent suppression of spermatogenesis in the testes of rats and mice [1–12]. Tamoxifen (Tx), one of triphenylethylene derivatives, inhibits estrogen action by competing with the hormone in binding the estrogen receptor. Tx, therefore, has been widely used for the therapy of estrogen-receptor positive human breast cancer [13, 14]. On the other hand, Tx has been reported as producing estrogenic effects on uteri and vaginae of various

MATERIALS AND METHODS

C57BL/Tw male mice were kept under 12 hr light/12 hr dark condition at 23–25°C temperature. Mice were given 5 daily subcutaneous injections of 100 μ g tamoxifen (Tx, mw=563.6) (Sigma, St. Louis, MO), suspended in 0.02 ml of saline and of the vehicle alone, starting within 24 hr after birth and killed by ether anesthesia at ages of 5, 10, 20, 30 and 60 days. Mice were also given daily injections of 100 μ g Tx and of the vehicle alone for 5 days starting on the day of birth (0 day), 3, 5, 7 and 10 days. In addition, two groups of mice were neonatally given 5 daily injections of 100 μ g clomiphene citrate (Clm, mw=598.1) (Sigma) and

100 μ g nafoxidine hydrochloride (Naf, mw=462.0) (Sigma) beginning on the day of birth, respectively. These animals were killed at 60 days.

Pairs of testes, seminal vesicles with coagulating glands and epididymides were weighed separately. These organs were fixed in Bouin's solution, embedded in paraffin and serially sectioned at 8 μ m. The sections were stained with Delafield's hematoxylin and eosin. In 5 transverse sections randomly selected from each testis, 20 seminiferous tubules were examined to count the number of seminiferous tubules containing mature spermatozoa. Percent ratio of the tubules showing active spermatogenesis was calculated for each mouse on the basis of 200 tubules and was used as the index of spermatogenic activity [5]. Diameters of seminiferous tubules were measured with a micrometer. Data were analysed by Duncan's multiple range test and Fisher's exact probability test.

RESULTS AND DISCUSSION

Weights of body, testes and epididymides in 60-day-old mice treated neonatally with a daily dose of 100 μ g of Tx, Clm or Naf were significantly

smaller than those in the controls except for the testis weight in Naf mice (Table 1). In mice given Clm injections neonatally, however, the body weights were significantly greater than in mice given Tx injections starting at 0 day. Weight of testes in mice given Tx starting at 5, 7 and 10 days, respectively, were significantly greater compared with that in mice given Tx starting at 0 day. Testes and epididymides in Naf mice, were also significantly heavier than those in mice given Tx from 0 day.

As shown in Figure 1, body weights in neonatally Tx-treated mice at ages of 10, 30 and 60 days were significantly smaller than those in the age-matched controls. Weights of epididymides (at 30 and 60 days), seminal vesicles with coagulating glands (at 60 days) and testes (at 30 and 60 days) were significantly smaller than those of the corresponding controls. The testes in 5-day-old Tx and control mice contained seminiferous tubules with spermatogonia and spermatocytes and interstitial cells.

Spermatozoa and spermatids were found in the tubules of control mice at 30 and 60 days. In the controls, the mean spermatogenic index was 30.6

TABLE 1. Body and organ weights in 60-day-old C57BL/Tw male mice treated with antiestrogens

Treatment and period (days of age)	No. of mice	Body weight (g)	Organ weights (mg/20 g body weight)	
			testes	epididymides
Saline				
*0-4	10	18.4 \pm 0.7 ^a	135.7 \pm 8.4	52.1 \pm 3.3
100 μ g tamoxifen				
0-4	10	12.4 \pm 0.9 ^b	43.8 \pm 5.6 ^b	20.4 \pm 3.0 ^b
3-7	15	12.3 \pm 0.9 ^b	63.2 \pm 5.0 ^b	18.5 \pm 1.9 ^b
5-9	10	14.3 \pm 0.9 ^b	68.1 \pm 7.1 ^{bc}	22.0 \pm 1.3 ^b
7-11	10	15.0 \pm 0.9 ^c	105.4 \pm 12.0 ^{cd}	34.9 \pm 3.3 ^{bd}
10-14	13	15.1 \pm 1.1 ^c	104.1 \pm 9.9 ^{cd}	33.7 \pm 1.8 ^{bd}
100 μ g clomiphene				
0-4	6	15.5 \pm 1.0 ^{ce}	66.6 \pm 4.3 ^b	23.2 \pm 1.3 ^b
100 μ g nafoxidine				
0-4	5	12.0 \pm 1.3 ^b	123.4 \pm 15.6 ^d	39.0 \pm 4.6 ^{bd}

* The day of birth is indicated as 0; a, Mean \pm S.E.

^b P<0.01 vs controls (Duncan's multiple range test)

^c P<0.05 vs controls (Duncan's multiple range test)

^d P<0.01 vs 100 μ g tamoxifen 0-4 (Duncan's multiple range test)

^e P<0.05 vs 100 μ g tamoxifen 0-4 (Duncan's multiple range test)

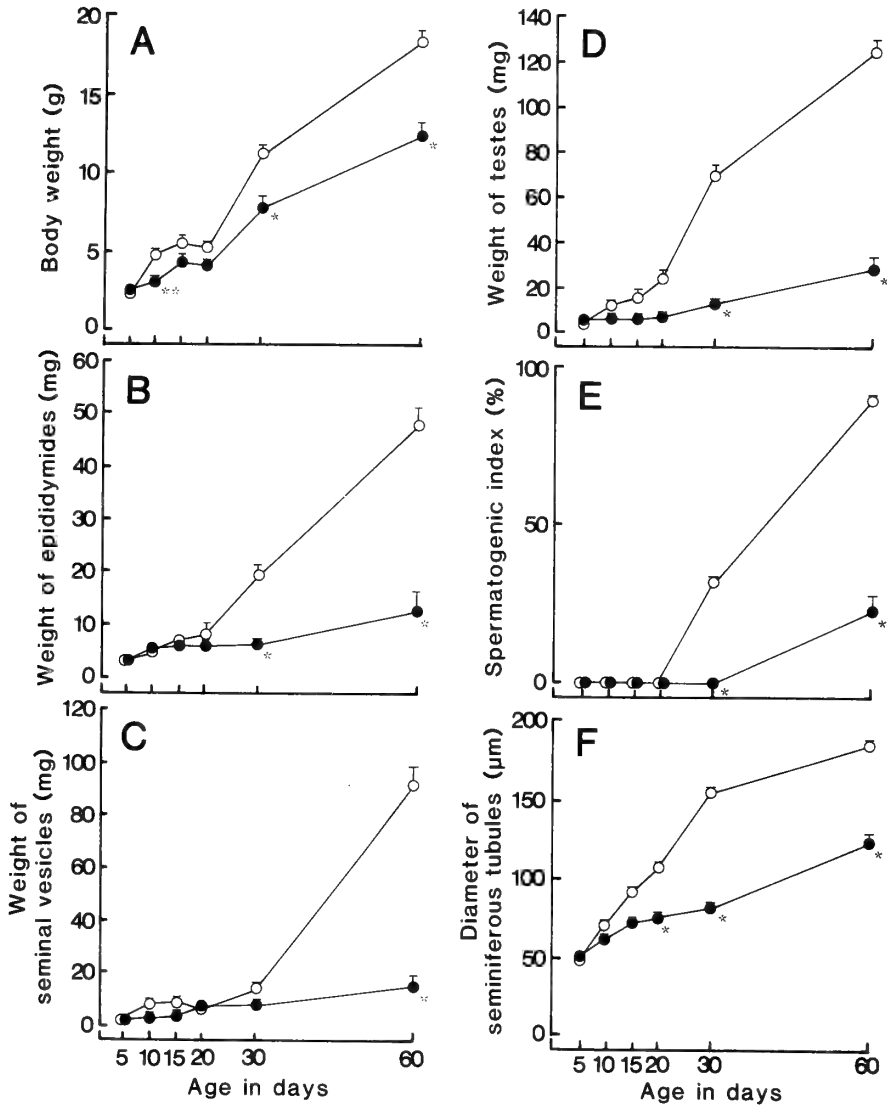


FIG. 1. Sequential changes in body weight (A), weights of epididymides (B), seminal vesicles with coagulating glands (C), testes (D), spermatogenic index (E) and diameters of seminiferous tubules (F) in mice given daily injections of 100 µg Tx (●) or the vehicle alone (○) starting on the day of birth. * $p < 0.01$, ** $p < 0.05$ vs respective controls.

$\pm 0.9\%$ at 30 days, and $88.7 \pm 1.9\%$ at 60 days. In contrast, the testis of Tx mice began to show spermatogenesis later than 30 days of age. Seminiferous tubules in Tx mice at ages of 20 and 30 days were smaller in diameter, lacking spermatids and spermatozoa. In 60-day-old Tx mice, spermatogenic index ($22.2 \pm 8.0\%$) was significantly lower than the value in the age-matched controls. In Clm and Naf mice at 60 days, spermatogenic indices

were not significantly lower than that in the controls (Table 2). Diameters of seminiferous tubules increased with age, from 5 to 60 days, in both control and Tx mice, though the diameters in Tx mice were significantly smaller than those in the corresponding controls after 20 days.

In all groups of 60-day-old mice given 5 daily Tx injections, spermatogenic indices and diameters of seminiferous tubules were significantly smaller

TABLE 2. Changes in genital organs in 60-day-old C57BL/Tw male mice treated neonatally with antiestrogens

Treatment and period (days of age)	No. of mice	No. of mice showing varying spermatogenic indices				Mean spermatogenic index (%)	Diameter of seminiferous tubules (μm)
		$\leq 25\%$	$\leq 50\%$	$\leq 75\%$	$> 75\%$		
Saline							
0-4	10	0	0	1	9	88.7 ± 1.9^a	183.0 ± 3.0
100 μg tamoxifen							
0-4	10	7 ^f	1	1	1	22.2 ± 8.0^b	121.2 ± 4.4^b
3-7	15	8 ^f	1	3	3	37.9 ± 9.1^b	118.4 ± 5.2^b
5-9	10	2	2	4	2	53.4 ± 8.9^{be}	142.4 ± 6.2^{be}
7-11	10	2	1	3	4	59.8 ± 9.0^{cd}	146.6 ± 7.5^{bd}
10-14	13	2	3	3	5	54.6 ± 8.1^{be}	155.4 ± 6.5^{bd}
100 μg clomiphene							
0-4	6	0	0	4	2	68.8 ± 4.4^d	145.3 ± 8.7^{bd}
100 μg nafoxidine							
0-4	5	0	0	3	2	74.4 ± 3.6^d	152.8 ± 6.3^{bd}

^a Mean \pm S.E.; b, $P < 0.01$ vs controls (Duncan's multiple range test)

^c $P < 0.05$ vs controls (Duncan's multiple range test)

^d $P < 0.01$ vs 100 μg tamoxifen 0-4 (Duncan's multiple range test)

^e $P < 0.05$ vs 100 μg tamoxifen 0-4 (Duncan's multiple range test)

^f $P < 0.01$ vs controls (Fisher's exact probability test)

than in the controls. Clm and Naf mice at 60 days also showed significantly smaller tubules diameter than those in the controls (Table 2). In mice given Tx starting at 0 and 3 days, the number of mice with spermatogenic indices lower than 25% was significantly larger compared to that of the controls ($p < 0.01$, Fisher's exact probability test).

In Tx mice at 60 days, epididymal ducts defective in stereocilia contained no spermatozoa in the lumen, while in the age-matched controls, epididymal ducts lined with a well-ciliated epithelium contained numerous spermatozoa. Seminal vesicles of these control mice contained a large amount of eosinophilic secretion in the lumen, whereas no such secretion was found in Tx mice at the same age. These findings suggest that the testis of 60-day-old Tx mice failed to secrete an amount of androgen sufficient for maintaining the sex accessory organs or that the testis was decreased in responsiveness to gonadotropin in Tx mice.

Previous studies have demonstrated that in neonatally estrogen-treated male rats and mice, the long-lasting suppression of spermatogenesis is caused by direct effects of estrogen on the testis

and/or by indirect effects through a permanent alteration of hypothalamo-hypophysial system [6, 9, 17, 25]. Male mice exposed neonatally to Tx also showed permanent suppression of the spermatogenesis and atrophy of the genital organs [24], suggesting that Tx has a side of estrogen agonist. It is presumable, therefore, that Tx acts directly and/or indirectly through the alteration of gonadotropin secretion (FSH and/or LH) on the testis.

The present study showed varying degrees of spermatogenesis suppression and genital organ abnormalities in male mice given Tx starting at 0, 3, 5, 7 and 10 days, the highest degree being found in two groups of mice given Tx beginning at 0 and 3 days. It is suggested, therefore, that in mice, the critical period of Tx induction of male genital organ dysfunction and abnormalities is present within 3 days after birth. Tx has been used for the therapy of estrogen-reactive human breast cancer; however, on the basis of the present study, the possibility cannot be excluded that male fetuses of pregnant women treated with Tx for the breast cancer exhibits postnatally a long-lasting testicular dysfunction, since neonatal mice are approximate-

ly at the same stage as that of the 16- to 20-week human fetuses [29].

ACKNOWLEDGMENTS

This work was supported by Grants-in-Aid from the Ministry of Education, Science and Culture, Japan.

REFERENCES

- 1 Takewaki, K. and Takasugi, N. (1953) *Annot. Zool. Japon.*, **26**: 99–105.
- 2 Arai, Y. (1964) *Endocrinol. Japon.*, **11**: 153–158.
- 3 Mori, T. (1967) *J. Fac. Sci. Univ. Tokyo, IV*, **11**: 243–254.
- 4 Takasugi, N. (1970) *Endocrinol. Japon.*, **17**: 277–281.
- 5 Takasugi, N. and Furukawa, M. (1972) *Endocrinol. Japon.*, **19**: 417–422.
- 6 Ohta, Y. and Takasugi, N. (1974) *Endocrinol. Japon.*, **21**: 183–190.
- 7 McLachlan, J. A., Newbold, R. R. and Bullock, B. (1975) *Science*, **190**: 991–992.
- 8 Jones, L. A. (1980) *Proc. Soc. Exp. Biol. Med.*, **165**: 17–25.
- 9 Arai, Y., Mori, T., Suzuki, Y. and Bern, H. A. (1983) *Int. Rev. Cytol.*, **84**: 235–268.
- 10 Takasugi, N., Tanaka, M. and Kato, C. (1983) *Endocrinol. Japon.*, **30**: 35–42.
- 11 Yasuda, Y., Kihara, T. and Tanimura, T. (1985) *Teratology*, **32**: 113–118.
- 12 Yasuda, Y., Ohara, I., Konishi, H. and Tanimura, T. (1988) *Am. J. Obstet. Gynecol.*, **159**: 1246–1250.
- 13 Jordan, V. C. and Dowse, L. J. (1976) *J. Endocr.*, **68**: 297–303.
- 14 Furr, B. J. A. and Jordan, V. C. (1984) *Pharmacol. Ther.*, **25**: 127–205.
- 15 Harper, M. J. K. and Walpole, A. L. (1967) *J. Reprod. Fert.*, **13**: 101–119.
- 16 Terenius, L. (1971) *Acta Endocrinol.*, **66**: 431–447.
- 17 Chamness, G. C., Bannayan, G. A., Landry Jr., L. A., Sheridan, P. J. and McGuire, M. L. (1979) *Biol. Reprod.*, **21**: 1087–1090.
- 18 Nguyen, B. L., Giambiagi, N., Mayrand, C., Lecerf, F. and Pasqualini, J. R. (1986) *Endocrinology*, **119**: 978–988.
- 19 Pasqualini, J. R. and Lecerf, F. (1985) *J. Endocr.*, **110**: 197–202.
- 20 Pasqualini, J. R., Giambiagi, Sumida, C., Nguyen, B.-L., Gelly, C., Mayrand, C. and Lecerf, F. (1986) *J. Steroid Biochem.*, **24**: 99–108.
- 21 Lecerf, F., Nguyen, B.-L. and Pasqualini, J. R. (1988) *Acta Endocrinol.*, **119**: 85–90.
- 22 Iguchi, T., Todoroki, R., Yamaguchi, S. and Takasugi, N. (1989) *Acta Anat.*, **136**: 146–154.
- 23 Ohta, Y., Iguchi, T. and Takasugi, N. (1989) *Reprod. Toxicol.*, **3**: 207–212.
- 24 Iguchi, T. and Hirokawa, M. (1986) *Proc. Japan Acad., Ser. B*, **62**: 157–160.
- 25 Iguchi, T., Hirokawa, M. and Takasugi, N. (1986) *Toxicology*, **42**: 1–11.
- 26 Iguchi, T., Irisawa, S., Uchima, F.-D. A. and Takasugi, N. (1988) *Reprod. Toxicol.*, **2**: 127–134.
- 27 Irisawa, S., Iguchi, T. and Takasugi, N. (1988) *Zool. Sci.* **5**: 1315.
- 28 Clark, J. H. and McCormack, S. A. (1980) *Science*, **197**: 164–165.
- 29 Kohrman, A. F. (1978) *Pediatrics* **62**: 1143–1150.

[COMMUNICATION]

Photoperiodic Influences on Pheromonal Delay of Puberty in Young Female Wild Mice

SUBHASH C. PANDEY and SHEO D. PANDEY

Department of Zoology, Christ Church College, Kanpur, India

ABSTRACT—Individually housed young females were painted on their external nares with distilled water or urine collected from donor females subjected to different photoperiodic treatments. Young painted with distilled water attained puberty significantly earlier than those painted with urine from donors under laboratory light condition or under short photoperiod. Urine of donors under long photoperiodic treatment did not delay the pubertal onset as the mean time taken for occurrence of first vaginal estrus in such urine-painted young was not significantly different from that of water-painted control young.

INTRODUCTION

Urinary pheromones in laboratory mice can accelerate or delay the onset of puberty in juvenile females. Sexual maturation of prepuberal females is accelerated by exposure to adult males or to their urine [1]. Young females living in groups or raised with adult females attain puberty later than those living in isolation [2]. The delaying effect is chemically mediated through urine collected from grouped females [3]. The acceleration and delay of puberty also occur in wild mice and the causative factors have been found to be present in the urine of male and female, respectively [4].

Naturally occurring variations in environmental factors influence the efficiency of different chemosignals modulating various physiological and behavioral activities in mammals [5]. Seasonal variation has been reported in pheromonal acceleration and delay of puberty in female laboratory mice [6]. Continuously breeding house mice

exhibit seasonal patterns of reproductive activity in certain regions [7]. Long diurnal photoperiod (16L:8D) abolishes mutual suppression of estrus in sparsely housed females at 36–38°C (our unpublished observations). For animals inhabiting wild, the interactions between social and environmental factors are potentially important. The present effort was therefore aimed to determine the relative influence of the day length and the puberty-delaying chemosignal of female origin on sexual maturation in young females.

MATERIALS AND METHODS

The wild mice, *Mus musculus domesticus*, employed in this study were trapped from the field and maintained in the laboratory on a diet consisting of soaked gram, boiled rice and milk. Water was available *ad libitum*. Forty eight prepuberal females (subject females) weighing 4.6 ± 0.58 g were randomly divided into 4 groups and housed individually in isolation cages (34×18×14 cm) under laboratory conditions of light (ca 13 hr) and temperature (30–38°C). There were 8 females in group A and D and 16 each in group B and C. The subject females were painted daily on the their external nares with distilled water (group A) or with diluted urine pooled from different donor females (group B, C and D; Table 1).

Adult females which served as donors were housed in colony cages (30×30×30 cm) at a density of 10 mice/cage. These donors were either held under laboratory light condition (LLC) or exposed to cool white fluorescent light of long (16L:8D) and short (8L:16D) duration at an

TABLE 1. Mean time taken for the occurrence of first vaginal estrus in young females painted with water or urine from donor females exposed to different photoperiods

Group	Painting material	Mean time (in days) taken for first vaginal oestrus to occur
A	Water (control)	27.3±0.78*
B	Urine of donors under long photoperiod (16L:8D)	28.4±0.35
C	Urine of donors under short photoperiod (8L:16D)	36.6±0.53*
D	Urine of donors under LLC	36.9±0.88

* Means connected with same vertical line are at par at 5% level of significance.

intensity of about 400 lux. The above photic treatments of donor females commenced 15 days before their urine was used in the experiment. Fresh urine was collected daily from all the donors by manual bladder palpation and diluted in distilled water (1:9). A drop (0.05 ml) of urine was applied twice daily at 9:00 and 17:00 hr with the help of a small paint brush and subjects were examined for the appearance of vaginal perforation. Starting on the day of vaginal perforation smears were collected daily until the occurrence of first vaginal estrus indicative of pubertal onset in females. The data were analysed by one way-analysis of variance.

RESULTS AND DISCUSSION

Onset of puberty as assessed by occurrence of the first vaginal estrus was delayed in subject females painted with urine of donors held under LLC or short-photoperiod. Control females painted with water exhibited first vaginal estrus significantly earlier than those painted with urine of above donors ($p < 0.01$). However, prepubertal females painted with urine of donors subjected to long photoperiodic treatment attained puberty at about the same time when it occurred in control females as the difference in mean time taken for first vaginal estrus in these two groups was not statistically significant (27.3 ± 0.78 days vs. 28.4 ± 0.35 days, C.D. = 2.25; Table 1).

Urine from adult donor females maintained under natural light: dark cycle exert a retardative effect on pubertal onset in young females. Results presented in the study demonstrate that the exposure of donor females to long day length

abolishes their puberty-delaying property. Exposure to short photoperiod is without any effect on the ability of donors to delay the sexual maturation. Evidently, the photoperiodic manipulations can alter the production/release of the delay chemosignal in adult donor females.

Seasonal breeding is a common reproductive strategy thought to increase the probability of survival of young [8]. In a seasonally changing environment, the day length has been suggested to be the most proximate signal that initiates reproductive activities in mammals [9]. Social factors acting in concert with environmental factors also influence puberty and reproductive processes in mammals [5, 6]. Adult females perhaps release the delay-chemosignal to communicate the adequacy of reproductive conditions to juvenile females [10]. Urine from isolated or sparsely housed adult females have been found ineffective in causing puberty delay in young female mice [11]. Seemingly, at higher population density when donor females release an effective amount of puberty-delaying chemosignal, long diurnal photoperiod (a signal of the onset of favorable breeding condition) diminishes the efficiency of the puberty-delaying cue in favor of propagation.

ACKNOWLEDGMENTS

This study was supported by a grant from the Department of Science and Technology to SDP and by an award of a Research Associateship to SCP from the Council of Scientific and Industrial Research of India.

REFERENCES

1. Bronson, F. H. and Maruniak, J. A. (1975) Biol.

- Reprod., **13**: 94–98.
- 2 Vadenbergh, J. G., Drickamer, L. C. and Colby, D. R. (1972) *J. Reprod. Fertil.*, **28**: 397–405.
 - 3 McIntosh, T. K. and Drickamer, L. C. (1977) *Anim. Behav.*, **25**: 99–104.
 - 4 Pandey, S. C. (1986) Studies on pheromones in wild mice. Ph.D. thesis, Kanpur Univ., Kanpur.
 - 5 Bronson, F. H. (1985) *Biol. Reprod.*, **32**: 1–26.
 - 6 Drickamer, L. C. (1984) *J. Reprod. Fertil.*, **72**: 55–58.
 - 7 Pelikan, J. (1981) *Symp. Zool. Soc. Lond.*, **47**: 205–230.
 - 8 Sadleir, R. M. F. S. (1969) *The Ecology of Reproduction in Wild and Domestic Mammals*. Methuen and Co., London.
 - 9 Negus, N. C. and Berger, P. J. (1972) In “Biology of Reproduction: Basic and Clinical Studies”. Ed. by J. T. Velardo and B. A. Kasprow, Third Pan American Congress on Anatomy, New Orleans, pp. 89–98.
 - 10 Drickamer, L. C. (1982) *Dev. Psychobiol.*, **15**: 433–442.
 - 11 Pandey, S. C. and Pandey, S. D. (1989) *Arch. Biol.*, (In press)

[COMMUNICATION]

Immunocytochemical and Ultrastructural Characterization of the Cells in the Pars Tuberalis of the Turtle, *Geoclemys reevesii*

YOSHIHIKO OOTA

*Biological Institute, Faculty of Science, Shizuoka University,
Shizuoka 422, Japan*

ABSTRACT—Using immunocytochemical and electron microscopical techniques, two distinct types of secretory cells were detected in the turtle pars tuberalis (PT). The cells showing positive immunoreaction to TSH-antiserum were exclusively found in the rostral PT, while those immunoreactive to FSH-antiserum were concentrated in the caudal PT.

INTRODUCTION

The identification of cell types producing different pituitary hormones has been established in the pars distalis (PD) of the reptilian pituitary gland by conventional staining methods [1–3], electron microscopy [2, 4, 5] and immunocytochemistry [5–8]. However, little attention has been paid to the pars tuberalis (PT), since PT is predominantly composed of chromophobic cells. A few ultrastructural studies showed the presence of secretory granules in some cells in the PT of the turtle [6, 8, 9]. Thus, to date, there is very little information concerning the functional significance of the PT. The present report describes the presence of cells immunoreactive to FSH- or TSH-antiserum in the turtle PT.

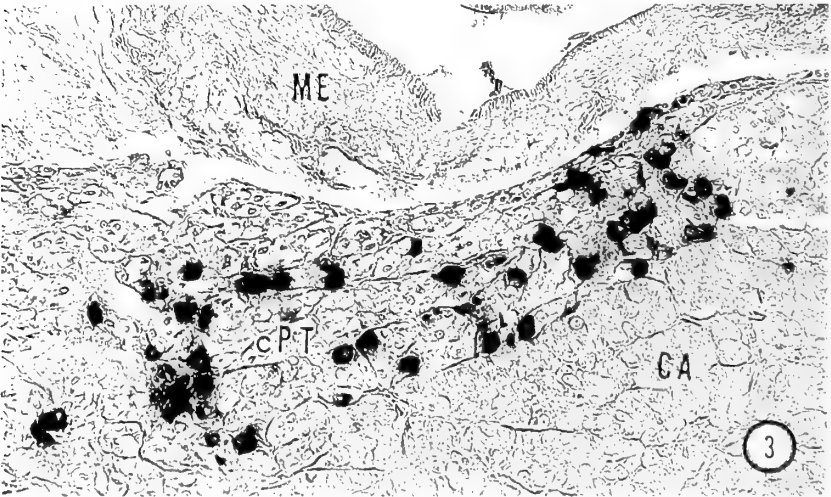
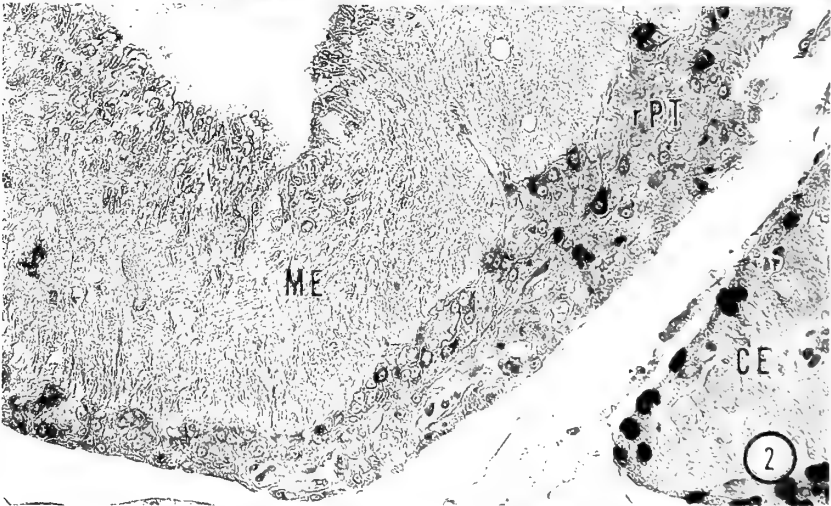
MATERIALS AND METHODS

Adult male and female turtles, *Geoclemys reevesii*, (carapace length, 160–200 mm) were obtained from a dealer. The hypothalamic regions of 6

animals were fixed in Bouin-Hollande sublimate solution. Sections were made at 6 μ m thickness through ordinary paraffin method. Some sections from each animal were stained with Azan or Gomori's paraldehyde fuchsin staining method. For immunocytochemical study, avidin-biotin-peroxidase complex method was used [10]. The following antisera raised against rabbits were used: anti-rat somatotropin, anti-rat prolactin, anti-rat TSH- β , anti-porcine ACTH, anti-bullfrog LH- β and anti-bullfrog FSH- β . All the primary antisera were kindly provided by Dr. K. Wakabayashi, Hormone Assay Center, Institute of Endocrinology, Gunma University. To ensure the specificity, all positive results were controlled by omission of the primary antisera and by a parallel incubation with antisera preabsorbed with the respective hormone. For electron microscopy, the hypothalamic regions of 8 animals were fixed in paraformaldehyde and glutaraldehyde, postfixed in 1% OsO₄, and embedded in Epon. Ultrathin sections were stained with uranyl acetate and lead citrate, and examined with a JEM-T8 electron microscope.

RESULTS AND DISCUSSION

In the turtle, the PT is well developed and can be divisible into rostral and caudal portions (Fig. 1). The rostral portion spreads under the median eminence as a thick layer of flattened epithelial cells. Between the rostral portion and the median eminence, lie capillaries of the primary plexus, whose blood drains into the hypophysial portal



vessels. The caudal portion is a thick cluster of cells situated dorsally to the anterior part of the PD. Histologically, the majority of the tuberal cells are chromophobic for the tinctorial stainings used in this study. A few cells showing slight affinity for AF appear only in the caudal portion of the PT, although there are numerous AF-positive cells in the PD.

In the rostral portion, some cells show a positive reaction to TSH-antiserum (Fig. 2). They are large and angular in shape. Cells reacting to FSH-antiserum are found to be concentrated mainly in the caudal portion, generally being spherical or ovoid in shape (Fig. 3). Preabsorption of the antisera with TSH and FSH and also omission of the respective primary antisera completely block the positive staining results. Throughout their distributions, the immunoreactive FSH-cells outnumber the immunoreactive TSH-cells (Figs. 2, 3). All the tuberal cells are non-reactive to other antisera than TSH- and FSH- antisera tested.

Although the PT tissue appears largely chromophobic with tinctorial staining methods it is very interesting to note that two types of cells were identified immunocytochemically: cells showing TSH-like immunoreactivity entirely in the rostral portion and cells showing FSH-like immunoreactivity largely in the caudal portion. In the PD, TSH- and FSH- immunoreactive cells have been frequently demonstrated in the caudal lobe of the turtle PD [5]. Since the turtle PT develops as a pair of lateral outgrowths from the anterior aspects of the pituitary anlage [7], it is possible that the cells reacting with TSH- and FSH- antisera in the PT might have migrated from the caudal lobe of the PD during embryogenesis.

Five secretory cell types have been recognized in the PD in various staining methods including immunocytochemical study [2, 5, 6, 11]. In this study, cells reacting with somatotropin-, prolactin-,

ACTH- and LH-antisera are frequently detected in the PD. However, cells immunoreacting to these antisera are undetectable in the PT.

Electron microscopically, two types of secretory cells can be distinguished. Type 1 cells are found in the rostral portion, although the number is not many. They are characterized by the presence of numerous granulated vesicles (150–200 nm in diameter) with variable electron densities (Fig. 4). The Golgi apparatus and rough endoplasmic reticulum are generally well developed. Type 2 cells are found in the caudal portion, and they contain electron-dense granules, mostly with diameters ranging 200 to 360 nm (Fig. 5). They present well developed Golgi apparatus, numerous and dilated cisternae of the rough endoplasmic reticulum. Ultrastructurally, presence of two types of secretory cells in the turtle PT has been reported previously [8]. Judging from the location and the difference in size of granules contained in respective cells and the present immunocytochemical findings, type 1 cells may be characterized as TSH-cells, whereas type 2 cells may be considered as FSH-cells.

The vascularization of the turtle hypophysis has been investigated previously, and portal vessels run through the rostral and caudal PT [12]. Although some cells of type 1 and type 2 are closely contacted with the capillaries of the portal system, extrusion of the secretory granules into the capillaries were not demonstrated. At present, it is not known to which extent these immunoreactive TSH- and FSH-cells in the PT are physiologically involved in the thyrotropic and gonadotropic functions of the pituitary. Presence of immunoreactive TSH- and FSH-cells has been reported in the PT of a variety of mammals [13].

FIGS. 1–3. Mid-sagittal sections through infundibulum and hypophysis. 1. Section stained with Azan stain. Pars tuberalis can be divisible into rostral (rPT) and caudal portion (cPT). Dotted line represents the boundary between rPT and cPT. CE, cephalic lobe of the pars distalis; ME, median eminence. Arrows indicate blood capillaries. $\times 115$. 2. Section immunostained with anti-TSH. Cells reacting to the antiserum are confined to the rPT. $\times 220$. 3. Section immunostained with anti-FSH. Cells reacting to the antiserum are common in the cPT. CA, caudal lobe of the pars distalis. $\times 220$.

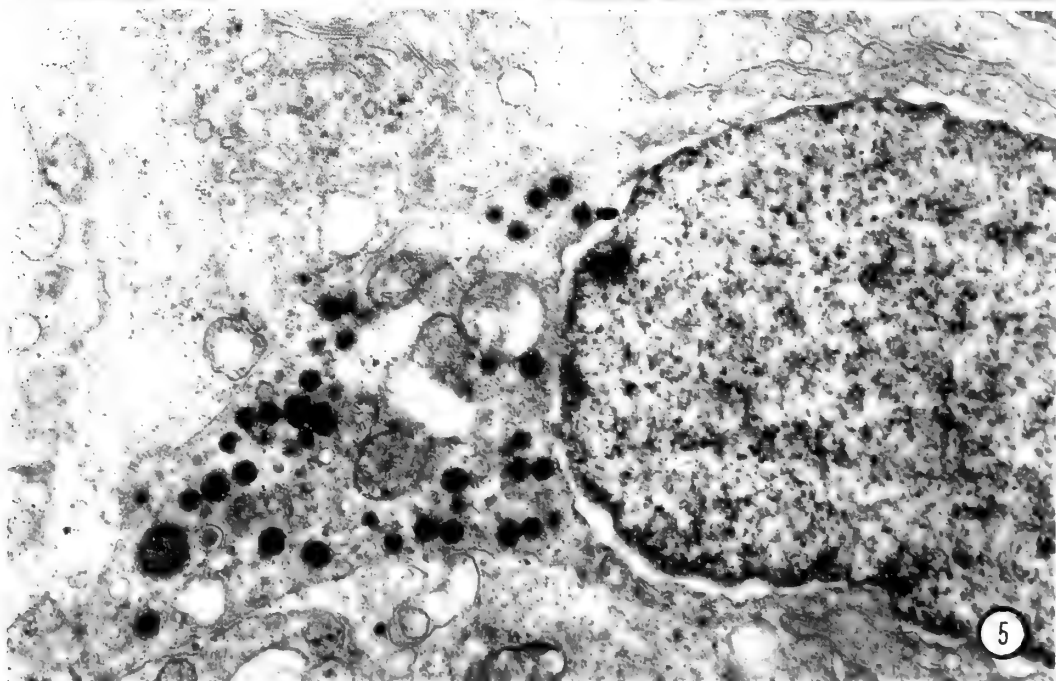
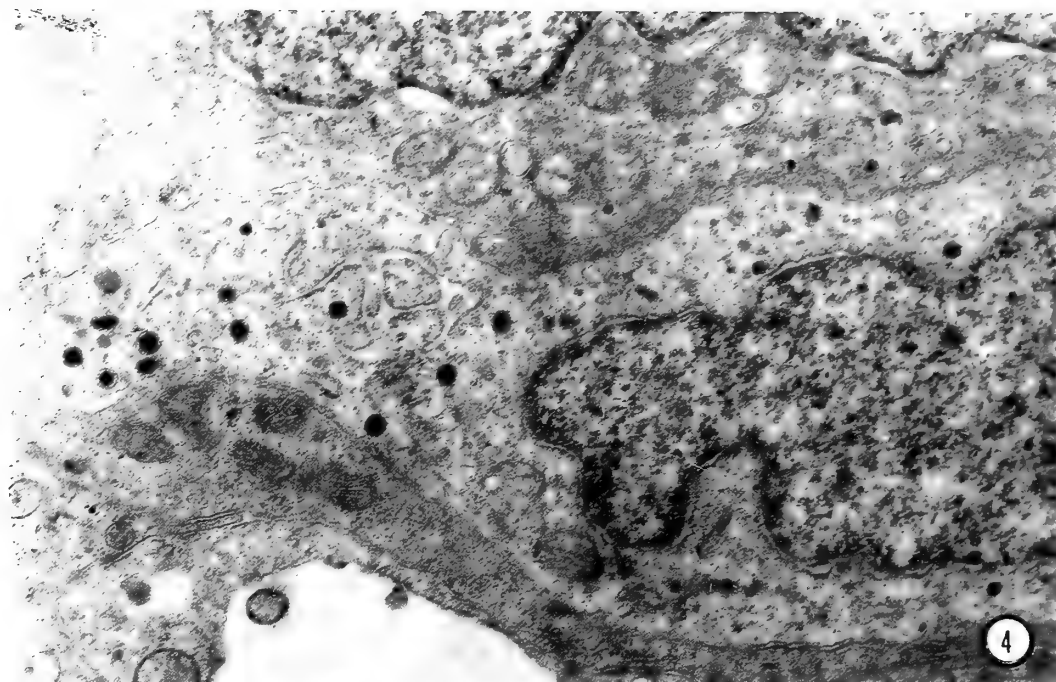


FIG. 4. Electron micrograph of the rostral portion of the PT. Note type 1 cell containing a few granulated vesicles. $\times 18,200$.

FIG. 5. Electron micrograph of outermost layer of the caudal portion of the PT. Note type 2 cell with many dark granules. $\times 18,200$.

REFERENCES

- 1 Saint Girons, H. (1970) In "Biology of the Reptilia". vol. 3, Ed. by C. Gans, Academic Press, London/New York, pp. 135-199.
- 2 Licht, P. and Pearson, A. K. (1978) *Int. Rev. Cytol., Suppl.*, **7**: 239-286.
- 3 Fitzgerald, K. T. (1979) *Gen. Comp. Endocrinol.*, **37**: 383-399.
- 4 Doerr-Schott, J. (1976) *Gen. Comp. Endocrinol.*, **28**: 513-529.
- 5 Mikami, S. (1986) In "Pars Distalis of the Pituitary Gland" Ed. by F. Yoshimura, and A. Gorbman, Elsevier Science Publ. B.V. pp. 71-79.
- 6 Pearson, A. K. and Licht, P. (1982) *Cell Tissue Res.*, **222**: 81-100.
- 7 Pearson, A. K. (1985) In "Biology of the Reptilia". vol. 14A Ed. by C. Gans, John Wiley & Sons, Inc., New York, pp. 681-719.
- 8 Oota, Y. (1980) *Rep. Fac. Sci., Shizuoka Univ.*, **14**: 63-74.
- 9 Dellmann, H.-D., Stoeckel, M. E., Hindelang-Gertner, C., Porte, A. and Stutinsky, F. (1974) *Cell Tissue Res.*, **148**: 313-329.
- 10 Hsu, S. M., Raine, L. and Fanger, H. (1981) *J. Histochem. Cytochem.*, **29**: 577-580.
- 11 Oota, Y. (1986) *Proc. Japan Acad.*, **62B**: 311-313.
- 12 Oota, Y. and Koshimizu, I. (1988) *Zool. Sci.*, **5**: 1013-1018.
- 13 Gross, D. S. (1984) *Gen. Comp. Endocrinol.*, **56**: 283-298.

[COMMUNICATION]

A Centrolenid-Like Anuran Larva from Southeast AsiaROBERT F. INGER and RICHARD J. WASSERSUG¹*Field Museum of Natural History, Roosevelt Road at Lake Shore Drive,
Chicago, Illinois 60605-2496, USA*

ABSTRACT—Vermiform tadpoles of the treefrog family, Centrolenidae, live buried in leaf litter on the margins of streams in the New World. These tadpoles have, among other features, long tails with reduced fins, small, subcutaneous eyes and highly vascularized, nearly pigmentless skin. We describe here the first tadpole from Southeast Asia with this morphology. The tadpole was collected in a microhabitat similar to the one in which centrolenid larvae have been found. Except for the fact that the Bornean larva has more denticle rows, the tadpoles are virtually identical in external morphology. The Bornean tadpole probably belongs to either a ranid or rhacophorid genus but, since no metamorphic individuals with adult diagnostic features have been found, the taxonomic assignment is uncertain.

INTRODUCTION

The Centrolenidae is a well-defined family of arboreal frogs restricted to Central and South America. Tadpoles have been described for less than a fifth of the 65 known species, yet those described are sufficiently similar to one another in ecology and morphology, while different enough from other known larvae to characterize the family [1].

Centrolenid tadpoles are found only in association with streams. Those collected in the field have been found burrowed into decaying vegetation at the edge of the water, not exposed to the current. These tadpoles are characterized by having long tails ($\geq 2 \times$ the head-body length) with reduced dorsal and ventral fins, depressed or cylindrical bodies, small dorsal eyes covered with skin, and

reduced pigmentation. All of these features seem directly related to their fossorial way of life.

In this paper, we describe a centrolenid-like tadpole from Borneo. At present we can identify the larva only to suborder. Subtle oral features distinguish this larva from true centrolenid larvae; otherwise the convergence in microhabitat use and overall morphology is among the most precise that we know of for amphibian larvae.

RESULTS

Four specimens have been collected (Table 1) from two localities (Danum Valley Field Centre, Lahad Datu District, Sabah and Nanga Takalit, Kapit District, Seventh Division, Sarawak) and deposited in the Field Museum of Natural History (FMNH). The following description is based on the largest specimen collected so far, a stage 31 of Gosner [2] individual.

The general body form is ovoidal, strongly depressed. The eyes are dorsal, extremely small, below the skin and far posterior from the tip of the snout. The eye-snout distance is one-third the head-body length. The pupils are directed obliquely dorsolateral. Eye diameter is 8% of head-body length; interorbital distance is 60% of the internarial distance. The nostrils are small ($< 1\%$ of head-body length), lack an elevated rim, and are exceptionally far forward. They are just dorsal to the lateral edge of the snout, above the corner of the mouth, at 11% of distance from snout back along the head-body.

The oral disc is ventral, subterminal. Its width is $2/3$ the maximum width of the body. The marginal

Accepted August 8, 1989

Received June 19, 1989

¹ Present address: Department of Anatomy, Dalhousie University, Halifax, Nova Scotia B3H 4H7, Canada

TABLE 1. Measurements¹ and denticle counts of fossorial stream-associated tadpoles from Borneo

Specimen(s)	FMNH #31452	FMNH #221024
Locality	Danum	N. Takalit
No. individuals	1	3
Stages ²	31	25
Head-body length	10.0	5.4-6.5
Head-body depth	5.2	3.3-4.0
Head-body depth	3.6	2.1-2.3
Eye diameter	0.8	0.3
Eye-snout	2.8	1.7-2.2
Nostril-snout	1.1	0.7(1)
Interorbital	1.4	1.1-1.2
Internarial	2.3	—
Snout-spiracle	7.1	4.5-4.8
Tail length	22.5	10.4-13.0
Tail depth	4.7	2.7-3.3
Denticles ³		
-upper	I:1-1	I:1-1
-lower	1-1:VIII	1-1:VIII

¹ Measurements made with ocular micrometer at 12×, given in mm; definitions of dimensions as in Inger and Frogner [15].

² According to Gosner [2].

³ Follows system used in Inger [3].

papillae are in a single row with a narrow median gap along the posterior free edge of the disc. The papillae are of moderate size. Papillae are absent along the anterodorsal edge of the disc, but are clustered on a small outwardly directed flap at the lateral corners of the mouth. A distinct notch separates these flaps from the ventral portion of the disc. The papillae on the lateral flaps are the largest and are in two rows, seven to nine papillae in an outer row and two to four in an inner row.

The dental formula, following the system of Inger [3], is I: 1-1/1-1: VIII. The denticles in the ventral rows decrease in size from the inner-most to outer-most rows and the four outer-most rows are distinctly shorter than the inner ones. The denticles are dense, spatulate and range from black (large) to brown (small) in color. They all curve toward the mouth. In microscopic detail, they most closely resemble the denticles illustrated for *Rana chalconota* and *Rana signata* in Inger [3].

The upper beak is a wide, gentle arch. The margin is finely serrated. The marginal serrations are of uniform size, smaller than the denticles, and

darkly pigmented. The lower beak is V-shaped, with an angle of 100° between the arms. The pigmented margin of the lower beak is slightly more extensive than that of the upper beak; its serrations are coarser than those of the upper beak, but still finer than the neighboring denticles.

The spiracle is sinistral, midway up the side of the body and far posterior (i.e., 70% of distance

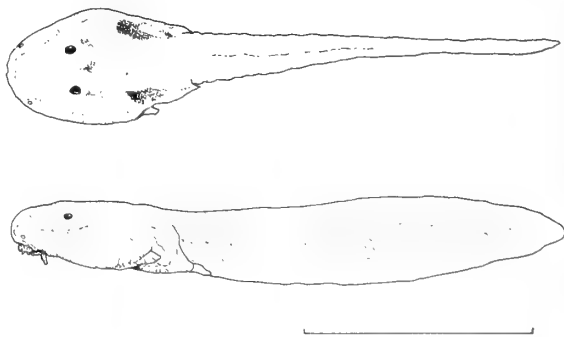


FIG. 1. Dorsal (above) and lateral (below) views of the fossorial ranoid tadpole described in this report. The illustration is of a stage 25 specimen (FMNH #221024) See Table 1. Scale line=5.0 mm.

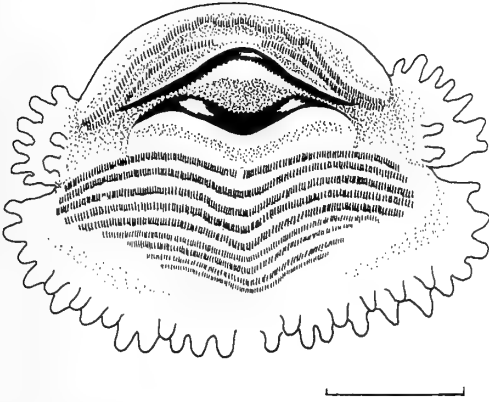


FIG. 2. Oral disc of the tadpole illustrated in Fig. 1. Scale line=0.5 mm.

from the snout tip to end of body). The spiracle has a short, free, terminal tube. The width of the spiracular opening is slightly greater than the diameter of the eye.

The anal tube is median and long.

The tail is long and slender, $2 \frac{1}{4}$ times the head-body length (Table 1). The tail tip is broadly rounded. The fin margins are very weakly convex. The maximum depth of the tail is at approximately $\frac{3}{5}$ of tail length. Both the dorsal and ventral fins are shallow. The dorsal fin begins on the tail just above the end of the anal tube. The ventral fin begins immediately behind the body proper and is slightly deeper than the dorsal fin in the proximal $\frac{1}{3}$ of the tail. The caudal musculature is deeper than either fin in the proximal $\frac{2}{3}$ of the tail.

The head-body of the preserved tadpole is pigmentless. The skin on the body has a shiny appearance. The skin overlying the caudal musculature has a faint, brownish reticulum. This pigment pattern extends up on to the dorsal fin near the base of the tail.

Neuromasts are present but not easily observed or counted. They are singular, not organized into stitches. Approximately 20 neuromasts are present in both the infraorbital and supraorbital rows on each side of the head.

The posterior $\frac{2}{3}$ of the intestines, along with a portion of the pancreas, are visible through the ventral body wall. We counted five coils of intestine from the center of the gut to the caudal edge of the body cavity.

Because the internal oral features of this tadpole are so similar to those of *Centrolenella fleischmanni* [4], only features that differ from *C. fleischmanni* are described here. Terminology follows Wassersug [4].

The medial pair of infralabial papillae are smaller. The lateral pair of infralabial papillae are larger with finger-like projections. There are four buccal floor arena papillae per side. The prenarial arena has a small, median knob anteriorly and a larger transverse ridge posterior to it. The long, longitudinally oriented, internal narial depression that characterizes *C. fleischmanni* is absent. The median ridge is smaller and more posterior. The postnarial papillae are much larger. They have rounded apices and project anteromedially over the medial half of the internal nares. Additional flap-like papillae of the anterior buccal roof are absent. The dorsal velum is not continuous across the midline. The glottis is smaller and not patent.

Qualitatively, the structure in the pharynx of this specimen looked indistinguishable from those of *C. fleischmanni*. Secretory ridges are present on the branchial food traps. Because of the small size of the specimen, no attempt was made to count gill filter rows.

The lungs at stage 31 are large, as long as the body cavity and flattened, indicating that they were not inflated in life. The skin is heavily vascularized.

Fine, heterogeneous particulate matter fills the alimentary tract. No macroscopic fragments of arthropods or plants are present. Some small mineral grains are visible, but most of the contents are unidentifiable organic debris.

Taxonomic considerations

The most mature tadpole collected so far is still too young to reveal any adult diagnostic characters. Adult frogs in the neighborhoods where these fossorial tadpoles were collected comprise pelobatids, bufonids, ranids, rhacophorids, and microhylids [5, 6]. The presence of denticles, a sinistral spiracle and perforated nares immediately exclude the tadpole from the Microhylidae [7]. The oral disc papillation, denticle row counts and denticle morphology are unlike any Bornean bufonids or pelobatids. The tadpole is by elimina-

tion tentatively classified as ranoid, either Ranidae or Rhacophoridae. Further assignment to family or genus is not possible at this time.

DISCUSSION

Our Bornean tadpoles were collected in deep leaf litter within but near edges of clear streams in lowland primary rain forest. The three in stage 25 were taken with larvae of two bufonids (*Ansonia leptopus* and *Pedostibes hosei*), and a pelobatid (*Leptobrachium montanum*). The stage 31 tadpole was found with larvae of *Rana signata*. All of these, except for the larval *Leptobrachium*, are commonly found in drifts of dead leaves [6].

Although Duellman and Trueb [1] claim that centrolenid tadpoles "develop in gravel or detritus in flowing water", to the best of our knowledge free-living centrolenid larvae avoid both flowing water and gravelly substrates. Rather they are found within the "accumulation of leaves, sticks and mud" [8] or occasionally even in the humus of a stream bank above the waterline [9] and out of the current. The common microhabitat of centrolenid larvae closely resembles the microhabitat where our unusual Bornean tadpoles were collected.

Except for the denticle formula and narial position, our Bornean tadpoles are externally identical to those of many centrolenid species [10]. The body profile, spiracle position, tail length, fin shape, and overall size and coloration are the same. So are the small nostrils and the small, dorsally positioned, sub-cutaneous eyes. The most conspicuous feature that distinguishes the Bornean tadpole from centrolenid larvae are the supernumerary, ventral denticle rows. Centrolenids all have two or fewer upper rows and three or fewer lower rows.

Internally our tadpole can be distinguished from *C. fleischmanni* by a variety of anatomical features, primarily anteriorly near the orifice of the mouth and the internal nares. These may be little more than internal reflections of differences in external oral morphology and narial position (slightly more anterior in the Bornean species). In key features, which reflect the filter-feeding capacity of the tadpoles—such as the pattern of papillae

on the buccal floor and roof, the shape of the ventral velum, filter plates, and gill filters—the tadpoles are indistinguishable.

Virtually all of the features that distinguish both the Bornean species and centrolenid tadpoles from typical ranoid and bufonid larvae can be understood as adaptations for a fossorial rather than either pelagic or demersal existence [9, 11, 12]. Not all fossorial tadpoles are associated with stream bank leaf litter, but all have cylindrical or depressed bodies and long tails with reduced fins. All have small dorsally located eyes and reduced pigmentation. Several arboreal tadpoles from a variety of anuran families fit this description [13]. The Bornean species is exceptional among all fossorial tadpoles in its high number of ventral denticle rows. We have no functional explanation for this distinctive feature. Another noteworthy feature in the Bornean species is the uninflated lung. This tadpole does not breathe air like certain arboreal and semi-terrestrial "fossorial" tadpoles [10, 13]. Villa [9, 14] suggested that centrolenid tadpoles, which are often reddish in life, appear so because of perfusion of skin for cutaneous respiration. Although the Bornean tadpoles were not particularly reddish in life, the extensive vascularization of their skin supports the idea that they rely heavily on cutaneous respiration.

As a final note, although we have formally described a single form of centrolenid-like tadpole from Southeast Asia, we suspect that other Old World species may have tadpoles of this type.

All other tadpoles collected with our fossorial form have been collected frequently and in large numbers in Bornean stream leaf litter [6]. The rarity of the fossorial form suggests that it may have been displaced into a slightly more aquatic situation than where it normally resides. Truly fossorial tadpoles are notoriously difficult to collect [9], as evidenced by the fact that larvae are known for less than 20% of centrolenid species in contrast to 25–30% for remaining anurans. Among tropical faunas the tadpoles of Borneo are well known [3], but even there tadpoles are known for only about 50% of the species.

ACKNOWLEDGMENTS

We thank Molly Ozaki and Brenda Zwicker for typing the manuscript, and V. Ann King for drafting the figures. Scott Pronych and Tracey Earle provided critical comments on early drafts. This work was supported by a National Science Foundation (USA) grant and an award from Marshall Field III Fund to R.F.I. The junior author was supported by the Natural Sciences and Engineering Research Council (CANADA).

REFERENCES

- 1 Duellman, W. E. and Trueb, L. (1986) *Biology of Amphibians*. McGraw Hill Book Company, New York.
- 2 Gosner, K. L. (1960) *Herpetologica*, **16**: 183–190.
- 3 Inger, R. F. (1985) *Fieldiana: Zool.*, New Series, **26**: 1–89.
- 4 Wassersug, R. J. (1980) *Univ. Kansas Mus. Nat. Hist. Miscellaneous Publ.*, **68**: 1–146.
- 5 Inger, R. F. (1966) *Fieldiana: Zool.*, **52**: 1–402.
- 6 Inger, R. F. Voris, H. K., and Frogner, K. J. (1986) *J. Tropical Ecol.*, **2**: 193–205.
- 7 Wassersug, R. J. (1989) *Fortschritte der Zool.* (In press)
- 8 Heyer, W. R. (1985) *Papeis Avulsos de Zoologia*, **36**: 1–21.
- 9 Villa, J. and Valerio, C. E. (1982) *Brenesia*, **19/20**: 1–16.
- 10 Altig, R. and Johnston, G. F. (1986) *Smithsonian Herp. Information Service*, **67**: 1–75.
- 11 Wassersug, R. J. and Heyer, W. R. (1983) *Canad. J. Zool.*, **61**: 761–769.
- 12 Wassersug, R. J. and Pyburn, W. F. (1987) *Zool. J. Linnean Soc.*, **91**: 137–169.
- 13 Lannoo, M. J., Townsend, D. S. and Wassersug, R. J. (1987) *Fieldiana: Zool.*, New Series, **38**: 1–31.
- 14 Villa, J. (1984) *Milwaukee Publ. Mus. Contrib. Bio. Geol.*, **55**: 1–50.
- 15 Inger, R. F. and Frogner, K. J. (1980) *Sarawak Mus. J.*, **27**: 311–324.

Development

Growth & Differentiation

Published Bimonthly by the Japanese Society of
Developmental Biologists
Distributed by Business Center for Academic
Societies Japan, Academic Press, Inc.

Papers in Vol. 32, No. 3. (June 1990)

30. **REVIEW:** T. Shinomura and K. Kimata: Precartilaginous condensation during skeletal pattern formation
 31. K. Yamamoto and S. Nemoto: Absence of species specificity of germinal vesicle factor required for the cytoplasmic cycle during meiotic division
 32. H. Nakayama, X. Ru, J. Fujita, T. Kasugai, H. Onoue, S. Hirota, H. Kuroda and Y. Kitamura: Growth competition between W mutant and wild-type cells in mouse aggregation chimeras
 33. C. Hui and Y. Suzuki: Homeodomain binding sites in the promoter region of silk protein genes
 34. Y. Kajiwar, T. Kuwana and M. Inoue: Pigmentation patterns of mouse chimeras following injection of embryonic cells into postimplantation embryos *in Utero*
 35. R. A. Raff, L. Herlands, V. B. Morris and J. Healy: Evolutionary modification of Echinoid sperm correlates with developmental mode
 36. K. Akasaka, Y. Akimoto, M. Sato, H. Hirano and H. Shimada: Histochemical detection of arylsulfatase activity in sea urchin embryos
 37. K. Akasaka, K. Yamada, K. Sekine and H. Shimada: Effects of aphidicolin on arylsulfatase gene expression in sea urchin embryos
 38. A. Fujiwara, K. Taguchi and I. Yasumasu: Fertilization membrane formation in sea urchin eggs induced by drugs known to cause Ca^{2+} release from isolated sarcoplasmic reticulum
 39. P. A. Veno, M. A. Strumski and W. H. Kinsey: Purification and characterization of echinonectin a carbohydrate-binding protein from sea urchin eggs
 40. I. Takahashi, T. Ueda, Y. Kameoka, K. Abe, N. Takagi and K. Hashimoto: Construction of a DNA library enriched with mouse 4 chromosome of T(X; 4)37H translocation
 41. K. Joseph and T. G. Baby: Changes in polyamine contents during development of the frog, *Microhyla ornata*
 42. K. Mitsunaga, S. Shinohara and I. Yasumasu: Probable contribution of protein phosphorylation by protein kinase C to spicule formation in sea urchin embryos
 43. N. Yoshizaki: Localization and characterization of lectins in yolk platelets of *Xenopus* oocytes
-

Development, Growth and Differentiation (ISSN 0012-1592) is published bimonthly by The Japanese Society of Developmental Biologists, Department of Developmental Biology, Mitsubishi Kasei Institute of Life Science, Minami-ohtani 11, Machida, Tokyo 194, Japan. 1989: Volume 31. Annual subscription for Vol. 32, 1990: U. S. \$ 148.00, U. S. and Canada: U. S. \$ 163.00, all other countries except Japan. All prices include postage, handling and air speed delivery except Japan. Second class postage paid at Jamaica, N.Y. 11431, U. S. A.

Outside Japan: Send subscription orders and notices of change of address to Academic Press, Inc., Journal Subscription Fulfillment Department, 1 East First Street, Duluth, MN 55802, U. S. A. Send notices of change of address at least 6-8 weeks in advance. Please include both old and new addresses. U. S. A. POSTMASTER: Send changes of address to *Development, Growth and Differentiation*, Academic Press, Inc., Journal Subscription Fulfillment Department, 1 East First Street, Duluth, MN 55802, U. S. A.

In Japan: Send nonmember subscription orders and notices of change of address to Business Center for Academic Societies Japan, 16-3, Hongo 6-chome, Bunkyo-ku, Tokyo 113, Japan. Send inquiries about membership to Business Center for Academic Societies Japan, 4-16, Yayoi 2-chome, Bunkyo-ku, Tokyo 113, Japan.

Air freight and mailing in the U. S. A. by Publications Expediting, Inc., 200 Meacham Avenue, Elmont, NY 11003, U. S. A.

NARISHIGE

THE ULTIMATE NAME IN MICROMANIPULATION

OUR NEW MODELS **WR-88** and **MO-102M**
MAKE PRECISION MICROMANIPULATION SO EASY!



SOME FEATURES of THE WR-88 WATER ROBOT MICROMANIPULATOR (3-DIMENSIONAL)

- * Drift-free, the new WR-88 has a DRIFT movement of less than 2 microns.
- * The new WR-88 has a SMOOTH MICRODRIVE MECHANISM.
- * An Aqua Purificate remote control ensures totally vibration-free operation.



NARISHIGE SCIENTIFIC INSTRUMENT LAB.

9-28 KASUYA 4-CHOME SETAGAYA-KU, TOKYO 157, JAPAN
PHONE (INT-L) 81-308-8233, FAX (INT-L) 81-3-308-2005
CABLE : NARISHIGE LABO, TELEX, NARISHIGE J27781

THE BOTANICAL MAGAZINE TOKYO

An international journal for plant sciences published quarterly by the Botanical Society of Japan. For a century, the journal has continuously published outstanding papers by Japanese as well as foreign botanical scientists. Contributors to the journal are not limited to the members of the Society and their papers are accepted by paying the page charge.

Papers in a Recent Issue :

DARNAEDI, D., M. KATO AND K. IWATSUKI : Electrophoretic Evidence for the Origin of *Dryopteris yakusilvicola* (Dryopteridaceae)

ZHANG, X., I. INOUE AND M. CHIHARA : An Unusual Short Flagellum in *Mallomonas guttata* (Synurophyceae, Chrysophyta)

TEROUCHI, N., S. HASEZAWA, H. MATSUSHIMA, Y. KANEKO AND K. SYÔNO : Observation by SEM of the Attachment of *Agrobacterium tumefaciens* to the Surface of Vinca, Asparagus and Rice Cells

TAKASO, T. AND H. TOBE : Seed Coat Morphology and Evolution in Celtidaceae and Ulmaceae (Urticales)

PJON, C.-J., S.-d. KIM AND J.-Y. PAK : Effects of Spermidine on Chlorophyll Content, Photosynthetic Activity and Chloroplast Ultrastructure in the Dark and under Light

FUJISHIMA, H., H. OKADA, Y. HORIO AND T. YAHARA : A Cytotaxonomy and Origin of *Ranunculus yaegatakenensis*, an Endemic Taxon of Yakushima Island

KAWAKUBO, N. : Dioecism of the Genus *Callicarpa* (Verbenaceae) in the Bonin (Ogasawara) Islands

AMANO, M. : Biosystematic Study of *Sedum* L. Subgenus *Aizoon* (Crassulaceae) I. Cytological and Morphological Variations of *Sedum aizoon* L. var. *floribundum* Nakai

RIDGE, R.W. : Cytochalasin-D Causes Abnormal Wall-Ingrowths and Organelle-Crowding in Legume Root Hairs

Order form

Send to

THE BOTANICAL SOCIETY OF JAPAN

Toshin Building
Hongo 2-27-2, Bunkyo-ku,
Tokyo 113, Japan

THE BOTANICAL MAGAZINE, TOKYO

☐ Individuals : ¥ 7,000 p.a.

☐ Institutions : ¥ 17,500 p.a.

Name (Please print) : _____

Address : _____

Date : _____ Signature : _____

(Contents continued from back cover)

rumen of Holstein-Friesian cattle (<i>Bos taurus taurus</i>) in Hokkaido, Japan, with the description of two new species	449
Watabe, H., X. C. Liang and W. X. Zhang: The <i>Drosophila polychaeta</i> and the <i>D. quadri-setata</i> species-groups (Diptera: Drosophilidae) from Yunnan Province, southern China	459
Sawada, I. and M. Harada: Cestodes of field micromammals (Insectivora) from central Honshu, Japan	469
Takeda, M. and N. Shikatani: Crabs of the genus <i>Calappa</i> from the Ryukyu Islands, with description of a new species	477
Ito, T. and M. J. Grygier: Description and complete larval development of a new species of <i>Baccalaureus</i> (Crustacea: Ascothoracida) parasitic in a zoanthid from Tanabe Bay, Honshu, Japan	485
Abé, H.: Three new species of the genus <i>Rhombognathus</i> (Acari, Halacaridae) from Japan	517
Inger, R. F. and R. J. Wassersug: A centrolenid-like anuran larva from southeast Asia (COMMUNICATION)	557

ZOOLOGICAL SCIENCE

VOLUME 7 NUMBER 3

JUNE 1990

CONTENTS

REVIEWS

- Plisetskaya, E. M.: Recent studies of fish pancreatic hormones: Selected topics 335
- Suzuki, N.: Structure and function of sea urchin egg jelly molecules 355

ORIGINAL PAPERS

Physiology

- Nakashima, H. and Y. Kamishima: Regulation of water permeability of the skin of the treefrog, *Hyla arborea japonica* 371
- Hori, K., Y. Furukawa and M. Kobayashi: Regulatory actions of 5-hydroxytryptamine and some neuropeptides on the heart of the African giant snail, *Achatina fulica* Férussac 377
- Kanui, T. I., K. Hole and J. O. Miaron: Nociception in crocodiles: Capsaicin instillation, formalin and hot plate tests (COMMUNICATION) 537

Cell Biology and Morphology

- Tamamaki, N.: Evidence for the phagocytotic removal of photoreceptive membrane by pigment cells in the eye of the planarian, *Dugesia japonica* 385
- Sato, M., H. Mitani and A. Shima: Eurythermic growth and synthesis of heat shock proteins of primary cultured goldfish cells 395
- Iga, T., J. Kinutani and N. Maeno: Motility of cultured iridophores from the freshwater goby, *Odontobutis obscura* 401

Biochemistry

- Ryuzaki, M. and M. Oonuki: Changes in lipid composition in the tail of *Rana catesbeiana* larvae during metamorphosis 409

Genetics

- Phang, V. P. E., A. A. Fernando and E. W. K. Chia: Inheritance of the color patterns of the blue snakeskin and red snakeskin varieties of the guppy, *Poecilia reticulata* 419

Developmental Biology

- Irisawa, S., T. Iguchi and N. Takasugi: Critical period of induction by tamoxifen of genital organ abnormalities in male mice (COMMUNICATION) 541

Reproductive Biology

- Pandey, S. C. and S. D. Pandey: Photoperiodic influences on pheromonal delay of puberty in young female wild mice (COMMUNICATION) 547

Endocrinology

- Oota, Y.: Immunocytochemical and ultrastructural characterization of the cells in the pars tuberalis of the turtle, *Geoclemys reevesii* (COMMUNICATION) 551
- Taniguchi, Y., S. Tanaka and K. Kurosumi: Distribution of immunoreactive thyrotropin-releasing hormone in the brain and hypophysis of larval bullfrogs with special reference to nerve fibers in the pars distalis ... 427
- Takei, Y. and T. X. Watanabe: Vasodepressor effect of atrial natriuretic peptides in the quail, *Coturnix coturnix japonica* 435

Taxonomy and Systematics

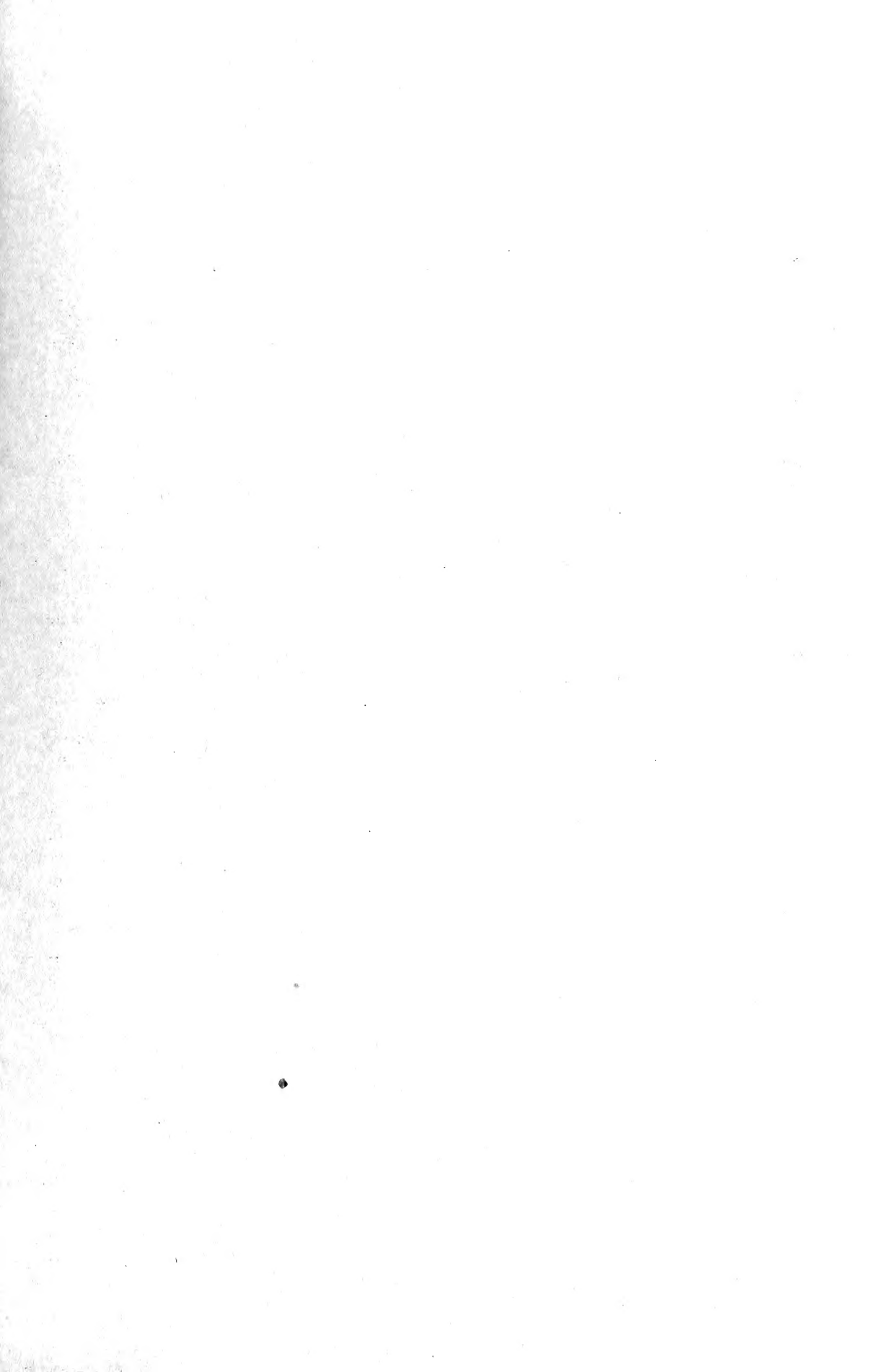
- Tanabe, T.: A new millipede of the genus *Riukiaria* from Is. Yaku-shima, Japan (Diplopoda; Polydesmida; Xystodesmidae) 443

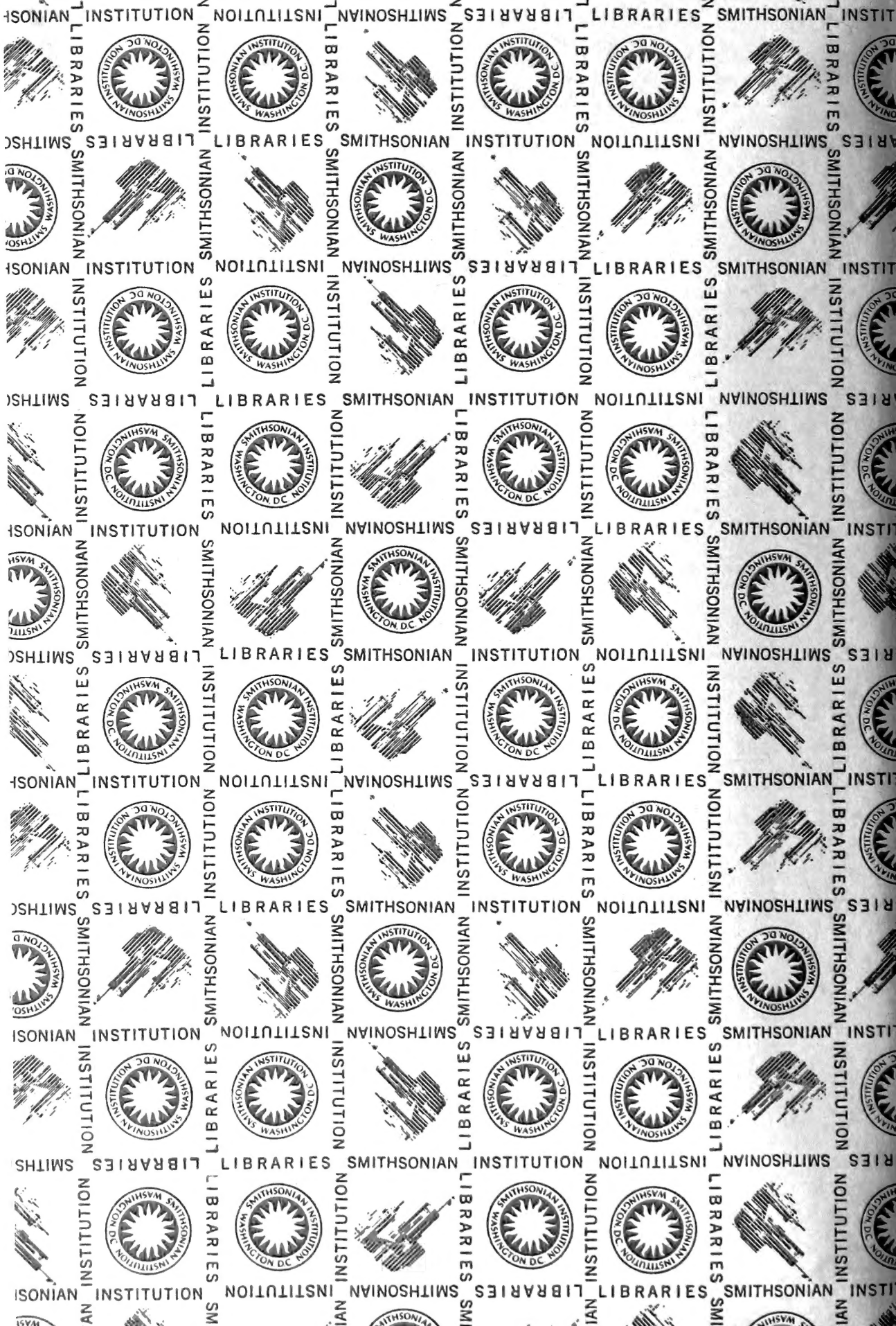
(Contents continued on inside back cover)

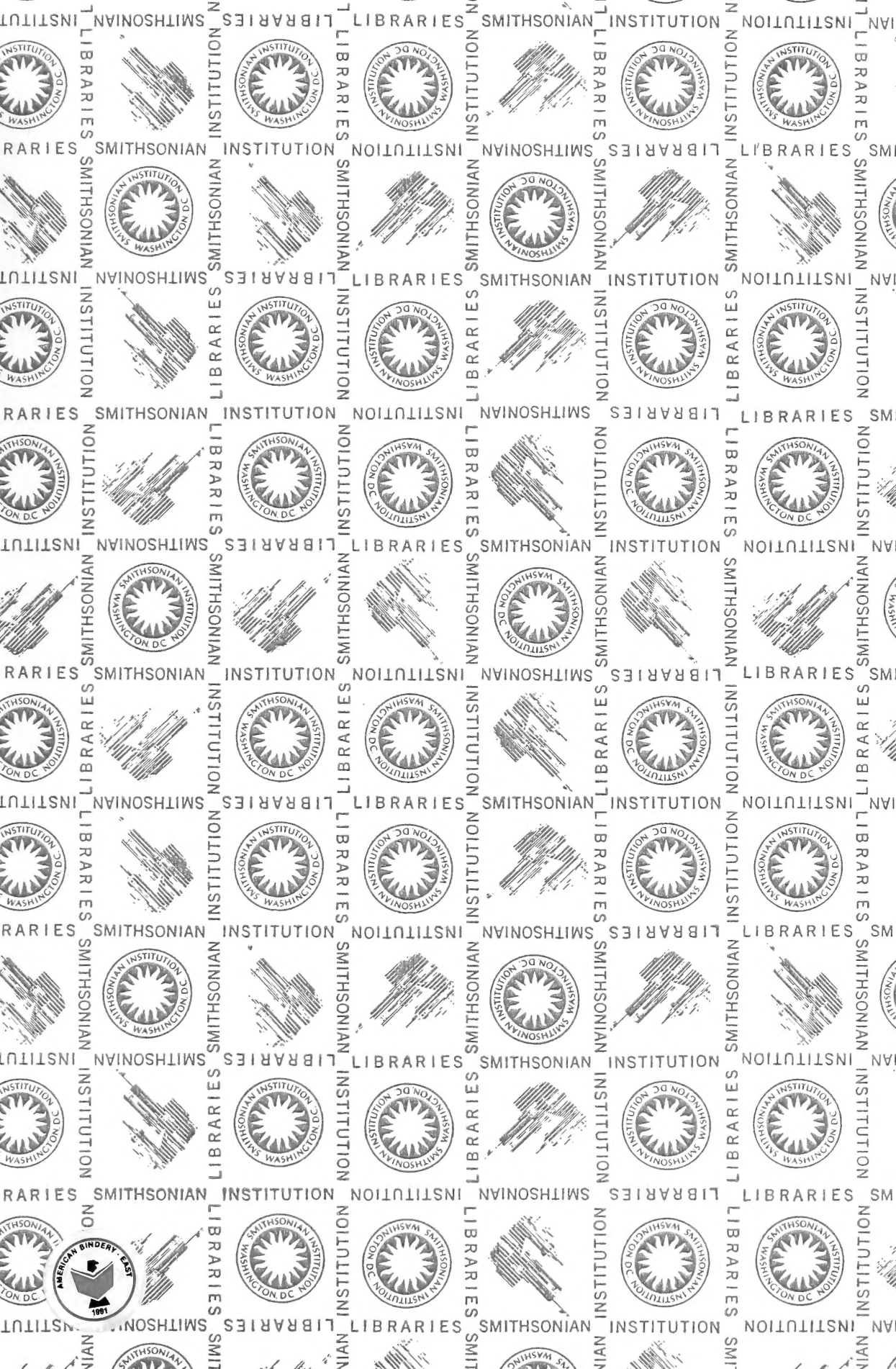
INDEXED IN:

Current Contents/LS and AB & ES,
Science Citation Index,
ISI Online Database,
CABS Database, INFOBIB

Issued on June 15
Printed by Daigaku Letterpress Co., Ltd.,
Hiroshima, Japan







SMITHSONIAN INSTITUTION LIBRARIES



3 9088 01261 2727